

The iminium-catalyzed (*E*)-polyene cyclization

Josephine M. Warnica

Department of Chemistry, McGill University

Montréal, Québec, Canada

April 2022

A thesis submitted to McGill University in partial fulfilment of the requirements
of the degree of Doctor of Philosophy

© Josephine M. Warnica 2022

Abstract

The biosynthesis of steroids and other terpenoid natural products proceeds through an enzymatic polyene cyclization; a cascade reaction that builds up a large amount of molecular complexity in a single step. Research into synthetic polyene cyclizations has been driven both by the intriguing mechanism of cascade olefin additions with complete chemo-, regio-, and stereocontrol, as well as the applicability of these reactions for the synthesis of medically relevant molecules.

Using a cyclic hydrazide catalyst and 2-formyl-1,5-diene substrates, our group had reported the first iminium-catalyzed Cope rearrangement. DFT calculations on the reaction pathway suggested a stepwise mechanism proceeding through a shallow energy cyclohexyl cation intermediate. We recognized a similar cyclohexadiene structure in the substrates for both the Cope rearrangement as well as the polyene cyclization. With the same cyclic hydrazide catalyst and polyene substrates containing this 2-formyl-1,5-diene, in addition to a stabilizing methyl group and a terminating aromatic ring, the first iminium-catalyzed polyene cyclization was reported.

In this thesis, a modular synthesis of substrates was developed, that was used for the investigation into the scope and limitations of the racemic iminium-catalyzed (*E*)-polyene cyclization. Through the investigation into the limitations of the reaction, it was found that the reaction worked well with substrates containing terminating groups of strong to intermediate nucleophilicities, including several heterocycles.

Investigation into the asymmetric reaction resulted in the development of two catalysts; one with improved reactivity and another that afforded high enantioselectivity. A modular synthetic route was developed to build a library of chiral hydrazide catalysts to screen the effects of different aromatic substitution. It was found that the addition of an extended aromatic substitution to the hydrazide catalyst did not promote selectivity in the reaction. However, the reactivity of the catalyst was drastically increased. With this more reactive catalyst, the scope of the racemic polyene cyclization could be expanded to include substrates with less nucleophilic terminating groups that had not been reactive under previous conditions.

Computational modelling indicated a preferred conformation in a chiral hydrazide catalyst with *m*-terphenyl substitution that could promote desired selectivity in the asymmetric reaction.

Therefore, *m*-terphenyl catalysts with different substitution patterns were synthesized and screened in the model (*E*)-polyene cyclization. It was found that, after optimization of reaction conditions, 3,5-*di**tert*-butyl substitution on the *m*-terphenyl moiety of the chiral hydrazide catalyst yielded *trans*-decalin product from the model substrate in 80% ee. Investigation into the limitations of the reaction both experimentally and with DFT calculations has provided evidence towards potential (*E*)-polyene substrates which would provide *trans*-decalin products with high enantioselectivity.

Resume

La biosynthèse des stéroïdes et autres produits naturels terpénoïdes passe par une cyclisation enzymatique des polyènes ; une réaction en cascade qui accumule une grande quantité de complexité moléculaire en une seule étape. La recherche sur les cyclisations de polyènes synthétiques a été motivée à la fois par le mécanisme intrigant des additions d'oléfines en cascade avec chimio-, régio- et stéréocontrôle complets, ainsi que par l'applicabilité de ces réactions pour la synthèse de molécules pertinentes sur le plan médical.

En utilisant un catalyseur d'hydrazide cyclique et des substrats de 2-formyl-1,5-diène, notre groupe avait rapporté le premier réarrangement de Cope catalysé par l'iminium. Les calculs DFT sur la voie de réaction ont suggéré un mécanisme par étapes passant par un intermédiaire de cation cyclohexyle à faible énergie. Nous avons reconnu une structure de cyclohexadiène similaire dans les substrats pour le réarrangement de Cope ainsi que pour la cyclisation du polyène. Avec le même catalyseur d'hydrazide cyclique et des substrats de polyène contenant ce 2-formyl-1,5-diène, en plus d'un groupe méthyle stabilisant et d'un cycle aromatique de terminaison, la première cyclisation de polyène catalysée par l'iminium a été rapportée.

Dans cette thèse, une synthèse modulaire de substrats a été développée, qui a été utilisée pour l'étude de la portée et des limites de la cyclisation racémique catalysée par l'iminium (*E*)-polyène. Grâce à l'enquête sur les limites de la réaction, il a été constaté que la réaction fonctionnait bien avec des substrats contenant des groupes terminaux de nucléophilie fortes à intermédiaires, y compris plusieurs hétérocycles.

L'étude de la réaction asymétrique a abouti au développement de deux catalyseurs; un avec une réactivité améliorée et un autre qui offrait une énantiosélectivité élevée. Une voie de synthèse modulaire a été développée pour construire une bibliothèque de catalyseurs hydrazides chiraux pour cribler les effets de différentes substitutions aromatiques. Il a été trouvé que l'addition d'une substitution aromatique étendue au catalyseur hydrazide ne favorisait pas la sélectivité dans la réaction. Cependant, la réactivité du catalyseur a été considérablement augmentée. Avec ce catalyseur plus réactif, la portée de la cyclisation du polyène racémique pourrait être élargie pour inclure des substrats avec des groupes de terminaison moins nucléophiles qui n'avaient pas été réactifs dans les conditions précédentes.

La modélisation informatique a indiqué une conformation préférée dans un catalyseur d'hydrazide chiral avec une substitution m-terphényle qui pourrait favoriser la sélectivité souhaitée dans la réaction asymétrique. Par conséquent, des catalyseurs de m-terphényle avec différents modèles de substitution ont été synthétisés et criblés dans le modèle de cyclisation (*E*)-polyène. Il a été constaté qu'après optimisation des conditions de réaction, la substitution 3,5-ditert-butyle sur le fragment m-terphényle du catalyseur hydrazide chiral a donné un produit trans-décaline à partir du substrat modèle à 80% ee. L'étude des limites de la réaction à la fois expérimentalement et avec des calculs DFT a fourni des preuves de substrats potentiels (*E*)-polyène qui fourniraient des produits trans-décaline avec une énantiosélectivité élevée.

Acknowledgements

Firstly, I'd like to thank my supervisor, Prof. Jim Gleason. Your excitement for chemistry was what drew me to your lab and has helped me continue when things weren't going as planned. Thank you for teaching the importance of having a broad knowledge of organic chemistry and taking the effort to train me in it. I would not have become the chemist that I am today without the training that I've received in your group.

Thank you to all of the McGill staff for your support in my research. Thank you, Nadim and Alex for all of your help with HRMS. Thank you, Robin, for your help with a vast amount of NMR questions. Thank you, Rick, Weihua, and J.P, for all of the help with instrument issues. Thank you to the departmental office staff, including Chantal, Chelsea, Linda, Sandra, and Nikoo,, for always knowing the answers to my questions.

Thank you to my committee members, Prof. Bruce Arndtsen and Prof. J.P. Lumb, for helping shape this thesis. Also, thank you to all the people who have gotten me here, including the people at the University of Guelph, Prof. Adrian Schwan and Prof. Steffen Graether, and Craig Bryant at the Centre of Forensic Sciences.

Thank you to all the Gleason group members, past and present, for the help that you have given me along the way. Special thanks to Jon, for your patience in training me and all the knowledge you passed on; Nick, for your guidance and commiseration on characterizing 7-membered rings; Adam, for your insane editing talent and listening ear; Sam, for being my polyene partner-in-crime; and Don, for being my left-hand man these past four years. You have given me many experiences during my time at McGill that I will remember fondly.

Finally, thank you to my family. Mom, Dad, Meg and Will, I couldn't have done this without you.

Contributions by the author

Aside from the work assigned below and throughout the thesis text, all other original work in this thesis was performed by the author, Josephine M. Warnica.

The initial inception of the iminium-catalyzed polyene cyclization was developed by Dainis Kaldre and Prof. James Gleason. Initial synthesis of the (*E*)-polyene model substrate was done by Dainis Kaldre and optimized by Samuel Plamondon. Optimization of the cyclization of the model (*E*)- and (*Z*)-polyene substrates was also done by Dainis Kaldre and Samuel Plamondon. All further work on the (*Z*)-polyene cyclization was performed by Samuel Plamondon.

Synthesis of previously screened chiral hydrazide catalysts was performed by Dainis Kaldre, Samuel Plamondon, and Nicklas Häggman (as assigned throughout the text). Screening of initial chiral catalysts in the (*E*)-polyene cyclization was performed by Dainis Kaldre and Samuel Plamondon. All other chiral catalysts have been designed and synthesized by the author.

DFT calculations on the (*Z*)-polyene cyclization were performed by Prof. James Gleason. Preliminary calculations for results presented on the (*E*)-polyene cyclization in Chapter 3 were performed by the author and optimized by Prof. James Gleason. All DFT calculations in Chapter 4 were performed by the author.

Table of contents

Abstract.....	ii
Resume.....	iv
Acknowledgements.....	vi
Contributions by the author	vii
Table of contents.....	viii
List of schemes	xiii
List of figures.....	xix
List of tables.....	xxii
List of abbreviations	xxiii
Chapter 1. Introduction	1
1.1 Biosynthesis of terpene and terpenoid natural products.....	1
1.1.1 Biosynthesis of steroids	2
1.1.2 Elucidation of the biosynthetic polyene cyclization.....	3
1.1.3 Biosynthetic polyene cyclization.....	5
1.1.4 Crystal structure of SHC and OSC.....	7
1.1.5 Mutagenesis experiments on SHC.....	8
1.1.6 Mechanism of the biosynthetic polyene cyclization.....	11
1.2 Cation- π interaction	12
1.2.1 Initial discoveries in cation- π interactions	13
1.2.2 Origin of attraction in cation- π interactions.....	14
1.3 Cation- π interactions in organic synthesis.....	16
1.3.1 Cation- π interactions in supramolecular catalysis	19
1.3.2 Cation- π interactions in small molecule catalysis.....	23
1.4 Synthetic polyene cyclizations	27

1.4.1 Racemic polyene cyclizations	28
1.4.2 Substrate-controlled diastereoselective cyclizations	29
1.4.3 Reagent/catalyst controlled enantioselective polyene cyclizations	31
1.4.3.1 Transition metal-catalyzed asymmetric polyene cyclizations	33
1.4.3.2 Organocatalyzed asymmetric polyene cyclizations	35
1.5 Organocatalysis	39
1.5.1 Amine catalysts.....	40
1.6 Iminium catalysis	41
1.6.1 Asymmetric iminium catalysis	42
1.6.1.1 Iminium catalysis with secondary amine catalysts	43
1.6.1.2 Hydrazone-type catalysts.....	45
1.6.2 Iminium-catalysis of α -branched enals	49
1.6.2.1 Primary amine catalysts with α -branched enals.....	50
1.7 Organocatalytic Cope rearrangement.....	53
1.7.1 The α -effect in hydrazone catalysts.....	56
1.7.2 Mechanism of the iminium-catalyzed Cope rearrangement.....	57
1.8 Iminium-catalyzed polyene cyclization	58
1.9 References	60
Chapter 2. Investigation into the racemic iminium-catalyzed (<i>E</i>)-polyene cyclization.....	80
2.1 Introduction	80
2.2 Initial work on the iminium-catalyzed polyene cyclization	81
2.3 Substrate synthesis	83
2.3.1 Modular substrate synthesis.....	84
2.4 Solvent screen	89
2.5 Substrate scope.....	92

2.6 Less nucleophilic substrates	96
2.6.1 Ether-bridged substrates	97
2.7 Proposed mechanism of the iminium-catalyzed polyene cyclization	102
2.8 Conclusions	104
2.9 References	105
Chapter 3. Exploration of cation- π interactions in the iminium-catalyzed (<i>E</i>)-polyene cyclization	107
3.1 Chiral catalyst design	107
3.2 Asymmetric iminium-catalyzed Cope rearrangement.....	108
3.3 Initial work on the asymmetric iminium-catalyzed polyene cyclization	111
3.4 Asymmetric (<i>Z</i>)-polyene cyclization.....	112
3.5 Incorporation of extended aromatics into chiral catalysts.....	113
3.5.1 Initial synthesis of chiral catalysts.....	114
3.5.2 Modular synthesis of catalysts with extended aromatic systems	115
3.5.3 Catalyst screening.....	123
3.6 Extended substrate scope	125
3.7 Mechanistic investigation.....	129
3.7.1 Reaction profiles.....	129
3.7.2 Conformational analysis of catalyst 3.47	133
3.8 Correlation of reactivity to σ^+	133
3.9 Conclusions	134
3.10 References	135
Chapter 4. Asymmetric iminium-catalyzed (<i>E</i>)-polyene cyclization	137
4.1 Introduction	137
4.2 DFT-mediated catalyst design.....	137

4.3 Substituted anthracene catalyst	140
4.4 <i>m</i> -Terphenyl catalyst	142
4.4.1 Synthesis of <i>m</i> -terphenyl catalyst	145
4.4.2 Screening of <i>m</i> -terphenyl catalyst	146
4.5 Substituted <i>m</i> -terphenyl catalysts	147
4.5.1 Synthesis of substituted <i>m</i> -terphenyl catalysts	149
4.5.2 Screening of substituted <i>m</i> -terphenyl catalysts	150
4.6 Investigation into bulkier carbamates	154
4.6.1 Synthesis of 3,5- <i>tert</i> -butyl- <i>m</i> -terphenyl catalysts with bulkier carbamates	154
4.6.2 Screening of 3,5- <i>tert</i> -butyl- <i>m</i> -terphenyl catalysts with bulkier carbamates	155
4.7 Alternate catalysts	156
4.7.1 4-Substituted <i>m</i> -terphenyl catalysts	156
4.7.2 6-Membered ring <i>m</i> -terphenyl catalyst	158
4.8 Optimization with 3,5-di- <i>tert</i> -butyl <i>m</i> -terphenyl catalyst 4.13	159
4.9 Investigations into substrate scope	163
4.9.1 Phenyl-terminated substrate	163
4.9.2 Analysis of EtOH-trapped products	165
4.9.3 3,5-Dimethylphenyl-terminated substrate	166
4.9.4 DFT investigation of reaction mechanism	167
4.9.5 Phenol-terminated substrate	171
4.9.6 Furan-terminated substrate	172
4.9.7 Future substrates	173
4.10 Conclusions	175
4.11 References	176
Contribution to knowledge and overall conclusion	179

Chapter 5. Experimental Procedures.....	179
5.1. General Experimental.....	181
5.2. Experimental Procedures from Chapter 2	182
5.3. Experimental Procedures from Chapter 3	221
5.4. Experimental Procedures from Chapter 4	249
5.5 References	283
Chapter 6. Density Functional Theory Calculations.....	288
6.1. DFT Calculations from Chapter 4.....	288
6.2 References	368
Chapter 7. NMR Spectra and HPLC Chromatograms	369
7.1. NMR Spectra of New Compounds	369
7.2. HPLC Chromatograms.....	506
Appendix I. Table of results for the model (<i>E</i>)-polyene cyclization with chiral hydrazide catalysts	514

List of schemes

Scheme 1.1. Combination of DMAPP and IPP units in the biosynthesis of terpenes.	1
Scheme 1.2. Monoterpene cyclizations and related natural products.	2
Scheme 1.3. Biosynthetic precursors of squalene and (3 <i>S</i>)-2,3-oxidosqualene.	3
Scheme 1.4. Early work by Linstead and Stork on the synthetic polyene cyclization.	4
Scheme 1.5. Schinz and Eschenmoser's evidence towards carbenium anti-parallel addition to an olefin.	5
Scheme 1.7. Biosynthesis of lanosterol from (3 <i>S</i>)-2,3-oxidosqualene.	6
Scheme 1.8. Hoshino's proposed mechanism of biosynthesis of hopene.....	12
Scheme 1.9. Cyclophane-catalyzed Menschutkin reaction.....	19
Scheme 1.10. Prins cyclization catalyzed by supramolecular assembly.	21
Scheme 1.11. (a) Cationic cyclization of geranyl acetate catalyzed by capsule 1.66 and (b) selective conversion of geranyl acetate in the presence of extended analogue 1.70	22
Scheme 1.12. Cationic sesquiterpene cyclizations catalyzed by capsule 1.66 (GC yields).....	23
Scheme 1.13. Tail-to-head cyclizations of neryl chloride derivatives.....	25
Scheme 1.14. Proposed mechanism of the thiourea-catalyzed polyene cyclization.....	25
Scheme 1.15. Screening of thiourea catalysts in the polyene cyclization of α -hydroxy lactam 1.87	26
Scheme 1.16. Chiral Bronsted acid-catalyzed polyene cyclization.	27
Scheme 1.17. Allylic alcohol-initiated polyene cyclization in Johnson's synthesis of progesterone.	28
Scheme 1.18. Tetracyclization achieved with incorporation of cation-stabilizing auxiliary.....	29
Scheme 1.19. Johnson's diastereomeric polyene cyclization initiated by the opening of a chiral acetal.	30
Scheme 1.20. Epoxide initiated polyene cyclization in Corey's synthesis of dammarenediol II.	30
Scheme 1.21. First reported enantioselective polyene cyclization.	31

Scheme 1.22. Enantioselective polyene cyclization with LBA 1.110 ·SnCl ₄	32
Scheme 1.23. Enantioselective tricyclization with LBA 1.120 ·SbCl ₅	33
Scheme 1.24. Gagne's asymmetric cationic Pt(II)-catalyzed polyene cyclization.	33
Scheme 1.25. Toste's asymmetric cation Au(I)-catalyzed polyene cyclization.	34
Scheme 1.26. Carreira's Ir(I)-catalyzed polyene cyclization.....	35
Scheme 1.27. LBBA-catalyzed polyene cyclization.....	36
Scheme 1.28. Yamamoto's enantioselective bromonium-initiated polyene cyclization.	37
Scheme 1.29. Denmark's enantioselective sulfenium-promoted polyene cyclization.	37
Scheme 1.30. Macmillan's enantioselective radical polyene cyclization.....	38
Scheme 1.31. Jacobsen's enantioselective thiourea-catalyzed polyene cyclization.	38
Scheme 1.32. Proline-catalyzed Hajos-Parrish-Eder-Sauer-Wiechert reaction.....	39
Scheme 1.33. Early examples of iminium reactivity.	42
Scheme 1.34. Early examples of asymmetric iminium catalysis.....	42
Scheme 1.35. MacMillan's iminium-catalyzed Diels-Alder reaction.	43
Scheme 1.36. Enantioinduction through electrostatic interaction in the iminium-catalyzed cyclopropanation.....	45
Scheme 1.37. Effect of an α -heteroatom substituted catalyst on the iminium-catalyzed Diels-Alder reaction.....	46
Scheme 1.38. Asymmetric hydrazide-catalyzed Diels-Alder reaction of α,β -unsaturated aldehydes.....	48
Scheme 1.39. Vinylogous Michael addition with α -branched enal.	49
Scheme 1.40. Preferred (<i>E</i>)-iminium formed with primary amine catalysts.	50
Scheme 1.41. Diels-Alder reaction of α -branched enals with primary amine catalyst 1.213	51
Scheme 1.42. Diels-Alder reaction of α -branched enals with BINOL-derived catalyst 1.216	51
Scheme 1.43. Diels-Alder reaction with α -branched enals with alkyl substitution.	51

Scheme 1.44. Friedel-Crafts alkylation with α -branched enals.	52
Scheme 1.45. Thermal and transition metal-catalyzed Cope rearrangements.	53
Scheme 1.46. Iminium-catalyzed Cope rearrangement of 1,5-hexadiene, 2-carboxaldehydes. ...	54
Scheme 1.47. Catalyst screen for the organocatalytic Cope rearrangement.	55
Scheme 1.48. Iminium-catalyzed Cope rearrangement.	56
Scheme 1.49. Comparison of relative second-order rate constants for the reaction amines, hydrazines, and hydrazides with benzhydrylium ion.	57
Scheme 1.50. Proposed mechanism of the iminium-catalyzed Cope rearrangement.	58
Scheme 1.51. Proposed iminium-catalyzed polyene cyclization.	59
Scheme 2.1. Iminium-catalyzed Cope rearrangement and proposed iminium-catalyzed polyene cyclization with 1,5-hexadiene-2-carboxaldehyde highlighted in blue.	80
Scheme 2.2. Model substrates for the iminium-catalyzed polyene cyclization.	81
Scheme 2.3. Preliminary results for iminium-catalyzed (<i>Z</i>)-polyene cyclization.	83
Scheme 2.4. Initial synthesis of model (<i>E</i>)-polyene substrates (work done by Dr. Samuel Plamondon).	84
Scheme 2.5. Initial retrosynthetic analysis of (<i>E</i>)-polyene substrates.	85
Scheme 2.6. Synthesis of iodide 2.17	85
Scheme 2.7. Attempted Kocienski rearrangement with iodide 2.17	86
Scheme 2.8. Second retrosynthetic analysis of (<i>E</i>)-polyene substrate synthesis.	87
Scheme 2.9. Carboalumination-iodination of 1-hexynol and 1-butyne.	87
Scheme 2.10. Revised synthesis of iodide coupling partner.	88
Scheme 2.11. Synthesis of iodide coupling partner.	88
Scheme 2.12. Final steps in the synthesis of (<i>E</i>)-polyene substrates.	89
Scheme 2.13 Possible side products from the polyene cyclization of substrate 2.46 in MeNO ₂	91
Scheme 2.14 Isolated product from solvent trapping of substrate 2.46 with EtOH.	91

Scheme 2.15. Cyclization of (<i>Z</i>)-polyene substrate 2.70	94
Scheme 2.16. Proposed cyclization of ether-bridged substrates.....	98
Scheme 2.17. Retrosynthetic analysis of ether-bridged substrates.....	98
Scheme 2.18. Synthesis of vinyl iodide coupling partner.....	99
Scheme 2.19. Synthesis of ether-bridged substrates 2.93 and 2.94	100
Scheme 2.20. Unsuccessful polyene cyclizations of ether-bridged substrates.....	101
Scheme 2.21. Proposed mechanism of isomerization in the iminium-catalyzed (<i>E</i>)-polyene cyclization.....	104
Scheme 3.1. Positions of possible chiral substitution on the 7-membered ring hydrazide catalyst.....	108
Scheme 3.2. Mechanism of Cope rearrangement of substrate 3.7	109
Scheme 3.3. Catalyst screen for the asymmetric iminium-catalyzed Cope rearrangement. (Work done by Dr. Dainis Kaldre).....	110
Scheme 3.4. Initial asymmetric polyene cyclization. (Work done by Dr. Samuel Plamondon).	111
Scheme 3.5. Asymmetric iminium-catalyzed (<i>Z</i>)-polyene cyclization. (Work done by Dr. Samuel Plamondon).....	113
Scheme 3.6. Iminium-catalyzed cyclization of (<i>E</i>)-polyene substrate 2.4 with bicyclic hydrazide catalyst 3.23 . (Work done by Dr. Samuel Plamondon).	113
Scheme 3.7. Original synthesis of catalyst 3.16 . (Work done by Dr. Nicklas Häggman).....	115
Scheme 3.8. Retrosynthetic analysis for the modular synthesis of catalysts 3.27 and 3.28	116
Scheme 3.9. Synthesis of benzyl and naphthyl catalysts 3.16 and 3.38	117
Scheme 3.10. Failed electrophile-electrophile cross-coupling attempt to synthesize anthracene catalyst.	117
Scheme 3.11. Synthesis of alkyl iodide 3.40	118
Scheme 3.12. Negishi cross-coupling of anthracenyl bromide with iodide 3.40	119
Scheme 3.13. Unsuccessful deprotection of Cbz groups in hydrazide 3.39	119

Scheme 3.14. Synthesis of anthracenyl catalyst 3.46 .	120
Scheme 3.15. Unrealized synthetic routes to catalyst 3.47 .	121
Scheme 3.16. Retrosynthetic analysis of anthracenyl catalyst 3.47 .	122
Scheme 3.17. Synthesis of anthracenyl catalyst 3.47 .	122
Scheme 3.18. Polyene cyclization of substrate 2.56 with catalyst 3.47 .	125
Scheme 3.19. Synthesis of substrates with less nucleophilic terminating groups.	126
Scheme 3.20. Stereospecificity in polyene cyclization of substrate 2.50 .	129
Scheme 4.1. Synthesis of 9-bromo-2,7-di- <i>tert</i> -butylanthracene.	141
Scheme 4.2. Synthesis of 2,7-di- <i>tert</i> -butylanthracene catalyst 4.4 .	141
Scheme 4.3. Polyene cyclization of 2.4 with catalyst 4.4 .	142
Scheme 4.5. Asymmetric polyene cyclization of 2.4 with <i>m</i> -terphenyl catalyst 4.5 .	147
Scheme 4.6. Final steps in the synthesis of substituted <i>m</i> -terphenyl catalysts.	150
Scheme 4.7. Screening of chiral catalysts with alkyl substituted <i>m</i> -terphenyls.	151
Scheme 4.8. Screening of <i>m</i> -terphenyl catalysts with electronically varied substitution.	152
Scheme 4.9. Screening of <i>m</i> -terphenyl catalysts with bulky substitution.	153
Scheme 4.10. Synthesis of 3,5- <i>tert</i> -butyl- <i>m</i> -terphenyl catalysts with bulkier protecting groups.	155
Scheme 4.11. Asymmetric cyclization of model substrate 2.4 with catalysts 4.20 and 4.21 .	156
Scheme 4.12. Synthesis of 4-substituted <i>m</i> -terphenyl catalysts 4.28 and 4.29 .	157
Scheme 4.13. Screening of asymmetric (<i>E</i>)-polyene cyclizations with catalysts 4.28 and 4.29 .	157
Scheme 4.14. Synthesis of 6-membered ring catalyst 4.34 .	158
Scheme 4.15. Polyene cyclization of model substrate 2.4 with catalyst 4.34 .	159
Scheme 4.16. Enantioselectivity of ethanol trapping with substrate 2.56 .	165
Scheme 4.17. Asymmetric cyclization was substrate 2.46 .	166

Scheme 4.18. Synthesis of phenol-terminated substrate 4.39	172
Scheme 4.19. Polyene cyclization of phenol substrate 4.39 with catalyst 4.13	172
Scheme 4.20. Synthesis of furan-terminated substrate 4.45	173
Scheme 4.21. Cyclization of furan-terminated substrate 4.44 with catalyst 4.13	173

List of figures

Figure 1.1. Steroid precursors in prokaryotes (hopene) and vertebrates/fungi (lanosterol).	2
Figure 1.2. Squalene as the biosynthetic precursor to cholesterol.	4
Figure 1.3. Active site of SHC, with 2-azasqualene shown in blue and binding site residues at 5Å shown in grey. ²³⁻²⁵ Arrow highlighting Asp376.	7
Figure 1.4. Cyclization products of squalene with SHC mutants.	9
Figure 1.5. Different views of the active site of SHC, with 2-azasqualene shown in blue and binding site residues at 5Å shown in grey.	10
Figure 1.6. Cyclophane macrocycle 1.42 with reported guest molecules.	13
Figure 1.7. a) Schematic representation of the quadrupole moment of benzene and hexafluorobenzene with b) related ESP maps.	14
Figure 1.8. Total interaction energy (E_{total} , difference between the energy of the complex and the summed energies of individual components) and electrostatic energy (E_{es} , interactions between distributed multipoles of monomers) for methane, ammonia, and ammonium-benzene complexes calculated at the CCSD(T) level of theory at the basis set limit.	15
Figure 1.9. Comparison of cation- π interaction with benzene and K^+ vs an alkyl ammonium and distribution of charge in tetramethylammonium.	16
Figure 1.10. Lowest energy conformations of iminium with imidazolidinone catalyst 1.47 calculated at the B3LYP/6-31G(d) level of theory.	17
Figure 1.11. Metal-ligand $[Ga_4L_6]^{12-}$ cluster.	20
Figure 1.12. Structure of hexameric resorcin(4)arene 1.66	21
Figure 1.13. (a) General structure of chiral thiourea catalyst and (b) representation of the crystal structure of 1.77 with ammonium chloride.	24
Figure 1.14. Iminium and enamine catalysis.	40
Figure 1.15. LUMO-lowering concept in iminium-catalyzed nucleophilic addition to α,β -unsaturated aldehydes.	41
Figure 1.16. Examples of imidazolidinone and proline-based secondary amine catalysts.	43

Figure 1.17. Relative energies for most stable iminium conformations with imidazolidinone catalyst x calculated at B3LYP/6-31G(d) level.	44
Figure 1.18. Iminium ion with Jorgensen's catalyst showing favoured face of nucleophilic attack.	45
Figure 1.19. Chiral hydrazine-based catalysts.	47
Figure 1.20. A-1,3 strain generated with iminium ion formation.	49
Figure 1.21. Computed energies of the iminium at the M06-2X/6-311G(d,p), SCRf=EtOH level and computational model of 1.250ii	57
Figure 2.1. Substrate scope of the racemic (<i>E</i>)-polyene cyclization.	93
Figure 2.2. Electrophilic substitution constants for methoxy substitution.	95
Figure 2.3. Terminating groups for substrates 2.4 , 2.46 , and 2.50	96
Figure 2.4. Orbital alignment and resonance donation in the transition state of a substrate with a methoxy-substituted arene vs. an ether-bridged substrate.	102
Figure 2.5. Proposed mechanism for the iminium-catalyzed polyene cyclization.	103
Figure 3.1. Comparison of the transition state for the first ring closure for (<i>Z</i>)- and (<i>E</i>)-polyene substrates with catalyst 3.21	112
Figure 3.2. Potential mode of enantioinduction in 7-membered ring hydrazide catalyst with extended aromatic substitution.	114
Figure 3.3. Reaction profile for substrates 2.56 and 3.63 calculated at the M06-2X/6-311G(d,p), SCRf=EtOH level of theory.	132
Figure 4.1. Low energy conformations of the transition state for the initial ring-closure in the reaction of substrate 3.64 with catalyst CO ₂ Me- 3.47 . Calculations at the M06-2X/6-31G(d), SRCF = EtOH level of theory.	138
Figure 4.2. Computational models of proximal <i>s-cis</i> and proximal <i>s-trans</i> conformations of the first transition state in the reaction of substrate 3.64 with catalyst CO ₂ Me- 3.47 . Calculations run at the M06-2X/6-31G(d), SRCF = EtOH level of theory.	140

Figure 4.3 Rotational isomers of <i>m</i> -terphenyl moiety as calculated in the proximal <i>s-trans</i> conformation of the first transition state of substrate 3.64 with catalyst CO ₂ Me- 4.5 . Calculations run at the M06-2X/6-31G(d), SRCF = EtOH level of theory. Free energies in kcal/mol.	144
Figure 4.4. Computational model of proximal <i>s-trans</i> and proximal <i>s-cis</i> conformations of the first transition state of substrate 3.64 with <i>m</i> -terphenyl catalyst CO ₂ Me- 4.5 . Calculations run at the M06-2X/6-31G(d), SRCF = EtOH level of theory.	145
Figure 4.5. Computational model of distal <i>s-trans</i> , proximal <i>s-trans</i> , and distal <i>s-cis</i> conformations of the first transition state of substrate 3.64 with 2,6-dimethyl <i>m</i> -terphenyl catalyst CO ₂ Me- 4.10 . Calculations run at the M06-2X/6-31G(d), SRCF = EtOH level of theory.	148
Figure 4.6. Calculated energy differences between proximal <i>s-trans</i> and distal <i>s-cis</i> conformations of the first transition state of substrate 3.64 with methyl substituted <i>m</i> -terphenyl catalysts. Calculations run at the M06-2X/6-31G(d), SRCF = EtOH level of theory.	149
Figure 4.7. Chiral catalysts with bulkier protecting groups.	154
Figure 4.8. Reaction profile of 3,5-dimethoxyphenyl terminated substrate 2.4 with catalyst CO ₂ Me- 4.13 . Calculations run at the M06-2X/6-311G(d,p), solvent = EtOH level of theory. Free energies in kcal/mol.	168
Figure 4.9. Lowest energy conformations of the first transition state of 3,5-dimethylphenyl terminated substrate 2.46 with catalyst CO ₂ Me- 4.13 . Calculations at the M06-2X/6-311G(d,p), solvent = EtOH level of theory.	169
Figure 4.10. Reaction profile of 3,5-dimethylphenyl terminated substrate 2.46 with catalyst CO ₂ Me- 4.13 . Calculations at the M06-2X/6-311G(d,p), solvent = EtOH level of theory. Free energies in kcal/mol.	170
Figure 4.11. Potential substrates for the asymmetric (<i>E</i>)-polyene cyclization.	175

List of tables

Table 1.1. Enantioselectivity of imidazolidinone-catalyzed Michael addition and molar ratio of iminium ions with varying aromatic substitution.	18
Table 2.1. Iminium-catalyzed polyene cyclization of model (<i>E</i>)-polyene substrate 2.4 (work done by Dr. Dainis Kaldre).....	82
Table 2.2. Solvent screen for polyene cyclization of 2.42	90
Table 2.3. Attempts at polyene cyclization of substrate 2.56	97
Table 3.1. Screening of chiral hydrazide catalysts 3.16 , 3.38 , 3.46 , and 3.47 in the asymmetric iminium-catalyzed (<i>E</i>)-polyene cyclization.	124
Table 3.2. Extended substrate scope of iminium-catalyzed (<i>E</i>)-polyene cyclizations using catalyst 1.241 and catalyst 3.47	127
Table 3.3. Free energies of transition states and intermediate cations for several substrates at the M06-2X/6-311G(d,p), SRCF=EtOH level of theory.	130
Table 4.1. Solvent screen with catalyst 4.13	160
Table 4.2. Co-acid screen with catalyst 4.13	161
Table 4.3. Screening of alcoholic solvents with catalyst 4.13	162
Table 4.4. Screening of conditions for cyclization of substrate 3.64	164

List of abbreviations

9-BBN	9-borabicyclo[3.3.1]nonane
σ^+	electrophilic substituent constant
A-1,3	1,3-allylic
Ac	acetyl
ACh	acetylcholine
AcOH	acetic acid
Ad	1-adamantyl
Ala	alanine
Anth	anthracenyl
APCI	atmospheric pressure chemical ionization
Ar	argon or aromatic group
Asn	asparagine
Asp	aspartic acid
BINOL	1,1'-bi-2-naphthol
Bn	benzyl
Boc	<i>tert</i> -butoxycarbonyl
Bu	butyl
cat.	catalytic amount
CBS	Corey-Bakshi-Shibata
Cbz	benzyloxycarbonyl
COSY	correlated spectroscopy
Cp	cyclopentadienyl
Cy	cyclohexyl

Cys	cysteine
d	day or doublet
D	debye
dba	dibenzylideneacetone
DBU	1,8-diazabicyclo[5.4.0]undec-7-ene
DCM	dichloromethane
DFT	density functional theory
DIAD	diisopropyl azodicarboxylate
DIBAL-H	diisobutylaluminum hydride
DMAP	N,N-dimethylaminopyridine
DMAPP	dimethyl allyl diphosphate
DMDO	dimethyldioxirane
DMF	dimethylformamide
DMP	Dess-Martin periodinane
DMPU	N, N'-dimethylpropyleneurea
DMSO	dimethyl sulfoxide
DPPA	diphenylphosphoryl azide
dppf	1,1'-bis(diphenylphosphino)ferrocene
dr	diastereomeric ratio
E	electrophile
ee	enantiomeric excess
equiv.	equivalents
ESI	electrospray ionization
ESP	electrostatic potential

Et	ethyl
Et ₂ O	diethyl ether
EtOAc	ethyl acetate
EtOH	ethanol
FPP	farnesyl pyrophosphate
GPP	geranyl pyrophosphate
H	hour
HFIP	1,1,1,3,3,3-hexafluoroisopropanol
HMBC	heteronuclear multiple bond correlation
HMDS	hexamethyldisilazane
HOMO	highest occupied molecular orbital
HPLC	high-performance liquid chromatography
HSQC	heteronuclear single quantum coherence
IgG	immunoglobulin G
IPP	isopentyl diphosphate
ⁱ Pr	isopropyl
ⁱ Pr	isopropanol
IR	infrared
IUPAC	International Union of Pure and Applied Chemistry
LA	Lewis acid
LBA	Lewis acid-assisted Brønsted acid
LBBA	Lewis base-assisted Brønsted acid
LDA	lithium diisopropylamide
Ln	ligand(s)

LUMO	lowest unoccupied molecular orbital
m	multiplet
<i>m</i>	<i>meta</i>
<i>m</i> -CPBA	<i>meta</i> -chloroperbenzoic acid
Me	methyl
MeCN	acetonitrile
MeNO ₂	nitromethane
MeOH	methanol
Mes	mesityl
min	minutes
MS	mass spectrometry or molecular sieves
Ms	methanesulfonyl
MTBE	<i>tert</i> -butyl methyl ether
Naph	naphthyl
NBS	N-bromosuccinimide
n.d.	not determined
NIS	N-iodosuccinimide
NMP	N-methyl-2-pyrrolidone
NMQ	N-methyl quinoline
NMR	nuclear magnetic resonance
NOESY	nuclear Overhauser effect spectroscopy
N.R.	no reaction
Nu	nucleophile
<i>o</i>	<i>ortho</i>

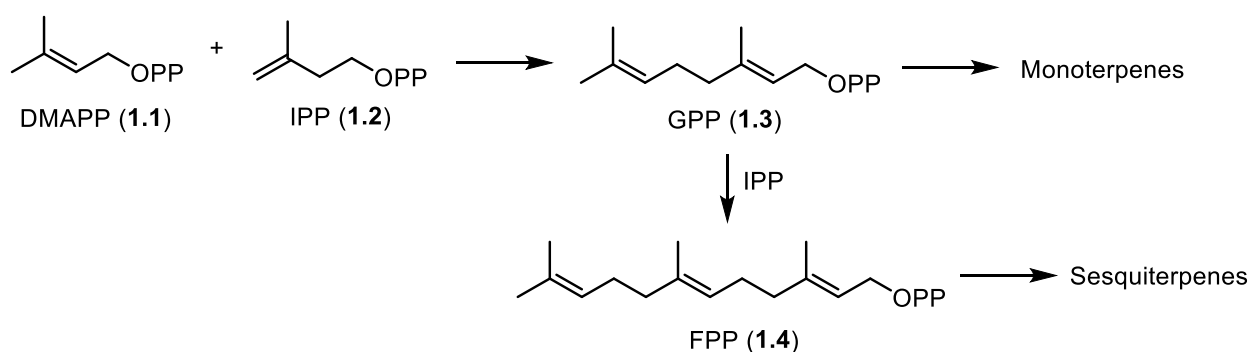
[O]	oxidation
OSC	oxidosqualene cyclase
<i>p</i>	<i>para</i>
Pd/C	palladium-on-carbon
Pd(OH) ₂ /C	palladium hydroxide-on-carbon
Ph	phenyl
Phe	phenylalanine
Piv	pivalyl
pyr.	pyridine
q	quartet
quant.	quantitative yield
R	generic functional group
R*	chiral functional group
recryst.	recrystallization
rt	room temperature
s	singlet
sept	septet
SHC	squalene-hopene cyclase
s.m.	starting material
t	time or triplet
T	temperature
TBAF	tetrabutylammonium fluoride
TBS	<i>tert</i> -butyldimethylsilyl
^t Bu	<i>tert</i> -butyl

tBu	<i>tert</i> -butanol
TEMPO	(2,2,6,6-tetramethylpiperidin-1-yl)oxyl
Tf	trifluoromethanesulfonyl
TFA	trifluoroacetic acid
TfOH	trifluoromethanesulfonic acid
THF	tetrahydrofuran
Thr	threonine
TIPS	triisopropylsilyl
TMEDA	N,N,N',N'-tetramethylethylenediamine
TMS	trimethylsilyl
Trp	tryptophan
Ts	<i>para</i> -toluenesulfonyl
Tyr	tyrosine
UV	ultraviolet
X	electronegative group

Chapter 1. Introduction

1.1 Biosynthesis of terpene and terpenoid natural products

Terpene and terpenoid natural products comprise an incredibly important class of molecules, with applications from flavour and fragrance to pharmaceuticals.¹⁻² The structures of these molecules contain one or multiple isoprene units resulting from their biosynthetic origins, dimethyl allyl diphosphate (DMAPP, **1.1**) and isopentyl diphosphate (IPP, **1.2**) (Scheme 1). The basic carbon skeletons initially built from these units are terpenes and further modifications, such as oxygenation and methyl shifts, result in terpenoid products.

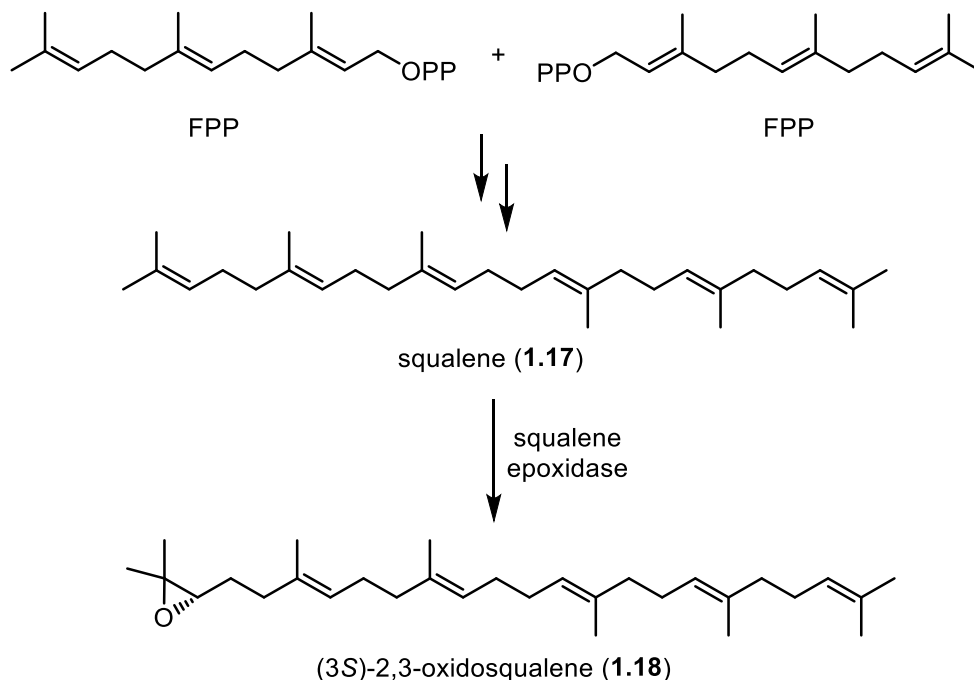


Scheme 1.1. Combination of DMAPP and IPP units in the biosynthesis of terpenes.

The addition of IPP to DMAPP with the elimination of a phosphate results in geranyl pyrophosphate (GPP, **1.3**), which is the precursor to monoterpene natural products. Further additions of IPP increases the number of isoprene units in the subsequent terpene natural products. For example, the addition of one IPP unit gives farnesyl pyrophosphate (FPP, **1.4**), which is the precursor to sesquiterpene natural products.³

Open chain terpenes, such as GPP, can undergo enzyme-controlled cationic cyclizations. In the biosynthesis of cyclic monoterpenes and terpenoids (Scheme 1.2), the elimination of pyrophosphate leads to the geranyl cation (**1.5**). After eventual isomerization to the linalyl cation (**1.6**), the geometry favours the addition of the internal olefin in a tail-to-head cyclization, forming the α -terpinyl cation (**1.7**). From this intermediate, different cationic cyclization pathways can be taken, leading to products with multiple different carbon skeletons, including the resulting natural products shown below.³⁻⁴ This complexity increases with the addition of further isoprene units, and the number of potential cyclization pathways leads to a diverse set of terpene and terpenoid structures with a wide variety of biological functions.⁵

The biosynthesis of steroids proceeds through the head-to-head combination of two FPP units to give squalene (**1.17**), a linear triterpene (Scheme 1.3). In prokaryotes, squalene can then undergo an enzyme-controlled polyene cyclization, forming nine contiguous stereocenters, to give the fused ring system of hopene. In humans and fungi, the enzymatic epoxidation of squalene gives (3*S*)-2,3-oxidosqualene (**1.18**), which undergoes a similar polyene cyclization to result in the fused ring system of lanosterol.



Scheme 1.3. Biosynthetic precursors of squalene and (3*S*)-2,3-oxidosqualene.

The biosynthesis of these steroid molecules has fascinated both chemists and biologists due to not only the importance of this family of molecules for medicinal applications, but also the complete enzymatic chemo-, regio-, and stereocontrol in the synthesis of these structurally complex molecules.⁶

1.1.2 Elucidation of the biosynthetic polyene cyclization

In the early 1900s, biosyntheses of cholesterol (**1.19**) were proposed that began with squalene as a precursor.⁷ In the 1950s, Bloch provided evidence of this biosynthetic pathway with experiments that discovered isotope incorporation in both squalene and cholesterol found in rats that were fed ¹⁴C-labelled acetate.⁸⁻⁹ These results led to the Bloch-Woodward proposal that squalene is cyclized first to lanosterol, followed by further modifications to result in cholesterol.¹⁰

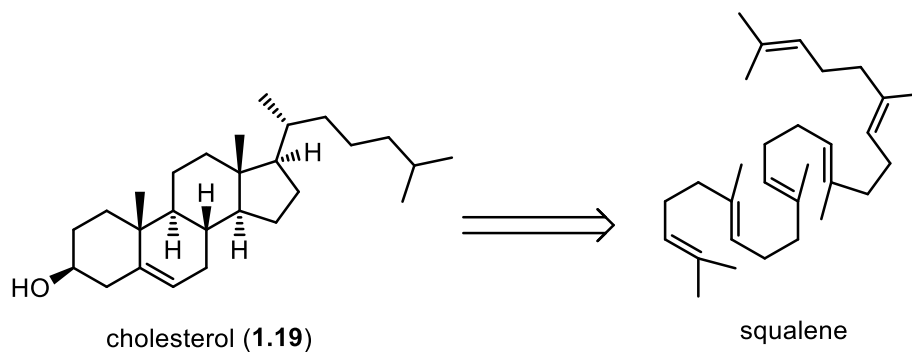
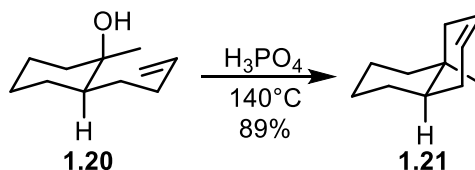


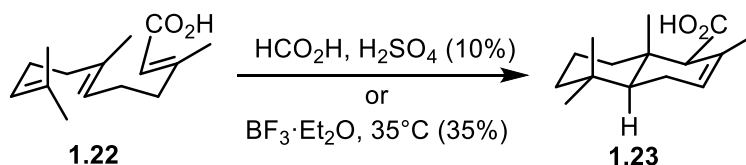
Figure 1.2. Squalene as the biosynthetic precursor to cholesterol.

To investigate the hypothesis of the biosynthetic origin of cholesterol, several groups launched experimental investigations into biomimetic cyclizations. Initial work by Linstead looked at decalin formation resulting from cyclization of an olefin onto a cyclohexyl cation formed from the acid dehydration of a tertiary alcohol (**1.20**, Scheme 1.4).¹¹⁻¹² Stork then built upon this work and synthesized the decalin product (**1.23**) through the acid-catalyzed cyclization of farnesic acid (**1.22**). After correction of the stereochemical assignment, the product was determined to be a *trans*-decalin.¹³⁻¹⁵

Linstead:



Stork:

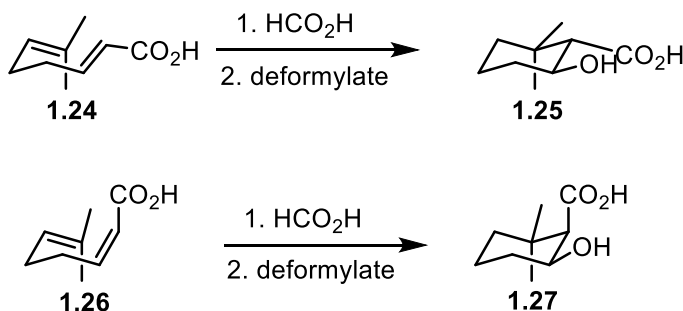


Scheme 1.4. Early work by Linstead and Stork on the synthetic polyene cyclization.

The diastereoselectivity of this cyclization prompted the hypothesis that addition was occurring anti-parallel across the internal olefin. Further evidence towards the anti-parallel addition hypothesis was provided in work by Schinz and Eschenmoser (Scheme 1.5), where cyclization across a *trans*- or *cis*-olefin (**1.24** or **1.26**) gave products of a single *anti*- or *syn*-

diastereomer (**1.25** or **1.27**), respectively.¹⁶ This work has resulted in the Stork-Eschenmoser hypothesis, which defines the stereospecific anti-parallel addition of carbenium ion and olefin to an alkene. This hypothesis has been observed in the synthesis of decalin ring systems, where an internal (*E*)-olefin results in the *trans*-decalin product and an internal (*Z*)-olefin results in the *cis*-decalin product.

Schinz and Eschenmoser:



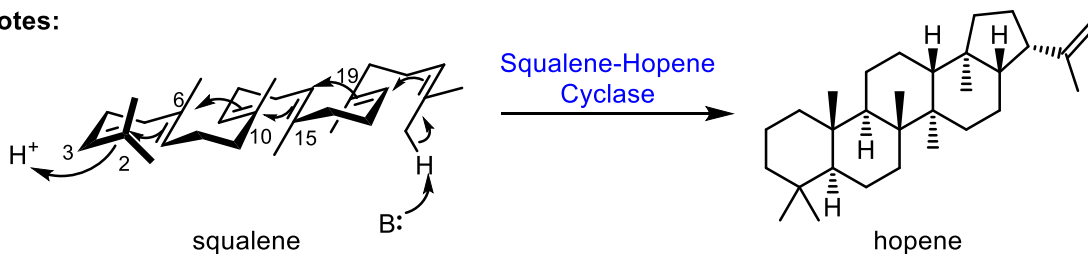
Scheme 1.5. Schinz and Eschenmoser's evidence towards carbenium anti-parallel addition to an olefin.

1.1.3 Biosynthetic polyene cyclization

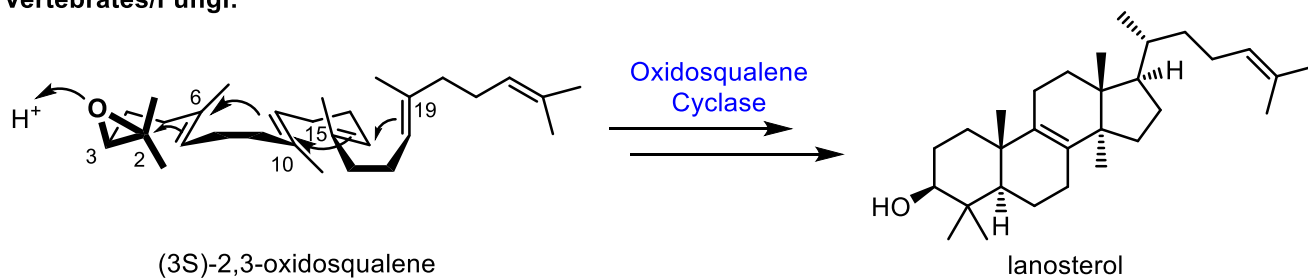
The cyclization of squalene in the biosynthesis of steroid molecules proceeds through a cationic cascade to form multiple carbon-carbon bonds in the fused ring system (Scheme 1.6). The enzymes that control these cyclizations belong to a class of cyclase enzymes, with the cyclization of squalene to hopene controlled by squalene-hopene cyclase (SHC) and the cyclization of 2,3-oxidosqualene to lanosterol controlled by oxidosqualene cyclase (OSC).⁶ In prokaryotes, the terminal olefin of squalene is protonated, followed by subsequent olefin additions before the cyclization is terminated by proton loss to give hopene. The *chair-chair-chair* conformation of squalene results in the *trans-anti-trans* ring system found in hopene. In vertebrates and fungi, the terminal olefin of squalene is first epoxidized to give (3*S*)-2,3-oxidosqualene. Protonation then initiates epoxide opening and the olefin addition cascade. OSC holds (3*S*)-2,3-oxidosqualene in a *chair-boat-chair* conformation, which results in the *trans-syn-trans* ring system found in the tricyclic intermediate **1.28** (Scheme 1.7). In the currently accepted mechanism, ring expansion and final ring closure gives the tetracyclic skeleton (**1.29**), which is followed by a series of 1,2-proton shifts, 1,2 methyl shifts, and a terminating deprotonation to result in lanosterol.^{15, 17-18} The

mechanism of these polyene cyclizations was originally proposed to proceed through a concerted pathway. However, recent evidence has suggested the presence of discrete carbocation intermediates and a stepwise mechanism,¹⁹ which will be discussed in later sections. The fascinating ability of cyclase enzymes to assert complete control over these reactions has driven significant research into their structure and function.

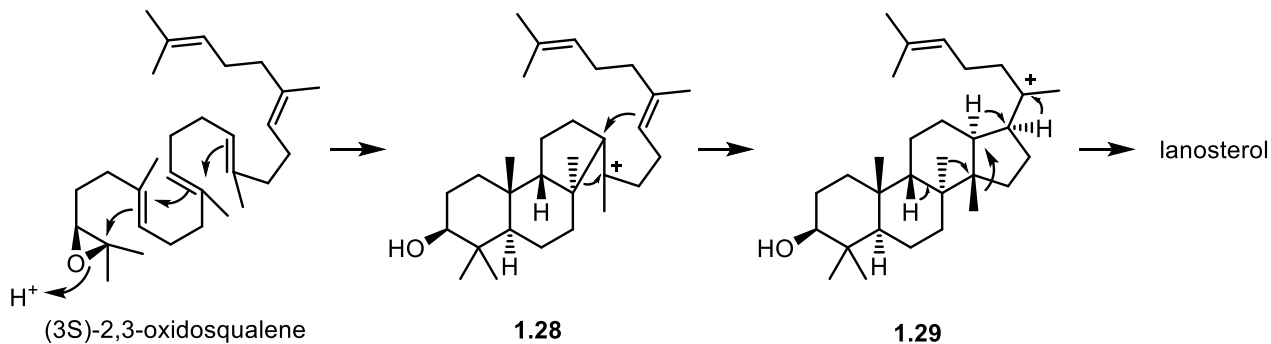
Prokaryotes:



Vertebrates/Fungi:



Scheme 1.6. Enzymatic polyene cyclizations in steroid biosynthesis with originally proposed mechanisms.



Scheme 1.7. Biosynthesis of lanosterol from (3S)-2,3-oxidosqualene.

1.1.4 Crystal structure of SHC and OSC

The first crystal structures of SHC and OSC were obtained in 1997 and 2004 respectively.²⁰⁻²¹ The elucidation of their structures showed that, in addition to providing similar functions, there are several analogous structural motifs. The binding pockets for both enzymes are mainly non-polar. However, one end contains a highly conserved aspartate-containing domain, of Asp-Asp-Thr-Ala in SHC and the analogous Asp-Cys-Thr in OSC. The crystallization of SHC with a stable squalene analogue (2-azasqualene) gave the position of Asp376 near C3 (Figure 1.3), suggesting the participation of these amino acid residues in the initial protonation step of the biosynthetic polyene cyclization.^{17, 22}

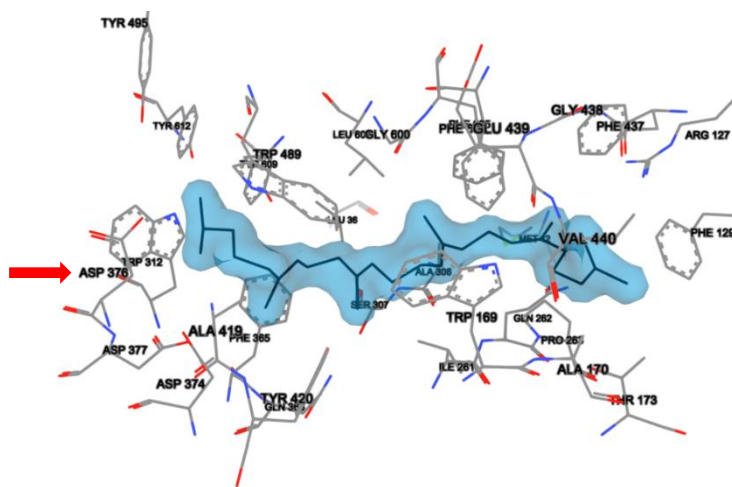


Figure 1.3. Active site of SHC, with 2-azasqualene shown in blue and binding site residues at 5Å shown in grey.²³⁻²⁵ Arrow highlighting Asp376.

The level of conservation of amino acid residues between SHC and OSC is high at the Asp376 end of the cavity (left, Figure 1.3) and lower at the other end. This is consistent with the respective steroids obtained from these enzymes, with similar initial cyclizations providing a 6,6-fused bicycle of the A and B rings, followed by the divergent reactivity resulting in the C/D/(E) rings.

The binding pockets of both SHC and OSC contain a large number of conserved aromatic amino acids. The conservation of these amino acids and their relative positioning to the respective cyclization substrates in the co-crystallized structures have suggested their importance in the stabilization of cationic intermediates in the polyene cyclization.

Prior to structural elucidation of OSC, site-directed mutagenesis and substrate-analogue compatibility experiments were conducted to investigate the enzyme mechanism and divergent cyclization behaviour from SHC.²⁶ More recently, efforts have been made into determining the relationship between the enzyme structure and function.²⁷⁻³⁰ However, there has been considerably more research into the structure and function relationship of SHC through site-directed mutagenesis experiments. Through this research, key amino acid interactions have been suggested that are integral to the current mechanistic understanding of the biosynthetic polyene cyclization.

1.1.5 Mutagenesis experiments on SHC

Site-directed mutagenesis experiments were conducted on SHC to investigate the importance of the conserved motif of polar amino-acids. Mutations of residue Asp376 to Glu gave 10% activity relative to the wild type enzyme and mutation to Arg rendered the enzyme inactive.²² With structural evidence obtained from the crystal structure, the placement of this residue relative to 2-azasqualene supports the theory that Asp376 initiates the cyclization of squalene through protonation of the C2-C3 olefin, with charge stabilization from the surrounding residues.^{17, 20}

Point-mutation experiments on Asp377 have shown it to be a key residue in the cyclization of squalene to hopene. Mutation of Asp377 to Cys or Asn resulted in monocyclic product **1.30** (Figure 1.4), suggesting its function in stabilization of the C10 cation (hopene labelling).³¹

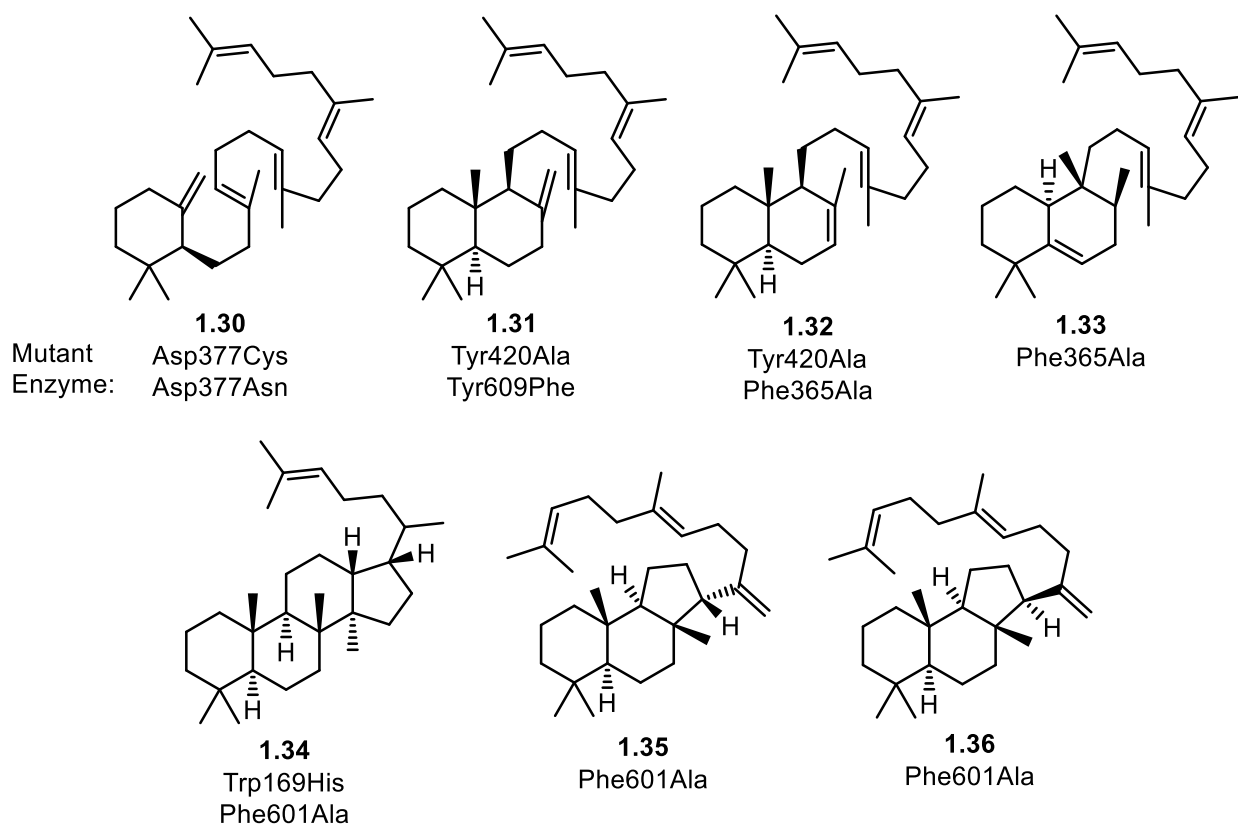


Figure 1.4. Cyclization products of squalene with SHC mutants.

Point-mutation experiments on aromatic amino acids in the binding pocket of SHC by replacing them with either non-aromatic amino acids or those with less π -electron density (i.e. replacing Tyr with Phe), have also resulted in the incomplete cyclization of squalene. Mutant SHC enzymes Tyr420Ala, Phe365Ala, and Tyr609Phe led to bicycles **1.31** and **1.32**, **1.32** and **1.33**, and **1.31**, respectively.³²⁻³⁴ The premature termination of the cyclization of squalene to yield these bicyclic products suggests that the aromatic side chains of Tyr420, Phe365, and Tyr609 participate in stabilization of a C8 cation.

To further investigate the importance of the π -density at aromatic amino acid residues Phe365 and Phe605, which have been proposed to stabilize cationic charge at C8 and C13, respectively, Hoshino incorporated site-specific mutations of natural and unnatural amino acids at these positions. Site-directed mutations incorporated residues with higher cation- π binding energies (as discussed in section 1.2.2), O-methyltyrosine, Tyr, and Trp, as well as those with lower cation- π binding energies, mono-, di-, and trifluorophenylalanines, and the effect of the resulting mutant enzymes on the kinetics of the polyene cyclization was observed.³⁷ The increased size of the Tyr and Trp residues in the mutant protein led to looser binding, which was more significant for Phe365. However, the Phe605 mutants showed increasing catalytic activity with mutations that increased cation- π binding strength (in the order Phe605Tyr, Phe605OMe-Tyr, Phe605Trp). Conversely, the activity of the fluorine-substituted mutants at both Phe365 and Phe605 decreased proportionally to the number of fluorine molecules incorporated.

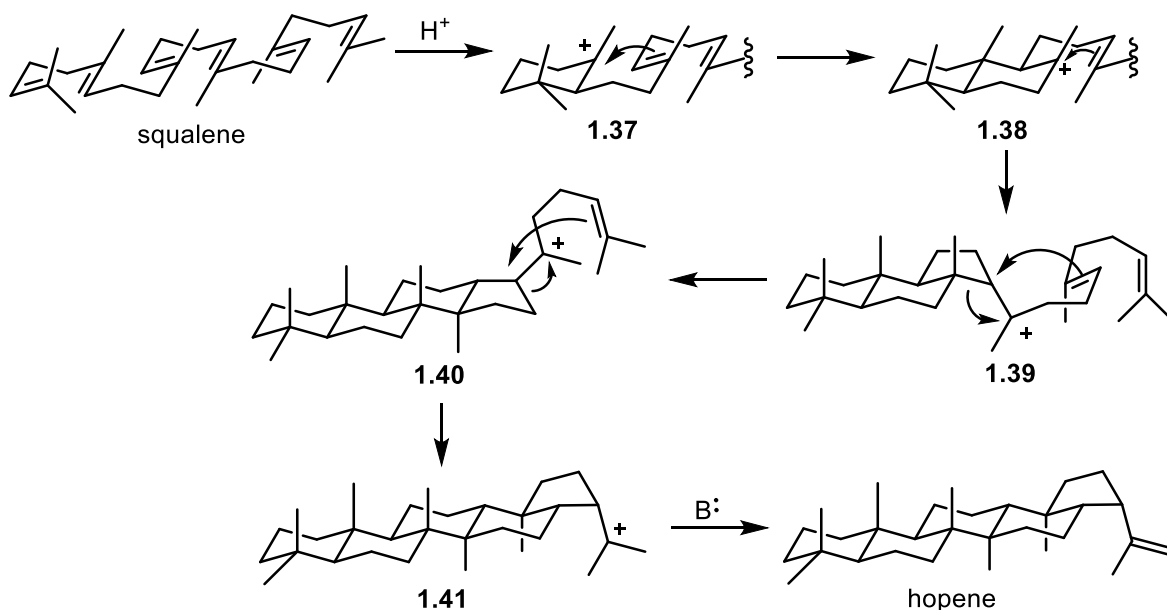
These mutagenesis studies show the importance of the π -electron density at Phe365 and Phe605, as well as aromatic residues at Tyr420, Tyr609, Trp169 and Phe601, for the complete polyene cyclization of squalene by SHC. These residues have been postulated to stabilize intermediate cations in the cyclization pathway, which has led to the proposal of a stepwise mechanism.

1.1.6 Mechanism of the biosynthetic polyene cyclization

The complete regio- and stereocontrol observed in the biosynthesis of hopene initially led to the postulation of a concerted cyclization mechanism proceeding from the *chair-chair-chair-chair* conformation of squalene seen in Scheme 1.6. This was the favoured hypothesis due to the lack of stereochemical erosion that would be more indicative of a stepwise mechanism. However, the energetically disfavoured non-Markovnikov additions required for this proposed mechanism prompted some dispute and both Stork and Eschenmoser noted the possibility of cationic intermediates in their early reports.³⁸⁻³⁹

With more recent evidence from point-mutation experiments, it has been accepted that both OSC- and SHC-catalyzed polyene cyclizations proceed through an asynchronous pathway with rigidly held carbocation intermediates. The non-Markovnikov addition in the synthesis of hopene to form the 6-membered C ring has been proposed by Hoshino to proceed through initial 6-6-5 ring formation (**1.39**, Scheme 1.8), followed by a ring expansion.⁴⁰ He has proposed a similar 5-

membered ring formation/expansion to form the D ring. Shulz has proposed an alternative mechanism where the 6-6-6-5 structure (**1.40**) can be formed directly with sequential cyclizations stabilized by the squalene binding structure, without requiring the first ring expansion.²³ He has then proposed the same ring expansion to result in the 6-membered D ring. The cyclization is then terminated in a proton loss to give hopene. Aromatic amino acids have proven integral to the complete cyclization, leading to the postulation that they provide stabilization through cation- π interaction with cationic intermediates along this mechanistic pathway.



Scheme 1.8. Hoshino's proposed mechanism of biosynthesis of hopene.

1.2 Cation- π interaction

The cation- π interaction that has been proposed between aromatic amino acid side chains and cationic intermediates in the biosynthetic polyene cyclization has been identified in many other areas of chemistry and biology.⁴¹⁻⁴² However, in comparison to other noncovalent interactions, such as hydrogen-bonding or π - π stacking, cation- π interactions have been underutilized in synthetic chemistry. This thesis will discuss our investigation into cation- π interactions for the stabilization of cationic intermediates and transition states in the iminium-catalyzed polyene cyclization. In sections 1.2 and 1.3, we will give overview of the significance of cation- π interactions and give relevant examples of their use in synthetic chemistry.

1.2.1 Initial discoveries in cation- π interactions

In the 1980s, an association enthalpy of 19 kcal/mol was reported between K^+ and benzene in the gas phase.⁴³ This was unusually high, considering the 18 kcal/mol binding enthalpy between K^+ and water. A report followed shortly after of a similarly high binding energy of quaternary ammonium salts with π -systems, in the range of 10-22 kcal/mol.⁴⁴ Although the term “cation- π interaction” wasn’t coined until several years later,⁴⁵ these observations marked the beginning of computational and experimental investigation into this noncovalent attraction.

Following these initial reports, cation- π interactions have been well documented in the solution phase. Dougherty’s program in host-guest chemistry led to the design of a cyclophane receptor, **1.42** (Figure 1.6).⁴⁶ Carboxylate groups on the exterior of cyclophane **1.42** promote water-solubility, while the aromatic-lined core desolvates organic molecules. Interestingly, in the investigation of potential guests, they determined that the cyclophane core had a strong affinity towards cationic ammonium ions, desolvating NMQ (**1.43**), nicotine (**1.45**) and ACh (**1.46**) from an aqueous solution.⁴⁷ Cationic charge was noted to play a large role in the molecular recognition, as demonstrated by the greater binding affinity of NMQ (**1.43**) ($\Delta G^\circ = -8.4$ kcal/mol) compared to a neutral, isostructural analogue 4-methyl quinoline (**1.44**) ($\Delta G^\circ = -5.9$ kcal/mol).

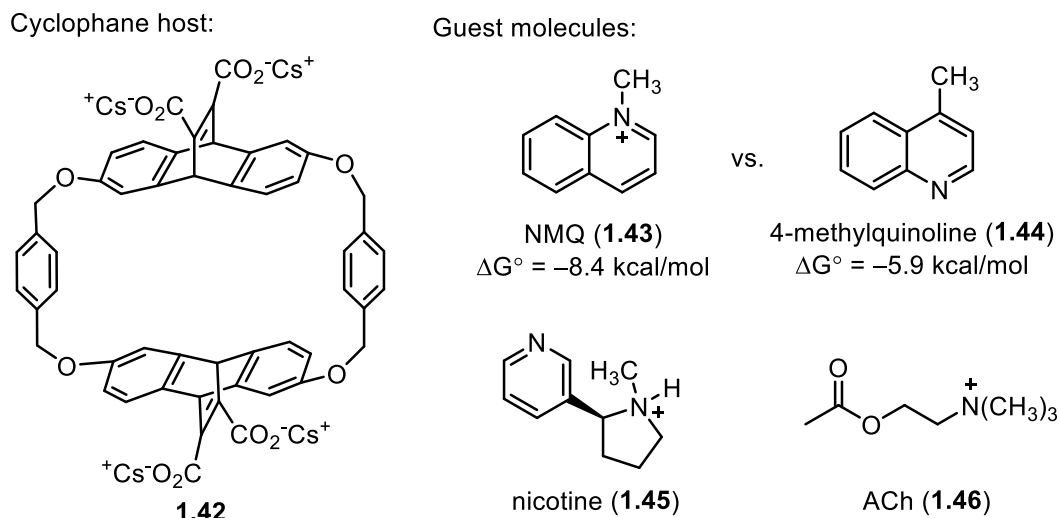


Figure 1.6. Cyclophane macrocycle **1.42** with reported guest molecules.

Early indications from structural biology and host-guest chemistry suggested that the nature of the interaction between π -systems and proximal cations differs from that of a typical

dipole–ion interaction. Since these initial observations, detailed investigations have been undertaken into the physical nature of the cation– π interaction.

1.2.2 Origin of attraction in cation– π interactions

The binding energy of cation– π interactions is largely attributed to electrostatic and inductive forces. However, the fundamental nature of the interaction is electrostatic and, in many cases, the interaction can be effectively modelled as an ion-quadrupole interaction.⁴⁸⁻⁵⁰ The strength of binding energy of a cation– π interaction can be predicted from the electrostatic potential (ESP) of an aromatic ring, with electron-donating substituents creating a more negative ESP and electron-withdrawing substituents creating a more positive ESP (e.g. benzene vs. hexafluorobenzene, Figure 1.7)^{41, 51}

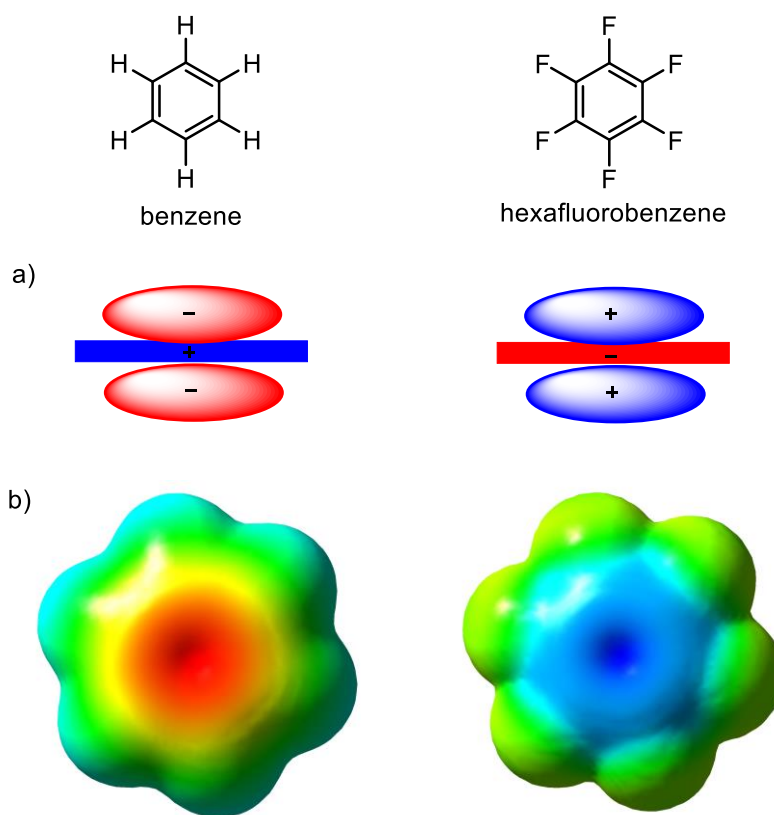


Figure 1.7. a) Schematic representation of the quadrupole moment of benzene and hexafluorobenzene with b) related ESP maps.

Computational and experimental evidence has demonstrated that the electronic nature of aromatic substitution and the size of the π -system can be predictors of the relative strength of cation- π interactions.⁵²⁻⁵⁵ However, the correlation between ESP maps and strength of cation- π interaction can only be interpreted qualitatively, as the effects of aromatic substitution on the polarization of aryl π -cloud can be overestimated.⁵⁶

In addition to electrostatic attraction, inductive forces can play a role in the overall binding energy of the cation- π interaction which depends on the polarizability of the aromatic. This is in contrast to π - π and CH- π interactions, where the interaction primarily consists of dispersion forces.⁵⁷ The overall binding energy computed for a positively charged ammonium or tetramethyl ammonium is larger in magnitude than that of a neutral CH- π or NH- π interaction, with the cation- π interaction defined with a significant portion attributed to electrostatic force (Figure 1.8).⁵⁸

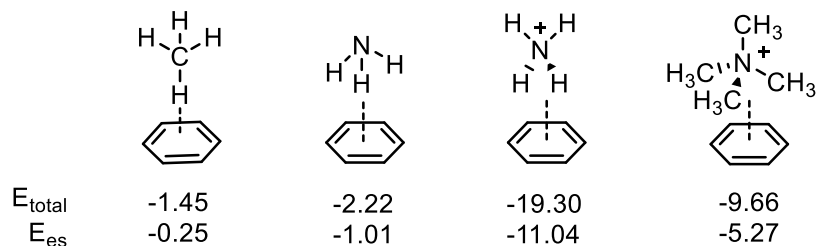


Figure 1.8. Total interaction energy (E_{total} , difference between the energy of the complex and the summed energies of individual components) and electrostatic energy (E_{es} , interactions between distributed multipoles of monomers) for methane, ammonia, and ammonium-benzene complexes calculated at the CCSD(T) level of theory at the basis set limit.

A further defining feature of the cation- π interaction is the distance dependence on the strength of interaction. A typical quadrupole-ion interaction would be expected to have a stabilization energy distance dependence of $1/r^3$, where r is the distance between the ion and the quadrupole. The stabilization energy of a cation- π interaction has a distance dependence of $1/r^n$, where $n < 2$, meaning that it provides stabilization at longer distances than would be expected for a true electrostatic interaction.⁵¹

The cation has been shown to have preference for the centre of an aromatic ring and perpendicular to the plane of atoms, optimizing ion-orbital interaction.⁵⁹⁻⁶¹ Metal cations can interact directly with the π system. However, in more complex systems such as alkyl ammonium

ions, the π system has been postulated to interact with the CH α to the nitrogen due to the distribution of charge in the molecule (Figure 1.9).⁴¹

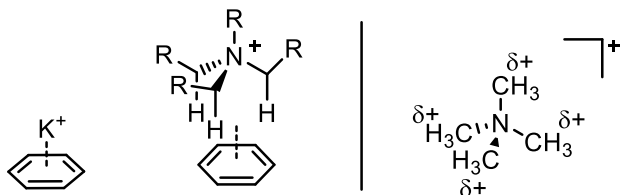


Figure 1.9. Comparison of cation- π interaction with benzene and K^+ vs an alkyl ammonium and distribution of charge in tetramethylammonium.

Experimental studies to investigate the thermodynamics of the cation- π interaction in solution have been performed on equilibrium systems. Through these, the magnitude of the interaction was determined to be dependant on the nature of the cation, the nature of the π -system, as well as other factors.^{54, 62-68} In the interaction of enzymes with cationic molecules, the cation- π interaction has been estimated to increase binding by 2.6-2.8 kcal/mol,⁶⁹⁻⁷⁰ placing it in comparable magnitude to other strong noncovalent interactions, such as hydrogen bonding.

1.3 Cation- π interactions in organic synthesis

With the recognition of cation- π attraction as a strong non-covalent interaction, recent investigation has been undertaken into its potential to promote reactivity and/or selectivity in synthetic chemistry.⁷¹⁻⁷² In substrates containing both cationic character and a neutral aromatic, cation- π interactions have been proposed to promote regioselectivity and stereoselectivity in both intra- and intermolecular reactions through the stabilization of favourable conformations.⁷³⁻⁷⁶ Similarly, catalysts incorporating both an aromatic and cationic element have been proposed to achieve reactivity and selectivity through cation- π stabilization of favoured conformations.⁷⁷

As an examples, cation- π interactions have been proposed to stabilize the favoured conformation of iminium **1.49**, formed from imidazolidinone catalyst **1.47** and aldehyde **1.48**. Catalyst **1.47** has been developed by MacMillan to promote iminium-catalyzed reactions of α,β -unsaturated aldehydes with high enantioselectivity.⁷⁸⁻⁷⁹ DFT calculations showed that the preferred conformation of iminium **1.49** was the (*E*)-isomer (Figure 1.10).⁸⁰⁻⁸¹ At the B3LYP/6-31G(d) level of theory, three low energy conformations were found, differing in the N-C-C-Ph dihedral angle. In the lowest energy conformation, **1.49i**, the phenyl group is stacked over the

imidazolidinone ring, with proposed stabilization through a favourable CH- π interaction with the geminal dimethyl group. The energy difference is only 0.3 kcal/mol between this isomer and **1.49ii**, with the phenyl group stacked over the iminium. Both conformations are significantly lower in energy than **1.49iii** (+1.3 kcal/mol), where the phenyl group is twisted away from the iminium, suggesting that an interaction with the phenyl group is stabilizing conformations **1.49i** and **1.49ii**.

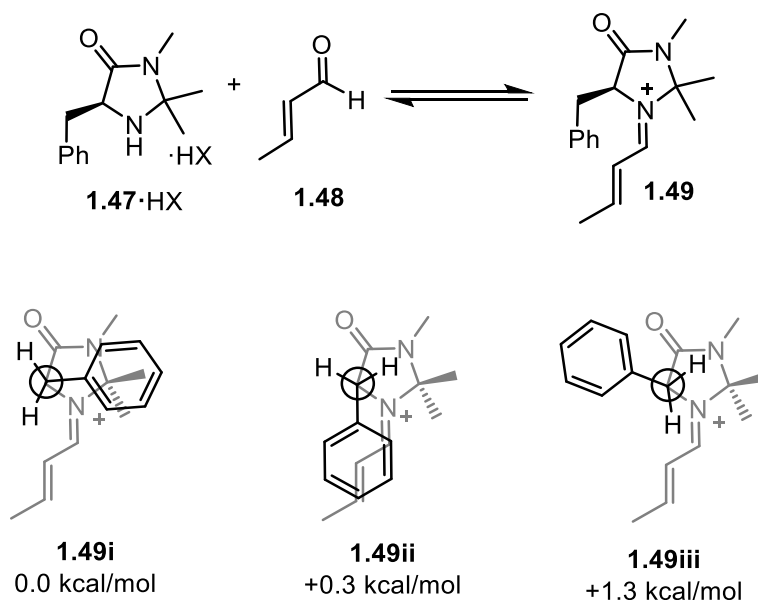
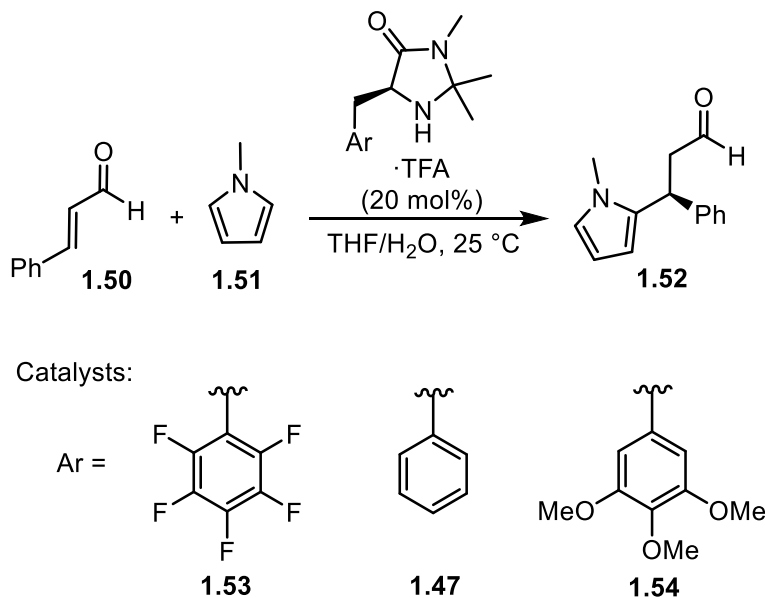


Figure 1.10. Lowest energy conformations of iminium with imidazolidinone catalyst **1.47** calculated at the B3LYP/6-31G(d) level of theory.

The effect of the electronics of the aromatic substitution on the imidazolidinone catalyst was studied further by Gilmour in the iminium-catalyzed Michael addition of N-methyl pyrrole (**1.51**) to cinnamaldehyde (**1.50**) (Table 1.1).⁸²⁻⁸⁴ A conformer population analysis was performed using spectroscopic data which determined the ground-state conformer population of the corresponding α,β -unsaturated iminium salts. Catalyst **1.53**, with electronegative fluorine substitution on the arene, showed an increased amount of conformer **iii** (47%), with the aromatic twisted away from the iminium, and resulted in product **1.52** with diminished enantioselectivity (65% ee) compared to that obtained with the phenyl substituted imidazolidinone **1.47** (23% of **iii**, **1.52** in 84% ee). Catalyst **1.54**, with a 3,4,5-trimethoxyphenyl substituent, showed a decreased amount of ground state iminium conformation **iii** (18%), and resulted in product **1.52** with increased enantioselectivity (94% ee). This evidence showed that both the ratio of ground-state conformers of the iminium as well as the enantioselectivity of the reaction were strongly dependant

on the arene quadrupole moment, suggesting a cation- π interaction in iminium conformations **i** and **ii** which results in greater shielding of one face of the α,β -unsaturation.

Table 1.1. Enantioselectivity of imidazolidinone-catalyzed Michael addition and molar ratio of iminium ions with varying aromatic substitution.



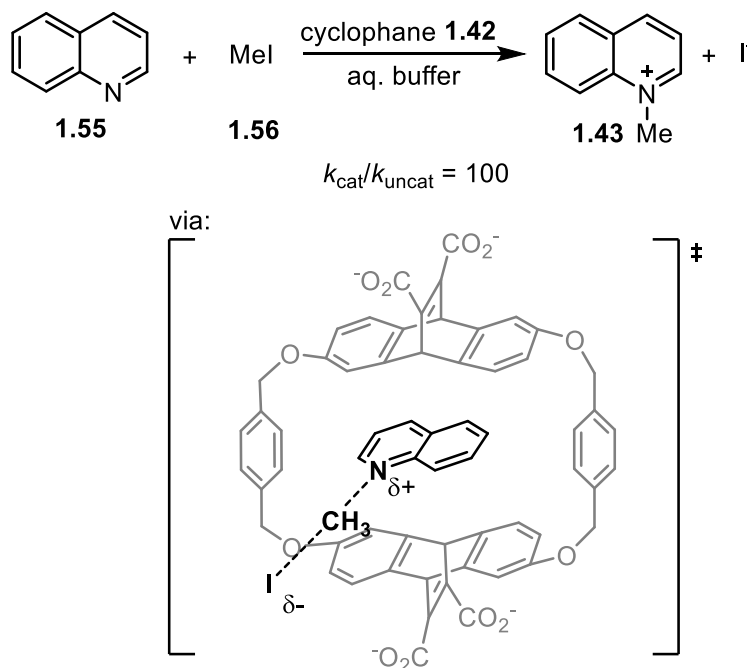
Entry	Catalyst	Q_{zz}	Iminium Ion Mole Fraction			ee of 1.52 (%)
			i	ii	iii	
1	1.53	+3.01	0.37	0.16	0.47	65
2	1.47	-3.46	0.75	0.03	0.23	84
3	1.54	-5.68	0.65	0.17	0.18	94

In addition to substrate-substrate and catalyst-catalyst interactions, aromatic substitution has also been strategically incorporated into catalyst designs to promote a favourable interaction with cationic substrates. In the following sections, relevant examples of cation- π interactions between catalyst/reagent and cationic intermediates or transition states of the substrate will be discussed, with a focus on those related to synthetic monoterpene or polyene cyclizations.

1.3.1 Cation- π interactions in supramolecular catalysis

The incorporation of aromatic molecules into the core of supramolecular hosts as a strategy for the molecular recognition of cationic molecules has been well established. Recent research has been done in the extension of this binding affinity for the stabilization of cationic transition states, with the goals of providing selectivity and rate enhancement in chemical reactions.

In a seminal paper, Dougherty showed that the reaction of quinoline (**1.55**) with methyl iodide (**1.56**) proceeded with a 100-fold increase in rate when sequestered inside cyclophane receptor **1.42** (Scheme 1.9). This increase in reactivity was proposed to occur due to the stabilization of the transition state through cation- π interaction with the cyclophane core.⁸⁵



Scheme 1.9. Cyclophane-catalyzed Menshutkin reaction.

This example demonstrated the possibilities of utilizing the binding properties of supramolecular hosts to lower kinetic barriers for reactivity. Further examples of the enhancement of rate and selectivity in organic reactions have been demonstrated with $[\text{Ga}_4\text{L}_6]^{12-}$ cluster **1.57** (Figure 1.11).⁸⁶ The host-guest chemistry of this cluster accommodates many mono-cationic species, such as tetraalkylammonium salts,⁸⁷ organometallic compounds,⁸⁸ and reactive

phosphonium species,⁸⁹ through binding interactions with the naphthalene bridges lining the inner cavity.⁹⁰

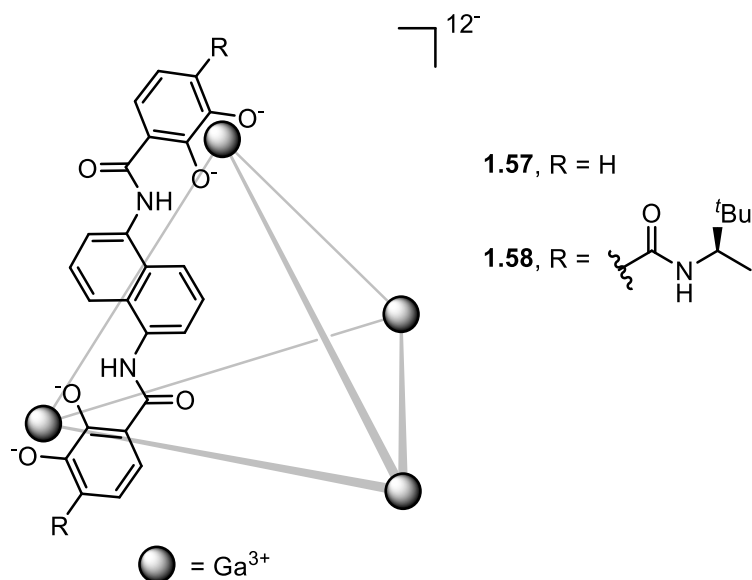
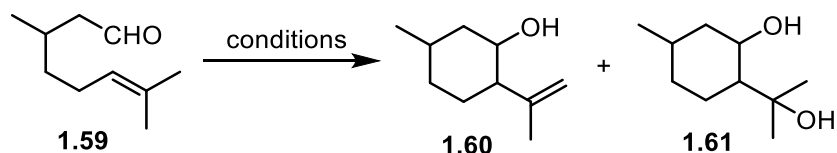


Figure 1.11. Metal–ligand $[\text{Ga}_4\text{L}_6]^{12-}$ cluster.

Encapsulation of cationic substrates and intermediates within the confined binding pocket of cluster **1.57** is postulated to lower the entropic barrier for reactivity. This allows energetically disfavoured reactions to proceed, such as the acid-hydrolysis of orthoformates and acetals in basic solution.⁹¹⁻⁹⁴ Rate acceleration of a reactions with cationic transition states, such as the Nazarov cyclization and aza-Cope rearrangement, have also been observed with cluster **1.57**.⁹⁵⁻⁹⁶

Monoterpene-like Prins-cyclizations of citronellal (**1.59**) and homologous aldehydes (**1.62**) were catalyzed selectively by the $[\text{Ga}_4\text{L}_6]^{12-}$ cluster (Scheme 1.10).⁹⁷ The reaction catalyzed by **1.57** showed opposite selectivity to the acid-catalyzed reaction, which resulted in mainly the water trapped product (**1.61**), due to affinity of the cationic intermediate to the hydrophobic core of the supramolecular assembly. Using enantiopure catalyst **1.58**, a modest enantioselectivity could be achieved with a gem-dimethyl substrate, **1.62**.⁹⁸ Reactivity and enantioselectivity in reactions catalyzed by the $[\text{Ga}_4\text{L}_6]^{12-}$ cluster were highly substrate-dependant, with the steric environment of the different substitution patterns having a large effect.



conditions:

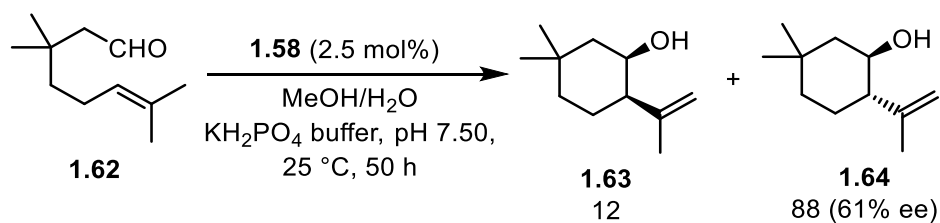
- A. catalyst **1.57** (10 mol%) in KH_2PO_4 buffer, pH 7.50, 60 °C, 28 h
 B. KH_2PO_4 , pH 3.20, 50 °C, 8h

97

9

3

91



Scheme 1.10. Prins cyclization catalyzed by supramolecular assembly.

More recently, the catalytic potential of the supramolecular assembly of resorcin(4)arene (**1.66**, Figure 1.12), has been demonstrated. In CDCl_3 , the self-assembly of resorcin(4)arene (**1.65**) occurs as a hexamer with the participation of four water molecules,⁹⁹⁻¹⁰⁰ and this supramolecular assembly (**1.66**) had previously demonstrated successful encapsulation of cationic tetraalkylammonium ions.¹⁰¹⁻¹⁰² Supramolecular assembly **1.66** acts as a reasonably strong acid, which can protonate substrates then selectively bind cationic intermediates within the internal cavity through cation- π interactions. With these properties, it has successfully been demonstrated to promote acid-catalyzed reactions, such as the selective hydrolysis of acetals.¹⁰³

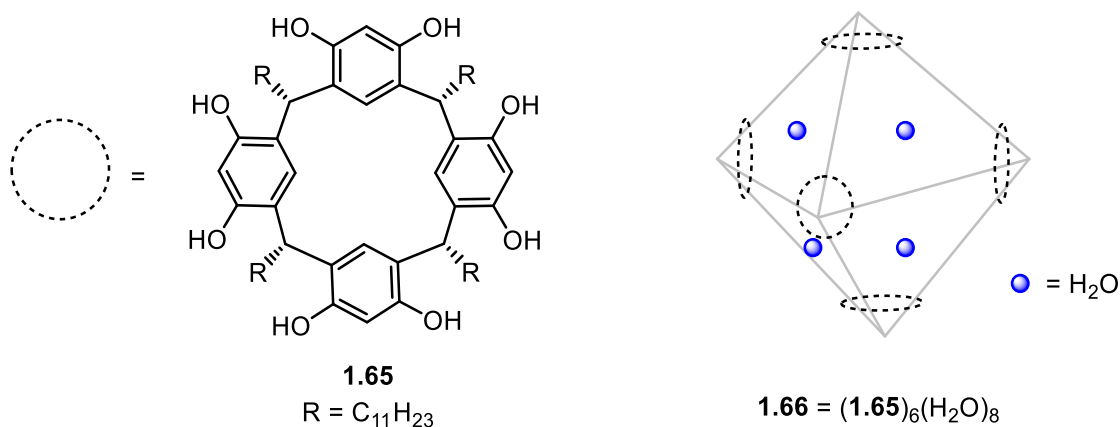
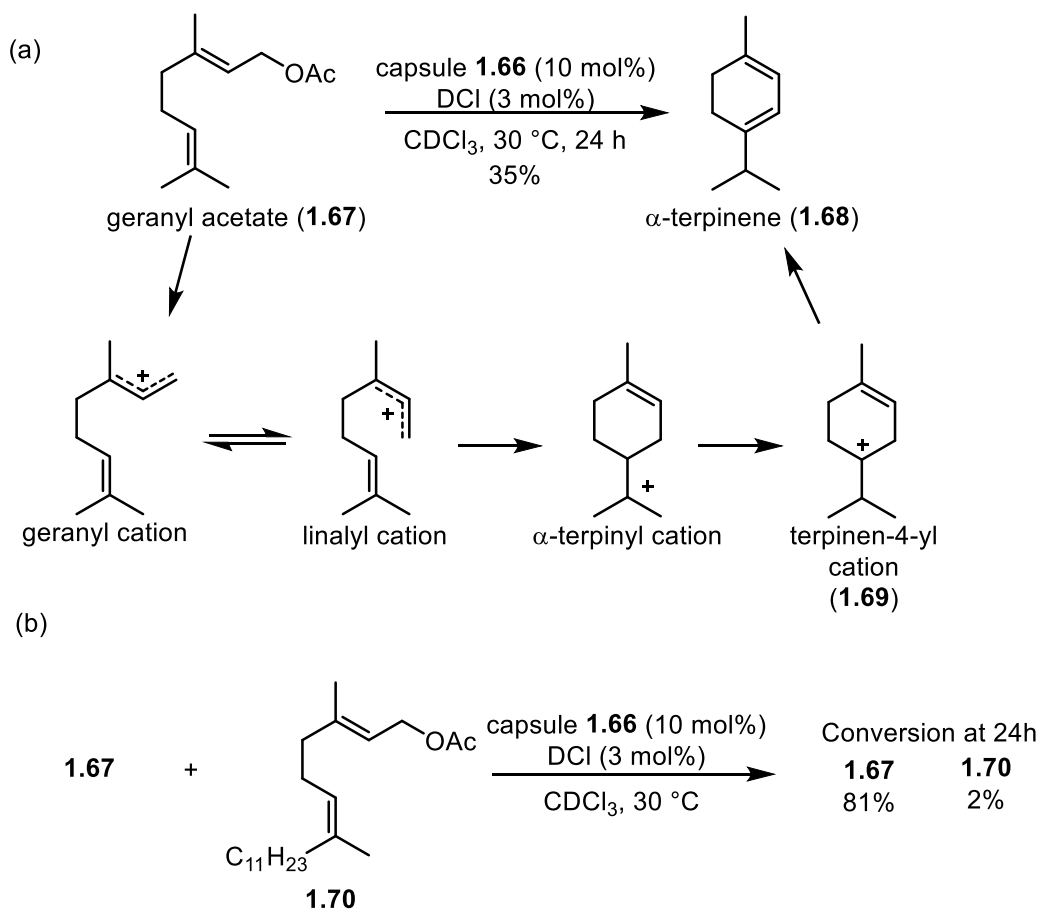


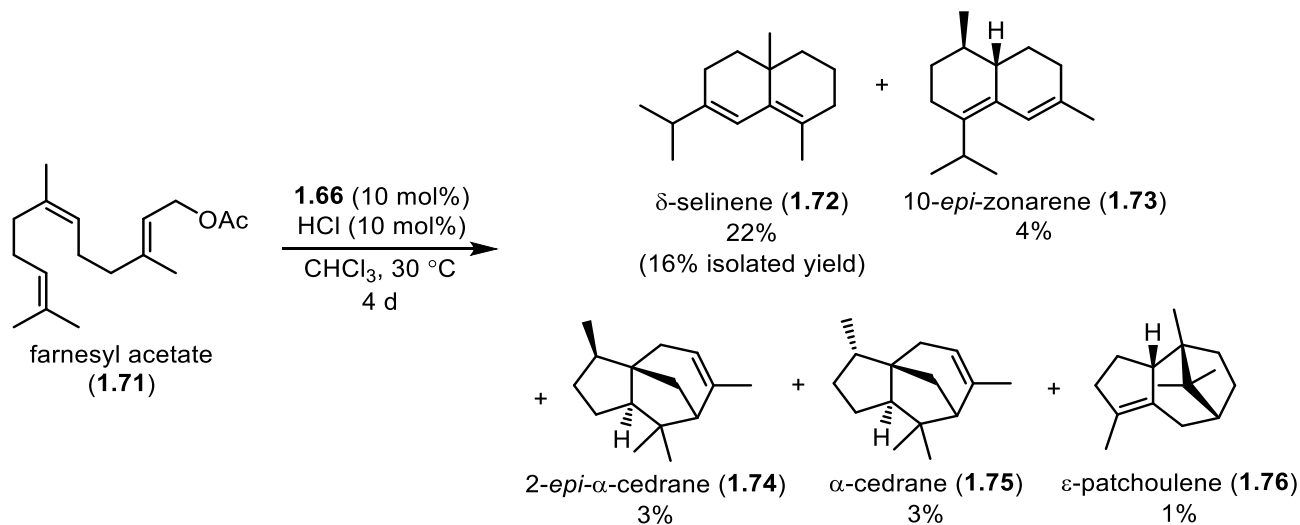
Figure 1.12. Structure of hexameric resorcin(4)arene **1.66**.

Capsule **1.66** has been demonstrated to catalyze other reactions with cationic intermediates, such as the cyclization of geranyl acetate (**1.67**, Scheme 1.11a).¹⁰⁴ This tail-to-head cyclization is the proposed biosynthetic pathway to α -terpinene (**1.68**), but has been challenging to replicate synthetically due to the low energy barriers to multiple alternate products. Within the capsule, the direct cyclization of geranyl acetate proceeds through protonation of the acetate, followed by an S_N1 type pathway. Stabilizing interactions within the aromatic-lined core have been proposed to lower the activation barrier for the isomerization from the geranyl cation to the linalyl cation. A cation- π interaction has also been proposed to stabilize the intermediate α -terpinyl cation, to allow the 1,2-hydride shift to proceed prior to elimination, leading to α -terpinene as the major product in 35% yield. The reaction was demonstrated to proceed inside the capsule through the size exclusion of extended substrate **1.70**, which failed to react (Scheme 1.11b).¹⁰⁵



Scheme 1.11. (a) Cationic cyclization of geranyl acetate catalyzed by capsule **1.66** and (b) selective conversion of geranyl acetate in the presence of extended analogue **1.70**.

Capsule **1.66** was demonstrated to catalyze the cyclization of a more complex polyene substrate with some selectivity (Scheme 1.12). The polyene cyclization of farnesyl acetate (**1.71**) proceeded to result in a mixture of several natural products (**1.72-1.76**), with an isolated yield of 16% of the major product, δ -selinene (**1.72**).¹⁰⁶ Additionally, capsule **1.66** has been demonstrated to catalyze other cationic cyclizations,^{104, 107-108} as well as an iminium-catalyzed 1,4-reduction.¹⁰⁹



Scheme 1.12. Cationic sesquiterpene cyclizations catalyzed by capsule **1.66** (GC yields).

The binding affinities for these supramolecular host-cationic guest complexes create interesting possibilities for their use in catalysis. However, most of the current examples of supramolecular catalysis are incredibly substrate specific. Only small deviations from the optimal substrate can be made without detrimental effects on the reactivity and selectivity. In addition, as shown by the polyene cyclization with capsule **1.66** (Scheme 1.12), selectivity issues in more complex reactions can lead to low yields of desired product.

1.3.2 Cation- π interactions in small molecule catalysis

In recent years, cation- π interactions have been incorporated into strategies for small molecule catalysis, with stabilization of cationic intermediates and transition states leading to regio- and stereoselectivity.⁷¹⁻⁷² A prominent catalyst design in this area is the chiral thiourea (e.g. **1.77** and **1.78**, Figure 1.13a) developed by Jacobsen. These thioureas recognize ion-pairs through anion-binding with the thiourea H-bond donor and cation-binding with a strategically placed aryl group. A crystal structure of catalyst **1.77** co-crystallized with ammonium chloride showed evidence of recognition of the ion pair, with the separation of the positively charged

tetramethylammonium and anionic chloride ion (Figure 1.13b). Successful rate acceleration and selectivity have been achieved using this group of catalysts in a range of reactions, including Friedel-Crafts alkylations,¹¹⁰⁻¹¹¹ acylations,¹¹² and rearrangements.¹¹³

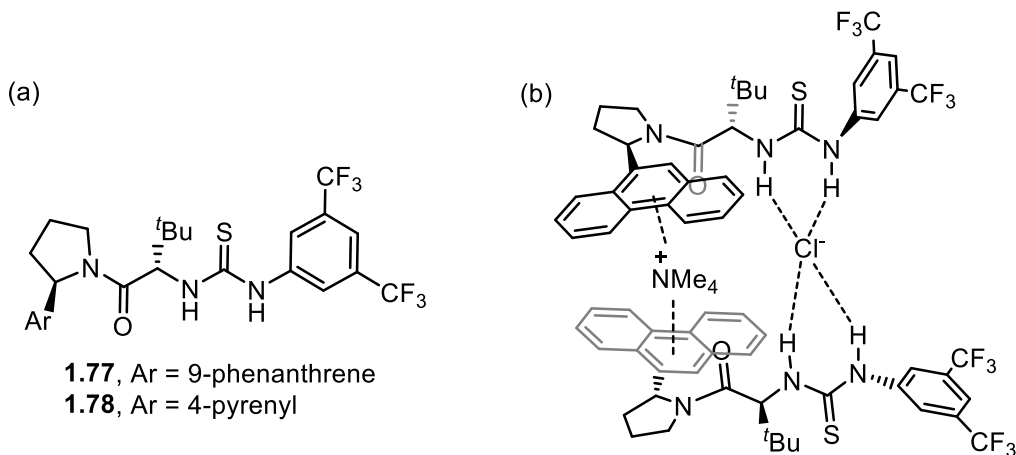
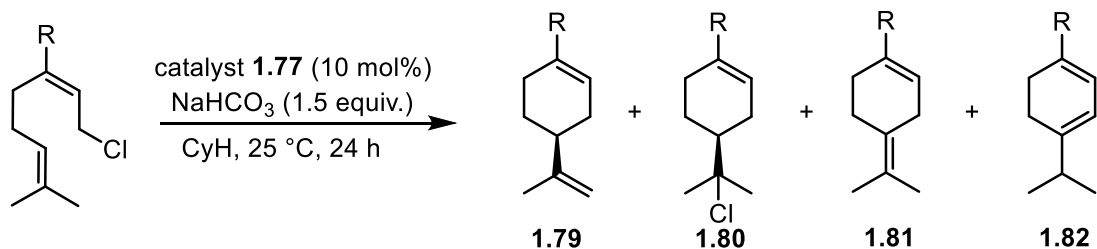
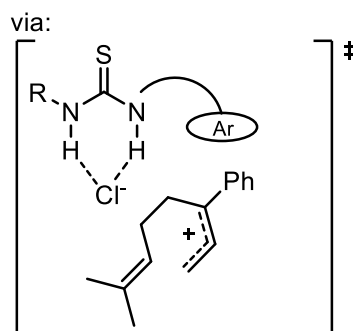


Figure 1.13. (a) General structure of chiral thiourea catalyst and (b) representation of the crystal structure of **1.77** with ammonium chloride.

Asymmetric tail-to-head cyclizations of neryl chloride derivatives have been reported using thiourea catalyst **1.77** (Scheme 1.13).¹¹⁴ Ionization of the allyl chloride results in the allylic cation, which has been proposed to participate in cation- π binding with the phenanthryl moiety on the catalyst. High enantioselectivity was obtained in substrates that had electron-deficient substitution on the distal olefin. The cyclization of substrate **1.83**, with electron-deficient *p*-cyanophenyl substitution, yielded 67% of corresponding product **1.79** in 92% ee and substrate **1.84**, with *p*-methylphenyl substitution, yielded 60% of corresponding product **1.79** in diminished 77% ee. Mechanistic analysis showed the direct involvement of the second olefin in the rate-determining step. Electron-deficient substrates were proposed to have more donation from the isoprene olefin due to less stabilization of the allylic cation by the substituent, which would lead to more highly ordered enantio-determining transition state.

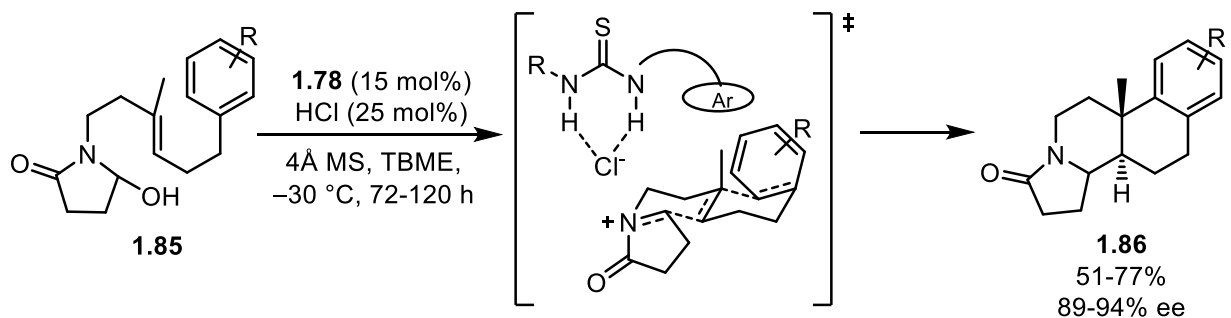


Substrate	yield of 1.79 (% ee)	yield of 1.80	yield of 1.81 + 1.82
1.83 , R = <i>p</i> -cyanophenyl	67 (92)	12	17
1.84 , R = <i>p</i> -methylphenyl	60 (77)	17	18



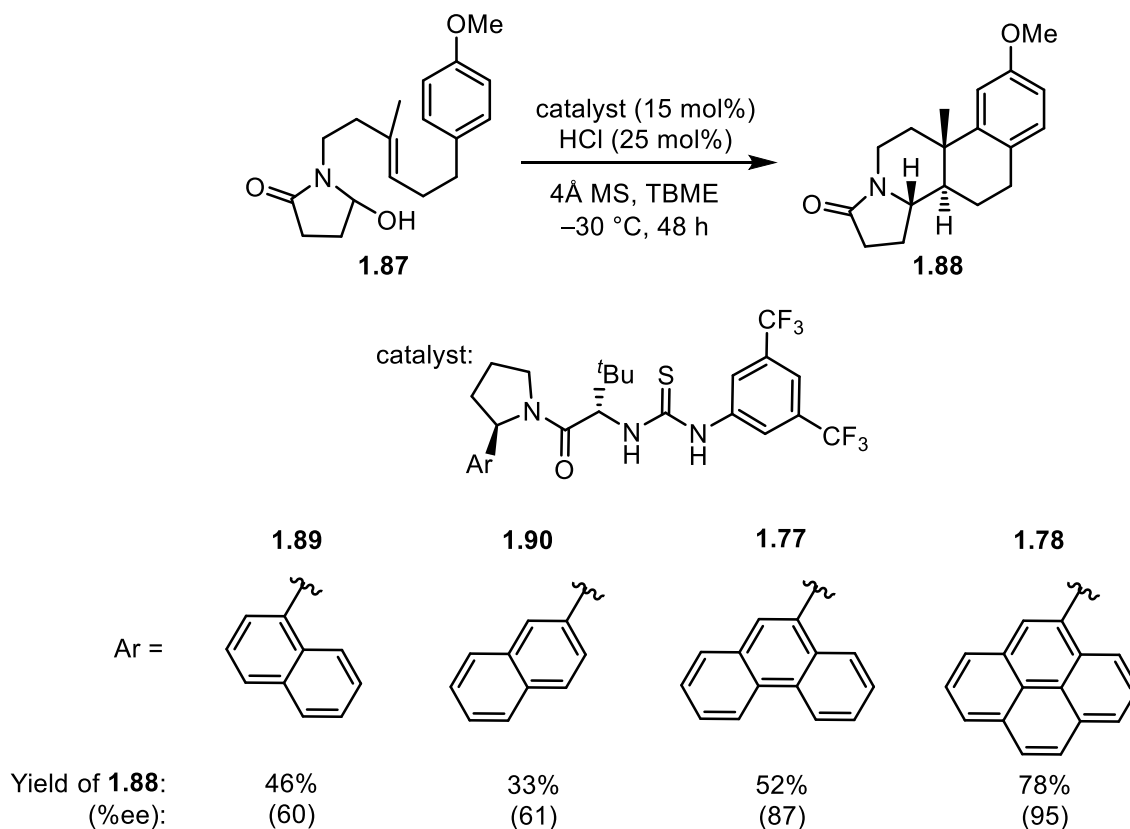
Scheme 1.13. Tail-to-head cyclizations of neryl chloride derivatives.

Thiourea catalyst **1.78**, with 4-pyrenyl substitution, was demonstrated to effectively catalyze the polyene cyclization of α -hydroxy lactam substrates (**1.85**, Scheme 1.14),¹¹⁵ giving products **1.86** in high yields (51-77%) and enantioselectivities (89-94% ee).¹¹⁶ Under hydrochloric acid conditions, the α -hydroxy lactam is ionized to give the corresponding acyl iminium ion with a chloride counterion. The thiourea is then proposed to perform co-operative catalysis, binding to the chloride anion with the thiourea moiety and to the cationic transition state through cation- π interaction with the pyrene. Mechanistic evidence suggested that the chiral catalyst selectively stabilizes the major diastereomeric transition state, leading to high levels of enantioselectivity.



Scheme 1.14. Proposed mechanism of the thiourea-catalyzed polyene cyclization.

In the polyene cyclization, both the reactivity and the enantioselectivity were highly dependant on the size of the extended aromatic (Scheme 1.15). With naphthyl substitution in **1.89** and **1.90**, product **1.88** was obtained in 46% and 36% yield with above 60% ee. With phenanthrene substitution in **1.77**, product **1.88** was obtained in 52% yield and 87% ee and the best results were obtained with anthracene substitution in **1.78**, which provided product **1.88** in 78% yield and 95% ee. This correlation between the enantioselectivity and the polarizability and quadrupole moment of the arenes provided strong evidence towards stabilization of the major transition state in the enantioselectivity-determining event.

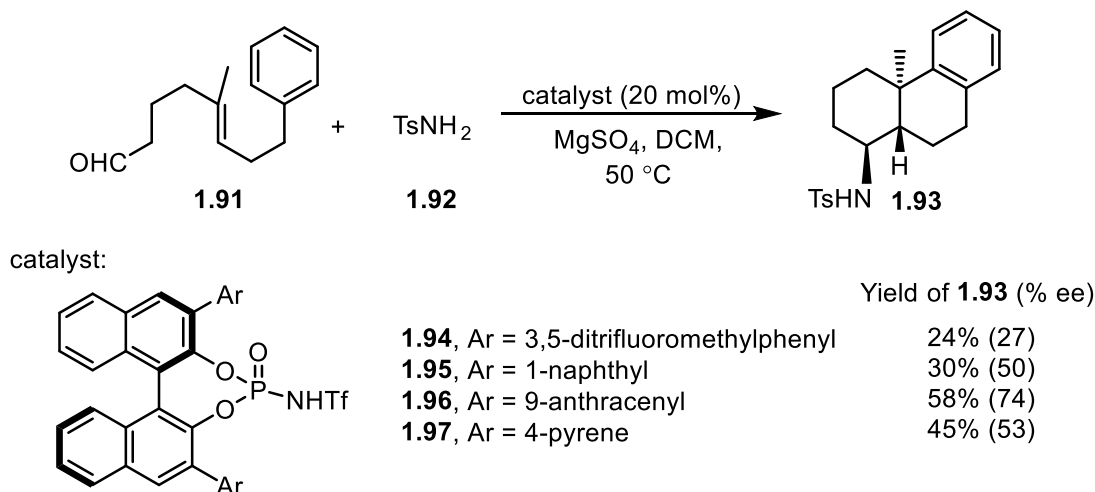


Scheme 1.15. Screening of thiourea catalysts in the polyene cyclization of α -hydroxy lactam

1.87.

In an iminium-promoted polyene cyclization catalyzed by chiral BINOL-derived phosphoramidate (Scheme 1.16), anthracenyl substitution on catalyst **1.96** provided optimal reactivity and enantioselectivity (**1.93** in 58% yield, 74% ee).¹¹⁷ The authors propose a cation- π interaction due to the relation between reactivity and the quadrupole moment of the aromatic groups on the catalyst. However, the mechanism of enantioinduction is unclear and could arise

from destabilization of the ground state as opposed to transition state stabilization. Anthracene has also been incorporated into a BINOL-derived thiophosphoramidate catalyst for the asymmetric bromonium-initiated polyene cyclization.¹¹⁸



Scheme 1.16. Chiral Bronsted acid-catalyzed polyene cyclization.

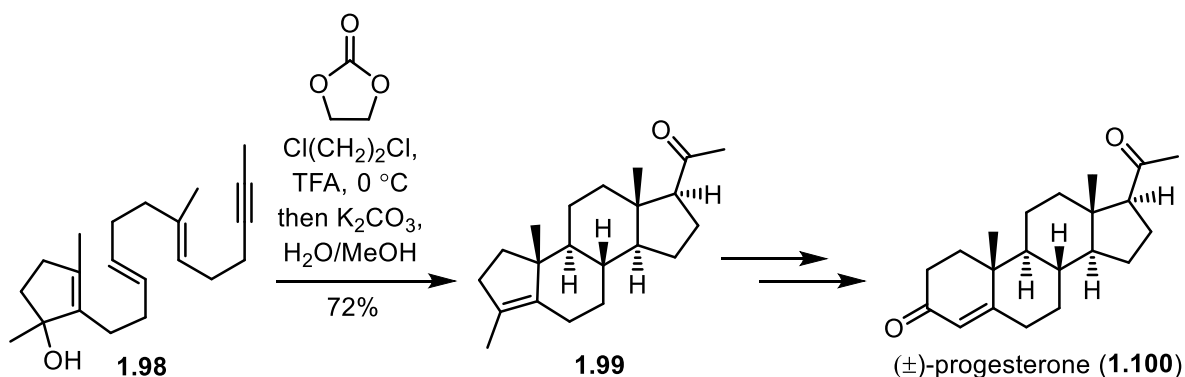
Harnessing cation- π interactions in the synthetic polyene cyclization is an attractive endeavour due to the role that they play in the complete regio- and stereocontrol achieved in steroid biosynthesis. The examples shown where cation- π interactions are proposed to stabilize cationic intermediates or transition states in monoterpene and polyene cyclizations demonstrate the viability of using this interaction to achieve reactivity and selectivity. Also made apparent is the difficulty in achieving selective termination of cyclizations where alternate termination pathways are possible that have low energy activation barriers.

1.4 Synthetic polyene cyclizations

Catalyst designs that incorporate extended aromatics to stabilize cation intermediates and transition states through cation- π interactions have been successfully used in several reactions. The polyene cyclization proceeds through multiple ring closures to result in the final fused ring products, each with a possibility of multiple alternate low energy pathways which could proceed instead. In the biosynthetic polyene cyclization, cation- π interactions have been postulated to stabilize cationic intermediates, contributing to the observed selectivity. There have been several strategies developed in attempts to achieve similar selectivity to that observed in nature, several of which will be discussed in this section.

1.4.1 Racemic polyene cyclizations

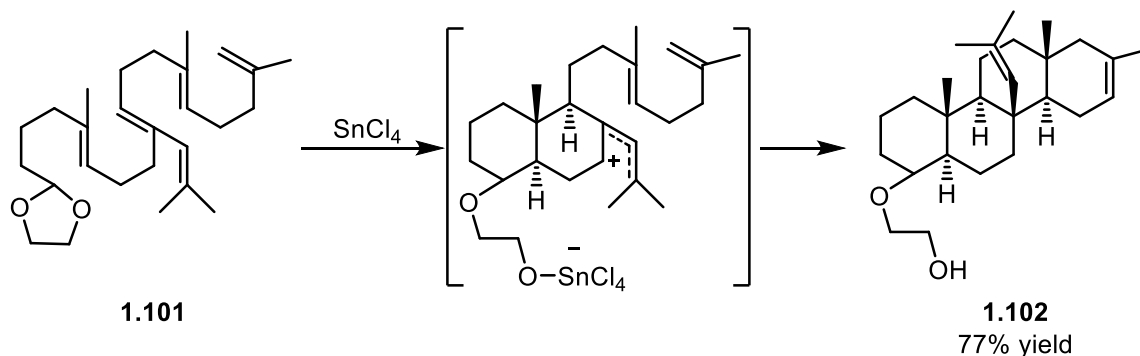
Initial investigations by Stork and Eschenmoser had initiated the polyene cyclization through electrophilic activation of the initial olefin, either by protonation or Lewis acid coordination. This method suffers poor selectivity for the initial olefin. Therefore, to expand the potential applicability of the polyene cyclization to the synthesis of terpene natural products, different initiation methods were developed. Johnson developed methods which initiated the racemic polyene cyclization through the Lewis or Bronsted acid activation of a sulfonate ester,¹¹⁹ acetal,¹²⁰ or allylic alcohol. The acid catalyzed dehydration of an allylic alcohol was used to promote the polyene cyclization in Johnson's total synthesis of progesterone (**1.100**, Scheme 1.17).¹²¹ Of note is the methyl group installed to favour the cyclization to the 6,6-bicycle (**1.99**), instead of the 6,5 ring system initially formed in the biosynthesis. Methods have also been developed which initiate the polyene cyclization through epoxide opening,¹²² analogous to that seen in the biosynthesis of lanosterol, as well as the ionization of an α -hydroxy lactam.¹¹⁵



Scheme 1.17. Allylic alcohol-initiated polyene cyclization in Johnson's synthesis of progesterone.

To expand the utility of the polyene cyclization for the synthesis of natural products, potential terminating groups have also been investigated. The use of aromatic rings to terminate the polyene cyclization is most prevalent, where varying substitution allows increased reactivity as well as promoting regioselectivity. However, there have been other terminating groups reported, such as alkenes (Scheme 1.18),^{121, 123} alcohols (Scheme 1.21),¹²⁴ propargyl silanes (Scheme 1.19),¹²⁵ and silyl enol ethers (Scheme 1.20).¹²⁶

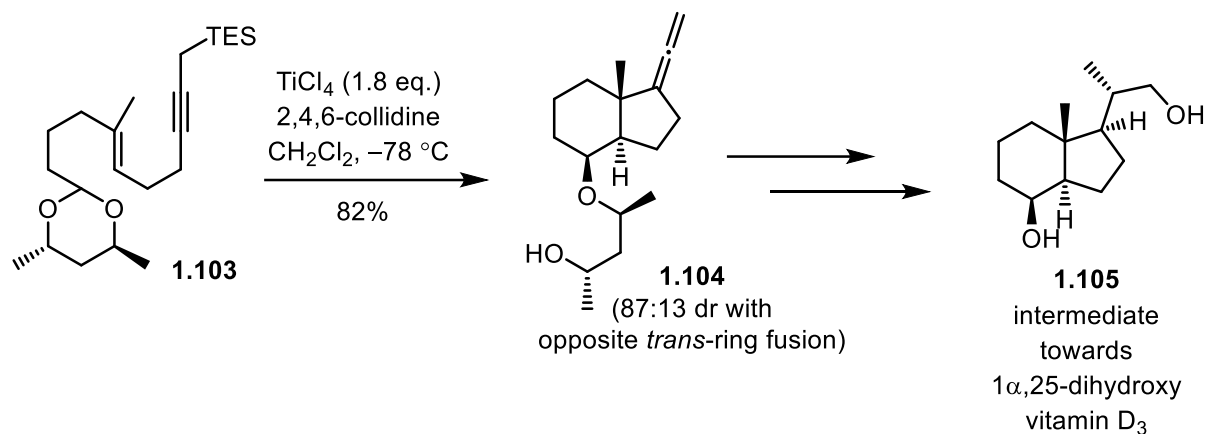
Reports of polyene cyclizations promoted by the acid activation of the terminal olefin were limited to mono- and bicyclizations, where further cyclizations led to very low yields of products with significant amounts of side products.¹⁵ These side products resulted from either low selectivity for activation of the initial olefin or premature termination of the cyclization. With the development of an acetal initiating group, Johnson demonstrated that good yields of a tricyclic product could be obtained.¹²⁷ However, using the same acetal initiating group in his effort towards the total synthesis of tetracyclic natural products, Johnson noted that products were generally obtained in poor yields or not at all.¹²⁸ He overcame this issue by stabilizing the intermediate cations to promote further cyclizations. With cation-stabilizing auxiliaries, such as allyl (Scheme 1.18) or fluorine groups, high yields of tetracyclized product could be achieved (e.g. 77% of product **1.102**).¹²⁹



Scheme 1.18. Tetracyclization achieved with incorporation of cation-stabilizing auxiliary.

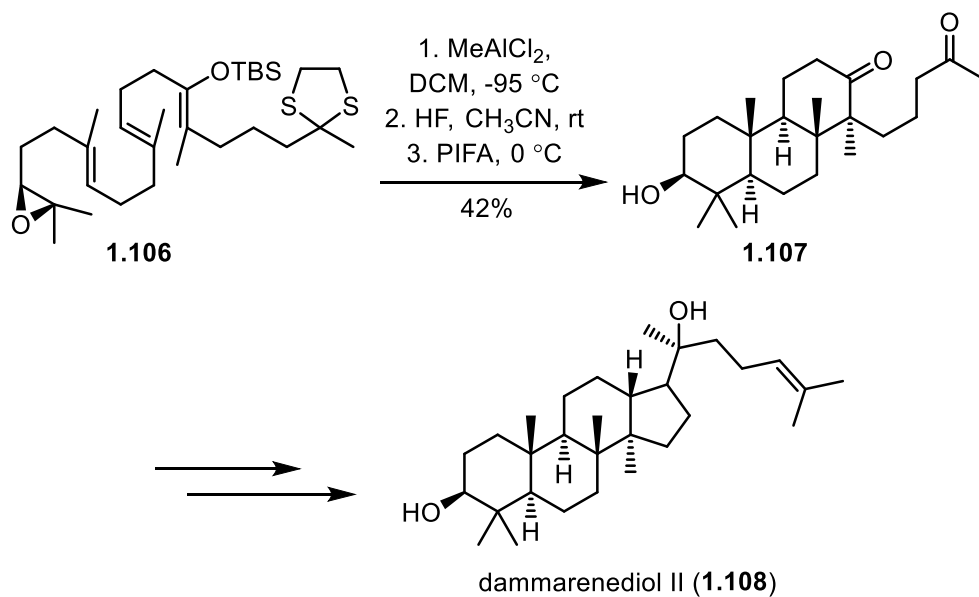
1.4.2 Substrate-controlled diastereoselective cyclizations

Initial reports of imparting asymmetry to cyclized products used chiral substrates which underwent diastereoselective polyene cyclizations. The first method to achieve this was reported by Johnson with the initiation of the polyene cyclization by the Lewis acid assisted opening of a chiral acetal.¹³⁰ This method was used in the asymmetric synthesis of a key intermediate towards $1\alpha,25$ -dihydroxy vitamin D_3 (**1.105**, Scheme 1.19), where the polyene cyclization gave an 87:13 diastereomeric ratio of separable products (**1.104** and diastereomer).¹³¹ An intermolecular approach to chiral acetal-promoted polyene cyclizations has also been reported.¹³²



Scheme 1.19. Johnson's diastereomeric polyene cyclization initiated by the opening of a chiral acetal.

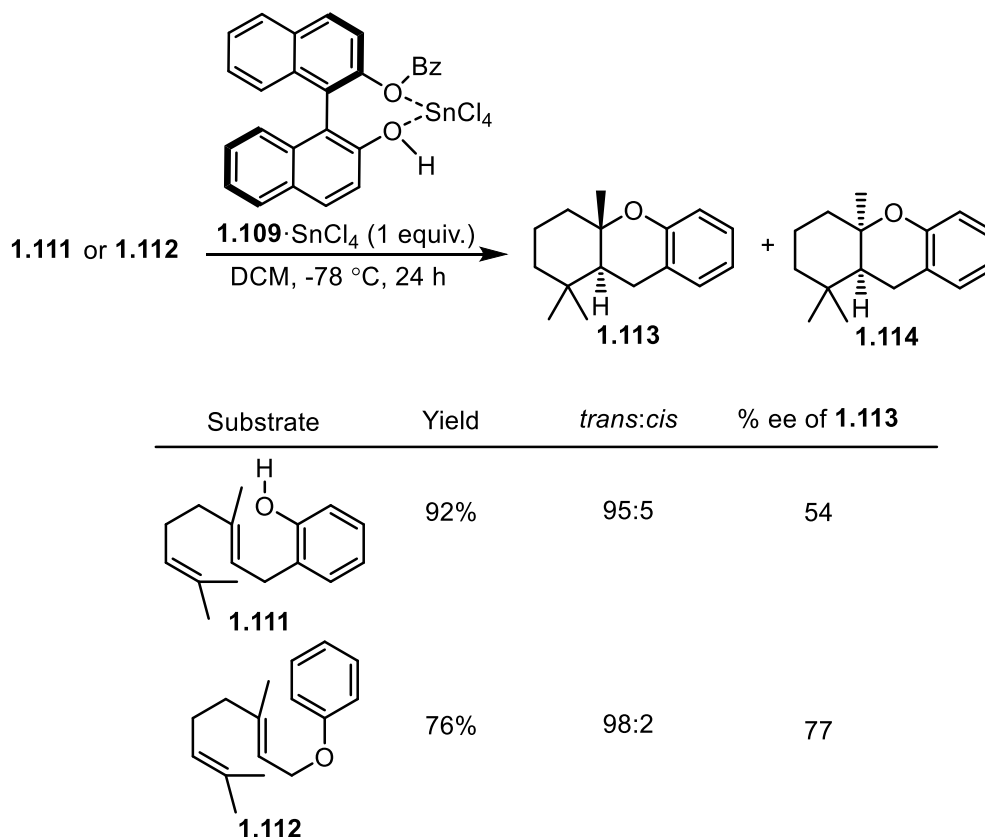
An asymmetric synthesis of dammarenediol (**1.108**) was achieved by Corey, who initiated the ring-forming polyene cyclization through Lewis acid-catalyzed opening of a chiral epoxide (**1.106**, Scheme 1.20).¹²⁶ The use of an epoxide initiating group mimics the polyene cyclization in the biosynthesis of dammarenediol. The chiral epoxide controls the stereochemistry in the final product, with the correct conformation for epoxide opening occurring with only one *chair-chair-chair* transition state. The regioselectivity of the third ring closure was obtained through addition of a silyl enol ether.



Scheme 1.20. Epoxide initiated polyene cyclization in Corey's synthesis of dammarenediol II.

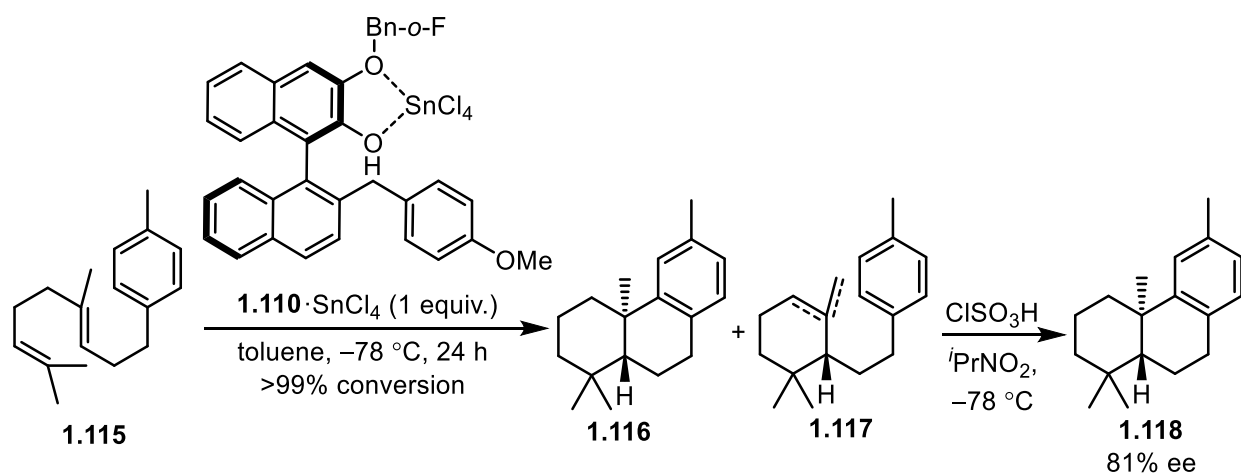
1.4.3 Reagent/catalyst controlled enantioselective polyene cyclizations

Yamamoto reported the first enantioselective polyene cyclization using SnCl_4 with a BINOL-derived Bronsted acid (**1.109**) to provide a chiral proton source as an initiator (Scheme 1.21).¹²⁴ With this Lewis acid-assisted Bronsted acid (LBA), the polyene cyclization of phenol substrate **1.111** provided *trans*-decalin product **1.113** in 54% ee in a ratio of 95:5 with *cis*-decalin product **1.114**. The cyclization of phenol ether substrate **1.112** resulted in the same products, with better enantioselectivity (77% ee) and diastereoselectivity (98:2 *trans*:*cis*). The co-ordination of a chiral Bronsted acid to a Lewis acid both increases the acidity of the proton and restricts its rotational flexibility. To achieve high stereoselectivity with this method, the conformation of the transition state must be restricted, either through a more concerted mechanism, participation of the internal olefin in the initiation step, or through strong association of the counter anion with an intermediate cation.

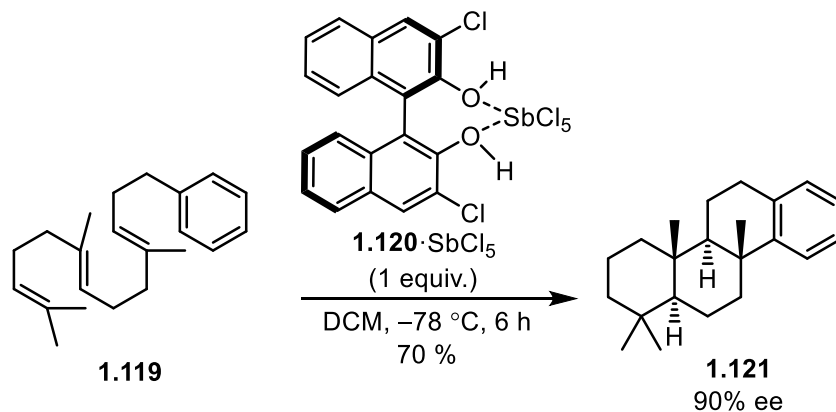


Scheme 1.21. First reported enantioselective polyene cyclization.

Chiral LBA **1.110**·SnCl₄ provided better enantioselectivity in the cyclization of substrates which were terminated by the π -system of an aromatic ring.¹³³ The cyclization of a *p*-methylphenyl terminated substrate **1.115** underwent the initial cyclization with >99% conversion (Scheme 1.22). However, this resulted in a mixture of the bicyclic product **1.116** and elimination product **1.117**. A second step with a strong acid was required to achieve complete bicyclization, affording product **1.118** in 81% ee. Further iterations of LBA catalysts provided higher enantioselectivity, also with the addition of a strong acid to complete the second cyclization.¹³⁴ Corey showed that the increased reactivity using SbCl₅ as the Lewis acid in catalyst **1.120**·SbCl₅ allowed the bicyclization to proceed without the addition of a strong acid.¹³⁵ Additionally this more reactive catalyst was successful at enantioselective tricyclizations, such as that of substrate **1.119** which provided product **1.121** in 70% yield and 90% ee (Scheme 1.23). Although modifications to LBA-promoted polyene have resulted in increased reactivity, these methods still have major limitations in that they require high catalysts loadings (usually stoichiometric) and cryogenic temperatures to achieve good yields of product and high enantioselectivity.



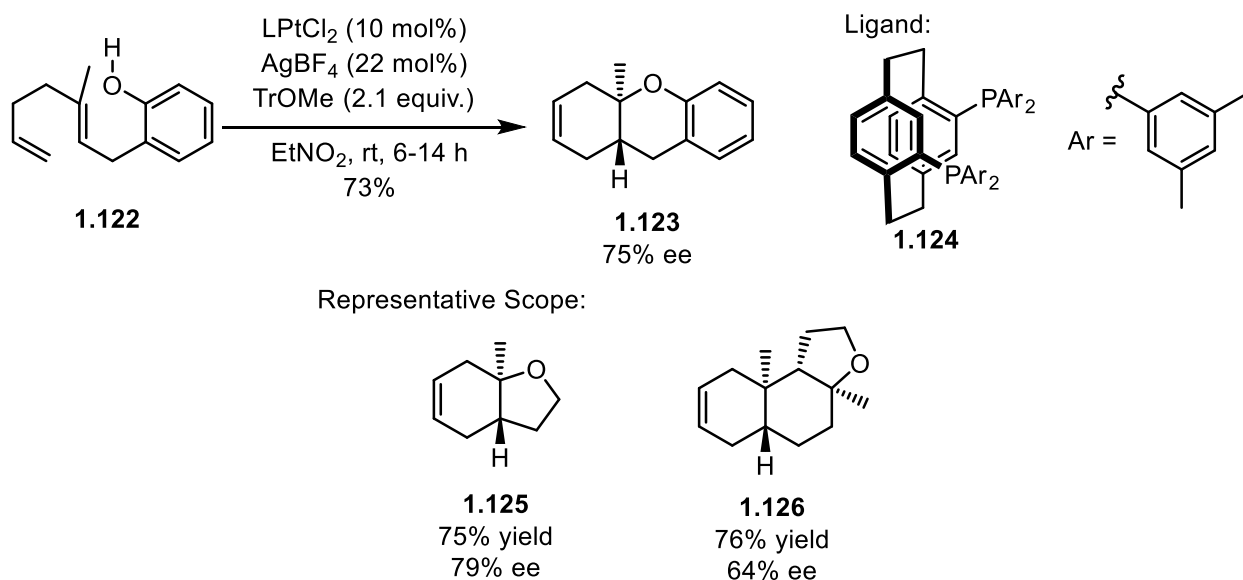
Scheme 1.22. Enantioselective polyene cyclization with LBA **1.110**·SnCl₄.



Scheme 1.23. Enantioselective tricyclization with LBA **1.120**·SbCl₅.

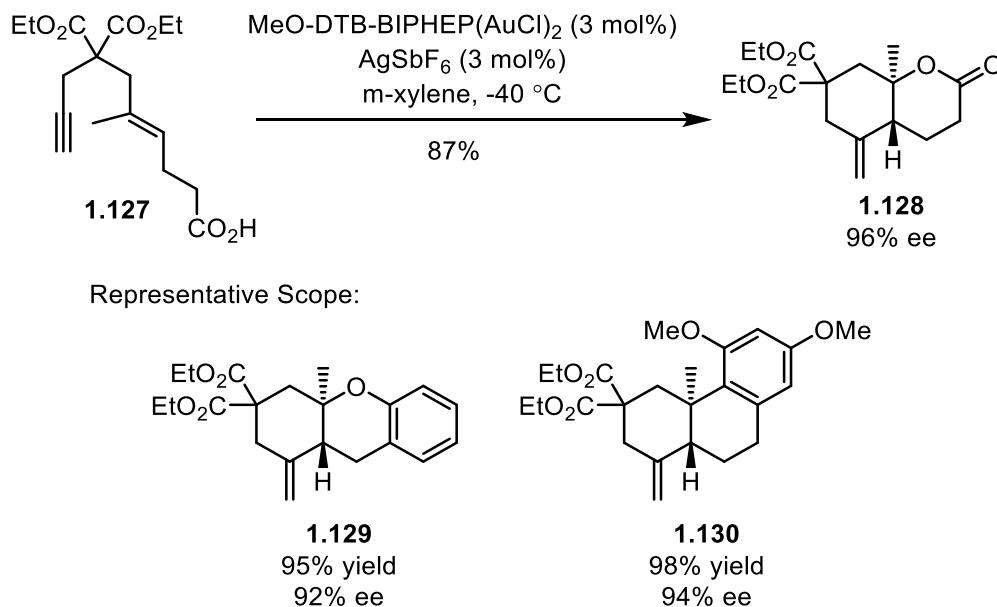
1.4.3.1 Transition metal-catalyzed asymmetric polyene cyclizations

The co-ordination of cationic metals to a terminal olefin as an initiating method for the polyene cyclization was first reported with stoichiometric mercury,¹³⁶ a method which was rendered enantioselective with the addition of a chiral bis-oxazolidinone ligand.¹³⁷ In the first asymmetric catalytic example of a polyene cyclization, Gagné reported a cationic Pt(II)-initiated bicyclization (Scheme 1.24).¹³⁸ A chiral phosphine ligand (**1.124**) provided a chiral environment which resulted in phenol ether product **1.123** in 75% ee. This method was also shown to effectively cyclize substrates which terminated via alcohol closure to form a 5-membered ring, yielding bicyclic product **1.125** (75% yield, 79% ee) and tricyclic product **1.126** (76% yield, 64% ee).



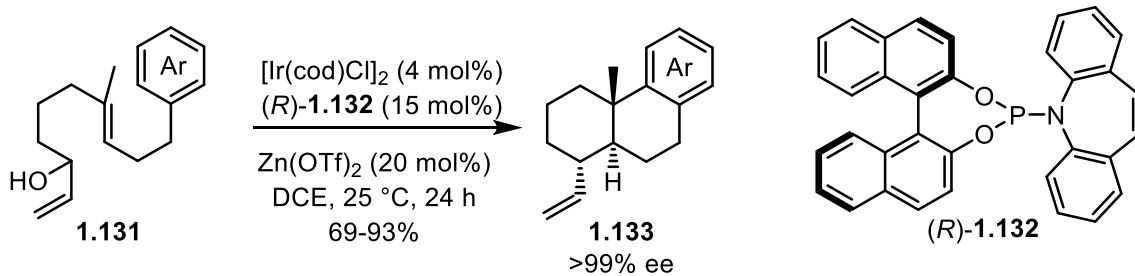
Scheme 1.24. Gagné's asymmetric cationic Pt(II)-catalyzed polyene cyclization.

Cationic Au(I) with a chiral ligand has also been demonstrated by Toste to catalyze the enantioselective polyene cyclization (Scheme 1.25).¹³⁹ Initiated by a 6-exo-dig cyclization, this methodology worked well in substrate **1.127**, which terminated with a carboxylic acid to give **1.128** (87%, 98% ee). Substrates with other electron-rich terminating groups, such as a phenol or dimethoxyphenyl, cyclized well to provide products **1.129** (95% yield, 92% ee) and **1.130** (92% yield, 94% ee) with high yields and enantioselectivity.

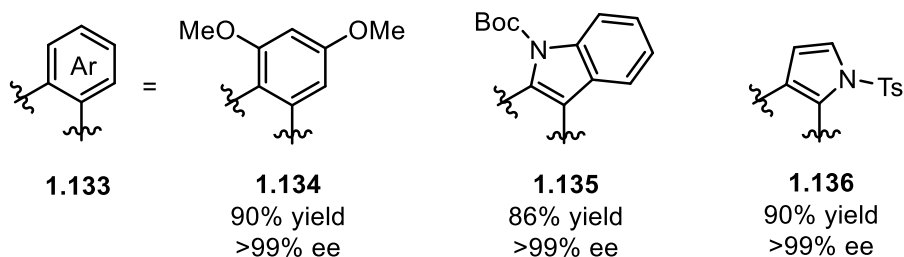


Scheme 1.25. Toste's asymmetric cation Au(I)-catalyzed polyene cyclization.

Carreira has reported an enantioselective polyene cyclization promoted by the Ir(I)-catalyzed activation of allylic alcohols (**1.131**), with the assistance of Zn(OTf)_2 (Scheme 1.26).¹⁴⁰ A chiral phosphoramidite ligand (**R**)-**1.132** is used to promote high enantioselectivities. This methodology provides products with high enantioselectivity (>99% ee) where the polyene cyclization is terminated by an electron-rich aromatic group, such as 3,5-dimethoxyphenyl (**1.134**, 90% yield), N-Boc indole (**1.135**, 86% yield), or N-tosyl pyrrole (**1.136**, 90% yield). In the transition metal catalyzed enantioselective polyene cyclizations reported, high levels of enantioinduction are achieved with the use of bulky ligands and generally require electron rich terminating groups to achieve high levels of enantioselectivity.



Representative Scope:

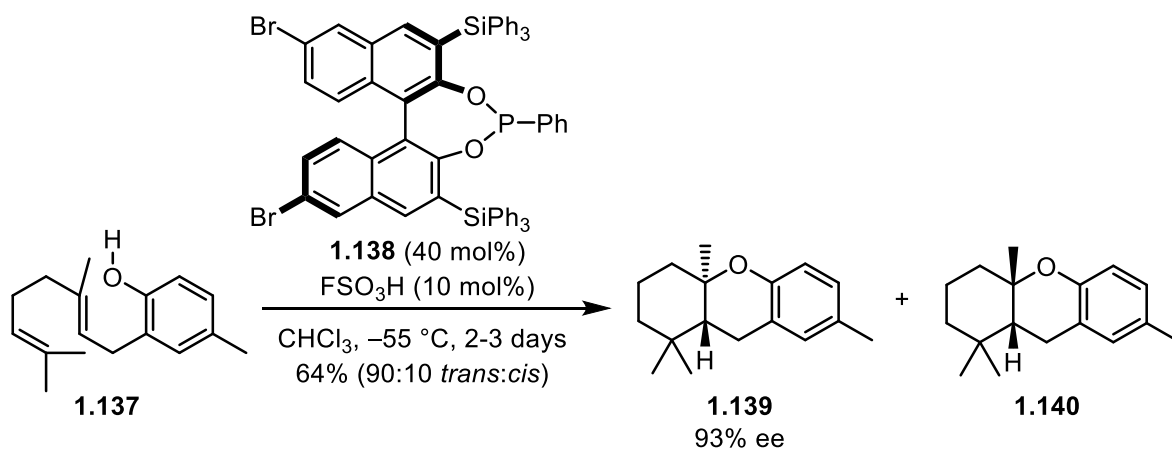


Scheme 1.26. Carreira's Ir(I)-catalyzed polyene cyclization.

1.4.3.2 Organocatalyzed asymmetric polyene cyclizations

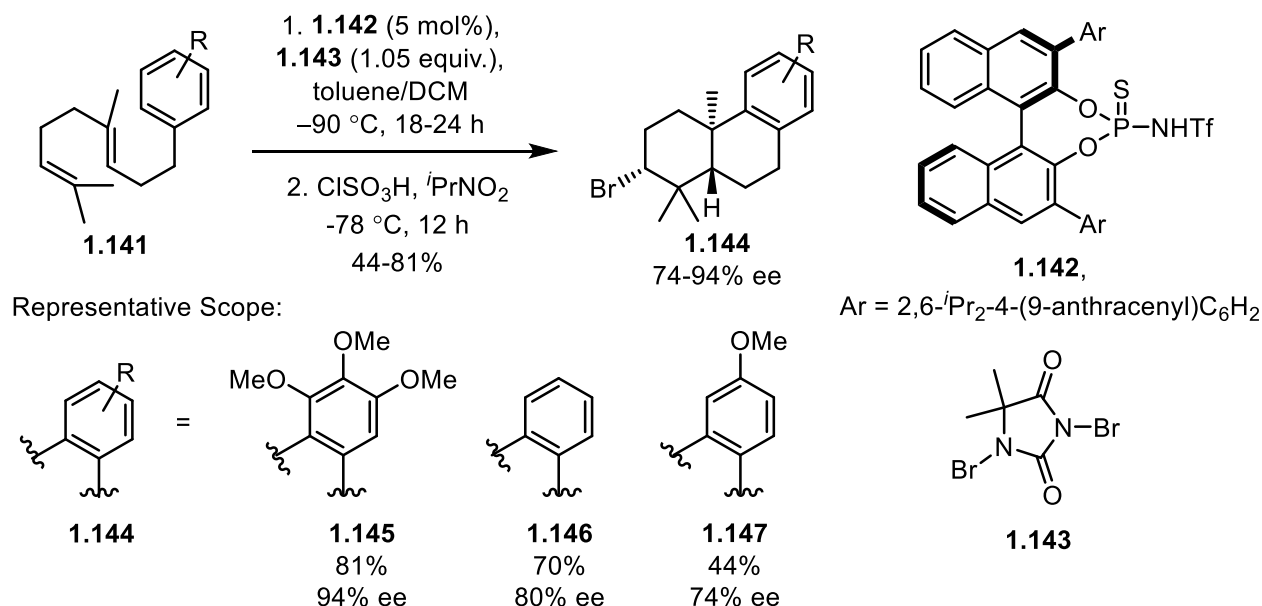
Organocatalysis has become a recognized method which provides a complementary approach to transition metal catalysis. Although organocatalysis has gained a recent surge in popularity, it has been underutilized as an approach in the asymmetric polyene cyclization. Of those examples reported, the most prevalent mode of initiating the cyclization has been through the electrophilic activation of the terminal olefin with either a proton or halonium co-ordinated to a chiral Lewis base.

A Lewis base-assisted Bronsted Acid (LBBA) catalyzed polyene cyclization was reported by Ishihara (Scheme 1.27).¹⁴¹ Using a chiral Lewis base **1.138** paired with an achiral Bronsted acid (fluorosulphonic acid), the cyclization of phenol-terminated polyenes, such as **1.137**, proceeded to give cyclized product in good yields (64%) and enantioselectivity (93% ee). This method suffered from erosion of diastereoselectivity, similarly seen in Yamamoto's LBA-promoted polyene cyclization (Scheme 1.20), providing a product mixture in a 90:10 ratio of *trans*:*cis* decalins (**1.139**:**1.140**).



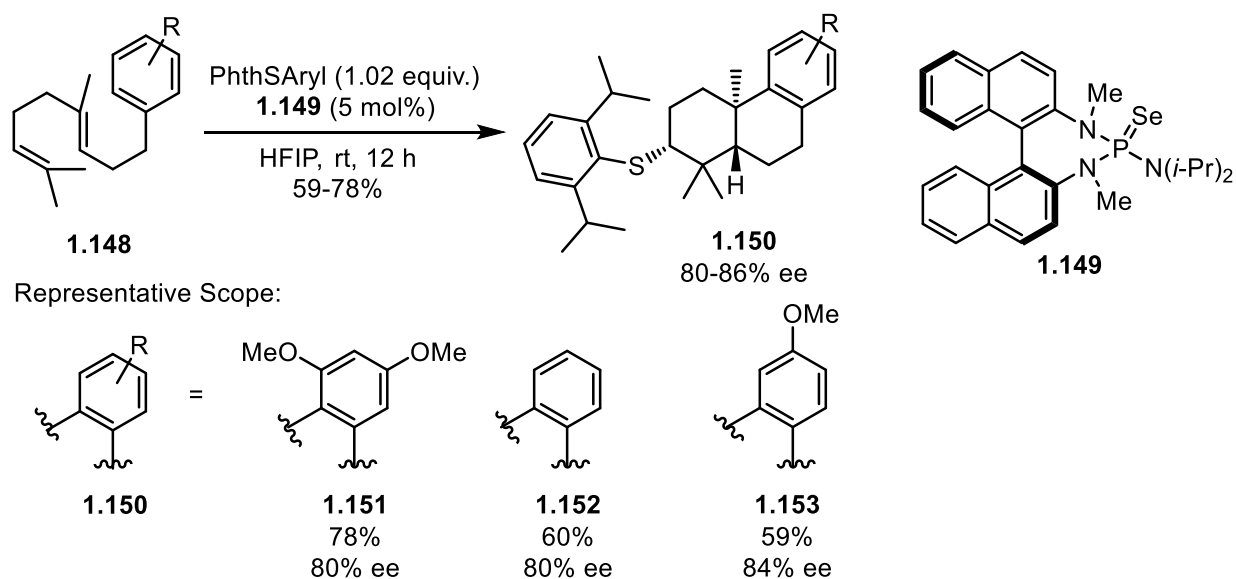
Scheme 1.27. LBBA-catalyzed polyene cyclization.

Electrophilic halogen sources had previously been used to initiate the polyene cyclization in a racemic fashion.¹⁴²⁻¹⁴⁴ The first enantioselective halonium-initiated polyene cyclization was reported by Ishihara, with a chiral iodonium species made from stoichiometric amounts BINOL-derived Lewis base with N-iodosuccinimide.¹⁴⁵ A similar asymmetric, catalytic bromonium-initiated cyclization was reported by Yamamoto (Scheme 1.28).¹¹⁸ BINOL-derived Lewis base **1.142** was used catalytically in conjunction with stoichiometric brominating reagent **1.143** to initiate the cyclization. Complete bicyclization required the addition of a strong acid. This methodology resulted in bicyclic products from substrates with electron-rich terminating groups (i.e. **1.145**) in good yield (81%) and enantioselectivity (94% ee). Termination by a phenyl ring resulted in product **1.146** in slightly diminished yields (70%) and enantioselectivity (80% ee) and a deactivating *p*-methoxy substituent on the terminating aromatic ring resulted in product **1.147** in moderate yield (44%) and enantioselectivity (74%).



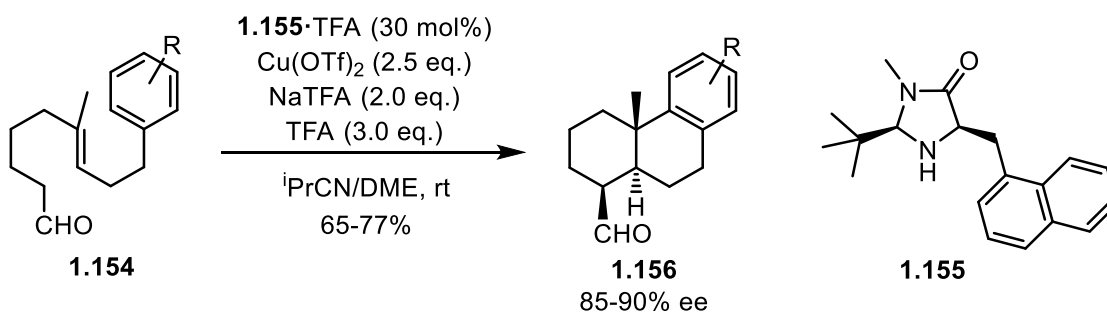
Scheme 1.28. Yamamoto's enantioselective bromonium-initiated polyene cyclization.

Denmark demonstrated that an electrophilic sulfur source, generated from a sulfur phthalimide and chiral Lewis base **1.149**, could initiate an enantioselective polyene cyclization (Scheme 1.29).¹⁴⁶ With HFIP as a solvent, the bicyclization proceeded in good yields without the addition of a second acid. Under these conditions, cyclization products with termination by aromatic groups of strong to weak nucleophilicity were obtained in good yields (78%, 60%, and 59%) and with good enantioselectivity (80%, 80% and 84% ee).



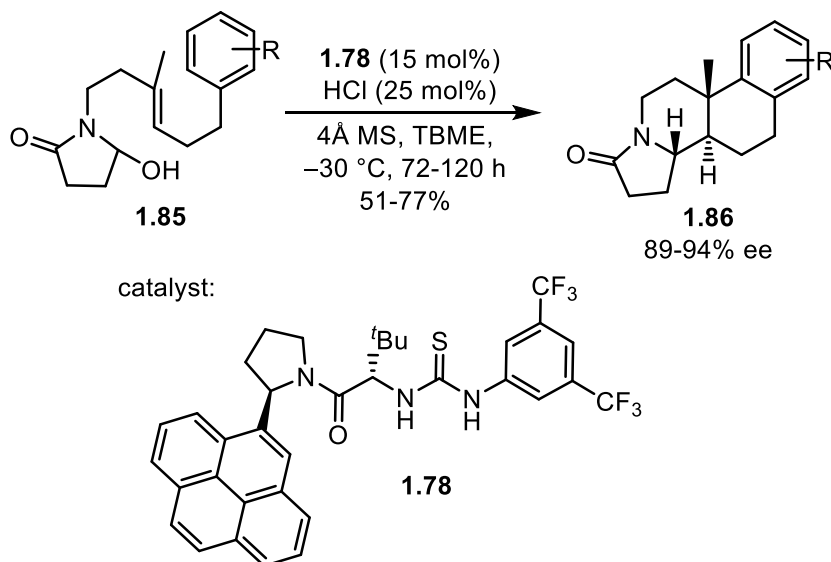
Scheme 1.29. Denmark's enantioselective sulfenium-promoted polyene cyclization.

Although the focus of this thesis is on cationic polyene cyclizations, MacMillan has reported a unique example using organocatalysis to induce enantioselectivity in a radical polyene cyclization (Scheme 1.30).¹⁴⁷ In this methodology, chiral imidazolidinone catalyst **1.155** condenses onto the carbonyl of **1.154**, initially forming the iminium. After isomerization to the enamine, oxidation with copper (II) triflate forms the α -imino radical intermediate, which initiates the cyclization cascade and provides cyclized products (**1.156**) in good yields (65-77%) and enantioselectivities (85-90% ee).



Scheme 1.30. Macmillan's enantioselective radical polyene cyclization.

As discussed in Section 1.3.2, Jacobsen has reported a thiourea-catalyzed polyene cyclization which incorporates both anion-binding catalysis and cation- π interactions to effect enantioselectivity (**1.78**, Scheme 1.31).¹¹⁶ This methodology incorporates a lactam ring into the decalin, providing products (**1.86**) in high yields (51-77%) and enantioselectivity (89-94% ee).

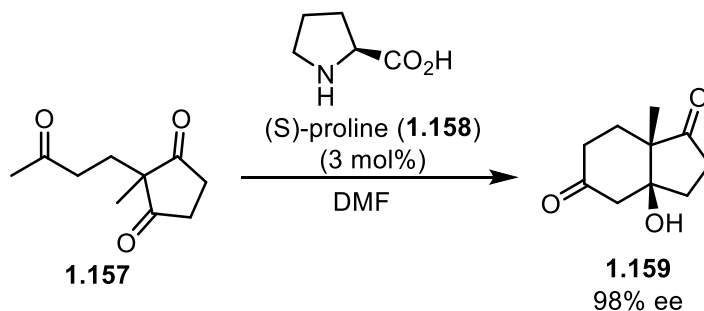


Scheme 1.31. Jacobsen's enantioselective thiourea-catalyzed polyene cyclization.

Recent interest in the asymmetric polyene cyclization has led to an increased number of methodologies in this area. However, as shown by the examples above, there continues to be area for improvement in the development of new initiation methods as well as catalysts to render the reaction asymmetric.

1.5 Organocatalysis

Organocatalysis is the use of a small organic molecules in substoichiometric amounts to accelerate a reaction. Although organocatalytic transformations have been reported in chemical literature for over 100 years, the proline-catalyzed intramolecular aldol addition of the Hajos-Parrish-Eder-Sauer-Wiechert reaction (Scheme 1.30)¹⁴⁸⁻¹⁴⁹ had remained one of very few reports of asymmetric organocatalysis¹⁵⁰⁻¹⁵⁵ until seminal papers in 2000 by MacMillan and List.^{78, 156} These reports were the beginning of the conceptualization of organocatalysis as a field of chemistry, which has grown to solidify its place as one of the main branches of enantioselective catalysis, along with transition metal catalysis and biocatalysis. The importance of the contributions in the field of organocatalysis were recognized with the awarding of the Nobel prize in Chemistry in 2021 to MacMillan and List.



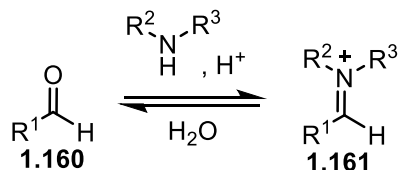
Scheme 1.32. Proline-catalyzed Hajos-Parrish-Eder-Sauer-Wiechert reaction.

There are two main advantages to organocatalysis. The first is that many organocatalysts are found in nature (i.e. proline) or are made from easily accessible pieces where the single enantiomer is found from a biological source. The second advantage is that many organocatalysts are insensitive to air and moisture, unlike many metal-based catalysts, allowing reactions to be run under atmospheric conditions. These advantages, along with the interesting reactivity that organocatalysis can provide, explain the recent rise in investigations towards further applications.

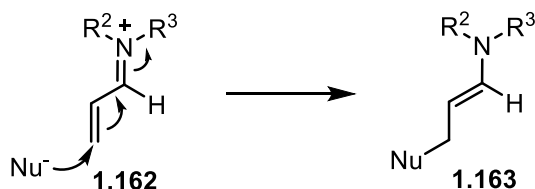
1.5.1 Amine catalysts

Amine catalysts have been the most widely explored class of organocatalysts. Condensation of an amine onto a carbonyl initially results in the formation of an iminium ion (**1.161**). As shown in Figure 1.14, amine catalysts are known to participate in two different modes of reactivity with either electrophilic or nucleophilic behaviour. If the carbonyl species is α,β -unsaturated, the formation of the iminium ion (**1.162**) increases the reactivity of the β -carbon towards a nucleophilic attack or of the entire unit to concerted cycloaddition. This mode is known as iminium catalysis. Alternatively, in enolizable substrates, formation of the iminium ion (**1.164**) can be followed by deprotonation of the α -carbon resulting in a nucleophilic enamine (**1.165**), which can add to an electrophilic species. Enamine catalysis has proven to be a useful method for the enantioselective α -functionalization of carbonyls (or to the γ -carbon in systems with further unsaturation)¹⁵⁷, with reports of cross aldol coupling,¹⁵⁶ intramolecular α -alkylation,¹⁵⁸ Mannich reactions,¹⁵⁹ Michael additions,¹⁶⁰ α -aminations,¹⁶¹⁻¹⁶² α -oxygenations,¹⁶³⁻¹⁶⁵ α -halogenation,¹⁶⁶⁻¹⁶⁹ α -sulphenylation,¹⁷⁰ and α -selenylation.¹⁷¹ As the work in this thesis focuses on iminium catalysis, only this branch of organocatalysis will be reviewed.

Iminium formation:



Iminium catalysis:



Enamine catalysis:

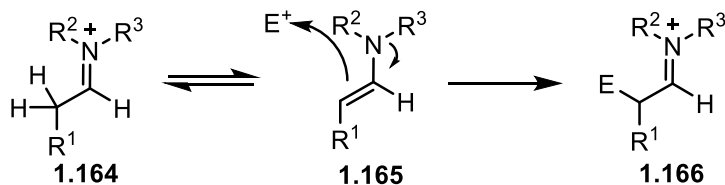


Figure 1.14. Iminium and enamine catalysis.

1.6 Iminium catalysis

Iminium catalysis increases the susceptibility for nucleophilic attack or cycloaddition onto α,β -unsaturated carbonyls by decreasing the energy of the lowest unoccupied molecular orbital (LUMO) of the π -system. This results in a smaller energy difference between the LUMO of the electrophilic α,β -unsaturated iminium and the highest occupied molecular orbital (HOMO) of the reacting nucleophile or cycloaddition partner, giving a greater gain in stabilization energy through bond formation (Figure 1.15).

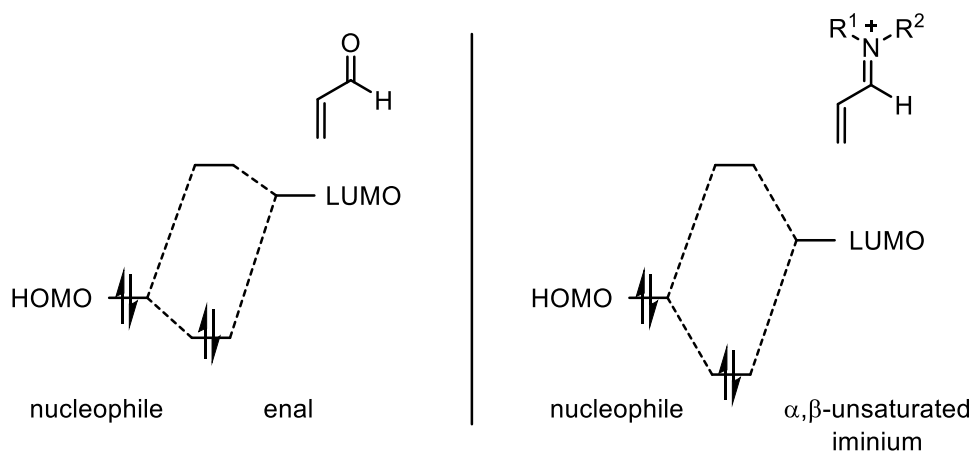
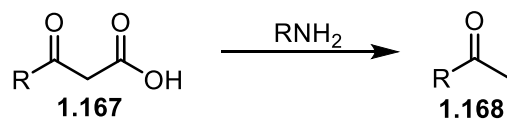


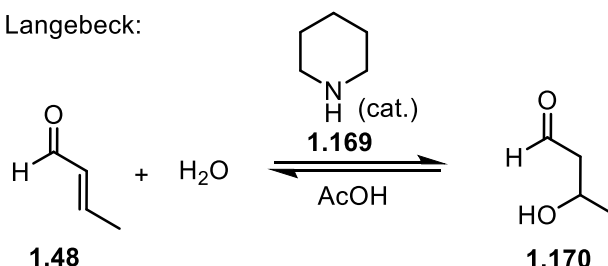
Figure 1.15. LUMO-lowering concept in iminium-catalyzed nucleophilic addition to α,β -unsaturated aldehydes.

Although the piperidine catalyzed Knoevenagel condensation was reported in the late 1800s,¹⁷² with the suggestion that the condensation of the amine and the aldehyde could play an important role in reactivity,¹⁷³ iminium ions as a reactive intermediate were not proposed until the early 1900s with a report of the decarboxylation of acetoacetic acid (**1.167**) catalyzed by amino acid and amine salts (Scheme 1.33).¹⁷⁴ A seminal paper was published by Langebeck in 1937, reporting the addition of water to crotonaldehyde catalyzed by piperidine (**1.169**) in the first iminium-catalyzed conjugate addition.¹⁷⁵

Pollak:



Langebeck:

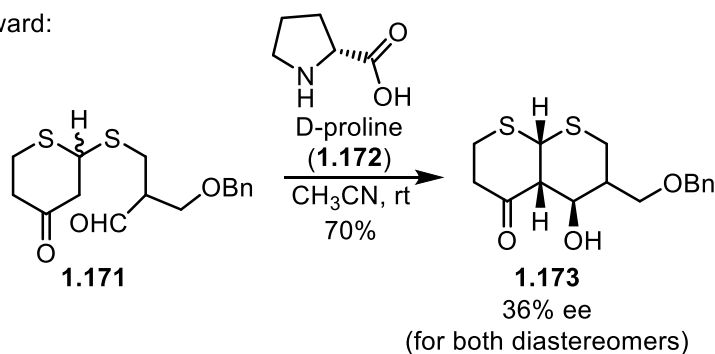


Scheme 1.33. Early examples of iminium reactivity.

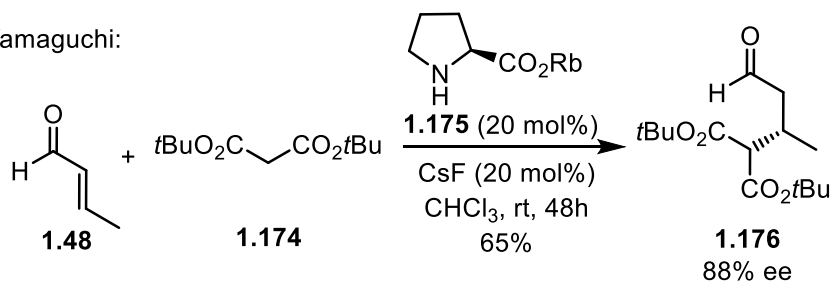
1.6.1 Asymmetric iminium catalysis

In the 1980s, Woodward reported the first use of asymmetric iminium catalysis, using proline (**1.172**) to effect an asymmetric deracemization and conjugate addition respectively (Scheme 1.34).¹⁷⁶ Shortly after, Yamaguchi published a series of papers on the asymmetric conjugate addition of malonates (**1.174**) and nitroesters to α,β -unsaturated aldehydes, catalyzed by proline salts (**1.175**).¹⁷⁷⁻¹⁸¹

Woodward:

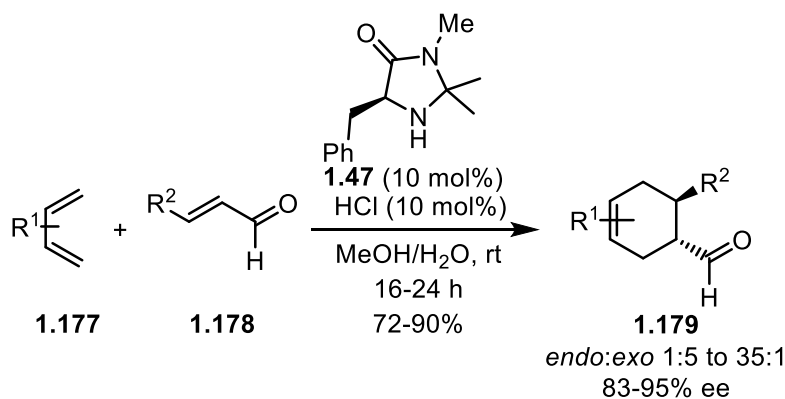


Yamaguchi:



Scheme 1.34. Early examples of asymmetric iminium catalysis.

Following these early reports of asymmetric iminium catalysis, MacMillan reported the first iminium-catalyzed Diels-Alder reaction in 2000 with imidazolidinone catalyst **1.47** (Scheme 1.35).⁷⁸ In this report, the iminiums formed with α,β -unsaturated aldehydes proceed to form the Diels-Alder adduct with unactivated dienes, giving cyclohexane products (**1.160**) in good yields (72-90%) and enantioselectivities (83-95% ee). The reversibility of the catalyst/substrate bond formation allowed facile catalyst turnover and reasonably low catalyst loadings (10 mol%). The wide applicability of iminium catalysis has since been demonstrated by many reports of iminium-catalyzed reactions, including conjugate additions,¹⁶⁰ conjugate reductions,¹⁸² cyclopropanations,¹⁸³ epoxidations,¹⁸⁴ Friedel-Crafts alkylation,⁷⁹ and dipolar cycloaddition¹⁸⁵.



Scheme 1.35. MacMillan's iminium-catalyzed Diels-Alder reaction.

1.6.1.1 Iminium catalysis with secondary amine catalysts

The most common amine catalysts are secondary amines, with the two major types being imidazolidinone type catalysts and proline-based catalysts. Some of the catalysts within these two classes that have been successful in iminium-catalyzed reactions are shown in Figure 1.16.

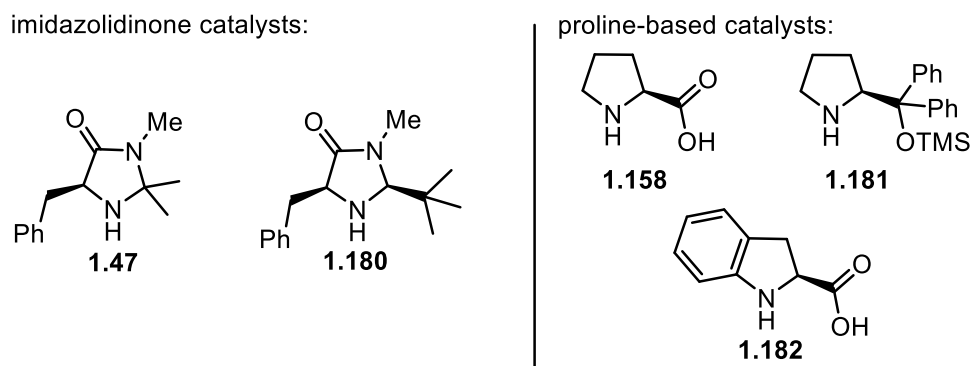


Figure 1.16. Examples of imidazolidinone and proline-based secondary amine catalysts.

Modifications have been made to the sterics and electronics of the imidazolidinone catalysts to achieve high reactivity and selectivity in different reactions. To investigate the origins of enantioselectivity following the success of catalyst **1.47** in the asymmetric Diels-Alder reaction, DFT calculations were performed on the iminium (**1.184**).⁸⁰⁻⁸¹ It was determined that the (*E*)-isomer of the iminium (**1.184i**), with the substrate pointed away from the sterically hindered geminal dimethyl substitution, was preferred by 1.2 kcal/mol calculated at the B3LYP/6-31G(d) level of theory (Figure 1.17). As discussed in section 1.3, the lowest energy conformation of the catalyst has the phenyl group stacked over the iminium, which blocks one face of the activated substrate. The cycloaddition then preferentially occurs on the opposite face, resulting in high levels of enantioselectivity.

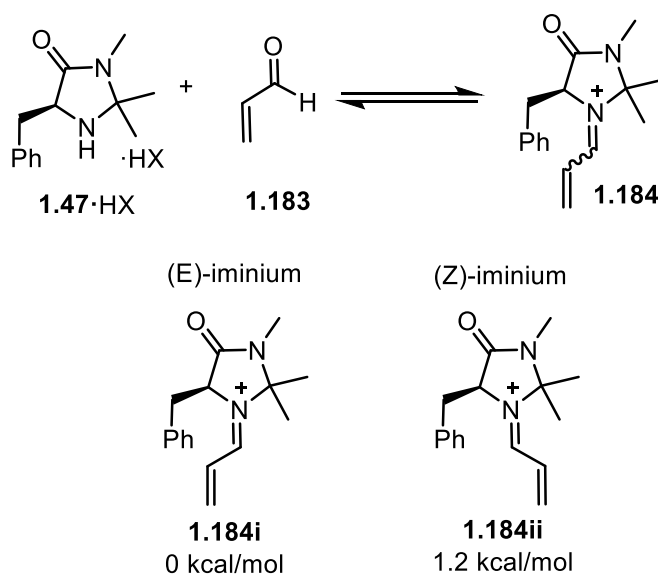
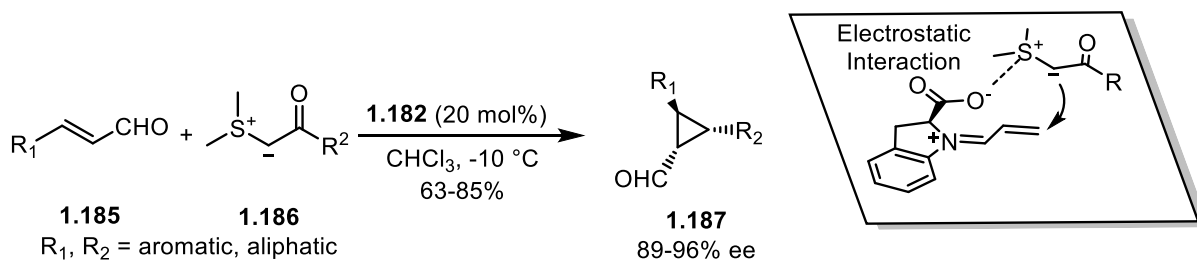


Figure 1.17. Relative energies for most stable iminium conformations with imidazolidinone catalyst **x** calculated at B3LYP/6-31G(d) level.

Proline-based catalysts with a carboxyl group (e.g. **1.158** and **1.182**) have been postulated to induce enantioselectivity with directed attack of the nucleophile through an electrostatic interaction with the carboxylic acid. MacMillan has reported an iminium-catalyzed cyclopropanation relying on the electrostatic interaction between a sulfur ylide (**1.186**) and the acid functionality in catalyst **1.182** to impart enantioselectivity (Scheme 1.36).¹⁸³ Initial investigations with proline (**1.158**) gave product with moderate enantioselectivity. Postulating that the erosion of enantioselectivity is due to the lack of a strong preference for the (*E*)- or (*Z*)-

iminium, catalyst **1.182** was designed to provide a preference for the (*E*)-isomer through steric hindrance of the (*Z*)-isomer by the phenyl substitution.



Scheme 1.36. Enantioinduction through electrostatic interaction in the iminium-catalyzed cyclopropanation.

Jorgensen showed that the addition of bulky aryl groups to the carboxylic acid functionality of proline and protection of the resulting alcohol resulted in catalyst **1.181**, which has a different mechanism of enantioinduction. Computational modelling of the iminium formed with catalyst **1.181** has shown that the (*E*)-isomer is favoured, with the bulky diaryl silyl ether blocking one face of the prochiral olefin to nucleophilic attack (Figure 1.18).¹⁸⁶

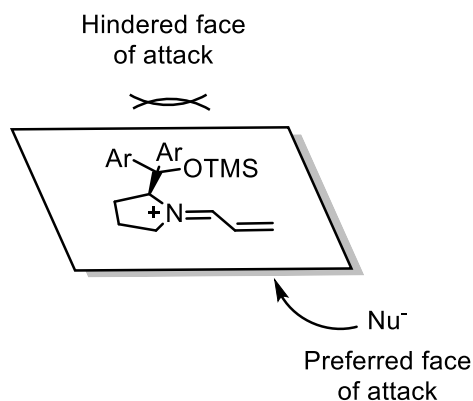


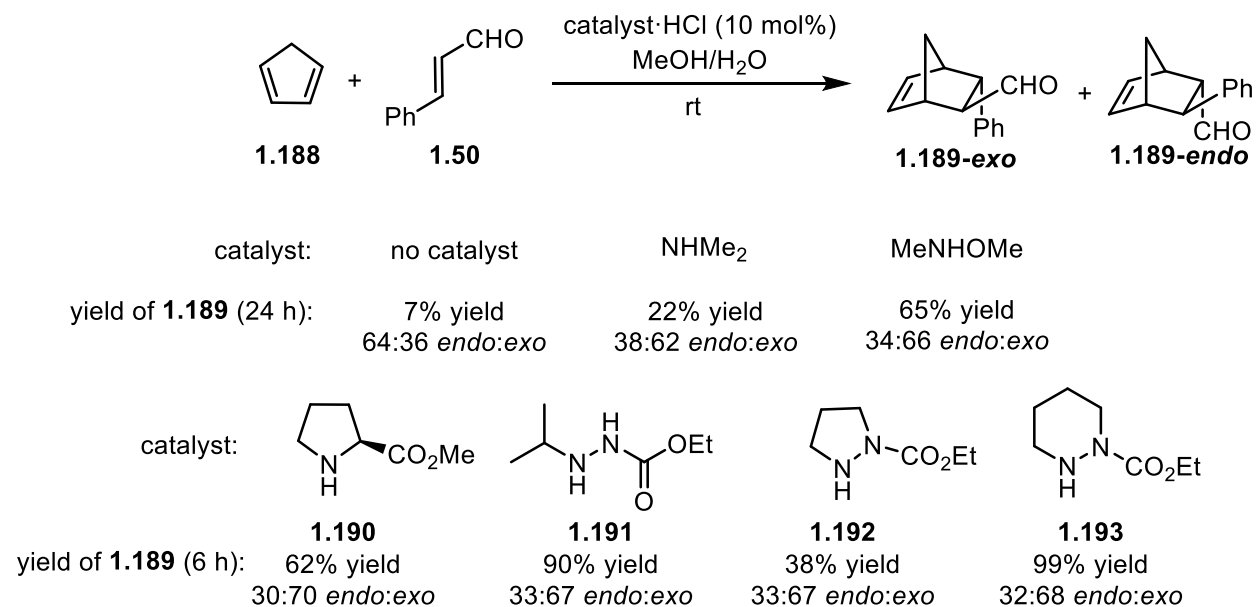
Figure 1.18. Iminium ion with Jorgensen's catalyst showing favoured face of nucleophilic attack.

1.6.1.2 Hydrazone-type catalysts

Following initial reports of asymmetric iminium catalysis by MacMillan, Tomkinson noted that most of the methodology reported had required an amine catalyst with a 5-membered ring scaffold. He hypothesized that the reactivity of these amine catalysts could be increased through α -heteroatom substitution (also known as the α -effect, where the nucleophilicity of a heteroatom is increased with the addition of an α -heteroatom).¹⁸⁷⁻¹⁸⁸ This new strategy would also create new

potential for chiral catalyst designs that varied from previously used 5-membered rings. The validity of the α -effect in hydrazides has come under more recent scrutiny, as discussed in Section 1.7.1.

In 2003, Tomkinson reported increased reactivity in the iminium-catalyzed Diels-Alder reaction with amine catalysts containing an α -heteroatom (Scheme 1.37).¹⁸⁹ In the Diels-Alder reaction of cyclopentadiene (**1.188**) with cinnamaldehyde (**1.50**), cycloaddition product (**1.189**) was obtained in 22% yield after 48 hours with dimethylamine hydrochloride, a simple secondary amine catalyst. The addition of an α -oxygen to the catalyst, in N,O-dimethylhydroxylamine, gave a significant increase in reactivity and resulted in a 65% yield of cycloaddition product in the same amount of time. Of the acyclic amine catalysts containing an α -heteroatom that were screened, the best results were obtained with catalyst **1.191**, which contains an electron-withdrawing ethyl carbamate. This catalyst gave a 90% yield of cycloaddition product **1.189** in only 6 hours.¹⁹⁰



Scheme 1.37. Effect of an α -heteroatom substituted catalyst on the iminium-catalyzed Diels-Alder reaction.

In a later study, Tomkinson investigated the Diels-Alder reaction with 5- and 6-membered ring hydrazides.¹⁹¹ He noted that the 6-membered ring hydrazide catalyst **1.193** had increased reactivity, giving a 99% yield of cycloaddition product in 6 hours, in comparison to the 5-membered ring hydrazide **1.192**, which gave a 38% yield of cycloaddition product in the same amount of time. Catalyst **1.193** was demonstrated to be even more reactive than the known proline

methyl ester (**1.190**), which gave the Diels-Alder adduct in 62% yield. Due to this surprisingly high reactivity, the electronic nature of the catalysts was investigated. DFT methods were used to determine the proton affinity, noting that the addition of an α -heteroatom lowers the proton affinity for the basic nitrogen. They proposed that enhanced iminium ion formation occurs in the hydrazide series of catalysts in comparison to their single nitrogen counterparts due to the increased acidity of the protonated catalyst. Additionally, it was noted that the calculated LUMO for the iminium ion formed with cinnamaldehyde and catalyst **1.190** was lower than that formed with catalyst **1.192** and higher than that formed with catalyst **1.193**, which corresponded to the reactivity trends observed.

Following the discovery by Tomkinson of highly reactive hydrazide catalysts, several reports were made of catalysts incorporating chirality into these scaffolds. The catalysts shown in Figure 1.19 have been reported to effect enantioselectivity in the Diels-Alder reaction¹⁹²⁻¹⁹⁶ as well as other chiral hydrazide catalysts with a 5-membered ring scaffold.¹⁹⁷⁻¹⁹⁹

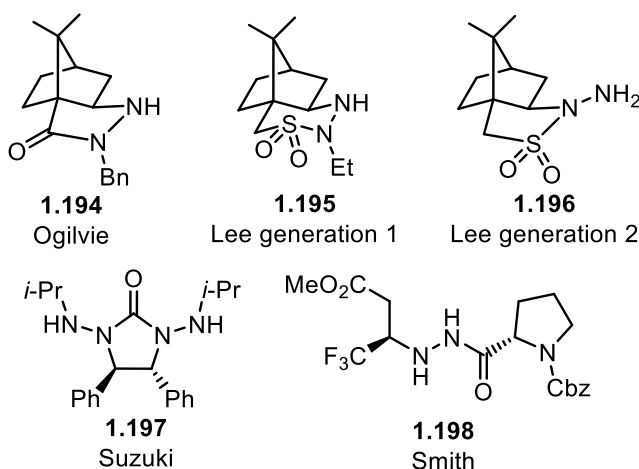
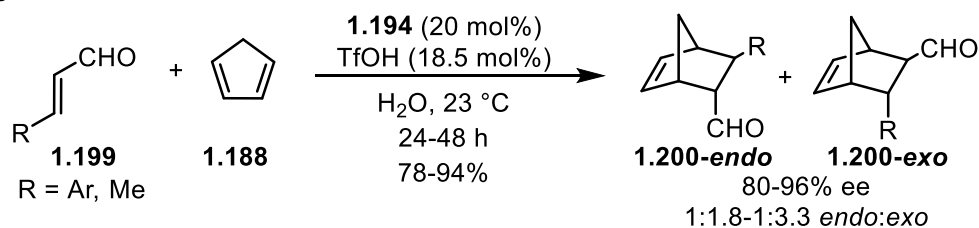


Figure 1.19. Chiral hydrazine-based catalysts.

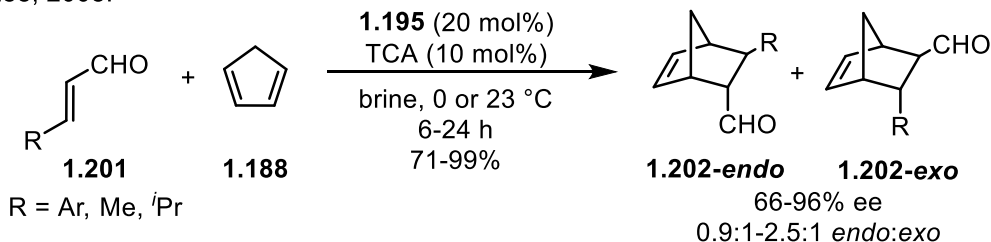
The first asymmetric hydrazide catalyst (**1.194**) was reported by Ogilvie, which incorporated a camphor-derived scaffold.^{192, 200} In the Diels-Alder reaction of cyclopentadiene with α,β -unsaturated aldehydes, this catalyst provided products in 78-94% yield with 80-96% ee (Scheme 1.43). Catalyst **1.194** was proposed to hold the iminium in a rigid conformation, with the camphor skeleton blocking the cycloaddition onto one face of the olefin and affording high enantioselectivity. However, catalyst **1.194** proved less reactive than imidazolidinone catalyst **1.48** in the Diels-Alder reaction, requiring longer reaction times (24-48 hours in comparison to 16-24

hours with catalyst **1.48**). Mechanistic studies on the reaction indicated that both the iminium ion formation and hydrolysis were very rapid processes, with the cycloaddition step being rate-limiting.²⁰¹ In 2008, camphor-derived catalyst **1.195** was reported by Lee, which gave greater reactivity in the Diels-Alder reaction of α,β -unsaturated aldehydes, providing products in 71-99% yield in 6-12 hours at 0 °C.¹⁹³ Lee's second generation hydrazine catalyst (**1.196**), which was designed with a less sterically-hindered primary hydrazine, successfully catalyzed the Diels-Alder reaction with α,β -unsaturated ketones, providing cycloaddition products in 70% yield and 88% ee with cyclopentadiene.¹⁹⁴

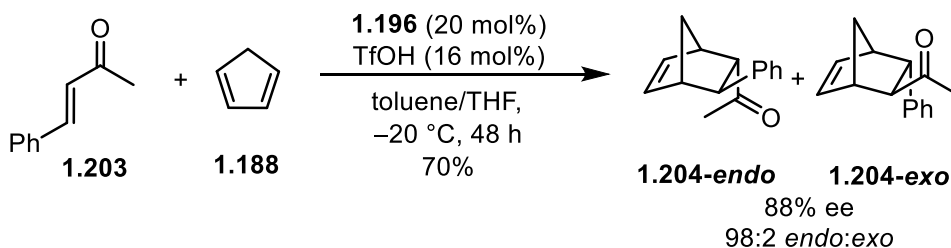
Ogilvie:



Lee, 2008:



Lee, 2010:



Scheme 1.38. Asymmetric hydrazide-catalyzed Diels-Alder reaction of α,β -unsaturated aldehydes.

1.6.2 Iminium-catalysis of α -branched enals

The observed increase in reactivity with hydrazone catalysts in the Diels-Alder reaction prompted our group's interest in their potential for other iminium-catalyzed reactions, particularly those requiring substrates where iminium-activation is difficult to achieve. Despite the rapid expansion in iminium-catalyzed methodology over the past 20 years, there has remained an obvious limitation with reactions of α -branched enals. Formation of an iminium ion from an α,β -unsaturated carbonyl generates allylic-1,3 strain with the substitution α to the carbonyl (Figure 1.20). If this is a hydrogen, the A-1,3 strain isn't significant and the energy of the iminium is low enough to provide significant concentration of this reactive intermediate. However, if this substitution is larger than hydrogen, the A-1,3 strain can disfavor the iminium ion from being formed.

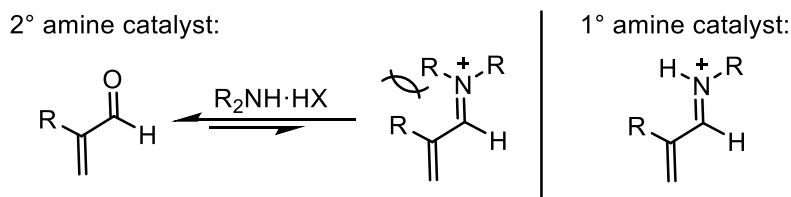
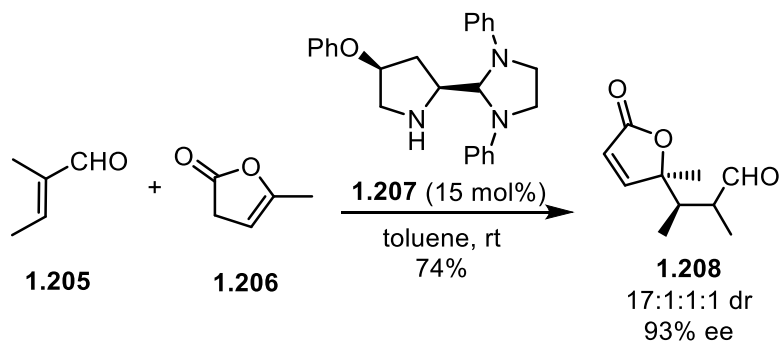


Figure 1.20. A-1,3 strain generated with iminium ion formation.

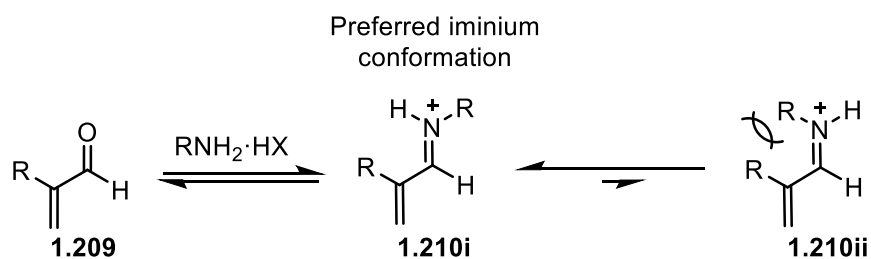
Due to the difficulties in generating the iminium ion, there have only been a couple of reported iminium-catalyzed reactions of α -branched enals with secondary amine catalysts. Small substrate scopes for the asymmetric epoxidation²⁰² and cyclopropanation²⁰³ of α -branched enals have been reported with catalyst **1.181** and a single example (**1.208**) was reported with high yield (74%) and enantioselectivity (93% ee) in the vinylogous Michael addition with catalyst **1.207** (Scheme 1.39).²⁰⁴



Scheme 1.39. Vinylogous Michael addition with α -branched enal.

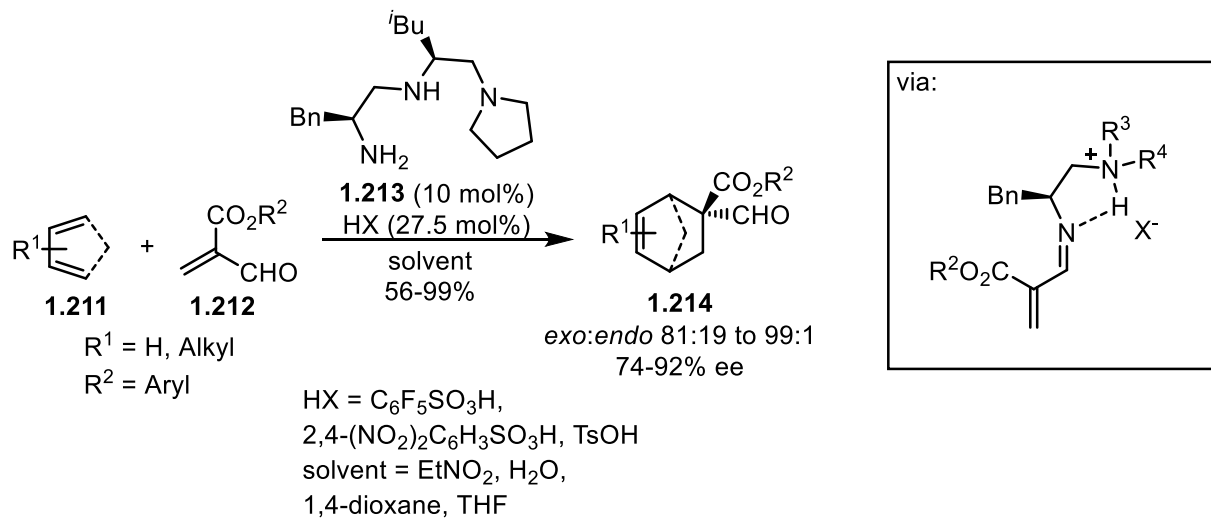
1.6.2.1 Primary amine catalysts with α -branched enals

Primary amine catalysts have less steric hindrance around the nitrogen and can form lower energy iminium intermediates. However, there have been few reported iminium-catalyzed reaction of α -branched enals with primary amine catalysts possibly due to the challenges of asymmetric catalysis. In general, with primary amines, the (*E*)-conformation of the iminium is preferred (**1.210i**, Scheme 1.40), which minimizes the A-1,3 strain between the catalyst and α -substitution on the iminium. This complicates enantioinduction with chiral primary amine catalysts, as the bulk of the catalyst is pointed away from the prochiral centre.

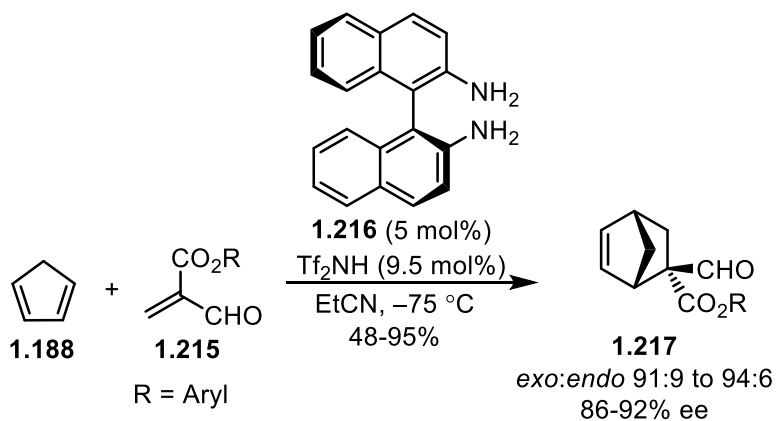


Scheme 1.40. Preferred (*E*)-iminium formed with primary amine catalysts.

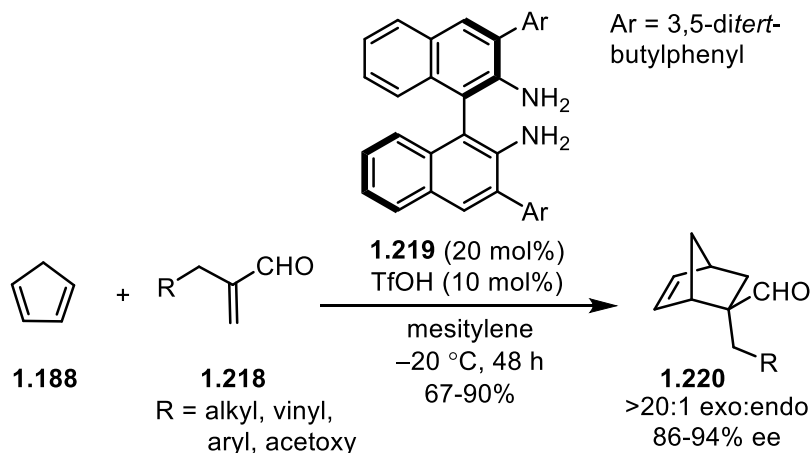
To circumvent this issue, primary amine catalysts have been designed with dual functionality. Ishihara reported a Diels-Alder reaction with α -branched enals (**1.212**) catalyzed by primary amine catalyst **1.213** (Scheme 1.41).²⁰⁵ The preferred iminium conformation is proposed to be the (*Z*)-conformer, which allows π -stacking of the benzyl group with the α,β -unsaturated iminium. Steric interactions between the bulky counterion of the co-acid and the α -substitution are proposed to disfavor the (*E*)-iminium conformation. Enantioselectivities were later improved in cycloadditions with cyclopentadiene using binaphthyl catalyst **1.216** (Scheme 1.42).²⁰⁶ Maruoka has reported the asymmetric Diels-Alder reaction of alkyl and benzyl α -substituted enals (**1.218**) using a substituted binaphthyl catalyst (**1.219**, Scheme 1.43).²⁰⁷ The iminium ion formation is proposed to proceed with assistance from the second primary amine for proton transfer.



Scheme 1.41. Diels-Alder reaction of α -branched enals with primary amine catalyst **1.213**.

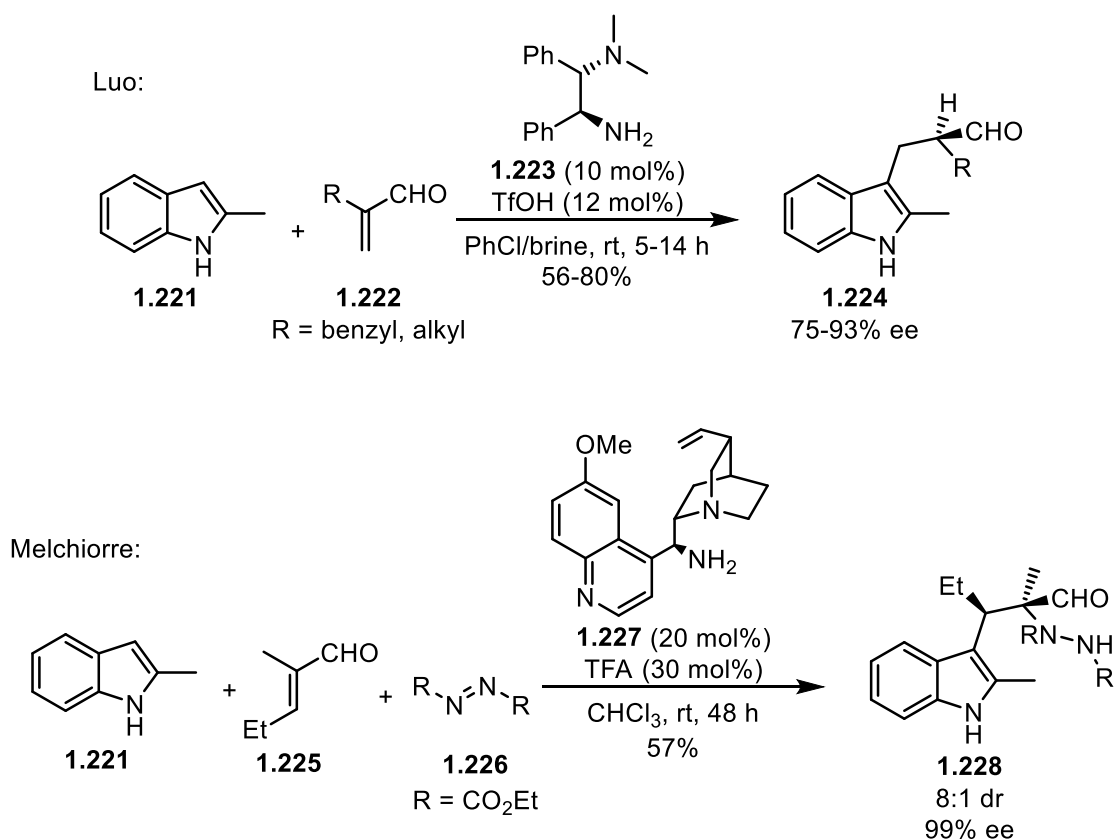


Scheme 1.42. Diels-Alder reaction of α -branched enals with BINOL-derived catalyst **1.216**.



Scheme 1.43. Diels-Alder reaction with α -branched enals with alkyl substitution.

Friedel-Crafts alkylations of indoles with α -branched enals have also been reported, including the example by Luo shown in Scheme 1.44.²⁰⁸⁻²⁰⁹ In the alkylation of indole **1.221** with α -branched enals, the protonation of the enamine resulting after nucleophilic attack was proposed to be the enantiodetermining step. This enantioselective protonation was also used to induce asymmetry in the conjugate additions of thiols²¹⁰ as well as malononitrile.²¹¹ Melchiorre expanded on this methodology to promote a cascade with trapping of the enamine by ethyl azodicarboxylate (**1.226**), forming products such as **1.228**.²¹²

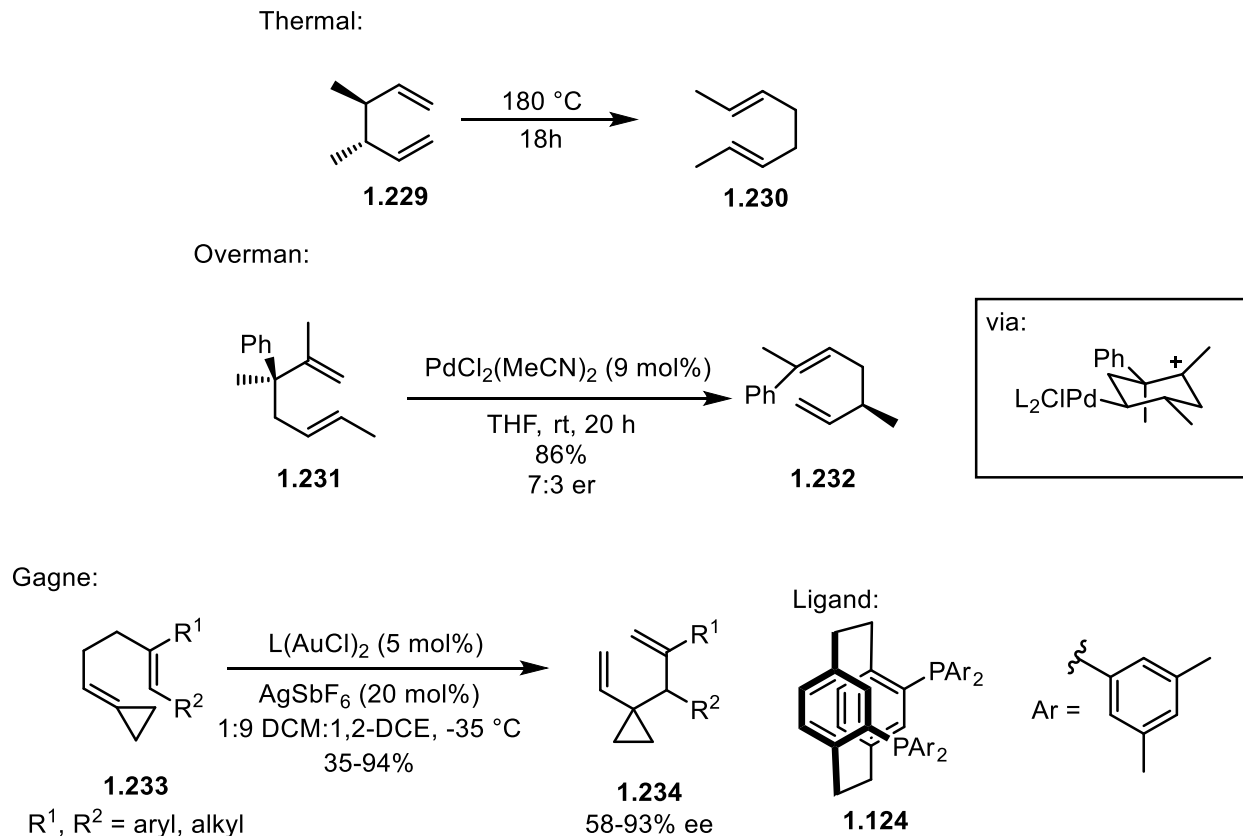


Scheme 1.44. Friedel-Crafts alkylation with α -branched enals.

Limited examples of iminium-catalyzed reactions have been reported with α -branched enals due to the difficulty in achieving iminium ion formation. Therefore, our group has noted a need for further investigation into amine catalysts that can promote these reactions to further explore the potential reactivity with this large class of substrates.

1.7 Organocatalytic Cope rearrangement

Pericyclic reactions are an important class of reactions that have seen prominent use in total synthesis.²¹³ Our group has been interested in developing iminium-catalyzed sigmatropic rearrangements, with initial focus on the Cope rearrangement. Although this reaction is thermally allowed, the high activation barrier requires very high temperatures to allow the reaction to proceed (i.e. 180 °C for the Cope rearrangement of substrate **1.229**, Scheme 1.45).²¹⁴

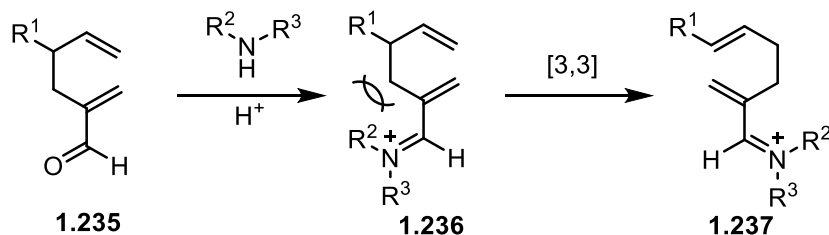


Scheme 1.45. Thermal and transition metal-catalyzed Cope rearrangements.

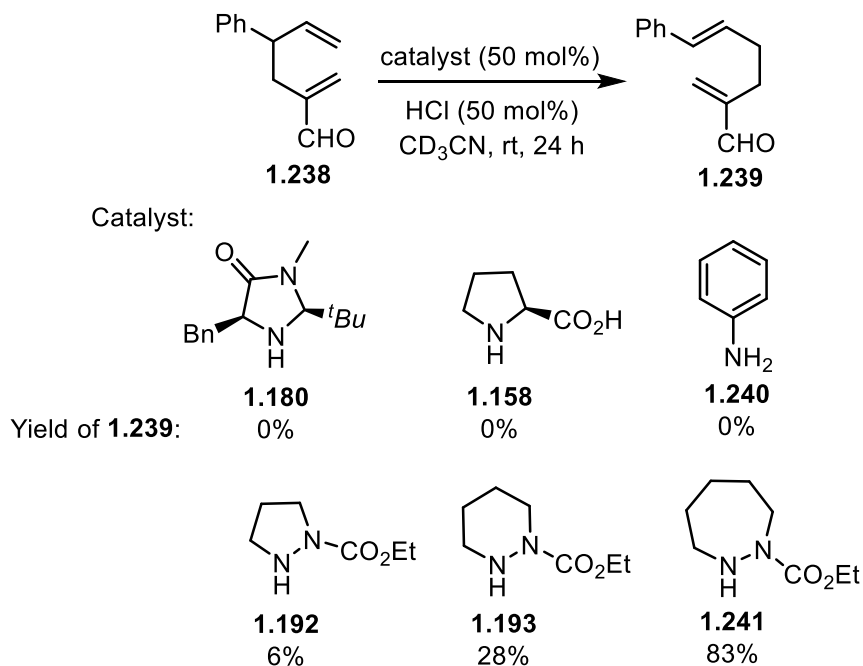
Transition-metals have previously been demonstrated to facilitate the Cope rearrangement, through alkene co-ordination and activation (Scheme 1.45). In the palladium-catalyzed Cope rearrangement, Overman proposed that the transfer of stereochemistry from substrate **1.231** to the product **1.232** suggested a mechanism proceeding through a cationic intermediate with similar chair topology to the thermal reaction.²¹⁵ Prior to our investigation, there had only been a one example reported for the catalytic asymmetric Cope rearrangement. This report by Gagne had used

a chiral cationic gold(I) complex to promote the Cope rearrangement.²¹⁶ Thermodynamic driving force for the reaction was provided by the strain release of a cyclopropylidene moiety in **1.233**.

Our group had hypothesized that iminium-activation could be used to lower the activation barrier for the Cope rearrangement (Scheme 1.46). Cope substrates (**1.235**) were designed with an electron-withdrawing formyl group at the 2-position of a cyclohexadiene, to allow the formation of an iminium ion with an amine catalyst. Initial investigation into the iminium-catalyzed Cope rearrangement with known amine catalysts was unsuccessful. Substrate **1.238** showed no reactivity with Macmillan's catalyst, proline, or aniline (Scheme 1.47) due to the significant A-1,3 strain generated with iminium ion formation. Inspired by reports of the increased reactivity of hydrazide catalysts, we screened several and found that the reaction proceeded with cyclic hydrazides, with a correlation between the reactivity of a series of cyclic catalysts (**1.192**, **1.193**, and **1.241**) and the ring size. The 5- and 6-membered ring catalysts **1.192** and **1.193** provided 6% and 28% of product, respectively, in 24 hours. An increased yield of 83% was provided by the 7-membered ring catalyst **1.241**, with complete consumption of starting material. Increasing the ring size by a methylene unit, to give the 8-membered ring catalyst provided product **1.239** in a slightly increased yield (89%). However, the 7-membered ring catalyst **1.241** was viewed as having the best balance between reactivity and accessibility and was thus chosen for further development.^{217 218}

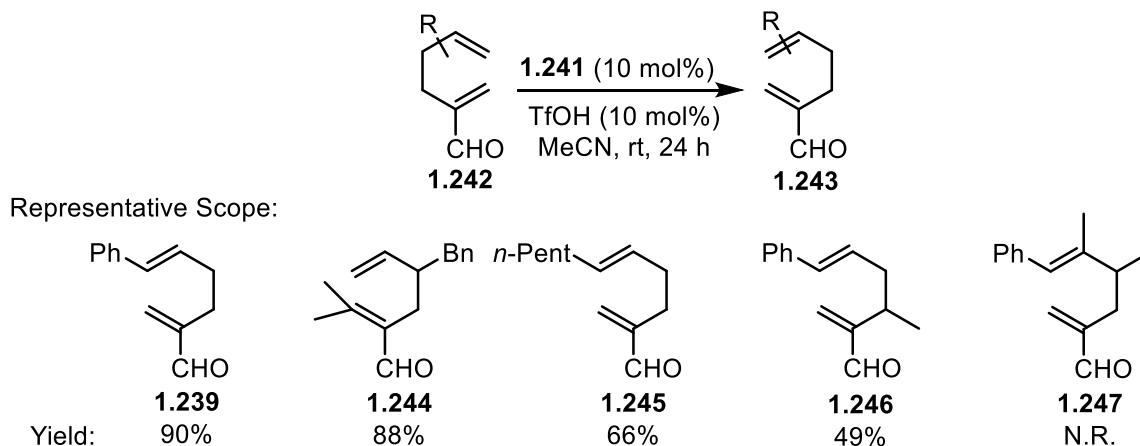


Scheme 1.46. Iminium-catalyzed Cope rearrangement of 1,5-hexadiene, 2-carboxaldehydes.



Scheme 1.47. Catalyst screen for the organocatalytic Cope rearrangement.

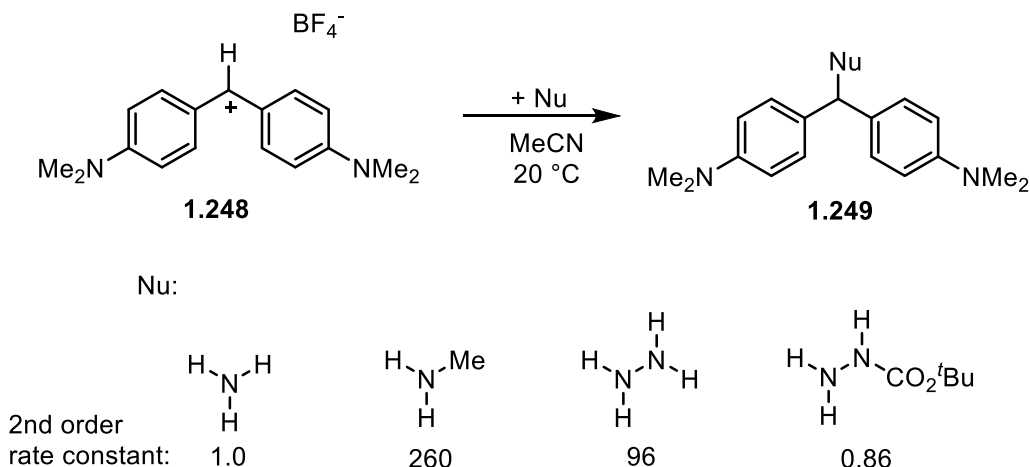
With the 7-membered ring hydrazide catalyst **1.241**, the iminium-catalyzed Cope rearrangement was shown to be successful with substrates that contained both aromatic and aliphatic substitution, where some of the resulting products are shown in Scheme 1.48. Under optimal conditions, substrate **1.238** provided product **1.239** in 90% yield. Aliphatic substitution at either methylene position provided product in good yields (**1.244**, 88% yield and **1.245**, 66% yield). Slightly diminished yields were achieved with β -substituted enals (**1.246**, 49% yield) and no reaction was observed when the olefin was trisubstituted (**1.247**, 0% yield). Following the success in the iminium-catalyzed Cope rearrangement, the 7-membered ring hydrazide catalyst **1.241** was also reported to promote the iminium-catalyzed Michael addition²¹⁹ and Diels-Alder reaction.²²⁰



Scheme 1.48. Iminium-catalyzed Cope rearrangement.

1.7.1 The α -effect in hydrazide catalysts

In initial reports by Tomkinson on the increased reactivity of hydrazide catalysts in the iminium-catalyzed Diels-Alder reaction (Section 1.6.1.2), it was postulated that the increased reactivity is due to the increased nucleophilicity of a heteroatom substituted with an α -heteroatom, known as the α -effect.¹⁸⁹⁻¹⁹⁰ This postulation has been brought under debate by recent work from Mayr on the validity of the α -effect through observations on the second order rate constants of the reaction of amine nucleophiles with benzhydrylium ion **1.248** (Scheme 1.49).²²¹ A higher second order rate constant was observed for the reaction of benzhydrylium ion with hydrazine ($k = 96$) than that for simple ammonia ($k = 1.0$). However, the addition of an alkyl group in methylamine provides an amine nucleophile with an even greater increase in rate constant ($k = 250$). In addition, an electron withdrawing *tert*-butyl carbamate on the hydrazine gives a nucleophile that results in a second order rate constant ($k = 0.86$) which is not significantly different to that of the reaction with simple ammonia. Therefore, hydrazides are not more nucleophilic than secondary amine catalysts and the reasons for their increased reactivity must lie elsewhere.



Scheme 1.49. Comparison of relative second-order rate constants for the reaction amines, hydrazines, and hydrazides with benzhydrylium ion.

1.7.2 Mechanism of the iminium-catalyzed Cope rearrangement

In our investigation into the mechanism of the iminium-catalyzed Cope rearrangement, DFT calculations were performed on a truncated iminium (**1.250**, Figure 1.21) At the M06-2X/6-311G(d,p) level of theory, the (*Z*)-iminium is calculated to be the preferred conformation by 2.6 kcal/mol. Interestingly, these results differ from the favoured iminium conformation observed with other known secondary amine catalysts (as discussed in Section 1.6.1.1). As suggested by the computational model of the lowest energy conformation (**1.250ii**), the N-N bond of the hydrazide catalyst can adopt a twist to more favourably accommodate the A-1,3 strain in the (*Z*)-conformation.

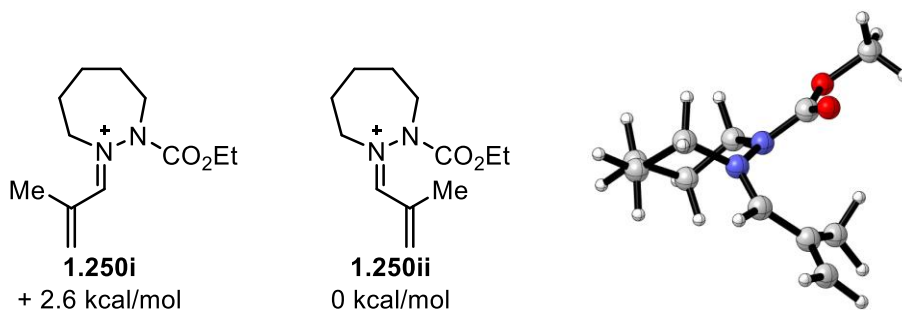
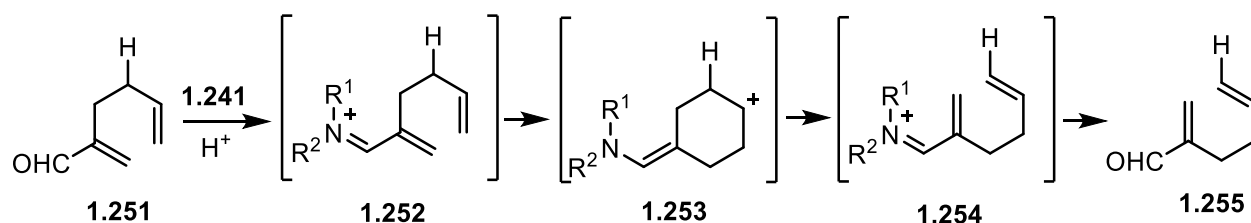


Figure 1.21. Computed energies of the iminium at the M06-2X/6-311G(d,p), SCRF=EtOH level and computational model of **1.250ii**.

Preliminary calculations on the Cope rearrangement of substrate **1.251** suggested that the iminium-catalyzed reaction proceeds through a stepwise mechanism with a shallow energy cyclohexyl cation intermediate (**1.253**, Scheme 1.50). Further computational analysis of the Cope rearrangement of substrate **1.238**, where the formation of product **1.239** conjugates the double bond with the phenyl group, has suggested that this substrate proceeds through a concerted rearrangement.²²² Evidence towards C-C bond formation being the rate-limiting step in this reaction has also been provided by ¹³C kinetic isotope effect (KIE) studies.²²² However, in simple substrates such as **1.251**, results indicated the presence of the cyclohexyl cation as previously observed.



Scheme 1.50. Proposed mechanism of the iminium-catalyzed Cope rearrangement.

1.8 Iminium-catalyzed polyene cyclization

Preliminary calculations at the B3LYP/6-31G(d) level of theory suggested that the cyclohexyl cation intermediate in the iminium-catalyzed Cope rearrangement was a shallow energy minimum (Figure 1.22). The blue pathway corresponding to the reaction of substrate **1.251** with ammonia gave an energy of the intermediate cyclohexyl cation of -0.4 kcal/mol relative to the first transition state. We hypothesized that this cation could be stabilized by the addition of a methyl group. In preliminary calculations on the ammonia catalyzed pathway, the addition of a methyl group (red pathway) stabilized the cation to give an energy for this intermediate of -3.4 kcal/mol relative to the first transition state.²¹⁷

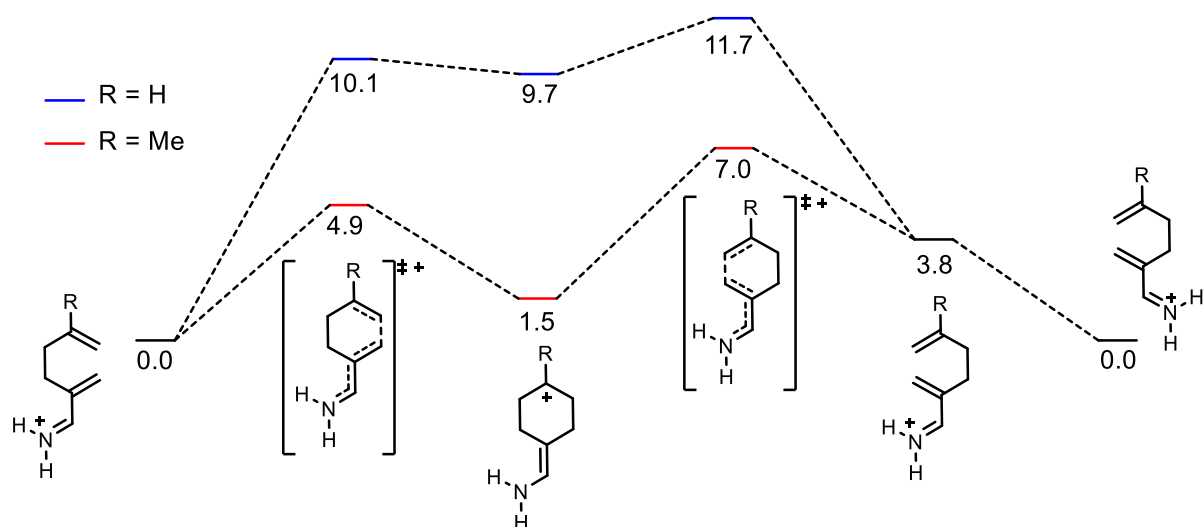
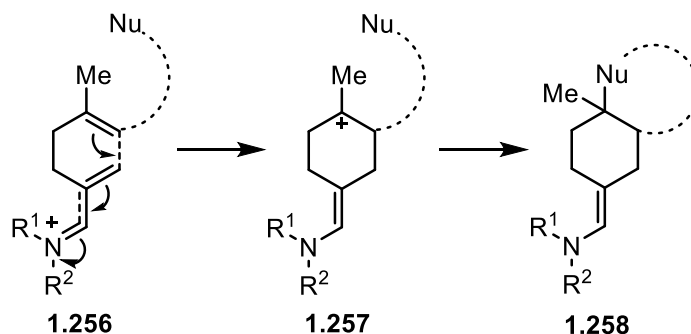


Figure 1.22. Reaction pathway of an iminium-catalyzed Cope rearrangement calculated at the B3LYP/6-31G(d) level of theory. Energies in kcal/mol. (Work done by Prof. James Gleason).

With the evidence of this intermediate cyclohexyl cation, we noted the similarities between the substrates for the Cope rearrangement and the initial ring formation in a polyene cyclization. We hypothesized that with a stabilized cyclohexyl cation intermediate, a cationic cyclization cascade could then proceed in substrates with a tethered nucleophilic aromatic ring to trap the cation. If successful, this would be the first example of an iminium-catalyzed polyene cyclization. Iminium catalysis would provide an initiation approach that is complementary to current methodology and these cyclic hydrazide catalysts could provide a scaffold which, with the incorporation of chiral substitution, has the potential to render the reaction asymmetric.



Scheme 1.51. Proposed iminium-catalyzed polyene cyclization.

In this thesis, we discuss the investigation of the iminium-catalyzed polyene cyclization of (*E*)-polyenes. In Chapter 2 we will discuss our development of the racemic iminium-catalyzed

polyene cyclization. In Chapter 3, we will discuss our initial investigation into the addition of extended aromatics onto the cyclic hydrazide catalyst scaffold, which has resulted in a more reactive catalyst. Finally, in Chapter 4, we will discuss our investigation into the asymmetric reaction with the addition of different aromatic substitution to the cyclic hydrazide catalyst, which has resulted in a highly enantioselective polyene cyclization.

1.9 References

1. Breitmaier, E., Terpenes : flavors, fragrances, pharmaca, pheromones. WILEY-VCH: Weinheim, Germany, 2006.
2. Nicolau, K. C.; Montagnon, T., *Molecules That Changed the World*. Wiley-VCH: 2008.
3. Dewick, P. M., Medicinal natural products : a biosynthetic approach. 2nd ed.; Wiley: West Sussex, England, 2002.
4. Degenhardt, J.; Köllner, T. G.; Gershenzon, J., Monoterpene and sesquiterpene synthases and the origin of terpene skeletal diversity in plants. *Phytochemistry* **2009**, *70* (15-16), 1621-1637.
5. Gershenzon, J.; Dudareva, N., The function of terpene natural products in the natural world. *Nat. Chem. Biol.* **2007**, *3* (7), 408-414.
6. Davis, E. M.; Croteau, R., Cyclization Enzymes in the Biosynthesis of Monoterpenes, Sesquiterpenes, and Diterpenes. Springer Berlin Heidelberg: 2000; pp 53-95.
7. Robinson, R., On the mechanism of the conversion of squalene to sterols. *Chem. Ind. (London)* **1934**, *53*, 1062-1075.
8. Langdon, R. G.; Bloch, K., The Biosynthesis of Squalene. *J. Biol. Chem.* **1953**, *200* (1), 129-134.
9. Little, H. N.; Bloch, K., Studies on the utilization of acetic acid for the biological synthesis of cholesterol. *J. Biol. Chem.* **1950**, *183* (1), 33-46.
10. Woodward, R. B.; Bloch, K., The Cyclization of Squalene in Cholesterol Synthesis. *J. Am. Chem. Soc.* **1953**, *75* (8), 2023-2024.
11. Hibbit, D. C.; Linstead, R. P., 112. Fused carbon rings. Part VII. The preparation of cyclic hydrocarbons from unsaturated tertiary alcohols. The synthesis of cis-9-methyl-octalin and -decalin, and a proof of the presence of the angular methyl group. *J. Chem. Soc. (resumed)* **1936**, 470-476.

12. Linstead, R. P.; Wang, A. B.-L.; Williams, J. H.; Errington, K. D., 239. Fused carbon rings. Part XII. A simple synthesis of derivatives of decalin from cyclohexanone, and observations on cyclo-hexanespirobutyrolactone and allied compounds. *J. Chem. Soc. (resumed)* **1937**, 1136-1140.
13. Stork, G.; Conroy, H., Elaboration of the 1-Substituted 7,8-Dimethoxy-2-tetralones Toward the 13-Alkyl Hydrophenanthrene System of Morphine. *J. Am. Chem. Soc.* **1951**, *73* (10), 4748-4751.
14. Stadler, P. A.; Eschenmoser, A.; Schinz, H.; Stork, G., Untersuchungen über den sterischen Verlauf säurekatalysierter Cyclisationen bei terpenoiden Polyenverbindungen. 3. Mitteilung. Zur Stereochemie der Bicyclofarnesyssäuren. *Helv. Chim. Acta* **1957**, *40* (7), 2191-2198.
15. Yoder, R. A.; Johnston, J. N., A Case Study in Biomimetic Total Synthesis: Polyolefin Carbocyclizations to Terpenes and Steroids. *Chem. Rev.* **2005**, *105* (12), 4730-4756.
16. Kappeler, H.; Stauffacher, D.; Eschenmoser, A.; Schinz, H., Synthese und Cyclisation der 3,7-Dimethyl-octadien-(2,7)-säure-(1) und über eine neue Herstellungsart der 5-Methyl-hexen-(5)-säure-(1). *Helv. Chim. Acta* **1954**, *37* (4), 957-964.
17. Wendt, K. U.; Schulz, G. E.; Corey, E. J.; Liu, D. R., Enzyme Mechanisms for Polycyclic Triterpene Formation. *Angew. Chem. Int. Ed.* **2000**, *39* (16), 2812-2833.
18. Christianson, D. W., Structural Biology and Chemistry of the Terpenoid Cyclases. *Chem. Rev.* **2006**, *106* (8), 3412-3442.
19. Pale-Grosdemange, C.; Feil, C.; Rohmer, M.; Poralla, K., Occurrence of Cationic Intermediates and Deficient Control during the Enzymatic Cyclization of Squalene to Hopanoids. *Angew. Chem. Int. Ed.* **1998**, *37* (16), 2237-2240.
20. Wendt, K. U., Structure and Function of a Squalene Cyclase. *Science* **1997**, *277* (5333), 1811-1815.
21. Thoma, R.; Schulz-Gasch, T.; D'Arcy, B.; Benz, J.; Aebi, J.; Dehmlow, H.; Hennig, M.; Stihle, M.; Ruf, A., Insight into steroid scaffold formation from the structure of human oxidosqualene cyclase. *Nature* **2004**, *432* (7013), 118-122.
22. Feil, C.; Sussmuth, R.; Jung, G.; Poralla, K., Site-Directed Mutagenesis of Putative Active-Site Residues in Squalene-Hopene Cyclase. *Eur. J. Biochem.* **1996**, *242* (1), 51-55.

23. Reinert, D. J.; Balliano, G.; Schulz, G. E., Conversion of Squalene to the Pentacarbocyclic Hopene. *Chem. Biol.* **2004**, *11* (1), 121-126.
24. Berman, H. M.; Westbrook, J.; Feng, Z.; Gilliland, G.; Bhat, T. N.; Weissig, H.; Shindyalov, I. N.; Bourne, P. E., The Protein Data Bank. *Nucleic Acids Res.* **2000**, *28* (1), 235-242.
25. Sehnal, D.; Bittrich, S.; Deshpande, M.; Svobodová, R.; Berka, K.; Bazgier, V.; Velankar, S.; Burley, S. K.; Koča, J.; Rose, A. S., Mol* Viewer: modern web app for 3D visualization and analysis of large biomolecular structures. *Nucleic Acids Res.* **2021**, *49* (W1), W431-W437.
26. Corey, E. J.; Cheng, H.; Baker, C. H.; Matsuda, S. P. T.; Li, D.; Song, X., Studies on the Substrate Binding Segments and Catalytic Action of Lanosterol Synthase. Affinity Labeling with Carbocations Derived from Mechanism-Based Analogs of 2,3-Oxidosqualene and Site-Directed Mutagenesis Probes. *J. Am. Chem. Soc.* **1997**, *119* (6), 1289-1296.
27. Oliaro-Bosso, S.; Schulz-Gasch, T.; Balliano, G.; Viola, F., Access of the Substrate to the Active Site of Yeast Oxidosqualene Cyclase: An Inhibition and Site-Directed Mutagenesis Approach. *ChemBioChem* **2005**, *6* (12), 2221-2228.
28. Takase, S.; Saga, Y.; Kurihara, N.; Naraki, S.; Kuze, K.; Nakata, G.; Araki, T.; Kushiro, T., Control of the 1,2-rearrangement process by oxidosqualene cyclases during triterpene biosynthesis. *Org. Biomol. Chem.* **2015**, *13* (26), 7331-7336.
29. Wu, T.-K.; Wen, H.-Y.; Chang, C.-H.; Liu, Y.-T., Protein Plasticity: A Single Amino Acid Substitution in the *Saccharomyces cerevisiae* Oxidosqualene–Lanosterol Cyclase Generates Protosta-13(17),24-dien-3 β -ol, a Rearrangement Product. *Org. Lett.* **2008**, *10* (12), 2529-2532.
30. Lodeiro, S.; Schulz-Gasch, T.; Matsuda, S. P. T., Enzyme Redesign: Two Mutations Cooperate to Convert Cycloartenol Synthase into an Accurate Lanosterol Synthase. *J. Am. Chem. Soc.* **2005**, *127* (41), 14132-14133.
31. Hoshino, T.; Kouda, M.; Abe, T.; Ohashi, S., New Cyclization Mechanism for Squalene: a Ring-expansion Step for the Five-membered C-ring Intermediate in Hopene Biosynthesis. *Biosci., Biotechnol., Biochem.* **1999**, *63* (11), 2038-2041.
32. Pale-Grosdemange, C.; Merkofer, T.; Rohmer, M.; Poralla, K., Production of bicyclic and tricyclic triterpenes by mutated squalene-hopene cyclase. *Tetrahedron Lett.* **1999**, *40* (33), 6009-6012.

33. Hoshino, T.; Sato, T., Functional analysis of phenylalanine 365 in hopene synthase, a conserved amino acid in the families of squalene and oxidosqualene cyclases†. *Chem. Commun.* **1999**, (19), 2005-2006.
34. Füll, C.; Poralla, K., Conserved Tyr residues determine functions of Alicyclobacillus acidocaldarius squalene–hopene cyclase. *FEMS Microbiol. Lett.* **2000**, *183* (2), 221-224.
35. Sato, T.; Hoshino, T.; Abe, T.; Hoshino, T., On the cyclization mechanism of squalene: a ring expansion process of the five-membered D-ring intermediate. *Chem. Commun.* **1998**, (23), 2617-2618.
36. Merkofer, T.; Pale-Grosdemange, C.; Wendt, K. U.; Rohmer, M.; Poralla, K., Altered product pattern of a squalene-hopene cyclase by mutagenesis of active site residues. *Tetrahedron Lett.* **1999**, *40* (11), 2121-2124.
37. Morikubo, N.; Fukuda, Y.; Ohtake, K.; Shinya, N.; Kiga, D.; Sakamoto, K.; Asanuma, M.; Hirota, H.; Yokoyama, S.; Hoshino, T., Cation– π Interaction in the Polyolefin Cyclization Cascade Uncovered by Incorporating Unnatural Amino Acids into the Catalytic Sites of Squalene Cyclase. *J. Am. Chem. Soc.* **2006**, *128* (40), 13184-13194.
38. Stork, G.; Burgstahler, A. W., The Stereochemistry of Polyene Cyclization. *J. Am. Chem. Soc.* **1955**, *77* (19), 5068-5077.
39. Stadler, P. A.; Nechvatal, A.; Frey, A. J.; Eschenmoser, A., Untersuchungen über den sterischen Verlauf säure-katalysierter Cyclisationen bei terpenoiden Polyenverbindungen. 1. Mitteilung. Cyclisation der 7,11-Dimethyl-2(trans), 6(trans), 10-dodecatrien-und der 7, 11-Dimethyl-2(cis), 6(trans), 10-dodecatrien-säure. *Helv. Chim. Acta* **1957**, *40* (5), 1373-1409.
40. Hoshino, T.; Sato, T., Squalene–hopene cyclase: catalytic mechanism and substrate recognition. *Chem. Commun.* **2002**, (4), 291-301.
41. Dougherty, D. A., The Cation– π Interaction. *Acc. Chem. Res.* **2013**, *46* (4), 885-893.
42. Mahadevi, A. S.; Sastry, G. N., Cation– π Interaction: Its Role and Relevance in Chemistry, Biology, and Material Science. *Chem. Rev.* **2013**, *113* (3), 2100-2138.
43. Sunner, J.; Nishizawa, K.; Kebarle, P., Ion-solvent molecule interactions in the gas phase. The potassium ion and benzene. *J. Phys. Chem.* **1981**, *85* (13), 1814-1820.
44. Meot-Ner, M.; Deakyne, C. A., Unconventional ionic hydrogen bonds. 2. $\text{NH}^+\cdots\text{C}\equiv\text{C}\cdots\text{N}^+$. Complexes of onium ions with olefins and benzene derivatives. *J. Am. Chem. Soc.* **1985**, *107* (2), 474-479.

45. Stauffer, D. A.; Barrans Jr, R. E.; Dougherty, D. A., Biomimetic Catalysis of an SN₂ Reaction Resulting from a Novel Form of Transition-State Stabilization. *Angew. Chem., Int. Ed. Engl.* **1990**, *29* (8), 915-918.
46. Petti, M. A.; Shepodd, T. J.; Dougherty, D. A., Design and synthesis of a new class of hydrophobic binding sites. *Tetrahedron Lett.* **1986**, *27* (7), 807-810.
47. Shepodd, T. J.; Petti, M. A.; Dougherty, D. A., Tight, oriented binding of an aliphatic guest by a new class of water-soluble molecules with hydrophobic binding sites. *J. Am. Chem. Soc.* **1986**, *108* (19), 6085-6087.
48. Kearney, P. C.; Mizoue, L. S.; Kumpf, R. A.; Forman, J. E.; McCurdy, A.; Dougherty, D. A., Molecular recognition in aqueous media. New binding studies provide further insights into the cation- π interaction and related phenomena. *J. Am. Chem. Soc.* **1993**, *115* (22), 9907-9919.
49. Mecozzi, S.; West, A. P.; Dougherty, D. A., Cation- π interactions in aromatics of biological and medicinal interest: electrostatic potential surfaces as a useful qualitative guide. *PNAS* **1996**, *93* (20), 10566-10571.
50. Mecozzi, S.; West, A. P.; Dougherty, D. A., Cation- π Interactions in Simple Aromatics: Electrostatics Provide a Predictive Tool. *J. Am. Chem. Soc.* **1996**, *118* (9), 2307-2308.
51. Ma, J. C.; Dougherty, D. A., The Cation- π Interaction. *Chem. Rev.* **1997**, *97* (5), 1303-1324.
52. Vijay, D.; Sastry, G. N., Exploring the size dependence of cyclic and acyclic π -systems on cation- π binding. *Phys. Chem. Chem. Phys.* **2008**, *10* (4), 582-590.
53. Gal, J.-F.; Maria, P.-C.; Decouzon, M.; M \acute{o} , O.; Y \acute{a} ñez, M.; Abboud, J. L. M., Lithium-Cation/ π Complexes of Aromatic Systems. The Effect of Increasing the Number of Fused Rings. *J. Am. Chem. Soc.* **2003**, *125* (34), 10394-10401.
54. Hunter, C. A.; Low, C. M. R.; Rotger, C.; Vinter, J. G.; Zonta, C., Substituent effects on cation- interactions: A quantitative study. *PNAS* **2002**, *99* (8), 4873-4876.
55. Raju, R. K.; Bloom, J. W. G.; An, Y.; Wheeler, S. E., Substituent Effects on Non-Covalent Interactions with Aromatic Rings: Insights from Computational Chemistry. *ChemPhysChem* **2011**, *12* (17), 3116-3130.

56. Wheeler, S. E.; Houk, K. N., Substituent Effects in Cation/ π Interactions and Electrostatic Potentials above the Centers of Substituted Benzenes Are Due Primarily to Through-Space Effects of the Substituents. *J. Am. Chem. Soc.* **2009**, *131* (9), 3126-3127.
57. Hunter, C. A.; Sanders, J. K. M., The nature of π - π interactions. *J. Am. Chem. Soc.* **1990**, *112* (14), 5525-5534.
58. Tsuzuki, S.; Fujii, A., Nature and physical origin of CH/ π interaction: significant difference from conventional hydrogen bonds. *Phys. Chem. Chem. Phys.* **2008**, *10* (19), 2584.
59. Estarellas, C.; Bauzá, A.; Frontera, A.; Quiñonero, D.; Deyà, P. M., On the directionality of anion- π interactions. *Phys. Chem. Chem. Phys.* **2011**, *13* (13), 5696.
60. Schwabacher, A. W.; Zhang, S.; Davy, W., Directionality of the cation- π effect: a charge-mediated size selectivity in binding. *J. Am. Chem. Soc.* **1993**, *115* (15), 6995-6996.
61. Marshall, M. S.; Steele, R. P.; Thanthiriwatte, K. S.; Sherrill, C. D., Potential Energy Curves for Cation- π Interactions: Off-Axis Configurations Are Also Attractive. *J. Phys. Chem. A* **2009**, *113* (48), 13628-13632.
62. Acharya, P.; Plashkevych, O.; Morita, C.; Yamada, S.; Chattopadhyaya, J., A Repertoire of Pyridinium-Phenyl-Methyl Cross-Talk through a Cascade of Intramolecular Electrostatic Interactions. *J. Org. Chem.* **2003**, *68* (4), 1529-1538.
63. Yamada, S.; Yamamoto, N.; Takamori, E., A Molecular Seesaw Balance: Evaluation of Solvent and Counteranion Effects on Pyridinium- π Interactions. *Org. Lett* **2015**, *17* (19), 4862-4865.
64. Yamada, S.; Yamamoto, N.; Takamori, E., Synthesis of Molecular Seesaw Balances and the Evaluation of Pyridinium- π Interactions. *J. Org. Chem.* **2016**, *81* (23), 11819-11830.
65. Hunter, C. A.; Low, C. M. R.; Vinter, J. G.; Zonta, C., Quantification of Functional Group Interactions in Transition States. *J. Am. Chem. Soc.* **2003**, *125* (33), 9936-9937.
66. Li, P.; Zhao, C.; Smith, M. D.; Shimizu, K. D., Comprehensive Experimental Study of N-Heterocyclic π -Stacking Interactions of Neutral and Cationic Pyridines. *J. Org. Chem.* **2013**, *78* (11), 5303-5313.
67. Rashkin, M. J.; Hughes, R. M.; Calloway, N. T.; Waters, M. L., Orientation and Alkylation Effects on Cation- π Interactions in Aqueous Solution. *J. Am. Chem. Soc.* **2004**, *126* (41), 13320-13325.

68. Gung, B. W.; Wekesa, F.; Barnes, C. L., Stacking Interactions between Nitrogen-Containing Six-Membered Heterocyclic Aromatic Rings and Substituted Benzene: Studies in Solution and in the Solid State. *J. Org. Chem.* **2008**, *73* (5), 1803-1808.
69. Ting, A. Y.; Shin, I.; Lucero, C.; Schultz, P. G., Energetic Analysis of an Engineered Cation- π Interaction in Staphylococcal Nuclease. *J. Am. Chem. Soc.* **1998**, *120* (28), 7135-7136.
70. Salonen, L. M.; Bucher, C.; Banner, D. W.; Haap, W.; Mary, J.-L.; Benz, J.; Kuster, O.; Seiler, P.; Schweizer, W. B.; Diederich, F., Cation- π Interactions at the Active Site of Factor Xa: Dramatic Enhancement upon Stepwise N-Alkylation of Ammonium Ions. *Angew. Chem. Int. Ed.* **2009**, *48* (4), 811-814.
71. Kennedy, C. R.; Lin, S.; Jacobsen, E. N., The Cation- π Interaction in Small-Molecule Catalysis. *Angew. Chem. Int. Ed.* **2016**, *55* (41), 12596-12624.
72. Yamada, S., Cation- π Interactions in Organic Synthesis. *Chem. Rev.* **2018**, *118* (23), 11353-11432.
73. Gutierrez, O.; Aubé, J.; Tantillo, D. J., Mechanism of the Acid-Promoted Intramolecular Schmidt Reaction: Theoretical Assessment of the Importance of Lone Pair-Cation, Cation- π , and Steric Effects in Controlling Regioselectivity. *J. Org. Chem.* **2012**, *77* (1), 640-647.
74. Yao, L.; Aubé, J., Cation- π Control of Regiochemistry of Intramolecular Schmidt Reactions en Route to Bridged Bicyclic Lactams. *J. Am. Chem. Soc.* **2007**, *129* (10), 2766-2767.
75. Stark, C. B. W.; Eggert, U.; Hoffmann, H. M. R., Chiral Allyl Cations in Cycloadditions to Furan: Synthesis of 2-(1'-Phenylethoxy)-8-oxabicyclo[3.2.1]oct-6-en-3-one in High Enantiomeric Purity. *Angew. Chem. Int. Ed.* **1998**, *37* (9), 1266-1268.
76. Krenske, E. H.; Houk, K. N.; Harmata, M., Origin of Stereoselectivity in the (4 + 3) Cycloadditions of Chiral Alkoxy Siloxyallyl Cations with Furan. *Org. Lett.* **2010**, *12* (3), 444-447.
77. Uyeda, C.; Jacobsen, E. N., Transition-State Charge Stabilization through Multiple Non-covalent Interactions in the Guanidinium-Catalyzed Enantioselective Claisen Rearrangement. *J. Am. Chem. Soc.* **2011**, *133* (13), 5062-5075.
78. Ahrendt, K. A.; Borths, C. J.; Macmillan, D. W. C., New Strategies for Organic Catalysis: The First Highly Enantioselective Organocatalytic Diels-Alder Reaction. *J. Am. Chem. Soc.* **2000**, *122* (17), 4243-4244.

79. Paras, N. A.; Macmillan, D. W. C., New Strategies in Organic Catalysis: The First Enantioselective Organocatalytic Friedel–Crafts Alkylation. *J. Am. Chem. Soc.* **2001**, *123* (18), 4370-4371.
80. Allemann, C.; Gordillo, R.; Clemente, F. R.; Cheong, P. H.-Y.; Houk, K. N., Theory of Asymmetric Organocatalysis of Aldol and Related Reactions: Rationalizations and Predictions. *Acc. Chem. Res.* **2004**, *37* (8), 558-569.
81. Gordillo, R.; Houk, K. N., Origins of Stereoselectivity in Diels–Alder Cycloadditions Catalyzed by Chiral Imidazolidinones. *J. Am. Chem. Soc.* **2006**, *128* (11), 3543-3553.
82. Holland, M. C.; Metternich, J. B.; Daniliuc, C.; Schweizer, W. B.; Gilmour, R., Aromatic Interactions in Organocatalyst Design: Augmenting Selectivity Reversal in Iminium Ion Activation. *Chem. Eur. J.* **2015**, *21* (28), 10031-10038.
83. Holland, M. C.; Metternich, J. B.; Mück-Lichtenfeld, C.; Gilmour, R., Cation– π interactions in iminium ion activation: correlating quadrupole moment & enantioselectivity. *Chem. Commun.* **2015**, *51* (25), 5322-5325.
84. Holland, M. C.; Paul, S.; Schweizer, W. B.; Bergander, K.; Mück-Lichtenfeld, C.; Lakhdar, S.; Mayr, H.; Gilmour, R., Noncovalent Interactions in Organocatalysis: Modulating Conformational Diversity and Reactivity in the MacMillan Catalyst. *Angew. Chem. Int. Ed.* **2013**, *52* (31), 7967-7971.
85. McCurdy, A.; Jimenez, L.; Stauffer, D. A.; Dougherty, D. A., Biomimetic catalysis of SN2 reactions through cation- π interactions. The role of polarizability in catalysis. *J. Am. Chem. Soc.* **1992**, *114* (26), 10314-10321.
86. Caulder, D. L.; Brückner, C.; Powers, R. E.; König, S.; Parac, T. N.; Leary, J. A.; Raymond, K. N., Design, Formation and Properties of Tetrahedral M4L4 and M4L6 Supramolecular Clusters. *J. Am. Chem. Soc.* **2001**, *123* (37), 8923-8938.
87. Davis, A. V.; Raymond, K. N., The Big Squeeze: Guest Exchange in an M4L6 Supramolecular Host. *J. Am. Chem. Soc.* **2005**, *127* (21), 7912-7919.
88. Fiedler, D.; Leung, D. H.; Bergman, R. G.; Raymond, K. N., Enantioselective Guest Binding and Dynamic Resolution of Cationic Ruthenium Complexes by a Chiral Metal–Ligand Assembly. *J. Am. Chem. Soc.* **2004**, *126* (12), 3674-3675.
89. Ziegler, M.; Brumaghim, J. L.; Raymond, K. N., Stabilization of a Reactive Cationic Species by Supramolecular Encapsulation. *Angew. Chem. Int. Ed.* **2000**, *39* (22), 4119-4121.

90. Pluth, M. D.; Johnson, D. W.; Szigethy, G.; Davis, A. V.; Teat, S. J.; Oliver, A. G.; Bergman, R. G.; Raymond, K. N., Structural Consequences of Anionic Host–Cationic Guest Interactions in a Supramolecular Assembly. *Inorg. Chem.* **2009**, *48* (1), 111-120.
91. Pluth, M. D.; Bergman, R. G.; Raymond, K. N., Acid Catalysis in Basic Solution: A Supramolecular Host Promotes Orthoformate Hydrolysis. *Science* **2007**, *316* (5821), 85-88.
92. Pluth, M. D.; Bergman, R. G.; Raymond, K. N., Supramolecular Catalysis of Orthoformate Hydrolysis in Basic Solution: An Enzyme-Like Mechanism. *J. Am. Chem. Soc.* **2008**, *130* (34), 11423-11429.
93. Pluth, M. D.; Bergman, R. G.; Raymond, K. N., Catalytic Deprotection of Acetals in Basic Solution with a Self-Assembled Supramolecular “Nanozyme”. *Angew. Chem. Int. Ed.* **2007**, *46* (45), 8587-8589.
94. Pluth, M. D.; Bergman, R. G.; Raymond, K. N., The Acid Hydrolysis Mechanism of Acetals Catalyzed by a Supramolecular Assembly in Basic Solution. *J. Org. Chem.* **2009**, *74* (1), 58-63.
95. Fiedler, D.; Bergman, R. G.; Raymond, K. N., Supramolecular Catalysis of a Unimolecular Transformation: Aza-Cope Rearrangement within a Self-Assembled Host. *Angew. Chem. Int. Ed.* **2004**, *43* (48), 6748-6751.
96. Hastings, C. J.; Pluth, M. D.; Bergman, R. G.; Raymond, K. N., Enzymelike Catalysis of the Nazarov Cyclization by Supramolecular Encapsulation. *J. Am. Chem. Soc.* **2010**, *132* (20), 6938-6940.
97. Hart-Cooper, W. M.; Clary, K. N.; Toste, F. D.; Bergman, R. G.; Raymond, K. N., Selective Monoterpene-like Cyclization Reactions Achieved by Water Exclusion from Reactive Intermediates in a Supramolecular Catalyst. *J. Am. Chem. Soc.* **2012**, *134* (43), 17873-17876.
98. Hart-Cooper, W. M.; Zhao, C.; Triano, R. M.; Yaghoubi, P.; Ozoires, H. L.; Burford, K. N.; Toste, F. D.; Bergman, R. G.; Raymond, K. N., The effect of host structure on the selectivity and mechanism of supramolecular catalysis of Prins cyclizations. *Chem. Sci.* **2015**, *6* (2), 1383-1393.
99. Macgillivray, L. R.; Atwood, J. L., A chiral spherical molecular assembly held together by 60 hydrogen bonds. *Nature* **1997**, *389* (6650), 469-472.
100. Avram, L.; Cohen, Y., The Role of Water Molecules in a Resorcinarene Capsule As Probed by NMR Diffusion Measurements. *Org. Lett.* **2002**, *4* (24), 4365-4368.

101. Yamanaka, M.; Shivanyuk, A.; Rebek, J., Kinetics and Thermodynamics of Hexameric Capsule Formation. *J. Am. Chem. Soc.* **2004**, *126* (9), 2939-2943.
102. Shivanyuk, A.; Rebek, J., Reversible encapsulation by self-assembling resorcinarene subunits. *PNAS* **2001**, *98* (14), 7662-7665.
103. Zhang, Q.; Tiefenbacher, K., Hexameric Resorcinarene Capsule is a Brønsted Acid: Investigation and Application to Synthesis and Catalysis. *J. Am. Chem. Soc.* **2013**, *135* (43), 16213-16219.
104. Zhang, Q.; Tiefenbacher, K., Terpene cyclization catalysed inside a self-assembled cavity. *Nat. Chem.* **2015**, *7* (3), 197-202.
105. Zhang, Q.; Catti, L.; Pleiss, J.; Tiefenbacher, K., Terpene Cyclizations inside a Supramolecular Catalyst: Leaving-Group-Controlled Product Selectivity and Mechanistic Studies. *J. Am. Chem. Soc.* **2017**, *139* (33), 11482-11492.
106. Zhang, Q.; Tiefenbacher, K., Sesquiterpene Cyclizations inside the Hexameric Resorcinarene Capsule: Total Synthesis of δ -Selinene and Mechanistic Studies. *Angew. Chem. Int. Ed.* **2019**, *58* (36), 12688-12695.
107. Catti, L.; Tiefenbacher, K., Brønsted Acid-Catalyzed Carbonyl-Olefin Metathesis inside a Self-Assembled Supramolecular Host. *Angew. Chem. Int. Ed.* **2018**, *57* (44), 14589-14592.
108. Catti, L.; Tiefenbacher, K., Intramolecular hydroalkoxylation catalyzed inside a self-assembled cavity of an enzyme-like host structure. *Chem. Commun.* **2015**, *51* (5), 892-894.
109. Bräuer, T. M.; Zhang, Q.; Tiefenbacher, K., Iminium Catalysis inside a Self-Assembled Supramolecular Capsule: Modulation of Enantiomeric Excess. *Angew. Chem. Int. Ed.* **2016**, *55* (27), 7698-7701.
110. Lin, S.; Jacobsen, E. N., Thiourea-catalysed ring opening of episulfonium ions with indole derivatives by means of stabilizing non-covalent interactions. *Nat. Chem.* **2012**, *4* (10), 817-824.
111. Yeung, C. S.; Ziegler, R. E.; Porco, J. A.; Jacobsen, E. N., Thiourea-Catalyzed Enantioselective Addition of Indoles to Pyrones: Alkaloid Cores with Quaternary Carbons. *J. Am. Chem. Soc.* **2014**, *136* (39), 13614-13617.
112. Birrell, J. A.; Desrosiers, J.-N.; Jacobsen, E. N., Enantioselective Acylation of Silyl Ketene Acetals through Fluoride Anion-Binding Catalysis. *J. Am. Chem. Soc.* **2011**, *133* (35), 13872-13875.

113. Brown, A. R.; Uyeda, C.; Brotherton, C. A.; Jacobsen, E. N., Enantioselective Thiourea-Catalyzed Intramolecular Cope-Type Hydroamination. *J. Am. Chem. Soc.* **2013**, *135* (18), 6747-6749.
114. Kutateladze, D. A.; Strassfeld, D. A.; Jacobsen, E. N., Enantioselective Tail-to-Head Cyclizations Catalyzed by Dual-Hydrogen-Bond Donors. *J. Am. Chem. Soc.* **2020**, *142* (15), 6951-6956.
115. Dijkink, J.; Speckamp, W. N., Simultaneous and stereospecific formation of two C • C bonds via α -acylimmonium cyclisation. *Tetrahedron Lett.* **1977**, *18* (11), 935-938.
116. Knowles, R. R.; Lin, S.; Jacobsen, E. N., Enantioselective Thiourea-Catalyzed Cationic Polycyclizations. *J. Am. Chem. Soc.* **2010**, *132* (14), 5030-5032.
117. Fan, L.; Han, C.; Li, X.; Yao, J.; Wang, Z.; Yao, C.; Chen, W.; Wang, T.; Zhao, J., Enantioselective Polyene Cyclization Catalyzed by a Chiral Brønsted Acid. *Angew. Chem. Int. Ed.* **2018**, *57* (8), 2115-2119.
118. Samanta, R. C.; Yamamoto, H., Catalytic Asymmetric Bromocyclization of Polyenes. *J. Am. Chem. Soc.* **2017**, *139* (4), 1460-1463.
119. Johnson, W. S.; Crandall, J. K., Olefinic Cyclizations. VII. Formolysis of cis- and trans-5,9-Decadienyl p-Nitrobenzenesulfonate and of Some Isomeric Monocyclic Esters*,1,2. *J. Org. Chem.* **1965**, *30* (6), 1785-1790.
120. Johnson, W. S.; Van Der Gen, A.; Swoboda, J. J., New Structural and Stereochemical Aspects of the Cyclization of Olefinic Acetals. *J. Am. Chem. Soc.* **1967**, *89* (1), 170-172.
121. Johnson, W. S.; Semmelhack, M. F.; Sultanbawa, M. U. S.; Dolak, L. A., A new approach to steroid total synthesis. A nonenzymic biogenetic-like olefinic cyclization involving the stereospecific formation of five asymmetric centers. *J. Am. Chem. Soc.* **1968**, *90* (11), 2994-2996.
122. Van Tamelen, E. E.; Seiler, M. P.; Wierenga, W., Biogenetic-type total synthesis. .delta.-Amyrin, .beta.-amyrin, and germanicol. *J. Am. Chem. Soc.* **1972**, *94* (23), 8229-8231.
123. Johnson, W. S.; Brinkmeyer, R. S.; Kapoor, V. M.; Yarnell, T. M., Asymmetric total synthesis of 11.alpha.-hydroxyprogesterone via a biomimetic polyene cyclization. *J. Am. Chem. Soc.* **1977**, *99* (25), 8341-8343.
124. Ishihara, K.; Nakamura, S.; Yamamoto, H., The First Enantioselective Biomimetic Cyclization of Polyprenoids. *J. Am. Chem. Soc.* **1999**, *121* (20), 4906-4907.

125. Schmid, R.; Huesmann, P. L.; Johnson, W. S., Propargylsilane function as a terminator of biomimetic polyene cyclizations leading to steroids. *J. Am. Chem. Soc.* **1980**, *102* (15), 5122-5123.
126. Corey, E. J.; Lin, S., A Short Enantioselective Total Synthesis of Dammarenediol II. *J. Am. Chem. Soc.* **1996**, *118* (36), 8765-8766.
127. Johnson, W. S.; Kinnel, R. B., Stereospecific Tricyclization of a Polyolefinic Acetal. *J. Am. Chem. Soc.* **1966**, *88* (16), 3861-3862.
128. Johnson, W. S.; Telfer, S. J.; Cheng, S.; Schubert, U., Cation-stabilizing auxiliaries: a new concept in biomimetic polyene cyclization. *J. Am. Chem. Soc.* **1987**, *109* (8), 2517-2518.
129. Johnson, W. S.; Chenera, B.; Tham, F. S.; Kullnig, R. K., Cation-stabilizing auxiliaries in polyene cyclizations. 4. The fluorine atom as a cation-stabilizing auxiliary in biomimetic polyene cyclizations. 1. Background and exploratory experiments. *J. Am. Chem. Soc.* **1993**, *115* (2), 493-497.
130. Johnson, W. S.; Harbert, C. A.; Stipanovic, R. D., Asymmetric induction of an olefinic acetal cyclization. *J. Am. Chem. Soc.* **1968**, *90* (19), 5279-5280.
131. Johnson, W. S.; Elliott, J. D.; Hanson, G., Asymmetric synthesis via acetal templates. 6. A stereoselective approach to a key intermediate for the preparation of vitamin D metabolites. *J. Am. Chem. Soc.* **1984**, *106* (4), 1138-1139.
132. Zhao, Y.-J.; Chng, S.-S.; Loh, T.-P., Lewis Acid-Promoted Intermolecular Acetal-Initiated Cationic Polyene Cyclizations. *J. Am. Chem. Soc.* **2007**, *129* (3), 492-493.
133. Ishibashi, H.; Ishihara, K.; Yamamoto, H., A New Artificial Cyclase for Polyrenoids: Enantioselective Total Synthesis of (-)-Chromazonarol, (+)-8-epi-Puupehedione, and (-)-11'-Deoxytaondiol Methyl Ether. *J. Am. Chem. Soc.* **2004**, *126* (36), 11122-11123.
134. Kumazawa, K.; Ishihara, K.; Yamamoto, H., Tin(IV) Chloride-Chiral Pyrogallol Derivatives as New Lewis Acid-Assisted Chiral Brønsted Acids for Enantioselective Polyene Cyclization. *Org. Lett* **2004**, *6* (15), 2551-2554.
135. Surendra, K.; Corey, E. J., Highly Enantioselective Proton-Initiated Polycyclization of Polyenes. *J. Am. Chem. Soc.* **2012**, *134* (29), 11992-11994.
136. Nishizawa, M.; Takenaka, H.; Hirotsu, K.; Higuchi, T.; Hayashi, Y., Synthesis and structure determination of isoaplysin-20. *J. Am. Chem. Soc.* **1984**, *106* (15), 4290-4291.

137. Snyder, S. A.; Treitler, D. S.; Schall, A., A two-step mimic for direct, asymmetric bromonium- and chloronium-induced polyene cyclizations. *Tetrahedron* **2010**, *66* (26), 4796-4804.
138. Mullen, C. A.; Campbell, A. N.; Gagné, M. R., Asymmetric Oxidative Cation/Olefin Cyclization of Polyenes: Evidence for Reversible Cascade Cyclization. *Angew. Chem. Int. Ed.* **2008**, *47* (32), 6011-6014.
139. Sethofer, S. G.; Mayer, T.; Toste, F. D., Gold(I)-Catalyzed Enantioselective Polycyclization Reactions. *J. Am. Chem. Soc.* **2010**, *132* (24), 8276-8277.
140. Schafroth, M. A.; Sarlah, D.; Krautwald, S.; Carreira, E. M., Iridium-Catalyzed Enantioselective Polyene Cyclization. *J. Am. Chem. Soc.* **2012**, *134* (50), 20276-20278.
141. Sakakura, A.; Sakuma, M.; Ishihara, K., Chiral Lewis Base-Assisted Brønsted Acid (LBBA)-Catalyzed Enantioselective Cyclization of 2-Geranylphenols. *Org. Lett* **2011**, *13* (12), 3130-3133.
142. Barluenga, J.; Trincado, M.; Rubio, E.; González, J. M., Intramolecular Arylation Reactions of Alkenes: A Flexible Approach to Chromans and Tetrahydroquinoline Derivatives. *J. Am. Chem. Soc.* **2004**, *126* (11), 3416-3417.
143. Snyder, S. A.; Treitler, D. S.; Brucks, A. P., Simple Reagents for Direct Halonium-Induced Polyene Cyclizations. *J. Am. Chem. Soc.* **2010**, *132* (40), 14303-14314.
144. Snyder, S. A.; Treitler, D. S., Et₂SBr·SbCl₅Br: An Effective Reagent for Direct Bromonium-Induced Polyene Cyclizations. *Angew. Chem. Int. Ed.* **2009**, *48* (42), 7899-7903.
145. Sakakura, A.; Ukai, A.; Ishihara, K., Enantioselective halocyclization of polyprenoids induced by nucleophilic phosphoramidites. *Nature* **2007**, *445* (7130), 900-903.
146. Tao, Z.; Robb, K. A.; Zhao, K.; Denmark, S. E., Enantioselective, Lewis Base-Catalyzed Sulfenocyclization of Polyenes. *J. Am. Chem. Soc.* **2018**, *140* (10), 3569-3573.
147. Rendler, S.; Macmillan, D. W. C., Enantioselective Polyene Cyclization via Organo-SOMO Catalysis. *J. Am. Chem. Soc.* **2010**, *132* (14), 5027-5029.
148. Hajos, Z. G.; Parrish, D. R., Asymmetric synthesis of bicyclic intermediates of natural product chemistry. *J. Org. Chem.* **1974**, *39* (12), 1615-1621.
149. Eder, U.; Sauer, G.; Wiechert, R., New Type of Asymmetric Cyclization to Optically Active Steroid CD Partial Structures. *Angew. Chem., Int. Ed. Engl.* **1971**, *10* (7), 496-497.

150. Tu, Y.; Wang, Z.-X.; Shi, Y., An Efficient Asymmetric Epoxidation Method for trans-Olefins Mediated by a Fructose-Derived Ketone. *J. Am. Chem. Soc.* **1996**, *118* (40), 9806-9807.
151. Denmark, S. E.; Wu, Z.; Crudden, C. M.; Matsushashi, H., Catalytic Epoxidation of Alkenes with Oxone. 2. Fluoro Ketones. *J. Org. Chem.* **1997**, *62* (24), 8288-8289.
152. Yang, D.; Yip, Y.-C.; Tang, M.-W.; Wong, M.-K.; Zheng, J.-H.; Cheung, K.-K., A C2 Symmetric Chiral Ketone for Catalytic Asymmetric Epoxidation of Unfunctionalized Olefins. *J. Am. Chem. Soc.* **1996**, *118* (2), 491-492.
153. Sigman, M. S.; Jacobsen, E. N., Schiff Base Catalysts for the Asymmetric Strecker Reaction Identified and Optimized from Parallel Synthetic Libraries. *J. Am. Chem. Soc.* **1998**, *120* (19), 4901-4902.
154. Corey, E. J.; Grogan, M. J., Enantioselective Synthesis of α -Amino Nitriles from N-Benzhydryl Imines and HCN with a Chiral Bicyclic Guanidine as Catalyst. *Org. Lett* **1999**, *1* (1), 157-160.
155. Miller, S. J.; Copeland, G. T.; Papaioannou, N.; Horstmann, T. E.; Ruel, E. M., Kinetic Resolution of Alcohols Catalyzed by Tripeptides Containing the N-Alkylimidazole Substructure. *J. Am. Chem. Soc.* **1998**, *120* (7), 1629-1630.
156. List, B.; Lerner, R. A.; Barbas, C. F., Proline-Catalyzed Direct Asymmetric Aldol Reactions. *J. Am. Chem. Soc.* **2000**, *122* (10), 2395-2396.
157. Bertelsen, S.; Marigo, M.; Brandes, S.; Dinér, P.; Jørgensen, K. A., Dienamine Catalysis: Organocatalytic Asymmetric γ -Amination of α,β -Unsaturated Aldehydes. *J. Am. Chem. Soc.* **2006**, *128* (39), 12973-12980.
158. Vignola, N.; List, B., Catalytic Asymmetric Intramolecular α -Alkylation of Aldehydes. *J. Am. Chem. Soc.* **2004**, *126* (2), 450-451.
159. List, B., The Direct Catalytic Asymmetric Three-Component Mannich Reaction. *J. Am. Chem. Soc.* **2000**, *122* (38), 9336-9337.
160. Hechavarria Fonseca, M. T.; List, B., Catalytic Asymmetric Intramolecular Michael Reaction of Aldehydes. *Angew. Chem. Int. Ed.* **2004**, *43* (30), 3958-3960.
161. Bøgevig, A.; Juhl, K.; Kumaragurubaran, N.; Zhuang, W.; Jørgensen, K. A., Direct Organo-Catalytic Asymmetric α -Amination of Aldehydes—A Simple Approach to Optically Active α -Amino Aldehydes, α -Amino Alcohols, and α -Amino Acids. *Angew. Chem. Int. Ed.* **2002**, *41* (10), 1790-1793.

162. List, B., Direct Catalytic Asymmetric α -Amination of Aldehydes. *J. Am. Chem. Soc.* **2002**, *124* (20), 5656-5657.
163. Zhong, G., A Facile and Rapid Route to Highly Enantiopure 1,2-Diols by Novel Catalytic Asymmetric α -Aminoxylation of Aldehydes. *Angew. Chem. Int. Ed.* **2003**, *42* (35), 4247-4250.
164. Brown, S. P.; Brochu, M. P.; Sinz, C. J.; Macmillan, D. W. C., The Direct and Enantioselective Organocatalytic α -Oxidation of Aldehydes. *J. Am. Chem. Soc.* **2003**, *125* (36), 10808-10809.
165. Hayashi, Y.; Yamaguchi, J.; Hibino, K.; Shoji, M., Direct proline catalyzed asymmetric α -aminoxylation of aldehydes. *Tetrahedron Lett.* **2003**, *44* (45), 8293-8296.
166. Enders, D.; Hüttl, M. R. M., Direct Organocatalytic α -Fluorination of Aldehydes and Ketones. *Synlett* **2005**, *2005* (06), 0991-0993.
167. Brochu, M. P.; Brown, S. P.; Macmillan, D. W. C., Direct and Enantioselective Organocatalytic α -Chlorination of Aldehydes. *J. Am. Chem. Soc.* **2004**, *126* (13), 4108-4109.
168. Halland, N.; Braunton, A.; Bachmann, S.; Marigo, M.; Jørgensen, K. A., Direct Organocatalytic Asymmetric α -Chlorination of Aldehydes. *J. Am. Chem. Soc.* **2004**, *126* (15), 4790-4791.
169. Bertelsen, S.; Halland, N.; Bachmann, S.; Marigo, M.; Braunton, A.; Jørgensen, K. A., Organocatalytic asymmetric α -bromination of aldehydes and ketones. *Chem. Commun.* **2005**, (38), 4821.
170. Marigo, M.; Wabnitz, T. C.; Fielenbach, D.; Jørgensen, K. A., Enantioselective Organocatalyzed α Sulfenylation of Aldehydes. *Angew. Chem. Int. Ed.* **2005**, *44* (5), 794-797.
171. Wang, W.; Wang, J.; Li, H., A Simple and Efficient l-Prolinamide-Catalyzed α -Selenenylation Reaction of Aldehydes. *Org. Lett* **2004**, *6* (16), 2817-2820.
172. Knoevenagel, E., Ueber eine Darstellungsweise der Glutarsäure. *Ber. Dtsch. Chem. Ges.* **1894**, *27* (2), 2345-2346.
173. Knoevenagel, E., Condensation von Malonsäure mit aromatischen Aldehyden durch Ammoniak und Amine. *Ber. Dtsch. Chem. Ges.* **1898**, *31* (3), 2596-2619.
174. Pollack, L., *Beitr. Chem. Physiol. Pathol.* **1907**, *10*, 232-250.
175. Langenbeck, W.; Sauerbier, R., Über organische Katalysatoren, XVII. Mitteil.: Die Hydratisierung des Crotonaldehyds zu Aldol. *Ber. Dtsch. Chem. Ges.* **1937**, *70* (7), 1540-1541.

176. Woodward, R. B.; Logusch, E.; Nambiar, K. P.; Sakan, K.; Ward, D. E.; Au-Yeung, B. W.; Balaram, P.; Browne, L. J.; Card, P. J.; Chen, C. H., Asymmetric total synthesis of erythromycin. 1. Synthesis of an erythronolide A secoacid derivative via asymmetric induction. *J. Am. Chem. Soc.* **1981**, *103* (11), 3210-3213.
177. Yamaguchi, M.; Igarashi, Y.; Reddy, R. S.; Shiraishi, T.; Hirama, M., Asymmetric Michael addition of nitroalkanes to prochiral acceptors catalyzed by proline rubidium salts. *Tetrahedron* **1997**, *53* (32), 11223-11236.
178. Yamaguchi, M.; Shiraishi, T.; Hirama, M., A Catalytic Enantioselective Michael Addition of a Simple Malonate to Prochiral α,β -Unsaturated Ketoses and Aldehydes. *Angew. Chem., Int. Ed. Engl.* **1993**, *32* (8), 1176-1178.
179. Yamaguchi, M.; Shiraishi, T.; Hirama, M., Asymmetric Michael Addition of Malonate Anions to Prochiral Acceptors Catalyzed by Proline Rubidium Salt. *J. Org. Chem.* **1996**, *61* (10), 3520-3530.
180. Yamaguchi, M.; Shiraishi, T.; Igarashi, Y.; Hirama, M., Catalytic asymmetric Michael addition of nitroalkane to enone and enal. *Tetrahedron Lett.* **1994**, *35* (44), 8233-8236.
181. Yamaguchi, M.; Yokota, N.; Minami, T., The Michael addition of dimethyl malonate to α,β -unsaturated aldehydes catalysed by proline lithium salt. *J. Chem. Soc., Chem. Commun.* **1991**, (16), 1088-1089.
182. Yang, J. W.; Hechavarria Fonseca, M. T.; List, B., A Metal-Free Transfer Hydrogenation: Organocatalytic Conjugate Reduction of α,β -Unsaturated Aldehydes. *Angew. Chem. Int. Ed.* **2004**, *43* (48), 6660-6662.
183. Kunz, R. K.; Macmillan, D. W. C., Enantioselective Organocatalytic Cyclopropanations. The Identification of a New Class of Iminium Catalyst Based upon Directed Electrostatic Activation. *J. Am. Chem. Soc.* **2005**, *127* (10), 3240-3241.
184. Marigo, M.; Franzén, J.; Poulsen, T. B.; Zhuang, W.; Jørgensen, K. A., Asymmetric Organocatalytic Epoxidation of α,β -Unsaturated Aldehydes with Hydrogen Peroxide. *J. Am. Chem. Soc.* **2005**, *127* (19), 6964-6965.
185. Jen, W. S.; Wiener, J. J. M.; Macmillan, D. W. C., New Strategies for Organic Catalysis: The First Enantioselective Organocatalytic 1,3-Dipolar Cycloaddition. *J. Am. Chem. Soc.* **2000**, *122* (40), 9874-9875.

186. Dinér, P.; Nielsen, M.; Marigo, M.; Jørgensen, K. A., Enantioselective Organocatalytic Conjugate Addition of N Heterocycles to α,β -Unsaturated Aldehydes. *Angew. Chem. Int. Ed.* **2007**, *46* (12), 1983-1987.
187. Jencks, W. P.; Carriuolo, J., General Base Catalysis of the Aminolysis of Phenyl Acetate. *J. Am. Chem. Soc.* **1960**, *82* (3), 675-681.
188. Jencks, W. P.; Carriuolo, J., Reactivity of Nucleophilic Reagents toward Esters. *J. Am. Chem. Soc.* **1960**, *82* (7), 1778-1786.
189. Cavill, J. L.; Peters, J.-U.; Tomkinson, N. C. O., Iminium ion catalysis: Use of the α -effect in the acceleration of the Diels–Alder reaction. *Chem. Commun.* **2003**, (6), 728-729.
190. Cavill, J. L.; Elliott, R. L.; Evans, G.; Jones, I. L.; Platts, J. A.; Ruda, A. M.; Tomkinson, N. C. O., The α -effect in iminium ion catalysis. *Tetrahedron* **2006**, *62* (2), 410-421.
191. Brazier, J. B.; Cavill, J. L.; Elliott, R. L.; Evans, G.; Gibbs, T. J. K.; Jones, I. L.; Platts, J. A.; Tomkinson, N. C. O., The α -effect in cyclic secondary amines: new scaffolds for iminium ion accelerated transformations. *Tetrahedron* **2009**, *65* (48), 9961-9966.
192. Lemay, M.; Ogilvie, W. W., Aqueous Enantioselective Organocatalytic Diels–Alder Reactions Employing Hydrazone Catalysts. A New Scaffold for Organic Acceleration. *Org. Lett.* **2005**, *7* (19), 4141-4144.
193. He, H.; Pei, B.-J.; Chou, H.-H.; Tian, T.; Chan, W.-H.; Lee, A. W. M., Camphor Sulfonyl Hydrazines (CaSH) as Organocatalysts in Enantioselective Diels–Alder Reactions. *Org. Lett.* **2008**, *10* (12), 2421-2424.
194. Li, Q.; Wong, W.-Y.; Chan, W.-H.; Lee, A. W. M., Second Generation CaSH (Camphor Sulfonyl Hydrazine) Organocatalysis. Asymmetric Diels–Alder Reactions and Isolation of the Catalytic Intermediate. *Adv. Synth. Catal.* **2010**, *352* (13), 2142-2146.
195. Suzuki, I.; Ando, M.; Shimabara, R.; Hirata, A.; Takeda, K., A novel hydrazone type organocatalyst for enantioselective Diels–Alder reactions. *Org. Biomol. Chem.* **2011**, *9* (8), 3033.
196. Gould, E.; Lebl, T.; Slawin, A. M. Z.; Reid, M.; Davies, T.; Smith, A. D., The development of highly active acyclic chiral hydrazides for asymmetric iminium ion organocatalysis. *Org. Biomol. Chem.* **2013**, *11* (45), 7877.
197. Jakob, F.; Herdtweck, E.; Bach, T., Synthesis and Properties of Chiral Pyrazolidines Derived from (+)-Pulegone. *Chem. Eur. J.* **2010**, *16* (25), 7537-7546.

198. Perez, F.; Leveille, T.; Bertolotti, M.; Rodriguez, J.; Coquerel, Y., Spirobicyclic and Tetracyclic Pyrazolidinones: Syntheses and Properties. *Eur. J. Org. Chem.* **2019**, 2019 (35), 6034-6043.
199. Gould, E.; Lebl, T.; Slawin, A. M. Z.; Reid, M.; Smith, A. D., Structural effects in pyrazolidinone-mediated organocatalytic Diels–Alder reactions. *Tetrahedron* **2010**, 66 (46), 8992-9008.
200. Lemay, M.; Aumand, L.; Ogilvie, W. W., Design of a Conformationally Rigid Hydrazide Organic Catalyst. *Adv. Synth. Catal.* **2007**, 349 (3), 441-447.
201. Lemay, M.; Ogilvie, W. W., Mechanistic Studies of Hydrazide-Catalyzed Enantioselective Diels–Alder Reactions. *J. Org. Chem.* **2006**, 71 (12), 4663-4666.
202. Bondzic, B. P.; Urushima, T.; Ishikawa, H.; Hayashi, Y., Asymmetric Epoxidation of α -Substituted Acroleins Catalyzed by Diphenylprolinol Silyl Ether. *Org. Lett* **2010**, 12 (23), 5434-5437.
203. Terrasson, V.; Van Der Lee, A.; Marcia De Figueiredo, R.; Campagne, J. M., Organocatalyzed Cyclopropanation of α -Substituted α,β -Unsaturated Aldehydes: Enantioselective Synthesis of Cyclopropanes Bearing a Chiral Quaternary Center. *Chem. Eur. J.* **2010**, 16 (26), 7875-7880.
204. Quintard, A.; Lefranc, A.; Alexakis, A., Highly Enantioselective Direct Vinylogous Michael Addition of γ -Butenolide to Enals. *Org. Lett* **2011**, 13 (6), 1540-1543.
205. Ishihara, K.; Nakano, K., Design of an Organocatalyst for the Enantioselective Diels–Alder Reaction with α -Acyloxyacroleins. *J. Am. Chem. Soc.* **2005**, 127 (30), 10504-10505.
206. Sakakura, A.; Suzuki, K.; Nakano, K.; Ishihara, K., Chiral 1,1'-Binaphthyl-2,2'-diammonium Salt Catalysts for the Enantioselective Diels–Alder Reaction with α -Acyloxyacroleins. *Org. Lett* **2006**, 8 (11), 2229-2232.
207. Kano, T.; Tanaka, Y.; Osawa, K.; Yurino, T.; Maruoka, K., Catalytic enantioselective construction of all-carbon quaternary stereocenters by an organocatalytic Diels–Alder reaction of α -substituted α,β -unsaturated aldehydes. *Chem. Commun.* **2009**, (15), 1956.
208. King, H. D.; Meng, Z.; Denhart, D.; Mattson, R.; Kimura, R.; Wu, D.; Gao, Q.; Macor, J. E., Enantioselective Synthesis of a Highly Potent Selective Serotonin Reuptake Inhibitor. An Application of Imidazolidinone Catalysis to the Alkylation of Indoles with an α,β -Disubstituted α,β -Unsaturated Aldehyde. *Org. Lett* **2005**, 7 (16), 3437-3440.

209. Fu, N.; Zhang, L.; Li, J.; Luo, S.; Cheng, J.-P., Chiral Primary Amine Catalyzed Enantioselective Protonation via an Enamine Intermediate. *Angew. Chem. Int. Ed.* **2011**, *50* (48), 11451-11455.
210. Fu, N.; Zhang, L.; Luo, S.; Cheng, J.-P., Asymmetric Sulfa-Michael Addition to α -Substituted Vinyl Ketones Catalyzed by Chiral Primary Amine. *Org. Lett* **2014**, *16* (17), 4626-4629.
211. Fu, N.; Zhang, L.; Luo, S., Chiral Primary Amine Catalyzed Asymmetric Michael Addition of Malononitrile to α -Substituted Vinyl Ketone. *Org. Lett* **2015**, *17* (2), 382-385.
212. Galzerano, P.; Pesciaioli, F.; Mazzanti, A.; Bartoli, G.; Melchiorre, P., Asymmetric Organocatalytic Cascade Reactions with α -Substituted α,β -Unsaturated Aldehydes. *Angew. Chem. Int. Ed.* **2009**, *48* (42), 7892-7894.
213. Nicolaou, K. C.; Sorensen, E. J., *Classics in total synthesis I : targets, strategies, methods*. VCH: Weinheim ;, 1996.
214. Cope, A. C.; Hardy, E. M., The Introduction of Substituted Vinyl Groups. V. A Rearrangement Involving the Migration of an Allyl Group in a Three-Carbon System1. *J. Am. Chem. Soc.* **1940**, *62* (2), 441-444.
215. Overman, L. E.; Jacobsen, E. J., Chair topology of the palladium dichloride catalyzed Cope rearrangement of acyclic 1,5-dienes. *J. Am. Chem. Soc.* **1982**, *104* (25), 7225-7231.
216. Felix, R. J.; Weber, D.; Gutierrez, O.; Tantillo, D. J.; Gagné, M. R., A gold-catalysed enantioselective Cope rearrangement of achiral 1,5-dienes. *Nat. Chem.* **2012**, *4* (5), 405-409.
217. Kaldre, D. Development of hybrid drugs for cancer treatment and studies in asymmetric organocatalysis. McGill University, 2016.
218. Kaldre, D.; Gleason, J. L., An Organocatalytic Cope Rearrangement. *Angew. Chem. Int. Ed.* **2016**, *55* (38), 11557-11561.
219. Larnaud, F.; Sulpizi, A.; Häggman, N. O.; Hughes, J. M. E.; Dewez, D. F.; Gleason, J. L., Organocatalytic Michael Addition of Indoles to α -Substituted Enals by Using a Diazepane Carboxylate Catalyst. *Eur. J. Org. Chem.* **2017**, *2017* (18), 2637-2640.
220. Häggman, N. O.; Zank, B.; Jun, H.; Kaldre, D.; Gleason, J. L., Diazepane Carboxylates as Organocatalysts in the Diels-Alder Reaction of α -Substituted Enals. *Eur. J. Org. Chem.* **2018**, *2018* (39), 5412-5416.

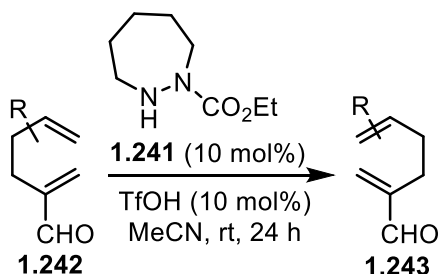
221. Nigst, T. A.; Antipova, A.; Mayr, H., Nucleophilic Reactivities of Hydrazines and Amines: The Futile Search for the α -Effect in Hydrazine Reactivities. *J. Org. Chem.* **2012**, *77* (18), 8142-8155.
222. Sanders, J. N.; Jun, H.; Yu, R. A.; Gleason, J. L.; Houk, K. N., Mechanism of an Organocatalytic Cope Rearrangement Involving Iminium Intermediates: Elucidating the Role of Catalyst Ring Size. *J. Am. Chem. Soc.* **2020**, *142* (39), 16877-16886.

Chapter 2. Investigation into the racemic iminium-catalyzed (*E*)-polyene cyclization

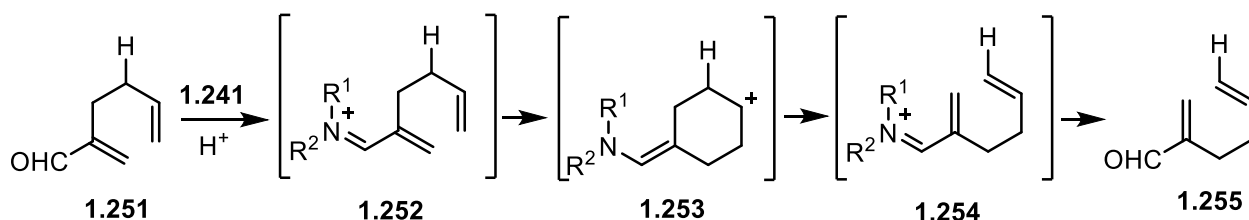
2.1 Introduction

As described in Section 1.7, an iminium-catalyzed Cope rearrangement of 1,5-hexadiene-2-carboxaldehydes was developed using cyclic hydrazide catalyst **1.241**.¹ Preliminary DFT calculations suggested that, with substrate **1.251**, the reaction proceeds by a stepwise mechanism with a shallow energy cyclohexyl cation intermediate. We hypothesized that, if the cyclohexyl cation was stabilized with a methyl group and a nucleophile was incorporated into the substrate, the ring opening to give the Cope product could be outcompeted by nucleophilic trapping. We envisioned that those substrates bearing a tethered, nucleophilic aromatic ring (**2.1**) would result in a cationic cascade giving us the first iminium-catalyzed polyene cyclization (Scheme 2.1).

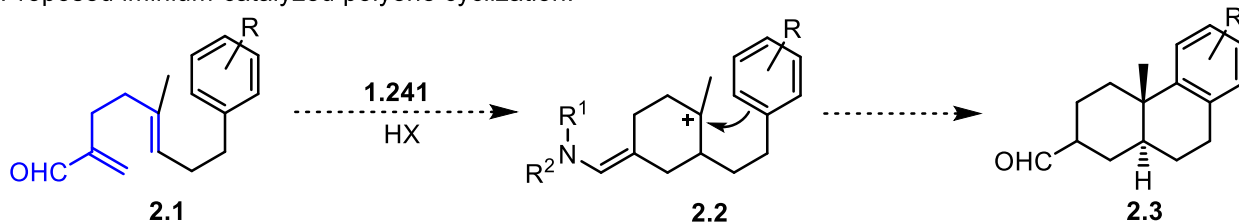
Iminium-catalyzed Cope rearrangement:



Mechanism of the iminium-catalyzed Cope rearrangement:



Proposed iminium-catalyzed polyene cyclization:

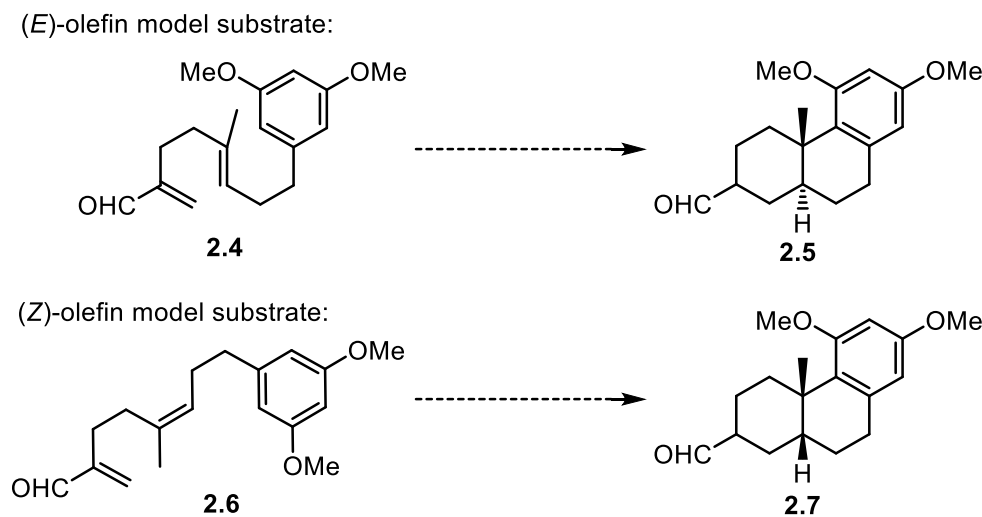


Scheme 2.1. Iminium-catalyzed Cope rearrangement and proposed iminium-catalyzed polyene cyclization with 1,5-hexadiene-2-carboxaldehyde highlighted in blue.

2.2 Initial work on the iminium-catalyzed polyene cyclization

Initial work on the iminium-catalyzed polyene cyclization was done by Dr. Dainis Kaldre and Dr. Samuel Plamondon. For initial investigation into the viability of the reaction, model (*E*)-polyene substrate **2.4** was designed with a 3,5-dimethoxyphenyl as a terminating group (Scheme 2.2). The trapping of the cation is an electrophilic aromatic substitution, which is expected to proceed more readily with electron-rich aromatic rings. The 3,5-dimethoxy substitution on the terminating phenyl ring makes it electron-rich and localizes the electron density at the desired site of reactivity, favouring the second ring closure onto the intermediate cyclohexyl cation.

In addition to investigating the cyclization of substrates with an internal (*E*)-olefin (e.g. **2.4**), we were also interested in investigating the cyclization of substrates containing the internal (*Z*)-olefin. We hypothesized that the two isomers would lead to the corresponding *trans*- or *cis*-decalin (e.g. **2.5** or **2.7**), according to the Stork-Eschenmoser hypothesis.

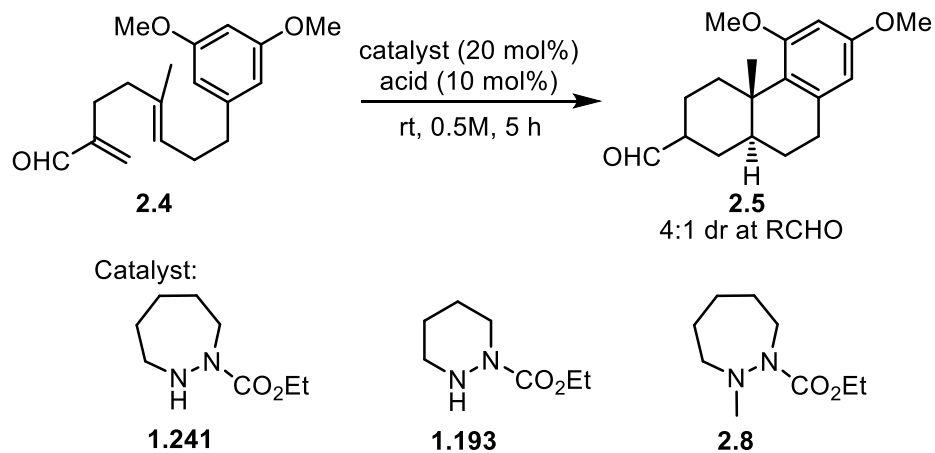


Scheme 2.2. Model substrates for the iminium-catalyzed polyene cyclization.

The polyene cyclization was initially examined under the optimum conditions for the Cope rearrangement using 7-membered ring hydrazide catalyst **1.241** as the TfOH salt in MeCN.² Under these conditions, substrate **2.4** afforded a 25% yield of cyclized product **2.5**, as determined by ¹H NMR (Table 2.1, entry 1). In an attempt to improve the reaction, MeNO₂ was screened as a solvent, as it had been the optimal solvent in the hydrazide-catalyzed Diels-Alder reaction.³ This solvent switch was found to provide a 55% yield of product **2.5**, as determined by ¹H NMR (entry 2). However, these conditions led to undesired side products which proved to be inseparable. The

hydrochloride salt of catalyst **1.241** was then screened under the same conditions (entry 3) and was found to give clean bicyclic product **2.5**, isolated in a 55% yield. Alternate solvent conditions of 15% *i*PrOH/DCM, which had been optimized by MacMillan for prior iminium-catalyzed reactions,⁴ gave a slightly decreased isolated yield of product (49%, entry 4). The 6-membered ring hydrazide catalyst **1.193** gave product in a lower yield (41%) under the same solvent and co-acid conditions (entry 5). No reaction was observed when N-methylated hydrazide catalyst **2.8**, as the triflic acid salt, was used in place of catalyst **1.241** (entry 6), suggesting that iminium ion formation was crucial for reactivity as opposed to an acid-catalyzed reaction. The cyclization of (*E*)-olefin substrate **2.4** results in the *trans*-decalin product and the stereochemistry at the α -position to the aldehyde is set post-cyclization, through hydrolysis of the resulting enamine. Due to this, the product **2.5** was isolated as a mixture of epimers at this position with a ratio of 4:1 and the major isomer being the thermodynamically preferred equatorial aldehyde.

Table 2.1. Iminium-catalyzed polyene cyclization of model (*E*)-polyene substrate **2.4** (work done by Dr. Dainis Kaldre).

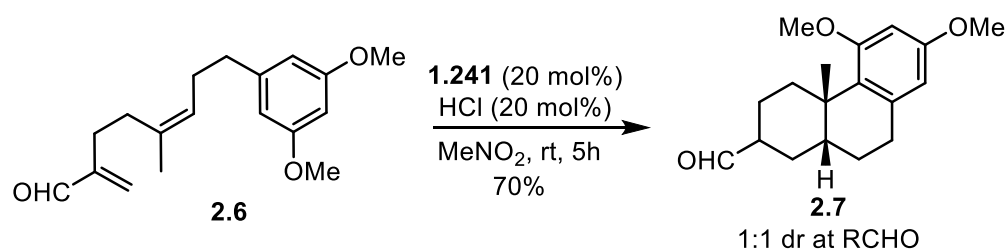


Entry	Catalyst	Solvent	Acid	¹ H NMR Yield (%)	Isolated Yield (%)
1	1.241	MeCN	TfOH	25 ^[a]	-
2	1.241	MeNO ₂	TfOH	55	-
3	1.241	MeNO ₂	HCl	66	55
4	1.241	15% <i>i</i> PrOH/DCM	HCl	-	49

5	1.193	MeNO ₂	HCl	56	41
6	2.8	MeNO ₂	TfOH	N.R.	

[a] After 24 h.

With these optimized conditions in entry 3, (*Z*)-olefin substrate **2.6** was found to cyclize to the *cis*-decalin product **2.7** in 70% yield (Scheme 2.3).⁵ The products were isolated as a thermodynamic mixture of epimers at the position α to the aldehyde in a thermodynamic ratio of 1:1. With the reaction conditions optimized for the model substrates, we were interested in investigating the scope and limitations of the polyene cyclization with substrates that contained different aromatic groups.

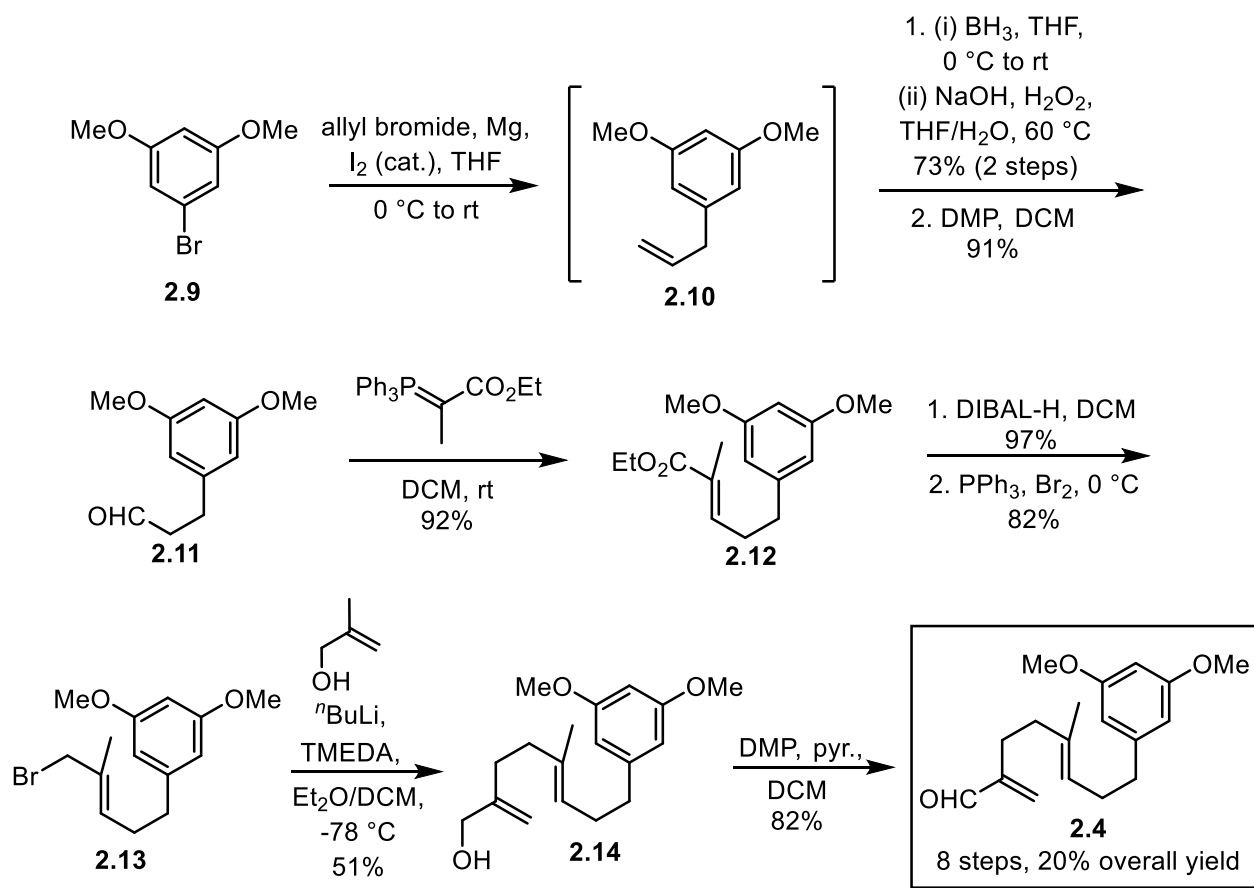


Scheme 2.3. Preliminary results for iminium-catalyzed (*Z*)-polyene cyclization.

2.3 Substrate synthesis

The initial synthesis of the model substrates had been developed by Dr. Dainis Kaldre and optimized by Dr. Samuel Plamondon. The initial route provided model (*E*)-olefin substrate **2.4** in 8 steps with 20% overall yield (Scheme 2.4). The synthesis began with 1-bromo-3,5-dimethoxybenzene (**2.9**). Addition of an allyl Grignard followed by a hydroboration/oxidation was performed in 73% yield over two steps and the resulting alcohol was then oxidized with DMP to provide aldehyde **2.11** in 91% yield. From aldehyde **2.11**, the internal (*E*)-olefin was synthesized through a stabilized Wittig olefination, giving product **2.12** in 92% yield. The ester was reduced with DIBAL-H in 97% yield and followed by an Appel reaction to provide bromide **2.13** in 82% yield. Addition of the dianion of methallyl alcohol displaced the bromide to give a 51% yield of alcohol **2.14** and a final oxidation with DMP buffered with pyridine provided final substrate **2.4** in 82% yield. Although the overall synthesis of this substrate was high yielding, it proceeded through multiple linear steps and built out from the terminal aromatic. To examine a substrate scope, we needed easy access to substrates with different terminating groups, which required the design of a

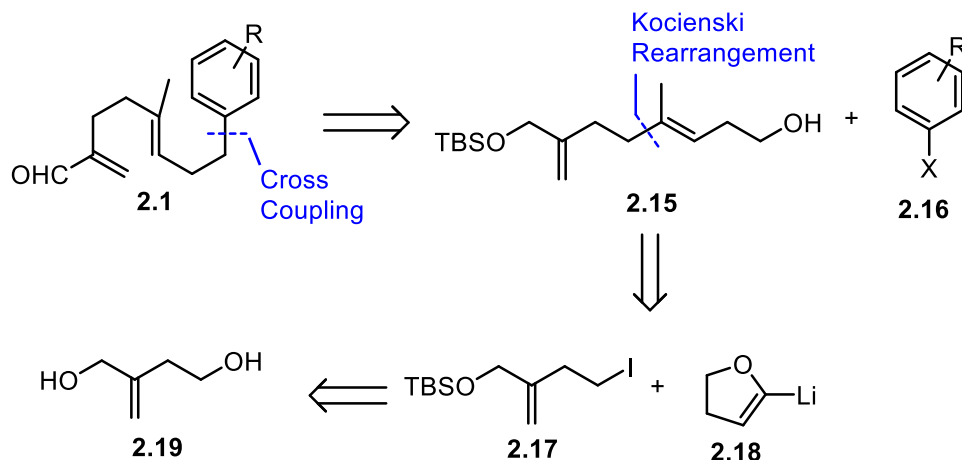
modular route to synthesize these polyenes. The development of this new route and all further experimentation in this chapter was completed by the author.



Scheme 2.4. Initial synthesis of model (*E*)-polyene substrates (work done by Dr. Samuel Plamondon).

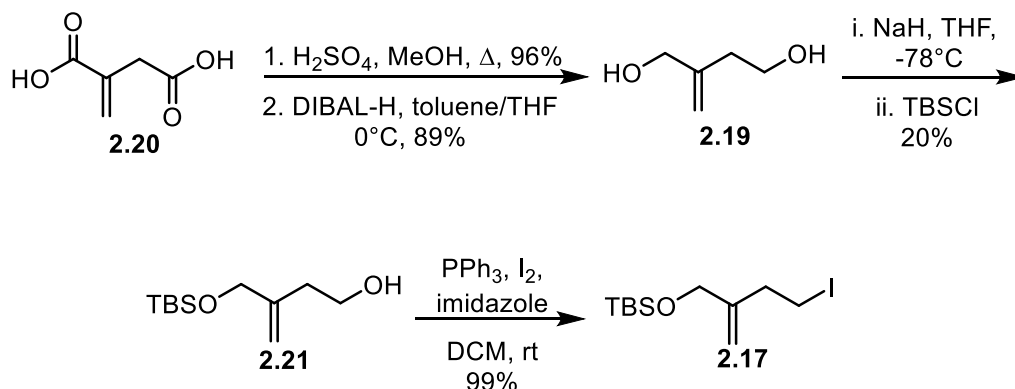
2.3.1 Modular substrate synthesis

A retrosynthesis was designed to synthesize (*E*)-polyene substrates in a modular fashion (Scheme 2.5). The final step in this synthesis would cross-couple the terminating aromatic ring with a halide synthesized from an Appel reaction on alcohol **2.15**. This route would provide a simple method to access a wide variety of terminating groups from a common intermediate. We initially envisioned that alcohol **2.15** could be made through a Kocienski rearrangement⁶ of lithiated dihydrofuran (**2.18**) and iodide **2.17**. Iodide **2.17** could be obtained from known diol **2.19** through mono-TBS protection followed by an Appel reaction.



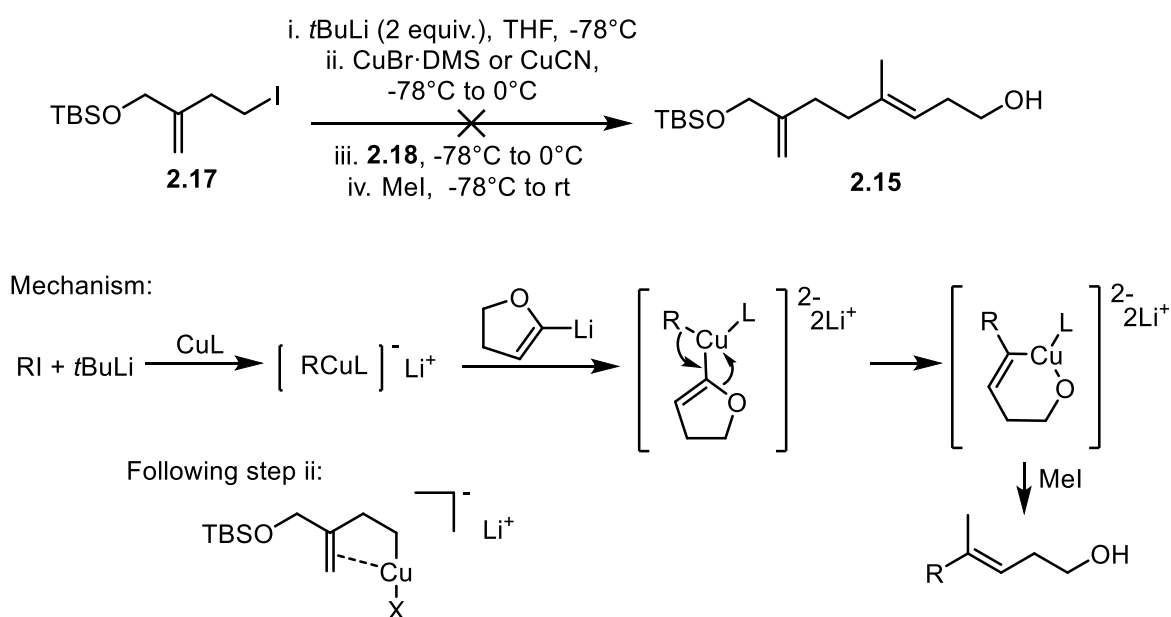
Scheme 2.5. Initial retrosynthetic analysis of (*E*)-polyene substrates.

The desired diol can be synthesized beginning with itaconic acid (**2.20**, Scheme 2.6). Fisher esterification of itaconic acid gave the dimethyl ester in 96% yield. A subsequent DIBAL-H reduction of the ester resulted in the known diol **2.19** in 89% yield. Mono-TBS protection of diol **2.19** proceeded well, with deprotonation by sodium hydride in THF at $-78\text{ }^{\circ}\text{C}$ giving the monoanion, followed by addition of TBSCl. However, there was no preference shown for protection of the allylic alcohol over the homo-allylic alcohol and a mixture of the two products was obtained. To aid in separation, MnO_2 oxidation was performed on the mixture to selectively oxidize the undesired unprotected allylic alcohol. However, due to these separation difficulties, product **2.21** was obtained in a poor yield of 20%. From alcohol **2.21**, the desired iodide **2.17** was obtained in 99% yield through an Appel reaction.



Scheme 2.6. Synthesis of iodide **2.17**.

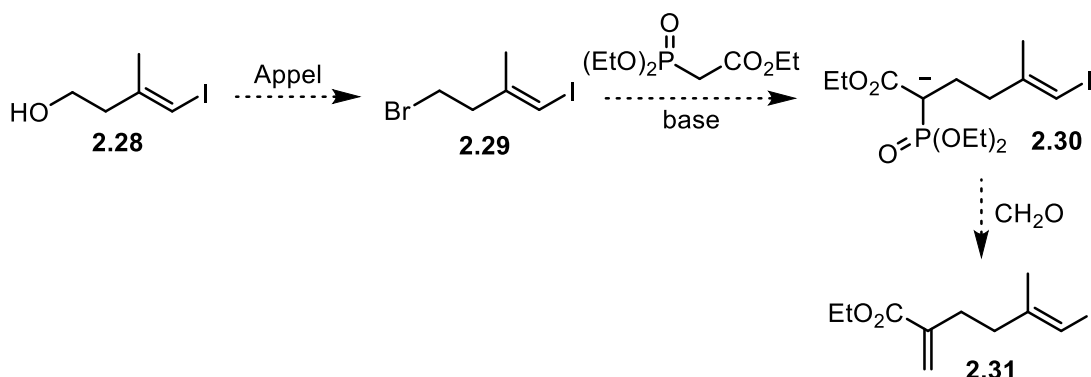
With iodide **2.17** in hand the Kocienski rearrangement was attempted under standard conditions (Scheme 2.7).⁶ Unfortunately, metal-halogen exchange of iodide **2.17** followed by attempted cross-coupling with lithiated furan in the presence of either CuBr·DMS or CuCN failed to give the desired product **2.15**. In both cases, the major product obtained was dehalogenated iodide. The accepted mechanism of the Kocienski rearrangement proceeds through formation of a higher order cuprate and subsequent cross-coupling/opening of the lithiated dihydrofuran followed by alkylation of the resulting vinyl cuprate with MeI.⁶⁻⁷ We suggest that this reaction does not proceed due to the terminal olefin in iodide **2.17**, which could co-ordinate to the metal centre following the addition to the Cu(I) species in step ii, as shown below, preventing the co-ordination of the lithiated dihydrofuran and poisoning the catalyst.



Scheme 2.7. Attempted Kocienski rearrangement with iodide **2.17**.

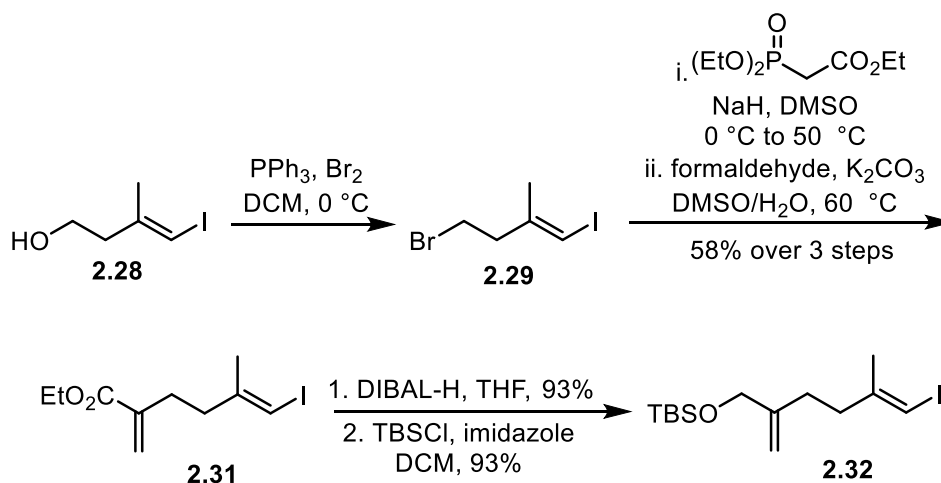
With the lack of desired reactivity in the Kocienski rearrangement, we concluded that this would not be a viable route to (*E*)-polyene substrates. A second retrosynthetic analysis was designed (Scheme 2.8), which incorporated a late-stage coupling of the aromatic group through a Suzuki cross-coupling. The aromatic cross-coupling partner **2.23** could be made from the hydroboration of commercially available styrenes. We envisioned that this could be cross-coupled to vinyl iodide **2.22** to provide the internal (*E*)-olefin. Iodide **2.22** could be made from alcohol **2.24** through oxidation and α -methylenation of the resulting aldehyde. Finally, alcohol **2.21** could be made through a carboalumination-iodination of 1-hexynol (**2.25**).

Vinyl iodide **2.28** is two methylene units shorter than vinyl iodide **2.24**, so revisions needed to be made to the original retrosynthesis (Scheme 2.10). To install the two-carbon unit, the alcohol could first be converted to bromide **2.29**, which could then be displaced with triethyl phosphonoacetate to form HWE reagent **2.30**. The terminal olefin of **2.31** could then be installed through an HWE reaction with formaldehyde.



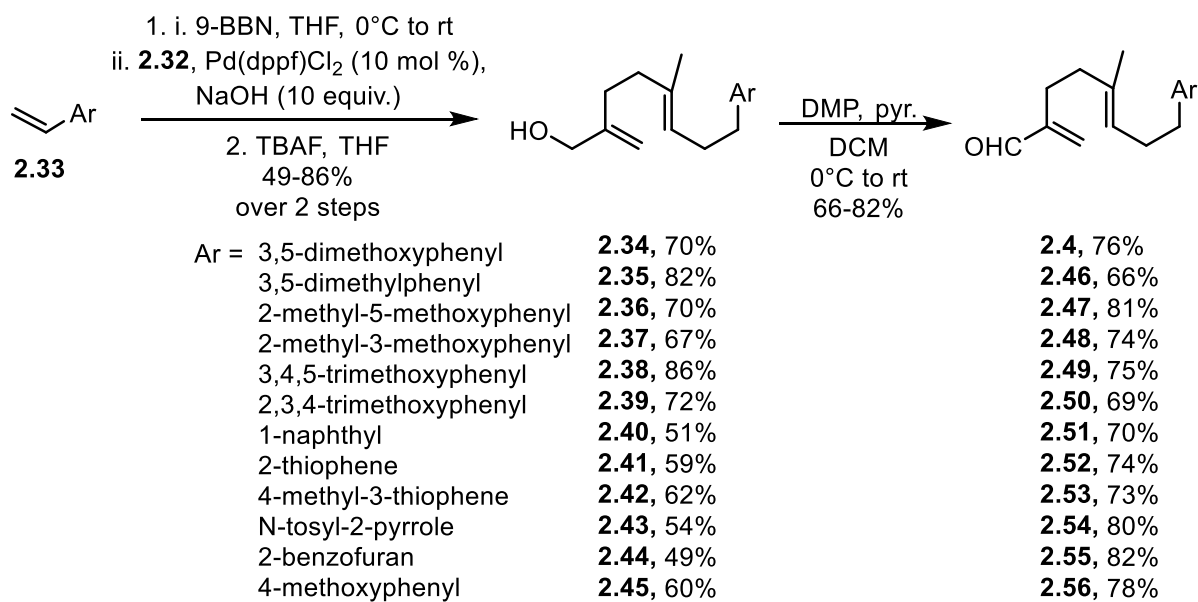
Scheme 2.10. Revised synthesis of iodide coupling partner.

With vinyl iodide **2.28** obtained as a single regioisomer, an Appel reaction was performed to convert the alcohol to bromide **2.29**, which was used in the next step after filtration through a silica plug. Deprotonated triethyl phosphonoacetate was alkylated with bromide **2.29**, forming an HWE reagent. An *in situ* HWE reaction was then performed with formaldehyde to result in α,β -unsaturated ester **2.31** in 58% yield over three steps. Ester **2.31** was then reduced with DIBAL-H in 93% yield and protected as the TBS ether in 93% yield to give the iodide coupling partner **2.32**.



Scheme 2.11. Synthesis of iodide coupling partner.

In the final steps of the substrate synthesis, iodide **2.29** was coupled to the aromatic terminating group (Scheme 2.12). The aromatic coupling partners were formed from the hydroboration of vinyl arenes using 9-BBN to obtain a single regioisomer. This was then coupled with vinyl iodide **2.32** under standard Suzuki cross-coupling conditions (Pd(dppf)Cl₂ with sodium hydroxide). To enable isolation of clean coupled products, TBAF-mediated deprotection yielded alcohols **2.34-2.45** in 49-86% over two steps. Final substrates **2.4** and **2.46-2.56** were then obtained through oxidation to the resulting aldehydes with DMP buffered with pyridine in yields of 66-82%.



Scheme 2.12. Final steps in the synthesis of (*E*)-polyene substrates.

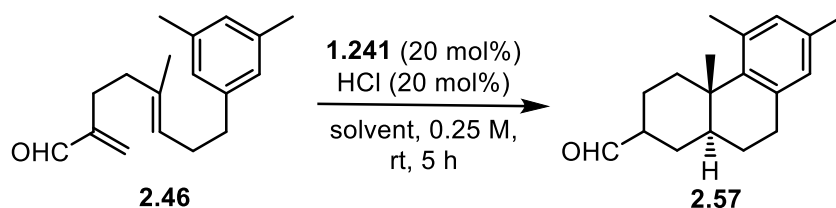
2.4 Solvent screen

In the polyene cyclization of model substrate **2.4**, the highest yields of product **2.5** were obtained using MeNO₂ as solvent in comparison to that obtained with MeCN or 15% *i*PrOH/DCM. Initial investigations into different substrates found that the substrate scope was limited by the nucleophilicity of the terminating group as well as the solvent conditions. For substrates with strongly nucleophilic terminating groups, such as model substrate **2.4**, the reaction performs well in MeNO₂. However, under the same conditions (Table 2.2, Entry 1), substrates with less nucleophilic terminating groups (e.g. **2.46**) resulted in a mixture of bicyclic product with undesired side products (44:56 ratio of **2.57**: undesired side products). The side products in the cyclization of **2.46** in MeNO₂ were not characterized as the mixture was inseparable. However, we presume

that they are a mixture of olefins seen in product **2.58** (Scheme 2.13) as a monocyclic olefin product has been isolated in the cyclization of substrates with terminating groups of lower nucleophilicity performed in MeNO₂. When EtOH was used as a solvent, a similar ratio of desired product to undesired side product was obtained (Entry 2, 43:57 ratio of **2.57** to undesired side products). In this instance it was possible to isolate one of the major side products which turned out to be ether **2.60** derived from trapping of the intermediate cyclohexyl cation with EtOH (Scheme 2.14).

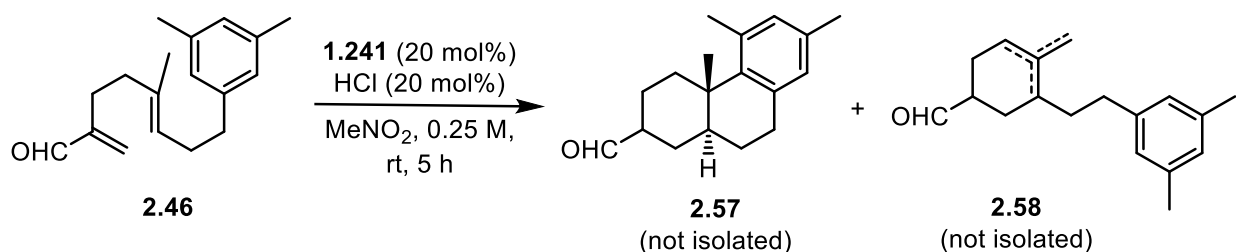
To identify conditions for the complete bicyclization of **2.46**, a solvent screen was performed in collaboration with Dr. Samuel Plamondon (who performed a more thorough solvent screen with the (*Z*)-polyene substrate). With DCM as the solvent, there was no reaction observed after 48 hours (Entry 3). In the (*Z*)-polyene cyclization, a mixture of HFIP/DCM was found to provide clean bicyclic product⁵ and when HFIP was added in a solvent mixture of 5% HFIP/DCM, bicyclic product **2.57** was obtained in a >99:1 ratio with undesired side products (Entry 4).

Table 2.2. Solvent screen for polyene cyclization of **2.42**.

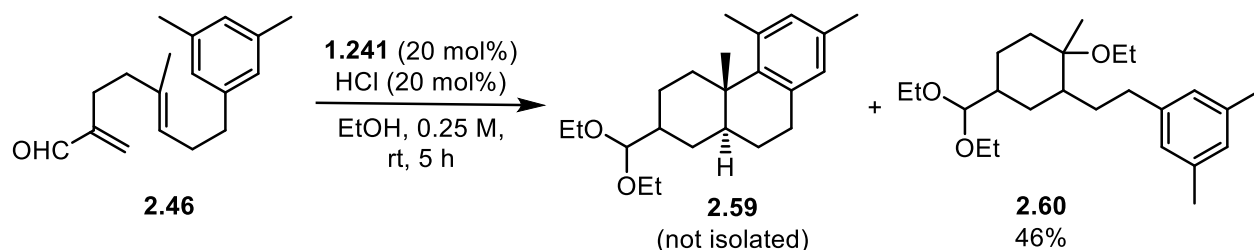


Entry	Solvent	2.57 : undesired side products ^[a]
1	MeNO ₂	44:56
2	EtOH	43:57 ^[b]
3	DCM	N.R. ^[c]
4	5% HFIP/DCM	>99:1

[a] Ratios determined by integration of aldehyde peak ratios in crude ¹H NMR. [b] Ratio of corresponding acetals **2.59** and **2.60** determined from aromatic peak ratios in crude ¹H NMR. [c] After 48 h.



Scheme 2.13 Possible side products from the polyene cyclization of substrate **2.46** in MeNO_2 .



Scheme 2.14 Isolated product from solvent trapping of substrate **2.46** with EtOH .

HFIP is a polar protic solvent with unique properties in comparison to other alcoholic solvents, such as $t\text{PrOH}$. It is a very polar solvent, with a relative polarity of 0.969 in comparison to 1 for H_2O and the much lower 0.546 for $t\text{PrOH}$.⁹ In addition, the trifluoromethyl groups on HFIP withdraw electron density from the alcohol, rendering it less nucleophilic than $t\text{PrOH}$. These properties have made HFIP a popular solvent in reactions with cationic intermediates, where it has been proposed to either aid in stabilization of the cationic charge or increase the persistence of cationic species.¹⁰⁻¹¹ The use of HFIP in electrophilic sulfur and halogen-initiated polyene cyclizations has been shown to decrease the formation of undesired side products.¹²⁻¹³ In these examples, the non-polar substrates are proposed to have a solvophobic effect with the HFIP, promoting highly organized chair-like conformations and lowering the entropic barrier towards cyclization. However, these reactions were run in undiluted HFIP, which would be significantly more polar than a 5% HFIP/DCM mixture.

Recent work has shown evidence of the participation of HFIP in proton transfer to help lower the activation barrier for these transformations.¹⁴ Participation of HFIP in proton transfer could be invoked to enhance iminium ion formation in the iminium-catalyzed polyene cyclization. However, based on side products obtained from premature termination of the cyclization in other solvents, we propose that the main role of HFIP is in the stabilization of the intermediate cyclohexyl cation to give a decreased propensity for alternate termination pathways. In

investigations done on the (*Z*)-polyene cyclization, it was found that concentrations of HFIP higher than 5% led to substrate degradation and lower yields of product.⁵ The pKa of HFIP is 9.3¹⁵ in comparison to 17.1 of ⁱPrOH,¹⁶ and it is possible that the increased acidity of a solvent mixture containing higher concentrations of HFIP promoted acid-mediated degradation of the substrate.

2.5 Substrate scope

Under these optimized conditions, (*E*)-polyene substrates cyclized to give *trans*-decalin products shown in Figure 2.1 in good yields.¹⁷ Decalin products were obtained as a thermodynamic mixture of diastereomers at the epimerizable position α to the aldehyde, as seen previously in the cyclization of model substrate **2.4**. This ratio (C3- β : α) was determined by integration of aldehyde peaks in the ¹H NMR. The *trans*- to *cis*-decalin ratio was also determined by integration of respective aldehyde peaks in the ¹H NMR. For products **2.67** and **2.68**, the aldehyde peaks for the *trans*- and *cis*-decalin products overlapped and therefore, the *trans*- to *cis*-decalin ratio could not be determined.

Under the optimal conditions, model substrate **2.4** cyclized to give **2.5** in 72% yield. Substrate **2.46**, with 3,5-dimethyl substitution, resulted in clean bicyclic product **2.57** in 75% yield. Substrates terminated by an aromatic ring with one methyl and one methoxy group were cyclized in good yields, with 2-methyl, 5-methoxy substitution giving product **2.61** in 72% yield and 2-methyl, 3-methoxy substitution giving product **2.62** in 75% yield. Substrates with three methoxy substituents cyclized to give **2.63**, with 3,4,5-trimethoxy substitution, in 69% yield and **2.64**, with 2,3,4-trimethoxy substitution, in 70% yield. Termination by a naphthyl ring gave high yield of product, providing 88% of **2.65**. Finally, termination by heterocycles was also well tolerated. The cyclization terminated with thiophene at the 3-position provided product **2.66** in 81% yield and at the 2-position provided product **2.67** in 43% yield. Heterocyclic substrates, such as **2.53**, that were prone to acid-mediated polymerization resulted in slightly lower yields of products due to the mildly acidic cyclization conditions. The closure of N-tosyl pyrrole at the 3-position provided product **2.68** in a slightly lower yield of 65%. Termination with benzofuran at the 3-position also worked well, providing product **2.69** in 82% yield. Although they were not included in the study, cyclization onto furan, pyrrole at the 2-position, and indole would be expected to work well (with the same potential lower yield resulting from acid-mediated polymerization as with thiophene) as they are more reactive to electrophilic substitution than thiophene.¹⁸

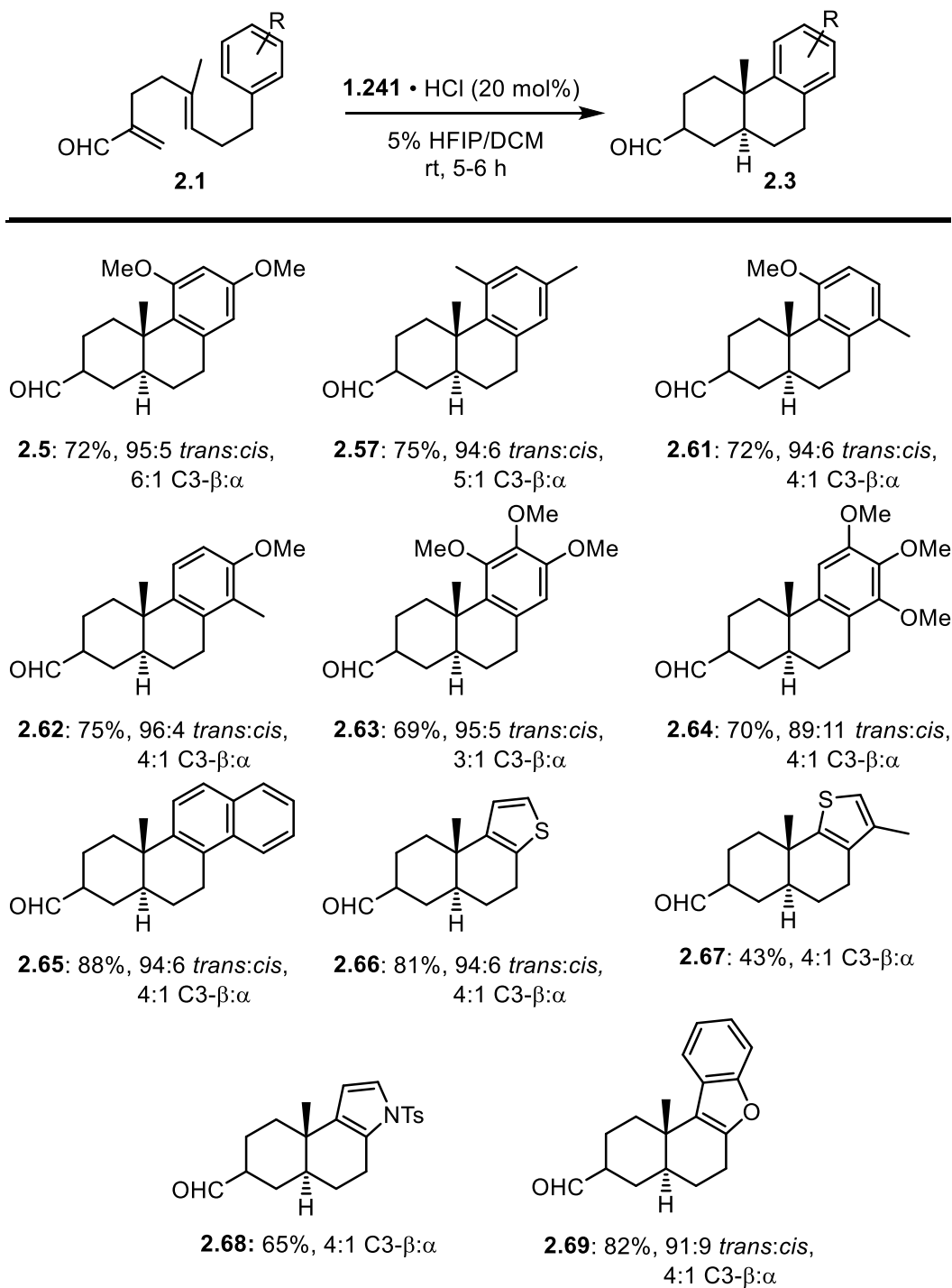
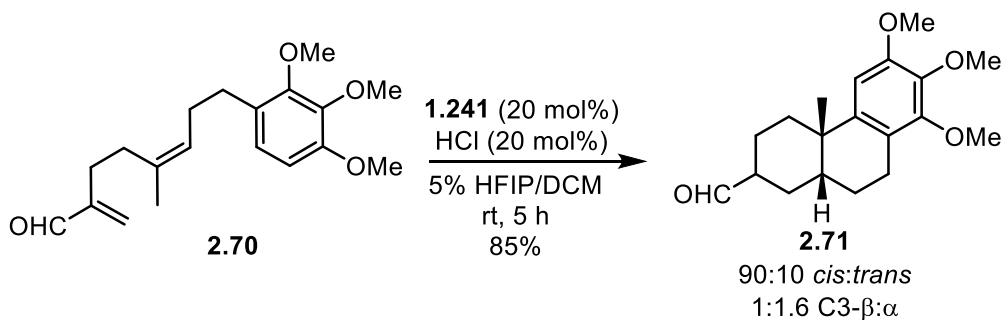


Figure 2.1. Substrate scope of the racemic (*E*)-polyene cyclization.

In the polyene cyclizations of (*E*)-olefin substrates, slight erosion of stereoselectivity was observed, with most products observed in approximately a 95:5 *trans*- to *cis*-decalin ratio. The amount of *cis*-decalin observed was slightly higher in substrates with less nucleophilic terminating

groups. The lowest observed ratio was 89:11 *trans*- to *cis*-decalin seen in cyclized product **2.64**. A similar observation was made in the cyclization of (*Z*)-olefin substrates, studied by Dr. Samuel Plamondon, which led to products with a small amount of the *trans*-decalin isomer.¹⁷ The amount of isomerization showed the same dependence on the nucleophilicity of the terminating group, with less nucleophilic terminating groups leading to a slightly lower ratio of *cis*- to *trans*-decalin products. The lowest observed ratio was 90:10 *cis*- to *trans*-decalin, seen in the cyclized product **2.71** of 2,3,4-trimethoxyphenyl terminated substrate **2.70** (Scheme 2.15).



Scheme 2.15. Cyclization of (*Z*)-polyene substrate **2.70**.

To help understand the results of the polyene cyclization, one can examine the electrophilic substituent constant (σ^+), a parameter that has been calculated from the solvolysis of substituted *t*-cumyl chlorides and can be correlated to the reactivity in electrophilic aromatic substitution reactions of substituted aromatic rings (Figure 2.2).¹⁹ The methoxy substitution is inductively withdrawing at all positions on the aromatic ring. However, the resonance donates electron density to the *ortho*- and *para*- positions. This is reflected in σ^+ , which for a *para*-methoxy substituent is -0.778 , indicating that it will react much faster in an electrophilic aromatic substitution than unsubstituted benzene ($\sigma^+ = 0$). A *meta*-methoxy substituent has a σ^+ of 0.047 , showing that it decreases the nucleophilicity of the aromatic ring for the desired position of reactivity. In contrast, methyl substitution is inductively donating, directing electron density to the *ortho*- and *para*- positions. This is reflected in σ^+ where a *para*-methyl substituent gives a σ^+ of -0.311 . Due to the inductively donating character of alkyl substitution, a methyl group will also slightly activate the *meta*-position, resulting in σ^+ of -0.066 .

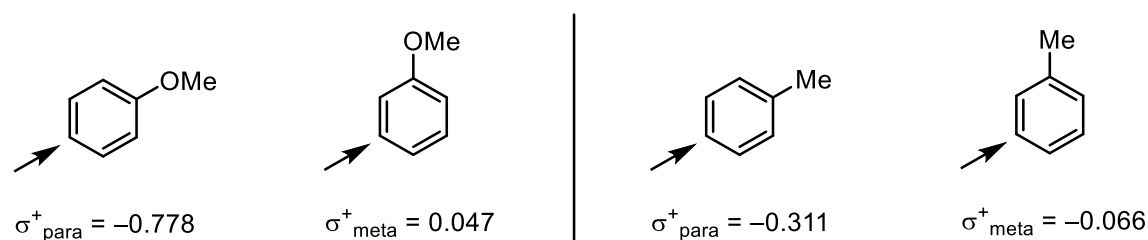


Figure 2.2. Electrophilic substitution constants for methoxy substitution.

The polyene cyclization is terminated through electrophilic substitution of the aromatic ring and so the kinetics of aromatic trapping can be correlated to σ^+ . Model substrate **2.4** is nucleophilic at the reacting site as it has one methoxy substituent *para*- to the desired site of reactivity as well as a methoxy substituent at the *ortho*-position that gives similar electronic effect to the *para*-methoxy but with additional steric hindrance (Figure 2.3). This substrate would be expected to react quickly in an electrophilic aromatic substitution and resulted in a 95:5 *trans*- to *cis*-decalin ratio of product **2.5**. Substrate **2.46** has two activating methyl substituents *ortho*- and *para*- to the desired site of reactivity. The inductively donating methyl substituents are not as activating as the resonance donating methoxy substituents. However, this terminating aromatic ring would still be expected to react relatively quickly in an electrophilic aromatic substitution and resulted in a 94:6 *trans*- to *cis*-decalin ratio of product **2.57**. Substrate **2.50** has two deactivating methoxy substituents *meta*- to the desired site of reactivity. In addition, the free rotation of the *para*-methoxy substituent is limited due to two *meta*-methoxy substituents, thus preventing necessary orbital alignment for resonance donation. Without resonance donation, the methoxy is considered an inductively withdrawing substituent. Therefore, due to the lower nucleophilicity of this terminating aromatic group, it would be expected to react slower in an electrophilic aromatic substitution than substrates **2.4** and **2.46**. Slow trapping by the terminating groups gives a higher probability that alternate pathways will be followed instead, including those that lead to the *cis*-decalin product as discussed in later sections. This was reflected in the lower *trans*- to *cis*-decalin ratio of 89:11 of product **2.64**.

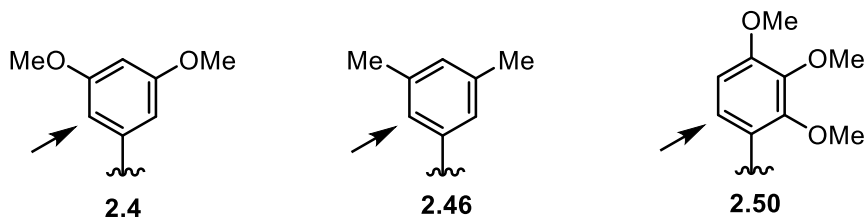
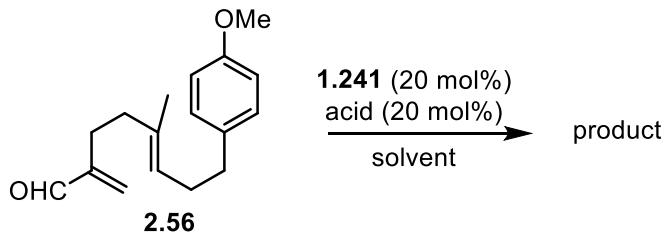


Figure 2.3. Terminating groups for substrates **2.4**, **2.46**, and **2.50**.

2.6 Less nucleophilic substrates

Under the standard conditions for the polyene cyclization, substrate **2.56** gave no desired product and only starting material was recovered (Table 2.3, Entry 1). This substrate is terminated by an aromatic ring with a methoxy substituent *meta*- to the desired site of reactivity and therefore is less nucleophilic at this position. Greater reactivity was observed in the iminium-catalyzed Cope rearrangement with either TfOH (pKa -14) or HClO₄ (pKa -10) as the co-acid.² Therefore, attempts to increase the reactivity in the cyclization of substrate **2.55** were performed using HClO₄ as a stronger co-acid. Although some reactivity was observed, these conditions only resulted in undesired monocyclic side products. When the reaction was run in MeNO₂, a non-nucleophilic polar solvent, the major product was isolated after reduction to the corresponding alcohol, giving **2.72** in 16% yield (Entry 2). This product is the result of either elimination at the cyclohexyl cation intermediate followed by sequential protonation/elimination steps or sequential 1,2 hydride shifts to give the thermodynamically favoured enal (prior to reduction). When run in EtOH, a nucleophilic solvent, the intermediate cyclohexyl cation was trapped with the solvent, resulting in ethyl ether **2.73** in 44% yield (Entry 3). A stronger co-acid results in a weakly co-ordinating counter anion, which gives greater cationic character to both the iminium and the cyclohexyl cation intermediates. However, in the reaction of **2.56**, alternate pathways with low activation barriers (e.g. solvent trapping or elimination) competed with the slow trapping of the aromatic ring.

Table 2.3. Attempts at polyene cyclization of substrate **2.56**.

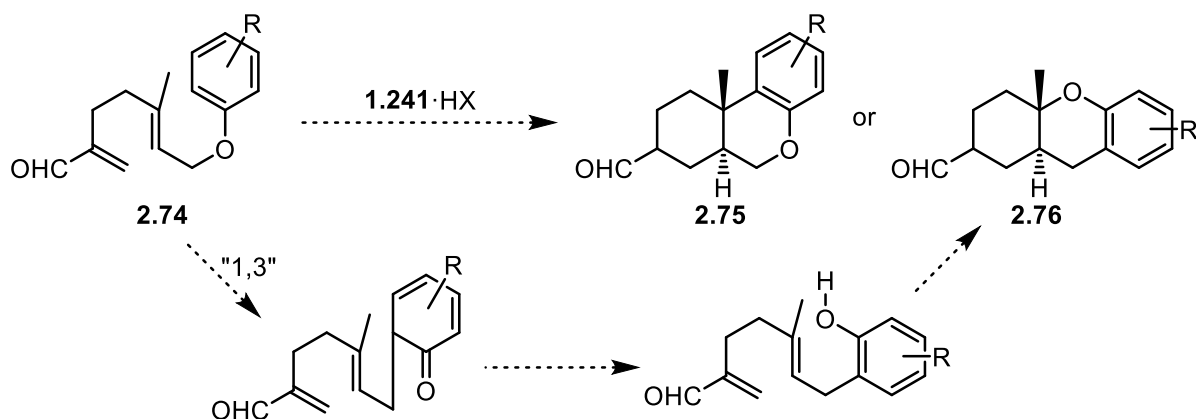


Entry	Acid	Solvent	Product
1	HCl	5% HFIP/DCM	N.R.
2	HClO ₄	MeNO ₂	<p style="text-align: center;">2.72, 16%^[a]</p>
3	HClO ₄	EtOH	<p style="text-align: center;">2.73, 44%^[b]</p>

[a] After NaBH₄ reduction. [b] After hydrolysis of ethyl acetal with CHCl₃/H₂O/TFA.

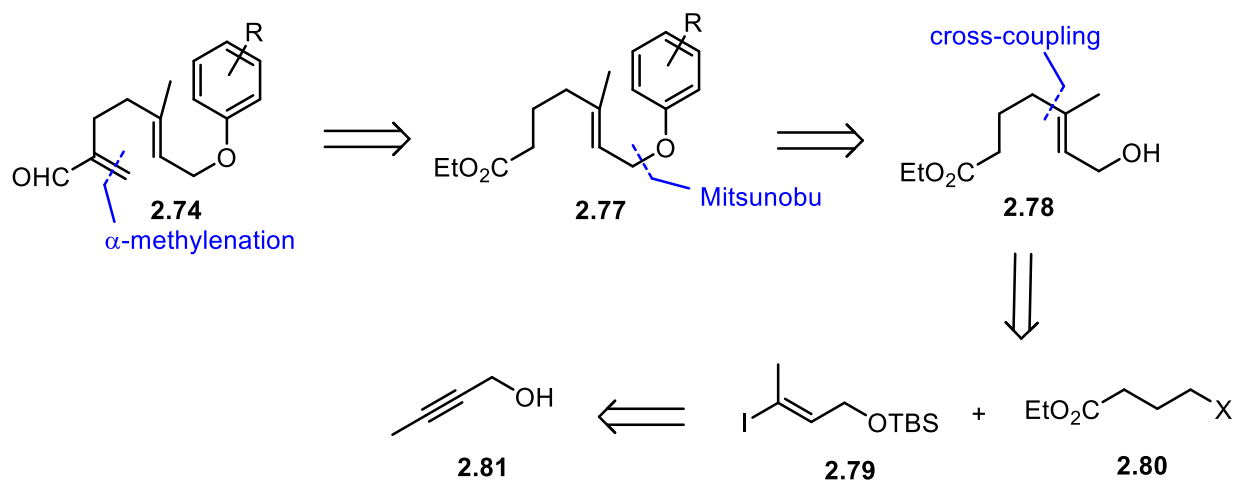
2.6.1 Ether-bridged substrates

With the observation that an aromatic terminating group with moderate to strong nucleophilicity was required, substrates were designed with an ether-bridge *ortho*- to the desired site of reactivity (**2.74**, Scheme 2.16). In these substrates, we presumed that the ether bridge would increase the nucleophilicity of the terminating aromatic ring. Substrates with skeletal ethers have previously been reported in synthetic polyene cyclization methodologies, either terminating by the aromatic ring²⁰ to give a ring system similar to product **2.75** or proceeding first through a formal 1,3-rearrangement prior to terminating with the resulting phenol²¹ to give a ring system similar to product **2.76**.



Scheme 2.16. Proposed cyclization of ether-bridged substrates.

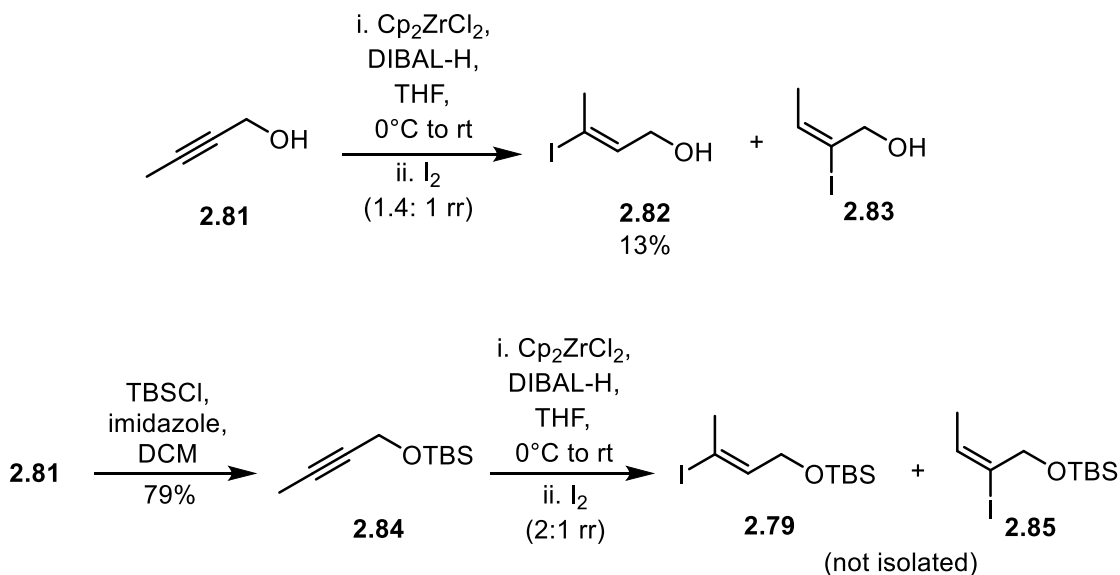
We envisioned that these ether-bridged substrates could also be made through a modular route (Scheme 2.17). In the final steps, the α,β -unsaturated aldehyde could be installed through reduction of ester **2.77** to the aldehyde, followed by α -methylenation. The ether-bridge in ester **2.77** could be made through a Mitsunobu reaction between allylic alcohol **2.78** and phenols with varying substitution. Allylic alcohol **2.78** could be made through a cross-coupling reaction between vinyl iodide **2.79** and alkyl halide **2.80**. Vinyl iodide could then be made through a hydrometallation-iodination from commercially available 2-butynol (**2.81**).



Scheme 2.17. Retrosynthetic analysis of ether-bridged substrates.

In the synthesis of vinyl iodide **2.79**, we initially performed a hydrozirconation with Cp_2ZrCl_2 and DIBAL-H to generate zirconocene hydrochloride *in situ*, followed by trapping of the resulting alkenyl metal species with iodine (Scheme 2.18). This hydrometallation-iodination suffered from low regioselectivity, providing desired vinyl iodide **2.82** in a 1.4:1 ratio with its

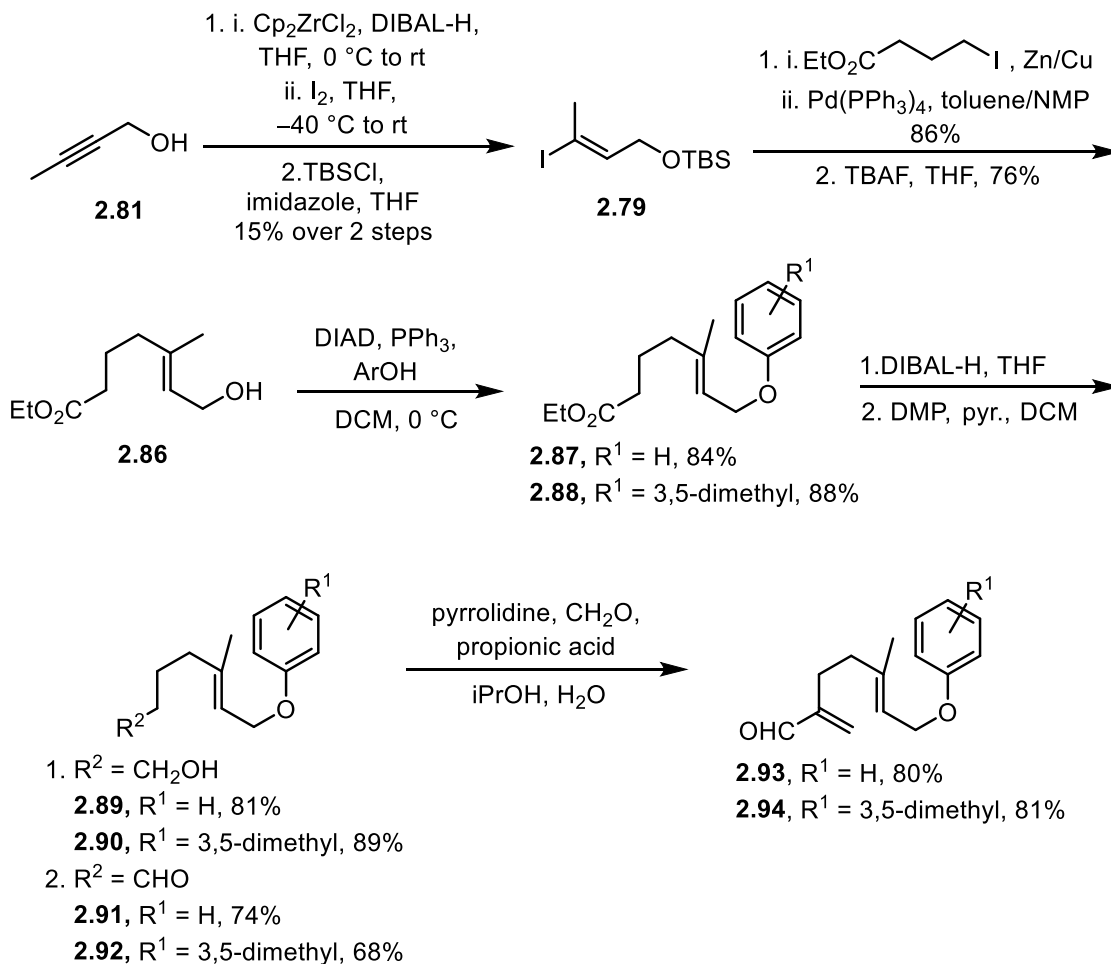
regioisomer **2.83**. A difficult separation of these regioisomers resulted in an isolated yield of 13% of the desired vinyl iodide **2.82**. The hydrometallation of **2.81** lacks a strong steric bias for the addition of the metal to either carbon of the alkyne. We attempted to increase this steric bias by initially protecting the alcohol as the bulky silyl ether **2.84**. In the hydrometallation-iodination of silyl ether **2.84**, the regioselectivity was slightly improved, providing a mixture of desired vinyl iodide **2.79** and its regioisomer **2.85** in a 2:1 ratio. However, these products were inseparable by column chromatography.



Scheme 2.18. Synthesis of vinyl iodide coupling partner.

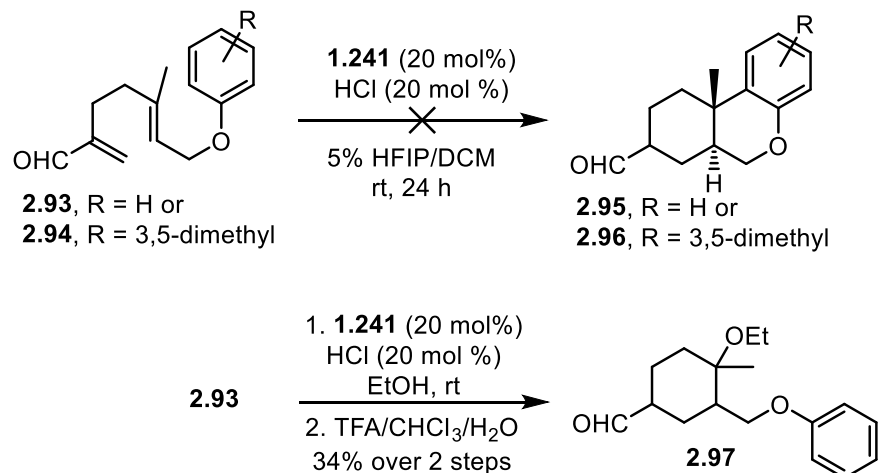
As the regioisomeric products were separable, the hydrometallation-iodination was performed on 2-butynol. To minimize volatility issues, protection of the alcohol as the silyl ether was performed prior to concentration of the solution of isolated product **2.82**, providing product **2.79** in 15% yield over two steps (Scheme 2.19). A Negishi cross-coupling was then performed between vinyl iodide **2.78** and the zinc halide formed from ethyl iodobutyrate to provide (*E*)-olefin in 86% yield. Deprotection of the silyl ether with TBAF gave the alcohol coupling partner **2.86** in 76% yield. A Mitsunobu reaction was then performed between a phenol and the allylic alcohol **2.86**. With phenol itself, this proceeded to give ester **2.87** in 85% yield while reaction with 3,5-dimethylphenol yielded ester **2.88** in 88% yield. Reduction of the ester with DIBAL-H proceeded to give alcohols **2.89** and **2.90** in 81% and 89% yield, respectively. This was followed by oxidation with DMP buffered with pyridine to give aldehydes **2.91** and **2.92** in 74% and 68% yields,

respectively. An α -methylenation by pyrrolidine-mediated aldol condensation with formaldehyde provided final ether-bridged substrates **2.93** and **2.94** in 80% and 81% yields, respectively.



Scheme 2.19. Synthesis of ether-bridged substrates **2.93** and **2.94**.

The polyene cyclization of ether-bridged substrates was attempted under the standard conditions (Scheme 2.20). No bicyclic product was obtained with substrate **2.93**, terminated by a phenyl ring, or substrate **2.94**, terminated by a 3,5-dimethylphenyl ring, with mostly starting material observed after 24 hours. When the reaction was run with EtOH as a solvent, no bicyclic product was observed in the reaction of **2.93**, and only EtOH trapped product **2.97** was isolated in a 34% yield after hydrolysis of the ethyl acetal.



Scheme 2.20. Unsuccessful polyene cyclizations of ether-bridged substrates.

The lack of expected reactivity can be explained by the alignment of the lone pair orbitals in the transition state for the closure of the second ring (Figure 2.4). A substrate with methoxy substitution *para*- to the site of desired reaction on the aromatic ring will lead to transition state **2.98**. The free rotation about the C-O bond of the aromatic ring and the methoxy oxygen allows proper orbital alignment for participation of the oxygen lone pair in resonance stabilization, as shown in the Newman projection below. A substrate with an ether bridge *ortho*- to the site of desired reaction will lead to transition state **2.99**, where the rotation about the C-O bond between the aromatic ring and the oxygen is restricted due to the chair-like conformation of the substrate. The restricted conformation places the orbitals of the lone pair electrons on the oxygen out of alignment for resonance donation, as shown in the Newman projection below. Without this resonance stabilization, only the inductively electron-withdrawing character of the oxygen is present, and the ether bridge lowers the nucleophilicity of the terminating aromatic.

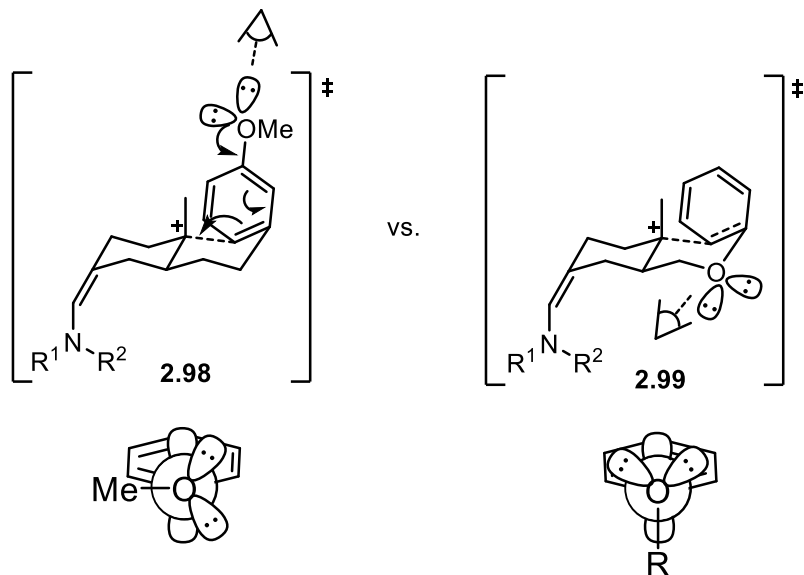


Figure 2.4. Orbital alignment and resonance donation in the transition state of a substrate with a methoxy-substituted arene vs. an ether-bridged substrate.

2.7 Proposed mechanism of the iminium-catalyzed polyene cyclization

Preliminary calculations on the Cope rearrangement had suggested that the reaction proceeded through a stepwise mechanism through a shallow energy intermediate cyclohexyl cation. The addition of a methyl group to the Cope substrate was shown to stabilize this intermediate. In the polyene cyclization, we propose that the reaction proceeds through a similar stepwise pathway (Figure 2.5). In the first step of our proposed mechanism, catalyst **1.241** condenses onto the aldehyde of the substrate to form the initial iminium **2.100**. This iminium then undergoes the first ring closure to give the intermediate cyclohexyl cation **2.2**. The second ring closure results in the arenium ion **2.103** and then deprotonation gives enamine **2.104**. Hydrolysis releases the catalyst as well as the final decalin product **2.3**. DFT calculations have further corroborated a stepwise pathway with substrates terminated by less nucleophilic aromatic rings and have suggested a concerted pathway following the first transition state for substrates terminated by strongly nucleophilic aromatic rings, as will be discussed in Chapters 3 and 4.

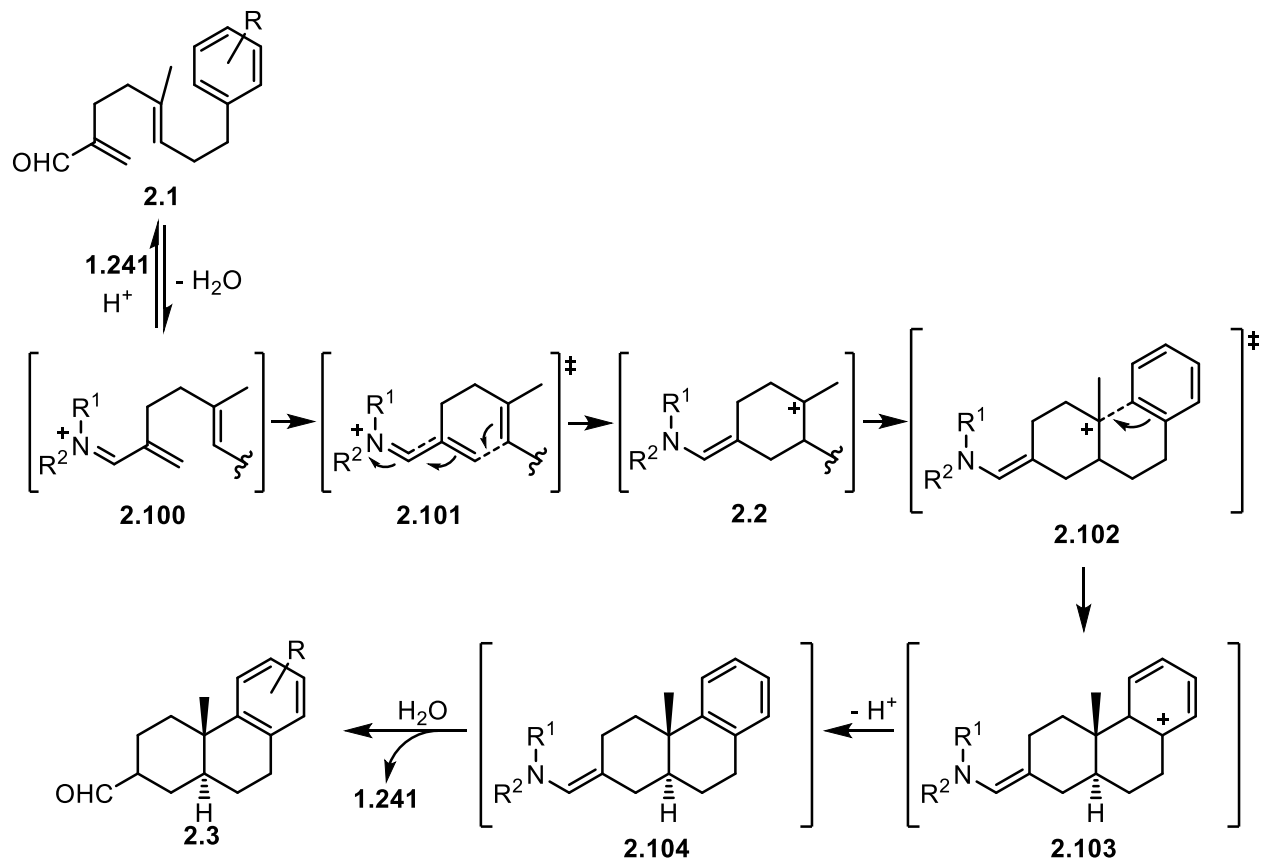
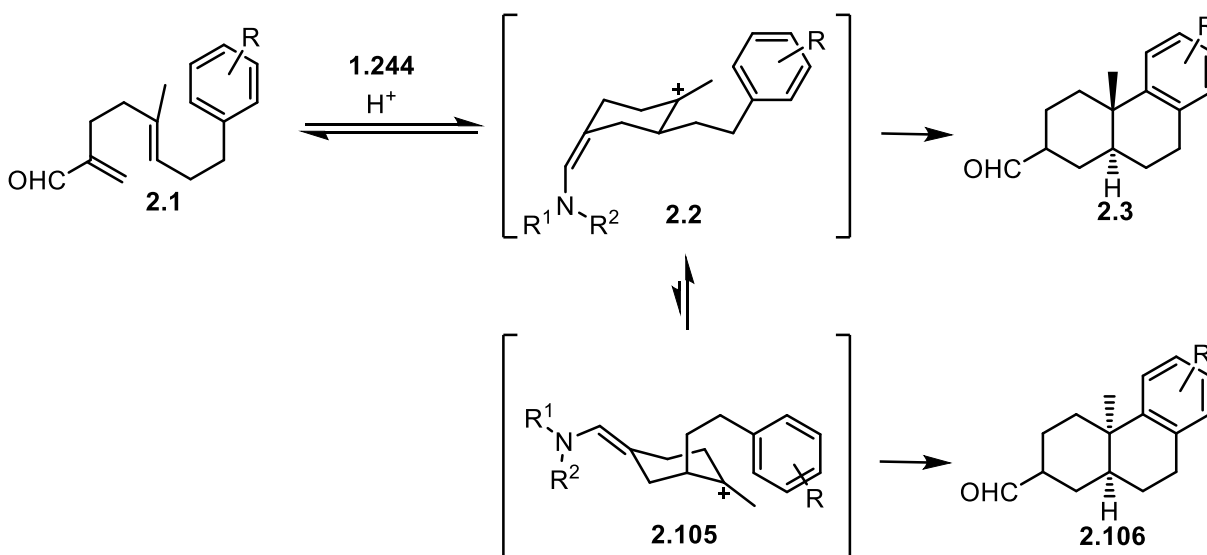


Figure 2.5. Proposed mechanism for the iminium-catalyzed polyene cyclization.

Experimental evidence of a stepwise pathway has also been observed. Monocyclic products isolated from the solvent trapping of substrates with less nucleophilic terminating groups in nucleophilic solvents as well as products from elimination in non-nucleophilic solvents suggest the presence of a cyclohexyl cation intermediate. Additionally, the small amount of isomerization to the *cis*-decalin products observed is further evidence of a cyclohexyl cation intermediate. We presume that the mechanism of isomerization is through a ring flip of the chair-like cyclohexyl cation intermediate (**2.2**), where trapping of the ring-flipped intermediate (**2.105**) would lead to the *cis*-decalin product **2.106** (Scheme 2.21). The activation barrier for trapping of the initial cyclohexyl cation intermediate **2.2** by the arene would be lower for more nucleophilic terminating groups and would therefore proceed more readily. In substrates with less nucleophilic terminating groups, the barrier would be higher, giving a greater propensity for the ring flip to occur and resulting in a higher amount of *cis*-decalin product from the (*E*)-olefin cyclization. Alternatively,

bond rotation of the aryl ethyl group would lead to an intermediate which would place the aryl group above the cyclohexyl cation and would also result in the *cis*-decalin product upon trapping.



Scheme 2.21. Proposed mechanism of isomerization in the iminium-catalyzed (*E*)-polyene cyclization.

2.8 Conclusions

Ethyl 1,2-diazepane-1-carboxylate (**1.241**) has proven to successfully catalyze the first iminium-catalyzed polyene cyclization. Polyene substrates were synthesized that contained a similar 1,5-hexadiene with a pendant formyl group at the 2-position as substrates for the iminium-catalyzed Cope rearrangement, with the addition of an aromatic ring as the terminating group. We have proposed a stepwise mechanism of the iminium-catalyzed polyene cyclization which proceeds through the formation of an intermediate cyclohexyl cation from the initial ring closure and is trapped by the terminating group. Solvent choice was important in the cyclization of substrates that had less nucleophilic terminating groups to minimize the formation of monocyclic side products. Through a solvent screen, the optimized solvent mixture of 5% DCM/HFIP was discovered, with which the scope of the iminium-catalyzed polyene cyclizations was expanded to include substrates with terminating groups with strong to intermediate nucleophilicities, including several heterocycles.

This methodology provides a complementary approach to other reported polyene cyclization methodology, where most of the current methodology relies on initiation through

electrophilic activation of an alkene or epoxide. Iminium catalysis promotes the polyene cyclization without the use of strong acids and does not require substitution of the initiating olefin, providing access to decalin systems without *gem*-dimethyl substitution. Limitations of the methodology include the increased isomerization to the *cis*-decalin systems and decreased reactivity with substrates terminated by less nucleophilic aromatic rings. Chapter 3 will investigate the incorporation of extended aromatics onto the hydrazone catalyst, which stabilizes cationic intermediates and transition states and overcomes some of these limitations.

2.9 References

1. Kaldre, D.; Gleason, J. L., An Organocatalytic Cope Rearrangement. *Angew. Chem. Int. Ed.* **2016**, *55* (38), 11557-11561.
2. Kaldre, D. Development of hybrid drugs for cancer treatment and studies in asymmetric organocatalysis. McGill University, 2016.
3. Häggman, N. O.; Zank, B.; Jun, H.; Kaldre, D.; Gleason, J. L., Diazepane Carboxylates as Organocatalysts in the Diels-Alder Reaction of α -Substituted Enals. *Eur. J. Org. Chem.* **2018**, *2018* (39), 5412-5416.
4. Austin, J. F.; Macmillan, D. W. C., Enantioselective Organocatalytic Indole Alkylations. Design of a New and Highly Effective Chiral Amine for Iminium Catalysis. *J. Am. Chem. Soc.* **2002**, *124* (7), 1172-1173.
5. Plamondon, S. J. Development of an asymmetric hydrazone-catalyzed polyene cyclization and its application to the total synthesis of (-)-3-oxoisotaxodione. McGill University, Montreal, 2021.
6. Kocienski, P.; Wadman, S.; Cooper, K., A stereoselective synthesis of functionalized alkenyllithiums and alkenyl cyanocuprates by the copper(I)-catalyzed coupling of organolithium reagents with α -lithiated cyclic enol ethers. *J. Am. Chem. Soc.* **1989**, *111* (6), 2363-2365.
7. Kocienski, P.; Barber, C., Synthetic applications of metallate rearrangements. *Pure Appl. Chem.* **1990**, *62* (10), 1933-1940.
8. Rand, C. L.; Van Horn, D. E.; Moore, M. W.; Negishi, E., A versatile and selective route to difunctional trisubstituted (E)-alkene synthons via zirconium-catalyzed carboalumination of alkynes. *J. Org. Chem.* **1981**, *46* (20), 4093-4096.
9. Reichardt, C.; Welton, T., Empirical Parameters of Solvent Polarity. In *Solvents and Solvent Effects in Organic Chemistry*, 2010; pp 425-508.

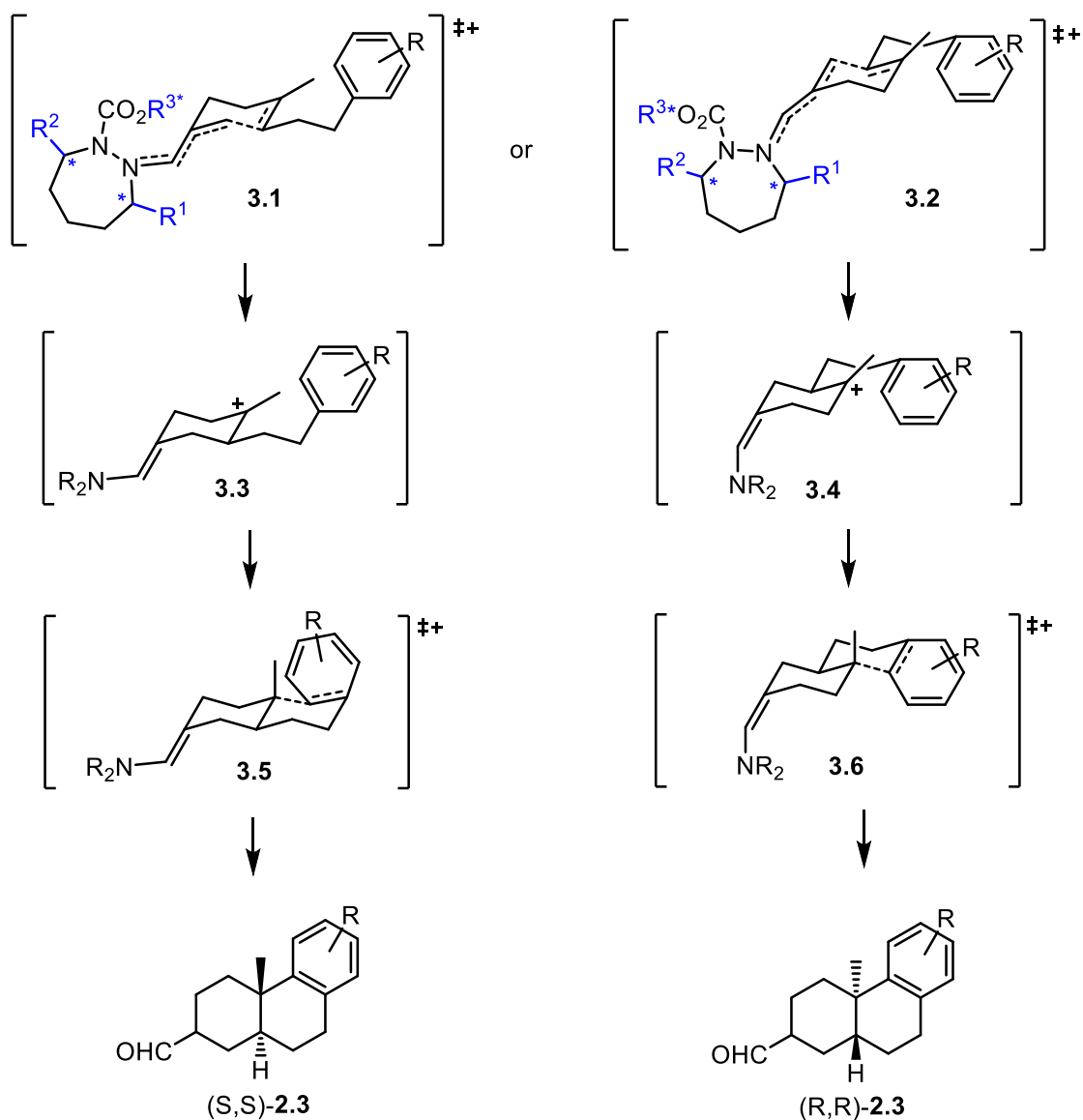
10. Colomer, I.; Chamberlain, A. E. R.; Haughey, M. B.; Donohoe, T. J., Hexafluoroisopropanol as a highly versatile solvent. *Nat. Rev. Chem.* **2017**, *1* (11), 0088.
11. Pozhydaiev, V.; Power, M.; Gandon, V.; Moran, J.; Lebœuf, D., Exploiting hexafluoroisopropanol (HFIP) in Lewis and Brønsted acid-catalyzed reactions. *Chem. Commun.* **2020**, *56* (78), 11548-11564.
12. Tao, Z.; Robb, K. A.; Zhao, K.; Denmark, S. E., Enantioselective, Lewis Base-Catalyzed Sulfenocyclization of Polyenes. *J. Am. Chem. Soc.* **2018**, *140* (10), 3569-3573.
13. Arnold, A. M.; Pöthig, A.; Drees, M.; Gulder, T., NXS, Morpholine, and HFIP: The Ideal Combination for Biomimetic Haliranium-Induced Polyene Cyclizations. *J. Am. Chem. Soc.* **2018**, *140* (12), 4344-4353.
14. Lemmerer, M.; Riomet, M.; Meyrelles, R.; Maryasin, B.; González, L.; Maulide, N., HFIP Mediates a Direct C–C Coupling between Michael Acceptors and Eschenmoser's salt. *Angew. Chem. Int. Ed.* **2022**.
15. Filler, R.; Schure, R. M., Highly acidic perhalogenated alcohols. A new synthesis of perfluoro-tert-butyl alcohol. *J. Org. Chem.* **1967**, *32* (4), 1217-1219.
16. International Union of, P.; Applied Chemistry. Commission on Equilibrium, D.; Serjeant, E. P.; Dempsey, B., *Ionisation constants of organic acids in aqueous solution*. Pergamon Press: Oxford ;, 1979.
17. Plamondon, S. J.; Warnica, J. M.; Kaldre, D.; Gleason, J. L., Hydrazide-Catalyzed Polyene Cyclization: Asymmetric Organocatalytic Synthesis of cis -Decalins. *Angew. Chem. Int. Ed.* **2020**, *59* (1), 253-258.
18. Joule, J. A.; Mills, K.; Smith, G. F., *Heterocyclic Chemistry*. **2020**.
19. Brown, H. C.; Okamoto, Y., Electrophilic Substituent Constants. *J. Am. Chem. Soc.* **1958**, *80* (18), 4979-4987.
20. Surendra, K.; Qiu, W.; Corey, E. J., A Powerful New Construction of Complex Chiral Polycycles by an Indium(III)-Catalyzed Cationic Cascade. *J. Am. Chem. Soc.* **2011**, *133* (25), 9724-9726.
21. Nakamura, S.; Ishihara, K.; Yamamoto, H., Enantioselective Biomimetic Cyclization of Isoprenoids Using Lewis Acid-Assisted Chiral Brønsted Acids: Abnormal Claisen Rearrangements and Successive Cyclizations. *J. Am. Chem. Soc.* **2000**, *122* (34), 8131-8140.

Chapter 3. Exploration of cation– π interactions in the iminium-catalyzed (*E*)-polyene cyclization

3.1 Chiral catalyst design

In Chapter 2, it was demonstrated that cyclic hydrazide catalyst **1.241** could mediate the iminium-catalyzed polyene cyclization of 1,5-hexadiene, 2-carboxaldehyde substrates with a terminating aromatic ring. The 7-membered ring scaffold of the hydrazide catalyst provided an opportunity for the design of a chiral catalyst for the asymmetric reaction. When considering catalyst designs for the asymmetric version, we initially looked at the transition state leading to the first ring closure (**3.1** and **3.2**, Scheme 3.1) that forms the first stereocenter in the decalin product ((*S,S*)-**2.3** or (*R,R*)-**2.3**). The second stereocenter is set by the *trans*-decalin like transition state of the second ring closure (**3.5** and **3.6**). The prochiral carbon on the polyene substrates is distanced from the catalyst and the flatness of the ring system has required bulky catalysts to provide remote induction of stereochemistry in previously reported examples of enantioselective polyene cyclizations (seen in Section 1.4.4). In the iminium-catalyzed polyene cyclization, there were several considerations in the design of a chiral catalyst. The first is the preferred conformation of the iminium ion. Computational analysis of the reaction with catalyst **1.241** had shown a preference for the (*Z*)-iminium, although it is possible that addition of steric bulk in a chiral catalyst would alter this preference. Additionally, the α,β -unsaturated iminium can be found in the *s-cis* or *s-trans* conformations. If one of these conformations is strongly preferred, then the enantioselectivity of the first ring closure depends on the facial selectivity of the addition to the terminal olefin. However, if both the *s-cis* and *s-trans* conformations are viable, enantioinduction becomes more difficult.

In the design of a chiral catalyst, there were three positions on the cyclic hydrazide scaffold that were considered for chiral substitution (highlighted in blue, Scheme 3.1). These positions, at the carbon α to the free N-H (R^1), the carbon α to the carbamate (R^2), and on the carbamate (R^3), were chosen due to their proximity to the bond formation in the first ring closure and thus were more likely to provide a discriminating interaction between diastereomeric conformations of this transition state. The other positions on the 7-membered ring were not considered for addition of chirality as they are further removed from the substrate.

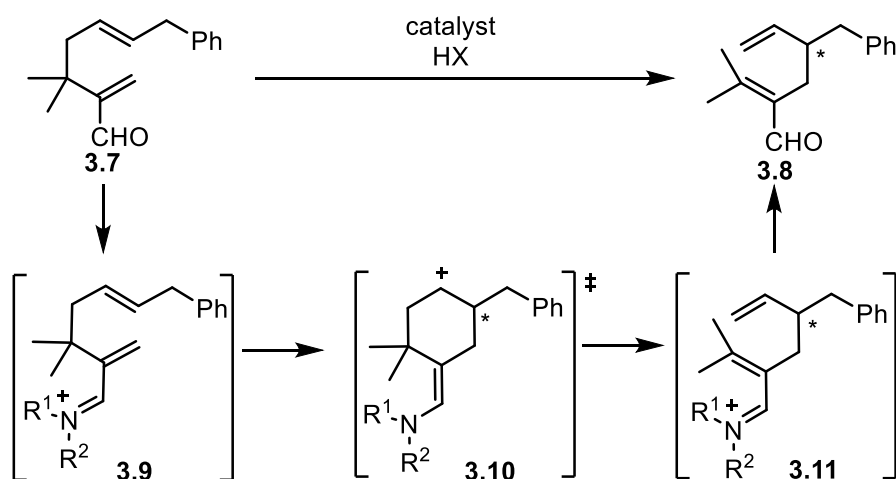


Scheme 3.1. Positions of possible chiral substitution on the 7-membered ring hydrazide catalyst.

3.2 Asymmetric iminium-catalyzed Cope rearrangement

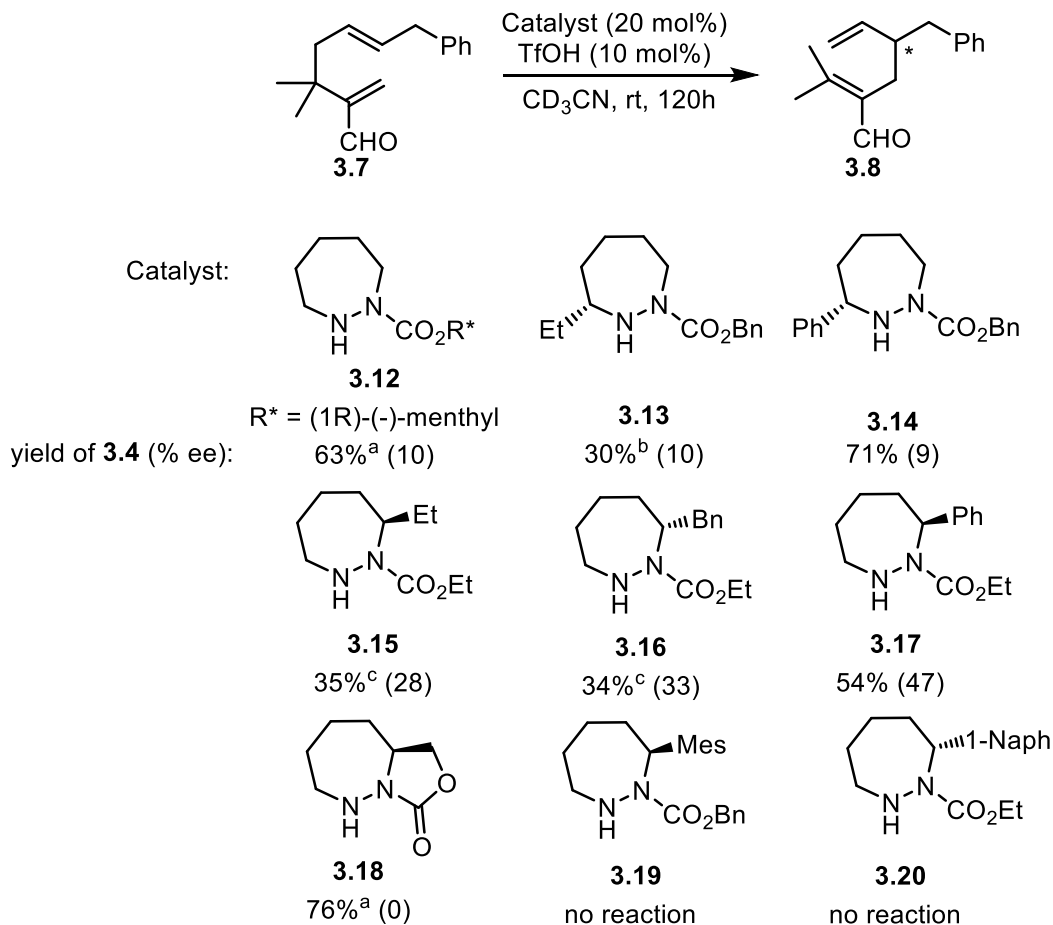
In the proposed mechanism of the asymmetric Cope rearrangement of model substrate **3.7**, following the formation of the α,β -unsaturated iminium ion (**3.9**), the reaction proceeds through closure of the ring to cyclohexyl cation **3.10** (Scheme 3.2). Due to the shared structural feature with the (*E*)-polyene cyclization of an enantiodetermining ring closure from the donation of the π -electrons from an (*E*)-olefin, we hypothesized that similar catalyst scaffolds would provide optimal enantioselectivity in both reactions. Therefore, in the initial investigation of the asymmetric (*E*)-

polyene cyclization, 7-membered ring catalysts with chiral substitution α to the carbamate were synthesized and screened.



Scheme 3.2. Mechanism of Cope rearrangement of substrate **3.7**.

Chiral catalysts, shown in Scheme 3.3, were synthesized for the induction of asymmetry in the iminium-catalyzed Cope rearrangement (work done by Dr. Dainis Kaldre). These catalysts were screened in the Cope rearrangement of substrate **3.7** to effect the enantioselective formation of product **3.8**. Chiral substitution at position R^3 gave very little enantioinduction, with the addition of a menthyl carbamate on catalyst **3.12** providing product **3.8** in 10% ee. Very little enantioinduction was also achieved with catalysts where the stereocenter was next to R^1 , such as the ethyl substituent in **3.13** providing product in 10% ee and bulkier phenyl substitution in **3.14** providing product in 9% ee. Out of the catalysts screened, those with substitution at R^2 gave the highest achieved enantioselectivity. Ethyl substitution in catalyst **3.15** provided product **3.8** in 28% ee and benzyl substitution at this position in catalyst **3.16** gave a similar 33% ee. With more sterically hindered phenyl substitution α to the carbamate in catalyst **3.17**, the highest enantioselectivity was observed, with product **3.8** obtained in a 47% ee. Finally, rigid bicyclic catalyst **3.18** provided a 76% yield of product **3.8**. However, no enantioselectivity was observed.



[a] After 24 h. [b] After 48 h. [c] After 72 h.

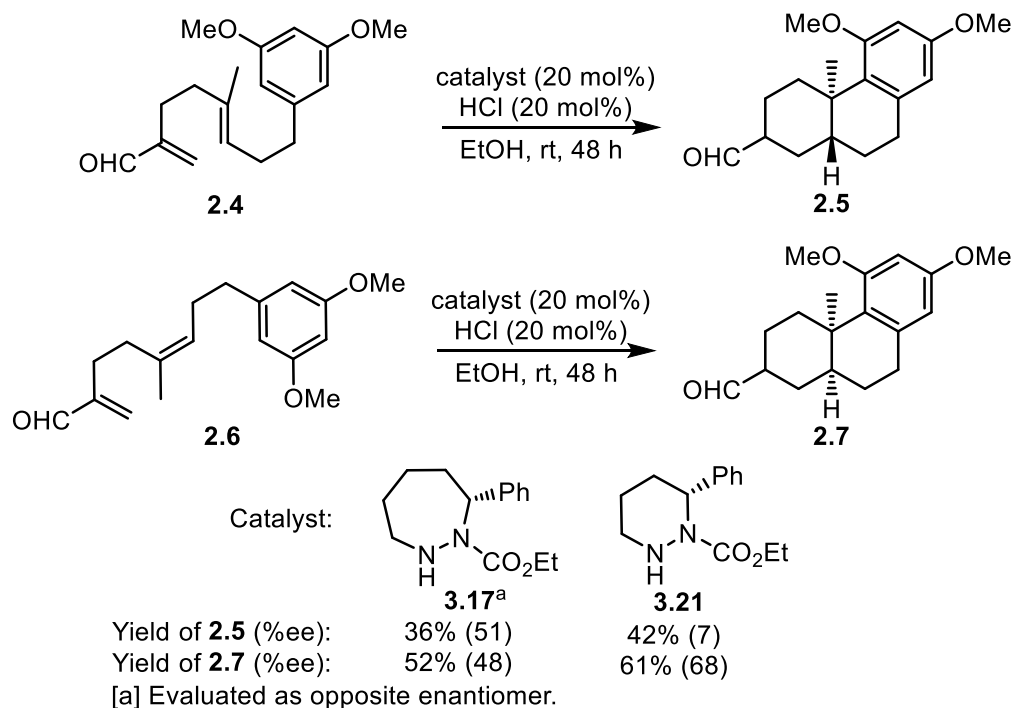
Scheme 3.3. Catalyst screen for the asymmetric iminium-catalyzed Cope rearrangement. (Work done by Dr. Dainis Kaldre).

It was interesting that catalyst **3.17** provided the highest enantioselectivity as, out of the substitution possibilities considered, it had a stereocenter furthest removed from the iminium. It was proposed that the bulky phenyl substituent in catalyst **3.17** geared the carbamate forward, partially blocking one face of the α,β -unsaturated iminium to induce enantioselectivity. Further attempts to increase the enantioselectivity were made by introducing larger substitution at this position. However, the addition of mesityl or naphthyl substitution in catalysts **3.19** and **3.20** resulted in no catalyst reactivity. Presumably these catalysts were too bulky to allow iminium ion formation.

3.3 Initial work on the asymmetric iminium-catalyzed polyene cyclization

Initial screening of chiral catalysts for the asymmetric (*E*)-polyene cyclization was done by Dr. Dainis Kaldre and Dr. Samuel Plamondon. For the initial screening of chiral catalysts, the polyene cyclization was performed on model substrates **2.4** and **2.6**, with nucleophilic terminating aromatic rings. As in the racemic iminium-catalyzed polyene cyclization, these substrates were chosen for screening due to the low activation barrier expected for the trapping of the aromatic ring, which reduces the possibility of reversibility in the first ring closure and potential equilibration.

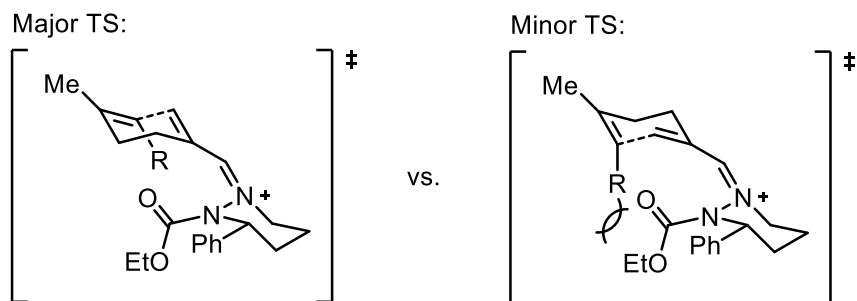
Phenyl catalyst **3.17**, which had achieved the highest enantioselectivity in the asymmetric Cope rearrangement, provided product **2.5** in 36% yield and 51% ee (Scheme 3.4). This catalyst gave similar results for both the (*E*)- and (*Z*)-polyene substrates, with the cyclization of the model (*Z*)-polyene substrate giving product **2.7** in 52% yield and 48% ee. Interestingly, the enantioselectivity of the cyclization for the two substrates diverged when investigating 6-membered ring catalysts. With phenyl substituted 6-membered ring catalyst **3.21**, the *trans*-decalin product **2.5** was obtained from (*E*)-polyene **2.4** in 7% ee, whereas the *cis*-decalin product **2.7** was obtained from (*Z*)-polyene **2.6** in 68% ee.



Scheme 3.4. Initial asymmetric polyene cyclization. (Work done by Dr. Samuel Plamondon).

The 6-membered ring catalysts can adopt more rigidly defined conformations, which should be beneficial in asymmetric synthesis. In the (*Z*)-polyene substrates, the steric bulk of the aryl ethyl group (*R*) lies in an axial configuration in the transition state leading to the first ring closure (Figure 3.1). In contrast, in the (*E*)-polyene substrates, the aryl ethyl group lies in an equatorial configuration, placing it further removed from potential steric interactions with the catalyst.

With (*Z*)-polyene substrates:



With (*E*)-polyene substrates:

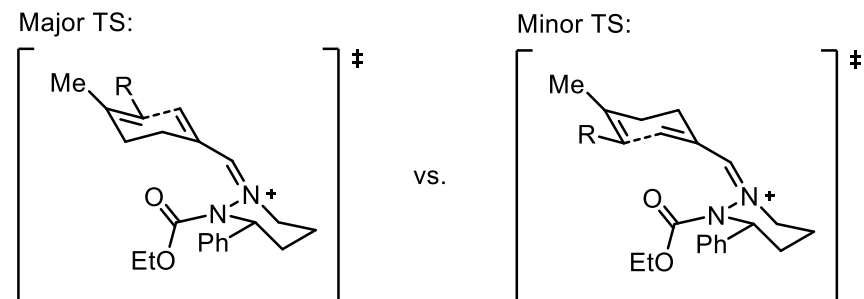
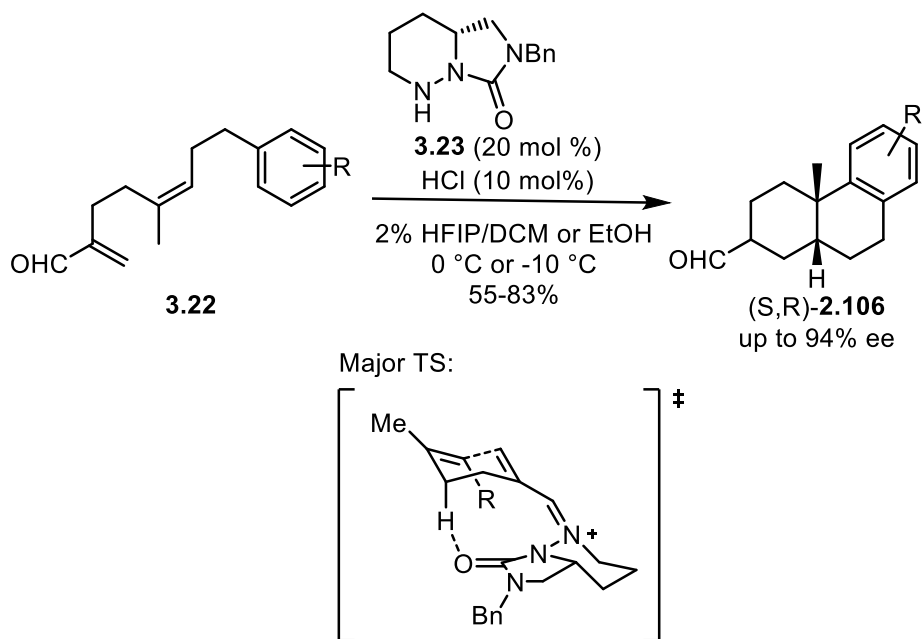


Figure 3.1. Comparison of the transition state for the first ring closure for (*Z*)- and (*E*)-polyene substrates with catalyst **3.21**.

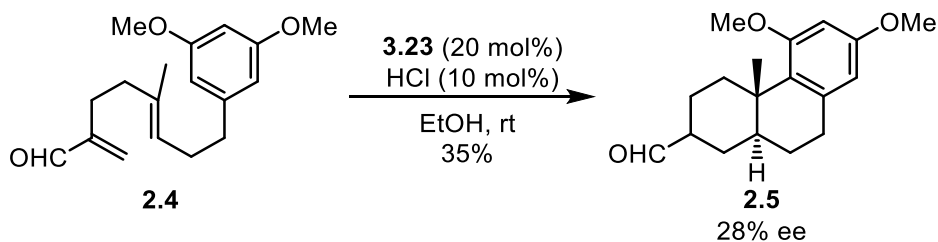
3.4 Asymmetric (*Z*)-polyene cyclization

With the 6-membered rings providing promising enantioselectivities in the (*Z*)-polyene cyclizations, Dr. Samuel Plamondon undertook further investigation.¹ Through this investigation, it was discovered that catalyst **3.23** effected the asymmetric cyclization of (*Z*)-polyene substrates (**3.22**) to give products ((*S,R*)-**2.106**) in yields of 55-83% and up to 94% ee (Scheme 3.5). Based on DFT calculations, evidence was found in the major transition state for an electrostatic interaction between the carbonyl of catalyst **3.23** and the axial C-H of the electron-poor substrate. This interaction was blocked by the aryl ethyl group of the substrate in the transition state with the

s-cis iminium conformation. In the polyene cyclization of (*E*)-olefin model substrate **2.4** with bicyclic catalyst **3.23**, this stabilizing interaction could occur in the first transition state in both *s-cis* and *s-trans* conformations, and product **2.5** was obtained in a significantly lower 28% ee (Scheme 3.6).



Scheme 3.5. Asymmetric iminium-catalyzed (*Z*)-polyene cyclization. (Work done by Dr. Samuel Plamondon).



Scheme 3.6. Iminium-catalyzed cyclization of (*E*)-polyene substrate **2.4** with bicyclic hydrazide catalyst **3.23**. (Work done by Dr. Samuel Plamondon).

3.5 Incorporation of extended aromatics into chiral catalysts

Based on preliminary results from the asymmetric iminium-catalyzed (*E*)-polyene cyclization, we hypothesized that the 7-membered ring hydrazide catalyst with substitution α to the carbamate would provide the highest levels of enantioselectivity. In the asymmetric Cope rearrangement, it had been found that any increases in steric bulk from a phenyl substituent had

shut down the reactivity of the catalyst presumably due to the difficult iminium ion formation. However, we hypothesized that the iminium ion formation would not be as hindered in the asymmetric polyene cyclization as substrates lacked the *gem*-dimethyl substitution as seen in Cope substrate **3.7**.

A successful catalyst had been designed for the (*Z*)-polyene cyclization which had induced high levels of enantioselectivity through a stabilizing interaction between the catalyst and substrate in the lowest energy conformation of the first transition state. With this success, and drawing inspiration from the enzymatic polyene cyclization, we hypothesized that we could effect enantioselectivity in the iminium-catalyzed (*E*)-polyene cyclization through selective stabilization in the first transition state. We postulated that the incorporation of extended aromatics in the catalyst could differentiate the energies of diastereomeric conformations of the first transition state by either electronic or steric effects (Figure 3.2), rendering the reaction asymmetric. As we were looking to provide selective stabilization of cationic charge in the substrate, the initial catalyst design incorporated an extra carbon into the side chain to decrease the distance between the aromatic and the substrate.

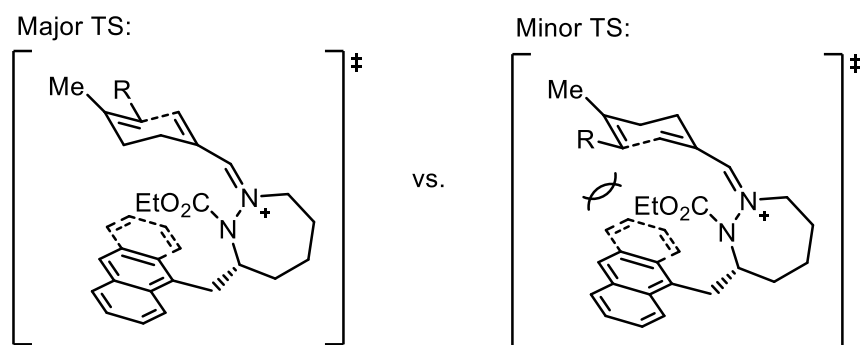
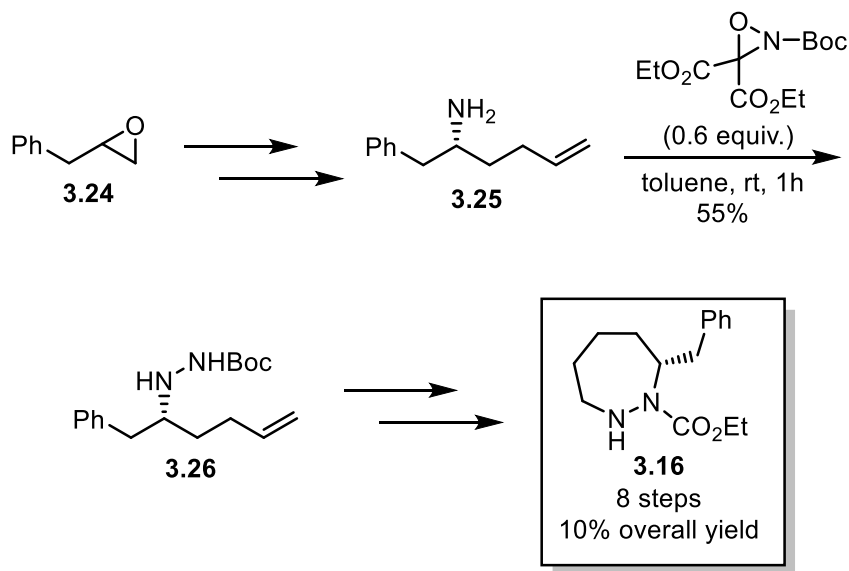


Figure 3.2. Potential mode of enantioinduction in 7-membered ring hydrazide catalyst with extended aromatic substitution.

3.5.1 Initial synthesis of chiral catalysts

Chiral 7-membered ring hydrazide catalysts shown in Scheme 3.3, were previously synthesized by Dr. Dainis Kaldre and Dr. Nicklas Häggman.²⁻³ The syntheses initially developed to build catalysts with bulky substitution at the carbon α to the free N-H (e.g. **3.14**) as well as α to the carbamate (e.g. **3.16** and **3.17**) built out from the substitution. As an example, the original synthesis of catalyst **3.16** was 8 steps from commercially available epoxide **3.24**, which

incorporated the benzyl substitution (Scheme 3.7). The N-N bond of this catalyst was formed by an electrophilic amination with oxaziridine that proceeded in a 55% yield to give hydrazide **3.26**. Further functionalization of the terminal alkene, followed by ring closure and protecting group manipulations resulted in the final catalyst in a 10% overall yield.

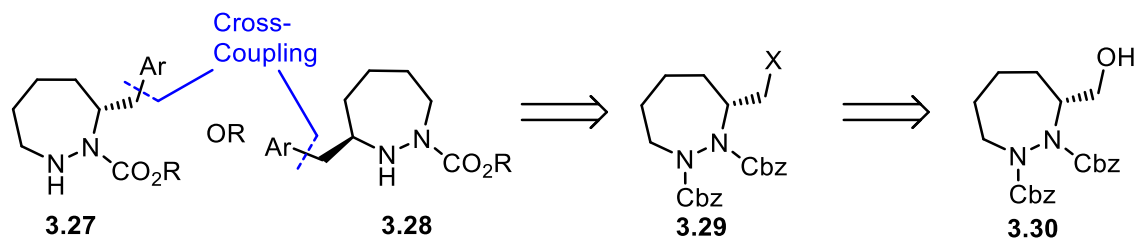


Scheme 3.7. Original synthesis of catalyst **3.16**. (Work done by Dr. Nicklas Häggman).

This route would be difficult to modify to allow the incorporation of different aromatic substitution on the catalyst, as the installation of the benzyl group was early in the synthesis and prior to the ring closure. Therefore, a modular route would be needed to screen different aromatic substitution at this position. All further catalyst design and experimental work has been performed by the author.

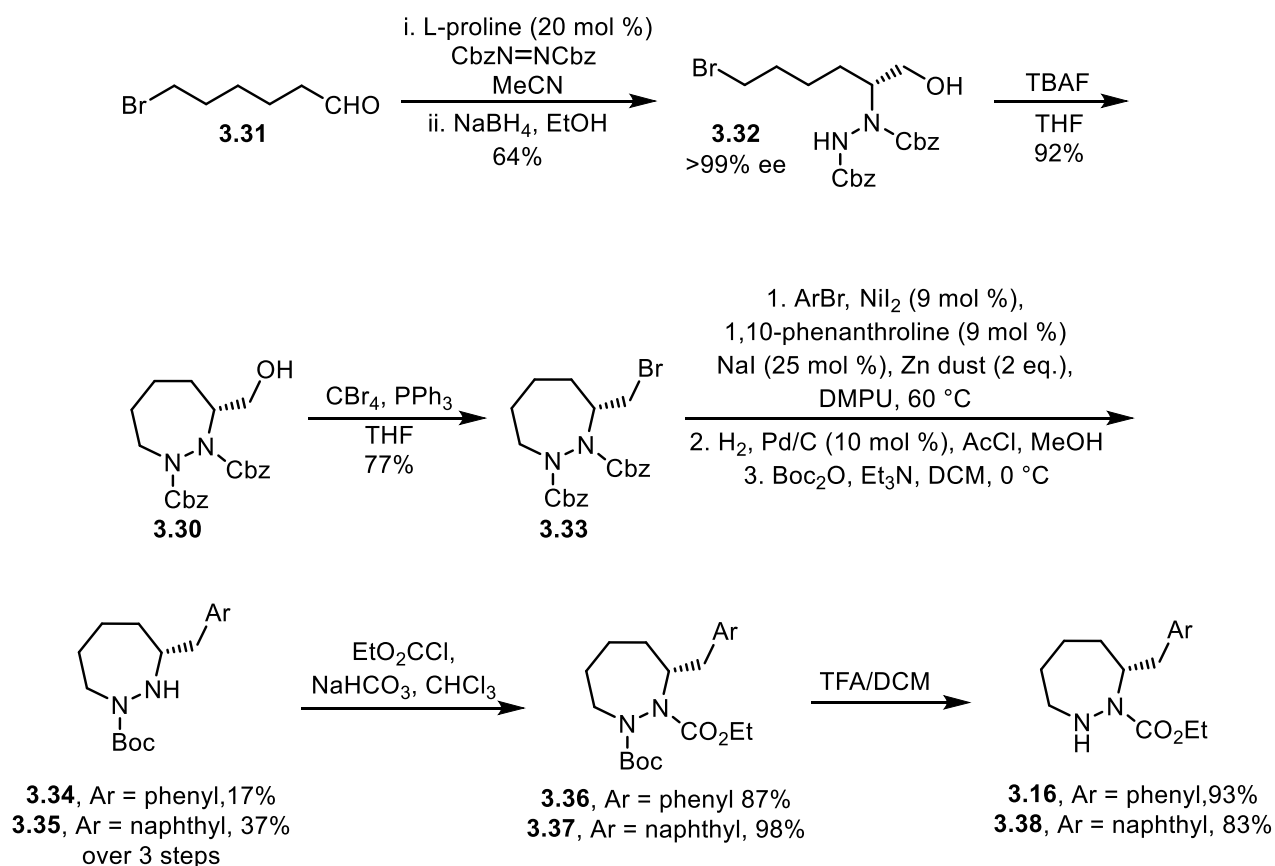
3.5.2 Modular synthesis of catalysts with extended aromatic systems

A retrosynthetic strategy was designed to enable modular synthesis of catalysts containing a variety of large aromatics substitution adjacent to the carbamate (e.g. catalyst **3.27** or **3.28**). To allow a range of catalysts to be prepared with maximum efficiency, a late-stage cross-coupling of the aromatic group was planned (Scheme 3.8). The halide coupling partner **3.29** was envisioned to be made from an Appel reaction on alcohol **3.30**, where a known synthesis had already been developed for the asymmetric iminium-catalyzed Diels-Alder reaction.³



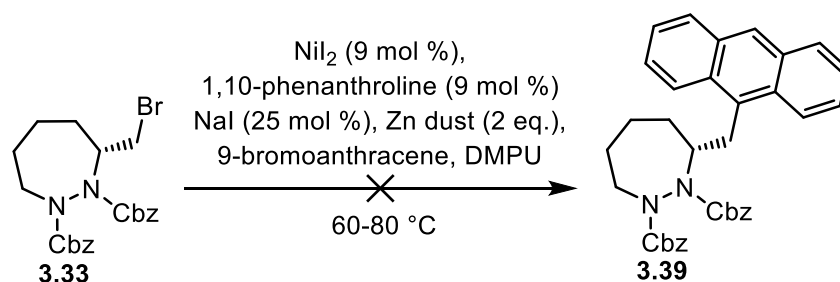
Scheme 3.8. Retrosynthetic analysis for the modular synthesis of catalysts **3.27** and **3.28**.

The synthesis of intermediate alcohol **3.30** began with a proline-catalyzed α -hydrazination of aldehyde **3.31** with dibenzyl azodicarboxylate to install the stereocenter (Scheme 3.9). *In situ* reduction of the resulting alcohol was required to prevent racemization. This reaction was optimized to provide product **3.32** in 64% yield and >99% ee. A TBAF-mediated intramolecular closure of the hydrazide onto the bromide formed the 7-membered ring of intermediate alcohol **3.30**. An Appel reaction then provided the bromide coupling partner **3.33** in 77% yield. Electrophile-electrophile cross-coupling conditions developed by the Weix group⁴ were employed to install the aromatic ring. Under these conditions, the cross-coupled products were formed but these co-eluted with the dehalogenated hydrazide. Deprotection of the benzyl carbamates under acidic conditions gave the free hydrazine as its salt, followed by protection of the less hindered nitrogen as the *tert*-butyl carbamate resulted in products **3.34** and **3.35**. The free base of the unprotected hydrazine is known to quickly oxidize to the corresponding hydrazone. Phenyl cross-coupled product **3.34** was obtained in 17% yield over these three steps and the naphthyl cross-coupled product **3.35** was obtained in 37% yield. Protection of the more hindered nitrogen as the ethyl carbamate led to products **3.36** and **3.37** in 87% and 98% yield, respectively, and the deprotection of the *tert*-butyl carbamate led to the final catalysts **3.16** and **3.38** in 93% and 83% yield, respectively.



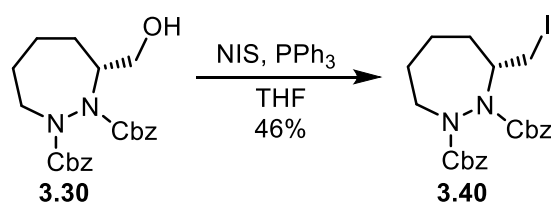
Scheme 3.9. Synthesis of benzyl and naphthyl catalysts **3.16** and **3.38**.

In the investigation of extended aromatic moieties in the chiral hydrazide catalyst, we attempted the synthesis outlined above with 9-bromoanthracene in the cross-coupling step. Under the Weix cross-coupling conditions, no desired product was obtained (Scheme 3.10). Increasing the temperature led to the dehalogenated product which results from Zn insertion into the alkyl halide bond and quenching upon workup.



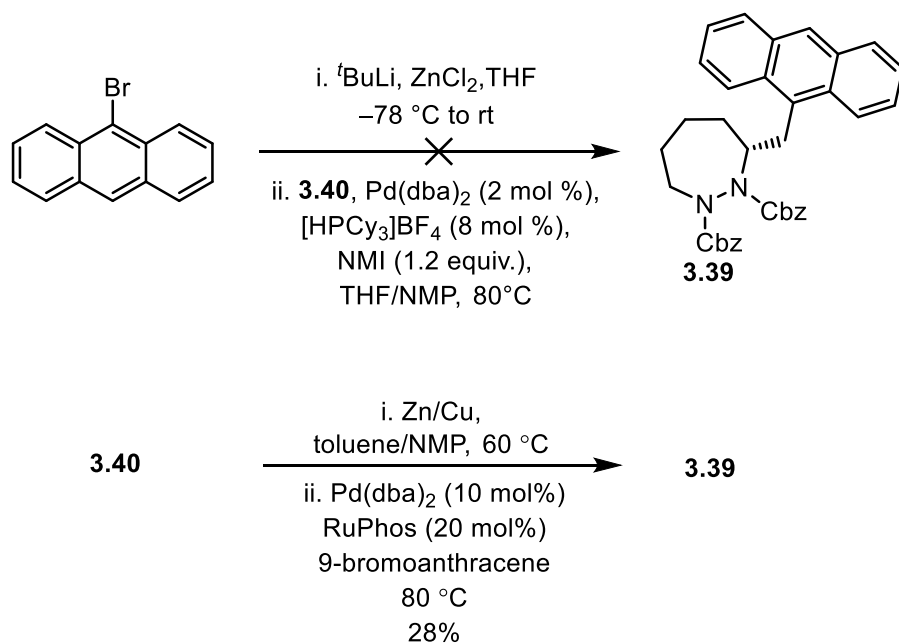
Scheme 3.10. Failed electrophile-electrophile cross-coupling attempt to synthesize anthracene catalyst.

The proposed mechanism of the Weix electrophile-electrophile cross-coupling reaction begins with the oxidative addition of the aryl bromide by a Ni(0) species. This is then followed by the addition of an alkyl radical formed from the reductive cleavage of the alkyl halide bond through a radical chain mechanism.⁵ The steric bulk of the anthracene could disfavour the oxidative addition into the aryl bromide as well as the addition of the alkyl radical. Heating up the reaction promoted the insertion of Zn into the alkyl halide bond, eventually leading to dehalogenated material after work-up. For further screening of cross-coupling conditions, alkyl iodide **3.40** was synthesized to allow for a more favourable oxidative addition into the alkyl halide bond (Scheme 3.11).



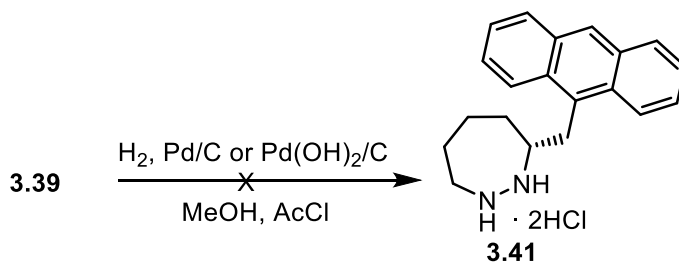
Scheme 3.11. Synthesis of alkyl iodide **3.40**.

Initially, we attempted cross-coupling conditions that avoided the oxidative addition of palladium into the anthracenyl bromide bond by forming the aryl zinc reagent. This was then cross-coupled to the alkyl iodide using conditions that have been developed by Fu to avoid β -hydride elimination of the palladium alkyl species.⁶ However, under these conditions, no desired product was obtained and only dehalogenated anthracene and starting iodide were observed (Scheme 3.12). Conditions were then screened for the Negishi cross-coupling of the alkyl zinc species with 9-bromoanthracene. Zinc/copper couple was used as an activated zinc reagent to reliably generate the aliphatic zinc species. The cross-coupling performed with palladium and an SPhos ligand was unsuccessful. Fortunately, switching to RuPhos as the ligand provided desired cross-coupled product **3.39**, albeit in a low yield of 28%.



Scheme 3.12. Negishi cross-coupling of anthracenyl bromide with iodide **3.40**.

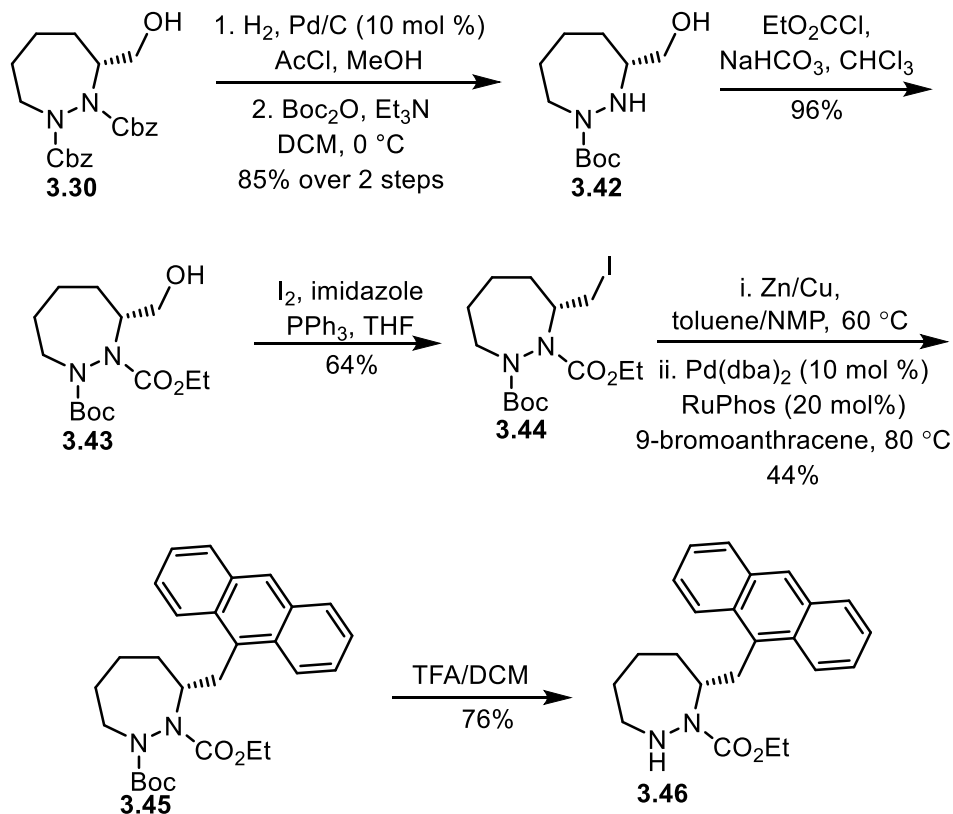
With conditions now developed to synthesize cross-coupled product **3.39**, we attempted to remove both benzyl carbamates. Unfortunately, hydrogenolysis with either Pd/C or Pd(OH)₂/C under acidic conditions and long reaction times led only to a small amount of mono-deprotected product in addition to decomposition of the substrate (Scheme 3.13).



Scheme 3.13. Unsuccessful deprotection of Cbz groups in hydrazide **3.39**.

To circumvent the need for deprotection of the very hindered benzyl carbamate protected hydrazide **3.39**, we performed protecting group manipulations prior to the coupling step (Scheme 3.14). As in the previous synthesis, deprotection of the benzyl carbamates of intermediate **3.30** under acidic conditions followed by protection of the less hindered nitrogen as the *tert*-butyl carbamate resulted in **3.42** in 85% yield over two steps. Protection of the more hindered nitrogen as the ethyl carbamate gave alcohol **3.43** in 96% yield and an Appel reaction provided iodide

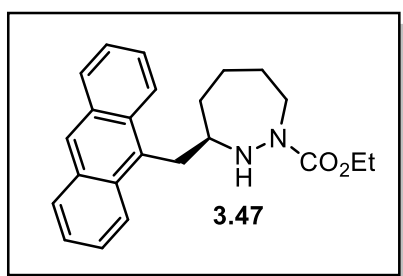
coupling partner **3.44** in 64% yield. The optimized Negishi cross-coupling conditions with anthracenyl bromide led to product **3.45** in 44% yield and deprotection of the *tert*-butyl carbamate led to the final anthracene catalyst **3.46** in 76% yield.



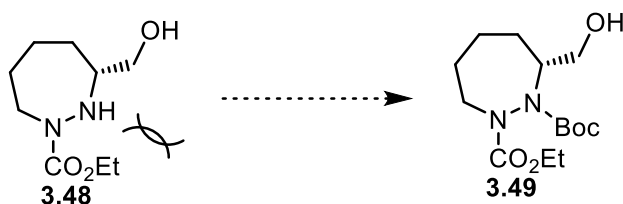
Scheme 3.14. Synthesis of anthracenyl catalyst **3.46**.

As will be discussed in Section 3.4, the addition of extended aromatic substitution α to the carbamate resulted in a more reactive catalyst. In an attempt to further increase reactivity, catalyst **3.47** was synthesized, with anthracenyl substitution α to the free N-H and closer to the substrate after iminium formation. In the initial synthesis of catalyst **3.47**, it was realized that the protecting group strategy was going to be a challenge. Synthesizing this catalyst with the same strategy as in the synthesis of catalyst **3.46** would have required the addition of a *tert*-butyl carbamate to a very hindered position (Scheme 3.15). Attempts to add a *tert*-butyl carbamate to a similar position in a 6-membered ring by Dr. Samuel Plamondon had been unsuccessful. This nitrogen has been protected with benzyl chloroformate (as will be shown in Chapter 4). However, after coupling with anthracenyl bromide, the benzyl carbamate in **3.50** is very hindered. The deprotection of a

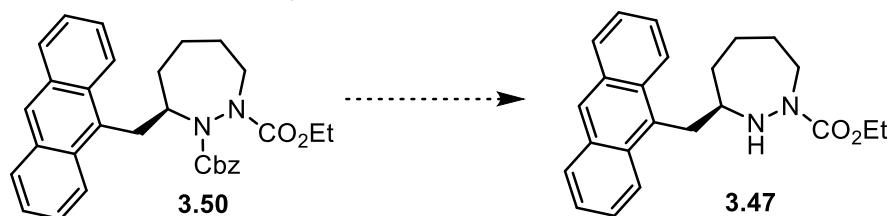
hindered benzyl carbamate at a similar position in hydrazide **3.39** had not been successful. Therefore, a different synthetic strategy was developed for catalyst **3.47**.



Hindered Boc Protection:

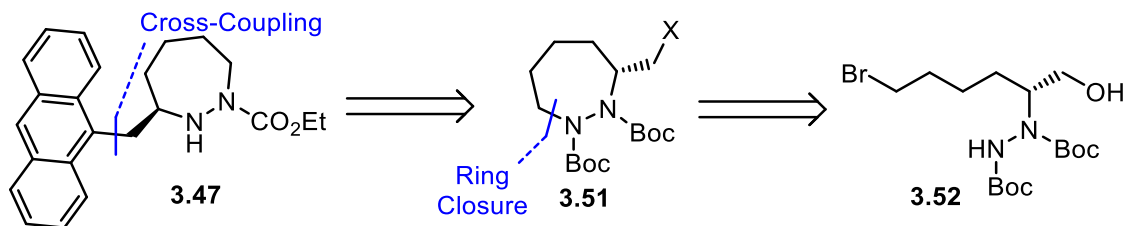


Hindered Cbz Deprotection:



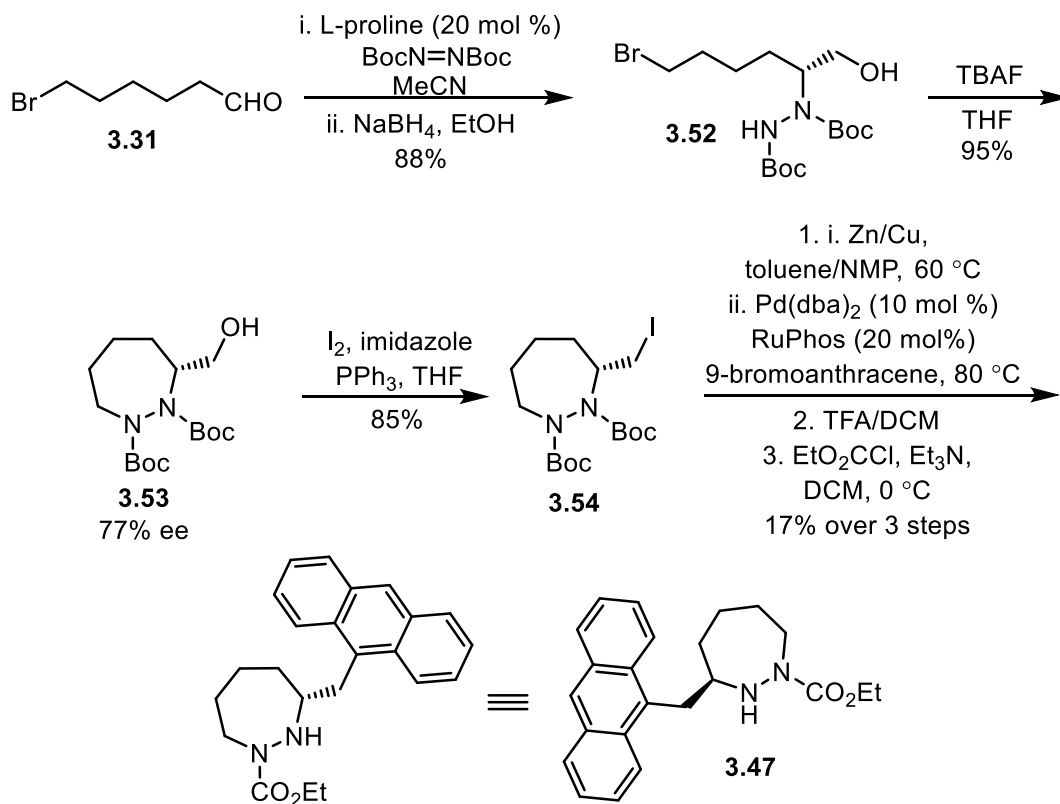
Scheme 3.15. Unrealized synthetic routes to catalyst **3.47**.

The deprotection of dibenzyl carbamates from catalyst **3.39** had been unsuccessful, as the sterically hindered environment of the hydrazide had prevented hydrogenation on a metal surface. Alternatively, the removal of di-*tert*-butyl carbamates proceeds through protonation of the carbamate, which is easier to perform in a sterically hindered environment. So a retrosynthetic analysis of catalyst **3.47** was designed that included a late-stage deprotection of di-*tert*-butyl carbamates (Scheme 3.16). The alkyl halide cross-coupling partner **3.51** could be made following a similar procedure from hydrazide **3.52** as designed for previous catalysts. The initial α -hydrazination to provide **3.52** would proceed with di-*tert*-butyl azodicarboxylate.



Scheme 3.16. Retrosynthetic analysis of anthracenyl catalyst **3.47**.

The initial α -hydrazination of aldehyde **3.31** with di-*tert*-butyl azodicarboxylate proceeded to give bromide **3.52** in 88% yield (Scheme 3.17). The additional steric bulk of the *tert*-butyl carbamates reduced the enantioselectivity of the reaction and, after TBAF-mediated ring closure in 95% yield, alcohol **3.53** was isolated in 77% ee. An Appel reaction resulted in the desired cross-coupling partner **3.54** in 85% yield. Following the previously optimized Negishi cross-coupling conditions resulted in a complicated product mixture. To isolate the desired product, removal of the di-*tert*-butyl carbamates followed by a selective mono-protection of the less hindered nitrogen as the ethyl carbamate resulted in final catalyst **3.47** in a 17% yield over three steps.



Scheme 3.17. Synthesis of anthracenyl catalyst **3.47**.

3.5.3 Catalyst screening

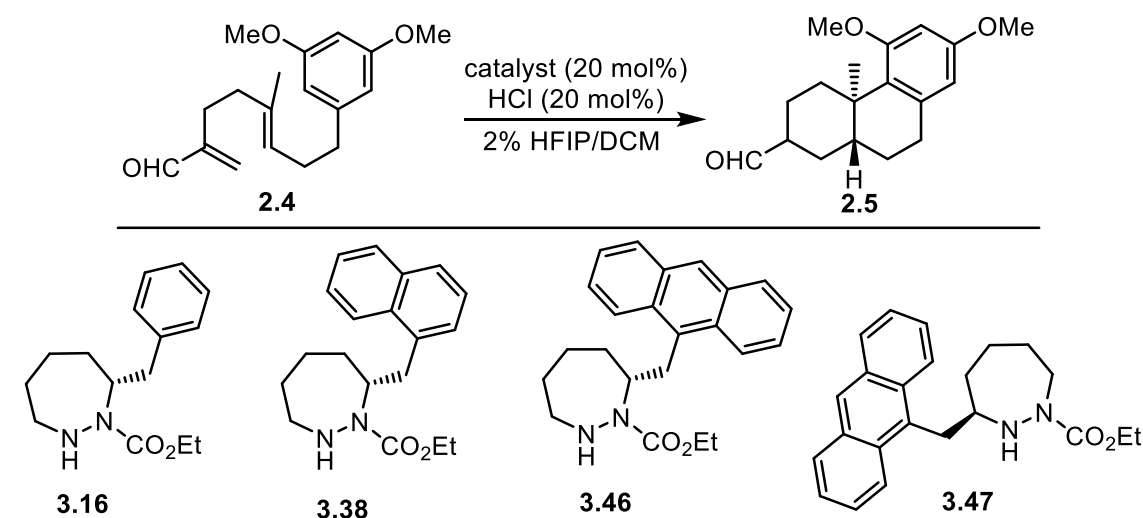
Catalysts **3.16**, **3.38**, **3.46**, and **3.47** were investigated in the polyene cyclization of model (*E*)-olefin substrate **2.4** (Table 4.1).⁷ For catalyst screening, 2% HFIP/DCM was used as a solvent system, as it had provided clean bicyclic product with high enantioselectivity in the asymmetric (*Z*)-polyene cyclization. Enantiomeric excess was measured by reduction to corresponding primary alcohol and analysis by chiral HPLC. Catalyst **3.16**, with benzyl substitution α to the carbamate, gave bicyclic product **2.5** in 19% ee (Entry 1). This was slightly lower than the enantioselectivity obtained with catalyst **3.16** in the asymmetric Cope rearrangement (33% ee), with MeCN as the solvent. However, we will show in Chapter 4 that enantioselectivity in the asymmetric (*E*)-polyene cyclization with other chiral hydrazide catalysts is largely affected by solvent polarity, and it is possible that this also applies with this catalyst. Increasing the number of fused aromatic rings from one in benzyl substitution to two in naphthyl substitution with catalyst **3.38** gave a small increase in enantioselectivity (25% ee, Entry 2). This increase was presumably due to the additional steric bulk of the naphthyl compared to the benzyl substitution. Increasing the number of fused aromatic rings from two in naphthyl substitution to three in anthracene substitution with catalyst **3.46** gave product **2.5** with negligible enantioselectivity (Entry 3). We have postulated that previous catalysts with steric bulk at this position have provided enantioselectivity through gearing of the carbamate, which then provides a steric interaction with the substrate. With catalyst **3.46**, any selectivity gained by the steric interaction of the substrate with the carbamate was negated by the stabilizing interaction of the cationic substrate with the anthracene substitution.

The yield of cyclized product **2.5** was higher in the reaction with catalyst **3.46** (67%) than with catalyst **3.16** (16%) or catalyst **3.38** (43%). This could be due to increased stabilization of cationic intermediates with the anthracene substitution. Stabilization of cationic intermediates would lower the probability of alternate outcomes, such as elimination after the initial ring closure. However, the screening for enantioselectivity was done at small scale (~10 mg) and monitored by taking aliquots for ¹H NMR. Therefore, significant conclusions cannot be taken from the yields.

Interestingly, the rate of reaction was drastically increased with catalyst **3.46**, with the reaction complete in only 4 hours, in comparison to 72 hours with catalysts **3.16** and **3.38**. We then hypothesized that, if this initial increase was the result of a stabilizing interaction between the

catalyst and substrate, moving the anthracene substitution closer to the substrate would potentially provide a further increase in reactivity. Accordingly, catalyst **3.47** provided a further increase in reactivity, with the reaction being complete in only 1 hour, although with negligible enantioselectivity (6% ee). As will be discussed in Chapter 4, the flat environment of the anthracene doesn't provide any steric differentiation between diastereomeric conformations of the first transition state, which has proven necessary for high enantioselectivity.

Table 3.1. Screening of chiral hydrazide catalysts **3.16**, **3.38**, **3.46**, and **3.47** in the asymmetric iminium-catalyzed (*E*)-polyene cyclization.



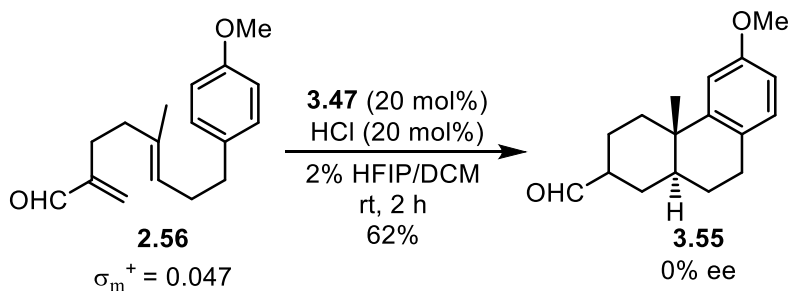
Entry	Catalyst	Time (h)	Yield (%)	% ee of 2.5 ^[a]
1	3.16	72	16	19 ^[b]
2	3.38	72	43	25
3	3.46	4	67	2
4	3.47	1	66	6 ^[b]

[a] Enantiomeric excess measured by reduction to corresponding primary alcohol and analysis by chiral HPLC. The % ee shown is the aggregate of C3 epimers for the major trans decalin isomer.

[b] Enantiomeric excess values normalized to catalyst enantiopurity, assuming no non-linear effects.

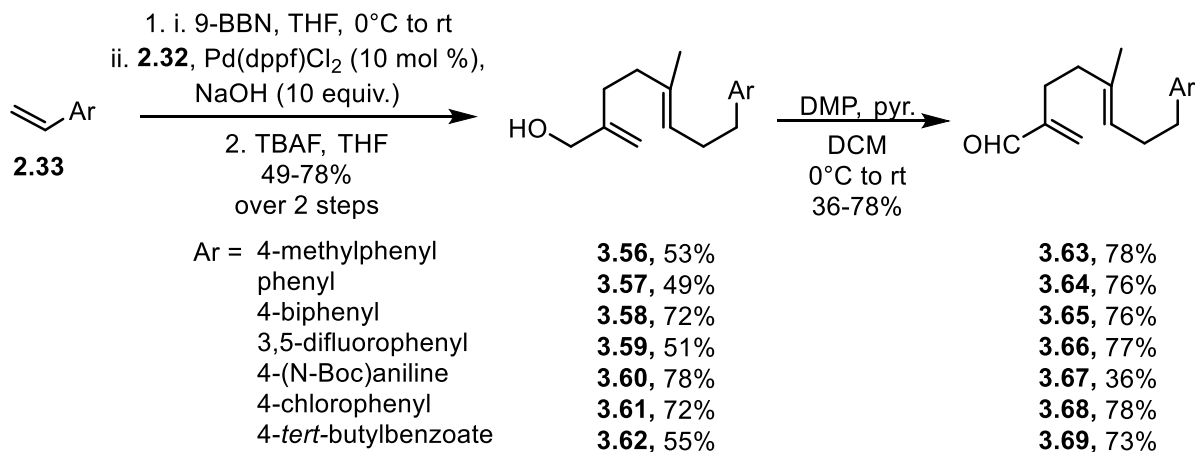
3.6 Extended substrate scope

The high reactivity of catalyst **3.47** was intriguing and we wondered whether this catalyst might be useful in expanding the substrate scope of the polyene cyclization. Attempts to achieve the bicyclization of substrate **2.56** with the simple 7-membered ring catalyst **1.241** had been unsuccessful. The low reactivity of a less nucleophilic terminating group had only resulted in prematurely trapped monocyclic products. The reactivity of the second ring closure was related to σ^+ , as discussed in Section 2.5, where the methoxy substituent *meta*- to the site of desired reactivity slightly deactivates the ring to electrophilic aromatic substitution ($\sigma_m^+ = 0.047$). With more reactive catalyst **3.47**, we again attempted this reaction (Scheme 3.18). Gratifyingly, we were able to obtain a 62% yield of bicyclic product **3.55** in only 2 hours. The enantioselectivity achieved in the bicyclization was also negligible and product **3.55** was obtained in 0% ee.



Scheme 3.18. Polyene cyclization of substrate **2.56** with catalyst **3.47**.

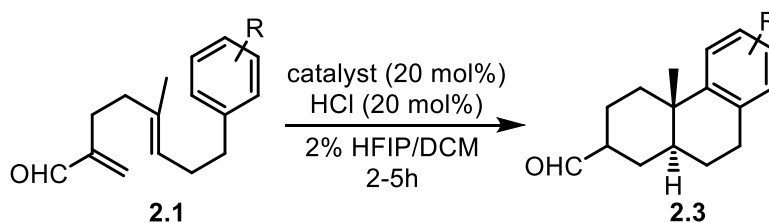
With the increased reactivity of catalyst **3.47** established, we were interested in investigating the extended substrate scope and limitations. Substrates with less nucleophilic terminating groups were synthesized by the same route as previous polyene substrates (Scheme 3.19). The hydroboration product of the corresponding styrene was cross-coupled under Suzuki conditions with iodide **2.29**. After TBAF deprotection of the cross-coupled product, alcohols **3.56-3.62** were obtained in 49-78% yield. Oxidation with DMP buffered with pyridine provided the final substrates **3.63-3.69** in 36-78% yield. Alcohol **3.60**, with a Boc-protected aniline terminating group, proved to be slightly unstable to oxidative conditions and resulted in a lower yield of product (36% of **3.67**).



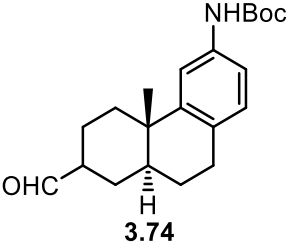
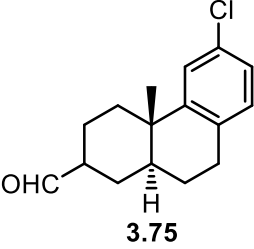
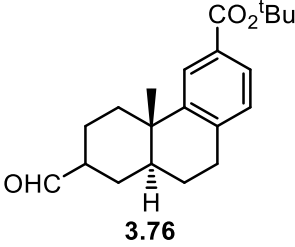
Scheme 3.19. Synthesis of substrates with less nucleophilic terminating groups.

The cyclization of substrates with less nucleophilic terminating groups was investigated with catalyst **1.241** as well as catalyst **3.47** (Table 3.2).⁷ In the cyclization of substrate **3.63**, with a moderately nucleophilic 4-methyl substituted terminating group, a low yield of product **3.70** (36%) was obtained with catalyst **1.241** in 24 h. However, with catalyst **3.47**, 78% yield of product **3.70** was obtained in only 3 hours. A simple phenyl terminated substrate **3.64** gave no reaction using catalyst **1.241** but gave a good yield of product **3.71** (58%) with catalyst **3.47**. Substrates **3.65**, **3.66**, and **3.67** gave similar results with catalyst **1.241**, with no bicyclization product obtained. Due to the longer reaction times required with catalyst **3.47** with these substrates, there was incomplete conversion due to catalyst decomposition.⁸ However, acceptable yields of product were still obtained, with 52% of product **3.72**, 39% of product **3.73**, and 40% of product **3.74**. The reactivity limits of catalyst **3.47** were hit when the terminating group has more strongly deactivating substituents, such as the 4-chloro- or 4-ester substitution seen in substrates **3.68** and **3.69**. With these substrates, no desired bicyclic products **3.75** or **3.76** were obtained with either catalyst **1.241** or catalyst **3.47**.

Table 3.2. Extended substrate scope of iminium-catalyzed (*E*)-polyene cyclizations using catalyst **1.241** and catalyst **3.47**.

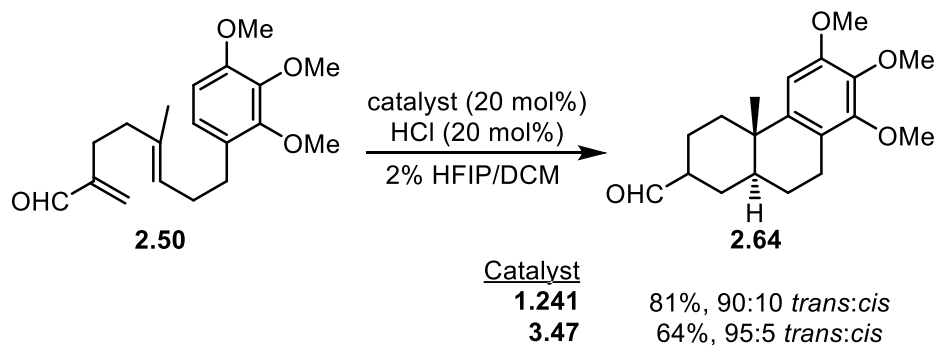


Entry	Substrate (σ_m^+ or σ_p^+) ^[a]	Product	Catalyst 1.241		Catalyst 3.47	
			Time	Yield	Time	Yield
1	3.63 (-0.066)		24 h	36%	3 h	78%
2	3.64 (0)		24 h	-	5 h	58%
3	3.65 (0.109)		24 h	-	5 h	52% ^[b]
4	3.66 (-0.073) ^[c]		24 h	-	5 h	39% ^[d]

5	3.67 (0.11) ^[e]		24 h	-	5 h	40% ^[f]
6	3.68 (0.399)		24 h	-	24 h	-
7	3.69 (0.366) ^[g]		24 h	-	24 h	-

[a] For use of σ_m^+ and σ_p^+ in electrophilic substitution see Ref. ⁹ [b] 72% conversion at 5 h. [c] Additional deactivating character from the *ortho* fluoro- substituent not taken into account. [d] 50% conversion at 5 h. [e] Ref. ¹⁰. σ_m^+ value for ethyl carbamate. [f] 52% conversion at 5 h. [g] σ_m^+ value for ethyl ester.

As seen in Chapter 2, the cyclizations of (*E*)-olefin substrates result in *trans*-decalin products and (*Z*)-olefin substrates result in *cis*-decalin products. However, due to the stepwise nature of the reaction, some erosion of stereospecificity occurs and small amounts of *cis*-decalin product are obtained from the (*E*)-polyene cyclization. The largest amount of isomerization was observed in substrate **2.50**, with two methoxy substituent at the *meta*- to the desired site of reactivity. With catalyst **1.241**, product was obtained in a 90:10 *trans*- to *cis*- decalin ratio. With catalyst **3.47**, although a slightly lower yield was obtained (64% compared to 81% with catalyst **1.241**), the stereoselectivity was improved; the product was obtained in a 95:5 *trans*- to *cis*- decalin ratio (Scheme 3.20).



Scheme 3.20. Stereospecificity in polyene cyclization of substrate **2.50**.

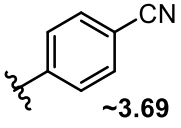
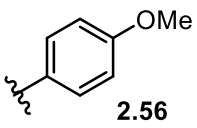
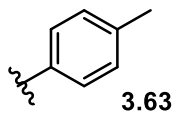
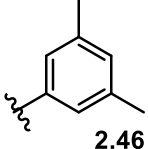
3.7 Mechanistic investigation

3.7.1 Reaction profiles

We were interested in investigating the difference in reactivity between catalyst **1.241** and **3.47**, so we performed DFT calculations on four substrates that represented the range of reactivities of the polyene cyclization (Table 3.3). A 4-cyanophenyl substrate (as an analog of 4-ester substrate **3.69**, Entry 1) would not be expected to produce bicyclic product with either catalyst. 4-methoxy substrate **2.56** produced bicyclic product only with more reactive catalyst **3.47** (Entry 2). 4-methyl substrate **3.63** produced bicyclic product with catalyst **3.47** and slowly with catalyst **1.241** (Entry 3). Finally, 3,5-dimethyl substrate **2.46** produced bicyclic product in a short time frame with catalyst **1.241** and would have been expected to provide product readily with catalyst **3.47** (Entry 4). Calculations were performed at the M06-2X/6-311G(d,p) level of theory, using the PCM solvation model for EtOH. We had previously found that the M06-2X functional performed well in predicting reactivity and selectivity in both the Cope rearrangement and polyene cyclization.¹

¹ Preliminary DFT calculations were performed by the author, final optimizations and energies were calculated by Prof. James Gleason.

Table 3.3. Free energies of transition states and intermediate cations for several substrates at the M06-2X/6-311G(d,p), SRCF=EtOH level of theory.^[a]

Entry	Substrate		TS1	Cation 1	TS2	Cation 2
	Terminating Group	Catalyst				
1		1.241	10.1	7.9	18.0	17.1
		3.47	7.6	4.0	14.5	14.3
2		1.241	9.3	6.0	12.5	11.2
		3.47	7.0	2.2	9.0	7.9
3		1.241	8.8	5.5	10.6	8.0
		3.47	6.8	1.6	7.1	4.6
4		1.241	8.8	6.1	8.4	4.5
		3.47	6.6	2.2	4.1	0.4

[a] Energies in kcal/mol.

The reaction profile, shown in Figure 3.3, displays the energetic pathway for the reaction of substrate **2.56** with both catalyst **1.241** and catalyst **3.47** (Table 3.3, Entry 2) as well as the reaction of substrate **3.63** with catalyst **1.241** (Entry 3, **1.241**). As discussed in Section 2.7, and shown by the reaction profile, the reaction proceeds in a stepwise fashion. Following the formation of the iminium ion, the first step is the addition of the central olefin onto the α,β -unsaturated iminium to afford a cyclohexyl cation. The second step is the trapping of the cation by the terminating aromatic ring. A deprotonation to rearomatize the aromatic ring then results in the enamine product and hydrolysis of the enamine results in the final *trans*-decalin product. For the reaction of substrates **2.56** and **3.63** with catalyst **1.241**, the activation barrier for the first step is similar. With both substrates, the activation barrier for the aromatic trapping is higher in energy than that for the first ring closure. The activation barrier with substrate **2.56** was calculated to be 1.9 kcal/mol higher in energy than with substrate **3.63** because of a deactivating methoxy substituent *meta*- to the site of electrophilic addition on the aromatic ring. Due to the challenges in

modelling a bimolecular proton transfer, the activation barriers for the deprotonation of the arenium intermediate were not calculated. Therefore, the rate-limiting step was determined to be either the electrophilic aromatic substitution or the deprotonation of the arenium intermediate. The reaction proceeds with substrate **3.63** but not with substrate **2.56**. As the activation barrier for the second ring closure is calculated to be lower in energy with substrate **3.63**, two possibilities are considered. The first is that the activation barrier for the deprotonation of substrate **3.63** is lower in energy than that with substrate **2.56**. This might be the case if the relative activation barriers for deprotonation are similar in magnitude. The second possibility is that, if the aromatic trapping is the rate-determining step with substrate **2.56**, the energy of this barrier is higher than the activation barrier for the deprotonation of substrate **3.63**.

We have previously observed that computed energies in the iminium-catalyzed Cope rearrangement were underestimated when compared to kinetic studies.¹¹ Therefore, while it is possible that the absolute energies for the cationic intermediates and transition states here may be underestimated, the relative energies are still instructive. In addition, it was determined that the rate-limiting step for the Cope rearrangement was the ring formation, not iminium ion formation or hydrolysis. Therefore, we assume that the ring formation will also be higher in energy than these steps in the polyene cyclization. Although the activation barrier for deprotonation of the arenium intermediate was not calculated, we expect that the calculated energies of this transition state would correlate to the relative energies of the arenium intermediate. The reaction proceeds when the energy of this intermediate is less than 8.0 kcal/mol, indicating that the following deprotonation step is also kinetically accessible. Assuming that the deprotonation of the arenium intermediate does not affect reactivity trends, we have determined the limits of reactivity with an activation barrier for the electrophilic aromatic substitution of ~10.5-11.0 kcal/mol.

In comparing the blue vs. red pathway in Figure 3.3, the incorporation of anthracene into catalyst **3.75** is shown to stabilize all intermediates along the reaction pathway. There is a moderate amount of stabilization for the iminium ion (2.1 kcal/mol) and the first transition state (2.3 kcal/mol) as well as greater stabilization at the intermediate cation (3.8 kcal/mol) and the second transition state (3.5 kcal/mol). The energy barrier for the second ring closure is calculated to be 9.0 kcal/mol with catalyst **3.47**, which now falls within the range of reactivity. With an energy barrier of 10.6 kcal/mol for the second step with *p*-methyl substrate **3.63** and catalyst **1.241** (green pathway), the reaction proceeded slowly. In contrast, energy values calculated with catalyst **3.47**

gave a drop of energy for the activation barrier for the electrophilic aromatic substitution to 7.1 kcal/mol (Table 3.3, Entry 3) and the reaction proceeded quickly.

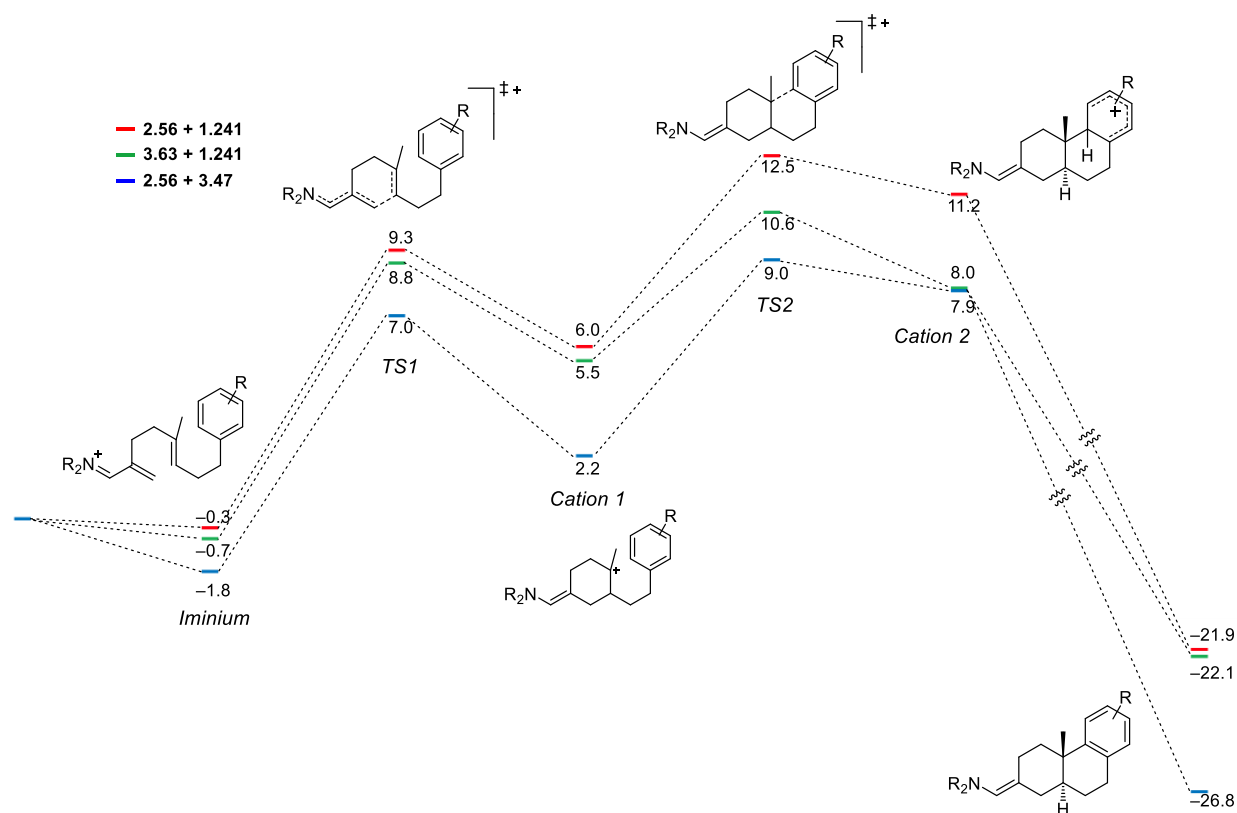


Figure 3.3. Reaction profile for substrates **2.56** and **3.63** calculated at the M06-2X/6-311G(d,p), SCRF=EtOH level of theory.

As shown in Table 3.3, the limit of reactivity with an activation barrier of 10.5-11.0 kcal/mol for the second ring closure correlates well with reactivity across several substrates. The 4-cyanophenyl substrate, a model for substrate **3.69**, was calculated to have a slightly higher barrier with catalyst **1.241** (10.1 kcal/mol) compared to that with catalyst **3.47** (7.6 kcal/mol) for the first cyclization. The second step is significantly higher in energy with catalyst **1.241** (18.0 kcal/mol) than those substrates that showed reactivity. With catalyst **3.47**, while the second step is lower in energy (14.5 kcal/mol), it is still higher than that observed for reactivity, and it was expected that the bicyclization would not proceed. Substrate **2.46**, which had shown high reactivity with catalyst **1.241**, has a sufficiently low activation barrier (8.4 kcal/mol) for the reaction to proceed.

For all of the substrates shown, the anthracene catalyst **3.47** has a stabilizing effect on the first transition state (2.0-2.5 kcal/mol), cyclohexyl cation intermediate (3.8-3.9 kcal/mol), second

transition state (3.5-4.3 kcal/mol), and arenium intermediate (2.8-4.1 kcal/mol). Stabilization is also expected to occur in the transition state for the deprotonation of the arenium intermediate.

3.7.2 Conformational analysis of catalyst 3.47

Conformational analysis of the intermediate cation of substrate **2.56** with anthracene catalyst, **3.47**, was performed computationally (Figure 3.4). The conformation where the substrate is directly above the anthracene ring is preferred, as the conformation with the substrate distal to the anthracene is higher in energy by 2.1 kcal/mol and the conformation with the anthracene turned away from the substrate is higher in energy by 4.1 kcal/mol. This suggests stabilization by cation- π interactions between the anthracene substitution and the catalyst. This energy difference between the preferred proximal and turned conformations is roughly similar to the stabilization of the cation moving from catalyst **1.241** to **3.47**. Additionally, the proximal conformation was preferred in both transition states as well as the second cation, suggesting that cation- π stabilization occurs throughout the reaction process.

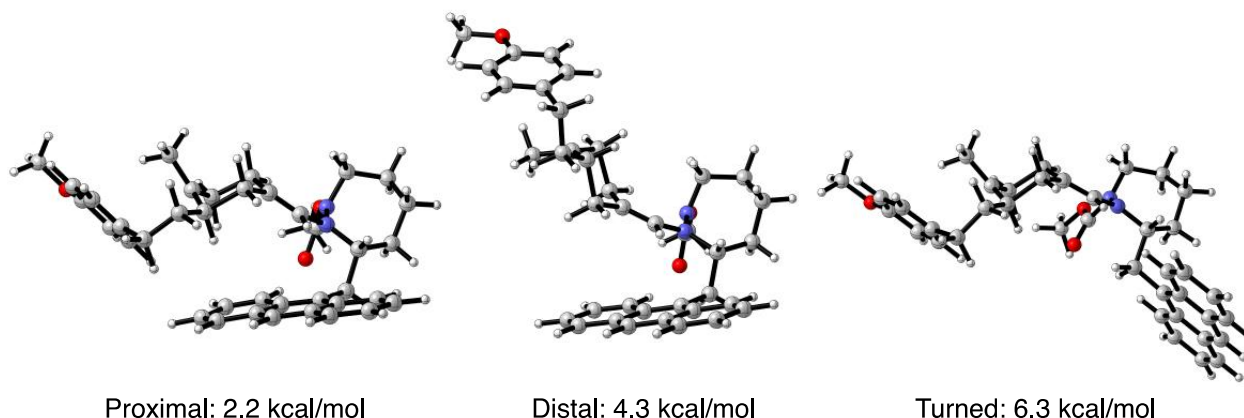


Figure 3.4. Conformational analysis of the intermediate cation of substrate **2.56** and catalyst **3.47** shows cation- π stacking is preferred.

3.8 Correlation of reactivity to σ^+

With the polyene substrates shown in Table 3.2, we observed a correlation between the σ^+ values for the substituents on the aryl terminating groups *m*- or *p*- to the reacting site and the reactivity of the substrates. The values of σ^+ have previously been used to predict reactivity patterns in electrophilic substitutions of aromatic rings,⁹ and we suggest that they can also be used to estimate reactivity in the iminium-catalyzed (*E*)-polyene cyclization.

We have estimated limits of reactivity of the catalysts **1.241** and **3.47** as a relation to the σ^+ of the terminating aromatic ring, to aid in the quick assessment of the viability of the reaction with a given substrate. The reactivity limit for catalyst **1.241** lies within the nucleophilicities of the methyl substituted aryl ring in substrate **3.63** (-0.07) and the unsubstituted aromatic ring in substrate **3.64** (0). With this catalyst, the reaction with a simple phenyl terminated substrate or aromatics with even slightly deactivating substitution would not be expected to proceed. In contrast, with catalyst **3.47** the reaction of the simple phenyl terminated substrate **3.64** proceeds in short reaction times, as well as that of the *p*-methoxy phenyl terminated substrate **2.55** (σ^+ constants up to about +0.05). For substrates with σ^+ constant of up to +0.11, the reaction proceeds with longer reaction times. Substituents above a σ^+ parameter of +0.11, such as the chloro- and ester substituents with $\sigma^+ \sim +0.3$ in substrates **3.68** and **3.69** do not react with this catalyst.

3.9 Conclusions

In this chapter, we have designed a modular route to hydrazide catalysts that has improved upon previous syntheses of chiral hydrazide catalysts and has allowed easy substitution with various aromatic rings. Through our investigation of the incorporation of extended aromatics into the chiral hydrazide catalyst, we have discovered catalyst **3.47**, that provided the bicyclized product **3.55** from substrate **2.56** in 62% yield in only 2 hours. This substrate is terminated by an aromatic ring of weak nucleophilicity and had only resulted in undesired monocyclic side products with catalyst **1.241**. With this more reactive catalyst (**3.47**), we have expanded the scope of the iminium-catalyzed (*E*)-polyene cyclization to substrates that contain weakly nucleophilic terminating groups in yields of 39-78%. The reactivity of these substrates was found to correlate to the σ^+ of the terminating aromatic ring. Reactivity limits of both catalysts have been estimated based on these σ^+ values, which have been suggested as a quick method to approximate the viability of a given substrate in the reaction.

DFT calculations were performed on the reaction profile with catalyst **1.241** and catalyst **3.47** and different substrates that showed a range of reactivity. Evidence was found for the stabilization of cationic species with this catalyst through potential cation- π interaction, which was corroborated with a conformational analysis of catalyst **3.47**.

Although the reactivity in the polyene cyclization was increased with catalyst **3.47**, product was obtained with negligible enantioselectivity. In Chapter 4, we further investigate this result

through computational analysis and synthesize catalysts with less rigid aromatic substitution to achieve a highly asymmetric reaction.

3.10 References

1. Plamondon, S. J.; Warnica, J. M.; Kaldre, D.; Gleason, J. L., Hydrazide-Catalyzed Polyene Cyclization: Asymmetric Organocatalytic Synthesis of cis -Decalins. *Angew. Chem. Int. Ed.* **2020**, *59* (1), 253-258.
2. Kaldre, D.; Gleason, J. L., An Organocatalytic Cope Rearrangement. *Angew. Chem. Int. Ed.* **2016**, *55* (38), 11557-11561.
3. Häggman, N. O.; Zank, B.; Jun, H.; Kaldre, D.; Gleason, J. L., Diazepane Carboxylates as Organocatalysts in the Diels-Alder Reaction of α -Substituted Enals. *Eur. J. Org. Chem.* **2018**, *2018* (39), 5412-5416.
4. Everson, D. A.; Jones, B. A.; Weix, D. J., Replacing Conventional Carbon Nucleophiles with Electrophiles: Nickel-Catalyzed Reductive Alkylation of Aryl Bromides and Chlorides. *J. Am. Chem. Soc.* **2012**, *134* (14), 6146-6159.
5. Biswas, S.; Weix, D. J., Mechanism and Selectivity in Nickel-Catalyzed Cross-Electrophile Coupling of Aryl Halides with Alkyl Halides. *J. Am. Chem. Soc.* **2013**, *135* (43), 16192-16197.
6. Zhou, J.; Fu, G. C., Palladium-Catalyzed Negishi Cross-Coupling Reactions of Unactivated Alkyl Iodides, Bromides, Chlorides, and Tosylates. *J. Am. Chem. Soc.* **2003**, *125* (41), 12527-12530.
7. Warnica, J. M.; Gleason, J. L., The stabilized iminium catalyzed (E)-polyene cyclization: trapping of non-activated terminating groups enabled by cation- π interactions. *Can. J. Chem.* **2021**, *100* (3), 212-216.
8. Catalyst decomposition occurred due to oxidation. Some decomposition was still observed when the reaction was run under argon.
9. Brown, H. C.; Okamoto, Y., Electrophilic Substituent Constants. *J. Am. Chem. Soc.* **1958**, *80* (18), 4979-4987.
10. Hall, H. K., Field and Inductive Effects on the Base Strengths of Amines. *J. Am. Chem. Soc.* **1956**, *78* (11), 2570-2572.

11. Sanders, J. N.; Jun, H.; Yu, R. A.; Gleason, J. L.; Houk, K. N., Mechanism of an Organocatalytic Cope Rearrangement Involving Iminium Intermediates: Elucidating the Role of Catalyst Ring Size. *J. Am. Chem. Soc.* **2020**, *142* (39), 16877-16886.

Chapter 4. Asymmetric iminium-catalyzed (E)-polyene cyclization

4.1 Introduction

As shown in Chapter 3, the addition of extended aromatic substitution α to the free N-H on 7-membered ring catalysts (e.g. catalyst **3.47**) resulted in increased reactivity in the iminium-catalyzed polyene cyclization. Evidence of a stabilizing interaction between the aromatic group at this position and the substrate was suggested with DFT studies. Unfortunately, catalyst **3.47** afforded product with virtually no enantioselectivity. In our efforts to render the reaction asymmetric, we sought to retain this stabilization while creating a favourable steric environment for enantioinduction.

4.2 DFT-mediated catalyst design

For our investigation into viable catalyst designs for the asymmetric reaction, we initially sought to determine the reasons for low enantioselectivity with catalyst **3.47**. DFT calculations were run to identify the lowest energy conformations of the transition state leading to the closure of the first ring, which sets the first stereocenter. There are four low energy conformations of this transition state which come from the attack of the central olefin onto the iminium in both the *s-trans* and *s-cis* conformations and the substrate both proximal and distal to the carbonyl of the catalyst. As seen in Figure 4.1, the proximal *s-trans* transition state and the distal *s-cis* transition state would lead to the same enantiomer ((R,R)-**3.71**) and the proximal *s-cis* transition state and the distal *s-trans* transition state would lead to the opposite enantiomer ((S,S)-**3.71**).

Of the four possible conformations, the proximal *s-trans* transition state was calculated to be the lowest in energy. The proximal *s-cis* conformation was the lowest energy conformation which would lead to the opposite enantiomer of product **3.71** and was higher in energy than the proximal *s-trans* conformation by 1.6 kcal/mol. These proximal transition states were both lower in energy than their distal counterparts, where the distal *s-cis* conformation was calculated to be 3.1 kcal/mol higher in energy and the distal *s-trans* conformation was calculated to be 2.3 kcal/mol higher in energy.

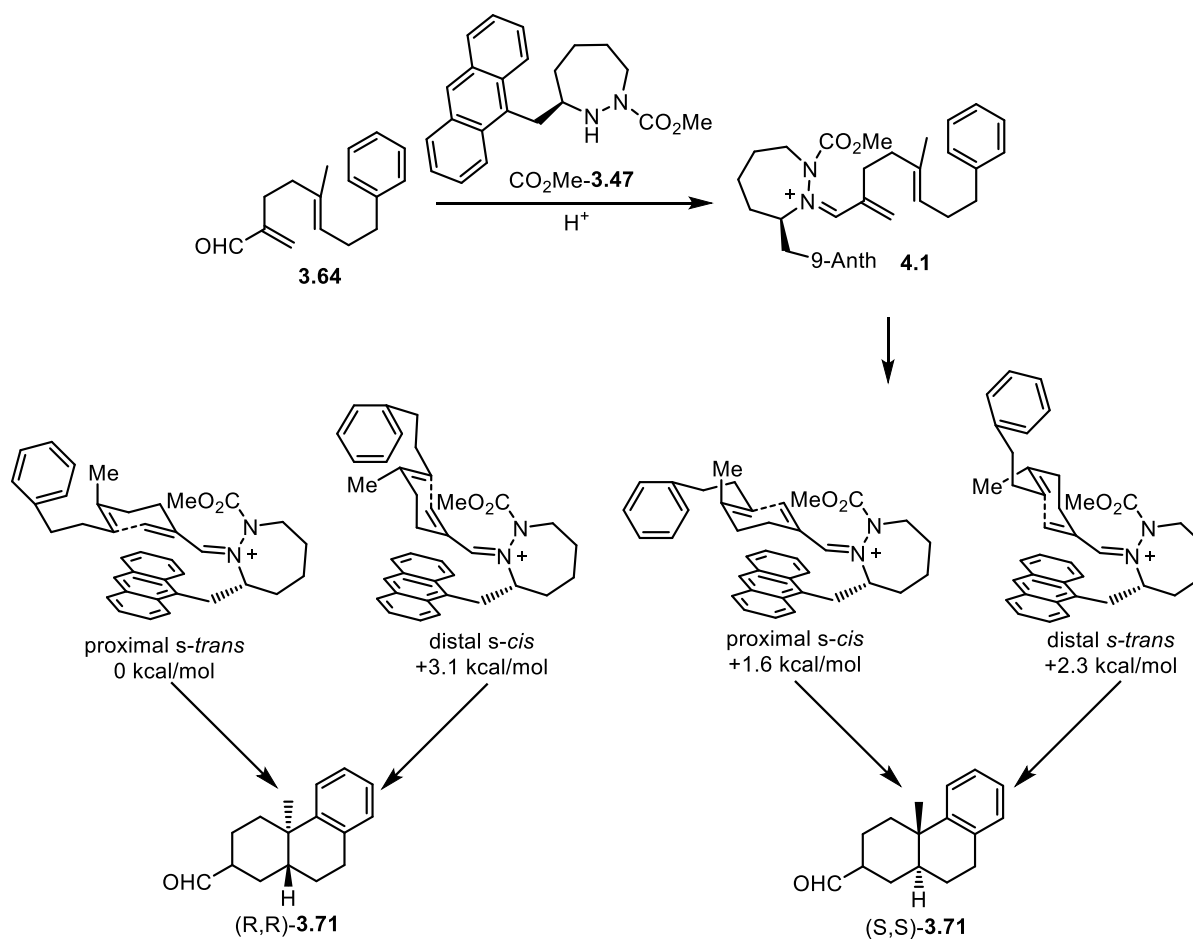


Figure 4.1. Low energy conformations of the transition state for the initial ring-closure in the reaction of substrate **3.64** with catalyst **CO₂Me-3.47**. Calculations at the M06-2X/6-31G(d), SRCF = EtOH level of theory.

For preliminary calculations, the M06-2X/6-31G(d) level of theory with the PCM solvation model for EtOH was chosen as this functional has been demonstrated to perform well when predicting relative reactivity and stereoselectivity of cyclic hydrazide catalysts in both polyene and Cope reactions.¹⁻² The basis set was chosen to use less computational resources for screening purposes. As the first ring closure sets the first stereocenter, the relative energies calculated are expected to correlate to the enantioselectivity that has been observed experimentally. However, as seen with the energies calculated for catalyst **3.47**, calculations at this level of theory overestimated the difference in transition state energies so that they could not be correlated to experimental results.

In a study by Dougherty on the computational analysis of cation- π interactions, the M06-2X functional was found to overestimate binding energies. Conversely, the M06 functional was found to reproduce experimental results for the binding of different cations to benzene with more accuracy.³ The diastereomeric conformations of the first transition state shown in Figure 4.1 were re-optimized and the energies calculated at the M06/6-31G(d,p), SRCF = EtOH level. These calculations provided energetics that more closely correlated to the lack of enantioselectivity seen with catalyst **3.47**, with a calculated energy difference between the proximal *s-trans* and proximal *s-cis* transition states of 0.1 kcal/mol. However, with further exploration into the addition of sterically bulky substitution on the aromatic rings of the catalyst, energies calculated with this functional failed to explain experimentally observed selectivity. Although the energy differences calculated with M06-2X functional could not be used for quantitative prediction of enantioselectivity, when used qualitatively the differences aligned with changes observed in enantioselectivity. Therefore, they are shown in this chapter for comparative purposes.

In the proximal *s-trans* and proximal *s-cis* conformations of the first transition state, the anthracene lies below the substrate and provides a stabilizing interaction with the building cationic charge (as discussed in Chapter 3). As seen in the computational models of these two conformations (Figure 4.2), the flat environment of the anthracene does not provide any sterically differentiating interactions. Therefore, we suggest that the lack of enantioselectivity isn't surprising as the anthracene has a similar observed interaction with the substrate in both conformations.

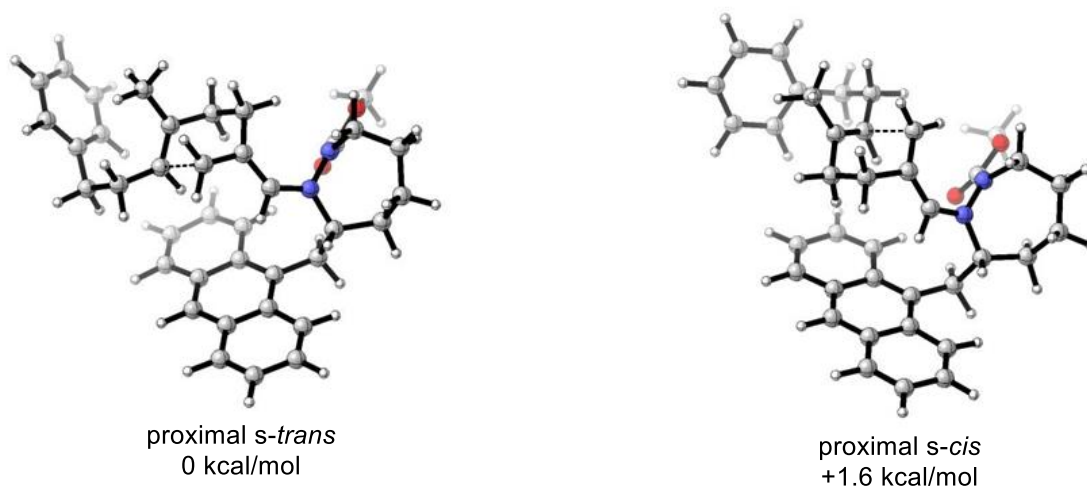
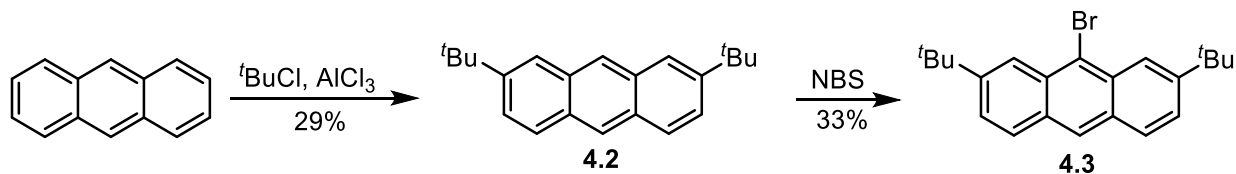


Figure 4.2. Computational models of proximal *s-cis* and proximal *s-trans* conformations of the first transition state in the reaction of substrate **3.64** with catalyst CO₂Me-**3.47**. Calculations run at the M06-2X/6-31G(d), SRCF = EtOH level of theory.

4.3 Substituted anthracene catalyst

The anthracene substitution in catalyst **3.47** had provided an increase in reactivity with evidence of stabilization of cationic intermediates and transition states. However, it had not provided product with any significant enantioselectivity. We had hoped to retain the reactivity gained by stabilization of cationic intermediates and transition states by the anthracene substitution, while additionally achieving enantioselectivity through destabilization of the minor conformation of the transition state leading to the first ring closure.

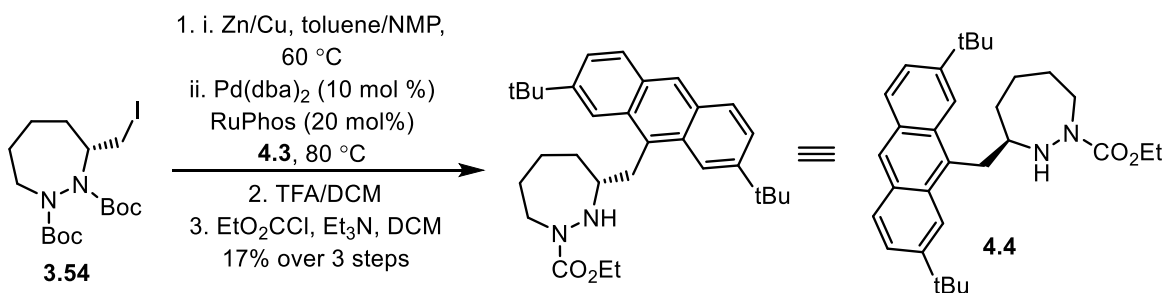
When considering which substitution pattern to pursue, we investigated the ease of synthesizing substituted anthracenyl bromide coupling partners. The simplest synthetic route considered began with the substitution of anthracene through a Friedel-Crafts alkylation with *tert*-butyl chloride. The Friedel-Crafts alkylation on anthracene gave a mixture of the 2,6- and 2,7-di-*tert*-butyl substitution patterns.⁴ However, 2,7-di-*tert*-butyl anthracene (**4.2**) could be separated by recrystallization in 29% overall yield (Scheme 4.1). Following the Friedel-Crafts alkylation, 2,7-di-*tert*-butyl anthracene was selectively brominated with NBS to afford 9-bromo-2,7-di-*tert*-butylanthracene (**4.3**) in 33% yield after recrystallization.



Scheme 4.1. Synthesis of 9-bromo-2,7-di-*tert*-butylanthracene.

In addition to being the simplest C_2 -symmetric substitution pattern on anthracene to synthesize, computational modelling of catalyst **3.47** (Figure 4.2) suggested that substitution at the 2,7-positions of the anthracene substitution would provide steric interference with the side chain in the proximal *s-cis* conformation of the first transition state. We hypothesized that this steric interaction could potentially provide selective destabilization of this conformation, leading to cyclized product with high enantioselectivity. Therefore, the synthesis of catalyst **4.4** was continued with 2,7-di-*tert*-butyl substituted anthracene.

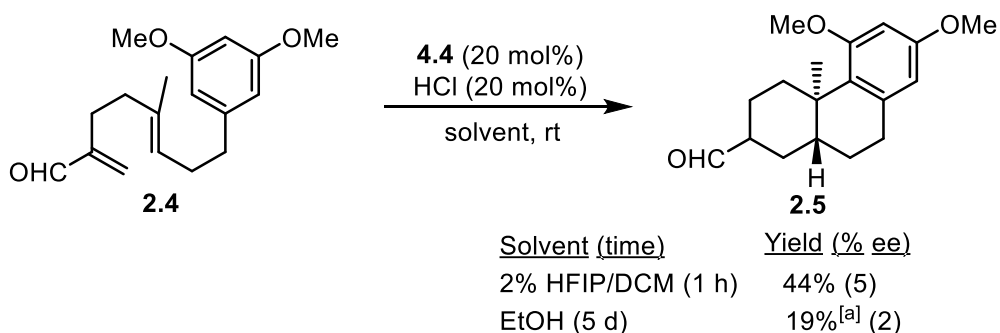
In the final steps of the synthesis, 9-bromo-2,7-di-*tert*-butylanthracene was coupled to iodide **3.54** following conditions that had been optimized in the synthesis of catalyst **3.47** (Scheme 4.2). After deprotection of the *tert*-butyl carbamates under acidic conditions and protection of the less hindered nitrogen as the ethyl carbamate, catalyst **4.4** was obtained in a 17% yield over 3 steps.



Scheme 4.2. Synthesis of 2,7-di-*tert*-butylanthracene catalyst **4.4**.

The polyene cyclization of model (*E*)-olefin substrate **2.4** was investigated with catalyst **4.4** (Scheme 4.3). In the solvent mixture of 2% HFIP/DCM, the starting material was completely consumed in one hour, which was similar reactivity as seen with the unsubstituted anthracene catalyst **3.47**. Under these conditions, product **2.5** was obtained in 44% yield and 5% ee. The catalyst was also screened with EtOH as a solvent, as this had provided significantly increased enantioselectivity with catalysts that will be discussed in later sections. In EtOH, the reaction took

5 days to complete and provided lower yields of product **2.5** (19%) with no increase in enantioselectivity (2% ee).



[a] After hydrolysis of ethyl acetal with $\text{CHCl}_3/\text{H}_2\text{O}/\text{TFA}$.

Scheme 4.3. Polyene cyclization of **2.4** with catalyst **4.4**.

Computational modelling had suggested that the addition of bulky *tert*-butyl substitution at the 2,7-positions on the anthracene would destabilize the proximal *s-cis* conformation of the first transition state and increase the preference for the conformation leading to the major enantiomer. However, it is possible this bulky substitution negates the stabilizing interaction of the proximal transition states and the distal transition states are preferred instead. Enantioinduction is difficult to achieve if these distal conformations are preferred, as there is little differentiation between the *s-cis* and *s-trans* iminium ions. Therefore, we suggest that the lack of enantioselectivity observed with catalyst **4.4** is likely due to the competing steric and electronic effects of the bulky *tert*-butyl substituents and the anthracene.

4.4 *m*-Terphenyl catalyst

As the addition of bulky substitution to the flat environment of the anthracene afforded product with negligible enantioselectivity, we considered the addition of aromatic substitution that was less rigid. We hypothesized that *m*-terphenyl substitution, such as that seen in catalyst **4.5** (Figure 4.3), could potentially provide a steric environment which would favour one conformation of the transition state leading to the first ring closure. In preliminary DFT studies, the proximal *s-trans* conformation of the first transition state was calculated to be lower in energy than the proximal *s-cis* conformation by 1.5 kcal/mol, which was not significantly different than the energy difference calculated for catalyst **3.47**. However, in the proximal *s-trans* conformation of the

transition state with catalyst **4.5**, the computational model showed a promising rotational preference for the phenyl groups of the *m*-terphenyl moiety.

There are four possible rotational isomers for the phenyl groups of the *m*-terphenyl moiety, as shown in Figure 4.3. In DFT studies performed with *m*-terphenyl catalysts, the energies of these four rotamers were calculated. In the proximal *s-trans* conformation of the first transition state in the reaction of substrate **3.64** with catalyst **4.5**, the lowest energy rotamer found was that with the *m*-terphenyl moiety in a cage-like conformation around the substrate. The rotamer that was found to be second highest in energy had the phenyl groups of the *m*-terphenyl moiety twisted clockwise. This rotamer was calculated to be 0.8 kcal/mol higher in energy than the cage-like rotamer, as the phenyl group near to the carbamate participates in a half-cage conformation around the substrate and the other phenyl group presumably provides a slight steric interaction. The third highest energy rotamer found had the phenyl groups twisted counter-clockwise and was calculated to be 2.3 kcal/mol higher in energy. Presumably, this rotamer provides an unfavourable steric interaction between the phenyl group closest to the carbamate and the substrate. The highest energy rotamer formed an inverse cage and was calculated to be 3.1 kcal/mol higher in energy. Presumably, this inverse cage-like rotamer provides an unfavourable steric interaction between the substrate and both phenyl groups in the *m*-terphenyl moiety. It is also possible that the rotation of the phenyl groups towards the cationic substrate provides a higher level of stabilization than when the phenyl groups are twisted outwards. The cage-like rotamer of the *m*-terphenyl moiety places the π -cloud of all three aromatic rings in closer proximity to the cationic substrate. Therefore, this rotamer has the potential to provide a stronger cation- π interaction than the rotamers with phenyl rings twisted outwards. Another factor in the consideration of energy differences between rotamer conformations is the confined pocket that is created for the substrate in the cage-like rotamer, which would potentially allow ring closure to be entropically more favourable.

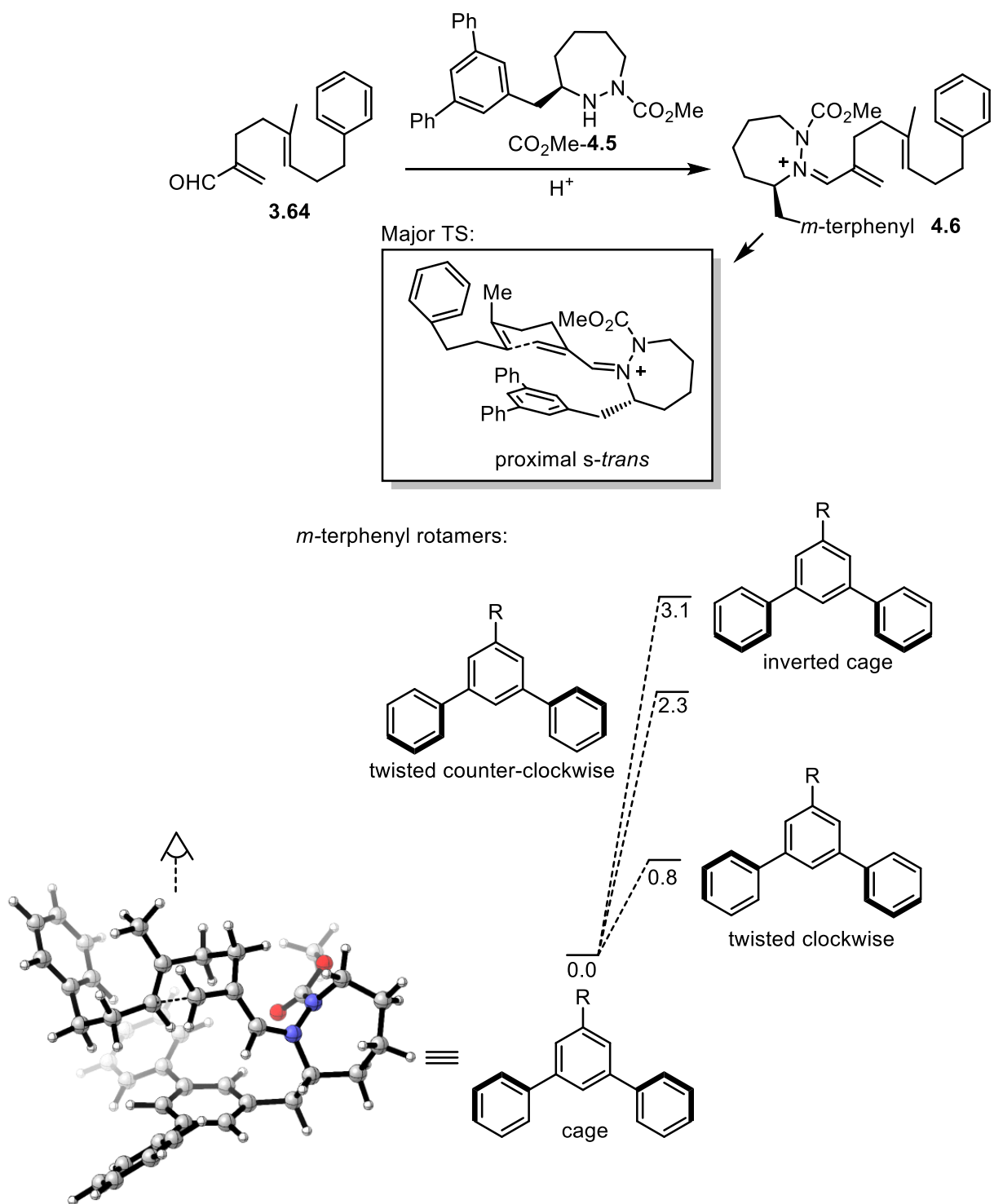


Figure 4.3 Rotational isomers of *m*-terphenyl moiety as calculated in the proximal *s-trans* conformation of the first transition state of substrate **3.64** with catalyst **CO₂Me-4.5**. Calculations run at the M06-2X/6-31G(d), SRCF = EtOH level of theory. Free energies in kcal/mol.

As described above, in the lowest energy conformation of the first transition state, the proximal *s-trans* conformation, the *m*-terphenyl substitution prefers the cage-like rotamer around the substrate. In contrast, in the proximal *s-cis* conformation, the cage-like rotamer of the *m*-terphenyl substituent would interfere with the side chain of the substrate (Figure 4.4). Instead, the preferred rotation of the *m*-terphenyl substituent is twisted counter-clockwise, resulting in a higher energy conformation. With this potential for more favourable interactions between the substrate and the *m*-terphenyl moiety in the proximal *s-trans* conformation, we proceeded to synthesize this catalyst and examine it experimentally.

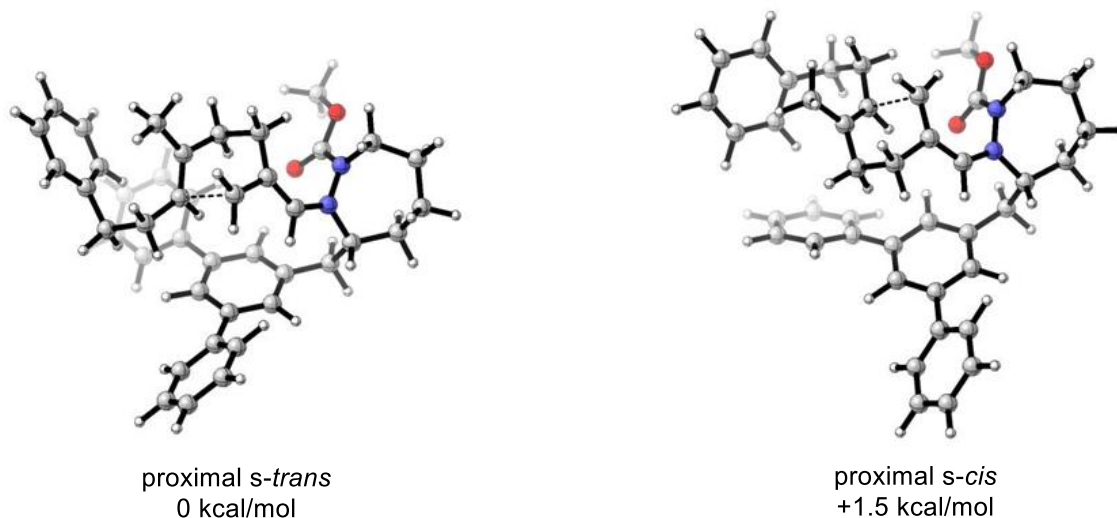


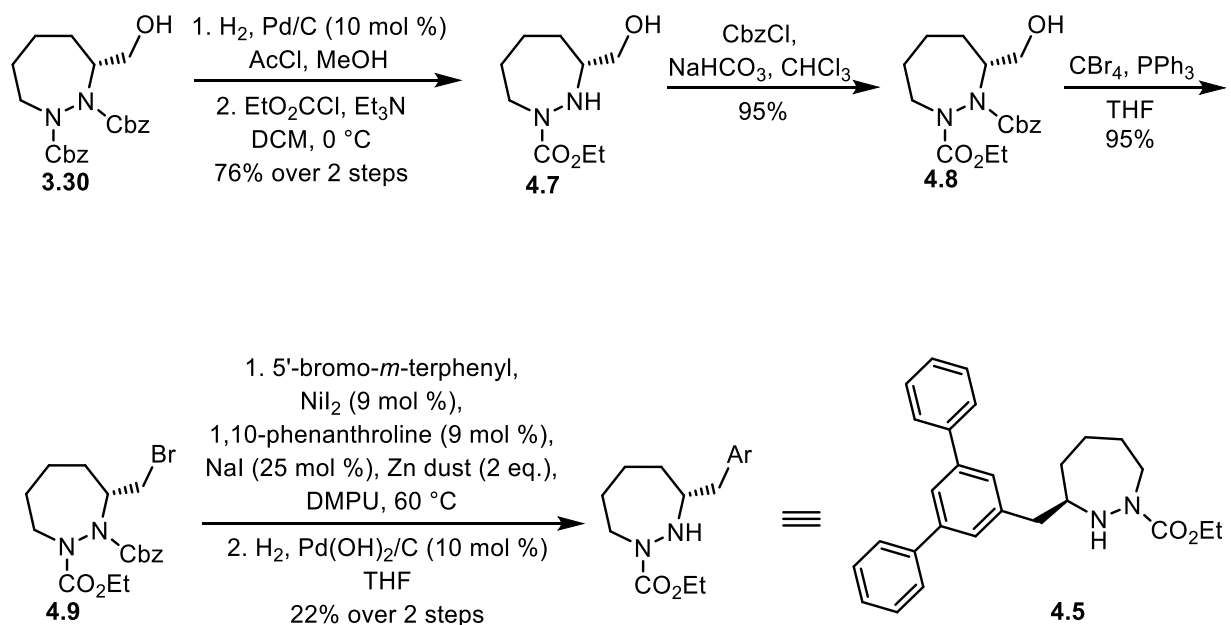
Figure 4.4. Computational model of proximal *s-trans* and proximal *s-cis* conformations of the first transition state of substrate **3.64** with *m*-terphenyl catalyst CO₂Me-**4.5**. Calculations run at the M06-2X/6-31G(d), SRCF = EtOH level of theory.

4.4.1 Synthesis of *m*-terphenyl catalyst

For catalyst **3.47**, with anthracene substitution α to the free N-H, the synthetic route had proceeded with the initial cross-coupling of anthracene to a di-*tert*-butyl carbamate protected hydrazide. This was then followed by global carbamate deprotection and subsequent mono-protection of the less hindered nitrogen to afford the final catalyst. This synthetic route was not ideal, as the proline-catalyzed α -hydrazination that had afforded the stereocenter proceeded with lower enantioselectivity with di-*tert*-butyl azodicarboxylate (77% ee) than with dibenzyl azodicarboxylate (>99% ee). Therefore, the synthesis of *m*-terphenyl catalyst **4.5** was designed to

proceed from intermediate alcohol **3.30** which could be prepared with high enantioselectivity (Scheme 3.9).

The deprotection of benzyl carbamates under acidic hydrogenation conditions followed by protection of the less hindered nitrogen as the ethyl carbamate resulted in hydrazide **4.7** in 76% yield over two steps (Scheme 4.4). Protection of the more hindered nitrogen as the benzyl carbamate afforded alcohol **4.8** in 95% yield and an Appel reaction resulted in the bromide coupling partner **4.9** in 95% yield. Cross-coupling with *m*-terphenyl bromide using Weix electrophile-electrophile cross-coupling conditions, followed by deprotection of the benzyl carbamate provided terphenyl catalyst **4.5** in 22% yield over two steps. The yields for the cross-coupling step were generally low. However, in comparison to the Negishi cross-coupling developed for catalysts **3.46** and **3.47**, it required a lower equivalence of the synthetically expensive alkyl halide as it was used in equimolar amounts with the cross-coupling partner. Therefore, for the purposes of synthesizing catalysts to be screened, it was continued to be used.

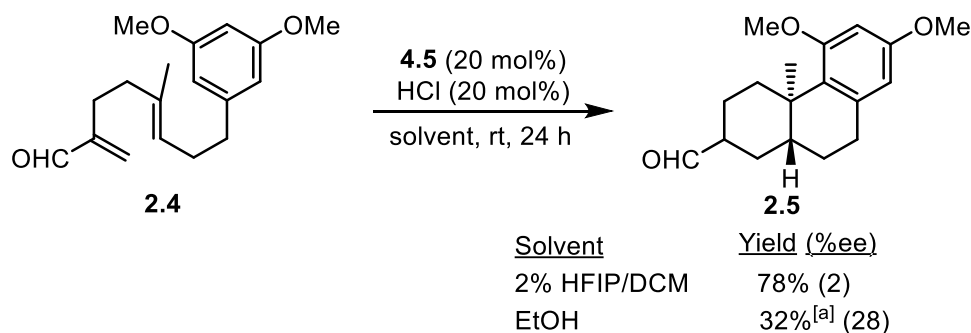


Scheme 4.4. Synthesis of *m*-terphenyl catalyst **4.5**.

4.4.2 Screening of *m*-terphenyl catalyst

Under the standard catalyst screening conditions, with 2% HFIP/DCM as a solvent, it was found that the cyclization of model (*E*)-polyene substrate **2.4** with *m*-terphenyl catalyst **4.5** gave product **2.5** in 78% yield with negligible enantioselectivity (Scheme 4.5). We had assumed that

the asymmetric (*E*)-polyene cyclization would show a similar solvent dependence to the asymmetric (*Z*)-polyene cyclization, where the enantioselectivity in 2% HFIP/DCM was only slightly attenuated in comparison to that found in EtOH. However, when the polyene cyclization with catalyst **4.5** was run in EtOH, although the yield was decreased (32%) it resulted in a significant increase in enantioselectivity to provide product **2.5** in 28% ee. As mentioned in Chapter 3, significant conclusions could not be taken from yields in reactions screening for enantioselectivity as these were done at small scale (~10 mg) and monitored by taking aliquots for ¹H NMR.



[a] After hydrolysis of ethyl acetal with CHCl₃/H₂O/TFA.

Scheme 4.5. Asymmetric polyene cyclization of **2.4** with *m*-terphenyl catalyst **4.5**.

In 2% HFIP/DCM, *m*-terphenyl substitution had not provided the desired increase in enantioselectivity that we were hoping to achieve. Although the enantioselectivity had increased when the reaction was run in EtOH, it was still relatively low. We presumed that the steric environment with catalyst **4.5** did not provide a significant difference in energies of diastereomeric conformations of the first transition state that would provide high enantioselectivity. We hypothesized that catalysts designed with bulkier substitution would destabilize the minor transition state and provide a desired increase in enantioselectivity.

4.5 Substituted *m*-terphenyl catalysts

In our initial investigations into bulkier aromatic substitution, we looked at substitution of the *m*-terphenyl moiety of catalyst **4.5**. DFT calculations were run on the *m*-terphenyl catalyst with methyl substitution at the 2,6-positions, 4-position, and 3,5-positions. With methyl substitution at the 2,6-position of the terphenyl in catalyst **4.10**, the distal conformations of the first transition state were preferred (Figure 4.5). The lowest energy conformation was the distal *s-trans*

conformation, with both the proximal *s-trans* and the distal *s-cis* conformations having similar energies that were calculated to be 1.3 kcal/mol higher. This was a smaller energy difference than that calculated for unsubstituted *m*-terphenyl catalyst **4.5** (1.5 kcal/mol). Therefore, catalysts with this substitution pattern were not synthesized as the preference for the *s-cis* and *s-trans* iminium ions is difficult to control in the distal conformations.

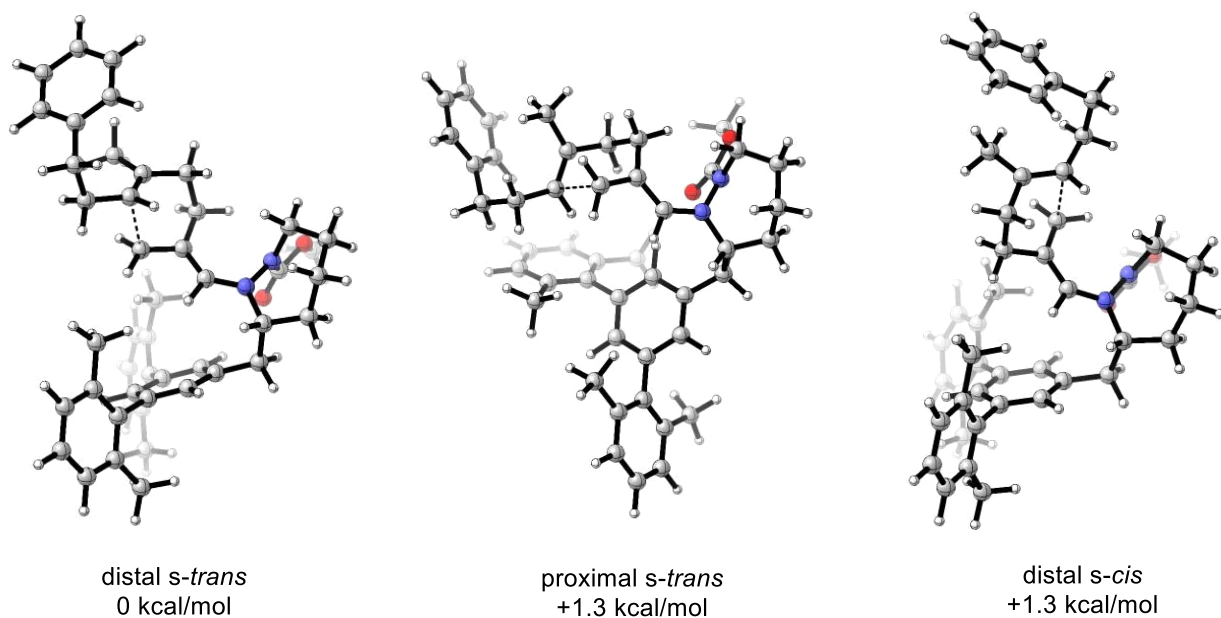
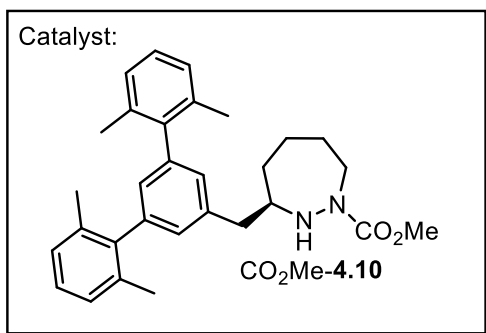


Figure 4.5. Computational model of distal *s-trans*, proximal *s-trans*, and distal *s-cis* conformations of the first transition state of substrate **3.64** with 2,6-dimethyl *m*-terphenyl catalyst CO₂Me-**4.10**. Calculations run at the M06-2X/6-31G(d), SRCF = EtOH level of theory.

In computational models of the catalysts with methyl substitution at the 4-position and at the 3,5-positions of the *m*-terphenyl, the proximal *s-trans* conformation was calculated to be the lowest energy conformation of the first transition state (Figure 4.6). The proximal *s-cis* conformation was calculated to be the lowest energy conformation leading to the opposite

enantiomer. With methyl substitution at the 4-position of the *m*-terphenyl in catalyst CO₂Me-**4.11**, there was a calculated energy difference between these two conformations of 1.7 kcal/mol. With 3,5-dimethyl substitution in catalyst CO₂Me-**4.12**, a slightly larger energy difference of 2.0 kcal/mol was calculated, and so this catalyst was synthesized and examined experimentally.

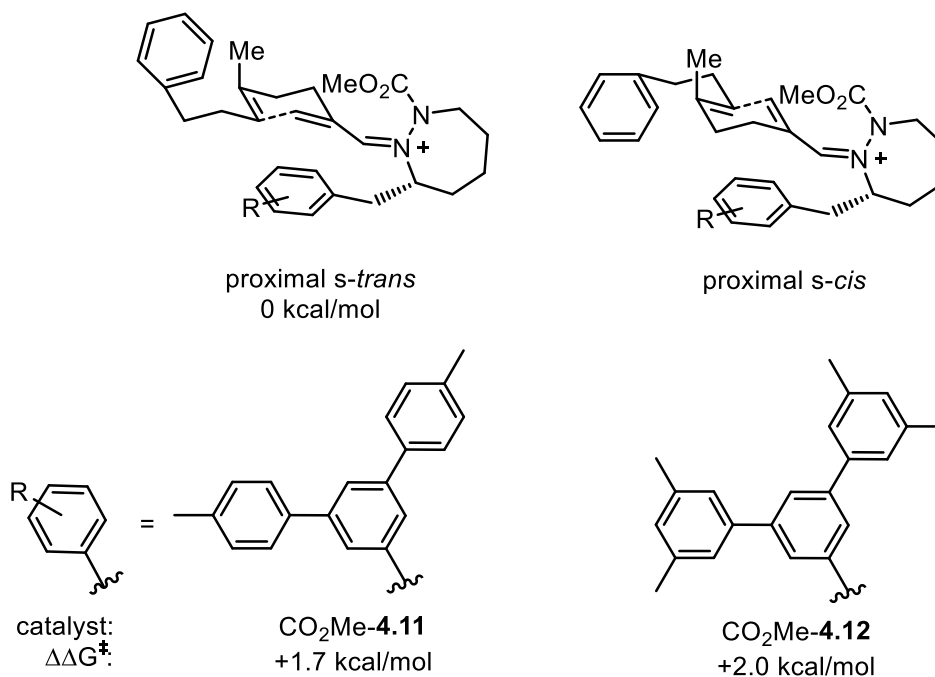
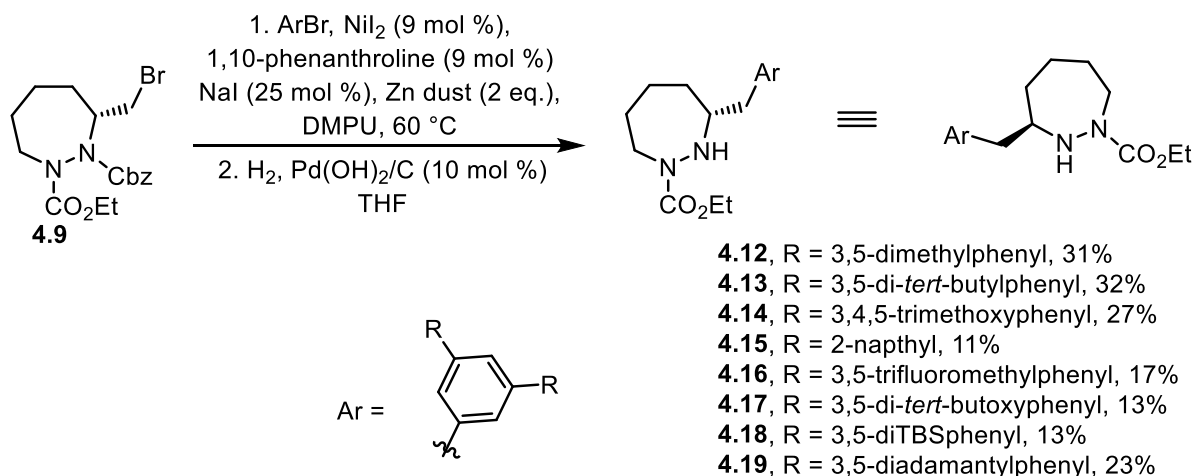


Figure 4.6. Calculated energy differences between proximal *s-trans* and distal *s-cis* conformations of the first transition state of substrate **3.64** with methyl substituted *m*-terphenyl catalysts. Calculations run at the M06-2X/6-31G(d), SRCF = EtOH level of theory.

4.5.1 Synthesis of substituted *m*-terphenyl catalysts

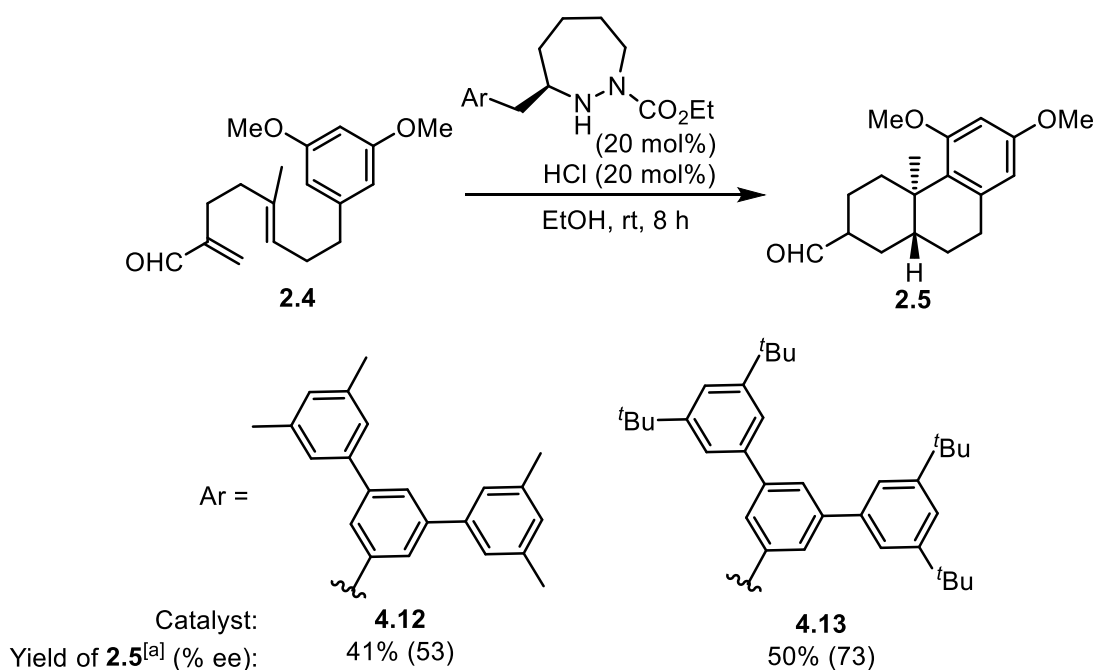
Substituted *m*-terphenyl catalysts were synthesized by the same route as *m*-terphenyl catalyst **4.5** (Scheme 4.6). *m*-Terphenyl bromides were synthesized through a Suzuki cross-coupling of 1,3,5-tribromobenzene with respective phenyl boronic acids to give separable mixtures of the mono-, di-, and tri-substituted products in a statistical ratio (details in experimental). Cross coupling of the intermediate bromide **4.9** with *m*-terphenyl bromides was performed under Weix electrophile-electrophile cross-coupling conditions. The benzyl carbamate of the cross-coupled products was then deprotected by hydrogenation, providing substituted *m*-terphenyl catalysts **4.12-4.19** in 11-32% yield over two steps.



Scheme 4.6. Final steps in the synthesis of substituted *m*-terphenyl catalysts.

4.5.2 Screening of substituted *m*-terphenyl catalysts

In comparison to the activation barrier for the first transition state with *m*-terphenyl catalyst **4.5**, the addition of methyl substitution at the 3,5-positions in *m*-terphenyl catalyst **4.12** was calculated to increase the $\Delta\Delta G^\ddagger$ by 0.5 kcal/mol. When this catalyst was screened with model substrate **2.4** in EtOH, it resulted in cyclized product **2.5** in 41% yield and 53% ee (Scheme 4.7), which was a 25% ee increase from that achieved with catalyst **4.5**. This result indicated that the addition of steric bulk was having the desired effect of destabilizing the minor conformation of the first transition state. With this promising result, we increased the steric bulk further and synthesized catalyst **4.13**, with *tert*-butyl substitution at the 3,5-positions of the *m*-terphenyl. We found that this increase in steric bulk provided a further increase in enantioselectivity, providing product **2.5** in 50% yield and 73% ee.

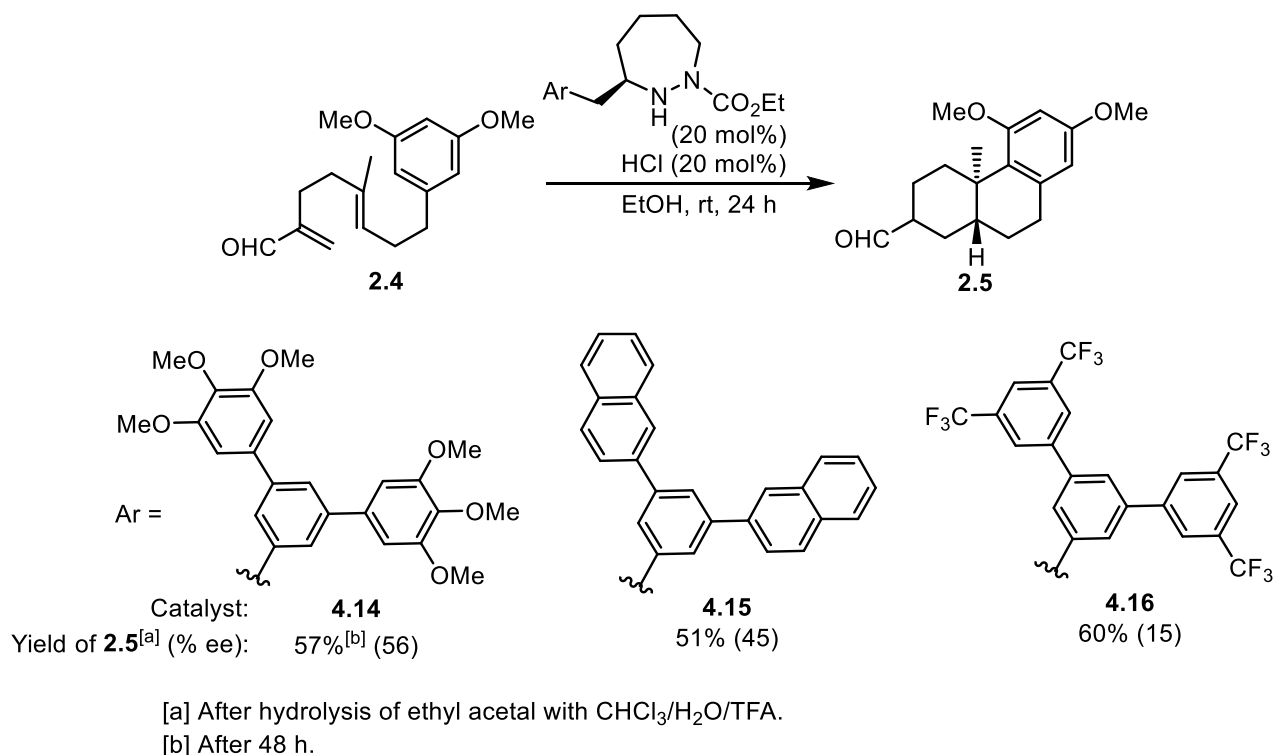


[a] After hydrolysis of ethyl acetal with $\text{CHCl}_3/\text{H}_2\text{O}/\text{TFA}$.

Scheme 4.7. Screening of chiral catalysts with alkyl substituted *m*-terphenyls.

To investigate whether cation- π interactions were strongly influencing the enantioselectivity through selective stabilization of the major conformation of the first transition state, we synthesized catalysts **4.14**, **4.15**, and **4.16** (Scheme 4.8). Catalyst **4.14**, with three electron-rich methoxy substituents, and catalyst **4.15**, with naphthyl groups, contain aromatic groups with more negative quadrupole moments than simple alkyl-substituted phenyl.⁵⁻⁶ Therefore, if cation- π interaction was strongly influencing the enantioselectivity, these catalysts would be expected to provide products in higher enantioselectivities. Catalyst **4.14** provided product **2.5** in 57% yield and 56% ee, which was similar that obtained with catalyst **4.12** (a catalyst with similar steric influence). Naphthyl substitution in catalyst **4.15** provided product in 51% yield and with higher enantioselectivity than phenyl substitution (45% ee vs. 28% ee). However, the naphthyl group is a larger substituent and is more comparable in size to catalyst **4.12**, which gave product with similar enantioselectivity. Catalyst **4.16** was substituted with 3,5-trifluoromethyl groups, which are expected to have a similar steric interaction as a methyl substitution but with strongly electron-withdrawing character. The corresponding quadrupole moment would be more positive, leading to weaker cation- π interaction. This catalyst provided product **2.5** in 60% yield and with significantly decreased enantioselectivity (15% ee).

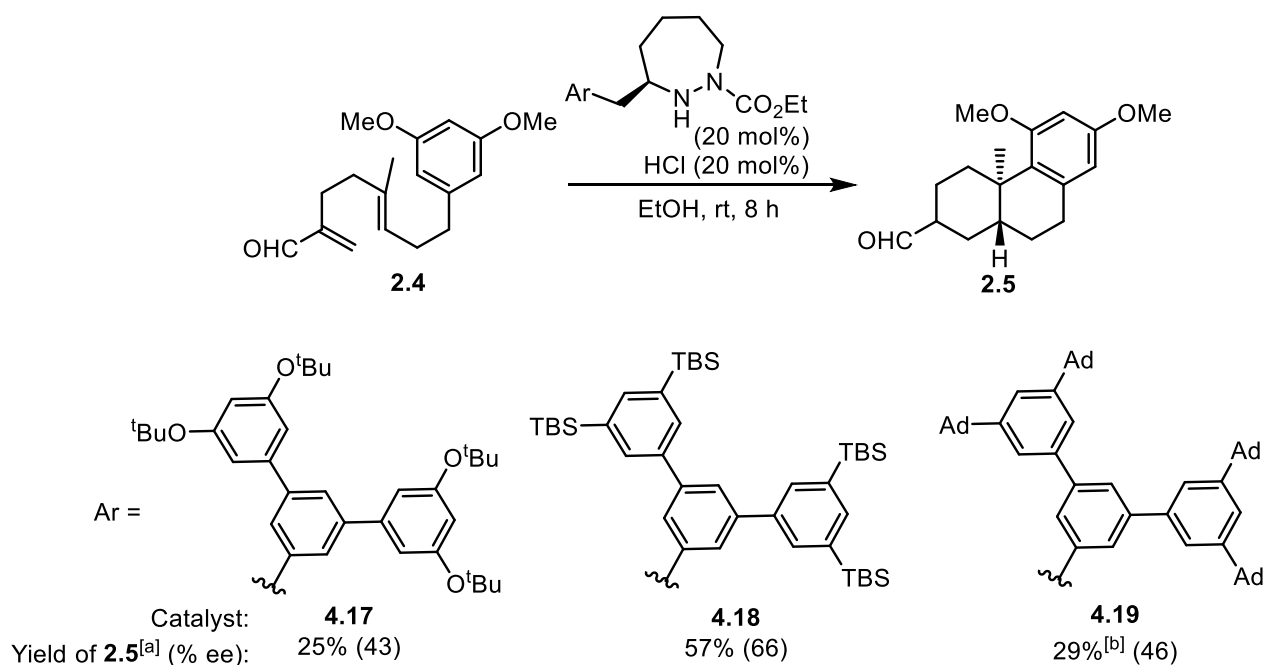
While increasing the strength of the cation– π interaction did not have any significant improvement on enantioselectivity, the negative effect of electron-withdrawing substituents suggests that decreasing the strength of the cation– π interaction has a detrimental effect. We propose that the cage-like conformation of the *m*-terphenyl catalyst around the substrate is favoured with moderate cation– π interactions present, while bulky substitution destabilizes the minor diastereomeric conformation of the first transition state. It is possible that there is less preference for this proximal conformation with a cage-like *m*-terphenyl moiety when there is weaker cation– π interaction, such as that achieved with catalyst **4.16**.



Scheme 4.8. Screening of *m*-terphenyl catalysts with electronically varied substitution.

Different large substituents were investigated with catalysts **4.17**, **4.18**, and **4.19** (Scheme 4.9). Catalyst **4.17**, with 3,5-di-*tert*-butyl ethers, was synthesized to investigate the addition of electron-rich substituents that also provided steric bulk. This catalyst resulted in product **2.5** in 25% yield and 43% ee, lower than the 73% ee obtained with *tert*-butyl catalyst **4.13**. The ether C–O bond in catalyst **4.17** presumably allows the rotation of the *tert*-butyl group away from the substrate, whereas in catalyst **4.13** the *tert*-butyl group is fixed, presumably in a position where it provides a more significant steric interaction with the minor transition state. Catalyst **4.18**, with

3,5-di-TBS substitution, provided product **2.5** in 57% yield and with a slightly diminished enantioselectivity (66%) in comparison to *tert*-butyl catalyst **4.13**. As C-Si bonds are longer than the C-C bonds in *tert*-butyl substitution, the silyl group would be expected to provide additional effective steric bulk. However, the C-Si bond to the terphenyl would also be increased in length, potentially providing a less ideal steric environment to effect enantioselectivity. Attempts to synthesize catalysts that had larger silyl groups (i.e. TIPS or TBDPS) were unsuccessful due to the difficulties in putting two bulky substituents *meta*- on the aromatic ring of the terphenyl. Bulky adamantyl groups in catalyst **4.19** provided product **2.5** in 29% yield and with significantly reduced enantioselectivity (46% ee). The adamantyl groups have the same number of C-C bonds from the initial carbon as the *tert*-butyl groups in catalyst **4.13**. However, these are pinned back in the adamantyl cage, which potentially provided a less favourable steric environment to effect enantioselectivity.



[a] After hydrolysis of ethyl acetal with CHCl₃/H₂O/TFA.

[b] After 24 h.

Scheme 4.9. Screening of *m*-terphenyl catalysts with bulky substitution.

4.6 Investigation into bulkier carbamates

With the success of 3,5-*tert*-butyl substitution on the *m*-terphenyl moiety of catalyst **4.13** in inducing higher levels of enantioselectivity, we proceeded to investigate whether different protecting groups on the nitrogen would have a further impact. Based on models of the lowest energy conformations of the first transition state with catalyst **4.5**, we hypothesized that a bulkier protecting group might provide a steric interaction with the aryl ethyl chain of the substrate in the minor conformation (proximal *s-cis*, Figure 4.4), which would lead to an increased preference for the major conformation. Therefore, catalysts **4.20** and **4.21** were synthesized that have either a Piv or Boc protecting group, respectively (Figure 4.7).

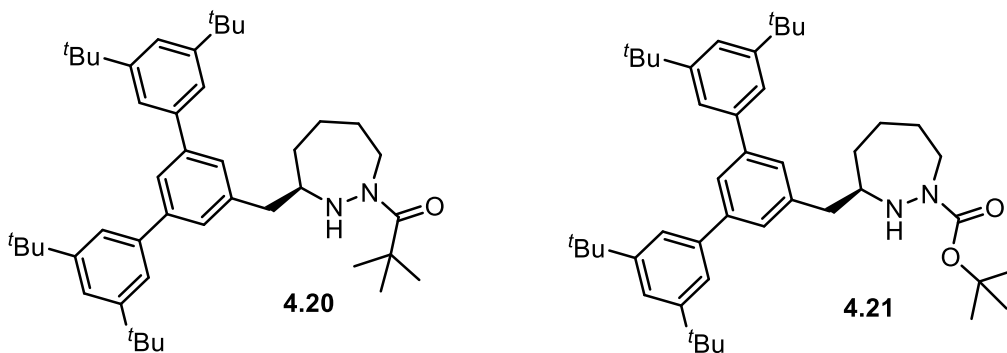
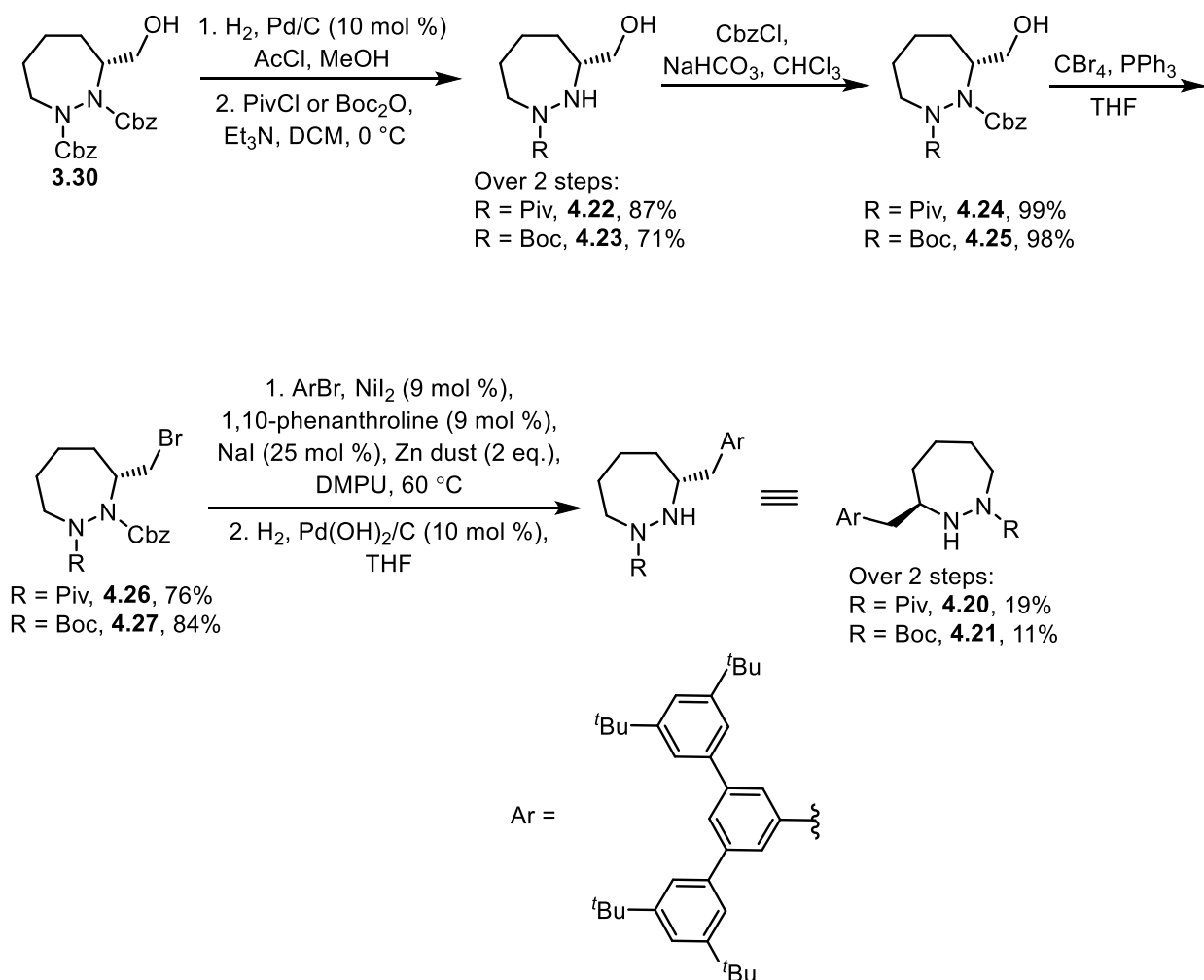


Figure 4.7. Chiral catalysts with bulkier protecting groups.

4.6.1 Synthesis of 3,5-*tert*-butyl-*m*-terphenyl catalysts with bulkier carbamates

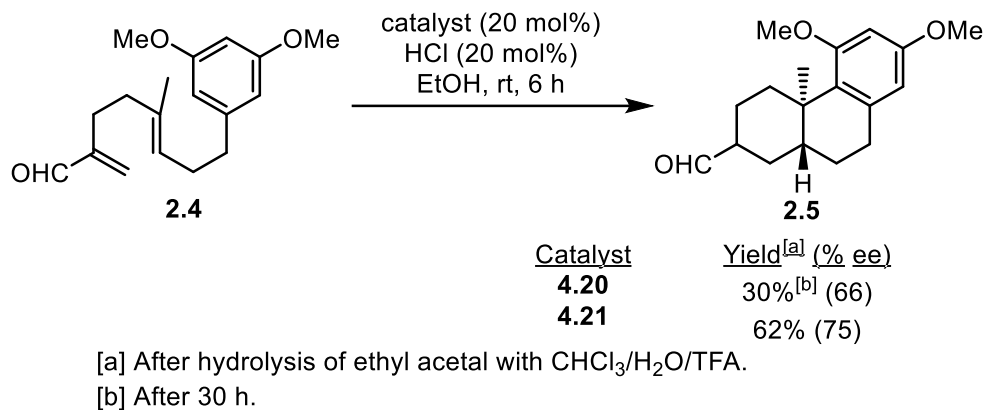
Catalysts **4.20** and **4.21** were synthesized by a similar route as catalyst **4.13**, starting from intermediate alcohol **3.30** (Scheme 4.10). Deprotection of benzyl carbamates under acidic hydrogenation conditions followed by protection of the less hindered nitrogen with either PivCl or Boc₂O resulted in amide **4.22** in 87% yield or hydrazide **4.23** in 71% yield over two steps. Protection of the more hindered nitrogen as the benzyl carbamate afforded hydrazides **4.24** and **4.25** in 99% and 98% yields, respectively. An Appel reaction then resulted in the bromide coupling partners **4.26** and **4.27** in 76% and 84% yield. Cross-coupling with the 3,5-*tert*-butyl-*m*-terphenyl bromide using Weix electrophile-electrophile cross-coupling conditions, followed by deprotection of the benzyl carbamate provided catalysts **4.20** and **4.21** in 19% and 11% yield, respectively, over two steps.



Scheme 4.10. Synthesis of 3,5-*tert*-butyl-*m*-terphenyl catalysts with bulkier protecting groups.

4.6.2 Screening of 3,5-*tert*-butyl-*m*-terphenyl catalysts with bulkier carbamates

Following the synthesis of catalysts **4.20** and **4.21**, they were investigated in the polyene cyclization of model (*E*)-olefin substrate **2.4** (Scheme 4.11). Catalyst **4.20** provided product **2.5** in 30% yield and 66% ee, where as catalyst **4.21** provided product **2.5** in 62% yield and 75% ee. The enantioselectivities observed with these catalysts were not significantly different from that observed with catalyst **4.13**.



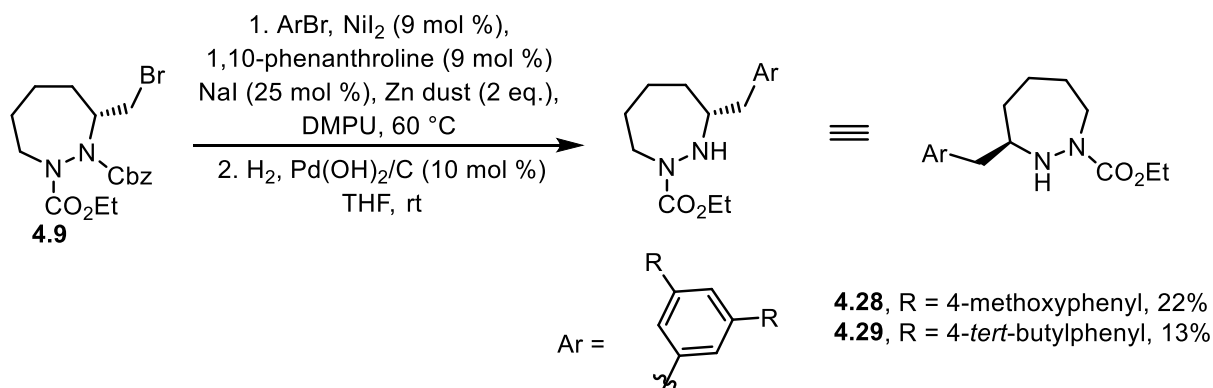
Scheme 4.11. Asymmetric cyclization of model substrate **2.4** with catalysts **4.20** and **4.21**.

In computational models of the proximal *s-trans* and *s-cis* conformations of the first transition state with unsubstituted *m*-terphenyl catalyst **4.5** (Figure 4.4), preference is shown for the carbamate rotamer that points the carbonyl towards the substrate. In this conformation, the bulk of the carbamate is pointed away from the substrate and back towards the 7-membered ring. Therefore, it is possible that the protecting groups in these catalysts were not large enough to interact with the substrate, resulting in a similar effective steric environment as that with ethyl carbamate catalyst **4.13**, which had provided similar enantioselectivities.

4.7 Alternate catalysts

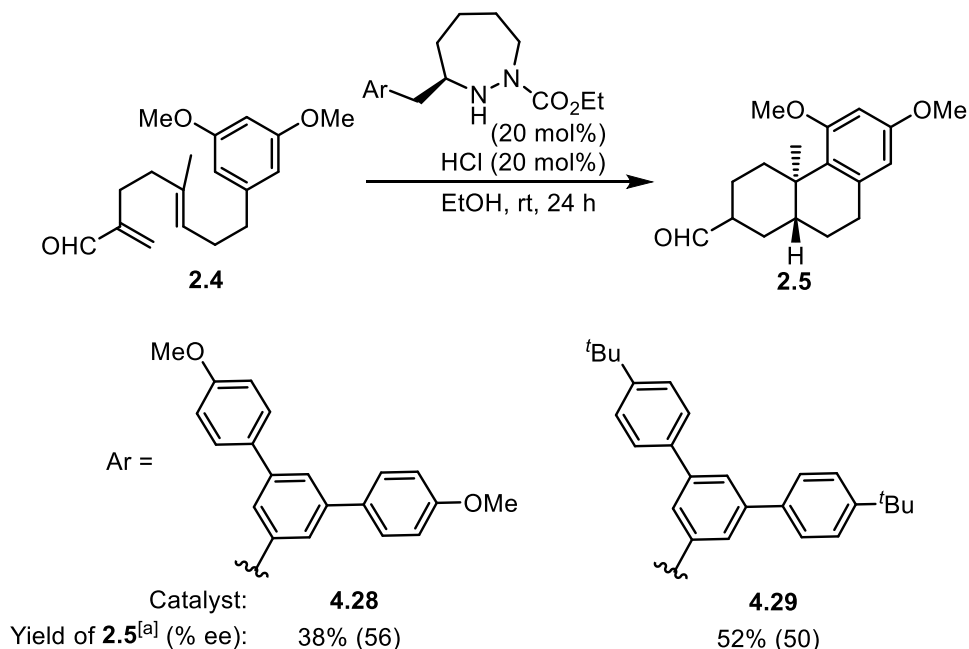
4.7.1 4-Substituted *m*-terphenyl catalysts

The calculated difference in $\Delta\Delta G^\ddagger$ for the first transition state between 4-methyl substituted *m*-terphenyl **4.11** and 3,5-dimethyl substituted *m*-terphenyl **4.12** had been small (0.3 kcal/mol, Figure 4.6). Therefore, there was a possibility that catalysts where the *m*-terphenyl was substituted at the 4-position would provide similar selectivity as catalysts substituted at the 3,5-positions of the *m*-terphenyl moiety. To investigate this possibility, we synthesized 4-methoxy substituted *m*-terphenyl catalyst **4.28** and 4-*tert*-butyl substituted *m*-terphenyl catalyst **4.29**. These were synthesized by the same route as catalyst **4.13**, where the Weix electrophile-electrophile cross-coupling of the *m*-terphenyl bromides with alkyl bromide **4.9** followed by deprotection of the benzyl carbamate resulted in catalyst **4.28** in 22% yield and catalyst **4.29** in 13% yield over two steps (Scheme 4.12).



Scheme 4.12. Synthesis of 4-substituted *m*-terphenyl catalysts **4.28** and **4.29**.

Following the synthesis of catalysts **4.28** and **4.29**, they were investigated in the polyene cyclization of model (*E*)-olefin substrate **2.4** (Scheme 4.13). Catalyst **4.28** provided product **2.5** in 38% yield and 56% ee, which was no different than the enantioselectivity observed with the 3,4,5-trimethoxy substituted *m*-terphenyl catalyst **4.14**. Increasing the steric bulk at the 4-position to *tert*-butyl groups in catalyst **4.29** provided product **2.5** in 52% yield and 50% ee. The lower enantioselectivity achieved with this catalyst in comparison to the 3,5-di-*tert*-butyl substituted *m*-terphenyl catalyst **4.13** aligns with the lower $\Delta\Delta G^\ddagger$ determined by DFT calculations.

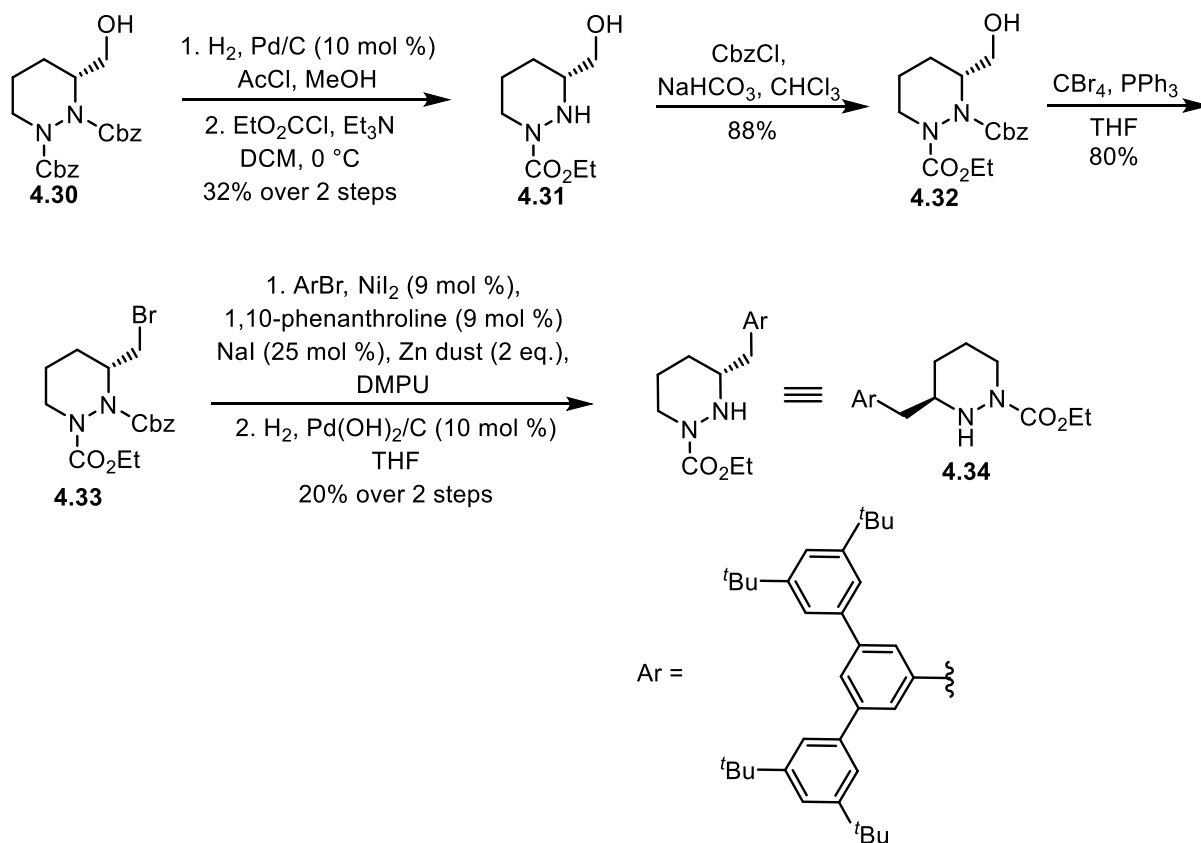


[a] After hydrolysis of ethyl acetal with CHCl₃/H₂O/TFA.

Scheme 4.13. Screening of asymmetric (*E*)-polyene cyclizations with catalysts **4.28** and **4.29**.

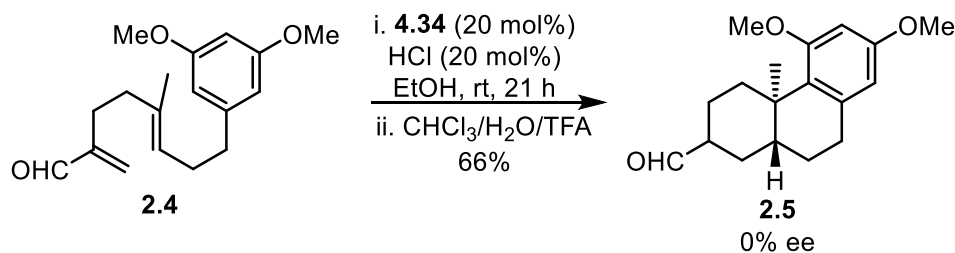
4.7.2 6-Membered ring *m*-terphenyl catalyst

The increased rigidity of a 6-membered ring catalyst scaffold is generally beneficial in asymmetric catalysis as it is expected to orient substitution on the ring more consistently than a 7-membered ring. Therefore, we were interested in investigating the asymmetric reaction with 6-membered ring hydrazide catalyst **4.34**, which is expected to hold the aromatic substitution in a more defined conformation. The synthesis of catalyst **4.34** proceeded through the same route as catalyst **4.13**, with one methylene unit less in the hydrazide ring (Scheme 4.14). Dibenzyl carbamate **4.30** was obtained from Dr. Samuel Plamondon. Hydrogenation of the benzyl carbamates under acidic conditions and subsequent protection of the less hindered nitrogen provided hydrazide **4.31** in 32% yield over two steps. Protection of the more hindered nitrogen as the benzyl carbamate provided alcohol **4.32** in 88% yield, which was followed by an Appel reaction to give bromide coupling partner **4.33** in 80% yield. Cross-coupling with 3,5-di-*tert*-butyl substituted *m*-terphenyl bromide followed by deprotection of the benzyl carbamate afforded the final catalyst **4.34** in 20% yield over two steps.



Scheme 4.14. Synthesis of 6-membered ring catalyst **4.34**.

Catalyst **4.34** was investigated in the polyene cyclization of model (*E*)-olefin substrate **2.4** and provided product **2.5** in 66% yield but with negligible enantioselectivity (Scheme 4.15). Preliminary DFT calculations suggested that 6-membered ring catalysts prefer the chair conformation where the aromatic substitution is in the axial position, in comparison to the pseudo-equatorial position that is the preferred conformation of the 7-membered ring catalysts. In this conformation of the 6-membered ring, the axial positioning places the *m*-terphenyl closer to the catalyst ring, providing a different steric environment around the substrate than that provided by the 7-membered ring catalyst. In catalyst **4.34**, this altered steric environment would potentially provide preferred conformations of the first transition state with the substrate distal to the aromatic substitution or with the *m*-terphenyl substitution twisted away from the substrate, both which would provide a lower preference for the *s-trans* or *s-cis* iminium ion.



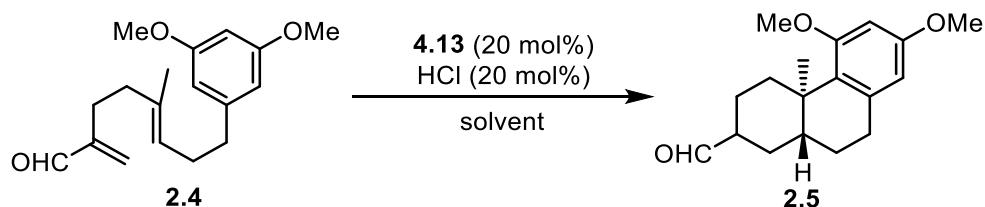
Scheme 4.15. Polyene cyclization of model substrate **2.4** with catalyst **4.34**.

4.8 Optimization with 3,5-di-*tert*-butyl *m*-terphenyl catalyst **4.13**

Under chiral catalyst screening conditions, catalyst **4.13** had provided cyclized product **2.5** from model (*E*)-polyene substrate **2.4** with the highest enantioselectivity. Therefore, further conditions were screened to optimize the selectivity with this catalyst. Initially, solvents were screened with the HCl salt of catalyst **4.13** (Table 4.1). It was found that higher enantioselectivity was achieved in polar solvents. The initial reaction had been run in EtOH (relative polarity of 0.654) and had provided product **2.5** in 48% yield and 73% ee (Entry 1). The addition of water to EtOH in a concentration of 10% H₂O/EtOH provided product **2.5** in 56% yield and with a slight increase in enantioselectivity to 75% ee (Entry 2). However, the reaction was difficult to perform as the catalyst had limited solubility under these conditions. With MeNO₂, a slightly less polar solvent (relative polarity of 0.481), the enantioselectivity was significantly lower and resulted in product **2.5** in 63% yield and 38% ee (Entry 3). The solvent mixture of 2% HFIP/DCM provided product **2.5** in 32% yield and a similar diminished enantioselectivity of 29% ee (Entry 4). Very

non-polar solvents, such a toluene (Entry 5) and cyclohexane (Entry 6) with relative polarities of 0.099 and 0.006, respectively, gave product **2.5** in yields of 70% and 48%. Low enantioselectivities were achieved in these non-polar solvents, with a slight preference for the opposite enantiomer (-29% and -27% ee, respectively). Additionally, in non-polar solvents there was significantly less reactivity, with the reaction taking 5-7 days to complete.

Table 4.1. Solvent screen with catalyst **4.13**.



Entry	Solvent	Relative Polarity ⁷	Reaction Time ⁸	Yield of 2.5	ee (%)
1	EtOH	0.654	8 h	48% ^[a]	73
2	10% H ₂ O/EtOH		28h	56% ^[a]	75
3	MeNO ₂	0.481	5 days	63%	38
4	2% HFIP/DCM		7 days	32%	29
5	toluene	0.099	7 days	70%	-29
6	cyclohexane	0.006	5 days	48%	-27

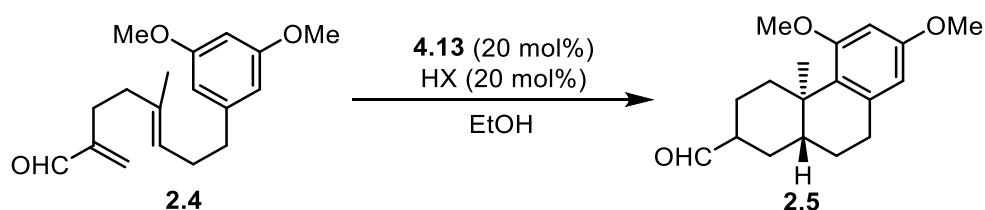
[a] After hydrolysis of ethyl acetal with CHCl₃/H₂O/TFA.

The results from this initial solvent screen indicated that polar solvents were necessary to obtain high enantioselectivity with catalyst **4.13**. As the substrate is a long, non-polar carbon chain, polar solvents are expected to promote substrate folding to give a closed conformation, potentially one that is pre-aligned for reactivity. The long reaction times and reversal of the major enantiomer obtained in the cyclization of **2.4** in non-polar solvents indicate that enantioinduction is occurring through a different interaction.

For catalyst screening, HCl (pK_a -8.0) was initially used as a co-acid as it had provided clean product in the original racemic iminium-catalyzed polyene cyclization. To optimize for enantioselectivity, the effect of the co-acid on the asymmetric reaction was investigated (Table

4.2). Acids were screened that were stronger (Tf₂NH, pK_a -11.9) and weaker (TFA, pK_a -0.25) than HCl. It was found that the enantioselectivity was not strongly dependant on the co-acid. Tf₂NH, a stronger co-acid, provided product **2.5** in 69% yield and a faster reaction time (3 hours) with slightly diminished enantioselectivity (67% ee, Entry 2). TFA, a weaker co-acid, provided product **2.5** in 48% yield and a slower reaction time (6 days), but with slightly higher enantioselectivity (80% ee, Entry 3).

Table 4.2. Co-acid screen with catalyst **4.13**.



Entry	Acid	pK _a ⁹⁻¹⁰	Reaction Time ⁷	Yield of 2.5 ^[a]	ee (%)
1	HCl	-8.0 (H ₂ O)	8 h	48%	73
2	Tf ₂ NH	-11.9 (DCE)	3 h	69%	67
3	TFA	-0.25 (H ₂ O)	6 days	48%	80

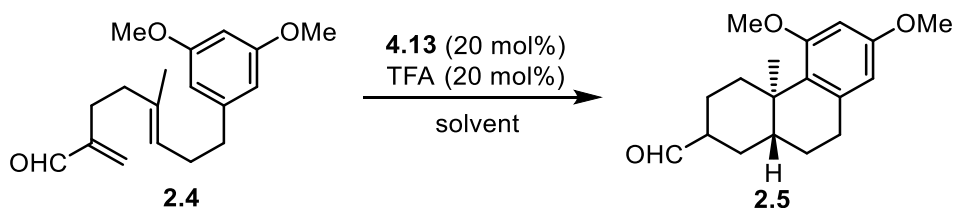
[a] After hydrolysis of ethyl acetal with CHCl₃/H₂O/TFA.

The role of the acid in these reactions is to protonate the carbonyl oxygen to facilitate iminium ion formation. The counteranion balances cationic charge or stabilizes partial cationic charge along the reaction pathway. A strong acid results in a weakly co-ordinating/nucleophilic counteranion which donates less electron density in an ionic bond and, in turn, provides more cationic character to the participating cation. In the reaction with Tf₂NH as the co-acid, the weakly co-ordinating counteranion would give more cationic character to the initial α,β-unsaturated iminium, the intermediate cyclohexyl cation, as well as the arenium ion. This would result in the observed increase in reactivity. A weak acid results in a strongly co-ordinating/nucleophilic counteranion after deprotonation, and the converse argument can be made for the observed reduced reactivity with TFA as a co-acid. Trapping of cationic intermediates with more nucleophilic counteranions is also a consideration. Although trifluoroacetate trapped products were not isolated,

it is possible that the reduced reactivity with TFA arises from an equilibrium of counterion trapped products with cationic intermediates.

As EtOH had provided the highest enantioselectivity in a solvent screen with the HCl salt of catalyst **4.13**, a second solvent screen was performed with other protic solvents using TFA as a co-acid (Table 4.3). With this solvent screen, we were interested in determining whether the protic character of the solvent or the polarity was influencing the enantioselectivity. Both 1,2-ethanediol (Entry 2) and 1,3-propanediol (Entry 3) resulted in irreversible formation of the acetal and gave no desired reactivity. MeOH, with a relative polarity higher than EtOH (0.762), provided 59% of product **2.5** in only 24 hours but with slightly diminished enantioselectivity (75% ee, Entry 4). *i*PrOH (Entry 5) and *t*BuOH (Entry 6), with lower relative polarities of 0.546 and 0.389, provided product **2.5** in 51% and 53% yields with lower enantioselectivities (72% and 53% ee, respectively). The results from this screen provided EtOH as the optimal solvent in this reaction, with the polarity of the solvent being an influencing factor on the enantioselectivity.

Table 4.3. Screening of alcoholic solvents with catalyst **4.13**.



Entry	Solvent	Relative Polarity ⁷	Reaction Time ⁷	Yield of 2.5 ^[a]	ee (%)
1	EtOH	0.654	6 days	48%	80
2	1,2-ethanediol		7 days	-	-
3	1,3-propanediol		7 days	-	-
4	MeOH	0.762	24 h	59%	75
5	<i>i</i> PrOH	0.546	11 days	51%	72
6	<i>t</i> BuOH	0.389	9 days	53%	53

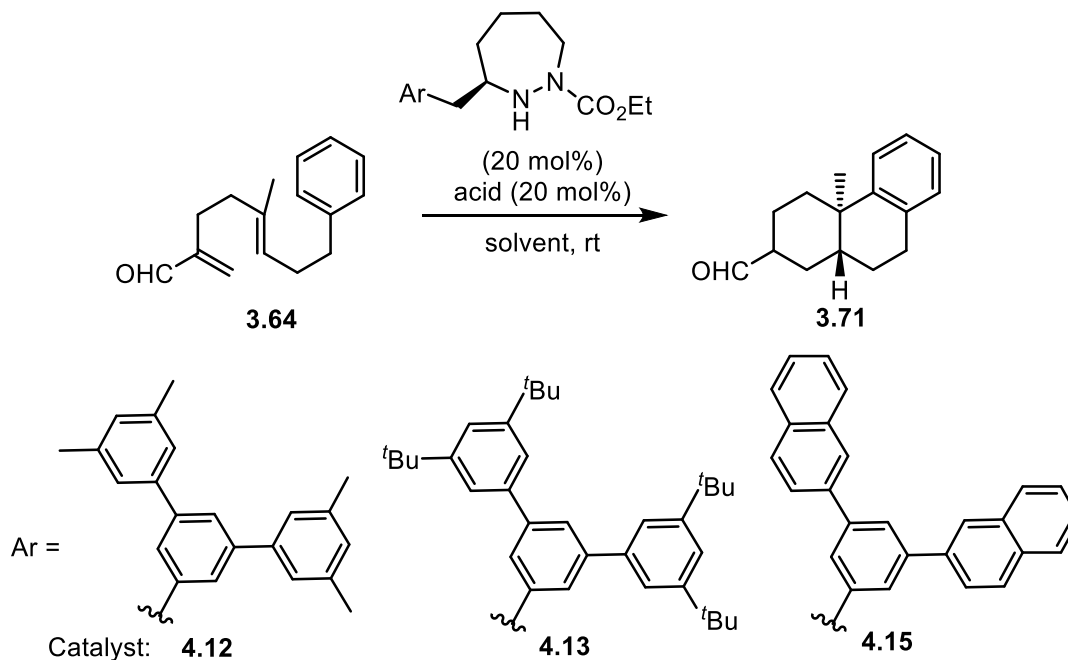
[a] After hydrolysis of corresponding acetal with CHCl₃/H₂O/TFA.

4.9 Investigations into substrate scope

4.9.1 Phenyl-terminated substrate

With the increased reactivity of anthracene catalyst **3.47**, we had successfully cyclized substrates with less nucleophilic terminating groups. In our initial investigations into the scope of the asymmetric reaction, we sought to determine whether *m*-terphenyl catalysts would show similar reactivity. For this investigation, we screened *m*-terphenyl catalysts in the polyene cyclization of substrate **3.64**, which is terminated by a less nucleophilic phenyl ring (Table 4.4). In the reaction with 3,5-dimethyl substituted *m*-terphenyl catalyst **4.12** as the HCl salt, run in the solvent mixture of 2% HFIP/DCM, no bicyclic product **3.71** was observed and only a minimal amount of starting material was consumed (Entry 1). With the same catalyst, the reaction run in EtOH resulted in monocyclic EtOH trapped product, with no observed bicyclic product **3.71** (Entry 2). With 3,5-di-*tert*-butyl-*m*-terphenyl catalyst **4.13** as the HCl salt, the reaction was run in *i*PrOH to reduce solvent trapping (Entry 3). However, the major product observed in this reaction was *i*PrOH trapped monocyclic product and no desired bicyclic product **3.71** was observed. To increase the reactivity of catalyst **4.13**, the Tf₂NH salt was screened. In MeNO₂, the reaction resulted in no desired product and only monocyclic side products resulting from elimination were observed (Entry 4). In MTBE, product **3.71** was isolated in 13% yield with low enantioselectivity (12% ee, Entry 5). We investigated whether a stronger cation- π interaction would stabilize the intermediate and allow the desired bicyclization to proceed by examining catalyst **4.15** in this reaction (Entry 6). Although the TFA salt of catalyst **4.15** provided product **3.71** in a low yield (20%) when run in MeNO₂, it provided low enantioselectivity (4% ee).

Table 4.4. Screening of conditions for cyclization of substrate **3.64**.



Entry	Catalyst	Solvent	Acid	Reaction Time	Yield of 3.71	ee (%)
1	4.12	2% HFIP/DCM	HCl	24 h	-	-
2	4.12	EtOH	HCl	24 h	-	_[a]
3	4.13	<i>i</i> PrOH	HCl	48 h	-	_[a]
4	4.13	MeNO ₂	Tf ₂ NH	30 min.	-	-
5	4.13	MTBE	Tf ₂ NH	5 days	13%	12
6	4.15	MeNO ₂	TFA	18 h	20%	4

[a] Only alcohol trapped monocyclic product was observed.

We had demonstrated that EtOH provided product with the highest enantioselectivity in the cyclization of substrate **2.4** with catalyst **4.13**, with less polar solvents having a detrimental effect (Tables 4.1 and 4.3). Although the asymmetric reaction of substrate **3.64** was attempted in EtOH, the solvent trapping outcompeted the intramolecular trapping of the cyclohexyl cation by the terminating group. Low enantioselectivity was observed in bicyclic product **3.71** obtained from the reaction in non-nucleophilic solvents, MTBE and MeNO₂. However, it was unclear whether

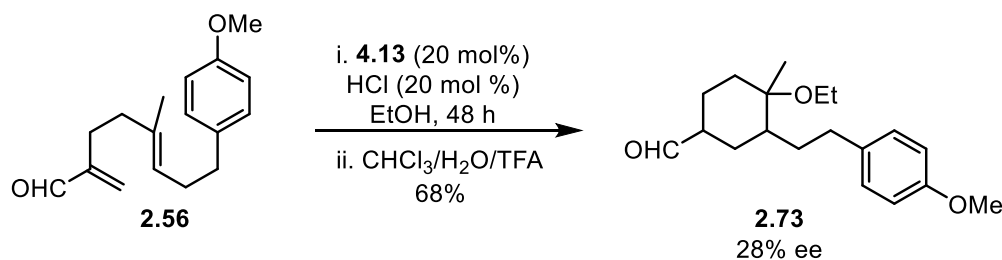
the low enantioselectivities observed in these reactions were innate to the substrate or due to solvent effects.

4.9.2 Analysis of EtOH-trapped products

As seen in Section 1.4.4, in LBA-catalyzed polyene cyclizations, the addition of a strong acid after the catalyst is necessary to complete the second ring closure. Prior to the addition of the strong acid, a mixture of monocyclic olefins is observed. The acid protonates these olefinic intermediates, which allows the intramolecular trapping of the resulting cation by the terminating group.

In the asymmetric iminium-catalyzed (*E*)-polyene cyclization of the model substrate **2.4**, EtOH had provided significantly higher enantioselectivity. However, with substrates that contained less nucleophilic terminating groups, the major product isolated was the result of EtOH trapping of the cyclohexyl cation intermediate. We envisioned that with EtOH trapped products (e.g. **4.35**, Scheme 4.16), a second step of the addition of a strong acid would reionize the ethyl ether and allow for intramolecular trapping by the aromatic terminating group. As the first stereocenter of the decalin product is set by the initial ring closure, which is followed by EtOH trapping, we assumed that the enantioselectivity achieved would be maintained in the bicyclic product after reionization and second ring closure.

Prior to investigating the reionization of EtOH trapped product **2.73**, we examined the enantioselectivity of the EtOH trapping with catalyst **4.13** to ensure that the second cyclization would provide bicyclic product in high enantiomeric excess (Scheme 4.16). EtOH trapped product **4.35**, which had been obtained after cyclization of substrate **2.56** with catalyst **4.13** in EtOH, was isolated in 68% yield but with low enantioselectivity of 28% ee.¹¹ As the EtOH trapping wasn't highly enantioselective, we did not proceed with attempts to re-ionize this species.



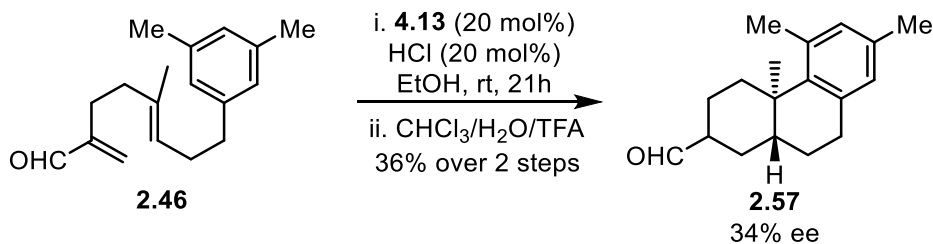
Scheme 4.16. Enantioselectivity of ethanol trapping with substrate **2.56**.

In this reaction, the initial ring closure sets the first stereocenter. However, for the enantioselectivity achieved in this step to be transferred to the product this must be the rate-limiting step. The low enantioselectivity observed in the EtOH trapping suggests that the first ring closure is not the rate-limiting step and that there is an element of reversibility in the reaction.

4.9.3 3,5-Dimethylphenyl-terminated substrate

The cyclization of model (*E*)-polyene substrate **2.4**, which was terminated by a 3,5-dimethoxyphenyl ring, had proceeded with high enantioselectivity to give product **2.5** with catalyst **4.13** in EtOH. Low yields of bicyclic product **3.71** with low enantioselectivity had resulted from the cyclization of substrate **3.64** with *m*-terphenyl catalysts in MTBE or MeNO₂. However, as this substrate was terminated by an unsubstituted phenyl ring, it was unclear whether the low enantioselectivity was attributed to the lower nucleophilicity of the terminating group, the lack of 3,5-substitution on the terminating group, or the solvent system.

To investigate the scope of the bicyclization with catalyst **4.13** in EtOH, we needed a substrate that was terminated by an aromatic ring that was less nucleophilic than that in model substrate **2.4**, but still nucleophilic enough so that the second ring closure could compete with EtOH trapping. Substrate **2.46** had provided a nearly equimolar amount of EtOH trapped product to bicyclic product with catalyst **1.241** (Section 2.4) and so we assumed that we would obtain some yield of bicyclic product in the asymmetric reaction. In addition, substrate **2.46** is terminated by a 3,5-dimethylphenyl ring, which would allow us to investigate whether high levels of enantioselectivity with substrate **2.4** were due to the steric environment achieved with substitution at the 3,5-positions. Therefore, the asymmetric reaction of substrate **2.46** was run with catalyst **4.13**. The resulting product **2.57** was obtained in a 36% yield with low enantioselectivity (34% ee, Scheme 4.17).



Scheme 4.17. Asymmetric cyclization of substrate **2.46**.

4.9.4 DFT investigation of reaction mechanism

To investigate the origins of the diminished enantioselectivity in the polyene cyclization of substrate **2.46**, we performed DFT calculations on the reaction profiles of substrates **2.4** and **2.46** with catalyst **4.13**. Final calculations were run with a larger basis set to provide greater accuracy, at the M06-2X/6-311G(d,p) level of theory and using the PCM solvation model for EtOH.

The calculated reaction profile for substrate **2.4** gave an activation barrier for the first ring closure in the proximal *s-trans* conformation of 4.8 kcal/mol (relative to the initial iminium, Figure 4.8). The activation barrier for the proximal *s-cis* conformation, which leads to the opposite enantiomer, was calculated to be 3.6 kcal/mol higher in energy (8.4 kcal/mol). At this level of theory, the calculations suggested that the bicyclization is a concerted, asynchronous process¹² with a $\Delta\Delta G^\ddagger$ that is somewhat consistent with the experimentally observed enantioselectivity. Absolute stereochemical assignment of enantioenriched product **2.5** has been done by Dr. Samuel Plamondon,¹³ and the results obtained are consistent with the major enantiomer that would be obtained from the proximal *s-trans* conformation of the first transition state.

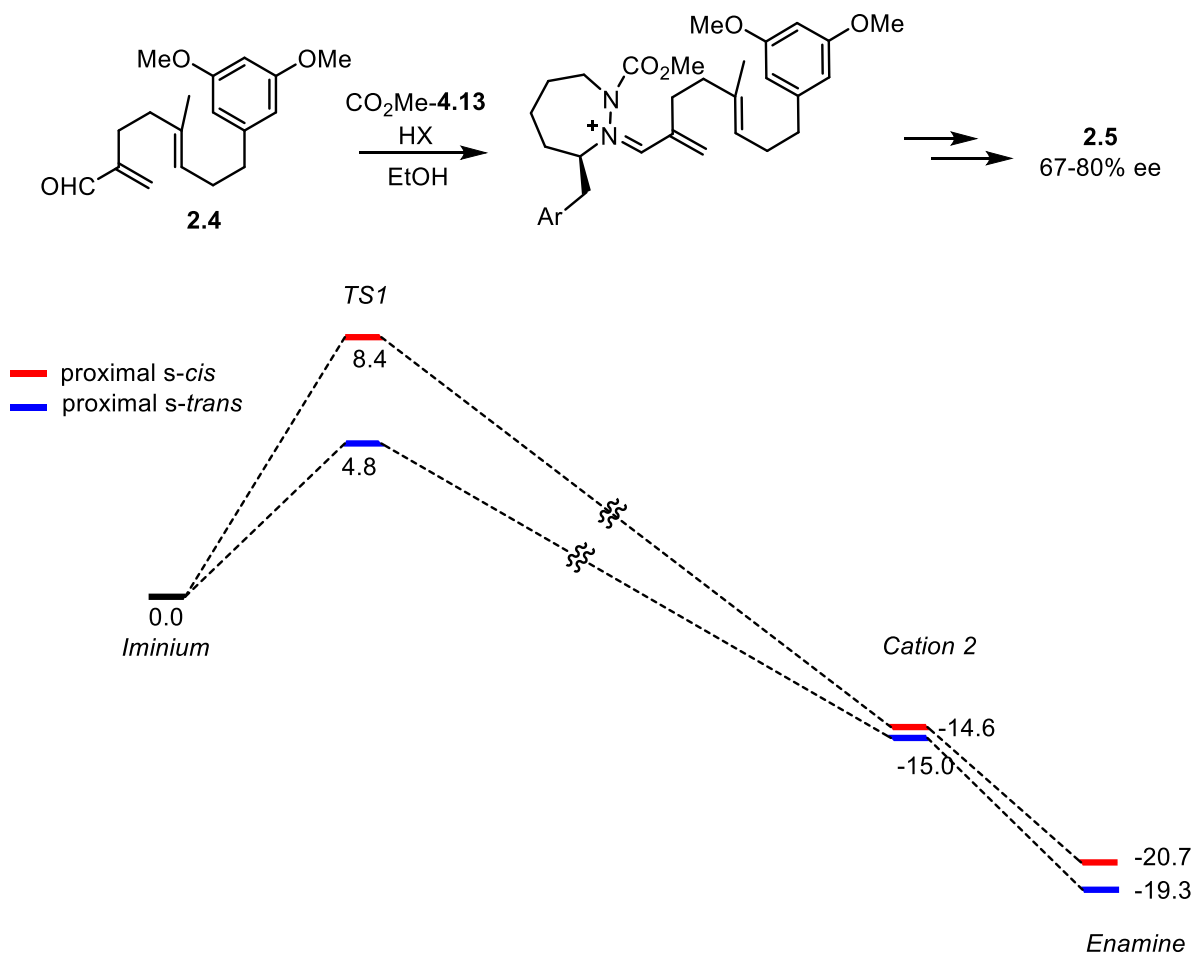


Figure 4.8. Reaction profile of 3,5-dimethoxyphenyl terminated substrate **2.4** with catalyst **CO₂Me-4.13**. Calculations run at the M06-2X/6-311G(d,p), solvent = EtOH level of theory. Free energies in kcal/mol.

The lowest energy conformation for the first transition state in the reaction of substrate **2.46** with catalyst **4.13** was found with a different *m*-terphenyl rotamer than the preferred cage-like rotamer in previously modelled *m*-terphenyl catalysts. This lowest energy conformation (proximal *s-trans* twist) preferred the 3,5-di-*tert*-butylphenyl groups of the *m*-terphenyl moiety twisted clockwise (see Figure 4.3), which gave a calculated activation barrier for the first ring closure of 5.2 kcal/mol relative to the initial iminium (Figure 4.9). The activation barrier for the cage-like rotamer in the proximal *s-trans* conformation was calculated to be 1.2 kcal/mol higher in energy, with an energy of 6.4 kcal/mol. The lowest energy proximal *s-cis* conformation, which leads to the minor enantiomer, was found with the cage-like rotamer of the *m*-terphenyl and was calculated to have an activation barrier of 9.5 kcal/mol.

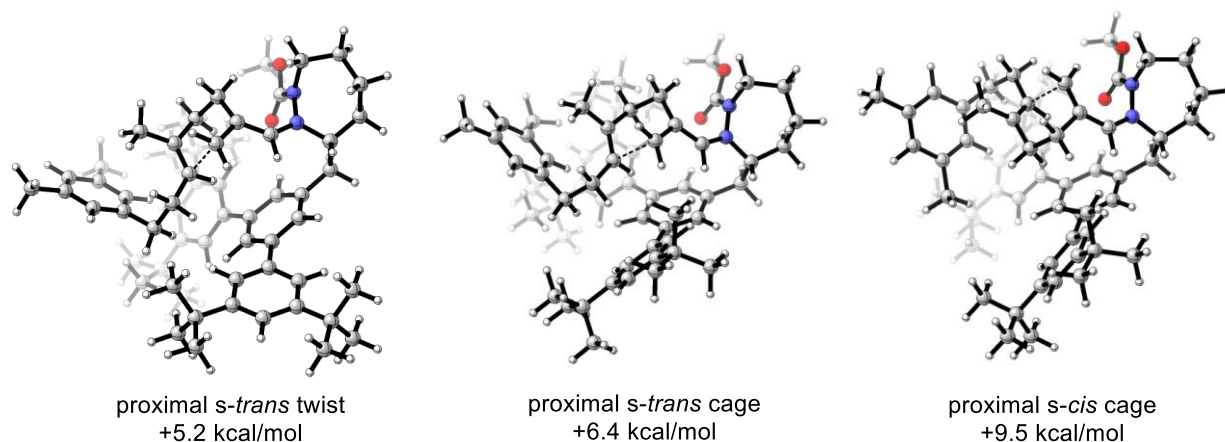


Figure 4.9. Lowest energy conformations of the first transition state of 3,5-dimethylphenyl terminated substrate **2.46** with catalyst CO₂Me-**4.13**. Calculations at the M06-2X/6-311G(d,p), solvent = EtOH level of theory.

Unlike substrate **2.4**, the reaction profile for substrate **2.46** was calculated to be stepwise (Figure 4.10). The cage-like rotamer of the *m*-terphenyl moiety was preferred for the cyclohexyl cation intermediate and the second transition state of the proximal *s-trans* conformation, giving energies of -0.8 kcal/mol and 2.4 kcal/mol. In comparison, the proximal *s-trans* conformation with the twisted *m*-terphenyl moiety had calculated energies of 1.3 kcal/mol and 5.5 kcal/mol for the cyclohexyl cation intermediate and second transition state. The rotational barrier for the 3,5-di-*tert*-butylphenyl ring distal to the carbamate, which is the barrier between the cage-like and twisted rotamers, was calculated to be 4.5 kcal/mol at the cyclohexyl cation intermediate. This barrier is lower than the 5.5 kcal/mol barrier for the second ring closure and the 5.2 kcal/mol barrier for the reverse reaction, which suggests that rotation of the phenyl group to result in the more stable proximal *s-trans* conformation with the cage-like *m*-terphenyl moiety would be a likely outcome. However, the rotational barrier is still relatively high in energy, providing a significant probability that alternate lower energy pathways would proceed instead.

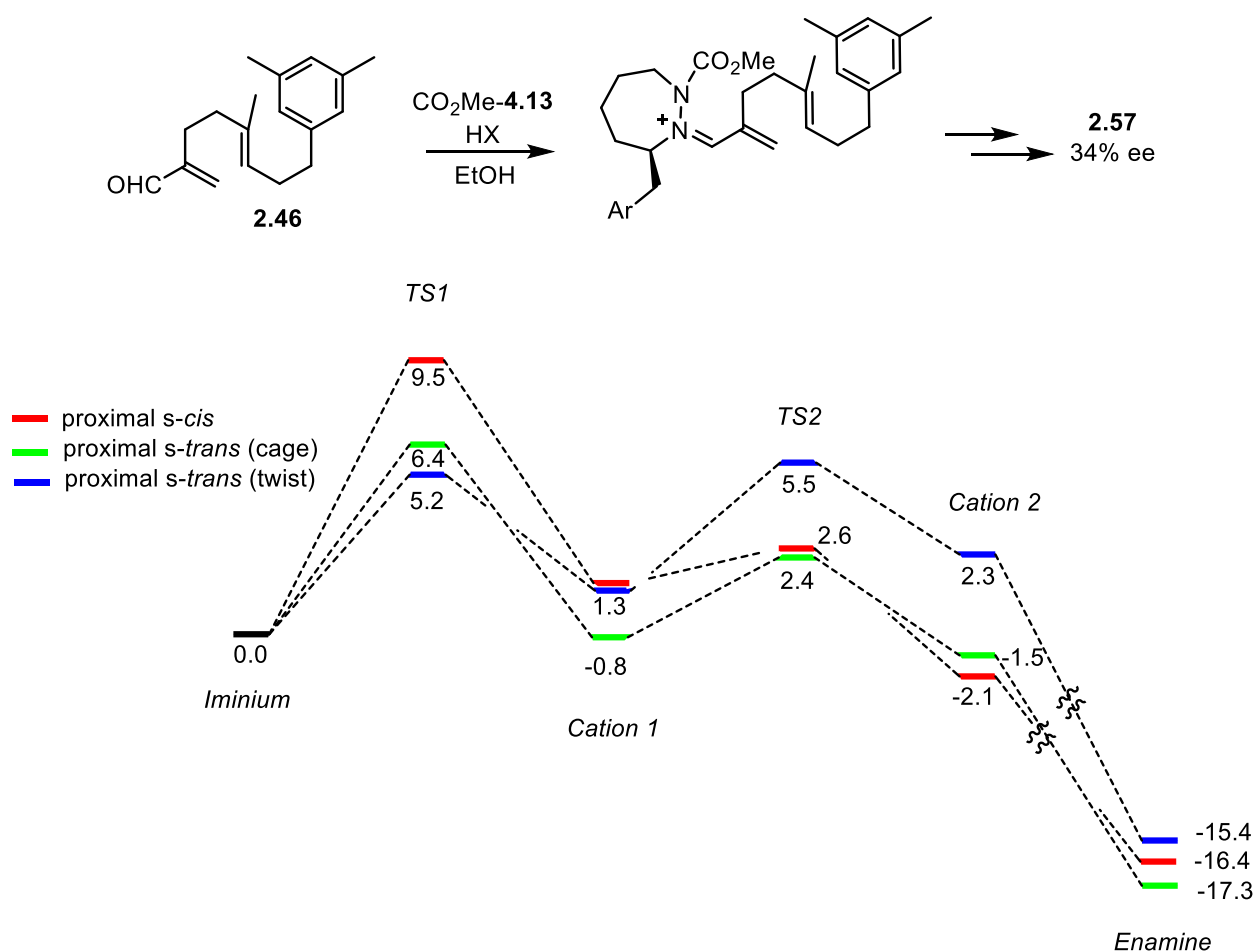


Figure 4.10. Reaction profile of 3,5-dimethylphenyl terminated substrate **2.46** with catalyst **CO₂Me-4.13**. Calculations at the M06-2X/6-311G(d,p), solvent = EtOH level of theory. Free energies in kcal/mol.

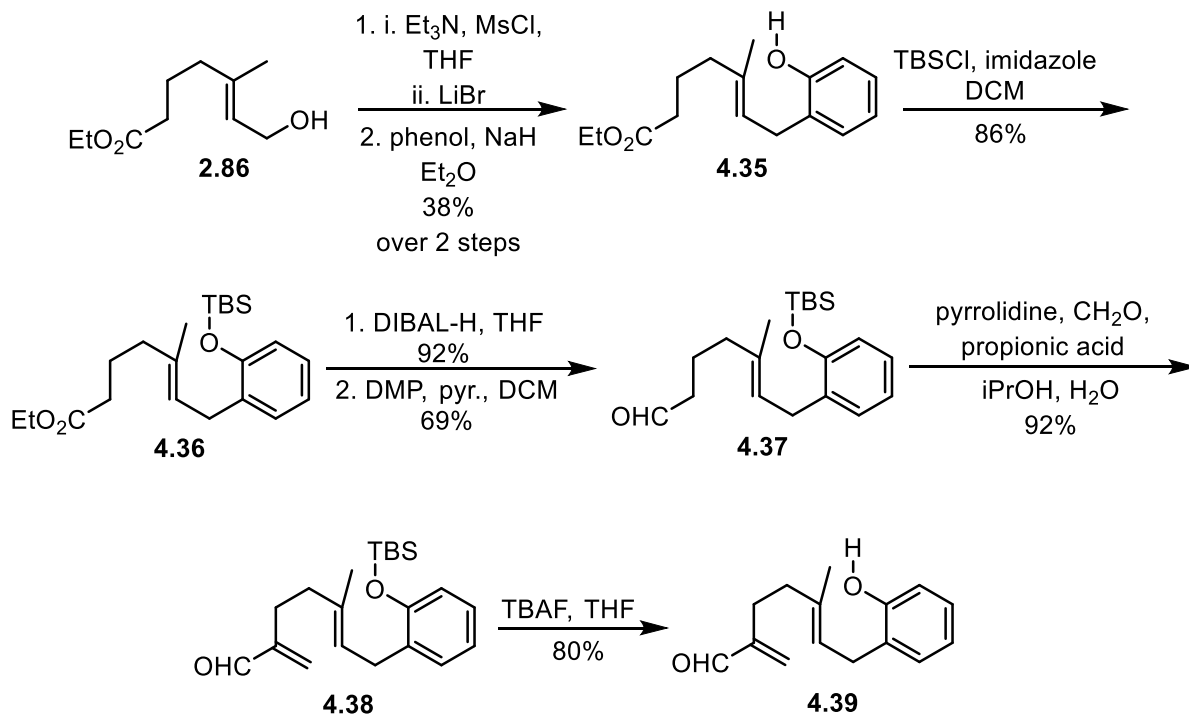
The activation barrier for the proximal *s-cis* conformation was calculated to be 4.3 kcal/mol higher than the lowest energy proximal *s-trans* conformation of the first transition state. The intermediate cyclohexyl cation was calculated to be 1.3 kcal/mol for this conformation and the second transition state was calculated to be 2.6 kcal/mol. Due to the challenges in modelling bimolecular proton transfer, the activation barrier for the deprotonation of the arenium intermediate was not calculated. In the reaction of substrate **2.4** with catalyst **4.13**, the low energy of the arenium ion suggests that the following deprotonation would not be rate-limiting and the enantioselectivity of the reaction should be closely correlated to the energy difference between the diastereomeric conformations of the first transition state. In contrast, the higher energies of the arenium ion with substrate **2.46** suggest a greater possibility that the deprotonation might be the

rate-limiting step. If this is the case, the reaction would be less likely to proceed to enamine product and there is a higher probability for alternate pathways to occur instead, such as the reverse reaction or solvent trapping, which could contribute to the erosion of enantioselectivity. Additionally, it is possible that the deprotonation of the arenium ion in the distal conformations would have a lower activation barrier than in the proximal conformations, as it would be a less hindered process. There is less steric differentiation between the *s-cis* and *s-trans* iminium ions in the distal conformations. Therefore, if the deprotonation is rate-limiting and provides a preference for these conformations over their proximal counterparts, lower enantioselectivity would be expected.

Based on these observations, we hypothesized that substrates with terminating groups of strong nucleophilicity are required to achieve high enantioselectivity with catalyst **4.13**. These substrates would be more likely to proceed through a concerted second ring closure and would also be expected to result in more stable arenium ions, decreasing the probability that arenium deprotonation is the rate-limiting step. Therefore, as the first ring closure should be the rate-limiting step with such substrates, a strong preference for one conformation of this transition state would be expected to lead to *trans*-decalin product with high enantioselectivity.

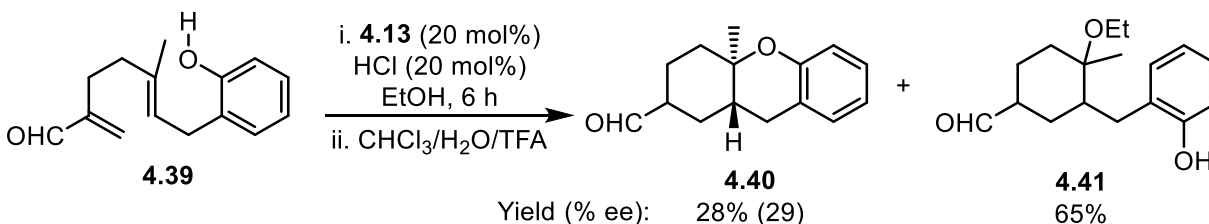
4.9.5 Phenol-terminated substrate

In our investigation into substrates with electron-rich terminating groups, we hypothesized that trapping by a phenol would be a low barrier process, as alcohol trapping of the intermediate cyclohexyl cation proceeded readily. Therefore, substrate **4.39** was designed and synthesized (Scheme 4.18). The synthesis proceeds from intermediate alcohol **2.86** through initial formation of the mesylate and displacement with lithium bromide. This bromide was then displaced by sodium phenolate, giving phenol **4.35** in 38% yield over two steps which was protected as the TBS ether to give ester **4.36** in 86% yield. The ester was reduced with DIBAL-H in 92% yield and subsequently oxidized with DMP buffered with pyridine to give aldehyde **4.37** in 69% yield. An α -methylenation proceeded to give enal **4.38** in 92% yield. This was followed by deprotection of the TBS ether to give phenol substrate **4.39** in 80% yield.



Scheme 4.18. Synthesis of phenol-terminated substrate **4.39**.

Substrate **4.39** was screened in the asymmetric polyene cyclization with catalyst **4.13** (Scheme 4.19). Under these conditions, product **4.40** was provided in 28% yield. The trapping was either slower than we had expected or was reversible, and trapping of the cyclohexyl cation by EtOH was competitive, providing product **4.41** in 65% yield. Low enantioselectivity was achieved in the bicyclization, providing product **4.40** in 29% ee.

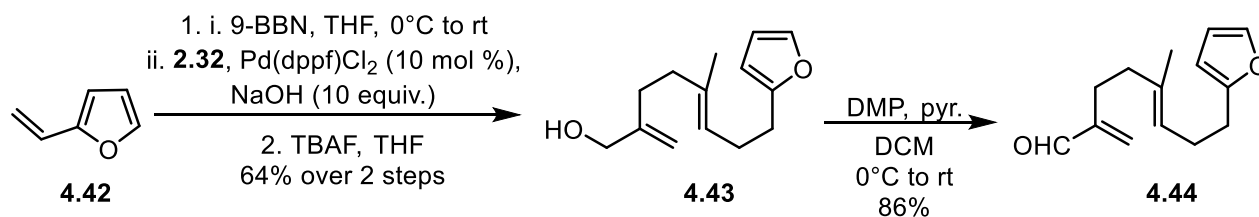


Scheme 4.19. Polyene cyclization of phenol substrate **4.39** with catalyst **4.13**.

4.9.6 Furan-terminated substrate

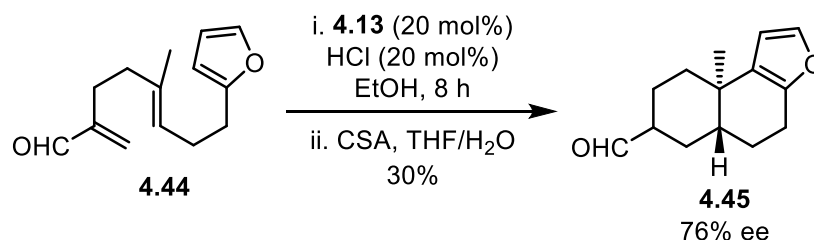
To investigate our hypothesis that substrates with strongly nucleophilic terminating groups would cyclize with high enantioselectivity, we investigated substrate **4.44**, which is terminated by an electron-rich furan ring. The synthesis of substrate **4.44** followed the same route as that was

used to synthesize (*E*)-polyene substrates in Chapters 2 and 3 (Scheme 4.20). The final steps in the synthesis proceeded with a Suzuki cross-coupling between the hydroboration product of styrene **4.42** and iodide **2.32**. Following deprotection of the TBS ether, alcohol **4.43** was isolated in 64% yield. Oxidation of the alcohol with DMP buffered with pyridine provided substrate **4.44** in 86% yield.



Scheme 4.20. Synthesis of furan-terminated substrate **4.45**.

Substrate **4.44** was examined in the asymmetric polyene cyclization with catalyst **4.13** (Scheme 4.21). Under these reaction conditions, we found that the acid sensitivity of the furan functional group resulted in a slightly diminished yield of product **4.45** (30% yield). However, product **4.45** was obtained with high enantioselectivity (76% ee).



Scheme 4.21. Cyclization of furan-terminated substrate **4.44** with catalyst **4.13**.

This result supported our hypothesis that substrates with more nucleophilic terminating groups would cyclize with high enantioselectivity in the asymmetric (*E*)-polyene cyclization with catalyst **4.13**. To provide further support for our hypothesis, we have determined a range of substrates to be assessed which we propose would cyclize with catalyst **4.13** to give *trans*-decalin products with high enantioselectivity.

4.9.7 Future substrates

We have designed catalyst **4.13** in our investigation into the asymmetric iminium catalyzed (*E*)-polyene cyclization, which has provided bicyclic products with high enantioselectivities with the model (*E*)-polyene substrate **2.4** as well as furan-terminated substrate **4.44**. The final steps in

this project will be to finish the investigation into the scope and limitations of the reaction. In our analysis of substrates that will potentially provide products with high enantioselectivities, we have considered two criteria. Evidence has shown that strongly nucleophilic terminating groups, e.g. those in substrates **2.4** and **4.44**, are required to provide *trans*-decalin products with high enantioselectivities. Therefore, this is the first criteria that we considered. Secondly, based on computational models with catalyst **4.13**, we presume that the terminating group needs to be similar in size or smaller than the 3,5-dimethoxyphenyl in substrate **2.4**. It is possible that substrates with much larger terminating groups would not fit into the cage-like binding pocket of the *m*-terphenyl moiety. The resulting steric interference could give a greater preference for the distal conformations of the first transition state, which have been correlated with lower enantioselectivities.

We suggest that the substrates shown in Figure 4.11 fulfill these two criteria. Substrates **2.47** and **2.48** are terminated by a strongly nucleophilic aromatic ring, with a methoxy and methyl substituent *para*- or *ortho*- to the desired site of reactivity. Both substrates had a lower degree of isomerization to give *cis*-decalin product in the racemic iminium-catalyzed (*E*)-polyene cyclization (96:4 and 94:6 *trans:cis*, respectively). Therefore, they are expected to have shorter lived cyclohexyl cation intermediates following the first ring closure. In addition, substrates with these terminating groups provided *cis*-decalin product with high enantioselectivity in the (*Z*)-polyene cyclization, where the enantioselectivity was also correlated to the nucleophilicity of the terminating group (albeit not to the same degree).

As substrate **4.44** provided product **4.45** with high enantioselectivity, we expect that substrates terminated by more reactive heterocycles than furan will produce similar results. It is known that electrophilic substitution of a 5-membered ring heterocycle will generally react faster at the 2-position than that at the 3-position. Although rates vary depending on the nature of the electrophile, general reactivity trends also indicate that pyrrole will react much faster than furan.¹⁴ Therefore, we presume that the cyclization of a substrate terminated by pyrrole at the 3- or 2-positions (as in substrates **4.46** and **4.47**) will proceed with high enantioselectivity. The reactivity of these substrates could be modulated through a protecting group on the pyrrole nitrogen.

Reactivity trends for the electrophilic substitution of iron tricarbonyl-complexed carbocation $[\text{C}_6\text{H}_7\text{Fe}(\text{CO})_3]^+$ suggest that electrophilic substitution of indole will occur at the 3-

position at a faster rate than the electrophilic substitution of furan.¹⁴ Therefore, assuming similar reactivity trends in the termination of the polyene cyclization, we expect that substrate **4.48** will also cyclize with high enantioselectivity.

Reaction rates of the electrophilic substitution of indole and benzofuran at the 2-position are generally slower than with the other heterocyclic terminating groups in Figure 4.11.¹⁴ However, substrates terminated by these heterocycles proceeded with good enantioselectivity in the iridium-catalyzed polyene cyclization, a reaction which was limited by the need for a strongly nucleophilic terminating group.¹⁵ Therefore, we presume that substrates terminated by these heterocycles (substrates **4.49**, **4.50**, and **4.51**) will proceed with high enantioselectivity in the asymmetric iminium-catalyzed (*E*)-polyene cyclization.

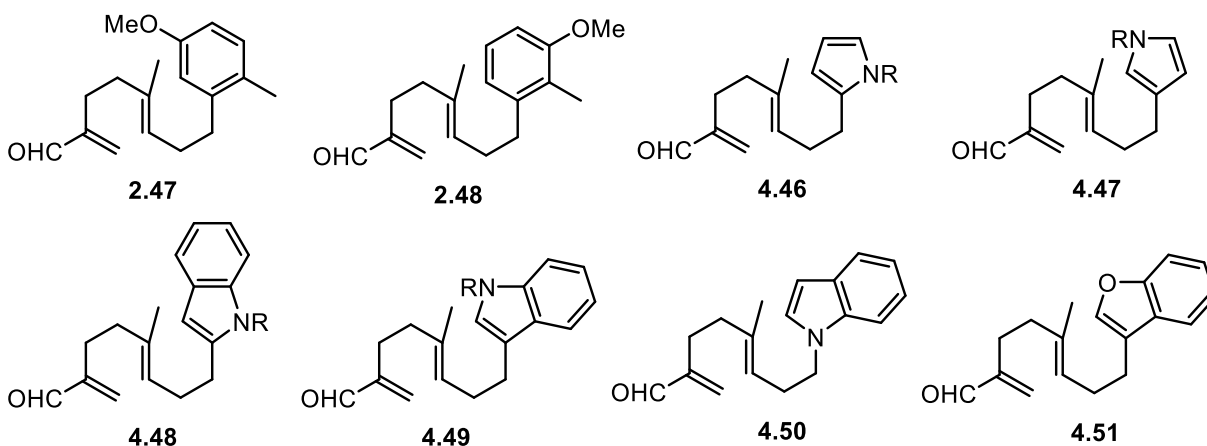


Figure 4.11. Potential substrates for the asymmetric (*E*)-polyene cyclization.

4.10 Conclusions

In this chapter, we have performed DFT calculations to investigate the relative energies of diastereomeric conformations of the transition state for the first ring closure in the asymmetric (*E*)-polyene cyclization, which sets the first stereocenter. Through this investigation, we modelled a catalyst with *m*-terphenyl substitution that showed a promising steric environment for the induction of asymmetry. Using a modular synthetic route similar to that developed for aromatic substituted cyclic hydrazides in Chapter 3, we synthesized a library of *m*-terphenyl catalysts with substitution that had varied steric and electronic effects. The cyclization of model (*E*)-polyene substrate **2.4** was investigated with this library of catalysts, the results of which are summarized in Appendix I. Catalyst **4.13**, with 3,5-di-*tert*-butyl substitution on the *m*-terphenyl moiety, was

identified as providing high enantioselectivity. With this catalyst, the reaction conditions were optimized to provide *trans*-decalin product **2.5** in up to 80% ee.

Experimental investigation into the scope of the reaction with catalyst **4.13** has suggested a correlation of the enantioselectivity with the nucleophilicity of the terminating group. DFT calculations on the reaction profile of catalyst **4.13** with substrate **2.4**, which is terminated by a strongly nucleophilic aromatic ring, provided evidence towards a concerted second ring closure with a lower energy arenium ion intermediate. The energy of the arenium intermediate suggested that it is unlikely that deprotonation of this intermediate is the rate-limiting step. Based on these calculations, the rate-limiting step is most likely the initial ring closure and we found that the observed enantioselectivity was somewhat consistent with the $\Delta\Delta G^\ddagger$ for this step.

We further investigated the scope of the reaction, with the hypothesis that strongly nucleophilic terminating groups are required to achieve high enantioselectivities. Substrate **4.44**, with an electron-rich terminating furan ring, provided *trans*-decalin product **4.45** in 76% ee. With these results, we have identified several substrates that we propose would also cyclize to give *trans*-decalin products with high enantioselectivity in the asymmetric (*E*)-polyene cyclization.

There is a significant number of natural products that contain a *trans*-decalin core, many of which have medicinal relevance. The enantioselective (*E*)-polyene cyclization developed in this chapter could be used to synthesize these natural products and other derivatives asymmetrically from simple achiral precursors. In addition to promoting the asymmetric polyene cyclization, the chiral catalyst developed has the potential for enantioinduction in other iminium-catalyzed reactions.

4.11 References

1. Plamondon, S. J.; Warnica, J. M.; Kaldre, D.; Gleason, J. L., Hydrazide-Catalyzed Polyene Cyclization: Asymmetric Organocatalytic Synthesis of *cis*-Decalins. *Angew. Chem. Int. Ed.* **2020**, *59* (1), 253-258.
2. Sanders, J. N.; Jun, H.; Yu, R. A.; Gleason, J. L.; Houk, K. N., Mechanism of an Organocatalytic Cope Rearrangement Involving Iminium Intermediates: Elucidating the Role of Catalyst Ring Size. *J. Am. Chem. Soc.* **2020**, *142* (39), 16877-16886.

3. Davis, M. R.; Dougherty, D. A., Cation- π interactions: computational analyses of the aromatic box motif and the fluorination strategy for experimental evaluation. *Phys. Chem. Chem. Phys.* **2015**, *17* (43), 29262-29270.
4. Whitton, A. J.; Kumberger, O.; Müller, G.; Schmidbaur, H., Preparation and characterisation of 9,10-dihydroanthracene and tert-butyl-9,10-dihydroanthracene complexes with one or two tricarbonylchromium units; crystal structure of tricarbonyl ($\eta^{1,2,3,4,4a,9a}$ -9,10-dihydroanthracene)chromium. *Chem. Ber.* **1990**, *123* (10), 1931-1939.
5. Holland, M. C.; Metternich, J. B.; Mück-Lichtenfeld, C.; Gilmour, R., Cation- π interactions in iminium ion activation: correlating quadrupole moment & enantioselectivity. *Chem. Commun.* **2015**, *51* (25), 5322-5325.
6. Heard, G. L.; Boyd, R. J., Calculation of Quadrupole Moments of Polycyclic Aromatic Hydrocarbons: Applications to Chromatography. *J. Phys. Chem. A* **1997**, *101* (29), 5374-5377.
7. Reichardt, C.; Welton, T., Empirical Parameters of Solvent Polarity. In *Solvents and Solvent Effects in Organic Chemistry*, 2010; pp 425-508.
8. Due to restrictions on laboratory availability during this time, longer reaction times may be overestimated.
9. Smith, M. O., March's advanced organic chemistry : reactions, mechanisms, and structure. 7th edition / ed.; Wiley: Hoboken, 2013.
10. Kütt, A.; Rodima, T.; Saame, J.; Raamat, E.; Mäemets, V.; Kaljurand, I.; Koppel, I. A.; Garlyauskayte, R. Y.; Yagupolskii, Y. L.; Yagupolskii, L. M.; Bernhardt, E.; Willner, H.; Leito, I., Equilibrium Acidities of Superacids. *J. Org. Chem.* **2011**, *76* (2), 391-395.
11. Product was obtained as two diastereomers which were reduced to corresponding alcohols and analyzed by chiral HPLC. Reported enantiomeric excess was the aggregate of both diastereomers. Further analysis of diastereomers was not conducted but presumably they were the C3 epimers in the cyclohexyl product with the ethyl ether trans to the aryl ethyl chain due to the steric hindrance of this bulky substitution favouring an anti addition of EtOH to the cyclohexyl cation.
12. In ref. 1, IRC calculations and coordinate scans were performed on a similar systems and have also suggested a concerted, asynchronous pathway.

13. Plamondon, S. J. Development of an asymmetric hydrazide-catalyzed polyene cyclization and its application to the total synthesis of (-)-3-oxoisotaxodione. McGill University, Montreal, 2021.
14. Katritzky, A. R., Handbook of heterocyclic chemistry. 3rd / ed.; Elsevier: Oxford, 2010.
15. Schafroth, M. A.; Sarlah, D.; Krautwald, S.; Carreira, E. M., Iridium-Catalyzed Enantioselective Polyene Cyclization. *J. Am. Chem. Soc.* **2012**, *134* (50), 20276-20278.

Contribution to knowledge and overall conclusion

This thesis investigates the scope and limitations of the first iminium catalyzed (*E*)-polyene cyclization. The methodology developed uses mildly acidic conditions to activate enal substrates and initiate the polyene cyclization, which is a complimentary approach to the widely used initiation method by electrophilic activation of an alkene or an epoxide. With a 7-membered ring hydrazide catalyst, the cyclization of (*E*)-polyene substrates terminated by aromatic rings of strong to intermediate nucleophilicity proceeded in high yields. With the simple 7-membered ring hydrazide catalyst, substrates with terminating groups of weaker nucleophilicities were unreactive or resulted in monocyclic side products. Further research into this polyene cyclization could investigate other terminating groups, such as enol ethers or alcohols, as well the extension of the cyclization to yield tricyclic products.

In the biosynthetic polyene cyclization, evidence has suggested the stabilization of cationic species through cation- π interactions with aromatic amino acid residues. Our initial strategy was to incorporate extended aromatics into our catalyst design to effect enantioselectivity, either through selective stabilization or steric differentiation of diastereomeric conformations of the cationic transition state which sets the first stereocenter. The incorporation of extended aromatic (anthracene) substitution into the cyclic hydrazide catalyst design provided negligible enantioselectivity. However, the reactivity was drastically increased. With this more reactive catalyst, we overcame some of the limitations of the reaction with the simple 7-membered ring catalyst and achieved bicyclization of substrates with weakly nucleophilic terminating groups. DFT calculations on the reaction mechanism suggested that the addition of anthracene substitution on the catalyst stabilized all cationic species along the reaction pathway. Increasing catalyst reactivity through the stabilization of intermediates and transition states is a useful strategy as it avoids the need for more reactive initiating methods that limit compatible substrate functionality. Evidence of stabilizing cation- π interactions with the incorporation of extended aromatics into catalyst design for the polyene cyclization has only been reported in one other methodology that incorporates a lactam ring into the bicyclic product.¹ In nature, there are many different polyene cyclization pathways leading to a diverse group of terpene natural products. Catalysts that stabilize cationic intermediates and transition states could potentially be used to access cyclization pathways other than those leading to decalin systems, which would be an interesting direction for future research.

To determine a viable catalyst design for the asymmetric reaction, we computationally modelled the transition state for the first ring closure, as this sets the first stereocenter in the final product. The lowest energy conformation of this transition state with a *m*-terphenyl substituted catalyst suggested that it could potentially provide high enantioselectivity in the polyene cyclization. A library of *m*-terphenyl catalysts with varied electronic and steric effects was synthesized and screened in the asymmetric iminium-catalyzed (*E*)-polyene cyclization. This has resulted in the development of a catalyst with 3,5-di-*tert*-butyl substitution on the *m*-terphenyl moiety that has promoted the cyclization of the model (*E*)-polyene substrate in up to 80% ee. Investigations into the scope of the reaction have provided evidence of a correlation between the nucleophilicity of the terminating group and the enantioselectivity observed. DFT studies on the reaction mechanism have suggested that the first ring closure is the rate-limiting step with substrates that cyclize with high enantioselectivity. However, it is possible that deprotonation of the arenium ion is rate-limiting with substrates that cyclize with lower enantioselectivity, potentially providing increased preference for pathways which erode the enantioselectivity. Further research could investigate the kinetics of the deprotonation of the arenium ion and whether this contributes to the lower enantioselectivity achieved in the cyclization of substrates with less nucleophilic terminating groups.

In conclusion, we have investigated the scope and limitations of the first iminium-catalyzed (*E*)-polyene cyclization and overcome some of these limitations by developing a catalyst with improved reactivity. Furthermore, we have developed a catalyst that promotes the asymmetric reaction with high enantioselectivity. This methodology promotes the cyclization of simple (*E*)-polyene precursors to provide structurally complex *trans*-decalin products, a motif commonly seen in terpene natural products. Therefore, this methodology has the potential applicability in the total synthesis of these complex natural products.

1. Knowles, R. R.; Lin, S.; Jacobsen, E. N., Enantioselective Thiourea-Catalyzed Cationic Polycyclizations. *J. Am. Chem. Soc.* **2010**, *132* (14), 5030-5032.

Chapter 5. Experimental Procedures

5.1. General Experimental

All reactions were performed under an inert argon atmosphere in oven- or flame-dried round bottom flasks fitted with rubber septa and using magnetic stirring, unless otherwise stated. Liquids and solutions were transferred via syringe or stainless-steel cannula under inert conditions. Reactions were frequently monitored by thin-layer chromatography (TLC), which was carried out on glass plates coated with 250 μm of 230-400 mesh silica gel that had been saturated with F-254 indicator. TLC plates were visualized using ultraviolet light and/or by exposure to various staining solutions followed by heating. Flash column chromatography was carried out on 230-400 mesh silica gel (Silicycle) using reagent-grade solvents. Room temperature (rt) indicates a temperature of approximately 22 °C.

All commercial reagents were used without further purification with the following exceptions: tetrahydrofuran and diethyl ether were distilled from sodium/benzophenone ketyl radical under a nitrogen atmosphere. Triethylamine was distilled from calcium hydride under a nitrogen atmosphere. Dichloromethane was distilled from calcium hydride under a dry air atmosphere. Pyridine, dimethylformamide, and dimethyl sulfoxide were stored over 4Å molecular sieves. Triphenylphosphine was recrystallized from methanol.

All polyene cyclization reactions were performed under air using reagent-grade solvents out of the bottle.

IR spectra were obtained using a Perkin-Elmer Spectrum One FT-IR spectrophotometer. NMR spectra were recorded on 400, 500 MHz Varian or 400, 500, 800 MHz Bruker spectrometers. Some NMR experiments were recorded at the Quebec/Eastern Canada High Field NMR Facility, supported by the Canada Foundation for Innovation, McGill University Faculty of Science and Department of Chemistry. Chemical shifts (δ) were internally referenced to the residual proton resonance of chloroform-*d* (δ 7.26 ppm). The following abbreviations were used for NMR peak multiplicities: s = singlet, d = doublet, t = triplet, q = quartet, sext = sextet, m = multiplet. Coupling constants (J) are reported in Hertz (Hz). High-resolution mass spectrometry was conducted by Dr. Nadim Saadé and Dr. Alexander Wahba in the Mass Spectrometry Facility in the Department of

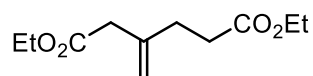
Chemistry, McGill University, using Thermo-Fisher Exactive Plus Orbitrap-API and Bruker Maxis API QqTOF mass spectrometers.

The following known compounds were synthesized following literature procedures: ethyl 1,2-diazepane-1-carboxylate¹ (**1.244**), Dess-Martin periodinane²⁻³.

Atom numbering for decalin compounds is based on IUPAC rules for the numbering of steroids, except for the numbering in the compounds' names, which uses general IUPAC nomenclature (as assigned by PerkinElmer ChemDraw).

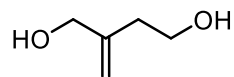
5.2. Experimental Procedures from Chapter 2

diethyl 3-methylenehexanedioate (**5.1**)



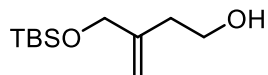
To a solution of itaconic acid (6.02 g, 46.2 mmol) in MeOH (18 mL) was added concentrated H₂SO₄ (0.81 mL). The solution was brought to 70 °C and stirred for 18 h. The solution was then cooled, diluted with water, and extracted with EtOAc (3 x 20 mL). Combined organic layers were washed with brine, dried with MgSO₄, filtered, and concentrated to obtain diethyl 3-methylenehexanedioate. Product was isolated as a colourless oil (7.06 g, 44.6 mmol, 96% yield) and used without further purification. Spectroscopic data were in accordance with previously reported literature.⁴

2-methylenebutane-1,4-diol (**2.19**)



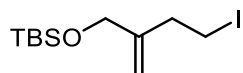
To a stirred solution of diethyl 3-methylenehexanedioate (5.09 g, 32.2 mmol) in THF (150 mL) at -78 °C was added DIBAL-H (1.0 M in DCM 140 mL, 140 mmol) dropwise. The solution was stirred for 2 h, then quenched water (5.6 mL), 15% KOH (5.6 mL), then water (14 mL) and let stir for 20 minutes. The solution was dried with MgSO₄ and filtered through celite. The filtrate was concentrated to provide 2-methylenebutane-1,4-diol, which was isolated as a colourless oil (2.94 g, 28.8 mmol, 89% yield) and used without further purification. Spectroscopic data were in accordance with previously reported literature.⁵

3-(((*tert*-butyldimethylsilyl)oxy)methyl)but-3-en-1-ol (**2.21**)



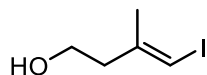
To a stirred solution of NaH (60% dispersion in mineral oil, 514 mg, 5.0 mmol) in THF (15 mL) at $-78\text{ }^{\circ}\text{C}$ was added a solution of 2-methylenebutane-1,4-diol (**2.17**) in THF (5 mL). The solution was stirred for 1 h, then TBSCl (789 mg, 5.2 mmol) in THF (5 mL) was added and the resulting solution was stirred for 3 h. The solution was quenched with water, extracted with EtOAc (3 x 20 mL). Combined organic layers were washed with brine, dried with MgSO_4 , filtered, and concentrated. The crude product was redissolved in DCM (40 mL), MnO_2 (9.5 g) was added, and the slurry was stirred for 24 h. The mixture was filtered through celite. The filtrate was concentrated and purified by silica gel column chromatography (gradient from 80:20 hexanes/ Et_2O to 75:25 hexanes/ Et_2O) to obtain 3-(((*tert*-butyldimethylsilyl)oxy)methyl)but-3-en-1-ol, which was isolated as a colourless oil (221 mg, 1.0 mmol, 20% yield). Spectroscopic data were in accordance with previously reported literature.⁶

tert-butyl(4-iodo-2-methylenebutoxy)dimethylsilane (**2.17**)



To a stirred solution of 3-(((*tert*-butyldimethylsilyl)oxy)methyl)but-3-en-1-ol (221 mg, 1.0 mmol) in THF (10 mL) at $0\text{ }^{\circ}\text{C}$ was added imidazole (171 mg, 2.5 mmol), PPh_3 (320.9 mg, 1.2 mmol), and I_2 (308 mg, 1.2 mmol). The solution was stirred for 1 h, diluted with hexanes and filtered through a silica plug (eluting with 8:1 hexanes/ Et_2O). The filtrate was concentrated to obtain *tert*-butyl(4-iodo-2-methylenebutoxy)dimethylsilane, which was isolated as a yellow oil (331 mg, 1.0 mmol, 99% yield). Spectroscopic data were in accordance with previously reported literature.⁶

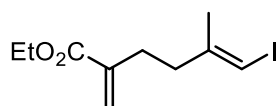
(*E*)-4-iodo-3-methylbut-3-en-1-ol (**2.28**)



To a stirred solution of Cp_2ZrCl_2 (836 mg, 2.9 mmol) in DCM (40 mL) at $0\text{ }^{\circ}\text{C}$ was added AlMe_3 (2.0 M in toluene, 18 mL, 36 mmol). The solution was brought to room temperature and let stir for 20 minutes, then brought to $0\text{ }^{\circ}\text{C}$ and 1-butynol (700 μL , 14.3 mmol) in DCM (10 mL) was added. The solution was brought to room temperature and let stir for 17 h, the brought to $-40\text{ }^{\circ}\text{C}$

and a solution of I₂ (4.42 g, 17.4 mmol) in THF (20 mL) was added. The solution was brought to room temperature and stirred for 2 h, then quenched with water at 0 °C. The aqueous layer was extracted with Et₂O (40 mL), then brought to pH 4 with 10% HCl and extracted with Et₂O (2 x 40 mL). The combined organic layers were washed with brine, dried with MgSO₄, filtered, and concentrated. The crude extracts were purified by silica gel column chromatography (gradient from hexanes to 80:20 hexanes/EtOAc) to obtain (*E*)-4-iodo-3-methylbut-3-en-1-ol, which was isolated as a colourless oil (1.13 g, 5.3 mmol, 37% yield over 2 steps). Spectroscopic data were in accordance with previously reported literature.⁷

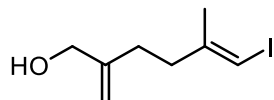
ethyl (*E*)-6-iodo-5-methyl-2-methylenehex-5-enoate (2.31)



To a stirred solution of PPh₃ (3.37 g, 12.8 mmol) in DCM (10 mL) at 0 °C was added bromine (600 μL, 11.7 mmol). The solution was stirred for 10 minutes, then a solution of (*E*)-4-iodo-3-methylbut-3-en-1-ol (2.08 g, 9.8 mmol) in DCM (40 mL) was added. The solution was stirred for 1 h, then concentrated. The crude bromide was purified by a silica gel plug (eluted with hexanes). Following the procedure of Serebryakov *et al*⁸: To a stirred solution of NaH (60% dispersion in mineral oil, 622 mg, 15.5 mmol) in DMSO (16 mL) at 0 °C was added triethyl phosphonoacetate (3.0 mL, 15.5 mmol) dropwise. When bubbling ceased, the solution was added to the bromide formed in the previous step. The solution was brought to 50 °C and stirred for 2 h. The solution was cooled to room temperature and K₂CO₃ (3.25 g, 23.2 mmol) and formaldehyde (37% in water, 3.5 mL, 47.0 mmol) were added. The mixture was brought to 60 °C and let stir for 1 h. The solution was diluted with water and extracted with Et₂O (3 x 20 mL). The combined organic layers were washed with brine, dried with MgSO₄, filtered, and concentrated. The crude extracts were purified by silica gel column chromatography (gradient from hexanes to 95:5 hexanes/ethyl acetate) to obtain ethyl (*E*)-6-iodo-5-methyl-2-methylenehex-5-enoate, which was isolated as a colourless oil (1.67 g, 5.7 mmol, 58% yield over 2 steps. IR (Film) 3057, 2980, 2930, 2854, 1712, 1630, 1445, 1408, 1369, 1306, 1267, 1185, 1134, 1095, 1025, 943, 888, 863, 843, 815, 780, 682, 662 cm⁻¹; ¹H NMR (500 MHz, CDCl₃) δ = 6.15 (d, J = 1.2 Hz, 1 H), 5.90 (q, J = 0.9 Hz, 1 H), 5.51 (d, J = 1.2 Hz, 1 H), 4.20 (qt, J = 7.1, 1.4 Hz, 2 H), 2.44 (t, J = 8.0 Hz, 2 H), 2.37 (t, J = 8.0 Hz, 2 H), 1.85 (d, J = 0.9 Hz, 3 H), 1.30 (tt, J = 7.0, 1.5 Hz, 3 H) ppm; ¹³C NMR (125 MHz, CDCl₃) δ = 166.8, 146.9,

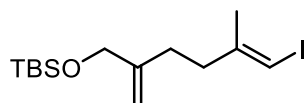
139.7, 125.2, 75.5, 60.7, 38.6, 30.3, 23.8, 14.2 ppm; MS (ESI) exact mass calculated for [M+Na] (C₁₀H₁₅INaO₂) requires m/z 317.0009, found m/z 317.0007.

(E)-6-iodo-5-methyl-2-methylenehex-5-en-1-ol (5.2)



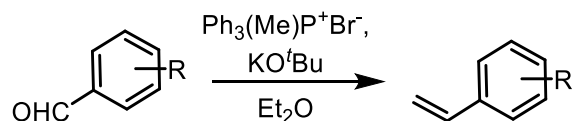
To a stirred solution of ethyl (*E*)-6-iodo-5-methyl-2-methylenehex-5-enoate (1.55 g, 5.3 mmol) in THF (20 mL) at 0 °C was added DIBAL-H (25 wt. % in toluene, 8 mL, 11.6 mmol) dropwise. The solution was stirred for 3 h, then quenched with a saturated solution of Rochelle's salt. The mixture was extracted with EtOAc (3 x 20 mL). The combined organic layers were washed with brine, dried with MgSO₄, filtered and concentrated. The crude extracts were purified by silica gel column chromatography (gradient from hexanes to 80:20 hexanes/EtOAc) to obtain (*E*)-6-iodo-5-methyl-2-methylenehex-5-en-1-ol, which was isolated as a colourless oil (1.24 g, 4.9 mmol, 93% yield). IR (Film) 3378, 3058, 2979, 2914, 2853, 1712, 1653, 1629, 1446, 1409, 1374, 1290, 1268, 1189, 1138, 1094, 1065, 1024, 945, 898, 864, 815, 780, 764, 742, 665, 598, 579 cm⁻¹; ¹H NMR (400 MHz, CDCl₃) δ = 5.93 (d, J = 0.9 Hz, 1 H), 5.06 (s, 1 H), 4.88 (d, J = 1.1 Hz, 1 H), 4.08 (d, J = 5.9 Hz, 2 H), 2.38 (dd, J = 8.4, 7.1 Hz, 2 H), 2.22 (dd, J = 8.4, 7.1 Hz, 2 H), 1.86 (s, 3 H), 1.39 (t, J = 6.1 Hz, 1 H) ppm; ¹³C NMR (125 MHz, CDCl₃) δ = 147.8, 147.4, 110.2, 75.2, 65.9, 37.9, 31.1, 23.9 ppm; MS (ESI) exact mass calculated for [M+Na] (C₈H₁₃INaO) requires m/z 274.9903, found m/z 274.9906.

(E)-tert-butyl((6-iodo-5-methyl-2-methylenehex-5-en-1-yl)oxy)dimethylsilane (2.32)



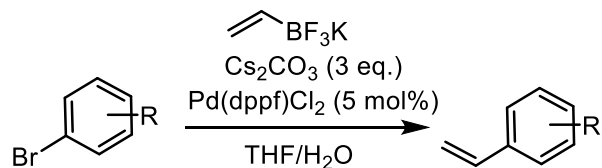
To a stirred solution of (*E*)-6-iodo-5-methyl-2-methylenehex-5-en-1-ol (1.30 g, 5.2 mmol) in DCM (20 mL) was added imidazole (717 mg, 10.5 mmol) and TBSCl (872 mg, 10.3 mmol). The resulting solution was stirred for 3 h, then concentrated and purified by silica gel column chromatography (gradient from hexanes to 93:7 hexanes/ethyl acetate) to obtain (*E*)-tert-butyl((6-iodo-5-methyl-2-methylenehex-5-en-1-yl)oxy)dimethylsilane, which was isolated as a colourless oil (1.7617 g, 4.8 mmol, 93% yield). IR (Film) 3075, 3056, 2953, 2928, 2895, 2856, 1654, 1618, 1471, 1462, 1388, 1377, 1361, 1252, 1141, 1107, 1081, 1006, 939, 899, 834, 774, 738, 705, 667,

583, 509 cm^{-1} ; ^1H NMR (400 MHz, CDCl_3) δ = 5.91 (d, J = 1.0 Hz, 1 H), 5.04 (s, 1 H), 4.82 (d, J = 1.2 Hz, 1 H), 4.07 (s, 2 H), 2.36 (dd, J = 8.8, 6.8 Hz, 2 H), 2.16 (dd, J = 8.7, 7.0 Hz, 2 H), 1.86 (d, J = 0.6 Hz, 3 H), 0.92 (s, 9 H), 0.09 (s, 6 H) ppm; ^{13}C NMR (125 MHz, CDCl_3) δ = 147.6, 147.6, 109.3, 75.0, 65.9, 38.0, 30.9, 25.9, 23.9, 18.4, -5.3 ppm; MS (ESI) exact mass calculated for $[\text{M}+\text{Na}]$ ($\text{C}_{14}\text{H}_{27}\text{INaOSi}$) requires m/z 389.0768, found m/z 389.0775.



Synthesis of vinylarenes (general procedure A)

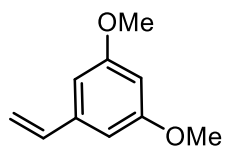
To a stirred suspension of methyltriphenylphosphonium bromide (1.82 g, 5.1 mmol) in Et_2O (20 mL) at 0 $^\circ\text{C}$ was added potassium *tert*-butoxide (505 mg, 4.5 mmol). The mixture was stirred 15 minutes and became bright yellow. A solution of aryl aldehyde (3.0 mmol) in Et_2O (10 mL) was added dropwise. The reaction mixture was removed from cooling, stirred overnight, cooled to 0 $^\circ\text{C}$, and quenched with saturated aqueous NH_4Cl (12 mL). The aqueous layer was diluted with water (6 mL) and extracted with Et_2O (2 x 12 mL). The organic layer and ether extracts were combined, washed with water and brine, dried with MgSO_4 , filtered, concentrated, and purified by flash chromatography to give the vinylarene.



Synthesis of vinylarenes (general procedure B)

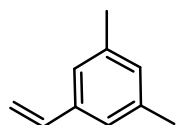
Following a modified procedure of Molander *et al.*⁹: To a 10 mL microwave vial containing aryl bromide, $\text{Pd}(\text{dppf})\text{Cl}_2$, CsCO_3 , and vinyl trifluoroborate was added $\text{THF}:\text{H}_2\text{O}$ (9:1). The solution was brought to 85 $^\circ\text{C}$ and let stir for 21 h. The reaction quenched with water (5 mL) and extracted with Et_2O (2 x 10 mL). The organic layer and ether extracts were combined, washed with brine, dried with MgSO_4 , filtered, concentrated, and purified by flash chromatography to give the vinylarene.

1,3-dimethoxy-5-vinylbenzene (5.3)



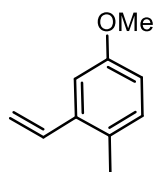
From 3,5-dimethoxybenzaldehyde (6.0 mmol), general procedure A was followed to give, after flash chromatography (gradient from 99:1 to 97:3 hexanes/EtOAc), 950 mg (5.8 mmol) of product **5.3** as a colourless oil (96% yield). Spectroscopic data were in accordance with previously reported literature.¹⁰

1,3-dimethyl-5-vinylbenzene (5.4)



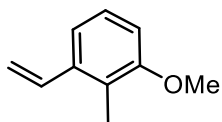
From 3,5-dimethylbenzaldehyde (3.0 mmol), general procedure A was followed to give, after flash chromatography (gradient from 97:3 to 95:5 pentane/DCM), 323 mg (2.4 mmol) of product **5.4** as a colourless oil (81% yield). Spectroscopic data were in accordance with previously reported literature.¹¹

4-methoxy-1-methyl-2-vinylbenzene (5.5)



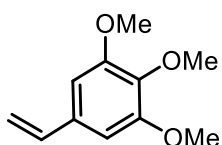
From 5-methoxy-2-methylbenzaldehyde (1.6 mmol), general procedure A was followed to give, after flash chromatography (gradient from 96:4 to 92:8 hexanes/DCM), 217 mg (1.5 mmol) of product **5.5** as a colourless oil (89% yield). Spectroscopic data were in accordance with previously reported literature.¹²

1-methoxy-2-methyl-3-vinylbenzene (5.6)



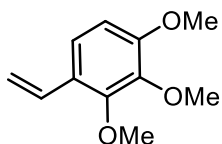
From 3-methoxy-2-methylbenzaldehyde (3.0 mmol), general procedure A was followed to give, after flash chromatography (gradient from 96:4 to 92:8 hexanes/DCM), 384 mg (2.6 mmol) of product **5.6** as a colourless oil (86% yield). Spectroscopic data were in accordance with previously reported literature.¹³

1,2,3-trimethoxy-5-vinylbenzene (5.7)



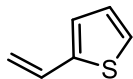
From 3,4,5-trimethoxybenzaldehyde (3.0 mmol), general procedure A was followed with the following modification: the aryl aldehyde was added as a solution in 5:1 Et₂O/DCM (12 mL). Purification by flash chromatography (gradient from 97:3 to 93:7 hexanes/EtOAc) gave 574 mg (3.0 mmol) of product **5.7** as a colourless oil (98% yield). Spectroscopic data were in accordance with previously reported literature.¹⁴

1,2,3-trimethoxy-4-vinylbenzene (5.8)



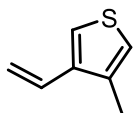
From 2,3,4-trimethoxybenzaldehyde (2.9 mmol), general procedure A was followed to give, after flash chromatography (gradient from 50:50 to 70:30 DCM/pentane), 545 mg (2.8 mmol) of product **5.8** as a colourless oil (97% yield). Spectroscopic data were in accordance with previously reported literature.¹⁵

2-vinylthiophene (5.9)



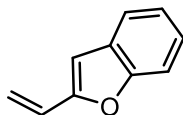
From thiophene-2-carbaldehyde (3.0 mmol), general procedure A was followed to give, after flash chromatography (pentane), 188 mg (1.7 mmol) of product **5.9** as a colourless oil (57% yield). Spectroscopic data were in accordance with previously reported literature.⁹

3-methyl-4-vinylthiophene (5.10)



From 3-bromo-4-methylthiophene (0.40 mmol), general procedure B was followed to give, after flash chromatography (pentane), 120 mg (1.6 mmol) of product **5.10** as a colourless oil (34% yield). Spectroscopic data were in accordance with previously reported literature.¹⁶

2-vinylbenzofuran (5.11)



From benzofuran-2-carbaldehyde (3.0 mmol), general procedure A was followed to give, after flash chromatography (gradient from 95:5 to 92:8 pentane/DCM), 386 mg (2.7 mmol) of product **5.11** as a yellow oil (89% yield). Spectroscopic data were in accordance with previously reported literature.¹⁷

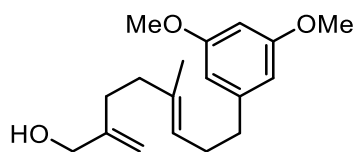
Synthesis of (*E*)-polyene alcohols (general procedure C)

Following the procedure of Zhao *et al*¹⁸: To a stirred solution of vinylarene (1.1 mmol) in tetrahydrofuran (400 μ L) at 0 °C was added a solution of 9-BBN (0.5 M in THF, 2.1 mL, 1.1 mmol). The mixture was brought to room temperature and stirred for 18 h. When the hydroboration was complete, the reaction was cooled to 0 °C and Pd(dppf)Cl₂ (40 mg, 0.054 mmol), NaOH (216 mg, 5.4 mmol), and a solution of (*E*)-*tert*-butyl((6-iodo-5-methyl-2-methylenehex-5-en-1-yl)oxy)dimethylsilane (198 mg, 0.54 mmol) in THF (400 μ L) were added sequentially. The mixture was brought to room temperature and stirred for 22 h. The reaction was quenched with

saturated aqueous NH_4Cl and extracted with EtOAc (3 x 10 mL). The combined organic layers were washed with brine, dried with MgSO_4 , filtered, and concentrated. The crude extracts were purified by silica gel column chromatography (gradient from hexanes to 94:6 hexanes/EtOAc) to obtain coupling product.

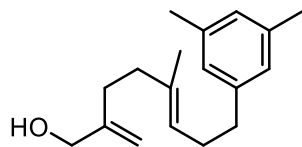
To a stirred solution of coupled product in THF was added a solution of TBAF (1.0 M in THF, 1.1 mL, 1.1 mmol) was added and the resulting solution was stirred for 1 h. The reaction was quenched with saturated aqueous NaHCO_3 and extracted with EtOAc (3 x 10 mL). The combined organic layers were washed with brine, dried with MgSO_4 , filtered, and concentrated. The crude extracts were purified by silica gel column chromatography (gradient from hexanes to 70:30 hexanes/EtOAc) to obtain alcohol product.

(E)-8-(3,5-dimethoxyphenyl)-5-methyl-2-methyleneoct-5-en-1-ol (2.34)



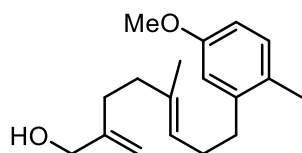
Followed general procedure C from 3,5-dimethoxystyrene on a 0.54 mmol scale and purified using silica gel column chromatography to give 98 mg (0.38 mmol, 70% yield over 2 steps) of (E)-8-(3,5-dimethoxyphenyl)-5-methyl-2-methyleneoct-5-en-1-ol as a colourless oil. IR (Film) 3393, 3083, 2933, 2838, 1594, 1459, 1428, 1204, 1148, 1065, 1026, 896, 829, 736, 694 cm^{-1} ; ^1H NMR (500 MHz, CDCl_3) δ = 6.36 (d, J = 2.2 Hz, 2 H), 6.31 (t, J = 2.2 Hz, 1 H), 5.20 (t, J = 6.9 Hz, 1 H), 5.02 (d, J = 1.1 Hz, 1 H), 4.86 (s, 1 H), 4.05 (s, 2 H), 3.78 (s, 6 H), 2.59 (t, J = 7.7 Hz, 2 H), 2.31 (td, J = 7.5, 6.8 Hz, 2 H), 2.15 (bs, 4 H), 2.09 (s, 1 H), 1.60 (s, 3 H) ppm; ^{13}C NMR (125 MHz, CDCl_3) δ = 160.5, 148.7, 144.6, 135.2, 123.8, 109.0, 106.5, 97.5, 65.6, 55.1, 37.7, 36.2, 31.4, 29.5, 15.8 ppm; HRMS (ESI) exact mass calculated for $[\text{M}+\text{Na}]$ ($\text{C}_{18}\text{H}_{26}\text{NaO}_3$) requires m/z 313.1774, found m/z 313.1784.

(E)-8-(3,5-dimethylphenyl)-5-methyl-2-methyleneoct-5-en-1-ol (2.35)



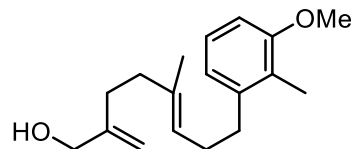
Followed general procedure C from 3,5-dimethylstyrene on a 0.54 mmol scale and purified using silica gel column chromatography to give 119 mg (0.46 mmol, 82% yield over 2 steps) of (*E*)-8-(3,5-dimethylphenyl)-5-methyl-2-methyleneoct-5-en-1-ol as a colourless oil. IR (Film) 3318, 3012, 2917, 2854, 1653, 1605, 1449, 1378, 1061, 1023, 895, 842, 701 cm^{-1} ; ^1H NMR (400 MHz, CDCl_3) δ = 6.84 (bs, 1H), 6.82 (bs, 2 H), 5.22 (t, J = 7.0 Hz, 1 H), 5.02 (d, J = 1.2 Hz, 1 H), 4.88 (s, 1 H), 4.07 (d, J = 5.0 Hz, 2 H), 2.57 (t, J = 7.9 Hz, 2 H), 2.30 (m, 8 H), 2.16 (bs, 4 H), 1.60 (s, 3 H), 1.39 (t, J = 5.1 Hz, 1 H) ppm; ^{13}C NMR (125 MHz, CDCl_3) δ = 149.0, 142.2, 138.0, 135.1, 127.3, 126.3, 124.3, 109.4, 66.0, 38.0, 35.9, 31.6, 30.0, 21.3, 15.9 ppm; HRMS (ESI) exact mass calculated for $[\text{M}+\text{Na}]$ ($\text{C}_{18}\text{H}_{24}\text{NaO}$) requires m/z 279.1719, found m/z 279.1712.

(E)-8-(5-methoxy-2-methylphenyl)-5-methyl-2-methyleneoct-5-en-1-ol (2.36)



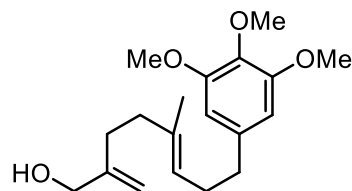
Followed general procedure C from 4-methoxy-2-methylstyrene on a 0.54 mmol scale and purified using silica gel column chromatography to give 103 mg (0.38 mmol, 70% yield over 2 steps) of (*E*)-8-(5-methoxy-2-methylphenyl)-5-methyl-2-methyleneoct-5-en-1-ol as a colourless oil. IR (Film) 3452, 3053, 1936, 2865, 2837, 1652, 1608, 1579, 1498, 1454, 1383, 1303, 1265, 1208, 1161, 1114, 1045, 896, 854, 803, 704 cm^{-1} ; ^1H NMR (500 MHz, CDCl_3) δ = 7.07 (d, J = 8.2 Hz, 1 H), 6.74 (d, J = 2.3 Hz, 1 H), 6.69 (dd, J = 8.2, 2.4 Hz, 1 H), 5.26 (t, J = 7.0 Hz, 1 H), 5.06 (s, 1 H), 4.90 (s, 1 H), 4.09 (s, 2 H), 3.80 (s, 3 H), 2.62 (t, J = 7.6 Hz, 2 H), 2.30 (m, 5 H), 2.18 (s, 4 H), 2.06 (s, 1 H), 1.62 (s, 3 H) ppm; ^{13}C NMR (125 MHz, CDCl_3) δ = 157.6, 148.8, 141.5, 135.2, 130.6, 127.9, 123.9, 114.8, 110.5, 109.1, 65.7, 55.1, 37.8, 33.5, 31.4, 28.4, 18.3, 15.8 ppm; HRMS (ESI) exact mass calculated for $[\text{M}+\text{Na}]$ ($\text{C}_{18}\text{H}_{26}\text{NaO}_2$) requires m/z 297.1825, found m/z 297.1815.

(E)-8-(3-methoxy-2-methylphenyl)-5-methyl-2-methyleneoct-5-en-1-ol (2.37)



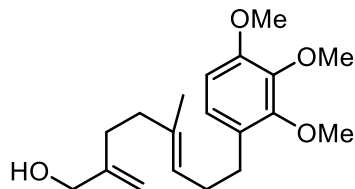
Followed general procedure C from 3-methoxy-2-methylstyrene on a 0.54 mmol scale and purified using silica gel column chromatography to give 101 mg (0.36 mmol, 67% yield over 2 steps) of (E)-8-(3-methoxy-2-methylphenyl)-5-methyl-2-methyleneoct-5-en-1-ol as a colourless oil. IR (Film) 3327, 3071, 2932, 2861, 2837, 1653, 1584, 1463, 1438, 1380, 1310, 1252, 1192, 1168, 1142, 1101, 1018, 895, 835, 778, 719, 678 cm^{-1} ; ^1H NMR (500 MHz, CDCl_3) δ = 7.12 (dd, J = 7.8, 7.8 Hz, 1 H), 6.81 (d, J = 7.7 Hz, 1 H), 6.74 (d, J = 8.0 Hz, 1 H), 5.27 (t, J = 7.0 Hz, 1 H), 5.05 (s, 1 H), 4.90 (s, 1 H), 4.09 (s, 2 H), 3.84 (s, 3 H), 2.66 (t, J = 7.6 Hz, 2 H), 2.29 (td, J = 7.6, 7.1 Hz, 2 H), 2.23 (s, 3 H), 2.18 (s, 4 H), 1.83 (s, 1 H), 1.62 (s, 3 H) ppm; ^{13}C NMR (125 MHz, CDCl_3) δ = 157.6, 148.8, 141.7, 135.1, 125.8, 124.4, 124.1, 121.4, 109.2, 107.8, 65.8, 55.4, 37.9, 33.6, 31.4, 28.8, 15.8, 11.2 ppm; HRMS (APCI) exact mass calculated for $[\text{M}+\text{H}]$ ($\text{C}_{18}\text{H}_{27}\text{O}_2$) requires m/z 267.1390, found m/z 267.1389.

(E)-5-methyl-2-methylene-8-(3,4,5-trimethoxyphenyl)oct-5-en-1-ol (2.38)



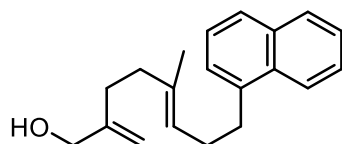
Followed general procedure C from 3,4,5-trimethoxystyrene on a 0.54 mmol scale and purified using silica gel column chromatography to give 144 mg (0.46 mmol, 86% yield over 2 steps) of (E)-5-methyl-2-methylene-8-(3,4,5-trimethoxyphenyl)oct-5-en-1-ol as a colourless oil. IR (Film) 3433, 3042, 2984, 2936, 2839, 1590, 1508, 1457, 1420, 1342, 1323, 1238, 1183, 1127, 1010, 896, 826, 778 cm^{-1} ; ^1H NMR (500 MHz, CDCl_3) δ = 6.41 (s, 2 H), 5.20 (t, J = 7.0 Hz, 1 H), 5.02 (d, J = 1.2, 1 H), 4.87 (d, J = 1.0 Hz, 1 H), 4.07 (d, J = 5.2 Hz, 2 H), 3.86 (s, 6 H), 3.83 (s, 3 H), 2.59 (t, J = 8.1 Hz, 2 H), 2.31 (td, J = 7.2, 8.1 Hz, 2 H), 2.16 (s, 4 H), 1.60 (s, 3 H), 1.38 (t, J = 5.4 Hz, 1 H) ppm; ^{13}C NMR (125 MHz, CDCl_3) δ = 152.8, 148.7, 137.9, 135.9, 135.3, 123.8, 109.1, 105.2, 65.6, 60.7, 55.9, 37.8, 36.2, 31.4, 29.7, 15.8 ppm; HRMS (APCI) exact mass calculated for $[\text{M}+\text{H}]$ ($\text{C}_{19}\text{H}_{29}\text{O}_4$) requires m/z 321.2060, found m/z 321.2059.

(E)-5-methyl-2-methylene-8-(2,3,4-trimethoxyphenyl)oct-5-en-1-ol (2.39)



Followed general procedure C from 2,3,4-trimethoxystyrene on a 0.54 mmol scale and purified using silica gel column chromatography to give 132 mg (0.41 mmol, 72% yield over 2 steps) of (E)-5-methyl-2-methylene-8-(2,3,4-trimethoxyphenyl)oct-5-en-1-ol as a colourless oil. IR (Film) 3461, 3054, 2938, 2853, 1653, 1602, 1494, 1466, 1417, 1265, 1232, 1199, 1144, 1099, 1049, 1018, 899, 800, 703 cm^{-1} ; ^1H NMR (500 MHz, CDCl_3) δ = 6.81 (d, J = 8.5 Hz, 1 H), 6.59 (d, J = 8.5 Hz, 1 H), 5.21 (t, J = 7.0 Hz, 1 H), 5.00 (d, J = 1.3 Hz, 1 H), 4.84 (d, 1.2 Hz, 1 H), 4.05 (s, 2 H), 3.87 (s, 3 H), 3.86 (s, 3 H), 3.82 (s, 3 H), 2.56 (t, J = 7.7 Hz, 2 H), 2.24 (td, J = 7.5, 7.2 Hz, 2 H), 2.13 (m, 4H), 1.98 (s, 1 H), 1.58 (s, 3 H) ppm; ^{13}C NMR (125 MHz, CDCl_3) δ = 151.8, 151.7, 148.8, 142.1, 135.0, 128.1, 124.2, 123.7, 109.1, 107.0, 65.7, 60.8, 60.6, 55.9, 37.8, 31.4, 29.7, 29.1, 15.8 ppm; HRMS (APCI) exact mass calculated for $[\text{M}+\text{H}]$ ($\text{C}_{19}\text{H}_{29}\text{O}_4$) requires m/z 321.2060, found m/z 321.2062.

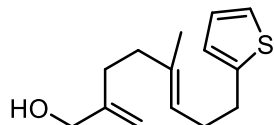
(E)-5-methyl-2-methylene-8-(naphthalen-1-yl)oct-5-en-1-ol (2.40)



Followed general procedure C from 1-vinylnaphthalene on a 0.54 mmol scale and purified using silica gel column chromatography to give 76 mg (0.27 mmol, 51% yield over 2 steps) of (E)-5-methyl-2-methylene-8-(naphthalen-1-yl)oct-5-en-1-ol as a yellow oil. IR (Film) 3398, 3065, 3046, 2926, 2854, 1718, 1654, 1596, 1509, 1448, 1395, 1166, 1061, 1019, 898, 797, 777 cm^{-1} ; ^1H NMR (400 MHz, CDCl_3) δ = 8.06 (d, J = 8.0 Hz, 1H), 7.86 (d, J = 8.0 Hz, 1 H), 7.71 (d, J = 8.0 Hz, 1 H), 7.51 (m, 2H), 7.40 (dd, J = 7.6, 7.6 Hz, 1 H), 7.32 (d, J = 6.9 Hz, 1 H), 5.31 (t, J = 7.1 Hz, 1 H), 5.04 (d, 1.5 Hz, 1 H), 4.88 (s, 1 H), 4.08 (d, J = 6.3 Hz, 2 H), 3.10 (t, J = 7.6, 2 H), 2.46 (td, J = 7.4, 6.9 Hz, 2H), 2.15 (s, 4H), 1.56 (s, 3H), 1.32 (t, J = 6.1 Hz, 1H) ppm; ^{13}C NMR (125 MHz, CDCl_3) δ = 148.9, 138.3, 135.4, 133.8, 131.9, 128.8, 126.5, 126.0, 125.7, 125.5, 125.4, 124.2,

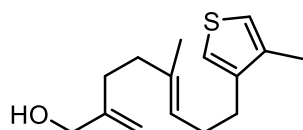
123.8, 109.4, 66.0, 38.0, 33.1, 31.5, 29.2, 16.0 ppm; HRMS (ESI) exact mass calculated for [M+Na] (C₂₀H₂₄NaO) requires m/z 303.1719, found m/z 303.1709.

(E)-5-methyl-2-methylene-8-(thiophen-2-yl)oct-5-en-1-ol (2.41)



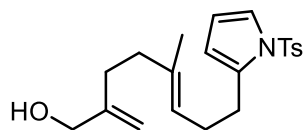
Followed general procedure C from 2-vinylthiophene on a 0.54 mmol scale and purified using silica gel column chromatography to give 74 mg (0.32 mmol, 59% yield over 2 steps) of (E)-5-methyl-2-methylene-8-(thiophen-2-yl)oct-5-en-1-ol as a colourless oil. IR (Film) 3319, 3099, 3071, 2921, 1651, 1439, 1383, 1237, 1060, 1025, 897, 849, 822, 692 cm⁻¹; ¹H NMR (500 MHz, CDCl₃) δ = 7.12 (dd, J = 5.1, 1.2 Hz, 1 H), 6.92 (dd, J = 5.1, 3.4 Hz, 1 H), 6.80 (dd, J = 3.4, 1.0 Hz, 1 H), 5.22 (td, J = 6.8, 0.8 Hz, 1 H), 5.02 (d, J = 1.2 Hz, 1 H), 4.88 (d, J = 1.1 Hz, 1 H), 4.07 (s, 2 H), 2.87 (t, J = 7.7 Hz, 2 H), 2.38 (td, J = 7.6, 6.9 Hz, 2 H), 2.17 (bs, 4 H), 1.62 (s, 4 H) ppm; ¹³C NMR (125 MHz, CDCl₃) δ = 148.8, 145.1, 135.8, 126.5, 124.0, 123.5, 122.9, 109.3, 65.8, 37.8, 31.4, 30.0, 30.0, 16.0 ppm; HRMS (ESI) exact mass calculated for [M+Na] (C₁₄H₂₀NaOS) requires m/z 259.1127, found m/z 259.1125.

(E)-5-methyl-2-methylene-8-(4-methylthiophen-3-yl)oct-5-en-1-ol (2.42)



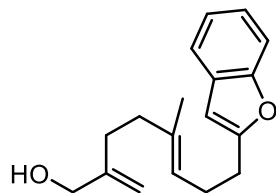
Followed general procedure C from 2-vinylthiophene on a 0.54 mmol scale and purified using silica gel column chromatography to give 82 mg (0.33 mmol, 62% yield over 2 steps) of (E)-5-methyl-2-methylene-8-(4-methylthiophen-3-yl)oct-5-en-1-ol as a colourless oil. IR (Film) 3330, 3085, 2921, 2856, 1652, 1445, 1383, 1060, 1022, 896, 861 cm⁻¹; ¹H NMR (500 MHz, CDCl₃) δ = 6.90 (m, 2 H), 5.25 (t, J = 6.8 Hz, 1 H), 5.04 (d, J = 1.2 Hz, 1 H), 4.89 (d, J = 1.0 Hz, 1 H), 4.08 (s, 2 H), 2.57 (t, J = 8.3 Hz, 2 H), 2.33 (td, J = 8.3, 6.8 Hz, 2 H), 2.20 (s, 3H), 2.18 (bs, 4 H), 1.75 (s, 1 H), 1.63 (s, 3H) ppm; ¹³C NMR (125 MHz, CDCl₃) δ = 148.8, 141.7, 136.9, 135.3, 124.0, 120.7, 120.2, 109.3, 65.8, 37.8, 31.4, 29.0, 27.8, 15.8, 14.4 ppm; HRMS (ESI) exact mass calculated for [M+Na] (C₁₅H₂₂NaOS) requires m/z 273.1284, found m/z 273.1279.

(E)-5-methyl-2-methylene-8-(1-tosyl-1H-pyrrol-2-yl)oct-5-en-1-ol (2.43)



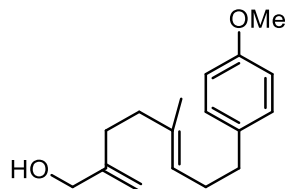
Followed general procedure C from 1-tosyl-2-vinyl-1H-pyrrole on a 0.54 mmol scale and purified using silica gel column chromatography to give 74 mg (0.32 mmol, 59% yield over 2 steps) of (*E*)-5-methyl-2-methylene-8-(1-tosyl-1H-pyrrol-2-yl)oct-5-en-1-ol as a colourless oil. IR (Film) 3555, 3373, 3155, 2922, 2855, 1652, 1597, 1448, 1362, 1185, 10990, 1053 cm^{-1} ; ^1H NMR (500 MHz, CDCl_3) δ = 7.62 (d, J = 8.8 Hz, 2 H), 7.27 (m, 3 H), 6.18 (dd, J = 3.3, 3.3 Hz, 1 H), 5.97 (m, 1 H), 5.11 (t, J = 6.9 Hz, 1 H), 5.01 (d, J = 1.1 Hz, 1 H), 4.85 (d, J = 1.0 Hz, 1 H), 4.05 (s, 2 H), 2.68 (t, J = 8.0 Hz, 2 H), 2.38 (s, 3 H), 2.25 (td, J = 8.0, 7.0 Hz, 2 H), 2.12 (m, 4 H), 1.78 (bs, 1 H), 1.56 (s, 3 H) ppm; ^{13}C NMR (125 MHz, CDCl_3) δ = 148.8, 144.6, 136.4, 135.6, 135.3, 128.9, 126.6, 123.5, 122.2, 112.0, 111.2, 109.2, 65.7, 37.8, 31.3, 27.2, 27.0, 21.5, 15.8 ppm; HRMS (ESI) exact mass calculated for $[\text{M}+\text{Na}]$ ($\text{C}_{21}\text{H}_{27}\text{NNaO}_3\text{S}$) requires m/z 396.1604, found m/z 396.1600.

(E)-8-(benzofuran-2-yl)-5-methyl-2-methyleneoct-5-en-1-ol (2.44)



Followed general procedure C from 2-vinylbenzofuran on a 0.54 mmol scale and purified using silica gel column chromatography to give 74 mg (0.26 mmol, 49% yield over 2 steps) of (*E*)-8-(benzofuran-2-yl)-5-methyl-2-methyleneoct-5-en-1-ol as a colourless oil. IR (Film) 3328, 3067, 3040, 2917, 2855, 1653, 1601, 1587, 1455, 1383, 1320, 1252, 1177, 1141, 1104, 1059, 1010, 944, 896, 795, 750, 704 cm^{-1} ; ^1H NMR (500 MHz, CDCl_3) δ = 7.50 (dd, J = 6.9, 1.4 Hz, 1 H), 7.44 (d, J = 7.9 Hz, 1 H), 7.21 (m, 2 H), 6.42 (s, 1 H), 5.24 (t, J = 7.2 Hz, 1 H), 5.00 (s, 1 H), 4.87 (s, 1 H), 4.05 (s, 2 H), 2.82 (t, J = 7.6 Hz, 2 H), 2.48 (td, J = 7.6, 7.1 Hz, 2 H), 2.16 (s, 4 H), 1.67 (s, 1 H), 1.65 (s, 3 H) ppm; ^{13}C NMR (125 MHz, CDCl_3) δ = 159.1, 154.6, 148.7, 135.9, 128.9, 123.2, 123.0, 122.3, 120.1, 110.6, 109.3, 102.0, 65.8, 37.8, 31.4, 28.5, 26.0, 15.9 ppm; HRMS (ESI) exact mass calculated for $[\text{M}+\text{Na}]$ ($\text{C}_{18}\text{H}_{22}\text{NaO}_2$) requires m/z 293.1512, found m/z 293.1502.

(E)-8-(4-methoxyphenyl)-5-methyl-2-methyleneoct-5-en-1-ol (2.45)

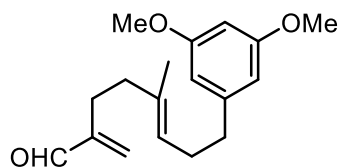


Followed general procedure C from 1-methoxy-4-vinylbenzene on a 0.54 mmol scale and purified using silica gel column chromatography to give 99 mg (0.38 mmol, 73% yield over 2 steps) of (*E*)-8-(4-methoxyphenyl)-5-methyl-2-methyleneoct-5-en-1-ol as a colourless oil. IR (Film) 3352, 3063, 2988, 2916, 2854, 1512, 1243, 1035 cm^{-1} ; ^1H NMR (400 MHz, CDCl_3) δ = 7.10 (d, J = 8.7 Hz, 2H), 6.82 (d, J = 8.7 Hz, 2H), 5.19 (t, J = 6.6 Hz, 1H), 5.01 (s, 1H), 4.87 (s, 1H), 4.07 (d, J = 5.3, 2H), 3.79 (s, 3H), 2.58 (t, J = 7.9 Hz, 2H), 2.26 (dt, J = 7.9, 6.6 Hz, 2H), 2.14 (s, 4H), 1.57 (s, 3H), 1.31 (t, J = 5.3 Hz, 1H) ppm; ^{13}C NMR (125 MHz, CDCl_3) δ = 157.8, 149.1, 135.4, 134.6, 129.5, 124.3, 113.8, 109.5, 66.1, 55.4, 38.1, 35.2, 31.7, 30.2, 16.1 ppm; HRMS (ESI) exact mass calculated for $[\text{M}+\text{Na}]$ ($\text{C}_{17}\text{H}_{24}\text{NaO}_2$) requires m/z 283.16685, found m/z 283.16681.

Synthesis of aldehydes (general procedure D)

To a solution of alcohol (0.30 mmol) in DCM (3 mL) was added pyridine (40 μL , 0.50 mmol) and Dess-Martin periodinane³ (170 mg, 0.40 mmol). The mixture was stirred for 1 h. The reaction was quenched with saturated aqueous sodium thiosulphate and extracted with DCM (3 x 10 mL). The combined organic layers were washed with brine, dried with MgSO_4 , filtered and concentrated. The crude extracts were purified by silica gel column chromatography (gradient from hexanes to 90:10 hexanes/EtOAc) to obtain aldehyde.

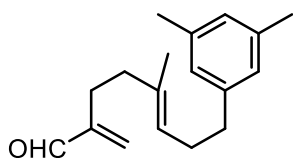
(E)-8-(3,5-dimethoxyphenyl)-5-methyl-2-methyleneoct-5-enal (2.4)



From (*E*)-8-(3,5-dimethoxyphenyl)-5-methyl-2-methyleneoct-5-en-1-ol, general procedure D was followed on a 0.30 mmol scale to give 73 mg (0.23 mmol, 76% yield) of (*E*)-8-(3,5-dimethoxyphenyl)-5-methyl-2-methyleneoct-5-enal as a colourless oil. IR (Film) 3083, 3056, 2992, 2932, 2838, 2694, 1687, 1594, 1460, 1428, 1347, 1315, 1293, 1204, 1150, 1066, 940, 830,

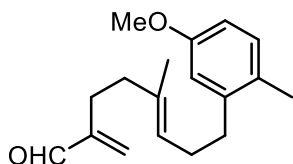
694 cm^{-1} ; ^1H NMR (500 MHz, CDCl_3) δ = 9.52 (s, 1 H), 6.37 (d, J = 2.2 Hz, 2 H), 6.32 (t, J = 2.2 Hz, 1 H), 6.22 (s, 1 H), 5.98 (s, 1 H), 5.18 (tq, J = 7.1, 0.9 Hz, 1 H), 3.80 (s, 6 H), 2.59 (t, J = 7.5 Hz, 2 H), 2.36 (t, J = 8.1 Hz, 2 H), 2.31 (td, J = 7.6, 7.3 Hz, 2 H), 2.14 (t, J = 7.9, 2 H), 1.61 (s, 3 H) ppm; ^{13}C NMR (125 MHz, CDCl_3) δ = 194.6, 160.7, 149.8, 144.7, 134.6, 134.2, 124.6, 106.5, 97.7, 55.2, 37.6, 36.3, 29.6, 26.3, 15.9 ppm; HRMS (ESI) exact mass calculated for $[\text{M}+\text{Na}]$ ($\text{C}_{18}\text{H}_{24}\text{NaO}_3$) requires m/z 311.1618, found m/z 311.1622.

(*E*)-8-(3,5-dimethylphenyl)-5-methyl-2-methyleneoct-5-enal (2.46)



From (*E*)-8-(3,5-dimethylphenyl)-5-methyl-2-methyleneoct-5-en-1-ol, general procedure D was followed on a 0.46 mmol scale to give 78 mg (30 μmol , 66% yield) of (*E*)-8-(3,5-dimethylphenyl)-5-methyl-2-methyleneoct-5-enal as a colourless oil. IR (Film) 3435, 3012, 2921, 2860, 1715, 1605, 1451, 1377, 1265, 1161, 1084, 1038, 946, 845, 734, 702 cm^{-1} ; ^1H NMR (500 MHz, CDCl_3) δ = 9.54 (s, 1 H), 6.85 (s, 1 H), 6.83 (s, 2 H), 6.23 (d, J = 0.7 Hz, 1 H), 6.00 (d, J = 0.5 Hz, 1 H), 5.21 (tq, J = 7.1, 1.1 Hz, 1 H), 2.57 (t, J = 7.8 Hz, 2 H), 2.37 (t, J = 7.6 Hz, 2 H), 2.32 – 2.27 (m, 8 H), 2.15 (t, J = 7.4 Hz, 2 H) 1.62 (s, 3 H) ppm; ^{13}C NMR (125 MHz, CDCl_3) δ = 194.6, 149.9, 142.2, 137.7, 134.4, 134.1, 127.4, 126.2, 124.9, 37.6, 35.9, 30.0, 26.4, 21.3, 15.8 ppm; HRMS (ESI) exact mass calculated for $[\text{M}+\text{Na}]$ ($\text{C}_{18}\text{H}_{24}\text{NaO}$) requires m/z 279.1719, found m/z 279.1712.

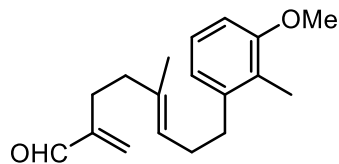
(*E*)-8-(5-methoxy-2-methylphenyl)-5-methyl-2-methyleneoct-5-enal (2.47)



From (*E*)-8-(5-methoxy-2-methylphenyl)-5-methyl-2-methyleneoct-5-en-1-ol, general procedure D was followed on a 0.30 mmol scale to give 72 mg (0.24 mmol, 81% yield) of (*E*)-8-(5-methoxy-2-methylphenyl)-5-methyl-2-methyleneoct-5-enal as a colourless oil. IR (Film) 3060, 2932, 2863, 2834, 2698, 1688, 1609, 1578, 1498, 1452, 1382, 1304, 1284, 1249, 1208, 1160, 1114, 1087, 1045, 997, 942, 868, 848, 801, 778, 713 cm^{-1} ; ^1H NMR (500 MHz, CDCl_3) δ = 9.55 (s, 1 H), 7.07 (d, 7.8 Hz, 1 H), 6.74 (d, J = 2.8 Hz, 1 H), 6.69 (dd, 7.8, 2.8 Hz, 1 H), 6.25 (s, 1 H), 6.01 (s, 1 H), 5.24

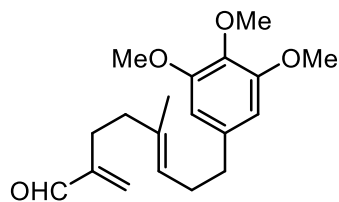
(tq, $J = 7.1, 1.0$ Hz, 1 H), 3.81 (s, 3 H), 2.61 (t, $J = 7.7$ Hz, 2 H), 2.39 (t, $J = 7.7$ Hz, 2 H), 2.31 – 2.27 (m, 5 H), 2.17 (t, $J = 7.7$ Hz, 2 H), 1.63 (s, 3 H) ppm; ^{13}C NMR (125 MHz, CDCl_3) $\delta = 194.6, 157.8, 149.9, 141.6, 134.6, 134.2, 130.8, 127.9, 124.7, 114.8, 110.8, 55.2, 37.7, 33.6, 28.5, 26.4, 18.4, 15.8$ ppm; HRMS (ESI) exact mass calculated for $[\text{M}+\text{Na}]$ ($\text{C}_{18}\text{H}_{24}\text{NaO}_2$) requires m/z 295.1669, found m/z 295.1678.

(*E*)-8-(3-methoxy-2-methylphenyl)-5-methyl-2-methyleneoct-5-enal (2.48)



From (*E*)-8-(3-methoxy-2-methylphenyl)-5-methyl-2-methyleneoct-5-en-1-ol, general procedure D was followed on a 0.35 mmol scale to give 72 mg (0.26 mmol, 74% yield) of (*E*)-8-(3-methoxy-2-methylphenyl)-5-methyl-2-methyleneoct-5-enal as a colourless oil. IR (Film) 2937, 2865, 2844, 2699, 1689, 1627, 1584, 1464, 1438, 1378, 1346, 1310, 1256, 1167, 1142, 1101, 1055, 1033, 1014, 942, 870, 838, 778, 720, 678 cm^{-1} ; ^1H NMR (500 MHz, CDCl_3) $\delta = 9.53$ (s, 1 H), 7.10 (t, 7.8 Hz, 1 H), 6.79 (d, $J = 7.6$ Hz, 1 H), 6.72 (d, $J = 8.0$ Hz, 1 H), 6.23 (s, 1 H), 5.98 (s, 1 H), 5.22 (tq, $J = 7.1, 1.2$ Hz, 1 H), 3.83 (s, 3 H), 2.63 (t, $J = 7.9$ Hz, 2 H), 2.37 (t, $J = 7.6$ Hz, 2 H), 2.26 (td, $J = 8.0, 7.2$ Hz, 2 H), 2.20 (s, 3 H), 2.15 (t, $J = 7.6$ Hz, 2 H), 1.61 (s, 3 H) ppm; ^{13}C NMR (125 MHz, CDCl_3) $\delta = 194.6, 157.6, 149.8, 141.7, 134.4, 134.1, 125.8, 124.7, 124.4, 121.4, 107.8, 55.4, 37.6, 33.6, 28.9, 26.3, 15.7, 11.2$ ppm; HRMS (APCI) exact mass calculated for $[\text{M}+\text{H}]$ ($\text{C}_{18}\text{H}_{25}\text{O}_2$) requires m/z 255.1743, found m/z 255.1751.

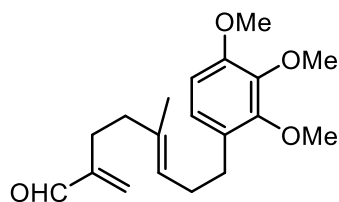
(*E*)-5-methyl-2-methylene-8-(3,4,5-trimethoxyphenyl)oct-5-enal (2.49)



From (*E*)-5-methyl-2-methylene-8-(3,4,5-trimethoxyphenyl)oct-5-en-1-ol, general procedure D was followed on a 0.40 mmol scale to give 101 mg (0.30 mmol, 75% yield) of (*E*)-5-methyl-2-methylene-8-(3,4,5-trimethoxyphenyl)oct-5-enal as a colourless oil. IR (Film) 3083, 2992, 2935, 2838, 2698, 1686, 1588, 1508, 1456, 1419, 1384, 1342, 1322, 1236, 1183, 1140, 1010, 946, 825,

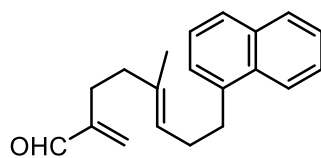
777, 743 cm^{-1} ; ^1H NMR (500 MHz, CDCl_3) δ = 9.49 (s, 1 H), 6.39 (s, 2 H), 6.19 (s, 1 H), 5.95 (s, 1 H), 5.16 (tq, J = 7.1, 1.1 Hz, 1 H), 3.84 (s, 6 H), 3.82 (s, 3 H), 2.56 (t, J = 7.4, 2 H), 2.36 – 2.26 (m, 4 H), 2.11 (t, J = 7.5 Hz, 2 H), 1.59 (s, 3 H) ppm; ^{13}C NMR (125 MHz, CDCl_3) δ = 194.5, 153.0, 149.8, 138.0, 136.1, 134.6, 134.1, 124.5, 105.4, 60.8, 56.0, 37.7, 36.3, 29.8, 26.4, 15.9 ppm; HRMS (APCI) exact mass calculated for $[\text{M}+\text{H}]$ ($\text{C}_{19}\text{H}_{27}\text{O}_4$) requires m/z 321.2060, found m/z 321.2059.

(*E*)-5-methyl-2-methylene-8-(2,3,4-trimethoxyphenyl)oct-5-enal (2.50)



From (*E*)-5-methyl-2-methylene-8-(2,3,4-trimethoxyphenyl)oct-5-en-1-ol, general procedure D was followed on a 0.37 mmol scale to give 82 mg (0.26 mmol, 69% yield) of (*E*)-5-methyl-2-methylene-8-(2,3,4-trimethoxyphenyl)oct-5-enal as a colourless oil. IR (Film) 3056, 2934, 2836, 2698, 1688, 1627, 1602, 1493, 1465, 1435, 1416, 1384, 1273, 1232, 1199, 1163, 1144, 1098, 1050, 1019, 943, 902, 839, 797, 736, 701 cm^{-1} ; ^1H NMR (500 MHz, CDCl_3) δ = 9.51 (s, 1 H), 6.82 (d, J = 8.6 Hz, 1 H), 6.60 (d, J = 8.6 Hz, 1 H), 6.22 (s, 1 H), 5.97 (s, 1 H), 5.20 (tq, J = 7.0, 1.2 Hz, 1 H), 3.88 (s, 3 H), 3.87 (s, 3 H), 3.84 (s, 3 H), 2.56 (t, J = 7.9 Hz, 2 H), 2.35 (t, J = 7.8 Hz, 2 H), 2.24 (td, J = 7.8, 7.0 Hz, 2 H), 2.12 (t, J = 7.8 Hz, 2 H), 1.59 (s, 3 H) ppm; ^{13}C NMR (125 MHz, CDCl_3) δ = 194.6, 151.9, 151.9, 149.9, 142.2, 134.4, 134.1, 128.2, 125.0, 123.8, 107.1, 60.9, 60.7, 56.0, 37.6, 29.9, 29.2, 26.3, 15.8 ppm; HRMS (APCI) exact mass calculated for $[\text{M}+\text{H}]$ ($\text{C}_{19}\text{H}_{27}\text{O}_4$) requires m/z 319.1904, found m/z 319.1904.

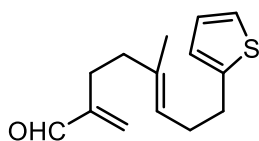
(*E*)-5-methyl-2-methylene-8-(naphthalen-1-yl)oct-5-enal (2.51)



From (*E*)-5-methyl-2-methylene-8-(naphthalen-1-yl)oct-5-en-1-ol, general procedure D was followed on a 0.27 mmol scale to give 53 mg (0.19 mmol, 70% yield) of (*E*)-5-methyl-2-methylene-8-(naphthalen-1-yl)oct-5-enal as a colourless oil. IR (Film) 3048, 2928, 2854, 2699,

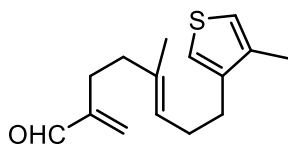
1687, 1627, 1596, 1510, 1439, 1395, 1351, 1265, 1225, 1165, 1078, 1020, 942, 866, 838, 790, 776, 734, 703 cm^{-1} ; ^1H NMR (500 MHz, CDCl_3) δ = 9.54 (s, 1 H), 8.08 (d, J = 8.1 Hz, 1 H), 7.87 (dd, J = 7.8, 1.3 Hz, 1 H), 7.73 (d, J = 8.5 Hz, 1 H), 7.54 (ddd, J = 7.9, 6.8, 1.4, 1 H), 7.49 (ddd, 8.1, 6.8, 1.4 Hz, 1 H), 7.42 (dd, J = 8.5, 7.1 Hz, 1 H), 7.33 (d, J = 7.1 Hz, 1 H), 6.22 (d, J = 0.6 Hz, 1 H), 5.98 (d, J = 0.6 Hz, 1 H), 5.30 (tq, J = 7.1, 1.3 Hz, 1 H), 3.11 (t, J = 7.7 Hz, 2 H), 2.47 (td, J = 7.7, 7.0 Hz, 2 H), 2.37 (t, J = 7.7 Hz, 2 H), 2.15 (t, J = 7.7 Hz, 2 H), 1.58 (s, 3 H) ppm; ^{13}C NMR (125 MHz, CDCl_3) δ = 194.6, 149.9, 138.3, 134.7, 134.2, 133.8, 131.9, 128.8, 126.5, 125.9, 125.7, 125.5, 125.4, 124.8, 123.8, 37.7, 33.1, 29.2, 26.4, 15.9 ppm; HRMS (ESI) exact mass calculated for $[\text{M}+\text{Na}]$ ($\text{C}_{20}\text{H}_{22}\text{NaO}$) requires m/z 301.1563, found m/z 301.1569.

(*E*)-5-methyl-2-methylene-8-(thiophen-2-yl)oct-5-enal (2.52)



From (*E*)-5-methyl-2-methylene-8-(thiophen-2-yl)oct-5-en-1-ol, general procedure D was followed on a 0.31 mmol scale to give 54 mg (0.23 mmol, 74% yield) of (*E*)-5-methyl-2-methylene-8-(thiophen-2-yl)oct-5-enal as a colourless oil. IR (Film) 3361, 3107, 3071, 2921, 2850, 2698, 1688, 1628, 1535, 1439, 1384, 1364, 1346, 1320, 1255, 1226, 1168, 1120, 1076, 1041, 942, 849, 823, 777, 692 cm^{-1} ; ^1H NMR (500 MHz, CDCl_3) δ = 9.52 (s, 1H), 7.11 (dd, J = 5.1, 0.8 Hz, 1 H), 6.92 (dd, J = 5.1, 3.4 Hz, 1 H), 6.79 (d, J = 3.2 Hz, 1 H), 6.21 (s, 1 H), 5.97 (s, 1 H), 5.19 (t, J = 6.9 Hz, 1 H), 2.86 (t, J = 7.6 Hz, 2 H), 2.40 – 2.35 (m, 4 H), 2.15 (t, J = 7.6 Hz, 2 H), 1.62 (s, 3 H) ppm; ^{13}C NMR (125 MHz, CDCl_3) δ = 194.6, 149.8, 145.1, 135.2, 134.2, 126.6, 124.1, 124.1, 123.0, 37.6, 30.1, 30.0, 26.3, 15.9 ppm; HRMS (ESI) exact mass calculated for $[\text{M}+\text{Na}]$ ($\text{C}_{14}\text{H}_{18}\text{NaOS}$) requires m/z 257.0971, found m/z 257.0975.

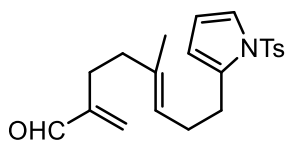
(*E*)-5-methyl-2-methylene-8-(4-methylthiophen-3-yl)oct-5-enal (2.53)



From (*E*)-5-methyl-2-methylene-8-(4-methylthiophen-3-yl)oct-5-en-1-ol, general procedure D was followed on a 0.32 mmol scale to give 58 mg (0.23 mmol, 73% yield) (*E*)-5-methyl-2-methylene-8-(4-methylthiophen-3-yl)oct-5-enal as a colourless oil. IR (Film) 3083, 2922, 2855,

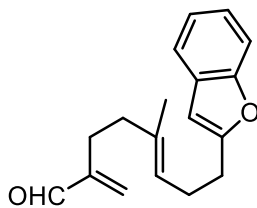
2699, 1688, 1627, 1444, 1383 cm^{-1} ; ^1H NMR (500 MHz, CDCl_3) δ = 9.53 (s, 1H), 6.89 (s, 2H), 6.22 (s, 1 H), 5.98 (s, 1 H) 5.21 (t, J = 7.0, 1 H), 2.53 (t, J = 8.2 Hz, 2 H), 2.37 (t, J = 7.5 Hz, 2 H), 2.30 (td, J = 7.6, 7.4 Hz, 2 H), 2.19 (s, 3 H), 2.14 (t, J = 7.5 Hz, 2 H), 1.62 (s, 3 H) ppm; ^{13}C NMR (125 MHz, CDCl_3) δ = 194.5, 149.8, 141.6, 136.8, 134.6, 134.1, 124.6, 120.7, 120.1, 37.6, 29.0, 27.8, 26.3, 15.8, 14.4 ppm; HRMS (ESI) exact mass calculated for $[\text{M}+\text{Na}]$ ($\text{C}_{15}\text{H}_{20}\text{NaOS}$) requires m/z 271.1127, found m/z 271.1127.

(*E*)-5-methyl-2-methylene-8-(1-tosyl-1H-pyrrol-2-yl)oct-5-enal (2.54)



From (*E*)-5-methyl-2-methylene-8-(1-tosyl-1H-pyrrol-2-yl)oct-5-en-1-ol, general procedure D was followed on a 0.28 mmol scale to give 83 mg (0.22 mmol, 80% yield) of (*E*)-5-methyl-2-methylene-8-(1-tosyl-1H-pyrrol-2-yl)oct-5-enal as a colourless oil. IR (Film) 3151, 3063, 2924, 2854, 2702, 1686, 1596, 1363, 1173, 945 cm^{-1} ; ^1H NMR (500 MHz, CDCl_3) δ = 9.49 (s, 1H), 7.61 (d, J = 7.0 Hz, 2 H), 7.27 (m, 3 H), 6.17 (m, 2 H), 5.95 (s, 2 H), 5.06 (t, J = 6.4 Hz, 1 H), 2.65 (t, J = 8.1 Hz, 2 H), 2.38 (s, 3 H), 2.31 (t, J = 8.1 Hz, 2 H), 2.22 (td, J = 7.2, 6.9 Hz, 2 H), 2.08 (t, J = 7.1 Hz, 2 H), 1.55 (s, 3 H) ppm; ^{13}C NMR (125 MHz, CDCl_3) δ = 194.5, 149.7, 144.6, 136.4, 135.3, 134.9, 134.2, 129.9, 126.6, 124.1, 122.2, 112.0, 111.2, 37.5, 27.2, 27.0, 26.2, 21.5, 15.8 ppm; HRMS (ESI) exact mass calculated for $[\text{M}+\text{Na}]$ ($\text{C}_{21}\text{H}_{25}\text{NNaO}_3\text{S}$) requires m/z 394.1447, found m/z 394.1434.

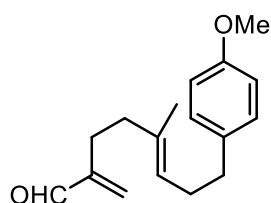
(*E*)-8-(benzofuran-2-yl)-5-methyl-2-methyleneoct-5-enal (2.55)



From (*E*)-8-(benzofuran-2-yl)-5-methyl-2-methyleneoct-5-en-1-ol, general procedure D was followed on a 0.25 mmol scale to give 55 mg (0.20 mmol, 82% yield) of (*E*)-8-(benzofuran-2-yl)-5-methyl-2-methyleneoct-5-enal as a colourless oil. IR (Film) 3063, 3040, 2921, 2848, 2699, 1688, 1627, 1601, 1587, 1455, 1348, 1319, 1304, 1252, 1225, 1177, 1141, 1105, 1009, 943, 880, 795,

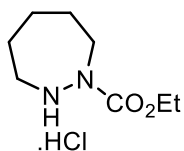
741, 705 cm^{-1} ; ^1H NMR (500 MHz, CDCl_3) δ = 9.50 (s, 1 H), 7.51 (d, J = 7.5 Hz, 1 H), 7.44 (d, J = 6.8 Hz, 1 H), 7.25 – 7.19 (m, 2 H), 6.40 (d, J = 0.8 Hz, 1 H), 6.19 (d, J = 0.8 Hz, 1 H), 5.92 (d, J = 0.8 Hz, 1 H), 5.21 (tq, J = 7.0, 1.3 Hz, 1 H), 2.82 (t, J = 7.1 Hz, 2 H), 2.47 (td, J = 7.1, 7.0 Hz, 2 H), 2.37 (t, J = 7.9 Hz, 2 H), 2.16 (t, J = 7.9 Hz, 2 H), 1.66 (s, 3 H) ppm; ^{13}C NMR (125 MHz, CDCl_3) δ = 194.6, 159.1, 154.6, 149.7, 135.3, 134.2, 129.0, 123.9, 123.1, 122.4, 120.2, 110.7, 102.1, 37.6, 28.6, 26.3, 26.1, 15.9 ppm; HRMS (APCI) exact mass calculated for $[\text{M}-\text{H}]$ ($\text{C}_{18}\text{H}_{19}\text{O}_2$) requires m/z 267.1390, found m/z 267.1388.

(*E*)-8-(4-methoxyphenyl)-5-methyl-2-methyleneoct-5-enal (2.56)



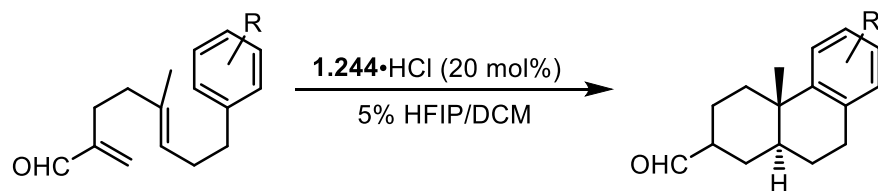
From (*E*)-8-(4-methoxyphenyl)-5-methyl-2-methyleneoct-5-en-1-ol, general procedure D was followed on a 0.38 mmol scale to give 76 mg (0.29 mmol, 77% yield) of (*E*)-8-(3-methoxy-2-methylphenyl)-5-methyl-2-methyleneoct-5-enal as a colourless oil. IR (Film) 3031, 2996, 2927, 2853, 2835, 1689, 1511, 1244, 1177, 1037 cm^{-1} ; ^1H NMR (400 MHz, CDCl_3) δ = 9.51 (s, 1H), 7.09 (d, J = 8.7 Hz, 2H), 6.82 (d, J = 8.7 Hz, 2H), 6.20 (s, 1H), 5.96 (s, 1H), 5.16 (t, J = 6.8 Hz, 1H), 3.79 (s, 3H), 2.56 (t, J = 8.6 Hz, 2H), 2.34 (t, J = 8.6 Hz, 2H), 2.25 (dt, J = 6.8, 6.7 Hz, 2H), 2.11 (t, J = 6.7 Hz, 2H), 1.56 (s, 3H) ppm; ^{13}C NMR (125 MHz, CDCl_3) δ = 194.8, 157.8, 150.0, 134.6, 134.5, 134.3, 129.4, 124.8, 113.8, 55.4, 37.8, 35.2, 30.2, 26.4, 16.0 ppm; HRMS (ESI) exact mass calculated for $[\text{M}+\text{Na}]$ ($\text{C}_{17}\text{H}_{22}\text{NaO}_2$) requires m/z 281.15120, found m/z 281.15227.

ethyl 1,2-diazepane-1-carboxylate hydrochloride (1.241·HCl)



Ethyl 1,2-diazepane-1-carboxylate (**1.241**) was synthesized by Dr. Samuel Plamondon according to literature.¹ Gaseous hydrochloric acid was bubbled through a stirred solution of freebase ethyl 1,2-diazepane-1-carboxylate in hexanes, causing an oil to crash out. The solvent was removed *in vacuo*, the residue was dissolved in a hexanes/dichloromethane mixture, and the solvent was again

removed. After three repetitions of this cycle, the oil was left under high vacuum for several days until all the material had solidified, giving an off-white powder.



Racemic polyene cyclization (general procedure E)

To a 1.8-mL or 3.7-mL vial containing aldehyde was added a solution of catalyst **1.241**·HCl (0.2 equiv.) in 5% HFIP/DCM (0.25 M in substrate). The mixture was briefly swirled to homogenize and let stand for 5 hours. The reaction mixture was concentrated and purified by silica gel column chromatography (gradient from hexanes to 93:7 hexanes/EtOAc) to obtain *trans*-decalin products as a mixture of diastereomers.

Racemic polyene cyclization (general procedure F)

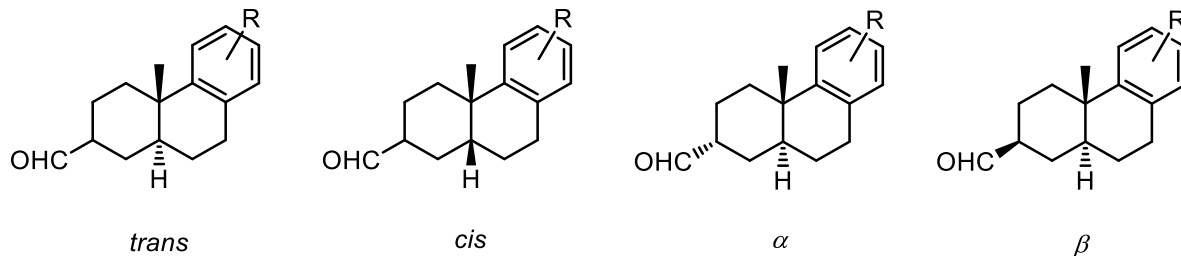
To a 1 mL vial containing aldehyde was added a solution of catalyst **1.241**·HCl (0.2 equiv.) in EtOH (0.25 M in substrate). The mixture was briefly swirled to homogenize and let stand for 4 h. The reaction mixture was concentrated and redissolved in CHCl₃ (0.5 mL); water (0.25 mL) and TFA (0.25 mL) were added. The biphasic mixture was stirred for 1 h, added dropwise to a saturated solution of NaHCO₃ (5 mL), extracted with DCM (5 mL), and concentrated. The reaction mixture was concentrated and purified by silica gel column chromatography (gradient from 97:3 to 90:10 hexanes/EtOAc) to obtain aldehyde product as a mixture of diastereomers.

¹H and ¹³C peaks for the α diastereomer of *trans*-decalin products are reported with an asterisk (*) where possible to distinguish from the β diastereomer peaks. The integrations are reported as a proportion of the total signal (i.e. 1 H x 0.5 for a signal that corresponds to one proton of one of the two diastereomers).

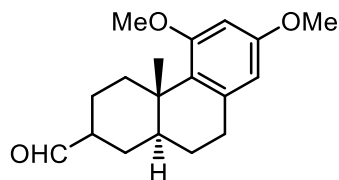
Note: NMR spectra show small ratios of *cis*-decalin products.

Stereochemical nomenclature for polyene cyclization products:

- *trans* and *cis* refer to ring fusion
- α and β refer to stereochemistry at C3



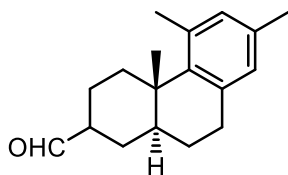
(4a*RS*,10a*RS*)-5,7-dimethoxy-4a-methyl-1,2,3,4,4a,9,10,10a-octahydrophenanthrene-2-carbaldehyde (2.5)



Prepared according to general procedure E from polyene **2.4** (49 mg, 0.17 mmol). The reaction was run for 5 h and product **2.5** was isolated as a colourless oil (35 mg, 0.12 mmol, 72% yield, *trans*:*cis* 95:5, *trans*- β : α 6:1). IR (Film) 2988, 2928, 2861, 2837, 2709, 1721, 1604, 1580, 1459, 1419, 1341, 1325, 1309, 1289, 1268, 1230, 1212, 1194, 1150, 1132, 1119, 1085, 1065, 1046, 1023, 941, 829, 736, 702 cm^{-1} ; ^1H NMR (500 MHz, CDCl_3) δ = 9.73* (s, 1 H x 0.2), 9.66 (d, J = 1.5 Hz, 1 H x 0.8), 6.30 (d, J = 2.4 Hz, 1 H x 0.8), 6.30* (d, J = 2.4 Hz, 1H x 0.2), 6.22 (d, J = 2.4 Hz, 1 H x 0.8), 6.21* (d, J = 2.4 Hz, 1 H x 0.2), 3.78 (s, 3 H x 0.8), 3.77 (s, 3 H x 0.8), 3.75* (s, 3 H x 0.2), 3.75* (s, 3 H x 0.2), 3.17 (dt, J = 13.4, 3.5 Hz, 1 H x 0.8), 2.99 – 2.91 (m, 1 H x 0.8), 2.99 – 2.91* (m, 2 H x 0.2), 2.77 (dd, J = 17.4, 4.5 Hz, 1 H x 0.8), 2.74* (dd, J = 17.3, 5.5 Hz, 1 H x 0.2), 2.43* (t, J = 6.2 Hz, 1 H x 0.2), 2.40 – 2.34 (m, 1 H x 0.8), 2.13* (d, J = 14.8, 1 H x 0.2), 2.01* (d, J = 14.0, 1 H x 0.2), 1.96 – 1.88* (m, 1 H x 0.2), 1.86 (m, 1 H x 0.8), 1.82 – 1.74* (m, 1 H x 0.2), 1.74 – 1.39 (m, 6 H x 0.8), 1.74 – 1.39* (m, 3 H x 0.2), 1.25 (td, J = 13.4, 3.8 Hz, 1 H x 0.8), 1.20* (s, 3 H x 0.2), 1.17 (s, 3 H x 0.8), 1.13* (td, J = 14.1, 4.2, 1 H x 0.2) ppm; ^{13}C NMR (125 MHz, CDCl_3) δ = 206.0*, 204.7, 160.0, 159.8*, 158.0, 158.0*, 138.8, 138.8*, 127.6*, 127.5, 105.0, 105.0*, 97.4, 97.4*, 55.1, 55.1*, 55.0, 55.0*, 50.8, 46.6*, 44.2, 41.5*, 37.4, 37.3*, 34.7, 32.8*,

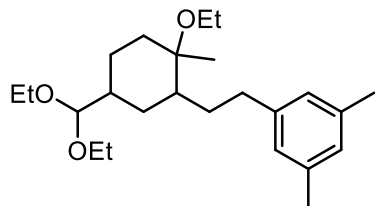
32.2, 32.0*, 28.2, 27.4*, 25.7, 25.7*, 22.0, 21.0*, 16.6, 16.1* ppm; MS (ESI) exact mass calculated for [M+Na] (C₁₈H₂₄NaO₃) requires m/z 311.1618, found m/z 311.1611.

(4aRS,10aRS)-4a,5,7-trimethyl-1,2,3,4,4a,9,10,10a-octahydrophenanthrene-2-carbaldehyde
(2.57)



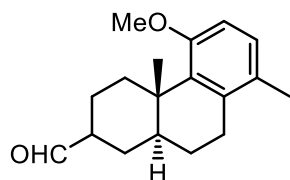
Prepared according to general procedure E from polyene **2.46** (48 mg, 0.18 mmol). The reaction was run for 5 h and product **2.57** was isolated as a colourless oil (35.6, 0.14 mmol, 75% yield, *trans:cis* 94:6, *trans-β:α* 5:1). IR (Film) 3050, 2973, 2926, 2860, 2712, 1722, 1611, 1463, 1440, 1382, 1266, 1166, 1044, 1016, 911, 849, 734, 703, 611 cm⁻¹; ¹H NMR (500 MHz, CDCl₃) δ = 9.73* (s, 1 H x 0.2), 9.68 (d, J = 1.5 Hz, 1 H x 0.8), 6.79 (s, 1 H x 0.8), 6.78 (s, 1 H x 0.8), 6.76* (s, 1 H x 0.2), 6.75* (s, 1 H x 0.2), 3.02 – 2.91* (m, 1 H x 0.2), 2.99 (ddd, J = 16.9, 12.2, 7.6 Hz, 1 H x 0.8), 2.87 (dt, J = 13.4, 3.4 Hz, 1 H x 0.8), 2.80 (dd, J = 17.0, 6.0 Hz, 1 H x 0.8), 2.80 – 2.74* (m, 1 H x 0.2), 2.66* (dt, J = 13.5, 2.7 Hz, 1 H x 0.2), 2.50 (s, 3 H x 0.8), 2.47* (s, 3 H x 0.2), 2.40 – 2.33 (m, 1 H x 0.8), 2.40 – 2.31* (m, 2 H x 0.2), 2.24 (s, 3 H x 0.8), 2.23 – 2.17* (m, 1 H x 0.2), 2.22* (s, 3 H x 0.2), 2.06 – 2.02* (m, 1 H x 0.2), 1.95 – 1.88* (m, 1 H x 0.2), 1.94 – 1.89 (m, 1 H x 0.8), 1.84 – 1.46* (m, 3 H x 0.2), 1.78 – 1.50 (m, 6 H x 0.8), 1.39 (ddd, J = 13.5, 13.5, 3.6 Hz, 1 H x 0.8), 1.31 – 1.27* (m, 1 H x 0.2), 1.27* (s, 3 H x 0.2), 1.24 (s, 3 H x 0.8) ppm; ¹³C NMR (125 MHz, CDCl₃) δ = 205.5*, 204.4, 142.0*, 141.9, 136.8, 136.8*, 136.2, 136.1*, 134.9, 134.8*, 131.8, 131.7*, 128.8, 128.7*, 50.3, 46.1*, 44.4, 41.6*, 38.5, 38.4*, 35.3, 33.2*, 31.7, 31.5*, 28.7, 27.8*, 25.8, 25.7*, 24.3, 24.2*, 22.0, 20.9*, 20.3, 20.3*, 17.4, 16.9* ppm; MS (ESI) exact mass calculated for [M+Na] (C₁₈H₂₄NaO) requires m/z 279.1719, found m/z 279.1713.

1-(2-(5-(diethoxymethyl)-2-ethoxy-2-methylcyclohexyl)ethyl)-3,5-dimethylbenzene (2.60)



Prepared according to general procedure E from polyene **2.46** (22 mg, 0.087 mmol) using EtOH as the solvent instead of HFIP/DCM. The reaction was run for 24 h and product **2.60** was isolated as a colourless oil (15 mg, 0.040 mmol, 46% yield). IR (Film) 3272, 2972, 2926, 2868, 1721, 1697, 1606, 1531, 1458, 1444, 1371, 1337, 1291, 1254, 1162, 1115, 1062, 1004, 951, 844, 702 cm^{-1} ; ^1H NMR (500 MHz, CDCl_3) δ = 6.82 (s, 2H), 6.81 (s, 1H), 4.16 (d, J = 7.2 Hz, 1 H), 3.70 – 3.64 (m, 2H), 3.54 – 3.48 (m, 2H), 3.37 – 3.27 (m, 2H), 2.68 – 2.63 (m, 1H), 2.46 – 2.40 (m, 1H), 2.28 (s, 6H), 2.05 – 2.04 (m, 1H), 2.00 – 1.97 (m, 1H), 1.78 – 1.72 (m, 2H), 1.64 – 1.59 (m, 1H), 1.54 – 1.46 (m, 2H), 1.23 (t, J = 7.2 Hz, 3H), 1.21 (t, J = 7.2 Hz, 3H), 1.18 – 1.12 (m, 2H), 1.12 (t, J = 7.2 Hz, 3H), 1.04 (s, 3H), 0.92 – 0.84 (m, 1H) ppm; ^{13}C NMR (125 MHz, CDCl_3) δ = 143.1, 137.6, 127.2, 126.2, 106.5, 76.8, 62.0, 62.0, 55.2, 43.1, 40.6, 35.8, 34.0, 31.5, 30.2, 25.3, 21.2, 18.0, 16.3, 15.4, 15.3 ppm; HRMS (ESI) exact mass calculated for $[\text{M}+\text{Na}]$ ($\text{C}_{24}\text{H}_{40}\text{NaO}_3$) requires m/z 399.2870, found m/z 399.2866.

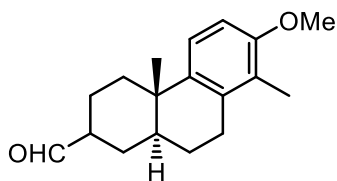
(4aRS,10aRS)-5-methoxy-4a,8-dimethyl-1,2,3,4,4a,9,10,10a-octahydrophenanthrene-2-carbaldehyde (2.61)



Prepared according to general procedure E from polyene **2.47** (48 mg, 0.17 mmol). The reaction was run for 5 h and product **2.61** was isolated as an off-white solid (34 mg, 0.12 mmol, 72% yield, *trans:cis* 94:6, *trans- β : α* 4:1). IR (Film) 2927, 2861, 2833, 1708, 1721, 1582, 1461, 1437, 1406, 1374, 1340, 1289, 1244, 1223, 1190, 1166, 1144, 1107, 1085, 1057, 1034, 1007, 948, 922, 907, 888, 801, 736, 722, 702 cm^{-1} ; ^1H NMR (500 MHz, CDCl_3) δ = 9.73* (s, 1 H x 0.2), 9.67 (d, J = 1.6 Hz, 1 H x 0.8), 6.97 (d, J = 8.1 Hz, 1 H x 0.8), 6.95* (d, J = 8.1 Hz, 1 H x 0.2), 6.68 (d, J = 8.1 Hz, 1 H x 0.8), 6.64* (d, J = 8.1 Hz, 1 H x 0.2), 3.79 (s, 3 H x 0.8), 3.77* (s, 3 H x 0.2), 3.26 (dt,

$J = 13.4, 3.3 \text{ Hz}, 1 \text{ H} \times 0.8$), 3.05^* (dt, $J = 13.7, 3.5 \text{ Hz}, 1 \text{ H} \times 0.2$), $2.70 - 2.64$ (m, $2 \text{ H} \times 0.8$), $2.65 - 2.60^*$ (m, $2 \text{ H} \times 0.2$), 2.46^* (t, $J = 6.5 \text{ Hz}, 1 \text{ H} \times 0.2$), $2.41 - 2.33$ (m, $1 \text{ H} \times 0.8$), 2.15 (s, $3 \text{ H} \times 0.8$), 2.13^* (s, $3 \text{ H} \times 0.2$), $2.05 - 2.00^*$ (m, $1 \text{ H} \times 0.2$), $1.99 - 1.90^*$ (m, $1 \text{ H} \times 0.2$), $1.90 - 1.83$ (m, $1 \text{ H} \times 0.8$), $1.84 - 1.76^*$ (m, $1 \text{ H} \times 0.2$), $1.77 - 1.54$ (m, $6 \text{ H} \times 0.8$), $1.77 - 1.54^*$ (m, $3 \text{ H} \times 0.2$), $1.48 - 1.39^*$ (m, $1 \text{ H} \times 0.8$), 1.27^* (s, $3 \text{ H} \times 0.2$), $1.26 - 1.20$ (m, $1 \text{ H} \times 0.8$), 1.23 (s, 3 H), 1.12^* (td, $J = 13.7, 4.1 \text{ Hz}, 1 \text{ H} \times 0.2$) ppm; ^{13}C NMR (125 MHz, CDCl_3) $\delta = 206.0^*, 204.7, 157.2, 157.2^*, 136.5, 136.5^*, 134.9, 134.8^*, 128.9, 128.9^*, 127.7, 127.6^*, 109.0, 109.0^*, 55.1, 55.0^*, 50.8, 46.5^*, 43.5, 40.8^*, 38.0, 37.9^*, 34.6, 32.6^*, 29.4, 29.2^*, 28.2, 27.4^*, 25.6, 25.6^*, 22.0, 21.0^*, 19.5, 19.5^*, 16.4, 15.8^*$ ppm; MS (ESI) exact mass calculated for $[\text{M}+\text{Na}]$ ($\text{C}_{18}\text{H}_{24}\text{NaO}_2$) requires m/z 295.1669, found m/z 295.1667.

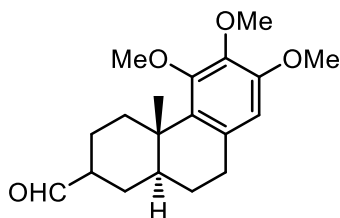
(4a*RS*,10a*RS*)-7-methoxy-4a,8-dimethyl-1,2,3,4,4a,9,10,10a-octahydrophenanthrene-2-carbaldehyde (2.62)



Prepared according to general procedure E from polyene **2.48** (48 mg, 0.18 mmol). The reaction was run for 5 h and product **2.62** was isolated as a white solid (36 mg, 0.13 mmol, 75% yield, *trans*:*cis* 96:4, *trans*- β : α 4:1). IR (Film) 3083, 3040, 2928, 2858, 2833, 2709, 1721, 1596, 1583, 1483, 1464, 1438, 1375, 1337, 1291, 1260, 1214, 1192, 1170, 1148, 1109, 1088, 1023, 999, 930, 899, 844, 802, 738, 706 cm^{-1} ; ^1H NMR (500 MHz, CDCl_3) $\delta = 9.72^*$ (s, $1 \text{ H} \times 0.2$), 9.70 (d, $J = 1.2 \text{ Hz}, 1 \text{ H} \times 0.8$), 7.15 (d, $J = 8.6 \text{ Hz}, 1 \text{ H} \times 0.8$), 7.09^* (d, $J = 8.6 \text{ Hz}, 1 \text{ H} \times 0.2$), 6.75 (d, $J = 8.6 \text{ Hz}, 1 \text{ H} \times 0.8$), 6.72^* (d, $J = 8.6 \text{ Hz}, 1 \text{ H} \times 0.2$), 3.81 (s, $3 \text{ H} \times 0.8$), 3.80^* (s, $3 \text{ H} \times 0.2$), $2.84 - 2.62$ (m, $2 \text{ H} \times 0.8$), $2.84 - 2.62^*$ (m, $2 \text{ H} \times 0.2$), 2.51^* (t, $J = 6.0 \text{ Hz}, 1 \text{ H} \times 0.2$), $2.42 - 2.32$ (m, $2 \text{ H} \times 0.8$), $2.30 - 2.23^*$ (m, $1 \text{ H} \times 0.2$), $2.20 - 2.14^*$ (m, $1 \text{ H} \times 0.2$), 2.11 (s, $3 \text{ H} \times 0.8$), 2.08^* (s, $3 \text{ H} \times 0.2$), $2.08 - 2.04^*$ (m, $1 \text{ H} \times 0.2$), $2.02 - 1.95$ (m, $1 \text{ H} \times 0.8$), $1.95 - 1.88^*$ (m, $1 \text{ H} \times 0.2$), $1.83 - 1.57$ (m, $5 \text{ H} \times 0.8$), $1.83 - 1.57^*$ (m, $3 \text{ H} \times 0.2$), $1.50 - 1.39$ (m, $2 \text{ H} \times 0.8$), $1.50 - 1.39^*$ (m, $1 \text{ H} \times 0.2$), 1.35^* (td, $J = 13.6, 4.2 \text{ Hz}, 1 \text{ H} \times 0.2$), 1.11^* (s, $3 \text{ H} \times 0.2$), 1.08 (s, $3 \text{ H} \times 0.8$) ppm; ^{13}C NMR (125 MHz, CDCl_3) $\delta = 205.4^*, 204.3, 155.2, 155.1^*, 139.7^*, 139.6, 135.2, 135.1^*, 124.4, 124.4^*, 122.3, 122.2^*, 108.0, 108.0^*, 55.5, 55.5^*, 50.5, 46.4^*, 40.7, 38.0^*, 37.1, 36.2, 36.0^*$,

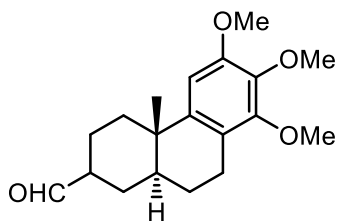
34.9*, 28.3, 27.4*, 27.3, 27.2*, 25.6*, 25.6, 22.0, 21.8, 21.3*, 20.8*, 11.1, 11.0* ppm; MS (APCI) exact mass calculated for [M-H] (C₁₈H₂₃O₂) requires m/z 271.1703, found m/z 271.1701.

(4aRS,10aRS)-5,6,7-trimethoxy-4a-methyl-1,2,3,4,4a,9,10,10a-octahydrophenanthrene-2-carbaldehyde (2.63)



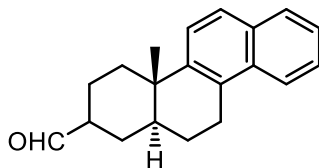
Prepared according to general procedure E from polyene **2.49** (49 mg, 0.15 mmol). The reaction was run for 5 h and product **2.63** was isolated as a white solid (34 mg, 0.11 mmol, 69% yield, *trans:cis* 95:5, *trans-β:α* 3:1). IR (Film) 2972, 2930, 2860, 2841, 2709, 1722, 1596, 1570, 1488, 1464, 1448, 1481, 1374, 1337, 1324, 1264, 1241, 1194, 1144, 1111, 1062, 1024, 982, 962, 942, 908, 868, 831, 789, 754, 667 cm⁻¹; ¹H NMR (500 MHz, CDCl₃) δ = 9.72* (s, 1 H x 0.2), 9.66 (d, J = 1.6 Hz, 1 H x 0.8), 6.36 (s, 1 H x 0.8), 6.33* (s, 1H x 0.2), 3.89 (s, 3 H x 0.8), 3.87* (s, 3 H x 0.2), 3.81 (s, 3 H x 0.8), 3.81 (s, 3 H x 0.8), 3.79* (s, 3 H x 0.2), 3.79* (s, 3 H x 0.2), 3.10 (dt, J = 13.3, 3.4 Hz, 1 H x 0.8), 2.96 – 2.82 (m, 1 H x 0.8), 2.96 – 2.82* (m, 1 H x 0.2), 2.74 (dd, J = 16.9, 5.1 Hz, 1 H x 0.8), 2.69* (dd, J = 17.5, 5.6 Hz, 1 H x 0.2), 2.46* (t, J = 5.6 Hz, 1 H x 0.2), 2.41 – 2.32 (m, 1 H x 0.8), 2.16* (d, J = 13.5 Hz, 1 H x 0.2), 2.01* (d, J = 14.3 Hz, 1 H x 0.2), 1.97 – 1.86* (m, 1 H x 0.2), 1.92 – 1.86 (m, 1 H x 0.8), 1.78* (td, J = 13.5, 5.6 Hz, 1 H x 0.2), 1.74 – 1.41 (m, 6 H x 0.8), 1.74 – 1.41* (m, 4 H x 0.2), 1.35 (dt, J = 13.5, 5.0 Hz, 1 H x 0.8), 1.24 – 1.19* (m, 1 H x 0.2), 1.20* (s, 3 H x 0.2), 1.17 (s, 3 H x 0.8) ppm; ¹³C NMR (125 MHz, CDCl₃) δ = 205.8*, 204.5, 153.6, 153.5*, 151.3, 151.2*, 140.6, 140.5*, 132.1*, 132.1, 132.0, 132.0*, 107.6, 107.5*, 60.5, 60.5*, 60.4, 60.4*, 55.6, 55.6*, 50.6, 46.5*, 43.7, 41.0*, 37.8, 37.7*, 35.3, 33.3*, 31.6, 31.4*, 28.2, 27.4*, 25.9, 25.9*, 22.0, 21.0*, 18.2, 17.6* ppm; MS (ESI) exact mass calculated for [M+Na] (C₁₉H₂₆NaO₄) requires m/z 341.1723, found m/z 341.1727.

(4a*RS*,10a*RS*)-6,7,8-trimethoxy-4a-methyl-1,2,3,4,4a,9,10,10a-octahydrophenanthrene-2-carbaldehyde (2.64)



Prepared according to general procedure E from polyene **2.50** (46 mg, 0.14 mmol). The reaction was run for 5 h and product **2.64** was isolated as a yellow solid (33 mg, 0.10 mmol, 70% yield, *trans*:*cis* 89:11, *trans*- β : α 4:1). IR (Film) 3056, 2932, 2859, 2711, 1722, 1599, 1576, 1492, 1464, 1451, 1404, 1376, 1341, 1318, 1273, 1222, 1194, 1165, 1133, 1113, 1056, 1034, 1313, 928, 901, 872, 850, 835, 792, 734, 702 cm^{-1} ; ^1H NMR (500 MHz, CDCl_3) δ = 9.71* (s, 1 H x 0.2), 9.68 (d, J = 1.2 Hz, 1 H x 0.8), 6.60 (s, 1 H x 0.8), 6.55* (s, 1 H x 0.2), 3.85 (s, 3 H x 0.8), 3.84 (s, 3 H x 0.8), 3.83 (s, 3 H x 0.8), 3.83* (s, 3 H x 0.2), 3.82* (s, 3 H x 0.2), 3.81* (s, 3 H x 0.2), 2.87 – 2.79 (m, 1 H x 0.8), 2.87 – 2.75* (m, 1 H x 0.2), 2.70 – 2.60 (m, 1 H x 0.8), 2.70 – 2.56* (m, 1 H x 0.2), 2.50* (t, J = 6.2 Hz, 1 H x 0.2), 2.40 – 2.28 (m, 1 H x 0.8), 2.40 – 2.28* (m, 1 H x 0.2), 2.28 – 2.22* (m, 1 H x 0.2), 2.09* (dt, J = 12.9, 3.0 Hz, 1 H x 0.2), 2.04* (dt, J = 13.7, 1.5 Hz, 1 H x 0.2), 1.98 (d, J = 13.7 Hz, 1 H x 0.8), 1.93 – 1.85* (m, 1 H x 0.2), 1.77 (d, J = 13.3 Hz, 1 H x 0.8), 1.73 – 1.55* (m, 3 H x 0.2), 1.70 – 1.55 (m, 4 H x 0.8), 1.52 – 1.36 (m, 2 H x 0.8), 1.52 – 1.36* (m, 1 H x 0.2), 1.09* (s, 3 H x 0.2), 1.06 (s, 3 H x 0.8) ppm; ^{13}C NMR (125 MHz, CDCl_3) δ = 205.3*, 204.2, 151.2, 151.1*, 151.0, 151.0*, 142.8*, 142.7, 140.0, 140.0*, 121.8, 121.8*, 103.8, 103.7*, 60.6, 60.6*, 60.1, 60.0*, 56.0, 56.0*, 50.4, 46.4*, 41.1, 38.3*, 36.8, 36.7, 36.5*, 34.6*, 28.3, 27.5*, 25.1*, 25.0, 23.0, 22.9*, 21.9, 21.5, 21.0*, 20.7* ppm; MS (APCI) exact mass calculated for $[\text{M}+\text{H}]$ ($\text{C}_{19}\text{H}_{27}\text{O}_4$) requires m/z 319.1904, found m/z 319.1901.

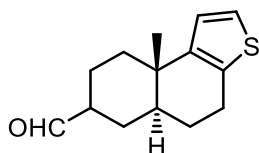
(4a*RS*,12a*RS*)-4a-methyl-1,2,3,4,4a,11,12,12a-octahydrochrysen-2-carbaldehyde (2.65)



Prepared according to general procedure E from polyene **2.51** (45 mg, 0.16 mmol). The reaction was run for 5 h and product **2.65** was isolated as a yellow solid (40 mg, 0.14 mmol, 88% yield,

trans:cis 94:6, *trans-β:α* 4:1). IR (Film) 3054, 2929, 2858, 2711, 1720, 1622, 1596, 1569, 1508, 1462, 1451, 1438, 1374, 1333, 1264, 1223, 1188, 1157, 1140, 1121, 1094, 1056, 1030, 1018, 998, 947, 864, 854, 842, 811, 777, 746, 734, 702, 672 cm⁻¹; ¹H NMR (500 MHz, CDCl₃) δ = 9.74* (s, 1 H x 0.2), 9.71 (d, J = 1.2 Hz, 1 H x 0.8), 7.99 (d, J = 8.5 Hz, 1 H x 0.8), 7.96* (d, J = 8.5 Hz, 1 H x 0.2), 7.80 (d, J = 8.1 Hz, 1 H x 0.8), 7.77* (d, J = 8.1 Hz, 1 H x 0.2), 7.69 (d, J = 8.5 Hz, 1 H x 0.8), 7.65* (d, J = 8.5 Hz, 1 H x 0.2), 7.53 – 7.42 (m, 3 H x 0.8), 7.53 – 7.42* (m, 3 H x 0.2), 3.31 (dd, J = 17.3, 5.7 Hz, 1 H x 0.8), 3.27 – 3.11* (m, 2 H x 0.2), 3.24 – 3.14 (m, 1 H x 0.8), 2.55* (t, J = 6.6 Hz, 1 H x 0.2), 2.51 (dt, J = 12.7, 3.2 Hz, 1 H x 0.8), 2.41 – 2.34 (m, 1 H x 0.8), 2.33 – 2.28* (m, 2 H x 0.2), 2.16 – 2.11* (m, 1 H x 0.2), 2.04 – 1.98 (m, 1 H x 0.8), 2.04 – 1.98* (m, 1 H x 0.2), 1.92 – 1.79 (m, 3 H x 0.8), 1.92 – 1.79* (m, 2 H x 0.2), 1.79 – 1.68 (m, 2 H x 0.8), 1.79 – 1.68* (m, 2 H x 0.2), 1.57 – 1.42 (m, 2 H x 0.8), 1.57 – 1.42* (m, 1 H x 0.2), 1.22* (s, 3 H x 0.2), 1.18 (s, 3 H x 0.8) ppm; ¹³C NMR (125 MHz, CDCl₃) δ = 205.4*, 204.2, 143.8*, 143.8, 132.4, 132.4*, 131.7, 131.7*, 129.8, 129.8*, 128.2, 128.2*, 126.2, 126.1*, 125.9, 125.8*, 125.0, 124.9*, 123.3, 123.3*, 123.2*, 123.2, 50.4, 46.4, 41.3, 38.6*, 37.0, 36.8*, 36.8, 34.6*, 28.2, 27.4*, 26.3, 26.2*, 25.4*, 25.4, 21.9, 21.1, 20.7*, 20.6* ppm; MS (APCI) exact mass calculated for [M+H] (C₂₀H₂₃O) requires m/z 279.1743, found m/z 279.1740.

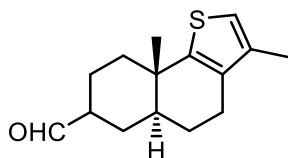
(5a*RS*,9a*RS*)-9a-methyl-4,5,5a,6,7,8,9,9a-octahydronaphtho[2,1-*b*]thiophene-7-carbaldehyde (2.66)



Prepared according to general procedure E from polyene **2.52** (46 mg, 0.19 mmol). The reaction was run for 5 h and product **2.66** was isolated as a yellow oil (37 mg, 0.16 mmol, 81% yield, *trans:cis* 94:6, *trans-β:α* 4:1). IR (Film) 3104, 3063, 2929, 2855, 2708, 1722, 1462, 1451, 1439, 1375, 1330, 1265, 1234, 1194, 1173, 1126, 1091, 1030, 1016, 986, 964, 910, 893, 855, 830, 729, 699 cm⁻¹; ¹H NMR (500 MHz, CDCl₃) δ = 9.71* (s, 1 H x 0.2), 9.67 (d, J = 1.3 Hz, 1 H x 0.8), 7.06 (d, J = 5.3 Hz, 1 H x 0.8), 7.02* (d, J = 5.3 Hz, 1 H x 0.2), 6.86 (d, J = 5.3 Hz, 1 H x 0.8), 6.81 (d, J = 5.3 Hz, 1 H x 0.8), 2.90 – 2.81 (m, 2 H x 0.8), 2.90 – 2.81* (m, 2 H x 0.2), 2.52* (t, J = 6.5 Hz, 1 H x 0.2), 2.37 (ttd, J = 12.6, 4.3, 1.2 Hz, 1 H x 0.8), 2.24 – 2.17* (m, 1 H x 0.2), 2.19 (dt, J = 12.9, 3.3 Hz, 1 H x 0.8), 2.05* (dq, J = 13.9, 1.7 Hz, 1 H x 0.2), 1.99 – 1.95* (m, 1 H x

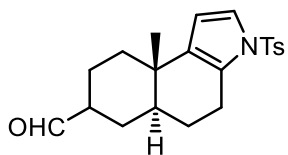
0.2), 1.97 – 1.90 (m, 1 H x 0.8), 1.87 – 1.58 (m, 5 H x 0.8), 1.87 – 1.58* (m, 5 H x 0.2), 1.55 – 1.34 (m, 2 H x 0.8), 1.55 – 1.34* (m, 1 H x 0.8) ppm; ^{13}C NMR (125 MHz, CDCl_3) δ = 205.3*, 204.1, 146.0*, 146.0, 134.4, 134.4*, 124.0, 124.0*, 122.4, 122.2*, 50.6, 46.6*, 42.0, 39.2*, 36.7, 36.0, 35.8*, 34.6*, 27.3, 26.5*, 26.1*, 26.1, 25.1, 25.0*, 21.5, 20.5, 20.3*, 20.0* ppm; MS (APCI) exact mass calculated for $[\text{M}+\text{H}]$ ($\text{C}_{14}\text{H}_{19}\text{OS}$) requires m/z 235.1155, found m/z 235.1151.

(5aRS,9aRS)-3,9a-dimethyl-4,5,5a,6,7,8,9,9a-octahydronaphtho[1,2-b]thiophene-7-carbaldehyde (2.67)



Prepared according to general procedure E from polyene **2.53** (49 mg, 0.20 mmol). The reaction was run for 5 h and product **2.67** was isolated as a white powder (21 mg, 0.084 mmol, 43% yield, *trans*- β : α 4:1). IR (Film) 3087, 2964, 1928, 1857, 2708, 1724, 1462, 1450, 1438, 1374, 1018 cm^{-1} ; ^1H NMR (500 MHz, CDCl_3) δ = 9.71* (s, 1 H x 0.2), 9.67 (s, 1 H x 0.8), 6.72 (x, 1 H x 0.8), 6.68* (s, 1 H x 0.2), 2.62 – 2.48 (m, 2 H), 2.44 – 2.36 (m, 1 H), 2.10 – 2.06 (m, 4 H), 1.96 – 1.89 (m, 1 H), 1.82 – 1.59 (m, 6 H), 1.52 – 1.42 (m, 1 H), 1.20* (s, 3 H x 0.2), 1.16 (s, 3 H x 0.8) ppm; ^{13}C NMR (125 MHz, CDCl_3) δ = 205.2*, 203.9, 148.1*, 147.9, 136.2, 136.2*, 133.1, 133.0*, 116.9, 116.8*, 50.8, 46.8*, 42.7, 40.0*, 38.6, 36.6, 36.6*, 36.5*, 27.4, 26.5*, 25.5*, 25.5, 24.7, 24.6*, 21.9, 21.6, 21.4*, 20.4*, 14.2, 14.2* ppm; MS (ESI) exact mass calculated for $[\text{M}+\text{Na}]$ ($\text{C}_{15}\text{H}_{20}\text{NaOS}$) requires m/z 271.1127, found m/z 271.1127.

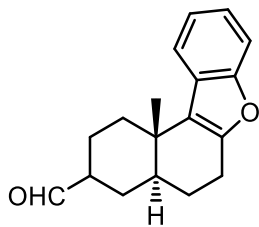
(5aRS,9aRS)-9a-methyl-3-tosyl-4,5,5a,6,7,8,9,9a-octahydro-3H-benzo[e]indole-7-carbaldehyde (2.68)



Prepared according to general procedure E from polyene **2.54** (48 mg, 0.13 mmol). The reaction was run for 5 h and product **2.68** was isolated as a white powder (31 mg, 0.084 mmol, 65% yield, *trans*- β : α 4:1). IR (Film) 3147, 3058, 2933, 2857, 2713, 1721, 1597, 1365, 1265, 1171, 1139, 1124, 1090, 1037, 813 cm^{-1} ; ^1H NMR (500 MHz, CDCl_3) δ = 9.65* (s, 1 H x 0.2), 9.63 (s, 1 H x 0.8),

7.65 – 7.61 (m, 2 H), 7.29 – 7.28 (m, 2 H), 7.16 (d, $J = 3.9$ Hz, 1 H x 0.8), 7.13* (d, $J = 3.9$ Hz, 1 H x 0.2), 6.12 (d, $J = 3.9$ Hz, 1 H x 0.8), 6.06 (d, $J = 3.9$ Hz, 1 H x 0.2), 2.90 – 2.81 (m, 1 H), 2.65 – 2.57 (m, 1 H x 0.8), 2.51 – 2.46* (m, 2 H x 0.2), 2.41 (s, 3 H), 2.35 – 2.28 (m, 1 H x 0.8), 2.12 – 1.96 (m, 1 H), 1.96 – 1.83 (m, 1 H), 1.71 – 1.52 (m, 4 H), 1.48 – 1.21 (m, 3 H), 0.99* (s, 3 H x 0.2), 0.95 (s, 2 H x 0.8) ppm; ^{13}C NMR (125 MHz, CDCl_3) $\delta = 205.5^*$, 204.0, 144.6, 144.5*, 136.5, 136.4*, 134.3*, 134.3, 130.0*, 129.9, 127.2(*), 126.8(*), 121.1, 121.0*, 108.3, 108.2*, 50.7, 46.7*, 41.9, 39.2*, 36.3, 34.2*, 33.6, 33.5*, 27.0, 26.1*, 25.4*, 25.3, 23.3, 23.0*, 21.6, 21.2, 20.4(*), 20.0*, 19.9* ppm; MS (ESI) exact mass calculated for $[\text{M}+\text{Na}]$ ($\text{C}_{21}\text{H}_{25}\text{NNaO}_3\text{S}$) requires m/z 394.1447, found m/z 394.1431.

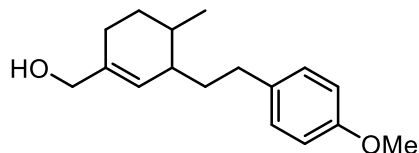
(4a*RS*,11c*RS*)-11c-methyl-1,2,3,4,4a,5,6,11c-octahydronaphtho[2,1-*b*]benzofuran-3-carbaldehyde (2.69)



Prepared according to general procedure E from polyene **2.55** (50 mg, 0.18 mmol). The reaction was run for 5 h and product **2.69** was isolated as a white solid (41 mg, 0.15 mmol, 82% yield, *trans:cis* 91:9, *trans-β:α* 4:1). IR (Film) 3053, 2935, 2859, 2813, 2712, 1722, 1624, 1610, 1451, 1376, 1316, 1266, 1235, 1210, 1179, 1149, 1109, 1049, 1015, 927, 864, 842, 710, 703 cm^{-1} ; ^1H NMR (500 MHz, CDCl_3) $\delta = 9.73^*$ (s, 1 H x 0.2), 9.69 (d, $J = 1.0$ Hz, 1 H x 0.8), 7.57 (dd, $J = 7.1$, 1.9 Hz, 1 H x 0.8), 7.52* (dd, $J = 7.0$, 1.2 Hz, 1 H x 0.2), 7.41 (dd, $J = 7.1$, 1.4 Hz, 1 H x 0.8), 7.38* (dd, $J = 7.5$, 1.6 Hz, 1 H x 0.2), 7.22 – 7.12 (m, 2 H x 0.8), 7.22 – 7.12* (m, 2 H x 0.2), 2.89 – 2.71 (m, 2 H x 0.8), 2.89 – 2.71* (m, 2 H x 0.2), 2.59 (dt, $J = 12.7$, 3.2 Hz, 1 H x 0.8), 2.57* (t, $J = 5.8$ Hz, 1 H x 0.2), 2.48 – 2.38 (m, 1 H x 0.8), 2.48 – 2.38* (m, 1 H x 0.2), 2.28 – 2.22* (m, 1 H x 0.2), 2.10 – 2.05* (m, 1 H x 0.2), 2.02 – 1.94 (m, 1 H x 0.8), 2.02 – 1.94* (m, 1 H x 0.2), 1.93 – 1.70 (m, 5 H x 0.8), 1.93 – 1.70* (m, 3 H x 0.2), 1.70 – 1.58 (m, 1 H x 0.8), 1.70 – 1.58* (m, 1 H x 0.2), 1.58 – 1.46 (m, 1 H x 0.8), 1.58 – 1.46* (m, 1 H x 0.2), 1.26* (s, 3 H x 0.2), 1.21 (s, 3 H x 0.8) ppm; ^{13}C NMR (125 MHz, CDCl_3) $\delta = 205.2^*$, 203.9, 154.7, 154.6*, 152.5, 152.5*, 127.0, 127.0*, 122.7, 122.6*, 122.3, 122.3*, 122.0, 121.9*, 119.8, 119.8*, 111.0, 111.0*, 50.8, 46.8*, 43.3, 40.6*, 35.7, 34.8, 34.7*, 33.8*, 27.0, 26.1*, 25.4*, 25.3, 23.9, 23.8*, 21.1, 19.9*, 18.8, 18.3*

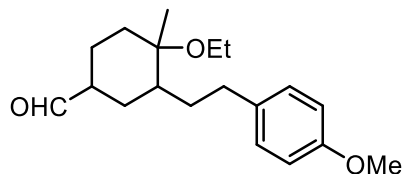
ppm; MS (APCI) exact mass calculated for [M-H] (C₁₈H₁₉O₂) requires m/z 267.1390, found m/z 267.1389.

(3-(4-methoxyphenethyl)-4-methylcyclohex-1-en-1-yl)methanol (2.72)



Prepared according to general procedure E from polyene **2.56** (40 mg, 0.15 mmol) with the HClO₄ salt of catalyst **1.241** and MeNO₂ as a solvent. The product was isolated as a mixture of aldehydes, and was redissolved in MeOH (2 mL), NaBH₄ (1 scoop) was added. Solution was let stir for 1 h, then quenched with saturated NH₄Cl and extracted with DCM (3 x 5 mL). The combined organic layers were washed with brine, dried with MgSO₄, filtered and concentrated. The crude extracts were purified by silica gel column chromatography (gradient from 90:10 to 80:20 hexanes/EtOAc). Product **2.72** was isolated as a colourless oil (8.1 mg, 0.031 mmol, 21% yield). IR (Film) 3340, 2920, 2857, 2835, 1610, 1454, 1243, 1110, 1036 cm⁻¹; ¹H NMR (500 MHz, CDCl₃) δ = 7.10 (d, J = 8.6 Hz, 2 H), 6.82 (d, J = 8.6 Hz, 2 H), 5.63 (s, 1 H x 0.8), 5.59 (s, 1 H x 0.2), 4.02 (s, 2 H), 3.79 (s, 3 H), 2.71 – 2.50 (m, 2 H), 2.03 – 1.90 (m, 2 H), 1.84 – 1.71 (m, 2 H), 1.62 – 1.52 (m, 2 H), 1.49 – 1.30 (m, 2 H), 0.96 (d, J = 6.6 Hz, 3 H x 0.8), 0.86* (d, J = 6.6 Hz, 3 H x 0.2) ppm; ¹³C NMR (125 MHz, CDCl₃) assigned for major diastereomer δ 157.7, 137.2, 134.9, 129.2, 126.2, 113.7, 67.5, 55.3, 41.8, 35.8, 32.6, 31.9, 29.9, 24.9, 19.8 ppm; HRMS (ESI) exact mass calculated for [M+Na] (C₁₇H₂₄NaO₂) requires m/z 283.16685 found m/z 283.16619.

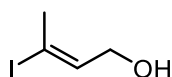
4-ethoxy-3-(4-methoxyphenethyl)-4-methylcyclohexane-1-carbaldehyde (2.73)



Prepared according to general procedure F from polyene **2.56** (12 mg, 0.046 mmol). The reaction was run for 4 h, and product **2.73** was isolated as a colourless oil (5.7 mg, 0.020 mmol, 43% yield). IR (Film) 2972, 2926, 2861, 1724, 1512, 1300 cm⁻¹; ¹H NMR (500 MHz, CDCl₃) δ = 9.66 (d, J = 1.2, 0.5H), 9.64 (d, J = 0.6 Hz, 0.5H), 7.11 (d, J = 8.6 Hz, 2H), 6.83 (d, J = 8.6 Hz, 2H), 3.79 (s, 3H), 3.40 – 3.18 (m, 2H), 2.74 – 2.64 (m, 1H), 2.52 – 2.43 (m, 1H), 2.40 – 2.20 (m, 1H), 2.17 –

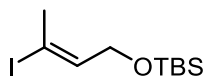
2.03 (m, 1.5H), 1.99 – 1.76 (m, 2H), 1.71 – 1.44 (m, 3.5H), 1.41 – 1.29 (m, 1H), 1.24 – 1.12 (m, 1H), 1.12 (t, J = 7.0 Hz, 3H), 1.08 (s, 1.5H), 1.05 (s, 1.5H) ppm; ¹³C NMR (125 MHz, CDCl₃) δ 205.3, 204.2, 157.9, 157.8, 134.9, 134.6, 129.4, 113.9, 113.9, 76.4, 75.7, 55.5, 55.4, 50.2, 45.0, 43.0, 40.2, 35.5, 33.4, 33.1, 31.7, 31.4, 31.1, 28.3, 25.4, 21.7, 20.7, 17.9, 16.4, 16.2 ppm; HRMS (ESI) exact mass calculated for [M+Na] (C₁₉H₂₈NaO₃) requires m/z 327.19307 found m/z 327.19310.

(E)-3-iodobut-2-en-1-ol (2.82)



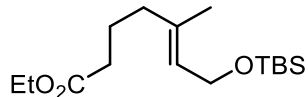
Following the procedure of Koskinen.¹⁹ To a solution of Cp₂ZrCl₂ (9.22 g, 31.5 mmol) in THF (40 mL) at 0 °C was added DIBAL-H (25 wt. % in toluene, 21.2 mL, 31.5 mmol), then a pre-mixed solution of 2-butyne-1-ol (1.99 g, 28.3 mmol) and DIBAL-H (25 wt. % in toluene, 19.2 mL, 28.3 mmol) in THF (40 mL). The resulting solution was brought to room temperature and let stir for 2 h. A solution of I₂ (18.32 g, 72.2 mmol) in THF (40 mL) was added at –78 °C. The resulting solution was brought to 0 °C and let stir for 1 h before it was quenched with saturated NH₄Cl and extracted with Et₂O (3 x 100 mL). The combined organic layers were washed with saturated sodium thiosulphate, washed with brine, dried with MgSO₄, filtered and concentrated. The crude extracts were purified by silica gel column chromatography (80:20 pentane/Et₂O). Before concentrating fully, (E)-3-iodobut-2-en-1-ol was used in the next procedure. Spectroscopic data were in accordance with previously reported literature.²⁰

(E)-tert-butyl((3-iodobut-2-en-1-yl)oxy)dimethylsilane (2.79)



Prior to purification, (E)-3-iodobut-2-en-1-ol column fractions were partially concentrated and redissolved in DCM (20 mL). Imidazole (765 mg, 11.2 mmol) and TBSCl (917 mg, 6.1 mmol) were added, and the resulting solution was let stir for 16 h. Solution was concentrated and purified by silica gel column chromatography (gradient from hexanes to 94:6 hexanes/EtOAc). (E)-tert-butyl((3-iodobut-2-en-1-yl)oxy)dimethylsilane was isolated as a colourless oil (1.3570 g, 4.3 mmol, 15% yield over two steps). Spectroscopic data were in accordance with previously reported literature.²¹

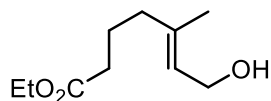
ethyl (*E*)-7-((*tert*-butyldimethylsilyl)oxy)-5-methylhept-5-enoate (5.12)



Following the procedure of Furkert *et al.*²²: To a stirred solution of cupric acetate (240 mg, 1.3 mmol) in acetic acid (4.0 mL) was added zinc dust (2.40 g, 36.7 mmol) at 100 °C. After 2 minutes, the solvent was cannulated off and the solid was washed with acetic acid (2 x 4.0 mL) and Et₂O (3 x 4.0 mL). Remaining solvent was removed under high vacuum.

To the dry solid was added a solution of ethyl-4-iodobutyrate (1.9315 g, 8.0 mmol) in toluene/NMP (36 mL/3.6 mL). The solution was brought to 50 °C and let stir for 1 h. The reaction was let cool until the solid was settled. The solvent was then cannulated into a flask containing Pd(PPh₃)₄ (460 mg, 0.40 mmol) and (*E*)-*tert*-butyl((3-iodobut-2-en-1-yl)oxy)dimethylsilane (1.2610 g, 4.0 mmol). The reaction was brought to 65 °C and let stir for 18 h. The reaction was then let cool, quenched with saturated NH₄Cl, and extracted with EtOAc. The combined extracts were washed with brine, dried with MgSO₄, filtered, concentrated, and purified by flash chromatography (gradient from hexanes to 90:10 hexane/EtOAc). Product **5.12** was isolated as colourless oil (1.0444 g, 3.5 mmol, 86% yield). IR (Film) ν 2954, 2929, 2856, 1735, 1006, 813 cm⁻¹; ¹H NMR (500 MHz, CDCl₃) δ = 5.31 (t, J = 6.1 Hz, 1 H), 4.18 (d, J = 6.3 Hz, 2 H), 4.12 (q, J = 7.1 Hz, 2 H), 2.27 (t, J = 7.7 Hz, 2 H), 2.02 (t, J = 7.6 Hz, 2 H), 1.75 (m, 2 H), 1.62 (s, 3 H), 1.25 (t, J = 7.1 Hz, 3 H), 0.90 (s, 9 H), 0.06 (s, 6 H) ppm; ¹³C NMR (125 MHz, CDCl₃) δ = 173.6, 135.9, 125.3, 60.2, 60.2, 38.8, 33.7, 26.0, 22.9, 18.4, 16.1, 14.2, -5.1 ppm; HRMS (ESI) exact mass calculated for [M+Na] (C₁₆H₃₂NaO₃Si) requires m/z 323.2013, found m/z 323.2001.

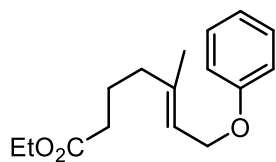
ethyl (*E*)-7-hydroxy-5-methylhept-5-enoate (2.86)



To a stirred solution of ethyl (*E*)-7-((*tert*-butyldimethylsilyl)oxy)-5-methylhept-5-enoate (1.0444 g, 3.5 mmol) in THF (11 mL) was added a solution of TBAF (1.0 M in THF, 7.0 mL, 7.0 mmol) was added and the resulting solution was stirred for 1 h. The reaction was quenched with saturated aqueous NaHCO₃ and extracted with EtOAc (3 x 10 mL). The combined organic layers were washed with brine, dried with MgSO₄, filtered, and concentrated. The crude extracts were purified

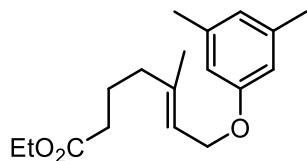
by silica gel column chromatography (gradient from hexanes to 50:50 hexanes/EtOAc). Product **2.86** was isolated as a colourless oil (495 mg, 2.6 mmol, 76% yield). IR (Film) $\nu = 3412, 2980, 2936, 2874, 1731, 1373, 1097 \text{ cm}^{-1}$; $^1\text{H NMR}$ (500 MHz, CDCl_3) $\delta = 5.35$ (t, $J = 6.9 \text{ Hz}$, 1 H), 4.06 (m, 4 H), 2.22 (t, $J = 7.8 \text{ Hz}$, 2 H), 1.99 (t, $J = 7.8 \text{ Hz}$, 2 H), 1.95 (s, 1 H), 1.70 (tt, $J = 7.8, 7.8 \text{ Hz}$, 2 H), 1.61 (s, 3 H), 1.98 (t, $J = 7.4 \text{ Hz}$, 3 H) ppm; $^{13}\text{C NMR}$ (125 MHz, CDCl_3) $\delta = 173.6, 138.0, 124.3, 60.1, 59.0, 38.6, 33.5, 22.6, 15.8, 14.1$ ppm; HRMS (ESI) exact mass calculated for $[\text{M}+\text{Na}]$ ($\text{C}_{10}\text{H}_{18}\text{NaO}_3$) requires m/z 209.1148, found m/z 209.1148.

ethyl (*E*)-5-methyl-7-phenoxyhept-5-enoate (2.87)



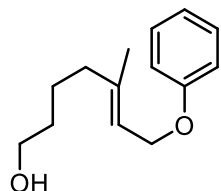
To a solution of ethyl (*E*)-7-hydroxy-5-methylhept-5-enoate (102 mg, 0.55 mmol), PPh_3 (158 mg, 0.60 mmol), and phenol (58 mg, 0.62 mmol) in THF (1.5 mL) at 0°C was added a solution of DIAD (133 mg, 0.66 mmol) in THF (1.5 mL). Solution was brought to room temperature and stirred for 2 h, then quenched with saturated NH_4Cl , and extracted with EtOAc. The combined extracts were washed with brine, dried with MgSO_4 , filtered, concentrated, and purified by flash chromatography (gradient from hexanes to 90:10 hexane/EtOAc). Product **2.87** was isolated as colourless oil (120 mg, 0.46 mmol, 84% yield). IR (Film) $\nu = 2930, 2855, 1715, 1454, 1305 \text{ cm}^{-1}$; $^1\text{H NMR}$ (500 MHz, CDCl_3) $\delta = 7.28$ (m, 2 H), 6.92 (m, 3 H), 5.50 (t, $J = 6.7 \text{ Hz}$, 1 H), 4.53 (d, $J = 5.0 \text{ Hz}$, 2 H), 4.13 (q, $J = 7.4 \text{ Hz}$, 2 H), 2.28 (t, $J = 8.0 \text{ Hz}$, 2 H), 2.10 (t, $J = 8.0 \text{ Hz}$, 2 H), 1.79 (tt, $J = 8.0, 8.0 \text{ Hz}$, 2 H), 1.73 (s, 3 H), 1.26 (t, $J = 7.4 \text{ Hz}$, 3 H) ppm; $^{13}\text{C NMR}$ (100 MHz, CDCl_3) $\delta = 173.5, 158.8, 140.0, 129.4, 120.6, 120.4, 114.7, 64.6, 60.2, 38.8, 33.7, 22.8, 16.4, 14.2$ ppm; HRMS (ESI) exact mass calculated for $[\text{M}+\text{Na}]$ ($\text{C}_{16}\text{H}_{22}\text{NaO}_3$) requires m/z 285.1461, found m/z 285.1462.

ethyl (*E*)-7-(3,5-dimethylphenoxy)-5-methylhept-5-enoate (2.88)



To a solution of ethyl (*E*)-7-hydroxy-5-methylhept-5-enoate (99 mg, 0.53 mmol), PPh₃ (155 mg, 0.59 mmol), and 3,5-dimethylphenol (75 mg, 0.62 mmol) in THF (1.5 mL) at 0 °C was added a solution of DIAD (130 mg, 0.66 mmol) in THF (1.5 mL). Solution was brought to room temperature and stirred for 2 h, then quenched with saturated NH₄Cl, and extracted with EtOAc. The combined extracts were washed with brine, dried with MgSO₄, filtered, concentrated, and purified by flash chromatography (gradient from hexanes to 90:10 hexane/EtOAc). Product **2.88** was isolated as colourless oil (122 mg, 0.47 mmol, 88% yield). IR (Film) $\nu = 2979, 2918, 2871, 1732, 1593, 1293, 1151, 990 \text{ cm}^{-1}$; ¹H NMR (500 MHz, CDCl₃) $\delta = 6.61 \text{ (s, 1 H)}, 6.56 \text{ (s, 2 H)}, 5.51 \text{ (t, } J = 6.9 \text{ Hz, 1 H)}, 4.52 \text{ (d, } J = 6.2 \text{ Hz, 2 H)}, 4.15 \text{ (q, } J = 7.0 \text{ Hz, 2 H)}, 2.30 \text{ (m, 8 H)}, 2.12 \text{ (t, } J = 7.6 \text{ Hz, 2 H)}, 1.80 \text{ (tt, } J = 8.0, 7.6 \text{ Hz, 2 H)}, 1.74 \text{ (s, 3 H)}, 1.28 \text{ (t, } J = 7.0 \text{ Hz, 3 H)}$ ppm; ¹³C NMR (100 MHz, CDCl₃) $\delta = 173.4, 158.8, 139.6, 139.0, 122.3, 120.6, 112.3, 64.4, 60.1, 38.7, 33.6, 22.7, 21.3, 16.2, 14.1$ ppm; HRMS (ESI) exact mass calculated for [M+Na] (C₁₈H₂₆NaO₃) requires m/z 313.17742, found m/z 313.17656.

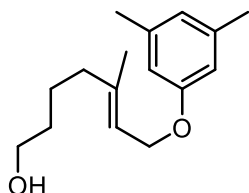
(*E*)-5-methyl-7-phenoxyhept-5-en-1-ol (2.89)



To a stirred solution of (*E*)-7-hydroxy-5-methylhept-5-enoate (23 mg, 0.087 mmol) in THF (0.45 mL) at 0 °C was added DIBAL-H (25 wt. % in toluene, 0.13 mL, 0.13 mmol) dropwise. The solution was stirred for 2 h, then quenched with a saturated solution of Rochelle's salt. The mixture was extracted with EtOAc (3 x 5 mL). The combined organic layers were washed with brine, dried with MgSO₄, filtered and concentrated. The crude extracts were purified by silica gel column chromatography (gradient from hexanes to 50:50 hexanes/EtOAc) to obtain product **2.89**, which was isolated as a colourless oil (16 mg, 0.070 mmol, 81% yield). IR (Film) $\nu = 3337, 2933, 2861, 1599, 1494, 1172, 1029 \text{ cm}^{-1}$; ¹H NMR (500 MHz, CDCl₃) $\delta = 7.28 \text{ (m, 2 H)}, 6.92 \text{ (m, 3 H)}, 5.50$

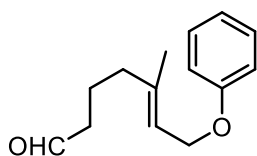
(t, $J = 7.6$ Hz, 1 H), 4.54 (d, $J = 6.6$ Hz, 2 H), 3.65 (t, $J = 6.4$ Hz, 2 H), 2.10 (t, $J = 7.0$ Hz, 2 H), 1.73 (s, 3 H), 1.55 (m, 4 H), 1.27 (s, 1H) ppm; ^{13}C NMR (125 MHz, CDCl_3) $\delta = 158.8, 140.9, 129.4, 120.6, 119.8, 114.7, 64.6, 62.8, 39.2, 32.3, 23.7, 16.5$ ppm; HRMS (ESI) exact mass calculated for $[\text{M}+\text{Na}]$ ($\text{C}_{14}\text{H}_{20}\text{NaO}_2$) requires m/z 243.1356, found m/z 243.1351.

(E)-7-(3,5-dimethylphenoxy)-5-methylhept-5-en-1-ol (2.90)



To a stirred solution of ethyl (*E*)-7-(3,5-dimethylphenoxy)-5-methylhept-5-enoate (121 mg, 0.42 mmol) in THF (1.5 mL) at 0 °C was added DIBAL-H (25 wt. % in toluene, 0.85 mL, 0.85 mmol) dropwise. The solution was stirred for 2 h, then quenched with a saturated solution of Rochelle's salt. The mixture was extracted with EtOAc (3 x 5 mL). The combined organic layers were washed with brine, dried with MgSO_4 , filtered and concentrated. The crude extracts were purified by silica gel column chromatography (gradient from hexanes to 50:50 hexanes/EtOAc) to obtain product **2.90**, which was isolated as a colourless oil (92 mg, 0.37 mmol, 89% yield). IR (Film) $\nu = 3345, 2933, 2862, 1593, 1459, 1292, 1151, 1002$ cm^{-1} ; ^1H NMR (400 MHz, CDCl_3) $\delta = 6.60$ (s, 1 H), 6.56 (s, 2 H), 5.50 (t, $J = 6.1$ Hz, 1 H), 4.51 (d, $J = 6.1$ Hz, 2 H), 3.64 (t, $J = 6.9$ Hz, 2 H), 2.3 (s, 6 H), 2.10 (t, $J = 7.0$ Hz, 2 H), 1.74 (s, 4 H), 1.55 (m, 4 H) ppm; ^{13}C NMR (100 MHz, CDCl_3) $\delta = 158.8, 140.6, 139.0, 122.3, 119.9, 112.4, 64.5, 62.6, 39.1, 32.2, 23.6, 21.3, 16.4$ ppm; HRMS (ESI) exact mass calculated for $[\text{M}+\text{Na}]$ ($\text{C}_{16}\text{H}_{24}\text{NaO}_2$) requires m/z 271.1669, found m/z 271.1676.

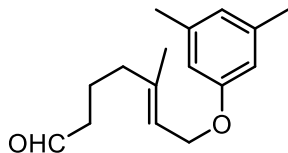
(E)-5-methyl-7-phenoxyhept-5-enal (2.91)



To a solution of (*E*)-5-methyl-7-phenoxyhept-5-en-1-ol (106 mg, 0.42 mmol) in DCM (2.5 mL) was added pyridine (70 μL , 0.88 mmol) and Dess-Martin periodinane³ (243 mg, 0.57 mmol). The mixture was stirred for 1 h. The reaction was quenched with saturated aqueous sodium thiosulfate and extracted with DCM (3 x 10 mL). The combined organic layers were washed with brine, dried

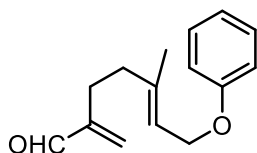
with MgSO_4 , filtered and concentrated. The crude extracts were purified by silica gel column chromatography (gradient from hexanes to 90:10 hexanes/EtOAc). Product **2.90** was isolated as a colourless oil (77 mg, 0.35 mmol, 73% yield). ^1H NMR (500 MHz, CDCl_3) δ = 9.76 (s, 1 H), 7.28 (m, 2 H), 6.91 (m, 3 H), 5.50 (t, J = 6.3 Hz, 1 H), 4.53 (d, J = 6.3 Hz, 2 H), 2.42 (t, J = 7.3 Hz, 2 H), 2.11 (t, J = 7.5 Hz, 2 H), 1.80 (tt, J = 7.5, 7.3 Hz, 2 H), 1.73 (s, 3 H) ppm.

(*E*)-7-(3,5-dimethylphenoxy)-5-methylhept-5-enal (2.92)



To a solution of (*E*)-7-(3,5-dimethylphenoxy)-5-methylhept-5-en-1-ol (91 mg, 0.41 mmol) in DCM (2.0 mL) was added pyridine (55 μL , 0.68 mmol) and Dess-Martin periodinane³ (217 mg, 0.51 mmol). The mixture was stirred for 1 h. The reaction was quenched with saturated aqueous sodium thiosulfate and extracted with DCM (3 x 10 mL). The combined organic layers were washed with brine, dried with MgSO_4 , filtered and concentrated. The crude extracts were purified by silica gel column chromatography (gradient from hexanes to 90:10 hexanes/EtOAc). Product **2.92** was isolated as a colourless oil (69 mg, 0.28 mmol, 68% yield). IR (Film) ν = 2918, 2722, 1722, 1611, 1458, 1292, 1151, 1054, 828 cm^{-1} ; ^1H NMR (500 MHz, CDCl_3) δ = 9.77 (s, 1 H), 6.61 (s, 1 H), 6.56 (s, 2 H), 5.50 (t, J = 6.2 Hz, 1 H), 4.51 (d, J = 6.6 Hz, 2 H), 2.42 (t, J = 7.1 Hz, 2 H), 2.30 (s, 6 H), 2.11 (t, J = 7.6 Hz, 2 H), 1.80 (tt, J = 7.6, 7.1 Hz, 2 H), 1.74 (s, 3 H) ppm; ^{13}C NMR (100 MHz, CDCl_3) δ = 202.1, 158.7, 139.5, 139.0, 122.3, 120.8, 112.4, 64.4, 43.0, 38.5, 21.3, 19.8, 16.3 ppm; HRMS (ESI) exact mass calculated for $[\text{M}+\text{Na}]$ ($\text{C}_{16}\text{H}_{22}\text{NaO}_2$) requires m/z 269.2512, found m/z 269.1501.

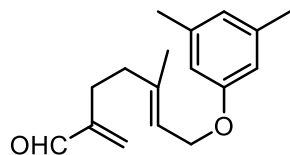
(*E*)-5-methyl-2-methylene-7-phenoxyhept-5-enal (2.93)



To a solution of (*E*)-5-methyl-7-phenoxyhept-5-enal (92 mg, 0.41 mmol) in *i*PrOH (4.2 mL) was added formaldehyde (37 wt. % in H_2O , 70 μL , 0.84 mmol), pyrrolidine (35 μL , 0.42 mmol) and propionic acid (100 μL of a 4.2 M solution in *i*PrOH, 0.42 mmol). Resulting solution was brought

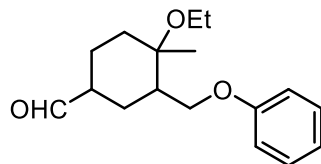
to 50 °C and let stir for 3 h before it was cooled and diluted with H₂O. The reaction was extracted with DCM (3 x 10 mL). The combined organic layers were washed with brine, dried with MgSO₄, filtered and concentrated. The crude extracts were purified by silica gel column chromatography (gradient from hexanes to 90:10 hexanes/EtOAc). Product **2.93** was isolated as a colourless oil (78 mg, 0.34 mmol, 80% yield). IR (Film) ν = 2958, 2930, 2848, 1750, 1690, 1495, 989 cm⁻¹; ¹H NMR (500 MHz, CDCl₃) δ = 9.52 (s, 1 H), 7.28 (m, 2 H), 6.94 (t, J = 7.3 Hz, 1 H), 6.90 (d, J = 8.6 Hz, 2 H), 6.23 (s, 1 H), 5.99 (s, 1 H), 5.49 (t, J = 6.5 Hz, 1 H), 4.53 (d, J = 6.4 Hz, 2 H), 2.42 (t, J = 6.7 Hz, 2 H), 2.22 (t, J = 6.7 Hz, 2 H), 1.75 (s, 3 H) ppm; ¹³C NMR (100 MHz, CDCl₃) δ = 194.5, 158.7, 149.5, 139.8, 134.4, 129.4, 120.6, 120.6, 114.7, 64.5, 37.5, 26.0, 16.5 ppm; HRMS (ESI) exact mass calculated for [M+Na] (C₁₅H₁₈NaO₂) requires m/z 253.1199, found m/z 253.1192.

(E)-7-(3,5-dimethylphenoxy)-5-methyl-2-methylenehept-5-enal (2.94)



To a solution of (*E*)-7-(3,5-dimethylphenoxy)-5-methylhept-5-enal (69 mg, 0.28 mmol) in *i*PrOH (2.8 mL) was added formaldehyde (37 wt. % in H₂O, 50 μ L, 0.56 mmol), pyrrolidine (100 μ L of a 2.8 M solution in *i*PrOH, 0.28 mmol) and propionic acid (100 μ L of a 2.8 M solution in *i*PrOH, 0.28 mmol). Resulting solution was brought to 50 °C and let stir for 3 h before it was cooled and diluted with H₂O. The reaction was extracted with DCM (3 x 10 mL). The combined organic layers were washed with brine, dried with MgSO₄, filtered and concentrated. The crude extracts were purified by silica gel column chromatography (gradient from hexanes to 90:10 hexanes/EtOAc). Product **2.94** was isolated as a colourless oil (59 mg, 0.23 mmol, 81% yield IR (Film) ν = 3052, 2978, 2933, 2865, 1705, 1676, 1258, 1156 cm⁻¹; ¹H NMR (500 MHz, CDCl₃) δ = 9.53 (s, 1 H), 6.60 (s, 1 H), 6.54 (s, 2 H), 6.25 (s, 1 H), 6.00 (s, 1 H), 5.49 (t, J = 6.5 Hz, 1 H), 4.51 (d, J = 6.5 Hz, 2 H), 2.42 (t, J = 6.9 Hz, 2 H), 2.30 (s, 6 H), 2.22 (t, J = 6.9 Hz, 2 H), 1.76 (s, 3 H) ppm; ¹³C NMR (100 MHz, CDCl₃) δ = 194.4, 158.8, 149.5, 139.5, 139.0, 134.3, 122.3, 120.8, 112.4, 64.4, 37.5, 26.0, 21.4, 16.4 ppm; HRMS (ESI) exact mass calculated for [M+Na] (C₁₇H₂₂NaO₂) requires m/z 281.1512, found m/z 281.1516.

4-ethoxy-4-methyl-3-(phenoxymethyl)cyclohexane-1-carbaldehyde (**2.97**)

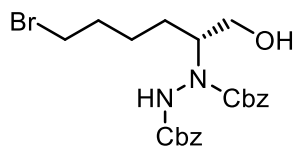


Prepared according to general procedure F from polyene **2.93** (8.1 mg, 0.035 mmol). The reaction was run for 24 h and purified by silica gel column chromatography after acetal deprotection (gradient from hexanes to 85:15 hexanes/EtOAc). Product **2.97** was isolated as a colourless oil (3.3 mg, 0.012 mmol, 34% yield). IR (Film) 3064, 3039, 2973, 2931, 2869, 2721, 1726, 1599, 1497, 1172, 829 cm^{-1} ; ^1H NMR (500 MHz, CDCl_3) δ = 9.68 (d, J = 1.1 Hz, 1 H x 0.6), 9.67* (s, 1 H x 0.4), 7.29 – 7.27 (m, 2 H), 6.94 – 6.90 (m, 3 H), 4.33 (dd, J = 9.2, 3.0 Hz, 1 H x 0.6), 4.12* (dd, J = 9.2, 3.0 Hz, 1 H x 0.4), 3.86* (dd, J = 9.2, 8.4 Hz, 1 H x 0.4), 3.72 (dd, J = 9.2, 9.2 Hz, 1 H x 0.6), 3.46 (m, 2 H x 0.6), 3.38* (qd, J = 7.0, 1.7 Hz, 2 H x 0.4), 2.47 – 2.20 (m, 2 H), 2.20 – 1.92 (m, 2 H), 1.87 – 1.55 (m, 2 H), 1.43 – 1.26 (m, 2 H), 1.19 – 1.14 (m, 6 H) ppm; ^{13}C NMR (125 MHz, CDCl_3) δ = 204.8*, 203.6, 159.0, 158.9*, 129.4*, 129.4, 120.7*, 120.5, 114.5*, 114.5, 75.1, 74.3*, 67.7*, 67.7, 55.7, 55.3*, 49.5, 45.1*, 43.9, 40.8*, 35.6, 32.5*, 26.8, 24.6*, 23.2, 21.3*, 20.7*, 18.0, 16.2, 16.0* ppm; HRMS (ESI) exact mass calculated for $[\text{M}+\text{Na}]$ ($\text{C}_{17}\text{H}_{24}\text{NaO}_3$) requires m/z 299.1618, found m/z 299.1610.

5.3. Experimental Procedures from Chapter 3

Note: due to restricted bond rotation, some catalyst intermediates display multiple rotamers and broad peaks in their ^1H and ^{13}C NMR spectra.

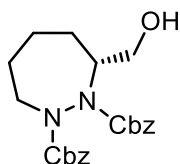
dibenzyl (*R*)-1-(6-bromo-1-hydroxyhexan-2-yl)hydrazine-1,2-dicarboxylate (**3.32**)



Following a modified procedure of Hamada *et al.*²³: To a stirred solution of 6-bromohexanal (1.9082 g, 10.7 mmol) and dibenzylazodicarboxylate (2.1298 g, 7.1 mmol) in MeCN (50 mL) at 0 °C was added (*S*)-proline (181 mg, 1.6 mmol) and the resulting reaction mixture was stirred at -5 °C for 17 h. EtOH (50 mL) and NaBH_4 (320 mg, 8.5 mmol) were added and the reaction mixture was stirred at 0 °C for 30 min. The reaction was quenched with saturated aqueous NH_4Cl and

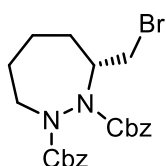
extracted with EtOAc (3 x 50 mL). The combined extracts were washed with brine, dried with Na₂SO₄, filtered, concentrated, and purified by flash chromatography (gradient from 80:20 to 60:40 hexanes/EtOAc) to give product **3.32** (2.20 g, 4.6 mmol, 64% yield) which was isolated as a colourless oil. Enantioselectivity was >99% ee, as determined by HPLC analysis using a CHIRACEL OD column (10% *i*PrOH in hexanes 40 min – tr 13.3 and 25.7 min). IR (thin film) ν 3272, 3033, 2956, 1712, 1252 cm⁻¹; ¹H NMR (500 MHz, CDCl₃) δ 7.43 – 7.20 (m, 10H), 6.64 – 6.48 (m, 1H), 5.35 – 5.02 (m, 4H), 4.55 – 4.00 (m, 2H), 3.64 – 3.21 (m, 4H), 1.96 – 1.60 (m, 2H), 1.48 – 1.16 (m, 4H) ppm; ¹³C NMR (125 MHz, CDCl₃) δ = 157.2, 156.2, 135.8, 135.1, 128.8, 128.8, 128.7, 128.4, 128.2, 127.9, 68.8, 68.4, 62.3, 33.7, 33.4, 32.1, 27.0, 24.5 ppm; HRMS (ESI) exact mass calculated for [M+Na] (C₂₂H₂₇N₂BrNaO₅) requires m/z 501.0996, found m/z 501.0975.

dibenzyl (R)-3-(hydroxymethyl)-1,2-diazepane-1,2-dicarboxylate (3.30)



To a stirred solution of dibenzyl (R)-1-(6-bromo-1-hydroxyhexan-2-yl)hydrazine-1,2-dicarboxylate (1.85 g, 3.8 mmol) in tetrahydrofuran (90 mL) was added tetrabutylammonium fluoride hydrate (1M in THF, 11.4 mL, 11.4 mmol). After 48 hours, saturated aqueous ammonium chloride was added, and the mixture was extracted with ethyl acetate. The combined extracts were washed with brine, dried with sodium sulfate, filtered, concentrated, and purified by flash chromatography (gradient from 80:20 to 65:35 hexanes/EtOAc) to give product **3.30** (1.4221 g, 3.6 mmol, 92% yield) which was isolated as a colourless oil. Spectroscopic data were in accordance with previously reported literature.²⁴

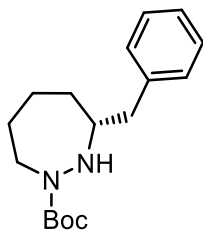
dibenzyl (R)-3-(bromomethyl)-1,2-diazepane-1,2-dicarboxylate (3.33)



To a stirred solution of PPh₃ (187 mg, 0.71 mmol) in THF (1.5 mL) at 0 °C was added CBr₄ (219 mg, 0.66 mmol). After 10 minutes, dibenzyl (R)-3-(hydroxymethyl)-1,2-diazepane-1,2-dicarboxylate (202 mg, 0.51 mmol) was added in THF (1.0 mL). The solution was brought to room

temperature and let stir for 23 h. The reaction was quenched with saturated aqueous NaHCO₃ and extracted with EtOAc. The combined extracts were washed with brine, dried with Na₂SO₄, filtered, concentrated, and purified by flash chromatography (gradient from 90:10 to 65:35 hexanes/EtOAc). Product **3.33** was isolated as a yellow oil (179 mg, 0.039 mmol, 77% yield). IR (Film) $\nu = 3065, 3033, 2937, 1857, 1703, 1392, 1321, 1156 \text{ cm}^{-1}$; ¹H NMR (500 MHz, CDCl₃) $\delta = 7.42 - 7.18 \text{ (m, 10H)}, 5.31 - 4.95 \text{ (m, 4H)}, 4.37 - 4.11 \text{ (m, 2H)}, 3.89 - 3.71 \text{ (m, 1H x 0.4)}, 3.64 - 3.52 \text{ (m, 1H x 0.4)}, 3.44 - 3.26 \text{ (m, 1H x 0.6)}, 3.10 - 2.82 \text{ (m, 1H + 1H x 0.6)}, 2.60 - 2.32 \text{ (m, 1H)}, 1.98 - 1.86 \text{ (m, 1H)}, 1.75 - 1.52 \text{ (m, 2H)}, 1.42 - 1.24 \text{ (m, 2H)}$ ppm; ¹³C NMR (125 MHz, CDCl₃) $\delta = 156.1, 155.8, 154.9, 154.8, 136.1, 136.0, 135.9, 135.6, 128.7, 128.6, 128.6, 128.5, 128.3, 128.3, 127.9, 127.6, 68.2, 68.2, 68.0, 68.0, 61.4, 61.0, 51.5, 50.6, 33.9, 33.6, 30.0, 29.8, 28.6, 28.1, 24.6, 24.6$ ppm; HRMS (ESI) exact mass calculated for [M+Na] (C₂₂H₂₅BrN₂NaO₄) requires m/z 483.0890, found m/z 483.0869.

***tert*-butyl (*R*)-3-benzyl-1,2-diazepane-1-carboxylate (3.34)**



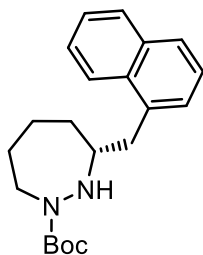
Following a modified procedure of Weix *et al.*²⁵: To a 10 mL microwave vial containing dibenzyl (*R*)-3-(bromomethyl)-1,2-diazepane-1,2-dicarboxylate (701 mg, 1.5 mmol), NiI₂ (44 mg, 0.13 mmol), 1,10-phenanthroline (27 mg, 0.13 mmol), NaI (67 mg, 0.38 mmol), and bromobenzene (243 mg, 1.5 mmol) was added DMPU (6.0 mL), pyridine (0.007 mL, 0.07 mmol), and Zn dust (201 mg, 3.0 mmol). The solution was brought to 60 °C and let stir for 48 hours, then the solution was brought to 80 °C and let stir for 24 hours. After cooling, the reaction was quenched with H₂O and extracted with EtOAc. The combined extracts were washed with water, dried with MgSO₄, filtered, concentrated, and purified by flash chromatography (gradient from 90:10 to 80:20 hexanes/EtOAc) to give a colourless oil (277 mg) which was isolated as a mixture with the dehalogenated hydrazide.

A stirred solution of the isolated mixture (63 mg) in MeOH (3 mL) was submitted to three cycles of vacuum/argon. AcCl (0.040 mL, 0.55 mmol) and 5% Pd/C (30 mg, 0.014 mmol) were added.

Argon flow was removed, and a needle attached to a hydrogen-filled balloon was inserted through the septum and into the reaction mixture. A second needle was inserted through the septum to allow gas efflux and the hydrogen was allowed to bubble through the mixture, with the balloon being refilled as needed. After 1 h, the balloon was removed and the mixture was filtered through diatomaceous earth, rinsing with MeOH. The filtrate was concentrated to give a yellow solid.

To a solution of the crude solid in DCM (1.4 mL) at 0 °C was added Et₃N (0.080 mL, 0.57 mmol) and di-*tert*-butyl dicarbonate (35 mg, 0.16 mmol). After 1 h, saturated aqueous NaHCO₃ was added, and the mixture was extracted with DCM (3 x 5 mL). The combined extracts were washed with water, dried with Na₂SO₄, filtered, concentrated, and purified by flash chromatography (gradient from 90:10 to 80:20 hexanes/EtOAc) to give product **3.34** (17 mg, 0.059 mmol, 17% yield over three steps) which was isolated as a colourless oil. IR (Film) ν = 3361, 3309, 2922, 2852, 1693, 1633, 1392, 1162 cm⁻¹; ¹H NMR (500 MHz, CDCl₃) δ = 7.38 – 7.13 (m, 5H), 5.13 – 4.34 (m, 1H), 3.99 – 3.60 (m, 1H), 3.35 – 3.05 (m, 2H), 2.88 – 2.46 (m, 2H), 1.94 – 1.59 (m, 4H), 1.55 – 1.20 (m, 11 H) ppm; ¹³C NMR (125 MHz, CDCl₃) δ = 156.2, 155.4, 138.9, 129.4, 128.6, 126.5, 80.2, 61.4, 60.6, 48.9, 47.3, 41.5, 41.2, 36.2, 34.4, 28.6, 27.8, 27.4, 23.5 ppm; HRMS (APCI) exact mass calculated for [M+Na] (C₁₇H₂₆N₂NaO₂) requires m/z 313.18865, found m/z 313.18892.

***tert*-butyl (*R*)-3-(naphthalen-1-ylmethyl)-1,2-diazepane-1-carboxylate (3.35)**



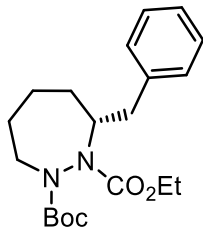
Following a modified procedure of Weix *et al.*²⁵: To a 20 mL microwave vial containing dibenzyl (*R*)-3-(bromomethyl)-1,2-diazepane-1,2-dicarboxylate (1.8796 g, 4.1 mmol), NiI₂ (113 mg, 0.36 mmol), 1,10-phenanthroline (68 mg, 0.37 mmol), NaI (154 mg, 1.0 mmol), and 1-bromonaphthalene (842 mg, 4.1 mmol) was added DMPU (16.5 mL), pyridine (0.017 mL, 0.21 mmol), and Zn dust (522 mg, 8.1 mmol). The solution was brought to 60 °C and let stir for 48 h, then the solution was brought to 80 °C and let stir for 24 h. After cooling, the reaction was quenched with H₂O and extracted with EtOAc. The combined extracts were washed with water,

dried with MgSO₄, filtered, concentrated, and purified by flash chromatography (gradient from 90:10 to 80:20 hexanes/EtOAc) to give a colourless oil (750 mg) which was isolated as a mixture with the dehalogenated hydrazide.

A stirred solution of the isolated mixture (128 mg) in MeOH (5 mL) was submitted to three cycles of vacuum/argon. AcCl (0.080 mL, 1.1 mmol) and 5% Pd/C (60 mg, 0.028 mmol) were added. Argon flow was removed, and a needle attached to a hydrogen-filled balloon was inserted through the septum and into the reaction mixture. A second needle was inserted through the septum to allow gas efflux and the hydrogen was allowed to bubble through the mixture, with the balloon being refilled as needed. After 1 h, the balloon was removed and the mixture was filtered through diatomaceous earth, rinsing with MeOH. The filtrate was concentrated to give a yellow solid

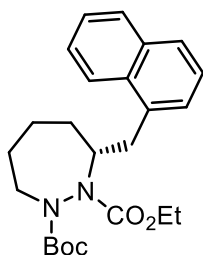
To a solution of the crude solid in DCM (2.5 mL) at 0 °C was added Et₃N (0.11 mL, 0.79 mmol) and di-*tert*-butyl dicarbonate (64 mg, 0.29 mmol). After 1 h, saturated aqueous NaHCO₃ was added, and the mixture was extracted with DCM (3 x 5 mL). The combined extracts were washed with water, dried with Na₂SO₄, filtered, concentrated, and purified by flash chromatography (gradient from 90:10 to 70:30 hexanes/EtOAc) to give product **3.35** (89 mg, 0.26 mmol, 37% yield over three steps) as a colourless oil. IR (Film) ν = 3324, 3045, 2975, 2928, 2863, 1686, 1390, 1364, 1154 cm⁻¹; ¹H NMR (500 MHz, CDCl₃) δ = 8.23 – 7.99 (m, 1H), 7.84 (d, J = 8.1 Hz, 1H), 7.73 (d, J = 8.1 Hz, 1H), 7.53 (dd, J = 8.1, 8.1 Hz, 1H), 7.48 (dd, J = 8.1, 8.1 Hz, 1H) 7.40 (dd, J = 8.3 Hz, 1H), 7.38 – 7.31 (m, 1H), 4.79 – 4.34 (m, 1H), 4.00 – 3.66 (m, 1H), 3.51 – 3.05 (m, 3H), 3.05 – 2.85 (m, 1H), 1.94 – 1.65 (m, 4H), 1.61 – 1.31 (m, 6H), 1.08 – 0.93 (m, 5H) ppm; ¹³C NMR (125 MHz, CDCl₃) δ = 156.3, 155.3, 134.9, 134.3, 132.4, 128.9, 127.6, 126.0, 125.7, 125.5, 124.4, 124.0, 80.1, 60.2, 48.8, 47.1, 38.6, 38.2, 36.9, 34.8, 28.6, 28.0, 27.3, 23.6 ppm; HRMS (ESI) exact mass calculated for [M+Na] (C₂₁H₂₈N₂NaO₂) requires m/z 363.2043, found m/z 363.2037.

1-(*tert*-butyl) 2-ethyl (*R*)-3-benzyl-1,2-diazepane-1,2-dicarboxylate (3.36)



To a stirred mixture of *tert*-butyl (*R*)-3-benzyl-1,2-diazepane-1-carboxylate (17 mg, 0.058 mmol) and NaHCO₃ (17 mg, 0.20 mmol) in CHCl₃ (0.60 mL) was added EtO₂CCl (0.020 mL, 0.21 mmol). After 19 h, water (2 mL) was added, and the mixture was extracted with DCM (3 x 2 mL). The combined extracts were dried with MgSO₄, filtered, concentrated, and purified by flash chromatography (gradient from 90:10 to 70:30 hexanes/EtOAc) to give product **3.36** (18 mg, 0.050 mmol, 87% yield) as a colourless oil. IR (Film) $\nu = 3019, 2977, 2932, 2857, 1702, 1366, 1154 \text{ cm}^{-1}$; ¹H NMR (500 MHz, CDCl₃) δ 7.32 – 7.15 (m, 5H), 4.41 – 4.01 (m, 4H), 3.48 – 3.12 (m, 1H), 2.97 – 2.79 (m, 1H), 2.69 – 2.45 (m, 1H), 1.87 – 1.59 (m, 4H), 1.55 – 1.26 (m, 14H) ppm; ¹³C NMR (125 MHz, CDCl₃) δ 155.5, 155.3, 139.6, 129.4, 128.5, 126.3, 81.2, 62.1, 62.0, 49.7, 41.4, 30.6, 28.5, 28.4, 24.9, 14.9 ppm; HRMS (ESI) exact mass calculated for [M+Na] (C₂₀H₃₀N₂NaO₄) requires *m/z* 385.20978, found *m/z* 385.20933.

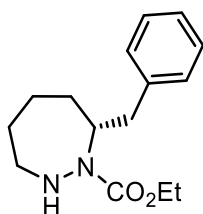
1-(*tert*-butyl) 2-ethyl (*R*)-3-(naphthalen-1-ylmethyl)-1,2-diazepane-1,2-dicarboxylate (3.37)



To a stirred mixture of *tert*-butyl (*R*)-3-(naphthalen-1-ylmethyl)-1,2-diazepane-1-carboxylate (57 mg, 0.17 mmol) and NaHCO₃ (51 mg, 0.60 mmol) in CHCl₃ (1.7 mL) was added EtO₂CCl (0.050 mL, 0.52 mmol). After 19 h, water (5 mL) was added and the mixture was extracted with dichloromethane (3 x 5 mL). The combined extracts were dried with MgSO₄, filtered, concentrated, and purified by flash chromatography (gradient from 90:10 to 70:30 hexanes/ethyl acetate) to give product **3.37** (68 mg, 0.16 mmol, 98% yield) as a colourless oil (98% yield). IR (Film) $\nu = 3052, 2976, 2932, 2857, 1701, 1392, 1367, 1155 \text{ cm}^{-1}$; ¹H NMR (500 MHz, CDCl₃) δ

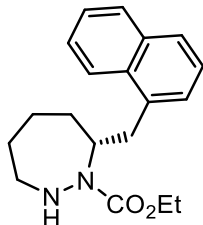
8.60 – 8.55 (m, 1H x 0.7), 8.30 (d, J = 7.6 Hz, 1H x 0.3), 7.90 – 7.81 (m, 1H), 7.77 – 7.70 (m, 1H), 7.64 – 7.44 (m, 2H), 7.42 – 7.28 (m, 2H), 4.51 – 4.24 (m, 4H), 3.94 – 3.71 (m, 1H), 3.17 – 2.80 (m, 2H), 1.74 – 1.29 (m, 18H) ppm; ^{13}C NMR (125 MHz, CDCl_3) δ 155.6, 155.6, 135.4, 134.0, 132.4, 128.6, 127.8, 127.3, 126.4, 125.8, 125.4, 124.8, 81.3, 62.1, 60.5, 49.8, 38.6, 31.0, 28.5, 18.4, 24.9, 15.0 ppm; HRMS (ESI) exact mass calculated for $[\text{M}+\text{Na}]$ ($\text{C}_{24}\text{H}_{32}\text{N}_2\text{NaO}_4$) requires m/z 435.22543, found m/z 435.22631.

ethyl (*R*)-7-benzyl-1,2-diazepane-1-carboxylate (3.16)



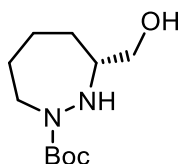
To a solution of 1-(*tert*-butyl) 2-ethyl (*R*)-3-benzyl-1,2-diazepane-1,2-dicarboxylate (15 mg, 0.042 mmol) in DCM (0.15 mL) at 0 °C was added TFA (0.080 mL). The solution was brought to room temperature and let stir for 2 h. The reaction was quenched with saturated aqueous NaHCO_3 and extracted with EtOAc. The combined extracts were washed with brine, dried with Na_2SO_4 , filtered, concentrated, and purified by flash chromatography (gradient from (90:10 to 70:30 hexanes/EtOAc) to give product **3.16** (10 mg, 0.039 mmol, 93% yield) as a colourless oil. IR (Film) $\nu = 3000, 2980, 2928, 2849, 1690, 1405, 1217\text{ cm}^{-1}$; ^1H NMR (500 MHz, CDCl_3) $\delta = 7.27 - 7.09$ (m, 5H), 4.30 – 4.01 (m, 2H), 3.95 – 3.88 (m, 1H x 0.5), 3.78 – 3.71 (m, 1H x 0.5), 3.05 – 2.94 (m, 1H), 2.86 – 2.70 (m, 2H), 2.70 – 2.57 (m, 1H), 1.99 – 1.88 (m, 1H), 1.81 – 1.62 (m, 2H), 1.59 – 1.46 (m, 2H), 1.33 – 0.97 (m, 4H) ppm; ^{13}C NMR (125 MHz, CDCl_3) $\delta = 157.0, 139.4, 129.4, 128.3, 126.2, 61.6, 58.8, 51.3, 41.1, 33.6, 31.2, 24.7, 14.5$ ppm; HRMS (ESI) exact mass calculated for $[\text{M}+\text{Na}]$ ($\text{C}_{15}\text{H}_{22}\text{N}_2\text{NaO}_2$) requires m/z 285.1573, found m/z 285.1567.

ethyl (*R*)-7-(naphthalen-1-ylmethyl)-1,2-diazepane-1-carboxylate (3.38)



To a solution of 1-(*tert*-butyl) 2-ethyl (*R*)-3-(naphthalen-1-ylmethyl)-1,2-diazepane-1,2-dicarboxylate (66 mg, 0.16 mmol) in DCM (0.50 mL) at 0 °C was added TFA (0.25 mL). The solution was brought to room temperature and let stir for 2 h. The reaction was quenched with the addition of saturated aqueous NaHCO₃ and extracted with EtOAc. The combined extracts were washed with brine, dried with Na₂SO₄, filtered, concentrated, and purified by flash chromatography (gradient from 90:10 to 70:30 hexanes/EtOAc) to give product **3.38** (42 mg, 0.013 mmol, 83% yield) as a white solid. IR (Film) $\nu = 3045, 2977, 2926, 2851, 1685, 1326, 1123, 1096 \text{ cm}^{-1}$; ¹H NMR (500 MHz, CDCl₃) $\delta = 8.36$ (d, *J* = 9.0 Hz, 1H x 0.2), 8.12 (d, *J* = 9.0 Hz, 1H x 0.8), 7.87 – 7.80 (m, 1H), 7.74 – 7.67 (m, 1H), 7.57 (t, *J* = 7.5 Hz, 1H x 0.2), 7.53 = 7.48 (m 1H x 0.8), 7.48 – 7.44 (m, 1H), 7.39 – 7.34 (m, 1H), 7.34 – 7.30 (m, 1H x 0.2), 7.24 (d, *J* = 6.7 Hz, 1H x 0.8), 4.83 – 4.68 (m, 1H x 0.8), 4.53 – 4.41 (m, 1H x 0.2), 4.38 – 4.28 (m, 1H x 0.8), 4.26 – 4.09 (m, 2H x 0.2), 3.83 – 3.72 (m, 1H x 0.8), 3.56 – 3.39 (m, 1H), 3.31 – 3.22 (m, 1 H x 0.8), 3.19 – 3.10 (m, 1H x 0.8), 3.08 – 2.96 (m, 1H + 1H x 0.2), 2.83 – 2.71 (m, 1H), 1.98 – 1.88 (m, 1H x 0.8), 1.83 – 1.50 (m, 4H + 2H x 0.2), 1.34 – 1.21 (m, 1H + 3H x 0.2), 0.72 (t, *J* = 6.6 Hz, 3H x 0.8) ppm; ¹³C NMR (125 MHz, CDCl₃) $\delta = 156.9, 135.4, 133.9, 132.4, 128.8, 127.6, 127.0, 125.8, 125.6, 125.5, 123.9, 61.5, 57.6, 51.4, 38.3, 31.3, 24.7, 13.9$ ppm; HRMS (ESI) exact mass calculated for [M+H] (C₁₉H₂₅N₂O₂) requires *m/z* 313.19105, found *m/z* 313.19135.

***tert*-butyl (*R*)-3-(hydroxymethyl)-1,2-diazepane-1-carboxylate (3.42)**

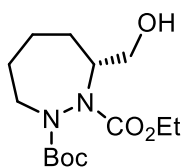


A stirred solution of dibenzyl (*R*)-3-(hydroxymethyl)-1,2-diazepane-1,2-dicarboxylate (426 mg, 1.1 mmol) in MeOH (10 mL) was submitted to three cycles of vacuum/argon. AcCl (0.30 mL, 4.2 mmol) and 5% Pd/C (234 mg, 0.11 mmol) were added. Argon flow was removed, and a needle

attached to a hydrogen-filled balloon was inserted through the septum and into the reaction mixture. A second needle was inserted through the septum to allow gas efflux and the hydrogen was allowed to bubble through the mixture, with the balloon being refilled as needed. After 1 h, the balloon was removed and the mixture was filtered through diatomaceous earth, rinsing with MeOH. The filtrate was concentrated to give crude (*R*)-(1,2-diazepan-3-yl)methanol hydrochloride as a yellow solid. (Note: benzyloxycarbonyl removal is performed under acidic conditions as the unprotected freebase is highly unstable to air oxidation.)

To a stirred suspension of crude (*R*)-(1,2-diazepan-3-yl)methanol in DCM (4.5 mL) at 0 °C was added Et₃N (0.38 mL, 2.7 mmol) and di-*tert*-butyl dicarbonate (216 mg, 0.99 mmol). After 1 h, saturated aqueous NaHCO₃ was added, and the mixture was extracted with DCM. The combined extracts were washed with water, dried with MgSO₄, filtered, concentrated, and purified by flash chromatography (gradient from 80:20 to 50:50 hexanes/EtOAc). Product **3.42** was isolated as a colourless oil (203 mg, 0.94 mmol, 85% yield over two steps). IR (Film) $\nu = 3429, 2976, 2929, 2863, 1689, 1669, 1391, 1365, 1163 \text{ cm}^{-1}$; ¹H NMR (500 MHz, CDCl₃) $\delta = 4.90 - 4.60 \text{ (m, 1 H)}, 4.02 \text{ (bs, 1 H)}, 3.52 - 3.19 \text{ (m, 4 H)}, 2.90 \text{ (bs, 1 H)}, 1.64 - 1.53 \text{ (m, 4 H)}, 1.34 \text{ (m, 10 H)}, 1.34 - 1.05 \text{ (m, 1 H)}$ ppm; ¹³C NMR (125 MHz, CDCl₃) $\delta = 156.7, 80.2, 63.9, 61.1, 49.2, 30.7, 28.1, 23.6$ (2 peaks overlapped) ppm; HRMS (ESI) exact mass calculated for [M+Na] (C₁₁H₂₂N₂NaO₃) requires *m/z* 253.1523, found *m/z* 253.1518.

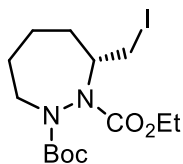
1-(*tert*-butyl) 2-ethyl (*R*)-3-(hydroxymethyl)-1,2-diazepane-1,2-dicarboxylate (**3.43**)



To a stirred mixture of *tert*-butyl (*R*)-3-(hydroxymethyl)-1,2-diazepane-1-carboxylate (188 mg, 0.81 mmol) and NaHCO₃ (252 mg, 3.0 mmol) in CHCl₃ (8 mL) was added EtO₂CCl (0.23 mL, 2.4 mmol). After 19 h, water was added (10 mL), and the mixture was extracted with DCM (3 x 10 mL). The combined extracts were dried with MgSO₄, filtered, concentrated, and purified by flash chromatography (gradient from 70:30 to 50:50 hexanes/EtOAc). Product **3.43** was isolated as a colourless oil (238 mg, 0.79 mmol, 96% yield). IR (Film) $\nu = 3428, 2979, 2935, 2881, 1691, 1368, 1320, 1149 \text{ cm}^{-1}$; ¹H NMR (500 MHz, CDCl₃) $\delta = 4.04 - 3.92 \text{ (m, 4H)}, 3.92 - 3.84 \text{ (m, 1H)}, 3.73 - 3.43 \text{ (m, 1H)}, 3.29 - 3.20 \text{ (m, 1H x 0.7)}, 2.95 - 2.87 \text{ (m, 1H x 0.3)}, 2.85 - 2.69 \text{ (m, 1H)}, 1.87 -$

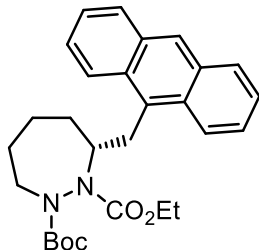
1.62 (m, 2H), 1.58 – 1.41 (m, 3H), 1.38 – 1.29 (m, 9H), 1.19 – 1.06 (m, 3H) ppm; ^{13}C NMR (100 MHz, CDCl_3) δ 157.1, 146.6, 155.3, 155.0, 82.1, 82.1, 81.8, 64.2, 63.1, 62.8, 62.2, 62.0, 61.9, 61.2, 61.1, 61.0, 50.8, 49.9, 49.5, 28.5, 28.5, 28.3, 28.0, 28.0, 24.7, 24.5, 14.5, 14.3 ppm; HRMS (ESI) exact mass calculated for $[\text{M}+\text{Na}]$ ($\text{C}_{14}\text{H}_{26}\text{N}_2 \text{NaO}_5$) requires m/z 325.17339, found m/z 325.17289.

***tert*-butyl (*S*)-2-(ethylperoxy)-3-(iodomethyl)-2 λ^3 -azepane-1-carboxylate (**3.44**)**



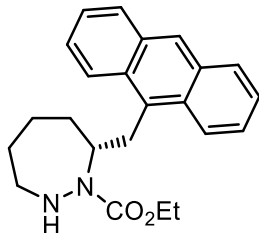
To a stirred solution of PPh_3 (240 mg, 0.91 mmol) and imidazole (52 mg, 0.76 mmol) in THF (5 mL) was added I_2 (209 mg, 0.82 mmol) at 0 °C. After 15 minutes, 1-(*tert*-butyl) 2-ethyl (*R*)-3-(hydroxymethyl)-1,2-diazepane-1,2-dicarboxylate (227 mg, 0.75 mmol) was added in THF (3 mL). The solution was brought to room temperature and stirred for 15 h. The reaction was quenched with the addition of saturated NaHCO_3 and extracted with EtOAc. The combined extracts were washed with brine, dried with Na_2SO_4 , filtered, concentrated, and purified by flash chromatography (gradient from 95:5 to 80:20 hexanes/EtOAc). Product **3.44** was isolated as a yellow oil (234 mg, 0.57 mmol, 64% yield). IR (Film) ν = 2975, 2932, 2857, 1703, 1366, 1308, 1148 cm^{-1} ; ^1H NMR (500 MHz, CDCl_3) δ = 4.28 – 3.94 (m, 4H), 3.64 – 3.32 (m, 1H), 3.07 – 2.85 (m, 1H), 2.85 – 2.66 (m, 1H), 2.57 – 2.40 (m, 1H), 1.90 – 1.79 (m, 1H), 1.65 – 1.45 (m, 2H), 1.45 – 1.34 (m, 9H) 1.32 – 1.10 (m, 5H) ppm; ^{13}C NMR (125 MHz, CDCl_3) δ = 155.3, 155.2, 155.0, 155.0, 154.9, 154.7, 154.3, 154.0, 81.4, 81.3, 81.3, 62.4, 62.4, 62.2, 62.2, 61.7, 61.4, 61.1, 51.2, 50.8, 49.4, 49.0, 31.2, 31.0, 30.9, 30.8, 28.6, 28.5, 28.4, 28.3, 28.2, 28.2, 24.8, 24.7, 24.7, 24.7, 14.7, 14.7, 13.6, 14.5, 8.8, 8.20, 7.65, 7.24 ppm; HRMS (ESI) exact mass calculated for $[\text{M}+\text{Na}]$ ($\text{C}_{14}\text{H}_{25}\text{IN}_2\text{NaO}_4$) requires m/z 435.07512, found m/z 435.07421.

1-(*tert*-butyl) 2-ethyl (*R*)-3-(anthracen-9-ylmethyl)-1,2-diazepane-1,2-dicarboxylate (3.45)



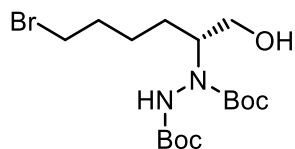
Following the procedure of Furkert *et al.*²²: To a stirred solution of Cu(OAc)₂ (16 mg, 0.088 mmol) in AcOH (1.0 mL) was added Zn dust (160 mg, 2.4 mmol) at 100 °C. After 2 minutes, the solvent was cannulated off and the solid was washed with AcOH (2 x 1.0 mL) and Et₂O (3 x 1.0 mL). Remaining solvent was removed under high vacuum. To the dry solid was added *tert*-butyl (*S*)-2-(ethylperoxy)-3-(iodomethyl)-2λ³-azepane-1-carboxylate (197 mg, 0.47 mmol) in toluene/NMP (0.67 mL/0.17 mL). The solution was brought to 60 °C and let stir for 1 h. The reaction was let cool until the solids settled. Then the solvent was cannulated into a flask containing Pd(dba)₂ (15 mg, 0.026 mmol), RuPhos (22 mg, 0.047 mmol), and 9-bromoanthracene (61 mg, 0.24 mmol). The reaction was brought to 100 °C and let stir for 16 h. The reaction was then let cool, quenched with water, and extracted with EtOAc (3 x 5 mL). The combined extracts were washed with brine, dried with Na₂SO₄, filtered, concentrated, and purified by flash chromatography (gradient from 90:10 to 80:20 hexane/EtOAc). Product **3.45** was isolated as a yellow oil (48 mg, 0.10 mmol, 44% yield). IR (Film) ν = 3052, 2978, 2933, 2865, 1705, 1676, 1258, 1156 cm⁻¹; ¹H NMR (500 MHz, CDCl₃) δ = 8.38 (s, 1H), 8.14 – 8.12 (m, 2H), 8.01 – 7.99 (m, 2H), 7.46 – 7.44 (m, 4H), 6.53 – 6.14 (m, 1H), 5.76 (s, 1H), 5.21 (s, 1H), 4.20 – 4.10 (m, 2H), 3.48 – 3.36 (m, 2H), 2.60 – 2.57 (m, 2H), 1.60 – 1.55 (m, 4H), 1.42 (s, 9H), 1.27 – 1.25 (m, 3H) ppm; ¹³C NMR (100 MHz, CDCl₃) δ = 156.4, 155.2, 146.7, 138.6, 131.5, 128.9, 128.6, 126.4, 126.0, 125.4, 125.2, 116.9, 81.2, 61.9, 50.5, 49.1, 38.9, 28.3, 27.6, 25.1, 14.6 ppm; HRMS (ESI) exact mass calculated for [M+Na] (C₂₈H₃₄N₂NaO₄) requires m/z 485.24108, found m/z 485.24057.

ethyl (R)-7-(anthracen-9-ylmethyl)-1,2-diazepane-1-carboxylate (3.46)



To a solution of 1-(*tert*-butyl) 2-ethyl (R)-3-(anthracen-9-ylmethyl)-1,2-diazepane-1,2-dicarboxylate (44 mg, 0.095 mmol) in DCM (0.30 mL) at 0 °C was added TFA (0.15 mL). The solution was brought to room temperature and let stir for 2 h. The reaction was quenched with the addition of saturated NaHCO₃ and extracted with EtOAc. The combined extracts were washed with brine, dried with Na₂SO₄, filtered, concentrated, and purified by flash chromatography (gradient from (90:10 to 60:40 hexanes/EtOAc). Product **3.46** was isolated as a yellow oil (26 mg, 0.072 mmol, 76% yield). IR (Film) ν = 3246, 3052, 2923, 2853, 1714, 1257, 1036 cm⁻¹; ¹H NMR (500 MHz, CDCl₃) δ = 8.38 (s, 1H), 8.16 – 8.09 (m, 2H), 8.03 – 7.97 (m, 2H), 7.50 – 7.39 (m, 4H), 6.51 – 5.86 (m, 1H), 5.76 (s, 1H), 5.20 (s, 1H), 4.14 (q, J = 7.8 Hz, 2H), 2.83 (bs, 2H), 2.56 (t, J = 8.9 Hz, 2H), 1.64 – 1.49 (m, 4H), 1.24 (t, J = 7.8 Hz, 3H) ppm; ¹³C NMR (125 MHz, CDCl₃) δ = 157.5, 146.7, 138.7, 131.5, 128.9, 128.6, 126.5, 126.0, 125.3, 125.2, 116.9, 61.4, 51.9, 39.0, 27.8, 25.4, 14.7 ppm; HRMS (ESI) exact mass calculated for [M+Na] (C₂₃H₂₆N₂NaO₂) requires m/z 385.1886, found m/z 385.1896.

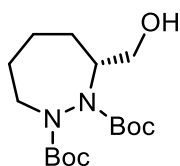
di-*tert*-butyl (R)-1-(6-bromo-1-hydroxyhexan-2-yl)-2 λ ²-diazane-1,2-dicarboxylate (3.52)



Following a modified procedure of Hamada *et al.*²³: To a stirred solution of 6-bromohexanal (2.54 g, 14.2 mmol) and di-*tert*-butyl azodicarboxylate (2.17 g, 9.4 mmol) in MeCN (100 mL) at 0 °C was added (*S*)-proline (251 mg, 2.2 mmol) and the resulting reaction mixture was brought to room temperature and stirred for 5 h. EtOH (40 mL) and NaBH₄ (358 mg, 9.5 mmol) were added and the reaction mixture was stirred at 0 °C for 1 h. The reaction was quenched with saturated aqueous NH₄Cl and extracted with EtOAc (3 x 100 mL), dried over Na₂SO₄, filtered and concentrated in vacuo. The crude product was purified by flash chromatography (gradient from 80:20 to 65:35

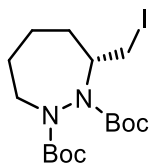
hexanes/EtOAc). Product **3.52** was isolated as a white solid (3.40g, 8.3 mmol, 88% yield). IR (Film) $\nu = 3270, 2978, 2933, 2867, 1708, 1393, 1367, 1283, 1253, 1153, 1060 \text{ cm}^{-1}$; $^1\text{H NMR}$ (500 MHz, CDCl_3) $\delta = 6.13$ (bs, 1H), 4.49 – 4.21 (m, 2H), 3.51 – 3.39 (m, 4H), 1.90 – 1.79 (m, 2H), 1.41 – 1.79 (m, 21H) ppm; $^{13}\text{C NMR}$ (125 MHz, CDCl_3) $\delta = 156.1, 155.3, 82.8, 82.6, 82.3, 81.6, 62.5, 62.3, 60.4, 58.1, 33.8, 33.4, 32.2, 28.4, 28.3, 28.2, 27.2, 27.0, 24.6$ ppm; HRMS (ESI) exact mass calculated for $[\text{M}+\text{Na}]$ ($\text{C}_{16}\text{H}_{30}\text{BrN}_2\text{NaO}_5$) requires m/z 433.1309, found m/z 433.1300.

di-*tert*-butyl (*R*)-3-(hydroxymethyl)-1,2-diazepane-1,2-dicarboxylate (3.53)



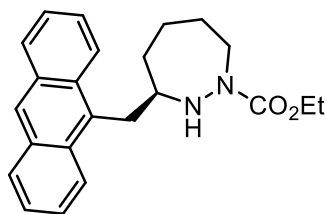
To a stirred solution of di-*tert*-butyl (*R*)-1-(6-bromo-1-hydroxyhexan-2-yl)-2,2-diazepane-1,2-dicarboxylate (1.53 g, 3.7 mmol) in THF (60 mL) was added TBAF hydrate (2.96 g, 11.3 mmol, anhydrous basis). After 48 h, saturated aqueous NH_4Cl was added, and the mixture was extracted with EtOAc (3 x 50 mL). The combined extracts were washed with brine, dried with Na_2SO_4 , filtered, concentrated, and purified by flash chromatography (gradient from 90:10 to 70:30 hexanes/EtOAc). Product **3.53** was isolated as a colourless oil (1.18 g, 3.6 mmol, 95% yield). Enantioselectivity was 77% ee, as determined by HPLC analysis of benzoyl ester using a CHIRACEL OJ-H column (5% i PrOH in hexanes in 40 min – tr 26.0 and 29.2 min). IR (Film) $\nu = 3430, 2976, 2933, 2881, 2861, 1703, 1393, 1366, 1333, 1253, 1148, 1115, 1049 \text{ cm}^{-1}$; $^1\text{H NMR}$ (500 MHz, CDCl_3) $\delta = 4.37$ -4.02 (m, 2H), 3.99-3.90 (m, 1H x 0.7), 3.83 – 3.66 (m, 0.7 x 1H), 3.65 – 3.43(m, 2H x 0.3), 3.40 – 3.28 (m, 1H x 0.7), 3.07 – 2.66 (m, 1H x 0.7 + 2H x 0.3), 1.87 – 1.69 (m, 2H), 1.64 – 1.52 (m, 3H), 1.52 – 1.37 (m, 19H) ppm; $^{13}\text{C NMR}$ (125 MHz, CDCl_3) $\delta = 157.4, 157.0, 155.3, 155.2, 154.5, 154.1, 82.2, 82.1, 81.7, 81.4, 81.0, 64.7, 64.1, 63.6, 63.2, 61.7, 60.7, 60.2, 50.8, 50.3, 49.7, 28.8, 28.6, 28.5, 28.4, 28.3, 28.2, 28.0, 24.9, 24.8$ ppm; HRMS (ESI) exact mass calculated for $[\text{M}+\text{Na}]$ ($\text{C}_{16}\text{H}_{30}\text{N}_2\text{NaO}_5$) requires m/z 353.2047, found m/z 353.2046.

di-tert-butyl (R)-3-(iodomethyl)-1,2-diazepane-1,2-dicarboxylate (3.54)



To a stirred solution of PPh_3 (1.12 g, 4.3 mmol) and imidazole (290 mg, 4.2 mmol) in THF (20 mL) was added I_2 (995 mg, 3.9 mmol) at 0 °C. After 15 minutes, di-tert-butyl (R)-3-(hydroxymethyl)-1,2-diazepane-1,2-dicarboxylate (1.18 g, 3.6 mmol) was added in THF (10 mL). The solution was brought to room temperature and stirred for 18 h. The reaction was quenched with the addition of saturated aqueous NaHCO_3 and extracted with EtOAc. The combined extracts were washed with brine, dried with Na_2SO_4 , filtered, concentrated, and purified by flash chromatography (gradient from 97:3 to 90:10 hexanes/EtOAc). Product **3.54** was isolated as a yellow oil (1.34 g, 3.0 mmol, 85% yield). IR (Film) $\nu = 2976, 2933, 2861, 1705, 1393, 1366, 1330, 1259, 1172, 1147 \text{ cm}^{-1}$; ^1H NMR (500 MHz, CDCl_3) $\delta = 4.27 - 3.96$ (m, 2H), 3.68 – 3.40 (m, 1H), 3.12 – 2.71 (m, 2H), 2.58 – 2.44 (m, 1H), 1.95 – 1.83 (m, 1H), 1.69 – 1.38 (m, 20H), 1.38 – 1.18 (m, 2H) ppm; ^{13}C NMR (125 MHz, CDCl_3) $\delta = 155.7, 155.1, 154.1, 153.6, 81.8, 81.3, 81.2, 81.2, 81.2, 81.1, 77.4, 77.2, 76.9, 62.1, 60.6, 60.6, 51.0, 49.4, 49.2, 31.1, 30.9, 30.8, 28.6, 28.5, 28.4, 28.4, 28.4, 28.3, 28.1, 24.9, 24.8, 24.7, 8.5, 8.1, 7.7$ ppm; HRMS (ESI) exact mass calculated for $[\text{M}+\text{Na}]$ ($\text{C}_{16}\text{H}_{29}\text{IN}_2\text{NaO}_4$) requires m/z 463.1064, found m/z 463.1080.

ethyl (R)-3-(anthracen-9-ylmethyl)-1,2-diazepane-1-carboxylate (3.47)

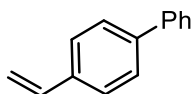


Following the procedure of Furkert *et al.*²²: To a stirred solution of $\text{Cu}(\text{OAc})_2$ (140 mg, 0.77 mmol) in AcOH (2.0 mL) was added Zn dust (1.40 g, 21 mmol) at 100 °C. After 2 minutes, the solvent was cannulated off and the solid was washed with AcOH (2 x 2.0 mL) and Et_2O (3 x 2.0 mL). Remaining solvent was removed under high vacuum. To the dry solid was added di-tert-butyl (R)-3-(iodomethyl)-1,2-diazepane-1,2-dicarboxylate (1.8551 g, 4.2 mmol) in toluene/NMP (11.5 mL/3.0 mL). The solution was brought to 60 °C and let stir for 1 h. The reaction was let cool until

the solids settled. Then the solvent was cannulated into a flask containing Pd(dba)₂ (241 mg, 0.42 mmol), RuPhos (399 mg, 0.85 mmol) and 9-bromoanthracene (532 mg, 2.1 mmol). The reaction was brought to 100 °C and let stir for 16 h. The reaction was then let cool, quenched with H₂O, and extracted with EtOAc (3 x 10 mL). The combined extracts were washed with brine, dried with Na₂SO₄, filtered, concentrated, and purified by flash chromatography (gradient from 95:5 to 80:20 hexane/EtOAc) to give a yellow oil of di-tert-butyl (*R*)-3-(anthracen-9-ylmethyl)-1,2-diazepane-1,2-dicarboxylate as a mixture with the dehalogenated hydrazide (593 mg).

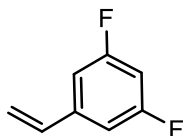
To a solution of the isolated mixture (353 mg) in DCM (3.1 mL) was added TFA (1.6 mL) at 0 °C. The solution was brought to room temperature and let stir for 4 h, then the solvent was removed under reduced pressure. The resulting red oil was redissolved in DCM (3.6 mL) and brought to 0 °C. EtO₂CCl (45 μL, 0.47 mmol), then Et₃N (300 μL, 2.1 mmol) were added and the reaction was let stir for 1 h. The reaction was then quenched with saturated aqueous NaHCO₃ and extracted with DCM (3 x 10 mL). The combined extracts were washed with brine, dried with Na₂SO₄, filtered, concentrated, and purified by flash chromatography (gradient from 80:20 to 65:35 hexanes/EtOAc). Product **3.47** was isolated as a yellow oil (75 mg, 0.21 mmol, 17% yield over 3 steps). IR (Film) ν = 3051, 2979, 2930, 2858, 1695, 1443, 1264, 1224, 1061 cm⁻¹; ¹H NMR (500 MHz, CDCl₃) δ = 8.38 (s, 1H), 8.13 – 8.11 (m, 2H), 8.01 – 7.99 (m, 2H), 7.46 – 7.44 (m, 4H), 5.75 (d, *J* = 1.3 Hz, 1H), 5.20 (bs, 1H), 4.10 (q, *J* = 5.7 Hz, 2H), 3.96 (bs, 1H), 3.35 (t, *J* = 7.1 Hz, 2H), 2.58 (t, *J* = 8.5 Hz, 2H), 1.64 – 1.52 (m, 4H), 1.20 (bs, 3H) ppm; ¹³C NMR (125 MHz, CDCl₃) δ = 157.9, 146.8, 138.7, 131.6, 129.0, 128.6, 126.5, 126.0, 125.4, 125.2, 116.9, 61.9, 50.3, 38.9, 27.7, 25.0, 14.8 ppm; HRMS (ESI) exact mass calculated for [M+H] (C₂₃H₂₇N₂O₂) requires *m/z* 363.20670, found *m/z* 363.20827.

4-vinyl-1,1'-biphenyl (**5.13**)



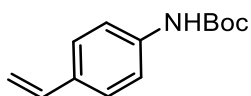
From [1,1'-biphenyl]-4-carbaldehyde (2.4 mmol), general procedure A was followed to give, after flash chromatography (hexanes), 390 mg (2.2 mmol) of product **5.13** as a colourless oil (92% yield). Spectroscopic data were in accordance with previously reported literature.²⁶

1,3-difluoro-5-vinylbenzene (**5.14**)



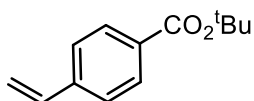
From 1-bromo-3,5-difluorobenzene (599 mg, 3.1 mmol), general procedure B was followed with Pd(dppf)Cl₂ (114 mg, 0.16 mmol), CsCO₃ (3.03 g, 5.8 mmol) and vinyl trifluoroborate (532 mg, 4.7 mmol) and THF: H₂O (5.4 mL:0.60 mL).to give, after flash chromatography (hexanes), 245 mg (1.7 mmol) of 1,3-difluoro-5-vinylbenzene (**5.14**) as a colourless oil (56% yield). IR (Film) 3094, 840, 1312, 1116 cm⁻¹; ¹H NMR (400 MHz, CDCl₃) δ = 6.92 – 6.90 (m, 2H), 6.72 – 6.69 (m, 1H), 6.63 (dd, J = 17.1, 7.0 Hz, 1H), 5.76 (d, J = 17.9 Hz, 1H), 5.36 (d, J = 10.8 Hz, 1H) ppm; ¹³C NMR (125 MHz, CDCl₃) δ = 163.3 (dd, J = 247.9, 13.1 Hz), 141.1 (t, J = 9.1 Hz), 135.2 (t, J = 3.5 Hz), 116.7, 109.1 (dd, J = 20.2 Hz, 5.5 Hz), 103.1 (t, J = 25.6 Hz) ppm; HRMS (APCI) exact mass calculated for [M+H] (C₈H₇F₂) requires m/z 141.0510, found m/z 141.0510.

tert-butyl (4-vinylphenyl)carbamate (**5.15**)



From *tert*-butyl (4-bromophenyl)carbamate (2.4 mmol), general procedure B was followed with Pd(dppf)Cl₂ (93 mg, 0.12 mmol), CsCO₃ (3.81 g, 7.2 mmol) and vinyl trifluoroborate (438 mg, 3.6 mmol) was added THF:H₂O (4.5 mL:0.50 mL).to give, after flash chromatography (gradient from 97:3 to 90:10 hexanes/EtOAc), 235 mg (1.1 mmol) of *tert*-butyl (4-vinylphenyl)carbamate (**5.15**) as a colourless oil (46% yield). Spectroscopic data were in accordance with previously reported literature.²⁷

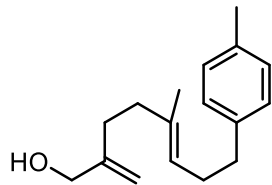
tert-butyl 4-vinylbenzoate (**5.16**)



From [1,1'-biphenyl]-4-carbaldehyde (2.4 mmol), general procedure A was followed to give, after flash chromatography (gradient from 90:10 to 70:30 hexanes/DCM), 367 mg (1.8 mmol) of

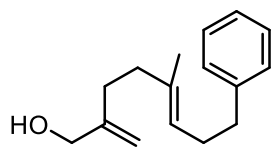
product **5.16** as a colourless oil (75% yield). Spectroscopic data were in accordance with previously reported literature.²⁸

(E)-5-methyl-2-methylene-8-(*p*-tolyl)oct-5-en-1-ol (3.56)



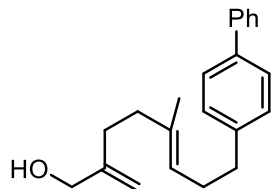
Followed general procedure C from 1-methyl-4-vinylbenzene on a 0.54 mmol scale and purified using silica gel column chromatography to give 71 mg (0.29 mmol, 53% yield over 2 steps) of (*E*)-5-methyl-2-methylene-8-(*p*-tolyl)oct-5-en-1-ol as a colourless oil. IR (Film) 3326, 3045, 3018, 2920, 2854, 1514, 1448 cm^{-1} ; ^1H NMR (500 MHz, CDCl_3) δ = 7.11 (s, 4H), 5.23 (t, J = 6.6 Hz, 1H), 5.04 (s, 1H), 4.89 (s, 1H), 4.08 (s, 2H), 2.62 (t, J = 8.2 Hz, 2H), 2.34 (s, 3H), 2.31 (dt, J = 8.3, 8.3 Hz, 2 H), 2.17 (bs, 4H), 1.62 (bs, 1H), 1.61 (s, 3H) ppm; ^{13}C NMR (100 MHz, CDCl_3) δ = 160.5, 148.7, 144.6, 135.2, 123.8, 109.0, 106.5, 97.5, 65.6, 55.1, 37.7, 36.2, 31.4, 29.5, 15.8; HRMS (ESI) exact mass calculated for $[\text{M}+\text{Na}]$ ($\text{C}_{17}\text{H}_{24}\text{NaO}$) requires m/z 267.1719, found m/z 267.1710.

(E)-5-methyl-2-methylene-8-phenyloct-5-en-1-ol (3.57)



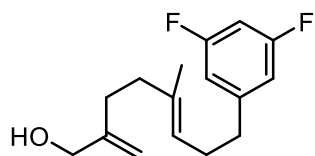
Followed general procedure C from styrene on a 0.54 mmol scale and purified using silica gel column chromatography to give 62 mg (0.27 mmol, 49% yield over 2 steps) of (*E*)-5-methyl-2-methylene-8-phenyloct-5-en-1-ol as a colourless oil. IR (Film) 3322, 3083, 3063, 3026, 2921, 2855, 1453, 1029 cm^{-1} ; ^1H NMR (500 MHz, CDCl_3) δ = 7.31 – 7.28 (m, 2H), 7.21 – 7.18 (m, 3H), 5.23 (t, J = 7.1 Hz, 1 H), 5.03 (s, 1H), 4.88 (s, 1H), 4.07 (s, 2H), 2.66 (t, J = 6.9 Hz, 2H), 2.33 (dt, J = 7.0, 7.0 Hz, 2H), 2.16 (bs, 4H), 1.66 (bs, 1H), 1.59 (s, 3H) ppm; ^{13}C NMR (125 MHz, CDCl_3) δ = 149.0, 142.4, 135.4, 128.6, 128.3, 125.8, 124.1, 109.4, 66.0, 38.0, 36.1, 31.6, 29.9, 16.0 ppm; HRMS (ESI) exact mass calculated for $[\text{M}+\text{Na}]$ ($\text{C}_{16}\text{H}_{22}\text{NaO}$) requires m/z 253.1563, found m/z 253.1565.

(E)-8-([1,1'-biphenyl]-4-yl)-5-methyl-2-methyleneoct-5-en-1-ol (3.58)



Followed general procedure C from 4-vinyl-1,1'-biphenyl on a 0.54 mmol scale and purified using silica gel column chromatography to give 120 mg (0.39 mmol, 72% yield over 2 steps) of (*E*)-8-(3,5-dimethoxyphenyl)-5-methyl-2-methyleneoct-5-en-1-ol as a colourless oil. IR (Film) 3351, 3089, 3058, 3030, 2977, 2934, 2850, 1487, 1073 cm^{-1} ; ^1H NMR (500 MHz, CDCl_3) δ = 7.62 (d, J = 7.0 Hz, 2H), 7.55 (d, J = 7.0 Hz, 2H), 7.46 (dd, J = 7.0, 7.0 Hz, 2H), 7.36 (dd, J = 7.0, 7.0 Hz, 1H), 7.29 (d, J = 7.0 Hz, 2H), 5.28 (t, J = 7.5 Hz, 1H), 5.05 (s, 1H), 4.9 (s, 1H), 4.09 (bs, 2H), 2.72 (t, J = 7.5 Hz, 2H), 2.39 (dt, J = 7.5, 7.5 Hz, 2H), 2.19 (bs, 4H), 1.64 (s, 4H) ppm; ^{13}C NMR (100 MHz, CDCl_3) δ = 149.0, 141.5, 141.2, 138.7, 135.5, 129.0, 128.8, 127.1, 127.0, 124.1, 109.5, 66.0, 38.0, 35.8, 31.6, 29.9, 16.0 ppm; HRMS (ESI) exact mass calculated for $[\text{M}+\text{Na}]$ ($\text{C}_{22}\text{H}_{26}\text{NaO}$) requires m/z 329.1876, found m/z 329.1880.

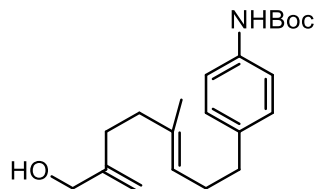
(E)-8-(3,5-difluorophenyl)-5-methyl-2-methyleneoct-5-en-1-ol (3.59)



Followed general procedure C from 1,3-difluoro-5-vinylbenzene on a 0.54 mmol scale and purified using silica gel column chromatography to give 74 mg (0.27 mmol, 51% yield over 2 steps) of (*E*)-8-(3,5-difluorophenyl)-5-methyl-2-methyleneoct-5-en-1-ol as a colourless oil. IR (Film) 3337, 1089, 2924, 2859, 1625, 1594, 1458, 1115 cm^{-1} ; ^1H NMR (500 MHz, CDCl_3) δ = 6.70 – 6.67 (m, 2H), 6.63 – 6.59 (m, 1H), 5.14 (t, J = 7.9 Hz, 1H), 5.01 (s, 1H), 4.86 (s, 1H), 4.06 (bs, 2H), 2.61 (t, J = 7.9 Hz, 2H), 2.29 (dt, J = 7.9, 7.9 Hz, 2H), 2.14 (bs, 4H), 1.60 (bs, 1H), 1.56 (s, 3H) ppm; ^{13}C NMR (100 MHz, CDCl_3) δ = 163.0 (dd, J = 247.2, 13.2 Hz), 148.9, 146.2 (t, J = 9.3 Hz), 136.2, 123.2, 111.3 (dd, J = 27.8, 6.0 Hz), 109.6, 101.2 (t, J = 25.0 Hz), 66.0, 37.9, 35.8,

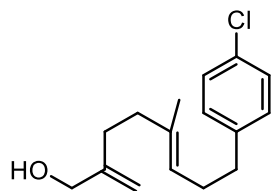
31.5, 29.2, 16.0 ppm; HRMS (ESI) exact mass calculated for [M+Na] (C₁₆H₂₀F₂NaO) requires m/z 289.1374, found m/z 289.1368.

***tert*-butyl (*E*)-(4-(7-(hydroxymethyl)-4-methylocta-3,7-dien-1-yl)phenyl)carbamate (3.60)**



Followed general procedure C from *tert*-butyl (4-vinylphenyl)carbamate on a 0.54 mmol scale and purified using silica gel column chromatography to give 143 mg (0.42 mmol, 78% yield over 2 steps) of *tert*-butyl (*E*)-(4-(7-(hydroxymethyl)-4-methylocta-3,7-dien-1-yl)phenyl)carbamate as a colourless oil. IR (Film) 3403, 3331, 2978, 2930, 2854, 1701, 1597, 1162 cm⁻¹; ¹H NMR (400 MHz, CDCl₃) δ = 7.14 (d, J = 9.2 Hz, 2H), 6.98 (d, J = 9.2 Hz, 2H), 6.45 (s, 1H), 5.06 (t, J = 7.0 Hz, 1H), 4.91 (s, 1H), 4.75 (s, 1H), 3.94 (s, 2H), 2.47 (t, J = 8.3 Hz, 2H), 2.16 (dt, J = 8.3, 7.0 Hz, 2H), 2.02 (s, 4H), 1.71 (s, 1H), 1.45 (s, 3H), 1.41 (s, 9H) ppm; ¹³C NMR (100 MHz, CDCl₃) δ = 153.1, 149.0, 137.1, 136.1, 135.4, 129.0, 124.0, 118.8, 109.4, 80.4, 65.9, 38.0, 35.4, 31.6, 29.9, 28.4, 16.0 ppm; HRMS (ESI) exact mass calculated for [M+Na] (C₂₁H₃₁NNaO₃) requires m/z 368.21962, found m/z 368.21898.

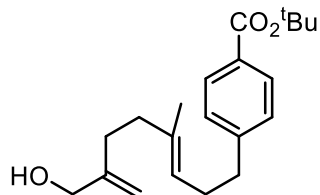
(*E*)-8-(4-chlorophenyl)-5-methyl-2-methyleneoct-5-en-1-ol (3.61)



Followed general procedure C from 1-chloro-4-vinylbenzene on a 0.54 mmol scale and purified using silica gel column chromatography to give 105 mg (0.39 mmol, 72% yield over 2 steps) of (*E*)-8-(4-chlorophenyl)-5-methyl-2-methyleneoct-5-en-1-ol as a colourless oil. IR (Film) 3315, 2925, 2855, 1491, 1448, 1015 cm⁻¹; ¹H NMR (500 MHz, CDCl₃) δ = 7.24 (d, J = 9.3 Hz, 2H), 7.10 (d, J = 9.3 Hz, 2H), 5.16 (t, J = 8.0 Hz, 1H), 5.01 (s, 1H), 4.86 (s, 1H), 4.06 (s, 2H), 2.60 (t, J = 8.0 Hz, 2H), 2.28 (dt, J = 8.0, 8.0 Hz, 2H), 2.14 (bs, 4H), 1.69 (bs, 1H), 1.56 (s, 3H) ppm; ¹³C NMR (100 MHz, CDCl₃) δ = 148.9, 140.8, 135.8, 131.5, 129.9, 128.4, 123.7, 109.5, 66.0, 38.0, 35.4,

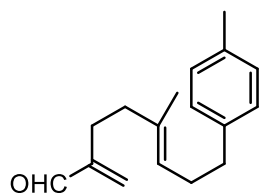
31.6, 29.8, 16.0 ppm; HRMS (ESI) exact mass calculated for [M+Na] (C₁₆H₂₁ClNaO) requires m/z 287.1173, found m/z 287.1165.

***tert*-butyl (*E*)-4-(7-(hydroxymethyl)-4-methylocta-3,7-dien-1-yl)benzoate (3.62)**



Followed general procedure C from *tert*-butyl 4-vinylbenzoate on a 0.54 mmol scale and purified using silica gel column chromatography to give 99 mg (0.30 mmol, 55% yield over 2 steps) of *tert*-butyl (*E*)-4-(7-(hydroxymethyl)-4-methylocta-3,7-dien-1-yl)benzoate as a colourless oil. IR (Film) 3403, 2977, 2928, 2856, 1711, 1610, 1165, 1063 cm⁻¹; ¹H NMR (500 MHz, CDCl₃) δ = 7.88 (d, J = 8.2 Hz, 2H), 7.21 (d, J = 8.2 Hz, 2H), 5.16 (t, J = 6.7 Hz, 1H), 5.01 (s, 1H), 4.85 (s, 1H), 4.06 (s, 2H), 2.67 (t, J = 7.7 Hz, 2H), 2.30 (dt, J = 7.7, 6.7 Hz, 2H), 2.13 (s, 4H), 1.58 (s, 9H), 1.55 (s, 4H) ppm; ¹³C NMR (125 MHz, CDCl₃) δ = 166.0, 149.0, 147.3, 135.8, 129.7, 129.5, 128.5, 123.6, 109.5, 80.8, 66.0, 38.0, 36.1, 31.6, 29.6, 28.3, 16.0 ppm; HRMS (ESI) exact mass calculated for [M+Na] (C₂₁H₃₀NaO₃) requires m/z 353.2087, found m/z 353.2082.

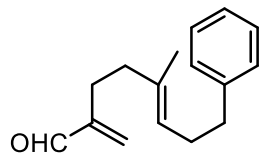
(*E*)-5-methyl-2-methylene-8-(*p*-tolyl)oct-5-enal (3.63)



From (*E*)-5-methyl-2-methylene-8-(*p*-tolyl)oct-5-en-1-ol, general procedure D was followed on a 0.29 mmol scale to give 55 mg (0.23 mmol, 78% yield) of (*E*)-5-methyl-2-methylene-8-(*p*-tolyl)oct-5-enal as a yellow oil. IR (Film) 3082, 2922, 2854, 2699, 1690, 1514, 1447 cm⁻¹; ¹H NMR (500 MHz, CDCl₃) δ = 9.52 (s, 1H), 7.09 (m, 4H), 6.21 (s, 1H), 5.97 (s, 1H), 5.18 (t, J = 7.6 Hz, 1H), 2.60 (t, J = 8.4 Hz, 2H), 2.36 (t, 8.4 Hz, 2H), 2.33 (s, 3H), 2.29 (dt, J = 7.6, 7.6 Hz, 2H), 2.13 (t, J = 7.6 Hz, 2H), 1.59 (s, 3H) ppm; ¹³C NMR (100 MHz, CDCl₃) δ = 194.7, 150.0, 139.3,

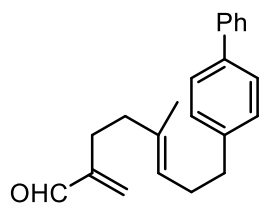
135.2, 134.6, 134.2, 129.0, 128.4, 124.9, 37.8, 35.7, 30.1, 26.4, 21.1, 16.0 ppm; HRMS (ESI) exact mass calculated for [M+Na] (C₁₇H₂₂NaO) requires m/z 265.1563, found m/z 265.1558.

(E)-5-methyl-2-methylene-8-phenyloct-5-enal (3.64)



From (*E*)-5-methyl-2-methylene-8-phenyloct-5-en-1-ol, general procedure D was followed on a 0.29 mmol scale to give 51 mg (0.22 mmol, 76% yield) of (*E*)-5-methyl-2-methylene-8-phenyloct-5-enal as a colourless oil. IR (Film) 3083, 3062, 3027, 2924, 2854, 2698, 1689, 1453 cm⁻¹; ¹H NMR (500 MHz, CDCl₃) δ = 9.51 (s, 1H), 7.28 (t, J = 7.8 Hz, 2H), 7.20 – 7.18 (m, 3H), 6.20 (s, 1H), 5.96 (s, 1H), 5.18 (t, J = 7.6 Hz, 1H), 2.64 (t, J = 8.5 Hz, 2H), 2.37 – 2.29 (m, 4H), 2.13 (t, J = 7.5 Hz, 2H), 1.58 (s, 3H) ppm; ¹³C NMR (125 MHz, CDCl₃) δ = 194.7, 149.9, 142.3, 134.7, 134.2, 128.6, 128.3, 125.8, 124.7, 37.7, 36.1, 29.9, 26.4, 15.9 ppm; HRMS (ESI) exact mass calculated for [M+Na] (C₁₆H₂₀NaO) requires m/z 251.1406, found m/z 251.1411.

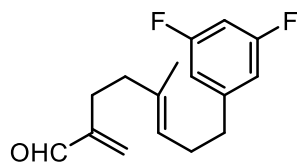
(E)-8-([1,1'-biphenyl]-4-yl)-5-methyl-2-methyleneoct-5-enal (3.65)



From (*E*)-8-(3,5-dimethoxyphenyl)-5-methyl-2-methyleneoct-5-en-1-ol, general procedure D was followed on a 0.39 mmol scale to give 91 mg (0.30 mmol, 76% yield) of (*E*)-8-([1,1'-biphenyl]-4-yl)-5-methyl-2-methyleneoct-5-enal as a colourless oil. IR (Film) 3055, 3027, 2924, 2853, 1690, 1519, 1486 cm⁻¹; ¹H NMR (500 MHz, CDCl₃) δ = 9.53 (s, 1H), 7.62 (d, J = 7.8 Hz, 2H), 7.55 (d, J = 8.1 Hz, 2H), 7.46 (t, J = 7.8 Hz, 2H), 7.35 (t, J = 7.7 Hz, 1H), 7.28 (d, J = 8.1 Hz, 2H), 6.22 (s,

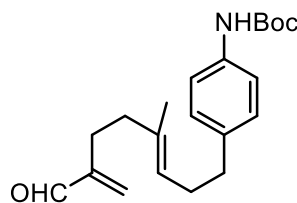
1H), 5.97 (s, 1H), 5.23 (t, J = 7.0 Hz, 1H), 2.71 (t, J = 7.5 Hz, 2H), 2.40 – 2.45 (m, 4H), 2.16 (t, J = 7.5 Hz, 2H), 1.63 (s, 3H) ppm; ¹³C NMR (100 MHz, CDCl₃) δ = 194.7, 149.9, 141.5, 141.2, 138.8, 134.8, 134.2, 129.0, 128.8, 127.1, 127.0, 124.7, 37.8, 35.7, 29.9, 26.4, 16.0 ppm; HRMS (ESI) exact mass calculated for [M+Na] (C₂₂H₂₄NaO) requires m/z 327.1719, found m/z 327.1719.

(E)-8-(3,5-difluorophenyl)-5-methyl-2-methyleneoct-5-enal (3.66)



From (*E*)-8-(3,5-difluorophenyl)-5-methyl-2-methyleneoct-5-en-1-ol, general procedure D was followed on a 0.28 mmol scale to give 57 mg (0.21 mmol, 77% yield) of (*E*)-8-(3,5-difluorophenyl)-5-methyl-2-methyleneoct-5-enal as a colourless oil. IR (Film) 3089, 2926, 2856, 2699, 1690, 1625, 1594, 1459, 1116 cm⁻¹; ¹H NMR (500 MHz, CDCl₃) δ = 9.50 (s, 1H), 6.67 (dd, J = 7.9, 1.4 Hz, 2H), 6.61 (tt, J = 9.0, 2.2 Hz, 1H), 6.19 (s, 1H), 5.96 (s, 1H), 5.10 (t, J = 7.0 Hz, 1H), 2.60 (t, J = 8.3 Hz, 2H), 2.33 (t, J = 8.3 Hz, 2H), 2.27 (dt, J = 7.6, 7.0 Hz, 2H), 2.11 (t, J = 7.6 Hz, 2H), 1.56 (s, 3H) ppm; ¹³C NMR (100 MHz, CDCl₃) δ = 194.6, 163.0 (dd, J = 247.4, 12.6 Hz), 149.9, 146.2 (t, J = 9.3 Hz), 135.5, 134.2, 123.8, 111.3 (dd, J = 18.5, 5.3 Hz), 101.2 (t, J = 21.4 Hz), 37.7, 35.8 (t, J = 2.1 Hz), 29.2, 26.4, 15.9 ppm; HRMS (ESI) exact mass calculated for [M+H] (C₁₆H₁₉F₂O) requires m/z 265.1398, found m/z 265.1398.

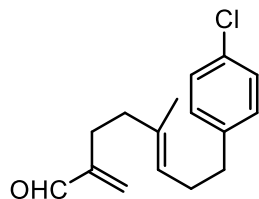
***tert*-butyl (*E*)-(4-(7-formyl-4-methylocta-3,7-dien-1-yl)phenyl)carbamate (3.67)**



From *tert*-butyl (*E*)-(4-(7-(hydroxymethyl)-4-methylocta-3,7-dien-1-yl)phenyl)carbamate general procedure D was followed on a 0.41 mmol scale to give 52 mg (0.15 mmol, 36% yield) of *tert*-butyl (*E*)-(4-(7-formyl-4-methylocta-3,7-dien-1-yl)phenyl)carbamate as a yellow oil. IR (Film) 3346, 2976, 2927, 2853, 1725, 1690, 1524, 1161 cm⁻¹; ¹H NMR (400 MHz, CDCl₃) δ = 9.50 (s, 1H), 7.25 (d, J = 8.6 Hz, 2H), 7.08 (d, J = 8.6 Hz, 2H), 6.48 (bs, 1H), 6.19 (s, 1H), 5.95 (s,

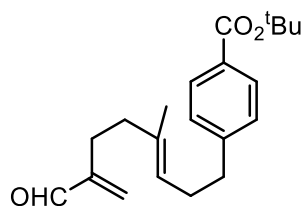
1H), 5.14 (t, J = 7.1 Hz, 1H), 2.56 (t, J = 7.8 Hz, 2H), 2.33 (t, J = 8.0 Hz, 2H), 2.24 (dt, J = 7.1, 7.1 Hz, 2H), 2.10 (t, J = 7.1 Hz, 2H), 1.55 (s, 3H), 1.51 (s, 9H) ppm; ¹³C NMR (100 MHz, CDCl₃) δ = 194.8, 153.0, 149.9, 137.1, 136.2, 134.6, 134.3, 129.0, 124.7, 118.7, 80.4, 37.7, 35.4, 30.0, 28.5, 26.4, 15.9 ppm; HRMS (ESI) exact mass calculated for [M+Na] (C₂₁H₂₉NNaO₃) requires m/z 366.20396, found m/z 366.20292.

(E)-8-(4-chlorophenyl)-5-methyl-2-methyleneoct-5-enal (3.68)



From (*E*)-8-(4-chlorophenyl)-5-methyl-2-methyleneoct-5-en-1-ol, general procedure D was followed on a 0.35 mmol scale to give 72 mg (0.27 mmol, 78% yield) of (*E*)-8-(4-chlorophenyl)-5-methyl-2-methyleneoct-5-enal as a colourless oil. IR (Film) 3050, 2925, 2855, 2699, 1688, 1491, 1015 cm⁻¹; ¹H NMR (500 MHz, CDCl₃) δ = 9.50 (s, 1H), 7.24 (d, J = 8.3 Hz, 2H), 7.09 (d, J = 8.3 Hz, 2H), 6.19 (s, 1H), 5.95 (s, 1H), 5.13 (t, J = 7.1 Hz, 1H), 2.59 (t, J = 7.6 Hz, 2H), 2.33 (t, J = 7.6 Hz, 2H), 2.26 (dt, J = 7.6, 7.1 Hz, 2H), 2.11 (t, J = 7.6 Hz, 2H), 1.55 (s, 3H) ppm; ¹³C NMR (100 MHz, CDCl₃) δ = 194.7, 149.9, 140.7, 135.1, 134.2, 131.5, 129.9, 128.4, 124.3, 37.8, 35.4, 29.8, 26.4, 16.0 ppm; HRMS (ESI) exact mass calculated for [M+Na] (C₁₆H₁₉ClNaO) requires m/z 285.1017, found m/z 285.1014.

***tert*-butyl (*E*)-4-(7-formyl-4-methylocta-3,7-dien-1-yl)benzoate (3.69)**



From *tert*-butyl (*E*)-4-(7-(hydroxymethyl)-4-methylocta-3,7-dien-1-yl)benzoate, general procedure D was followed on a 0.13 mmol scale to give 26 mg (0.09 mmol, 73% yield) of *tert*-butyl (*E*)-4-(7-formyl-4-methylocta-3,7-dien-1-yl)benzoate as a colourless oil. IR (Film) 2974, 2926, 2855, 1710, 1693, 1255, 1114 cm⁻¹; ¹H NMR (500 MHz, CDCl₃) δ = 9.50 (s, 1H), 7.89 (d, J = 8.5 Hz, 2H), 7.20 (d, J = 8.5 Hz, 2H), 6.19 (s, 1H), 5.95 (s, 1H), 5.13 (t, J = 6.8 Hz, 1H), 2.66

(t, J = 8.6 Hz, 2H), 2.34 – 2.29 (m, 4H), 2.10 (t, J = 7.6 Hz, 2H), 1.59 (s, 9H), 1.55 (s, 3H) ppm; ^{13}C NMR (125 MHz, CDCl_3) δ = 194.7, 166.0, 149.9, 147.3, 135.1, 134.3, 129.7, 129.6, 128.4, 124.3, 80.8, 37.8, 36.1, 29.6, 28.4, 16.4, 16.0 ppm; HRMS (ESI) exact mass calculated for $[\text{M}+\text{Na}]$ ($\text{C}_{21}\text{H}_{28}\text{NaO}_3$) requires m/z 351.1931, found m/z 351.1926.

General procedure for the formation of chiral hydrazide salts

AcOH (70 μL) was added slowly to methanol in a 10-mL volumetric flask. The flask was topped up with MeOH and shaken. An aliquot of the resulting 0.1M methanolic HCl solution (1 equiv.) was taken up in a microsyringe and added dropwise to a vial containing a solution of hydrazide freebase (1 equiv.) in MeOH. The solution was briefly swirled, left for 10 minutes, and concentrated to give the HCl salt.

Asymmetric polyene cyclization: catalyst screen (general procedure G)

To a 1 mL vial containing aldehyde (0.035 mmol) was added a solution of catalyst (0.007 mmol, as hydrochloride salt) in solvent (140 μL , 0.25M in substrate). The mixture was briefly swirled to homogenize and let stand. When the reaction was determined complete by ^1H NMR, the reaction was concentrated, and purified by flash chromatography to obtain aldehyde product as a mixture of diastereomers. The enantiomeric excess of the product was determined by reduction to the corresponding alcohol and chiral HPLC analysis (see section 7.2 for chromatographic conditions).

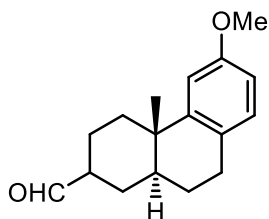
Racemic polyene cyclization (general procedure H)

To a 1 mL vial containing aldehyde (25 mg) was added a solution of catalyst **3.47**·HCl (0.2 equiv.) in 5% HFIP/DCM (0.25M in substrate). The mixture was briefly swirled to homogenize and let stand for 2-5 h (until done as monitored by ^1H NMR). The reaction mixture was concentrated and purified by silica gel column chromatography (gradient from 97:3 hexanes/EtOAc to 90:10 hexanes/EtOAc) to obtain aldehyde product as a mixture of diastereomers.

^1H and ^{13}C peaks for the α diastereomer of *trans*-decalin products are reported with an asterisk (*) where possible to distinguish from the β diastereomer peaks. The integrations are reported as a proportion of the total signal (i.e. 1H x 0.5 for a signal that corresponds to one proton of one of the two diastereomers).

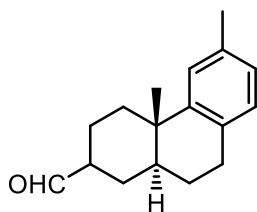
Note: NMR spectra show small ratios of *cis*-decalin products.

(4a*RS*,10a*RS*)-6-methoxy-4a-methyl-1,2,3,4,4a,9,10,10a-octahydrophenanthrene-2-carbaldehyde (3.55)



Prepared according to general procedure H from polyene **2.56** (25 mg, 0.098 mmol). The reaction was run for 2 h and product **3.55** was isolated as a colourless oil (16 mg, 0.060 mmol, 62% yield, *trans*- β : α 2:1). IR (Film) 2929, 2858, 2836, 2713, 1723, 1610, 1176 cm^{-1} ; ^1H NMR (500 MHz, CDCl_3) δ = 9.72* (s, 1 H x 0.3), 9.68 (d, J = 1.5 Hz, 1 H x 0.7), 6.99 (d, J = 8.6 Hz, 1 H x 0.7), 6.96* (d, J = 8.6 Hz, 1 H x 0.3), 6.82 (d, J = 2.3 Hz, 1 H x 0.7), 6.77* (d, J = 2.3 Hz, 1H x 0.3), 6.69 (dd, J = 8.6, 2.3 Hz, 1H x 0.7), 6.66* (dd, J = 8.6, 2.3 Hz, 1H x 0.3), 3.79 (s, 3H x 0.7), 3.77 (s, 3H x 0.3), 2.90 – 2.77 (m, 2H x 0.7), 2.53 – 2.47* (m, 1H x 0.3), 2.40 – 2.31 (m, 2H x 0.7), 2.31 – 2.22* (m, 3H x 0.3), 2.15 – 2.09* (m, 1H x 0.3), 2.08 – 2.01 (m, 2H x 0.3), 2.01 – 1.95 (m, 1H x 0.7 + 1H x 0.3), 1.80 – 1.75 (m, 1H x 0.7 + 1H x 0.3), 1.72 – 1.60 (m, 4H x 0.7 + 1H x 0.3), 1.54 – 1.40 (m, 2H x 0.7 + 2H x 0.3), 1.10* (s, 3H x 0.3), 1.08 (s, 3H x 0.7) ppm; ^{13}C NMR (100 MHz, CDCl_3) δ 205.6, 204.4*, 157.8, 157.8*, 148.5*, 148.5, 130.3, 130.2*, 127.6, 127.6*, 111.2, 111.2*, 110.6, 110.4*, 55.4, 55.4*, 50.7, 46.6*, 41.4, 38.7*, 37.0, 36.9*, 36.7, 34.6*, 28.6, 28.5, 28.5*, 27.7*, 25.9*, 25.8, 22.1, 21.6, 21.2*, 20.9* ppm; HRMS (ESI) exact mass calculated for $[\text{M}+\text{Na}]$ ($\text{C}_{17}\text{H}_{22}\text{NaO}_2$) requires m/z 281.1512, found m/z 281.1506.

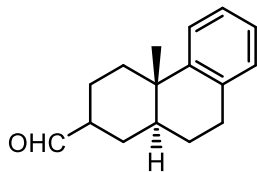
(4a*RS*,10a*RS*)-4a,6-dimethyl-1,2,3,4,4a,9,10,10a-octahydrophenanthrene-2-carbaldehyde (3.70)



Prepared according to general procedure E from polyene **3.63** (21 mg, 0.088 mmol). The reaction was run for 24 h and product **3.70** was isolated as a colourless oil (7.7 mg, 0.032 mmol, 36% yield, *trans*- β : α 5:1).

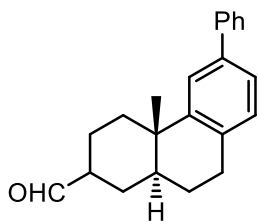
Prepared according to general procedure H from polyene **3.63** (26 mg, 0.10 mmol). The reaction was run for 3 h and product **3.70** was isolated as a colourless oil (20 mg, 0.082 mmol, 78% yield, *trans*- β : α 3:1). IR (Film) 2925, 2856, 1723, 1692, 1489, 1170 cm^{-1} ; ^1H NMR (500 MHz, CDCl_3) δ = 9.72* (s, 1H x 0.25), 9.69 (d, J = 1.6 Hz, 1H x 0.75), 7.10 – 7.08 (m, 1H x 0.75 + 1H x 0.25), 6.98 – 6.93 (m, 2H x 0.75 + 2H x 0.25), 2.93 – 2.71 (m, 2H x 0.75), 2.52 – 2.48* (m, 1H x 0.25), 2.43 – 2.32 (m, 2H x 0.75 + 2H x 0.25), 2.31 (s, 3H x 0.75), 2.29* (s, 3H x 0.25), 2.24 – 2.14* (m, 3H x 0.25), 2.07 – 2.03* (m, 1H x 0.25), 2.01 – 1.94 (m, 1H x 0.75 + 1H x 0.25), 1.80 – 1.75 (m, 1H x 0.75 + 1H x 0.25), 1.71 – 1.61 (m, 4H x 0.75 + 1H x 0.25), 1.52 – 1.42 (m, 2H x 0.75 + 2H x 0.25), 1.10* (s, 3H x 0.25), 1.08 (s, 3H x 0.75) ppm; ^{13}C NMR (125 MHz, CDCl_3) δ 205.6*, 204.5, 147.1*, 147.0, 135.1, 135.0*, 132.3, 132.3*, 129.4, 129.4*, 126.7, 126.6*, 125.3, 125.2*, 50.7, 46.6*, 41.5, 38.7*, 36.8, 36.7, 36.6*, 34.5*, 29.0, 28.9*, 28.5, 27.7*, 25.9*, 25.8, 22.1, 21.7, 21.4, 21.2*, 21.1*, 20.9* ppm; HRMS (ESI) exact mass calculated for $[\text{M}+\text{Na}]$ ($\text{C}_{17}\text{H}_{22}\text{NaO}$) requires m/z 265.1563, found m/z 265.1556.

(4a*RS*,10a*RS*)-4a-methyl-1,2,3,4,4a,9,10,10a-octahydrophenanthrene-2-carbaldehyde (3.71)



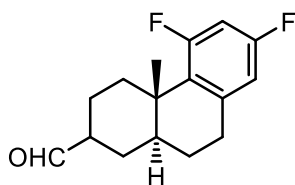
Prepared according to general procedure H from polyene **3.64** (25 mg, 0.11 mmol). The reaction was run for 5 h and product **3.71** was isolated as a colourless oil (15 mg, 0.064 mmol, 58% yield, *trans*- β : α 6:1). IR (Film) 3061, 3025, 2929, 2858, 1724, 1686, 1449 cm^{-1} ; ^1H NMR (500 MHz, CDCl_3) δ = 9.72* (s, 1H x 0.15), 9.69 (d, J = 1.4 Hz, 1H x 0.85), 7.29 – 7.27 (m, 1H x 0.85 + 1H x 0.15), 7.24 – 7.02 (m, 4H x 0.85 + 4H x 0.15), 2.95 – 2.86 (m, 2H x 0.85), 2.54 – 2.49* (m, 1H x 0.15), 2.42 – 2.23 (m, 2H x 0.85 + 1H x 0.15), 2.23 – 2.14* (m, 2H x 0.15), 2.00 – 1.97 (m, 1H x 0.85 + 4H x 0.15) 1.82 – 1.60 (m, 5H x 0.85 + 2H x 0.15), 1.56 – 1.40 (m, 2H x 0.85 + 2H x 0.15), 1.11 (s, 3H x 0.15), 1.08 (3H x 0.85) ppm; ^{13}C NMR (125 MHz, CDCl_3): δ 205.6*, 204.4, 147.2*, 147.2, 135.5, 135.4*, 129.5, 129.5*, 128.5, 128.5*, 125.8, 125.7*, 124.7, 124.6*, 50.7, 46.6*, 41.4, 38.6*, 36.8, 36.7, 35.4*, 34.5*, 29.4, 29.3*, 28.5, 27.6*, 25.8*, 25.7, 22.1, 21.7, 21.2*, 20.9* ppm; HRMS (ESI) exact mass calculated for $[\text{M}+\text{H}]$ ($\text{C}_{16}\text{H}_{21}\text{O}$) requires m/z 229.1587, found m/z 229.1581.

(4a*RS*,10a*RS*)-4a-methyl-6-phenyl-1,2,3,4,4a,9,10,10a-octahydrophenanthrene-2-carbaldehyde (3.72)



Prepared according to general procedure H from polyene **3.65** (25 mg, 0.083 mmol). The reaction was run for 5 h and product **3.72** was isolated as a colourless oil (13 mg, 0.043 mmol, 52% yield, *trans*- β : α 1.2:1). IR (Film) 3051, 3027, 2929, 2859, 1723, 1400 cm^{-1} ; ^1H NMR (500 MHz, CDCl_3) δ = 9.73 (s, 0.5H), 9.70 (0.5H), 7.62 – 7.50 (m, 2H), 7.46 – 7.39 (m, 3H), 7.39 – 7.30 (m, 2H), 7.20 – 7.10 (m, 1H), 3.03 – 2.85 (m, 2H), 2.55 – 2.48 (m, 1H), 2.38 – 2.24 (m, 2H), 2.14 – 1.94 (m, 2H), 1.84 – 1.63 (m, 3H), 1.58 – 1.41 (m, 2H), 1.16 (s, 1.5H), 1.13 (s, 1.5H) ppm; ^{13}C NMR (125 MHz, CDCl_3) δ 205.5, 204.4, 147.6, 147.6, 141.8, 141.7, 138.9, 138.8, 134.7, 134.7, 130.0, 129.9, 128.9, 128.9, 128.8, 128.8, 127.3, 127.2, 127.2, 127.1, 127.1, 127.0, 124.7, 124.6, 123.7, 123.6, 50.7, 46.6, 41.5, 38.7, 37.0, 36.8, 36.7, 34.6, 29.1, 29.0, 28.5, 27.6, 25.8, 25.7, 22.1, 21.8, 21.3, 20.9 ppm; HRMS (APCI) exact mass calculated for $[\text{M}+\text{H}]$ ($\text{C}_{22}\text{H}_{25}\text{O}$) requires m/z 305.18999, found m/z 305.19004.

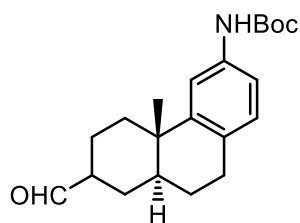
(4a*RS*,10a*RS*)-5,7-difluoro-4a-methyl-1,2,3,4,4a,9,10,10a-octahydrophenanthrene-2-carbaldehyde (3.73)



Prepared according to general procedure H from polyene **3.66** (25 mg, 0.096 mmol). The reaction was run for 5 h and product **3.73** was isolated as a colourless oil (9.8 mg, 0.037 mmol, 39% yield, *trans*- β : α 4:1). IR (Film) 3050, 2930, 2865, 1725, 1623, 1594, 1460, 1117 cm^{-1} ; ^1H NMR (500 MHz, CDCl_3) δ = 9.72* (s, 1H x 0.2), 9.66 (d, J = 1.0 Hz, 1H x 0.8), 6.77 – 6.48 (m, 2H x 0.8 + 2H x 0.2), 2.97-2.86 (m, 1H x 0.8+ 1H x 0.2), 2.85 – 2.77 (m, 2H x 0.8), 2.45 – 2.33 (m, 1H x 0.8 + 2H x 0.2), 1.96 – 1.88 (m, 1H x 0.8 + 2H x 0.2), 1.77 – 1.49 (m, 6H x 0.8 + 6H x 0.2), 1.48 – 1.41 (1H x 0.8 + 1H x 0.2), 1.20* (3H x 0.2), 1.17 (s, 3H x 0.8) ppm; ^{13}C NMR (100 MHz, CDCl_3)

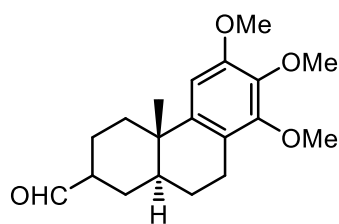
(assigned for major diastereomer): δ 204.3, 162.13 (dd, $J = 251.4, 9.6$ Hz), 160.61 (dd, $J = 243.7, 15.5$ Hz), 140.5 (dd, $J = 8.6, 7.0$ Hz), 129.5 (dd, $J = 12.1, 4.4$ Hz), 111.6 (dd, $J = 19.7, 3.3$ Hz), 102.2 (dd, $J = 29.0, 24.7$ Hz), 50.6 (d, $J = 1.1$ Hz), 43.2, 37.2 (d, $J = 3.1$ Hz), 35.3 (d, $J = 11.2$ Hz), 31.2 (t, $J = 2.0$ Hz), 28.0, 25.4, 21.9, 18.1 ppm; HRMS (ESI) exact mass calculated for $[M+Na]$ ($C_{16}H_{18}F_2NaO$) requires m/z 287.1218, found m/z 287.1215.

***tert*-butyl ((4*bRS*,8*aRS*)-7-formyl-4*b*-methyl-4*b*,5,6,7,8,8*a*,9,10-octahydrophenanthren-3-yl)carbamate (3.74)**



Prepared according to general procedure H from polyene **3.67** (26 mg, 0.10 mmol). The reaction was run for 5 h and product **3.74** was isolated as a colourless oil (10 mg, 0.029 mmol, 40% yield, *trans*- $\beta:\alpha$ 1:1). IR (Film) 3055, 2930, 2862, 1723, 1690, 1123 cm^{-1} ; 1H NMR (500 MHz, $CDCl_3$) $\delta = 9.71$ (s, 0.5H), 9.69 (d, $J = 1.4$ Hz, 0.5H), 7.12 – 6.91 (m, 3H), 6.43 – 6.33 (m, 1H), 2.89 – 2.75 (m, 1H), 2.51 – 2.46 (m, 0.5H), 2.40 – 2.31 (m, 1H), 2.29 – 2.10 (m, 2H), 2.07 – 1.88 (m, 2H), 1.79 – 1.57 (m, 3.5H), 1.51 (s, 4.5H), 1.50 (s, 4.5H), 1.46 – 1.35 (m, 2H), 1.10 (s, 1.5H), 1.07 (s, 1.5H) ppm; ^{13}C NMR (125 MHz, $CDCl_3$) δ 205.6, 204.5, 147.9, 147.9, 136.1, 136.1, 129.9, 129.8, 129.1, 129.0, 119.9, 119.0, 116.7, 115.3, 80.52, 80.4, 50.7, 46.6, 41.4, 38.6, 37.0, 36.8, 36.7, 36.7, 34.6, 28.8, 28.7, 28.5, 28.5, 27.6, 25.8, 25.7, 22.0, 21.6, 21.1, 20.9 ppm; HRMS (ESI) exact mass calculated for $[M+Na]$ ($C_{21}H_{29}NNaO_3$) requires m/z 366.20396, found m/z 366.20330.

(4aRS,10aRS)-6,7,8-trimethoxy-4a-methyl-1,2,3,4,4a,9,10,10a-octahydrophenanthrene-2-carbaldehyde (2.64)

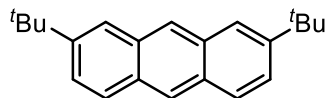


Prepared according to general procedure E from polyene **2.50** (25 mg, 0.078 mmol) in 2% HFIP/DCM as a solvent. The reaction was run for 4 h and product **2.64** was isolated as a colourless oil (20. mg, 0.064 mmol, 81% yield, *trans*- β : α 4:1).

Prepared according to general procedure H from **2.50** (25 mg, 0.078 mmol). The reaction was run for 5 h and product **2.64** was isolated as a colourless oil (16 mg, 0.051 mmol, 64% yield, *trans*- β : α 2:1).

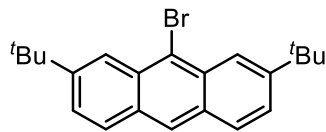
5.4. Experimental Procedures from Chapter 4

2,7-di-*tert*-butylanthracene (4.2)



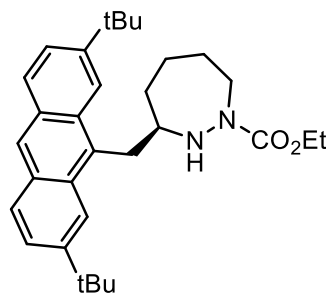
Following the procedure of Schmidbaur,²⁹ to a solution of anthracene (3.02 g, 16.8 mmol) in CHCl₃ (15 mL) was added *tert*-butyl chloride (5.3 mL, 48.7 mmol), then AlCl₃ (120 mg, 0.90 mmol). The solution was brought to reflux and let stir for 17 h. The reaction was then cooled and washed with water (2 x 3 mL). Solvent was evaporated and solid was redissolved in DCM and filtered. The solids were collected and recrystallized from hexanes to provide 2,7-di-*tert*-butylanthracene as white needle-like crystals (1.43 g, 4.9 mmol, 29% yield). Spectroscopic data were in accordance with previously reported literature.²⁹

9-bromo-2,7-di-*tert*-butylanthracene (4.3)



To a solution of 2,7-di-*tert*-butylanthracene (658 mg, 2.3 mmol) in CHCl_3 (20 mL) was added FeCl_3 (24 mg, 0.11 mmol) and NBS (136 mg, 0.78 mmol). The solution was brought to reflux and let stir for 30 minutes. NBS (136 mg, 0.78 mmol) was added, and the solution was let stir for 30 minutes. NBS (136 mg, 0.78 mmol) was added, and the solution was let stir for 2 h before it was cooled to room temperature. Solvent was evaporated and the crude solid was washed with MeOH. Crude product was recrystallized from EtOH to provide 9-bromo-2,7-di-*tert*-butylanthracene as yellow needle-like crystals (274 mg, 0.74 mmol, 33% yield). Spectroscopic data were in accordance with previously reported literature.³⁰

ethyl (*R*)-3-((2,7-di-*tert*-butylanthracen-9-yl)methyl)-1,2-diazepane-1-carboxylate (4.4)

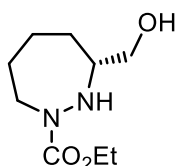


Following the procedure of Furkert *et al.*²²: To a stirred solution of $\text{Cu}(\text{OAc})_2$ (35 mg, 0.19 mmol) in AcOH (1.0 mL) was added Zn dust (350 mg, 5.3 mmol) at 100 °C. After 2 minutes, the solvent was cannulated off and the solid was washed with AcOH (2 x 1.0 mL) and Et_2O (3 x 1.0 mL). Remaining solvent was removed under high vacuum. To the dry solid was added di-*tert*-butyl (*R*)-3-(iodomethyl)-1,2-diazepane-1,2-dicarboxylate (392 mg, 0.89 mmol) in toluene/NMP (1.4 mL/0.4 mL). The solution was brought to 60 °C and let stir for 1 h. The reaction was let cool until the solid was settled. Then the solvent was cannulated into a flask containing $\text{Pd}(\text{dba})_2$ (32 mg, 0.056 mmol), RuPhos (49 mg, 0.10 mmol) and 9-bromo-2,7-di-*tert*-butylanthracene (193 mg, 0.52 mmol). The reaction was brought to 100 °C and let stir for 16 h. The reaction was then let cool, quenched with water, and extracted with EtOAc. The combined extracts were washed with brine,

dried with Na₂SO₄, filtered, concentrated, and purified by flash chromatography (gradient from 95:5 to 85:15 hexane/EtOAc) to give a yellow oil.

To a solution of the isolated mixture (48 mg) in DCM (800 μL) was added TFA (60 μL) at 0 °C. The solution was brought to room temperature and let stir for 4 h, then the solvent was removed under reduced pressure. The resulting red oil was redissolved in DCM (800 μL) and brought to 0 °C. EtO₂CCl (5 μL, 0.052 mmol), then Et₃N (30 μL, 0.22 mmol) were added and the reaction was let stir for 1 h. The reaction was then quenched with saturated NaHCO₃ and extracted with DCM. The combined extracts were washed with brine, dried with Na₂SO₄, filtered, concentrated, and purified by flash chromatography (gradient from 90:10 to 70:30 hexanes/EtOAc). Product **4.4** was isolated as a yellow oil (9.6 mg, 0.088 mmol, 29% yield over 3 steps). IR (Film) ν = 2960, 2866, 1699, 1629, 1455, 1381, 1259, 1200, 1057 cm⁻¹; ¹H NMR (500 MHz, CDCl₃) δ = 8.27 (s, 1 H), 8.01 (s, 2 H), 7.91 (d, J = 9.1 Hz, 2 H), 7.53 (d, J = 9.1 Hz, 2 H), 5.78 (s, 1 H), 5.20 (s, 1 H), 4.21 – 4.06 (m, 3 H), 3.37 – 3.34 (m, 2 H), 2.61 – 2.58 (m, 2 H), 1.66 – 1.52 (m, 4 H), 1.42 (s, 18 H), 1.28 – 1.20 (m, 3 H) ppm; ¹³C NMR (125 MHz, CDCl₃) δ = 156.2, 147.1, 137.8, 129.7, 128.8, 124.6, 124.1, 120.5, 116.8, 116.6, 62.3, 62.0, 61.7, 50.2, 38.6, 35.1, 29.7, 27.7, 25.3, 14.7, 14.4 ppm; HRMS (ESI) exact mass calculated for [M+Na] (C₃₁H₄₂N₂NaO₂) requires m/z 497.3138, found m/z 497.3145.

ethyl (*R*)-3-(hydroxymethyl)-1,2-diazepane-1-carboxylate (**4.7**)

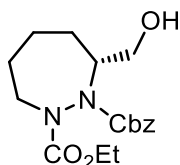


A stirred solution of dibenzyl (*R*)-3-(hydroxymethyl)-1,2-diazepane-1,2-dicarboxylate (1.5040 g, 3.8 mmol) in MeOH (40 mL) was submitted to three cycles of vacuum/argon. AcCl (1.1 mL, 15.2 mmol) and 10% Pd/C (454 mg, 0.43 mmol) were added. Argon flow was removed, and a needle attached to a hydrogen-filled balloon was inserted through the septum and into the reaction mixture. A second needle was inserted through the septum to allow gas efflux and the hydrogen was allowed to bubble through the mixture, with the balloon being refilled as needed. After 1 h, the balloon was removed and the mixture was filtered through diatomaceous earth, rinsing with MeOH. The filtrate was concentrated to give crude (*R*)-(1,2-diazepan-3-yl)methanol

hydrochloride as a yellow solid. (Note: benzyloxycarbonyl removal is performed under acidic conditions as the unprotected freebase is highly unstable to air oxidation.)

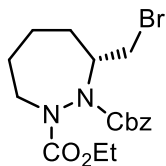
To a stirred suspension of crude (*R*)-(1,2-diazepan-3-yl)methanol in DCM (4.5 mL) at 0 °C was added Et₃N (1.6 mL, 11.4 mmol) and EtO₂CCl (340 μL, 3.6 mmol). After 1 h, saturated aqueous NaHCO₃ was added, and the mixture was extracted with DCM (3 x 5 mL). The combined extracts were washed with water, dried with MgSO₄, filtered, concentrated, and purified by flash chromatography (gradient from 70:30 to 20:80 hexanes/EtOAc). Product **4.7** was isolated as a colourless oil (582 mg, 2.9 mmol, 76% yield over two steps). IR (Film) ν = 3430, 3329, 2981, 2928, 2864, 1672, 1410, 1380, 1211, 1096, 1034 cm⁻¹; ¹H NMR (500 MHz, CDCl₃) δ = 4.93 (bs, 1 H), 4.17 (q, *J* = 7.5 Hz, 2 H), 3.73 – 3.70 (m, 1 H), 3.49 (bs, 2 H), 3.37 – 3.32 (m, 2 H), 3.03 (bs, 1 H), 1.80 – 1.61 (m, 5 H), 1.28 (t, *J* = 7.6 Hz, 3 H), 1.22 – 1.20 (m, 1 H) ppm; ¹³C NMR (125 MHz, CDCl₃) δ = 157.7, 156.7, 64.0, 61.8, 61.4, 49.2, 30.7, 28.1, 27.4, 23.7, 14.4 ppm; HRMS (ESI) exact mass calculated for [M+Na] (C₉H₁₈N₂NaO₃) requires *m/z* 225.1210, found *m/z* 225.1200.

2-benzyl 1-ethyl (*R*)-3-(hydroxymethyl)-1,2-diazepane-1,2-dicarboxylate (**4.8**)



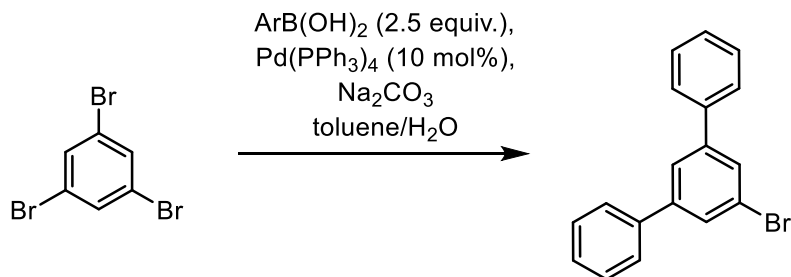
To a stirred solution of ethyl (*R*)-3-(hydroxymethyl)-1,2-diazepane-1-carboxylate (582 mg, 2.9 mmol) and NaHCO₃ (874 mg, 10.4 mmol) in CHCl₃ (30 mL) was added benzyl chloroformate (0.020 mL, 0.21 mmol). After 19 h, the reaction was quenched with water and extracted with DCM (3 x 30 mL). The combined extracts were dried with MgSO₄, filtered, concentrated, and purified by flash chromatography (gradient from 70:30 to 90:10 hexanes/EtOAc) to give product **4.8** (947 mg, 2.8 mmol, 95% yield) as a colourless oil. IR (Film) ν = 3429, 2935, 1693, 1320, 1212, 1051 cm⁻¹; ¹H NMR (500 MHz, CDCl₃) δ 7.36 – 7.28 (m, 5 H), 5.29 – 5.12 (m, 2 H), 4.27 – 4.13 (m, 3 H), 4.12 – 3.87 (m, 2 H), 3.74 – 3.36 (m, 2 H), 3.11 – 2.92 (m, 1 H), 1.88 – 1.40 (m, 6 H), 1.32 – 1.11 (m, 3H) ppm; ¹³C NMR (125 MHz, CDCl₃) δ 158.1, 157.5, 155.0, 155.0, 136.0, 135.7, 68.0, 67.6, 63.1, 63.0, 62.9, 62.8, 61.5, 61.3, 50.8, 49.7, 28.5, 28.4, 28.2, 27.9, 24.6, 24.3, 14.3, 14.2, 14.0 ppm; HRMS (ESI) exact mass calculated for [M+Na] (C₁₇H₂₄N₂NaO₅) requires *m/z* 359.1577, found *m/z* 359.1577.

2-benzyl 1-ethyl (*R*)-3-(bromomethyl)-1,2-diazepane-1,2-dicarboxylate (**4.9**)



To a stirred solution of PPh_3 (357 mg, 1.4 mmol) in THF (10 mL) at 0 °C was added CBr_4 (412 mg, 1.2 mmol). After 15 minutes, 2-benzyl 1-ethyl (*R*)-3-(hydroxymethyl)-1,2-diazepane-1,2-dicarboxylate (325 mg, 0.97 mmol) was added in THF (5 mL). The solution was brought to room temperature and stirred for 17 h. The reaction was quenched with the addition of saturated aqueous NaHCO_3 and extracted with EtOAc (3 x 10 mL). The combined extracts were washed with brine, dried with Na_2SO_4 , filtered, concentrated, and purified by flash chromatography (gradient from 90:10 to 80:20 hexanes/EtOAc). Product **4.9** was isolated as a colourless oil (367 mg, 0.92 mmol, 95% yield). IR (Film) $\nu = 2934, 2857, 1705, 1350, 1229, 1210, 1078 \text{ cm}^{-1}$; $^1\text{H NMR}$ (400 MHz, CDCl_3) $\delta = 7.37 - 7.28$ (m, 5 H), 5.30 – 5.07 (m, 2 H), 4.30 – 3.90 (m, 4 H), 3.85 – 3.54 (m, 1 H), 3.33 – 3.14 (m, 1 H), 3.02 – 2.81 (m, 1 H), 2.56 – 2.34 (m, 1 H), 1.95 – 1.88 (m, 1 H), 1.70 – 1.50 (m, 2 H), 1.40 – 1.29 (m, 2 H), 1.29 – 1.04 (m, 3H) ppm; $^{13}\text{C NMR}$ (100 MHz, CDCl_3) $\delta = 156.2, 156.1, 155.9, 155.7, 154.7, 154.6, 154.2, 154.0, 135.9, 135.8, 135.7, 135.6, 128.4, 128.4, 128.3, 128.3, 128.1, 128.1, 127.8, 127.7, 127.6, 127.3, 68.0, 68.0, 67.6, 62.4, 62.4, 62.2, 61.6, 61.2, 61.1, 60.7, 51.0, 50.4, 50.0, 49.4, 34.2, 33.7, 33.6, 33.3, 30.3, 30.0, 29.8, 29.6, 28.5, 28.3, 28.2, 28.0, 24.4, 24.3, 14.4, 14.4, 14.2, 14.2$ ppm; HRMS (ESI) exact mass calculated for $[\text{M}+\text{Na}]$ ($\text{C}_{17}\text{H}_{23}\text{BrN}_2\text{NaO}_4$) requires m/z 421.0733, found m/z 421.0734.

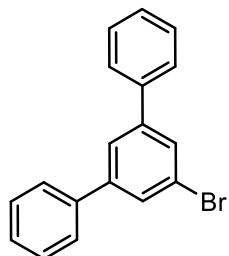
Synthesis of *m*-terphenyls (general procedure I)



Toluene and 1M aqueous Na_2CO_3 were degassed by bubbling argon through for 1 h. To a solution of 1,3,5-tribromobenzene (1 mmol) and aryl boronic acid (2.2-2.5 mmol) in toluene (4 mL) was added $\text{Pd}(\text{PPh}_3)_4$ (0.1 mmol) then 1 M aqueous Na_2CO_3 (3.0 mL). The solution was brought to

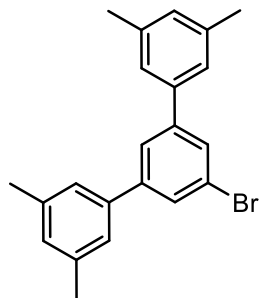
reflux and let stir for 17 h before it was cooled, diluted with water and extracted with DCM (3 x 10 mL). The combined extracts were washed with brine, dried with MgSO₄, filtered, concentrated, and purified by flash chromatography (hexanes).

5'-bromo-1,1':3',1''-terphenyl (5.17)



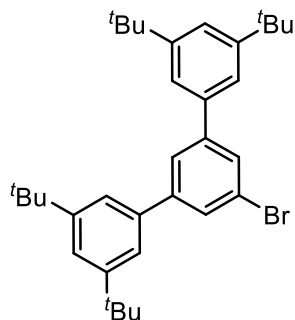
From phenylboronic acid (695 mg, 5.6 mmol), general procedure I was followed to give, after flash chromatography (hexanes), product **5.17** (227 mg, 0.44 mmol, 18% yield) as a white foam. Spectroscopic data were in accordance with previously reported literature.³¹

5'-bromo-3,3',5,5''-tetramethyl-1,1':3',1''-terphenyl (5.18)



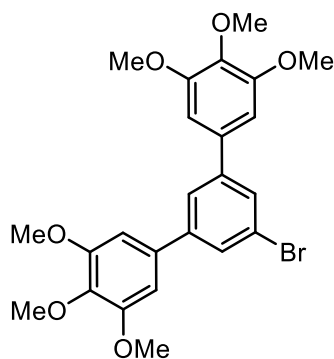
From 3,5-dimethylphenylboronic acid (741 mg, 4.9 mmol), general procedure I was followed to give, after flash chromatography (hexanes), product **5.18** (347 mg, 0.95 mmol, 43% yield) of a white foam. Spectroscopic data were in accordance with previously reported literature.³²

5'-bromo-3,3'',5,5''-tetra-*tert*-butyl-1,1':3',1''-terphenyl (5.19)



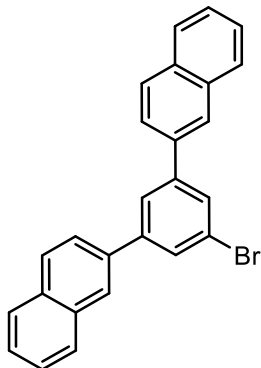
From 3,5-*tert*-butylphenylboronic acid (458 mg, 1.9 mmol), general procedure I was followed to give, after flash chromatography (hexanes), product **5.19** (187 mg, 0.35 mmol, 37% yield) as a white foam. Spectroscopic data were in accordance with previously reported literature.³³

5'-bromo-3,3'',4,4'',5,5''-hexamethoxy-1,1':3',1''-terphenyl (5.20)



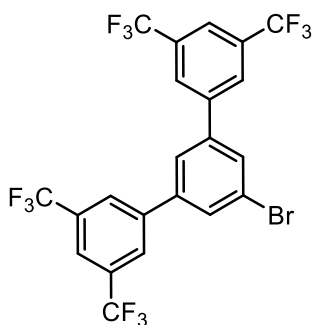
From (3,4,5-trimethoxyphenyl)boronic acid (144 mg, 0.68 mmol), general procedure I was followed to give, after flash chromatography (90:10 to 70:30 hexanes/EtOAc), product **5.20** (70 mg, 0.15 mmol, 74% yield) as a white foam. IR (Film) $\nu = 3050, 2935, 2838, 1718, 1508, 1407, 1344, 1124, 1006 \text{ cm}^{-1}$; $^1\text{H NMR}$ (500 MHz, CDCl_3) $\delta = 7.64$ (s, 2 H), 7.59 (s, 1 H), 6.76 (s, 4 H), 3.93 (s, 12 H), 3.90 (s, 6 H) ppm; $^{13}\text{C NMR}$ (125 MHz, CDCl_3) $\delta = 153.6, 143.9, 138.2, 135.6, 128.9, 124.8, 123.0, 104.6, 61.0, 56.3$ ppm; HRMS (ESI) exact mass calculated for $[\text{M}+\text{Na}]$ ($\text{C}_{24}\text{H}_{25}\text{BrNaO}_6$) requires m/z 511.07267, found m/z 511.07275.

2,2'-(5-bromo-1,3-phenylene)dinaphthalene (5.21)



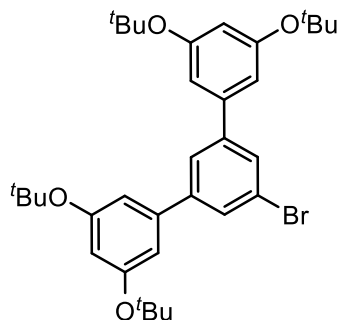
From 2-naphthylboronic acid (493 mg, 2.9 mmol), general procedure I was followed to give, after flash chromatography (98:2 to 95:5 hexanes/EtOAc), product **5.21** (123 mg, 0.30 mmol, 25% yield) as a white foam. Spectroscopic data were in accordance with previously reported literature.³⁴

5'-bromo-3,3'',5,5''-tetrakis(trifluoromethyl)-1,1':3',1''-terphenyl (5.22)



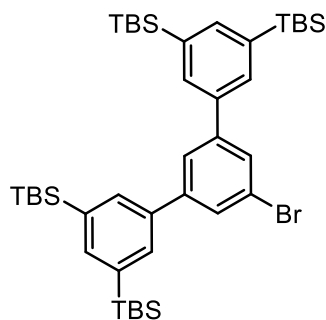
From 3,5-bis(trifluoromethyl)phenylboronic acid (999 mg, 3.9 mmol), general procedure I was followed to give, after flash chromatography (hexanes), product **5.22** (252 mg, 0.43 mmol, 43% yield) as a white foam. Spectroscopic data were in accordance with previously reported literature.³⁵

5'-bromo-3,3',5,5''-tetra-*tert*-butoxy-1,1':3',1''-terphenyl (5.23)



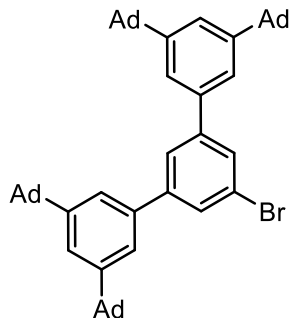
From (3,5-di-*tert*-butoxyphenyl)boronic acid (710 mg, 2.6 mmol), general procedure I was followed to give, after flash chromatography (98:2 to 90:10 hexanes/EtOAc), product **5.23** (182 mg, 0.30 mmol, 28% yield) as a white foam. IR (Film) $\nu = 2975, 2932, 2873, 1582, 1474, 1389, 1365, 1174, 1130, 1012 \text{ cm}^{-1}$; $^1\text{H NMR}$ (500 MHz, CDCl_3) $\delta = 7.64$ (d, $J = 1.5 \text{ Hz}$, 2 H), 7.61 (t, $J = 1.3 \text{ Hz}$, 1 H), 6.97 (d, $J = 2.0 \text{ Hz}$, 4 H), 6.70 (t, $J = 2.0 \text{ Hz}$, 2 H), 1.39 (s, 36 H) ppm; $^{13}\text{C NMR}$ (125 MHz, CDCl_3) $\delta = 156.2, 143.2, 140.3, 128.9, 124.7, 123.0, 119.5, 118.3, 78.9, 28.9$ ppm; HRMS (ESI) exact mass calculated for $[\text{M}+\text{H}]$ ($\text{C}_{34}\text{H}_{46}\text{BrO}_4$) requires m/z 597.25740, found m/z 597.25857.

(5'-bromo-[1,1':3',1''-terphenyl]-3,3',5,5''-tetrayl)tetrakis(*tert*-butyldimethylsilane) (5.24)



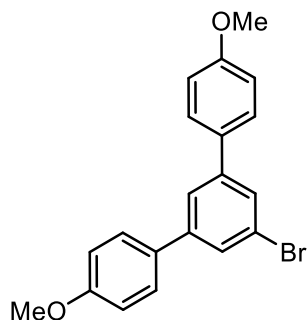
From (3,5-bis(*tert*-butyldimethylsilyl)phenyl)boronic acid (717 mg, 2.0 mmol), general procedure I was followed to give, after flash chromatography (hexanes), product **5.24** (166 mg, 0.22 mmol, 26% yield) as a white foam. IR (Film) $\nu = 3026, 2952, 2927, 2884, 2955, 1470, 1249, 860, 767 \text{ cm}^{-1}$; $^1\text{H NMR}$ (500 MHz, CDCl_3) $\delta = 7.72 - 7.70$ (m, 9 H), 0.93 (s, 36 H), 0.35 (s, 24 H) ppm; $^{13}\text{C NMR}$ (125 MHz, CDCl_3) $\delta = 144.5, 140.4, 137.8, 137.2, 133.7, 128.8, 125.6, 123.2, 26.5, 16.9, -6.2$ ppm.

1,1',1'',1'''-(5'-bromo-[1,1':3',1''-terphenyl]-3,3'',5,5''-tetrayl)tetrakis(adamantane) (5.25)



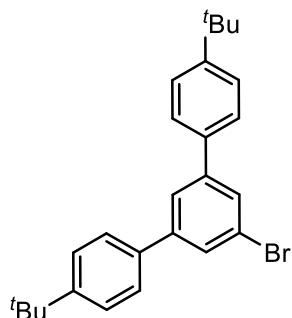
From (3,5-di((3*R*,5*R*,7*R*)-adamantan-1-yl)phenyl)boronic acid (732 mg, 1.9 mmol), general procedure I was followed to give, after flash chromatography (hexanes), product **5.25** (489 mg, 0.58 mmol, 62% yield) as a white foam. IR (Film) $\nu = 3062, 2900, 2847, 1589, 1449, 1344, 1103$ cm^{-1} ; $^1\text{H NMR}$ (500 MHz, CDCl_3) $\delta = 7.69$ (s, 1 H), 7.66 (s, 2 H), 7.44 (s, 2 H), 7.39 (s, 4 H), 2.12 (s, 12 H), 2.00 (s, 24 H), 1.80 (s, 24 H) ppm; $^{13}\text{C NMR}$ (125 MHz, CDCl_3) $\delta = 151.6, 145.1, 139.6, 128.9, 127.4, 125.8, 121.6, 121.2, 43.3, 36.8, 29.0$ ppm; HRMS (APCI) exact mass calculated for $[\text{M}+\text{H}]$ ($\text{C}_{58}\text{H}_{70}\text{Br}$) requires m/z 845.46554, found m/z 845.46425.

5'-bromo-4,4''-dimethoxy-1,1':3',1''-terphenyl (5.26)



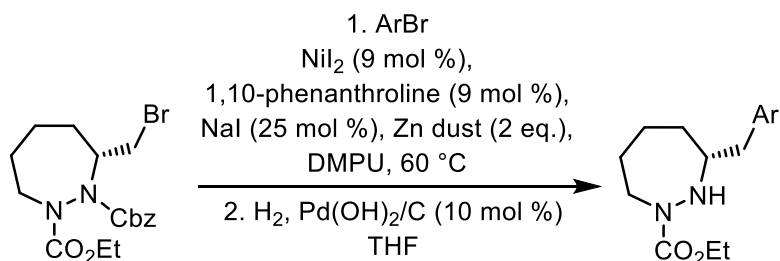
From (4-methoxyphenyl)boronic acid (510 mg, 3.4 mmol), general procedure I was followed to give, after flash chromatography (95:5 to 85:15 hexanes/EtOAc), product **5.26** (104 mg, 0.28 mmol, 30% yield) as a white foam. Spectroscopic data were in accordance with previously reported literature.³⁶

5'-bromo-4,4''-di-*tert*-butyl-1,1':3',1''-terphenyl (5.27)



From (4-(*tert*-butyl)phenyl)boronic acid (732 mg, 4.1 mmol), general procedure I was followed to give, after flash chromatography (hexanes), product **5.27** (326 mg, 0.77 mmol, 47% yield) of a white foam. Spectroscopic data were in accordance with previously reported literature.³⁷

Synthesis of *m*-terphenyl catalysts (general procedure J)

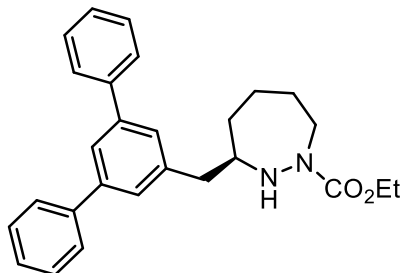


Following a modified procedure of Weix *et al.*²⁵: To a 1 mL HPLC vial containing bromo-*m*-terphenyl (0.25 mmol), NiI₂ (0.025 mmol), 1,10-phenanthroline (0.025 mmol), and NaI (0.063 mmol) was added a solution of 2-benzyl 1-ethyl (*R*)-3-(bromomethyl)-1,2-diazepane-1,2-dicarboxylate (0.25 mmol) in DMPU (1 mL). Zn dust (0.50 mmol) was added, vial was capped, and the solution was brought to 60 °C. After 72 h, the reaction was purified by flash chromatography (gradient from 95:5 to 85:15 hexanes/EtOAc) to give coupled product which was isolated as a mixture with the dehalogenated hydrazide.

A stirred solution of the isolated mixture in THF (2.0 mL) was submitted to three cycles of vacuum/argon and 10% Pd(OH)₂/C (0.050 mmol) was added. Argon flow was removed, and a needle attached to a hydrogen-filled balloon was inserted through the septum and into the reaction mixture. A second needle was inserted through the septum to allow gas efflux and the hydrogen was allowed to bubble through the mixture, with the balloon being refilled as needed. After 6 h, the balloon was removed and the mixture was filtered through diatomaceous earth, rinsing with

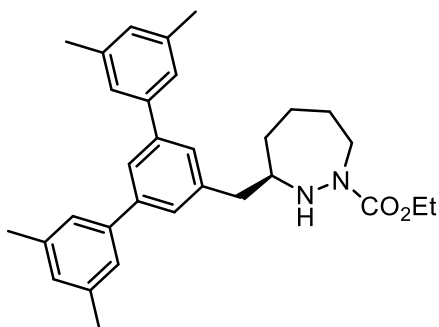
DCM. The filtrate was concentrated and purified by flash chromatography (gradient from 80:20 to 50:50 hexanes/EtOAc) to give desired product.

ethyl (*R*)-3-([1,1':3',1''-terphenyl]-5'-ylmethyl)-1,2-diazepane-1-carboxylate (4.5)



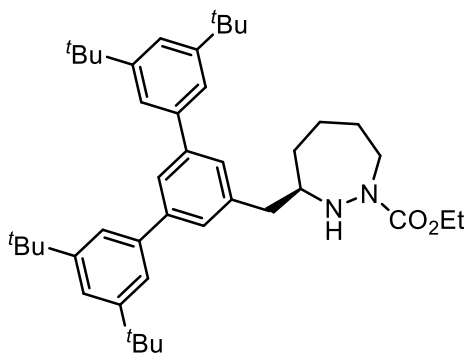
Prepared according to general procedure J from 5'-bromo-1,1':3',1''-terphenyl (82 mg, 0.26 mmol). Product **4.5** was isolated as a colourless oil (22 mg, 0.053 mmol, 22% yield). IR (Film) $\nu = 3325, 2058, 3033, 2927, 2854, 1688, 1596, 1261, 1028 \text{ cm}^{-1}$; $^1\text{H NMR}$ (500 MHz, CDCl_3) $\delta = 7.68 - 7.64$ (m, 5 H), $7.48 - 7.44$ (m, 6 H), $7.38 - 7.36$ (t, $J = 7.5 \text{ Hz}$, 2 H), 4.62 (bs, 1 H), 4.15 (bs, 1 H), 3.82 (bs, 2 H), $3.39 - 3.14$ (m, 2 H), $2.93 - 2.65$ (m, 2 H), $1.84 - 1.76$ (m, 4 H), $1.42 - 1.26$ (m, 3 H), 0.84 (bs, 2 H) ppm; $^{13}\text{C NMR}$ (125 MHz, CDCl_3) $\delta = 156.8, 156.0, 142.0, 141.0, 139.6, 128.8, 127.4, 127.2, 127.1, 124.3, 62.1, 61.3, 60.5, 48.3, 47.4, 41.2, 37.1, 35.0, 27.5, 26.9, 23.8, 14.4$ ppm; $^1\text{H NMR}$ (400 MHz, DMSO-d_6 , $80 \text{ }^\circ\text{C}$) $\delta = 7.75 - 7.72$ (m, 5 H), $7.51 - 7.46$ (m, 6 H), 7.38 (t, $J = 7.2 \text{ Hz}$, 2 H), 4.82 (s, 1 H), 3.95 (q, $J = 6.6 \text{ Hz}$, 2 H), $3.73 - 3.66$ (m, 1 H), $3.26 - 3.18$ (m, 2 H), $2.83 - 2.73$ (m, 2 H), $1.81 - 1.67$ (m, 4 H), $1.41 - 1.35$ (m, 2 H), 1.05 (t, $J = 6.6 \text{ Hz}$, 3 H) ppm; $^{13}\text{C NMR}$ (100 MHz, DMSO-d_6 , $80 \text{ }^\circ\text{C}$) $\delta = 155.4, 140.6, 140.0, 139.9, 128.3, 127.0, 126.5, 126.3, 122.6, 60.2, 47.9, 40.0, 34.5, 26.6, 23.0, 13.9$ ppm; HRMS (ESI) exact mass calculated for $[\text{M}+\text{Na}]$ ($\text{C}_{27}\text{H}_{30}\text{N}_2\text{NaO}_2$) requires m/z 437.2199, found m/z 437.2200.

ethyl (*R*)-3-((3,3'',5,5''-tetramethyl-[1,1':3',1''-terphenyl]-5'-yl)methyl)-1,2-diazepane-1-carboxylate (4.12)



Prepared according to general procedure J from 5'-bromo-3,3'',5,5''-tetramethyl-1,1':3',1''-terphenyl (94 mg, 0.26 mmol). Product **4.12** was isolated as a colourless oil (38 mg, 0.080 mmol, 31% yield). IR (Film) $\nu = 2927, 2865, 1696, 1593, 1447, 1408, 1380, 1336, 1212, 1112, 1025 \text{ cm}^{-1}$; $^1\text{H NMR}$ (500 MHz, CDCl_3) $\delta = 7.65$ (s, 1 H), 7.41 (s, 2 H), 7.28 (s, 4 H), 7.02 (s, 2 H), 4.89 – 4.50 (m, 1 H), 4.18 (bs, 1 H), 3.85 (bs, 2 H), 3.41 – 3.15 (m, 2 H), 2.89 – 2.64 (m, 2 H), 2.41 (s, 12 H), 1.95 – 1.69 (m, 4 H), 1.47 – 1.24 (m, 3 H), 0.87 (bs, 2 H) ppm; $^{13}\text{C NMR}$ (125 MHz, CDCl_3) $\delta = 156.8, 156.0, 142.0, 141.1, 139.3, 138.2, 129.0, 126.9, 125.1, 124.3, 62.2, 61.3, 60.4, 48.2, 47.4, 41.2, 37.1, 34.9, 27.5, 27.1, 26.9, 23.8, 23.5, 21.4, 14.7, 14.4$ ppm; HRMS (ESI) exact mass calculated for $[\text{M}+\text{Na}]$ ($\text{C}_{31}\text{H}_{38}\text{N}_2\text{NaO}_2$) requires m/z 493.2825, found m/z 493.2822.

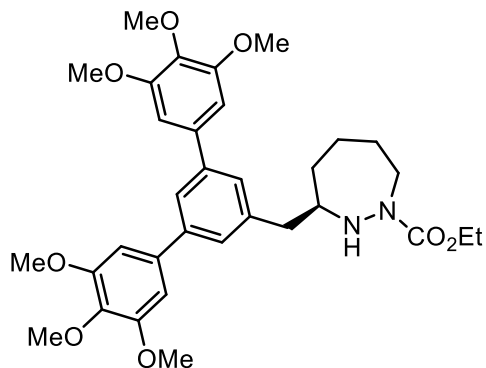
ethyl (R)-3-((3,3'',5,5''-tetra-*tert*-butyl-[1,1':3',1''-terphenyl]-5'-yl)methyl)-1,2-diazepane-1-carboxylate (4.13)



Prepared according to general procedure J from 5'-bromo-3,3'',5,5''-tetra-*tert*-butyl-1,1':3',1''-terphenyl (171 mg, 0.32 mmol). Product **4.13** was isolated as a colourless oil (65 mg, 0.10 mmol, 37% yield). IR (Film) $\nu = 2962, 2865, 1697, 1590, 1476, 1464, 1408, 1248, 1111 \text{ cm}^{-1}$; $^1\text{H NMR}$ (500 MHz, CDCl_3) $\delta = 7.64$ (bs, 1 H), 7.47 – 7.46 (m, 6 H), 7.39 (bs, 2 H), 4.66 (bs, 1 H), 4.16 (bs, 1 H), 3.84 (bs, 2 H), 3.44 – 3.24 (m, 2 H), 2.89 – 2.67 (m, 2 H), 1.85 – 1.77 (m, 4 H), 1.43 – 1.40 (m, 39 H), 0.87 (bs, 2 H) ppm; $^{13}\text{C NMR}$ (125 MHz, CDCl_3) $\delta = 156.8, 156.0, 151.2, 143.3, 140.8, 139.2, 127.2, 125.2, 121.9, 121.6, 62.2, 61.2, 60.1, 48.2, 47.4, 41.1, 37.1, 35.0, 31.5, 27.6, 26.9, 23.8, 14.6$ ppm; $^1\text{H NMR}$ (400 MHz, $\text{DMSO-d}_6, 80 \text{ }^\circ\text{C}$) $\delta = 7.58$ (s, 1 H), 7.47 – 7.46 (m, 4 H), 7.45 – 7.43 (m, 4 H), 4.80 (s, 1 H), 3.97 (q, $J = 7.5 \text{ Hz}$, 2 H), 3.74 – 3.67 (m, 1 H), 3.28 (bs, 1 H), 3.23 – 3.17 (m, 1 H), 2.85 – 2.73 (m, 2 H), 1.82 – 1.65 (m, 4 H), 1.42 – 1.37 (m, 38 H), 1.06 (t, $J = 7.5 \text{ Hz}$, 3 H) ppm; $^{13}\text{C NMR}$ (100 MHz, $\text{DMSO-d}_6, 80 \text{ }^\circ\text{C}$) $\delta = 155.4, 150.5, 141.9, 139.8, 139.5, 126.3, 123.4, 120.8, 120.6, 60.2, 60.0, 47.8, 40.0, 34.7, 34.2, 30.9, 26.6, 23.0, 14.0$ ppm;

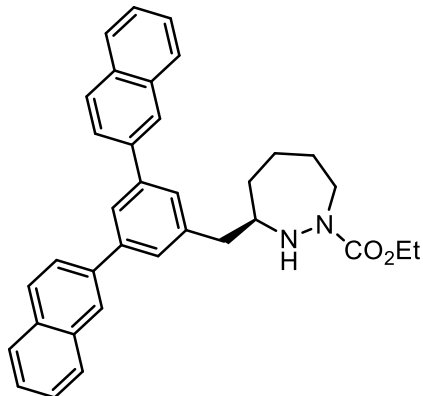
HRMS (ESI) exact mass calculated for $[M+Na]$ ($C_{43}H_{62}N_2NaO_2$) requires m/z 661.4703, found m/z 661.4710.

ethyl **(R)-3-((3,3'',4,4'',5,5''-hexamethoxy-[1,1':3',1''-terphenyl]-5'-yl)methyl)-1,2-diazepane-1-carboxylate (4.14)**



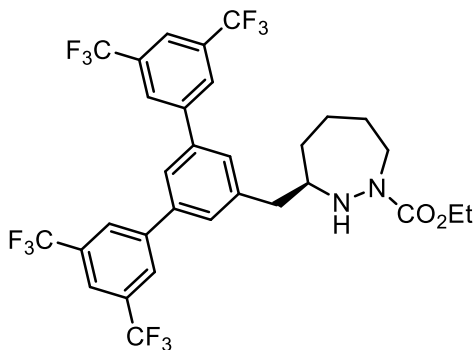
Prepared according to general procedure J from 5'-bromo-3,3'',4,4'',5,5''-hexamethoxy-1,1':3',1''-terphenyl (202 mg, 0.45 mmol). Product **4.14** was isolated as a colourless oil (42 mg, 0.071 mmol, 14% yield). IR (Film) $\nu = 2933, 2865, 1691, 1581, 1430, 1409, 1240, 1127 \text{ cm}^{-1}$; $^1\text{H NMR}$ (500 MHz, CDCl_3) $\delta = 7.54$ (s, 1 H), 7.40 (s, 2 H), 6.83 (s, 4 H), 4.71 (bs, 1 H), 4.12 (bs, 1 H), 3.94 – 3.84 (m, 20 H), 3.48 – 3.23 (m, 2 H), 2.84 – 2.67 (m, 2 H), 1.84 – 1.75 (m, 4 H), 1.45 – 1.39 (m, 2 H), 1.27 – 1.24 (m, 2 H), 0.91 (bs, 1 H) ppm; $^{13}\text{C NMR}$ (125 MHz, CDCl_3) $\delta = 156.8, 156.0, 153.5, 142.2, 139.3, 137.8, 137.2, 127.1, 124.3, 104.7, 61.9, 61.4, 60.9, 59.5, 56.3, 48.1, 47.5, 41.0, 36.9, 35.7, 27.4, 23.6, 14.6$ ppm; HRMS (ESI) exact mass calculated for $[M+Na]$ ($C_{33}H_{42}N_2NaO_8$) requires m/z 617.2833, found m/z 617.2812.

ethyl (*R*)-3-(3,5-di(naphthalen-2-yl)benzyl)-1,2-diazepane-1-carboxylate (4.15)



Prepared according to general procedure J from 2,2'-(5-bromo-1,3-phenylene)dinaphthalene (103 mg, 0.25 mmol). Product **4.15** was isolated as a colourless oil (30 mg, 0.059 mmol, 24% yield). IR (Film) $\nu = 3053, 3017, 2929, 2854, 1693, 1593, 1506, 1447, 1408, 1212, 1112 \text{ cm}^{-1}$; $^1\text{H NMR}$ (800 MHz, CDCl_3) $\delta = 8.10$ (s, 2 H), 7.92 – 7.91 (m, 5 H), 7.87 – 7.86 (m, 2 H), 7.79 (s, 2 H), 7.63 (s, 2 H), 7.52 – 7.48 (m, 4 H), 4.28 – 3.99 (m, 4 H), 3.84 – 3.46 (m, 2 H), 3.19 (bs, 1 H), 2.00 – 1.92 (m, 4 H), 1.58 (bs, 2 H), 1.28 – 1.18 (m, 3 H) ppm; $^{13}\text{C NMR}$ (200 MHz, CDCl_3) $\delta = 155.2, 153.6, 142.3, 137.9, 133.6, 132.7, 128.5, 128.2, 127.6, 127.3, 126.3, 126.0, 126.0, 125.5, 64.2, 63.6, 47.2, 38.8, 30.6, 26.6, 22.9, 14.4$ ppm; HRMS (ESI) exact mass calculated for $[\text{M}+\text{Na}]$ ($\text{C}_{35}\text{H}_{34}\text{N}_2\text{NaO}_2$) requires m/z 537.2512, found m/z 537.2534.

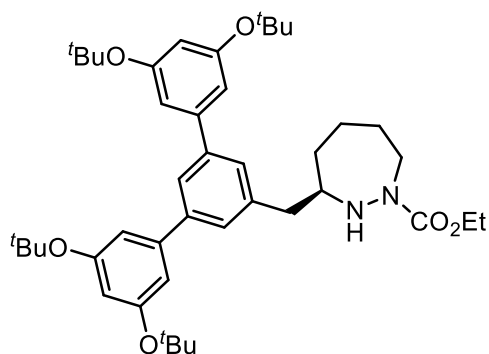
ethyl (*R*)-3-((3,3',5,5'-tetrakis(trifluoromethyl)-[1,1':3,1''-terphenyl]-5'-yl)methyl)-1,2-diazepane-1-carboxylate (4.16)



Prepared according to general procedure J from 5'-bromo-3,3',5,5'-tetrakis(trifluoromethyl)-1,1':3,1''-terphenyl (114 mg, 0.20 mmol). Product **4.16** was isolated as a colourless oil (34 mg, 0.050 mmol, 17% yield). IR (Film) $\nu = 3029, 2933, 1692, 1600, 1410, 1299, 1172, 1130 \text{ cm}^{-1}$; $^1\text{H NMR}$

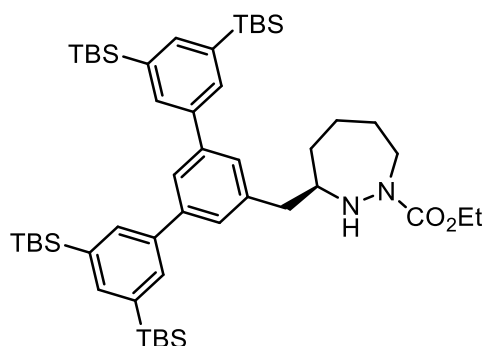
NMR (500 MHz, CDCl₃) δ = 8.13 (s, 4 H), 7.91 (s, 2 H), 7.62 (s, 3 H), 4.63 (bs, 1 H), 4.17 – 3.76 (m, 3 H), 3.55 – 3.22 (m, 2 H), 3.02 – 2.95 (m, 1 H), 2.83 – 2.75 (m, 1 H), 1.90 – 1.73 (m, 4 H), 1.50 – 1.20 (m, 4 H), 1.00 – 0.78 (m, 1 H) ppm; ¹³C NMR (125 MHz, CDCl₃) δ = 156.8, 142.8, 140.4, 139.7, 132.2 (q, J = 34.7 Hz), 128.8, 127.6, 124.5, 123.5 (q, J = 253.1 Hz), 121.3, 61.6, 59.4, 47.7, 40.7, 36.6, 27.2, 23.7, 14.6 ppm; HRMS (ESI) exact mass calculated for [M+Na] (C₃₁H₂₆F₁₂N₂NaO₂) requires m/z 709.1695, found m/z 709.1668.

ethyl (R)-3-((3,3'',5,5''-tetra-*tert*-butoxy-[1,1':3',1''-terphenyl]-5'-yl)methyl)-1,2-diazepane-1-carboxylate (4.17)



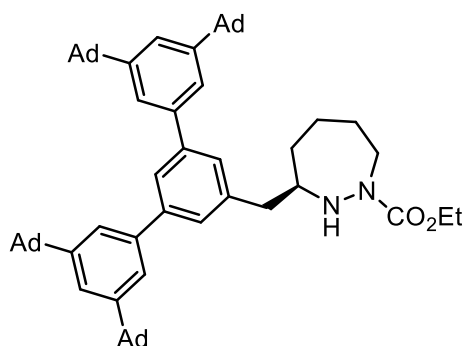
Prepared according to general procedure J from 5'-bromo-3,3'',5,5''-tetra-*tert*-butoxy-1,1':3',1''-terphenyl (169 mg, 0.28 mmol). Product **4.17** was isolated as a colourless oil (26 mg, 0.038 mmol, 13% yield). IR (Film) ν = 2975, 2929, 2873, 1694, 1579, 1259, 1036, 1012 cm⁻¹; ¹H NMR (500 MHz, CDCl₃) δ = 7.57 (s, 1 H), 7.37 (s, 2 H), 7.00 (s, 4 H), 6.67 (s, 2 H), 4.58 (bs, 1 H), 4.17 – 4.13 (m, 1 H), 3.83 (bs, 2 H), 3.40 – 3.14 (m, 2 H), 3.01 – 2.61 (m, 2 H), 1.84 – 1.75 (m, 4 H), 1.39 – 1.25 (m, 39 H), 0.86 – 0.84 (m, 2 H) ppm; ¹³C NMR (125 MHz, CDCl₃) δ = 156.7, 156.0, 141.6, 141.5, 139.6, 127.0, 124.2, 119.0, 118.4, 78.8, 62.0, 61.2, 48.2, 47.4, 41.1, 37.0, 35.2, 28.9, 27.5, 26.9, 24.0, 23.8, 14.5 ppm; HRMS (ESI) exact mass calculated for [M+Na] (C₄₃H₆₂N₂NaO₆) requires m/z 725.4500, found m/z 725.4510.

ethyl (*R*)-3-((3,3'',5,5''-tetrakis(*tert*-butyldimethylsilyl)-[1,1':3,1''-terphenyl]-5'-yl)methyl)-1,2-diazepane-1-carboxylate (4.18)



Prepared according to general procedure J from (5'-bromo-[1,1':3,1''-terphenyl]-3,3'',5,5''-tetrayl)tetrakis(*tert*-butyldimethylsilane) (224 mg, 0.29 mmol). Product **4.18** was isolated as a colourless oil (52 mg, 0.059 mmol, 22% yield). IR (Film) $\nu = 3027, 2952, 2927, 2884, 2856, 2698, 1597, 1470, 1361, 1249, 1176 \text{ cm}^{-1}$; $^1\text{H NMR}$ (500 MHz, CDCl_3) $\delta = 7.74$ (s, 4 H), 7.68 (s, 2 H), 7.62 (s, 1 H), 7.40 (s, 2 H), 4.70 – 4.57 (m, 1 H), 4.16 – 4.13 (m, 1 H), 3.92 – 3.76 (m, 2 H), 3.50 – 3.12 (m, 2 H), 2.97 – 2.66 (m, 2 H), 1.95 – 1.75 (m, 4 H), 1.48 – 1.22 (m, 3 H), 0.92 – 0.86 (m, 38 H), 0.33 (s, 24 H) ppm; $^{13}\text{C NMR}$ (125 MHz, CDCl_3) $\delta = 156.8, 156.0, 142.8, 139.8, 139.6, 139.0, 137.0, 133.8, 126.9, 125.2, 62.3, 61.2, 60.1, 48.3, 47.4, 41.1, 37.0, 35.0, 26.5, 23.8, 23.5, 16.9, 14.5, -6.2$ ppm; HRMS (ESI) exact mass calculated for $[\text{M}+\text{Na}]$ ($\text{C}_{51}\text{H}_{86}\text{N}_2\text{NaSi}_4\text{O}_2$) requires m/z 893.56586, found m/z 893.56383.

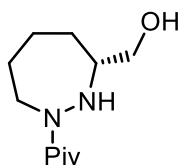
ethyl (*R*)-3-((3,3'',5,5''-tetra(adamantan-1-yl)-[1,1':3,1''-terphenyl]-5'-yl)methyl)-1,2-diazepane-1-carboxylate (4.19)



Prepared according to general procedure J from 1,1',1'',1'''-(5'-bromo-[1,1':3,1''-terphenyl]-3,3'',5,5''-tetrayl)tetrakis(1-adamantane) (198 mg, 0.23 mmol). Product **4.19** was isolated as a

colourless oil (52 mg, 0.054 mmol, 23% yield). IR (Film) ν = 2979, 2905, 2950, 1731, 1588, 1450, 1374, 1178, 1154 cm^{-1} ; ^1H NMR (500 MHz, CDCl_3) δ = 7.66 (bs, 1 H), 7.43 (s 6 H), 2.08 (s, 2 H), 4.60 (bs, 1 H), 4.16 (bs, 1 H), 3.84 (bs, 2 H), 3.44 – 3.23 (m, 2 H), 2.93 – 2.65 (m, 2 H), 2.13 (s, 12 H), 2.01 (s, 24 H), 1.83 – 1.78 (m, 28 H), 1.44 – 1.41 (m, 2 H), 1.27 – 1.25 (m, 1 H), 0.86 (s, 2 H) ppm; ^{13}C NMR (125 MHz, CDCl_3) δ = 156.8, 156.0, 151.4, 143.4, 140.9, 139.0, 127.0, 126.2, 125.4, 121.6, 120.6, 62.1, 61.3, 60.5, 48.5, 47.3, 43.3, 41.1, 36.8, 29.0, 23.8, 14.6 ppm; HRMS (APCI) exact mass calculated for $[\text{M}+\text{H}]$ ($\text{C}_{67}\text{H}_{87}\text{N}_2\text{O}_8$) requires m/z 951.67621, found m/z 951.67554.

(R)-1-(3-(hydroxymethyl)-1,2-diazepan-1-yl)-2,2-dimethylpropan-1-one (4.22)

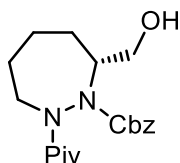


A stirred solution of dibenzyl (*R*)-3-(hydroxymethyl)-1,2-diazepane-1,2-dicarboxylate (558 mg, 1.4 mmol) in MeOH (7 mL) was submitted to three cycles of vacuum/argon. AcCl (400 μL , 5.6 mmol) and 10% Pd/C (154 mg, 0.14 mmol) were added. Argon flow was removed, and a needle attached to a hydrogen-filled balloon was inserted through the septum and into the reaction mixture. A second needle was inserted through the septum to allow gas efflux and the hydrogen was allowed to bubble through the mixture, with the balloon being refilled as needed. After 1 h, the balloon was removed and the mixture was filtered through diatomaceous earth, rinsing with MeOH. The filtrate was concentrated to give crude (*R*)-(1,2-diazepan-3-yl)methanol hydrochloride as a yellow solid. (Note: benzyloxycarbonyl removal is performed under acidic conditions as the unprotected freebase is highly unstable to air oxidation.)

To a stirred suspension of crude (*R*)-(1,2-diazepan-3-yl)methanol in DCM (7 mL) at 0 $^\circ\text{C}$ was added Et_3N (600 μL , 4.3 mmol) and PivCl (175 μL , 1.4 mmol). After 1 h, saturated aqueous NaHCO_3 was added, and the mixture was extracted with DCM (3 x 10 mL). The combined extracts were washed with water, dried with MgSO_4 , filtered, concentrated, and purified by flash chromatography (gradient from 60:40 to 80:20 hexanes/EtOAc). Product **4.22** was isolated as a colourless oil (264 mg, 1.2 mmol, 87% yield over two steps). IR (Film) ν = 3396, 3268, 2927, 2861, 1603, 1403, 1356, 1211, 989 cm^{-1} ; ^1H NMR (500 MHz, CDCl_3) δ 5.56 (bs, 1 H), 4.00 (bs, 1 H), 3.65 – 3.63 (m, 1 H), 3.42 – 3.38 (m, 2 H), 3.23 (bs, 1 H), 1.71 – 1.43 (m, 5 H), 1.14 (s, 9 H)

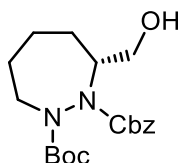
ppm; ^{13}C NMR (125 MHz, CDCl_3) δ = 178.3, 64.3, 61.5, 51.1, 38.4, 29.8, 27.8, 24.0 ppm; HRMS (ESI) exact mass calculated for $[\text{M}+\text{Na}]$ ($\text{C}_{11}\text{H}_{22}\text{N}_2\text{NaO}_2$) requires m/z 237.1573, found m/z 237.1576.

benzyl (*R*)-7-(hydroxymethyl)-2-pivaloyl-1,2-diazepane-1-carboxylate (**4.24**)



To a stirred mixture (*R*)-1-(3-(hydroxymethyl)-1,2-diazepan-1-yl)-2,2-dimethylpropan-1-one (264 mg, 1.2 mmol) and NaHCO_3 (407 mg, 4.8 mmol) in CHCl_3 (6.0 mL) was added benzyl chloroformate (600 μL , 4.2 mmol). After 19 h, reaction was quenched with H_2O and extracted with DCM (3 x 10 mL). The combined extracts were dried with MgSO_4 , filtered, concentrated, and purified by flash chromatography (gradient from 80:20 to 50:50 hexanes/ EtOAc) to give product **4.24** (429 mg, 1.2 mmol, 99% yield) as a colourless oil. IR (Film) ν = 3420, 3035, 2934, 2861, 1710, 1636, 1401, 1351, 1028 cm^{-1} ; ^1H NMR (500 MHz, CDCl_3) δ 7.31 – 7.30 (m, 5 H), 5.26 – 5.10 (m, 2 H), 4.34 – 3.99 (m, 3 H), 3.90 – 3.64 (m, 1 H), 3.32 – 3.06 (m, 2 H), 1.95 – 1.38 (m, 6 H), 1.34 (s, 3 H), 1.18 (s, 6 H) ppm; ^{13}C NMR (125 MHz, CDCl_3) δ 179.9, 179.2, 154.4, 154.1, 135.7, 135.4, 128.1, 127.9, 127.8, 127.7, 127.6, 127.1, 67.5, 67.3, 63.0, 62.6, 60.4, 60.3, 52.8, 51.8, 38.2, 38.2, 29.4, 29.2, 27.8, 27.5, 27.4, 27.2, 23.9, 23.7 ppm; HRMS (ESI) exact mass calculated for $[\text{M}+\text{Na}]$ ($\text{C}_{19}\text{H}_{28}\text{N}_2\text{NaO}_4$) requires m/z 371.1941, found m/z 371.1954.

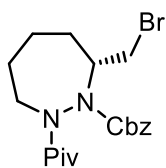
2-benzyl 1-(*tert*-butyl) (*R*)-3-(hydroxymethyl)-1,2-diazepane-1,2-dicarboxylate (**4.25**)



To a stirred mixture of *tert*-butyl (*R*)-3-(hydroxymethyl)-1,2-diazepane-1-carboxylate (251 mg, 1.1 mmol) and NaHCO_3 (341 mg, 4.0 mmol) in chloroform (5.5 mL) was added benzyl chloroformate (500 μL , 0.21 mmol). After 19 h, the reaction was quenched with H_2O and extracted with DCM (3 x 10 mL). The combined extracts were dried with MgSO_4 , filtered, concentrated, and purified by flash chromatography (gradient from 80:20 to 60:40 hexanes/ EtOAc) to give product **4.25** (390 mg, 1.1 mmol, 98% yield) as a colourless oil. IR (Film) ν = 3420, 2976, 2928,

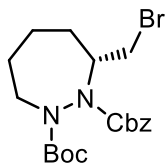
2862, 1686, 1477, 1450, 1162, 1120, 1032 cm^{-1} ; ^1H NMR (500 MHz, CDCl_3) δ 7.38 – 7.30 (m, 5 H), 5.30 – 5.11 (m, 2 H), 4.29 – 4.15 (m, 2 H), 4.10 – 3.56 (m, 2 H), 3.77 – 3.36 (m, 2 H), 3.08 – 2.84 (m, 1 H), 1.87 – 1.53 (m, 6 H), 1.42 – 1.36 (m, 9 H) ppm; ^{13}C NMR (125 MHz, CDCl_3) δ 156.8, 156.3, 154.9, 154.7, 135.8, 135.6, 128.2, 128.1, 128.0, 127.9, 127.8, 127.6, 127.6, 127.4, 127.1, 82.0, 82.0, 67.6, 67.4, 67.3, 64.0, 63.0, 62.6, 61.3, 61.2, 61.2, 50.8, 49.7, 49.4, 28.3, 28.3, 28.0, 27.8, 27.8, 27.7, 27.6, 24.5, 24.2 ppm; HRMS (ESI) exact mass calculated for $[\text{M}+\text{Na}]$ ($\text{C}_{19}\text{H}_{28}\text{N}_2\text{NaO}_5$) requires m/z 387.1890, found m/z 387.1872.

benzyl (*R*)-7-(bromomethyl)-2-pivaloyl-1,2-diazepane-1-carboxylate (4.26)



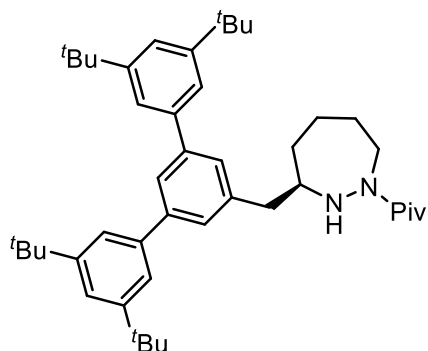
To a stirred solution of PPh_3 (522 mg, 2.0 mmol) in THF (7 mL) was added CBr_4 (611 mg, 1.8 mmol) at 0 °C. After 15 minutes, benzyl (*R*)-7-(hydroxymethyl)-2-pivaloyl-1,2-diazepane-1-carboxylate (494 mg, 1.4 mmol) was added in THF (4 mL). The solution was brought to room temperature and stirred for 15 h. The reaction was quenched with the addition of saturated NaHCO_3 and extracted with EtOAc (3 x 10 mL). The combined extracts were washed with brine, dried with Na_2SO_4 , filtered, concentrated, and purified by flash chromatography (gradient from (90:10 to 80:20 hexanes/EtOAc). Product **4.26** was isolated as a yellow oil (444 mg, 1.1 mmol, 76% yield). IR (Film) $\nu = 3034, 2933, 2859, 1709, 1660, 1398, 1304, 1024, 1012, 985 \text{ cm}^{-1}$; ^1H NMR (500 MHz, CDCl_3) $\delta = 7.34 – 7.26$ (m, 5 H), 5.21 – 5.04 (m, 2 H), 4.26 – 4.16 (m, 2 H), 3.90 – 3.77 (m, 1 H), 3.15 – 3.07 (m, 2 H), 2.54 – 2.51 (m, 1 H), 1.94 – 1.92 (m, 1 H), 1.75 – 1.72 (m, 1 H), 1.66 – 1.55 (m, 1 H), 1.43 – 1.35 (m, 1 H), 1.30 (s, 3 H), 1.24 – 1.17 (m, 1 H), 1.15 (s, 6 H) ppm; ^{13}C NMR (125 MHz, CDCl_3) $\delta = 177.7, 177.2, 154.5, 153.7, 135.6, 135.5, 128.3, 128.1, 127.9, 127.9, 127.8, 127.2, 67.7, 67.6, 61.0, 60.4, 52.8, 52.3, 38.2, 38.1, 34.8, 34.2, 29.8, 29.4, 29.1, 27.6, 27.6, 27.4, 24.0, 23.8$ ppm; HRMS (ESI) exact mass calculated for $[\text{M}+\text{H}]$ ($\text{C}_{19}\text{H}_{28}\text{BrN}_2\text{O}_3$) requires m/z 411.12778, found m/z 411.12691.

2-benzyl 1-(*tert*-butyl) (*R*)-3-(bromomethyl)-1,2-diazepane-1,2-dicarboxylate (4.27)



To a stirred solution of PPh_3 (392 mg, 1.5 mmol) in THF (7 mL) was added CBr_4 (459 mg, 1.4 mmol) at 0 °C. After 15 minutes, 2-benzyl 1-(*tert*-butyl) (*R*)-3-(hydroxymethyl)-1,2-diazepane-1,2-dicarboxylate (390 mg, 1.1 mmol) was added in THF (4 mL). The solution was brought to room temperature and stirred for 15 h. The reaction was quenched with the addition of saturated NaHCO_3 and extracted with EtOAc (3 x 10 mL). The combined extracts were washed with brine, dried with Na_2SO_4 , filtered, concentrated, and purified by flash chromatography (gradient from 90:10 to 80:20 hexanes/EtOAc). Product **4.27** was isolated as a yellow oil (383 mg, 0.90 mmol, 84% yield). IR (Film) $\nu = 3033, 2974, 2932, 2857, 1704, 1450, 1305, 1018 \text{ cm}^{-1}$; $^1\text{H NMR}$ (500 MHz, CDCl_3) $\delta = 7.38 - 7.26$ (m, 5 H), $5.32 - 5.08$ (m, 2 H), $4.27 - 4.00$ (m, 2 H), $3.86 - 3.51$ (m, 1 H), $3.40 - 3.13$ (m, 1 H), $2.96 - 2.75$ (m, 1 H), $2.53 - 2.37$ (m, 1 H), $1.98 - 1.86$ (m, 1 H), $1.67 - 1.52$ (m, 2 H), $1.50 - 1.29$ (m, 11 H) ppm; $^{13}\text{C NMR}$ (125 MHz, CDCl_3) $\delta = 154.8, 154.7, 154.6, 154.5, 135.9, 135.7, 128.4, 128.4, 18.3, 128.2, 128.0, 128.0, 128.0, 127.9, 127.8, 127.8, 127.5, 127.3, 81.3, 81.2, 81.2, 67.8, 67.6, 67.5, 61.1, 61.1, 60.8, 51.2, 49.4, 48.7, 33.8, 33.4, 30.2, 29.6, 29.5, 28.3, 28.3, 28.0, 28.0, 27.9, 27.8, 24.4, 24.4, 24.3$ ppm; HRMS (ESI) exact mass calculated for $[\text{M}+\text{Na}]$ ($\text{C}_{19}\text{H}_{27}\text{BrN}_2\text{NaO}_4$) requires m/z 449.10464, found m/z 449.10345.

(R)-2,2-dimethyl-1-(3-((3,3'',5,5''-tetra-*tert*-butyl-[1,1':3,1''-terphenyl]-5'-yl)methyl)-1,2-diazepan-1-yl)propan-1-one (4.20)

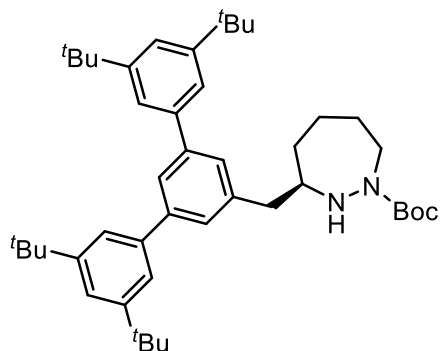


Following a modified procedure of Weix *et al.*²⁵: To a 1 mL HPLC vial containing 5'-bromo-3,3'',5,5''-tetra-*tert*-butyl-1,1':3,1''-terphenyl (130 mg, 0.24 mmol), NiI₂ (12 mg, 0.039 mmol), 1,10-phenanthroline (7.9 mg, 0.044 mmol), and NaI (17 mg, 0.11 mmol) was added a solution of benzyl (*R*)-7-(bromomethyl)-2-pivaloyl-1,2-diazepane-1-carboxylate (100 mg, 0.24 mmol) in DMPU (1 mL). Zn dust (48 mg, 0.73 mmol) was added, vial was capped, and the solution was brought to 60 °C. After 72 h, the reaction was purified by flash chromatography (gradient from 95:5 to 85:15 hexanes/EtOAc) to give coupled product which was isolated as a mixture with the dehalogenated hydrazide.

A stirred solution of the isolated mixture in THF (2.0 mL) was submitted to three cycles of vacuum/argon and 20% Pd(OH)₂/C (34 mg, 0.048 mmol) was added. Argon flow was removed, and a needle attached to a hydrogen-filled balloon was inserted through the septum and into the reaction mixture. A second needle was inserted through the septum to allow gas efflux and the hydrogen was allowed to bubble through the mixture, with the balloon being refilled as needed. After 6 h, the balloon was removed and the mixture was filtered through diatomaceous earth, rinsing with DCM. The filtrate was concentrated and purified by flash chromatography (gradient from 95:5 to 85:15 hexanes/EtOAc) to give product **4.20** as a colourless oil (31 mg, 0.047 mmol, 19% yield over 2 steps). IR (Film) $\nu = 3272, 3032, 2953, 2866, 1714, 1697, 1589, 1318, 1306, 1213, 1185 \text{ cm}^{-1}$; ¹H NMR (500 MHz, CDCl₃) $\delta = 7.62$ (bs, 1 H), 7.48 (m, 2 H), 7.45 (m, 4 H), 7.38 (m, 2 H), 3.67 (bs, 2 H), 3.32 – 3.31 (m, 1 H), 3.02 – 2.98 (m, 1 H), 2.86 (bs, 1 H), 1.90 – 1.74 (m, 4 H), 1.40 (s, 38 H), 1.32 (s, 9 H) ppm; ¹³C NMR (125 MHz, CDCl₃) $\delta = 178.5, 151.2, 143.2, 140.8, 139.4, 127.3, 125.2, 121.5, 62.3, 50.8, 42.1, 39.0, 37.1, 35.0, 33.4, 31.5, 28.0, 27.0,$

26.4 ppm; HRMS (ESI) exact mass calculated for $[M+Na]$ ($C_{45}H_{66}N_2NaO$) requires m/z 673.50674, found m/z 673.50646.

***tert*-butyl (R)-3-((3,3'',5,5''-tetra-*tert*-butyl-[1,1':3',1''-terphenyl]-5'-yl)methyl)-1,2-diazepane-1-carboxylate (4.21)**

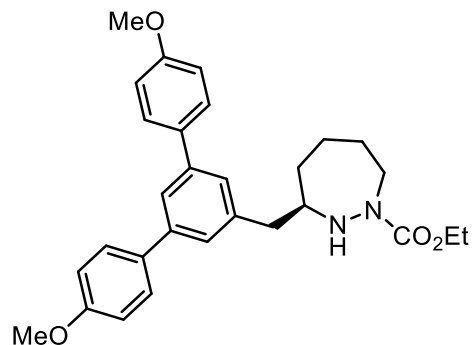


Following a modified procedure of Weix *et al.*²⁵: To a 1 mL HPLC vial containing 5'-bromo-3,3'',5,5''-tetra-*tert*-butyl-1,1':3',1''-terphenyl (125 mg, 0.23 mmol), NiI_2 (12 mg, 0.038 mmol), 1,10-phenanthroline (7.8 mg, 0.044 mmol), and NaI (16 mg, 0.11 mmol) was added a solution of 2-benzyl 1-(*tert*-butyl) (*R*)-3-(bromomethyl)-1,2-diazepane-1,2-dicarboxylate (125 mg, 0.24 mmol) in DMPU (1 mL). Zn dust (48 mg, 0.73 mmol) was added, vial was capped, and the solution was brought to 60 °C. After 72 h, the reaction was purified by flash chromatography (gradient from 95:5 to 85:15 hexanes/EtOAc) to give coupled product which was isolated as a mixture with the dehalogenated hydrazide.

A stirred solution of the isolated mixture in THF (2.0 mL) was submitted to three cycles of vacuum/argon and 20% $Pd(OH)_2/C$ (34 mg, 0.048 mmol) was added. Argon flow was removed, and a needle attached to a hydrogen-filled balloon was inserted through the septum and into the reaction mixture. A second needle was inserted through the septum to allow gas efflux and the hydrogen was allowed to bubble through the mixture, with the balloon being refilled as needed. After 6 h, the balloon was removed and the mixture was filtered through diatomaceous earth, rinsing with DCM. The filtrate was concentrated and purified by flash chromatography (gradient from 95:5 to 85:15 hexanes/EtOAc) to give product **4.21** as a colourless oil (18 mg, 0.026 mmol, 11% yield over 2 steps). IR (Film) $\nu = 3323, 3033, 2952, 2932, 2866, 1713, 1696, 1664, 1589, 1399, 1319, 1026\text{ cm}^{-1}$; 1H NMR (500 MHz, $CDCl_3$) $\delta = 7.61$ (bs, 1 H), 7.47 (bs, 2 H), 7.44 (bs, 4 H), 7.36 (bs, 2 H), 4.67 (bs, 1 H), 3.92 – 3.77 (m, 1 H), 3.43 – 3.18 (m, 2 H), 2.93 – 2.74 (m, 2 H),

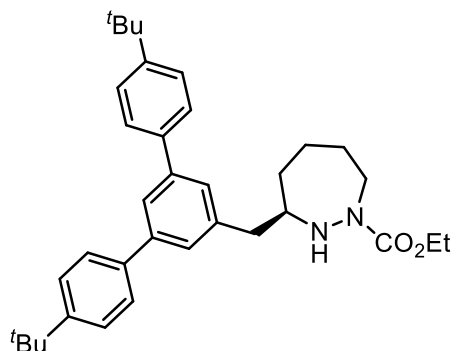
1.82 – 1.70 (m, 4 H), 1.48 – 1.25 (m, 47 H) ppm; ^{13}C NMR (125 MHz, CDCl_3) δ = 156.0, 155.2, 151.2, 143.4, 143.1, 140.9, 139.5, 127.2, 125.2, 121.9, 121.5, 80.0, 61.9, 60.3, 48.8, 47.0, 41.5, 41.2, 36.4, 35.0, 31.5, 28.4, 27.7, 27.1, 23.5 ppm; HRMS (ESI) exact mass calculated for $[\text{M}+\text{Na}]$ ($\text{C}_{45}\text{H}_{66}\text{N}_2\text{NaO}_2$) requires m/z 689.50165, found m/z 689.50088.

ethyl **(*R*)-3-((4,4''-dimethoxy-[1,1':3',1''-terphenyl]-5'-yl)methyl)-1,2-diazepane-1-carboxylate (4.28)**



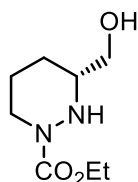
Prepared according to general procedure J from 5'-bromo-4,4''-dimethoxy-1,1':3',1''-terphenyl (104 mg, 0.23 mmol). Product **4.28** was isolated as a colourless oil (24 mg, 0.12 mmol, 22% yield). IR (Film) ν = 2930, 2836, 1687, 1608, 1512, 1451, 1440, 1247, 1177, 1032 cm^{-1} ; ^1H NMR (500 MHz, CDCl_3) δ 7.58 (d, J = 7.9 Hz, 5 H), 7.35 (s, 2 H), 6.99 (d, J = 7.9 Hz, 4 H), 4.71 – 4.55 (m, 1 H), 4.15 (bs, 1 H), 3.86 – 3.78 (m, 8 H), 3.39 – 3.13 (m, 2 H), 2.85 – 2.61 (m, 2 H), 1.83 – 1.77 (m, 4 H), 1.41 – 1.26 (m, 3 H), 0.84 (bs, 2 H) ppm; ^{13}C NMR (125 MHz, CDCl_3) δ = 159.2, 156.8, 156.0, 141.4, 139.5, 133.6, 128.2, 126.1, 123.4, 114.2, 62.2, 61.3, 60.4, 55.3, 48.2, 47.4, 41.2, 37.1, 34.9, 27.5, 26.9, 23.8, 14.6 ppm; HRMS (ESI) exact mass calculated for $[\text{M}+\text{Na}]$ ($\text{C}_{29}\text{H}_{34}\text{N}_2\text{NaO}_4$) requires m/z 497.2411, found m/z 497.2408.

ethyl (R)-3-((4,4''-di-*tert*-butyl-[1,1':3',1''-terphenyl]-5'-yl)methyl)-1,2-diazepane-1-carboxylate (4.29)



Prepared according to general procedure J from 5'-bromo-4,4''-di-*tert*-butyl-1,1':3',1''-terphenyl (106 mg, 0.25 mmol). Product **4.29** was isolated as a colourless oil (18 mg, 0.034 mmol, 13% yield). IR (Film) $\nu = 3307, 3031, 2933, 2862, 1709, 1597, 1322, 1308, 1080, 1063 \text{ cm}^{-1}$; $^1\text{H NMR}$ (500 MHz, CDCl_3) $\delta = 7.68$ (s, 1 H), 7.58 (d, $J = 8.0$ Hz, 4 H), 7.48 (d, $J = 8.0$ Hz, 4 H), 7.40 (s, 2 H), 4.61 (bs, 1 H), 4.16 (bs, 1 H), 3.84 (bs, 2 H), 3.37 – 3.12 (m, 2 H), 2.86 – 2.63 (m, 2 H), 1.83 – 1.77 (m, 4 H), 1.38 – 1.25 (m, 21 H), 0.84 (bs, 2 H) ppm; $^{13}\text{C NMR}$ (125 MHz, CDCl_3) $\delta = 156.8, 156.0, 150.4, 141.7, 139.5, 138.2, 126.8, 125.7, 124.0, 62.2, 61.3, 48.3, 47.4, 41.2, 37.1, 34.5, 31.4, 27.1, 26.9, 24.0, 23.8, 14.4$ ppm; HRMS (ESI) exact mass calculated for $[\text{M}+\text{Na}]$ ($\text{C}_{35}\text{H}_{46}\text{N}_2\text{NaO}_2$) requires m/z 549.3451, found m/z 549.3475.

ethyl (R)-3-(hydroxymethyl)tetrahydropyridazine-1(2H)-carboxylate (4.31)

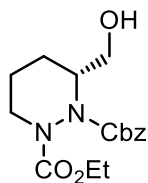


A stirred solution of dibenzyl (R)-3-(hydroxymethyl)tetrahydropyridazine-1,2-dicarboxylate (290 mg, 0.76 mmol, obtained from Dr. Samuel Plamondon) in MeOH (7.0 mL) was submitted to three cycles of vacuum/argon. AcCl (0.20 mL, 2.8 mmol) and 10% Pd/C (76 mg, 0.07 mmol) were added. Argon flow was removed, and a needle attached to a hydrogen-filled balloon was inserted through the septum and into the reaction mixture. A second needle was inserted through the septum to allow gas efflux and the hydrogen was allowed to bubble through the mixture, with the balloon being refilled as needed. After 1 h, the balloon was removed and the mixture was filtered through

diatomaceous earth, rinsing with MeOH. The filtrate was concentrated to give crude (*R*)-(hexahydropyridazin-3-yl)methanol hydrochloride as a yellow solid. (Note: benzyloxycarbonyl removal is performed under acidic conditions as the unprotected freebase is highly unstable to air oxidation.)

To a stirred suspension of crude (*R*)-(hexahydropyridazin-3-yl)methanol hydrochloride in DCM (4.5 mL) at 0 °C was added Et₃N (320 μL, 2.7 mmol) and EtO₂CCl (, 0.99 mmol). After 1 h, saturated aqueous NaHCO₃ was added, and the mixture was extracted with DCM (3 x 5 mL). The combined extracts were washed with water, dried with MgSO₄, filtered, concentrated, and purified by flash chromatography (gradient from 80:20 to 50:50 hexanes/EtOAc). Product **4.31** was isolated as a colourless oil (50 mg, 0.26 mmol, 32% yield over two steps). IR (Film) $\nu = 3422, 2982, 2935, 2860, 1693, 1408, 1264, 1180, 1050, 970 \text{ cm}^{-1}$; ¹H NMR (400 MHz, CDCl₃) $\delta = 4.14$ (q, *J* = 7.3 Hz, 2 H), 4.20 – 3.94 (bs, 1 H), 3.77 – 3.71 (m, 1 H), 3.52 – 3.50 (m, 2 H), 3.31 – 3.26 (m, 1 H), 2.94 – 2.88 (m, 1 H), 1.68 – 1.64 (m, 2 H), 1.54 – 1.51 (m, 1H), 1.40 – 1.30 (m, 2 H), 1.24 (t, *J* = 7.3 Hz, 3 H) ppm; ¹³C NMR (100 MHz, CDCl₃) $\delta = 155.8, 63.1, 61.9, 57.6, 45.0, 25.8, 22.7, 14.6$ ppm; HRMS (ESI) exact mass calculated for [M+Na] (C₈H₁₆N₂NaO₃) requires *m/z* 211.1053, found *m/z* 211.1049.

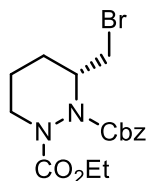
2-benzyl 1-ethyl (*R*)-3-(hydroxymethyl)tetrahydropyridazine-1,2-dicarboxylate (**4.32**)



To a stirred mixture of ethyl (*R*)-3-(hydroxymethyl)tetrahydropyridazine-1(2H)-carboxylate (49 mg, 0.26 mmol) and NaHCO₃ (86 mg, 1.0 mmol) in CHCl₃ (3.0 mL) was added benzyl chloroformate (110 μL, 0.77 mmol). After 19 h, reaction was quenched with water and extracted with DCM (3 x 5 mL). The combined extracts were dried with MgSO₄, filtered, concentrated, and purified by flash chromatography (gradient from 70:30 to 30:70 hexanes/EtOAc) to give product **4.32** (74 mg, 0.23 mmol, 88% yield) as a colourless oil. IR (Film) $\nu = 3399, 3067, 3035, 2954, 2929, 2856, 1686, 1595, 1489, 1454, 1254, 929 \text{ cm}^{-1}$; ¹H NMR (400 MHz, CDCl₃) $\delta 7.35 - 7.28$ (m, 5 H), 5.30 – 5.20 (m, 2 H), 4.56 – 4.45 (m, 1 H), 4.30 – 4.03 (m, 3 H), 3.81 – 3.63 (m, 1 H), 3.58 – 3.46 (m, 1 H + 1 H x 0.6), 3.12 – 3.02 (m, 1 H), 2.42 – 2.37 (m, 1 H x 0.4), 1.87 – 1.47 (m,

4 H), 1.34 – 1.16 (m, 3 H) ppm; ^{13}C NMR (100 MHz, CDCl_3) δ 156.7, 156.0, 155.6, 154.8, 136.1, 135.8, 128.4, 128.4, 128.2, 127.9, 127.7, 127.4, 68.0, 62.8, 62.6, 60.3, 60.2, 59.8, 56.0, 54.8, 45.5, 45.1, 43.8, 22.8, 22.4, 19.5, 19.2, 14.4, 14.2 ppm; HRMS (ESI) exact mass calculated for $[\text{M}+\text{Na}]$ ($\text{C}_{16}\text{H}_{22}\text{N}_2\text{NaO}_5$) requires m/z 345.1421, found m/z 345.1421.

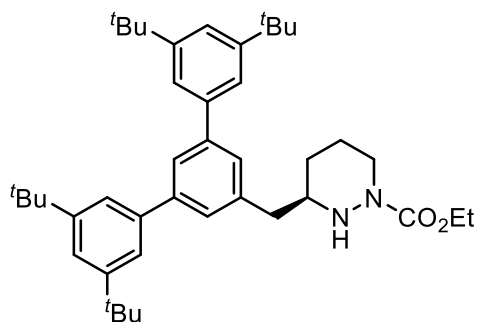
2-benzyl 1-ethyl (*R*)-3-(bromomethyl)tetrahydropyridazine-1,2-dicarboxylate (**4.33**)



To a stirred solution of PPh_3 (112 mg, 0.34 mmol) in THF (1.5 mL mL) was added CBr_4 (79 mg, 0.30 mmol) at 0 °C. After 15 minutes, 2-benzyl 1-ethyl (*R*)-3-(hydroxymethyl)tetrahydropyridazine-1,2-dicarboxylate (73 mg, 0.23 mmol) was added in THF (0.8 mL). The solution was brought to room temperature and stirred for 15 h. The reaction was quenched with the addition of saturated NaHCO_3 and extracted with EtOAc. The combined extracts were washed with brine, dried with Na_2SO_4 , filtered, concentrated, and purified by flash chromatography (gradient from 90:10 to 60:40 hexanes/EtOAc). Product **4.33** was isolated as a yellow oil (71 mg, 0.18 mmol, 80% yield). IR (Film) ν = 3035, 2953, 1704, 1451, 1298, 2360, 1209, 1094 cm^{-1} ; ^1H NMR (400 MHz, CDCl_3) δ = 7.39 – 7.29 (m, 5 H), 5.28 – 5.09 (m, 2 H), 4.65 – 4.45 (m, 1 H), 4.23 – 3.95 (m, 3 H), 3.68 – 3.53 (m, 1 H), 3.39 – 3.32 (m, 1 H), 3.22 – 2.98 (m, 1 H), 1.87 – 1.78 (m, 3 H), 1.52 – 1.50 (m, 1 H), 1.27 – 1.12 (m, 3 H) ppm; ^{13}C NMR (100 MHz, CDCl_3) δ = 155.4, 155.1, 135.8, 128.4, 128.2, 127.7, 67.9, 62.2, 54.8, 43.9, 30.3, 24.4, 18.7, 14.3 ppm; HRMS (ESI) exact mass calculated for $[\text{M}+\text{Na}]$ ($\text{C}_{16}\text{H}_{21}\text{BrN}_2\text{NaO}_4$) requires m/z 407.0577, found m/z 407.0568.

ethyl

(*R*)-3-((3,3',5,5''-tetra-*tert*-butyl-[1,1':3',1''-terphenyl]-5'-yl)methyl)tetrahydropyridazine-1(2H)-carboxylate (**4.34**)

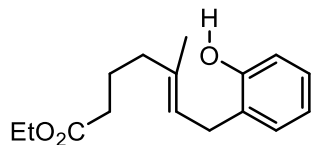


Following a modified procedure of Weix *et al.*²⁵: To a 1 mL HPLC vial containing 5'-bromo-3,3'',5,5''-tetra-*tert*-butyl-1,1':3',1''-terphenyl (103 mg, 0.19 mmol), NiI₂ (8.5 mg, 0.027 mmol), 1,10-phenanthroline (5.1 mg, 0.028 mmol), and sodium iodide (22 mg, 0.14 mmol) was added a solution of 2-benzyl 1-ethyl (*R*)-3-(bromomethyl)tetrahydropyridazine-1,2-dicarboxylate (71 mg, 0.18 mmol) in DMPU (720 μ L). Zn dust (34 mg, 0.52 mmol) was added, vial was capped, and the solution was brought to 60 °C. After 72 h, the reaction was purified by flash chromatography (gradient from 90:10 to 80:20 hexanes/EtOAc) to give coupled product which was isolated as a mixture with the dehalogenated hydrazide.

A stirred solution of the isolated mixture in THF (2.0 mL) was submitted to three cycles of vacuum/argon and 20% Pd(OH)₂/C (27 mg, 0.038 mmol) was added. Argon flow was removed, and a needle attached to a hydrogen-filled balloon was inserted through the septum and into the reaction mixture. A second needle was inserted through the septum to allow gas efflux and the hydrogen was allowed to bubble through the mixture, with the balloon being refilled as needed. After 6 h, the balloon was removed and the mixture was filtered through diatomaceous earth, rinsing with DCM. The filtrate was concentrated and purified by flash chromatography (gradient from 95:5 to 80:20 hexanes/EtOAc) to give product **4.34** as a colourless oil (23 mg, 0.036 mmol, 20% yield over 2 steps). IR (Film) ν = 2961, 2906, 2967, 1694, 1589, 1476, 1346, 1303, 1178 cm⁻¹; ¹H NMR (500 MHz, CDCl₃) δ = 7.64 (s, 1 H), 7.48 – 7.47 (m, 2 H), 7.47 – 7.46 (m, 4 H), 7.39 (m, 2 H), 4.86 (bs, 1 H), 4.07 – 4.04 (m, 3 H), 3.11 – 3.06 (m, 2 H), 2.90 – 2.79 (m, 2 H), 1.87 – 1.85 (m, 1 H), 1.73 – 1.71 (m, 1 H), 1.62 – 1.36 (m, 38 H), 1.12 (bs, 3 H) ppm; ¹³C NMR (125 MHz, CDCl₃) δ = 155.3, 151.1, 143.3, 140.8, 138.4, 127.0, 125.3, 121.9, 121.5, 61.6, 57.9, 44.9,

40.8, 35.0, 31.5, 30.6, 24.1, 14.5 ppm; HRMS (ESI) exact mass calculated for $[M+Na]$ ($C_{42}H_{60}N_2NaO_2$) requires m/z 647.4547, found m/z 647.4537.

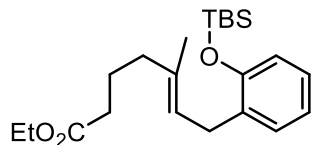
ethyl (*E*)-7-(2-hydroxyphenyl)-5-methylhept-5-enoate (4.35)



Following a modified procedure by Luo *et al.*,³⁸ To a solution of ethyl (*E*)-7-hydroxy-5-methylhept-5-enoate (190 mg, 1.0 mmol) in THF (3.5 mL) at -40 °C was added Et_3N (210 μ L, 1.5 mmol), then $MsCl$ (100 μ L, 1.3 mmol). Solution was let stir for 1 h, then a solution of $LiBr$ (485 mg, 5.6 mmol) in THF (3.5 mL) was added. Solution was let stir for 1 h, then quenched with water and extracted with $EtOAc$ (3 x 10 mL). The combined extracts were washed with saturated aqueous $NaHCO_3$, washed with brine, dried with magnesium sulfate, filtered, concentrated.

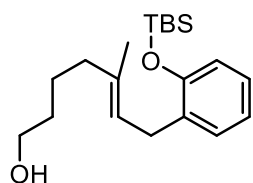
To a solution of phenol (94 mg, 1.0 mmol) in Et_2O (3 mL) at 0 °C was added NaH (60% dispersion in mineral oil, 44 mg, 1.1 mmol). The solution was brought to room temperature and let stir for 1 h. A solution of crude product from the first step in Et_2O (2 mL) was added. The solution was brought to 50 °C and let stir for 15 h then cooled, quenched with saturated aqueous NH_4Cl and extracted with DCM (3 x 5 mL). The combined extracts were washed with washed with brine, dried with $MgSO_4$, filtered, concentrated. Crude product was purified by flash chromatography (gradient from 90:10 to 75:25 hexanes/ $EtOAc$) to give product **4.35** as a colourless oil (102 mg, 0.39 mmol, 38% yield). IR (Film) $\nu = 3053, 2982, 1728, 1656, 1265, 1154, 1028$ cm^{-1} ; 1H NMR (400 MHz, $CDCl_3$) δ 7.12 – 7.07 (m, 2 H), 6.86 (ddd, $J = 7.4, 7.4, 1.1$ Hz, 1 H), 6.80 (d, $J = 7.9$ Hz, 1 H), 5.65 (s, 1 H), 5.36 (t, $J = 7.3$ Hz, 1 H), 4.14 (q, $J = 7.6$ Hz, 2 H), 3.37 (d, $J = 7.3$ Hz, 2 H), 2.30 (t, $J = 7.6$ Hz, 2 H), 2.09 (t, $J = 7.6$ Hz, 2 H), 1.79 (tt, $J = 7.6, 7.6$ Hz, 2 H), 1.75 (s, 3 H), 1.26 (t, $J = 7.5$ Hz, 3 H) ppm; ^{13}C NMR (100 MHz, $CDCl_3$) δ 174.0, 154.1, 136.5, 129.7, 127.2, 127.0, 122.7, 120.5, 115.4, 60.4, 38.9, 33.7, 29.0, 23.0, 15.9, 14.1 ppm; HRMS (ESI) exact mass calculated for $[M-H]$ ($C_{16}H_{21}O_3$) requires m/z 261.1496, found m/z 261.1492.

ethyl (*E*)-7-(2-((*tert*-butyldimethylsilyl)oxy)phenyl)-5-methylhept-5-enoate (4.36)



To a stirred solution of ethyl (*E*)-7-(2-hydroxyphenyl)-5-methylhept-5-enoate (102 mg, 0.39 mmol) in DCM (4 mL) was added imidazole (63 mg, 0.92 mmol) and TBSCl (68 mg, 0.45 mmol). The resulting solution was stirred for 2 h, then concentrated and purified by silica gel column chromatography (gradient from hexanes to 93:7 hexanes/ethyl acetate) to obtain product **4.36**, which was isolated as a colourless oil (87 mg, 0.23 mmol, 60% yield). IR (Film) $\nu = 2955, 2930, 2858, 1735, 1488, 1389, 1250 \text{ cm}^{-1}$; $^1\text{H NMR}$ (400 MHz, CDCl_3) δ 7.13 (d, $J = 7.4 \text{ Hz}$, 1 H), 7.07 (dd, $J = 7.6, 7.4 \text{ Hz}$, 1 H), 6.89 (dd, $J = 7.6, 7.4 \text{ Hz}$, 1 H), 6.80 (d, $J = 7.4 \text{ Hz}$, 1 H), 5.36 (t, $J = 7.4 \text{ Hz}$, 1 H), 4.14 (q, $J = 7.5 \text{ Hz}$, 2 H), 3.34 (d, $J = 7.4 \text{ Hz}$, 2 H), 2.30 (t, $J = 7.6 \text{ Hz}$, 2 H), 2.09 (t, $J = 7.6 \text{ Hz}$, 2 H), 1.79 (tt, $J = 7.6, 7.6 \text{ Hz}$, 2 H), 1.70 (s, 3 H), 1.26 (t, $J = 7.5 \text{ Hz}$, 3 H), 1.04 (s, 9 H), 0.26 (s, 6 H) ppm; $^{13}\text{C NMR}$ (100 MHz, CDCl_3) δ 173.7, 153.3, 135.1, 132.0, 129.5, 126.6, 123.5, 121.0, 118.3, 60.1, 38.9, 33.8, 28.4, 25.8, 23.1, 18.2, 15.9, 14.2, -4.2 ppm; HRMS (ESI) exact mass calculated for $[\text{M}+\text{Na}]$ ($\text{C}_{22}\text{H}_{36}\text{NaO}_3\text{Si}$) requires m/z 399.1577, found m/z 399.1577.

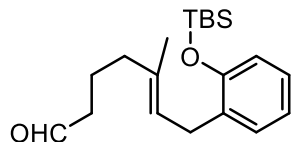
(*E*)-7-(2-((*tert*-butyldimethylsilyl)oxy)phenyl)-5-methylhept-5-en-1-ol (5.28)



To a stirred solution of ethyl (*E*)-7-(2-((*tert*-butyldimethylsilyl)oxy)phenyl)-5-methylhept-5-enoate (87 mg, 0.23 mmol) in THF (1.8 mL) at 0 °C was added DIBAL-H (25 wt. % in toluene, 510 μL , 0.51 mmol) dropwise. The solution was stirred for 2 h, then quenched with a saturated aqueous solution of Rochelle's salt. The mixture was extracted with EtOAc (3 x 5 mL). The combined organic layers were washed with brine, dried with MgSO_4 , filtered and concentrated. The crude extracts were purified by silica gel column chromatography (gradient from (90:10 to 80:20 hexanes/ EtOAc) to obtain product **5.28** which was isolated as a colourless oil (72 mg, 0.21 mmol, 92% yield). IR (Film) $\nu = 3351, 2930, 2858, 1488, 1451, 1252, 927 \text{ cm}^{-1}$; $^1\text{H NMR}$ (400 MHz, CDCl_3) $\delta = 7.13$ (d, $J = 7.6 \text{ Hz}$, 1 H), 7.07 (dd, $J = 7.7, 7.7 \text{ Hz}$, 1 H), 6.89 (dd, $J = 7.7, 7.6$

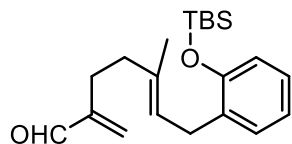
Hz, 1 H), 6.79 (d, $J = 7.7$ Hz, 1 H), 5.35 (t, $J = 6.9$ Hz, 1 H), 3.65 (t, $J = 7.0$ Hz, 2 H), 3.33 (d, $J = 7.0$ Hz, 2 H), 2.07 (t, $J = 7.0$ Hz, 2 H), 1.69 (s, 3 H), 1.59 – 1.49 (m, 4 H), 1.42 (s, 1 H), 1.03 (s, 9 H), 0.25 (s, 6 H) ppm; ^{13}C NMR (125 MHz, CDCl_3) $\delta = 153.3, 135.9, 132.1, 129.5, 126.5, 122.7, 121.0, 118.4, 62.9, 39.3, 32.4, 28.4, 25.8, 24.0, 18.2, 16.0, -4.2$ ppm. HRMS (ESI) exact mass calculated for $[\text{M}+\text{Na}]$ ($\text{C}_{20}\text{H}_{34}\text{NaO}_2\text{Si}$) requires m/z 357.22203, found m/z 357.22153.

(*E*)-7-(2-((*tert*-butyldimethylsilyl)oxy)phenyl)-5-methylhept-5-enal (4.37)



To a solution of (*E*)-7-(2-((*tert*-butyldimethylsilyl)oxy)phenyl)-5-methylhept-5-en-1-ol (72 mg, 0.21 mmol) in DCM (2.0 mL) was added pyridine (30 μL , 0.37 mmol) and Dess-Martin periodinane³ (109 mg, 0.25 mmol). The mixture was stirred for 1 h. The reaction was quenched with saturated aqueous sodium thiosulfate and extracted with DCM (3 x 5 mL). The combined organic layers were washed with brine, dried with MgSO_4 , filtered and concentrated. The crude extracts were purified by silica gel column chromatography (gradient from hexanes to 93:7 hexanes/EtOAc). Product **4.37** was isolated as a colourless oil (49 mg, 0.15 mmol, 69% yield). IR (Film) $\nu = 2954, 2930, 2895, 2858, 2712, 1726, 1489, 1252, 1008$ cm^{-1} ; ^1H NMR (400 MHz, CDCl_3) $\delta = 9.77$ (t, $J = 1.7$ Hz, 1 H), 7.11 (d, $J = 7.5$ Hz, 1 H), 7.07 (dd, $J = 7.5, 7.5$ Hz, 1 H), 6.88 (dd, $J = 7.5, 7.5$ Hz, 1 H), 6.79 (d, $J = 7.5$ Hz, 1 H), 5.35 (t, 7.0 Hz, 1 H), 3.33 (d, $J = 7.0$ Hz, 2 H), 2.41 (td, $J = 7.4, 1.7$ Hz, 2 H), 2.08 (t, $J = 7.5$ Hz, 2 H), 1.78 (tt, $J = 7.5, 7.4$ Hz, 2 H), 1.69 (s, 3 H), 1.02 (s, 9H), 0.24 (s, 6 H) ppm; ^{13}C NMR (100 MHz, CDCl_3) $\delta = 202.6, 153.3, 134.8, 131.9, 129.5, 126.6, 123.8, 121.0, 118.4, 43.2, 38.8, 28.4, 25.8, 20.2, 18.2, 15.9, -4.2$ ppm; HRMS (ESI) exact mass calculated for $[\text{M}+\text{Na}]$ ($\text{C}_{20}\text{H}_{32}\text{NaO}_2\text{Si}$) requires m/z 355.20638, found m/z 355.20565.

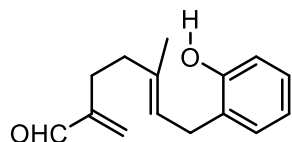
(*E*)-7-(2-((*tert*-butyldimethylsilyl)oxy)phenyl)-5-methyl-2-methylenehept-5-enal (4.38)



To a solution of (*E*)-7-(2-((*tert*-butyldimethylsilyl)oxy)phenyl)-5-methylhept-5-enal (47 mg, 0.15 mmol) in *i*PrOH (1.5 mL) was added formaldehyde (37 wt. % in H_2O , 25 μL , 0.30 mmol),

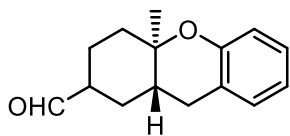
pyrrolidine (100 μ L of a 1.5 M solution in *i*PrOH, 0.15 mmol) and propionic acid (100 μ L of a 1.5 M solution in *i*PrOH, 0.15 mmol). Resulting solution was brought to 50 $^{\circ}$ C and let stir for 3 h before it was cooled and diluted with H₂O. The reaction was extracted with DCM (3 x 10 mL). The combined organic layers were washed with brine, dried with MgSO₄, filtered and concentrated. The crude extracts were purified by silica gel column chromatography (gradient from hexanes to 93:7 hexanes/EtOAc). Product **4.38** was isolated as a colourless oil (47 mg, 0.14 mmol, 92% yield). IR (Film) ν = 2955, 2929, 2857, 1692, 1489, 1451, 1252, 928, 838 cm^{-1} ; ¹H NMR (400 MHz, CDCl₃) δ = 9.52 (s, 1 H), 7.10 – 7.04 (m, 2 H), 6.87 (dd, *J* = 7.4, 7.4 Hz, 1 H), 6.78 (d, *J* = 7.4 Hz, 1 H), 6.22 (s, 1 H), 5.98 (s, 1 H), 5.33 (t, *J* = 6.9 Hz, 1 H), 3.31 (d, *J* = 7.0 Hz, 2 H), 2.39 (t, *J* = 7.4 Hz, 2 H), 2.18 (t, *J* = 7.4 Hz, 2 H), 1.71 (s, 3 H), 1.02 (s, 9 H), 0.24 (s, 6 H) ppm; ¹³C NMR (100 MHz, CDCl₃) δ = 194.6, 153.3, 149.8, 134.8, 134.1, 131.9, 129.5, 126.6, 123.6, 121.0, 118.4, 37.7, 28.4, 26.3, 25.8, 18.2, 16.0, -4.2 ppm; HRMS (ESI) exact mass calculated for [M+Na] (C₂₁H₃₂NaO₂Si) requires *m/z* 367.2064, found *m/z* 367.2072.

(*E*)-7-(2-hydroxyphenyl)-5-methyl-2-methylenehept-5-enal (4.39)



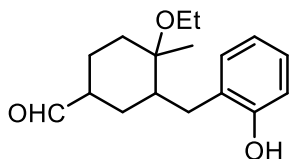
To a stirred solution of (*E*)-7-(2-((*tert*-butyldimethylsilyl)oxy)phenyl)-5-methyl-2-methylenehept-5-enal (47 mg, 0.14 mmol) in THF (1 mL) was added a solution of TBAF (1.0 M in THF, 180 μ L, 0.18 mmol) and the resulting solution was stirred for 1 h. The reaction was quenched with saturated aqueous NaHCO₃ and extracted with EtOAc (3 x 5 mL). The combined organic layers were washed with brine, dried with MgSO₄, filtered, and concentrated. The crude extracts were purified by silica gel column chromatography (gradient from 85:15 to 75:25 hexanes/EtOAc). Product **4.39** was isolated as a colourless oil (25 mg, 0.11 mmol, 80%). IR (Film) ν = 3399, 3067, 3035, 2954, 2929, 2856, 1686, 1594, 1454, 1254, 929, 839 cm^{-1} ; ¹H NMR (400 MHz, CDCl₃) δ = 9.51 (s, 1 H), 7.12 – 7.08 (m, 2 H), 6.86 (t, *J* = 7.5 Hz, 1 H), 6.80 (d, *J* = 7.5 Hz, 1 H), 6.24 (s, 1 H), 6.00 (s, 1 H), 5.32 (t, *J* = 7.1 Hz, 1 H), 5.09 (s, 1 H), 3.36 (d, *J* = 7.1 Hz, 2 H), 2.40 (t, *J* = 7.5 Hz, 2 H), 2.20 (t, *J* = 7.5 Hz, 2 H), 1.78 (s, 3 H) ppm; ¹³C NMR (100 MHz, CDCl₃) δ = 194.6, 154.1, 149.6, 136.8, 134.5, 129.9, 127.4, 126.7, 122.7, 120.7, 115.6, 37.7, 29.3, 26.3, 16.0 ppm; HRMS (ESI) exact mass calculated for [M+Na] (C₁₅H₁₈NaO₂) requires *m/z* 253.1199, found *m/z* 253.1197.

(4a*S*,9a*R*)-4a-methyl-2,3,4,4a,9,9a-hexahydro-1*H*-xanthene-2-carbaldehyde (4.40)



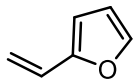
Followed general procedure G from (*E*)-7-(2-hydroxyphenyl)-5-methyl-2-methylenehept-5-enal (0.035 mmol) with catalyst **4.13**. The reaction was run for 6 h and, after acetal deprotection, (4a*S*,9a*R*)-4a-methyl-2,3,4,4a,9,9a-hexahydro-1*H*-xanthene-2-carbaldehyde was isolated as a colourless oil (2.3 mg, 0.010 mmol, 28% yield, 29% ee determined from major diastereomer) and 4-ethoxy-3-(2-hydroxybenzyl)-4-methylcyclohexane-1-carbaldehyde as a colourless oil (6.3 mg, 0.023 mmol, 65%). IR (Film) $\nu = 3308, 2972, 2928, 1902, 1723, 1488, 1393, 1380, 1173, 1113$ cm^{-1} ; ^1H NMR (500 MHz, CDCl_3) $\delta = 9.73^*$ (s, 1 H x 0.3), 9.69 (s, 1 H x 0.7), 7.11 – 7.03 (m, 2 H), 6.85 – 6.76 (m, 2 H), 2.70 – 2.62 (m, 1 H), 2.56 – 2.46 (m, 1 H), 2.46 – 2.30 (m, 1 H), 2.13 – 2.02 (m, 2 H), 1.94 – 1.89 (m, 1 H), 1.83 – 1.69 (m, 2 H), 1.56 – 1.44 (m, 1H), 1.29 – 1.22 (m, 1 H), 1.17* (s, 3 H x 0.3), 1.15 (s, 3 H x 0.7) ppm; ^{13}C NMR (125 MHz, CDCl_3) assigned for major diastereomer $\delta = 203.2, 153.4, 129.4, 127.5, 121.5, 120.0, 117.3, 76.3, 49.9, 38.6, 38.0, 29.1, 29.0, 23.1, 16.3$ ppm; HRMS (ESI) exact mass calculated for $[\text{M}+\text{Na}]$ ($\text{C}_{15}\text{H}_{18}\text{NaO}_2$) requires m/z 253.1199, found m/z 253.1197.

4-ethoxy-3-(2-hydroxybenzyl)-4-methylcyclohexane-1-carbaldehyde (4.41)



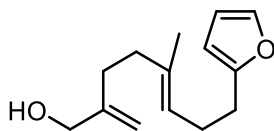
IR (Film) $\nu = 3305, 3034, 2975, 2932, 2867, 2716, 1722, 1584, 1488, 1455, 1379, 1305, 1264, 1180, 1074$ cm^{-1} ; ^1H NMR (500 MHz, CDCl_3) $\delta = 9.62$ (s, 1 H x 0.8), 9.49* (s, 1 H x 0.2), 7.70 (s, 1 H x 0.8), 7.52* (s, 1 H x 0.2), 7.15 – 7.01 (m, 2 H), 6.90 – 6.78 (m, 2 H), 3.56 – 3.42 (m, 2 H), 3.18 – 3.12 (m, 1 H), 2.41 – 2.17 (m, 1 H), 2.16 – 2.10 (m, 2 H), 2.01 – 1.92 (m, 2 H), 1.58 – 1.52 (m, 1 H), 1.44 – 1.21 (m, 9 H) ppm; ^{13}C NMR (125 MHz, CDCl_3) assigned for major diastereomer $\delta = 203.1, 154.8, 129.8, 128.1, 127.3, 119.4, 116.2, 77.8, 56.6, 49.7, 48.6, 35.6, 32.0, 29.1, 23.1, 15.7, 14.8$ ppm; HRMS (ESI) exact mass calculated for $[\text{M}+\text{Na}]$ ($\text{C}_{17}\text{H}_{24}\text{NaO}_3$) requires m/z 299.1618, found m/z 299.1620.

2-vinylfuran (4.42)



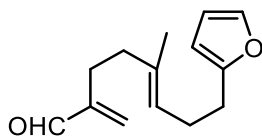
From furan-2-carbaldehyde (1.0 mL, 12.1 mmol), general procedure A was followed to give, after flash chromatography (90:10 pentane/Et₂O), 760 mg (8.1 mmol) of product **4.42** as a yellow oil (33% yield). Spectroscopic data were in accordance with previously reported literature.³⁹

(*E*)-8-(furan-2-yl)-5-methyl-2-methyleneoct-5-en-1-ol (4.43)



Followed general procedure C from 2-vinylfuran on a 0.54 mmol scale and purified using silica gel column chromatography to give 78 mg (0.35 mmol, 64% yield over 2 steps) of (*E*)-8-(furan-2-yl)-5-methyl-2-methyleneoct-5-en-1-ol (**4.43**) as a colourless oil. IR (Film) 3331, 2915, 2853, 1383, 1072 cm⁻¹; ¹H NMR (500 MHz, CDCl₃) δ = 7.29 (d, J = 2.2 Hz, 1 H), 6.27 (dd, J = 3.1, 2.2 Hz, 1 H), 5.97 (d, J = 3.1 Hz, 1 H), 5.18 (t, J = 7.0 Hz, 1 H), 5.01 (s, 1 H), 4.86 (s, 1 H), 4.06 (s, 2 H), 2.64 (t, J = 7.2 Hz, 2 H), 2.33 (dt, J = 7.2, 7.0 Hz, 2 H), 2.14 (s, 4 H), 1.60 (s, 4 H) ppm; ¹³C NMR (125 MHz, CDCl₃) δ = 156.0, 148.8, 140.7, 135.6, 123.5, 110.0, 109.3, 104.8, 65.8, 37.8, 21.4, 28.1, 26.4, 15.8 ppm; HRMS (ESI) exact mass calculated for [M+Na] (C₁₄H₂₀NaO₂) requires m/z 243.13555, found m/z 243.13547.

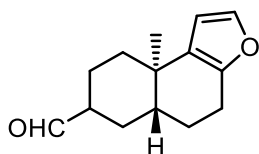
(*E*)-8-(furan-2-yl)-5-methyl-2-methyleneoct-5-enal (4.44)



From (*E*)-8-(furan-2-yl)-5-methyl-2-methyleneoct-5-en-1-ol, general procedure D was followed on a 0.20 mmol scale to give 38 mg (0.17 mmol, 86% yield) of (*E*)-8-(furan-2-yl)-5-methyl-2-methyleneoct-5-enal as a colourless oil. IR (Film) 2959, 2921, 2851, 1749, 1689, 1476, 1073 cm⁻¹; ¹H NMR (500 MHz, CDCl₃) δ = 9.50 (s, 1 H), 7.29 (d, J = 1.1 Hz, 1 H), 6.27 (dd, J = 3.0, 1.1 Hz, 1 H), 6.20 (s, 1 H), 5.96 (m, 2 H), 5.14 (t, J = 7.2 Hz, 1 H), 2.63 (t, J = 7.3 Hz, 2 H), 2.36 – 2.30 (m, 4 H), 2.12 (t, J = 7.3 Hz, 2 H), 1.60 (s, 3 H) ppm; ¹³C NMR (125 MHz, CDCl₃) δ = 194.6,

155.9, 149.8, 140.7, 134.9, 134.1, 124.1, 110.0, 104.8, 37.6, 28.1, 26.4, 26.2, 15.7 ppm; HRMS (ESI) exact mass calculated for $[M+Na]$ ($C_{14}H_{18}NaO_2$) requires m/z 241.1199, found m/z 241.1190.

(5a*S*,9a*S*)-9a-methyl-4,5,5a,6,7,8,9,9a-octahydronaphtho[2,1-*b*]furan-7-carbaldehyde (4.45)



Followed general procedure G from (E)-8-(furan-2-yl)-5-methyl-2-methyleneoct-5-enal with catalyst **4.13** in EtOH as a solvent. The reaction was run for 8 h and acetal deprotection was conducted with CSA in THF/water. Product **4.44** was isolated as a colourless oil (2.3 mg, 0.010, 30% yield, 76% ee determined from major diastereomer). IR (Film) $\nu = 2929, 2854, 1721, 1614, 1368, 1279, 1138 \text{ cm}^{-1}$; $^1\text{H NMR}$ (500 MHz, CDCl_3) δ 9.70* (s, 1 H x 0.2), 9.67 (s, 1 H x 0.8), 7.23 (s, 1 H x 0.8) 7.19* (s, 1 H x 0.2), 6.23 (s, 1 H x 0.8), 6.18* (s, 1 H x 0.2), 2.68 – 2.65 (m, 2 H), 2.40 – 2.33 (m, 1 H), 2.05 – 2.00 (m, 1 H), 1.92 – 1.86 (m, 1 H), 1.84 – 1.56 (m, 5 H), 1.47 – 1.37 (m, 2 H), 1.06* (s, 3 H x 0.2), 1.02 (s, 3 H x 0.8) ppm; $^{13}\text{C NMR}$ (125 MHz, CDCl_3) $\delta = 205.4^*, 204.1, 148.9, 148.8^*, 140.7, 140.6^*, 128.0, 127.9^*, 107.1, 107.0^*, 50.9, 46.8^*, 42.8, 40.1^*, 36.4, 34.4^*, 33.3, 33.1^*, 27.1, 26.2^*, 25.6^*, 25.5, 23.4, 23.3^*, 21.2, 20.2, 20.0^*, 19.7^*$ ppm; HRMS (APCI) exact mass calculated for $[M+H]$ ($C_{14}H_{19}NaO_2$) requires m/z 219.13796, found m/z 219.13728.

5.5 References

1. Kaldre, D.; Gleason, J. L., An Organocatalytic Cope Rearrangement. *Angew. Chem. Int. Ed.* **2016**, *55* (38), 11557-11561.
2. Frigerio, M.; Santagostino, M.; Sputore, S., A User-Friendly Entry to 2-Iodoxybenzoic Acid (IBX). *J. Org. Chem.* **1999**, *64* (12), 4537-4538.
3. Boeckman, R. K.; Shao, P.; Mullins, J. J., The Dess-Martin periodinane: 1,1,1-triacetoxy-1,1-dihydro-1,2-benziodoxol-3(1H)-one. *Org. Synth.* **2000**, *77*, 141.
4. Tran, N. C.; Dhondt, H.; Flipo, M.; Deprez, B.; Willand, N., Synthesis of functionalized 2-isoxazolines as three-dimensional fragments for fragment-based drug discovery. *Tetrahedron Lett.* **2015**, *56* (27), 4119-4123.

5. Fuchs, J.; Szeimies, G., Synthese von [n .1.1]Propellanen (n = 2, 3, 4). *Chem. Ber.* **1992**, *125* (11), 2517-2522.
6. Ogura, Y.; Ishigami, K.; Watanabe, H., Total synthesis of (±)-lysidicin A. *Tetrahedron* **2012**, *68* (6), 1723-1728.
7. Rand, C. L.; Van Horn, D. E.; Moore, M. W.; Negishi, E., A versatile and selective route to difunctional trisubstituted (E)-alkene synthons via zirconium-catalyzed carboalumination of alkynes. *J. Org. Chem.* **1981**, *46* (20), 4093-4096.
8. Vasil'Ev, A. A.; Engman, L.; Serebryakov, E. P., Synthesis of (3S*,4R*,6E,10Z)-3,4,7,11-tetramethyltrideca-6,10-dienal (faranal) using stereospecific 1,4-cis-hydrogenation of conjugated double bonds. *J. Chem. Soc., Perkin Trans. I* **2000**, (14), 2211-2216.
9. Molander, G. A.; Brown, A. R., Suzuki–Miyaura Cross-Coupling Reactions of Potassium Vinyltrifluoroborate with Aryl and Heteroaryl Electrophiles. *J. Org. Chem.* **2006**, *71* (26), 9681-9686.
10. Roberts, J. C.; Pincock, J. A., Methoxy-Substituted Stilbenes, Styrenes, and 1-Arylpropenes: Photophysical Properties and Photoadditions of Alcohols. *J. Org. Chem.* **2006**, *71* (4), 1480-1492.
11. Odell, L. R.; Lindh, J.; Gustafsson, T.; Larhed, M., Continuous Flow Palladium(II)-Catalyzed Oxidative Heck Reactions with Arylboronic Acids. *Eur. J. Org. Chem.* **2010**, *2010* (12), 2270-2274.
12. Médard, G., A route to the 9,10-secosteroid astrogorgiadiol featuring a key sp²–sp³ Suzuki type cross-coupling. *Tetrahedron* **2014**, *70* (2), 186-196.
13. A. Yoshida, K. O., T. Kasai, T. Koga, K. Hasegawa Preparation of diareno(thio)pyrans for treatment of arteriosclerosis. 1993.
14. Faler, C. A.; Joullié, M. M., The Kulinkovich Reaction in the Synthesis of Constrained N,N-Dialkyl Neurotransmitter Analogues. *Org. Lett* **2007**, *9* (10), 1987-1990.
15. Sun, B.; Hoshino, J.; Jermihov, K.; Marler, L.; Pezzuto, J. M.; Mesecar, A. D.; Cushman, M., Design, synthesis, and biological evaluation of resveratrol analogues as aromatase and quinone reductase 2 inhibitors for chemoprevention of cancer. *Bioorg. Med. Chem.* **2010**, *18* (14), 5352-5366.
16. Liwen Ji, B. Y., Younes Ansari, Giulia Canton Silicon-anode lithium-ion batteries with thiophene-based electrolyte additives improving stability. 2020.

17. Luca, L. D.; Giacomelli, G.; Nieddu, G., Synthesis of Substituted Benzofurans via Microwave-Enhanced Catch and Release Strategy. *J. Comb. Chem.* **2008**, *10* (4), 517-520.
18. Fan, L.; Han, C.; Li, X.; Yao, J.; Wang, Z.; Yao, C.; Chen, W.; Wang, T.; Zhao, J., Enantioselective Polyene Cyclization Catalyzed by a Chiral Brønsted Acid. *Angew. Chem. Int. Ed.* **2018**, *57* (8), 2115-2119.
19. Konstantinova, O.; Koskinen, A., Synthesis of the C1–C12 Fragment of Calyculin C. *Synthesis* **2019**, *51* (01), 285-295.
20. Zurwerra, D.; Glaus, F.; Betschart, L.; Schuster, J.; Gertsch, J.; Ganci, W.; Altmann, K.-H., Total Synthesis of (–)-Zampanolide and Structure–Activity Relationship Studies on (–)-Dactylolide Derivatives. *Chem. Eur. J.* **2012**, *18* (52), 16868-16883.
21. Karier, P.; Ungeheuer, F.; Ahlers, A.; Anderl, F.; Wille, C.; Fürstner, A., Metathesis at an Implausible Site: A Formal Total Synthesis of Rhizoxin D. *Angew. Chem. Int. Ed.* **2019**, *58* (1), 248-253.
22. Pantin, M.; Brimble, M. A.; Furkert, D. P., Total Synthesis of (–)-Peniphenone A. *J. Org. Chem.* **2018**, *83* (13), 7049-7059.
23. Henmi, Y.; Makino, K.; Yoshitomi, Y.; Hara, O.; Hamada, Y., Highly efficient synthesis of (R)- and (S)-piperazic acids using proline-catalyzed asymmetric α -hydrazination. *Tetrahedron: Asymmetry* **2004**, *15* (21), 3477-3481.
24. Häggman, N. O.; Zank, B.; Jun, H.; Kaldre, D.; Gleason, J. L., Diazepane Carboxylates as Organocatalysts in the Diels–Alder Reaction of α -Substituted Enals. *Eur. J. Org. Chem.* **2018**, *2018* (39), 5412-5416.
25. Everson, D. A.; Jones, B. A.; Weix, D. J., Replacing Conventional Carbon Nucleophiles with Electrophiles: Nickel-Catalyzed Reductive Alkylation of Aryl Bromides and Chlorides. *J. Am. Chem. Soc.* **2012**, *134* (14), 6146-6159.
26. Bejot, R.; He, A.; Falck, J. R.; Mioskowski, C., Chromium–Carbyne Complexes: Intermediates for Organic Synthesis. *Angew. Chem. Int. Ed.* **2007**, *46* (10), 1719-1722.
27. Klauk, F. J. R.; Yoon, H.; James, M. J.; Lautens, M.; Glorius, F., Visible-Light-Mediated Deaminative Three-Component Dicarbofunctionalization of Styrenes with Benzylic Radicals. *ACS Catal.* **2019**, *9* (1), 236-241.

28. Denmark, S. E.; Butler, C. R., Vinylation of Aromatic Halides Using Inexpensive Organosilicon Reagents. Illustration of Design of Experiment Protocols. *J. Am. Chem. Soc.* **2008**, *130* (11), 3690-3704.
29. Whitton, A. J.; Kumberger, O.; Müller, G.; Schmidbaur, H., Preparation and characterisation of 9,10-dihydroanthracene and tert-butyl-9,10-dihydroanthracene complexes with one or two tricarbonylchromium units; crystal structure of tricarbonyl ($\eta^{1,2,3,4,4a,9a}$ -9,10-dihydroanthracene)chromium. *Chem. Ber.* **1990**, *123* (10), 1931-1939.
30. Hoffend, C.; Schödel, F.; Bolte, M.; Lerner, H.-W.; Wagner, M., Boron-Doped Tri(9,10-anthrylene)s: Synthesis, Structural Characterization, and Optoelectronic Properties. *Chem. Eur. J.* **2012**, *18* (48), 15394-15405.
31. Higuchi, T.; Matsumoto, K.; Hatano, K.; Umezawa, N., Synthesis of a New, Bulky Tetraarylphosphonium, a Tetraarylborate, and Their Salt. *Synthesis* **2004**, *2004* (13), 2181-2185.
32. Spivey, A. C.; Fekner, T.; Spey, S. E., Axially Chiral Analogues of 4-(Dimethylamino)pyridine: Novel Catalysts for Nonenzymatic Enantioselective Acylations. *J. Org. Chem.* **2000**, *65* (10), 3154-3159.
33. Tiefenbacher, K.; Dube, H.; Ajami, D.; Rebek, J., A transparent photo-responsive organogel based on a glycoluril supergelator. *Chem. Commun.* **2011**, *47* (26), 7341.
34. Zhao, T.-Y.; Li, K.; Yang, L.-L.; Zhu, S.-F.; Zhou, Q.-L., Nickel-Catalyzed Desymmetrizing Cyclization of 1,6-Dienes to Construct Quaternary Stereocenters. *Org. Lett.* **2021**, *23* (10), 3814-3817.
35. Takagi, R.; Yamasaki, Y., Chiral Calcium Bis-sulfonimide Catalyzed Diels-Alder Reactions of 1-Acryloyl-pyrazole. *Chem. Lett.* **2021**, *50* (10), 1781-1783.
36. Jang, C.-J.; Ryu, J.-H.; Lee, J.-D.; Sohn, D.; Lee, M., Synthesis and Supramolecular Nanostructure of Amphiphilic Rigid Aromatic-Flexible Dendritic Block Molecules. *Chem. Mater.* **2004**, *16* (22), 4226-4231.
37. Greco, G. E.; Schrock, R. R., Synthesis of Triamidoamine Ligands of the Type (ArylNHCH₂CH₂)₃N and Molybdenum and Tungsten Complexes That Contain an [(ArylNCH₂CH₂)₃N]₃- Ligand. *Inorg. Chem.* **2001**, *40* (16), 3850-3860.
38. Yang, Z.; Li, H.; Zhang, L.; Zhang, M.-T.; Cheng, J.-P.; Luo, S., Organic Photocatalytic Cyclization of Polyenes: A Visible-Light-Mediated Radical Cascade Approach. *Chem. Eur. J.* **2015**, *21* (42), 14723-14727.

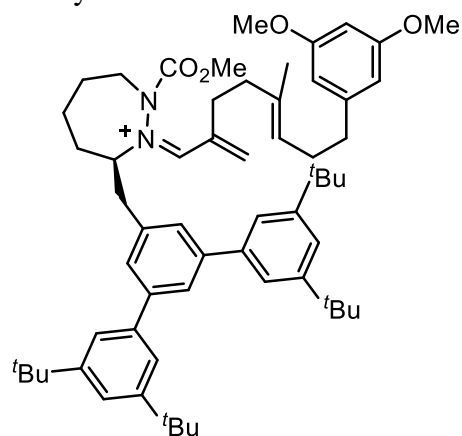
39. Waser, J.; Gaspar, B.; Nambu, H.; Carreira, E. M., Hydrazines and Azides via the Metal-Catalyzed Hydrohydrazination and Hydroazidation of Olefins. *J. Am. Chem. Soc.* **2006**, *128* (35), 11693-11712.

Chapter 6. Density Functional Theory Calculations

All DFT calculations were conducted using Gaussian 16, Revision B.01.¹ Structures were optimized at the M06-2X/6-311G(d,p) with EtOH solvation using the PCM model. All thermochemistry was determined using frequency calculations on stationary points. Conformations for the starting iminium ions were identified by a GMMX conformational search using the MMFF94 force field, substituting carbon for the iminium nitrogen, as the MMFF94 force field is not parameterized for iminium ions. GMMX structures within 5 kcal/mol of the global minimum were then converted back to iminium ions and reoptimized by DFT. In addition, simple iminium ion structures relaxing from the transition state were also assessed. Both proximal and distal transition states with *s-cis* and *s-trans* α,β -unsaturated iminium ions were assessed. In all cases the *s-trans* proximal structure was the global minimum.

6.1. DFT Calculations from Chapter 4

Catalyst **4.13** / **2.4** Iminium



EE = -2746.1340 a.u.

ΔG^0 = -2744.9166 a.u.

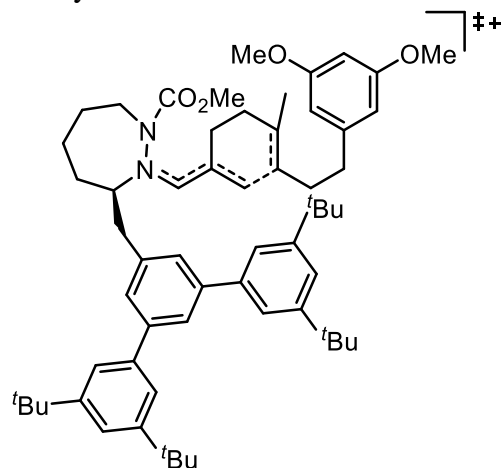
C	-0.6807	-3.01893	-0.49981
N	1.67968	-3.61437	-0.01807
C	-1.38653	-4.36047	-0.70037
C	-0.21039	-2.35704	-1.79759
H	-1.37844	-2.34088	0.0089
C	0.28676	-2.93284	1.73943
C	1.85539	-4.98313	-0.56048
C	2.84593	-2.89424	0.22143
C	-0.55304	-5.47651	-1.31916
H	-1.78407	-4.68595	0.27068
H	-2.24896	-4.1487	-1.33852

H	-1.05282	-2.44773	-2.49344
H	0.62615	-2.91138	-2.23425
C	1.24307	-3.19896	2.81778
H	-0.66957	-2.46925	1.98398
C	0.63842	-5.88833	-0.4567
H	2.69243	-5.41958	-0.00822
H	2.16402	-4.88697	-1.60614
O	2.64506	-1.75133	0.86807
O	3.91702	-3.31151	-0.15335
H	-1.20876	-6.3424	-1.45177
H	-0.20809	-5.19327	-2.32141
H	0.32039	-6.00342	0.58749
H	0.99426	-6.8727	-0.77502
C	3.84786	-1.03017	1.19646
H	3.50855	-0.09894	1.64733
H	4.44046	-1.61682	1.90131
H	4.42393	-0.82395	0.29278
C	1.54579	-2.08416	3.79648
H	2.0375	-2.53637	4.66172
H	2.28147	-1.41696	3.33318
C	1.74058	-4.43515	2.94163
H	1.51241	-5.2332	2.24248
H	2.36781	-4.68977	3.79008
C	-1.60379	-0.23532	3.1305
H	-2.22249	-0.83998	3.79594
C	0.35041	-1.2462	4.27489
H	-0.41518	-1.89658	4.71254
H	0.73166	-0.61612	5.08971
C	-0.27302	-0.33889	3.23517
C	-2.32314	0.71775	2.2135
H	-1.84376	0.73523	1.22782
H	-2.23457	1.74078	2.60919
C	0.66543	0.47848	2.37867
H	1.55084	0.781	2.95081
H	0.18408	1.38412	1.99968
H	1.01777	-0.08876	1.50346
C	-3.81186	0.39491	2.02708
H	-4.28025	0.24328	3.00683
H	-4.29802	1.26103	1.56261
C	-4.03229	-0.8146	1.15011
C	-4.22847	-0.6262	-0.21613
C	-4.01728	-2.11144	1.6682
C	-4.42855	-1.71923	-1.05988
H	-4.23171	0.37296	-0.64192
C	-4.23782	-3.2015	0.8218
H	-3.88266	-2.29736	2.72924

C	-4.46264	-3.01945	-0.54803
H	-4.65401	-3.86543	-1.19408
C	0.14172	-0.90056	-1.61074
C	-0.87846	0.03295	-1.41416
C	-0.58898	1.37705	-1.16046
H	-1.91651	-0.29468	-1.44095
C	1.7862	0.85783	-1.28587
C	0.7508	1.77331	-1.0875
H	0.98914	2.81819	-0.90562
C	-1.69149	2.3451	-0.92944
C	-1.58499	3.29274	0.09317
C	-2.86679	2.27626	-1.68346
H	-0.67159	3.32183	0.67923
C	-3.9457	3.12243	-1.41539
H	-2.92816	1.54537	-2.48428
C	3.20653	1.25841	-1.13543
C	3.57747	2.13959	-0.1171
C	4.19921	0.69347	-1.9394
H	2.80142	2.54849	0.52652
C	5.55155	0.96987	-1.72449
H	3.90468	0.02229	-2.74243
C	1.46539	-0.47636	-1.56791
H	2.26594	-1.19512	-1.72907
C	-3.81096	4.04018	-0.36838
H	-4.64711	4.69681	-0.13997
C	-2.64567	4.14688	0.3986
C	5.88767	1.84902	-0.68818
H	6.9318	2.06975	-0.50711
C	4.91805	2.4491	0.1234
C	-2.58388	5.16367	1.54214
C	-3.70889	4.86465	2.54793
H	-4.69697	4.93519	2.08297
H	-3.6009	3.85613	2.96299
H	-3.67354	5.58165	3.37552
C	-1.24619	5.11472	2.28773
H	-1.07174	4.1321	2.74103
H	-0.40497	5.34285	1.62442
H	-1.25031	5.85737	3.09179
C	-2.77131	6.58077	0.97417
H	-3.73361	6.68616	0.46359
H	-2.73641	7.31771	1.78411
H	-1.97796	6.81902	0.25796
C	-5.25661	3.06849	-2.2068
C	-5.21552	2.02379	-3.32732
H	-4.41983	2.24125	-4.0482
H	-5.06494	1.00998	-2.9397

H	-6.16809	2.03695	-3.8671
C	-5.52888	4.44421	-2.83869
H	-4.72163	4.72143	-3.52483
H	-6.46661	4.41714	-3.40452
H	-5.61596	5.22903	-2.08103
C	-6.40791	2.70977	-1.25091
H	-6.51007	3.44607	-0.44748
H	-7.35507	2.67564	-1.80067
H	-6.24304	1.72747	-0.79352
C	5.27497	3.39177	1.27728
C	6.78274	3.64458	1.37744
H	7.17691	4.09797	0.46179
H	6.98091	4.33262	2.20536
H	7.3361	2.71977	1.57178
C	4.57057	4.7434	1.07075
H	3.48223	4.63207	1.03905
H	4.8152	5.42293	1.89448
H	4.89274	5.20926	0.13362
C	4.80042	2.76727	2.601
H	5.05072	3.42616	3.43984
H	3.71633	2.61283	2.60746
H	5.28582	1.7993	2.76831
C	6.60424	0.2837	-2.60065
C	8.03053	0.71179	-2.2408
H	8.28213	0.45179	-1.20717
H	8.73995	0.19763	-2.89691
H	8.17295	1.78985	-2.3712
C	6.49203	-1.23916	-2.40775
H	5.50012	-1.60924	-2.68639
H	7.23304	-1.75371	-3.02953
H	6.67207	-1.51122	-1.36172
C	6.35334	0.63199	-4.07739
H	5.36407	0.30302	-4.40958
H	6.42501	1.71276	-4.23836
H	7.1006	0.14014	-4.70968
N	0.45784	-3.18508	0.48058
O	-4.58184	-1.42383	-2.37683
O	-4.21308	-4.4264	1.41247
C	-4.61439	-5.54574	0.64032
H	-3.92004	-5.73296	-0.18714
H	-4.602	-6.39832	1.3181
H	-5.62489	-5.40633	0.24176
C	-4.79706	-2.49379	-3.28043
H	-4.89409	-2.04009	-4.2658
H	-3.94846	-3.18756	-3.28035
H	-5.71482	-3.03917	-3.03639

Catalyst **4.13** / **2.4** Transition state 1



Proximal *s-trans*

EE = -2746.1293 a.u.

ΔG^0 = -2744.9089 a.u.

C	-2.59172	4.27206	0.10397
N	-0.45821	4.96726	-0.92579
C	-2.88117	5.76833	0.2045
C	-2.37703	3.6522	1.49613
H	-3.44441	3.78374	-0.38059
C	-1.37456	2.87688	-1.49264
C	-0.6512	5.93106	-2.02027
C	0.66584	4.83749	-0.14254
C	-2.97624	6.5149	-1.13437
H	-2.12473	6.2427	0.84218
H	-3.83128	5.8474	0.74214
H	-1.55033	4.17618	1.98675
H	-3.286	3.85916	2.07318
C	-0.42926	2.40539	-2.40503
H	-2.24997	2.25086	-1.33849
C	-1.62894	7.03532	-1.64374
H	0.32717	6.33648	-2.27709
H	-1.01793	5.35723	-2.8795
O	1.52895	5.82262	-0.39103
O	0.84749	3.93417	0.64936
H	-3.64494	7.37106	-1.00617
H	-3.44135	5.86818	-1.89086
H	-1.16951	7.66572	-0.87276
H	-1.78217	7.66392	-2.52728
C	2.7617	5.74365	0.3389
H	2.56428	5.74025	1.41149
H	3.3043	4.83825	0.0596
H	3.32247	6.63032	0.05234

C	0.97957	2.85318	-2.63381
H	1.23844	2.74328	-3.6923
H	1.19598	3.88395	-2.35835
N	-1.43985	4.00461	-0.79619
C	-0.71143	1.12519	-2.90022
H	-0.26526	0.78532	-3.83072
H	-1.63432	0.61721	-2.62638
C	0.54574	-0.16518	-1.61202
H	0.14965	0.28204	-0.70054
C	1.90184	1.8815	-1.7945
H	2.94634	2.14074	-1.99215
H	1.68602	2.04654	-0.73588
C	1.60608	0.47709	-2.19939
C	0.08535	-1.57311	-1.86579
H	-0.99135	-1.62203	-1.66394
H	0.22983	-1.86611	-2.91137
C	2.35877	-0.0556	-3.37842
H	2.48848	0.72511	-4.13776
H	3.36235	-0.35792	-3.05049
H	1.886	-0.92736	-3.83358
C	0.81381	-2.58081	-0.94766
H	0.68758	-2.2747	0.09789
H	0.34364	-3.56406	-1.06669
C	2.28347	-2.66423	-1.27701
C	3.20474	-1.89701	-0.5647
C	2.70887	-3.44665	-2.34955
C	4.55277	-1.91887	-0.9309
H	2.89087	-1.26936	0.2648
C	4.05502	-3.45521	-2.7152
H	2.00757	-4.04955	-2.91943
C	4.99283	-2.69026	-2.01177
H	6.0371	-2.70541	-2.29065
C	-2.09146	2.16881	1.47676
C	-3.04652	1.2418	1.05031
C	-2.75496	-0.12813	1.01354
H	-4.02635	1.59047	0.72956
C	-0.49949	0.35574	1.81484
C	-1.47504	-0.55251	1.39345
H	-1.24306	-1.61359	1.36752
C	-3.77946	-1.11884	0.58478
C	-5.13807	-0.88447	0.81492
C	-3.40497	-2.31095	-0.04238
H	-5.43352	0.02213	1.33618
C	-4.34905	-3.25848	-0.44212
H	-2.35156	-2.50214	-0.22831
C	0.87796	-0.07808	2.16951

C	1.9462	0.81444	2.02365
C	1.14089	-1.36805	2.63899
H	1.75362	1.80963	1.62965
C	2.44007	-1.78199	2.94412
H	0.31384	-2.05942	2.77866
C	-0.83476	1.71345	1.86445
H	-0.10788	2.43708	2.21273
C	3.25012	0.45476	2.37026
C	3.47628	-0.84946	2.8235
H	4.4863	-1.15216	3.06672
C	-5.69965	-2.98177	-0.20506
H	-6.44506	-3.70408	-0.51184
C	-6.11533	-1.80248	0.4227
C	4.36878	1.49245	2.23615
C	4.43187	1.98951	0.78253
H	4.58822	1.1511	0.09469
H	3.5059	2.50382	0.50474
H	5.25793	2.70116	0.6651
C	4.06119	2.68648	3.15659
H	3.99933	2.36876	4.20292
H	4.85354	3.43911	3.07179
H	3.11248	3.16298	2.88638
C	5.73486	0.9162	2.61769
H	6.50673	1.68035	2.47893
H	5.76064	0.60001	3.66624
H	5.98466	0.05544	1.98983
C	2.68104	-3.22801	3.38906
C	4.17328	-3.54189	3.53935
H	4.64016	-2.93352	4.32101
H	4.29821	-4.5935	3.8164
H	4.71145	-3.37185	2.59978
C	1.98739	-3.46865	4.74008
H	0.90874	-3.29427	4.67266
H	2.14318	-4.50339	5.06525
H	2.3929	-2.80187	5.50839
C	2.09752	-4.18728	2.33609
H	1.01543	-4.06218	2.22519
H	2.56111	-4.01483	1.35808
H	2.28482	-5.2256	2.63161
C	-3.87437	-4.55254	-1.11232
C	-3.08688	-4.21285	-2.38912
H	-3.70989	-3.65213	-3.09383
H	-2.19765	-3.6128	-2.16888
H	-2.75411	-5.13367	-2.88052
C	-2.959	-5.31791	-0.14091
H	-2.08094	-4.72596	0.13817

H	-3.49814	-5.57815	0.77601
H	-2.60654	-6.24419	-0.60786
C	-5.04074	-5.46843	-1.49764
H	-5.62199	-5.77221	-0.62072
H	-5.7167	-4.98323	-2.20978
H	-4.64966	-6.37491	-1.97034
C	-7.59023	-1.49535	0.70474
C	-7.79816	-1.35096	2.22205
H	-7.52918	-2.27772	2.73967
H	-7.19161	-0.54055	2.63783
H	-8.84941	-1.12955	2.43707
C	-7.97801	-0.17864	0.01027
H	-9.03084	0.05261	0.20605
H	-7.37656	0.66129	0.37162
H	-7.83906	-0.25625	-1.07325
C	-8.52221	-2.59945	0.1948
H	-8.43288	-2.73503	-0.88829
H	-8.31686	-3.55854	0.68181
H	-9.55968	-2.32807	0.41432
O	5.38761	-1.15002	-0.1803
O	4.37698	-4.24262	-3.77441
C	5.73293	-4.28596	-4.18084
H	5.77047	-4.96304	-5.0334
H	6.08711	-3.29509	-4.48592
H	6.37442	-4.67105	-3.38061
C	6.73253	-1.02165	-0.60647
H	7.26372	-1.97736	-0.53979
H	6.78574	-0.64488	-1.63384
H	7.19571	-0.30191	0.06853

Catalyst **4.13** / **2.4** Transition state 1 proximal *s-cis*

EE = -2746.121 a.u.

ΔG^0 = -2744.9033 a.u.

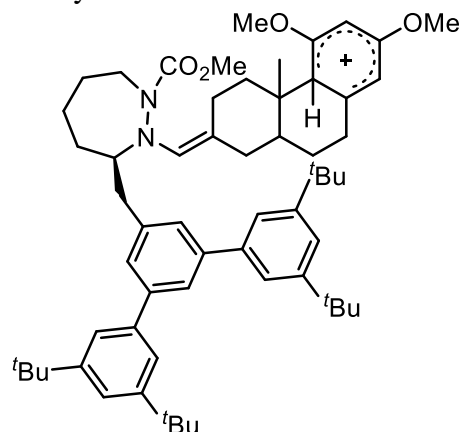
C	3.17118	4.08202	-0.7159
N	1.46134	4.90576	0.87644
C	3.44374	5.55839	-0.99109
C	2.53779	3.40453	-1.94825
H	4.119	3.59106	-0.48118
C	2.49884	2.83431	1.27133
C	1.99804	5.9338	1.78557
C	0.20585	4.89584	0.31374
C	3.95632	6.37075	0.20672
H	2.5393	6.02557	-1.39511
H	4.18269	5.57461	-1.7953
C	2.09504	1.97745	-1.73164

H	1.68106	3.99783	-2.27346
H	3.29077	3.4537	-2.74107
C	1.86402	2.40707	2.44177
H	3.30548	2.20179	0.9179
C	2.83524	6.97476	1.0571
H	1.15265	6.38907	2.29685
H	2.59608	5.40005	2.5295
O	-0.46646	5.98987	0.66313
O	-0.22517	4.00239	-0.37646
H	4.57575	7.18691	-0.16922
H	4.60766	5.74749	0.83061
H	2.17957	7.57507	0.41864
H	3.25891	7.64645	1.80793
C	-1.80593	6.07925	0.15213
C	2.54326	-0.31776	-1.07013
C	0.27677	0.36054	-1.65793
H	-1.79615	6.0197	-0.93497
H	-2.41863	5.27742	0.56174
H	-2.17409	7.04578	0.48111
C	1.18257	-0.60654	-1.21775
H	0.82	-1.58685	-0.92927
C	0.68007	2.90929	2.97399
H	0.41962	2.65118	3.99426
H	0.18362	3.78995	2.58984
N	2.34332	3.90666	0.51141
C	2.23789	1.0367	2.91578
H	2.21784	0.96979	4.00545
H	3.22606	0.72292	2.57821
C	-0.84032	1.48361	2.10351
H	-0.49917	1.71404	1.09381
C	-0.17822	0.49776	2.78601
C	-0.6168	-0.04713	4.10906
H	-1.40392	0.53325	4.58551
H	-1.00154	-1.06221	3.95206
H	0.23677	-0.12913	4.78891
C	1.15882	0.04777	2.31831
H	1.23899	0.07548	1.23249
H	1.38287	-0.9626	2.66711
C	-2.19458	2.02471	2.46696
H	-2.27281	3.05948	2.12168
H	-2.34132	2.03571	3.5489
C	-3.33095	1.21406	1.80182
H	-4.28464	1.66627	2.08578
H	-3.22852	1.2968	0.71865
C	-3.30732	-0.24432	2.17961
C	-2.58838	-1.14106	1.39289

C	-3.93966	-0.68894	3.33674
C	-2.48147	-2.47538	1.77898
H	-2.09968	-0.8185	0.48037
C	-3.8418	-2.02833	3.71133
H	-4.50758	-0.01176	3.96475
C	-3.10778	-2.93668	2.94077
H	-3.03268	-3.9722	3.23423
C	0.75515	1.65011	-1.90564
H	0.07586	2.42373	-2.23677
C	2.99081	0.97719	-1.34859
H	4.05011	1.20574	-1.27103
C	3.47123	-1.36337	-0.5649
C	4.53794	-1.02918	0.27229
C	3.27046	-2.70496	-0.89409
H	4.69662	0.0114	0.53393
C	4.09676	-3.70983	-0.39155
H	2.46094	-2.96147	-1.56833
C	-1.16539	0.047	-1.83708
C	-2.12751	1.05588	-1.72445
C	-1.57705	-1.25901	-2.11886
H	-1.80727	2.05582	-1.45641
C	-2.92555	-1.57497	-2.26938
H	-0.82757	-2.03188	-2.22289
C	-3.48257	0.78563	-1.92496
C	-3.85507	-0.53449	-2.18689
H	-4.90452	-0.76191	-2.33777
C	5.15018	-3.33834	0.44899
H	5.79662	-4.10602	0.84811
C	5.39278	-2.00413	0.78845
C	6.55917	-1.584	1.68922
C	7.32318	-2.78816	2.24941
H	8.13088	-2.43339	2.89352
H	6.67362	-3.43296	2.84709
H	7.77128	-3.38794	1.45358
C	6.03233	-0.75612	2.8737
H	5.57961	0.18067	2.54183
H	5.28582	-1.31856	3.44072
H	6.85685	-0.5031	3.54538
C	7.53756	-0.72607	0.86859
H	7.93318	-1.29498	0.02346
H	7.04995	0.17023	0.47832
H	8.37651	-0.41147	1.49548
C	3.82386	-5.16665	-0.7794
C	3.95288	-5.31819	-2.30469
H	3.24024	-4.68211	-2.83386
H	4.96005	-5.05069	-2.63429

H	3.76007	-6.35497	-2.59357
C	2.39654	-5.54747	-0.34869
H	1.64735	-4.92203	-0.83911
H	2.19256	-6.58846	-0.61382
H	2.27773	-5.43791	0.73249
C	4.80255	-6.13925	-0.11391
H	5.83468	-5.93966	-0.41275
H	4.74053	-6.08959	0.97623
H	4.558	-7.15961	-0.41777
C	-4.54783	1.88825	-1.92215
C	-3.99401	3.23035	-1.4277
H	-3.19866	3.60372	-2.07761
H	-4.79617	3.97206	-1.42354
H	-3.59871	3.15745	-0.4106
C	-5.74277	1.4951	-1.03682
H	-6.47475	2.30698	-1.0279
H	-6.24715	0.60134	-1.4081
H	-5.42966	1.30524	-0.0081
C	-5.04226	2.07397	-3.36844
H	-5.48042	1.15085	-3.75524
H	-5.80428	2.85751	-3.40695
H	-4.21662	2.36175	-4.0242
C	-3.41425	-3.00426	-2.51923
C	-2.26071	-4.01209	-2.53115
H	-2.66069	-5.0174	-2.68333
H	-1.55275	-3.80814	-3.33874
H	-1.72349	-3.99779	-1.57955
C	-4.1403	-3.07152	-3.87278
H	-4.49443	-4.08977	-4.05594
H	-5.00442	-2.40404	-3.8998
H	-3.46612	-2.79036	-4.686
C	-4.38312	-3.40472	-1.39273
H	-5.2573	-2.751	-1.35866
H	-4.73276	-4.42901	-1.55011
H	-3.87672	-3.35286	-0.42571
O	-4.49205	-2.37361	4.85148
O	-1.74372	-3.27273	0.96018
C	-4.42755	-3.7258	5.2746
H	-3.39139	-4.06823	5.34391
H	-4.88422	-3.75307	6.26055
H	-4.98531	-4.37787	4.5969
C	-1.65744	-4.6527	1.2774
H	-1.04385	-5.10338	0.50099
H	-1.18023	-4.80549	2.24926
H	-2.64751	-5.11819	1.27542

Catalyst **4.13** / **2.4** Cation 2



Proximal *s-trans*

EE = -2746.1693 a.u.

$\Delta G^0 = -2744.9397$ a.u.

C	-1.54535	4.48503	-0.52317
N	0.83051	4.38213	-1.1699
C	-1.3682	5.98766	-0.72854
C	-1.95205	4.18005	0.94264
H	-2.36777	4.15674	-1.16972
C	-0.53701	2.46299	-1.51255
C	1.01734	4.99449	-2.49233
C	1.65433	4.61012	-0.10577
C	-1.07651	6.416	-2.17529
H	-0.58552	6.3616	-0.05813
H	-2.30099	6.44991	-0.39571
H	-1.22833	4.6569	1.60813
H	-2.93301	4.63098	1.11709
C	0.29843	1.59909	-2.10922
H	-1.57295	2.15301	-1.4216
C	0.40557	6.38746	-2.55783
H	2.08224	5.01775	-2.71901
H	0.53517	4.3179	-3.20304
O	2.74016	5.30336	-0.48307
O	1.45835	4.24419	1.03455
H	-1.44436	7.4348	-2.31734
H	-1.64732	5.78039	-2.86268
H	0.96667	7.04838	-1.88861
H	0.53213	6.77417	-3.57285
C	3.61681	5.6899	0.58204
H	3.09165	6.33826	1.283
H	3.99189	4.81242	1.10729
H	4.43193	6.22665	0.10555
C	1.78704	1.67118	-2.33039
H	1.9901	1.62613	-3.40831

H	2.22407	2.60055	-1.96689
N	-0.35359	3.71886	-0.94066
C	-0.26433	0.26103	-2.52197
H	-0.13461	0.08927	-3.59803
H	-1.33865	0.21461	-2.31844
C	0.42048	-0.85972	-1.7263
H	0.28306	-0.59894	-0.66746
C	2.51467	0.50632	-1.62852
H	3.57316	0.55756	-1.88842
H	2.4375	0.65595	-0.54948
C	1.95313	-0.88741	-1.96625
C	-0.24982	-2.20864	-1.94672
H	-1.32384	-2.11278	-1.777
H	-0.12221	-2.55416	-2.97731
C	2.33515	-1.28439	-3.39643
H	1.86844	-0.61564	-4.12043
H	3.41674	-1.20732	-3.53593
H	2.03588	-2.30415	-3.64552
C	0.32818	-3.23336	-0.96191
H	0.09975	-2.90076	0.05764
H	-0.09732	-4.2272	-1.10571
C	1.80932	-3.27191	-1.14213
C	2.53992	-1.98127	-0.933
C	2.43353	-4.37933	-1.58459
C	4.02314	-2.1241	-1.0208
H	2.3045	-1.5835	0.06591
C	3.84915	-4.3726	-1.80426
H	1.90264	-5.3022	-1.78123
C	4.64286	-3.25434	-1.51033
H	5.71495	-3.30623	-1.60945
C	-1.9825	2.69732	1.2026
C	-3.0766	1.90694	0.85986
C	-2.98606	0.51103	0.89807
H	-3.99268	2.37435	0.51009
C	-0.67604	0.69112	1.64829
C	-1.77431	-0.08473	1.26382
H	-1.70088	-1.16768	1.25466
C	-4.1559	-0.32565	0.52358
C	-5.44134	0.02221	0.94023
C	-3.98642	-1.47261	-0.25132
H	-5.56651	0.9045	1.559
C	-5.06695	-2.27553	-0.61459
H	-2.98741	-1.72203	-0.58831
C	0.63867	0.09315	2.01475
C	1.79844	0.86786	1.90336
C	0.75634	-1.21781	2.48605

H	1.72506	1.87907	1.51843
C	1.99761	-1.75688	2.83824
H	-0.13966	-1.81498	2.61762
C	-0.81661	2.07979	1.64124
H	0.01071	2.71777	1.91855
C	3.04807	0.379	2.27875
C	3.13028	-0.94285	2.72727
H	4.09245	-1.34171	3.01327
C	-6.34027	-1.9	-0.17608
H	-7.18829	-2.51249	-0.44539
C	-6.54944	-0.75597	0.60018
C	4.25259	1.32797	2.25957
C	4.43292	1.96067	0.87005
H	4.61721	1.19851	0.1133
H	3.54823	2.52916	0.56927
H	5.28365	2.64823	0.88891
C	3.99096	2.45746	3.27316
H	3.81996	2.05196	4.27364
H	4.8554	3.12704	3.31506
H	3.11726	3.04607	2.9808
C	5.55147	0.61277	2.64159
H	6.38796	1.31182	2.56978
H	5.51692	0.23648	3.66712
H	5.75392	-0.23002	1.97552
C	2.0733	-3.18667	3.38712
C	3.51609	-3.63503	3.64281
H	4.00411	-3.01838	4.40133
H	3.51338	-4.6661	4.00342
H	4.11417	-3.59929	2.72772
C	1.30076	-3.25182	4.71602
H	0.24879	-2.99167	4.57989
H	1.35001	-4.26371	5.12758
H	1.73175	-2.5614	5.44539
C	1.44327	-4.16805	2.38611
H	0.39059	-3.94319	2.20191
H	1.97651	-4.14043	1.43103
H	1.50219	-5.18726	2.77718
C	-4.82532	-3.50313	-1.49881
C	-4.33776	-3.03222	-2.88007
H	-5.08993	-2.39949	-3.35805
H	-3.41166	-2.45749	-2.80387
H	-4.15081	-3.8944	-3.5263
C	-3.75312	-4.40208	-0.85972
H	-2.79927	-3.88162	-0.74627
H	-4.07328	-4.74275	0.12821
H	-3.58137	-5.28014	-1.48808

C	-6.09478	-4.33837	-1.69411
H	-6.49382	-4.68978	-0.73905
H	-6.87484	-3.7728	-2.20946
H	-5.86023	-5.21337	-2.30467
C	-7.93893	-0.33818	1.09268
C	-7.94752	-0.31671	2.63074
H	-7.71382	-1.30671	3.03071
H	-7.21815	0.39247	3.02739
H	-8.9363	-0.02336	2.99392
C	-8.26388	1.06841	0.56141
H	-9.25436	1.3777	0.90615
H	-7.53949	1.80758	0.90965
H	-8.26187	1.07684	-0.53162
C	-9.03748	-1.29547	0.61951
H	-9.09515	-1.33453	-0.47126
H	-8.87801	-2.30925	0.99552
H	-10.00301	-0.94764	0.99393
O	4.68574	-1.07606	-0.60236
O	4.32972	-5.49442	-2.25994
C	5.73733	-5.63254	-2.52131
H	5.85563	-6.63609	-2.91469
H	6.05181	-4.89576	-3.26006
H	6.29834	-5.52137	-1.59367
C	6.11812	-1.04759	-0.71713
H	6.55584	-1.83052	-0.09672
H	6.41006	-1.16807	-1.7606
H	6.41847	-0.06904	-0.35542

Catalyst **4.13** / **2.4** Cation 2 proximal *s-cis*

EE = -2746.1674 a.u.

ΔG^0 = -2744.9404 a.u.

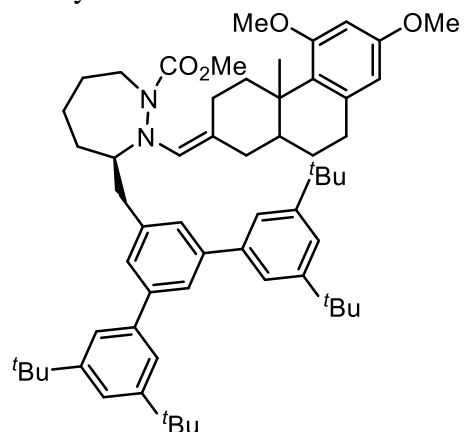
C	0.76847	4.74472	-0.89188
N	-1.20166	4.61663	0.56819
C	0.3972	6.22093	-1.01887
C	0.65475	4.03277	-2.26136
H	1.81583	4.69118	-0.57118
C	0.57463	3.05112	0.89759
C	-1.13226	5.60086	1.65531
C	-2.34705	4.26558	-0.08719
C	0.4883	7.02401	0.28793
H	-0.61068	6.3099	-1.44029
H	1.07827	6.64622	-1.76034
C	0.87286	2.54542	-2.1436
H	-0.33974	4.22231	-2.67235
H	1.39197	4.48273	-2.93378

C	0.08826	2.21408	1.8254
H	1.62098	2.93527	0.6344
C	-0.78783	6.99048	1.13487
H	-2.08155	5.602	2.18766
H	-0.35937	5.23612	2.33772
O	-3.39825	4.93997	0.4056
O	-2.42744	3.45508	-0.98512
H	0.70573	8.06615	0.0429
H	1.3353	6.65979	0.88157
H	-1.62787	7.36017	0.53718
H	-0.68042	7.66277	1.99071
C	-4.66187	4.6232	-0.18651
C	2.27683	0.66045	-1.54
C	-0.0942	0.31598	-1.97747
H	-4.62168	4.76166	-1.26631
H	-4.93682	3.59319	0.03926
H	-5.373	5.31176	0.26049
C	1.16299	-0.17893	-1.62035
H	1.27618	-1.21765	-1.32888
C	-1.32865	2.04427	2.30716
H	-1.35451	2.09009	3.40362
H	-2.00023	2.8221	1.9483
N	-0.00924	4.07241	0.15782
C	0.99422	1.12678	2.3477
H	1.05915	1.16731	3.44146
H	2.01108	1.24782	1.96401
C	-1.8729	0.68089	1.84082
H	-1.81839	0.69137	0.74249
C	-0.98324	-0.50014	2.31744
C	-1.05019	-0.72562	3.83363
H	-2.05781	-0.92713	4.19608
H	-0.41542	-1.56774	4.12092
H	-0.6804	0.15265	4.36368
C	0.47698	-0.25329	1.90446
H	0.55909	-0.31139	0.81653
H	1.1197	-1.03204	2.32393
C	-3.33532	0.49678	2.23862
H	-3.92748	1.32083	1.83141
H	-3.44251	0.5418	3.32621
C	-3.90236	-0.83313	1.70647
H	-4.89761	-1.03128	2.10656
H	-3.97557	-0.76258	0.61615
C	-2.97818	-1.9669	2.00627
C	-1.57466	-1.78271	1.53827
C	-3.33223	-3.03908	2.74065
C	-0.72304	-2.98935	1.686

H	-1.56451	-1.50238	0.47733
C	-2.36621	-4.05791	3.03768
H	-4.32944	-3.16562	3.14272
C	-1.06516	-4.04403	2.50439
H	-0.39861	-4.87774	2.65795
C	-0.21258	1.6828	-2.24623
H	-1.17205	2.10784	-2.50463
C	2.12296	2.02061	-1.81846
H	2.98409	2.68049	-1.75588
C	3.58426	0.11808	-1.0892
C	4.3704	0.84142	-0.1909
C	4.03482	-1.12647	-1.53272
H	4.00781	1.80092	0.16361
C	5.25309	-1.65282	-1.1004
H	3.42872	-1.67333	-2.24742
C	-1.29378	-0.56612	-2.00827
C	-2.57616	-0.0198	-1.8986
C	-1.16061	-1.9553	-2.13224
H	-2.68024	1.04902	-1.75762
C	-2.27313	-2.79248	-2.11885
H	-0.17224	-2.37814	-2.24784
C	-3.71871	-0.82435	-1.95053
C	-3.54213	-2.20553	-2.03641
H	-4.41256	-2.8497	-2.05384
C	6.01125	-0.90343	-0.19528
H	6.95391	-1.30056	0.15173
C	5.58844	0.34395	0.27356
C	6.40385	1.17096	1.27267
C	7.69445	0.46356	1.69763
H	8.23201	1.09306	2.41041
H	7.48738	-0.49314	2.18406
H	8.35478	0.28401	0.84546
C	5.55744	1.42797	2.53151
H	4.65182	1.99301	2.3003
H	5.26156	0.48412	2.997
H	6.13637	2.00393	3.25858
C	6.77898	2.51667	0.62881
H	7.38232	2.35903	-0.26881
H	5.89182	3.08812	0.34748
H	7.35994	3.11854	1.33303
C	5.72006	-3.00912	-1.63975
C	5.86051	-2.92446	-3.16933
H	4.91043	-2.67804	-3.6477
H	6.59074	-2.16002	-3.44668
H	6.20004	-3.88509	-3.5662
C	4.68206	-4.08677	-1.28364

H	3.70387	-3.86183	-1.71534
H	5.00414	-5.0578	-1.66943
H	4.57207	-4.16874	-0.19884
C	7.07115	-3.43509	-1.05637
H	7.86074	-2.7229	-1.30871
H	7.02742	-3.53443	0.03124
H	7.35133	-4.40625	-1.47072
C	-5.11862	-0.20023	-2.0077
C	-5.17692	1.14932	-1.27745
H	-4.52239	1.89746	-1.72796
H	-6.19837	1.53666	-1.31711
H	-4.89685	1.0488	-0.22483
C	-6.18899	-1.12456	-1.40752
H	-7.14971	-0.60455	-1.39738
H	-6.32091	-2.03488	-1.99504
H	-5.94699	-1.41079	-0.38064
C	-5.45275	0.0365	-3.49275
H	-5.43425	-0.90455	-4.04816
H	-6.45	0.47556	-3.5883
H	-4.72929	0.71801	-3.94709
C	-2.15731	-4.31712	-2.20156
C	-0.70025	-4.78102	-2.28899
H	-0.66727	-5.87257	-2.31053
H	-0.21292	-4.41184	-3.19493
H	-0.12265	-4.44216	-1.42485
C	-2.90407	-4.82628	-3.44591
H	-2.81408	-5.9137	-3.51508
H	-3.96667	-4.57797	-3.40886
H	-2.48198	-4.38765	-4.35354
C	-2.78439	-4.93433	-0.93988
H	-3.8358	-4.65926	-0.83326
H	-2.72051	-6.02504	-0.98357
H	-2.25295	-4.59813	-0.04479
O	-2.81297	-5.01356	3.80317
O	0.36863	-2.94392	0.96596
C	-1.95284	-6.09869	4.19161
H	-1.07882	-5.71047	4.71401
H	-2.55094	-6.71038	4.85799
H	-1.66086	-6.6729	3.31237
C	1.34222	-3.99333	1.07635
H	2.13757	-3.71804	0.39085
H	1.72089	-4.04151	2.09803
H	0.89923	-4.94609	0.78246

Catalyst **4.13** / **2.4** Enamine



Proximal *s-trans*

EE = -2745.7498 a.u.

$\Delta G^0 = -2744.5341$ a.u.

C	-1.54535	4.48503	-0.52317
N	0.83051	4.38213	-1.1699
C	-1.3682	5.98766	-0.72854
C	-1.95205	4.18005	0.94264
H	-2.36777	4.15674	-1.16972
C	-0.53701	2.46299	-1.51255
C	1.01734	4.99449	-2.49233
C	1.65433	4.61012	-0.10577
C	-1.07651	6.416	-2.17529
H	-0.58552	6.3616	-0.05813
H	-2.30099	6.44991	-0.39571
H	-1.22833	4.6569	1.60813
H	-2.93301	4.63098	1.11709
C	0.29843	1.59909	-2.10922
H	-1.57295	2.15301	-1.4216
C	0.40557	6.38746	-2.55783
H	2.08224	5.01775	-2.71901
H	0.53517	4.3179	-3.20304
O	2.74016	5.30336	-0.48307
O	1.45835	4.24419	1.03455
H	-1.44436	7.4348	-2.31734
H	-1.64732	5.78039	-2.86268
H	0.96667	7.04838	-1.88861
H	0.53213	6.77417	-3.57285
C	3.61681	5.6899	0.58204
H	3.09165	6.33826	1.283
H	3.99189	4.81242	1.10729
H	4.43193	6.22665	0.10555
C	1.78704	1.67118	-2.33039
H	1.9901	1.62613	-3.40831

H	2.22407	2.60055	-1.96689
N	-0.35359	3.71886	-0.94066
C	-0.26433	0.26103	-2.52197
H	-0.13461	0.08927	-3.59803
H	-1.33865	0.21461	-2.31844
C	0.42048	-0.85972	-1.7263
H	0.28306	-0.59894	-0.66746
C	2.51467	0.50632	-1.62852
H	3.57316	0.55756	-1.88842
H	2.4375	0.65595	-0.54948
C	1.95313	-0.88741	-1.96625
C	-0.24982	-2.20864	-1.94672
H	-1.32384	-2.11278	-1.777
H	-0.12221	-2.55416	-2.97731
C	2.33515	-1.28439	-3.39643
H	1.86844	-0.61564	-4.12043
H	3.41674	-1.20732	-3.53593
H	2.03588	-2.30415	-3.64552
C	0.32818	-3.23336	-0.96191
H	0.09975	-2.90076	0.05764
H	-0.09732	-4.2272	-1.10571
C	1.80932	-3.27191	-1.14213
C	2.53992	-1.98127	-0.933
C	2.43353	-4.37933	-1.58459
C	4.02314	-2.1241	-1.0208
C	3.84915	-4.3726	-1.80426
H	1.90264	-5.3022	-1.78123
C	4.64286	-3.25434	-1.51033
H	5.71495	-3.30623	-1.60945
C	-1.9825	2.69732	1.2026
C	-3.0766	1.90694	0.85986
C	-2.98606	0.51103	0.89807
H	-3.99268	2.37435	0.51009
C	-0.67604	0.69112	1.64829
C	-1.77431	-0.08473	1.26382
H	-1.70088	-1.16768	1.25466
C	-4.1559	-0.32565	0.52358
C	-5.44134	0.02221	0.94023
C	-3.98642	-1.47261	-0.25132
H	-5.56651	0.9045	1.559
C	-5.06695	-2.27553	-0.61459
H	-2.98741	-1.72203	-0.58831
C	0.63867	0.09315	2.01475
C	1.79844	0.86786	1.90336
C	0.75634	-1.21781	2.48605
H	1.72506	1.87907	1.51843

C	1.99761	-1.75688	2.83824
H	-0.13966	-1.81498	2.61762
C	-0.81661	2.07979	1.64124
H	0.01071	2.71777	1.91855
C	3.04807	0.379	2.27875
C	3.13028	-0.94285	2.72727
H	4.09245	-1.34171	3.01327
C	-6.34027	-1.9	-0.17608
H	-7.18829	-2.51249	-0.44539
C	-6.54944	-0.75597	0.60018
C	4.25259	1.32797	2.25957
C	4.43292	1.96067	0.87005
H	4.61721	1.19851	0.1133
H	3.54823	2.52916	0.56927
H	5.28365	2.64823	0.88891
C	3.99096	2.45746	3.27316
H	3.81996	2.05196	4.27364
H	4.8554	3.12704	3.31506
H	3.11726	3.04607	2.9808
C	5.55147	0.61277	2.64159
H	6.38796	1.31182	2.56978
H	5.51692	0.23648	3.66712
H	5.75392	-0.23002	1.97552
C	2.0733	-3.18667	3.38712
C	3.51609	-3.63503	3.64281
H	4.00411	-3.01838	4.40133
H	3.51338	-4.6661	4.00342
H	4.11417	-3.59929	2.72772
C	1.30076	-3.25182	4.71602
H	0.24879	-2.99167	4.57989
H	1.35001	-4.26371	5.12758
H	1.73175	-2.5614	5.44539
C	1.44327	-4.16805	2.38611
H	0.39059	-3.94319	2.20191
H	1.97651	-4.14043	1.43103
H	1.50219	-5.18726	2.77718
C	-4.82532	-3.50313	-1.49881
C	-4.33776	-3.03222	-2.88007
H	-5.08993	-2.39949	-3.35805
H	-3.41166	-2.45749	-2.80387
H	-4.15081	-3.8944	-3.5263
C	-3.75312	-4.40208	-0.85972
H	-2.79927	-3.88162	-0.74627
H	-4.07328	-4.74275	0.12821
H	-3.58137	-5.28014	-1.48808
C	-6.09478	-4.33837	-1.69411

H	-6.49382	-4.68978	-0.73905
H	-6.87484	-3.7728	-2.20946
H	-5.86023	-5.21337	-2.30467
C	-7.93893	-0.33818	1.09268
C	-7.94752	-0.31671	2.63074
H	-7.71382	-1.30671	3.03071
H	-7.21815	0.39247	3.02739
H	-8.9363	-0.02336	2.99392
C	-8.26388	1.06841	0.56141
H	-9.25436	1.3777	0.90615
H	-7.53949	1.80758	0.90965
H	-8.26187	1.07684	-0.53162
C	-9.03748	-1.29547	0.61951
H	-9.09515	-1.33453	-0.47126
H	-8.87801	-2.30925	0.99552
H	-10.00301	-0.94764	0.99393
O	4.68574	-1.07606	-0.60236
O	4.32972	-5.49442	-2.25994
C	5.73733	-5.63254	-2.52131
H	5.85563	-6.63609	-2.91469
H	6.05181	-4.89576	-3.26006
H	6.29834	-5.52137	-1.59367
C	6.11812	-1.04759	-0.71713
H	6.55584	-1.83052	-0.09672
H	6.41006	-1.16807	-1.7606
H	6.41847	-0.06904	-0.35542

Catalyst **4.13** / **2.4** Enamine proximal *s-cis*

EE = -2745.7478 a.u.

ΔG^0 = -2744.532 a.u.

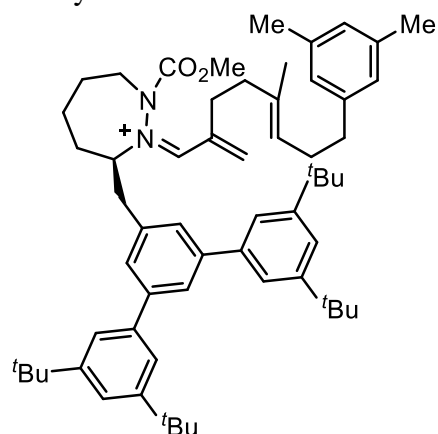
C	3.02365	-3.45114	-1.85766
N	4.05794	-2.88699	0.29262
C	4.30568	-4.24196	-2.12373
C	2.88665	-2.31936	-2.89958
H	2.17494	-4.13612	-1.99613
C	1.73104	-3.31888	0.22007
C	4.48479	-4.10301	0.9945
C	4.80736	-1.74831	0.24257
C	4.555	-5.42781	-1.18174
H	5.16601	-3.55916	-2.09289
H	4.23791	-4.59762	-3.15803
C	1.82474	-1.30046	-2.56719
H	3.84956	-1.80187	-2.97455
H	2.69025	-2.78308	-3.8746
C	1.19002	-2.66155	1.25084

H	1.26704	-4.24669	-0.1243
C	5.2878	-5.044	0.10558
H	5.05662	-3.80852	1.87452
H	3.56672	-4.58848	1.34098
O	5.94589	-1.89345	0.95213
O	4.52181	-0.72607	-0.35637
H	5.15358	-6.17816	-1.70876
H	3.59879	-5.91086	-0.93537
H	6.24192	-4.56467	-0.14853
H	5.52405	-5.94518	0.68308
C	6.78699	-0.74006	0.97511
C	-0.48799	-0.6477	-2.18578
C	1.30165	0.96497	-1.83859
H	7.078	-0.45784	-0.03872
H	6.27469	0.10052	1.44882
H	7.66119	-1.02842	1.55637
C	-0.05533	0.63968	-1.8443
H	-0.78653	1.36572	-1.49723
C	1.62818	-1.30296	1.71892
H	2.07591	-1.35373	2.72314
H	2.38881	-0.89593	1.04198
N	2.90272	-2.9441	-0.48059
C	-0.00652	-3.22128	1.9673
H	0.27086	-3.47957	2.99943
H	-0.3269	-4.15789	1.49514
C	0.42022	-0.34951	1.71839
H	0.06221	-0.32773	0.67598
C	-0.78515	-0.84275	2.56551
C	-0.43769	-0.97197	4.06127
H	-0.20746	0.00153	4.50339
H	-1.29284	-1.38989	4.60043
H	0.42205	-1.62855	4.22805
C	-1.17765	-2.22929	1.99647
H	-1.54922	-2.082	0.97337
H	-1.99007	-2.66668	2.5768
C	0.80664	1.07789	2.0775
H	1.73608	1.35807	1.56986
H	0.99238	1.167	3.15533
C	-0.31222	2.00901	1.63259
H	-0.2135	2.99737	2.09766
H	-0.21842	2.17636	0.5524
C	-1.70324	1.47512	1.92193
C	-1.93279	0.17451	2.40709
C	-2.75846	2.363	1.70069
C	-3.26486	-0.13314	2.77209
C	-4.06551	1.99807	1.98823

H	-2.56366	3.35973	1.31334
C	-4.32676	0.74605	2.54629
H	-5.33465	0.46435	2.81435
C	2.22304	-0.01269	-2.22299
H	3.28163	0.2217	-2.22079
C	0.46236	-1.6117	-2.54471
H	0.13279	-2.61455	-2.8111
C	-1.93143	-0.9743	-2.05931
C	-2.33343	-2.20209	-1.52458
C	-2.90149	-0.02263	-2.39272
H	-1.56671	-2.91875	-1.24532
C	-4.25797	-0.26469	-2.17546
H	-2.57544	0.91577	-2.82838
C	1.78546	2.2688	-1.32188
C	2.96448	2.29844	-0.58037
C	1.05733	3.45414	-1.49867
H	3.50128	1.36652	-0.41571
C	1.48717	4.65013	-0.92942
H	0.14741	3.42069	-2.0894
C	3.43307	3.4835	-0.00214
C	2.68103	4.6425	-0.18627
H	3.01852	5.57244	0.26066
C	-4.61951	-1.49445	-1.61583
H	-5.67101	-1.68929	-1.41858
C	-3.68172	-2.47652	-1.2836
C	-4.15574	-3.77034	-0.61534
C	-5.19296	-4.47169	-1.50759
H	-5.54268	-5.3905	-1.02394
H	-6.06539	-3.83786	-1.69318
H	-4.75456	-4.73867	-2.47507
C	-4.79491	-3.41291	0.73835
H	-4.07284	-2.89062	1.37728
H	-5.66673	-2.76234	0.60911
H	-5.12403	-4.3216	1.25591
C	-3.00302	-4.74615	-0.36003
H	-2.49289	-5.02083	-1.28972
H	-2.26464	-4.32083	0.3281
H	-3.39403	-5.66215	0.09457
C	-5.34332	0.76776	-2.49645
C	-4.76815	2.02969	-3.14787
H	-4.0574	2.53642	-2.48609
H	-4.26051	1.80074	-4.09102
H	-5.58113	2.73018	-3.36443
C	-6.04416	1.17882	-1.18975
H	-5.33553	1.65825	-0.50518
H	-6.85041	1.89111	-1.40131

H	-6.48198	0.31437	-0.67892
C	-6.37264	0.15304	-3.45949
H	-5.89336	-0.15144	-4.39598
H	-6.85982	-0.7256	-3.02573
H	-7.15127	0.88703	-3.69486
C	4.71798	3.43095	0.82929
C	5.86045	2.86382	-0.03134
H	6.03866	3.49447	-0.90905
H	6.78596	2.82308	0.55535
H	5.6334	1.84836	-0.3736
C	4.49542	2.49578	2.03099
H	5.40478	2.44355	2.64165
H	3.67671	2.858	2.66291
H	4.24826	1.48019	1.70006
C	5.1302	4.81076	1.34912
H	4.36853	5.23622	2.0113
H	6.05994	4.72439	1.92072
H	5.30364	5.51365	0.52699
C	0.69976	5.95701	-1.06757
C	-0.57092	5.78141	-1.9056
H	-1.09836	6.73839	-1.97226
H	-0.34021	5.45319	-2.92463
H	-1.25334	5.05275	-1.45396
C	1.58046	7.02287	-1.74091
H	1.02602	7.96307	-1.83731
H	2.48597	7.22428	-1.16033
H	1.88337	6.69857	-2.74213
C	0.28703	6.44528	0.33193
H	1.15774	6.63362	0.96755
H	-0.28174	7.37852	0.25271
H	-0.34291	5.69975	0.83003
O	-3.47706	-1.33309	3.38667
O	-5.03034	2.92122	1.71688
C	-6.36327	2.60234	2.07058
H	-6.96673	3.46242	1.78151
H	-6.71642	1.71464	1.5334
H	-6.45701	2.43541	3.14964
C	-4.77844	-1.64461	3.8454
H	-5.49217	-1.70386	3.01619
H	-4.69971	-2.62197	4.3214
H	-5.12743	-0.90654	4.57618

Catalyst **4.13** / **2.46** Iminium



EE = -2595.7259 a.u.

ΔG^0 = -2594.5144 a.u.

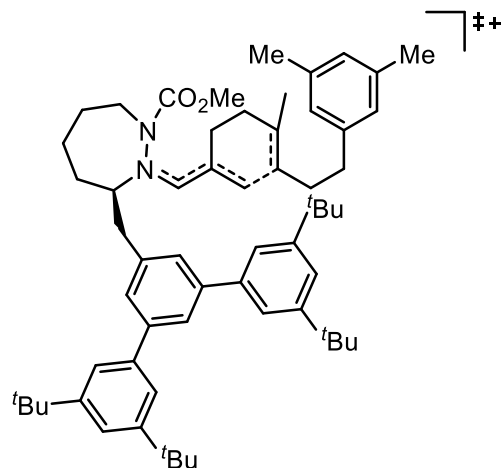
C	-0.17963	3.93227	-2.9307
N	-1.52376	3.75788	-0.8661
C	-0.5116	5.29135	-3.55049
C	-1.02806	2.78133	-3.4679
H	0.87768	3.72167	-3.10789
C	0.7349	4.30817	-0.69641
C	-2.67153	4.65587	-1.1091
C	-1.67222	2.71518	0.04134
C	-1.93798	5.78892	-3.31974
H	-0.31754	5.20087	-4.62419
H	0.20096	6.02799	-3.16083
H	-2.09103	3.02925	-3.40099
H	-0.79083	2.72018	-4.53681
C	0.74454	4.49881	0.75405
H	1.68164	4.35464	-1.23343
C	-2.31824	5.94423	-1.84422
H	-3.08425	4.89015	-0.12368
H	-3.43458	4.09722	-1.66215
O	-0.54779	2.04306	0.25524
O	-2.74508	2.49907	0.55932
H	-2.0252	6.76602	-3.80359
H	-2.664	5.13638	-3.81867
H	-3.21736	6.56349	-1.77639
H	-1.53232	6.49254	-1.30854
C	-0.64208	0.98167	1.22314
H	0.32536	0.47817	1.20307
H	-0.84233	1.40285	2.21213
H	-1.43876	0.28958	0.94293
C	1.84499	3.73346	1.45303
H	2.81875	4.14444	1.15463
H	1.82199	2.69866	1.0871

C	-0.12886	5.32878	1.33316
H	-0.08401	5.53126	2.39767
H	-0.88665	5.86036	0.76643
C	2.22487	1.49547	3.92746
H	1.16496	1.27932	3.78085
C	1.70599	3.70913	2.97908
H	0.67589	3.43293	3.23352
H	1.88564	4.71382	3.383
C	2.66239	2.71218	3.58933
C	3.05017	0.36351	4.48492
H	3.67198	0.71231	5.31798
H	3.74714	-0.00938	3.71975
C	4.0917	3.16029	3.73575
H	4.76079	2.33516	3.99077
H	4.17362	3.92539	4.51776
H	4.45813	3.61634	2.80854
C	2.16922	-0.79925	4.96997
H	2.81176	-1.57366	5.40383
H	1.51239	-0.44113	5.7709
C	1.33063	-1.40033	3.86409
C	1.94247	-2.10208	2.82294
C	-0.05835	-1.2542	3.84526
C	1.19697	-2.66809	1.78654
H	3.02416	-2.23205	2.83011
C	-0.83433	-1.80817	2.82291
H	-0.54734	-0.70103	4.646
C	-0.19182	-2.51254	1.80223
H	-0.79364	-2.94727	1.00436
C	-0.77402	1.45458	-2.79066
C	-1.84718	0.71465	-2.29493
C	-1.64726	-0.50909	-1.64557
H	-2.85882	1.09665	-2.41706
C	0.74659	-0.26488	-2.01036
C	-0.34117	-0.99238	-1.5274
H	-0.15208	-1.92022	-0.99497
C	-2.77825	-1.24826	-1.0295
C	-2.76762	-2.65054	-0.97139
C	-3.83861	-0.55268	-0.45273
H	-1.94565	-3.18311	-1.43861
C	-4.90096	-1.22543	0.1668
H	-3.81193	0.53379	-0.44555
C	2.12339	-0.79392	-1.82024
C	2.50092	-1.99683	-2.42041
C	3.02714	-0.10403	-1.01016
H	1.77382	-2.51504	-3.03735
C	4.31093	-0.60586	-0.78279

H	2.69878	0.82094	-0.54523
C	0.52335	0.96335	-2.63559
H	1.3765	1.52061	-3.01742
C	-4.85441	-2.61714	0.21191
H	-5.65561	-3.15871	0.70384
C	-3.78965	-3.35132	-0.33846
C	4.66484	-1.80221	-1.41645
H	5.6641	-2.2	-1.2552
C	3.78355	-2.51724	-2.23474
C	-3.76921	-4.8746	-0.1846
C	-2.56728	-5.51265	-0.88905
H	-2.57259	-5.30434	-1.96431
H	-1.61771	-5.15788	-0.47241
H	-2.60279	-6.59861	-0.75645
C	-3.68323	-5.20989	1.31511
H	-2.77236	-4.78487	1.75294
H	-4.54136	-4.81188	1.86603
H	-3.66079	-6.29592	1.45891
C	-5.0527	-5.48106	-0.77517
H	-5.13331	-5.25256	-1.84312
H	-5.04021	-6.57008	-0.65704
H	-5.94966	-5.10116	-0.27701
C	-6.02339	-0.4083	0.81229
C	-6.60721	0.57502	-0.21646
H	-5.85542	1.28832	-0.5684
H	-7.00522	0.03999	-1.0852
H	-7.42318	1.14774	0.2376
C	-5.43739	0.38296	1.99472
H	-4.60915	1.02474	1.67558
H	-6.2112	1.01555	2.44475
H	-5.06391	-0.30108	2.76476
C	-7.16078	-1.29318	1.33172
H	-6.81799	-1.97123	2.12021
H	-7.94836	-0.66208	1.75575
H	-7.6032	-1.8924	0.52842
C	4.24114	-3.83549	-2.86589
C	3.14277	-4.47805	-3.71876
H	2.8408	-3.82672	-4.54576
H	3.51487	-5.41422	-4.1469
H	2.25541	-4.7121	-3.12055
C	5.46417	-3.57719	-3.76173
H	6.29967	-3.15662	-3.19356
H	5.80294	-4.51581	-4.2139
H	5.21396	-2.87844	-4.56697
C	4.62367	-4.82323	-1.75012
H	4.96188	-5.76977	-2.18625

H	5.43135	-4.43298	-1.12298
H	3.76227	-5.03051	-1.10564
C	5.31891	0.08974	0.13577
C	5.73569	-0.88104	1.25351
H	6.22783	-1.77395	0.85605
H	6.43239	-0.38868	1.94123
H	4.85788	-1.20362	1.82442
C	6.55856	0.4954	-0.67894
H	6.28667	1.19736	-1.47432
H	7.29433	0.9808	-0.02829
H	7.03754	-0.37345	-1.14114
C	4.73512	1.34503	0.79243
H	4.4399	2.09405	0.04826
H	3.8612	1.11108	1.41475
H	5.49321	1.79872	1.43894
C	-2.33469	-1.65628	2.82367
H	-2.80587	-2.38813	3.49081
H	-2.62914	-0.66056	3.1712
H	-2.74751	-1.80702	1.82122
C	1.89193	-3.44849	0.70009
H	2.76126	-2.90142	0.31889
H	2.24968	-4.41136	1.08315
H	1.22442	-3.6537	-0.14312
N	-0.29029	4.02264	-1.43088

Catalyst **4.13** / **2.46** Transition State 1



Proximal *s-trans* cage

EE = -2595.7159 a.u.

$\Delta G^0 = -2594.5042$ a.u.

C	-1.07959	4.61372	-1.21985
N	-2.64825	4.02669	0.60522
C	-1.93261	5.8704	-1.36792
C	-1.22218	3.69914	-2.454
H	-0.03345	4.91487	-1.11875
C	-0.43104	3.2606	0.70963
C	-2.81538	5.13022	1.56603
C	-3.62938	3.15235	0.20473
C	-1.94267	6.80729	-0.15116
H	-2.9582	5.58655	-1.62684
H	-1.53057	6.39578	-2.23718
H	-2.28352	3.52721	-2.64482
H	-0.82095	4.26282	-3.30155
C	-0.4643	2.52148	1.89314
H	0.54505	3.39634	0.25573
C	-3.02828	6.46882	0.87459
H	-3.65407	4.87672	2.21071
H	-1.90976	5.14316	2.179
O	-4.79848	3.48398	0.74707
O	-3.44444	2.20334	-0.52125
H	-2.11332	7.82647	-0.50253
H	-0.95722	6.80521	0.32952
H	-4.00413	6.45968	0.37896
H	-3.06457	7.24254	1.64563
C	-5.89792	2.62257	0.41082
H	-6.04207	2.60552	-0.66845
H	-5.71031	1.61334	0.7755

H	-6.76169	3.05409	0.90663
C	-1.63697	1.86175	2.54533
H	-1.5218	1.8761	3.63155
H	-2.60196	2.30125	2.31353
N	-1.38834	3.89839	0.05113
C	0.78191	2.0445	2.30474
H	0.9451	1.75083	3.33556
H	1.68261	2.28227	1.74499
C	0.76459	-0.09094	1.56216
H	0.52689	0.24572	0.55754
C	-1.61085	0.35883	2.05998
H	-2.42361	-0.17591	2.55578
H	-1.78224	0.34423	0.9808
C	-0.28884	-0.23356	2.42109
C	2.15118	-0.64511	1.7343
H	2.86322	-0.00986	1.19679
H	2.44967	-0.66001	2.78537
C	-0.17226	-0.79143	3.80495
H	-0.73654	-0.17855	4.51432
H	-0.61438	-1.79465	3.8188
H	0.85765	-0.88203	4.14625
C	2.25216	-2.08096	1.16255
H	1.99223	-2.06481	0.10077
H	3.29356	-2.40389	1.23499
C	1.35637	-3.04134	1.90151
C	0.05966	-3.29902	1.45568
C	1.78449	-3.60904	3.102
C	-0.81073	-4.09792	2.2004
H	-0.28853	-2.85594	0.52357
C	0.94058	-4.41589	3.86323
H	2.79157	-3.40519	3.45713
C	-0.35722	-4.64328	3.40164
H	-1.03083	-5.25695	3.99346
C	-0.52123	2.36993	-2.31526
C	0.85994	2.28224	-2.13133
C	1.47543	1.05172	-1.87672
H	1.46251	3.18501	-2.17279
C	-0.69368	-0.03927	-2.05539
C	0.68524	-0.10212	-1.86725
H	1.13477	-1.05491	-1.61488
C	2.90467	0.96364	-1.47542
C	3.50053	2.00233	-0.76475
C	3.64629	-0.20099	-1.72129
H	2.92936	2.90239	-0.56464
C	4.94732	-0.33955	-1.25231
H	3.19039	-0.99425	-2.29916

C	-1.54916	-1.23998	-1.88634
C	-2.81082	-1.0944	-1.30581
C	-1.1164	-2.51218	-2.25986
H	-3.13017	-0.10656	-0.99036
C	-1.92843	-3.63374	-2.07735
H	-0.13777	-2.62143	-2.71557
C	-1.27996	1.20564	-2.291
H	-2.35036	1.27685	-2.42859
C	5.50931	0.72609	-0.53189
H	6.52358	0.62506	-0.16853
C	4.81124	1.90365	-0.28206
C	-3.19416	-3.44916	-1.51202
H	-3.83124	-4.30925	-1.36186
C	-3.64891	-2.18965	-1.10909
C	5.41707	3.07687	0.49382
C	5.50527	4.29996	-0.43486
H	6.1463	4.08565	-1.29363
H	4.52068	4.59047	-0.80833
H	5.92753	5.15082	0.10671
C	4.52165	3.41716	1.69774
H	3.53901	3.77578	1.38208
H	4.38299	2.54176	2.33871
H	4.98332	4.20956	2.29258
C	6.82236	2.76166	1.01588
H	7.51851	2.55503	0.19937
H	7.20278	3.62385	1.56798
H	6.81616	1.90367	1.6932
C	5.79118	-1.58863	-1.52284
C	4.98086	-2.69676	-2.20319
H	4.12314	-2.99615	-1.59382
H	4.6183	-2.3878	-3.18655
H	5.61671	-3.57363	-2.34427
C	6.3457	-2.14448	-0.20039
H	5.53289	-2.41394	0.47835
H	6.93779	-3.04195	-0.39765
H	6.99036	-1.42545	0.30816
C	6.96407	-1.20379	-2.4412
H	7.59814	-0.44403	-1.97851
H	7.58106	-2.08248	-2.64826
H	6.59565	-0.80927	-3.39154
C	-5.01588	-1.95998	-0.45669
C	-4.82287	-1.28609	0.91337
H	-4.31141	-0.32504	0.81425
H	-5.7963	-1.10644	1.37918
H	-4.23505	-1.91909	1.58375
C	-5.84694	-1.02396	-1.35172

H	-5.99481	-1.46347	-2.34144
H	-6.82843	-0.84953	-0.9012
H	-5.35269	-0.05655	-1.47447
C	-5.78811	-3.26595	-0.25157
H	-6.74615	-3.04962	0.22677
H	-5.9933	-3.76565	-1.20169
H	-5.2388	-3.95849	0.3928
C	-1.40141	-5.01312	-2.48615
C	-2.43262	-6.12259	-2.25676
H	-3.34228	-5.95201	-2.83835
H	-2.00784	-7.07911	-2.56973
H	-2.70706	-6.20862	-1.20224
C	-1.03262	-5.00304	-3.97933
H	-0.25387	-4.27014	-4.19938
H	-0.66148	-5.98739	-4.27733
H	-1.90739	-4.76602	-4.59031
C	-0.1493	-5.33556	-1.65185
H	0.63815	-4.5935	-1.80641
H	-0.38895	-5.35273	-0.58495
H	0.24636	-6.31522	-1.93401
C	1.42162	-5.04451	5.14611
H	0.60344	-5.15957	5.85864
H	1.83575	-6.03846	4.95531
H	2.20463	-4.44317	5.6101
C	-2.21079	-4.36511	1.71279
H	-2.57524	-3.53382	1.10818
H	-2.24046	-5.25979	1.08215
H	-2.89658	-4.52526	2.54691

Catalyst **4.13** / **2.46** Transition state 1 proximal *s-trans* rotated

EE = -2595.7162 a.u.

ΔG^0 = -2594.5061 a.u.

C	1.20591	4.65644	-0.2888
N	-0.99254	4.8318	0.832
C	1.08117	6.1662	-0.47529
C	1.1108	3.92265	-1.63779
H	2.17347	4.44089	0.17215
C	0.47522	3.09994	1.44306
C	-1.00793	5.87631	1.87011
C	-2.07326	4.39861	0.10087
C	1.03651	6.98911	0.82067
H	0.19824	6.38453	-1.08505
H	1.94855	6.46071	-1.07014
H	0.17001	4.1993	-2.11904
H	1.92437	4.30986	-2.25843

C	-0.26835	2.44858	2.42774
H	1.4791	2.72332	1.27337
C	-0.37542	7.17181	1.3846
H	-2.04315	6.02691	2.16818
H	-0.46218	5.47024	2.72727
O	-3.13898	5.15605	0.34423
O	-2.05561	3.447	-0.64597
H	1.45041	7.97792	0.6152
H	1.686	6.53101	1.57584
H	-1.0179	7.61304	0.61612
H	-0.35149	7.86868	2.22614
C	-4.33638	4.76837	-0.34926
H	-4.17123	4.7978	-1.42512
H	-4.63505	3.7648	-0.04762
H	-5.08607	5.49593	-0.05504
C	-1.73628	2.50752	2.70306
H	-1.91666	2.38206	3.77328
H	-2.23293	3.4239	2.39746
N	0.20037	4.15021	0.68506
C	0.37099	1.32779	2.96331
H	0.05367	0.91793	3.91555
H	1.38728	1.0782	2.67224
C	-0.52227	-0.31249	1.76391
H	-0.29944	0.19092	0.82619
C	-2.3844	1.27968	1.9433
H	-3.44784	1.24948	2.18819
H	-2.26529	1.44933	0.87268
C	-1.69446	0.03223	2.37903
C	0.34132	-1.5082	2.04676
H	1.3713	-1.24824	1.78444
H	0.3371	-1.76964	3.10825
C	-2.22801	-0.64025	3.60396
H	-2.58542	0.1022	4.324
H	-3.08712	-1.25991	3.31997
H	-1.50136	-1.29406	4.08441
C	-0.09992	-2.73576	1.21926
H	-0.15733	-2.4624	0.16109
H	0.6593	-3.51767	1.32156
C	-1.43692	-3.25755	1.68074
C	-2.60827	-2.93849	0.9902
C	-1.52174	-4.01182	2.84874
C	-3.85077	-3.37079	1.45344
H	-2.54764	-2.34865	0.07776
C	-2.75289	-4.44456	3.34359
H	-0.6119	-4.26166	3.38953
C	-3.90661	-4.11355	2.63499

H	-4.87192	-4.44922	3.00433
C	1.19876	2.41729	-1.54521
C	2.37003	1.76736	-1.15181
C	2.42666	0.3705	-1.07615
H	3.24754	2.35433	-0.89727
C	0.08582	0.26234	-1.74714
C	1.27503	-0.36627	-1.37455
H	1.31494	-1.44811	-1.32196
C	3.68406	-0.32688	-0.69057
C	4.92834	0.22233	-1.00607
C	3.64521	-1.55168	-0.02021
H	4.96562	1.15361	-1.55991
C	4.81126	-2.22501	0.3428
H	2.68443	-1.98832	0.2282
C	-1.16551	-0.49874	-2.00376
C	-2.40122	0.12188	-1.79884
C	-1.14421	-1.82111	-2.44993
H	-2.42473	1.13943	-1.4234
C	-2.32496	-2.5261	-2.69043
H	-0.18941	-2.30256	-2.63069
C	0.07617	1.6561	-1.84942
H	-0.81964	2.16748	-2.17217
C	-3.60034	-0.53001	-2.08373
C	-3.54139	-1.85532	-2.52555
H	-4.46311	-2.37887	-2.73746
C	6.03795	-1.6383	0.02015
H	6.95049	-2.14575	0.29659
C	6.11816	-0.41739	-0.65591
C	-4.91568	0.23671	-1.90965
C	-5.04992	0.68947	-0.44622
H	-4.9814	-0.15925	0.24012
H	-4.26215	1.40069	-0.1892
H	-6.01379	1.18363	-0.29322
C	-4.88999	1.48707	-2.80769
H	-4.78218	1.20801	-3.85897
H	-5.82371	2.04531	-2.6933
H	-4.06458	2.15139	-2.53942
C	-6.13956	-0.60266	-2.28861
H	-7.04059	0.00397	-2.17271
H	-6.09047	-0.93416	-3.32897
H	-6.24809	-1.48259	-1.64989
C	-2.24501	-3.99223	-3.12675
C	-3.62959	-4.63945	-3.23252
H	-4.24547	-4.15687	-3.99544
H	-3.5162	-5.68956	-3.51133
H	-4.16221	-4.59939	-2.27781

C	-1.55697	-4.07817	-4.49924
H	-0.54465	-3.66944	-4.46523
H	-1.4906	-5.12165	-4.81937
H	-2.12462	-3.52286	-5.2503
C	-1.42613	-4.78486	-2.09198
H	-0.40341	-4.40956	-2.00943
H	-1.89098	-4.72309	-1.1041
H	-1.37451	-5.83656	-2.38657
C	4.70238	-3.5664	1.07525
C	3.94898	-3.36466	2.40116
H	4.4741	-2.64947	3.03942
H	2.93478	-2.99295	2.23687
H	3.87445	-4.31508	2.93652
C	3.92693	-4.56272	0.19598
H	2.918	-4.20657	-0.02568
H	4.44591	-4.72431	-0.75218
H	3.83969	-5.52403	0.7095
C	6.07483	-4.16979	1.39001
H	6.64902	-4.3592	0.47959
H	6.66165	-3.5174	2.04161
H	5.93918	-5.12349	1.90504
C	7.45549	0.22778	-1.03437
C	7.53851	0.36212	-2.5645
H	7.47266	-0.61922	-3.04115
H	6.73442	0.98725	-2.95821
H	8.49084	0.81897	-2.84711
C	7.54628	1.62348	-0.39397
H	8.4987	2.09231	-0.65575
H	6.74286	2.27793	-0.73846
H	7.48595	1.5521	0.69507
C	8.65527	-0.59742	-0.55845
H	8.66077	-0.7098	0.52878
H	8.66504	-1.59227	-1.01077
H	9.57806	-0.08942	-0.84768
C	-5.11417	-3.04587	0.69945
H	-4.87677	-2.59278	-0.26331
H	-5.70587	-3.94671	0.52112
H	-5.74145	-2.3483	1.26173
C	-2.82492	-5.2788	4.59713
H	-3.81936	-5.23541	5.04273
H	-2.60362	-6.32633	4.37516
H	-2.09792	-4.93939	5.33696

Catalyst **4.13** / **2.46** Transition state 1 proximal *s-cis*

EE = -2595.7091 a.u.

ΔG^0 = -2594.4993 a.u.

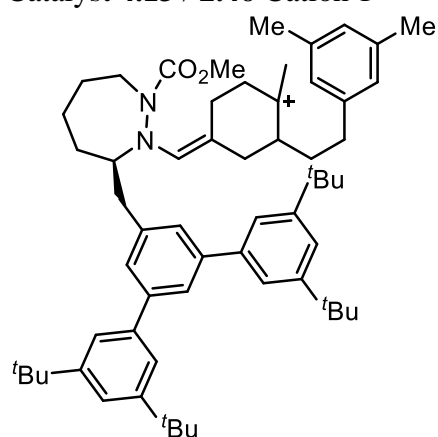
C	1.6726	4.23308	-1.53434
N	-0.03149	4.78553	0.17609
C	1.55622	5.70012	-1.93896
C	1.10979	3.31575	-2.63891
H	2.72758	3.99809	-1.3726
C	1.49722	3.05359	0.59782
C	0.3256	5.98904	0.94784
C	-1.29374	4.43222	-0.24193
C	1.96802	6.71789	-0.86593
H	0.53251	5.90518	-2.27004
H	2.19173	5.81118	-2.82031
C	1.05342	1.85279	-2.27272
H	0.10714	3.65732	-2.90286
H	1.74999	3.46663	-3.51366
C	1.09088	2.61234	1.86225
H	2.39263	2.58461	0.20464
C	0.8191	7.1231	0.06189
H	-0.55326	6.28218	1.51794
H	1.0994	5.67825	1.65552
O	-2.17566	5.36549	0.10737
O	-1.55738	3.40463	-0.82058
H	2.33504	7.61636	-1.36512
H	2.80569	6.32411	-0.27852
H	-0.01716	7.4951	-0.53834
H	1.13818	7.94037	0.71357
C	-3.53659	5.09517	-0.26448
C	2.11598	-0.19109	-1.49703
C	-0.29307	-0.13142	-1.85888
H	-3.60913	4.95887	-1.34234
H	-3.8958	4.2029	0.24633
H	-4.09873	5.96818	0.05137
C	0.8613	-0.80911	-1.46233
H	0.78127	-1.81602	-1.06777
C	-0.1183	2.89132	2.48987
H	-0.21327	2.68513	3.54979
H	-0.84501	3.58954	2.09769
N	1.02581	3.98577	-0.21384
C	1.82236	1.4192	2.39588
H	1.93263	1.46822	3.48115
H	2.81576	1.30064	1.96259
C	-1.34477	1.06031	1.92535
H	-1.16459	1.24835	0.86634
C	-0.4013	0.34229	2.60942
C	-0.56288	-0.12539	4.02216
H	-1.41002	0.3218	4.53826

H	-0.71676	-1.21146	4.01143
H	0.35063	0.06558	4.59347
C	0.95155	0.15485	2.022
H	0.91485	0.07727	0.93571
H	1.44047	-0.73399	2.42688
C	-2.75037	1.30757	2.39597
H	-3.11635	2.24355	1.96396
H	-2.79308	1.41713	3.48164
C	-3.70452	0.16978	1.95792
H	-4.71014	0.41254	2.31139
H	-3.72935	0.14082	0.8675
C	-3.27203	-1.17982	2.46741
C	-2.3965	-1.95622	1.70305
C	-3.65662	-1.63616	3.72504
C	-1.87311	-3.1487	2.19624
H	-2.1036	-1.60949	0.71459
C	-3.17116	-2.84331	4.23466
H	-4.33832	-1.03862	4.3251
C	-2.27247	-3.5804	3.46436
H	-1.87399	-4.51143	3.85832
C	-0.17511	1.20311	-2.25652
H	-1.05455	1.75554	-2.55812
C	2.20031	1.13651	-1.9266
H	3.17362	1.61458	-1.9925
C	3.32197	-0.91946	-1.02357
C	4.35224	-0.23982	-0.36944
C	3.43237	-2.2999	-1.19858
H	4.27062	0.83346	-0.22995
C	4.53541	-3.00834	-0.72232
H	2.64799	-2.82346	-1.73368
C	-1.62672	-0.78724	-1.84245
C	-2.78288	-0.02212	-1.65912
C	-1.74342	-2.16855	-2.02888
H	-2.68108	1.04117	-1.47449
C	-2.98872	-2.79463	-2.01681
H	-0.84691	-2.74919	-2.20563
C	-4.04924	-0.60936	-1.69232
C	-4.12346	-1.9938	-1.85676
H	-5.09909	-2.46621	-1.87553
C	5.54405	-2.29559	-0.06726
H	6.40349	-2.8308	0.30878
C	5.4753	-0.91134	0.1153
C	6.58136	-0.11774	0.81875
C	7.69877	-1.0223	1.34825
H	8.45243	-0.40832	1.84643
H	7.31996	-1.74567	2.07493

H	8.19327	-1.56745	0.54055
C	5.98625	0.65692	2.00696
H	5.25264	1.39673	1.67939
H	5.49817	-0.02396	2.70931
H	6.77933	1.19003	2.53795
C	7.19569	0.87871	-0.17939
H	7.63095	0.35109	-1.0318
H	6.44721	1.57875	-0.55752
H	7.98551	1.45699	0.30789
C	4.60028	-4.52421	-0.93506
C	4.57852	-4.82786	-2.44284
H	3.6669	-4.45682	-2.91576
H	5.43452	-4.36563	-2.94103
H	4.62753	-5.90795	-2.60556
C	3.38155	-5.18224	-0.26464
H	2.44282	-4.82038	-0.6901
H	3.41936	-6.26601	-0.40418
H	3.37278	-4.97355	0.80838
C	5.86873	-5.14196	-0.33823
H	6.77122	-4.7339	-0.8003
H	5.92666	-4.97922	0.74104
H	5.86078	-6.21997	-0.51451
C	-5.33906	0.21722	-1.62714
C	-5.07473	1.68073	-1.25112
H	-4.44557	2.18169	-1.99106
H	-6.02507	2.21767	-1.20375
H	-4.58984	1.77007	-0.27518
C	-6.32857	-0.38213	-0.61323
H	-7.22174	0.24576	-0.55916
H	-6.64908	-1.38439	-0.90276
H	-5.89067	-0.44145	0.38517
C	-5.98638	0.19037	-3.0243
H	-6.22595	-0.83192	-3.32645
H	-6.91212	0.77263	-3.01963
H	-5.31191	0.61864	-3.7701
C	-3.1565	-4.30847	-2.17545
C	-1.81866	-5.02476	-2.3868
H	-1.99921	-6.09599	-2.5014
H	-1.31191	-4.67207	-3.28882
H	-1.14684	-4.89074	-1.5353
C	-4.05418	-4.60648	-3.38833
H	-4.17682	-5.68692	-3.50258
H	-5.0469	-4.16618	-3.27665
H	-3.60655	-4.21256	-4.30441
C	-3.81369	-4.86725	-0.90103
H	-4.80454	-4.43626	-0.74101

H	-3.9243	-5.95216	-0.98185
H	-3.20244	-4.64479	-0.02188
C	-0.86199	-3.92937	1.39544
H	-1.08855	-4.9982	1.39426
H	-0.83852	-3.57767	0.36209
H	0.14032	-3.80601	1.81604
C	-3.62494	-3.34227	5.58294
H	-4.5884	-3.85272	5.49969
H	-2.90895	-4.04956	6.00319
H	-3.75051	-2.51662	6.28548

Catalyst **4.13** / **2.46** Cation 1



Proximal *s-trans* cage

EE = -2595.7279 a.u.

ΔG^0 = -2594.5157 a.u.

C	-1.26944	4.48649	-1.15845
N	-2.7032	3.77343	0.72207
C	-2.20271	5.69251	-1.23236
C	-1.33901	3.65787	-2.46522
H	-0.24231	4.86367	-1.05453
C	-0.43939	3.0305	0.63239
C	-2.78802	4.84131	1.72791
C	-3.78458	3.06515	0.26984
C	-2.17327	6.61511	-0.00472
H	-3.22982	5.35191	-1.42183
H	-1.90034	6.25296	-2.12337
H	-2.39098	3.48509	-2.71523
H	-0.90032	4.26641	-3.26483
C	-0.39267	2.0611	1.56814
H	0.5098	3.42105	0.26966
C	-3.12876	6.19341	1.1146
H	-3.52821	4.54641	2.47262
H	-1.8081	4.86522	2.21557
O	-4.90528	3.45034	0.8963

O	-3.74127	2.18208	-0.56732
H	-2.44469	7.6271	-0.32137
H	-1.1472	6.67552	0.38354
H	-4.15257	6.15276	0.72232
H	-3.11992	6.9442	1.91253
C	-6.07654	2.70742	0.54189
H	-6.27358	2.79826	-0.5275
H	-5.95094	1.65363	0.80027
H	-6.8856	3.14887	1.12008
C	-1.5477	1.25757	2.07974
H	-1.75931	1.45458	3.13778
H	-2.46001	1.42585	1.50851
N	-1.51035	3.66245	0.03962
C	0.95778	1.63905	2.06398
H	1.09443	1.78147	3.14358
H	1.77002	2.16823	1.55487
C	1.20036	0.08549	1.72304
H	0.98008	0.00661	0.65471
C	-1.24189	-0.2966	1.93569
H	-2.00721	-0.85717	2.47871
H	-1.26902	-0.54101	0.8701
C	0.10102	-0.47484	2.50359
C	2.62388	-0.38101	1.99165
H	3.31185	0.28897	1.46236
H	2.87077	-0.32635	3.05783
C	0.2075	-0.76343	3.94712
H	-0.53581	-0.16116	4.48604
H	-0.08324	-1.81174	4.11394
H	1.20167	-0.60042	4.36041
C	2.82806	-1.82086	1.46996
H	2.72939	-1.81524	0.37745
H	3.8497	-2.13364	1.70575
C	1.83386	-2.76752	2.08637
C	0.56311	-2.93326	1.51449
C	2.10798	-3.38998	3.30573
C	-0.43268	-3.68249	2.15719
H	0.34308	-2.49052	0.54142
C	1.14315	-4.15775	3.95898
H	3.08694	-3.25846	3.76212
C	-0.12822	-4.27846	3.37929
H	-0.89426	-4.85209	3.89733
C	-0.63557	2.3298	-2.33849
C	0.74887	2.24399	-2.17406
C	1.36469	1.02565	-1.86477
H	1.35551	3.14407	-2.25655
C	-0.80944	-0.06895	-1.96557

C	0.57339	-0.12779	-1.78107
H	1.03509	-1.07402	-1.50394
C	2.80715	0.95994	-1.51184
C	3.41396	2.01574	-0.83177
C	3.56623	-0.18343	-1.80506
H	2.82449	2.89939	-0.59795
C	4.90052	-0.28316	-1.41993
H	3.09679	-0.98737	-2.36207
C	-1.67507	-1.2607	-1.78194
C	-2.93878	-1.09749	-1.20602
C	-1.26206	-2.54022	-2.16003
H	-3.23922	-0.10339	-0.88046
C	-2.09741	-3.64903	-1.99414
H	-0.2841	-2.66123	-2.61999
C	-1.39553	1.16829	-2.24837
H	-2.47052	1.23586	-2.37018
C	5.47122	0.79634	-0.72528
H	6.51091	0.72482	-0.42439
C	4.75407	1.9535	-0.42537
C	-3.36839	-3.44466	-1.44191
H	-4.02485	-4.29539	-1.30637
C	-3.80131	-2.17942	-1.02735
C	5.37054	3.14095	0.32077
C	5.36844	4.37026	-0.60394
H	5.96508	4.18008	-1.50215
H	4.35358	4.63367	-0.91867
H	5.7963	5.23369	-0.08266
C	4.53751	3.45094	1.57639
H	3.51765	3.75739	1.32132
H	4.48015	2.57637	2.23473
H	4.99673	4.27214	2.13734
C	6.81249	2.86413	0.75812
H	7.46726	2.68224	-0.10042
H	7.20205	3.73392	1.29621
H	6.87078	1.99929	1.42774
C	5.76794	-1.49869	-1.76258
C	4.96414	-2.60643	-2.45131
H	4.13926	-2.9567	-1.82025
H	4.55025	-2.2718	-3.40816
H	5.61937	-3.45997	-2.65187
C	6.38559	-2.08139	-0.48081
H	5.60413	-2.42926	0.20249
H	7.02405	-2.93563	-0.73093
H	7.00081	-1.34783	0.04845
C	6.89523	-1.0527	-2.71029
H	7.532	-0.29322	-2.24571

H	7.52581	-1.90916	-2.97334
H	6.48184	-0.63295	-3.63333
C	-5.15873	-1.92775	-0.36429
C	-4.93088	-1.32086	1.03178
H	-4.39731	-0.36523	0.96636
H	-5.89308	-1.13631	1.52349
H	-4.34765	-1.99952	1.66443
C	-5.96029	-0.92384	-1.21134
H	-6.13004	-1.31247	-2.22107
H	-6.93545	-0.73664	-0.74674
H	-5.43474	0.03408	-1.29255
C	-5.97562	-3.21326	-0.20989
H	-6.93163	-2.9843	0.27161
H	-6.19017	-3.67292	-1.18052
H	-5.45262	-3.94819	0.41231
C	-1.59673	-5.03053	-2.42923
C	-2.58519	-6.14557	-2.07308
H	-3.54416	-6.0153	-2.58524
H	-2.17098	-7.11071	-2.38135
H	-2.77356	-6.18933	-0.99447
C	-1.38945	-5.03339	-3.95369
H	-0.65711	-4.27946	-4.25932
H	-1.0252	-6.01297	-4.28282
H	-2.33074	-4.8241	-4.47267
C	-0.25594	-5.33435	-1.73725
H	0.51561	-4.60658	-2.00692
H	-0.36315	-5.3226	-0.64683
H	0.10142	-6.32619	-2.03507
C	1.4531	-4.84825	5.26114
H	0.60233	-4.79815	5.94605
H	1.67272	-5.90754	5.0888
H	2.32214	-4.40209	5.75013
C	-1.80359	-3.80615	1.54861
H	-1.99901	-2.98665	0.85025
H	-1.90917	-4.7404	0.98462
H	-2.57813	-3.80265	2.32213

Catalyst **4.13** / **2.46** Cation 1 proximal *s-trans* rotated

EE = -2595.7229 a.u.

ΔG^0 = -2594.5056 a.u.

C	-0.57849	4.53409	-0.59382
N	1.74783	3.98913	-1.2395
C	-0.13286	5.97453	-0.83023
C	-1.03563	4.33333	0.87523
H	-1.44332	4.34181	-1.23893

C	0.06753	2.33595	-1.49416
C	2.03202	4.53508	-2.57556
C	2.58196	4.14522	-0.16708
C	0.22739	6.31602	-2.28487
H	0.70371	6.21661	-0.16445
H	-0.96796	6.6016	-0.50845
H	-0.24646	4.69682	1.53745
H	-1.92792	4.94618	1.02857
C	0.74041	1.31329	-2.05764
H	-1.0071	2.21458	-1.40803
C	1.67866	6.01338	-2.66689
H	3.08304	4.36264	-2.8024
H	1.4336	3.94209	-3.27199
O	3.76812	4.63016	-0.55595
O	2.3078	3.87655	0.98316
H	0.05065	7.38204	-2.44418
H	-0.45214	5.78377	-2.96092
H	2.35241	6.57528	-2.01154
H	1.86887	6.35101	-3.68925
C	4.68822	4.91636	0.50578
H	4.2695	5.67211	1.16952
H	4.90823	4.01268	1.07252
H	5.58398	5.29003	0.01889
C	2.21671	1.13597	-2.26682
H	2.45625	1.14036	-3.33624
H	2.81371	1.9133	-1.79506
N	0.46126	3.5594	-0.99838
C	-0.07718	0.13216	-2.50096
H	-0.00398	-0.04795	-3.5798
H	-1.13435	0.25775	-2.25552
C	0.40763	-1.16907	-1.74282
H	0.39559	-0.90821	-0.67934
C	2.71819	-0.24046	-1.67451
H	3.75174	-0.40242	-1.98531
H	2.6568	-0.17676	-0.58737
C	1.81175	-1.28982	-2.20096
C	-0.50261	-2.36076	-1.98084
H	-1.52429	-2.07672	-1.72474
H	-0.51471	-2.65565	-3.03302
C	2.13412	-1.8292	-3.54604
H	2.34598	-0.97282	-4.19829
H	3.0582	-2.41319	-3.51179
H	1.34256	-2.42906	-3.98521
C	-0.06236	-3.54374	-1.09532
H	-0.19745	-3.26756	-0.0453
H	-0.68721	-4.41389	-1.30343

C	1.37857	-3.85223	-1.36761
C	2.38193	-3.065	-0.76131
C	1.74634	-4.80815	-2.30741
C	3.7455	-3.30703	-1.03124
H	2.11907	-2.41575	0.0713
C	3.08653	-5.01658	-2.63257
H	0.97743	-5.39769	-2.79669
C	4.07322	-4.2594	-1.98162
H	5.11788	-4.44192	-2.21525
C	-1.31392	2.88157	1.16031
C	-2.52386	2.27502	0.83235
C	-2.65976	0.88259	0.88488
H	-3.35589	2.88157	0.48646
C	-0.34006	0.69492	1.602
C	-1.55214	0.10154	1.23485
H	-1.65217	-0.97948	1.23655
C	-3.96152	0.24524	0.55495
C	-5.15833	0.82022	0.98449
C	-4.01	-0.93955	-0.17901
H	-5.11652	1.72916	1.57498
C	-5.22036	-1.55919	-0.48812
H	-3.07816	-1.37011	-0.52493
C	0.87137	-0.09391	1.96101
C	2.13381	0.4933	1.81756
C	0.79428	-1.39339	2.46863
H	2.20805	1.49171	1.40059
C	1.94347	-2.1011	2.83528
H	-0.18046	-1.84477	2.61814
C	-0.26005	2.08796	1.59743
H	0.6589	2.58569	1.87304
C	3.29784	-0.16057	2.21651
C	3.18276	-1.46333	2.713
H	4.07714	-1.99095	3.01285
C	-6.39947	-0.95697	-0.03941
H	-7.34586	-1.42503	-0.26762
C	-6.39093	0.23183	0.69642
C	4.62917	0.60209	2.16321
C	4.90986	1.1295	0.74475
H	5.04762	0.316	0.02945
H	4.10076	1.77337	0.38776
H	5.82877	1.72248	0.75156
C	4.5216	1.81056	3.11307
H	4.28472	1.48403	4.12879
H	5.47383	2.34902	3.13808
H	3.74498	2.50364	2.77915
C	5.81459	-0.26076	2.60686

H	6.73183	0.32932	2.54613
H	5.70073	-0.5948	3.64109
H	5.94094	-1.1413	1.97152
C	1.80838	-3.51441	3.41425
C	3.16954	-4.18792	3.61831
H	3.77991	-3.65751	4.35296
H	3.01623	-5.20474	3.98664
H	3.72817	-4.24866	2.67964
C	1.09582	-3.42315	4.77481
H	0.09641	-2.99444	4.67157
H	0.99522	-4.42019	5.2124
H	1.66606	-2.79823	5.46672
C	0.97998	-4.40017	2.46875
H	-0.02714	-4.00639	2.31683
H	1.46788	-4.49097	1.494
H	0.88266	-5.40236	2.89429
C	-5.21421	-2.84377	-1.32326
C	-4.6815	-2.52073	-2.72999
H	-5.32321	-1.78736	-3.22488
H	-3.66898	-2.11212	-2.69184
H	-4.65925	-3.4276	-3.34063
C	-4.30256	-3.89051	-0.66017
H	-3.27054	-3.5414	-0.57843
H	-4.65884	-4.13147	0.34457
H	-4.29794	-4.80882	-1.25341
C	-6.6134	-3.45151	-1.46571
H	-7.04615	-3.69292	-0.49144
H	-7.29463	-2.77785	-1.99112
H	-6.54755	-4.3758	-2.04426
C	-7.67567	0.89584	1.20281
C	-7.64118	0.9619	2.73931
H	-7.57118	-0.04186	3.16621
H	-6.79091	1.54555	3.09816
H	-8.55525	1.43166	3.11273
C	-7.76933	2.32184	0.63353
H	-8.68511	2.80434	0.98574
H	-6.92289	2.93673	0.94637
H	-7.79054	2.29978	-0.4591
C	-8.93279	0.12763	0.78279
H	-9.02281	0.06685	-0.30482
H	-8.93962	-0.88689	1.18923
H	-9.81532	0.64653	1.16382
C	4.81355	-2.5535	-0.29257
H	4.38053	-1.73773	0.2843
H	5.3282	-3.21813	0.40761
H	5.56384	-2.15249	-0.97856

C	3.47856	-6.02431	-3.6756
H	4.3762	-6.56666	-3.37518
H	2.67605	-6.7384	-3.85795
H	3.70159	-5.51664	-4.61831

Catalyst **4.13** / **2.46** Cation 1 proximal *s-cis*

EE = -2595.7251 a.u.

ΔG^0 = -2594.512 a.u.

C	2.13515	-4.16096	-1.32077
N	3.55066	-3.2465	0.49179
C	3.31402	-5.09245	-1.58449
C	1.85302	-3.2716	-2.55333
H	1.25016	-4.78467	-1.14699
C	1.1832	-3.11196	0.66623
C	3.96288	-4.34121	1.38547
C	4.42678	-2.32851	-0.02294
C	3.61953	-6.08301	-0.45176
H	4.20659	-4.50103	-1.82034
H	3.06512	-5.64225	-2.49577
C	0.91324	-2.12659	-2.26471
H	2.80122	-2.86531	-2.91341
H	1.44668	-3.91579	-3.33883
C	0.97769	-2.22419	1.6547
H	0.35533	-3.76668	0.40367
C	4.54872	-5.52657	0.62921
H	4.67791	-3.94084	2.1017
H	3.06252	-4.63063	1.9327
O	5.65635	-2.5245	0.46927
O	4.14018	-1.45171	-0.80807
H	4.0898	-6.97024	-0.8815
H	2.6793	-6.41772	0.00227
H	5.49434	-5.21865	0.17209
H	4.78216	-6.31103	1.35436
C	6.65221	-1.59476	0.0267
C	-1.27247	-1.23795	-1.69826
C	0.6416	0.25851	-1.85327
H	6.69506	-1.57612	-1.06138
H	6.42948	-0.59703	0.40209
H	7.58912	-1.95588	0.44028
C	-0.71914	0.04253	-1.62424
H	-1.36867	0.86731	-1.34995
C	1.86207	-1.0742	2.02195
H	2.23502	-1.12764	3.04961
H	2.70834	-0.96835	1.34283
N	2.30581	-3.3596	-0.09411

C	-0.33907	-2.27567	2.35934
H	-0.23405	-2.43715	3.43627
H	-0.97417	-3.07361	1.97146
C	1.0472	0.30274	1.85942
H	0.77674	0.32305	0.80014
C	-0.15793	0.06434	2.66417
C	-0.26984	0.39587	4.09443
H	0.57207	0.94321	4.50491
H	-1.18947	0.98225	4.23056
H	-0.43608	-0.53236	4.65354
C	-1.11559	-0.90569	2.14134
H	-1.29545	-0.79504	1.07114
H	-2.04937	-0.9246	2.70523
C	1.89347	1.51952	2.21558
H	2.83594	1.44536	1.66632
H	2.14836	1.51835	3.2778
C	1.20257	2.84591	1.81946
H	1.77835	3.67973	2.22788
H	1.226	2.93219	0.73276
C	-0.22807	2.91736	2.28153
C	-1.21536	2.2768	1.5241
C	-0.59754	3.53309	3.47741
C	-2.54824	2.2124	1.94955
H	-0.9428	1.85345	0.56098
C	-1.9154	3.48788	3.92849
H	0.15614	4.0396	4.07292
C	-2.87572	2.81078	3.16139
H	-3.90234	2.77456	3.51379
C	1.43634	-0.83996	-2.18694
H	2.49262	-0.70229	-2.37472
C	-0.44759	-2.32082	-2.01569
H	-0.87551	-3.31792	-2.0787
C	-2.71729	-1.40453	-1.39239
C	-3.14436	-2.36931	-0.47959
C	-3.65783	-0.55452	-1.97554
H	-2.40051	-3.01658	-0.0247
C	-5.01502	-0.65649	-1.66841
H	-3.31485	0.18203	-2.69496
C	1.25111	1.60349	-1.68587
C	2.58733	1.71697	-1.28364
C	0.49525	2.76182	-1.88705
H	3.15182	0.81223	-1.08539
C	1.04641	4.02699	-1.68609
H	-0.53244	2.66468	-2.21217
C	3.17945	2.96846	-1.10928
C	2.39261	4.10381	-1.31998

H	2.83587	5.08175	-1.1661
C	-5.40669	-1.62405	-0.73819
H	-6.45283	-1.71044	-0.48411
C	-4.49141	-2.48892	-0.13078
C	-4.91437	-3.52347	0.91682
C	-6.43549	-3.59053	1.08908
H	-6.67988	-4.3598	1.8251
H	-6.84424	-2.64346	1.4496
H	-6.93395	-3.85011	0.15164
C	-4.29243	-3.1367	2.26946
H	-3.2014	-3.14254	2.21856
H	-4.6159	-2.13643	2.5709
H	-4.59688	-3.84713	3.04283
C	-4.41606	-4.91877	0.50513
H	-4.8388	-5.20918	-0.45995
H	-3.32763	-4.95621	0.42605
H	-4.72247	-5.65704	1.25085
C	-6.01773	0.26691	-2.36857
C	-5.94239	0.02821	-3.88657
H	-4.94881	0.25336	-4.27955
H	-6.17642	-1.01246	-4.12494
H	-6.66311	0.66998	-4.40056
C	-5.66887	1.73379	-2.06693
H	-4.6532	1.98246	-2.38399
H	-6.35891	2.39555	-2.59738
H	-5.75394	1.93763	-0.99657
C	-7.45851	0.01516	-1.91239
H	-7.78093	-1.00437	-2.13863
H	-7.57677	0.18716	-0.83945
H	-8.12672	0.70155	-2.4374
C	4.63935	3.13352	-0.67811
C	5.4502	1.85267	-0.8945
H	5.46798	1.55062	-1.94466
H	6.48068	2.01947	-0.57009
H	5.04531	1.0162	-0.31713
C	4.70069	3.49563	0.81574
H	5.74155	3.62463	1.12452
H	4.16778	4.42395	1.03161
H	4.26079	2.70171	1.42562
C	5.28043	4.26271	-1.50271
H	4.76622	5.21368	-1.34703
H	6.32637	4.39092	-1.21087
H	5.24644	4.02651	-2.56925
C	0.21841	5.30966	-1.79331
C	-1.22198	5.0341	-2.2367
H	-1.7664	5.97895	-2.29995

H	-1.25352	6.38497	-2.12912
H	-1.9867	3.71055	-2.71313
H	-0.43848	4.326	-3.30735
C	0.09214	2.07405	1.47348
H	1.04874	3.41748	0.2016
C	-2.25696	6.45092	1.18411
H	-2.69576	4.85476	2.58557
H	-0.98281	5.00827	2.18625
O	-4.29265	3.90061	1.13781
O	-3.40086	2.57404	-0.44803
H	-1.55603	7.80884	-0.31329
H	-0.30116	6.75409	0.31018
H	-3.30411	6.50316	0.86877
H	-2.11995	7.19788	1.9709
C	-5.56768	3.30679	0.86398
H	-5.83654	3.45401	-0.18138
H	-5.54475	2.24003	1.08763
H	-6.27071	3.8177	1.51506
C	-1.11301	1.34102	1.98437
H	-1.32188	1.58192	3.03219
H	-2.0016	1.56823	1.39815
N	-0.97393	3.76109	0.01147
C	1.42021	1.56817	1.96262
H	1.56341	1.72847	3.03726
H	2.24914	2.05477	1.44458
C	1.55637	0.02085	1.66333
H	1.34871	-0.08493	0.59625
C	-0.91416	-0.21717	1.86881
H	-1.71866	-0.71867	2.4092
H	-0.95923	-0.47516	0.80984
C	0.41973	-0.52583	2.43824
C	2.94409	-0.5205	1.96263
H	3.67114	0.04243	1.37026
H	3.20516	-0.38698	3.01601
C	0.4994	-0.67582	3.91128
H	-0.04527	0.16831	4.35279
H	-0.03385	-1.57496	4.23343
H	1.51407	-0.69445	4.29872
C	3.03687	-2.01374	1.57471
H	2.98345	-2.09717	0.48508
H	4.0032	-2.4064	1.89539
C	1.92273	-2.78691	2.2144
C	0.63422	-2.75272	1.64172
C	2.09655	-3.43501	3.43357
C	-0.45177	-3.41415	2.25205
H	0.50627	-2.36457	0.63428

C	1.02771	-4.06014	4.0736
H	3.07911	-3.44804	3.89444
C	-0.24056	-4.03743	3.47031
H	-1.06918	-4.53375	3.9668
C	-0.35775	2.37356	-2.3888
C	1.01316	2.14049	-2.28049
C	1.50682	0.86883	-1.97419
H	1.7047	2.96943	-2.40056
C	-0.77212	0.01652	-1.97212
C	0.60093	-0.18987	-1.84006
H	0.96487	-1.17622	-1.56865
C	2.94811	0.65532	-1.6755
C	3.69486	1.65623	-1.05826
C	3.56529	-0.57097	-1.96276
H	3.21661	2.60188	-0.82613
C	4.89677	-0.80196	-1.63646
H	2.98864	-1.33362	-2.47025
C	-1.75337	-1.07014	-1.72601
C	-2.94385	-0.7633	-1.0637
C	-1.51593	-2.38643	-2.12246
H	-3.10709	0.25806	-0.7327
C	-2.45676	-3.3919	-1.88637
H	-0.59603	-2.61566	-2.65024
C	-1.23356	1.30453	-2.24938
H	-2.2977	1.4889	-2.31858
C	5.61353	0.2286	-1.0078
H	6.65134	0.0544	-0.75483
C	5.03925	1.46258	-0.71618
C	-3.64784	-3.04647	-1.2383
H	-4.38236	-3.81539	-1.04524
C	-3.90377	-1.74032	-0.80811
C	5.81706	2.60077	-0.048
C	5.88628	3.79466	-1.01556
H	6.40156	3.51373	-1.93748
H	4.88894	4.1549	-1.27797
H	6.43389	4.61978	-0.55197
C	5.09755	3.0353	1.2402
H	4.10434	3.43979	1.03224
H	4.99095	2.19423	1.93133
H	5.67341	3.81825	1.74058
C	7.24641	2.18863	0.31746
H	7.82508	1.9124	-0.56737
H	7.75194	3.02958	0.79729
H	7.25531	1.34734	1.01548
C	5.61228	-2.1135	-1.97475
C	4.66756	-3.14344	-2.60226

H	3.8392	-3.39018	-1.93187
H	4.25411	-2.78793	-3.54923
H	5.22073	-4.0634	-2.80436
C	6.21112	-2.72728	-0.69834
H	5.42403	-2.96717	0.02032
H	6.74007	-3.6515	-0.94579
H	6.92163	-2.05335	-0.2159
C	6.74371	-1.81803	-2.97495
H	7.47789	-1.12675	-2.55535
H	7.26128	-2.74472	-3.23742
H	6.34234	-1.37611	-3.89044
C	-5.17418	-1.33439	-0.05563
C	-4.78272	-0.73482	1.30691
H	-4.15419	0.1518	1.18352
H	-5.68081	-0.43832	1.8567
H	-4.23664	-1.46413	1.91112
C	-5.92278	-0.2634	-0.86856
H	-6.19944	-0.64806	-1.85358
H	-6.83731	0.02986	-0.3444
H	-5.30803	0.63037	-1.00411
C	-6.1109	-2.52096	0.18435
H	-6.99503	-2.18134	0.72879
H	-6.44637	-2.96402	-0.75683
H	-5.62648	-3.29931	0.7805
C	-2.15787	-4.81916	-2.35711
C	-3.22571	-5.81747	-1.89865
H	-4.2059	-5.58318	-2.32089
H	-2.94983	-6.81976	-2.23418
H	-3.31414	-5.83885	-0.80886
C	-2.10268	-4.83605	-3.89449
H	-1.32295	-4.17053	-4.27167
H	-1.88884	-5.84756	-4.25087
H	-3.0585	-4.51637	-4.31726
C	-0.79914	-5.27805	-1.79867
H	0.01948	-4.64735	-2.15088
H	-0.79741	-5.25687	-0.70566
H	-0.59354	-6.30236	-2.12065
C	1.21059	-4.73718	5.40271
H	2.24667	-4.68527	5.73511
H	0.58348	-4.25605	6.15812
H	0.9087	-5.78472	5.34744
C	-1.80027	-3.43243	1.59082
H	-1.87264	-2.6778	0.80655
H	-1.98621	-4.40434	1.12455
H	-2.59538	-3.26618	2.32136

Catalyst **4.13** / **2.46** Transition State 2 proximal *s-trans* rotated

EE = -2595.7229 a.u.

ΔG^0 = -2594.5056 a.u.

C	-0.57849	4.53409	-0.59382
N	1.74783	3.98913	-1.2395
C	-0.13286	5.97453	-0.83023
C	-1.03563	4.33333	0.87523
H	-1.44332	4.34181	-1.23893
C	0.06753	2.33595	-1.49416
C	2.03202	4.53508	-2.57556
C	2.58196	4.14522	-0.16708
C	0.22739	6.31602	-2.28487
H	0.70371	6.21661	-0.16445
H	-0.96796	6.6016	-0.50845
H	-0.24646	4.69682	1.53745
H	-1.92792	4.94618	1.02857
C	0.74041	1.31329	-2.05764
H	-1.0071	2.21458	-1.40803
C	1.67866	6.01338	-2.66689
H	3.08304	4.36264	-2.8024
H	1.4336	3.94209	-3.27199
O	3.76812	4.63016	-0.55595
O	2.3078	3.87655	0.98316
H	0.05065	7.38204	-2.44418
H	-0.45214	5.78377	-2.96092
H	2.35241	6.57528	-2.01154
H	1.86887	6.35101	-3.68925
C	4.68822	4.91636	0.50578
H	4.2695	5.67211	1.16952
H	4.90823	4.01268	1.07252
H	5.58398	5.29003	0.01889
C	2.21671	1.13597	-2.26682
H	2.45625	1.14036	-3.33624
H	2.81371	1.9133	-1.79506
N	0.46126	3.5594	-0.99838
C	-0.07718	0.13216	-2.50096
H	-0.00398	-0.04795	-3.5798
H	-1.13435	0.25775	-2.25552
C	0.40763	-1.16907	-1.74282
H	0.39559	-0.90821	-0.67934
C	2.71819	-0.24046	-1.67451
H	3.75174	-0.40242	-1.98531
H	2.6568	-0.17676	-0.58737
C	1.81175	-1.28982	-2.20096
C	-0.50261	-2.36076	-1.98084

H	-1.52429	-2.07672	-1.72474
H	-0.51471	-2.65565	-3.03302
C	2.13412	-1.8292	-3.54604
H	2.34598	-0.97282	-4.19829
H	3.0582	-2.41319	-3.51179
H	1.34256	-2.42906	-3.98521
C	-0.06236	-3.54374	-1.09532
H	-0.19745	-3.26756	-0.0453
H	-0.68721	-4.41389	-1.30343
C	1.37857	-3.85223	-1.36761
C	2.38193	-3.065	-0.76131
C	1.74634	-4.80815	-2.30741
C	3.7455	-3.30703	-1.03124
H	2.11907	-2.41575	0.0713
C	3.08653	-5.01658	-2.63257
H	0.97743	-5.39769	-2.79669
C	4.07322	-4.2594	-1.98162
H	5.11788	-4.44192	-2.21525
C	-1.31392	2.88157	1.16031
C	-2.52386	2.27502	0.83235
C	-2.65976	0.88259	0.88488
H	-3.35589	2.88157	0.48646
C	-0.34006	0.69492	1.602
C	-1.55214	0.10154	1.23485
H	-1.65217	-0.97948	1.23655
C	-3.96152	0.24524	0.55495
C	-5.15833	0.82022	0.98449
C	-4.01	-0.93955	-0.17901
H	-5.11652	1.72916	1.57498
C	-5.22036	-1.55919	-0.48812
H	-3.07816	-1.37011	-0.52493
C	0.87137	-0.09391	1.96101
C	2.13381	0.4933	1.81756
C	0.79428	-1.39339	2.46863
H	2.20805	1.49171	1.40059
C	1.94347	-2.1011	2.83528
H	-0.18046	-1.84477	2.61814
C	-0.26005	2.08796	1.59743
H	0.6589	2.58569	1.87304
C	3.29784	-0.16057	2.21651
C	3.18276	-1.46333	2.713
H	4.07714	-1.99095	3.01285
C	-6.39947	-0.95697	-0.03941
H	-7.34586	-1.42503	-0.26762
C	-6.39093	0.23183	0.69642
C	4.62917	0.60209	2.16321

C	4.90986	1.1295	0.74475
H	5.04762	0.316	0.02945
H	4.10076	1.77337	0.38776
H	5.82877	1.72248	0.75156
C	4.5216	1.81056	3.11307
H	4.28472	1.48403	4.12879
H	5.47383	2.34902	3.13808
H	3.74498	2.50364	2.77915
C	5.81459	-0.26076	2.60686
H	6.73183	0.32932	2.54613
H	5.70073	-0.5948	3.64109
H	5.94094	-1.1413	1.97152
C	1.80838	-3.51441	3.41425
C	3.16954	-4.18792	3.61831
H	3.77991	-3.65751	4.35296
H	3.01623	-5.20474	3.98664
H	3.72817	-4.24866	2.67964
C	1.09582	-3.42315	4.77481
H	0.09641	-2.99444	4.67157
H	0.99522	-4.42019	5.2124
H	1.66606	-2.79823	5.46672
C	0.97998	-4.40017	2.46875
H	-0.02714	-4.00639	2.31683
H	1.46788	-4.49097	1.494
H	0.88266	-5.40236	2.89429
C	-5.21421	-2.84377	-1.32326
C	-4.6815	-2.52073	-2.72999
H	-5.32321	-1.78736	-3.22488
H	-3.66898	-2.11212	-2.69184
H	-4.65925	-3.4276	-3.34063
C	-4.30256	-3.89051	-0.66017
H	-3.27054	-3.5414	-0.57843
H	-4.65884	-4.13147	0.34457
H	-4.29794	-4.80882	-1.25341
C	-6.6134	-3.45151	-1.46571
H	-7.04615	-3.69292	-0.49144
H	-7.29463	-2.77785	-1.99112
H	-6.54755	-4.3758	-2.04426
C	-7.67567	0.89584	1.20281
C	-7.64118	0.9619	2.73931
H	-7.57118	-0.04186	3.16621
H	-6.79091	1.54555	3.09816
H	-8.55525	1.43166	3.11273
C	-7.76933	2.32184	0.63353
H	-8.68511	2.80434	0.98574
H	-6.92289	2.93673	0.94637

H	-7.79054	2.29978	-0.4591
C	-8.93279	0.12763	0.78279
H	-9.02281	0.06685	-0.30482
H	-8.93962	-0.88689	1.18923
H	-9.81532	0.64653	1.16382
C	4.81355	-2.5535	-0.29257
H	4.38053	-1.73773	0.2843
H	5.3282	-3.21813	0.40761
H	5.56384	-2.15249	-0.97856
C	3.47856	-6.02431	-3.6756
H	4.3762	-6.56666	-3.37518
H	2.67605	-6.7384	-3.85795
H	3.70159	-5.51664	-4.61831

Catalyst **4.13** / **2.46** Transition State 2 proximal *s-cis*

EE = -2595.7247 a.u.

ΔG^0 = -2594.5103 a.u.

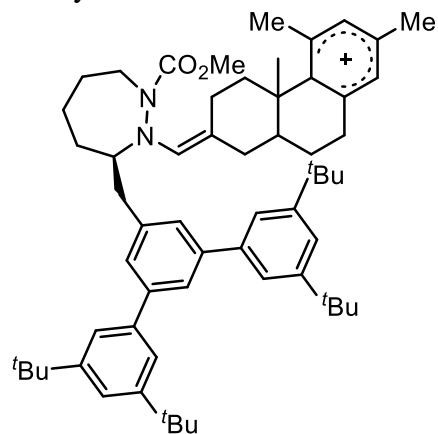
C	2.53503	-3.92254	-1.32508
N	3.95719	-2.8493	0.38855
C	3.77234	-4.76254	-1.628
C	2.12546	-3.09073	-2.56194
H	1.71312	-4.61154	-1.09598
C	1.59685	-2.9121	0.69194
C	4.50761	-3.87852	1.28484
C	4.71919	-1.86861	-0.18668
C	4.21681	-5.6923	-0.48971
H	4.5998	-4.10694	-1.92396
H	3.52477	-5.35619	-2.51173
C	1.10141	-2.02476	-2.25742
H	3.01909	-2.61233	-2.96977
H	1.74539	-3.78563	-3.31691
C	1.36524	-2.02716	1.67494
H	0.8136	-3.636	0.4784
C	5.1517	-5.03126	0.5256
H	5.22211	-3.40005	1.95211
H	3.66463	-4.22732	1.88623
O	5.9835	-1.93685	0.25099
O	4.31693	-1.03979	-0.97349
H	4.73589	-6.55044	-0.92244
H	3.33235	-6.08896	0.02276
H	6.04238	-4.65823	0.01016
H	5.48865	-5.77353	1.25449
C	6.86486	-0.92859	-0.2568
C	-1.12793	-1.31618	-1.6138
C	0.63547	0.33886	-1.89523

H	6.86116	-0.93629	-1.34591
H	6.56185	0.05352	0.10354
H	7.84882	-1.18591	0.12393
C	-0.68966	0.01029	-1.60119
H	-1.39883	0.78251	-1.32112
C	2.1725	-0.80573	1.997
H	2.54047	-0.80585	3.0288
H	3.02096	-0.67971	1.3253
N	2.6979	-3.08059	-0.12617
C	0.07242	-2.14575	2.42082
H	0.22612	-2.26854	3.49723
H	-0.50543	-3.0057	2.07859
C	1.27378	0.48747	1.78246
H	0.98734	0.44733	0.72764
C	0.06942	0.25007	2.61779
C	0.03828	0.56601	4.06441
H	0.79888	1.26816	4.38939
H	-0.95284	0.94332	4.33851
H	0.15598	-0.37948	4.60839
C	-0.80304	-0.85681	2.18424
H	-1.0326	-0.80783	1.11846
H	-1.71873	-0.91588	2.77511
C	2.03106	1.77698	2.06565
H	2.93553	1.7863	1.45243
H	2.3552	1.81631	3.10835
C	1.18458	3.02295	1.70917
H	1.67945	3.91793	2.092
H	1.13802	3.10709	0.62266
C	-0.21297	2.92729	2.24943
C	-1.13513	2.08913	1.59727
C	-0.60979	3.57705	3.41695
C	-2.45604	1.93535	2.06879
H	-0.87366	1.68174	0.62514
C	-1.8911	3.40023	3.93194
H	0.09444	4.21946	3.93601
C	-2.80114	2.57102	3.24879
H	-3.80653	2.45924	3.64315
C	1.50991	-0.69513	-2.23668
H	2.5411	-0.47204	-2.47498
C	-0.22386	-2.33107	-1.93928
H	-0.56231	-3.36375	-1.95315
C	-2.53424	-1.6013	-1.22624
C	-2.82319	-2.56835	-0.26238
C	-3.57671	-0.85588	-1.77742
H	-2.00053	-3.12968	0.17041
C	-4.90022	-1.06209	-1.38685

H	-3.34044	-0.1156	-2.5349
C	1.12991	1.73632	-1.7839
C	2.47065	1.97735	-1.46032
C	0.2631	2.81891	-1.95872
H	3.12524	1.1318	-1.27913
C	0.70847	4.13218	-1.81012
H	-0.76798	2.62518	-2.22397
C	2.95673	3.27979	-1.34039
C	2.06049	4.33634	-1.52269
H	2.42248	5.35273	-1.41139
C	-5.15332	-2.02962	-0.41007
H	-6.17218	-2.19669	-0.09309
C	-4.13324	-2.7926	0.16663
C	-4.4059	-3.81906	1.2706
C	-5.90431	-4.03554	1.50806
H	-6.03921	-4.79957	2.27701
H	-6.39533	-3.12375	1.85651
H	-6.40857	-4.37699	0.60038
C	-3.77855	-3.30888	2.57927
H	-2.69571	-3.20345	2.48311
H	-4.19431	-2.33476	2.85202
H	-3.97803	-4.01103	3.3934
C	-3.77955	-5.17262	0.89672
H	-4.20288	-5.54783	-0.03841
H	-2.69644	-5.10276	0.77743
H	-3.9817	-5.90426	1.68339
C	-6.01577	-0.24168	-2.04291
C	-6.00404	-0.49654	-3.56002
H	-5.05647	-0.19589	-4.01157
H	-6.16316	-1.55658	-3.77355
H	-6.80322	0.07526	-4.03939
C	-5.77727	1.25395	-1.77587
H	-4.80707	1.58297	-2.15595
H	-6.5518	1.84793	-2.26863
H	-5.81505	1.46387	-0.70387
C	-7.40237	-0.60883	-1.50474
H	-7.64367	-1.65758	-1.69574
H	-7.4793	-0.42459	-0.43009
H	-8.15574	0.0047	-2.00407
C	4.41889	3.58261	-1.0005
C	5.23479	2.30507	-0.78249
H	5.24974	1.67088	-1.6724
H	6.26587	2.57337	-0.53799
H	4.83681	1.70644	0.0421
C	4.48874	4.42481	0.28506
H	5.53118	4.65127	0.52468

H	3.954	5.37117	0.18083
H	4.05621	3.88132	1.12955
C	5.04917	4.37192	-2.16051
H	4.53098	5.31856	-2.32888
H	6.09611	4.59361	-1.93614
H	5.01018	3.79174	-3.08589
C	-0.2365	5.3335	-1.89097
C	-1.66548	4.92351	-2.26145
H	-2.29457	5.81511	-2.31072
H	-1.7029	4.43091	-3.23658
H	-2.09746	4.25136	-1.5147
C	0.26892	6.33401	-2.94267
H	-0.40573	7.19282	-2.9926
H	1.26708	6.70598	-2.70343
H	0.30549	5.86796	-3.93061
C	-0.27228	6.00918	-0.50802
H	0.7176	6.36213	-0.20949
H	-0.94951	6.86752	-0.52657
H	-0.62633	5.30607	0.25252
C	-3.44569	1.12886	1.27353
H	-4.43594	1.15646	1.72903
H	-3.52287	1.52335	0.25646
H	-3.14254	0.08033	1.17815
C	-2.3171	4.07944	5.20361
H	-3.10769	4.8058	5.00407
H	-2.71853	3.34667	5.90825
H	-1.48175	4.5924	5.67873

Catalyst **4.13** / **2.46** Cation 2



Proximal *s-trans* cage

EE = -2595.7354 a.u.

ΔG^0 = -2594.5178 a.u.

C	-1.36399	4.40823	-1.15666
N	-2.7471	3.66433	0.73883

C	-2.32686	5.59185	-1.20549
C	-1.41316	3.61719	-2.48833
H	-0.34887	4.81158	-1.04969
C	-0.45139	3.0173	0.65271
C	-2.79711	4.71954	1.76008
C	-3.84244	2.95963	0.33113
C	-2.28405	6.51468	0.02155
H	-3.34845	5.2282	-1.36683
H	-2.0619	6.16121	-2.10032
H	-2.45902	3.44514	-2.75485
H	-0.96522	4.24282	-3.2665
C	-0.35504	2.00758	1.52525
H	0.46401	3.53121	0.36588
C	-3.18918	6.06895	1.17241
H	-3.49203	4.41269	2.53968
H	-1.7955	4.75811	2.19536
O	-4.92642	3.30279	1.04521
O	-3.8573	2.12101	-0.54561
H	-2.59039	7.51766	-0.28461
H	-1.24979	6.59958	0.37623
H	-4.2241	6.0104	0.81951
H	-3.16308	6.81433	1.97231
C	-6.1204	2.58398	0.71764
H	-6.37565	2.73059	-0.33141
H	-5.98935	1.51961	0.91358
H	-6.89315	2.99692	1.35951
C	-1.46386	1.08091	1.94062
H	-1.7395	1.25554	2.98783
H	-2.35762	1.24671	1.33901
N	-1.58192	3.53682	0.00979
C	0.99994	1.65595	2.0824
H	1.04212	1.81611	3.16686
H	1.76879	2.29522	1.64058
C	1.35658	0.19342	1.76498
H	1.29471	0.09266	0.67481
C	-1.06815	-0.39768	1.7447
H	-1.86066	-1.01484	2.17224
H	-1.03637	-0.59172	0.66947
C	0.2934	-0.76448	2.35355
C	2.78777	-0.12644	2.17038
H	3.46977	0.54986	1.64823
H	2.93485	0.01794	3.24537
C	0.22634	-0.74304	3.8807
H	-0.08765	0.24357	4.22301
H	-0.51119	-1.46021	4.24665
H	1.18358	-0.96667	4.35256

C	3.1475	-1.57339	1.7778
H	3.1624	-1.63724	0.68344
H	4.13134	-1.84944	2.15827
C	2.10301	-2.48389	2.31702
C	0.72366	-2.28505	1.8266
C	2.35842	-3.36728	3.32631
C	-0.25764	-3.30492	2.24219
H	0.70105	-2.16379	0.73771
C	1.32885	-4.17976	3.84661
H	3.36047	-3.4598	3.72928
C	0.04288	-4.15566	3.27208
H	-0.69633	-4.87165	3.61414
C	-0.70663	2.29067	-2.38141
C	0.67561	2.20863	-2.21756
C	1.29622	0.99336	-1.9134
H	1.27385	3.11205	-2.29173
C	-0.87136	-0.10647	-2.02204
C	0.51003	-0.16179	-1.83256
H	0.97019	-1.10354	-1.54878
C	2.73958	0.94008	-1.55828
C	3.34163	2.01236	-0.90383
C	3.50517	-0.20315	-1.83088
H	2.74445	2.88849	-0.67514
C	4.8415	-0.2828	-1.45494
H	3.03956	-1.02185	-2.36451
C	-1.73768	-1.29442	-1.81298
C	-2.80474	-1.1957	-0.91684
C	-1.50152	-2.50971	-2.45559
H	-2.95898	-0.25731	-0.39242
C	-2.32185	-3.61835	-2.22816
H	-0.67971	-2.57721	-3.16106
C	-1.46171	1.12763	-2.30031
H	-2.53658	1.19558	-2.40844
C	5.41234	0.81921	-0.79872
H	6.45489	0.76552	-0.51301
C	4.68845	1.97556	-0.52138
C	-3.39321	-3.47955	-1.33894
H	-4.03487	-4.3292	-1.15353
C	-3.64524	-2.27822	-0.66711
C	5.31233	3.19806	0.15985
C	5.29959	4.3753	-0.83072
H	5.87892	4.13238	-1.72505
H	4.28177	4.62371	-1.14028
H	5.73947	5.26128	-0.36457
C	4.49776	3.58107	1.40668
H	3.4752	3.86748	1.15148

H	4.45642	2.7517	2.1183
H	4.96452	4.43505	1.90461
C	6.75938	2.9438	0.59366
H	7.40469	2.72586	-0.26078
H	7.14989	3.837	1.08641
H	6.82551	2.11228	1.3004
C	5.7149	-1.50141	-1.77019
C	4.91425	-2.63521	-2.41866
H	4.10068	-2.97309	-1.77022
H	4.49019	-2.33285	-3.37923
H	5.57526	-3.48595	-2.59912
C	6.34807	-2.04269	-0.47742
H	5.57672	-2.3762	0.22091
H	6.98896	-2.89733	-0.71001
H	6.96105	-1.29111	0.0236
C	6.83	-1.07525	-2.74103
H	7.46554	-0.30176	-2.30424
H	7.46027	-1.93433	-2.9868
H	6.40375	-0.68381	-3.66818
C	-4.78648	-2.09822	0.33846
C	-4.19996	-1.69823	1.7039
H	-3.62731	-0.76907	1.63327
H	-5.00722	-1.5465	2.42665
H	-3.54171	-2.48087	2.08998
C	-5.71338	-0.96947	-0.14712
H	-6.12742	-1.20449	-1.1311
H	-6.54376	-0.84333	0.55416
H	-5.17686	-0.01924	-0.21157
C	-5.6112	-3.37546	0.51596
H	-6.40632	-3.19601	1.24334
H	-6.07839	-3.6848	-0.42258
H	-4.99727	-4.20128	0.88593
C	-2.02474	-4.92994	-2.96273
C	-2.9546	-6.06568	-2.52421
H	-3.99988	-5.84172	-2.75073
H	-2.68565	-6.97882	-3.06011
H	-2.86713	-6.26554	-1.45266
C	-2.2038	-4.71098	-4.4748
H	-1.52754	-3.9393	-4.84901
H	-1.99378	-5.63823	-5.0151
H	-3.22862	-4.40536	-4.70025
C	-0.57439	-5.36116	-2.68228
H	0.14478	-4.61708	-3.03061
H	-0.41397	-5.51472	-1.61171
H	-0.35997	-6.30123	-3.19766
C	1.61547	-5.08583	4.99238

H	2.6384	-5.46031	4.95529
H	1.51457	-4.50245	5.91536
H	0.9099	-5.91342	5.04024
C	-1.56505	-3.4354	1.53004
H	-1.63583	-2.79337	0.655
H	-1.69296	-4.47398	1.21165
H	-2.39237	-3.21402	2.2108

Catalyst **4.13** / **2.46** Cation 2 proximal *s-trans* rotated

EE = -2595.7311 a.u.

ΔG^0 = -2594.5107 a.u.

C	-0.36488	4.55962	-0.61191
N	1.92837	3.90988	-1.25062
C	0.14702	5.97811	-0.84859
C	-0.84656	4.38644	0.85379
H	-1.23384	4.40901	-1.2633
C	0.1602	2.34899	-1.55649
C	2.23035	4.42722	-2.59318
C	2.77258	4.05229	-0.18742
C	0.51968	6.29897	-2.30494
H	0.99553	6.18108	-0.18476
H	-0.65655	6.64554	-0.52685
H	-0.05257	4.73074	1.52095
H	-1.72136	5.02701	0.9953
C	0.77647	1.2944	-2.11202
H	-0.9232	2.30882	-1.51073
C	1.95145	5.92123	-2.69397
H	3.2691	4.19958	-2.82812
H	1.59655	3.85919	-3.27878
O	3.97899	4.47925	-0.59081
O	2.49694	3.82547	0.97257
H	0.39679	7.37242	-2.46643
H	-0.1888	5.80031	-2.97697
H	2.6568	6.45313	-2.04674
H	2.15121	6.24285	-3.71985
C	4.90564	4.77084	0.46222
H	4.51764	5.57175	1.09118
H	5.0857	3.88466	1.06924
H	5.81873	5.08554	-0.0345
C	2.24508	0.99414	-2.25989
H	2.50342	0.95701	-3.32584
H	2.8746	1.76165	-1.81069
N	0.62789	3.5325	-0.99385
C	-0.09296	0.16111	-2.59686
H	0.01828	0.01037	-3.67801

H	-1.14867	0.38212	-2.41437
C	0.25329	-1.14065	-1.85583
H	0.14003	-0.91805	-0.78502
C	2.61476	-0.35595	-1.60392
H	3.66366	-0.55899	-1.8272
H	2.51541	-0.24294	-0.52089
C	1.73641	-1.52981	-2.06879
C	-0.72177	-2.25449	-2.20183
H	-1.74509	-1.90903	-2.04522
H	-0.6418	-2.53776	-3.25561
C	2.07292	-1.91085	-3.51193
H	1.83697	-1.0851	-4.18409
H	3.1406	-2.11668	-3.6138
H	1.52491	-2.78694	-3.86066
C	-0.45688	-3.47235	-1.30021
H	-0.65477	-3.18375	-0.26189
H	-1.10204	-4.31288	-1.55727
C	0.97481	-3.84841	-1.45545
C	1.9941	-2.84027	-1.08096
C	1.33439	-5.01799	-2.05889
C	3.39326	-3.31397	-1.13223
H	1.78031	-2.41939	-0.08838
C	2.6938	-5.33389	-2.2675
H	0.57427	-5.72124	-2.37972
C	3.70062	-4.48386	-1.77489
H	4.7351	-4.8004	-1.84962
C	-1.17038	2.94632	1.1499
C	-2.40155	2.3764	0.8396
C	-2.58089	0.98973	0.91252
H	-3.21778	3.00429	0.49386
C	-0.26173	0.73321	1.61133
C	-1.49799	0.17723	1.264
H	-1.63784	-0.8988	1.27695
C	-3.90655	0.39256	0.6038
C	-5.07441	0.99602	1.07137
C	-4.00617	-0.77897	-0.14727
H	-4.98974	1.89574	1.67146
C	-5.24267	-1.35835	-0.43305
H	-3.09301	-1.22546	-0.5244
C	0.92972	-0.09291	1.95974
C	2.18969	0.51468	2.01171
C	0.84168	-1.45851	2.24589
H	2.28668	1.56101	1.74655
C	1.97196	-2.20619	2.5967
H	-0.12853	-1.94291	2.22733
C	-0.13929	2.12284	1.58774

H	0.7953	2.599	1.84641
C	3.33322	-0.1884	2.38037
C	3.20461	-1.55027	2.67188
H	4.08252	-2.11186	2.95768
C	-6.39164	-0.72931	0.05644
H	-7.35671	-1.16702	-0.15265
C	-6.33071	0.44779	0.8076
C	4.66471	0.5678	2.47827
C	5.00443	1.23994	1.13534
H	5.16659	0.5038	0.34523
H	4.21071	1.91979	0.81371
H	5.92466	1.82184	1.24008
C	4.52257	1.66687	3.54746
H	4.24285	1.2354	4.51185
H	5.47448	2.19258	3.66888
H	3.76329	2.39836	3.25869
C	5.8266	-0.35047	2.86829
H	6.74803	0.23406	2.91822
H	5.66599	-0.80663	3.84834
H	5.97652	-1.14868	2.13573
C	1.82425	-3.70051	2.91087
C	3.15143	-4.34081	3.33066
H	3.55478	-3.87704	4.23423
H	2.98799	-5.40013	3.54121
H	3.90113	-4.26937	2.53781
C	0.81609	-3.88375	4.05819
H	-0.17538	-3.51398	3.78971
H	0.72357	-4.94455	4.30563
H	1.14981	-3.34953	4.95123
C	1.31445	-4.44236	1.66355
H	0.36581	-4.0312	1.31005
H	2.04755	-4.38359	0.85234
H	1.1569	-5.4991	1.89517
C	-5.30638	-2.61971	-1.30088
C	-4.8998	-2.24873	-2.73753
H	-5.58879	-1.50859	-3.15227
H	-3.8927	-1.82689	-2.771
H	-4.92052	-3.1361	-3.37642
C	-4.34063	-3.68463	-0.75518
H	-3.30538	-3.33744	-0.75579
H	-4.60521	-3.9584	0.26932
H	-4.38943	-4.58336	-1.3758
C	-6.71189	-3.2295	-1.33954
H	-7.0664	-3.48099	-0.33654
H	-7.43395	-2.55406	-1.80413
H	-6.68965	-4.14755	-1.93124

C	-7.58252	1.14181	1.35438
C	-7.50581	1.19226	2.88992
H	-7.45254	0.18293	3.30598
H	-6.63045	1.74875	3.23104
H	-8.3963	1.68347	3.29166
C	-7.65084	2.57524	0.80042
H	-8.54195	3.08062	1.18262
H	-6.77824	3.16224	1.09437
H	-7.70327	2.56412	-0.29131
C	-8.87135	0.4129	0.96126
H	-8.99265	0.36648	-0.124
H	-8.89501	-0.60547	1.35738
H	-9.72856	0.95153	1.37166
C	4.48703	-2.54929	-0.46027
H	4.10064	-1.75915	0.17645
H	5.07442	-3.23905	0.15184
H	5.16883	-2.12281	-1.20327
C	3.0537	-6.58511	-2.98742
H	4.07941	-6.88902	-2.78785
H	2.36322	-7.39194	-2.74038
H	2.95683	-6.39442	-4.06278

Catalyst **4.13** / **2.46** Cation 2 proximal *s-cis*

EE = -2595.7343 a.u.

ΔG^0 = -2594.5168 a.u.

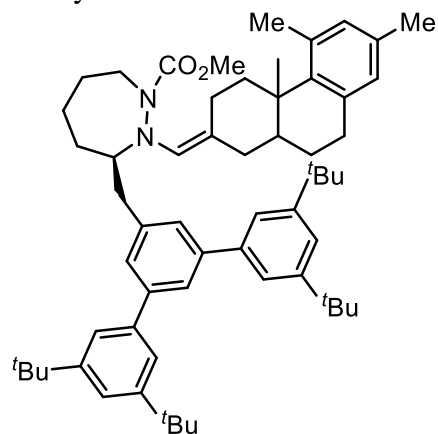
C	2.07406	-4.10483	-1.40834
N	3.51194	-3.30151	0.41995
C	3.22081	-5.0703	-1.69956
C	1.83225	-3.18112	-2.62326
H	1.16719	-4.70407	-1.25886
C	1.14441	-3.1786	0.6594
C	3.8864	-4.42911	1.28528
C	4.40482	-2.3698	-0.0273
C	3.49474	-6.10409	-0.59795
H	4.13353	-4.50258	-1.91605
H	2.95599	-5.58479	-2.6271
C	0.91285	-2.02332	-2.32373
H	2.79601	-2.78619	-2.95436
H	1.42673	-3.7932	-3.43499
C	0.9344	-2.29723	1.64238
H	0.34902	-3.8864	0.43239
C	4.44105	-5.60888	0.49762
H	4.60721	-4.0739	2.01947
H	2.97388	-4.70966	1.81705
O	5.62402	-2.59689	0.48909

O	4.15373	-1.45353	-0.7806
H	3.93532	-6.99364	-1.0542
H	2.5445	-6.42089	-0.15148
H	5.39512	-5.31457	0.04845
H	4.6517	-6.42131	1.19889
C	6.63241	-1.65399	0.11328
C	-1.26781	-1.1061	-1.77805
C	0.67227	0.35924	-1.88607
H	6.71359	-1.59662	-0.97152
H	6.3974	-0.66845	0.51358
H	7.55582	-2.02854	0.54552
C	-0.69562	0.16513	-1.68276
H	-1.32871	1.0012	-1.40228
C	1.80371	-1.12279	1.99746
H	2.14962	-1.19272	3.0367
H	2.68568	-1.07295	1.35694
N	2.26276	-3.33256	-0.16937
C	-0.37752	-2.33494	2.3755
H	-0.22509	-2.47322	3.45104
H	-0.97646	-3.18321	2.03547
C	1.02211	0.19497	1.79134
H	0.81153	0.24351	0.71633
C	-0.35066	0.20285	2.51046
C	-0.23841	0.27462	4.03497
H	0.33669	1.12829	4.3882
H	-1.22874	0.31851	4.49388
H	0.25453	-0.62403	4.40761
C	-1.1573	-1.03757	2.11159
H	-1.37687	-1.0001	1.03982
H	-2.10569	-1.0607	2.65616
C	1.87365	1.40441	2.15965
H	2.79101	1.39448	1.56767
H	2.1676	1.3616	3.21207
C	1.12731	2.72628	1.86933
H	1.66135	3.58013	2.28904
H	1.07174	2.85481	0.78326
C	-0.26142	2.66467	2.40118
C	-1.10857	1.55807	1.91094
C	-0.71283	3.48502	3.39686
C	-2.53579	1.62109	2.28234
H	-1.00279	1.42114	0.83038
C	-2.017	3.33331	3.91107
H	-0.06664	4.25197	3.80824
C	-2.91914	2.41658	3.32743
H	-3.95172	2.42214	3.65688
C	1.45619	-0.74686	-2.21924

H	2.51979	-0.62627	-2.37826
C	-0.45372	-2.19714	-2.09692
H	-0.89414	-3.18746	-2.17492
C	-2.71424	-1.26672	-1.47761
C	-3.15589	-2.29368	-0.64101
C	-3.64201	-0.35241	-1.97849
H	-2.42157	-2.98356	-0.23505
C	-4.99773	-0.44596	-1.6619
H	-3.29106	0.43276	-2.64002
C	1.30197	1.68782	-1.67085
C	2.69592	1.80809	-1.70891
C	0.52364	2.81468	-1.38911
H	3.29162	0.9198	-1.89187
C	1.11327	4.05272	-1.13299
H	-0.55413	2.71534	-1.38468
C	3.31632	3.03714	-1.48109
C	2.50665	4.13926	-1.19381
H	2.97812	5.09679	-1.00038
C	-5.40391	-1.479	-0.81221
H	-6.44935	-1.56206	-0.55378
C	-4.50248	-2.41174	-0.28996
C	-4.93852	-3.51559	0.67844
C	-6.45916	-3.5664	0.85955
H	-6.71286	-4.38682	1.5347
H	-6.84568	-2.64326	1.29832
H	-6.97086	-3.74074	-0.09046
C	-4.2966	-3.24504	2.04969
H	-3.20661	-3.25518	1.98397
H	-4.60647	-2.26891	2.43416
H	-4.60071	-4.01187	2.76752
C	-4.4713	-4.88403	0.15568
H	-4.90861	-5.09173	-0.82419
H	-3.38467	-4.9346	0.06228
H	-4.78481	-5.67152	0.8461
C	-5.98116	0.5682	-2.25574
C	-5.9014	0.51304	-3.79107
H	-4.90434	0.7705	-4.15371
H	-6.14843	-0.48814	-4.15318
H	-6.61149	1.22147	-4.22601
C	-5.60839	1.98138	-1.77635
H	-4.58064	2.24034	-2.04253
H	-6.27312	2.71858	-2.23486
H	-5.71339	2.05832	-0.69079
C	-7.42902	0.28811	-1.84062
H	-7.76044	-0.69725	-2.17804
H	-7.55611	0.34516	-0.75658

H	-8.08408	1.03593	-2.29347
C	4.83722	3.21205	-1.52973
C	5.55985	1.89537	-1.82989
H	5.26138	1.47454	-2.79327
H	6.63781	2.07529	-1.85555
H	5.36283	1.13782	-1.06587
C	5.34282	3.74631	-0.17857
H	6.42579	3.89123	-0.21827
H	4.88402	4.70401	0.07606
H	5.12468	3.03924	0.62652
C	5.18871	4.22017	-2.63748
H	4.73809	5.19708	-2.44928
H	6.2728	4.35186	-2.69173
H	4.8359	3.86256	-3.60811
C	0.29762	5.29332	-0.75964
C	-1.20979	5.02055	-0.76904
H	-1.74323	5.9345	-0.49829
H	-1.55605	4.71004	-1.75816
H	-1.48356	4.24708	-0.04638
C	0.5898	6.42808	-1.75522
H	0.01	7.31575	-1.48841
H	1.64607	6.70455	-1.75595
H	0.31415	6.12953	-2.76981
C	0.70013	5.7362	0.65843
H	1.76039	5.99327	0.71282
H	0.12184	6.61557	0.95497
H	0.50634	4.93683	1.37989
C	-3.55634	0.92083	1.44795
H	-4.5014	0.80751	1.97885
H	-3.73366	1.55514	0.56932
H	-3.23001	-0.04226	1.05721
C	-2.45591	4.17094	5.06048
H	-3.53679	4.3027	5.07405
H	-2.17178	3.64859	5.98207
H	-1.95422	5.13806	5.06402

Catalyst **4.13** / **2.46** Enamine



Proximal *s-trans* cage

EE = -2595.336 a.u.

ΔG^0 = -2594.1266 a.u.

C	-1.97287	3.87577	-1.66204
N	-3.53466	3.35112	0.15814
C	-3.04415	4.87128	-2.10529
C	-1.74486	2.82338	-2.77194
H	-1.03516	4.43143	-1.53545
C	-1.19499	3.2251	0.57577
C	-3.88742	4.5763	0.88746
C	-4.43119	2.3705	-0.14575
C	-3.30895	6.02461	-1.12731
H	-3.97835	4.3351	-2.30958
H	-2.70799	5.27431	-3.06442
H	-2.71842	2.43999	-3.08884
H	-1.29424	3.33415	-3.62911
C	-1.05519	2.41181	1.62567
H	-0.41554	3.96016	0.37674
C	-4.3375	5.69421	-0.0438
H	-4.65982	4.33558	1.61493
H	-2.98805	4.86741	1.43577
O	-5.64844	2.66526	0.34627
O	-4.19423	1.35584	-0.76814
H	-3.67026	6.88755	-1.69179
H	-2.36535	6.3312	-0.65966
H	-5.28201	5.40308	-0.51558
H	-4.53901	6.58428	0.5592
C	-6.63965	1.65242	0.15317
H	-6.75787	1.43037	-0.90705
H	-6.35947	0.7416	0.68369
H	-7.55868	2.06266	0.56202
C	-1.92033	1.23466	1.96049

H	-2.34072	1.35666	2.96694
H	-2.75639	1.13916	1.26689
N	-2.25393	3.24732	-0.36038
C	0.1744	2.49477	2.48384
H	-0.08909	2.64502	3.53829
H	0.79596	3.34484	2.18597
C	0.99102	1.20786	2.3128
H	1.18918	1.12215	1.2337
C	-1.1041	-0.07275	1.89001
H	-1.76798	-0.87029	2.21274
H	-0.85929	-0.25894	0.84329
C	0.21541	-0.08308	2.70126
C	2.34325	1.28273	3.00228
H	2.79861	2.26035	2.82615
H	2.23436	1.17594	4.08537
C	-0.10669	-0.12219	4.20827
H	-0.66704	0.76117	4.52375
H	-0.71629	-0.99661	4.4445
H	0.79818	-0.18564	4.81413
C	3.22341	0.18976	2.42182
H	3.59866	0.51868	1.44451
H	4.10293	0.01041	3.04722
C	2.49991	-1.12891	2.21557
C	1.10694	-1.30368	2.34916
C	3.32799	-2.19879	1.86079
C	0.60343	-2.6244	2.19244
C	2.83844	-3.47574	1.65688
H	4.39318	-2.01132	1.75988
C	1.47245	-3.66107	1.85339
H	1.06575	-4.66162	1.75182
C	-0.8877	1.66357	-2.33296
C	0.47601	1.8004	-2.07668
C	1.23066	0.73325	-1.57331
H	0.95976	2.75312	-2.27096
C	-0.76293	-0.65425	-1.60957
C	0.59753	-0.49413	-1.34186
H	1.14798	-1.3055	-0.87348
C	2.67183	0.91537	-1.25335
C	3.15124	2.14738	-0.81289
C	3.57301	-0.14845	-1.39833
H	2.44571	2.95605	-0.65208
C	4.92903	0.01224	-1.13443
H	3.19505	-1.10058	-1.74751
C	-1.50025	-1.89578	-1.26208
C	-2.55707	-1.80454	-0.35312
C	-1.18033	-3.1372	-1.81051

H	-2.78531	-0.83658	0.08339
C	-1.92588	-4.27768	-1.49632
H	-0.36189	-3.19917	-2.52086
C	-1.48504	0.42853	-2.11445
H	-2.54722	0.32412	-2.297
C	5.3796	1.27891	-0.73272
H	6.43799	1.41916	-0.55643
C	4.51303	2.35556	-0.5631
C	-2.9731	-4.15204	-0.57719
H	-3.55102	-5.02756	-0.31771
C	-3.29605	-2.92616	0.01403
C	4.99387	3.73979	-0.11621
C	4.57264	4.78885	-1.15945
H	5.00623	4.55651	-2.13551
H	3.48744	4.83519	-1.27096
H	4.92247	5.77876	-0.85413
C	4.357	4.08394	1.23972
H	3.26556	4.07417	1.18472
H	4.66776	3.36263	2.00046
H	4.67234	5.0806	1.56095
C	6.51662	3.80471	0.0393
H	7.02632	3.58066	-0.90134
H	6.80437	4.81304	0.34584
H	6.87393	3.10862	0.80232
C	5.94158	-1.12028	-1.33323
C	5.25198	-2.47068	-1.55828
H	4.57124	-2.70879	-0.73606
H	4.68446	-2.48464	-2.49191
H	6.00631	-3.25901	-1.61759
C	6.85336	-1.24647	-0.10104
H	6.26828	-1.43719	0.80146
H	7.54786	-2.07909	-0.24065
H	7.44646	-0.34548	0.06472
C	6.80704	-0.79624	-2.56339
H	7.34978	0.14239	-2.4274
H	7.53773	-1.593	-2.72959
H	6.18579	-0.70559	-3.45804
C	-4.41974	-2.75892	1.04041
C	-3.84008	-2.14149	2.32591
H	-3.41889	-1.15053	2.13522
H	-4.62785	-2.03582	3.07785
H	-3.05091	-2.77609	2.74015
C	-5.48425	-1.80711	0.46701
H	-5.90759	-2.21367	-0.45544
H	-6.2968	-1.67679	1.18883
H	-5.05712	-0.82399	0.25279

C	-5.08629	-4.09045	1.39617
H	-5.86548	-3.91806	2.14244
H	-5.55595	-4.551	0.52319
H	-4.36725	-4.79888	1.81648
C	-1.59336	-5.60744	-2.18351
C	-2.56997	-6.72378	-1.79882
H	-3.59693	-6.47243	-2.07631
H	-2.29354	-7.64041	-2.32521
H	-2.54161	-6.9336	-0.72667
C	-1.65754	-5.42275	-3.70969
H	-0.92643	-4.69183	-4.06033
H	-1.44845	-6.37328	-4.20807
H	-2.65123	-5.08516	-4.01528
C	-0.1776	-6.0501	-1.78271
H	0.56608	-5.28307	-2.01255
H	-0.13679	-6.25292	-0.70951
H	0.096	-6.9655	-2.3153
C	3.73057	-4.62394	1.26197
H	3.57447	-5.48472	1.9161
H	3.51765	-4.94861	0.23924
H	4.78326	-4.33994	1.31185
C	-0.84353	-3.04734	2.36106
H	-1.43643	-2.7956	1.47794
H	-0.88693	-4.13093	2.48322
H	-1.32333	-2.60047	3.23125

Catalyst **4.13** / **2.46** Enamine proximal *s-trans* rotated

EE = -2595.3315 a.u.

ΔG^0 = -2594.1235 a.u.

C	-0.15869	4.69576	-0.32542
N	2.01448	3.96044	-1.19802
C	0.40426	6.09996	-0.53562
C	-0.49941	4.46539	1.16822
H	-1.09908	4.6263	-0.8872
C	0.10846	2.60718	-1.60505
C	2.24211	4.54543	-2.52567
C	2.96976	3.92898	-0.22757
C	0.66891	6.48198	-2.00004
H	1.31869	6.2224	0.05672
H	-0.32967	6.7883	-0.10801
H	0.37165	4.73931	1.76892
H	-1.32407	5.13301	1.43454
C	0.6486	1.42225	-1.9131
H	-0.88521	2.85699	-1.97419
C	2.04288	6.05568	-2.5227

H	3.24527	4.28009	-2.85455
H	1.52875	4.05749	-3.19385
O	4.15451	4.35041	-0.70659
O	2.80948	3.57782	0.92377
H	0.58771	7.56713	-2.0987
H	-0.11637	6.05239	-2.6338
H	2.82435	6.51145	-1.90543
H	2.18112	6.42588	-3.54257
C	5.20534	4.43368	0.26129
H	4.93803	5.13863	1.04832
H	5.40143	3.45598	0.70035
H	6.07536	4.78672	-0.285
C	1.95881	0.95001	-1.34067
H	2.7955	1.24852	-1.98816
H	2.11753	1.4544	-0.38329
N	0.71404	3.63068	-0.84842
C	-0.05857	0.50876	-2.88642
H	0.34318	0.64695	-3.89862
H	-1.11798	0.78177	-2.94155
C	0.05322	-0.97177	-2.5131
H	-0.44666	-1.09684	-1.53931
C	2.00816	-0.56786	-1.10069
H	3.02098	-0.81126	-0.79913
H	1.36799	-0.81869	-0.25011
C	1.5278	-1.41577	-2.29786
C	-0.67335	-1.86751	-3.5037
H	-1.65977	-1.45678	-3.73776
H	-0.125	-1.92101	-4.44911
C	2.37008	-1.13553	-3.56027
H	2.39668	-0.07233	-3.80433
H	3.4007	-1.46472	-3.42987
H	1.97196	-1.67053	-4.42456
C	-0.80768	-3.24646	-2.88383
H	-1.56454	-3.20868	-2.09015
H	-1.16776	-3.97651	-3.61348
C	0.48829	-3.75849	-2.28131
C	1.59381	-2.93171	-1.99383
C	0.52868	-5.13179	-2.02062
C	2.76415	-3.56531	-1.49203
C	1.65285	-5.7481	-1.49943
H	-0.35181	-5.72752	-2.24783
C	2.76263	-4.94178	-1.26529
H	3.6707	-5.40316	-0.88645
C	-0.85754	3.02689	1.42515
C	-2.11517	2.51631	1.11618
C	-2.35381	1.13964	1.17516

H	-2.90303	3.18433	0.77943
C	-0.04574	0.77518	1.87321
C	-1.31052	0.28199	1.53139
H	-1.50108	-0.78449	1.53193
C	-3.68781	0.58642	0.82544
C	-4.8553	1.21897	1.2548
C	-3.79229	-0.57801	0.06377
H	-4.76755	2.11438	1.86112
C	-5.03351	-1.12268	-0.26587
H	-2.88124	-1.04895	-0.29156
C	1.09568	-0.13672	2.17015
C	2.39159	0.20417	1.77093
C	0.88893	-1.39619	2.73672
H	2.57116	1.16075	1.29516
C	1.9176	-2.33203	2.83988
H	-0.10002	-1.66579	3.08545
C	0.14652	2.15646	1.83593
H	1.11128	2.58444	2.06642
C	3.45712	-0.68465	1.90286
C	3.19961	-1.95464	2.42709
H	4.00893	-2.66651	2.50788
C	-6.18243	-0.4666	0.18544
H	-7.15071	-0.87746	-0.06086
C	-6.11574	0.70605	0.94436
C	4.84778	-0.25025	1.42248
C	4.8227	-0.04397	-0.10245
H	4.61562	-0.98289	-0.62235
H	4.06027	0.6856	-0.39027
H	5.79617	0.32188	-0.44353
C	5.22865	1.08306	2.08972
H	5.21122	0.99236	3.17887
H	6.23791	1.37463	1.78466
H	4.54551	1.88381	1.79645
C	5.92577	-1.28687	1.75375
H	6.8982	-0.91736	1.41966
H	5.98543	-1.47282	2.82946
H	5.74102	-2.23834	1.24757
C	1.60607	-3.72702	3.39183
C	2.78242	-4.69187	3.2077
H	3.66016	-4.37802	3.77815
H	2.49424	-5.68502	3.5612
H	3.06087	-4.77573	2.15308
C	1.28482	-3.61663	4.89125
H	0.43018	-2.95794	5.06376
H	1.04288	-4.60285	5.29796
H	2.14069	-3.21726	5.44177

C	0.39089	-4.31369	2.64968
H	-0.52035	-3.74508	2.84731
H	0.56437	-4.32418	1.57029
H	0.21664	-5.34232	2.97944
C	-5.08724	-2.39549	-1.11693
C	-4.4343	-2.10978	-2.4796
H	-4.98961	-1.33787	-3.01886
H	-3.40539	-1.76481	-2.36028
H	-4.41906	-3.01714	-3.09073
C	-4.31311	-3.51867	-0.4056
H	-3.26862	-3.24714	-0.23687
H	-4.76525	-3.74308	0.56396
H	-4.33133	-4.42783	-1.01315
C	-6.52041	-2.8786	-1.35852
H	-7.02929	-3.11199	-0.41973
H	-7.11081	-2.13357	-1.89772
H	-6.49682	-3.78824	-1.96323
C	-7.36692	1.43107	1.45142
C	-7.34419	1.4685	2.98911
H	-7.33295	0.45513	3.39863
H	-6.46668	1.99825	3.36554
H	-8.23487	1.98099	3.36311
C	-7.37668	2.86989	0.90749
H	-8.2671	3.39663	1.26159
H	-6.4997	3.4307	1.23733
H	-7.38984	2.86821	-0.18549
C	-8.66055	0.74111	1.00693
H	-8.74348	0.70476	-0.08233
H	-8.72676	-0.27867	1.39447
H	-9.51689	1.30093	1.39007
C	4.07271	-2.87887	-1.14347
H	4.03842	-2.48299	-0.12362
H	4.88244	-3.60877	-1.18239
H	4.3362	-2.05833	-1.80649
C	1.68043	-7.21841	-1.1758
H	1.56792	-7.37361	-0.09856
H	0.86987	-7.74898	-1.67696
H	2.62821	-7.67063	-1.4743

Catalyst **4.13** / **2.46** Enamine proximal *s-cis* rotated

EE = -2595.3341 a.u.

ΔG^0 = -2594.1252 a.u.

C	1.85626	-3.9267	-1.75557
N	3.40457	-3.49485	0.09953
C	2.91911	-4.91545	-2.23273

C	1.65637	-2.8155	-2.81042
H	0.90983	-4.4749	-1.66686
C	1.06078	-3.36982	0.49902
C	3.74836	-4.75256	0.77579
C	4.32592	-2.54579	-0.23385
C	3.16227	-6.11064	-1.30024
H	3.86153	-4.38345	-2.4093
H	2.58516	-5.27439	-3.20999
C	0.80483	-1.67186	-2.31988
H	2.63803	-2.42594	-3.09171
H	1.21141	-3.27291	-3.7002
C	0.9096	-2.60462	1.5826
H	0.27544	-4.08543	0.25627
C	4.1886	-5.83709	-0.19882
H	4.52374	-4.54763	1.51139
H	2.84709	-5.05676	1.31359
O	5.54841	-2.89723	0.20722
O	4.10457	-1.52116	-0.84338
H	3.51602	-6.95512	-1.89655
H	2.2116	-6.42291	-0.85105
H	5.13882	-5.53841	-0.65377
H	4.37626	-6.75348	0.36822
C	6.58609	-1.94962	-0.05621
C	-1.31082	-0.76007	-1.54116
C	0.68198	0.62819	-1.53328
H	6.64847	-1.73973	-1.12349
H	6.40021	-1.02286	0.48578
H	7.50243	-2.41634	0.29405
C	-0.68123	0.46044	-1.27505
H	-1.24061	1.25679	-0.79077
C	1.7727	-1.45451	2.00238
H	2.17041	-1.63315	3.01121
H	2.62529	-1.32322	1.33143
N	2.12854	-3.36555	-0.42253
C	-0.32824	-2.72735	2.41773
H	-0.06493	-2.90933	3.46679
H	-0.93311	-3.57788	2.09132
C	0.96726	-0.13902	1.98594
H	0.73102	0.05671	0.93499
C	-0.40704	-0.1638	2.72719
C	-0.2302	-0.16809	4.25847
H	0.18575	0.7755	4.61694
H	-1.20151	-0.30505	4.74234
H	0.42936	-0.97552	4.58903
C	-1.16031	-1.44317	2.30396
H	-1.48334	-1.33571	1.26347

H	-2.04989	-1.57862	2.91445
C	1.84013	0.99699	2.49616
H	2.77104	1.01638	1.92287
H	2.12086	0.79511	3.53422
C	1.13311	2.34781	2.36756
H	1.32006	2.95847	3.25788
H	1.55583	2.9063	1.52734
C	-0.36847	2.29243	2.15
C	-1.15194	1.13829	2.33791
C	-0.94994	3.50775	1.77605
C	-2.56014	1.27869	2.20076
C	-2.31652	3.64944	1.61753
H	-0.29657	4.36212	1.62361
C	-3.09495	2.51827	1.84711
H	-4.17313	2.60957	1.76565
C	1.40347	-0.44392	-2.06237
H	2.4642	-0.33678	-2.2502
C	-0.55832	-1.81731	-2.06565
H	-1.04668	-2.76455	-2.2774
C	-2.7515	-0.94882	-1.22782
C	-3.19517	-2.1378	-0.64466
C	-3.68043	0.0558	-1.50155
H	-2.4605	-2.89848	-0.39807
C	-5.03928	-0.1174	-1.23119
H	-3.33063	0.97377	-1.96246
C	1.39864	1.88463	-1.19476
C	2.53852	1.82791	-0.38411
C	0.96505	3.11743	-1.68449
H	2.84479	0.86572	0.01321
C	1.66383	4.29253	-1.401
H	0.08609	3.14103	-2.31641
C	3.24887	2.98376	-0.06546
C	2.7992	4.19869	-0.59247
H	3.35578	5.1019	-0.36665
C	-5.4465	-1.31907	-0.64442
H	-6.49377	-1.46584	-0.42392
C	-4.54005	-2.33704	-0.33275
C	-4.96351	-3.62732	0.37581
C	-6.48175	-3.72255	0.55721
H	-6.72722	-4.66675	1.04889
H	-6.86534	-2.91203	1.18179
H	-7.00283	-3.69686	-0.40344
C	-4.30526	-3.65885	1.76625
H	-3.21614	-3.6182	1.68957
H	-4.63335	-2.80597	2.36724
H	-4.57788	-4.57817	2.29236

C	-4.49932	-4.84735	-0.43698
H	-4.94418	-4.83693	-1.43535
H	-3.41336	-4.87223	-0.54759
H	-4.80596	-5.76812	0.06661
C	-6.02754	0.99526	-1.59792
C	-5.91025	1.30898	-3.09942
H	-4.91211	1.6648	-3.36175
H	-6.1234	0.4187	-3.69669
H	-6.62776	2.08717	-3.37358
C	-5.69458	2.25658	-0.78496
H	-4.66276	2.57939	-0.94426
H	-6.35957	3.07597	-1.07251
H	-5.82876	2.06389	0.28254
C	-7.47993	0.60569	-1.30408
H	-7.78091	-0.2797	-1.87003
H	-7.6375	0.40829	-0.24076
H	-8.13829	1.42879	-1.59166
C	4.47121	2.96954	0.85665
C	4.84543	1.55076	1.29658
H	5.06719	0.90482	0.44331
H	5.73306	1.59471	1.93355
H	4.04386	1.07579	1.86936
C	4.15851	3.80342	2.11141
H	5.016	3.79679	2.79026
H	3.93567	4.84184	1.85548
H	3.29521	3.39193	2.64237
C	5.6799	3.57847	0.1263
H	5.49472	4.6119	-0.1735
H	6.55426	3.57097	0.78298
H	5.91815	3.00012	-0.77011
C	1.26899	5.6453	-2.00348
C	-0.08947	5.57825	-2.70893
H	-0.37457	6.5767	-3.04936
H	-0.05766	4.92416	-3.58371
H	-0.86651	5.21204	-2.03297
C	2.33929	6.05097	-3.0321
H	2.07419	7.00613	-3.49447
H	3.3186	6.15964	-2.55964
H	2.42159	5.29724	-3.81932
C	1.19257	6.72781	-0.91416
H	2.14498	6.85861	-0.39756
H	0.92639	7.68651	-1.36742
H	0.43255	6.48462	-0.1683
C	-3.59642	0.1949	2.43637
H	-4.59129	0.64123	2.39895
H	-3.56071	-0.58453	1.67279

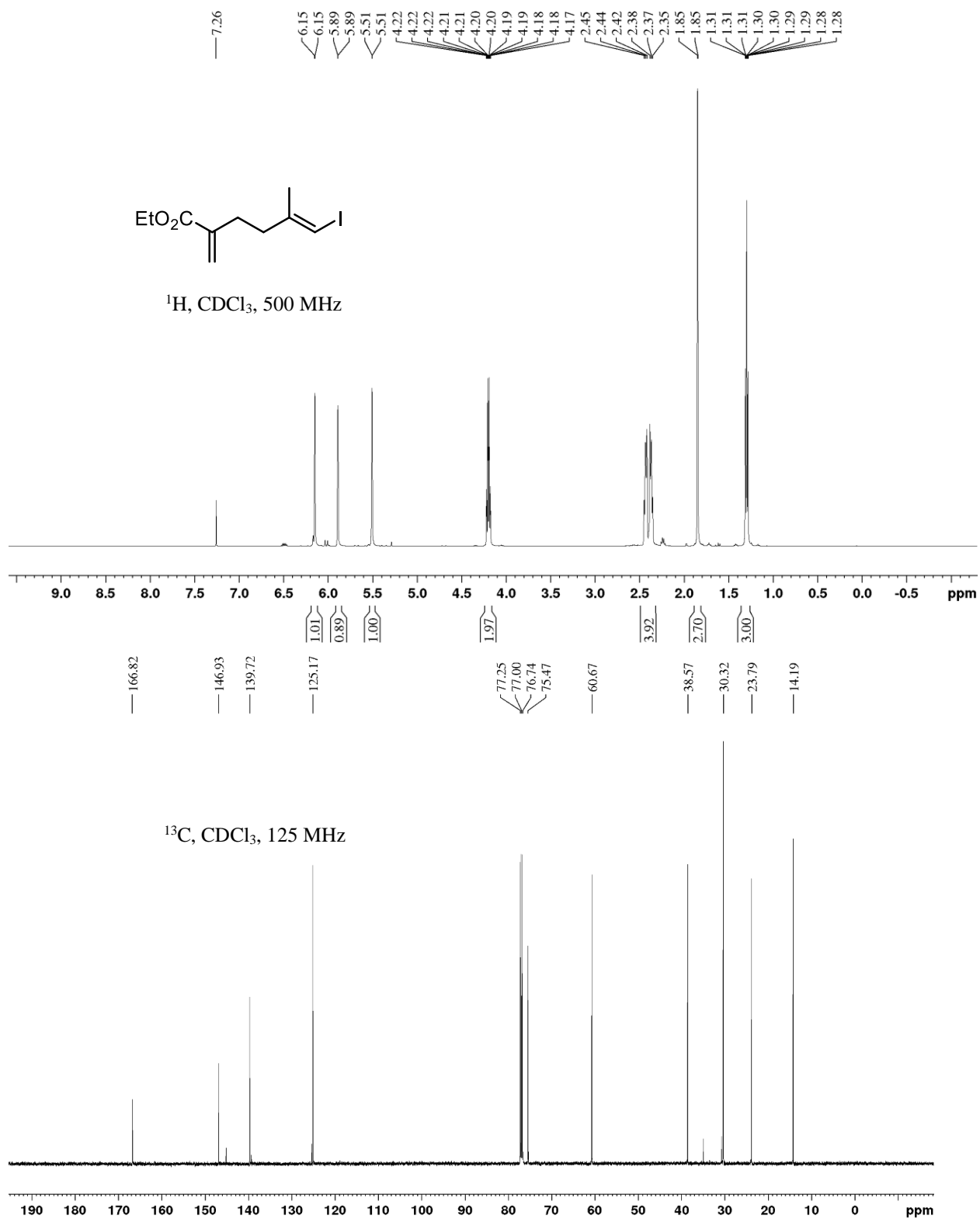
H	-3.48862	-0.27739	3.41441
C	-2.95635	4.96309	1.24741
H	-3.41162	4.91436	0.25404
H	-3.74747	5.22133	1.95513
H	-2.22435	5.77266	1.24366

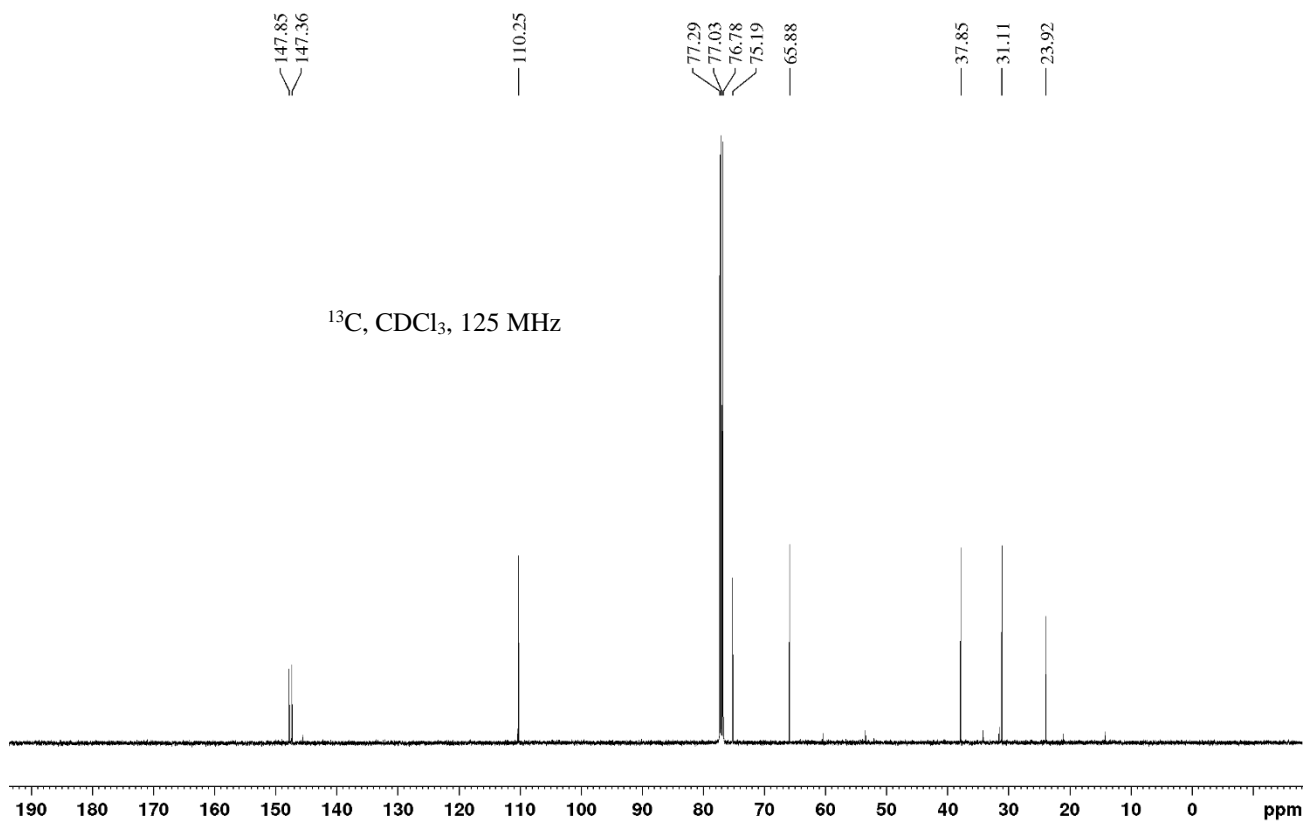
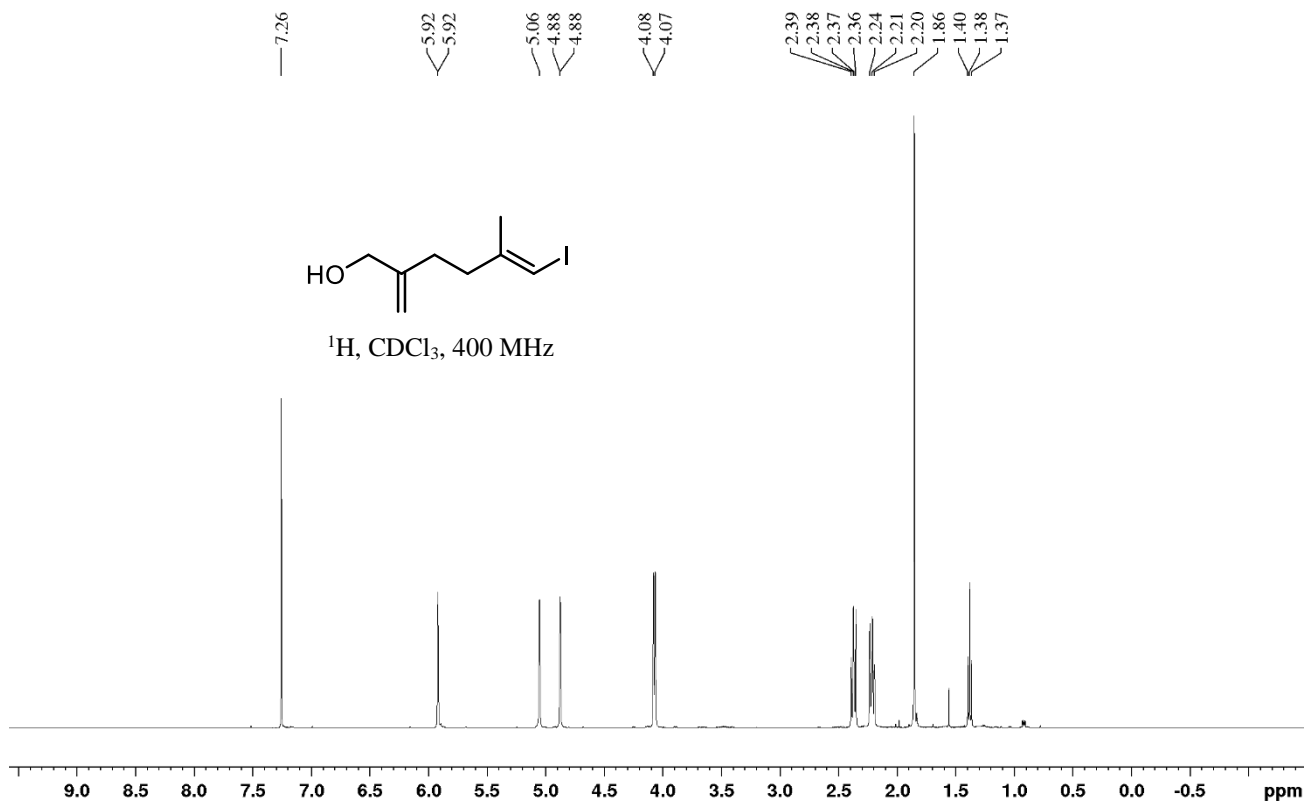
6.2 References

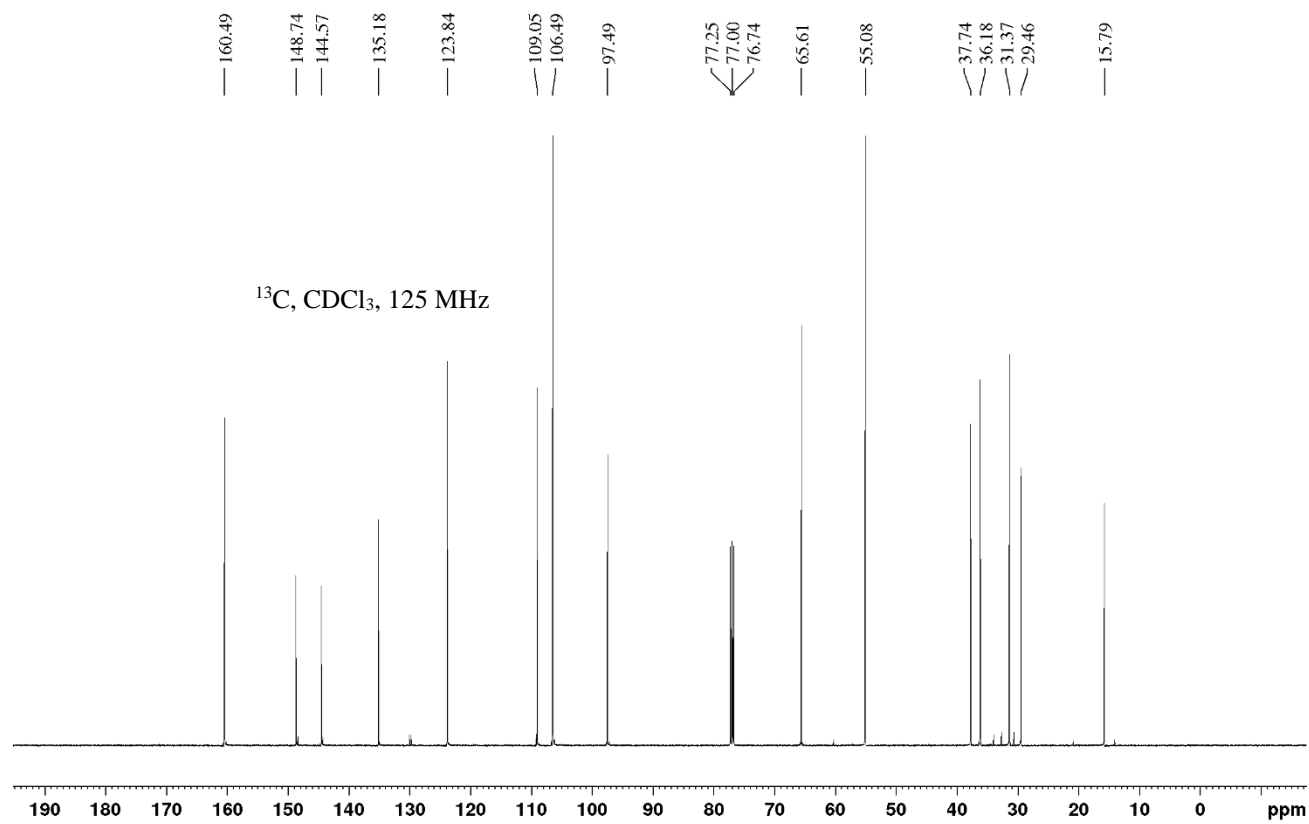
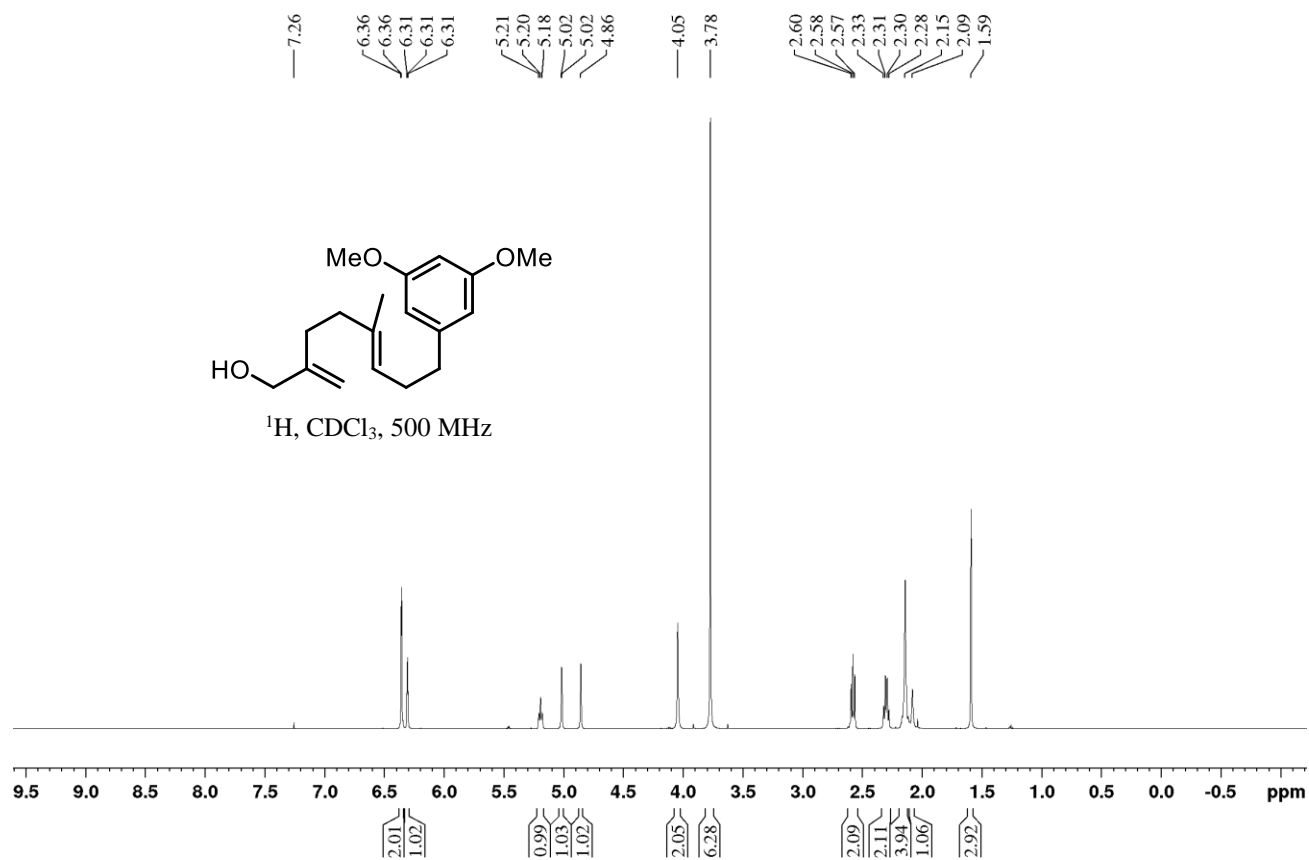
1. Gaussian 16, Revision B.01, M. J. Frisch, G. W. Trucks, H. B. Schlegel, G. E. Scuseria, M. A. Robb, J. R. Cheeseman, G. Scalmani, V. Barone, G. A. Petersson, H. Nakatsuji, X. Li, M. Caricato, A. V. Marenich, J. Bloino, B. G. Janesko, R. Gomperts, B. Mennucci, H. P. Hratchian, J. V. Ortiz, A. F. Izmaylov, J. L. Sonnenberg, D. Williams-Young, F. Ding, F. Lipparini, F. Egidi, J. Goings, B. Peng, A. Petrone, T. Henderson, D. Ranasinghe, V. G. Zakrzewski, J. Gao, N. Rega, G. Zheng, W. Liang, M. Hada, M. Ehara, K. Toyota, R. Fukuda, J. Hasegawa, M. Ishida, T. Nakajima, Y. Honda, O. Kitao, H. Nakai, T. Vreven, K. Throssell, J. A. Montgomery, Jr., J. E. Peralta, F. Ogliaro, M. J. Bearpark, J. J. Heyd, E. N. Brothers, K. N. Kudin, V. N. Staroverov, T. A. Keith, R. Kobayashi, J. Normand, K. Raghavachari, A. P. Rendell, J. C. Burant, S. S. Iyengar, J. Tomasi, M. Cossi, J. M. Millam, M. Klene, C. Adamo, R. Cammi, J. W. Ochterski, R. L. Martin, K. Morokuma, O. Farkas, J. B. Foresman, and D. J. Fox, Gaussian, Inc., Wallingford CT, 2016.

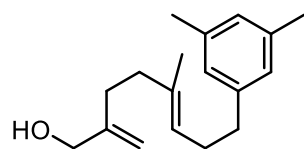
Chapter 7. NMR Spectra and HPLC Chromatograms

7.1. NMR Spectra of New Compounds

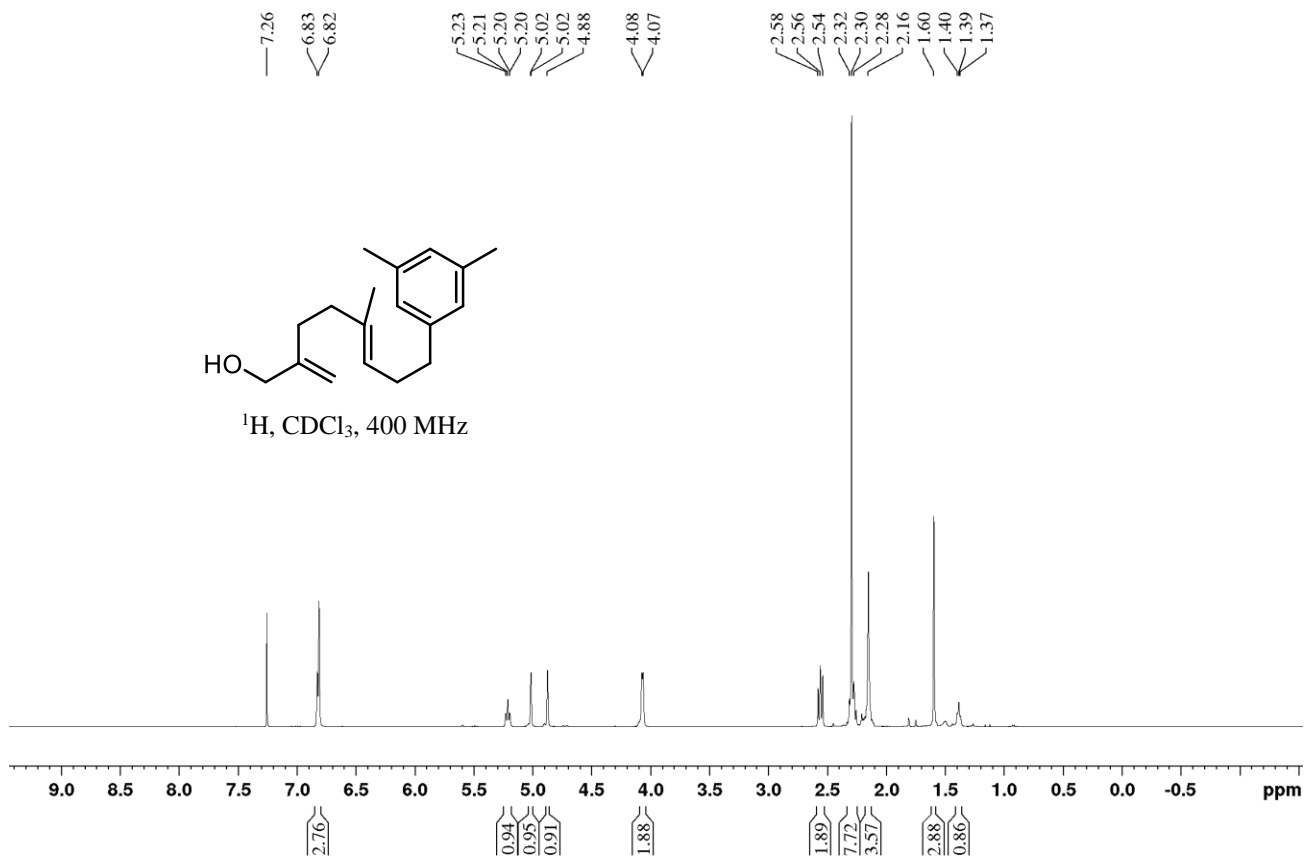




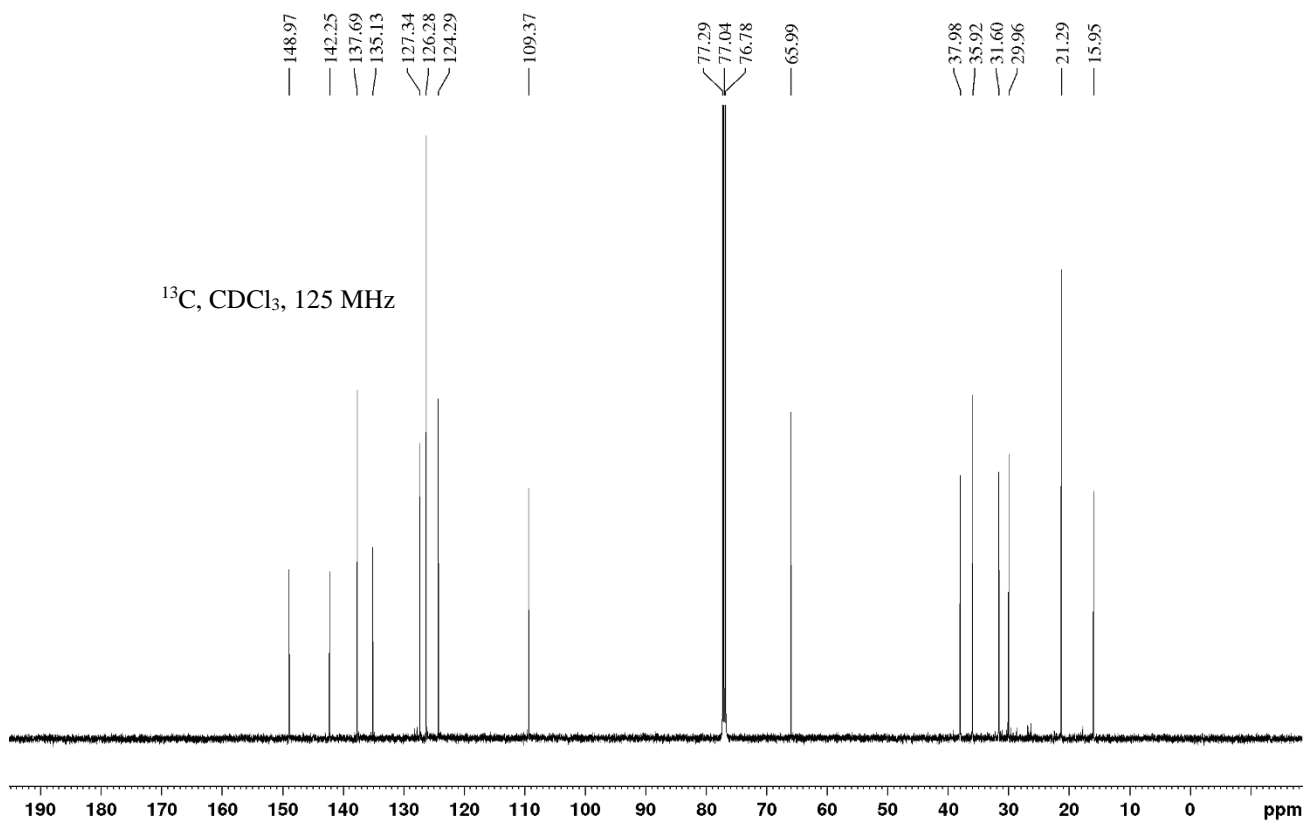


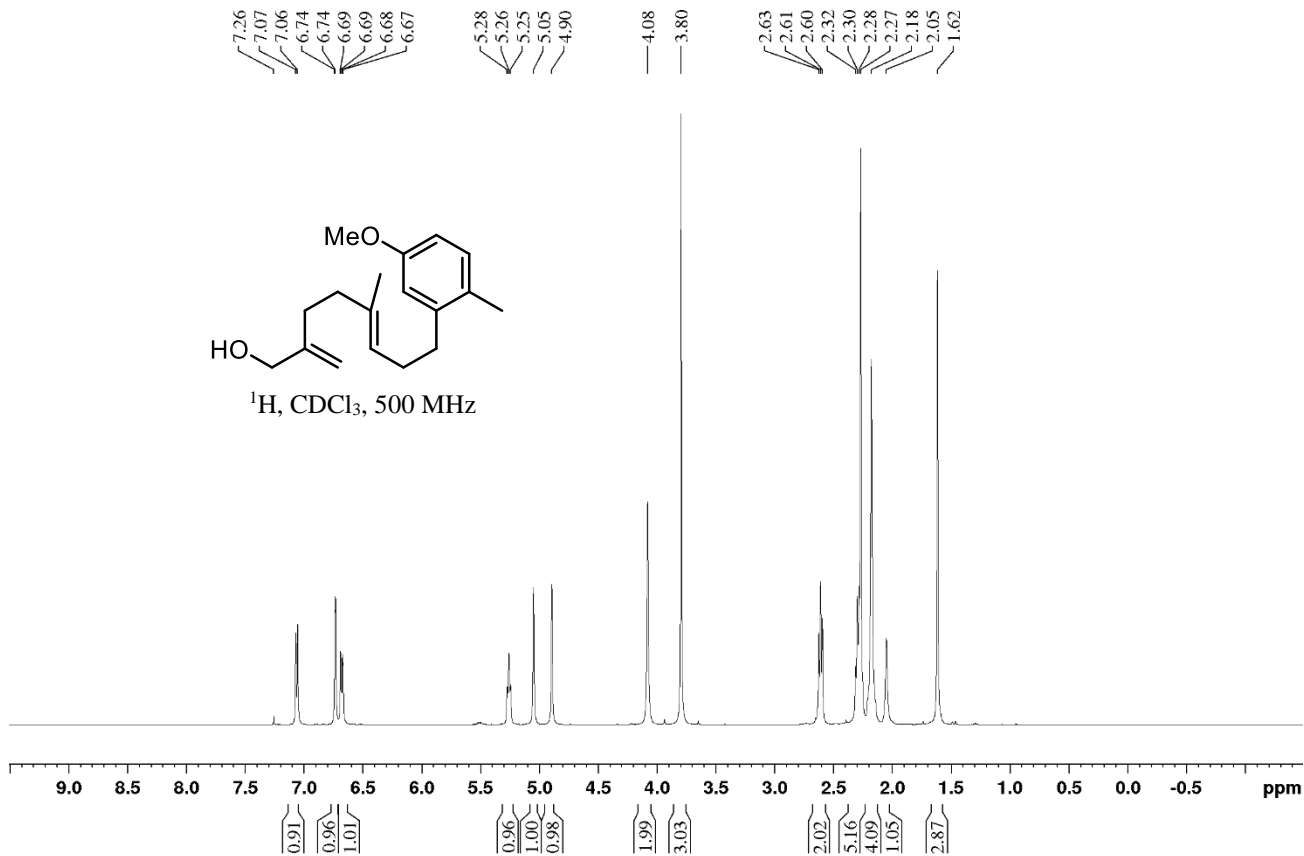
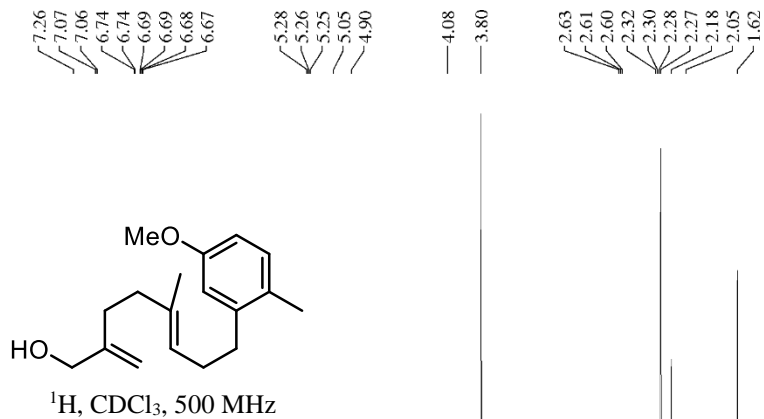


^1H , CDCl_3 , 400 MHz

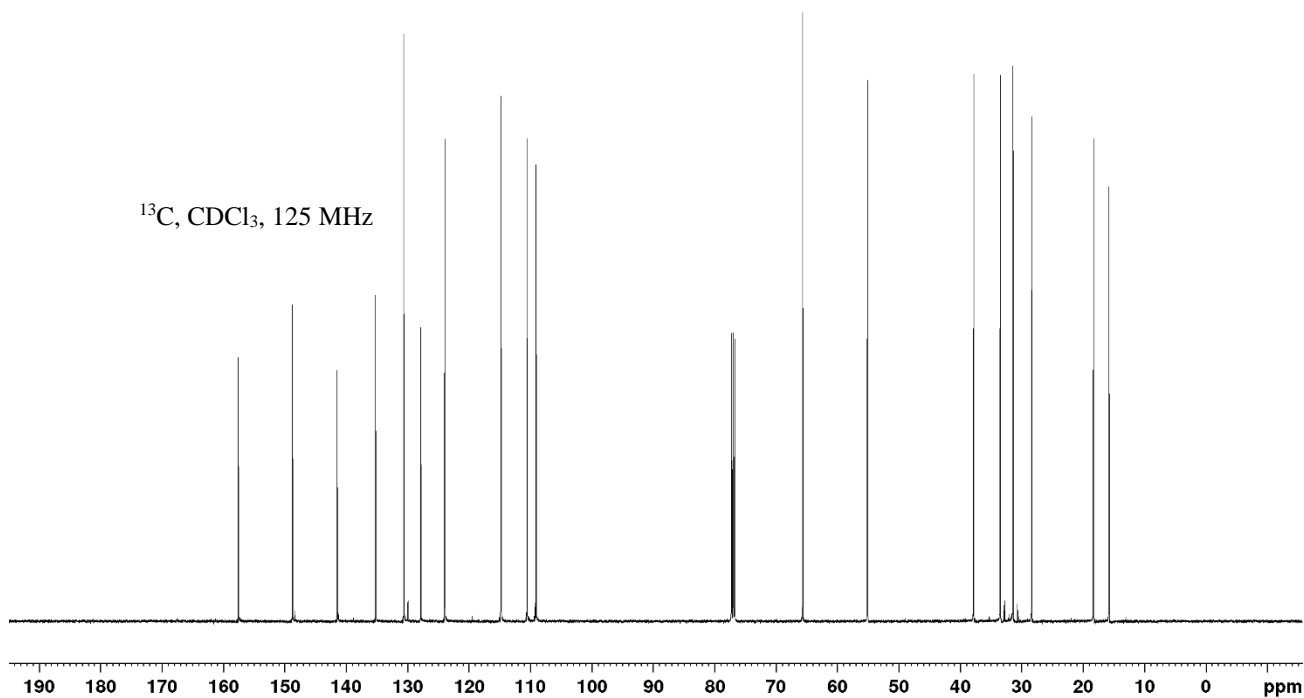


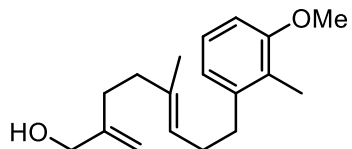
^{13}C , CDCl_3 , 125 MHz



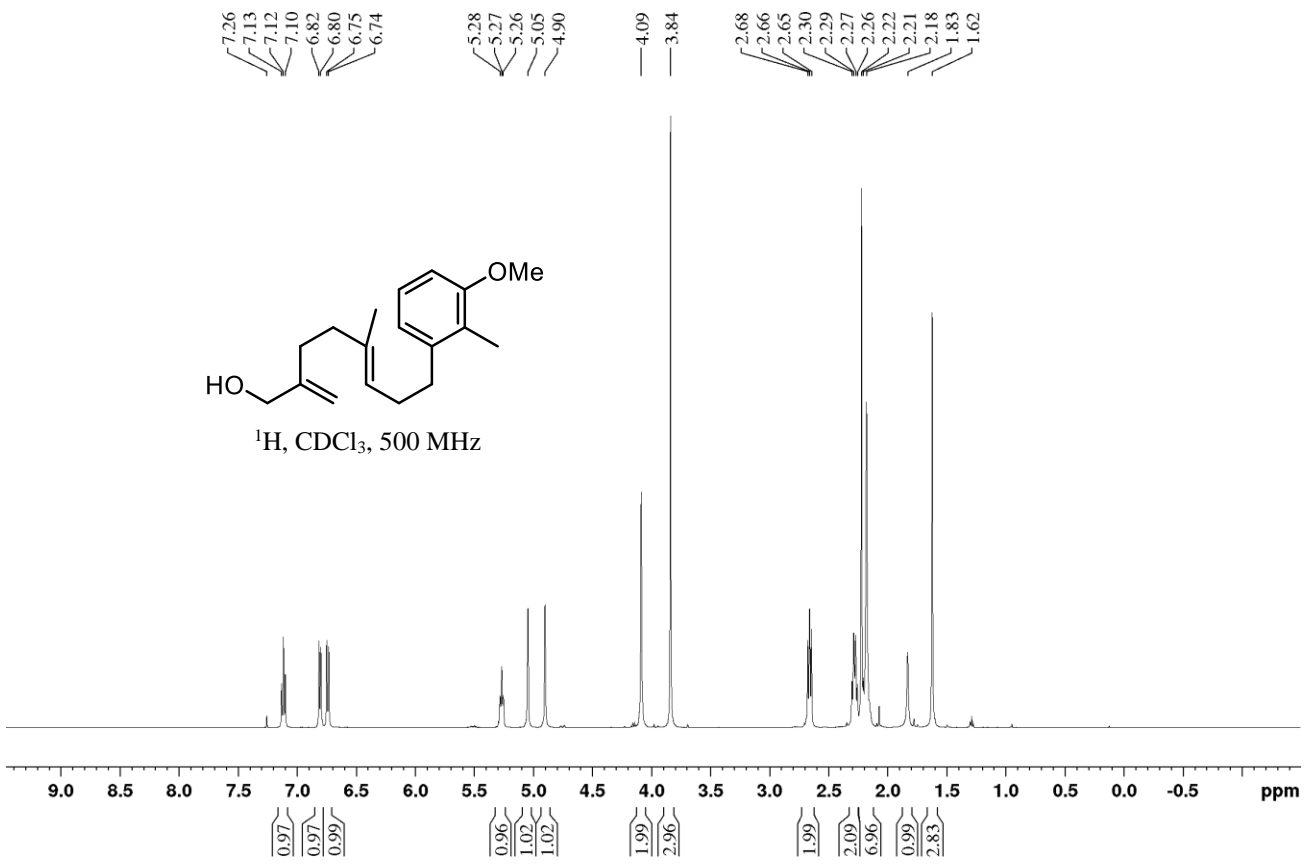


¹³C, CDCl₃, 125 MHz

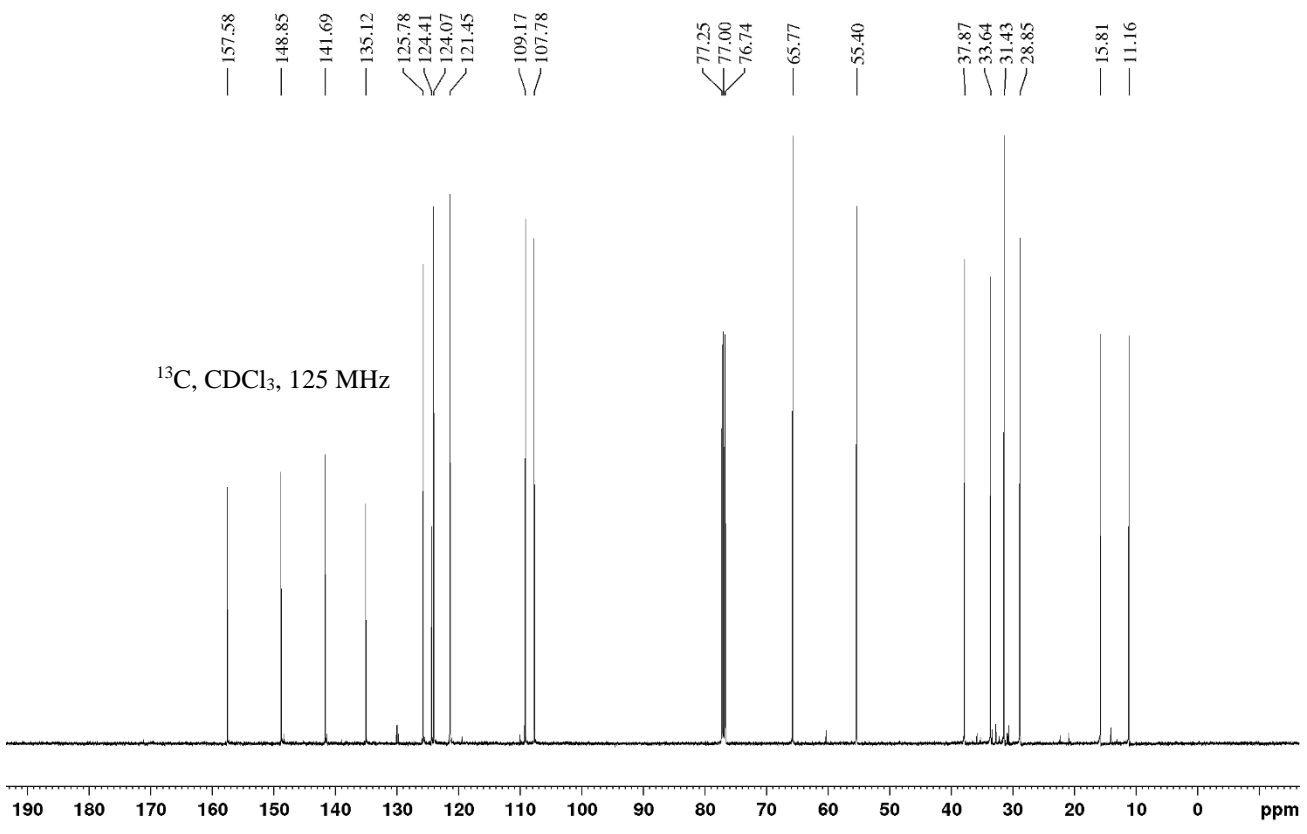


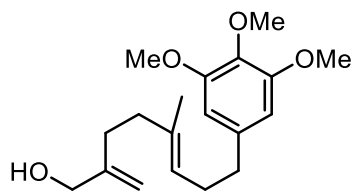


¹H, CDCl₃, 500 MHz

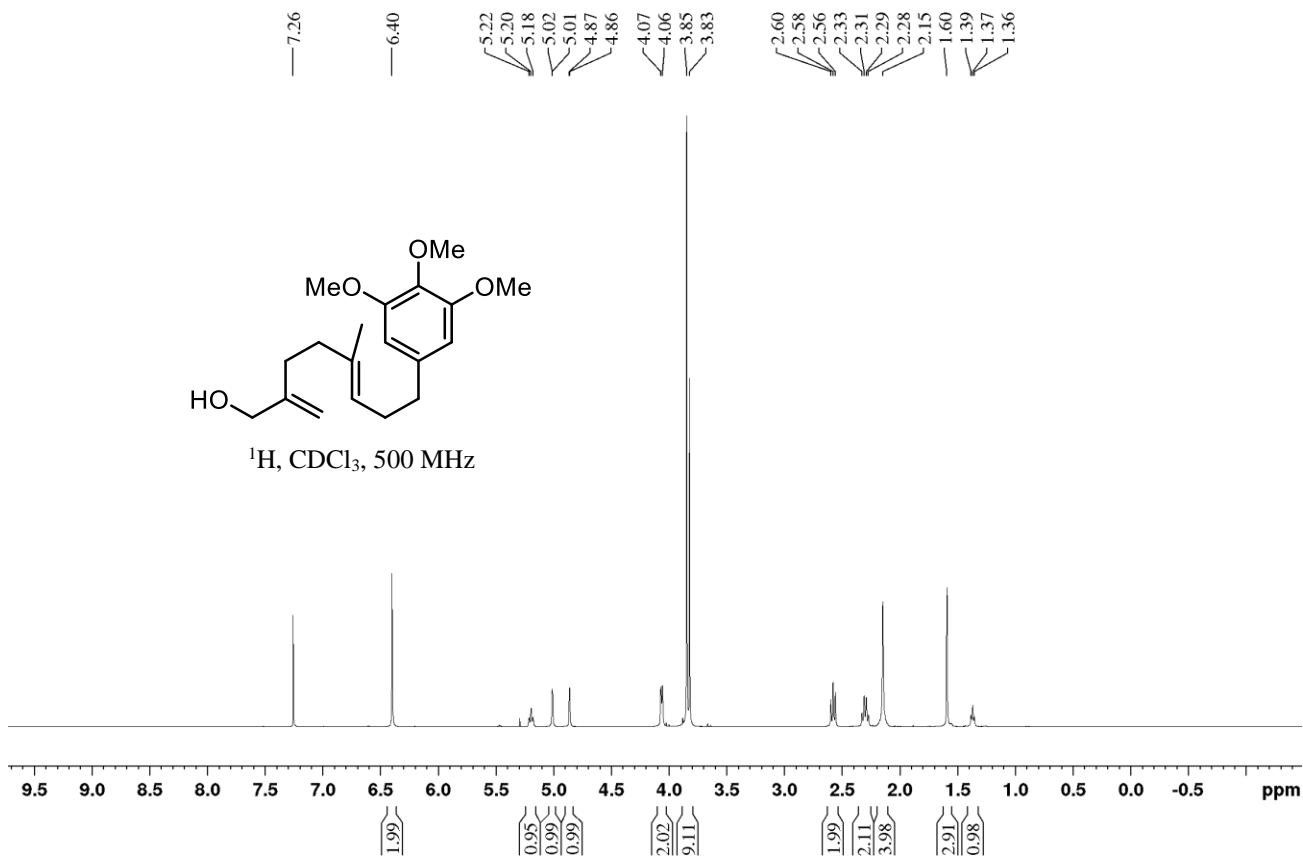


¹³C, CDCl₃, 125 MHz

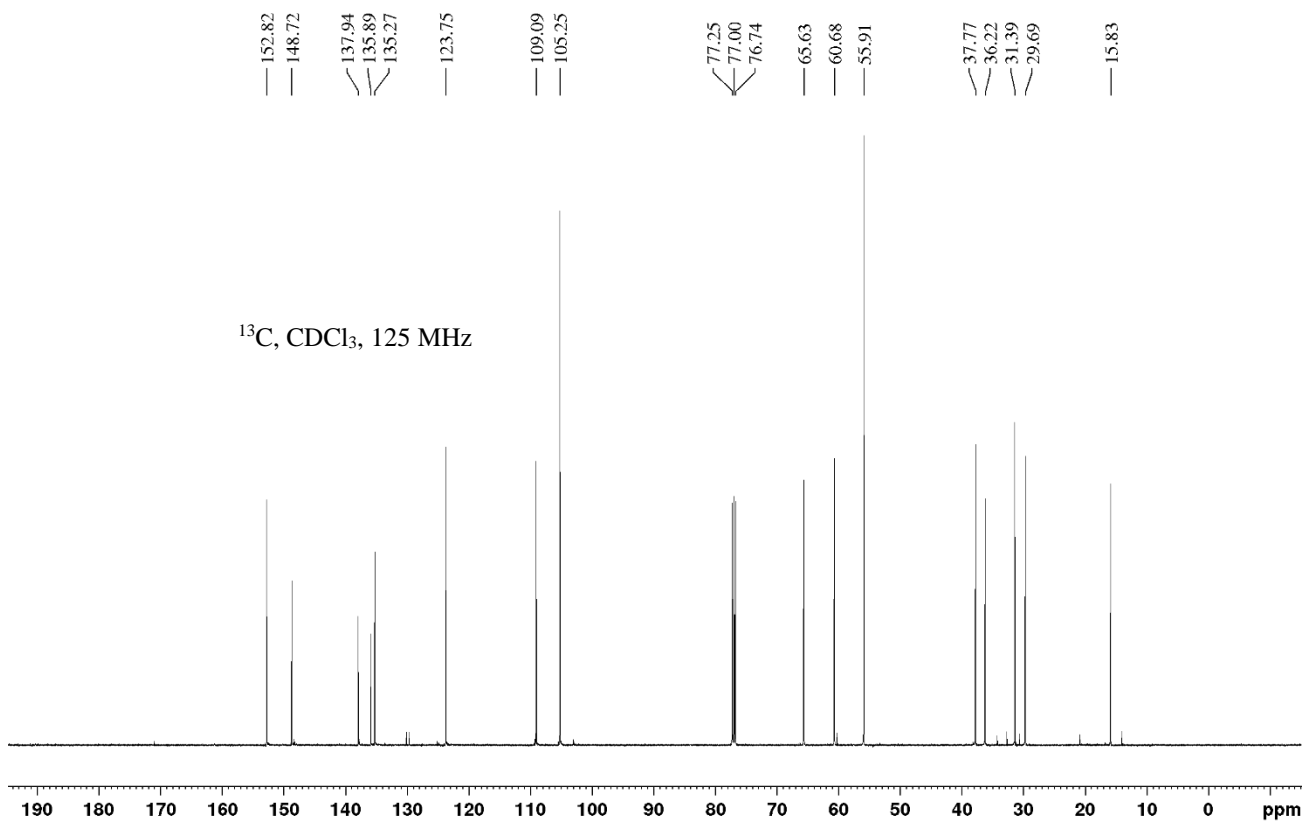


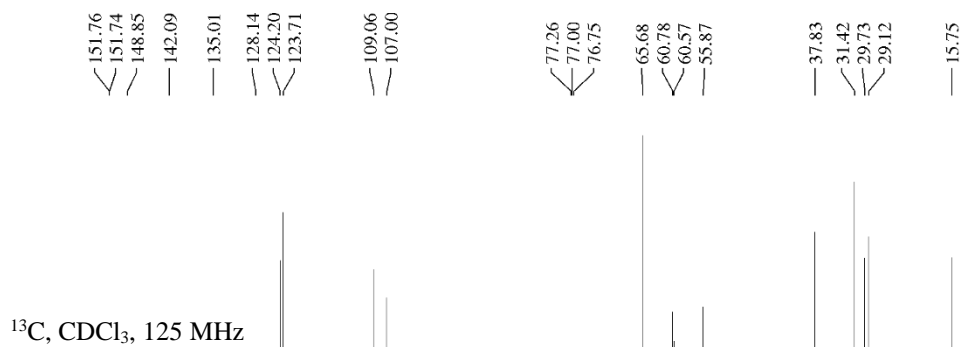
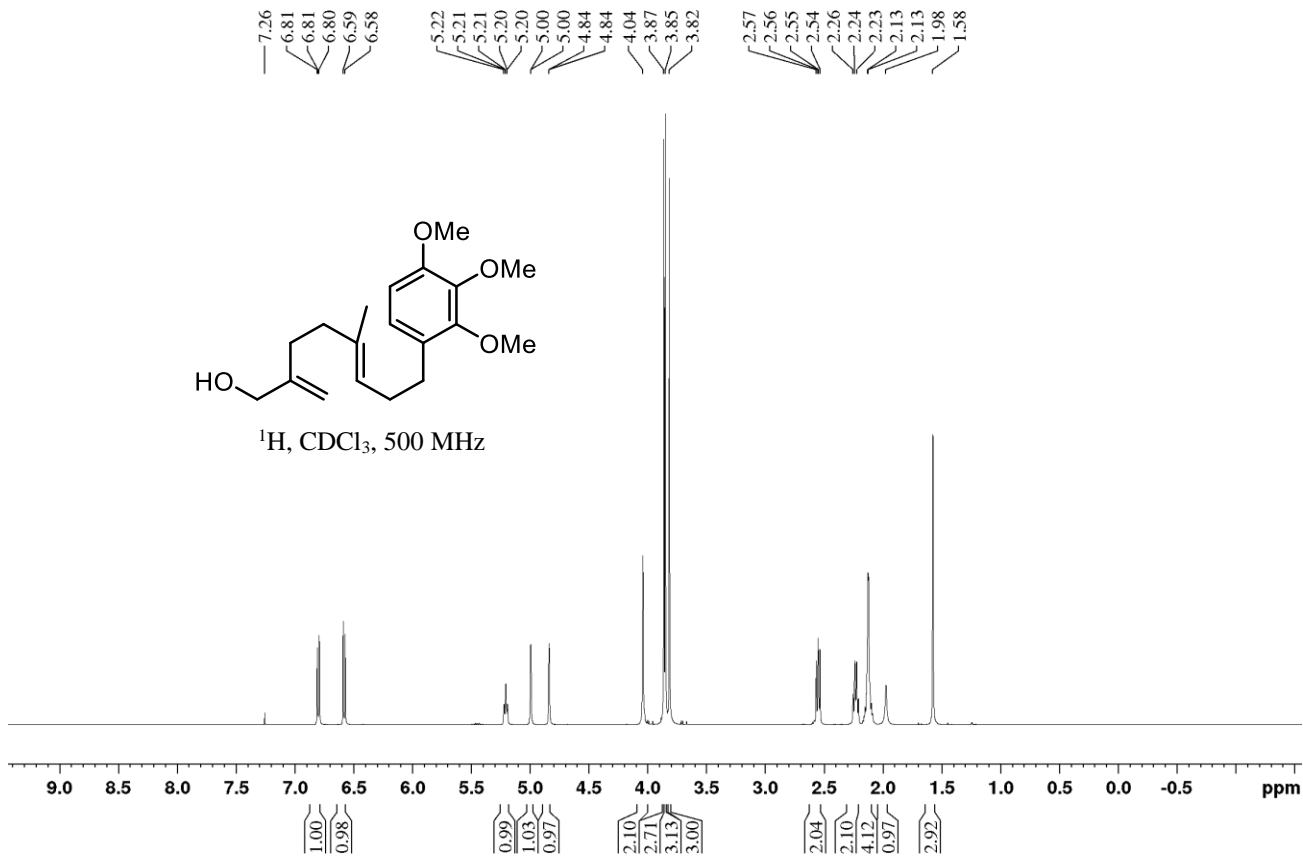
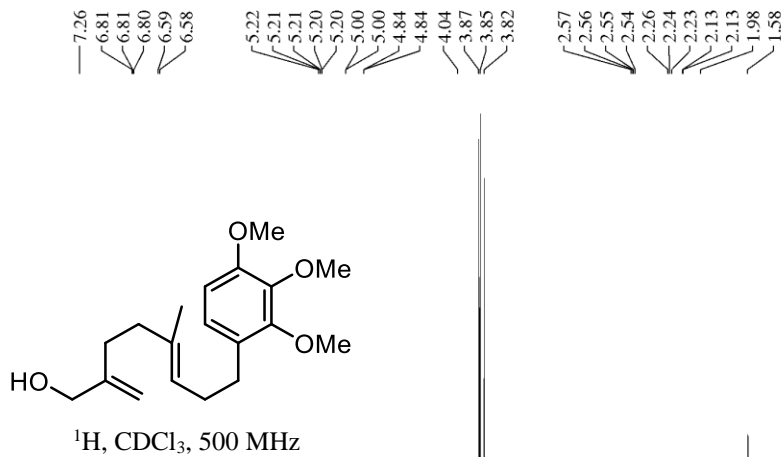


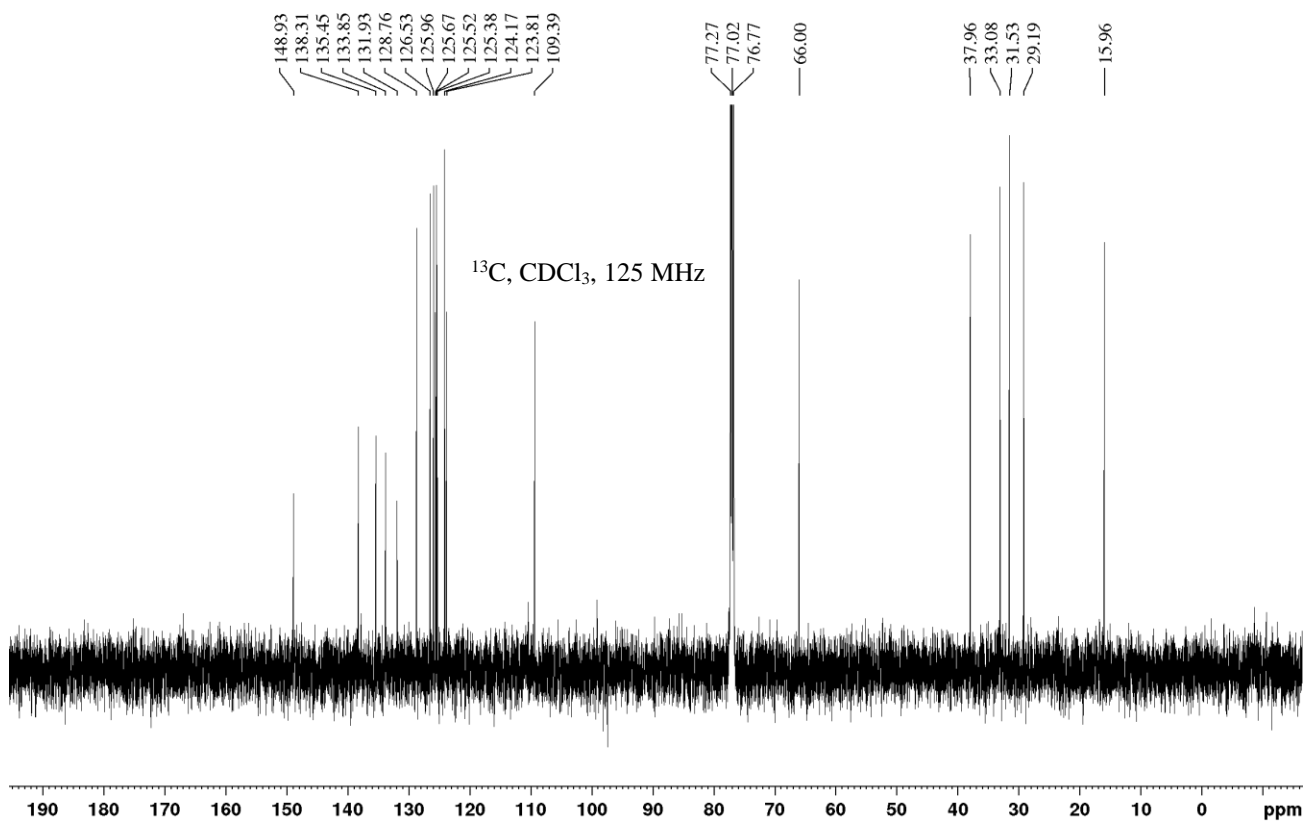
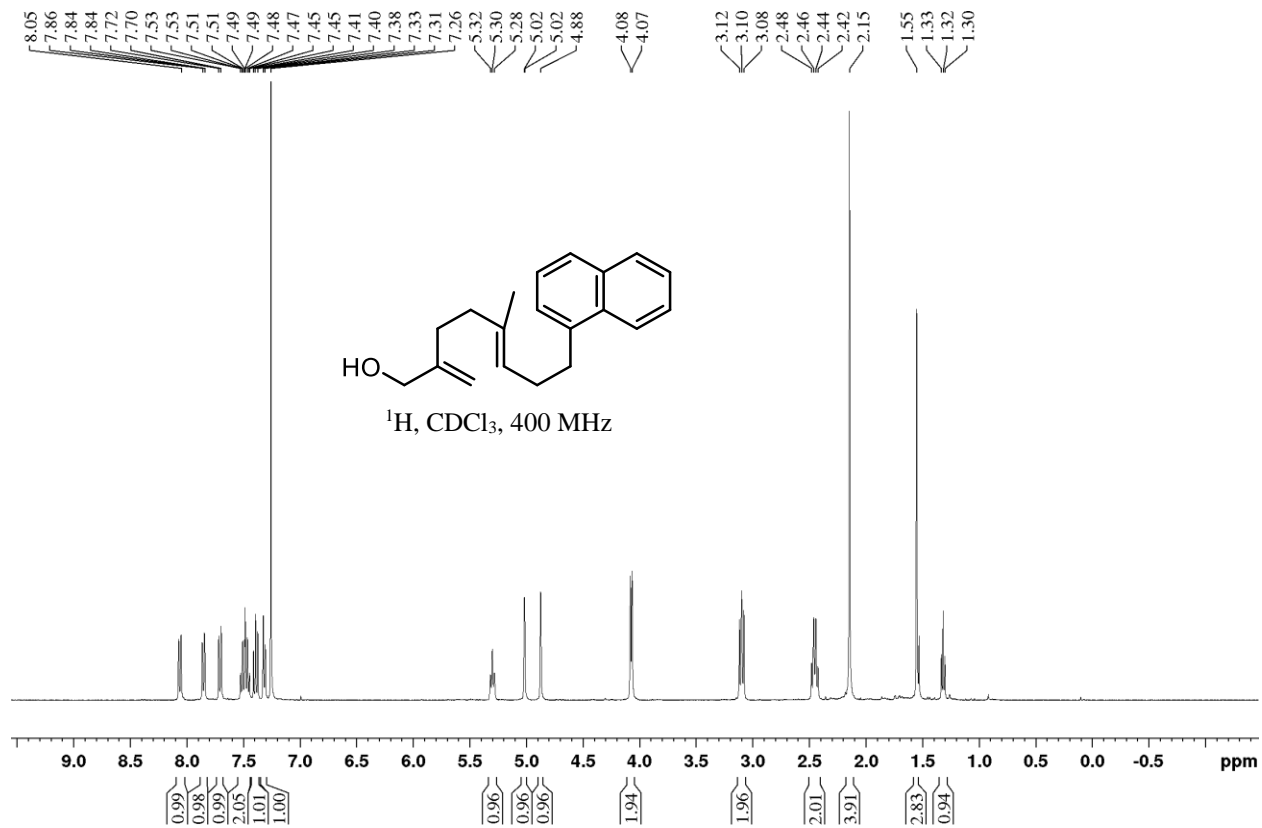
^1H , CDCl_3 , 500 MHz



^{13}C , CDCl_3 , 125 MHz

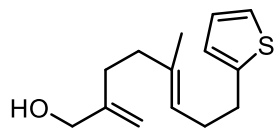




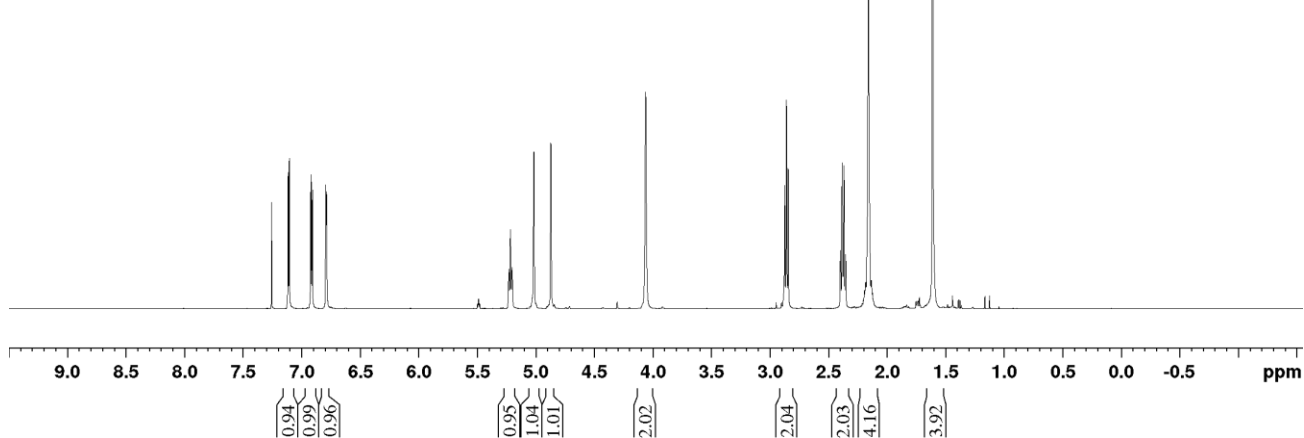


7.26
7.12
7.12
7.11
7.11
6.93
6.92
6.91
6.80
6.80
6.79
6.79
5.23
5.23
5.22
5.21
5.20
5.02
5.02
4.88
4.87
4.07

2.88
2.88
2.86
2.85
2.40
2.39
2.37
2.36
2.16
1.61



^1H , CDCl_3 , 500 MHz

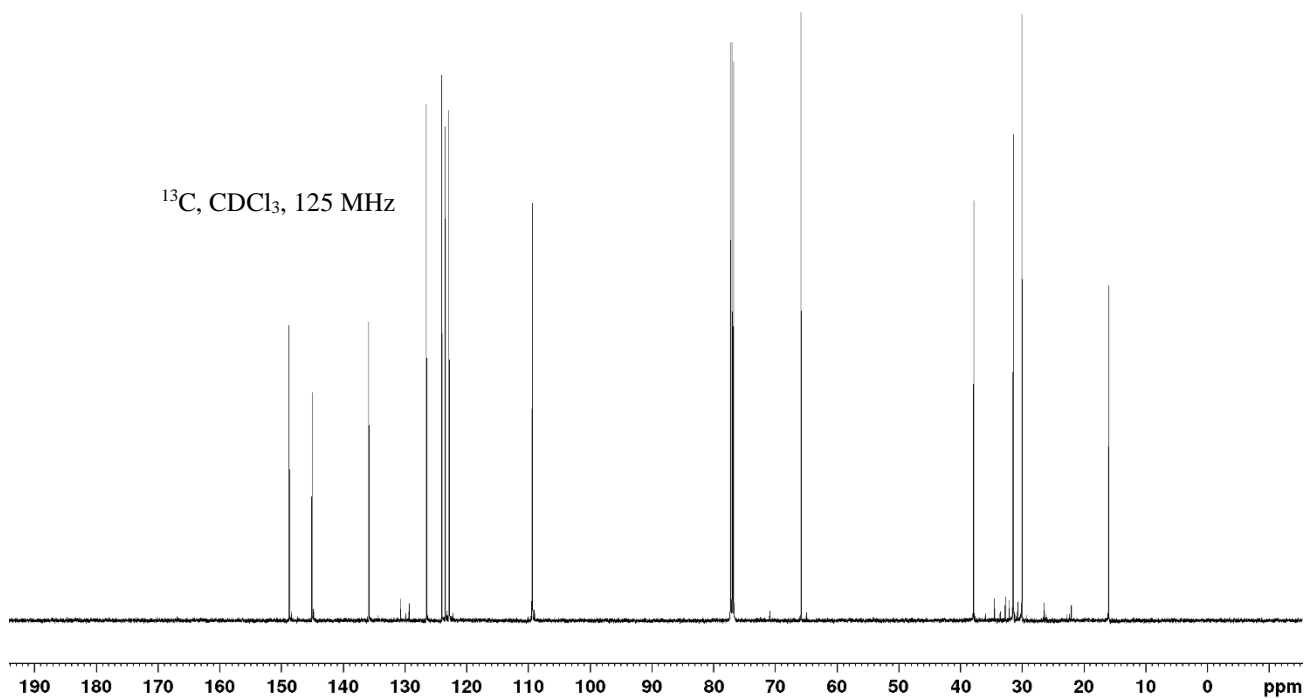


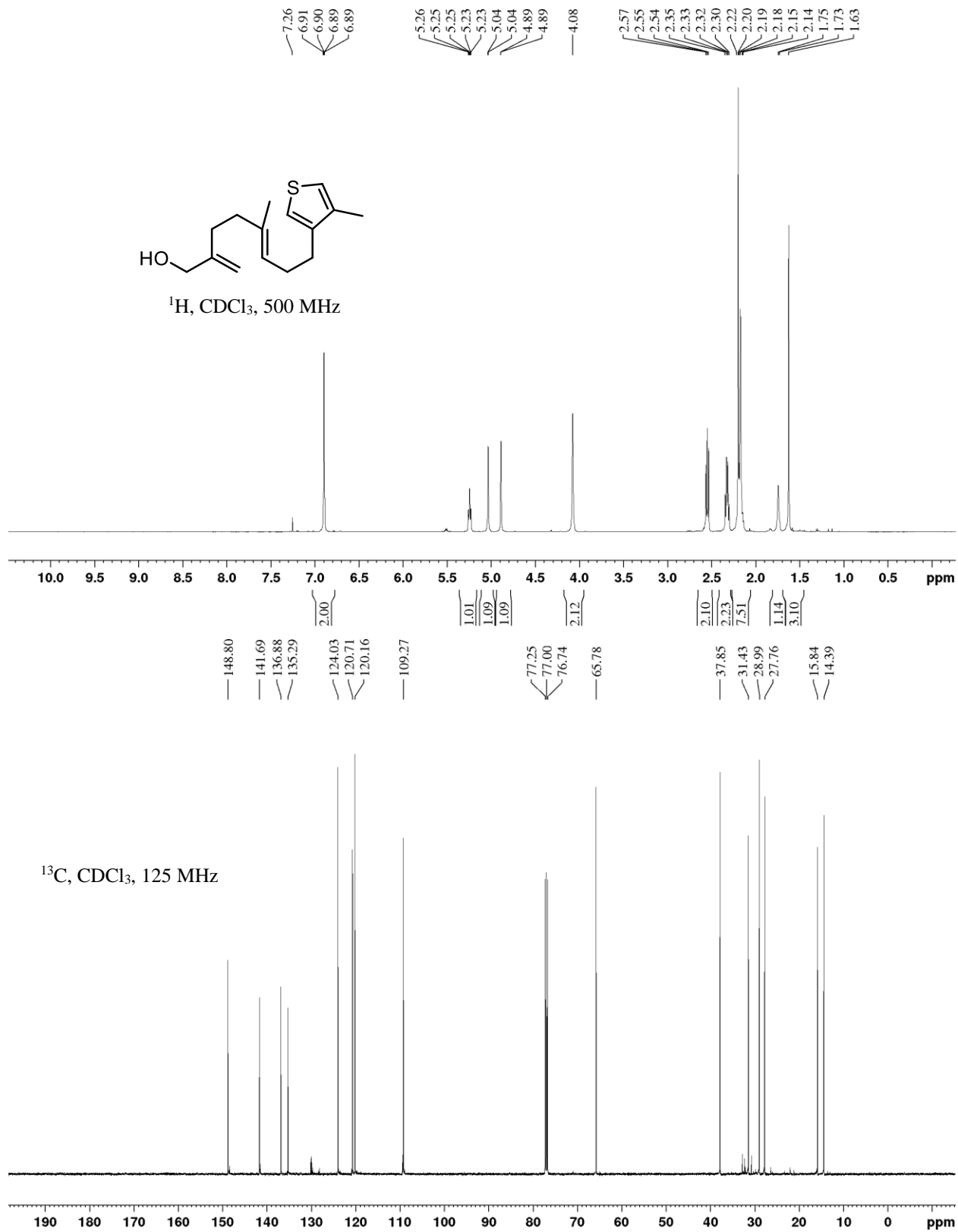
148.78
145.07
135.84
126.54
124.05
123.48
122.89
109.33

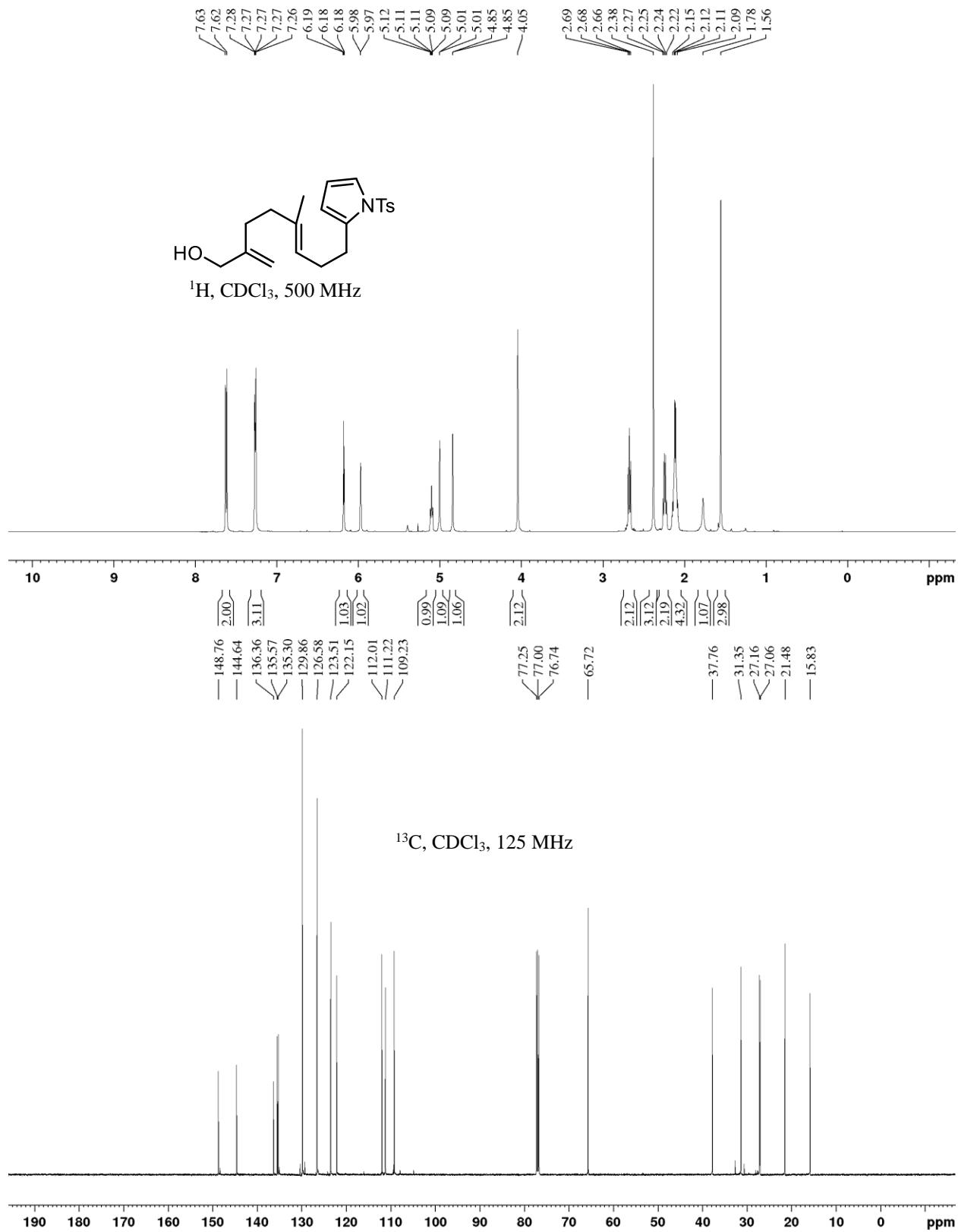
77.25
77.00
76.74
65.83

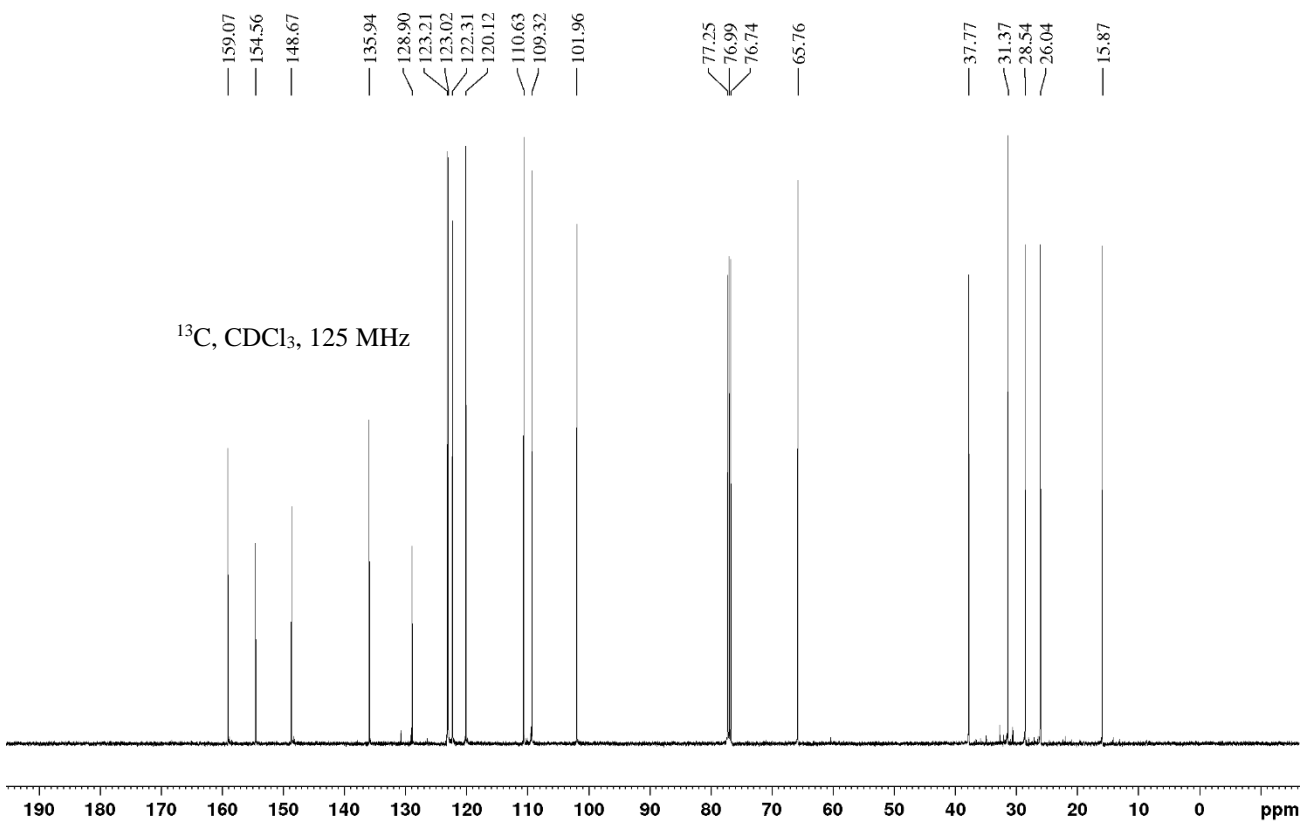
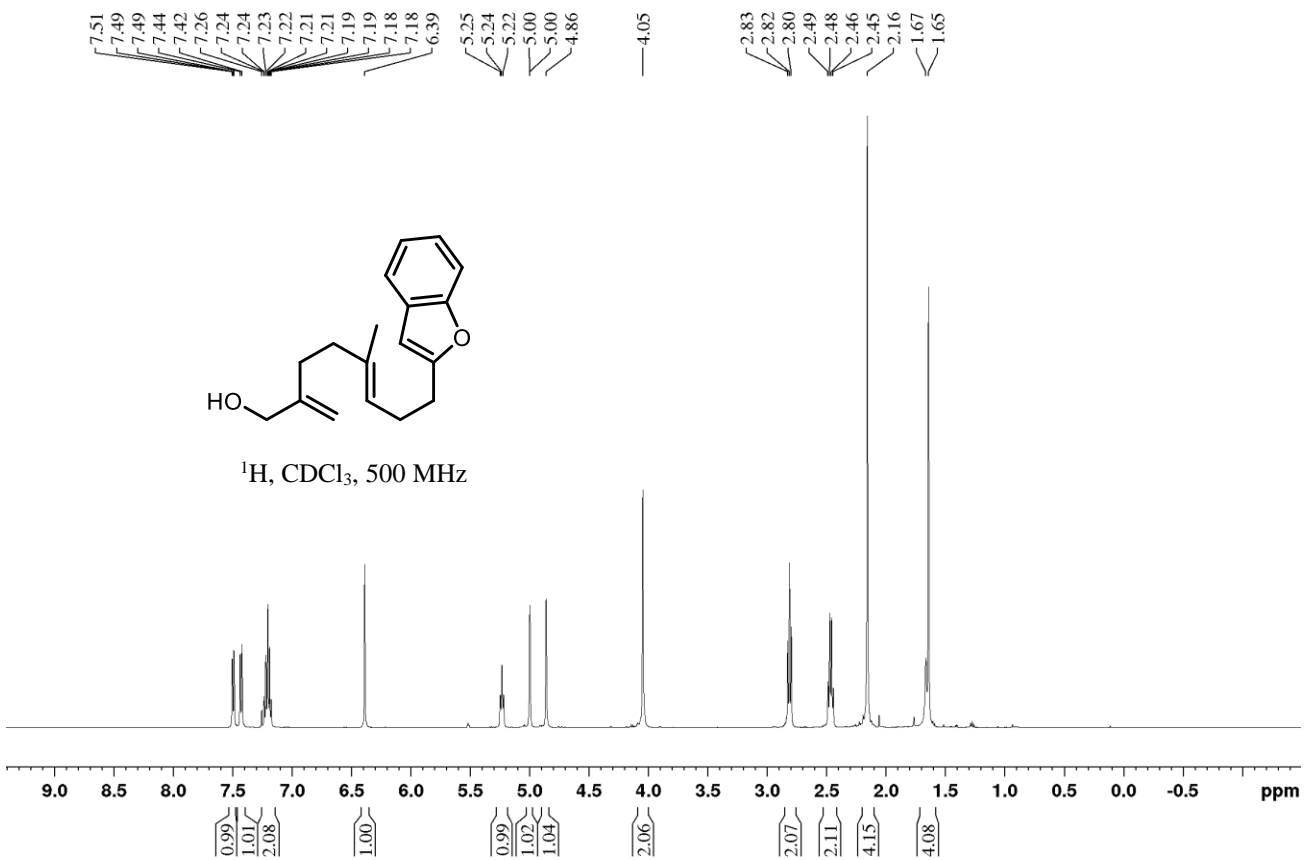
37.85
31.41
30.04
30.00
15.95

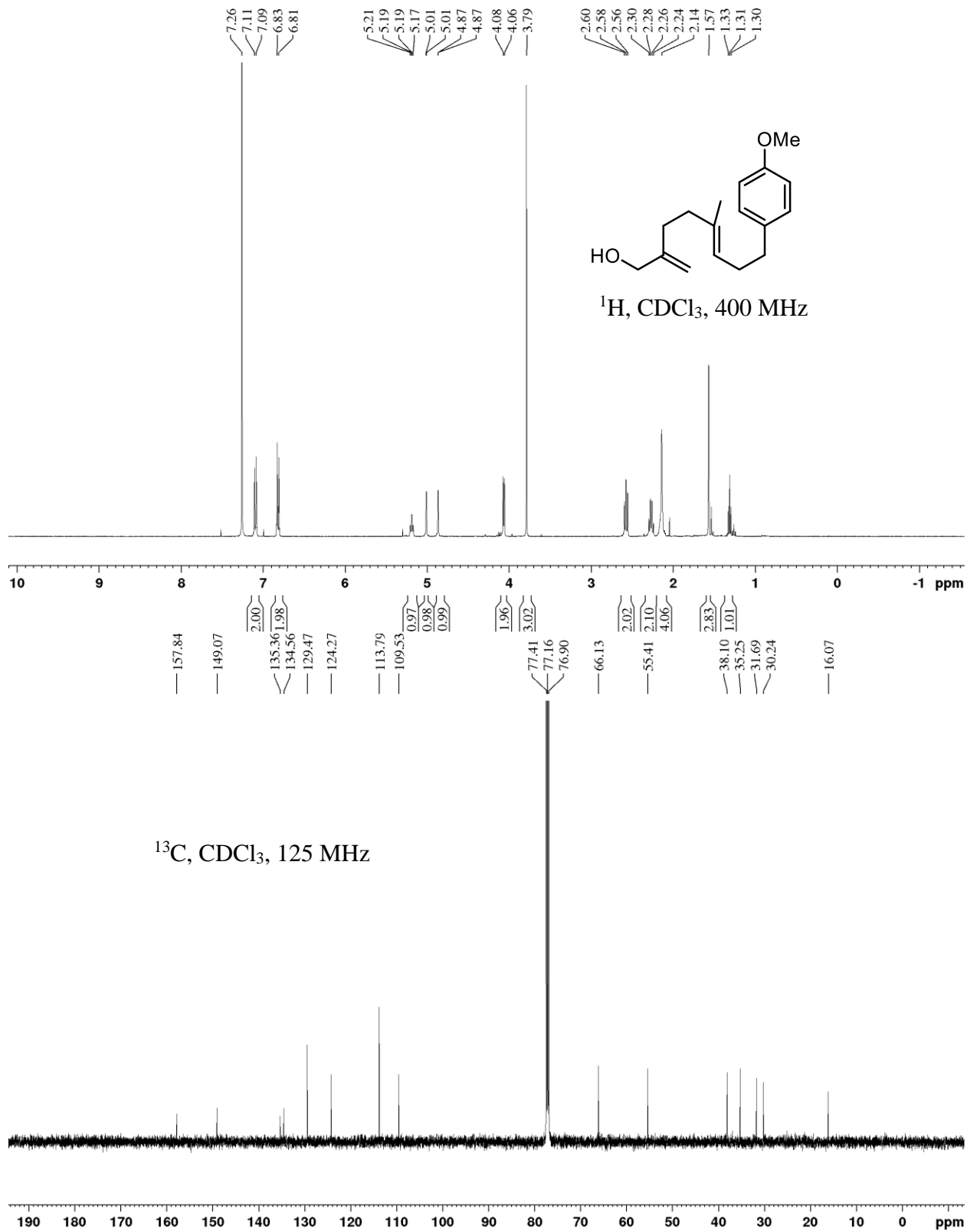
^{13}C , CDCl_3 , 125 MHz

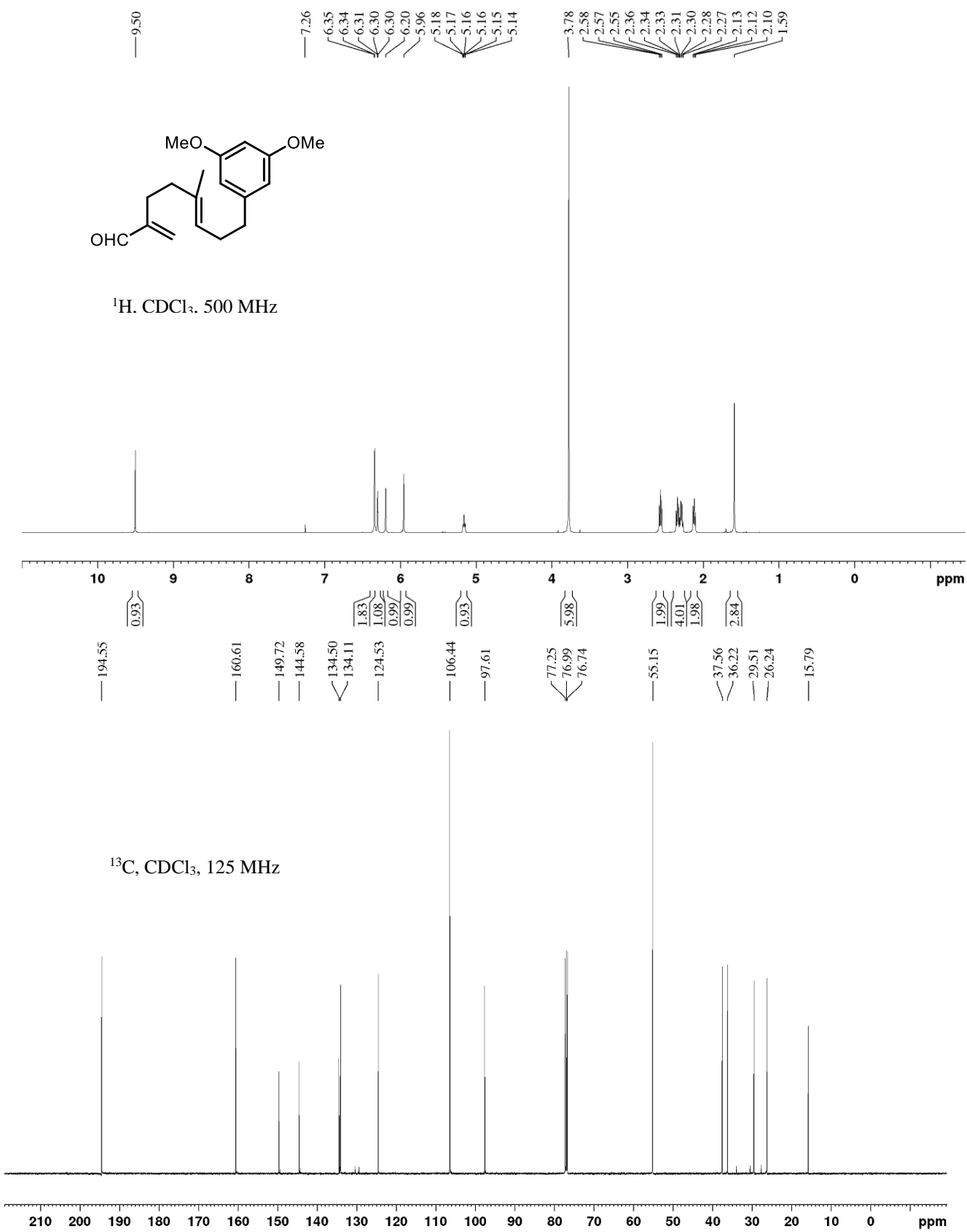


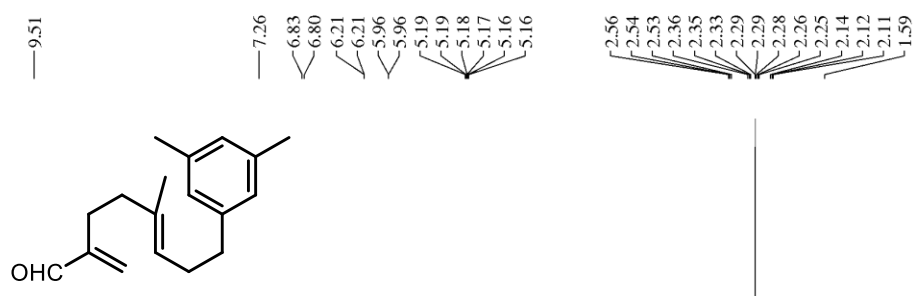




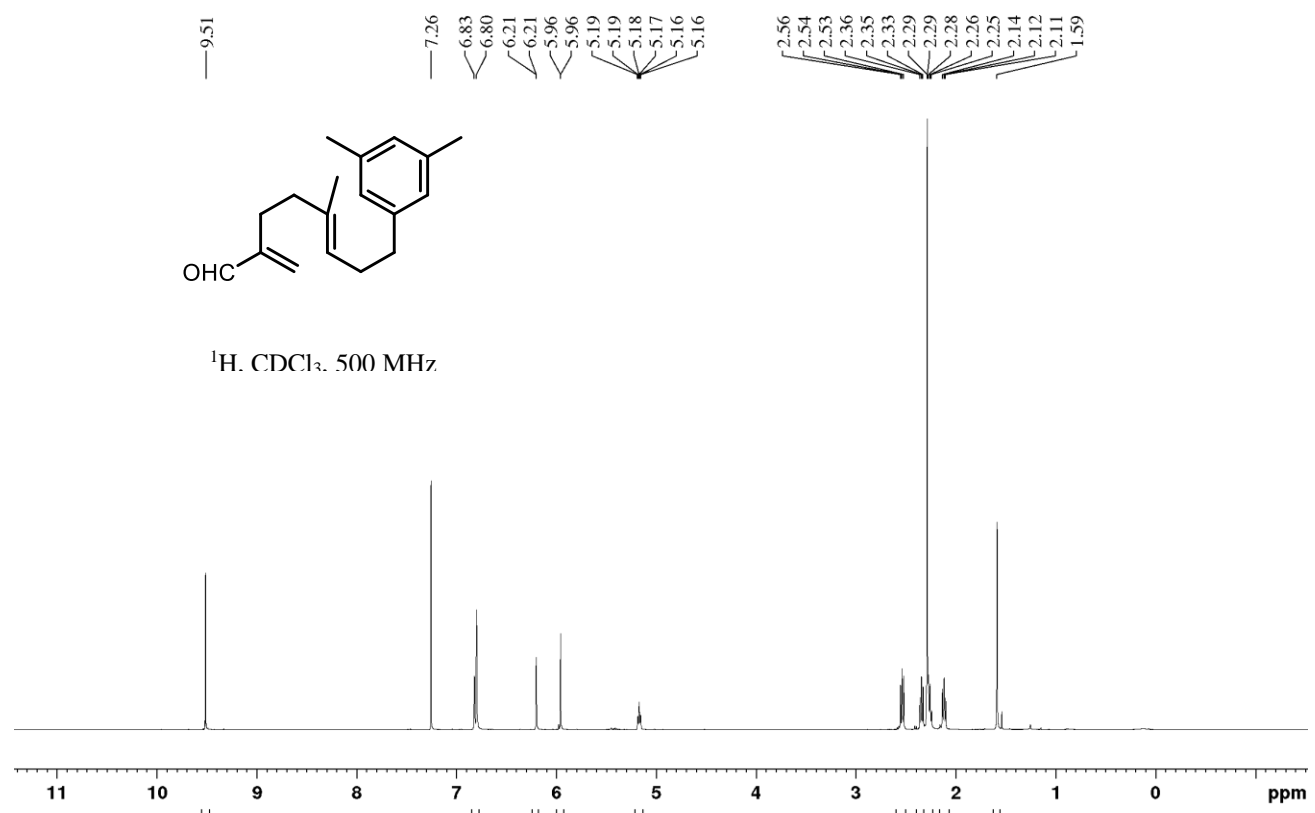




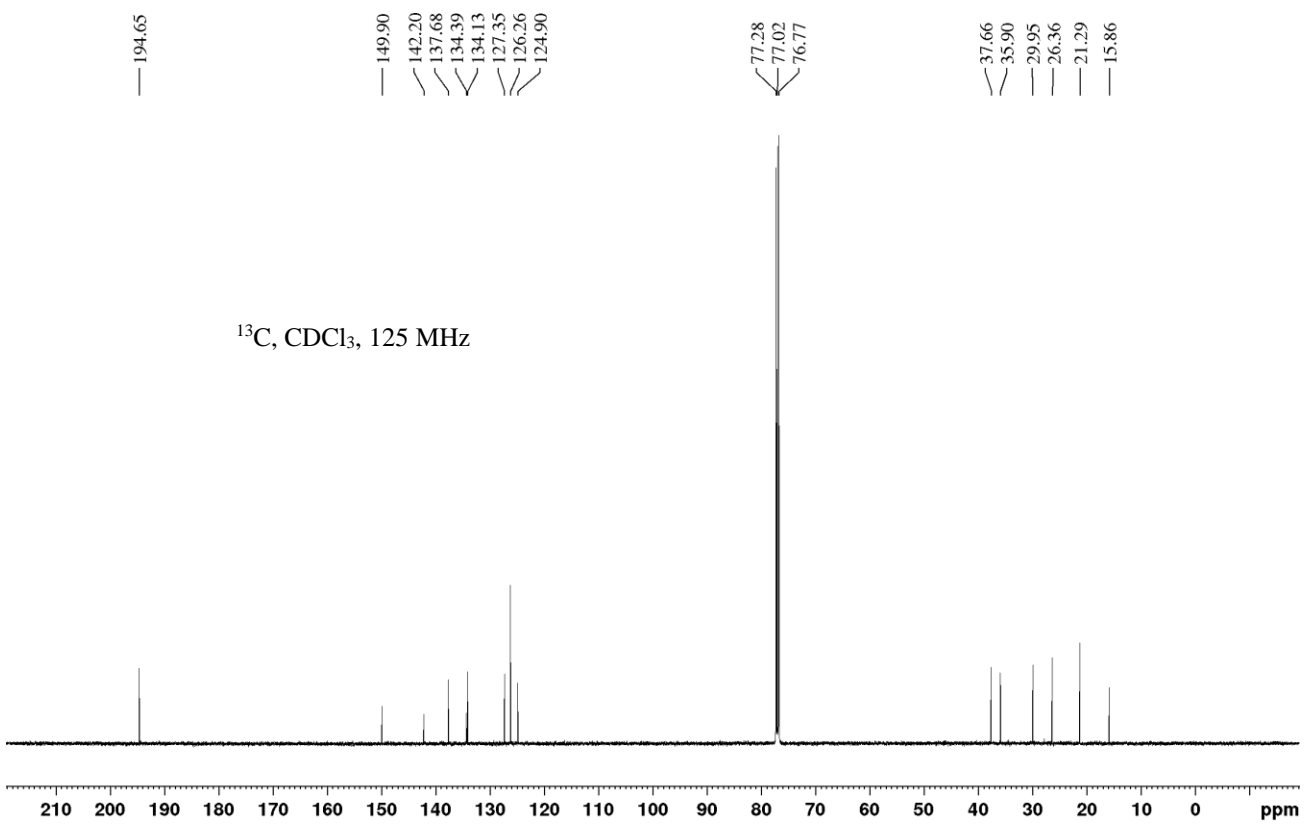


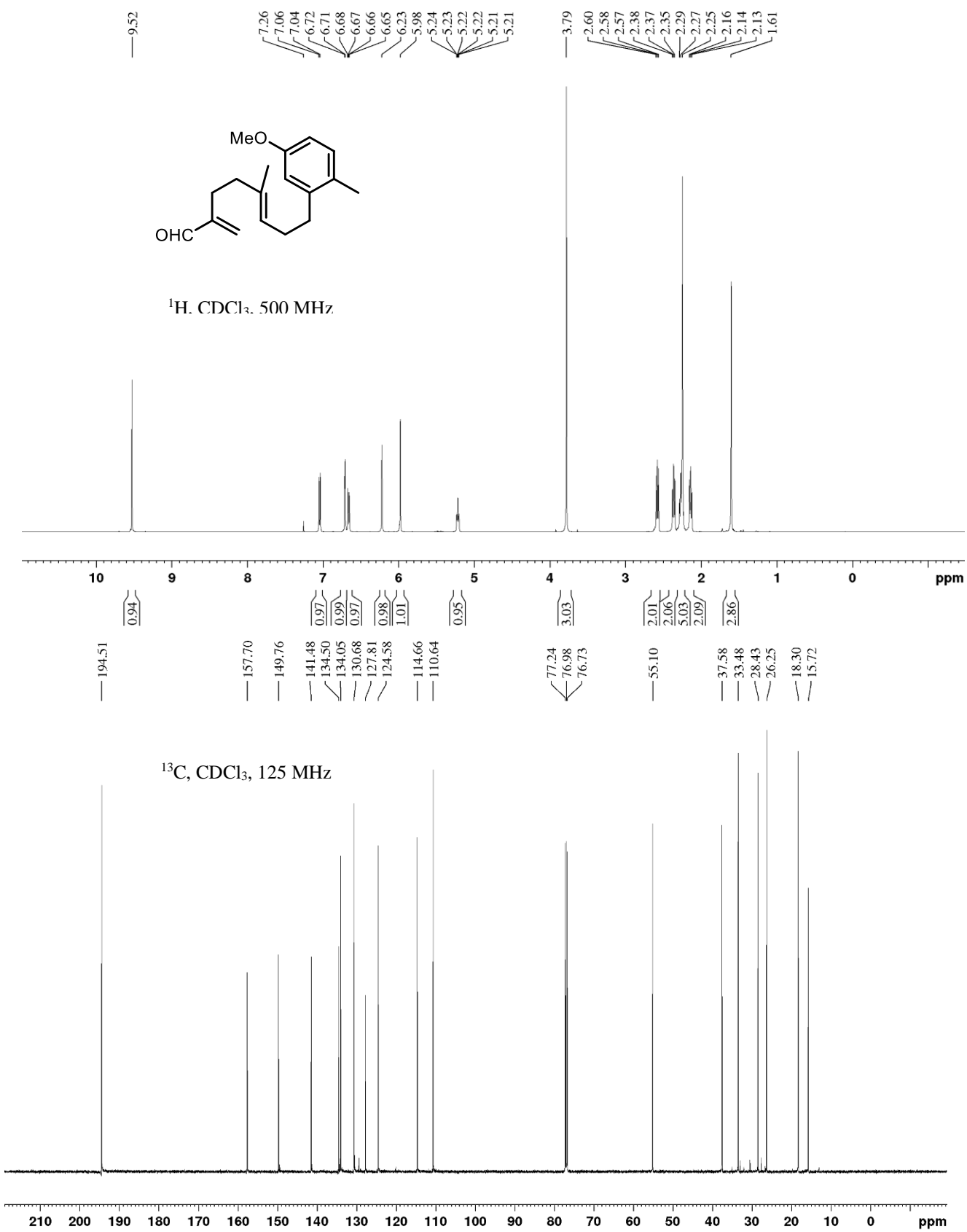


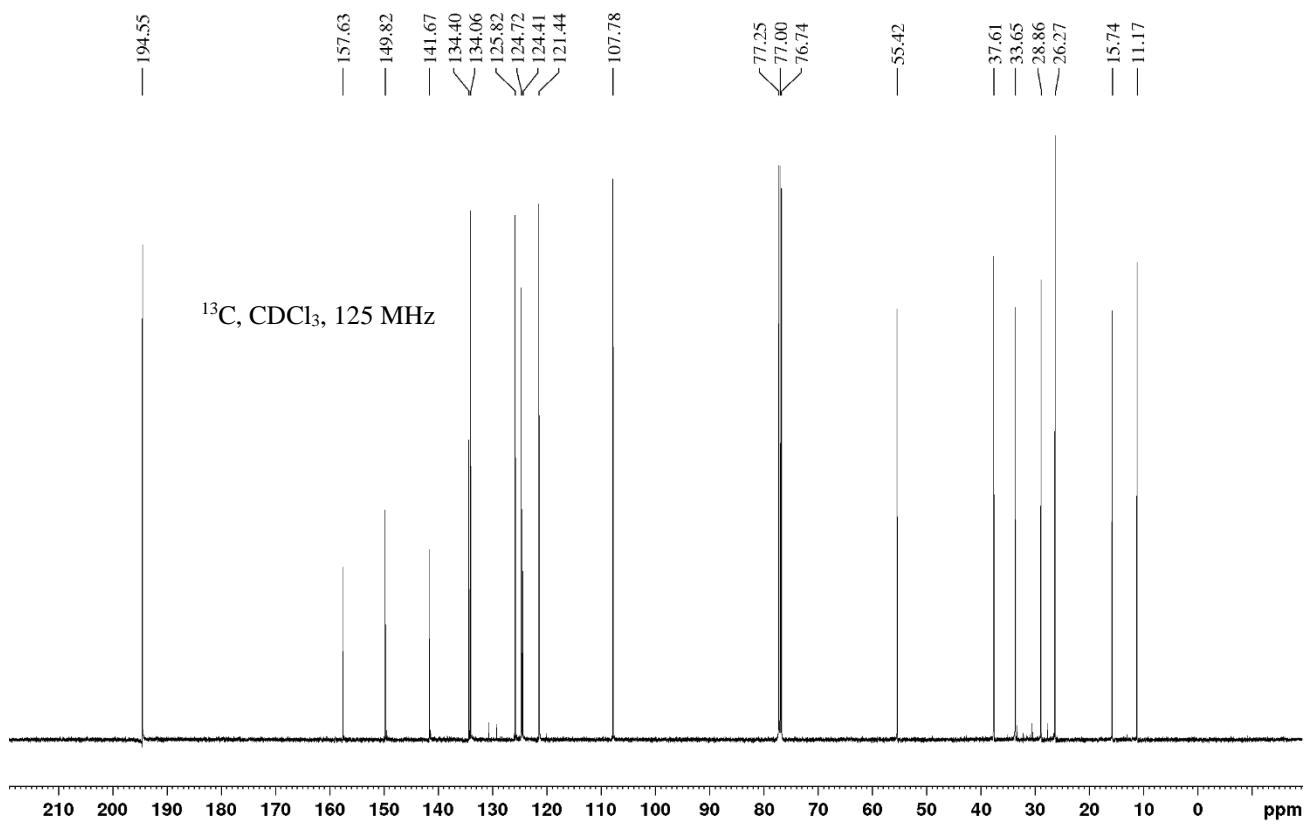
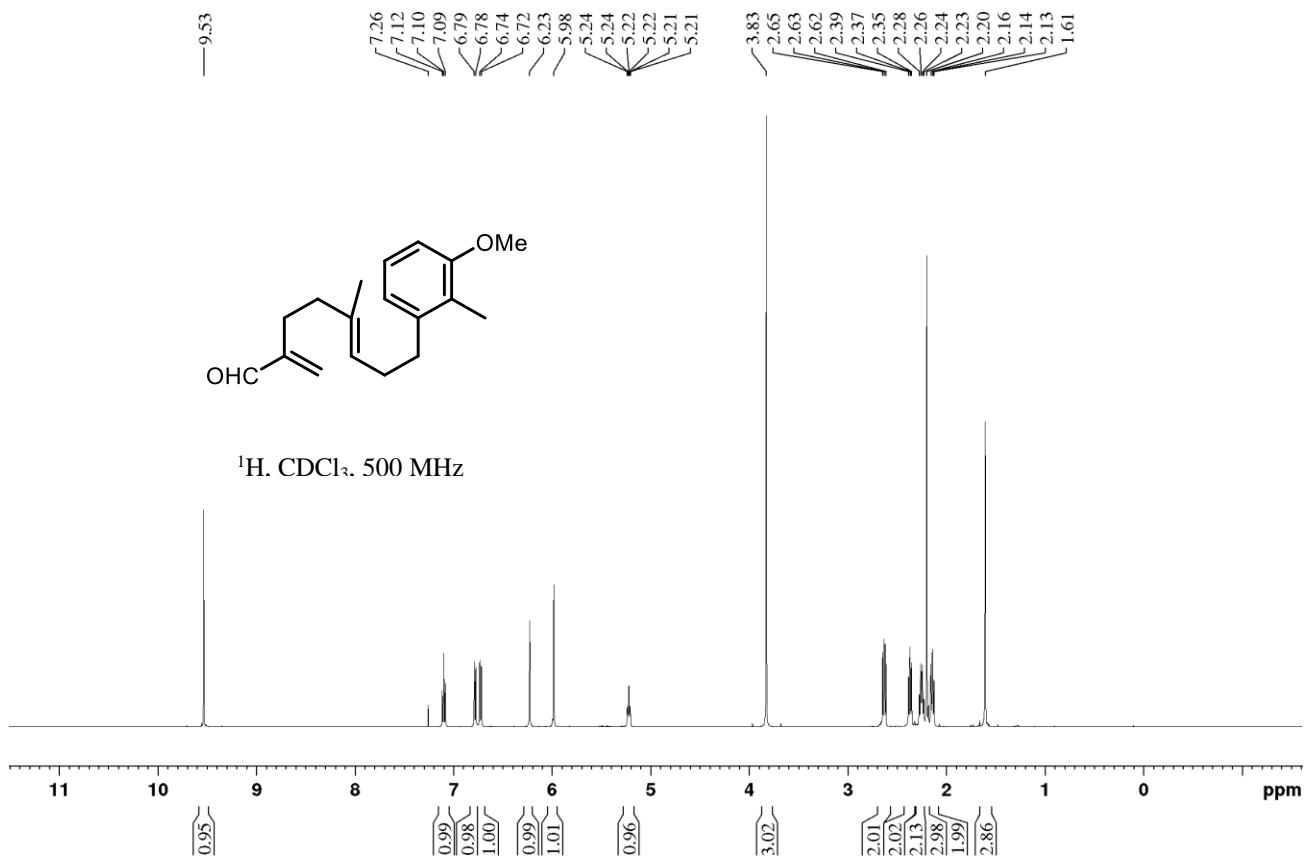
^1H , CDCl_3 , 500 MHz

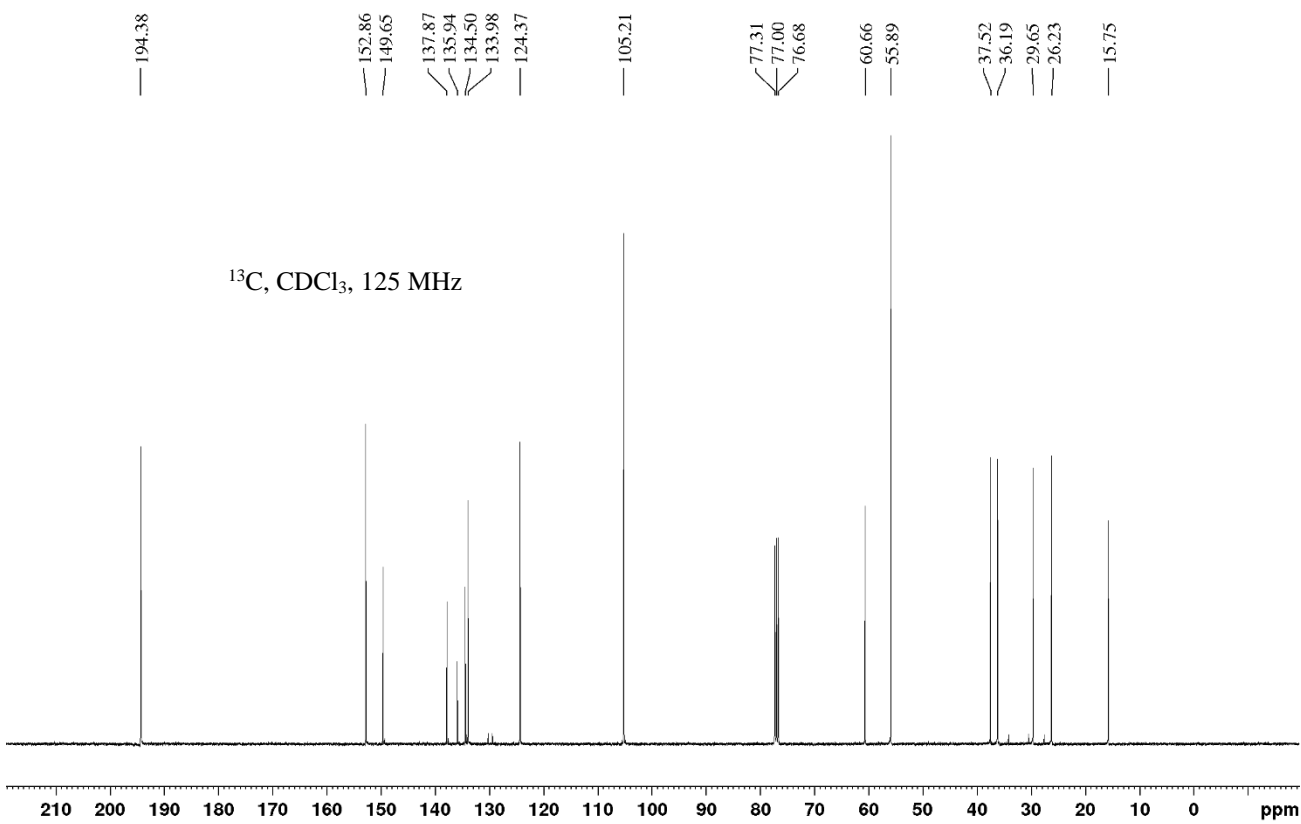
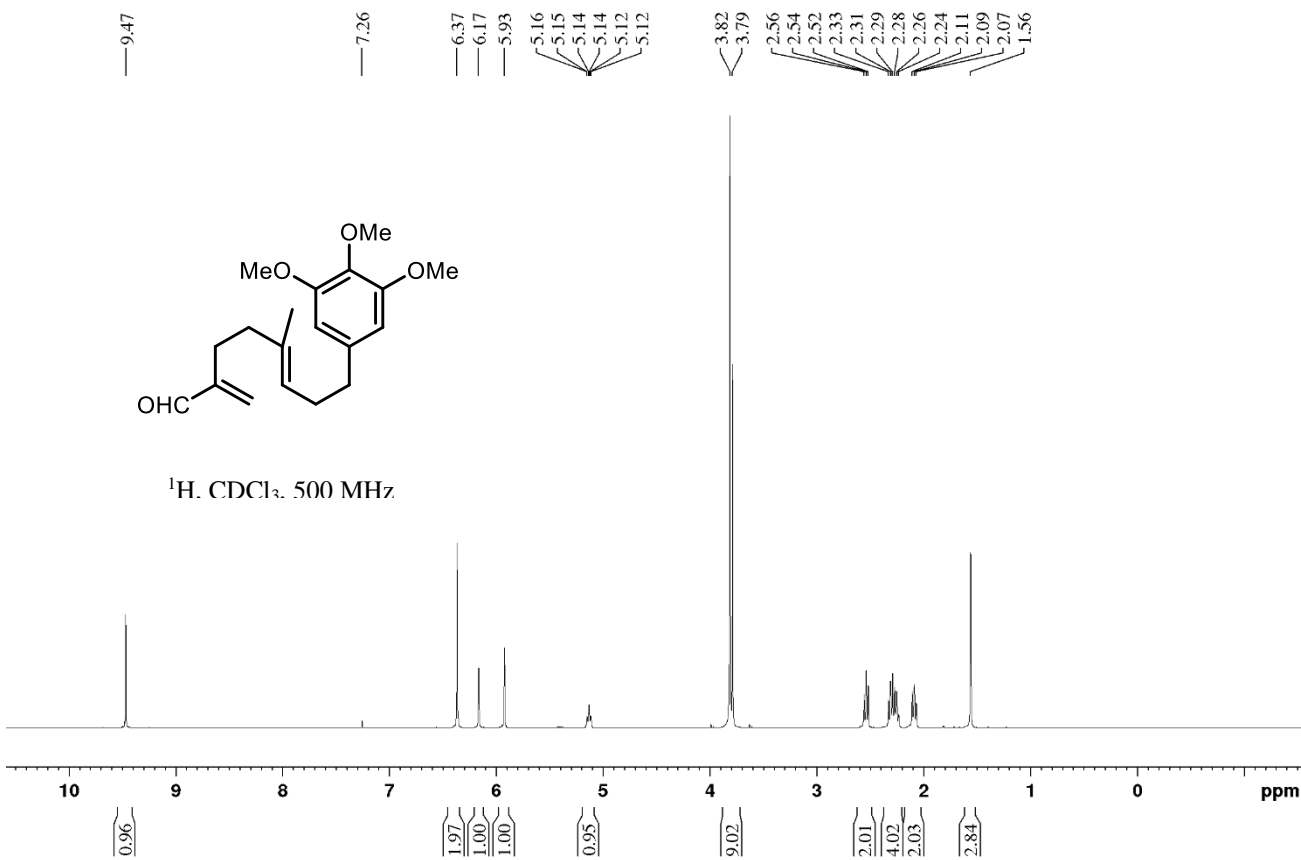


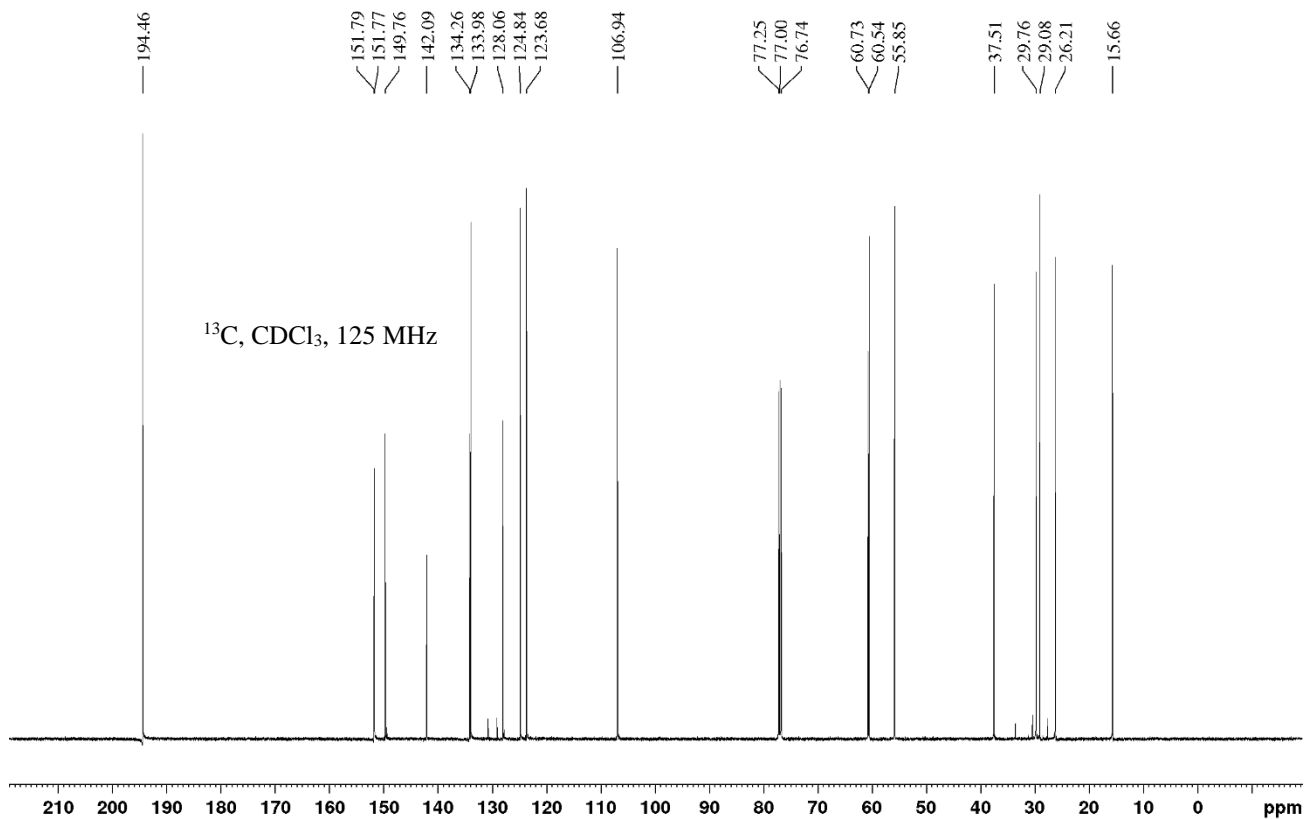
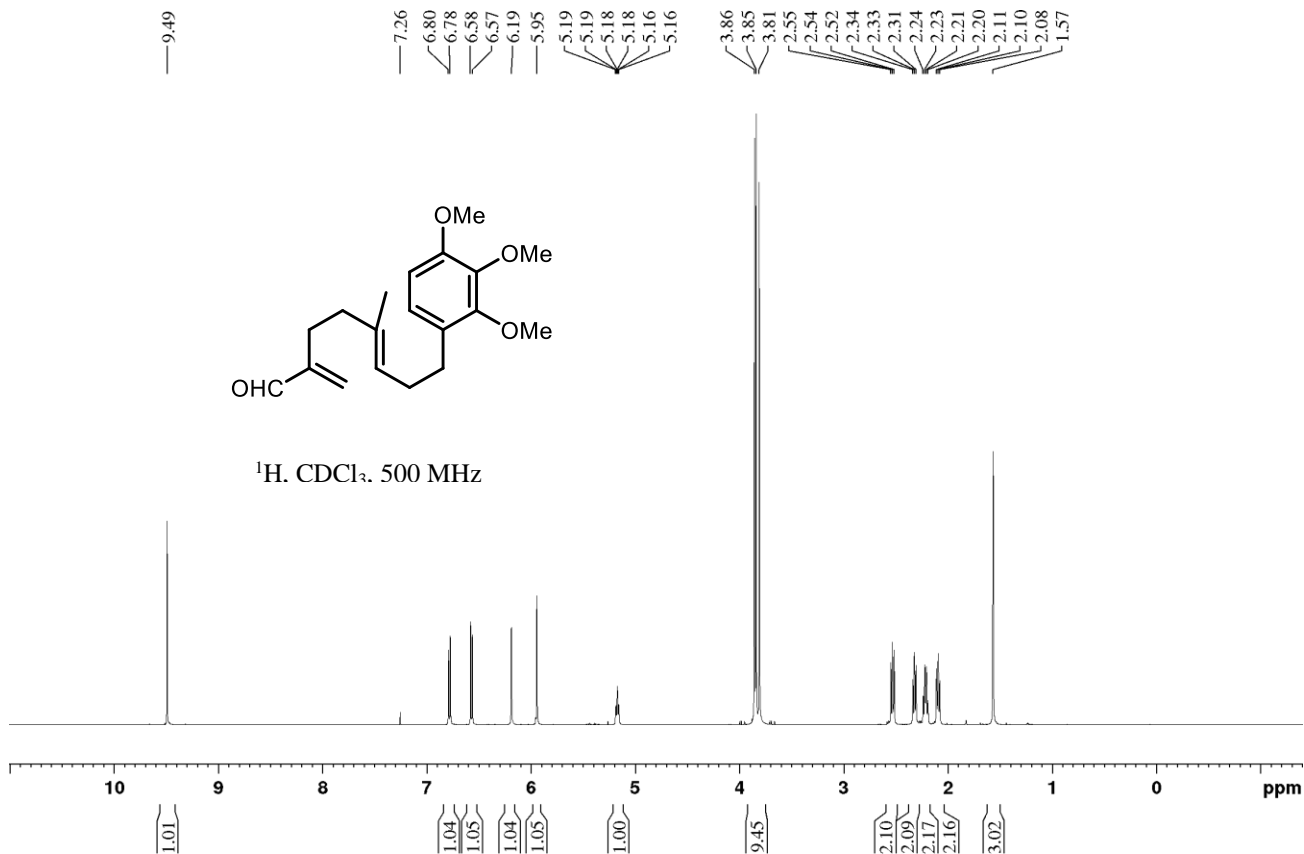
^{13}C , CDCl_3 , 125 MHz

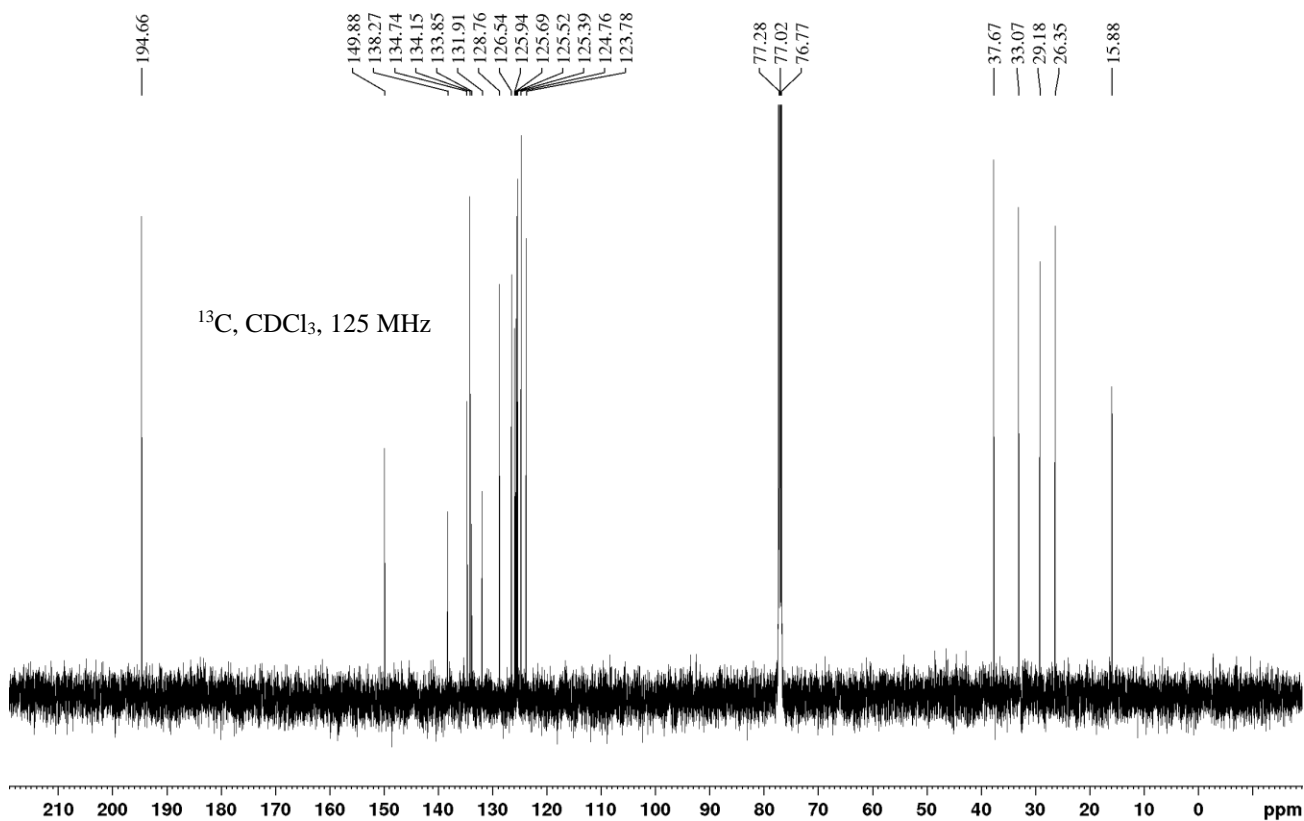
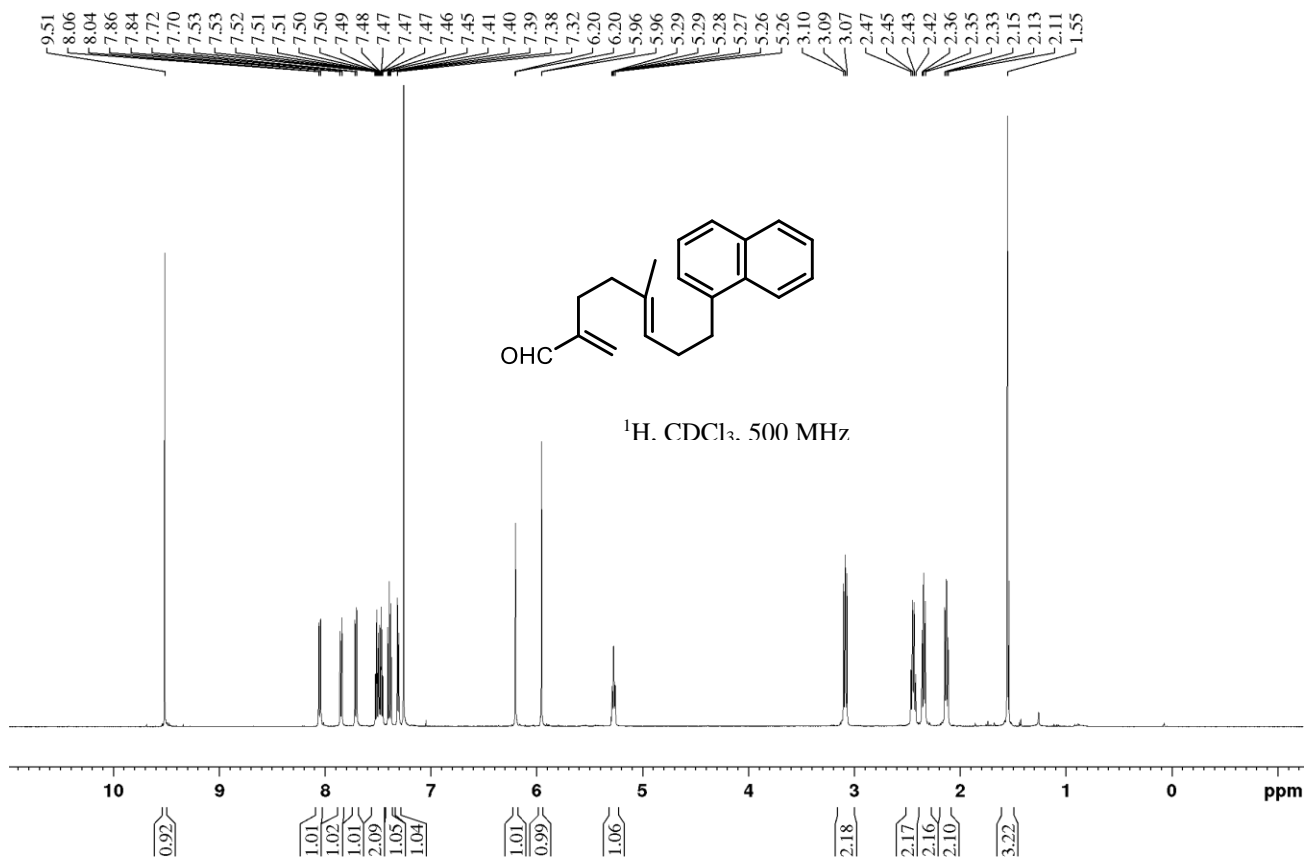


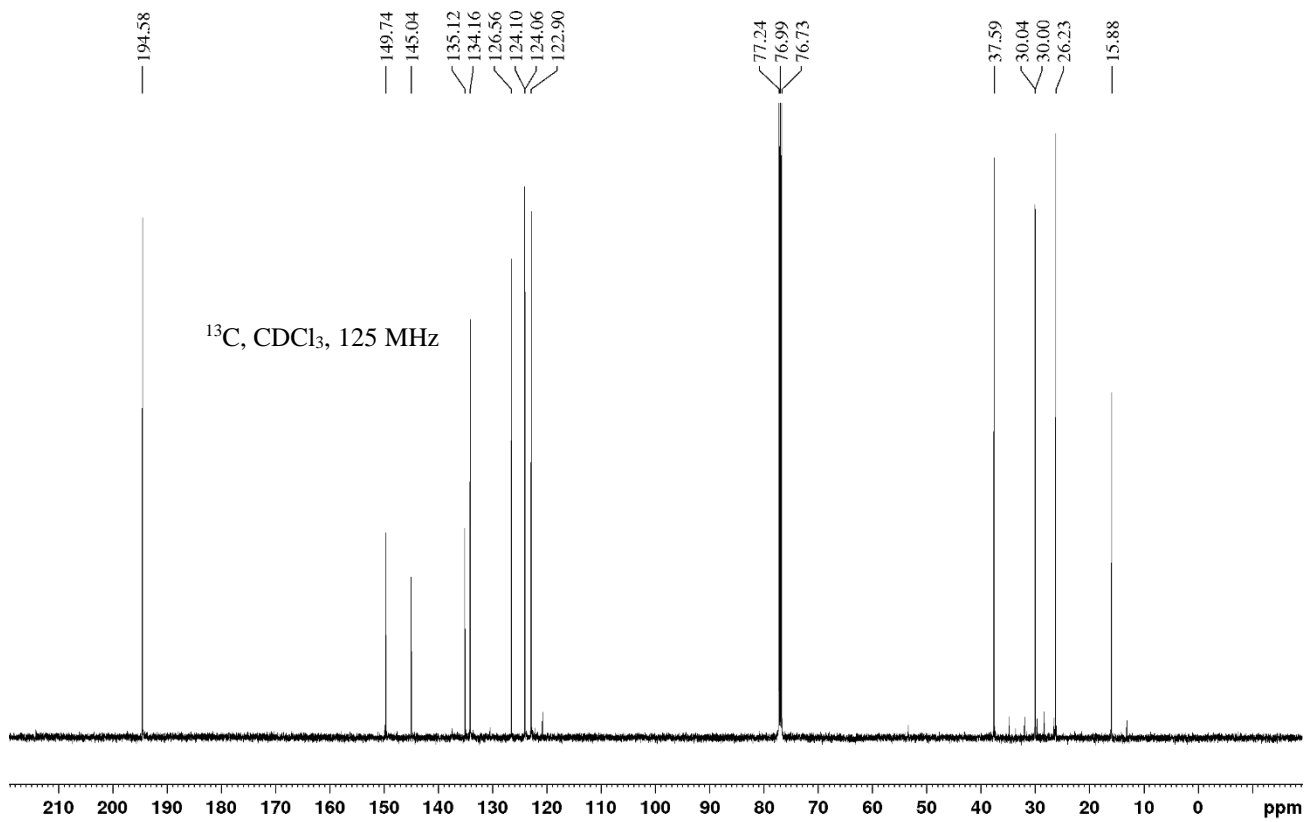
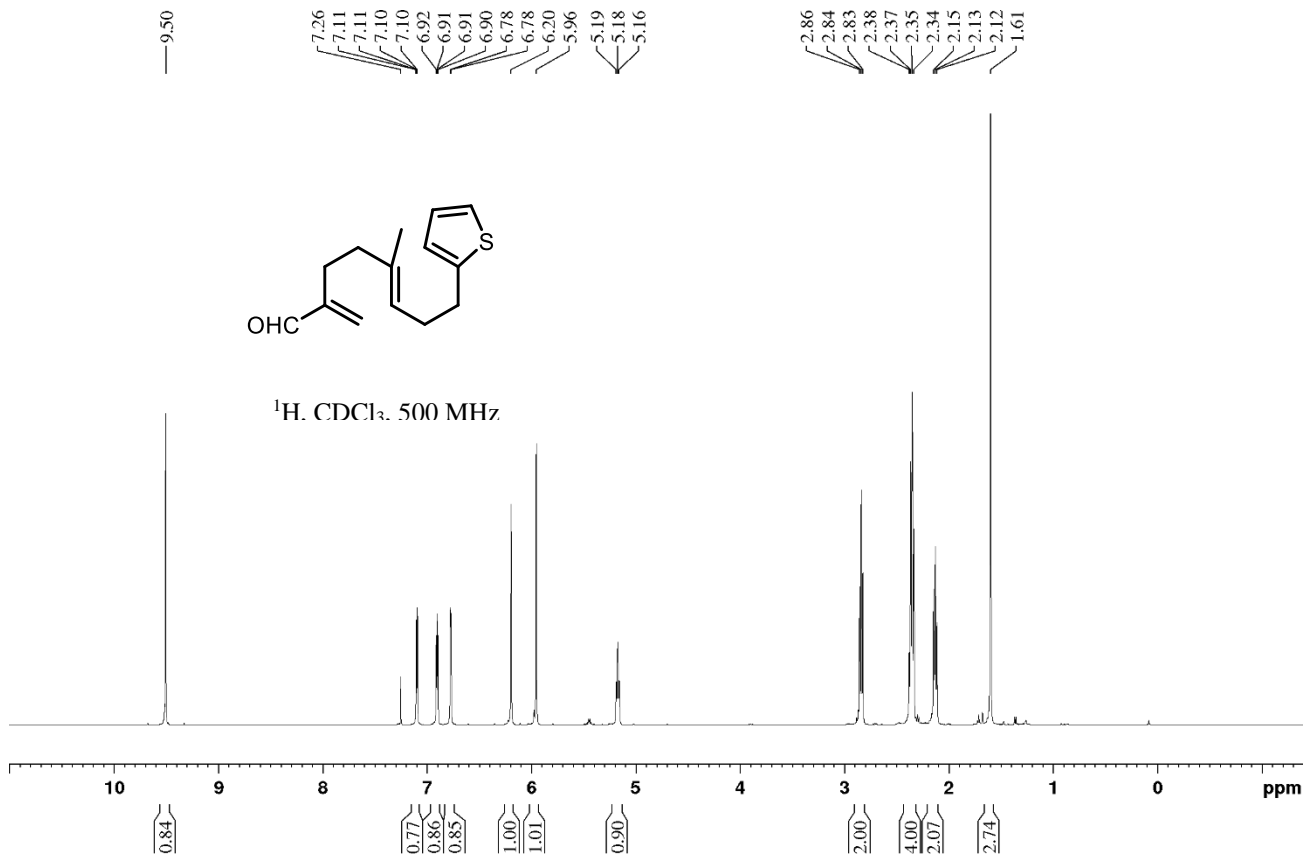


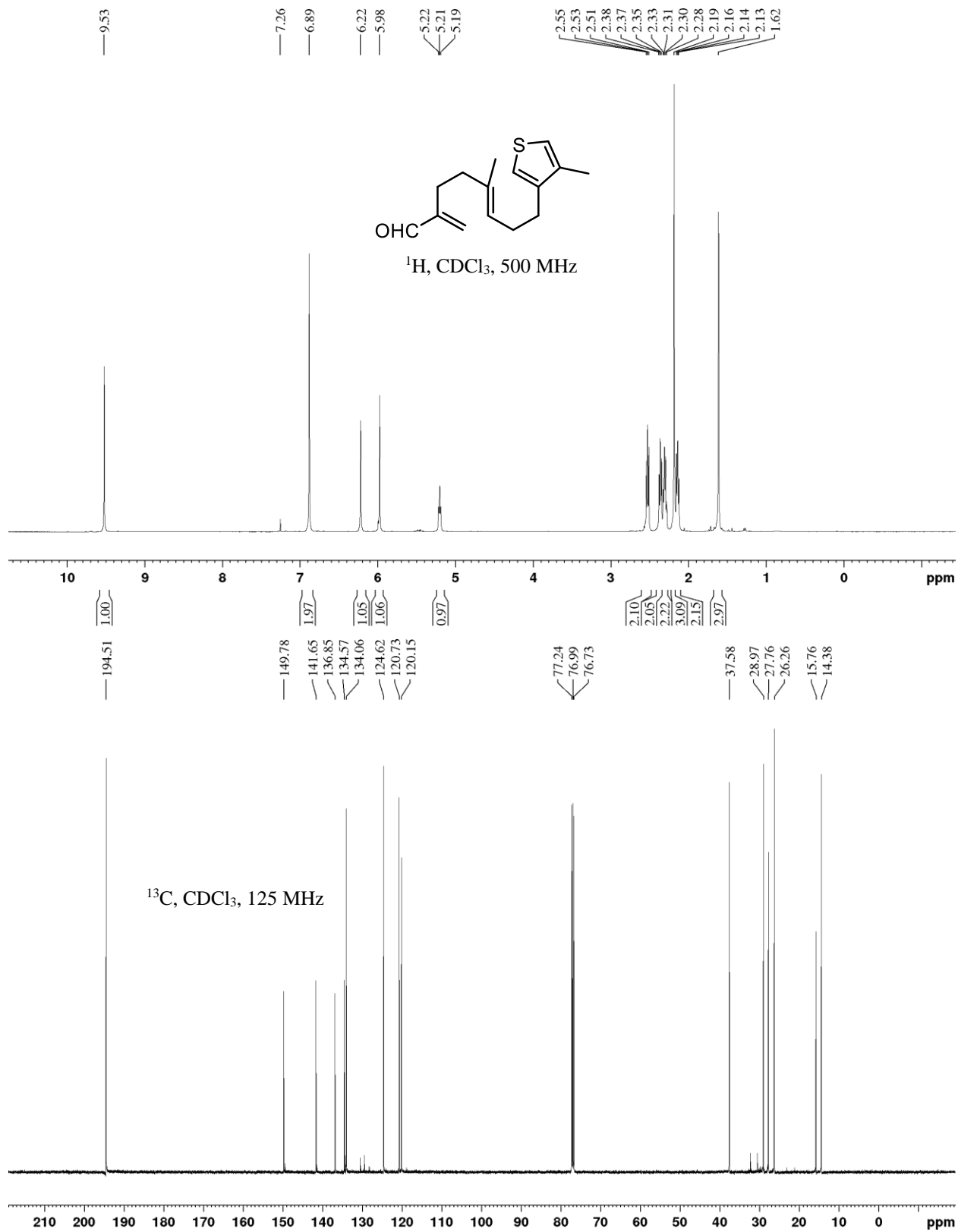


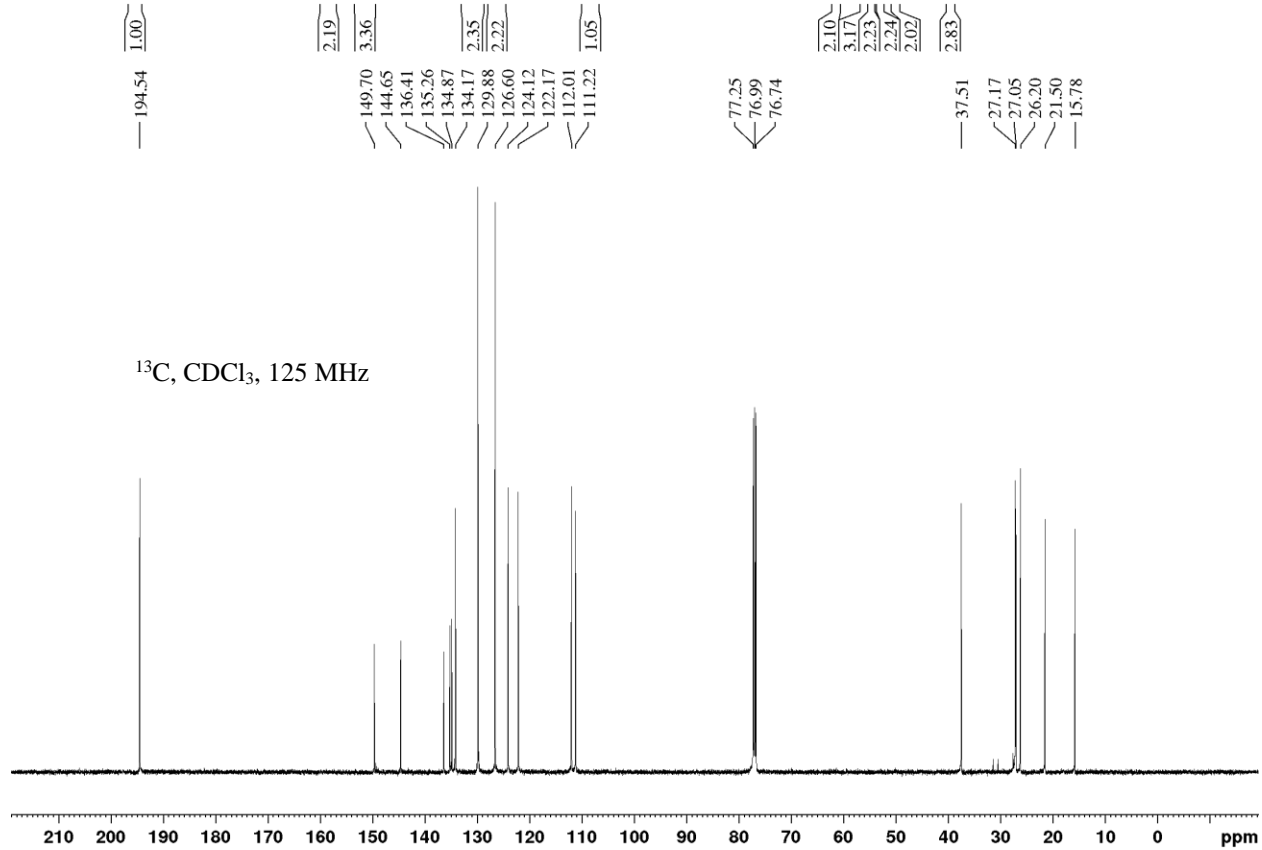
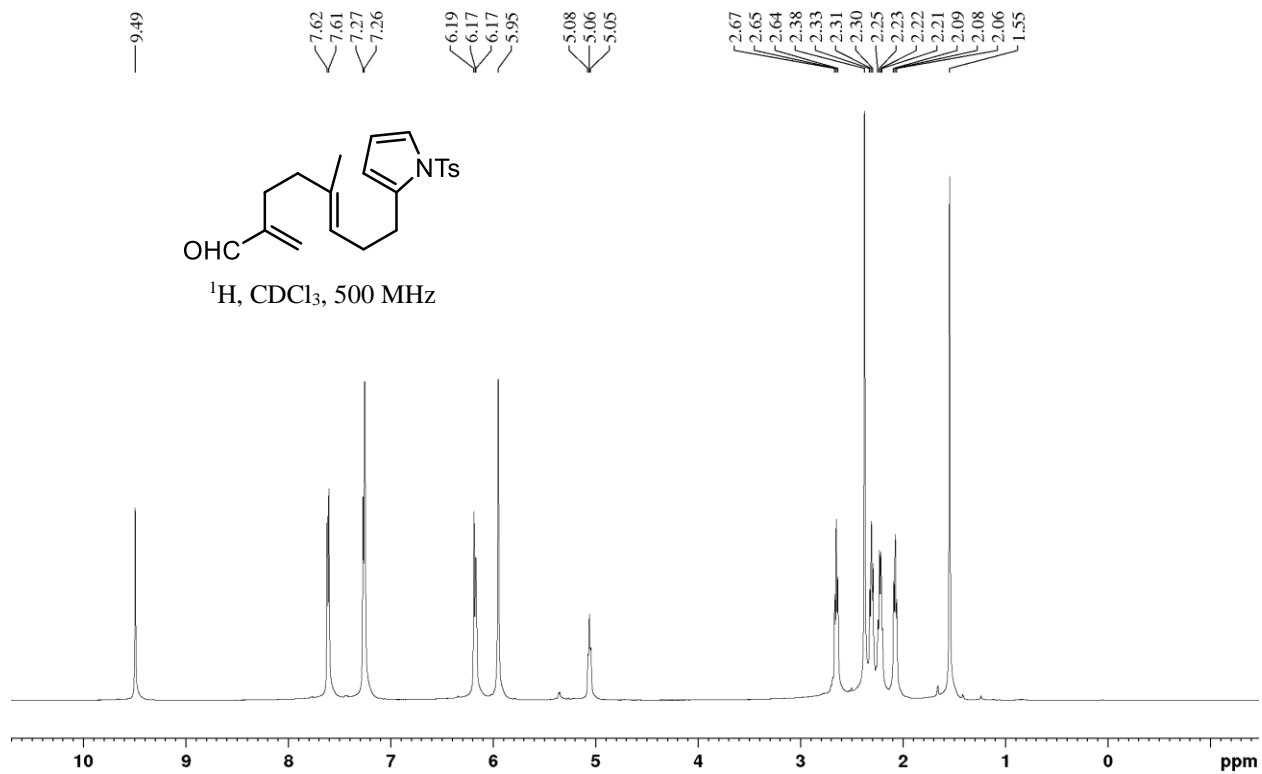


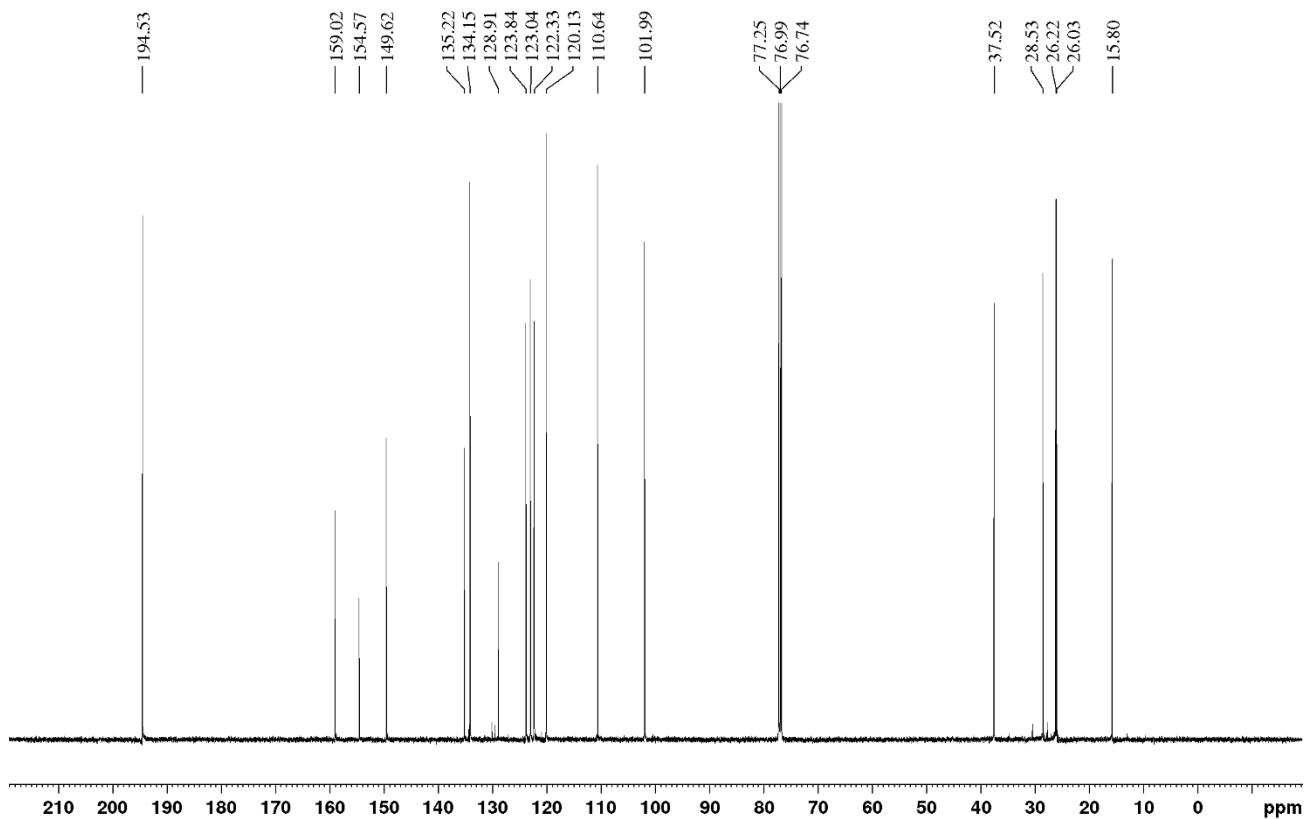
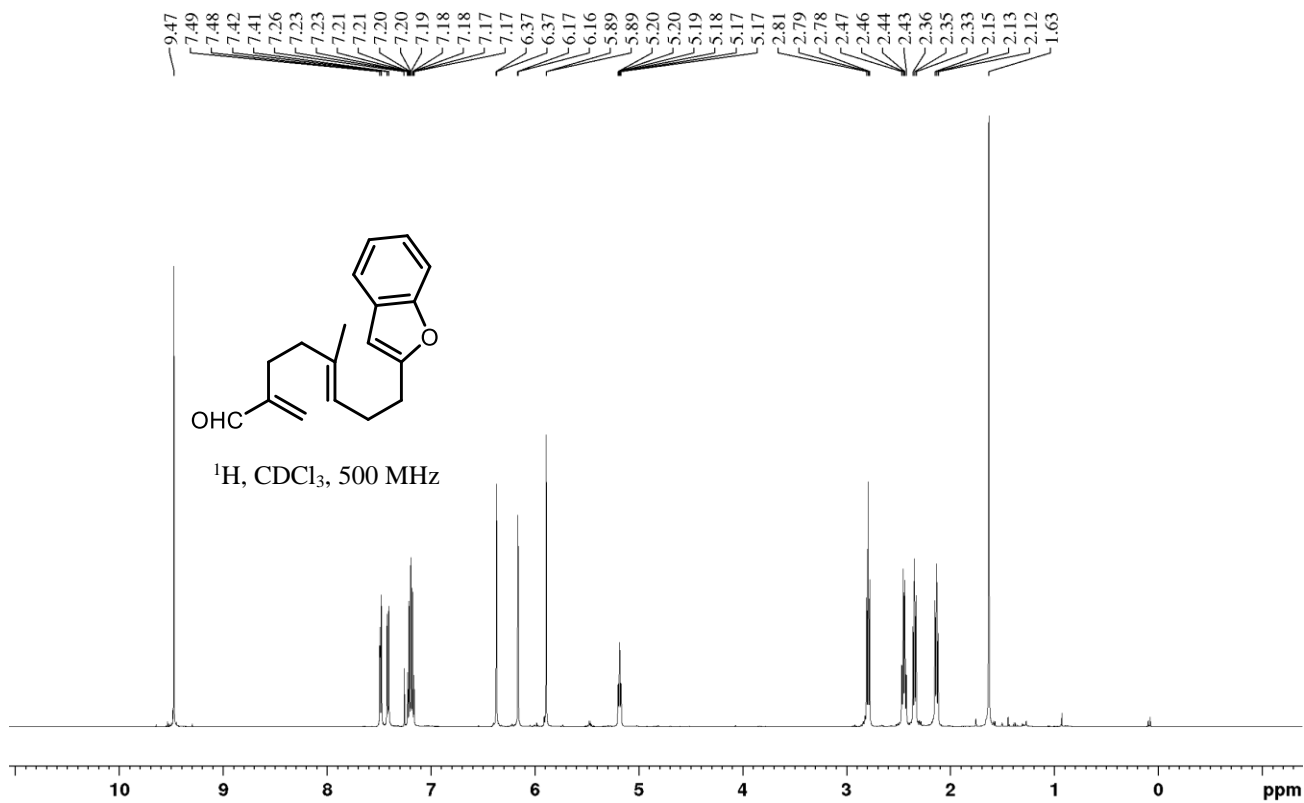


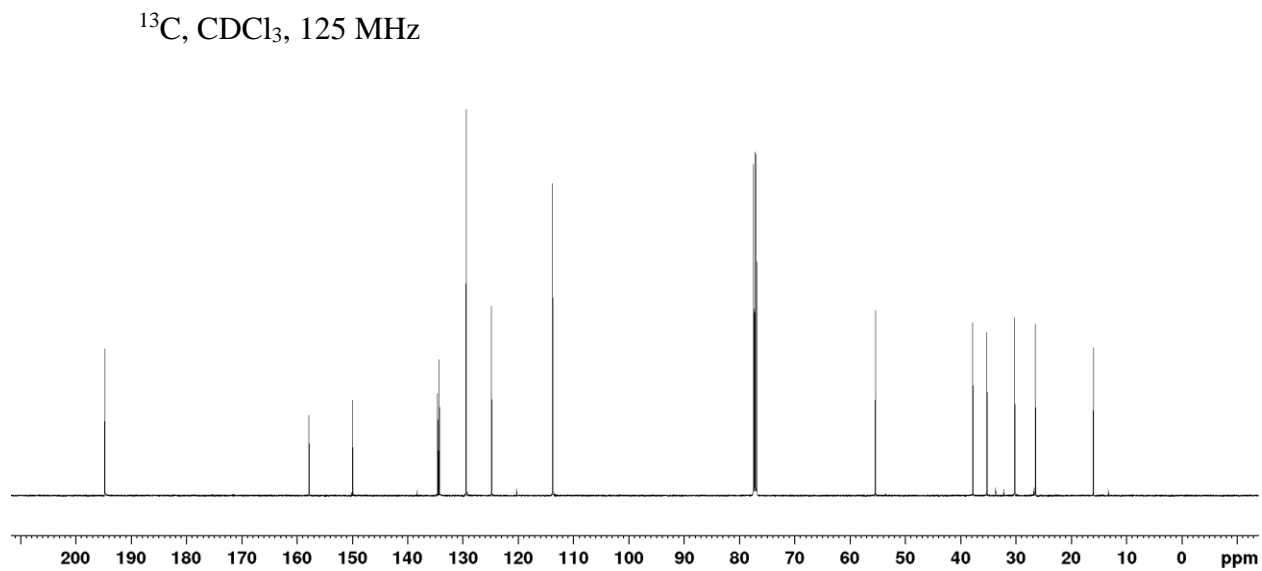
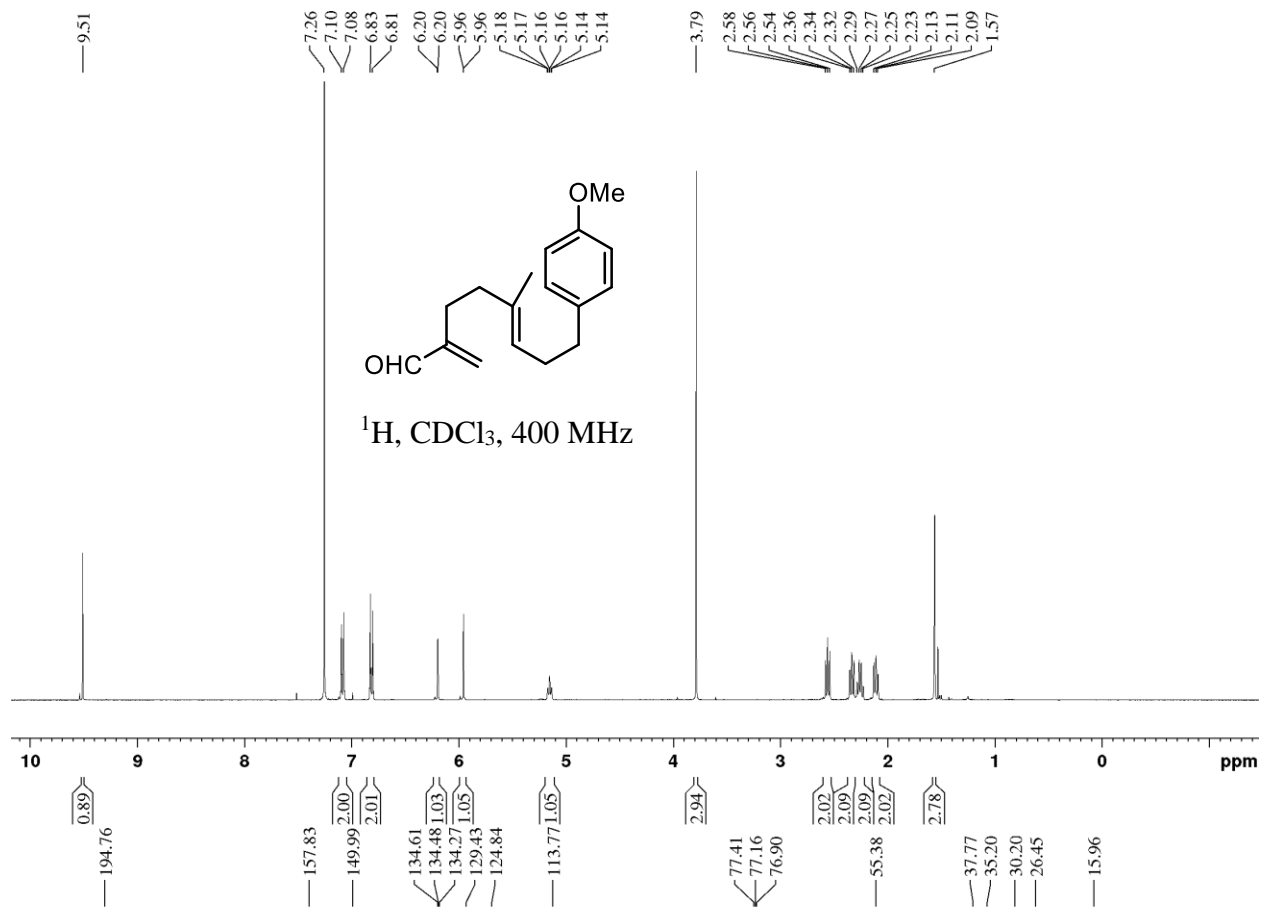


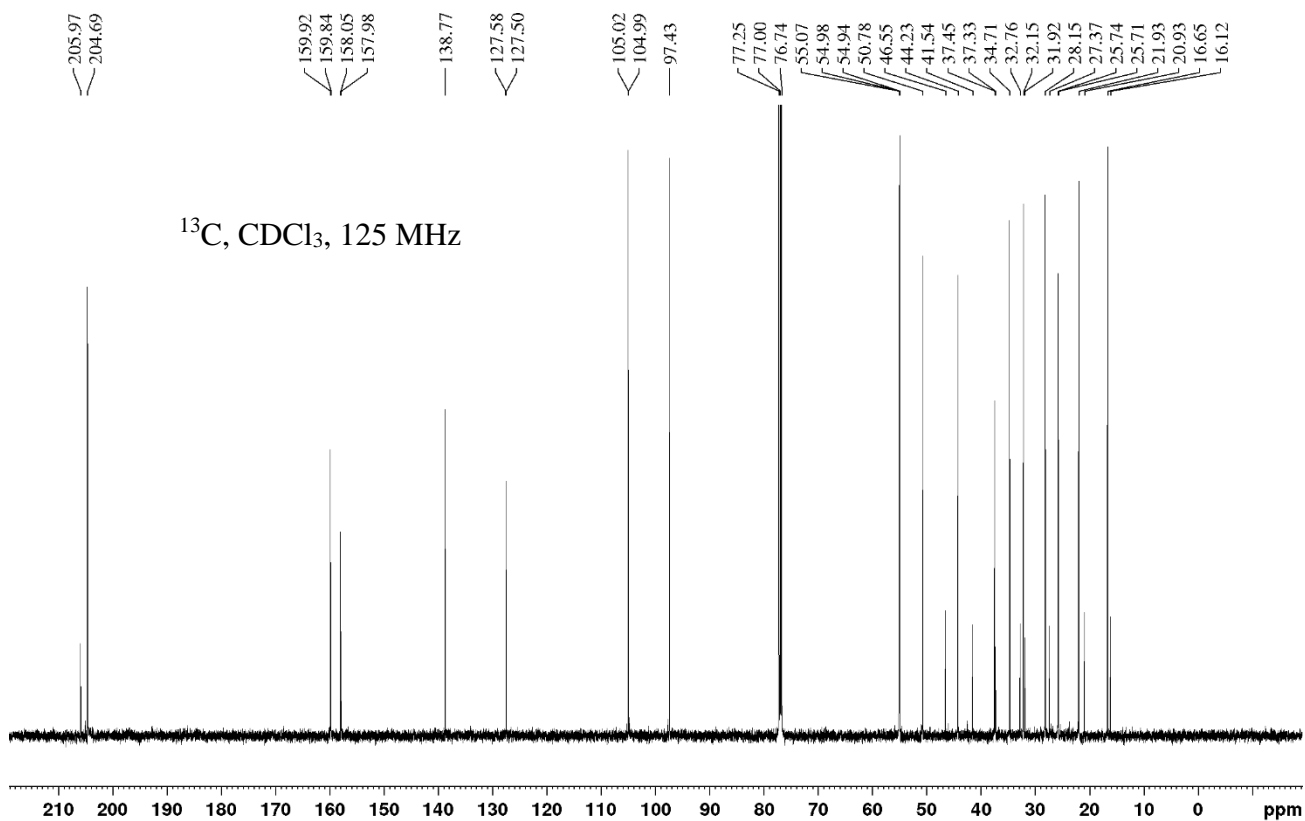
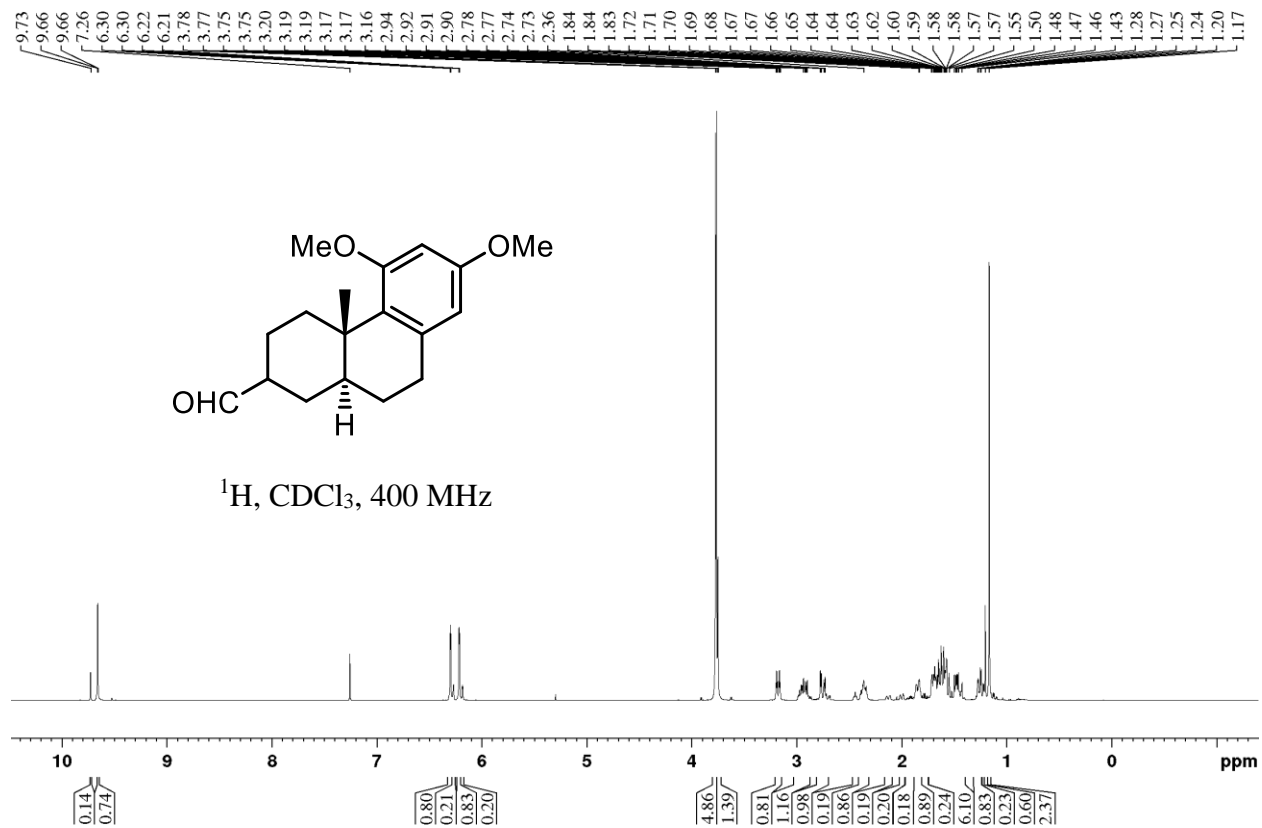


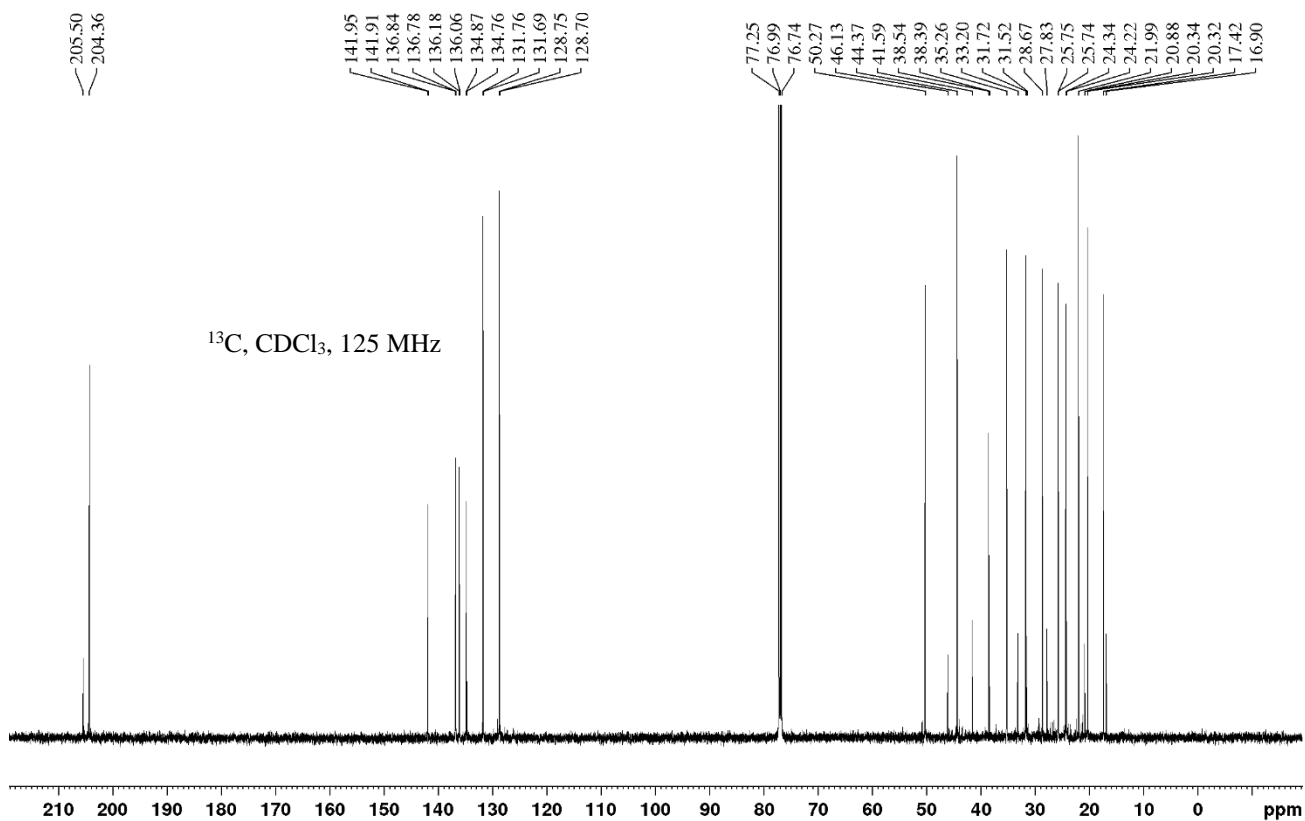
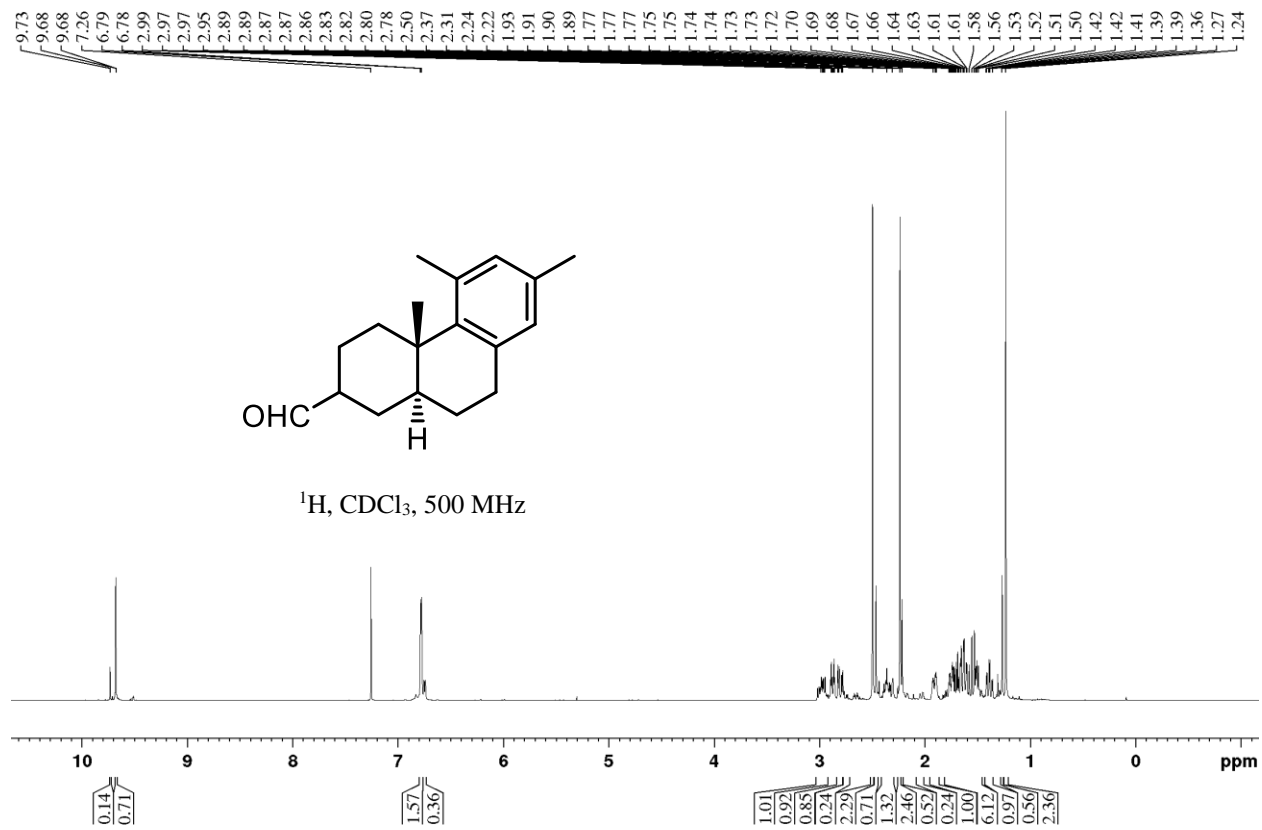




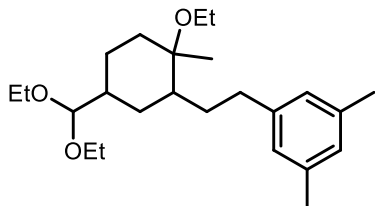




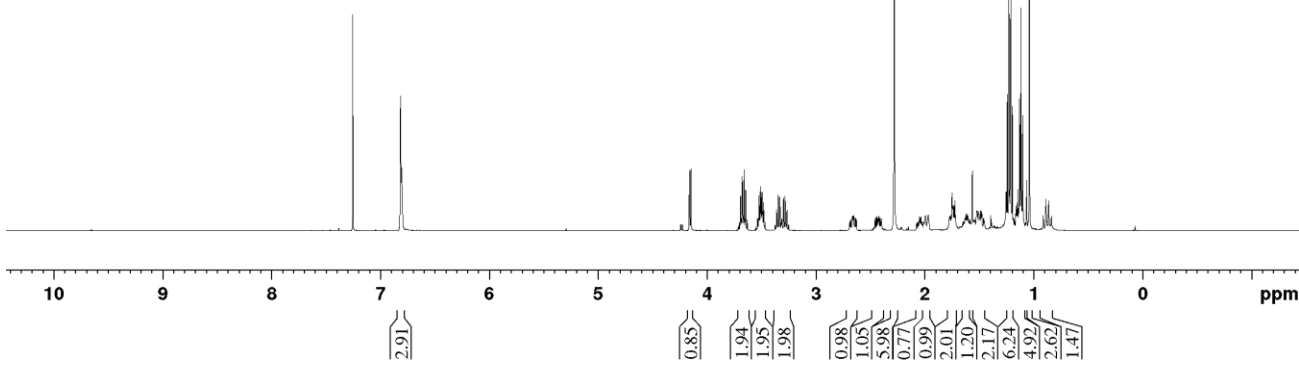




7.26
6.82
6.81
4.17
4.15
3.70
3.68
3.67
3.66
3.65
3.53
3.52
3.51
3.51
3.50
3.50
3.50
3.49
3.37
3.35
3.35
3.34
3.30
3.29
3.28
3.27
2.28
1.97
1.76
1.75
1.75
1.74
1.74
1.73
1.72
1.63
1.61
1.61
1.53
1.52
1.52
1.51
1.51
1.49
1.48
1.26
1.25
1.23
1.23
1.22
1.21
1.20
1.20
1.17
1.17
1.16
1.15
1.14
1.13
1.12
1.11
1.04
0.89
0.87

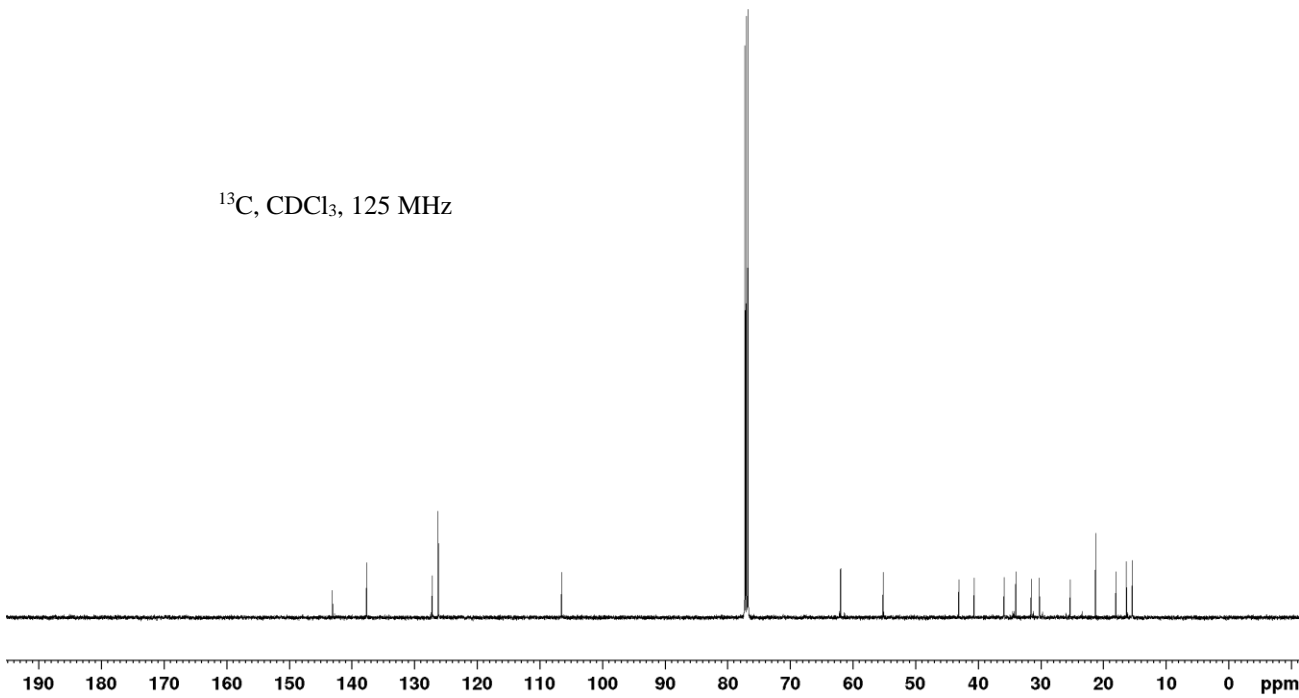


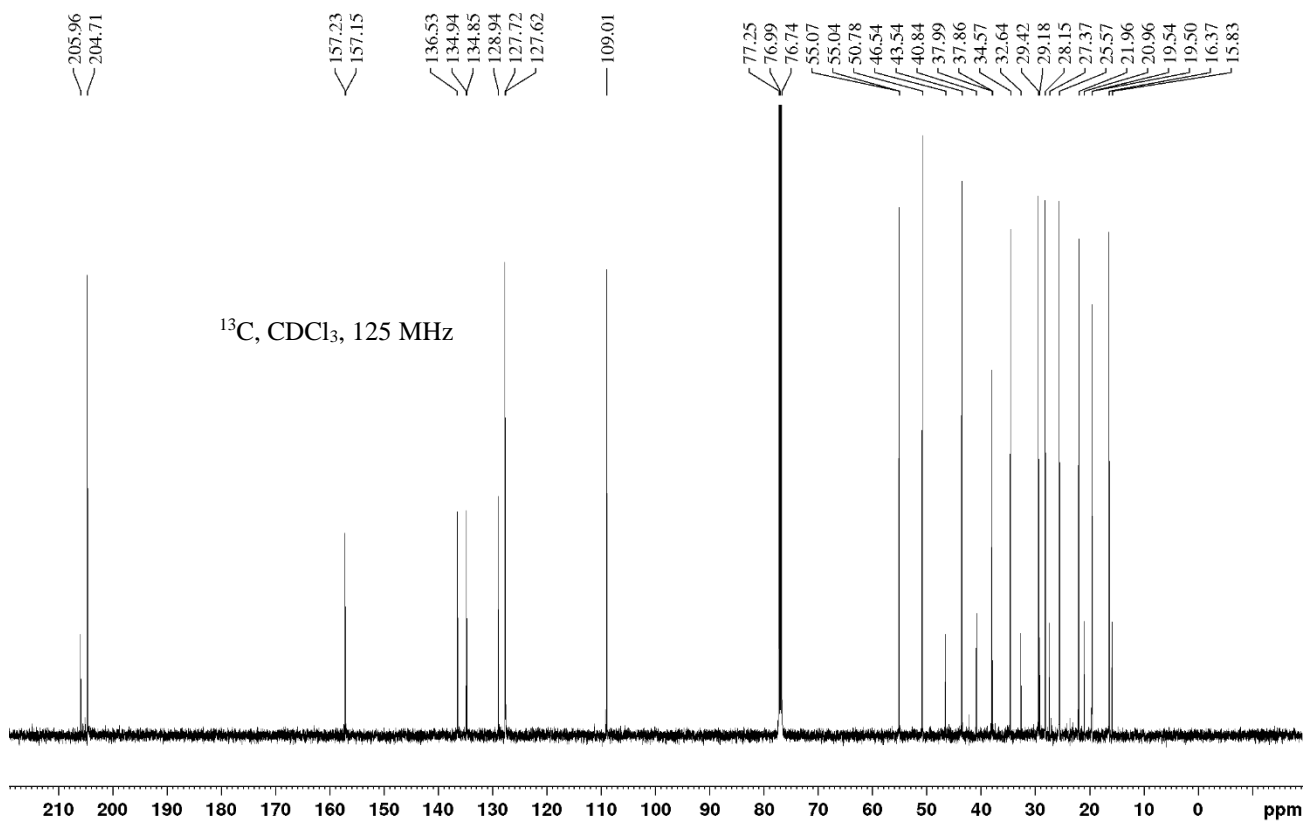
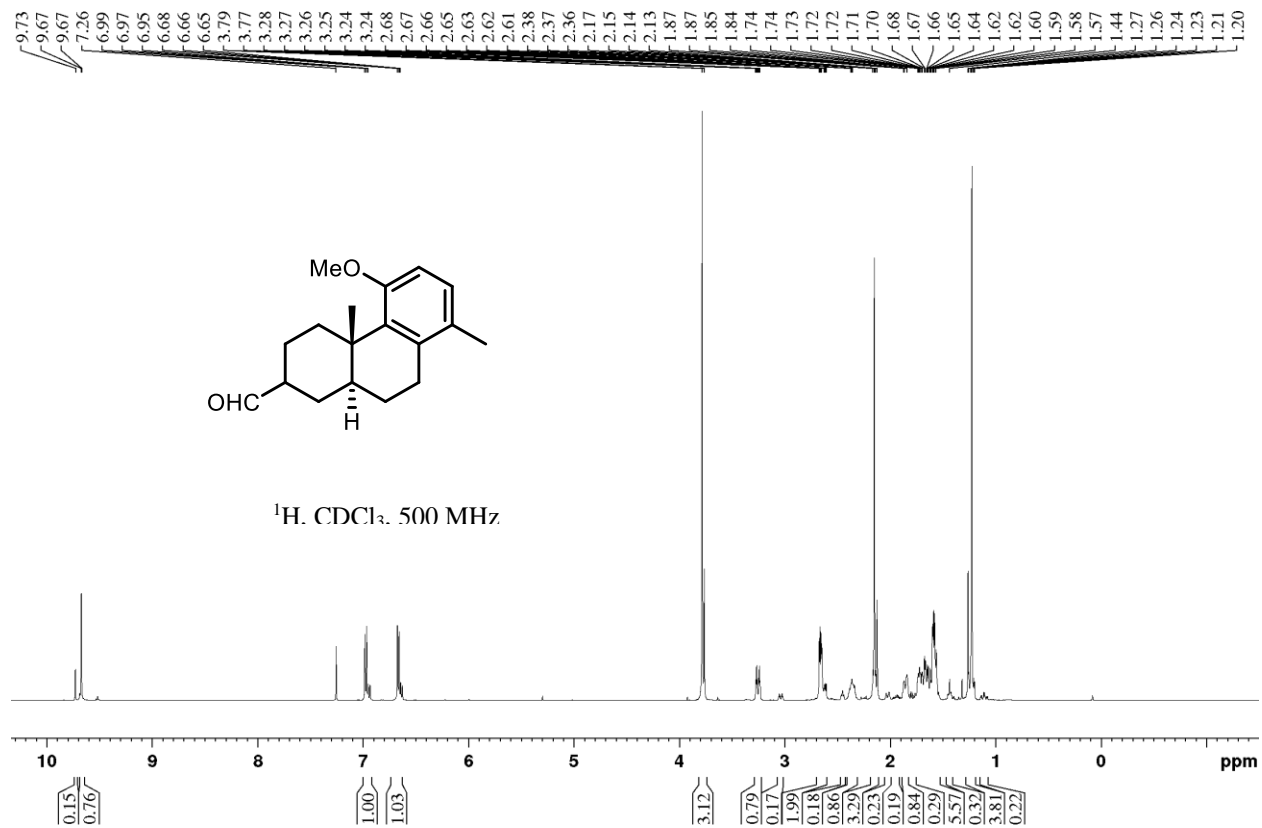
^1H , CDCl_3 , 500 MHz

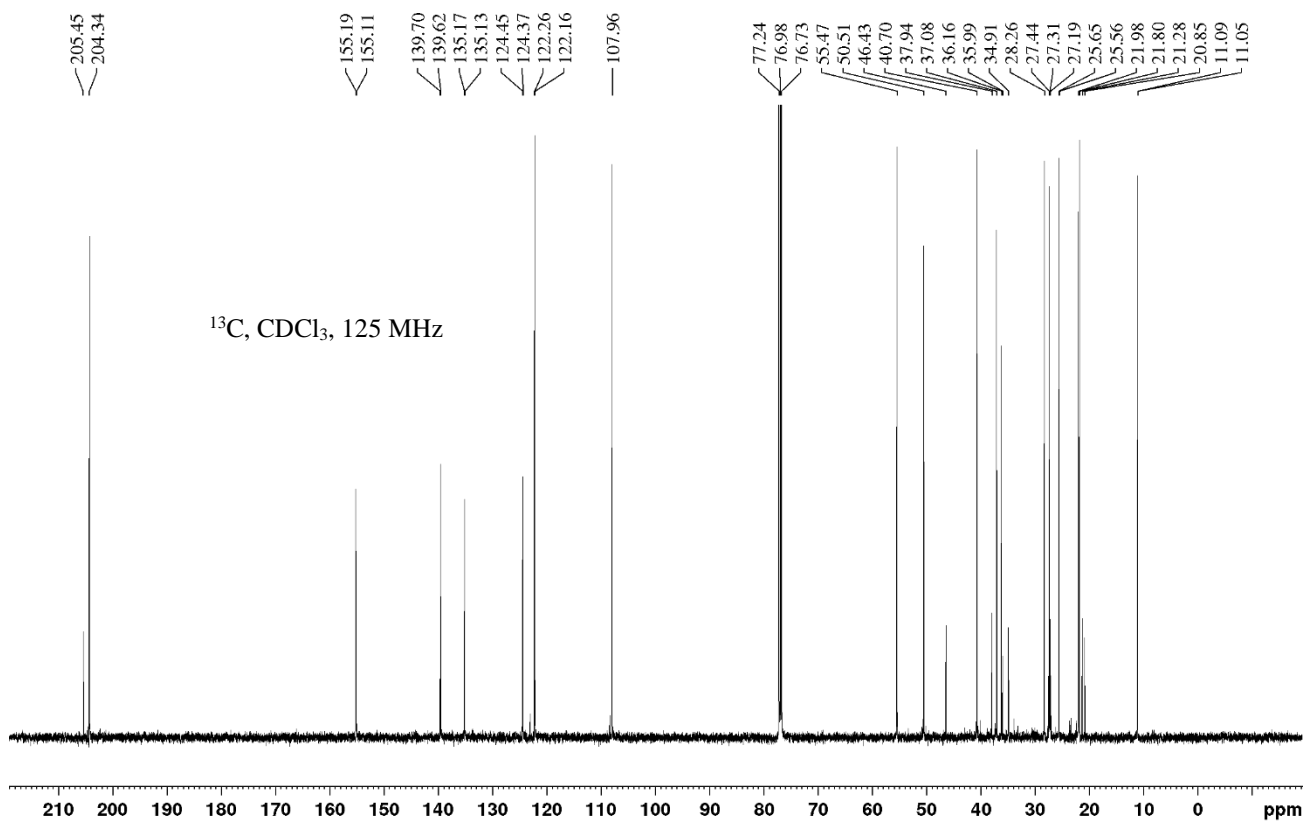
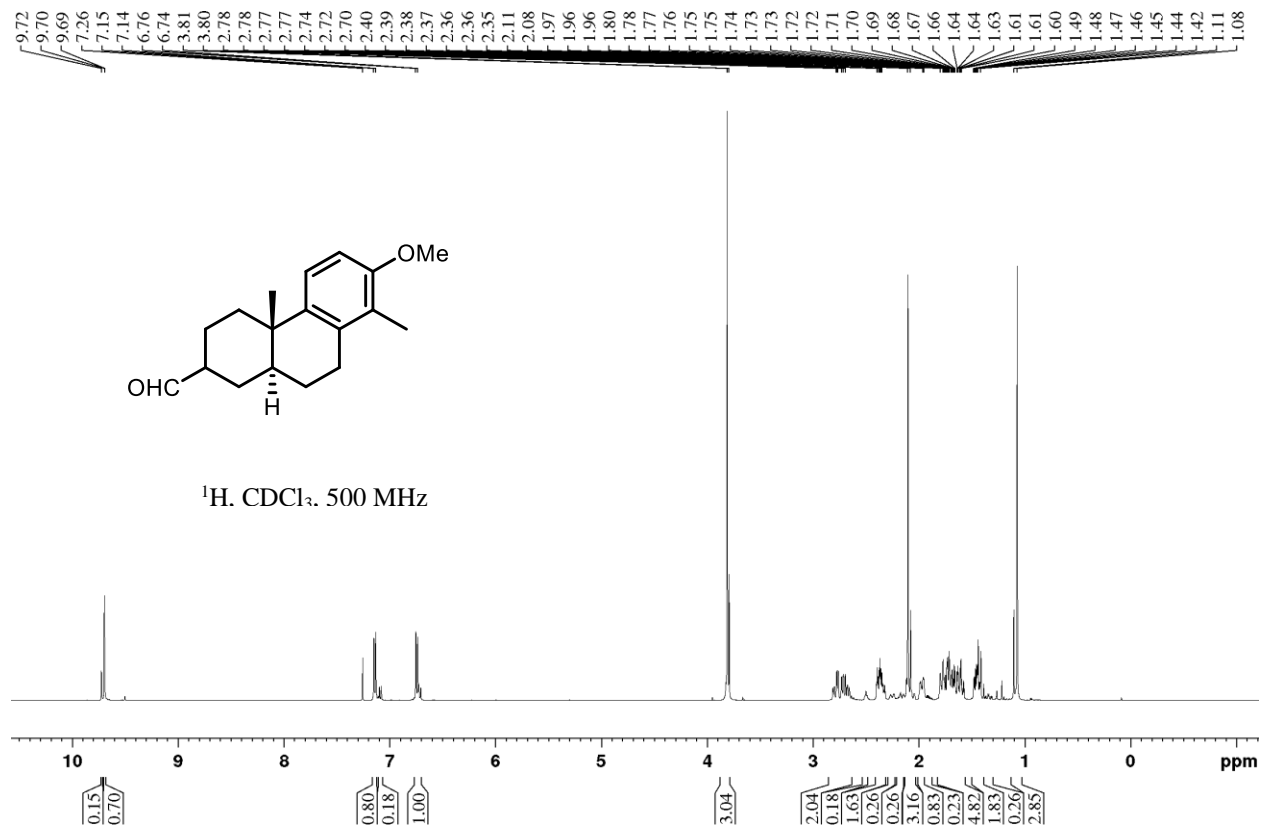


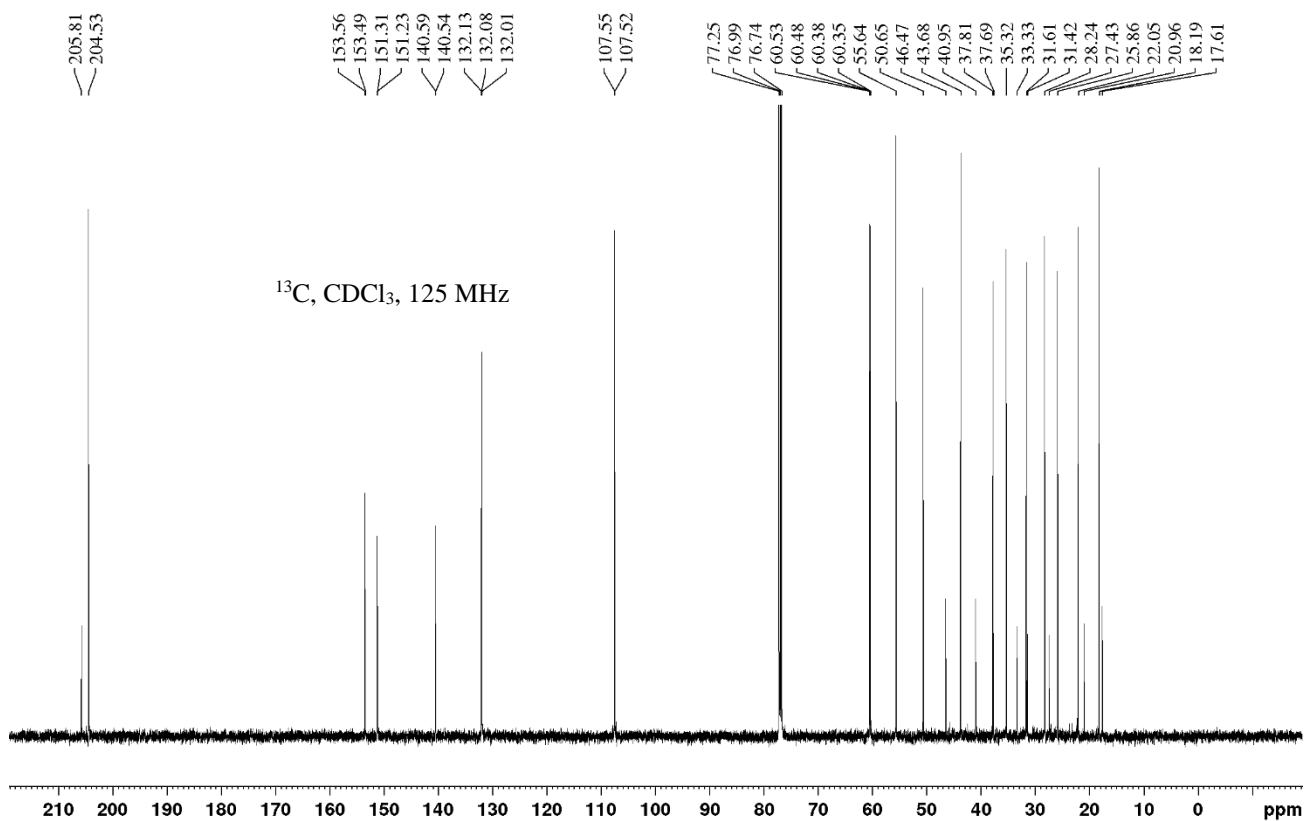
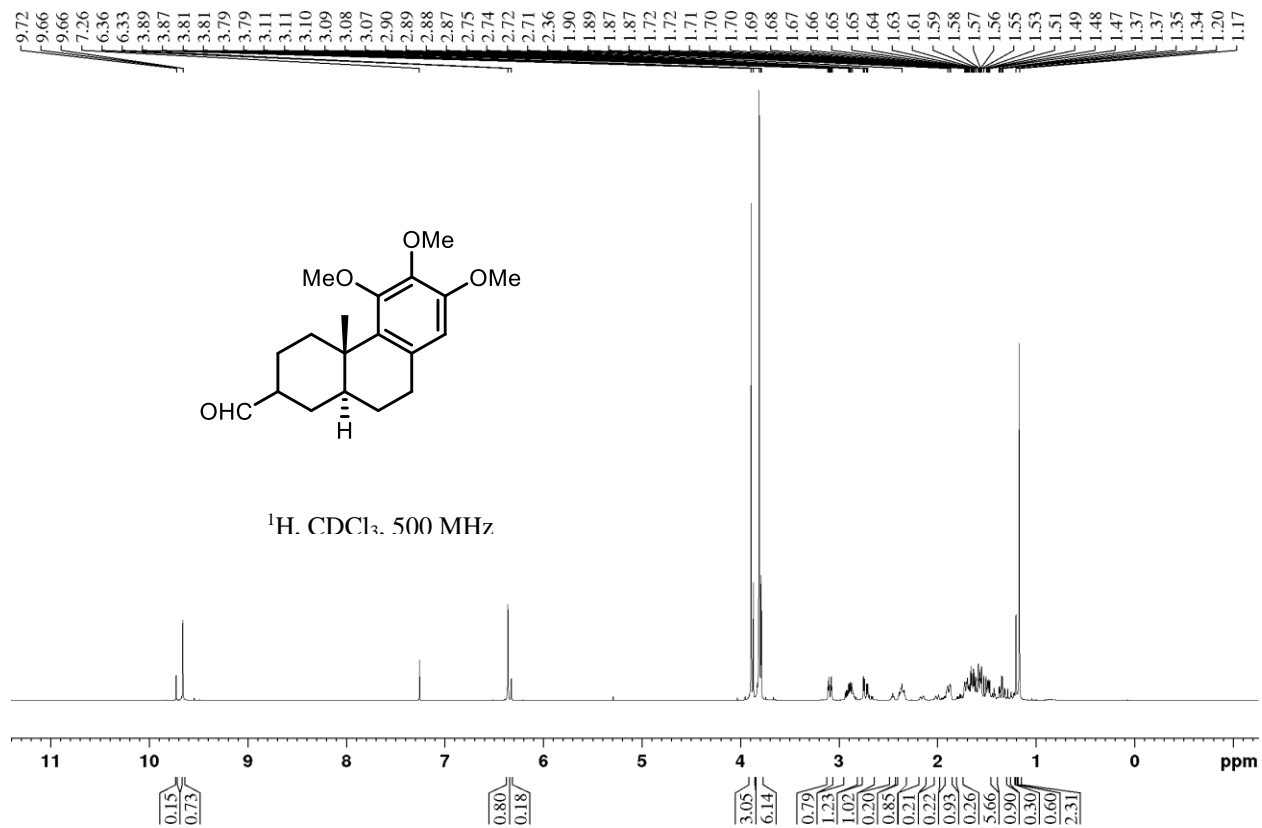
143.13
137.63
127.17
126.22
106.51
77.24
76.99
76.84
76.74
61.99
61.92
55.16
43.09
40.64
35.82
33.98
31.49
30.22
25.28
21.25
17.98
16.31
15.36
15.32

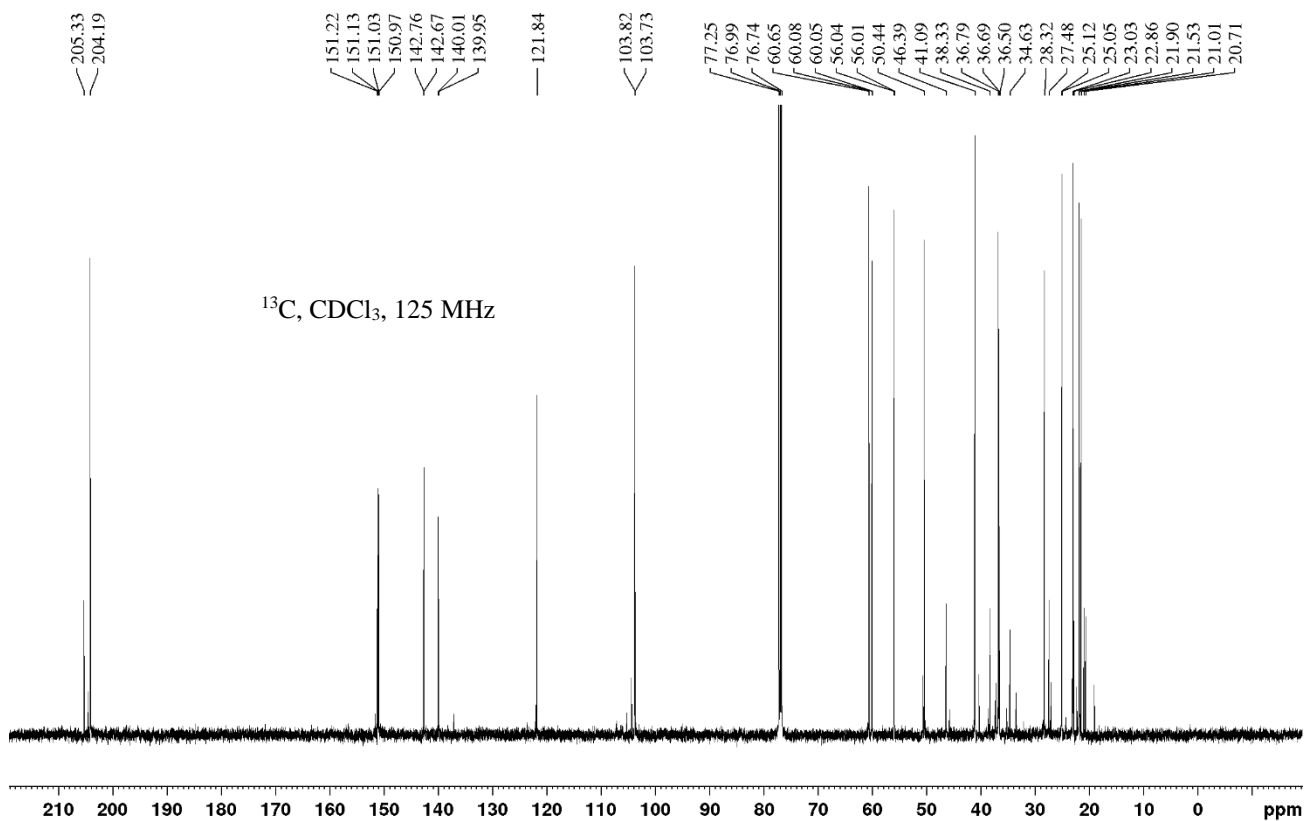
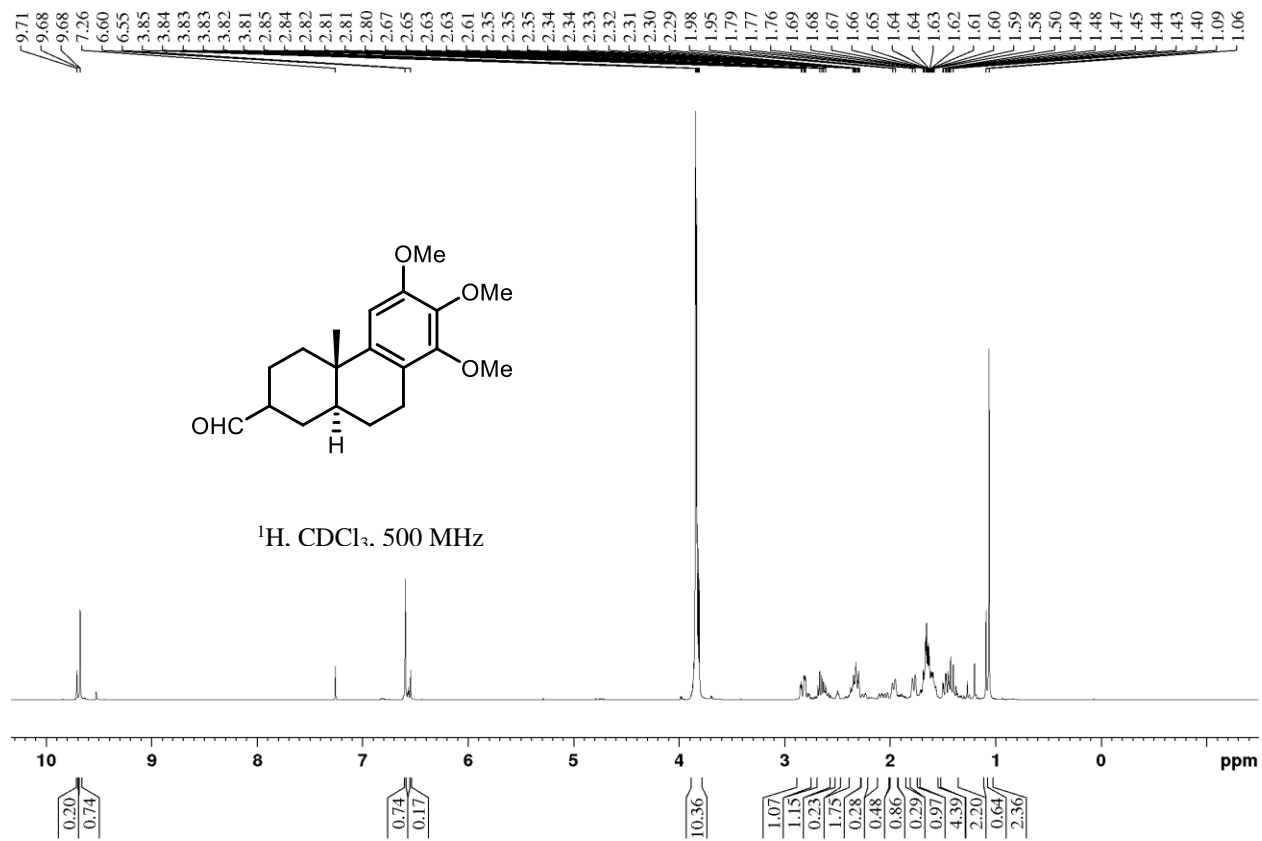
^{13}C , CDCl_3 , 125 MHz

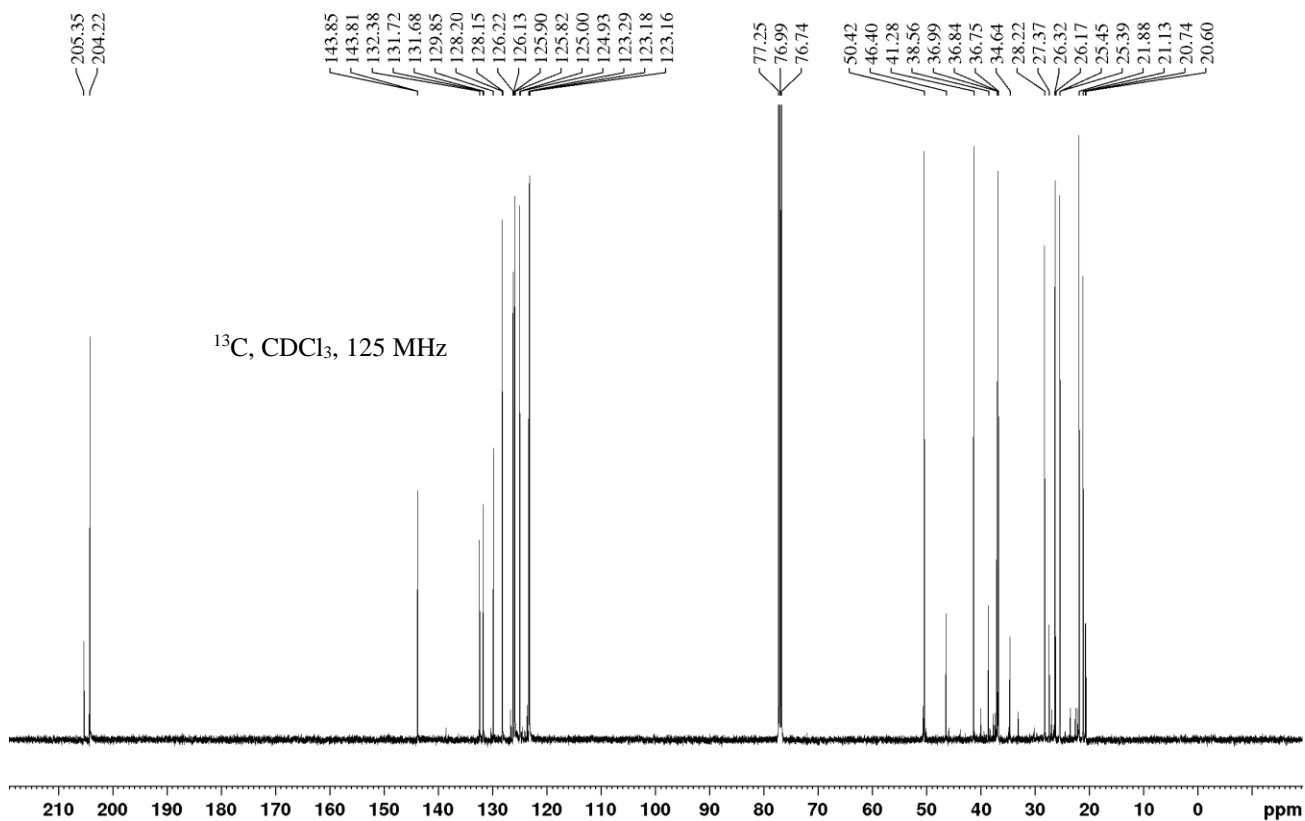
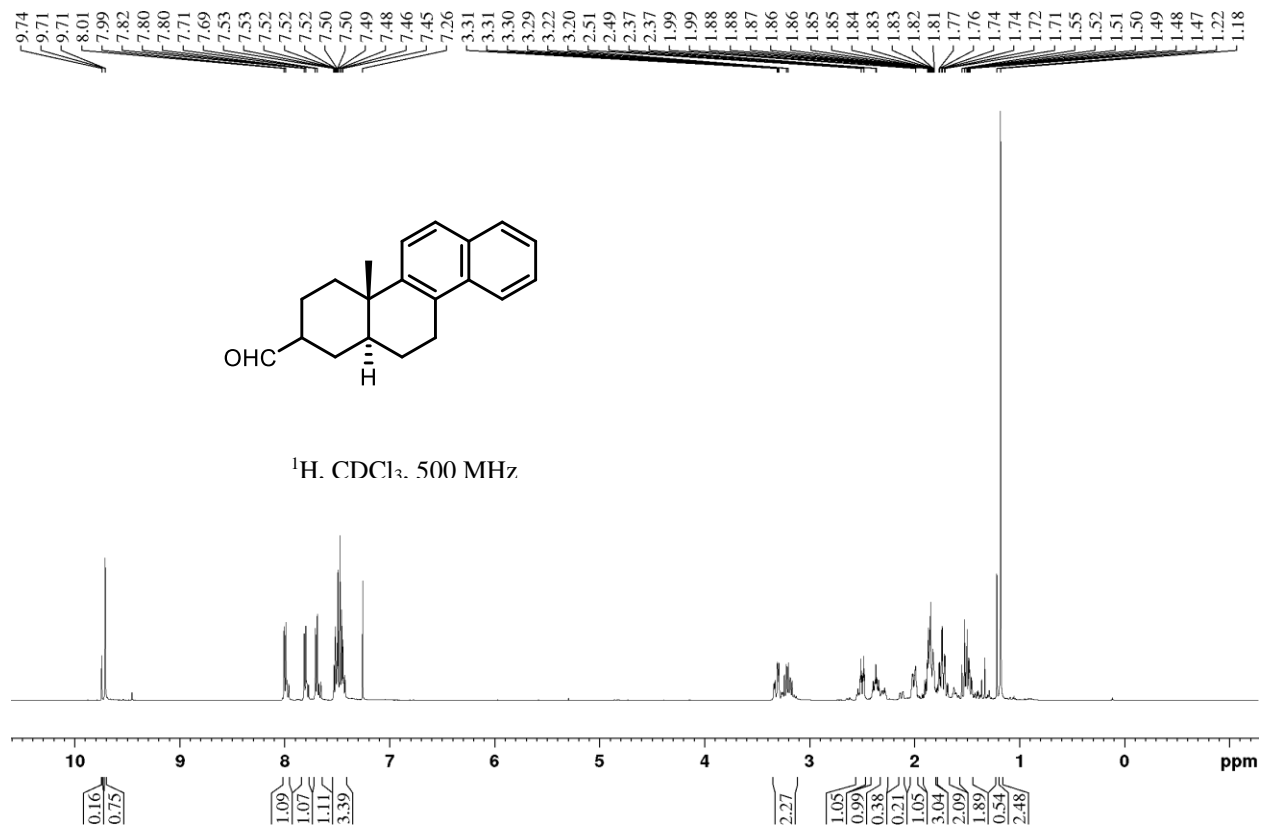


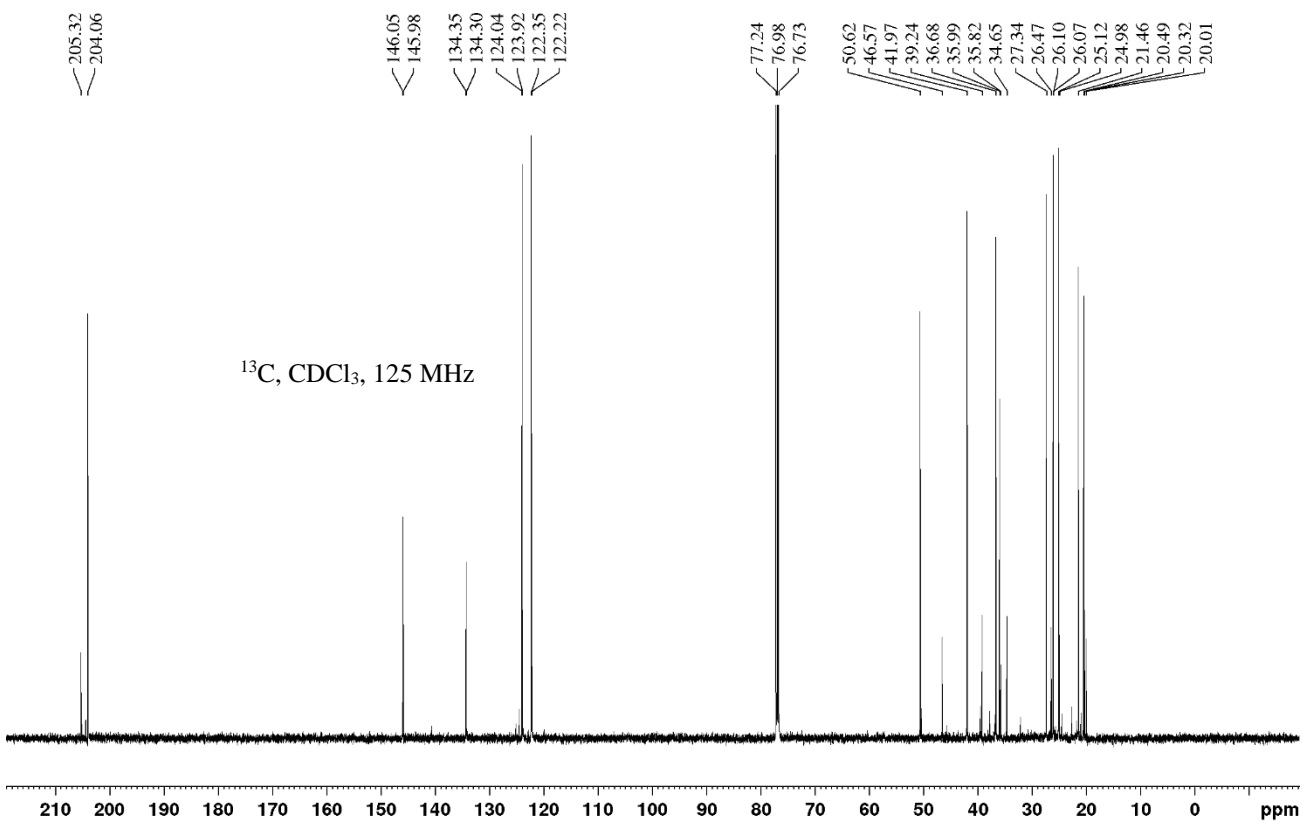
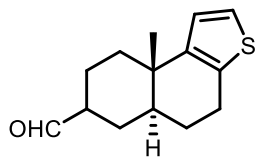
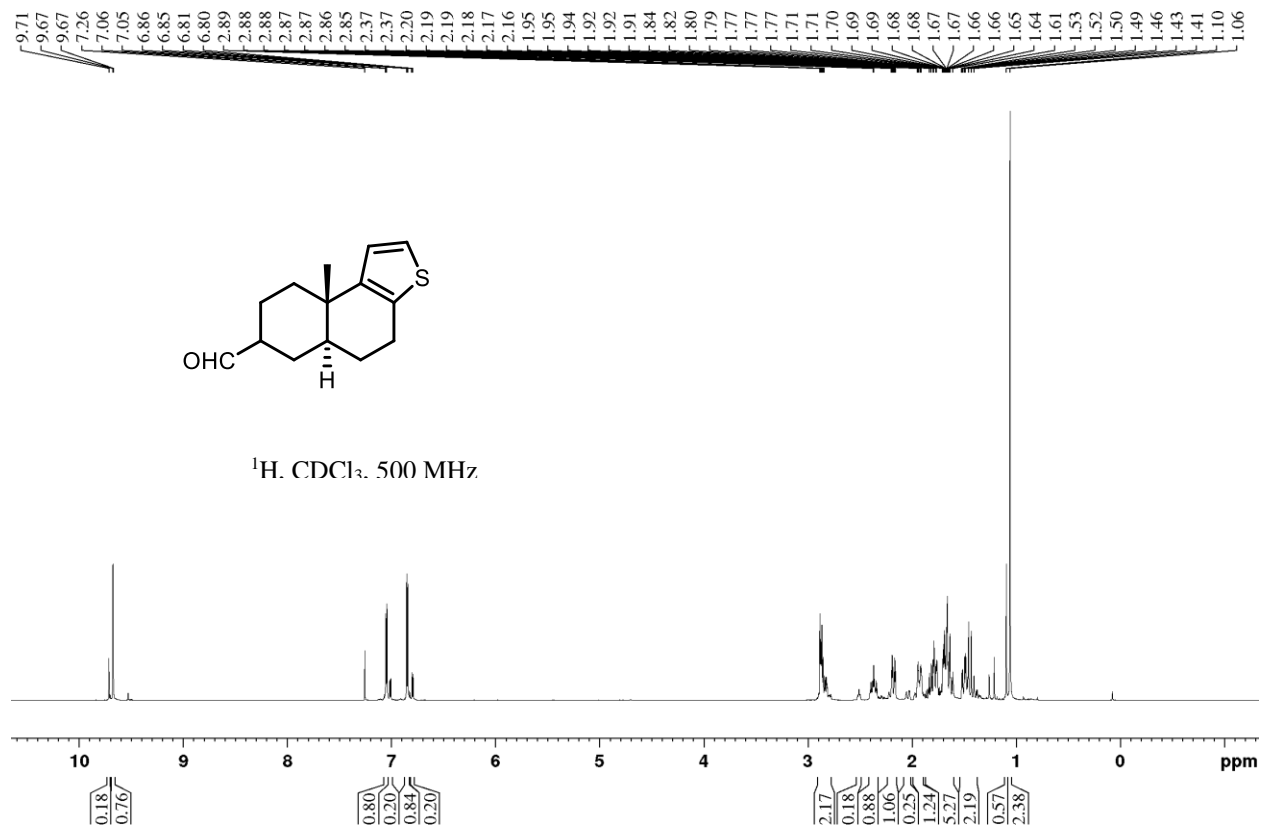


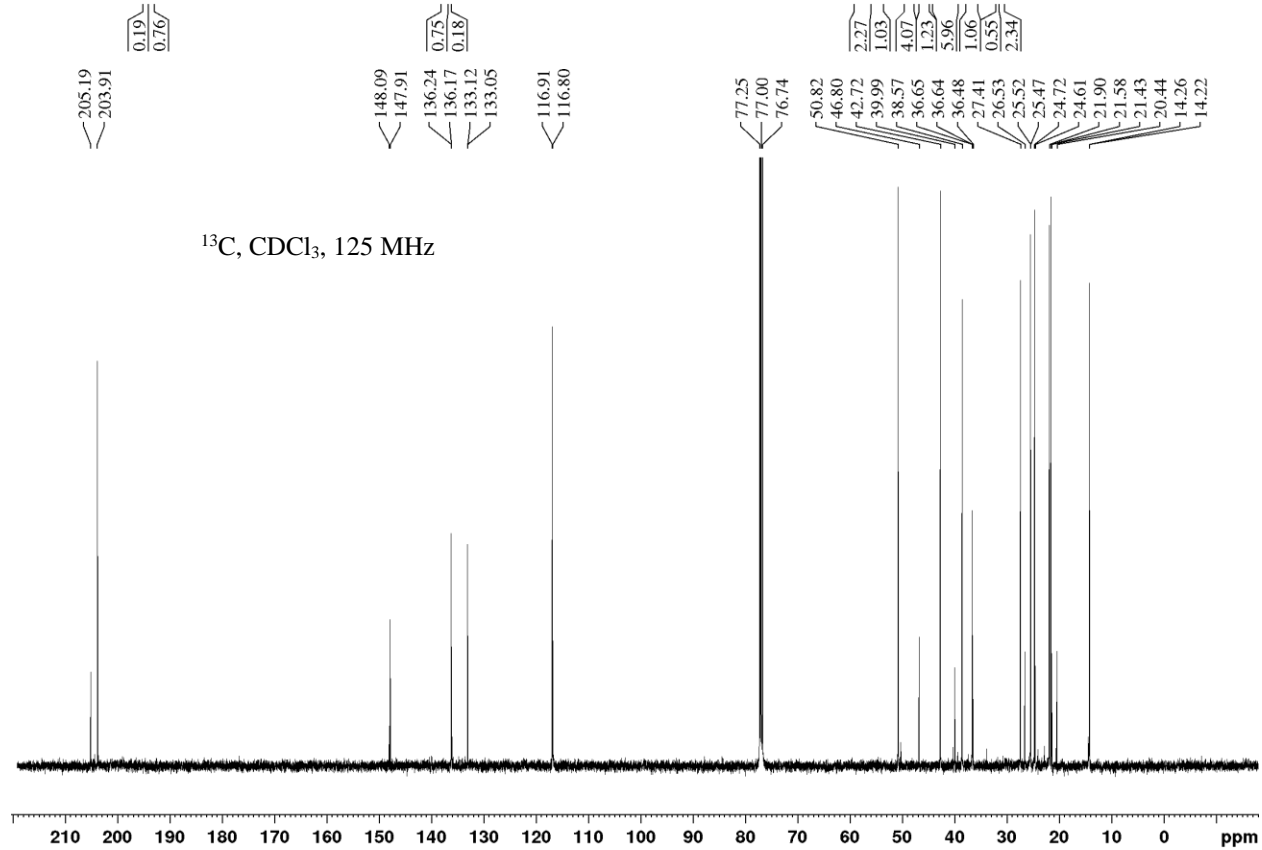
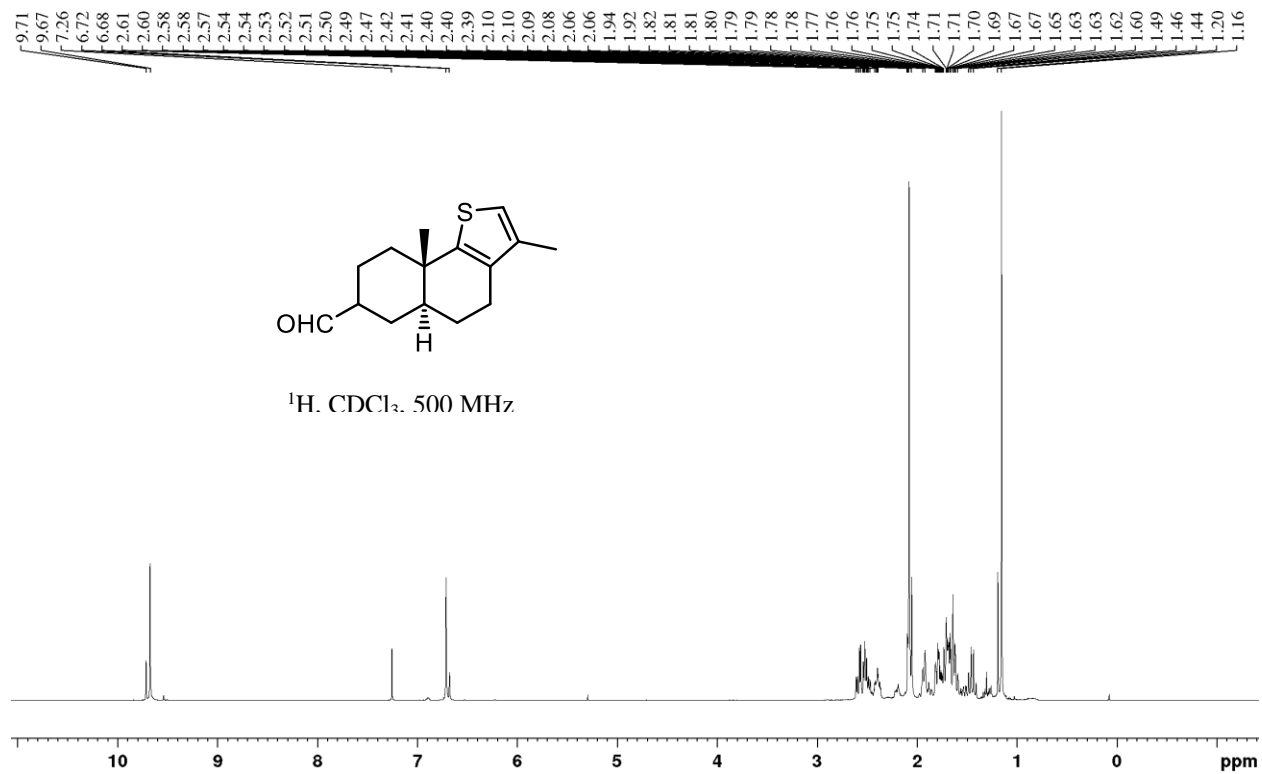


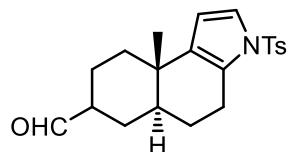
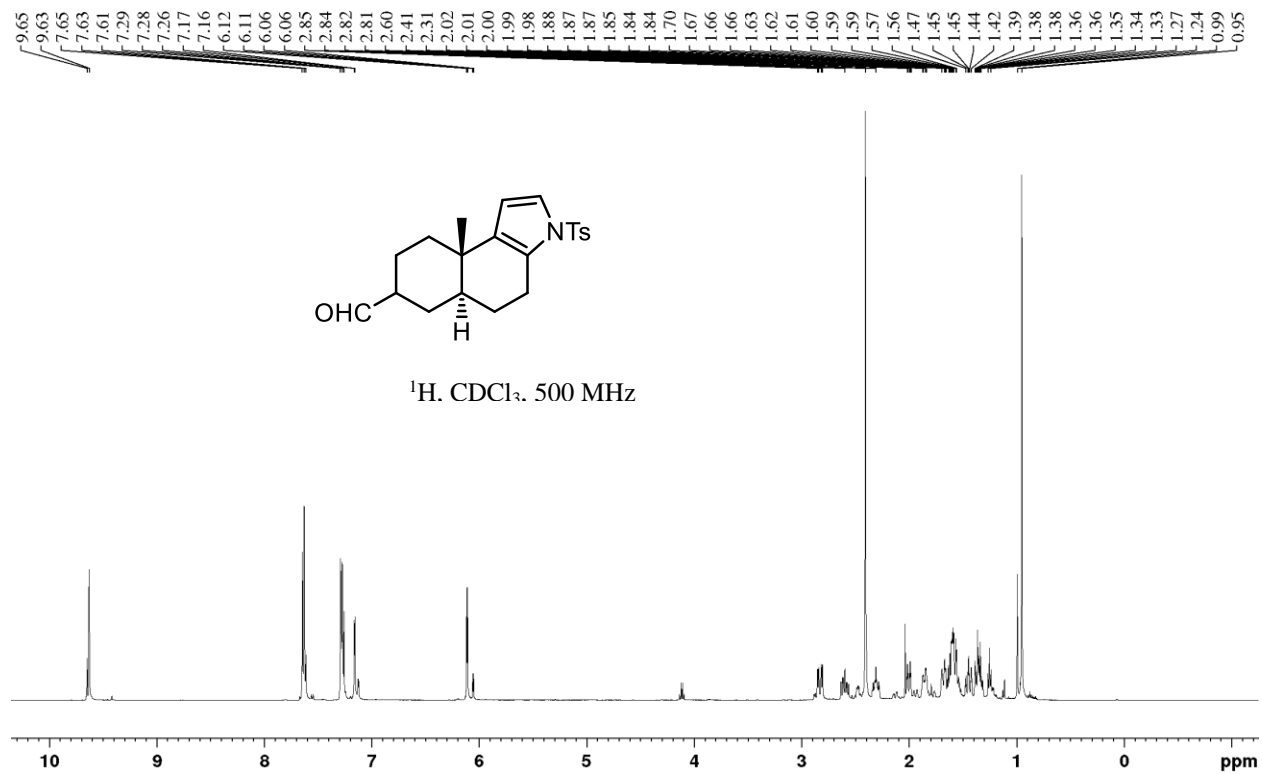




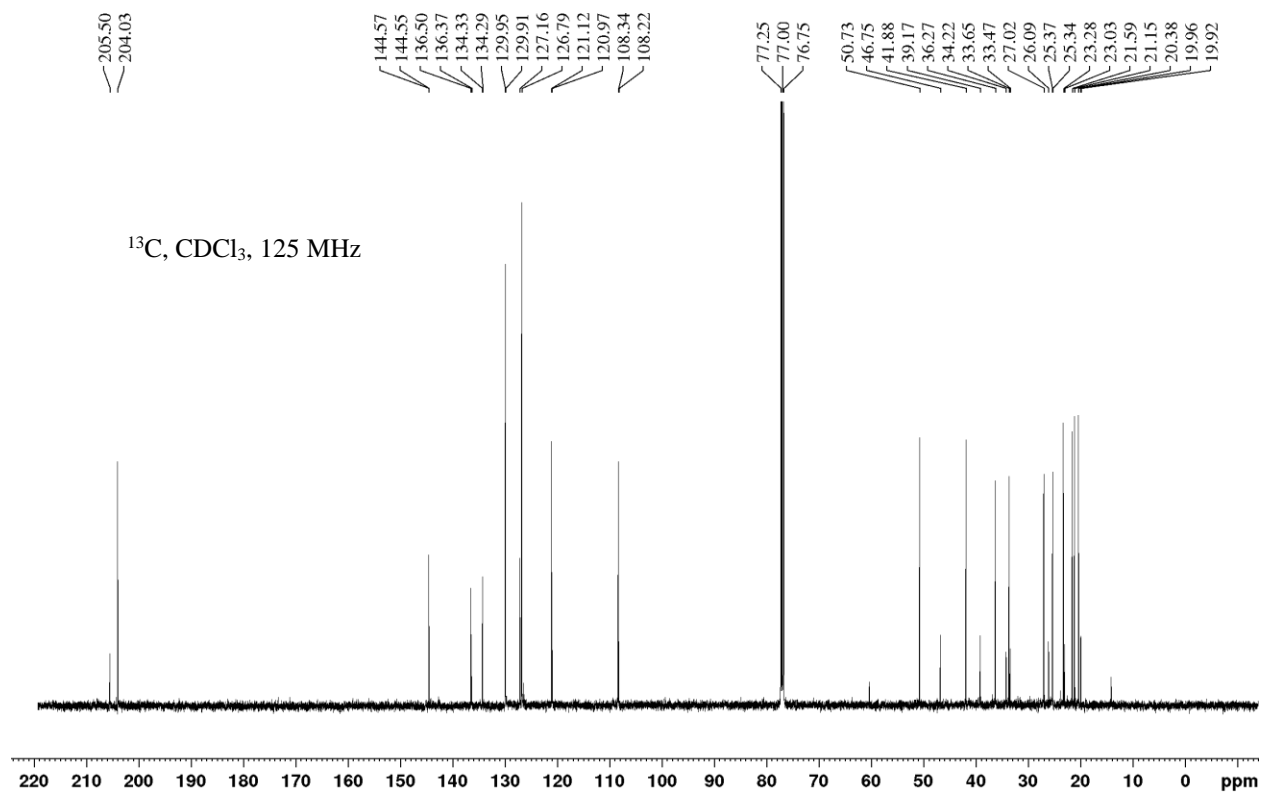




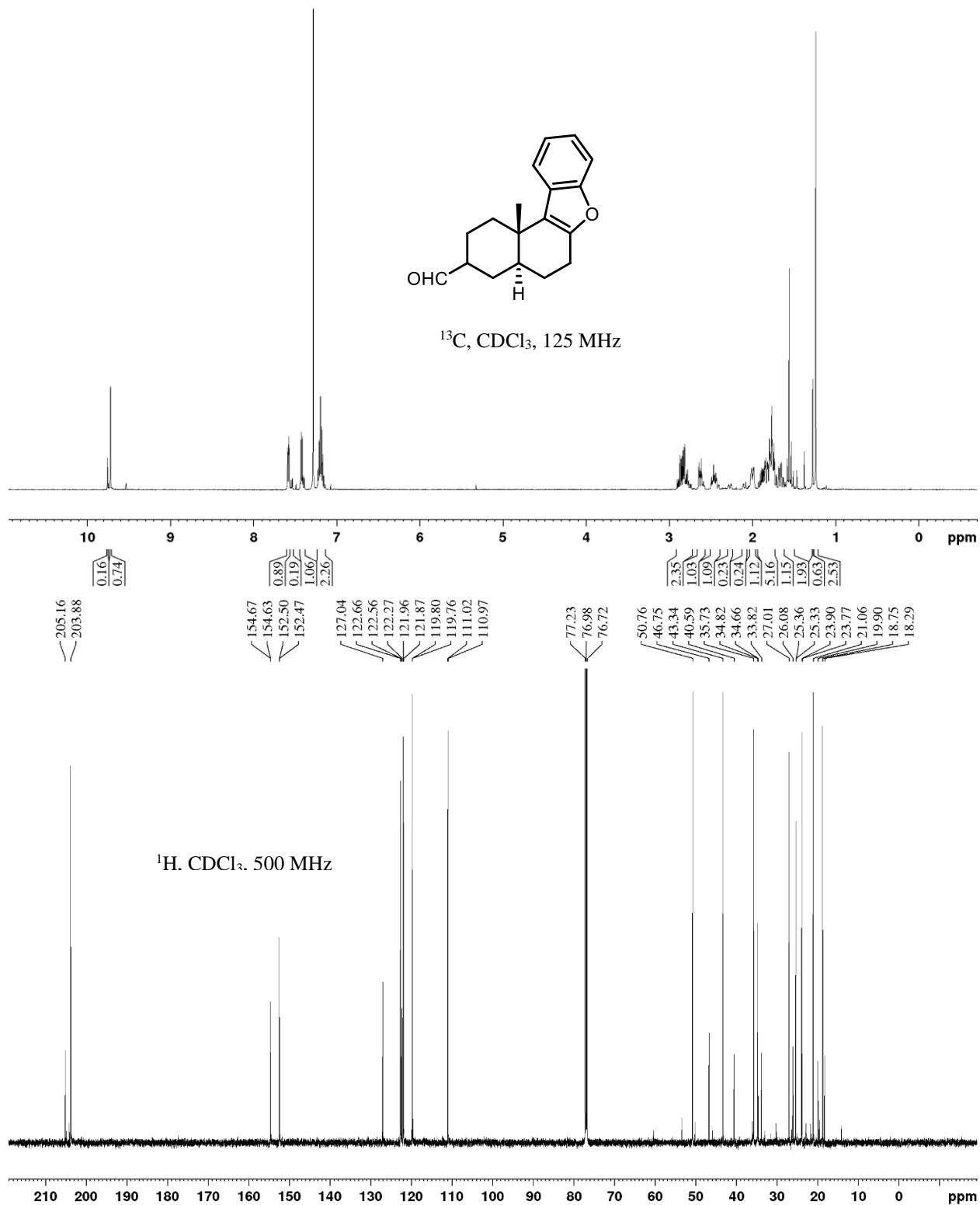


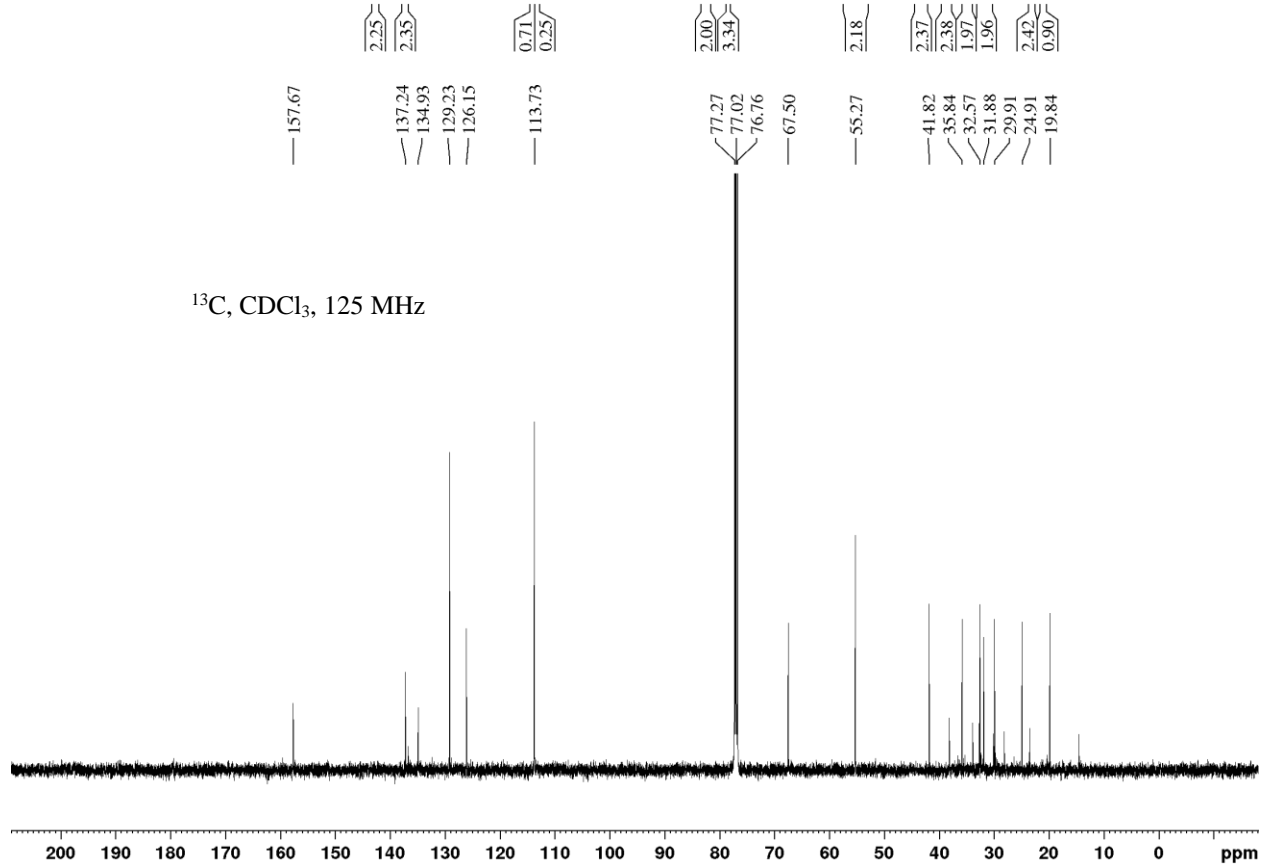
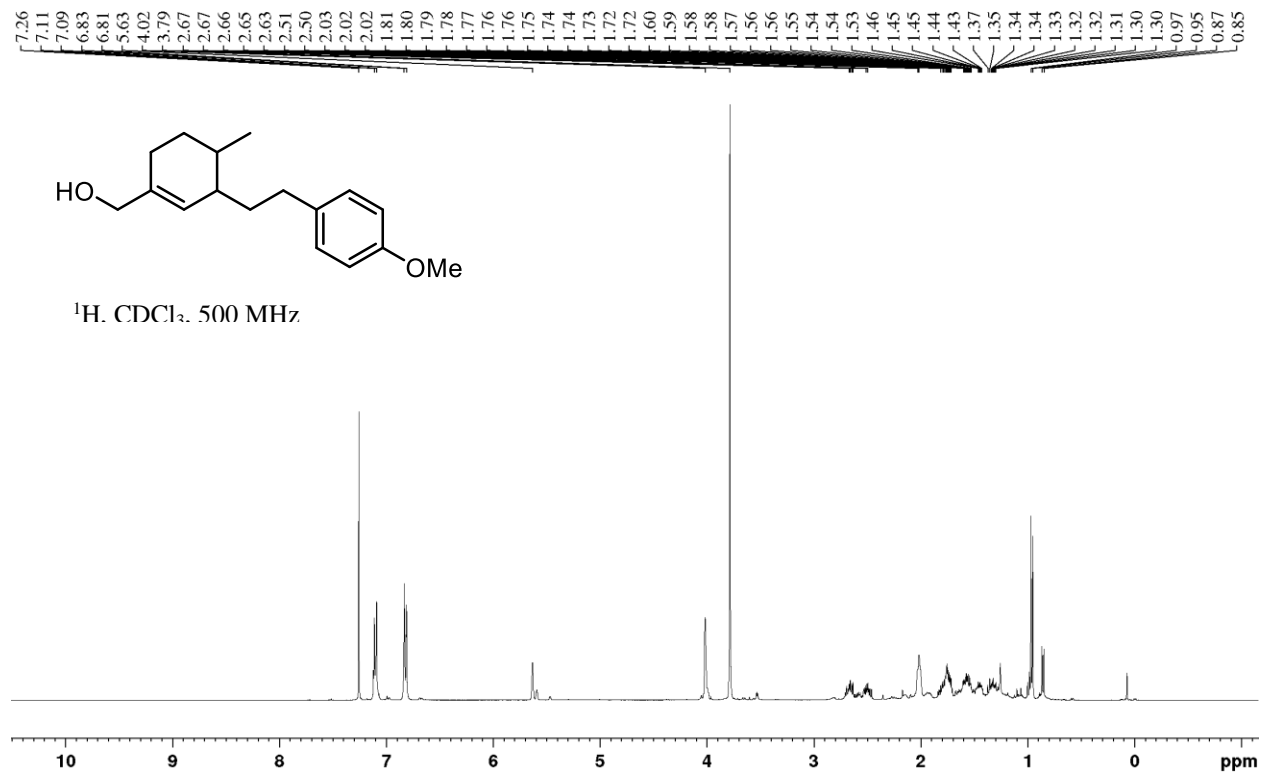


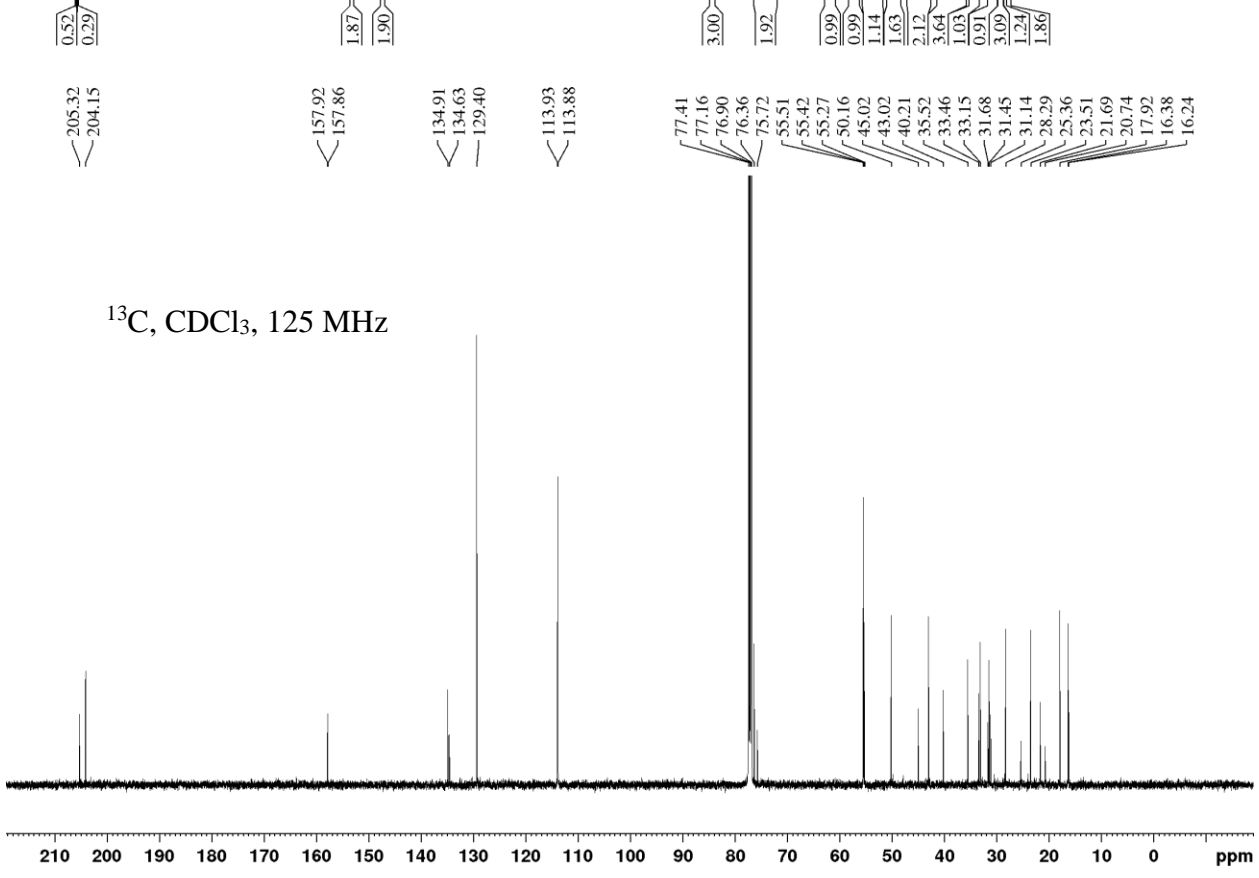
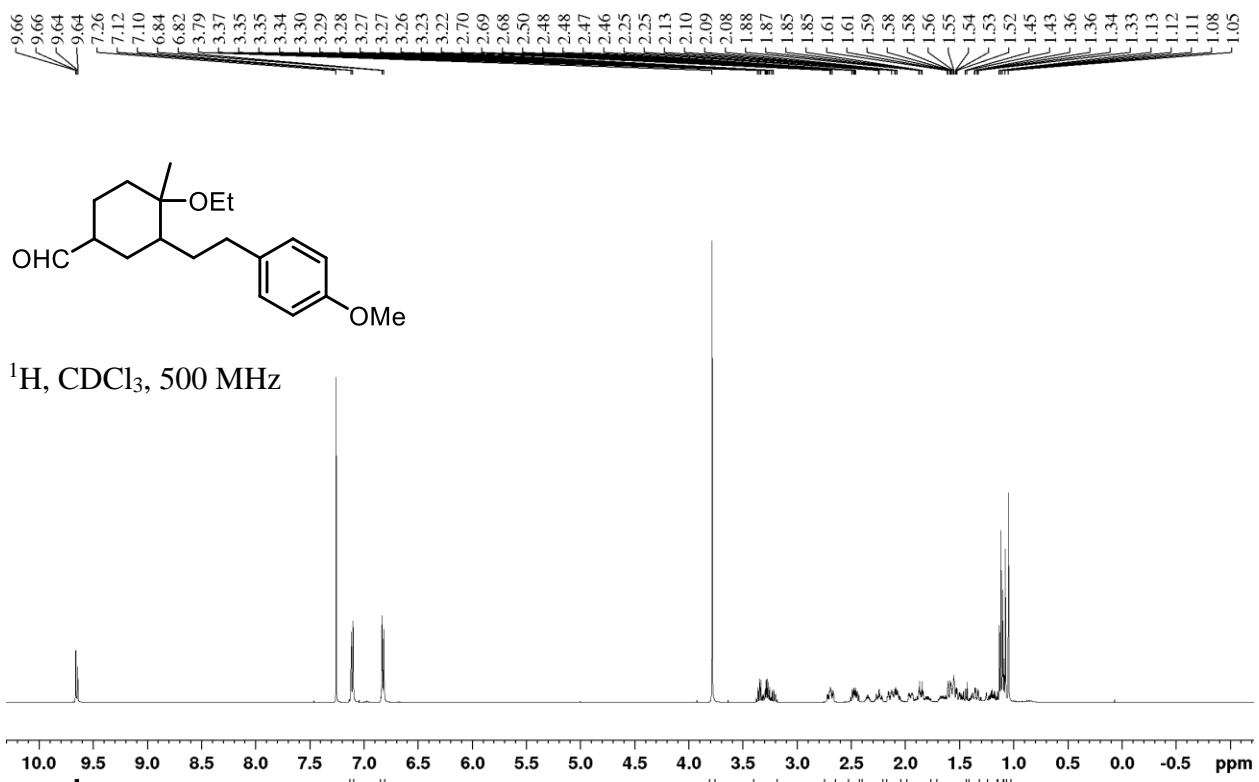
^1H , CDCl_3 , 500 MHz

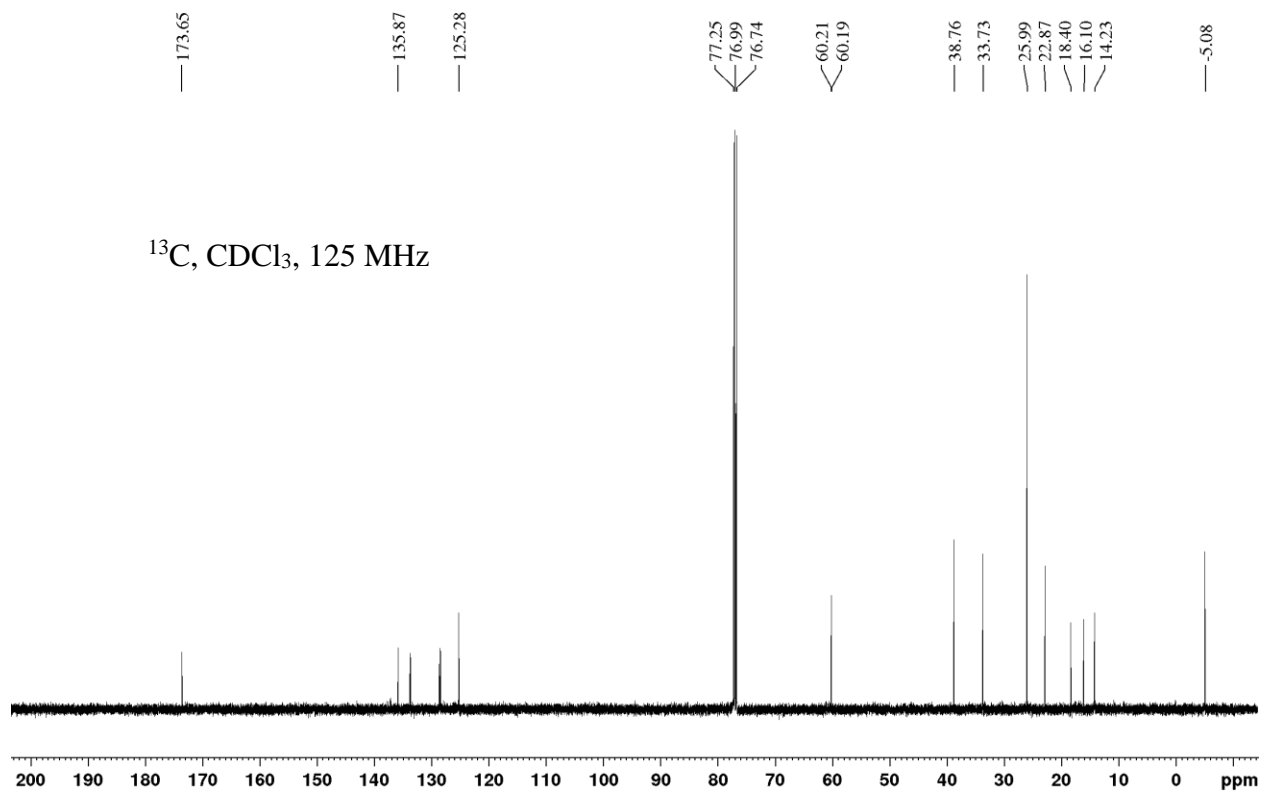
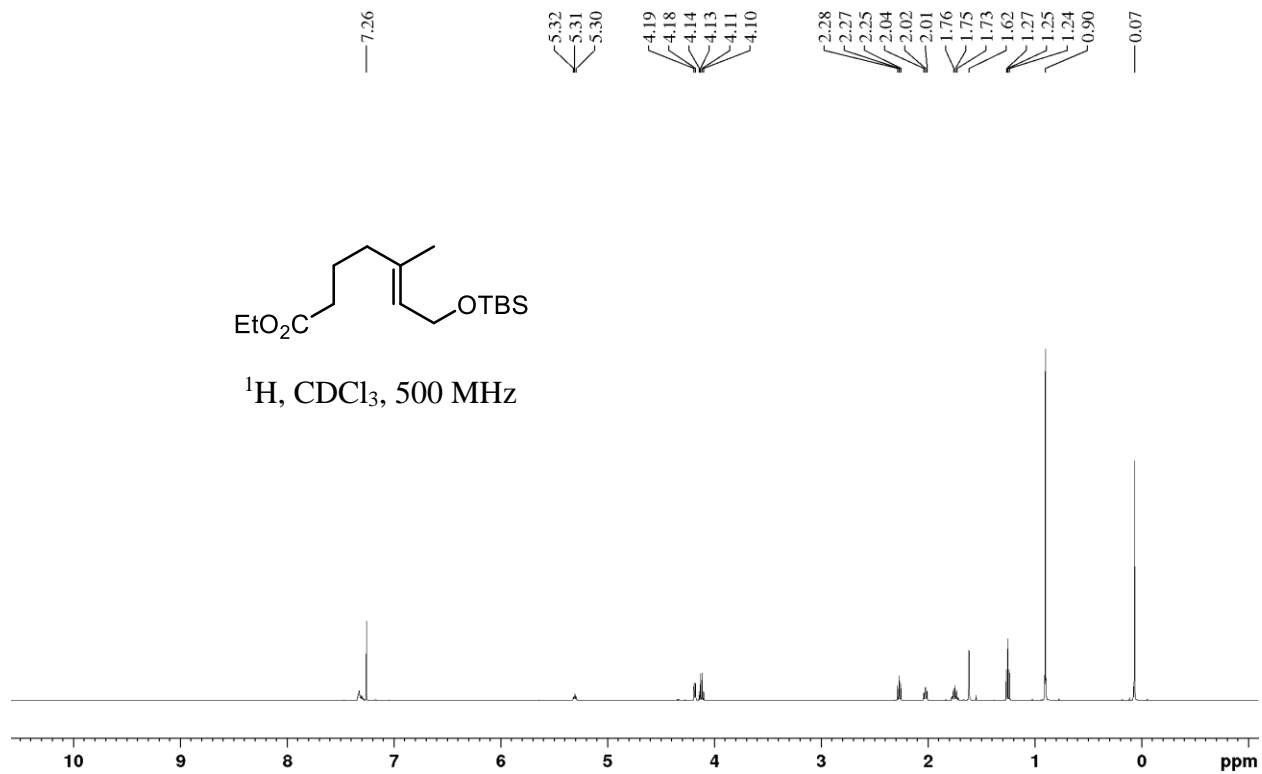


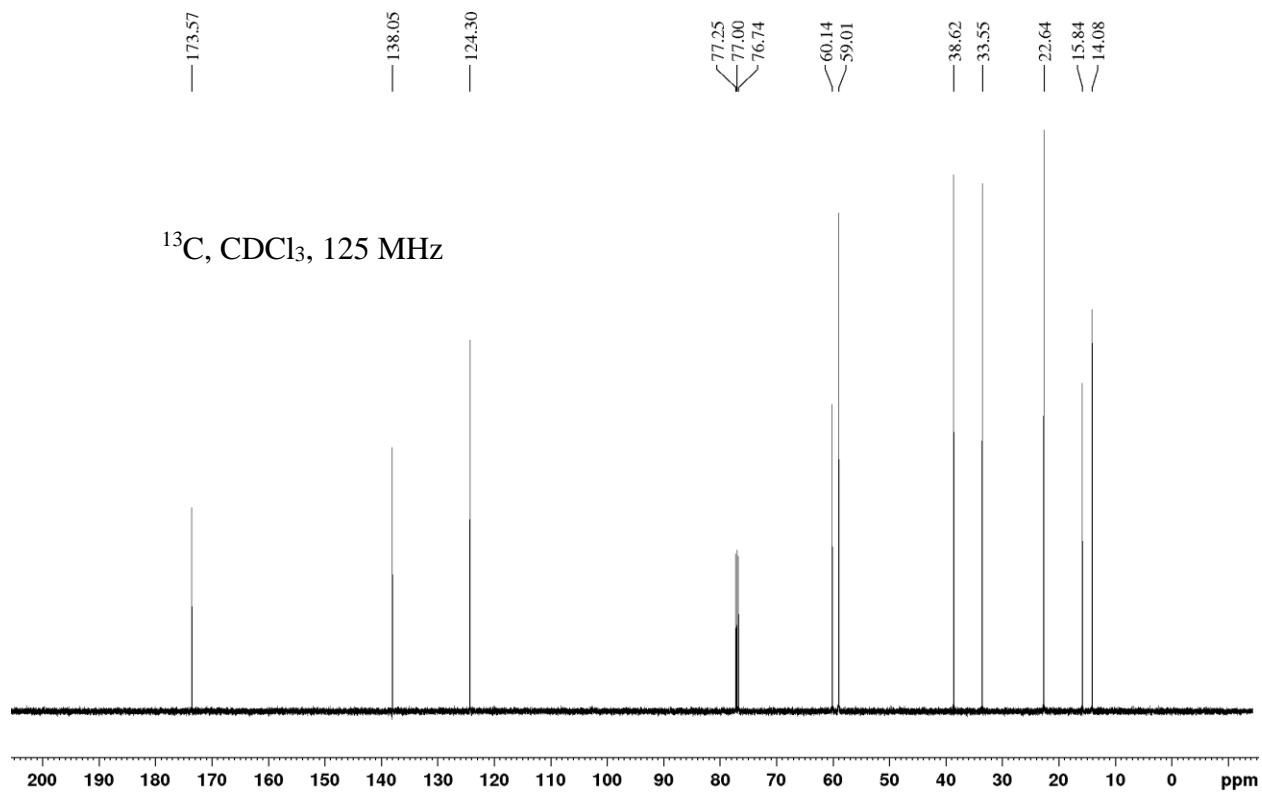
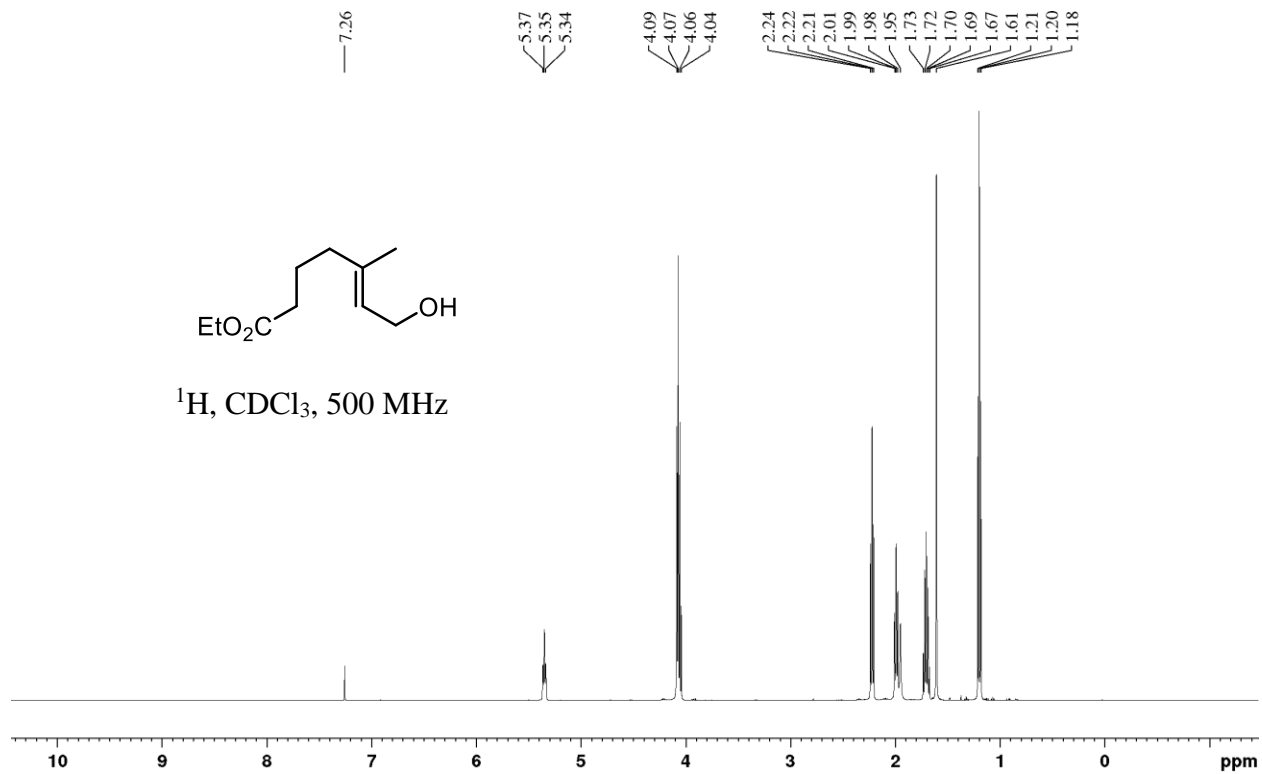
^{13}C , CDCl_3 , 125 MHz

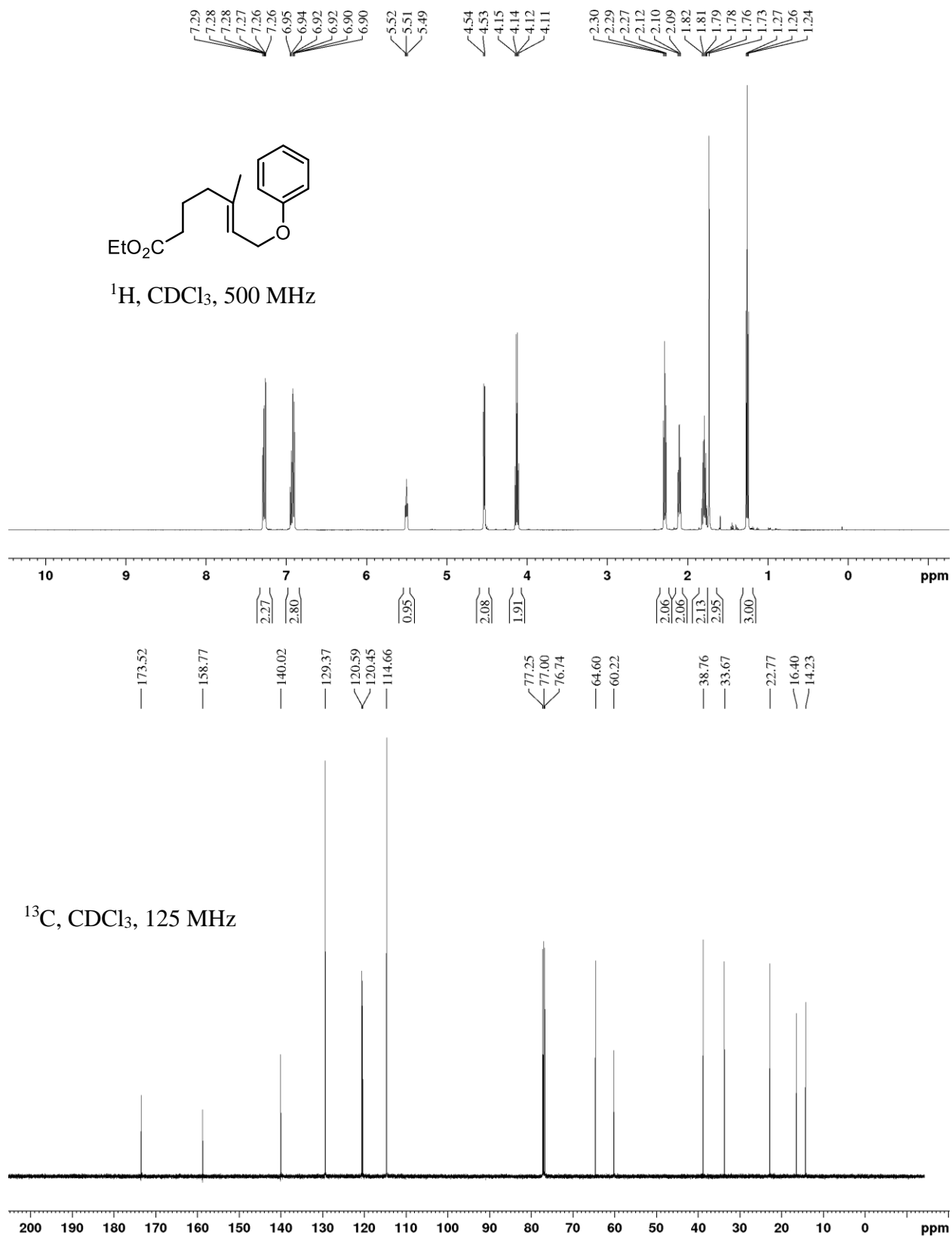


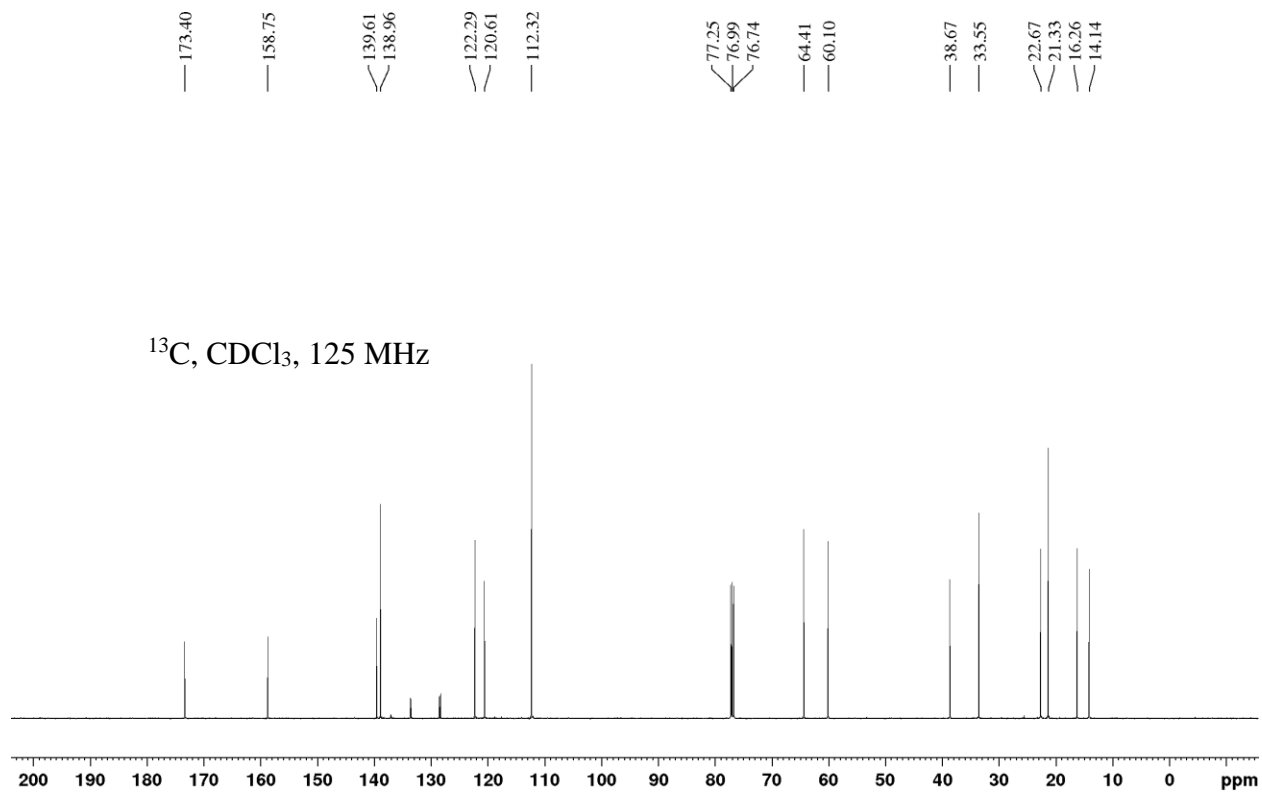
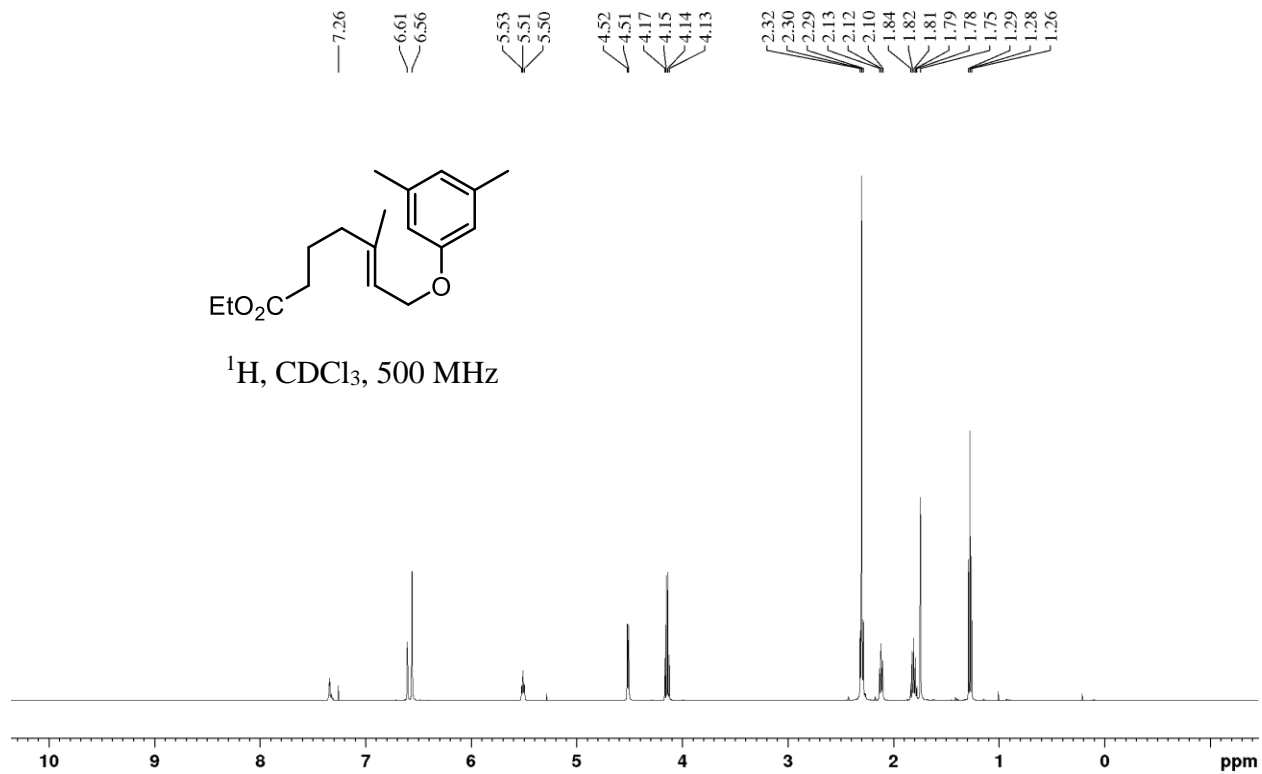




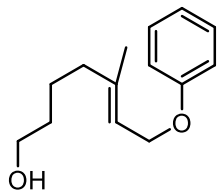




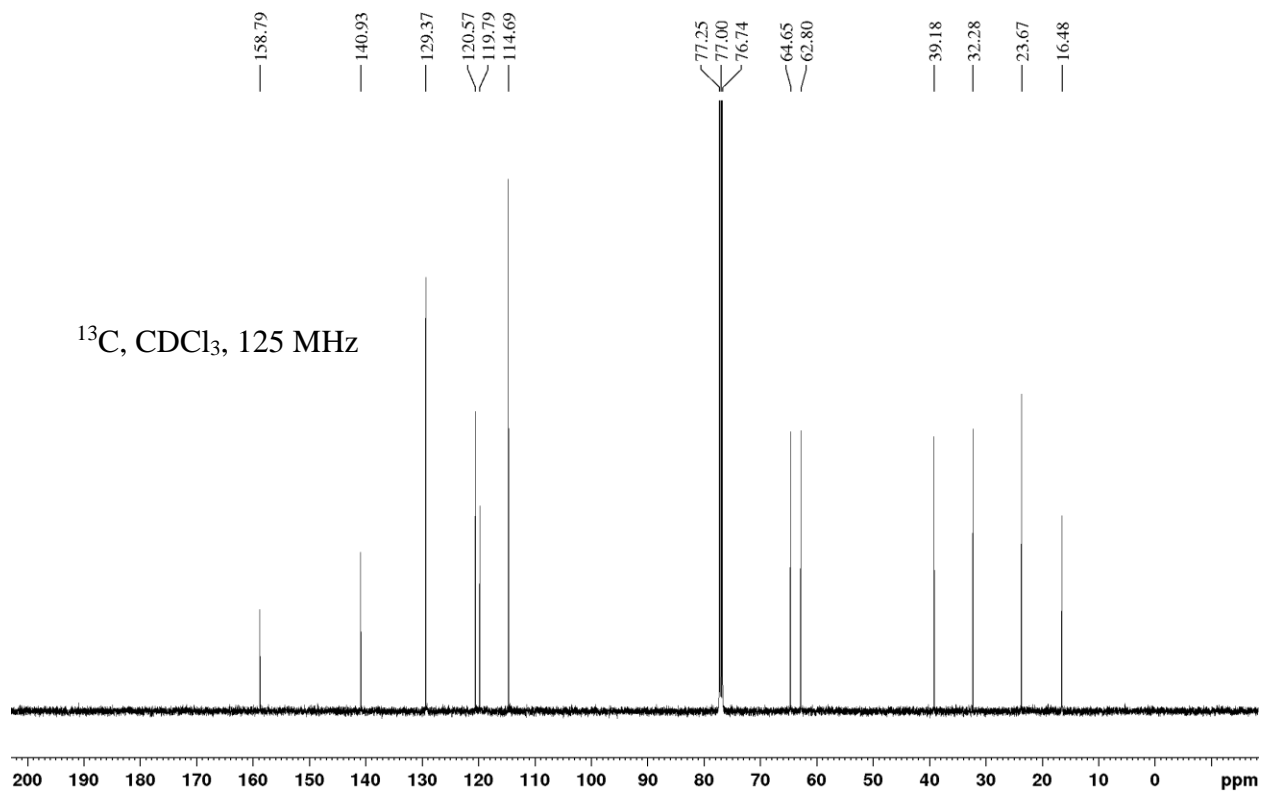
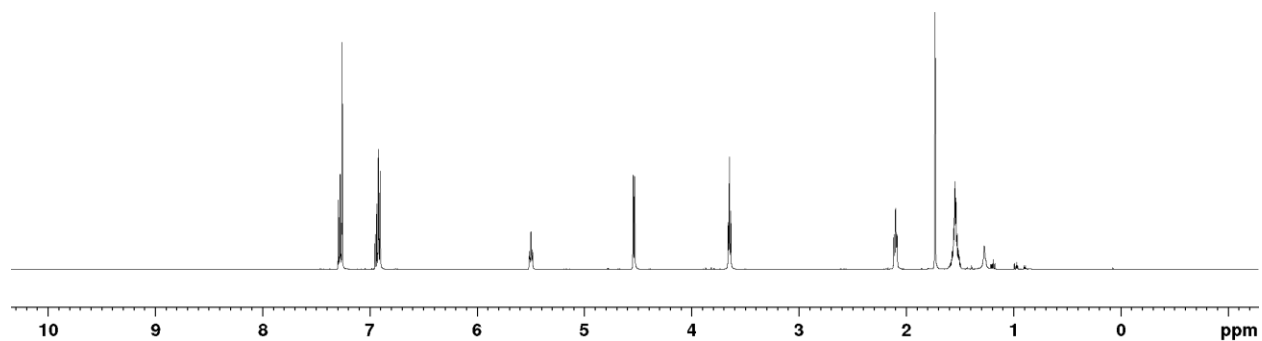




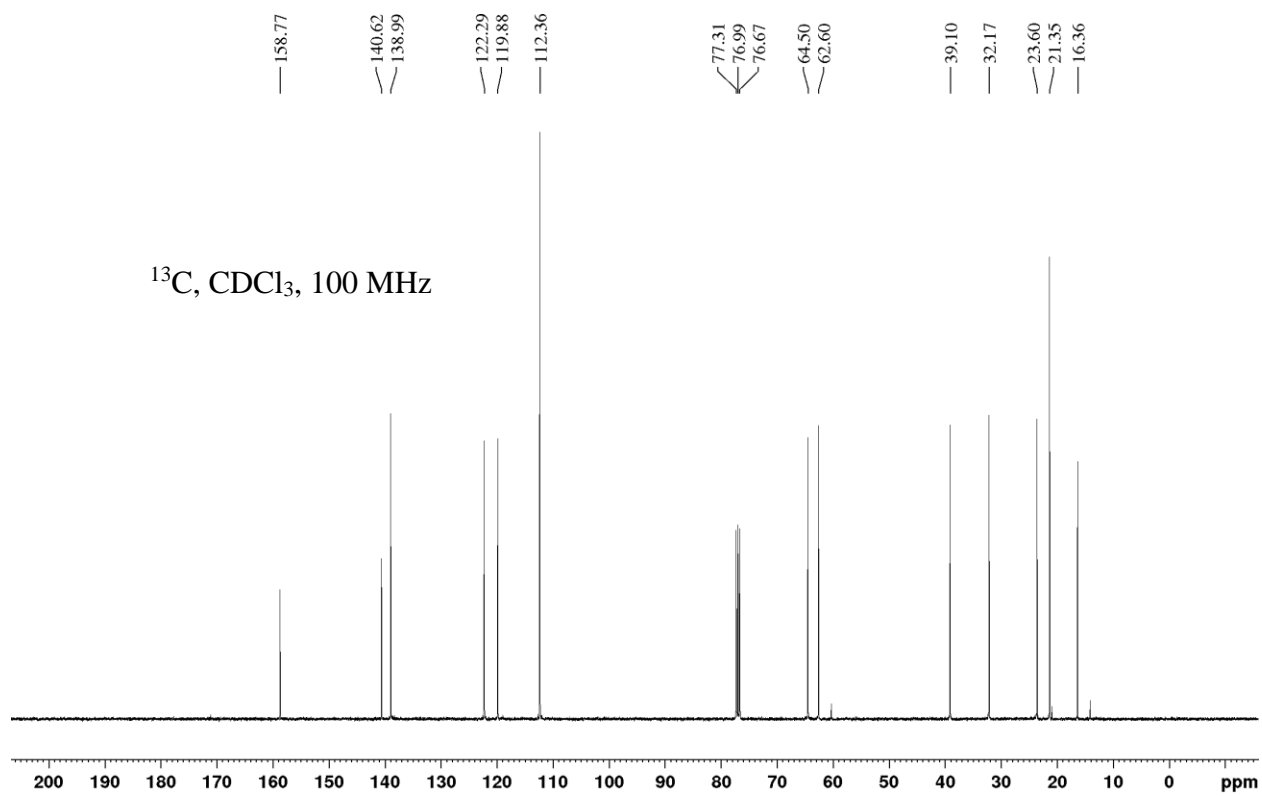
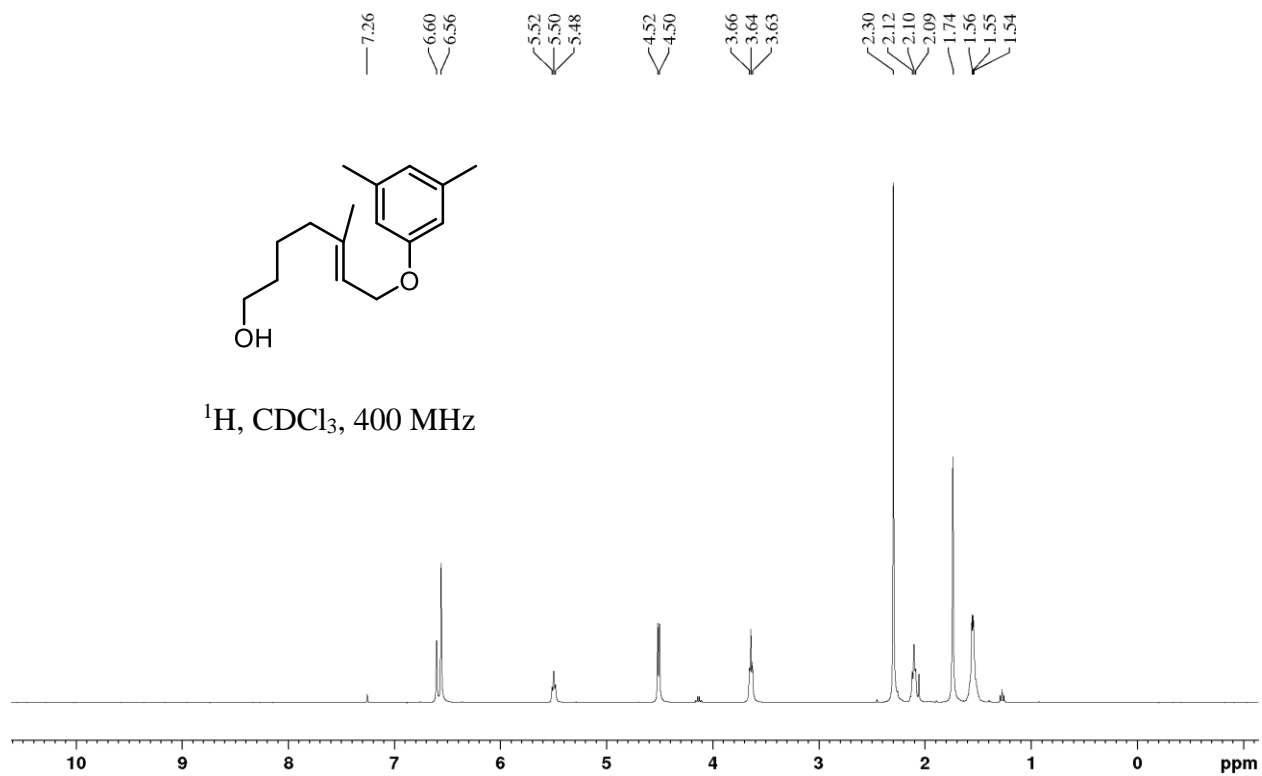
7.30
7.29
7.28
7.28
7.27
7.27
7.26
7.26
6.95
6.95
6.94
6.94
6.94
6.93
6.92
6.92
6.91
6.91
6.91
5.51
5.50
5.49
4.55
4.53
3.66
3.65
3.64
2.11
2.10
2.09
1.73
1.57
1.56
1.56
1.55
1.55
1.55
1.54
1.54
1.54
1.53
1.53
1.52
1.27

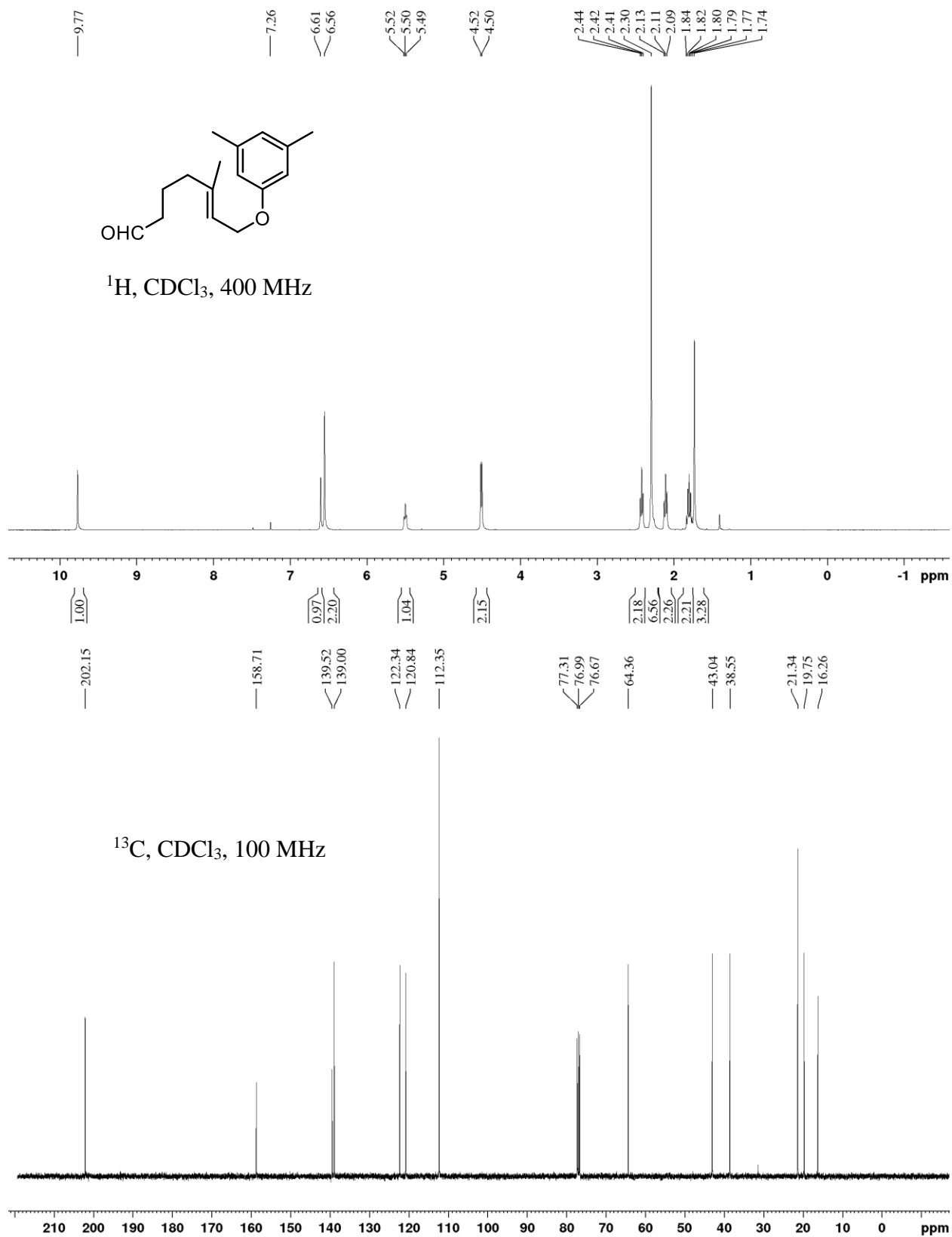


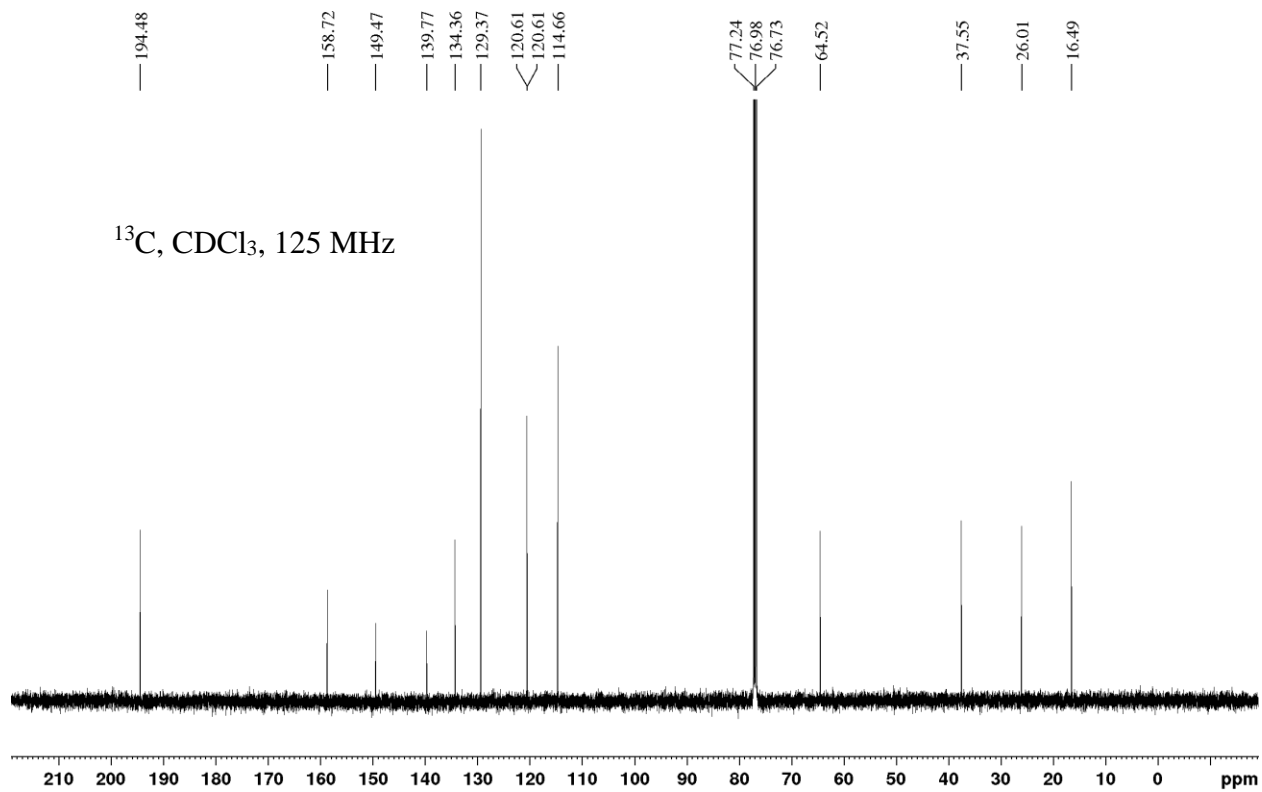
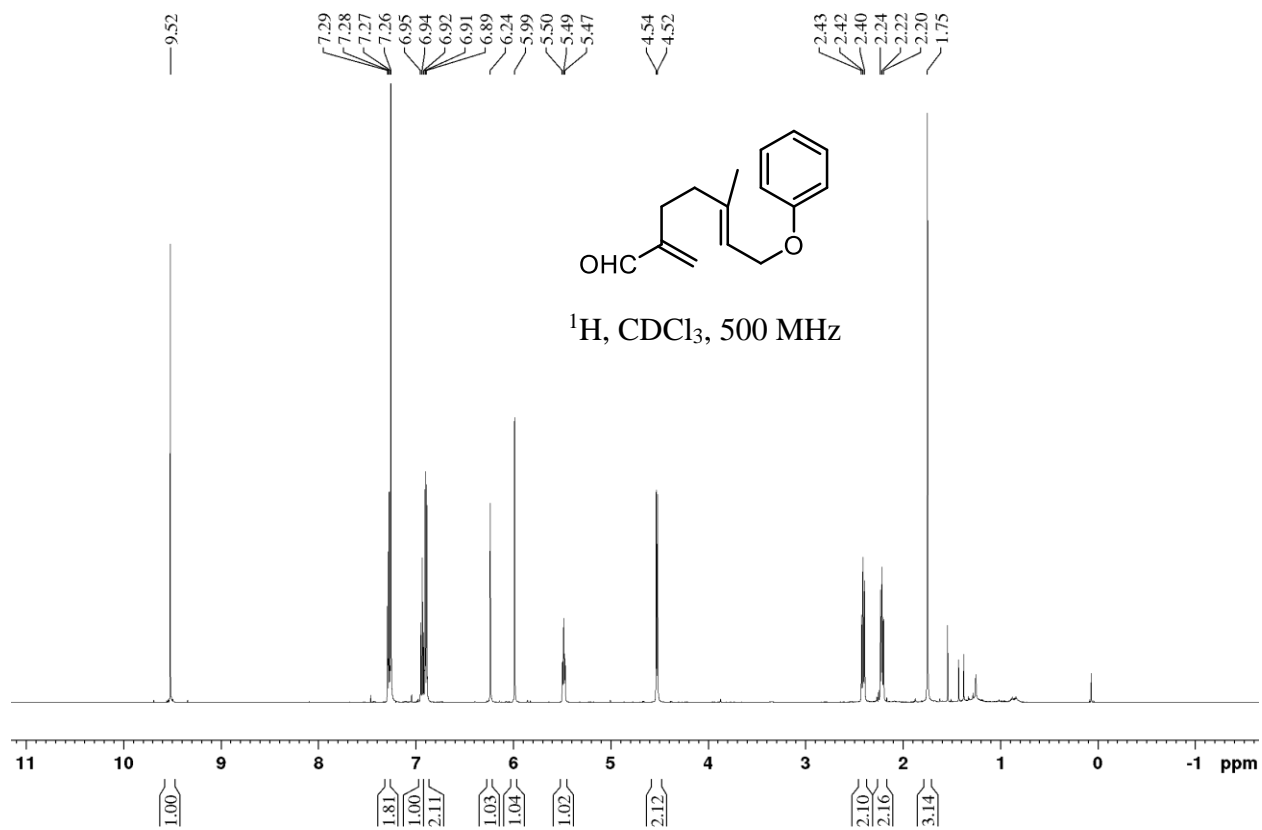
^1H , CDCl_3 , 500 MHz

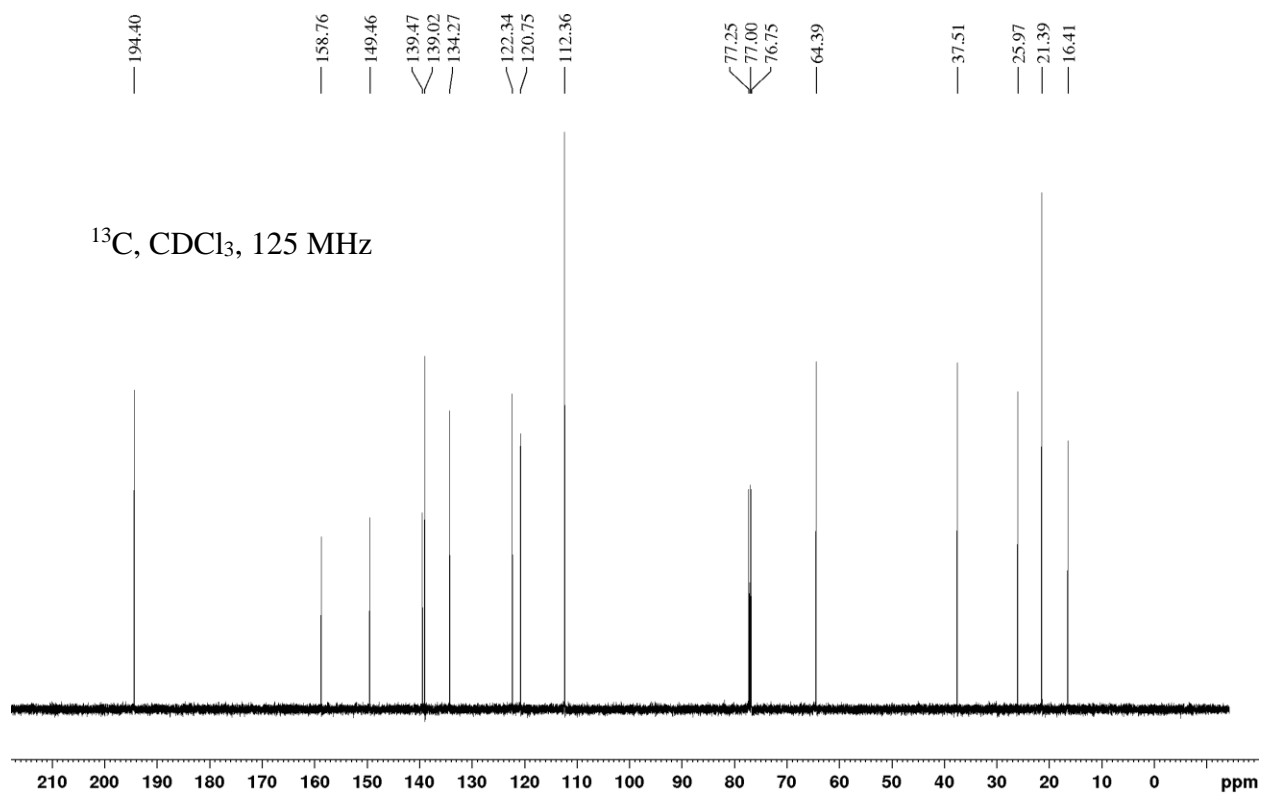
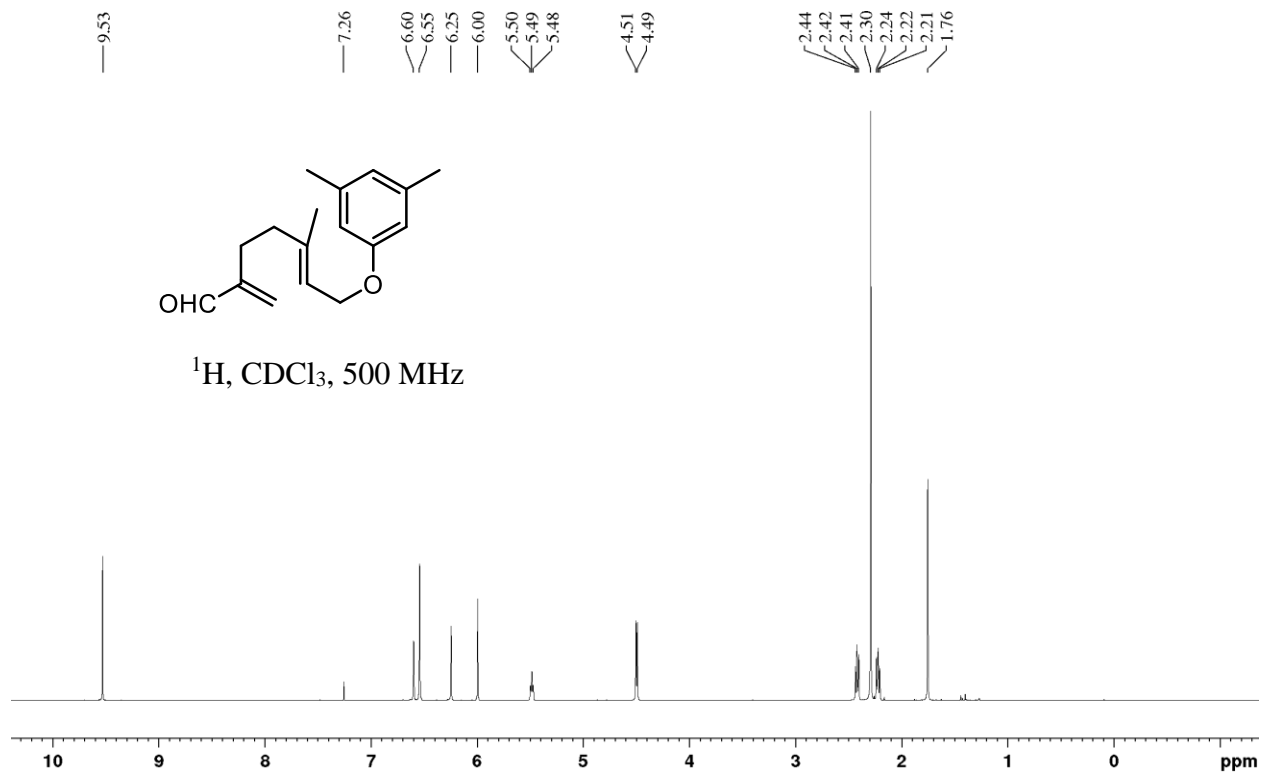


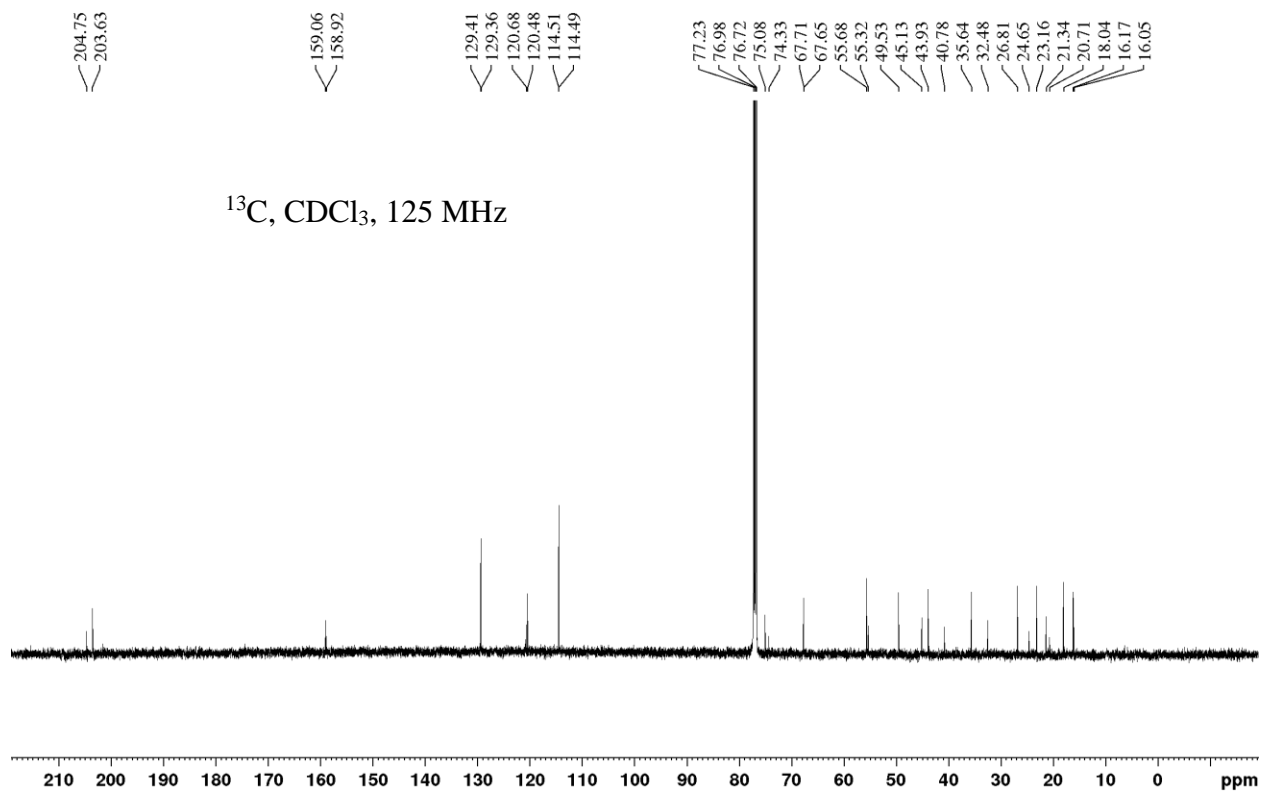
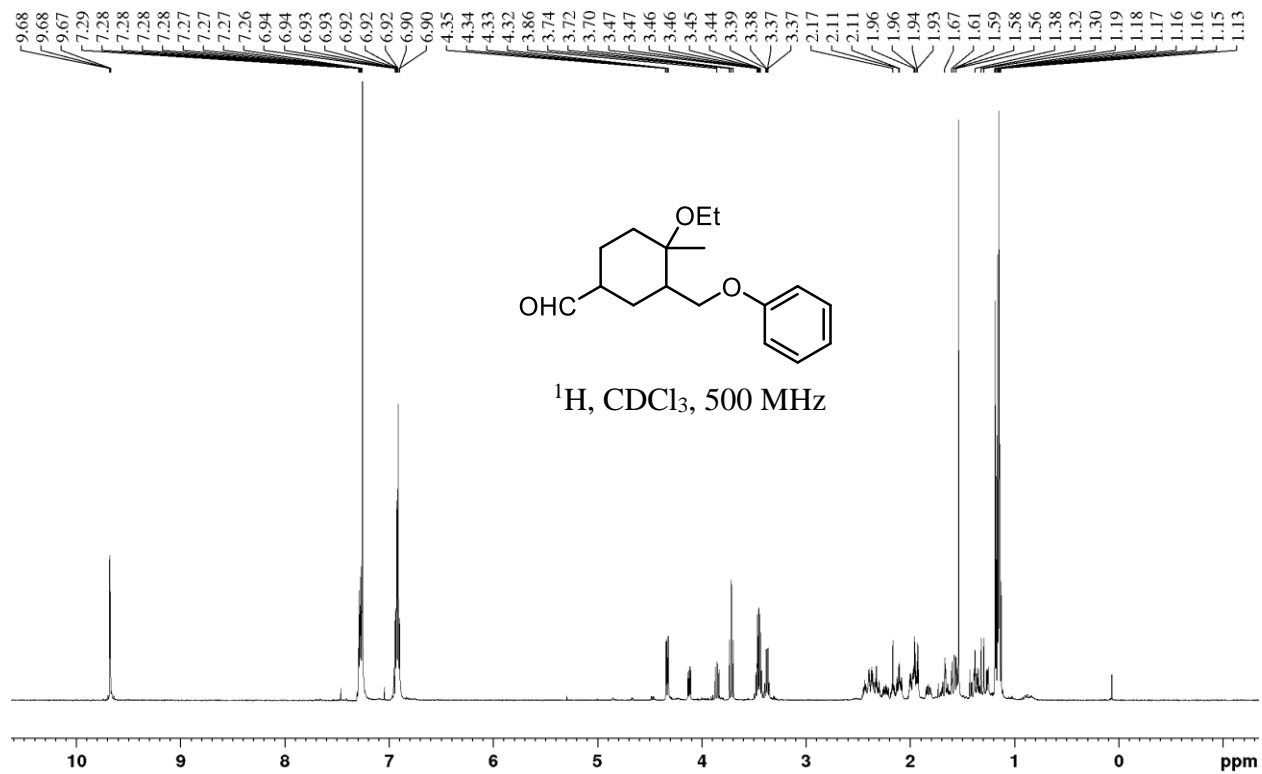
^{13}C , CDCl_3 , 125 MHz

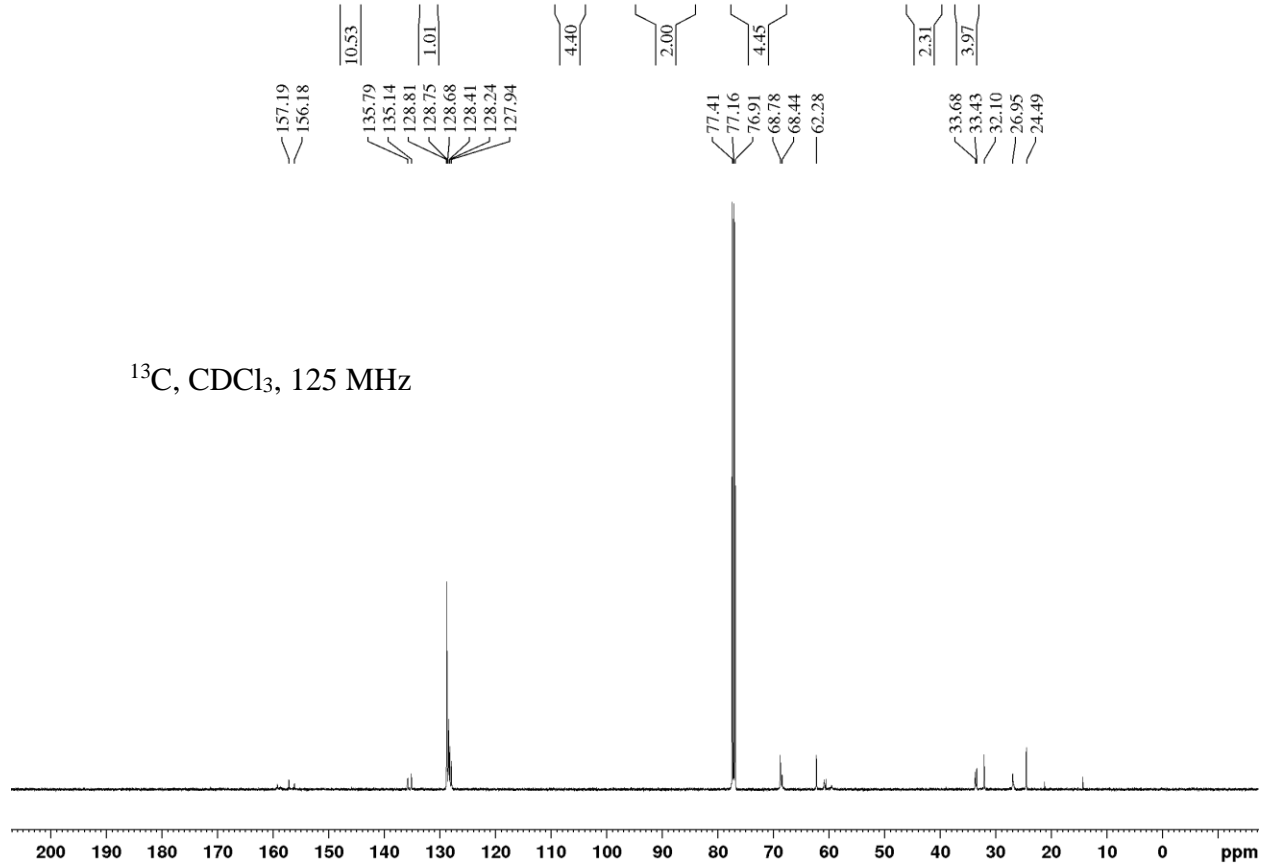
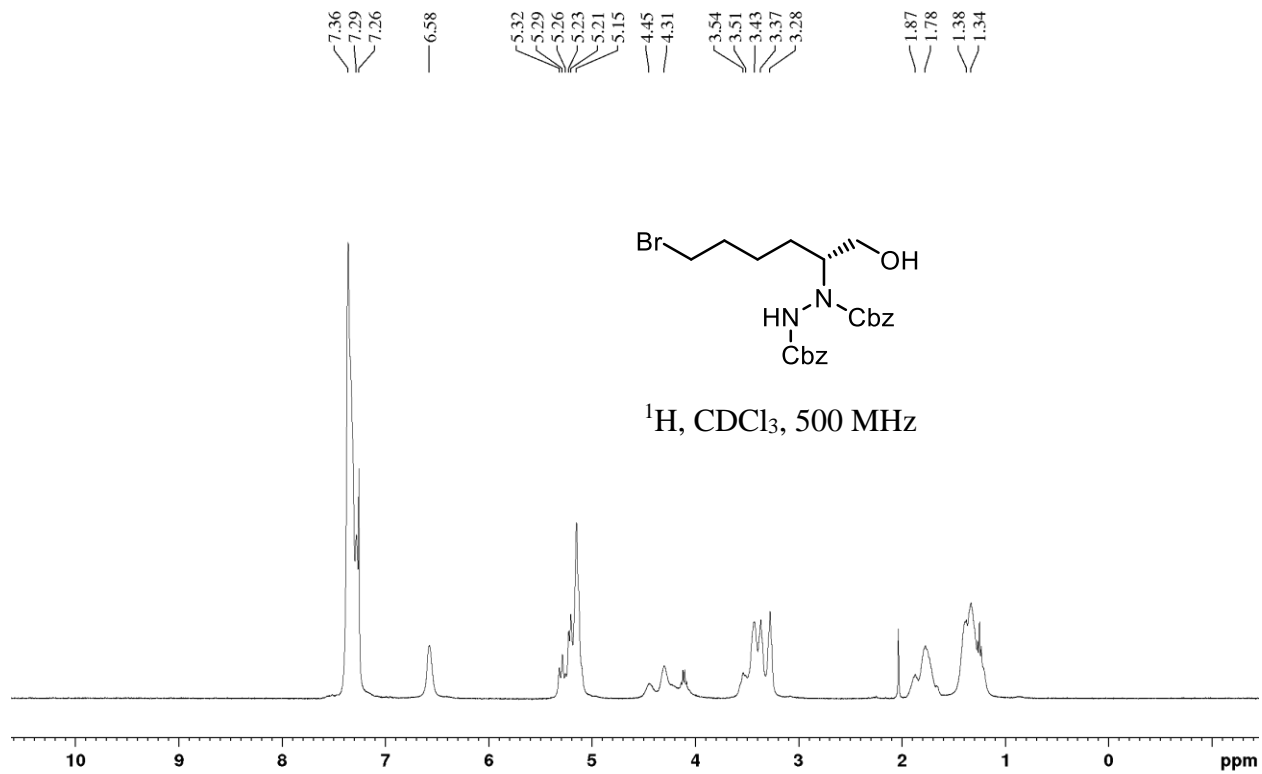


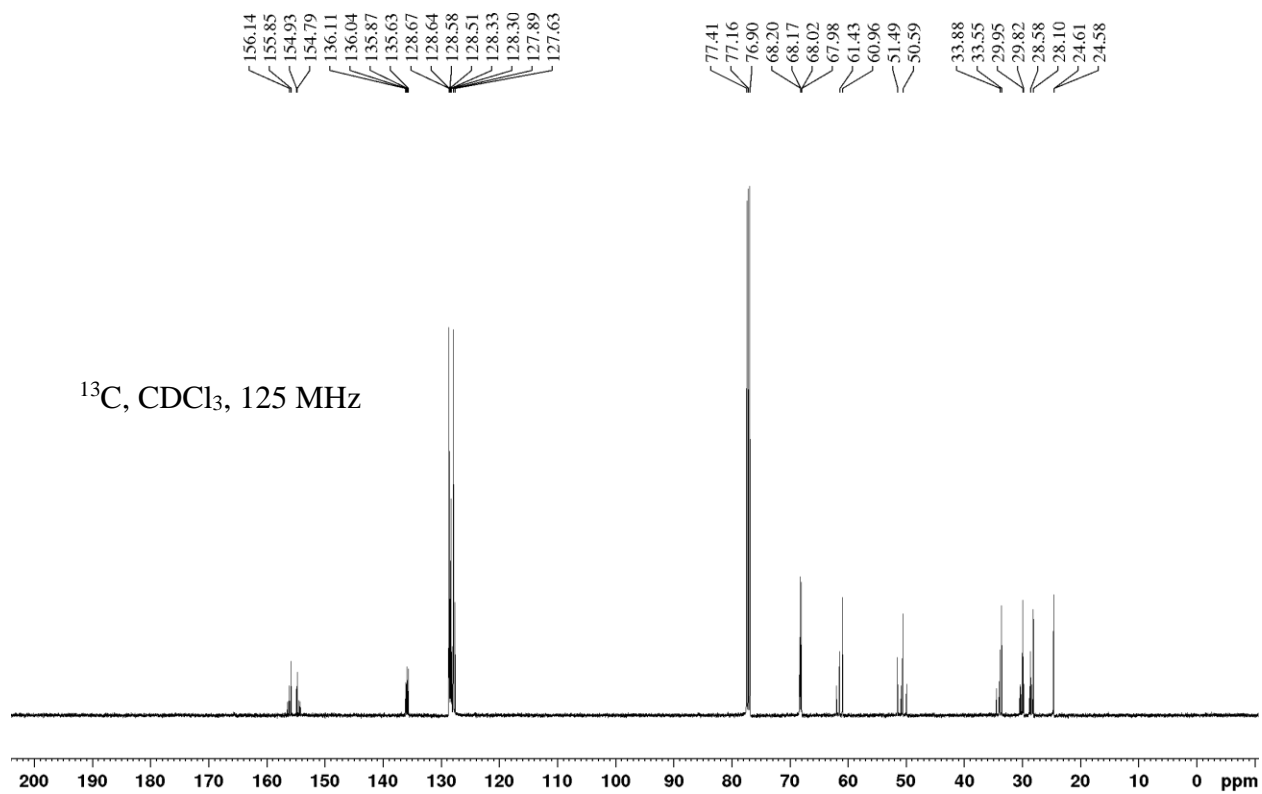
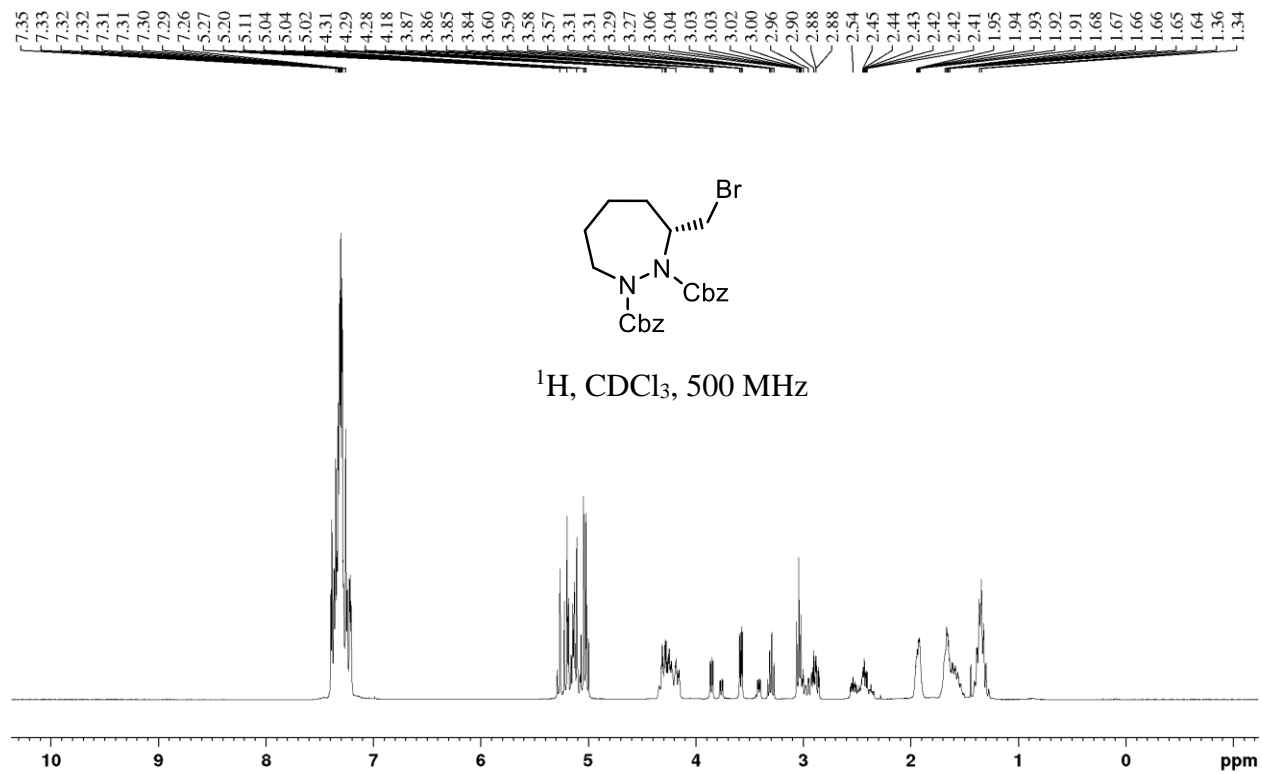


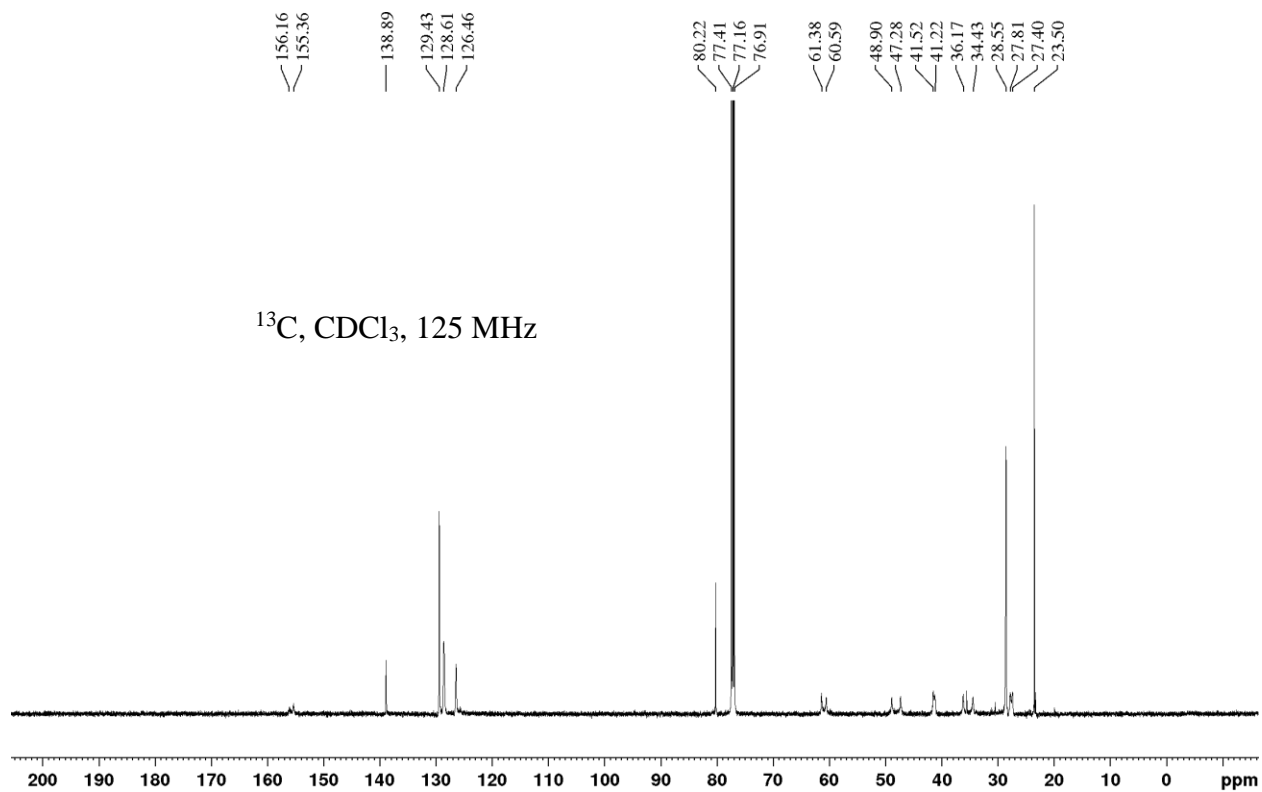
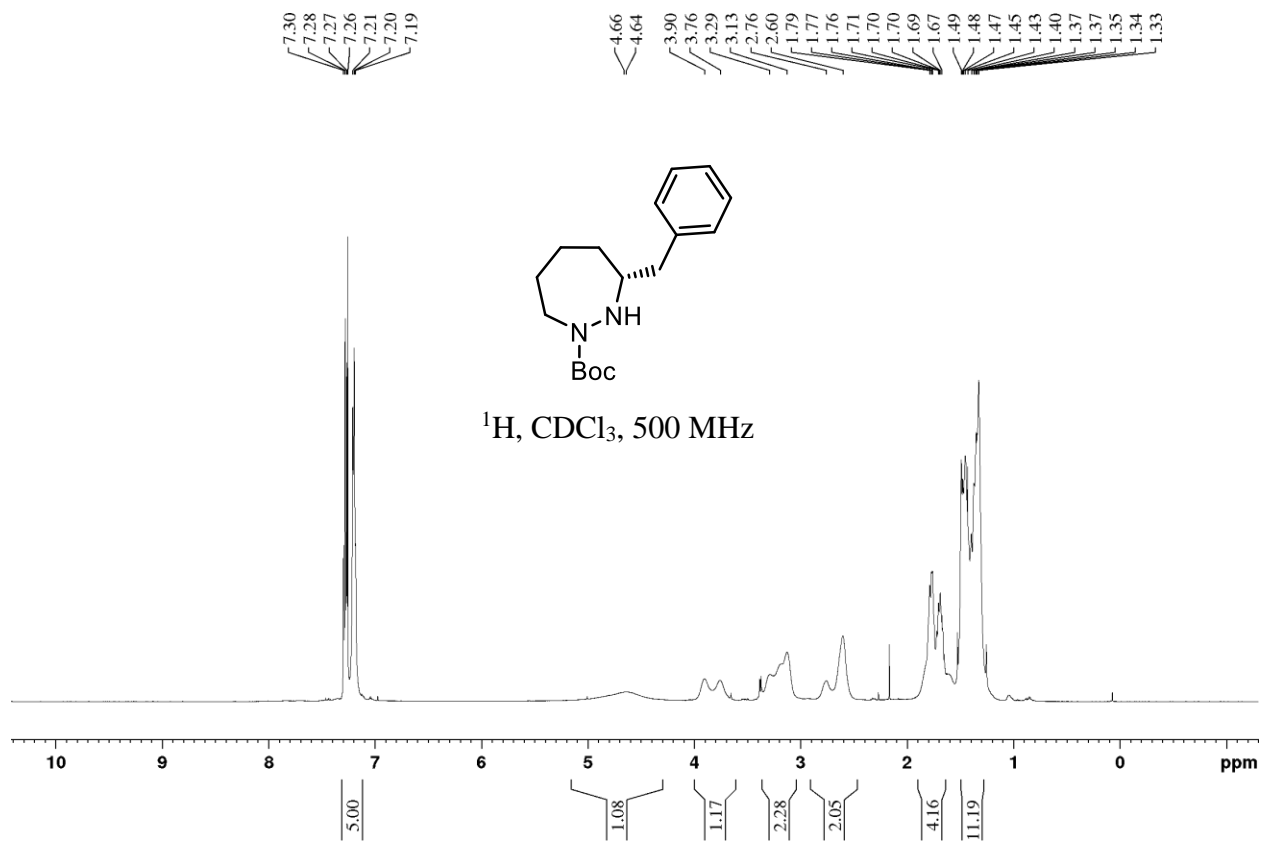


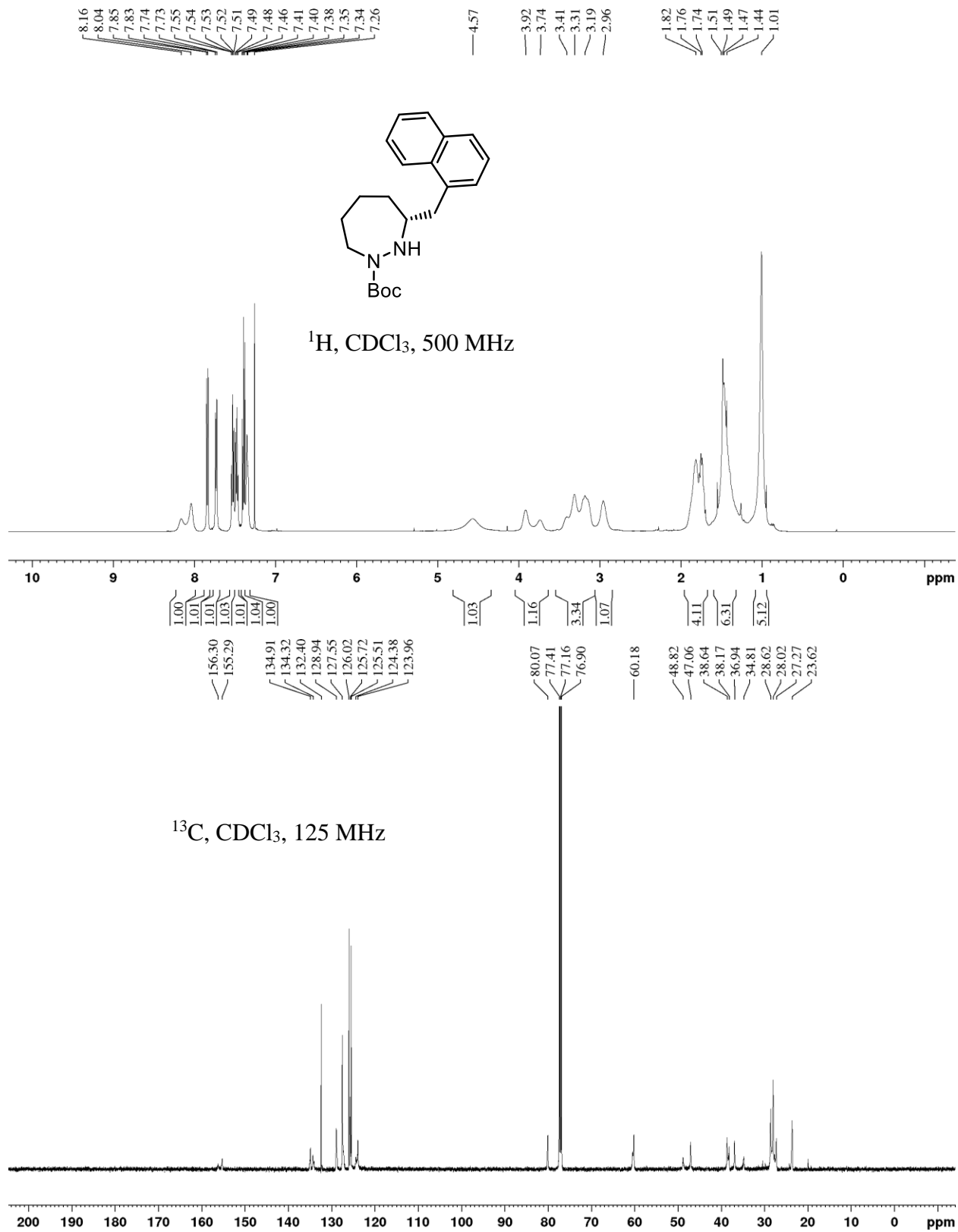


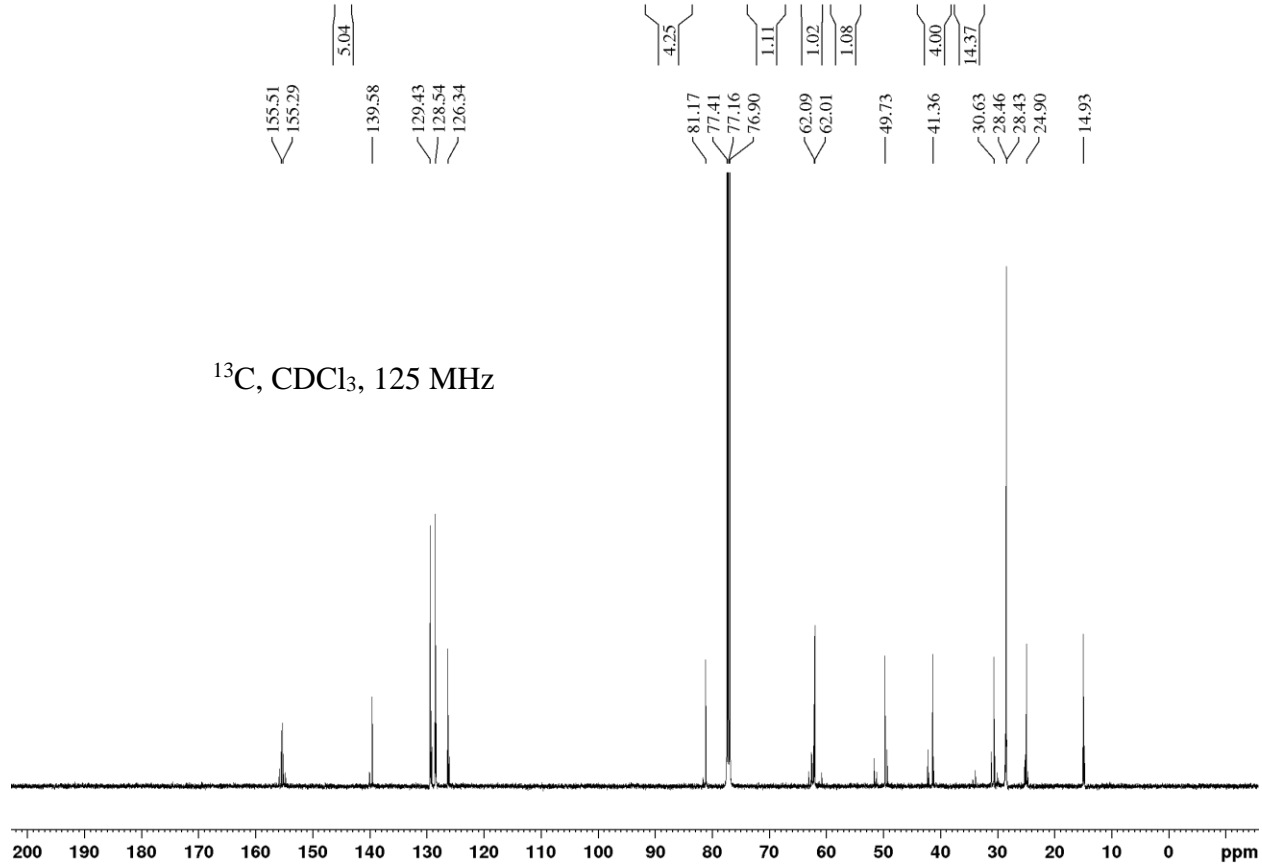
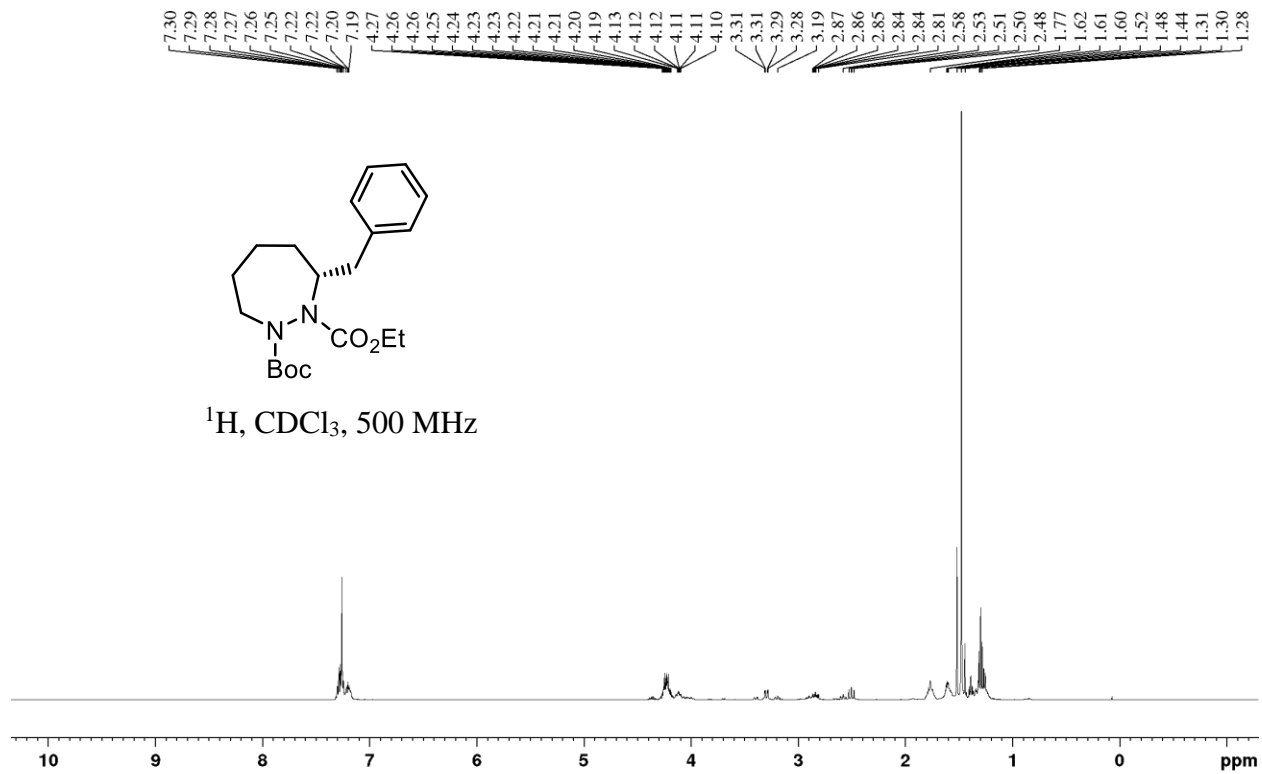


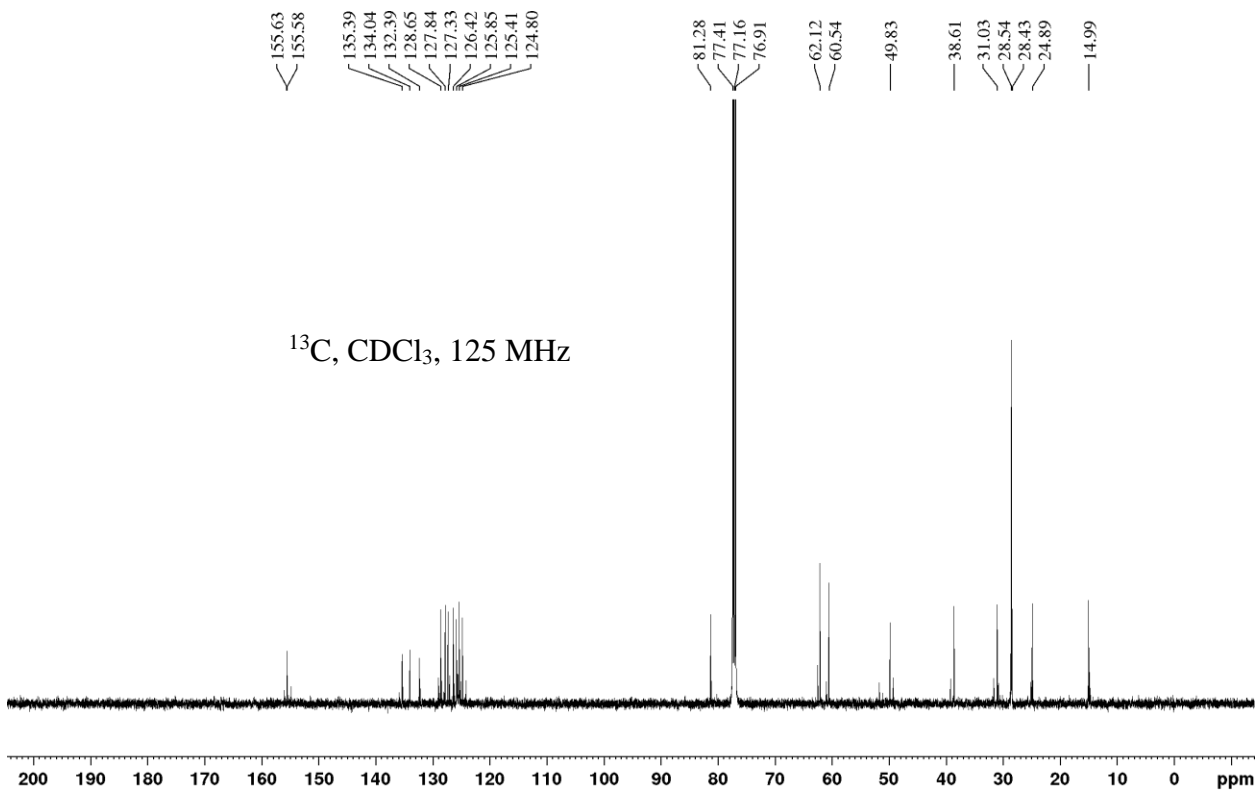
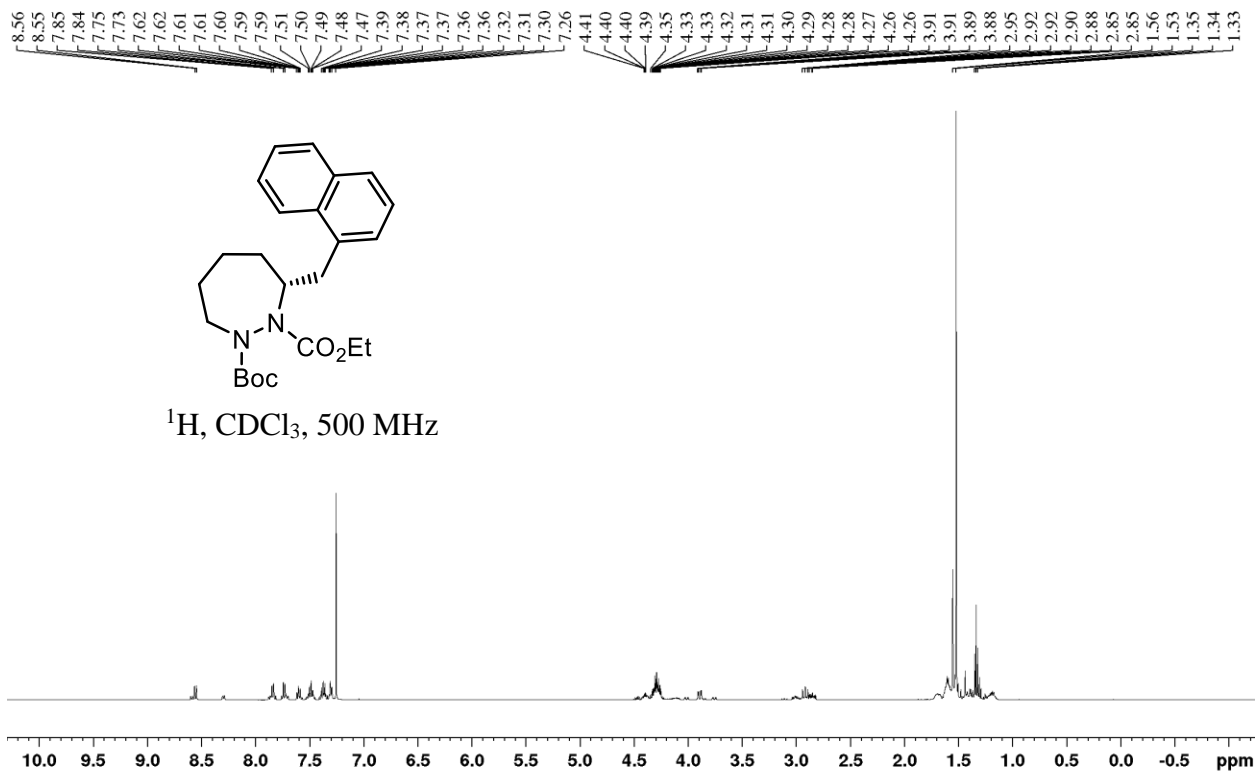


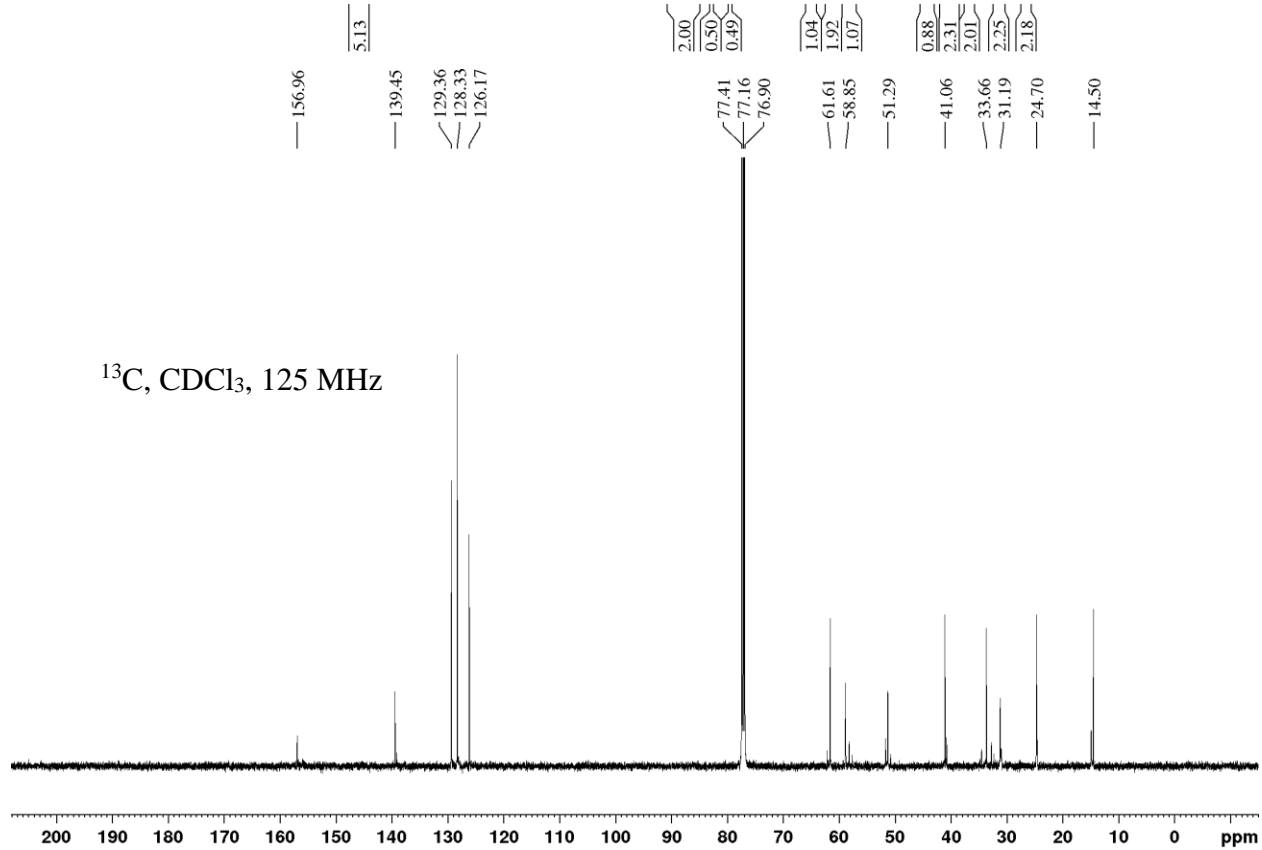
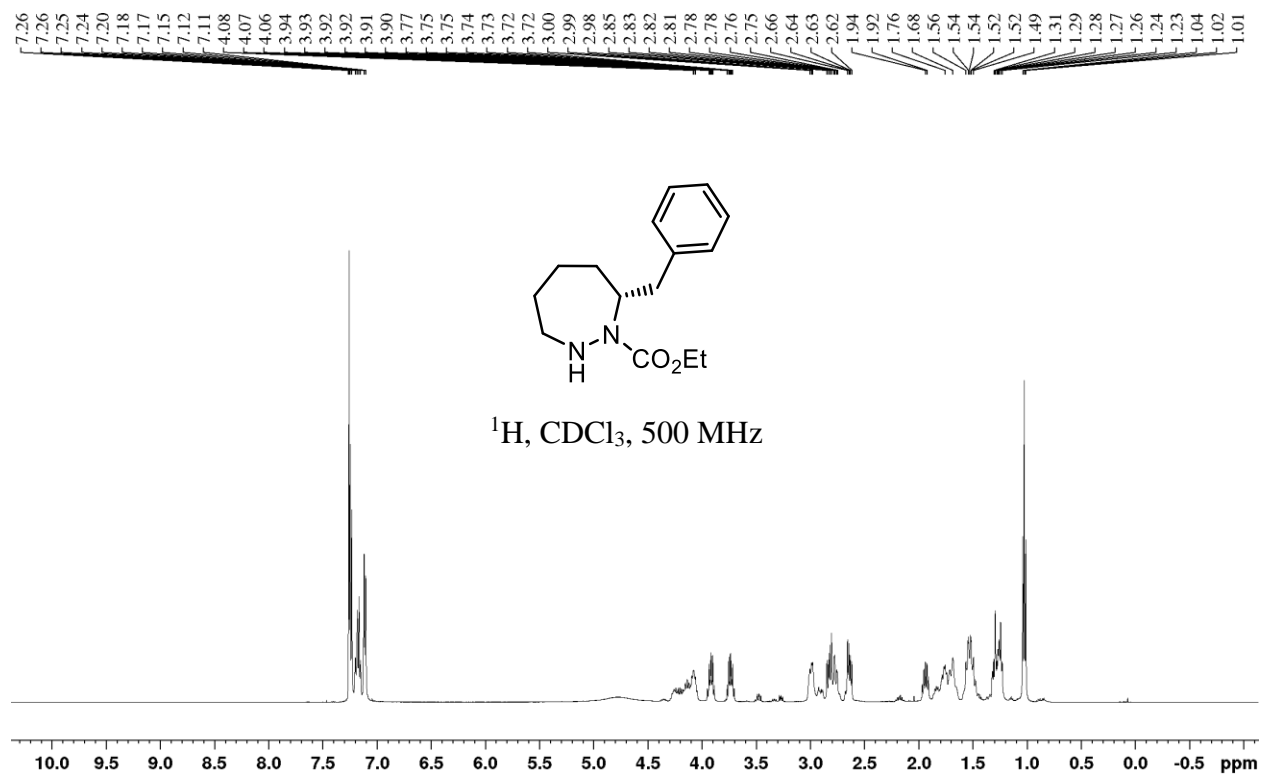




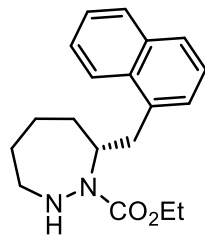




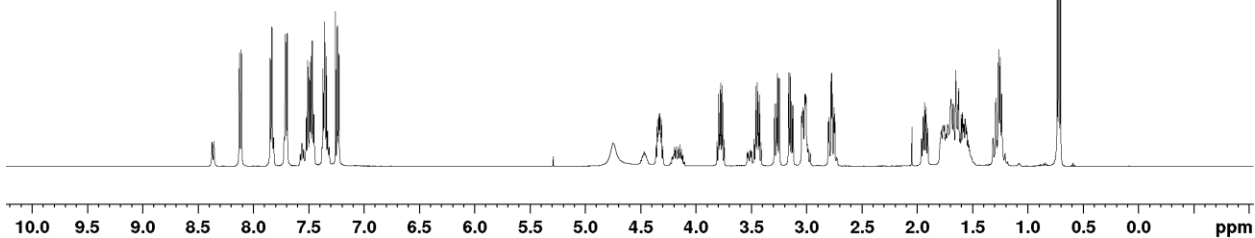




8.13
8.11
7.85
7.84
7.71
7.70
7.51
7.51
7.50
7.49
7.49
7.48
7.47
7.46
7.45
7.37
7.36
7.34
7.26
7.24
7.23
4.33
4.33
3.80
3.78
3.77
3.76
3.46
3.45
3.44
3.43
3.29
3.27
3.26
3.25
3.16
3.15
3.13
3.12
3.04
3.03
3.02
3.01
2.78
2.77
1.95
1.93
1.92
1.69
1.67
1.65
1.63
1.62
1.60
1.59
1.29
1.25
1.24
0.73
0.70



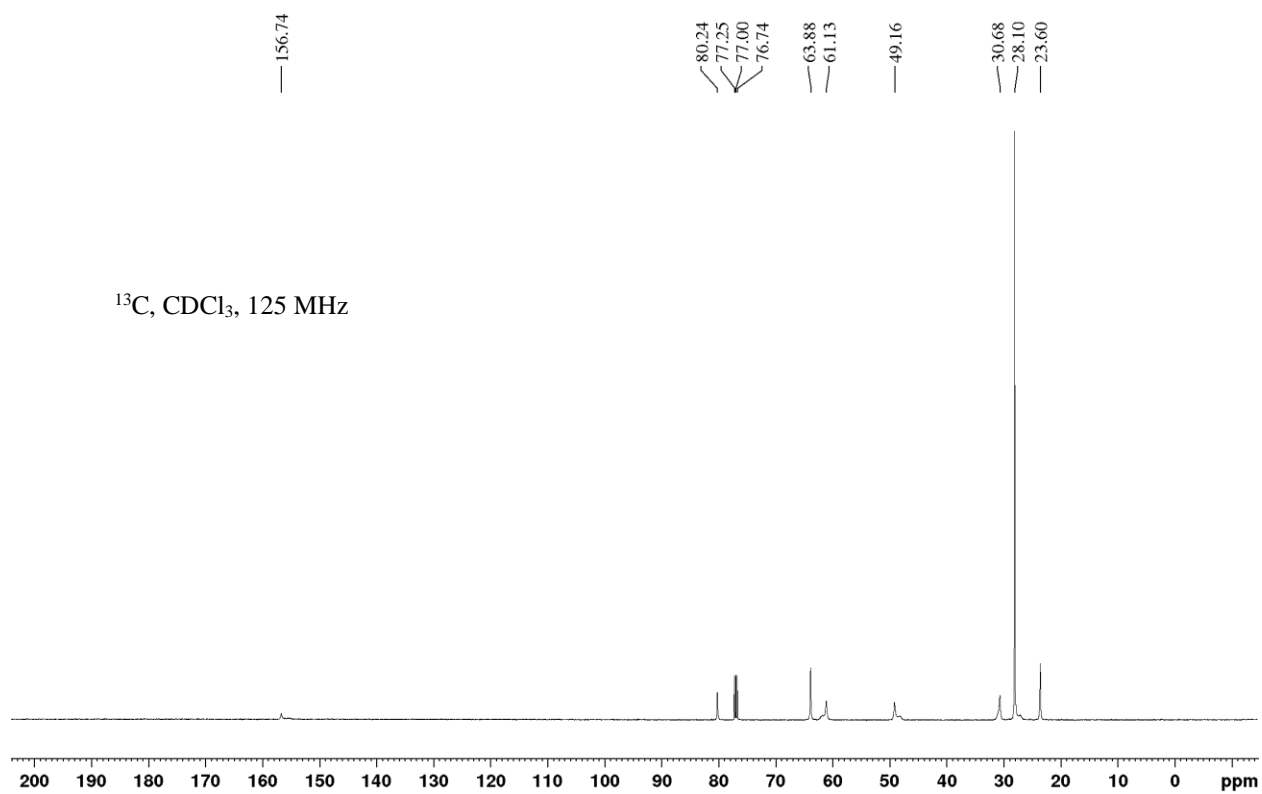
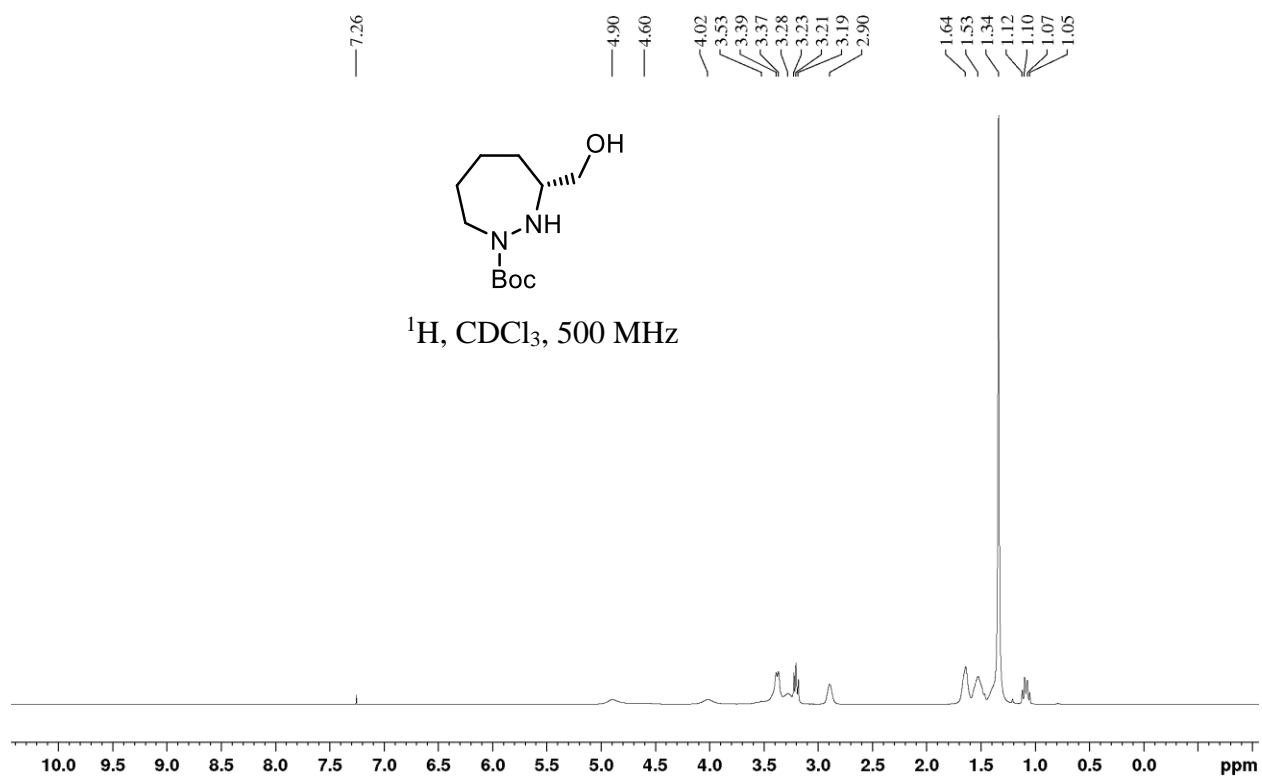
^1H , CDCl_3 , 500 MHz

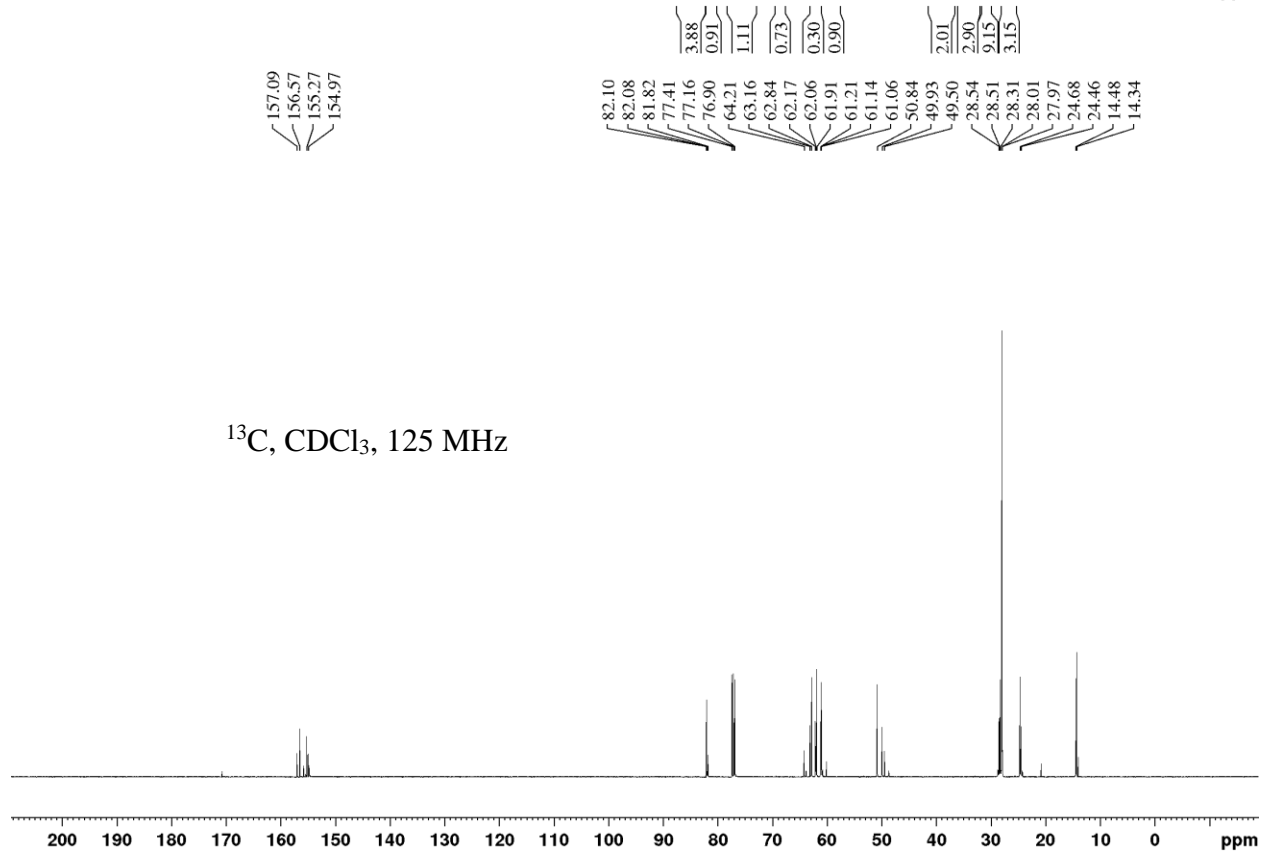
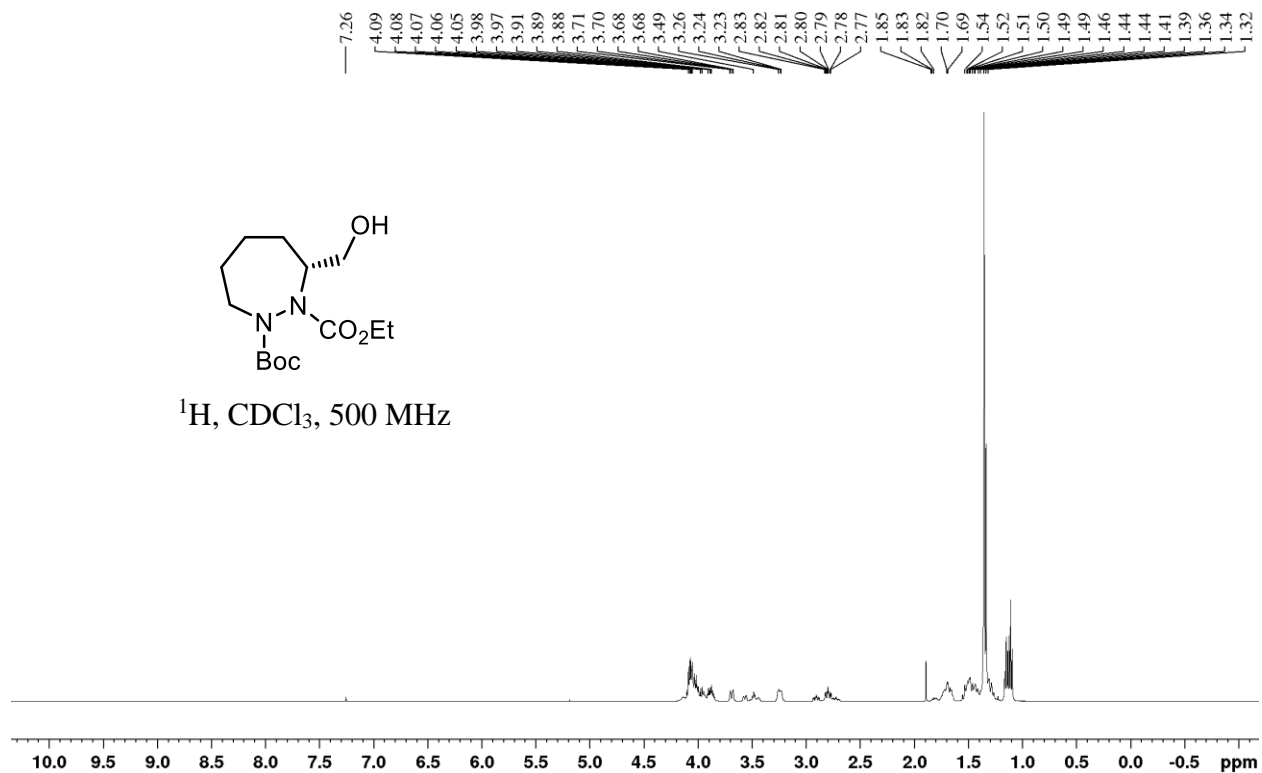


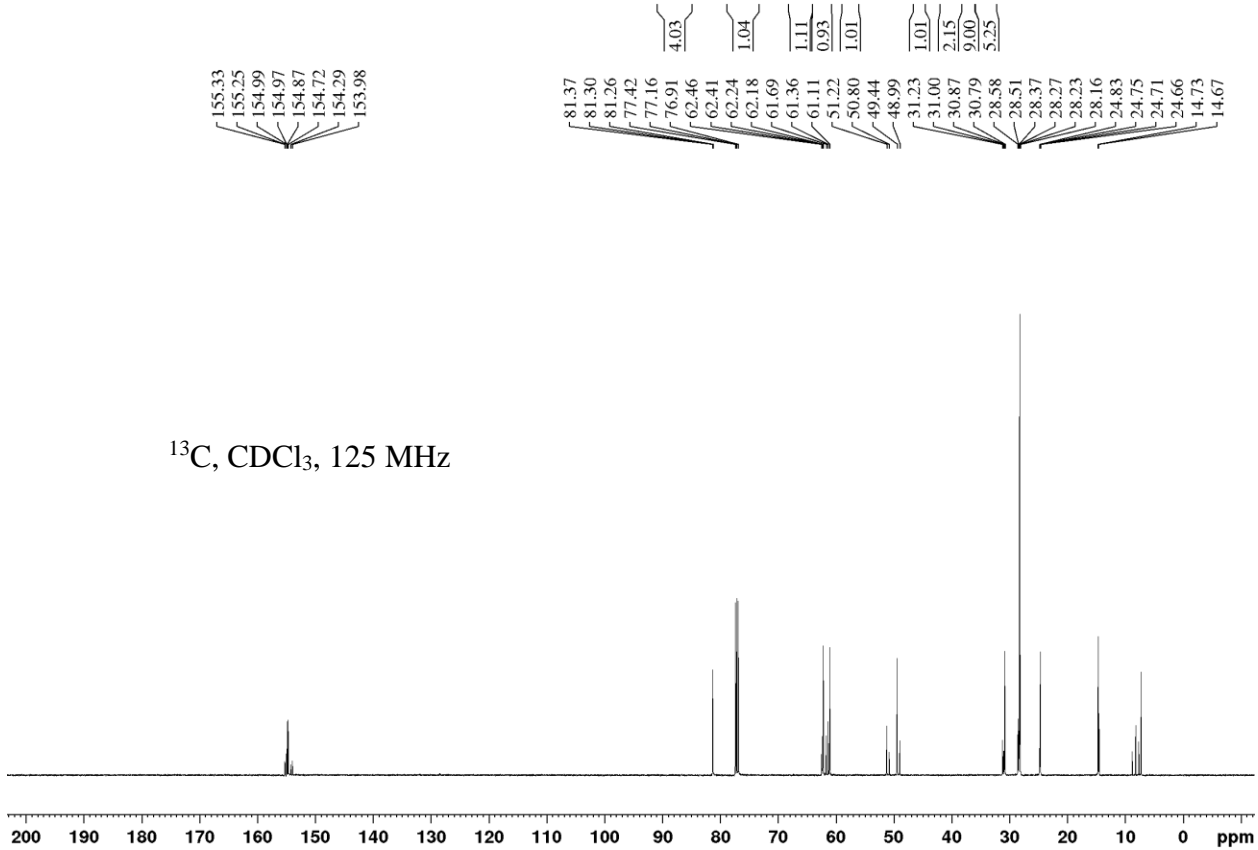
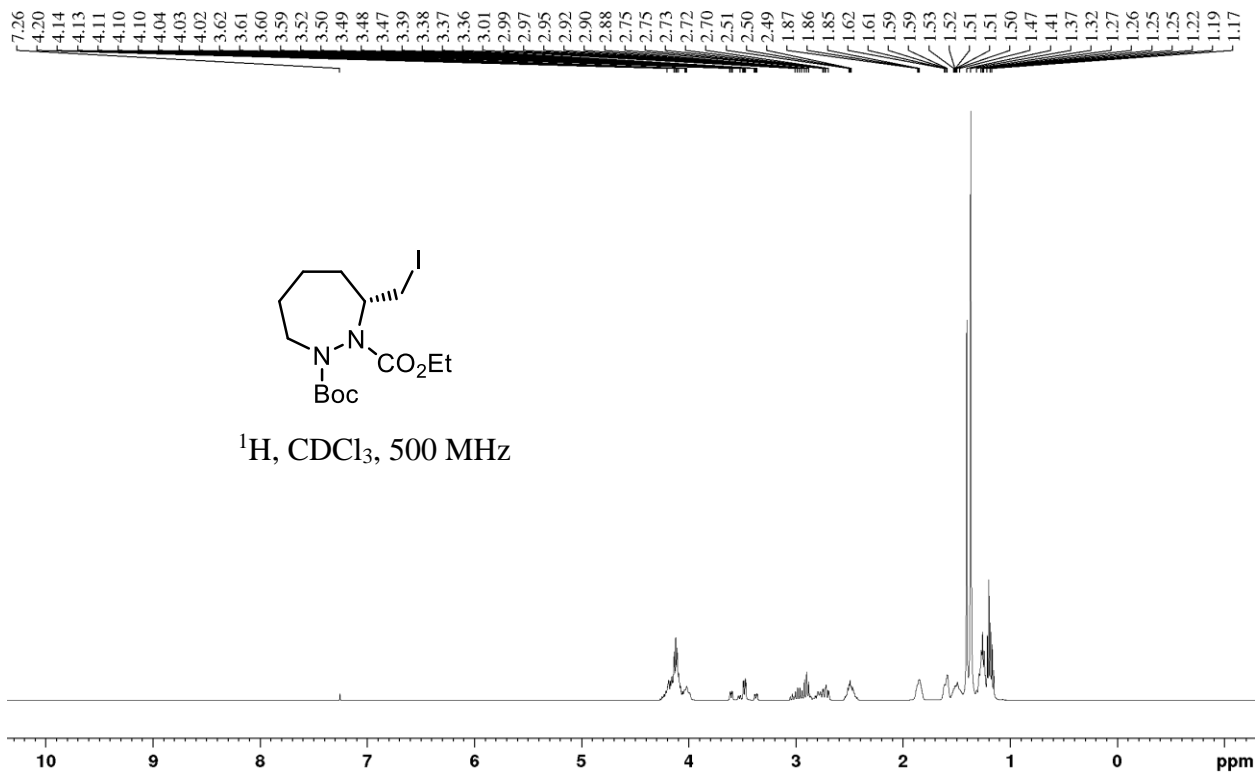
0.20
0.79
0.99
1.00
0.22
0.84
0.99
1.02
0.23
0.78
156.95
135.44
133.93
132.41
128.82
127.59
127.03
125.79
125.59
125.53
123.91
77.41
77.16
76.91
61.50
57.56
51.42
38.30
33.83
31.29
24.71
13.89

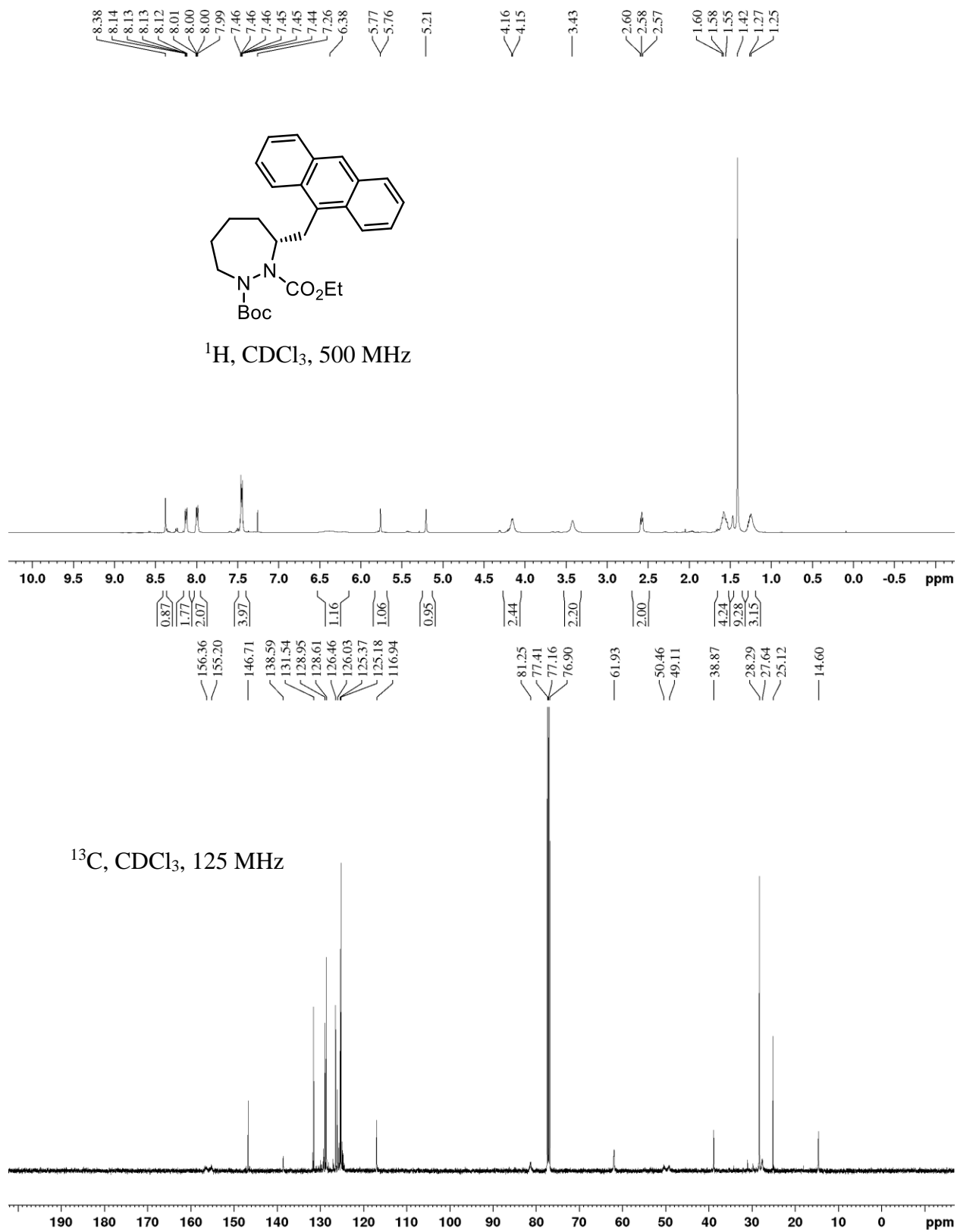
^{13}C , CDCl_3 , 125 MHz

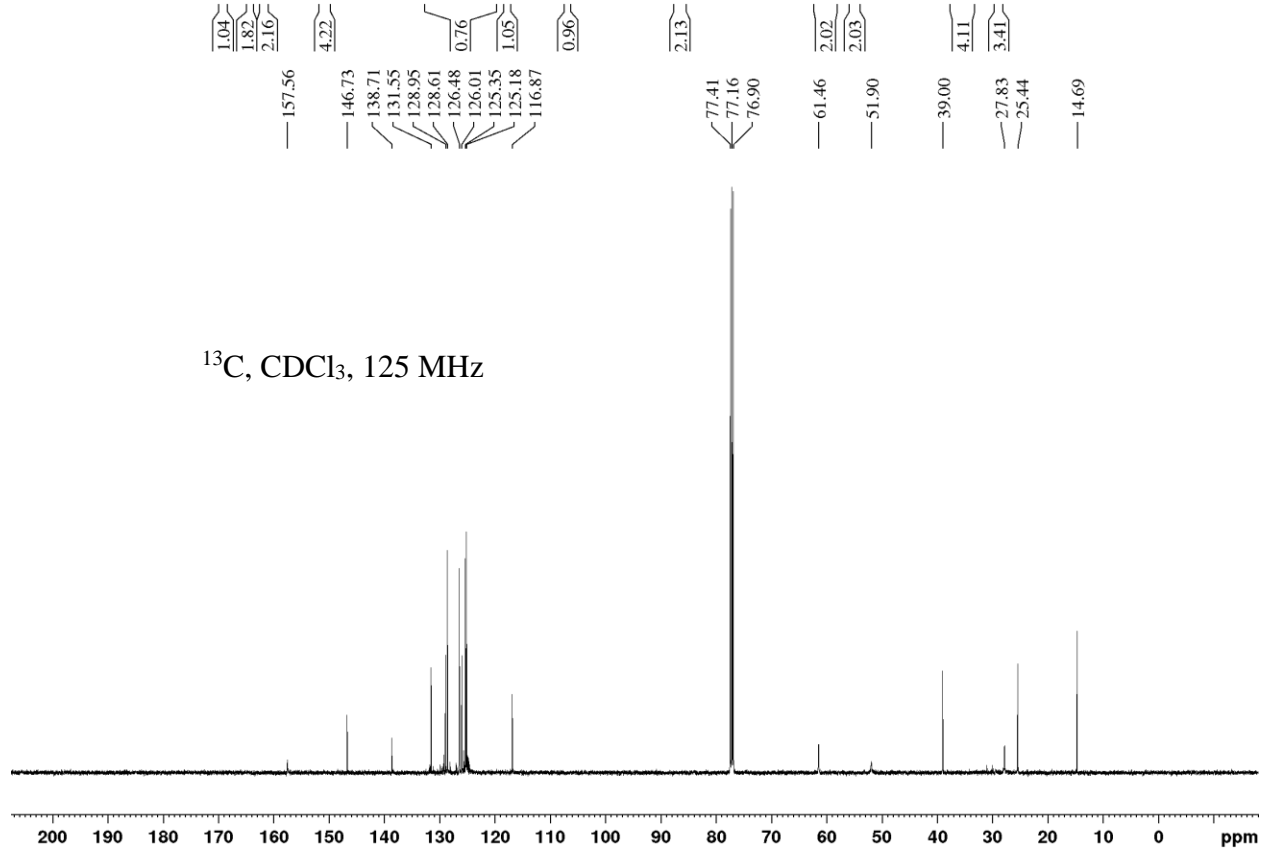
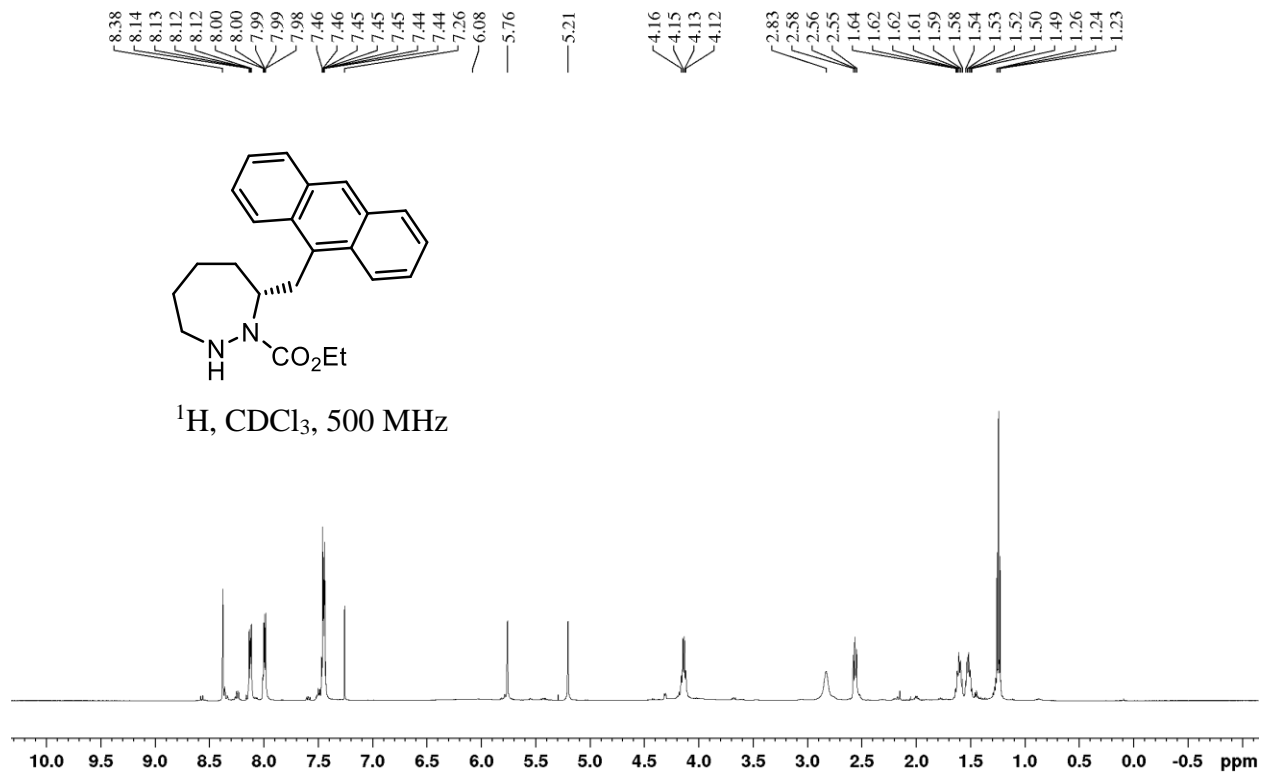


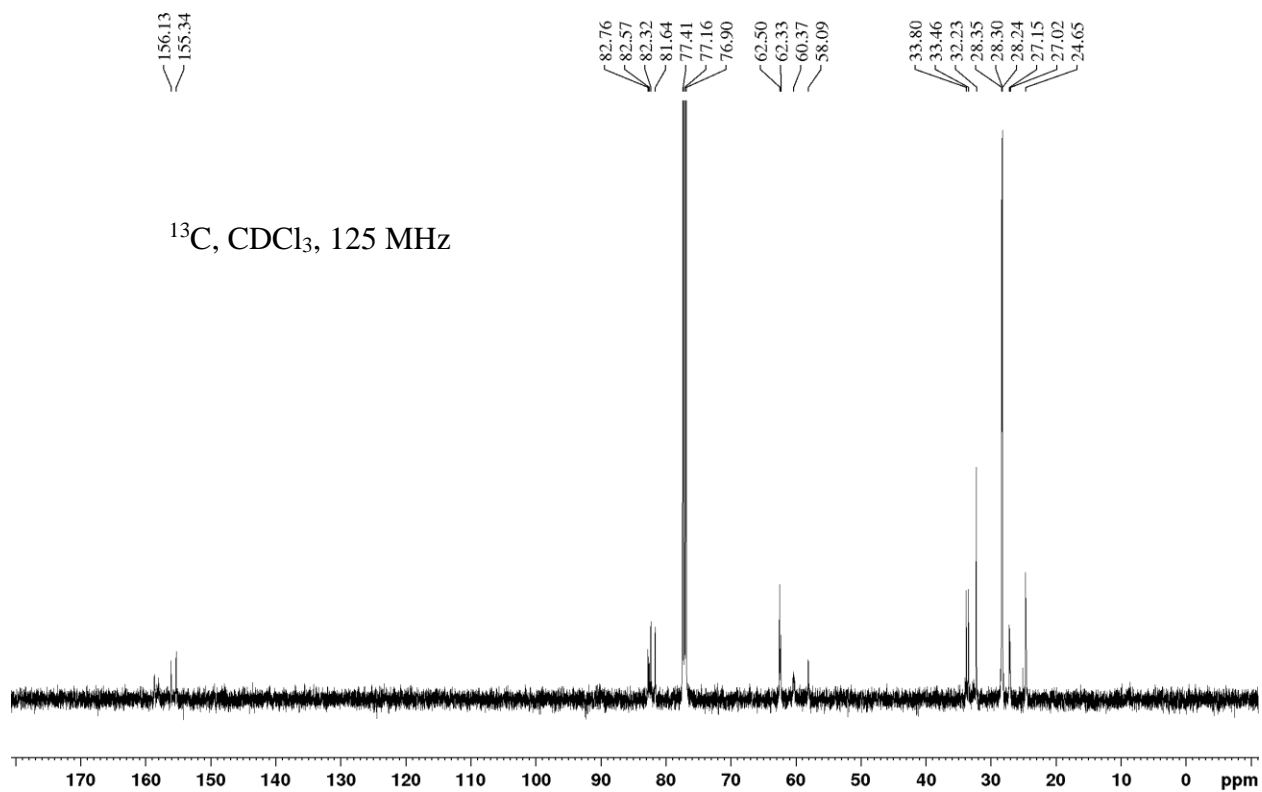
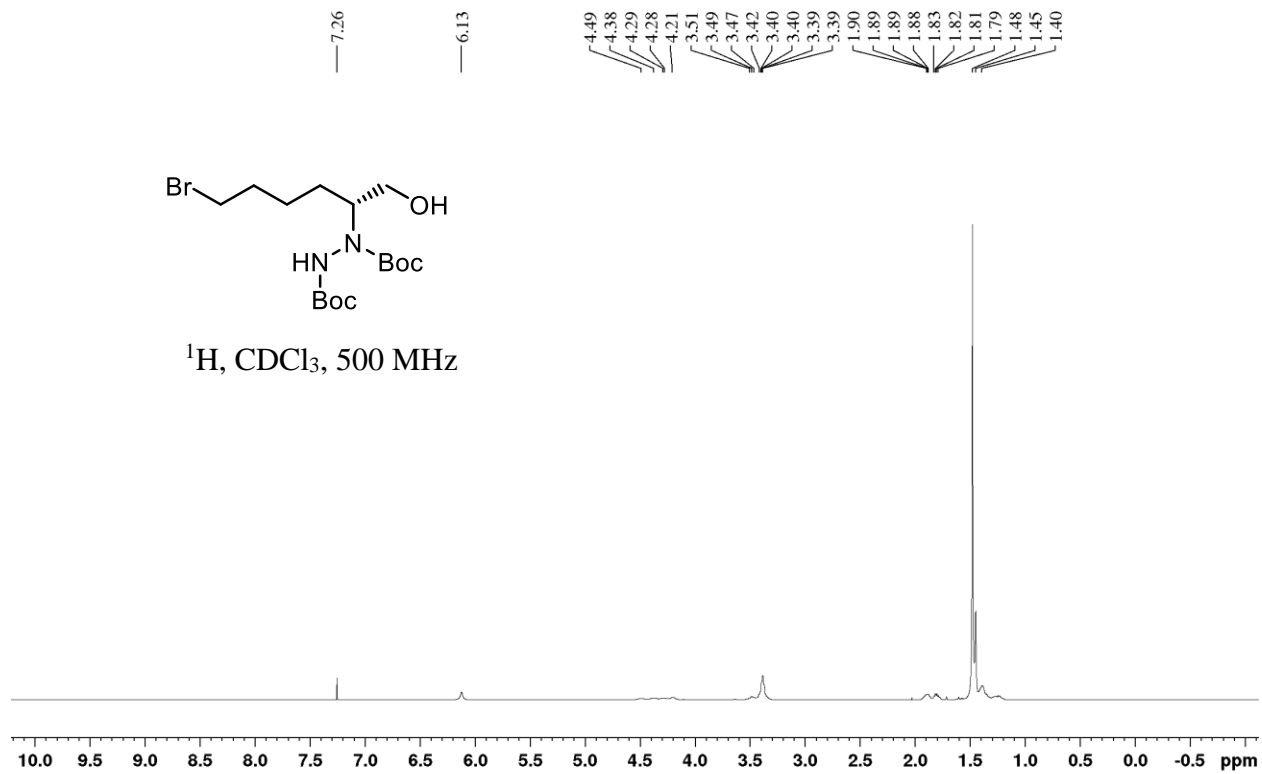


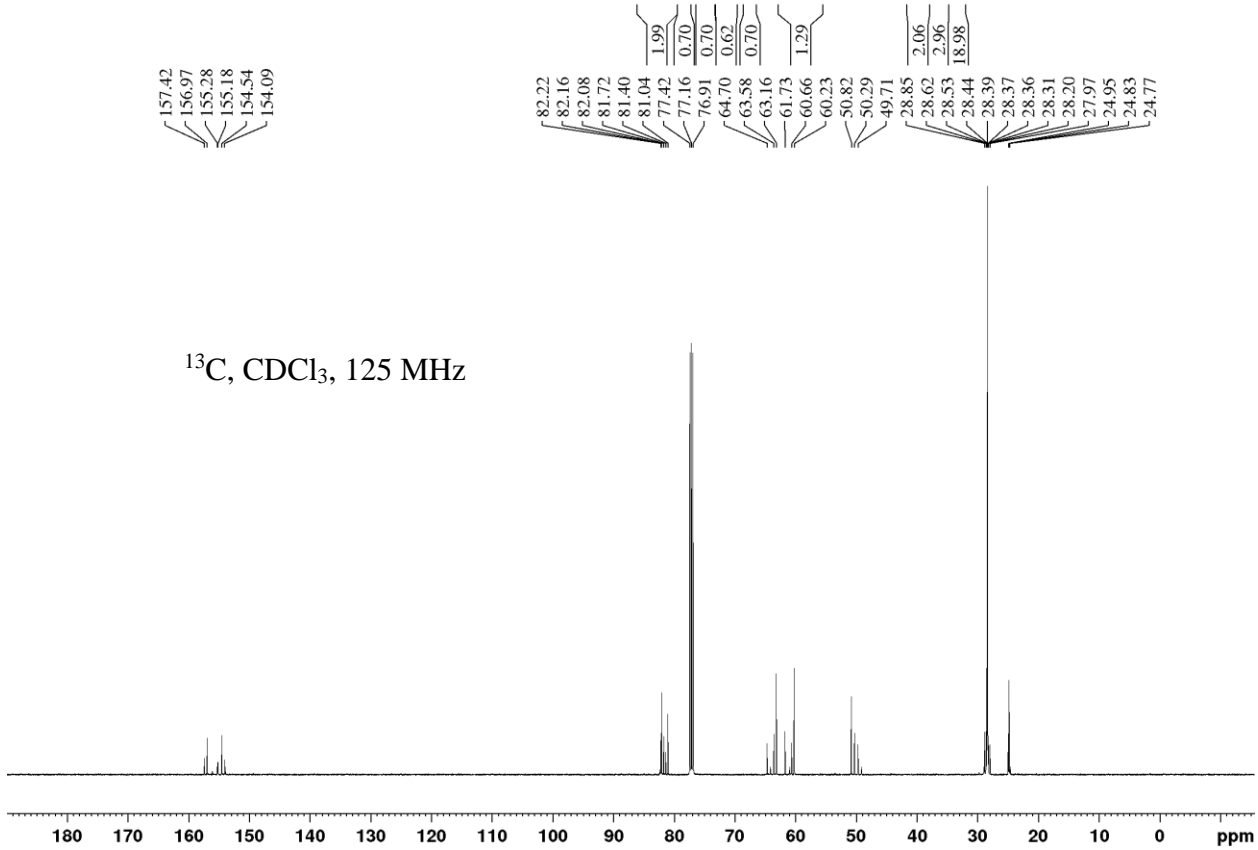
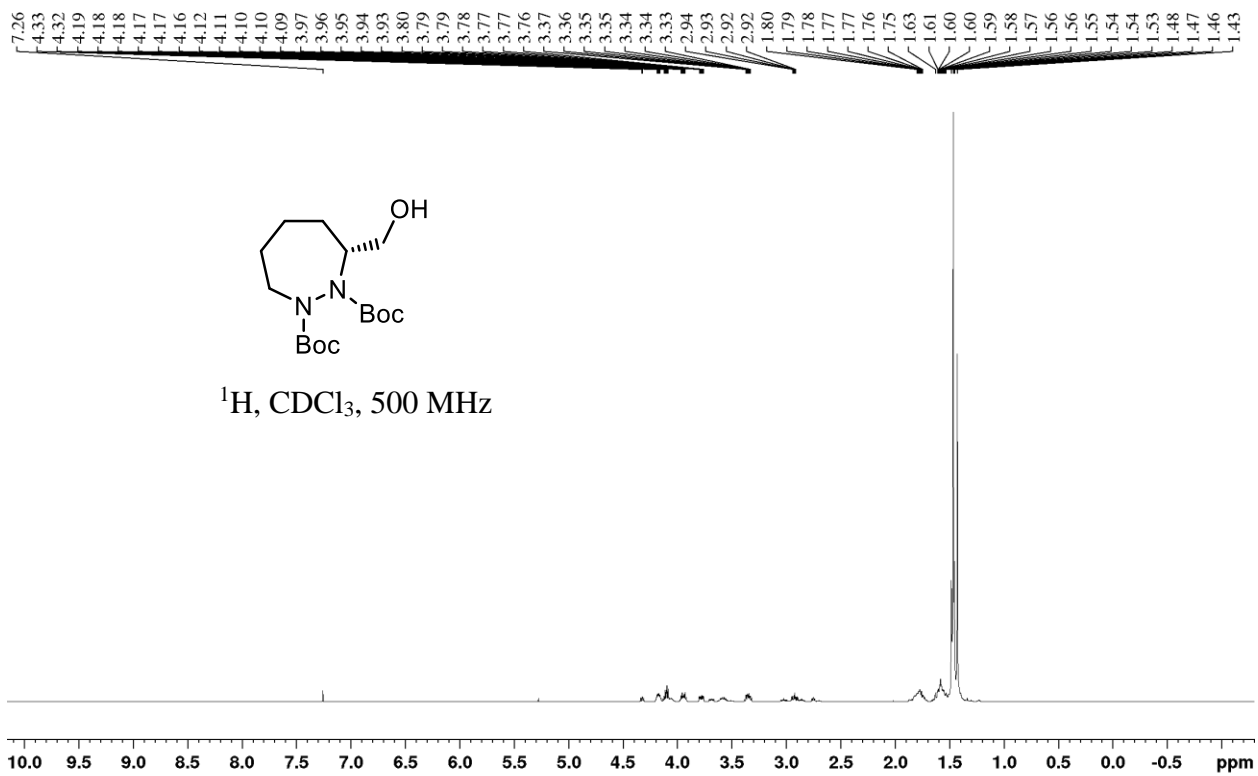


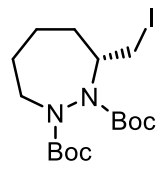
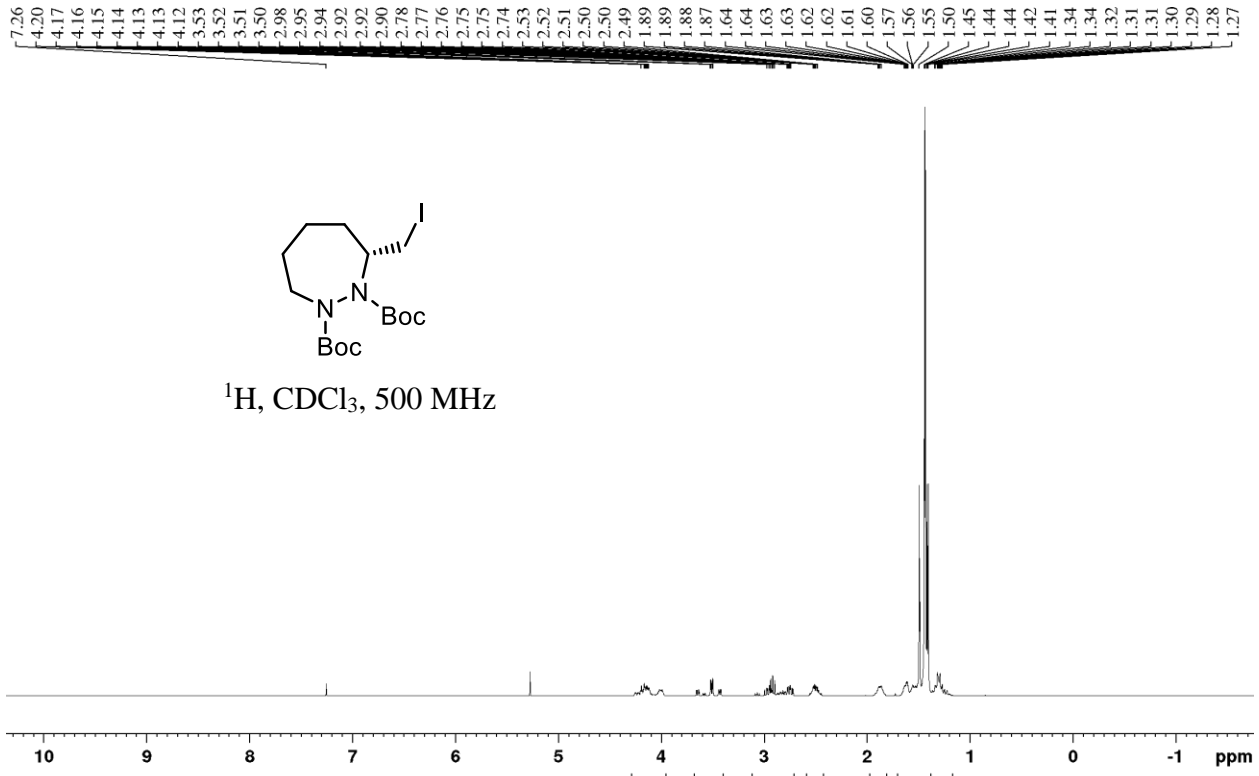




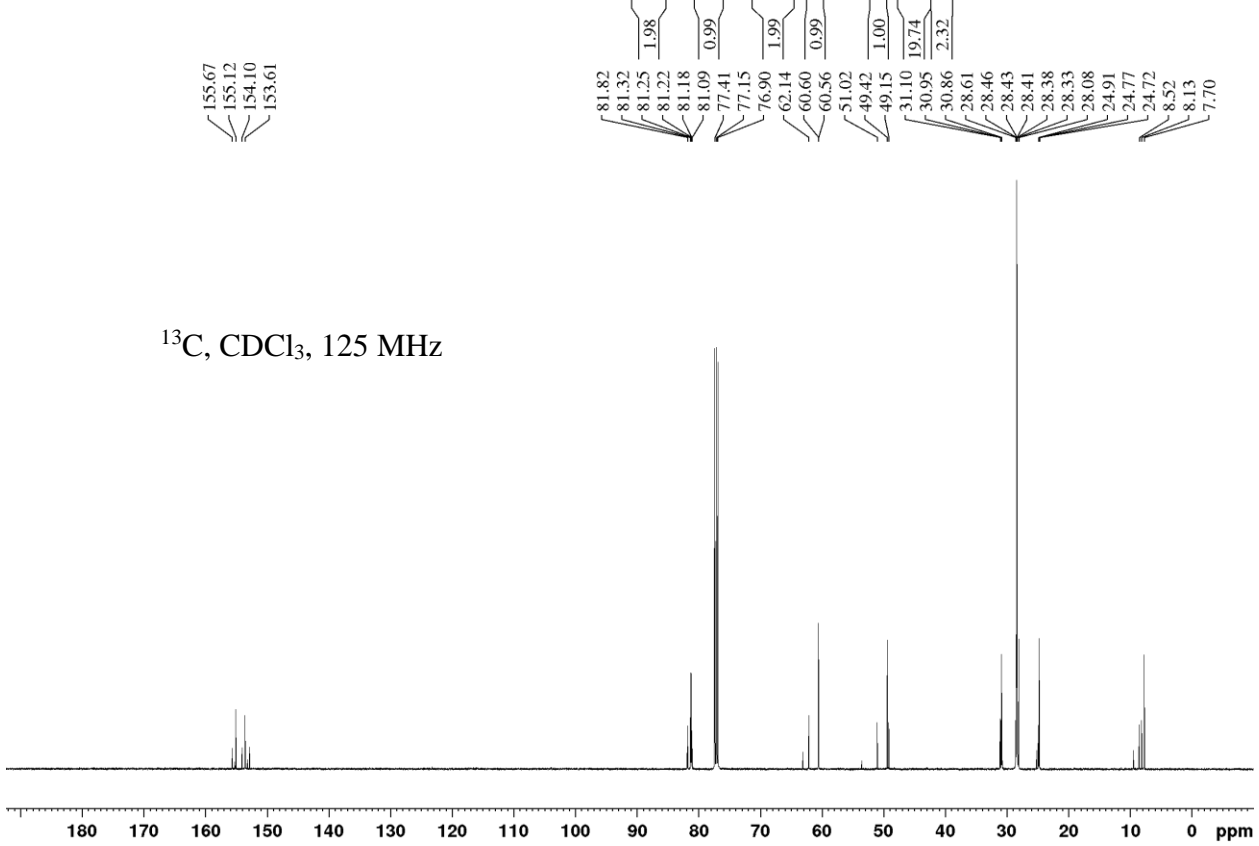


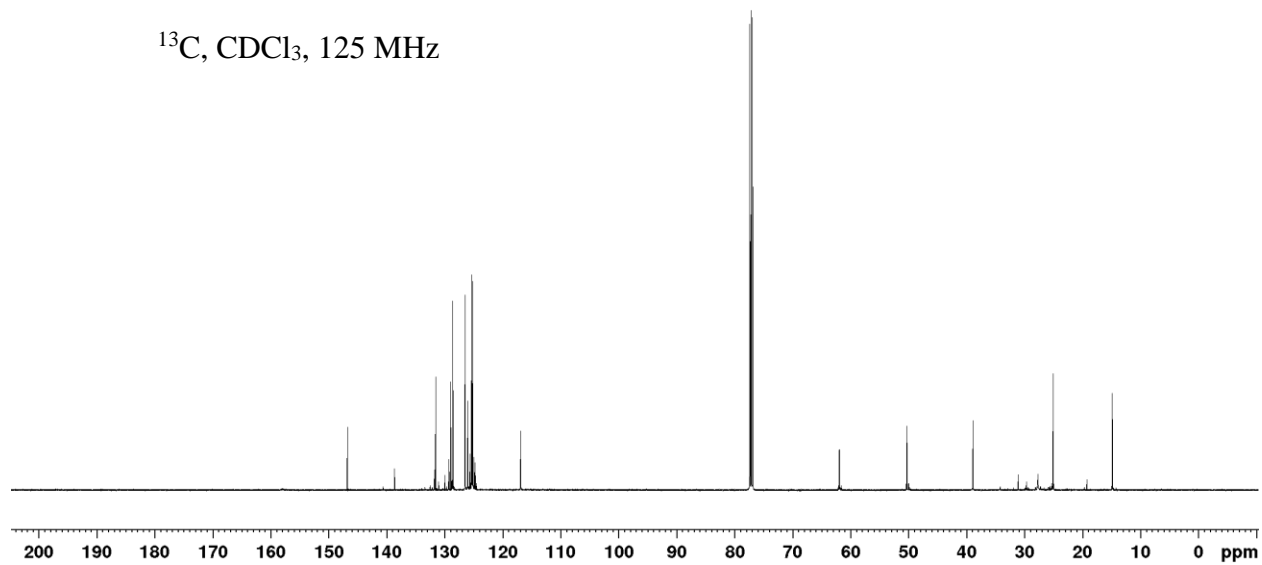
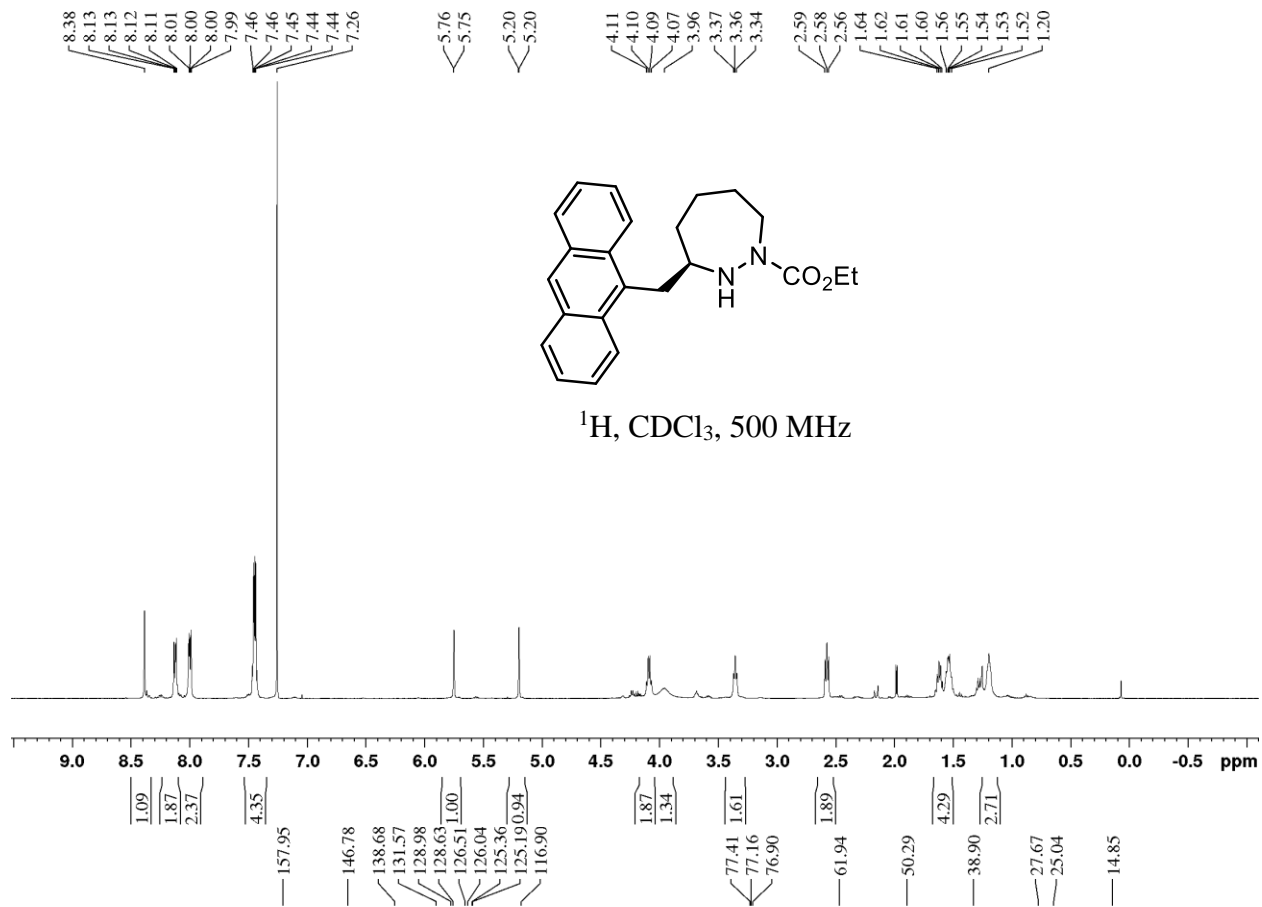


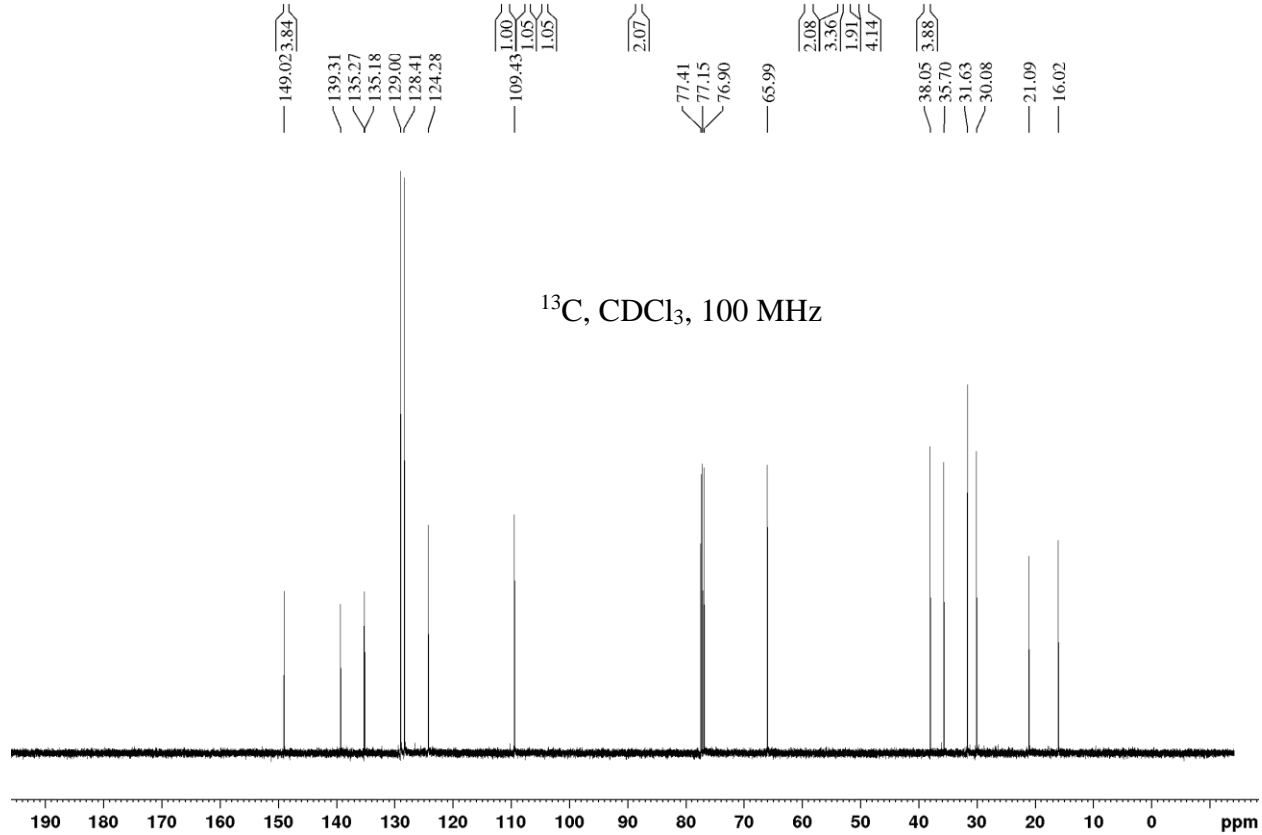
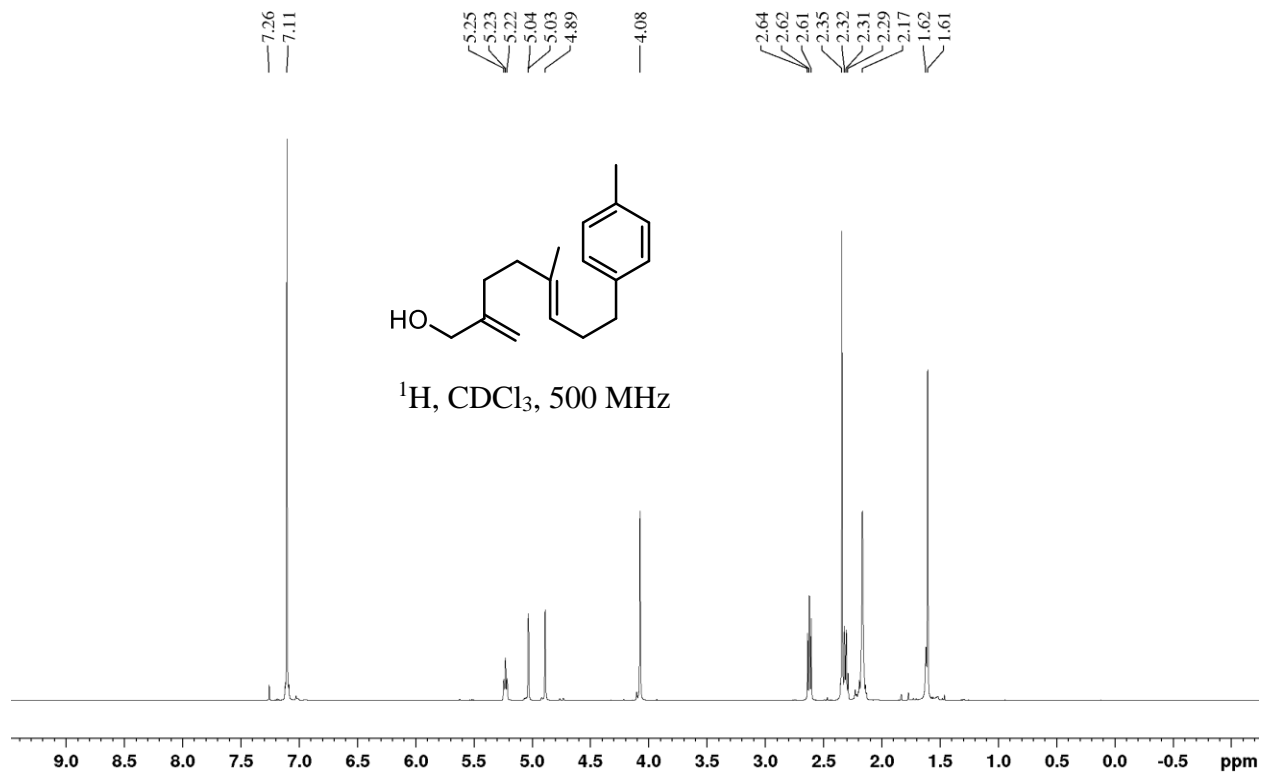


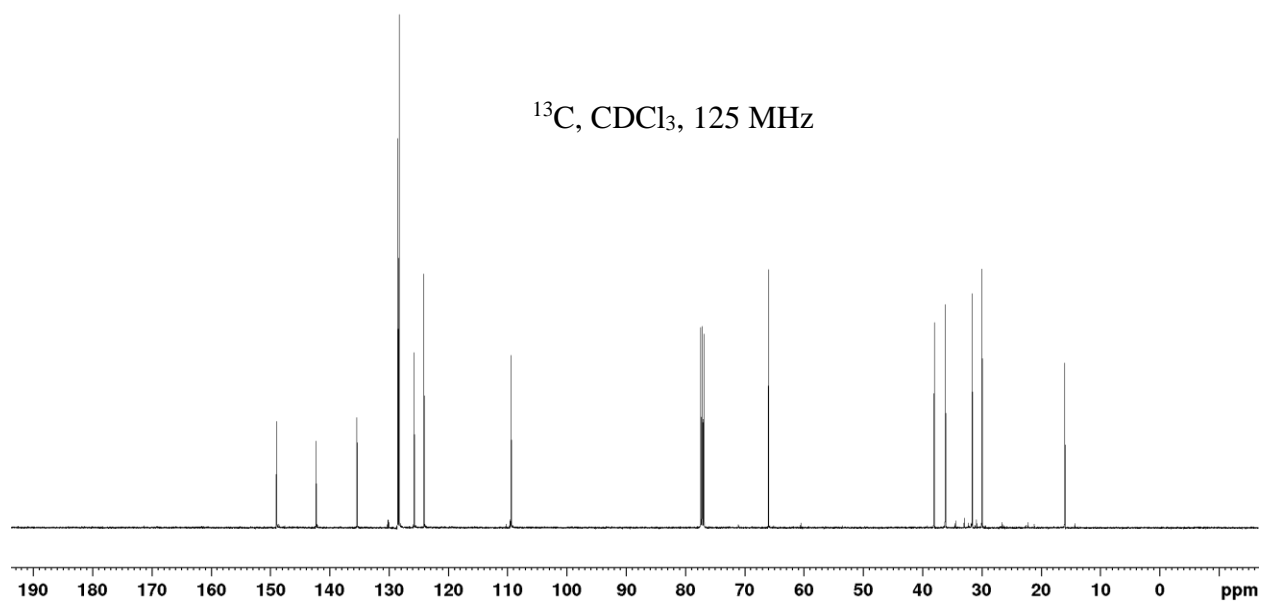
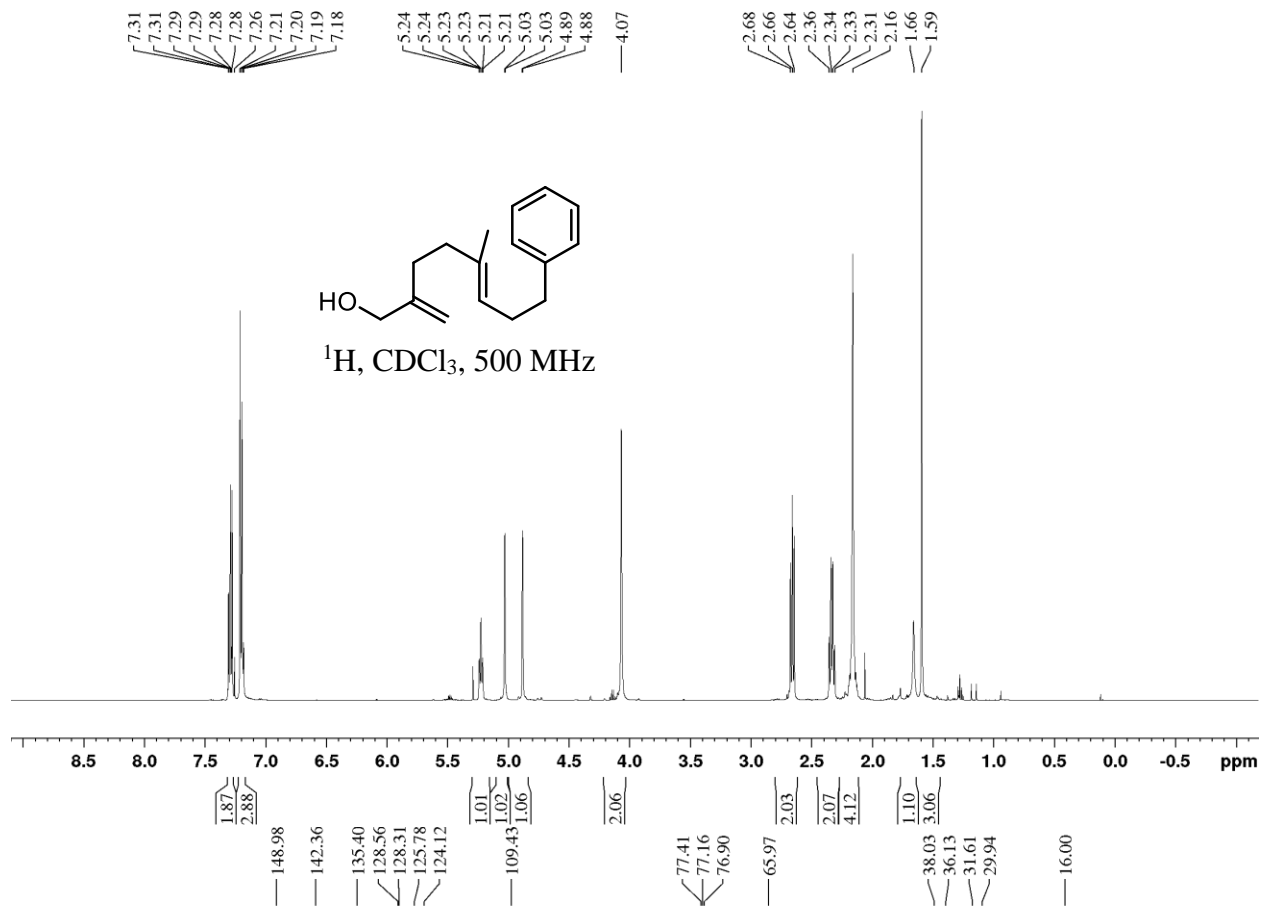


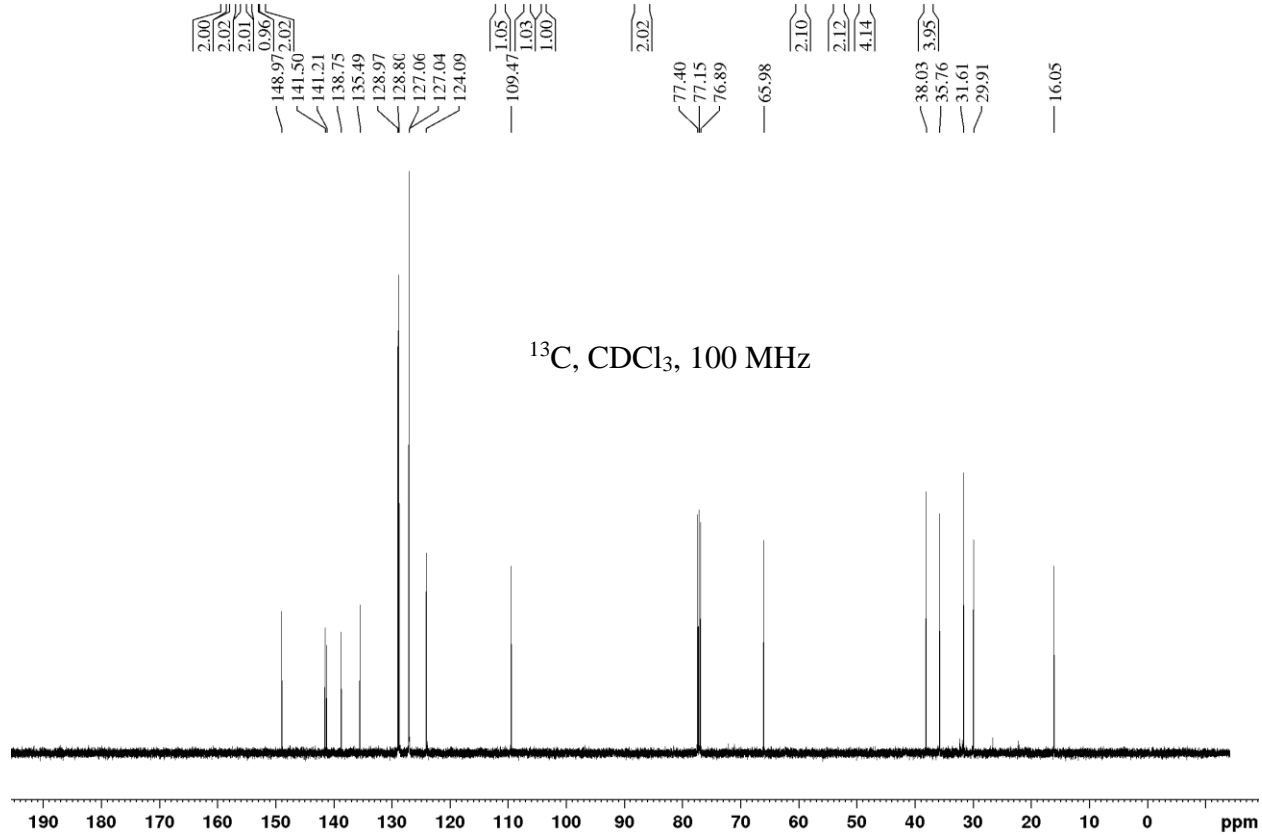
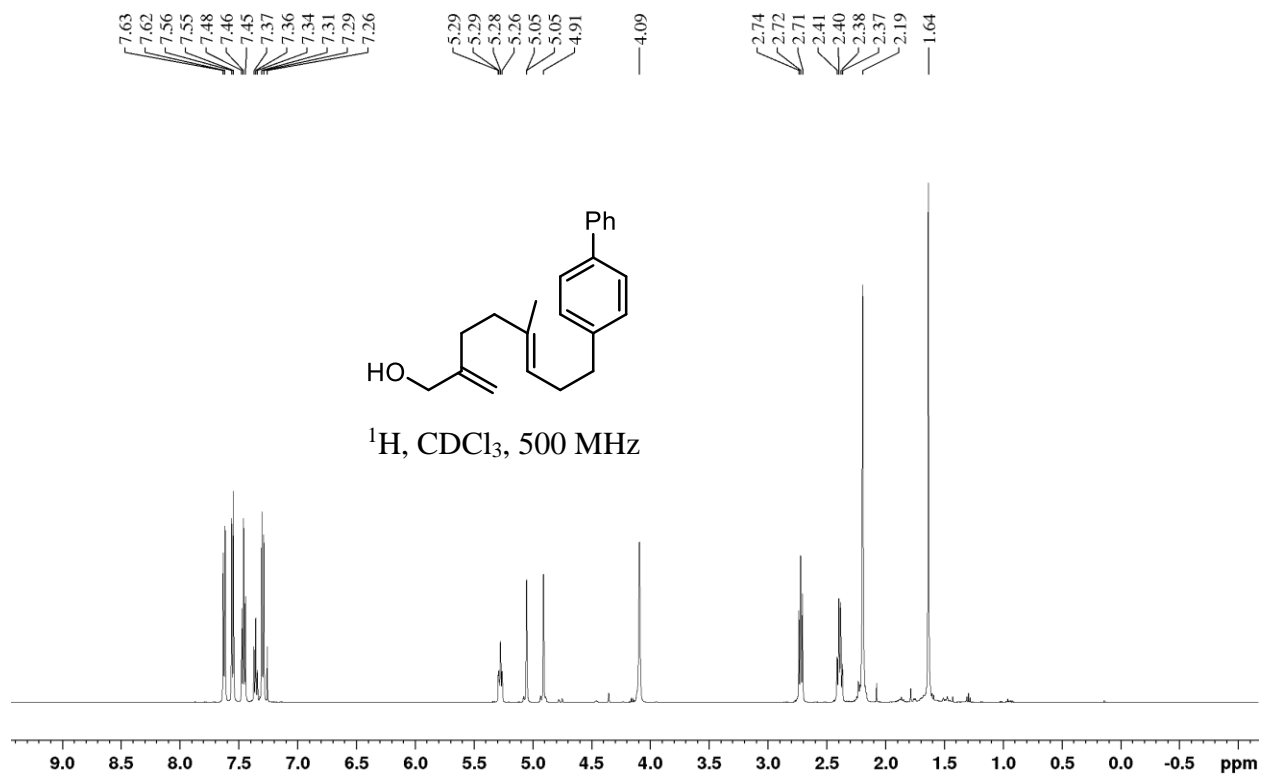
¹H, CDCl₃, 500 MHz

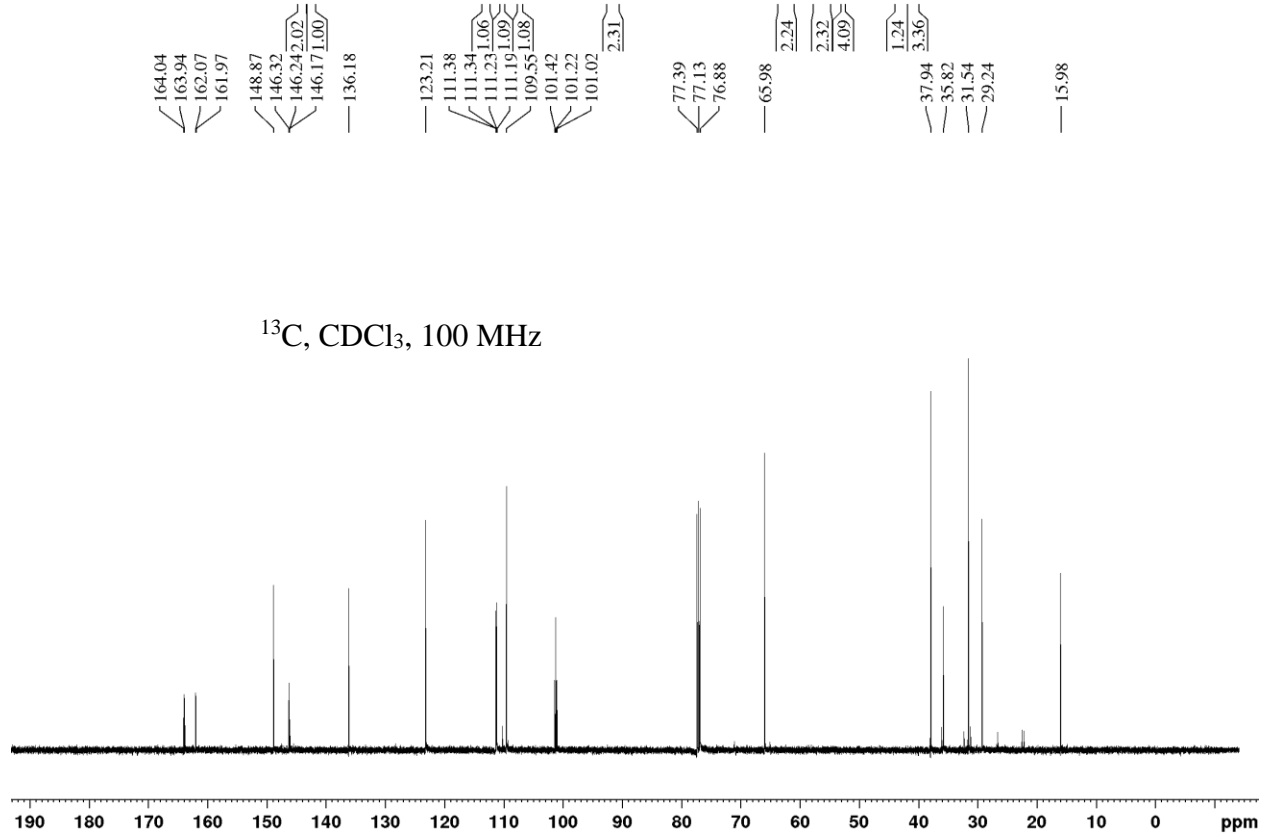
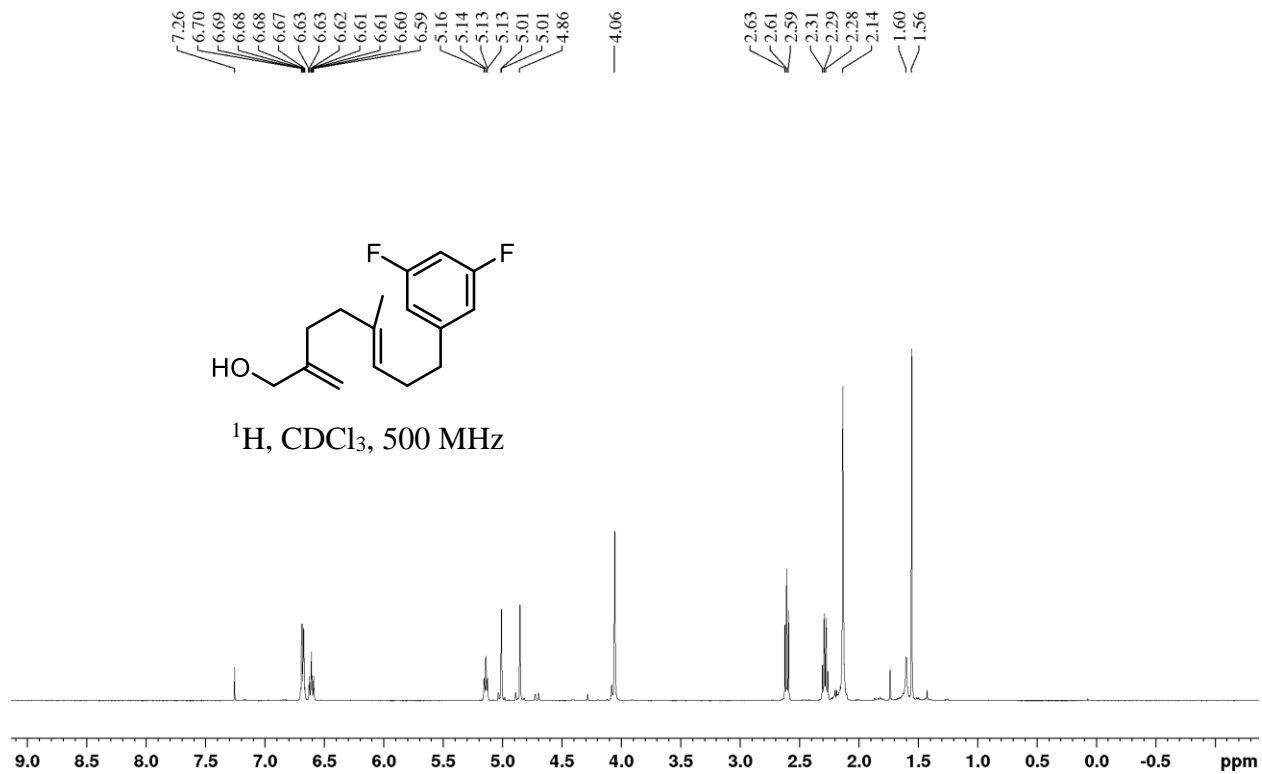


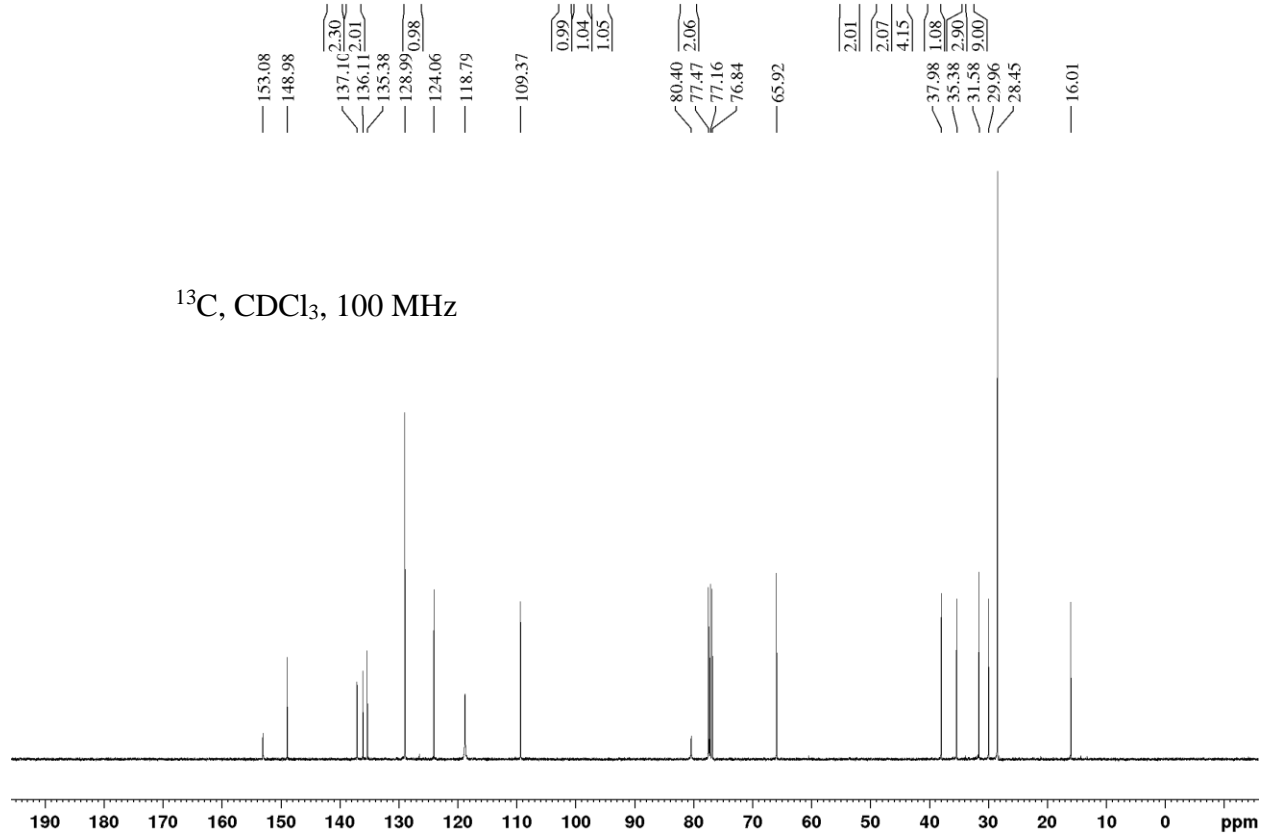
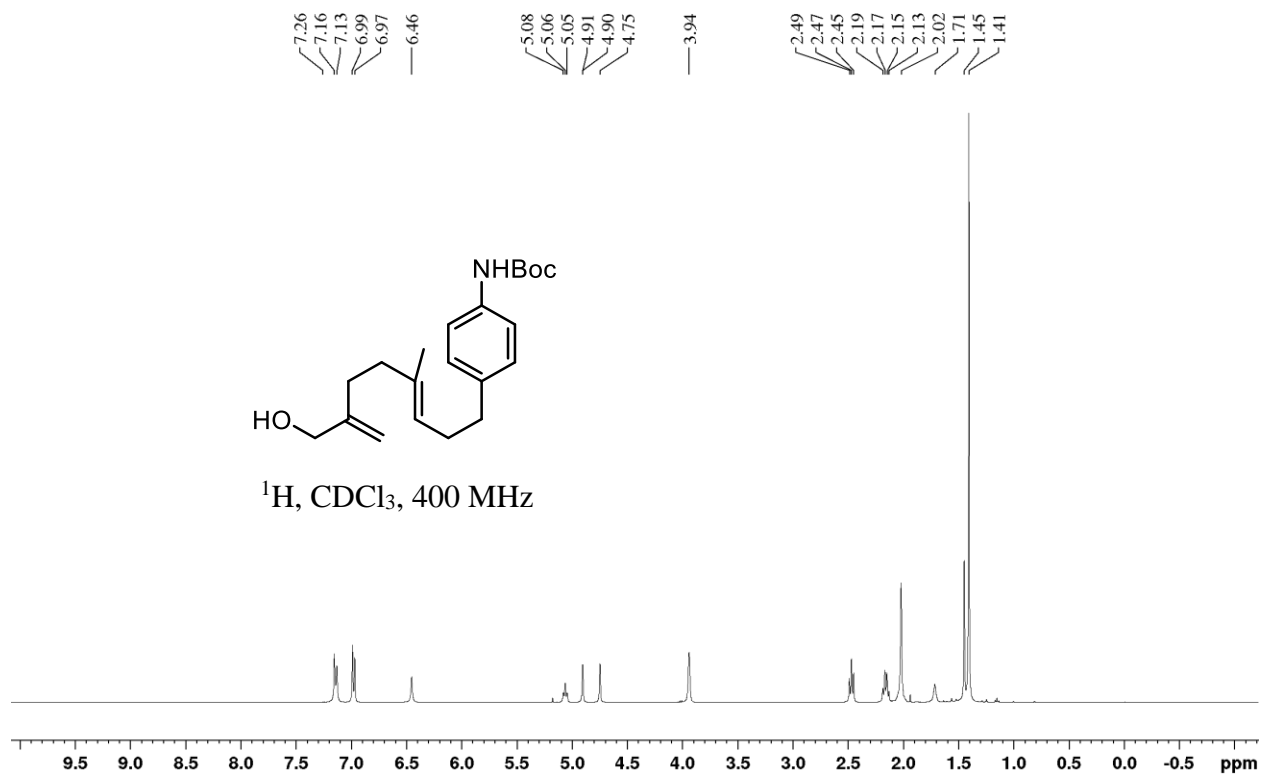


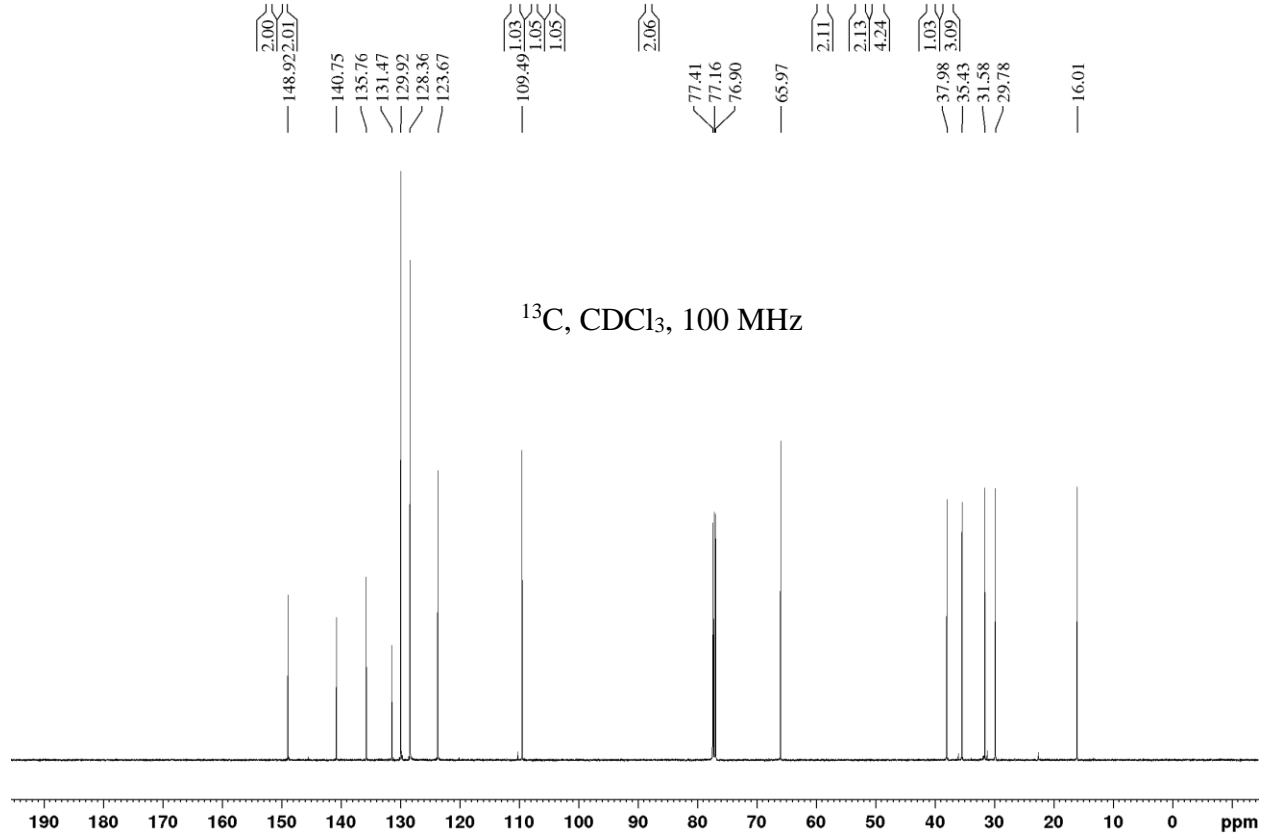
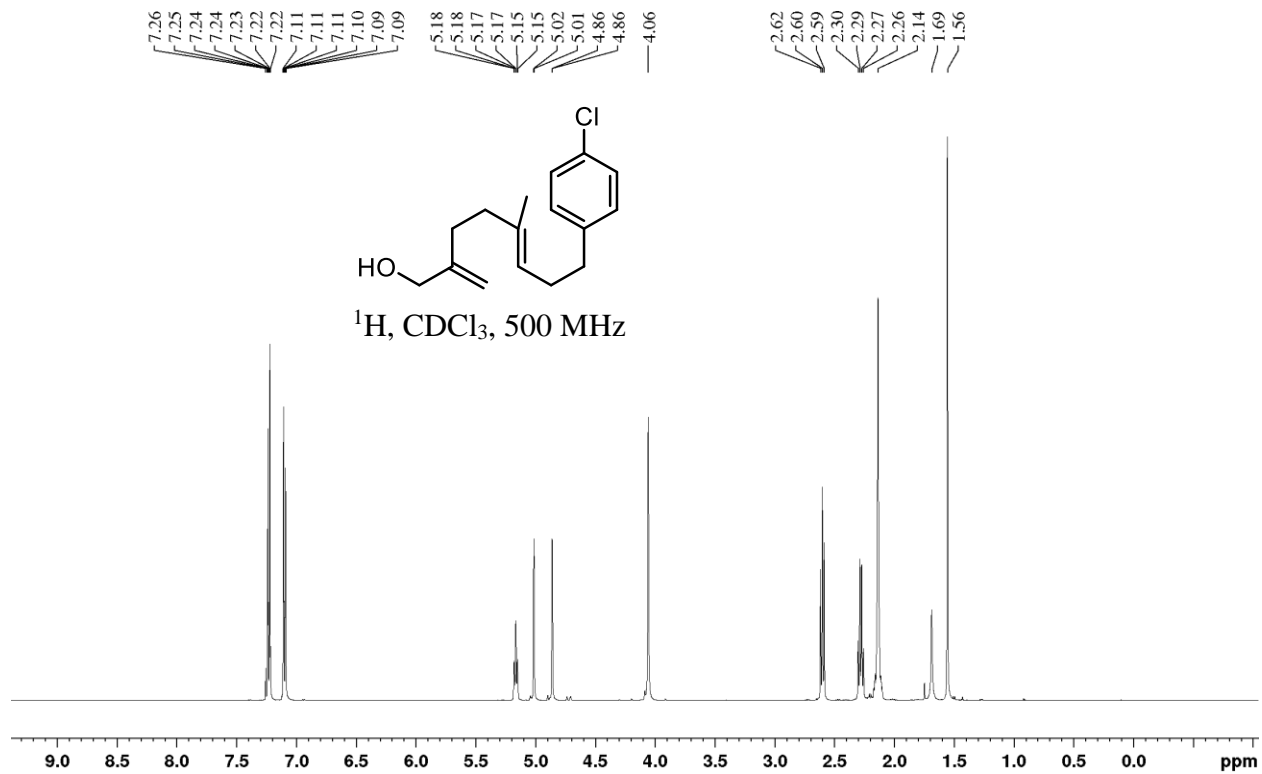


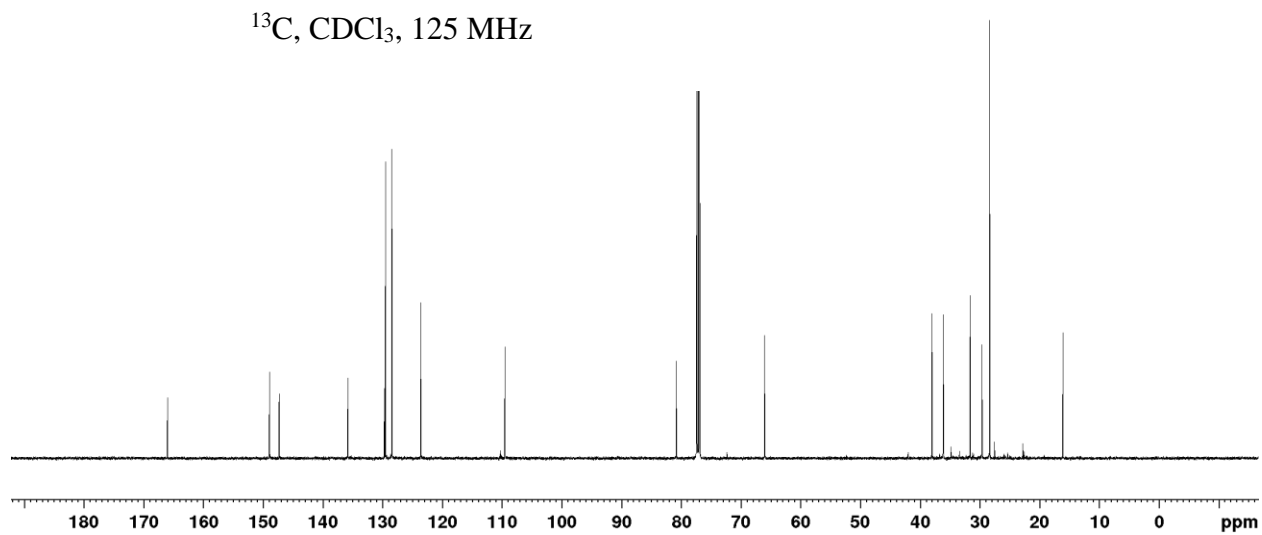
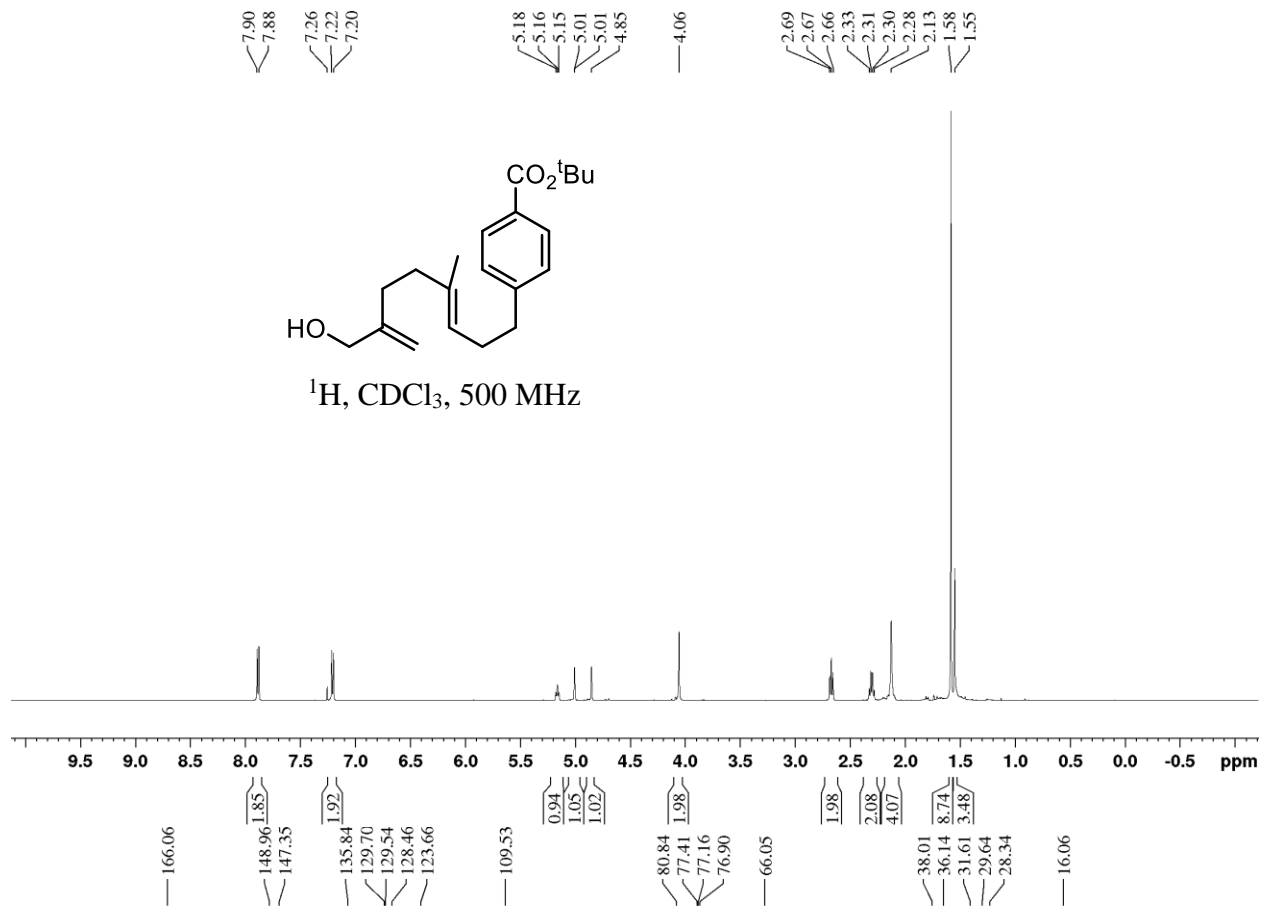


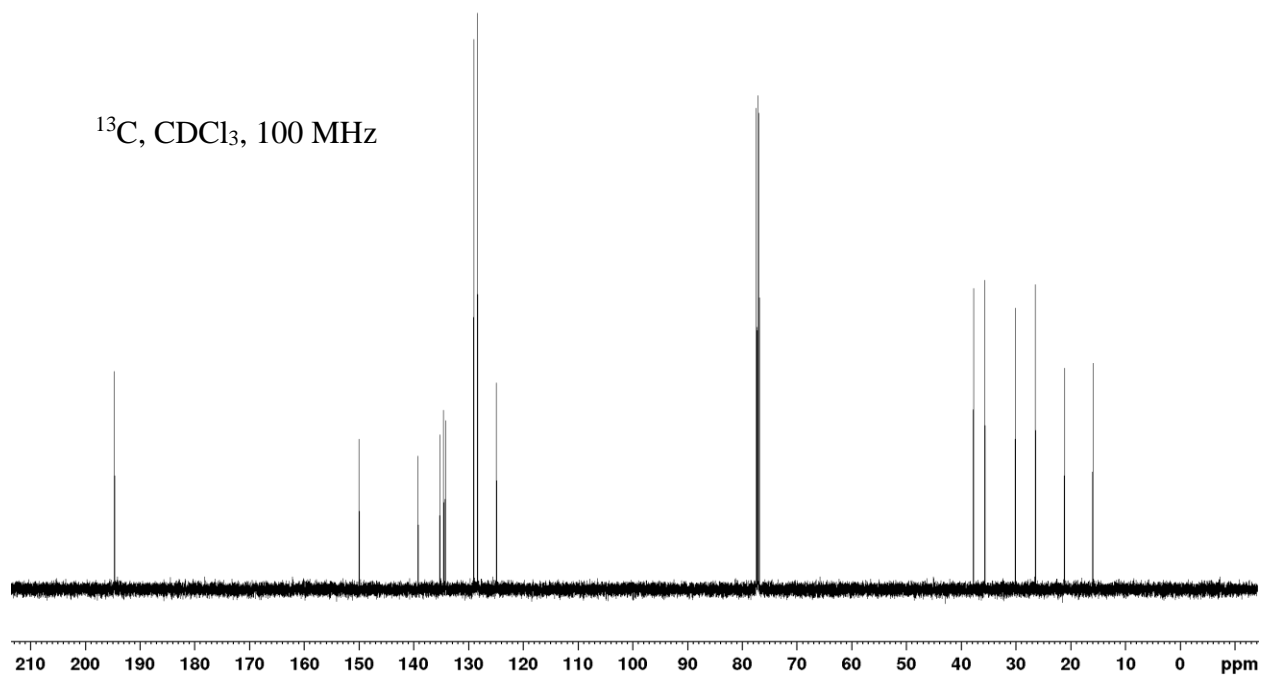
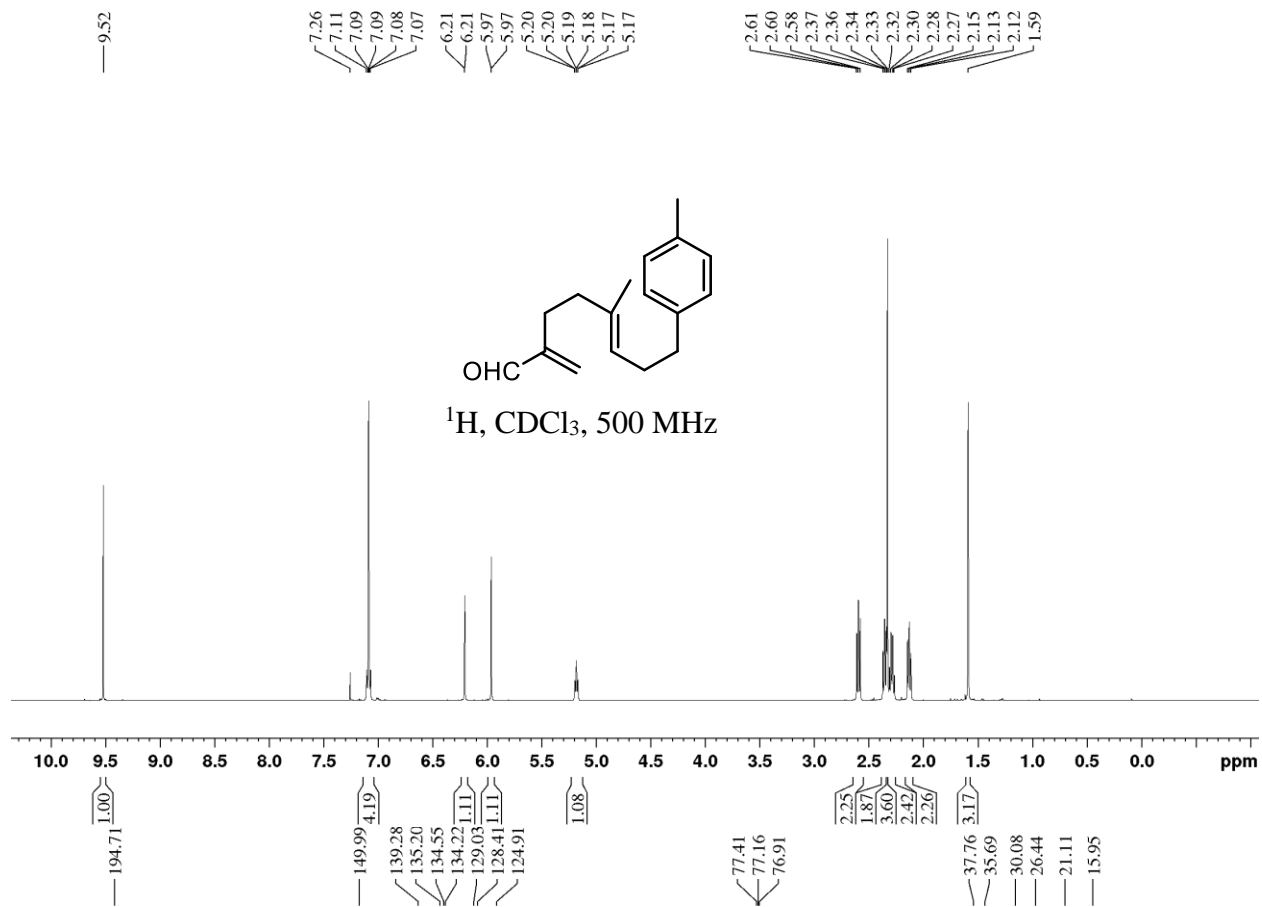


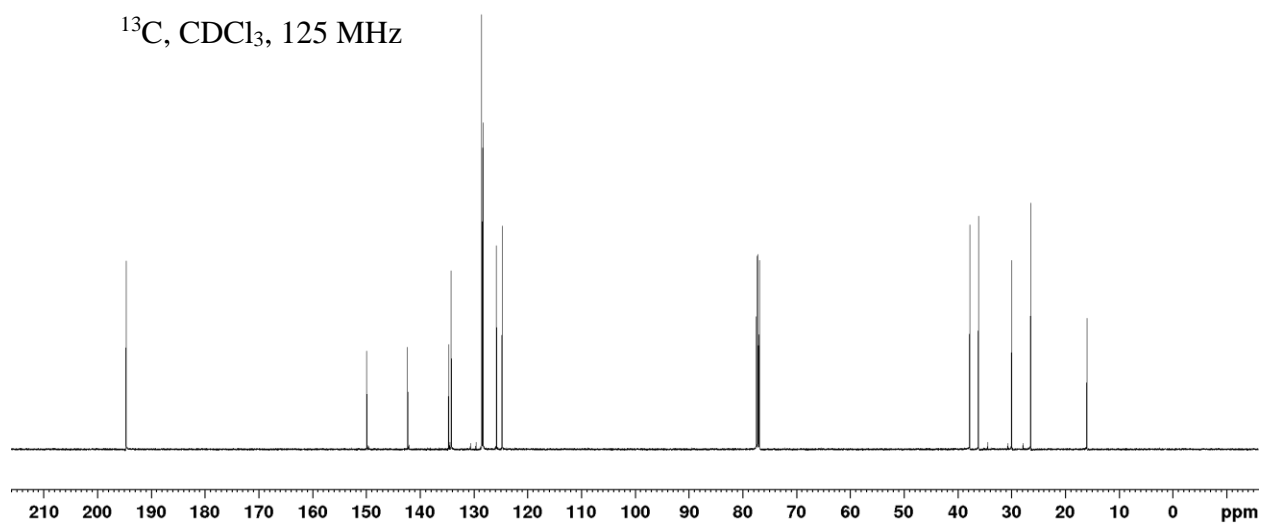
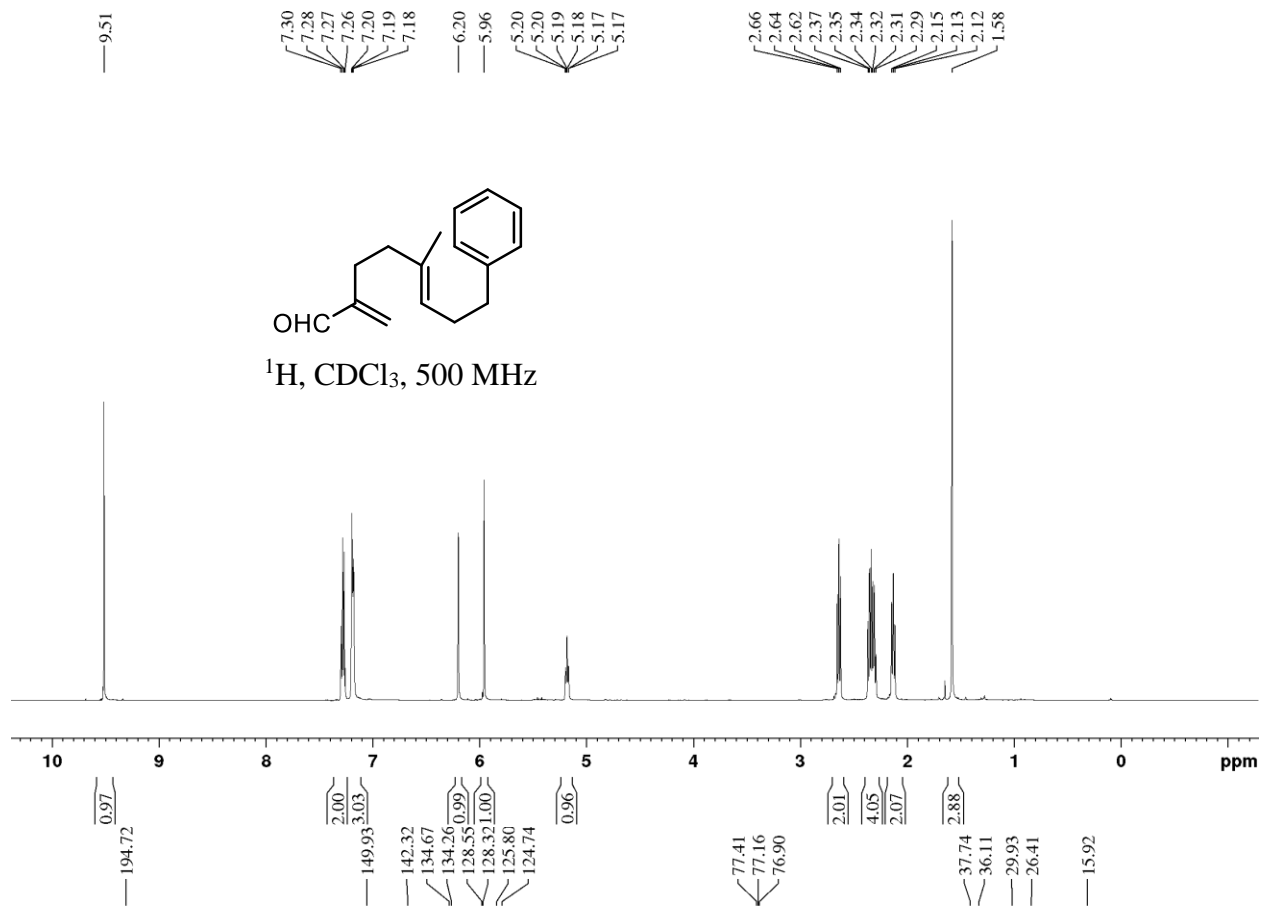


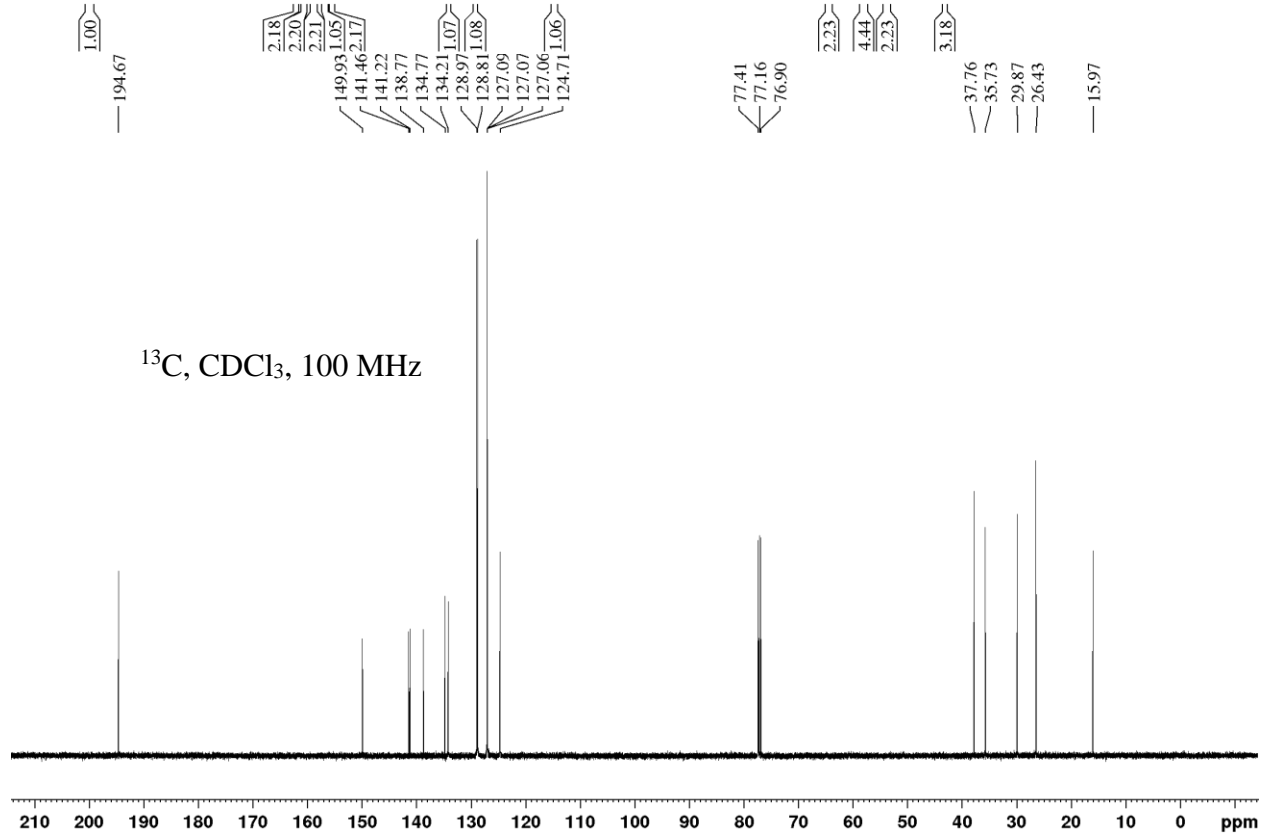
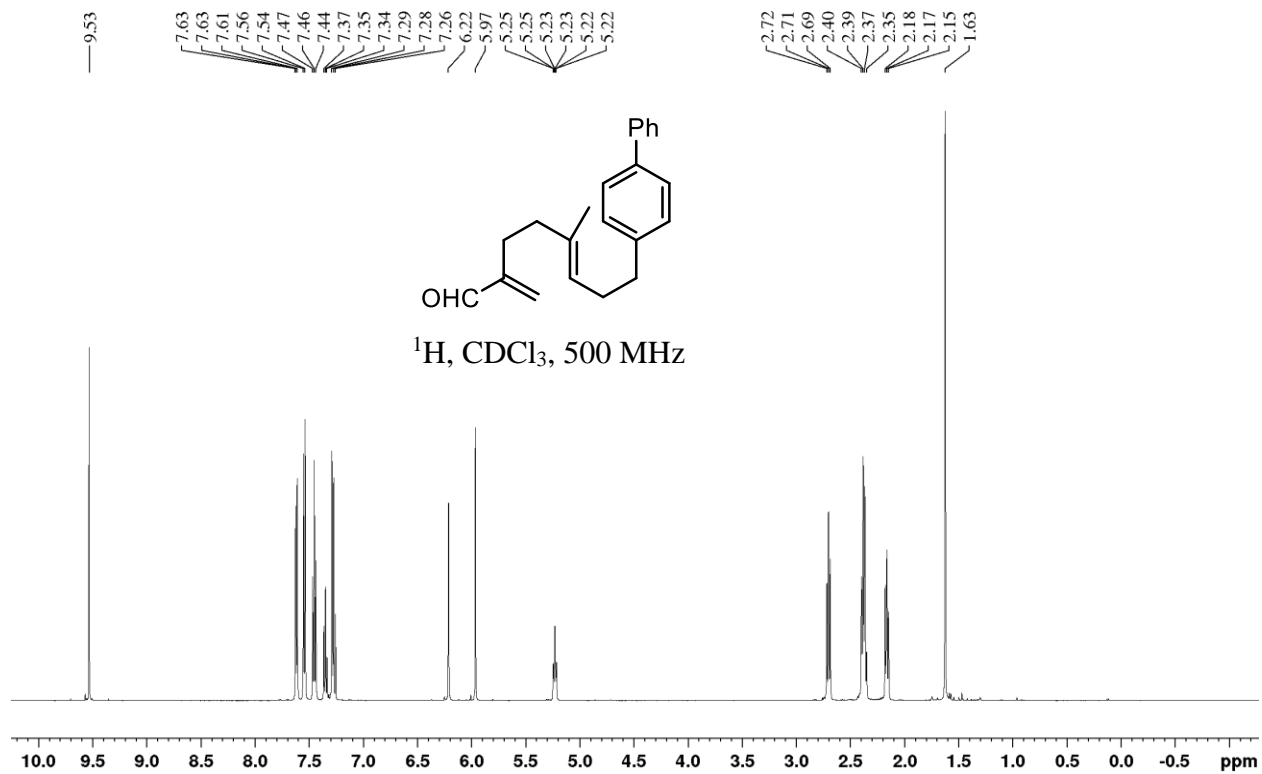


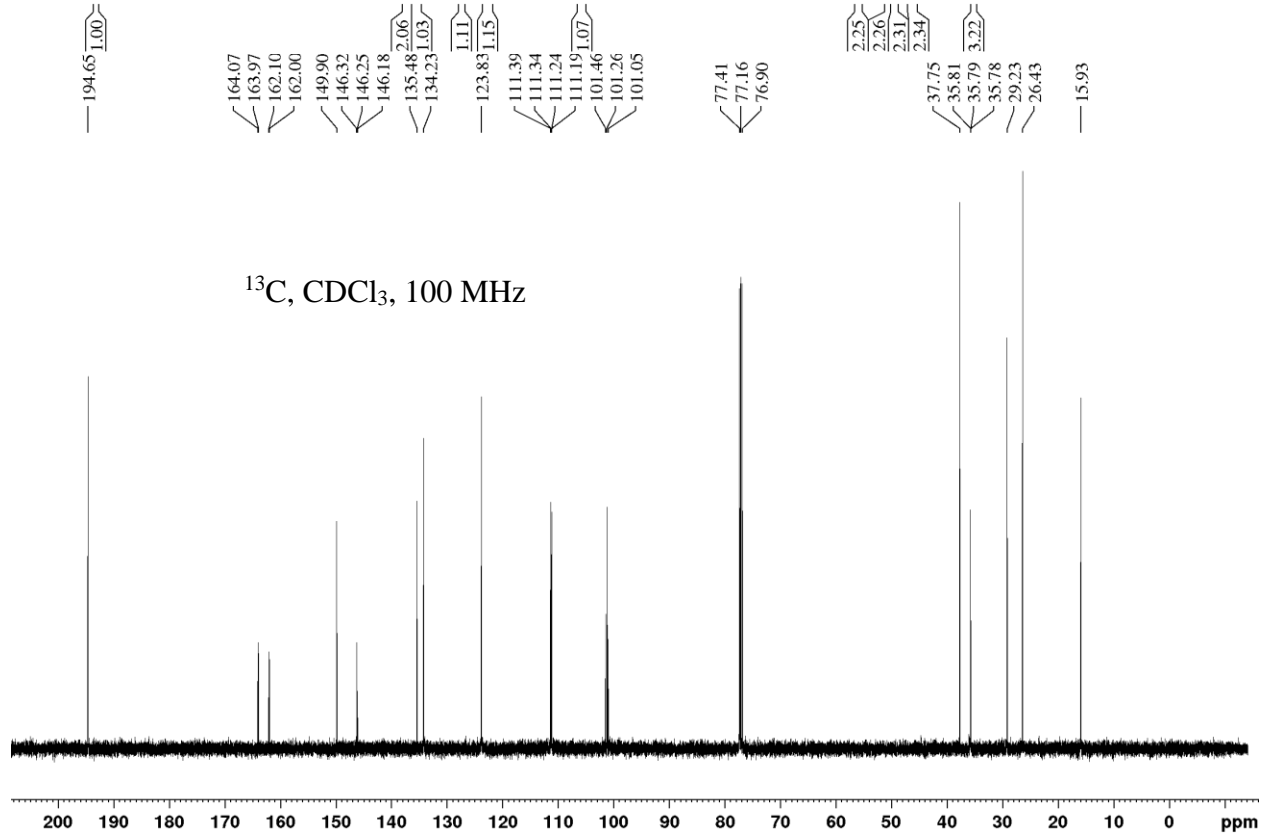
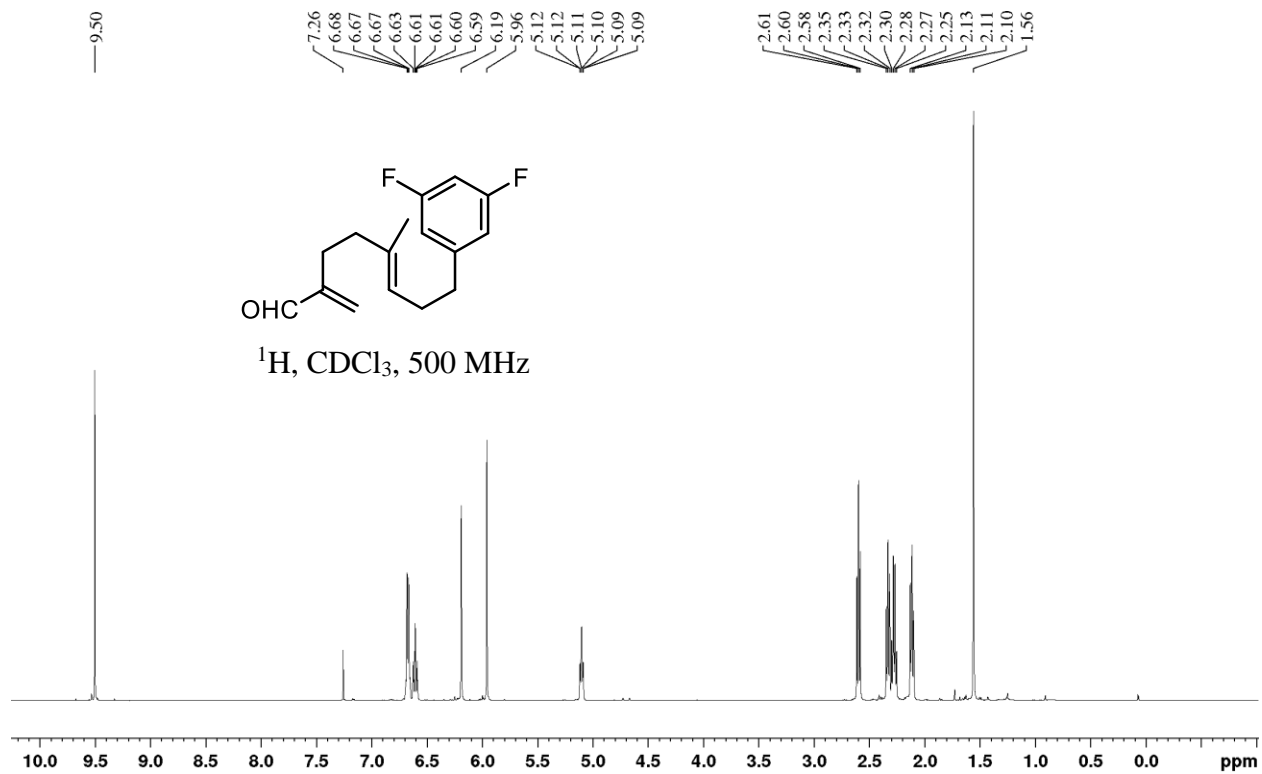


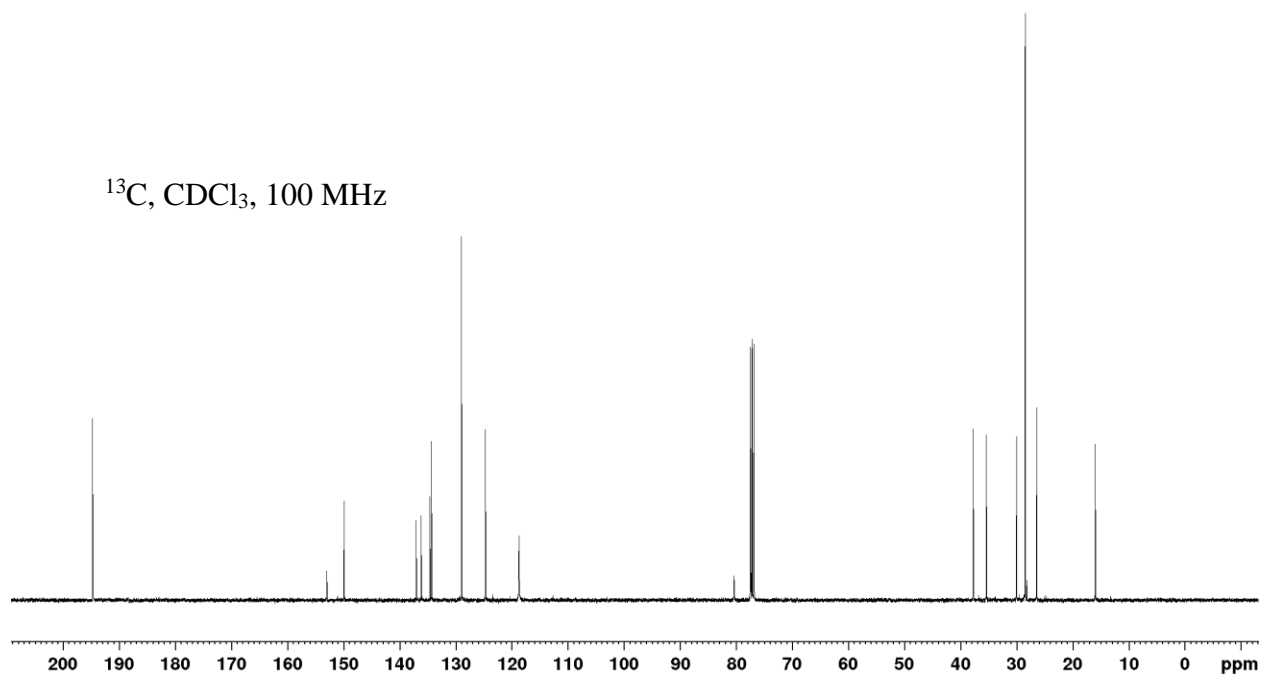
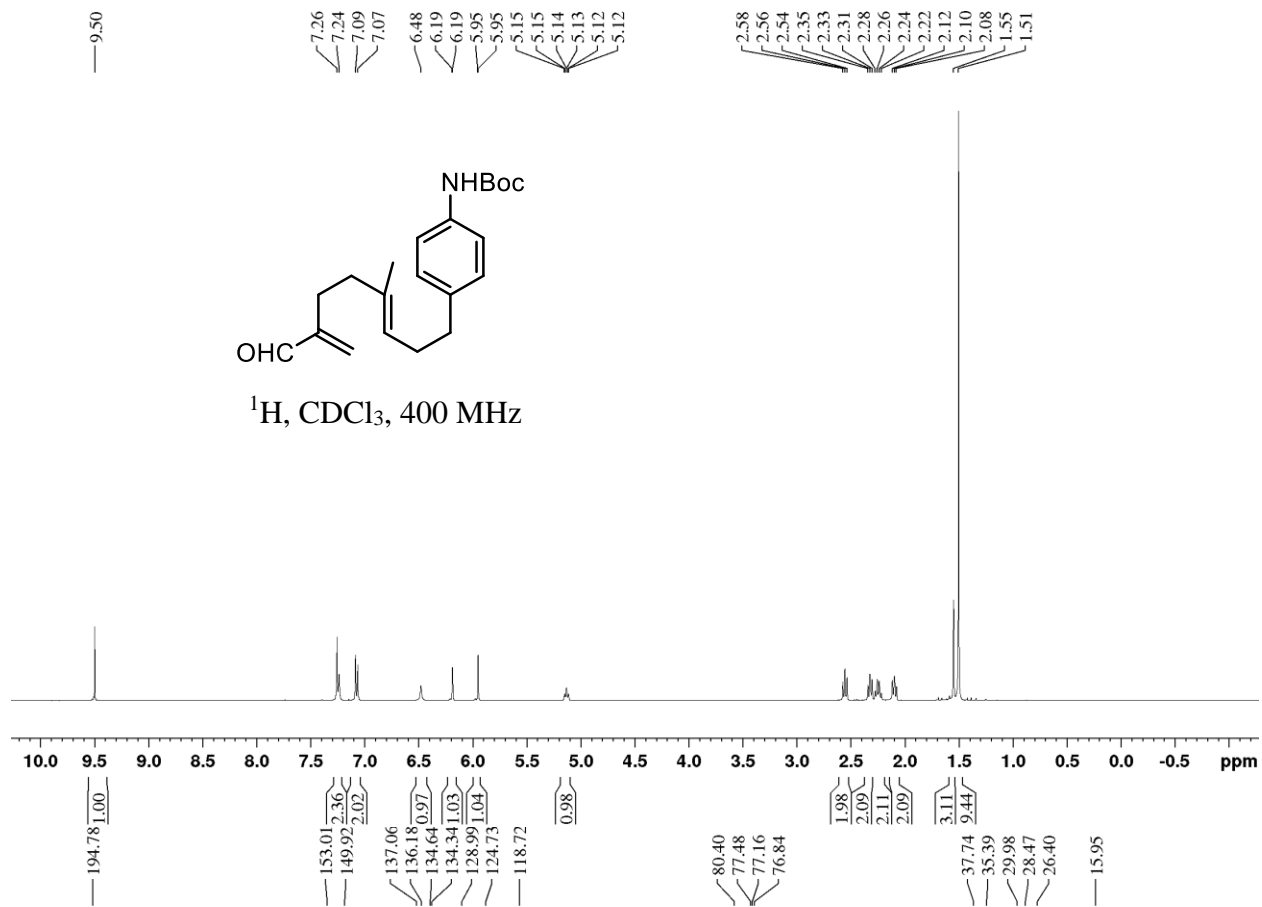


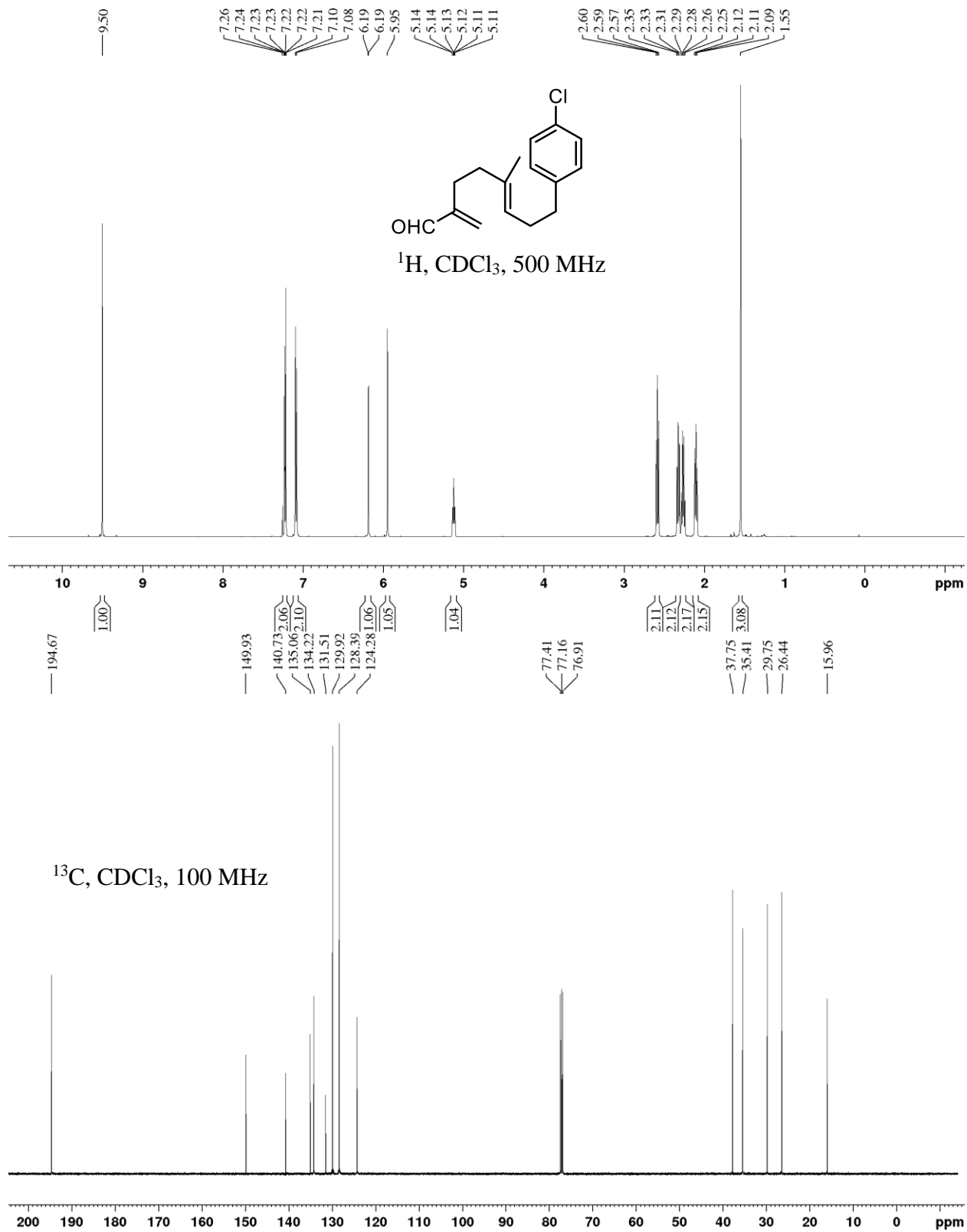


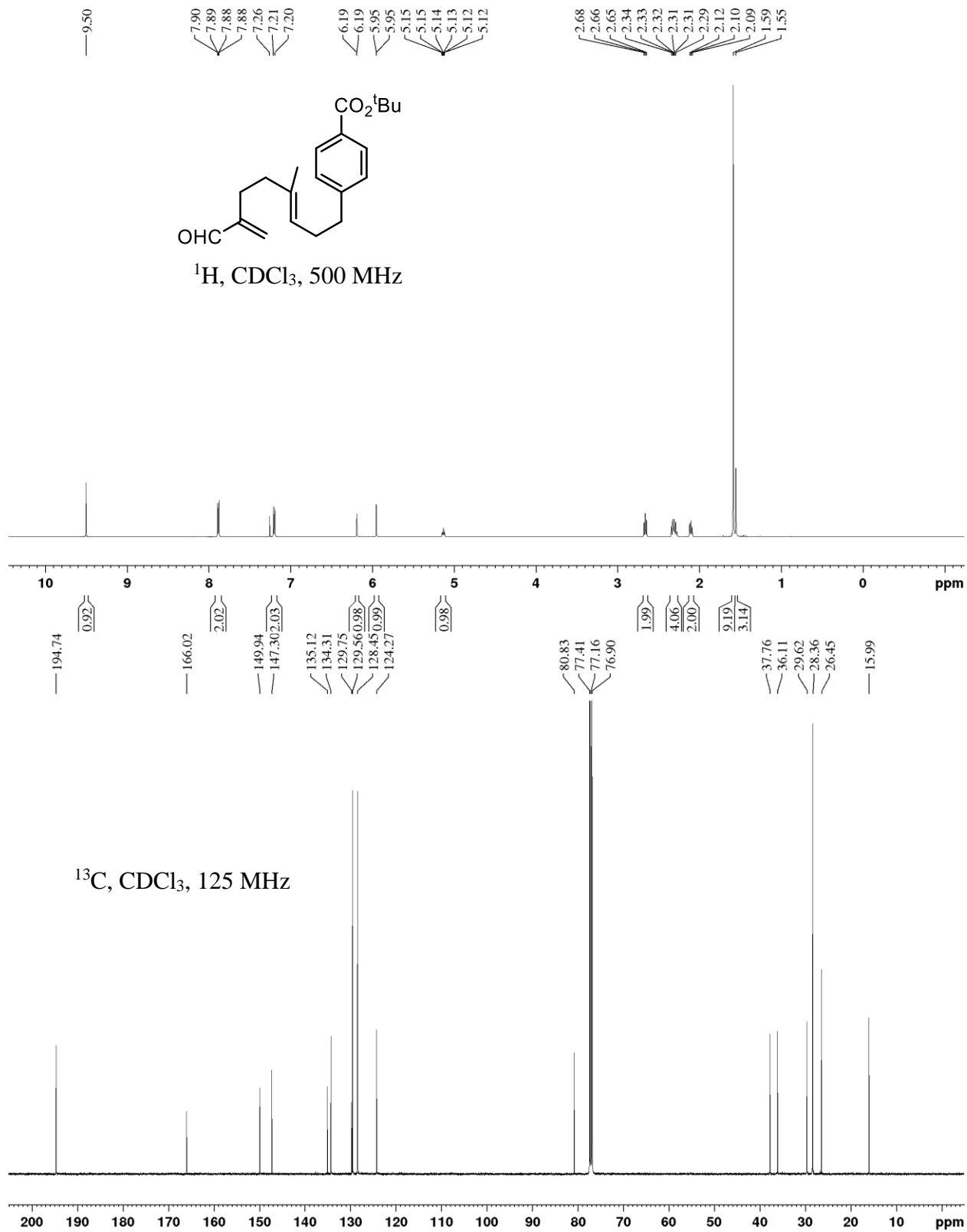


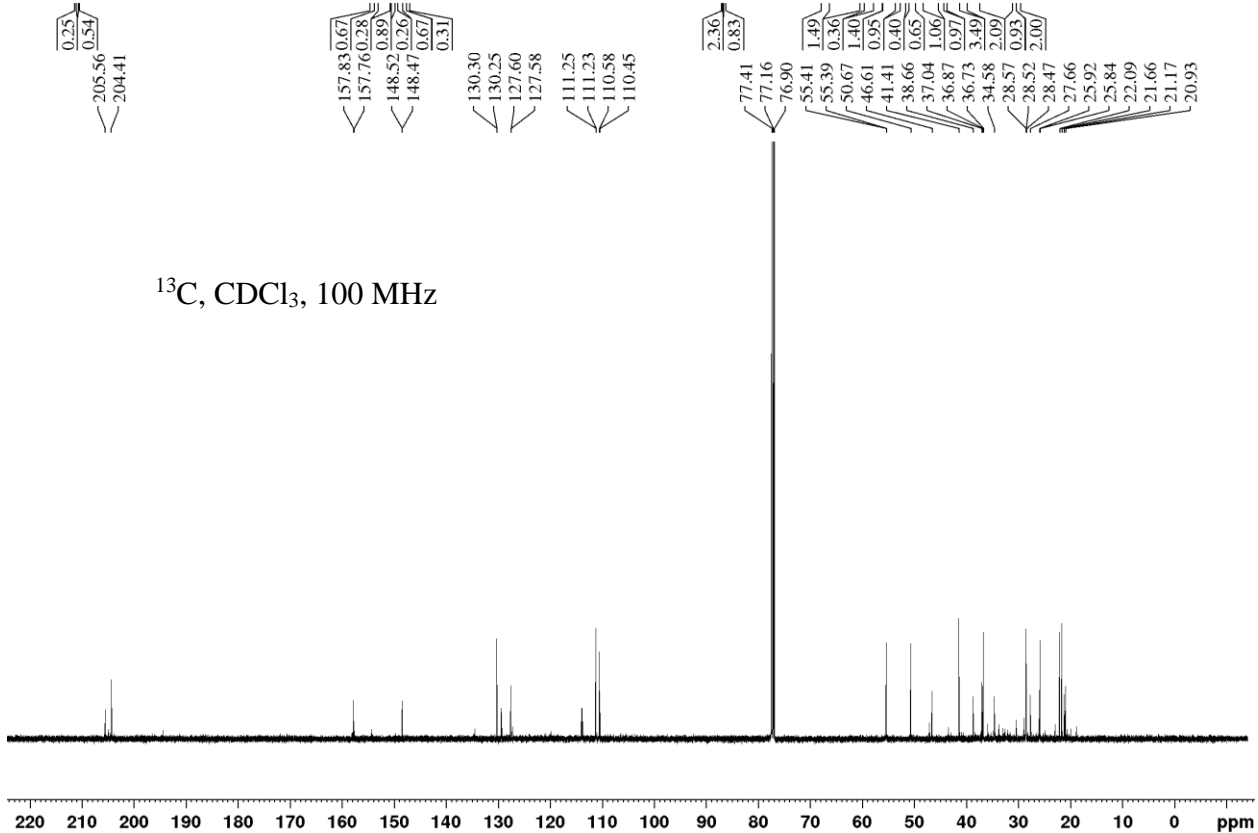
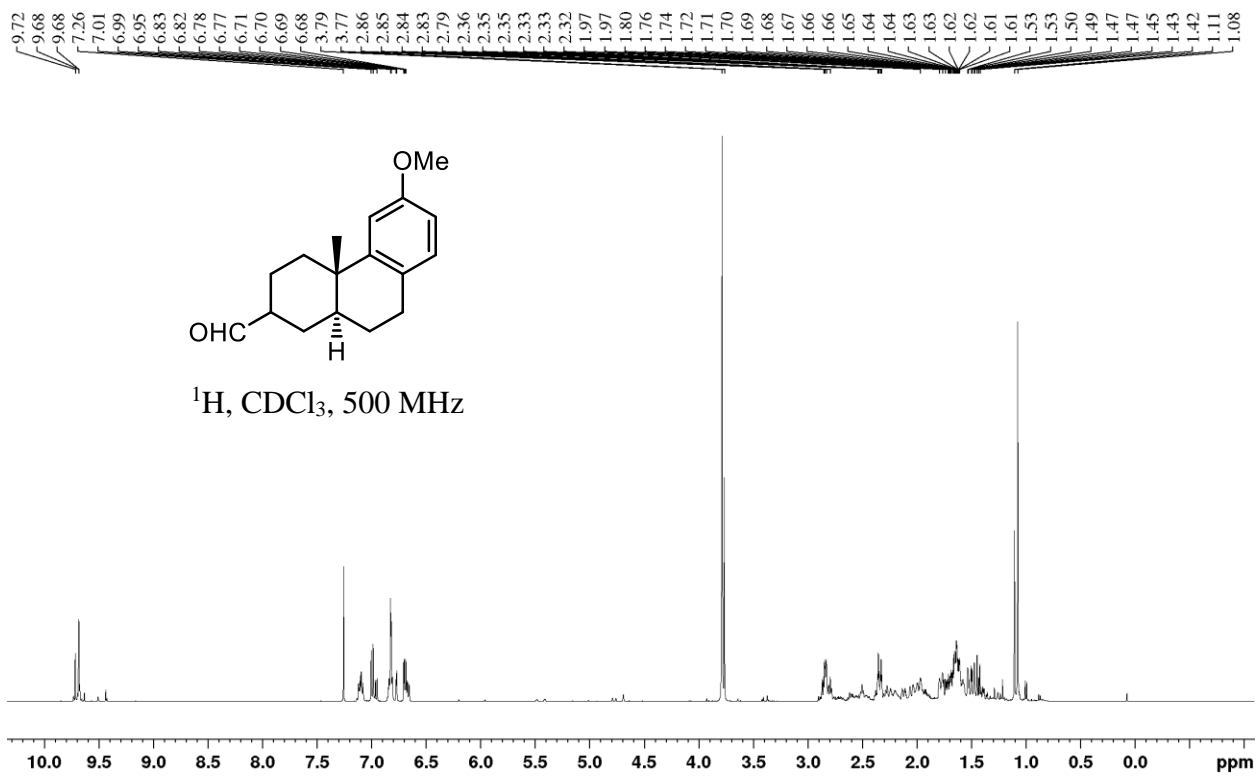




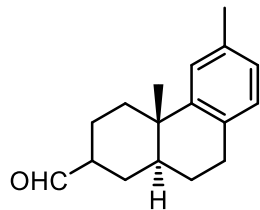




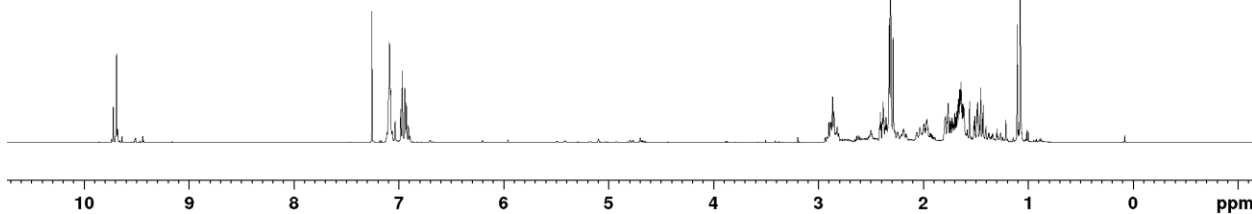




9.72 9.69 7.26 7.10 7.09 7.08 6.98 6.97 6.94 6.94 6.93 2.89 2.87 2.85 2.41 2.39 2.38 2.38 2.36 2.36 2.32 2.32 2.31 2.29 1.97 1.97 1.96 1.79 1.79 1.77 1.78 1.76 1.75 1.74 1.73 1.72 1.70 1.69 1.68 1.67 1.66 1.66 1.65 1.65 1.65 1.64 1.63 1.63 1.62 1.61 1.61 1.52 1.51 1.49 1.48 1.48 1.45 1.44 1.43 1.11 1.08

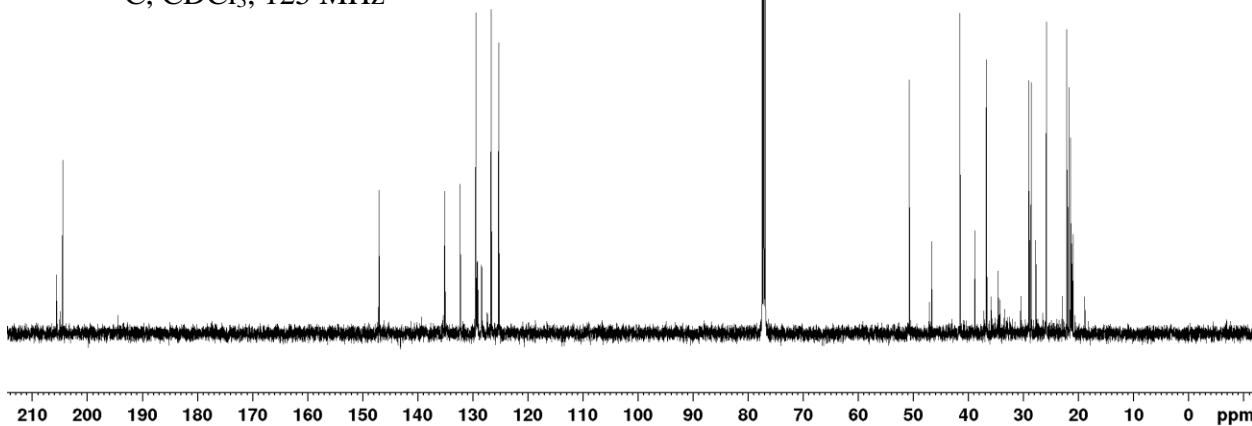


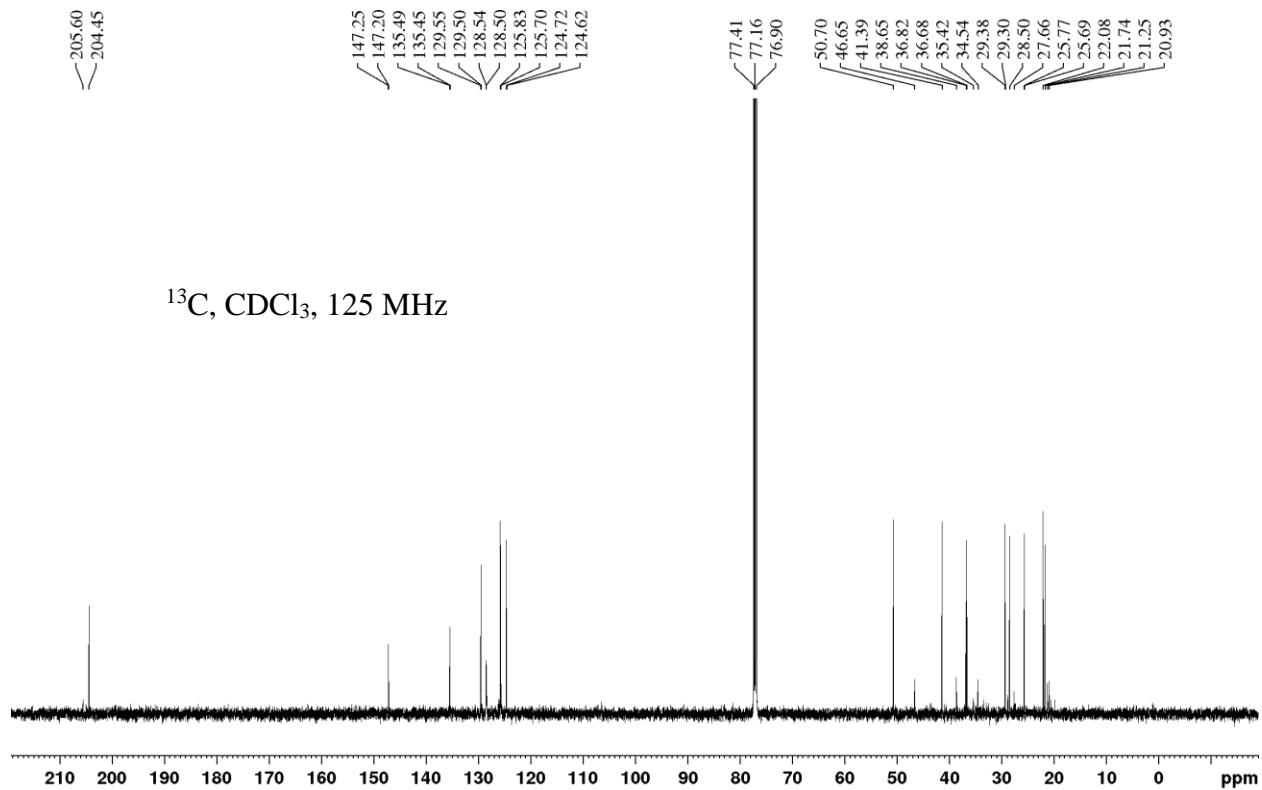
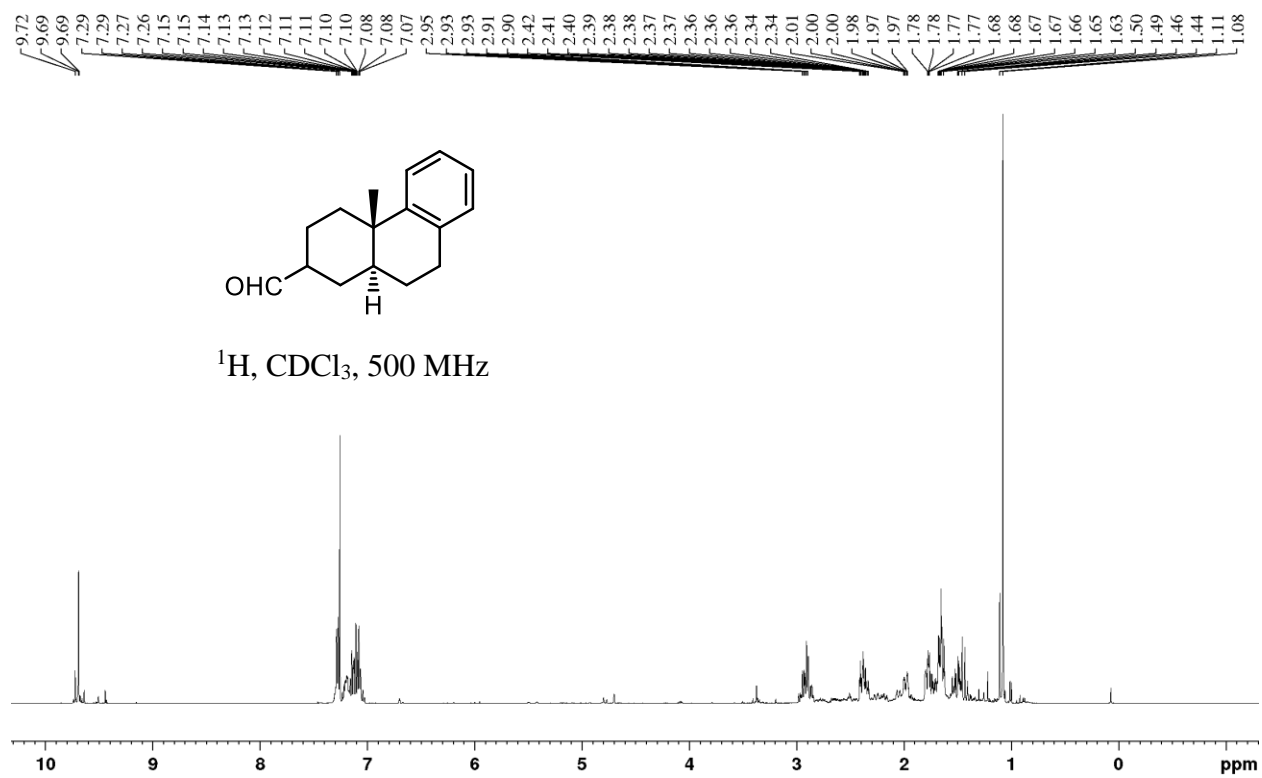
^1H , CDCl_3 , 500 MHz

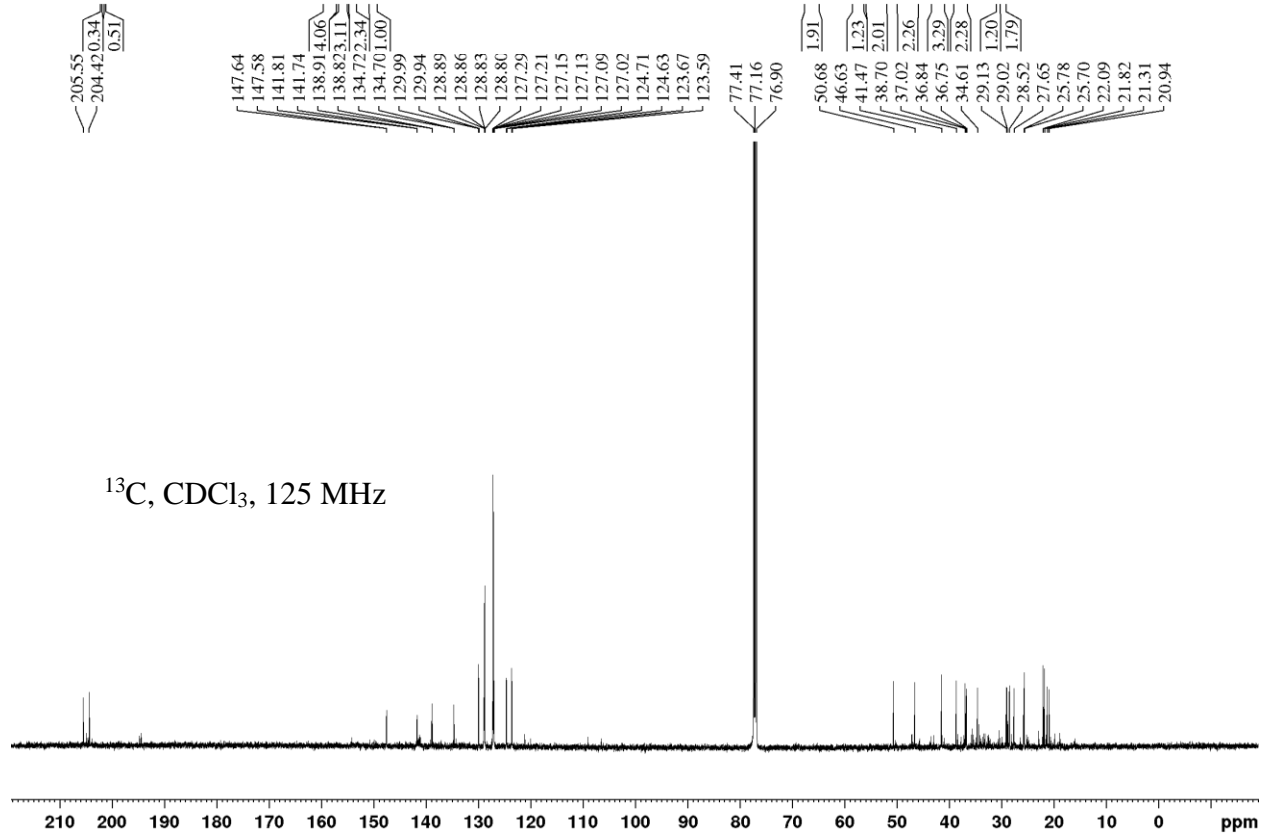
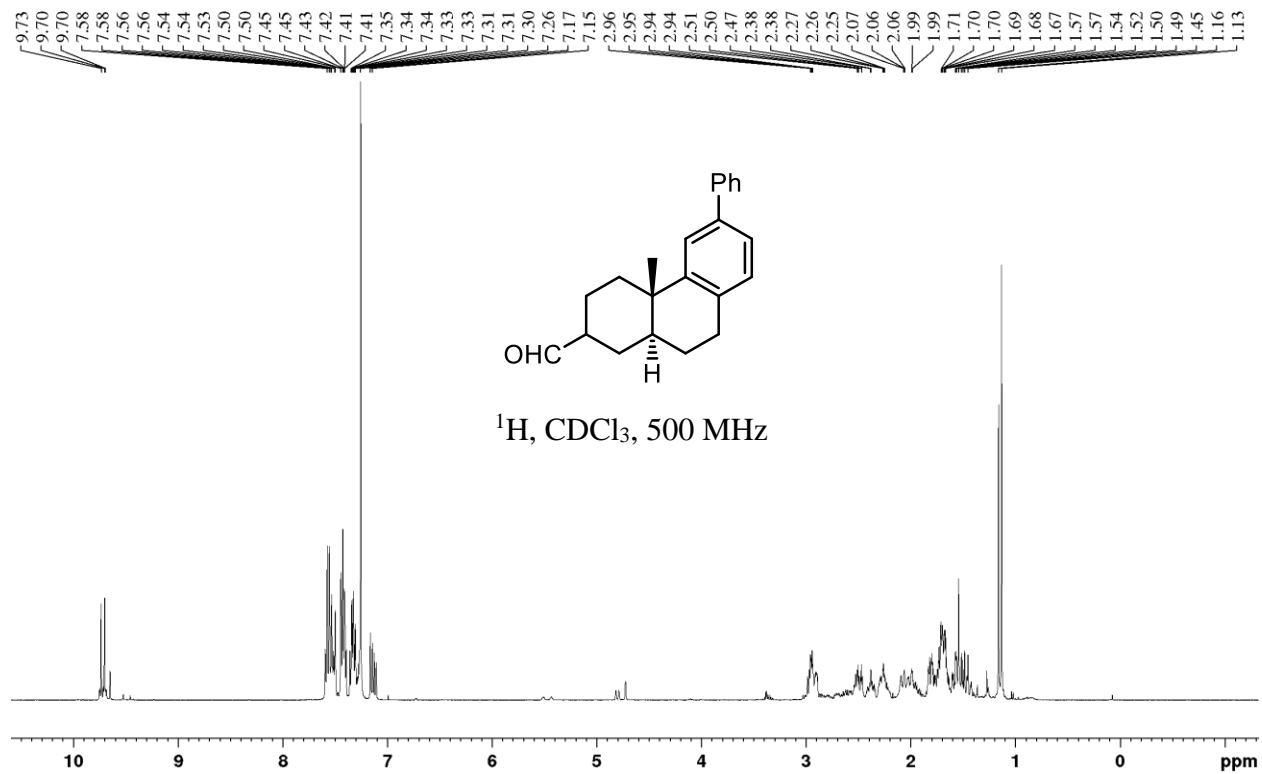


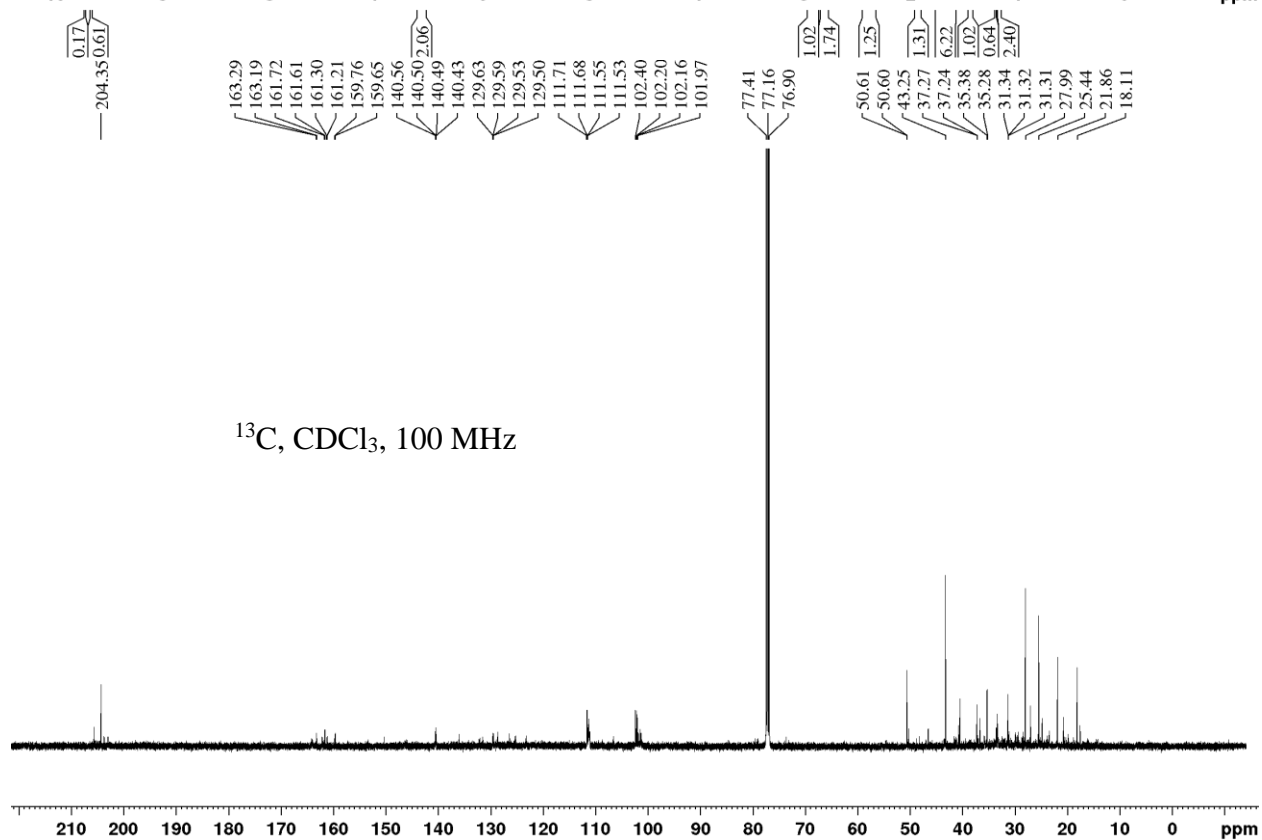
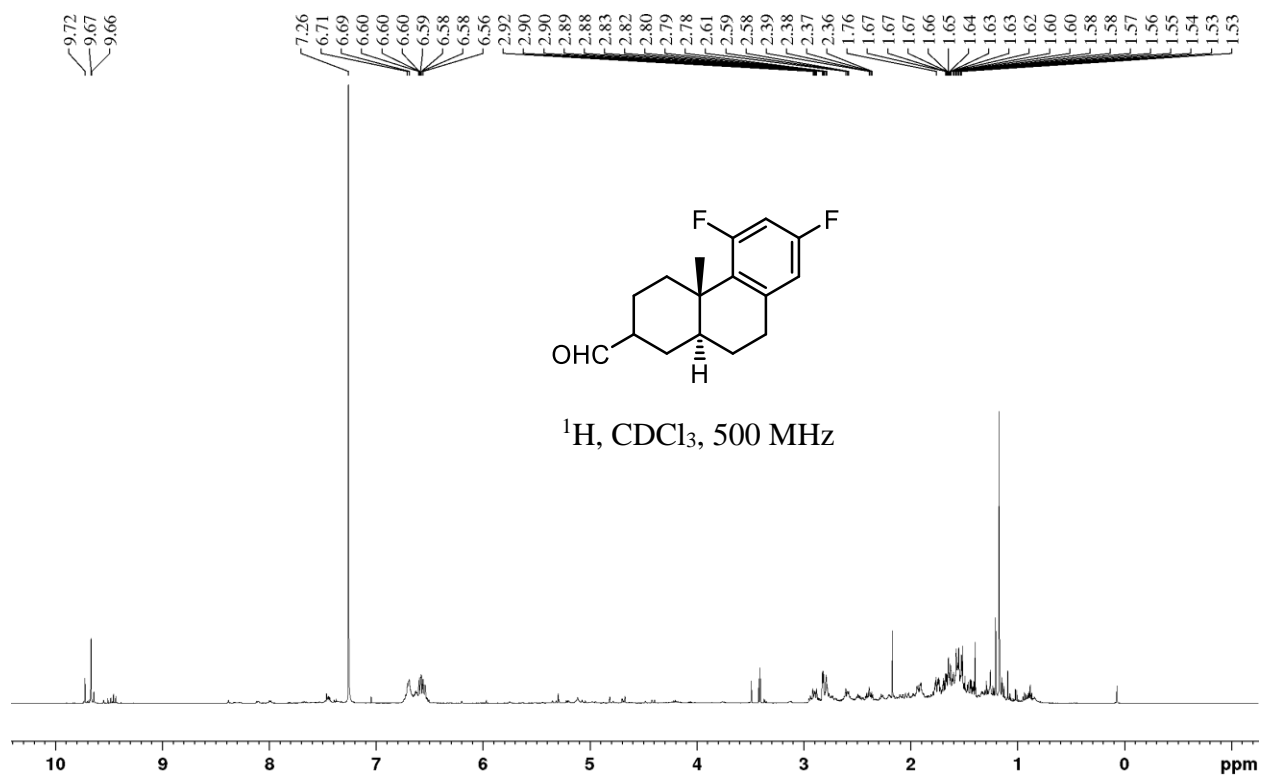
205.62 204.49 0.18 0.60 147.08 147.02 135.11 135.00 132.28 129.44 129.39 126.68 126.59 125.30 125.20 77.41 77.16 76.91 1.58 0.27 46.64 41.50 38.74 36.75 36.69 36.57 34.55 29.00 28.89 28.53 27.70 25.87 25.79 22.08 21.72 21.39 21.22 21.14 20.94

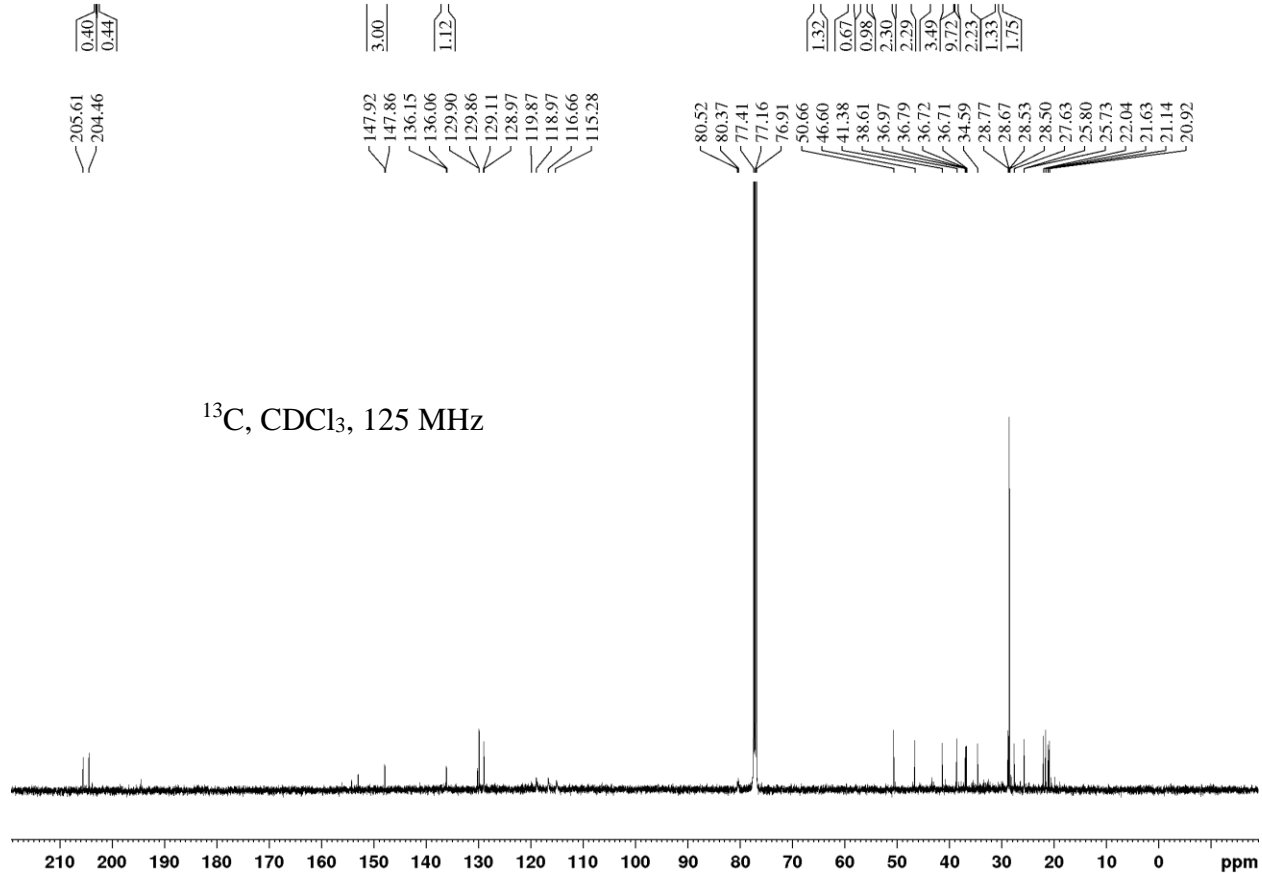
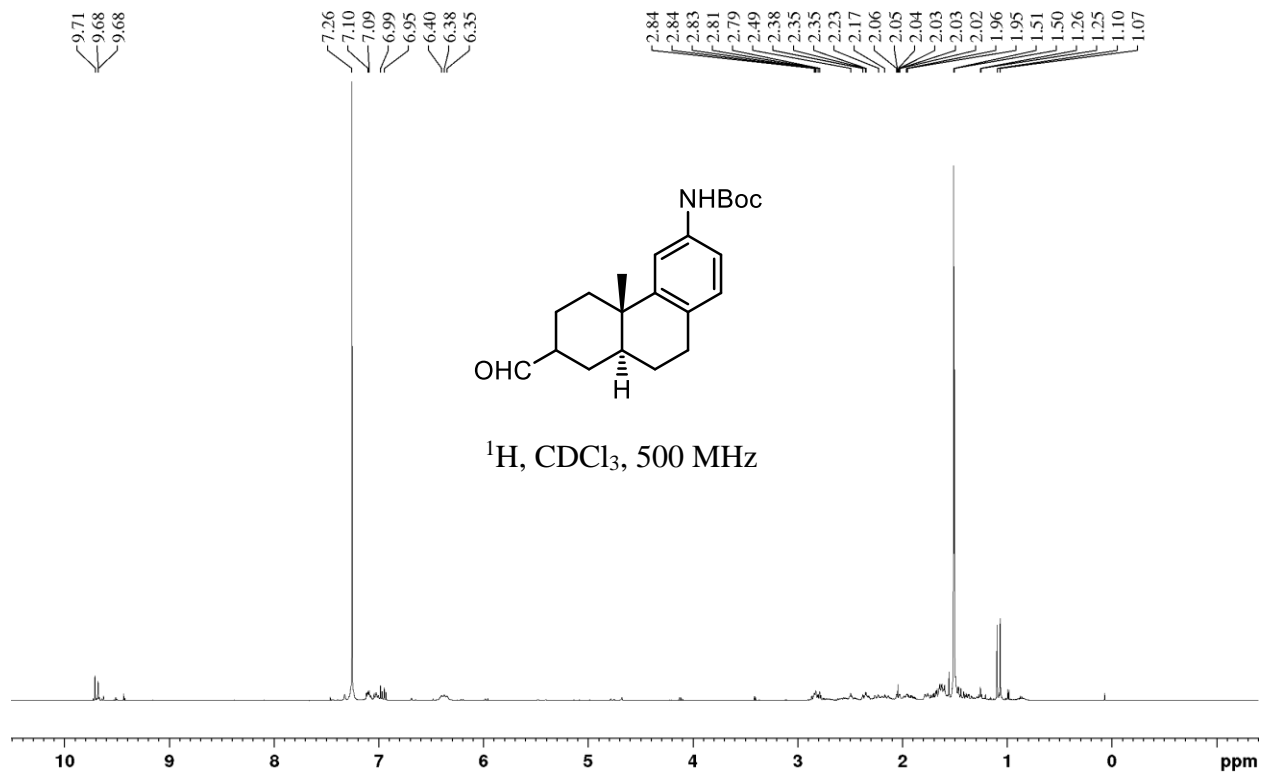
^{13}C , CDCl_3 , 125 MHz







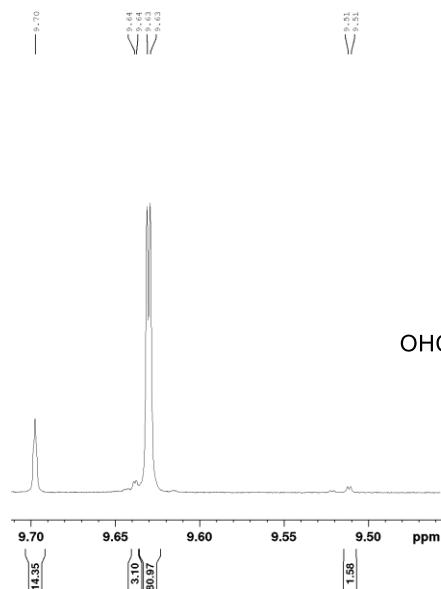




Diastereomeric ratios of polyene cyclization products in Chapter 2

Diastereomeric ratios were calculated from the relative integration of aldehyde peaks in the ^1H NMR obtained in either CDCl_3 or $(\text{CD}_3)_2\text{CO}$. Aldehyde peaks measured in the related *cis*-decalin products obtained from the (*Z*)-polyene cyclization are shown for comparison. Spectra for *cis*-decalin products were obtained from Samuel Plamondon.

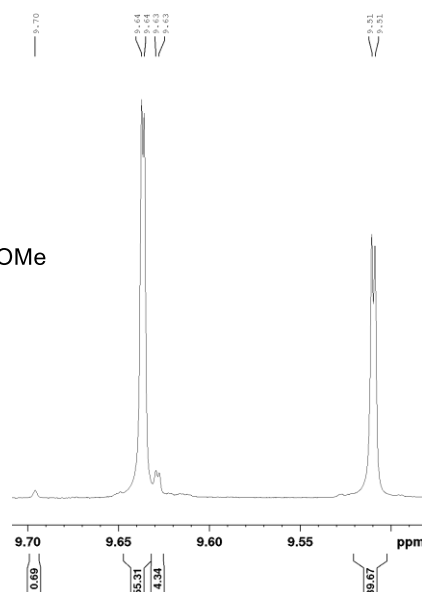
2.5:



^1H NMR (800 MHz, $(\text{CD}_3)_2\text{CO}$)
trans:*cis* 95:5, *trans*- β : α 6:1

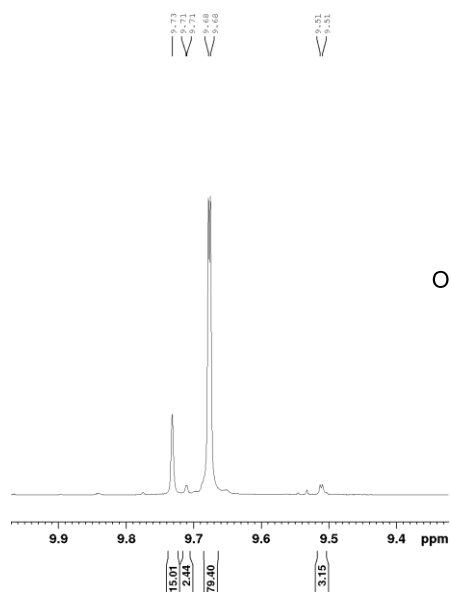
:

cis-2.5:



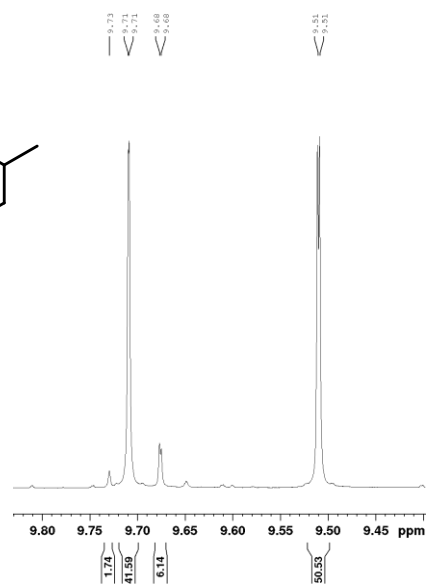
^1H NMR (800 MHz, $(\text{CD}_3)_2\text{CO}$)
cis:*trans* 95:5, *cis*- β : α 1.4:1

2.57:



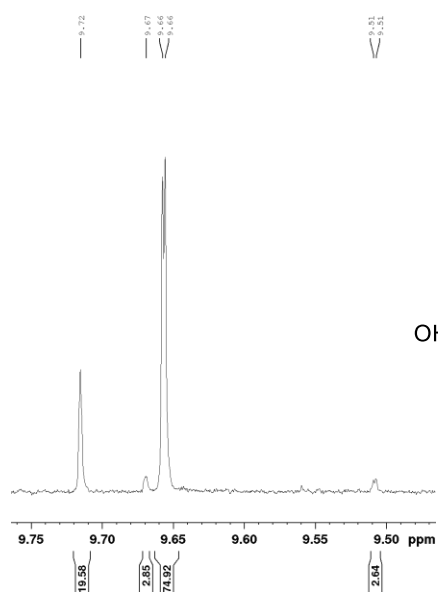
¹H NMR (500 MHz, CDCl₃)
trans:cis 94:6, *trans-β:α* 5:1

cis-2.57:



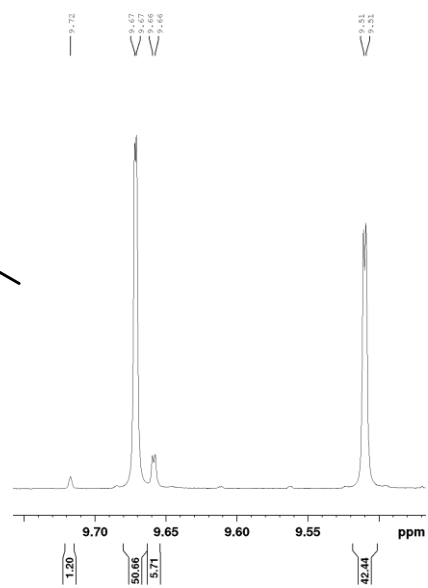
¹H NMR (800 MHz, CDCl₃)
cis:trans 92:8, *cis-α:β* 1.2:1

2.61:



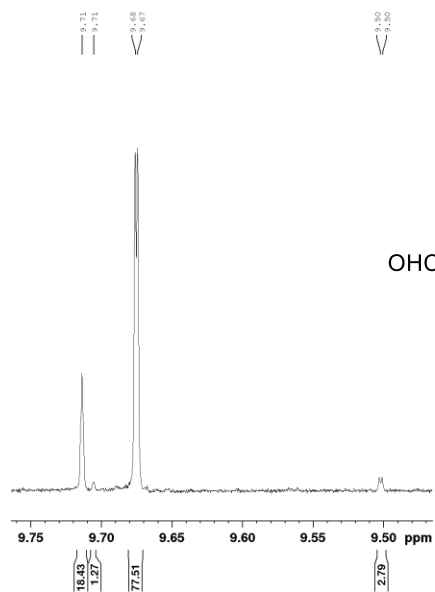
¹H NMR (800 MHz, (CD₃)₂CO)
trans:cis 94:6, *trans-β:α* 4:1

cis-2.61:



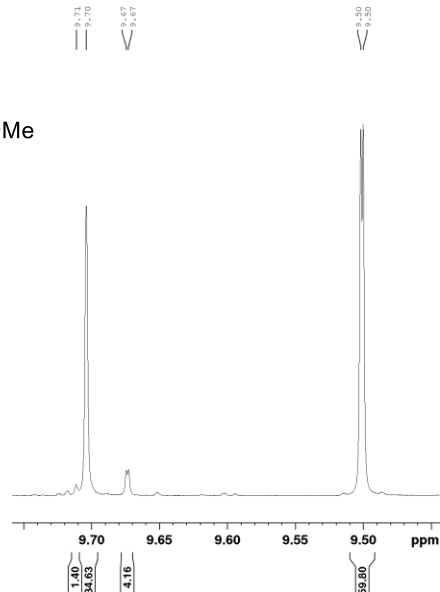
¹H NMR (800 MHz, (CD₃)₂CO)
cis:trans 93:7, *cis-β:α* 1.2:1

2.62:



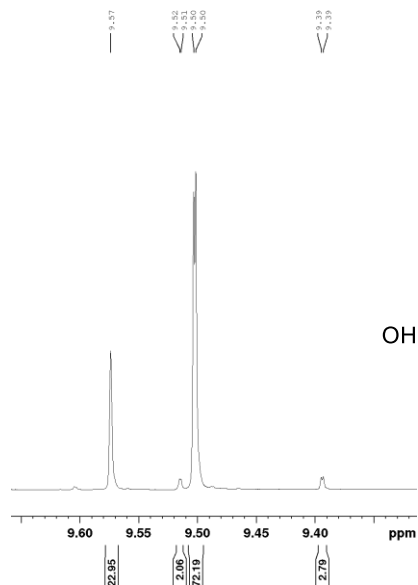
¹H NMR (800 MHz, (CD₃)₂CO)
trans:*cis* 96:4, *trans*-β:α 4:1

cis-2.62:



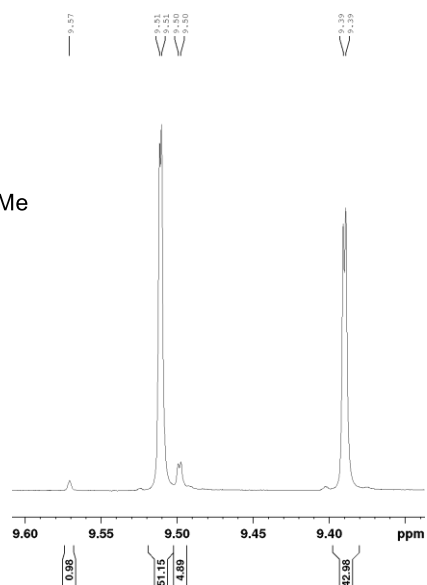
¹H NMR (800 MHz, (CD₃)₂CO)
cis:*trans* 94:6, *cis*-α:β 1.7:1

2.63:



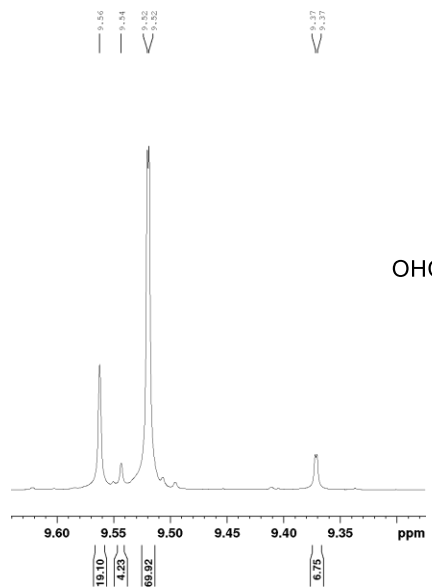
¹H NMR (800 MHz, (CD₃)₂CO)
trans:*cis* 95:5, *trans*-β:α 3:1

cis-2.63:



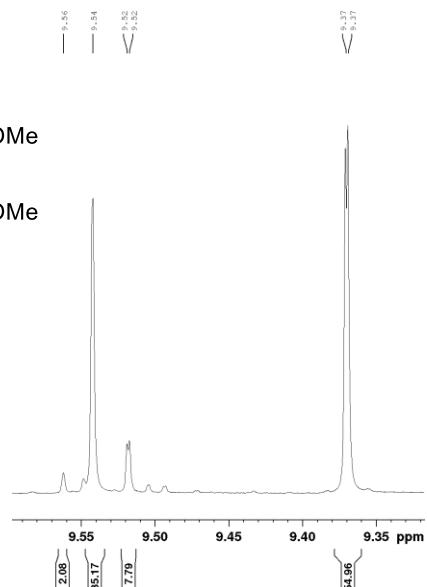
¹H NMR (800 MHz, (CD₃)₂CO)
cis:*trans* 94:6, *cis*-β:α 1.2:1

2.64:

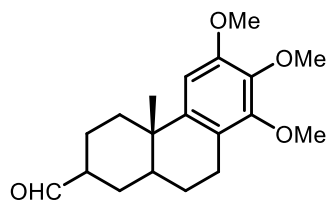


¹H NMR (800 MHz, (CD₃)₂CO)
trans:*cis* 89:11, *trans*-β:α 4:1

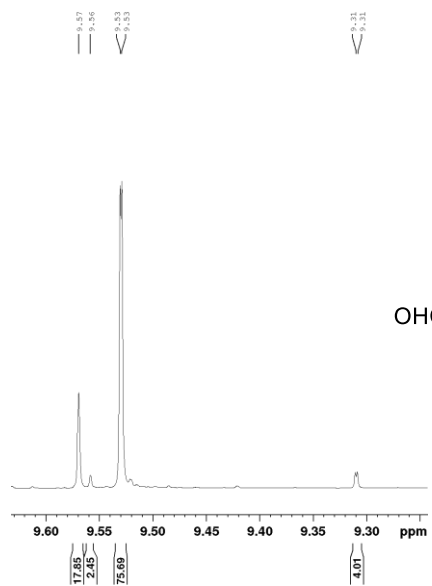
cis-2.64:



¹H NMR (800 MHz, (CD₃)₂CO)
cis:*trans* 90:10, *cis*-α:β 1.6:1

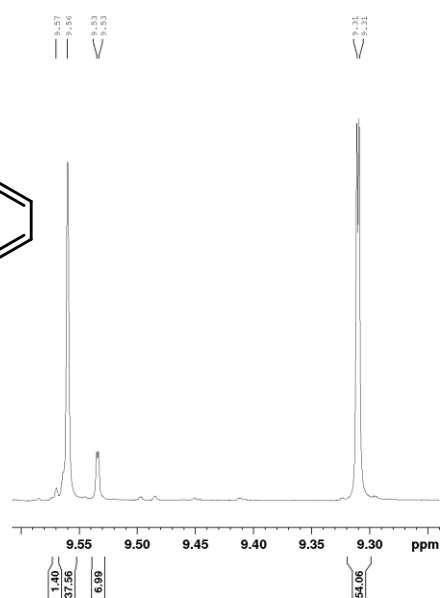


2.65:

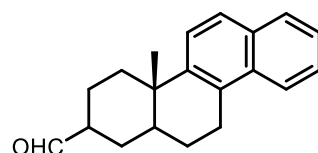


¹H NMR (800 MHz, (CD₃)₂CO)
trans:*cis* 94:6, *trans*-β:α 4:1

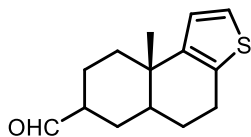
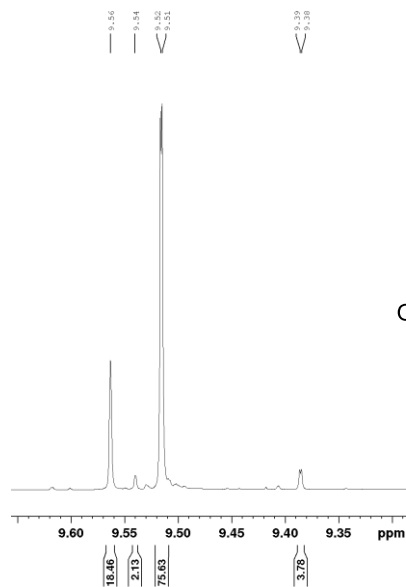
cis-2.65:



¹H NMR (800 MHz, (CD₃)₂CO)
cis:*trans* 92:8, *cis*-α:β 1.4:1

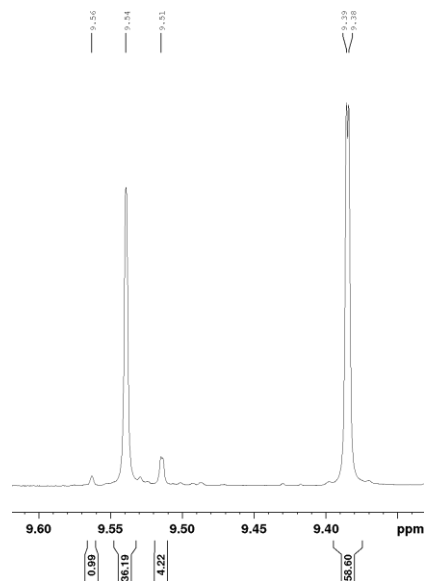


2.66:



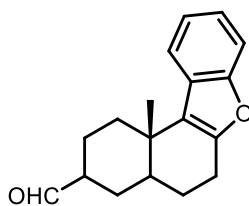
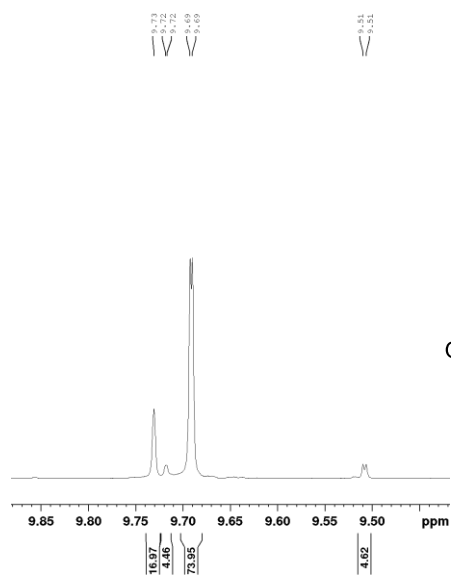
^1H NMR (800 MHz, $(\text{CD}_3)_2\text{CO}$)
trans:cis 94:6, *trans*- β : α 4:1

***cis*-2.66:**



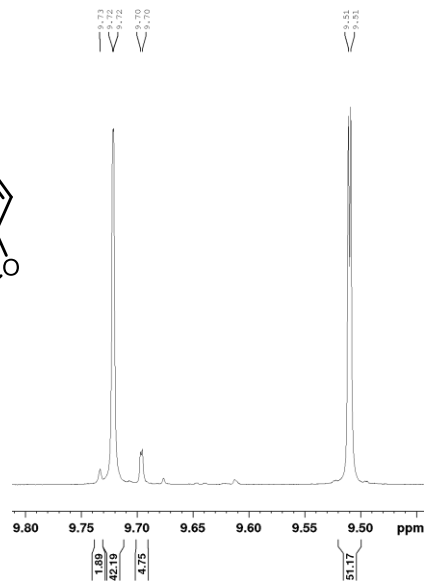
^1H NMR (800 MHz, $(\text{CD}_3)_2\text{CO}$)
cis:trans 95:5, *cis*- α : β 1.6:1

2.69:



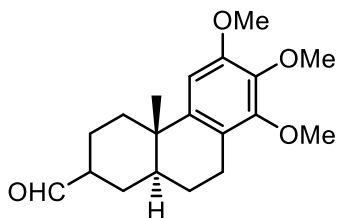
^1H NMR (500 MHz, CDCl_3)
trans:cis 91:9, *trans*- β : α 4:1

***cis*-2.69:**

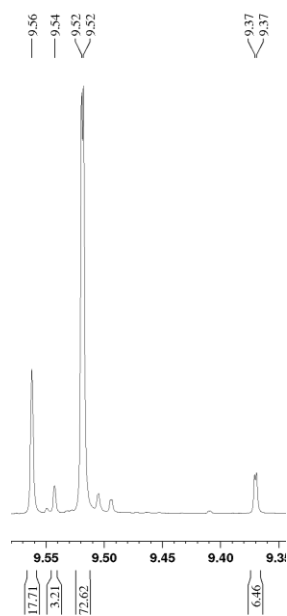


^1H NMR (800 MHz, CDCl_3)
cis:trans 93:7, *cis*- α : β 1.2:1

Diastereomeric ratios of polyene cyclization product in Chapter 3

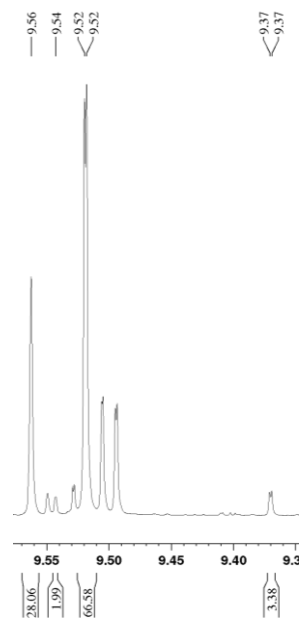


With catalyst **1.241**:

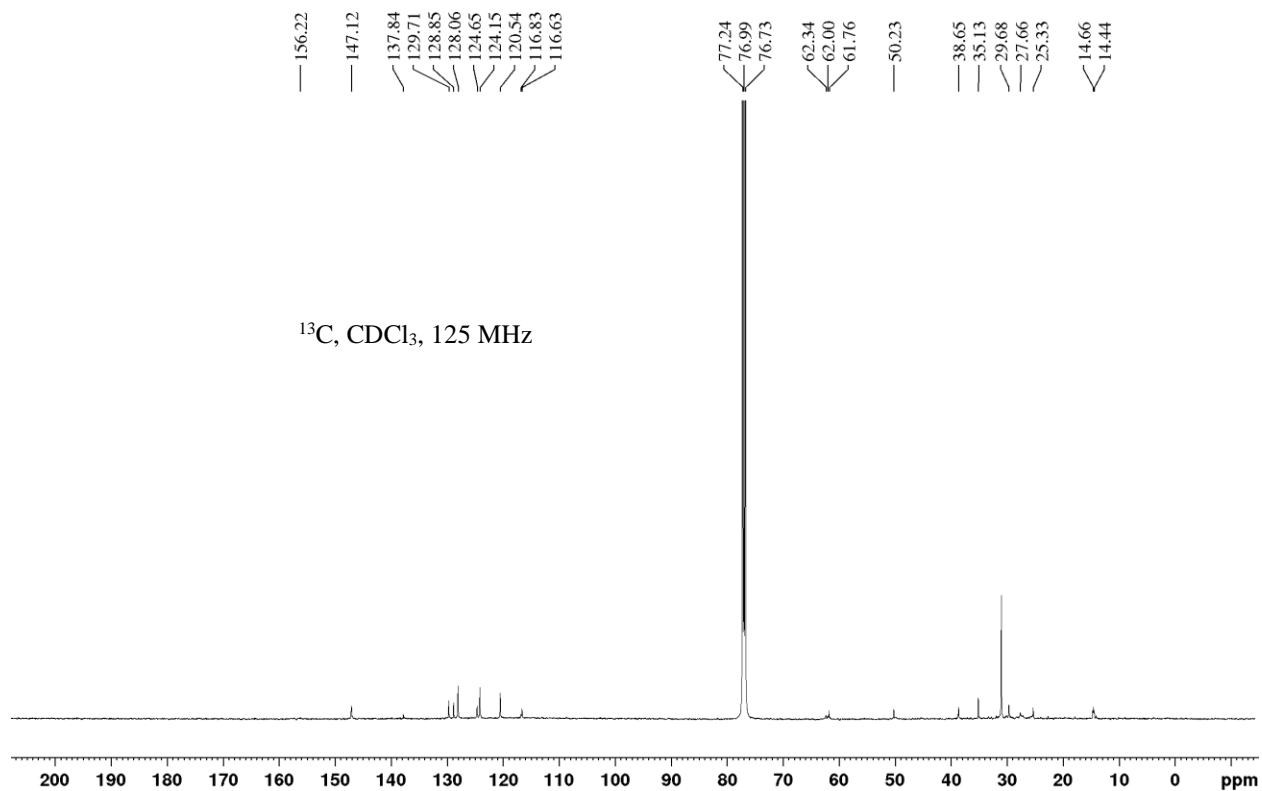
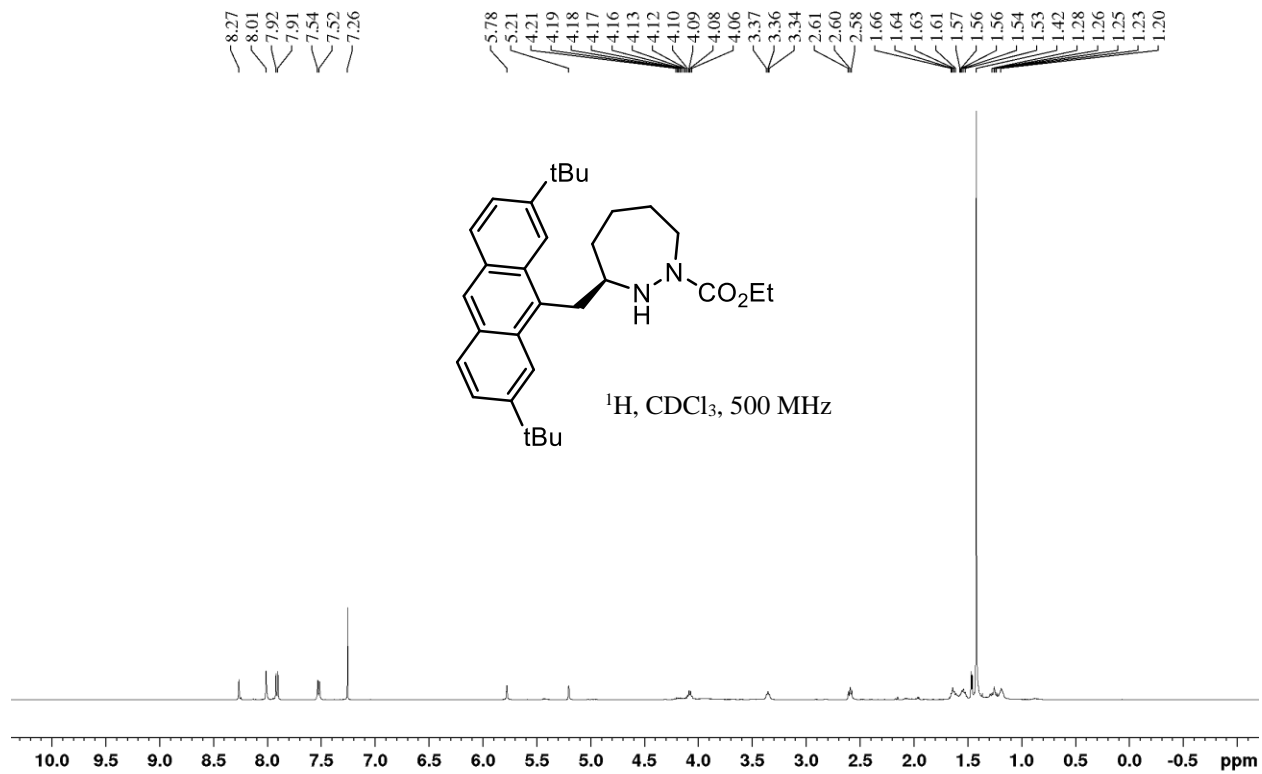


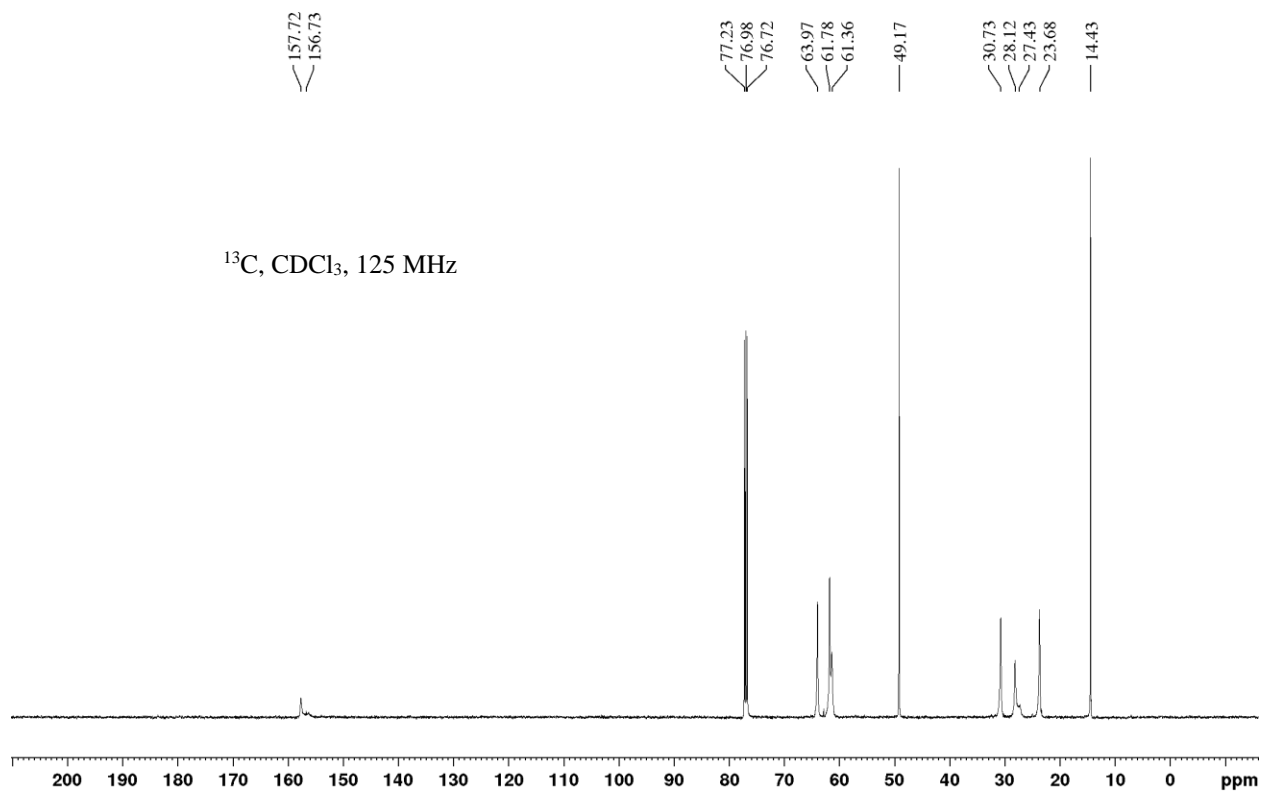
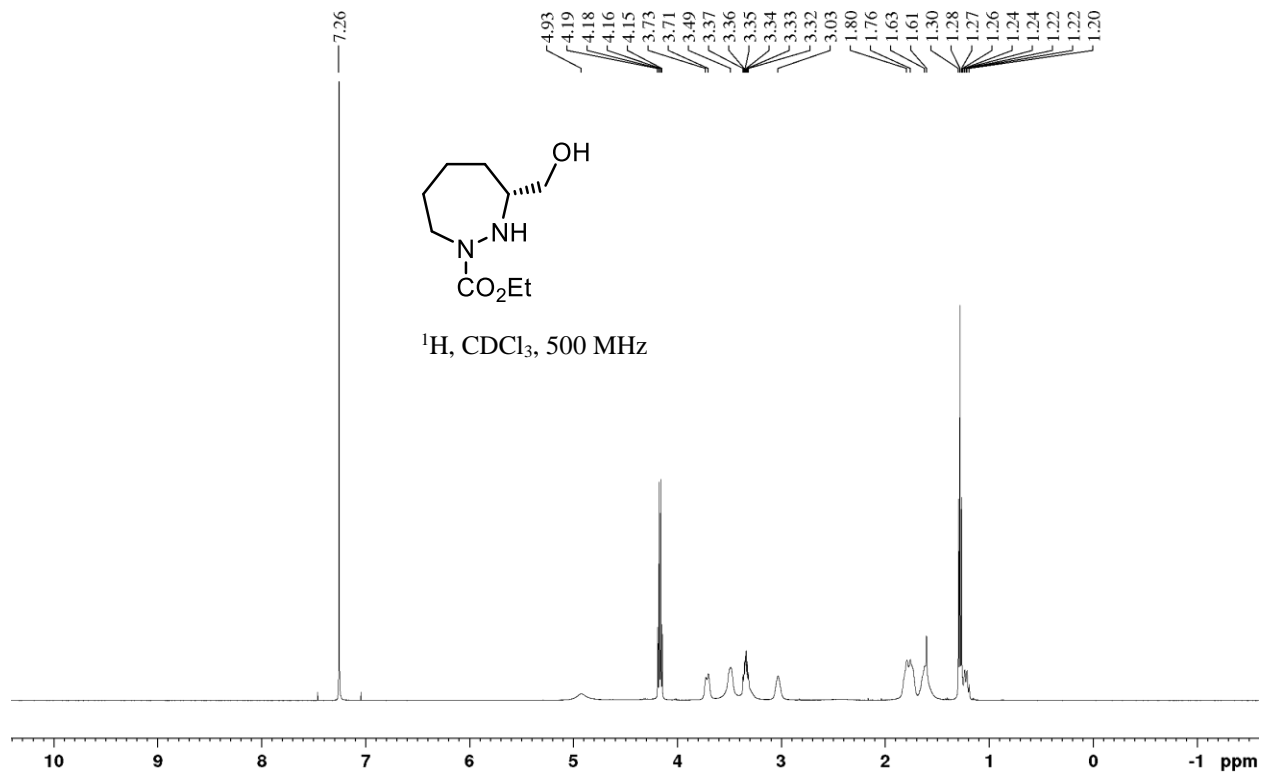
^1H NMR (800 MHz, $(\text{CD}_3)_2\text{CO}$)
trans:cis 90:10, *trans*- β : α 4:1

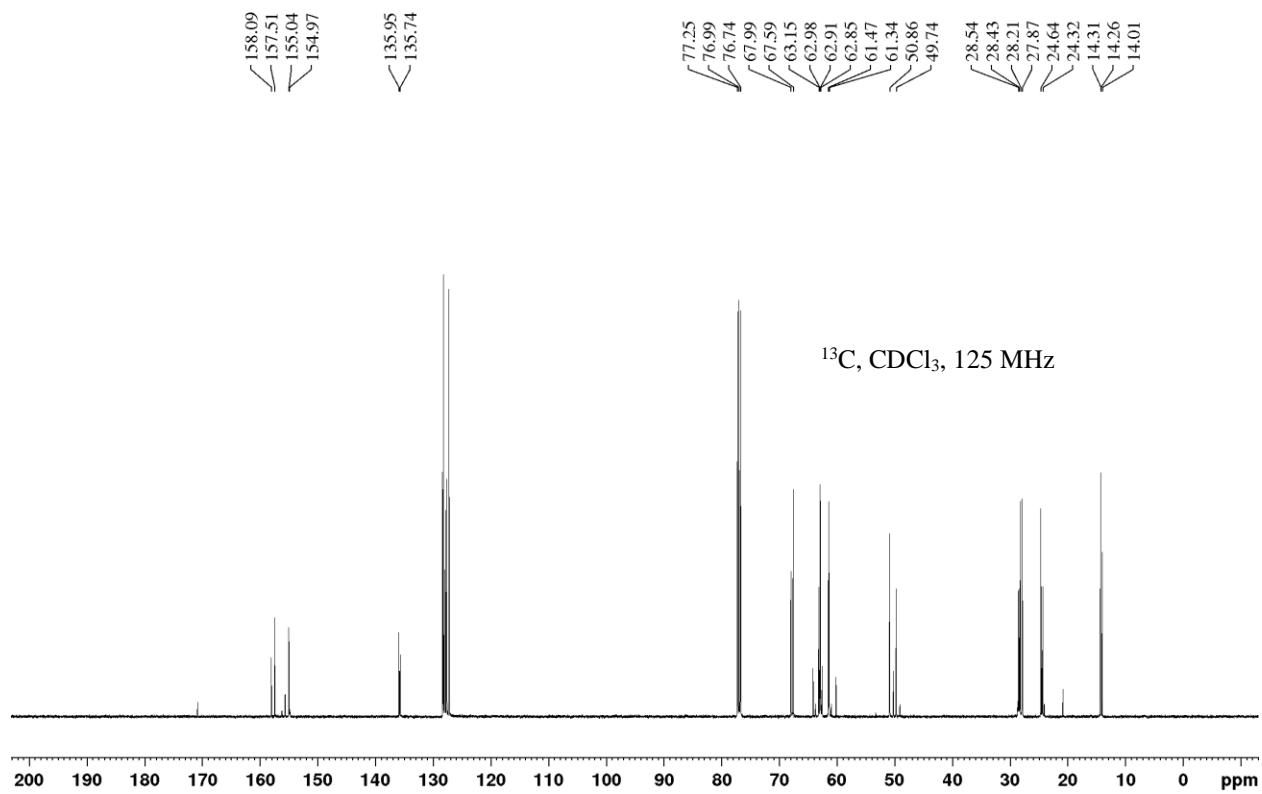
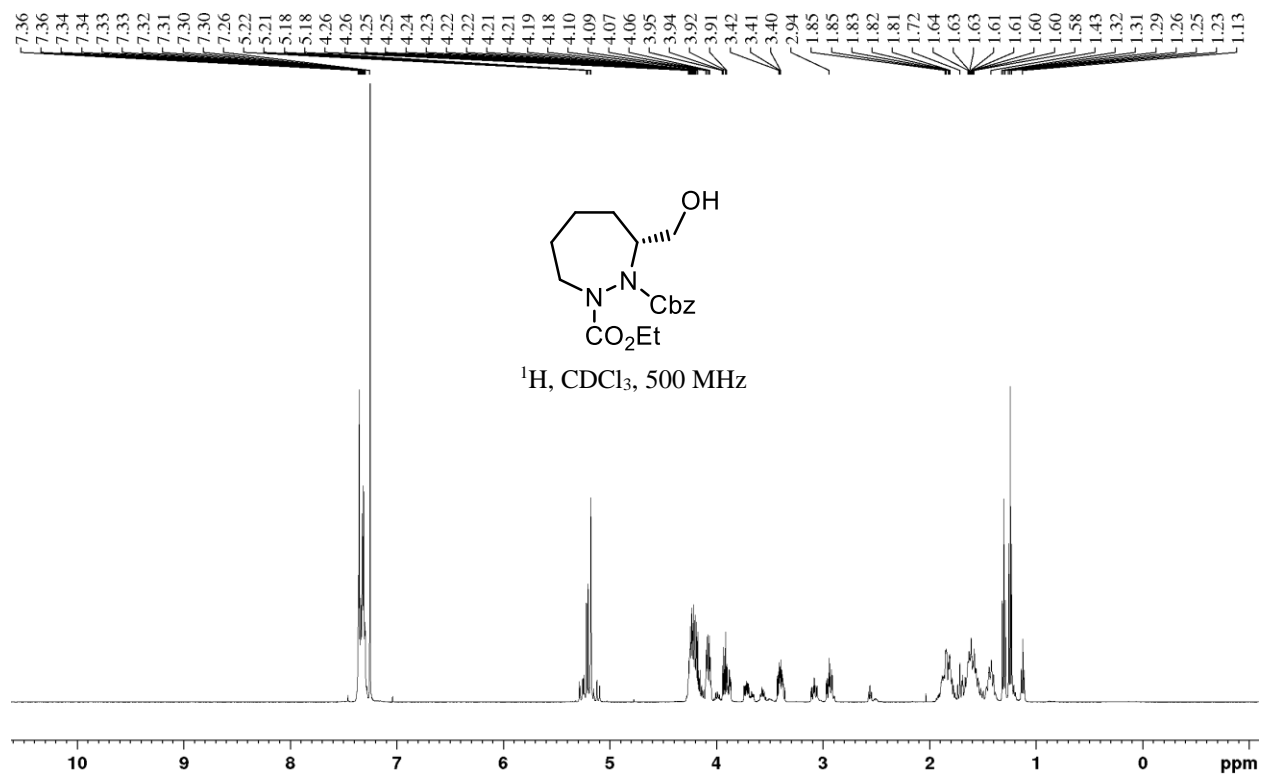
With catalyst **3.74**:

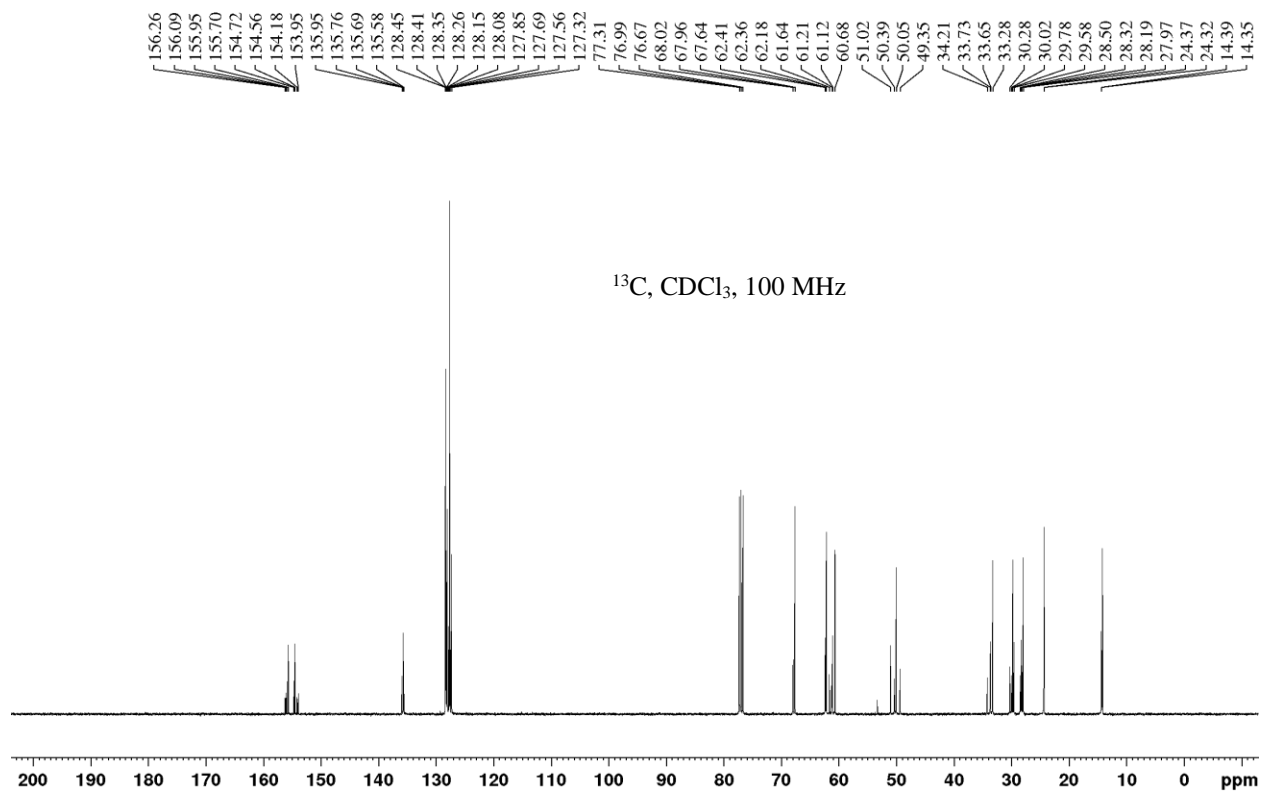
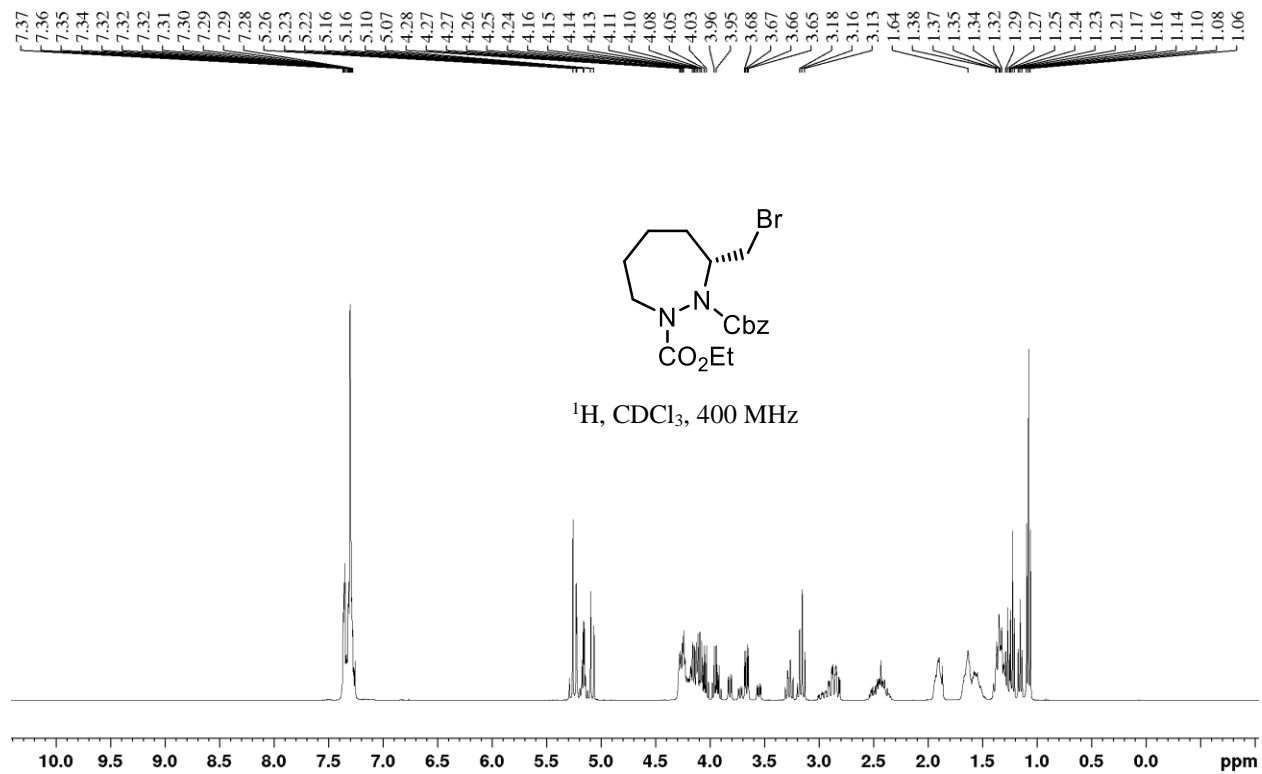


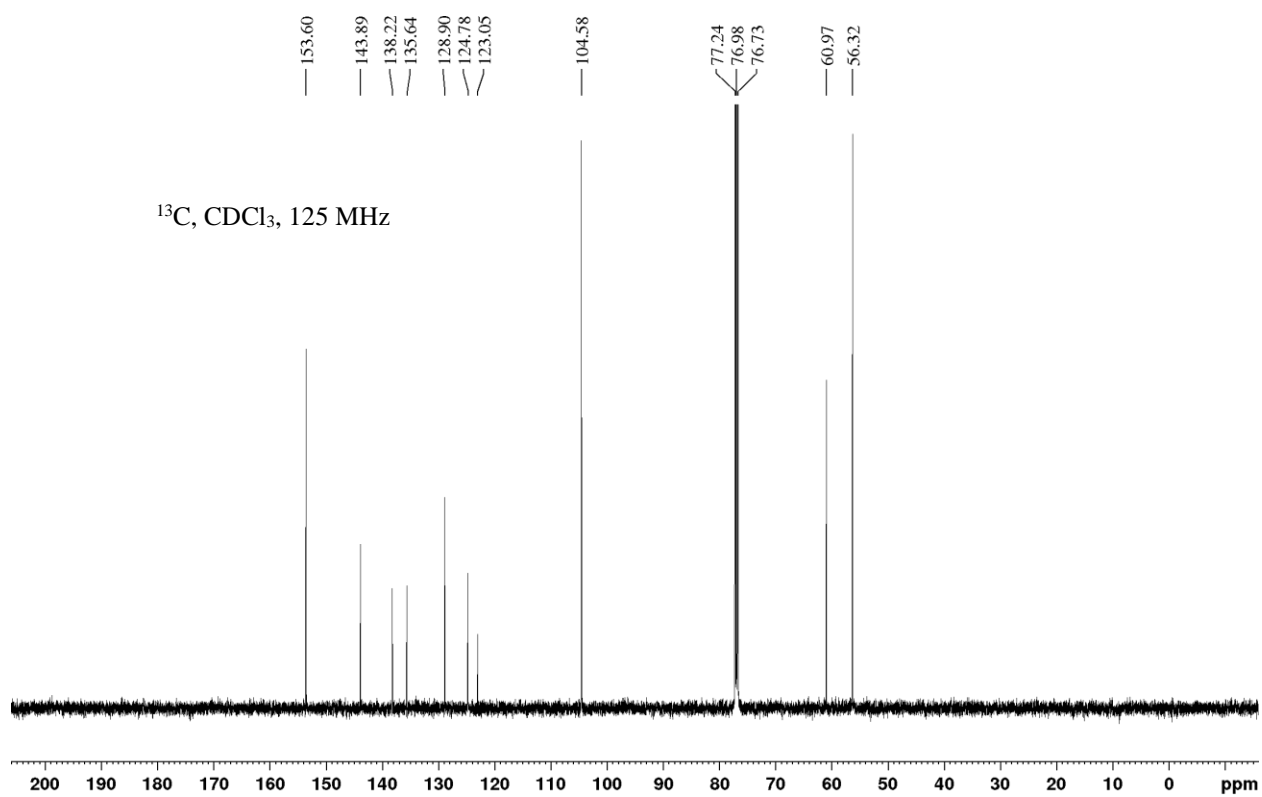
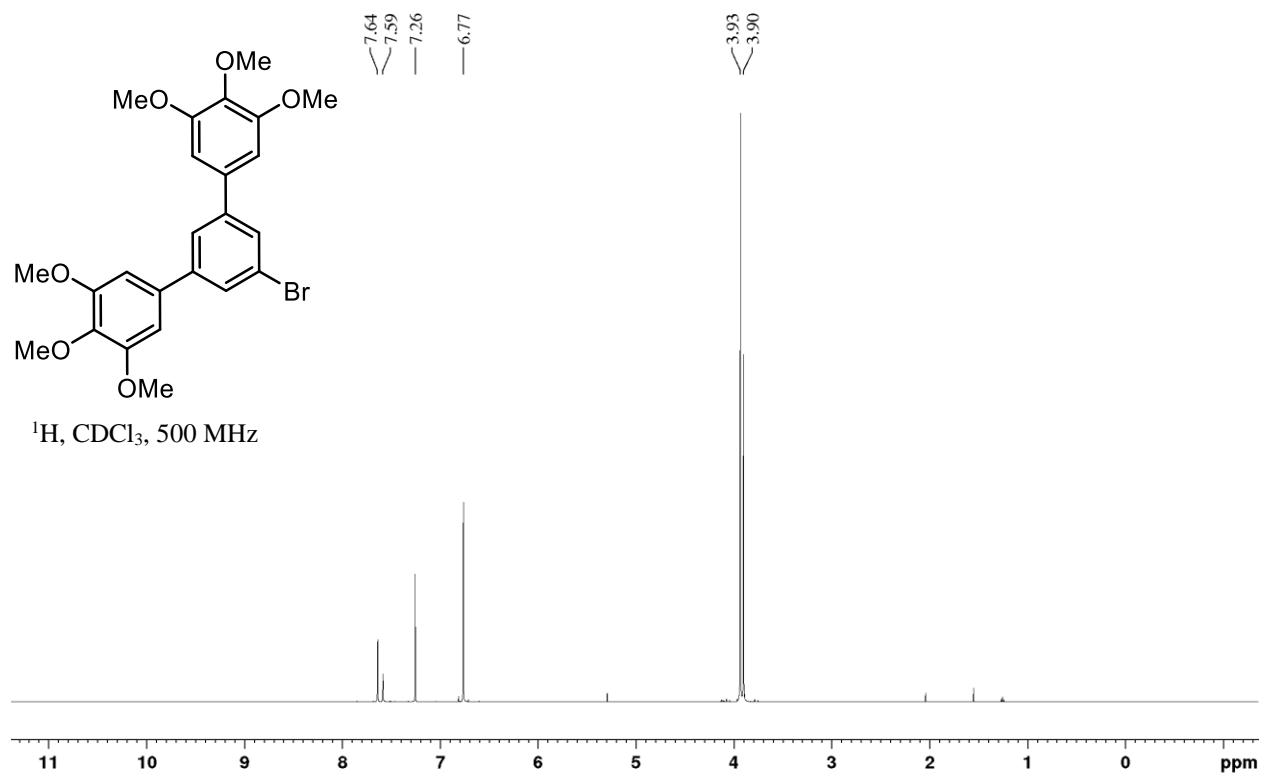
^1H NMR (800 MHz, $(\text{CD}_3)_2\text{CO}$)
trans:cis 95:5, *trans*- β : α 2:1
(before purification)

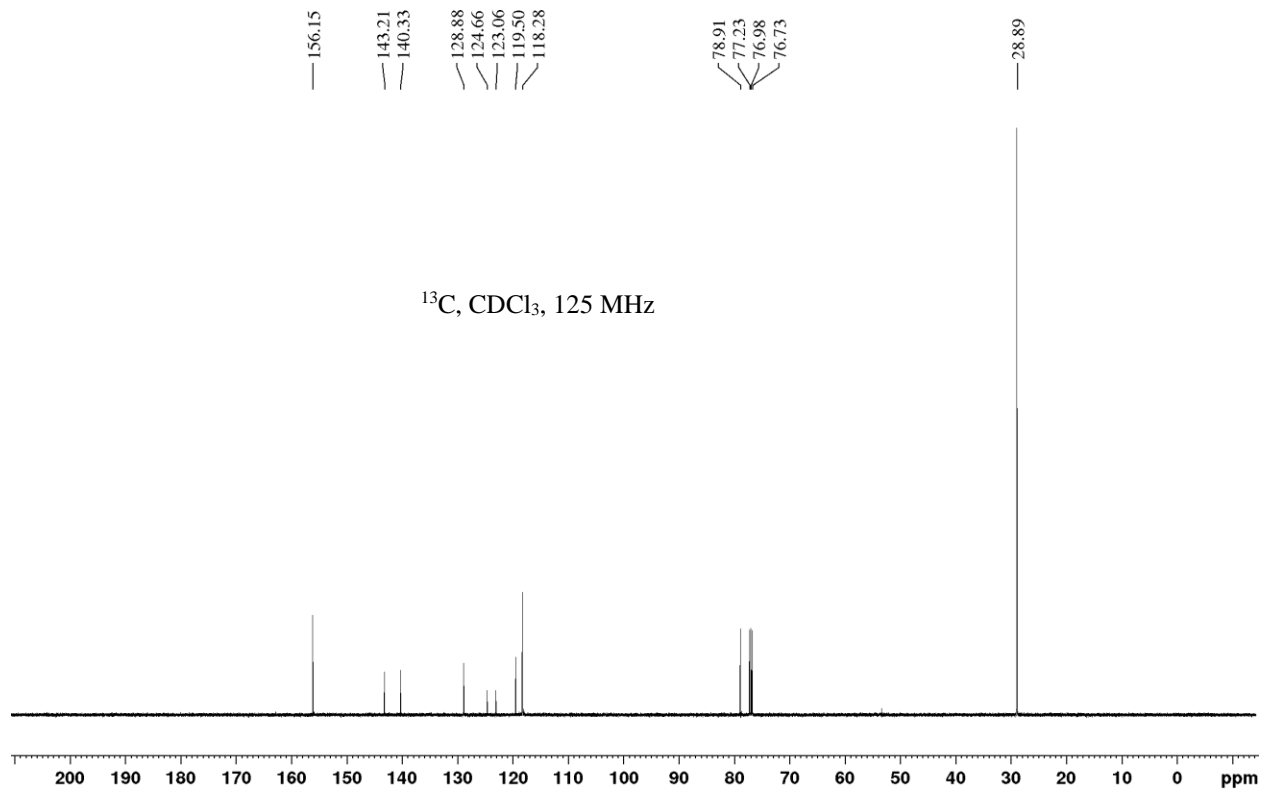
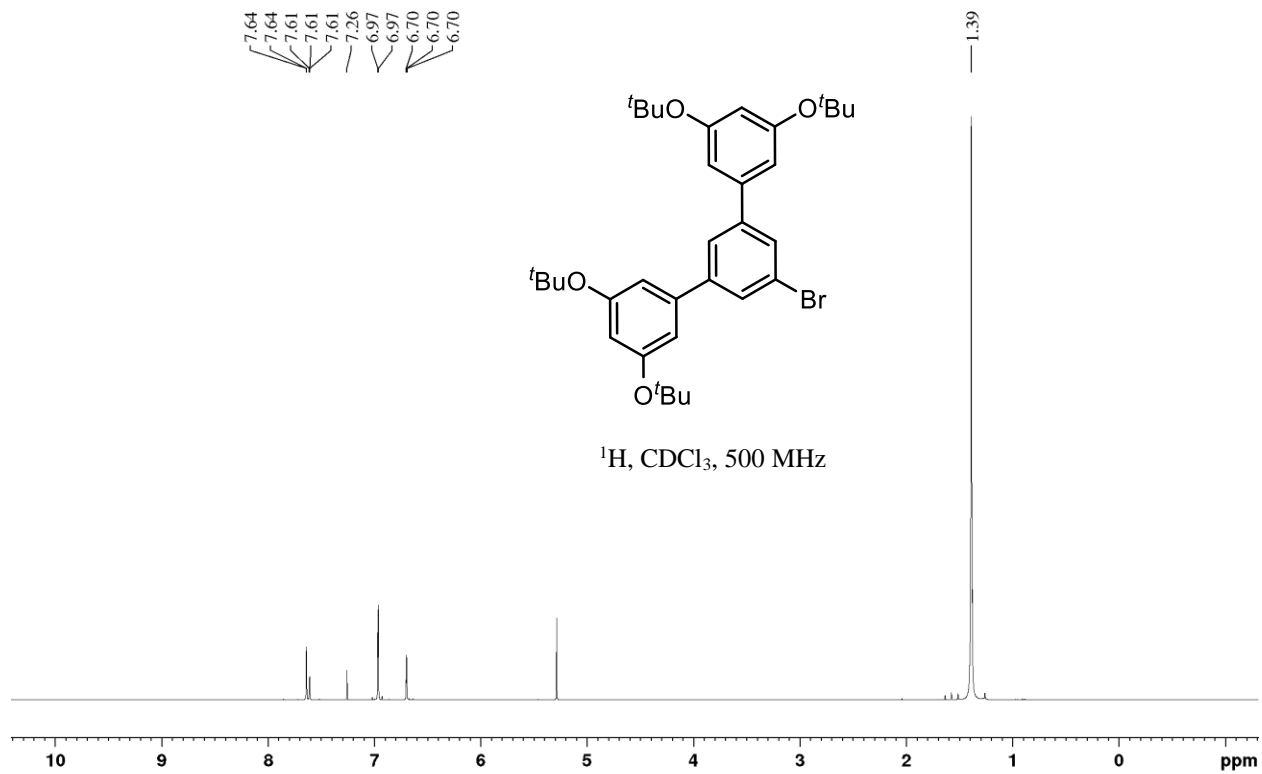


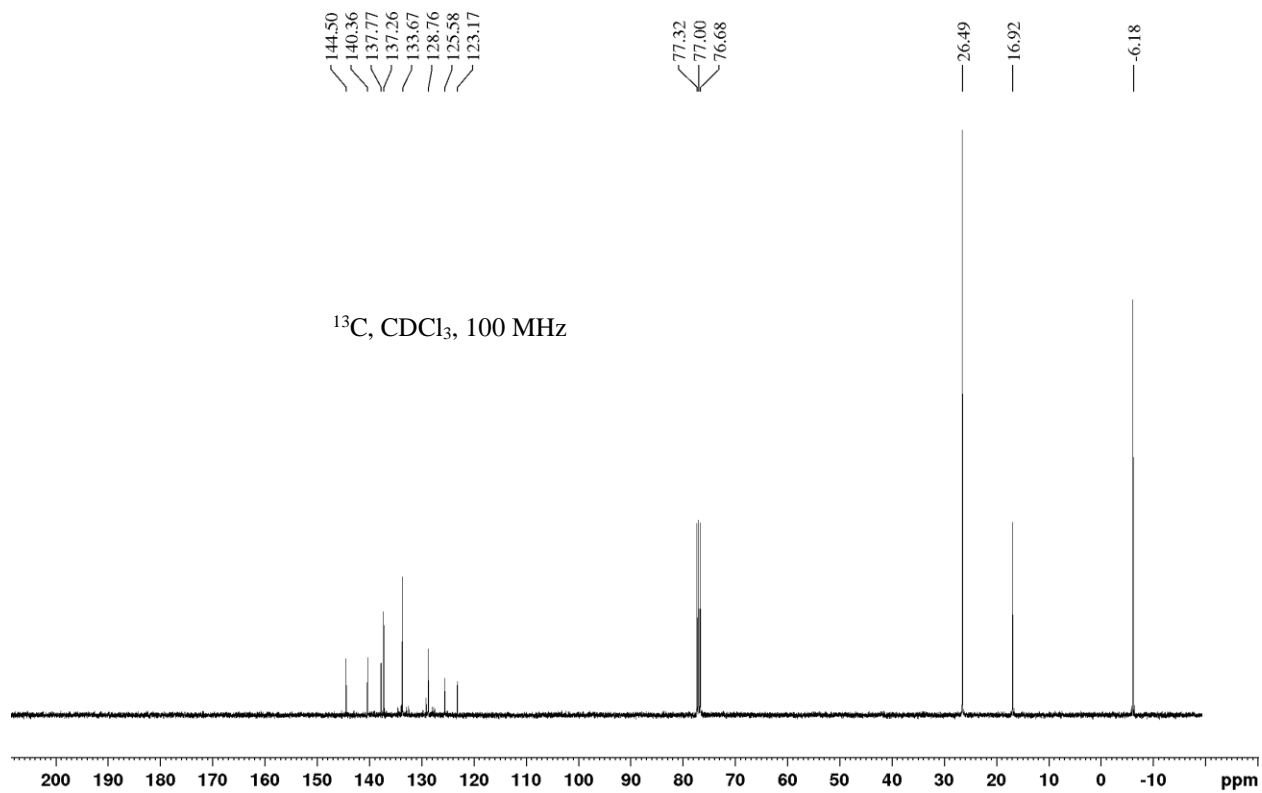
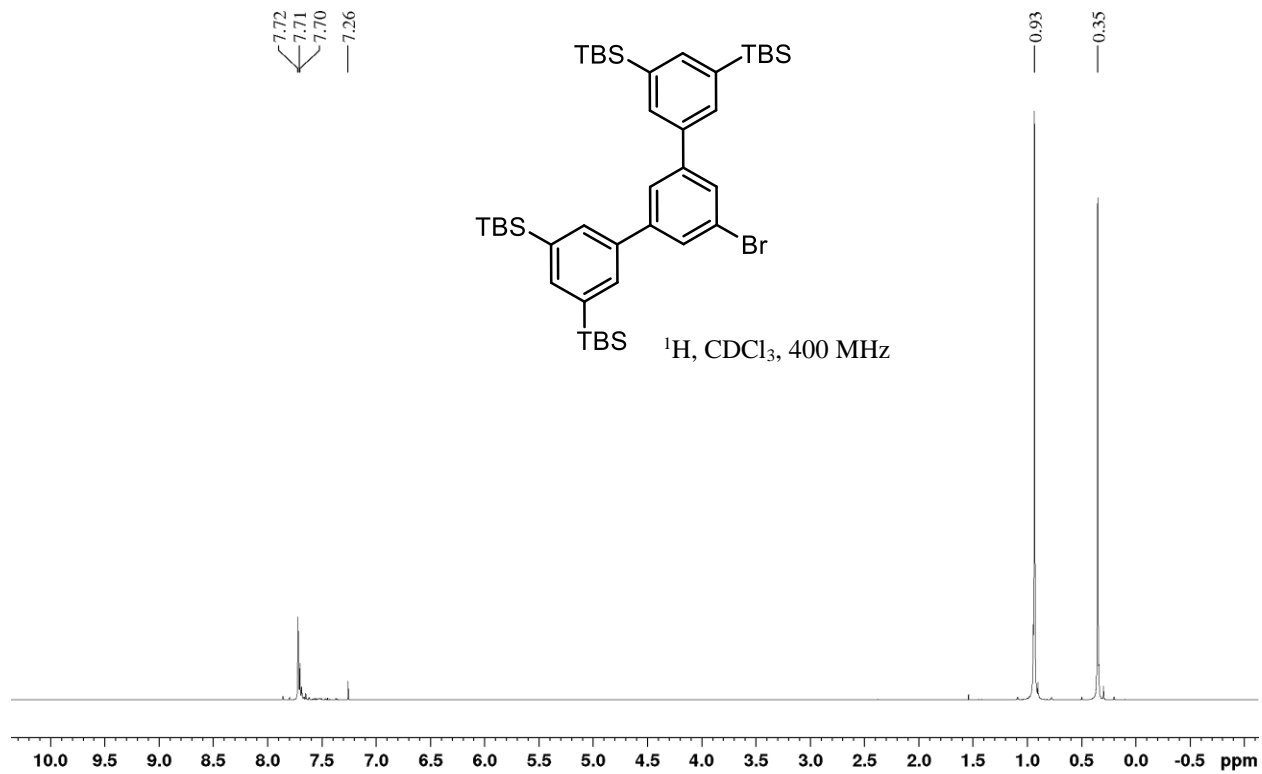


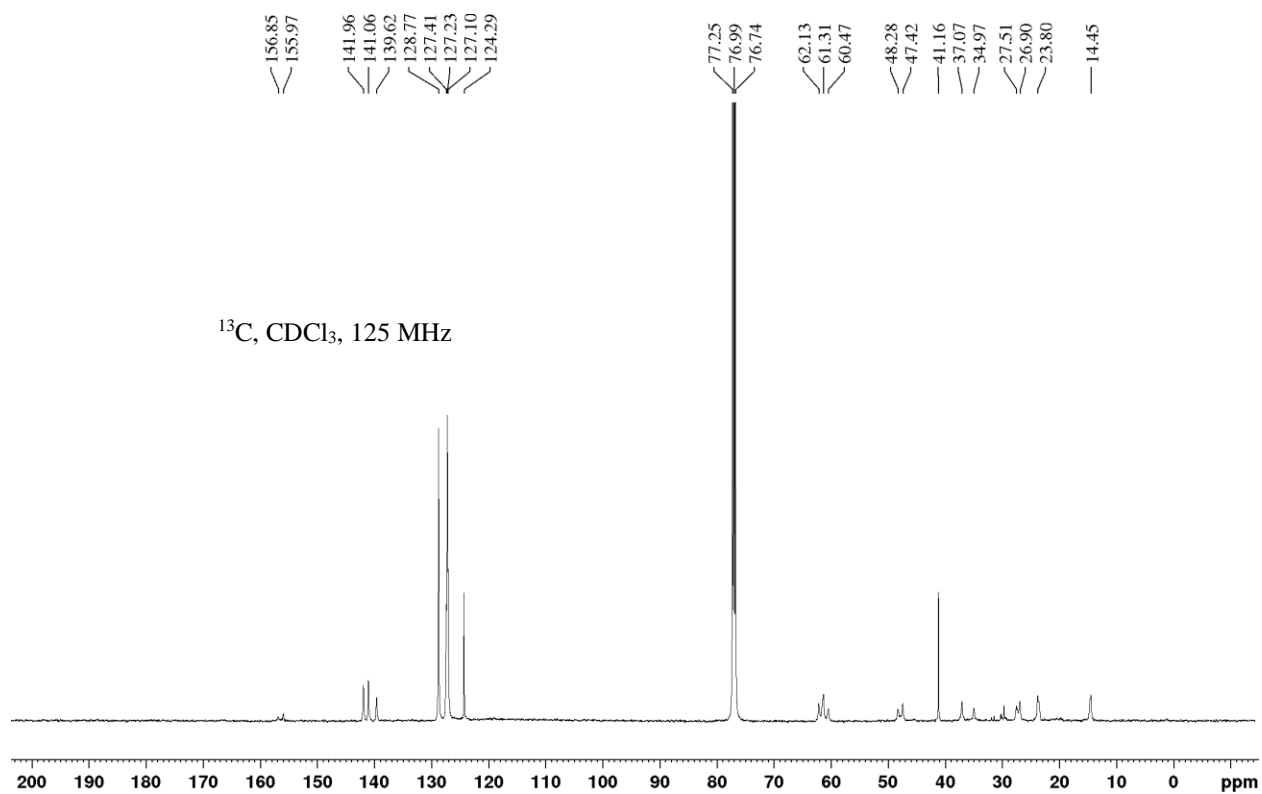
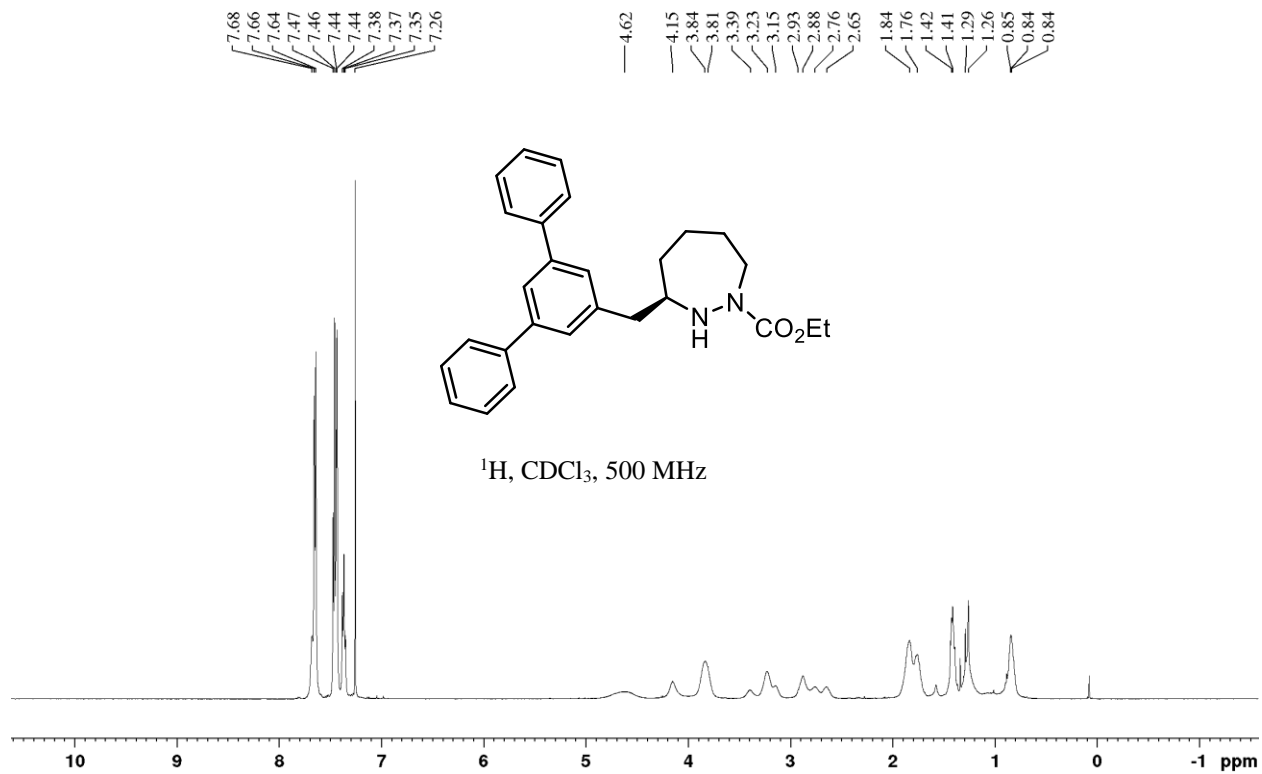


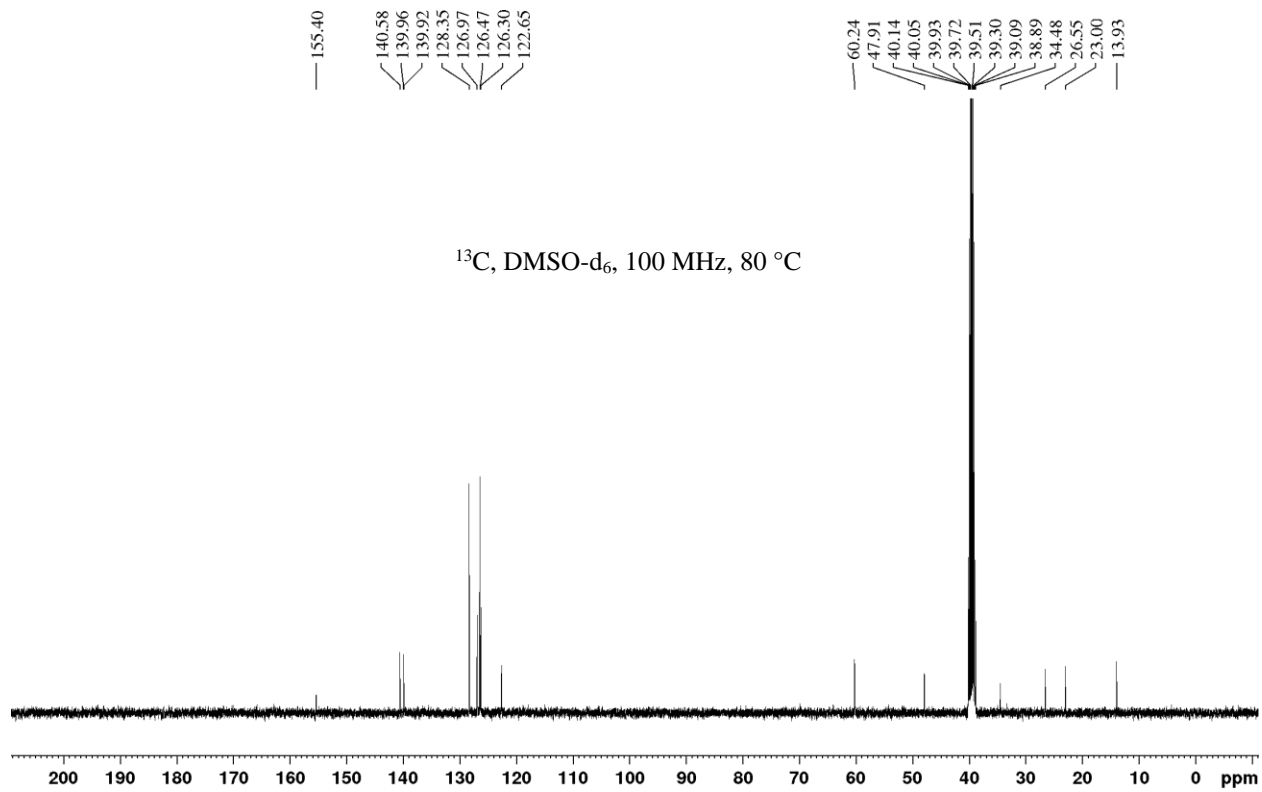
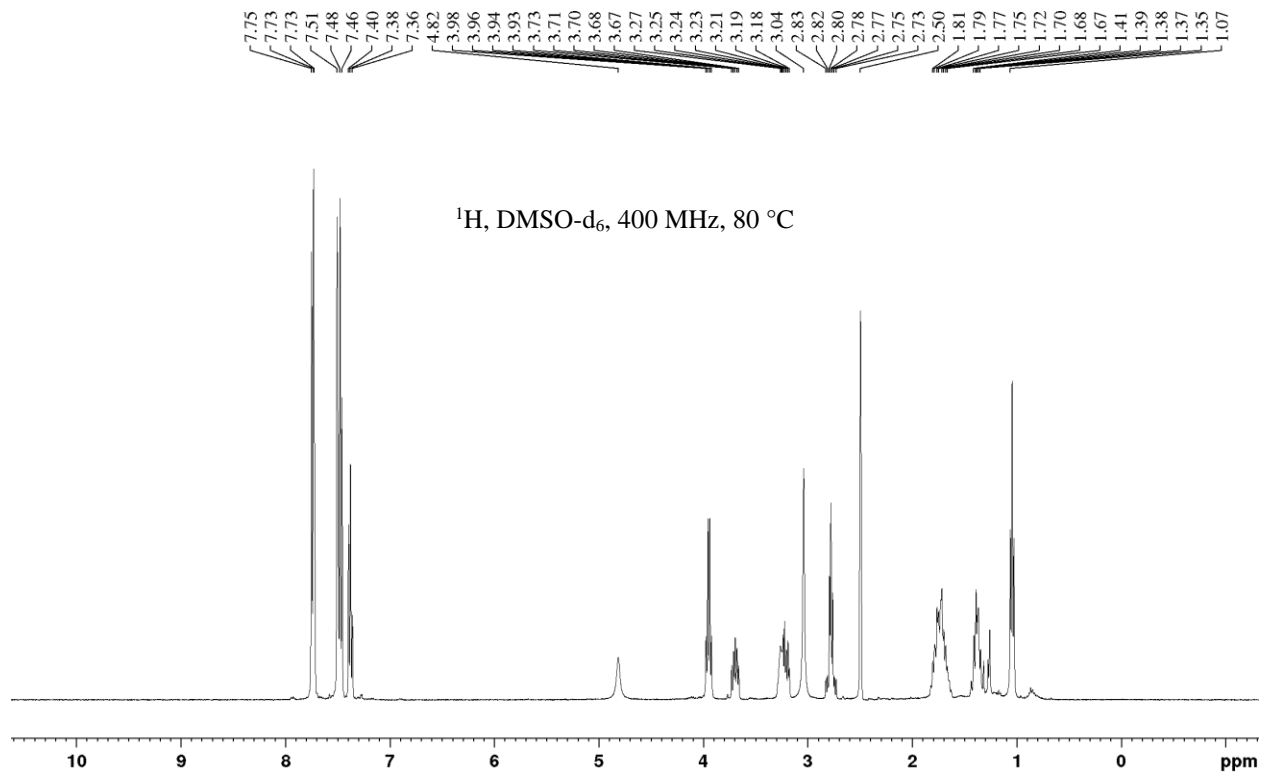




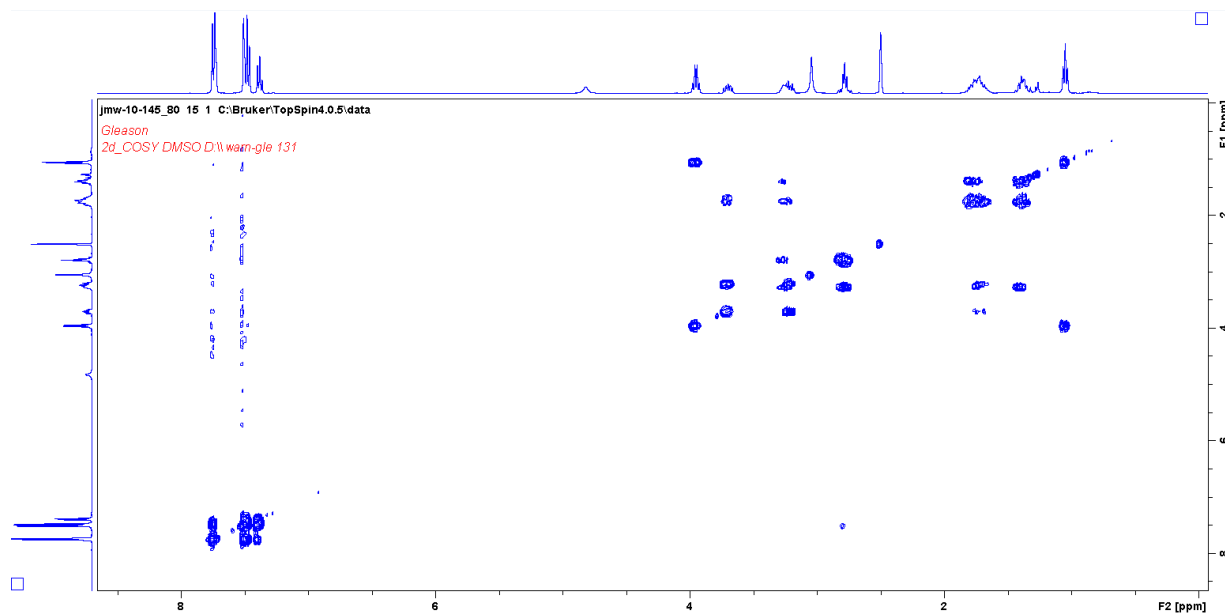




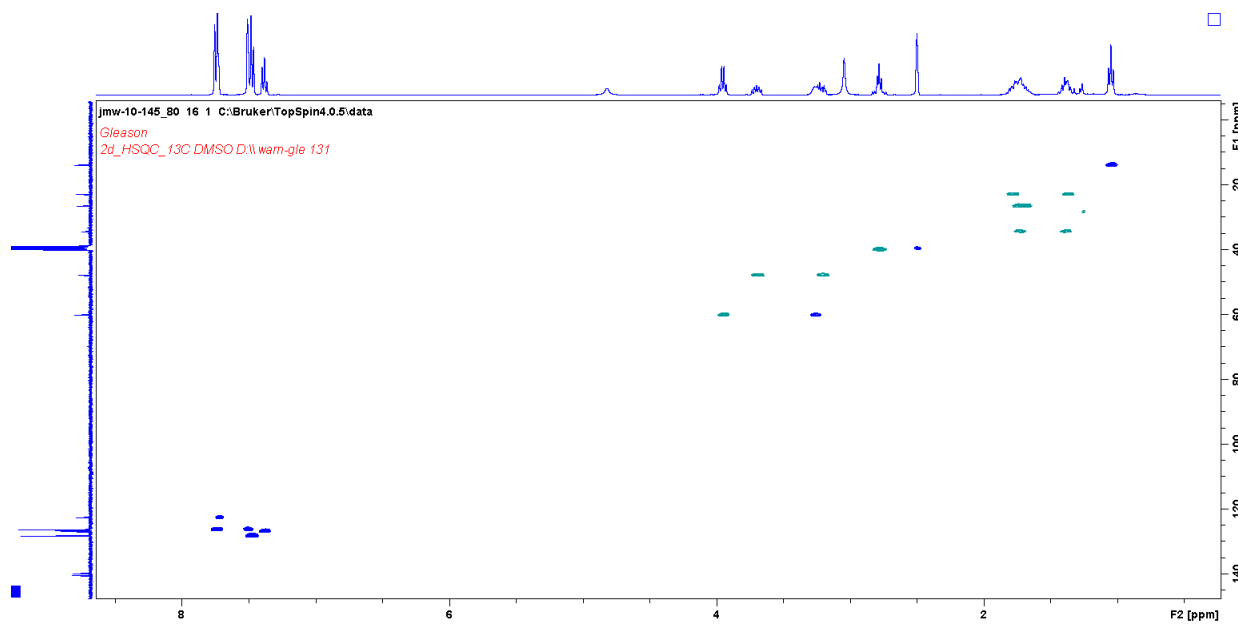




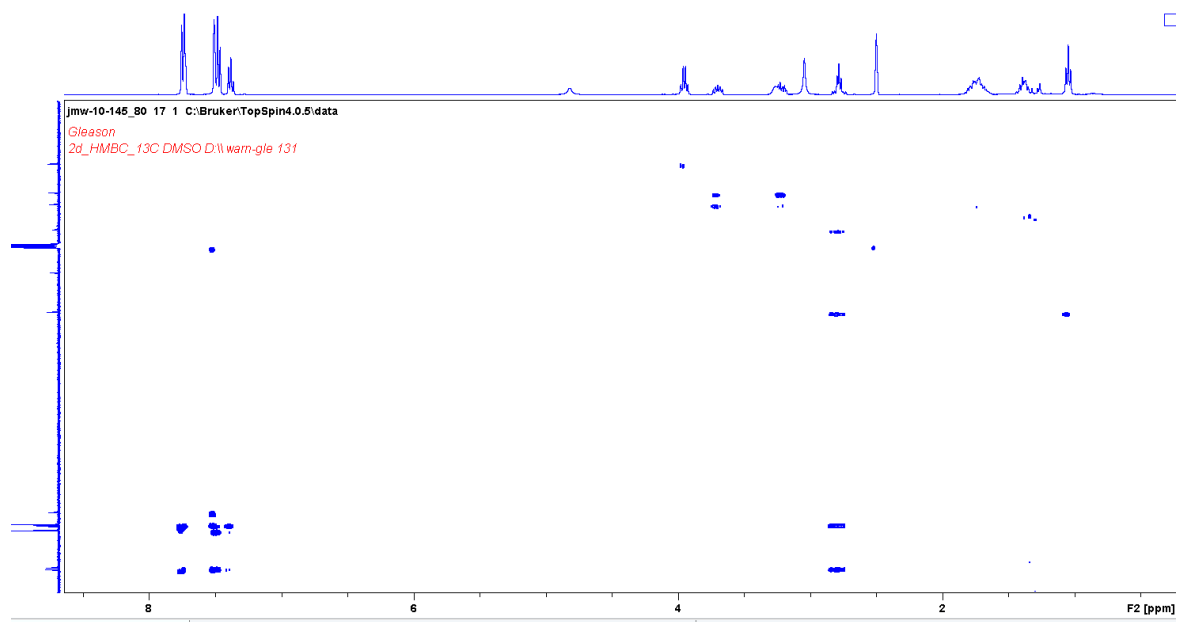
COSY, DMSO-d₆, 80 °C

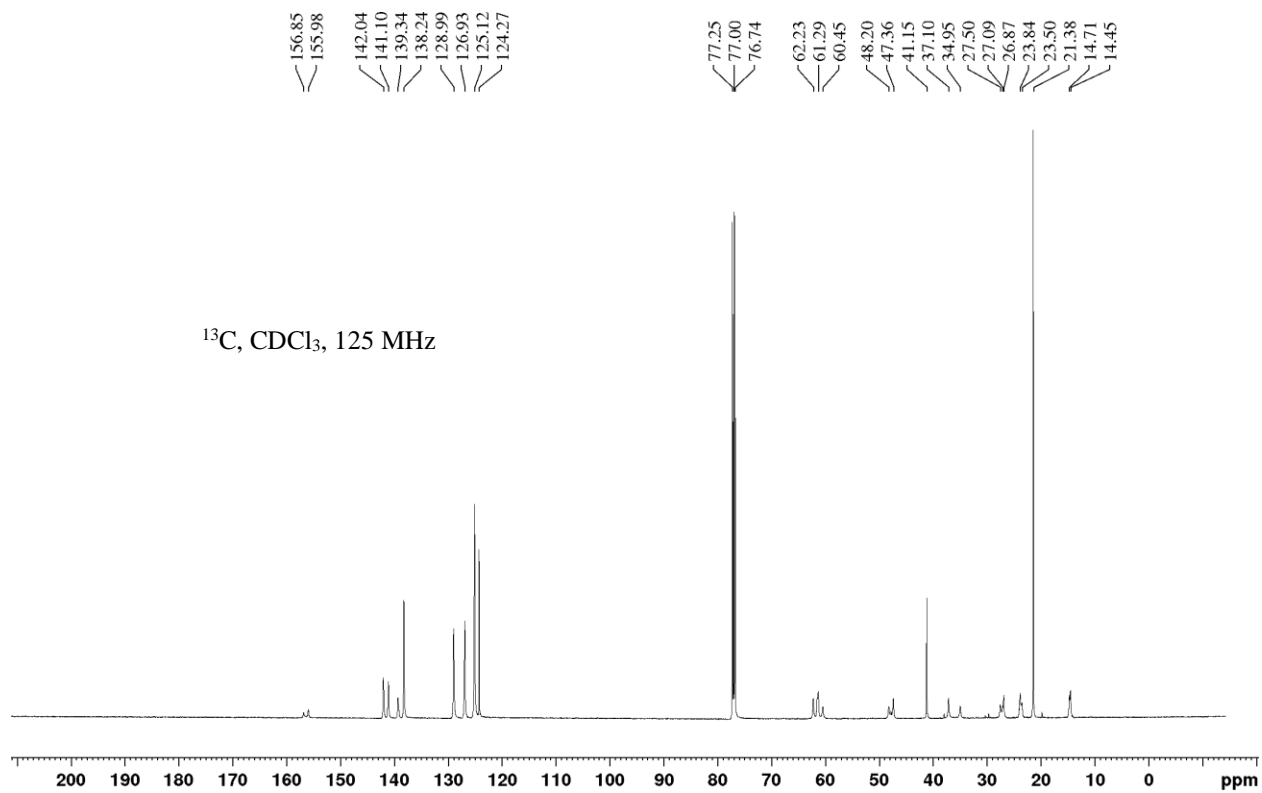
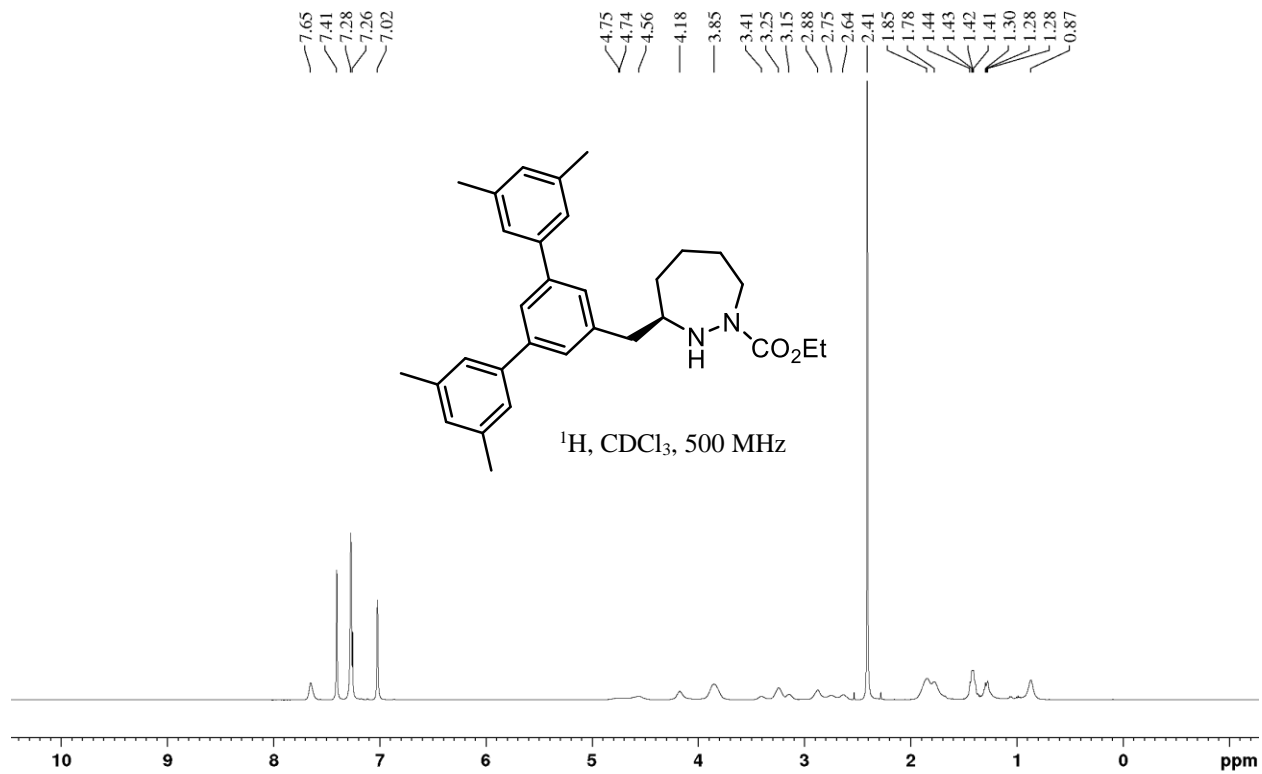


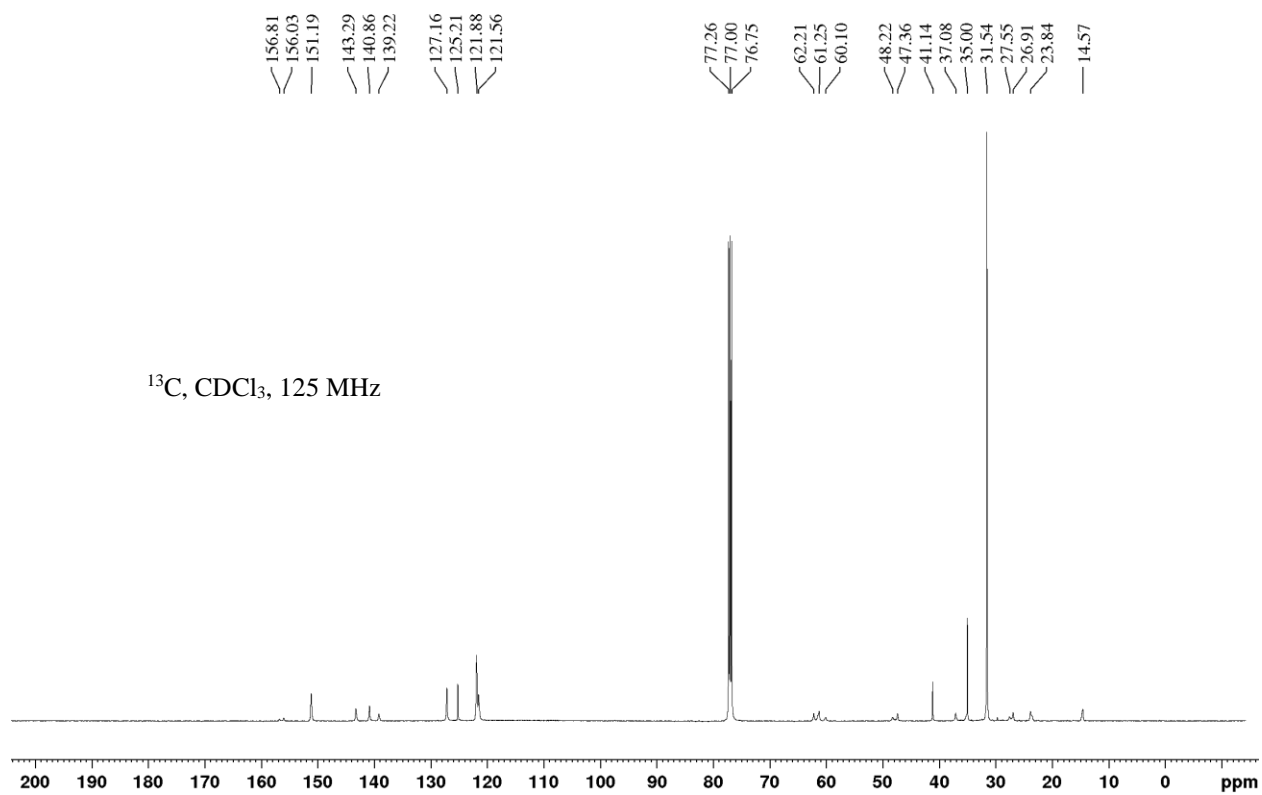
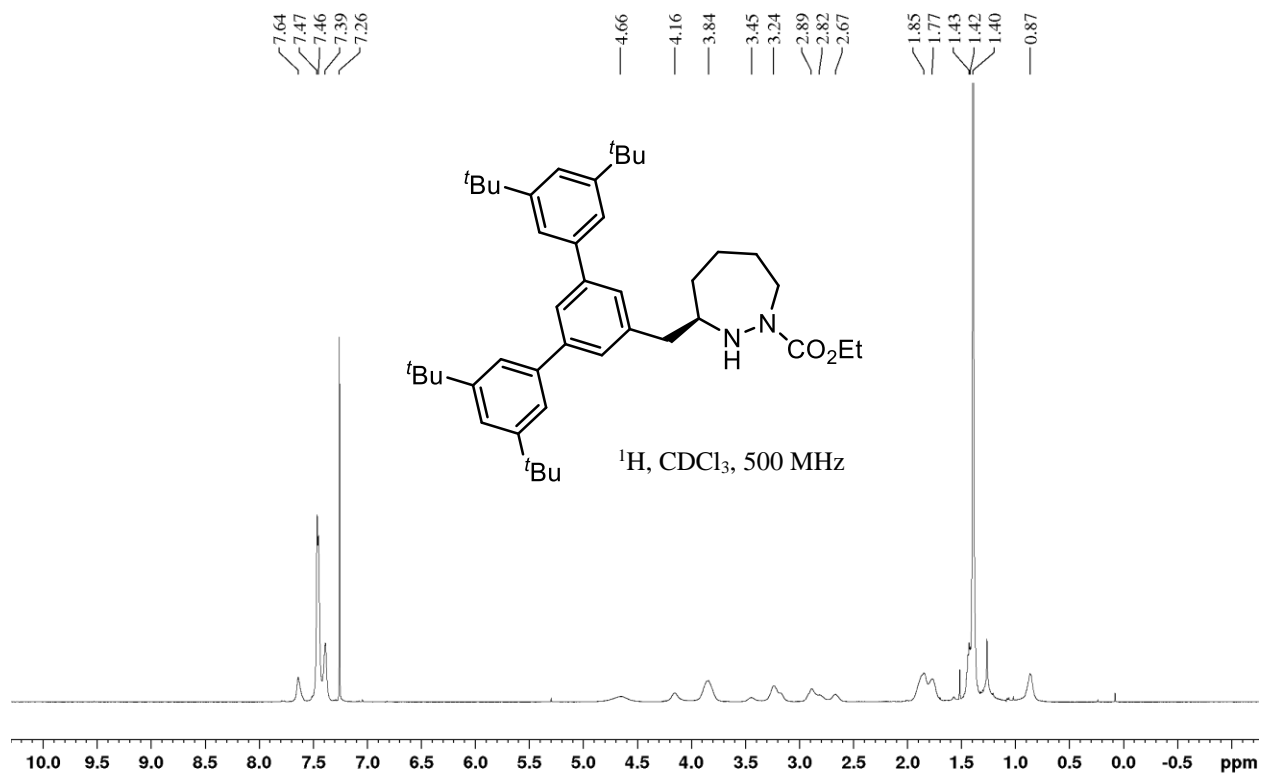
HSQC, DMSO-d₆, 80 °C

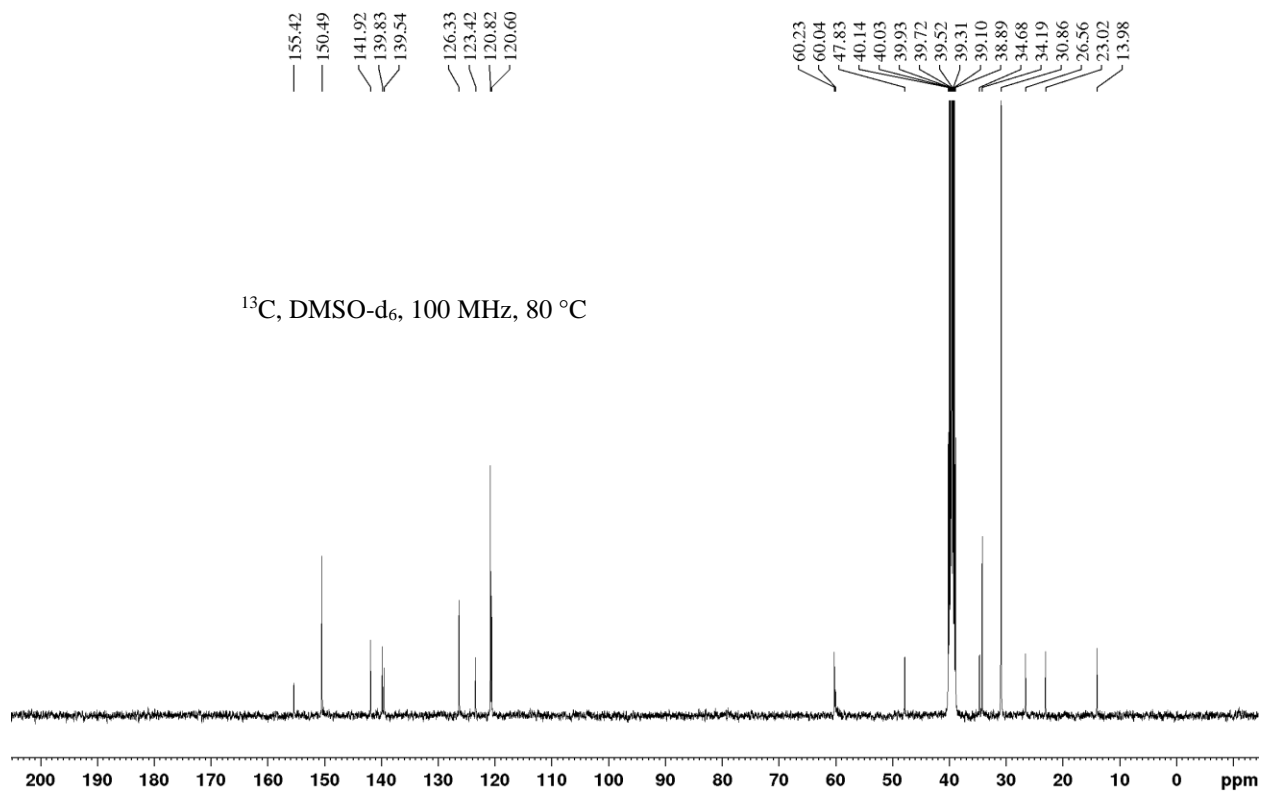
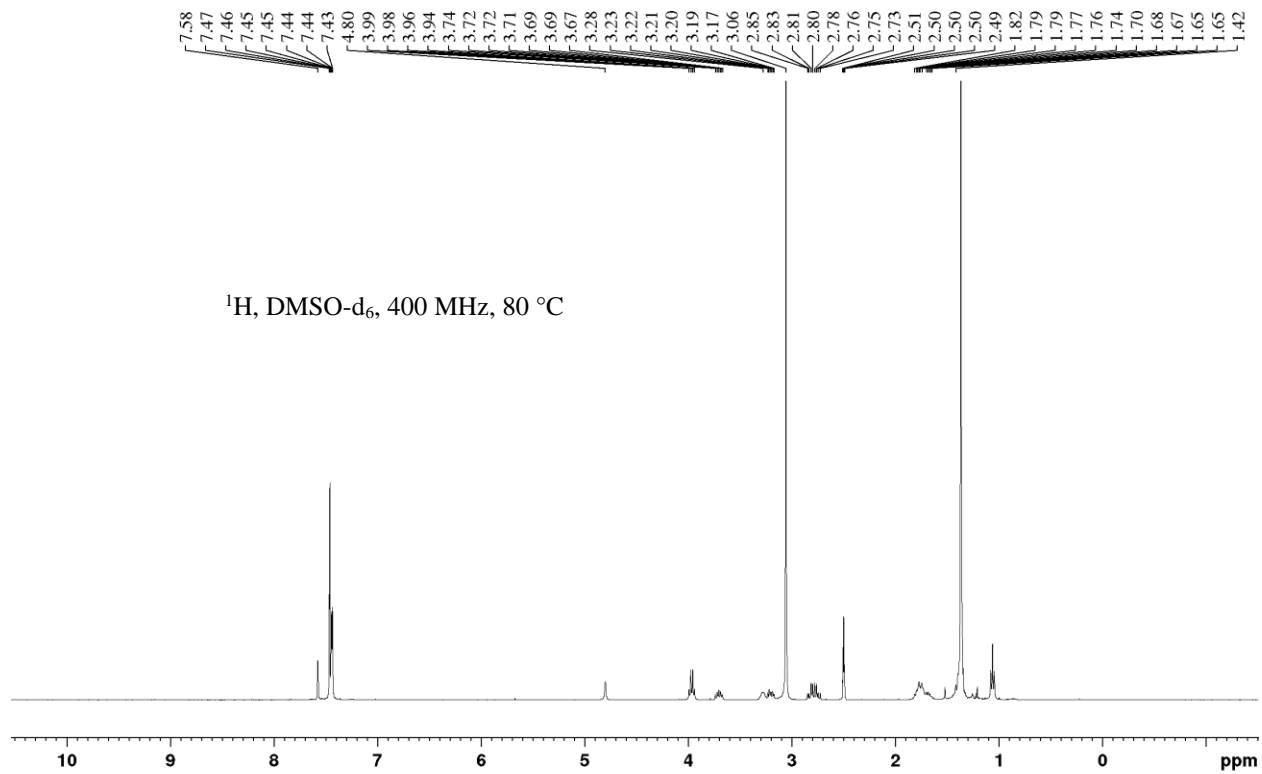


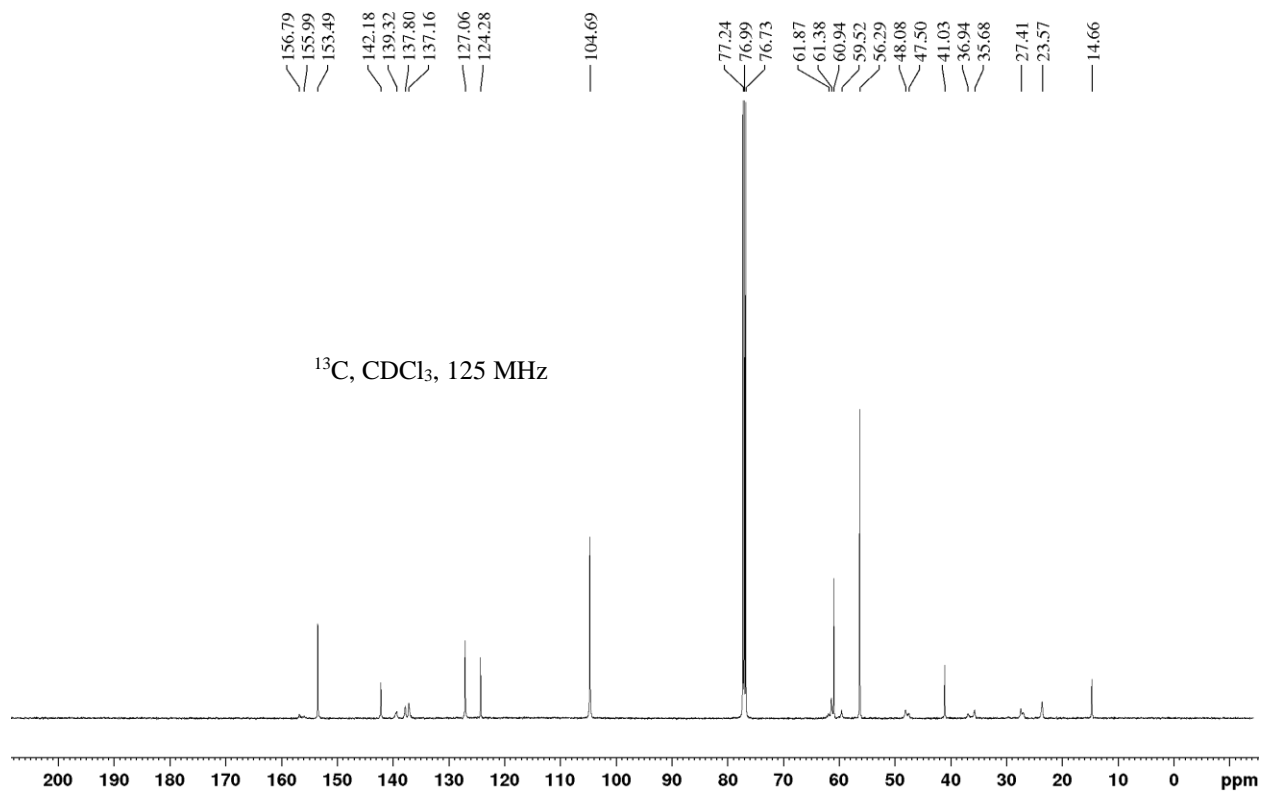
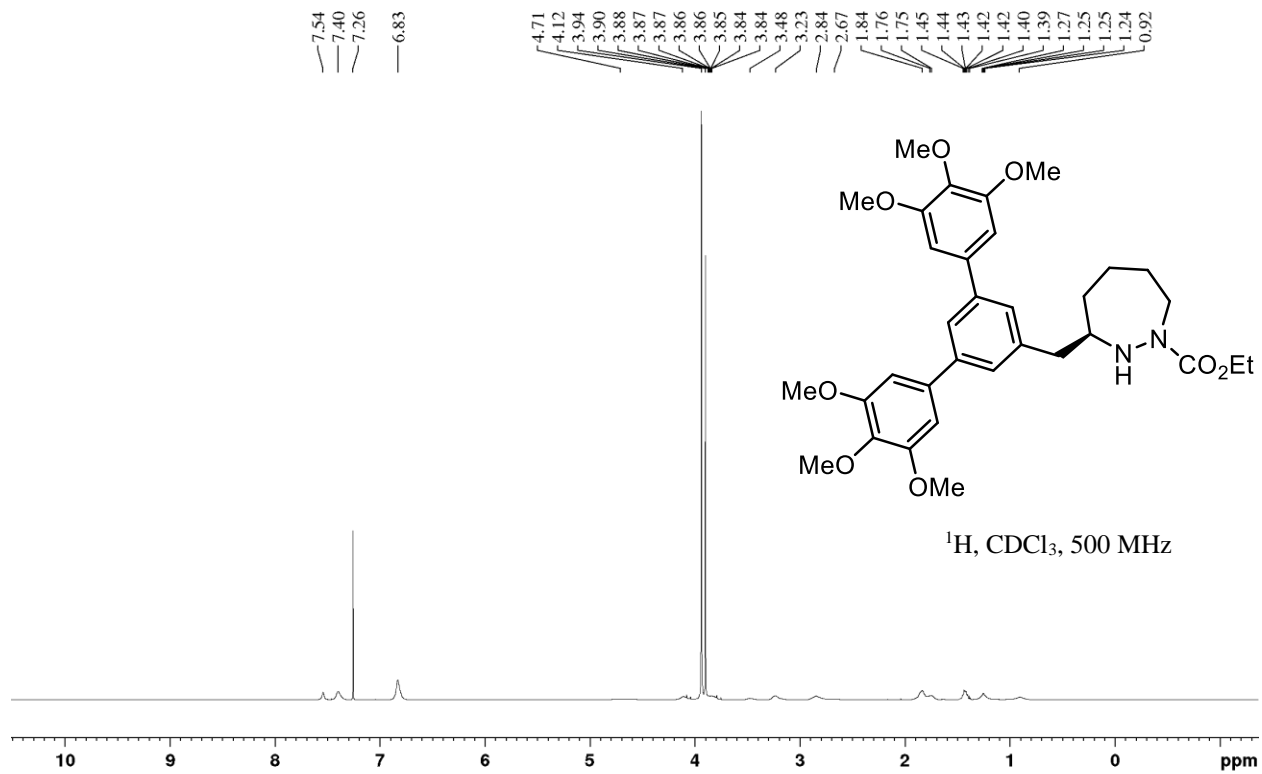
HMBC, DMSO-d₆, 80 °C

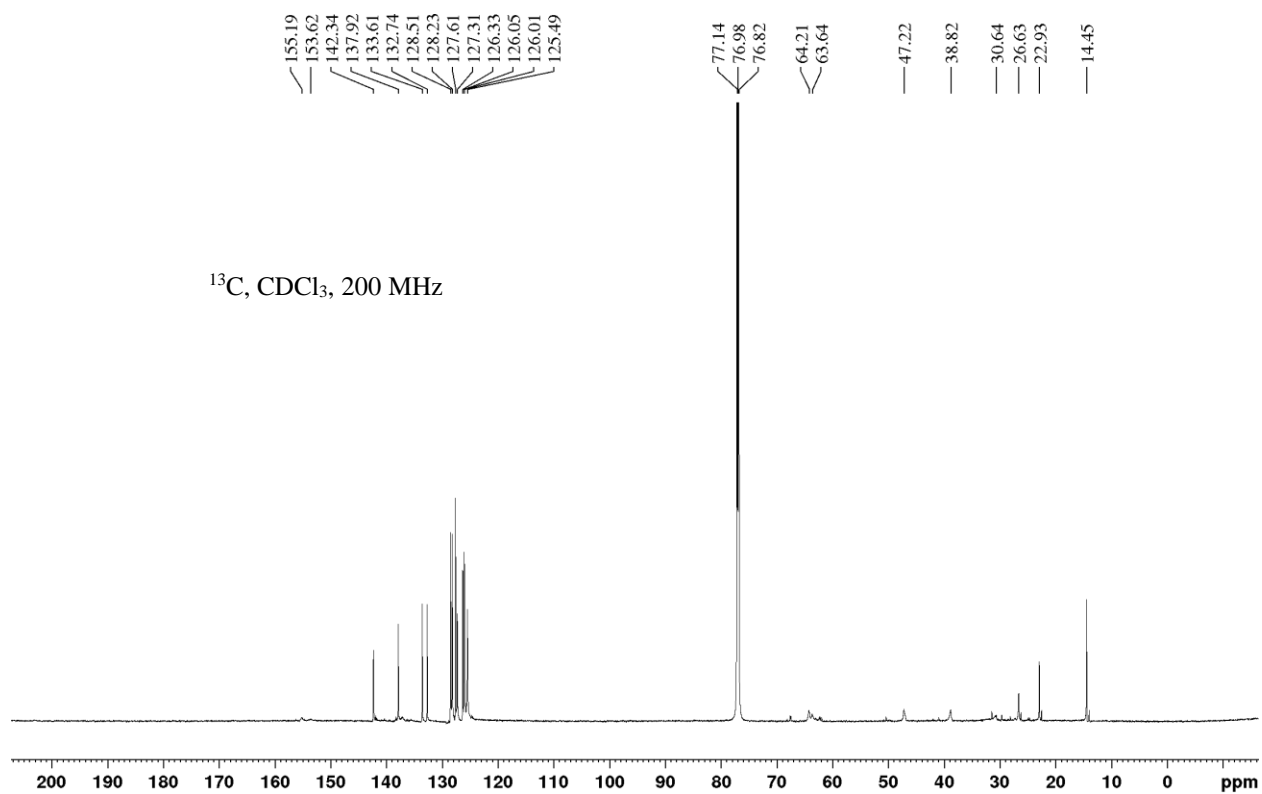
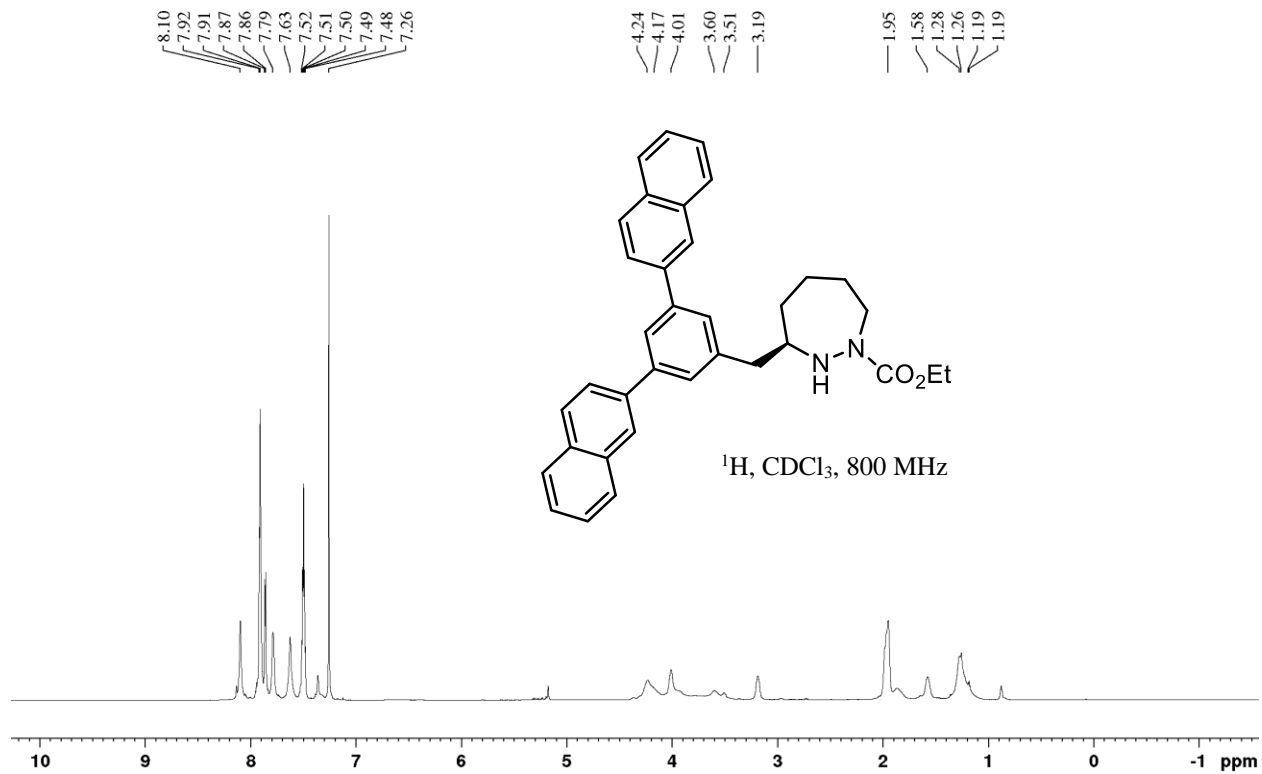


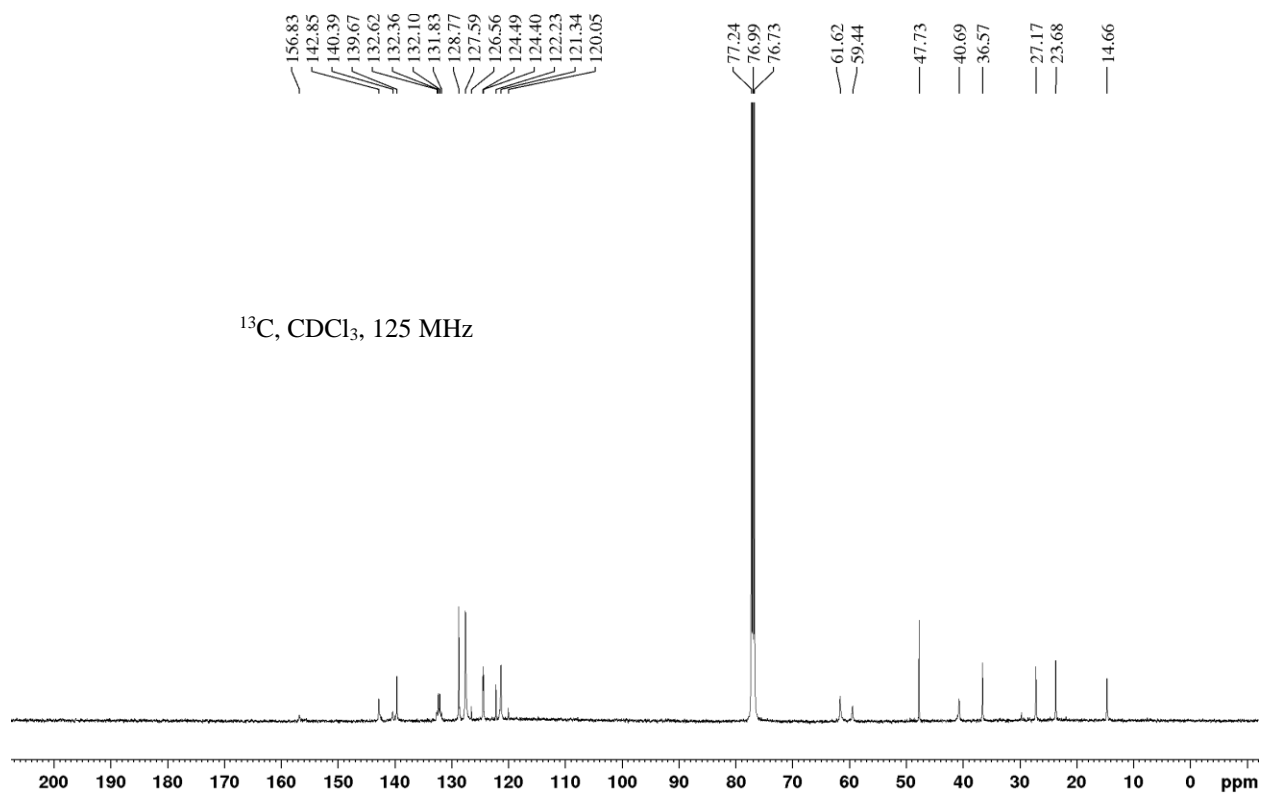
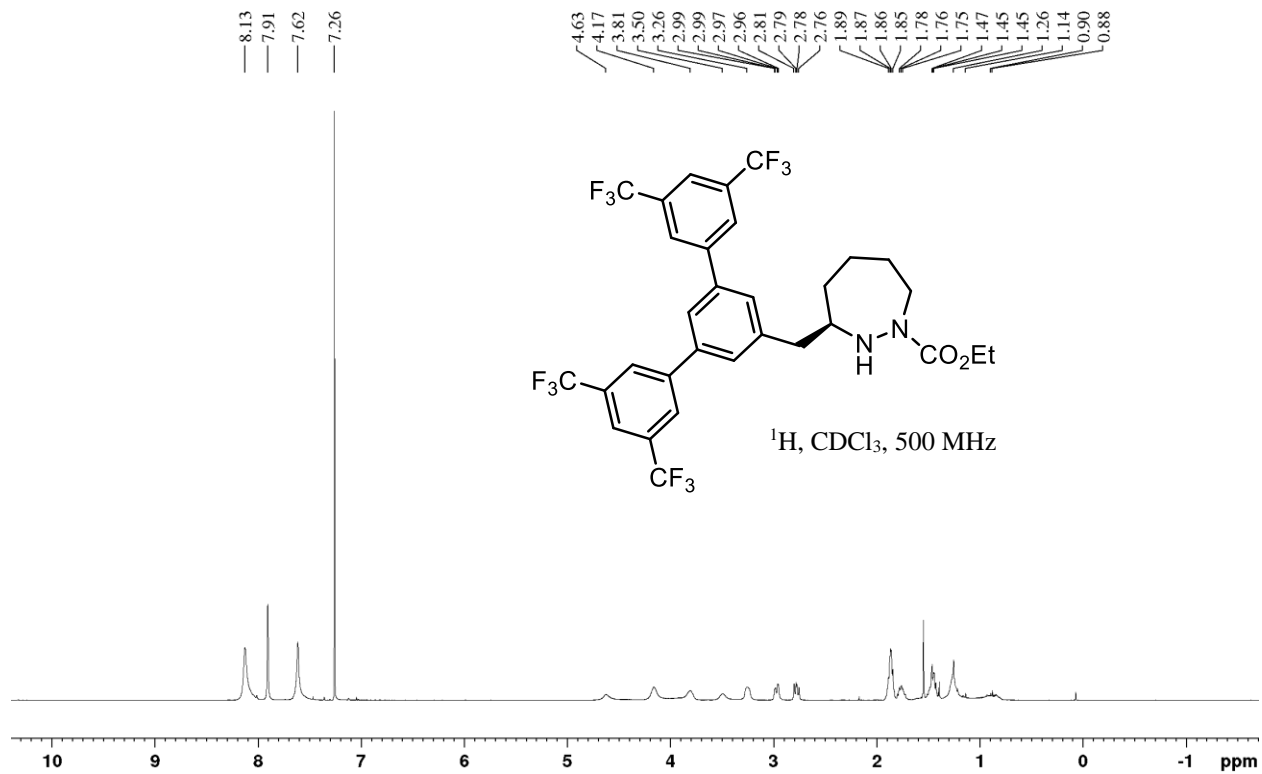


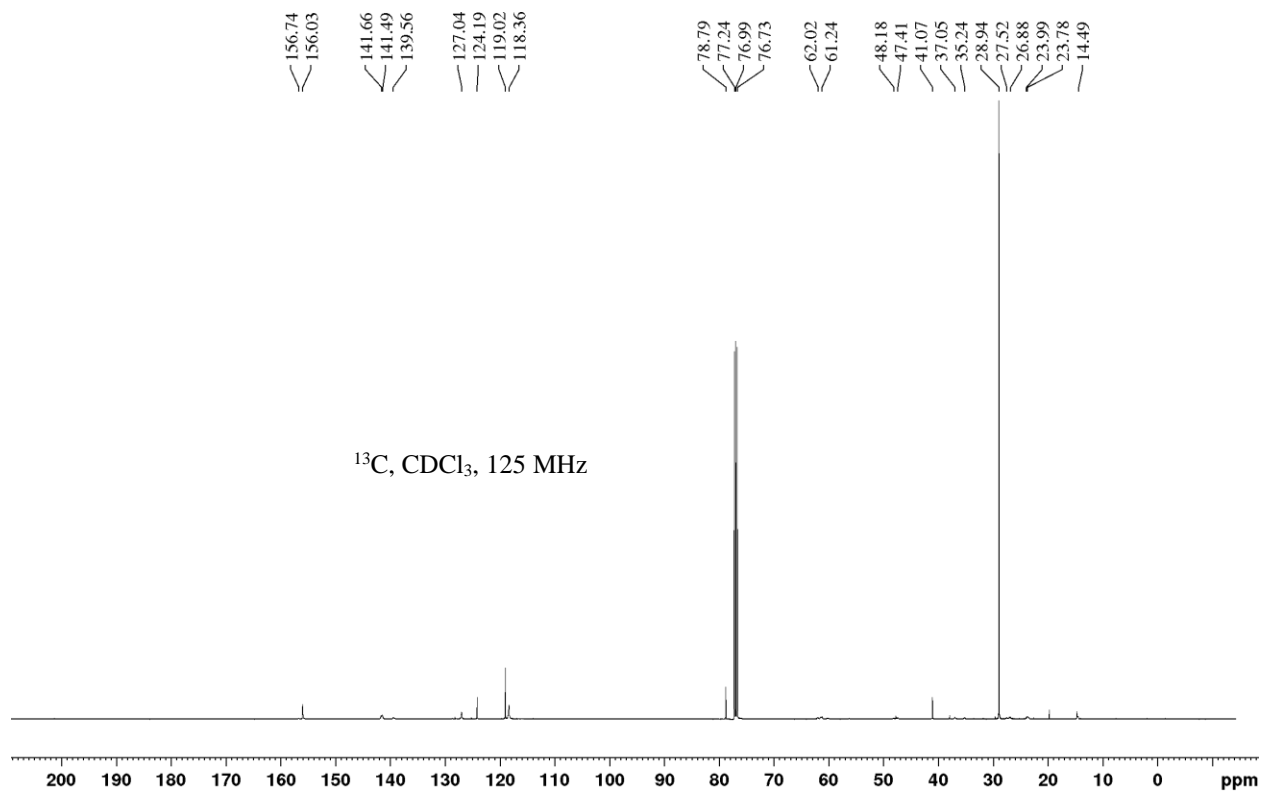
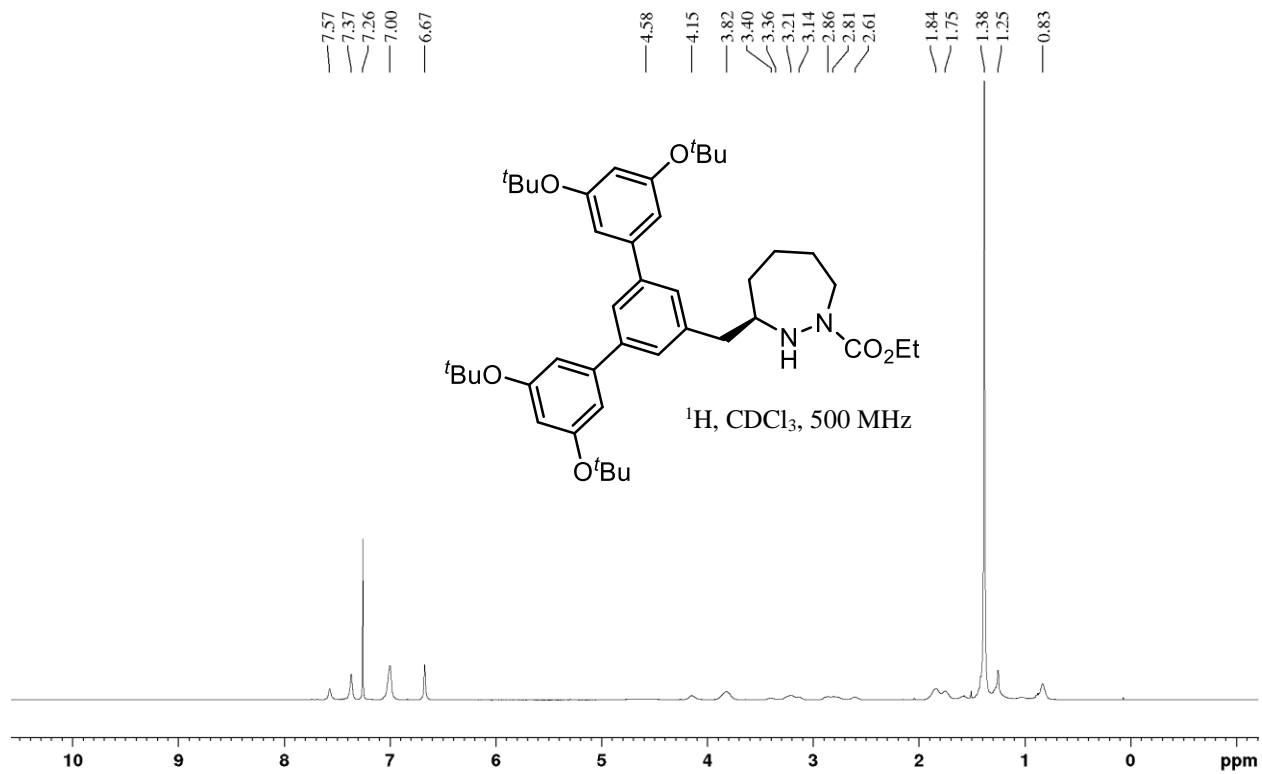


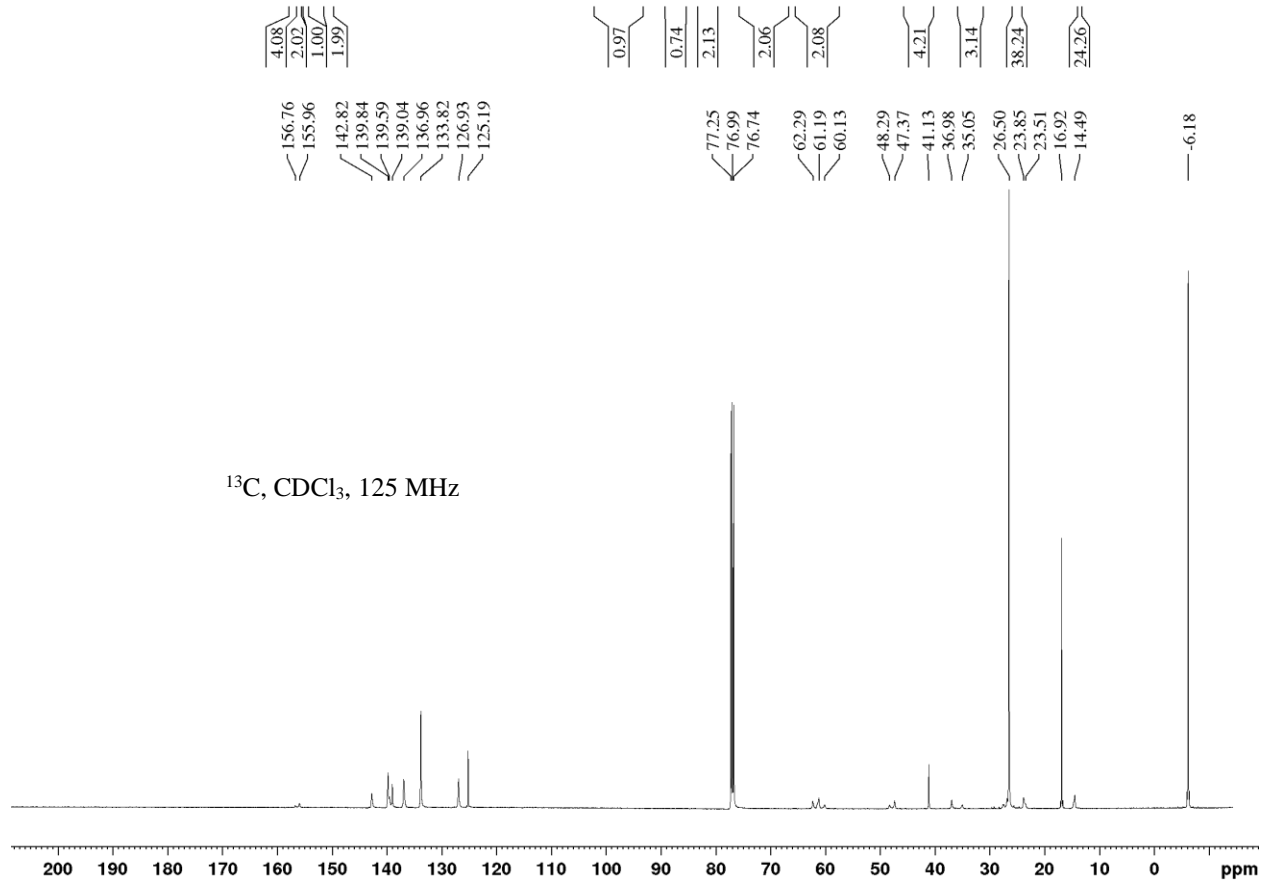
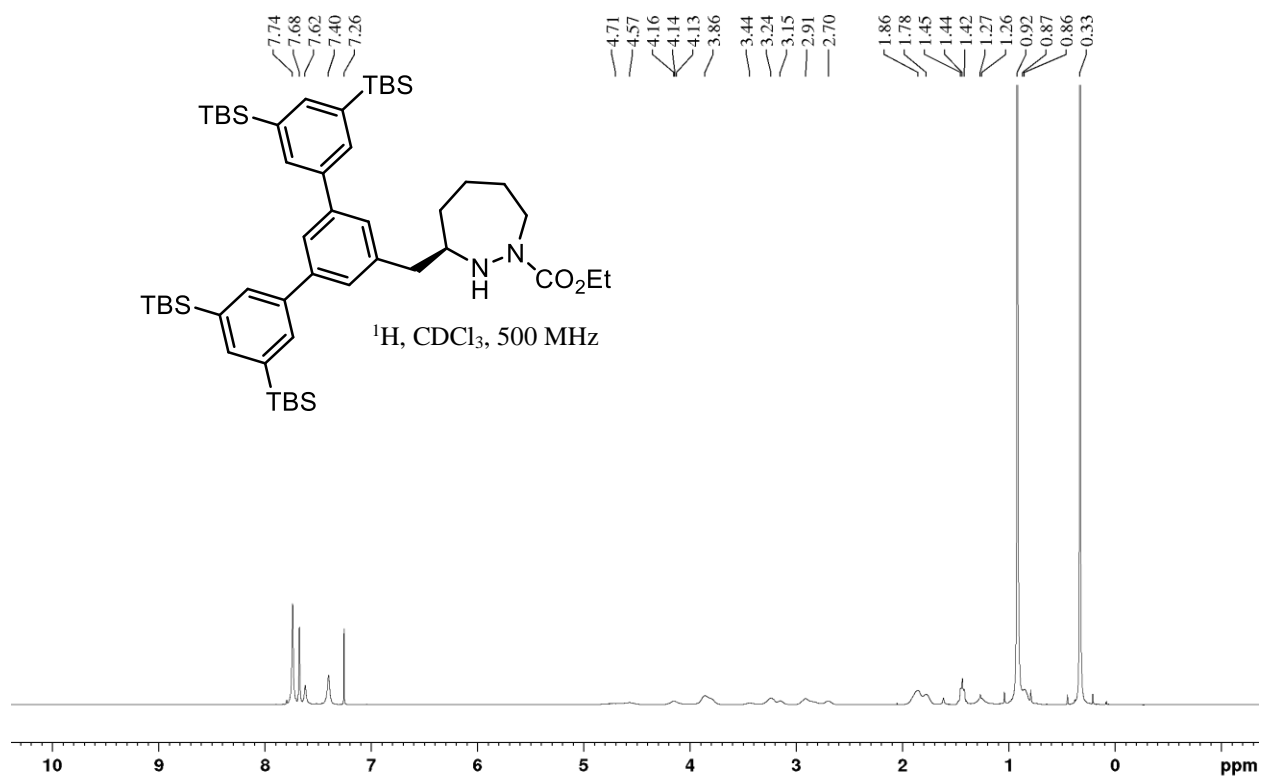


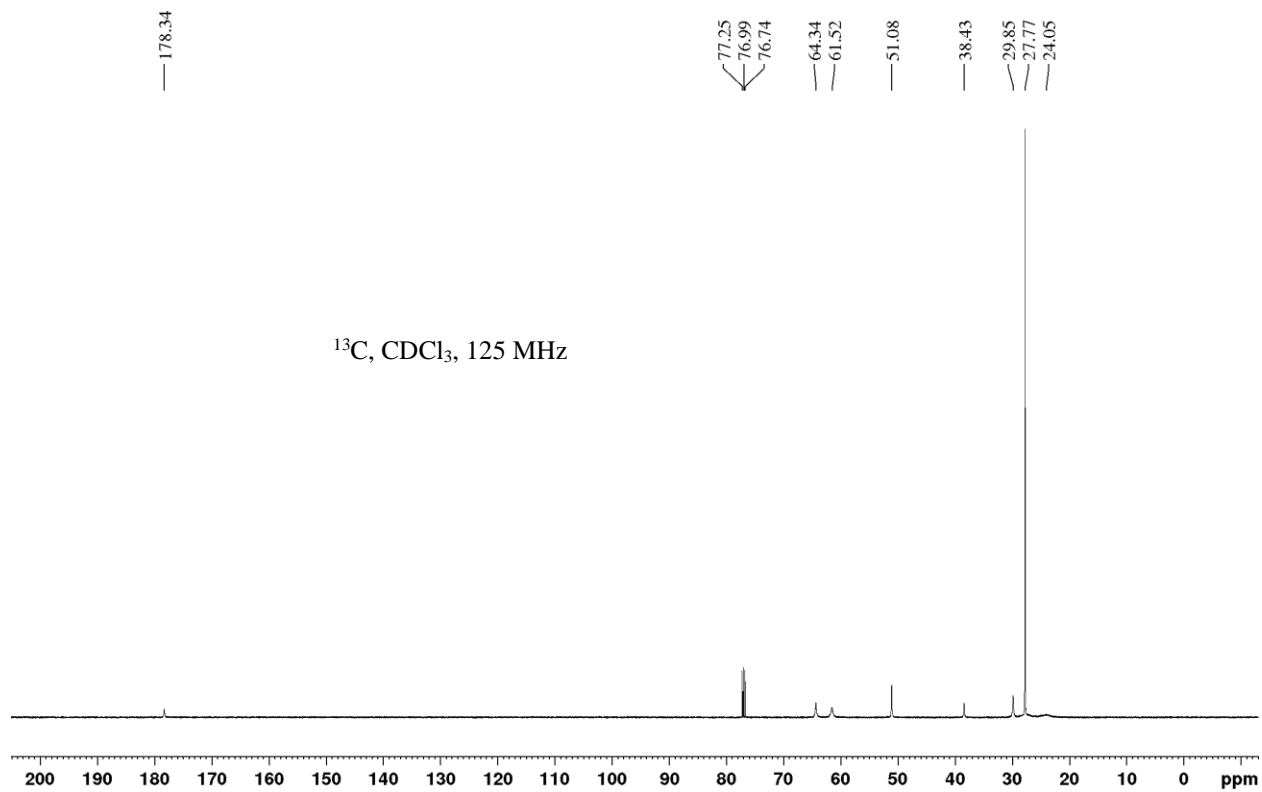
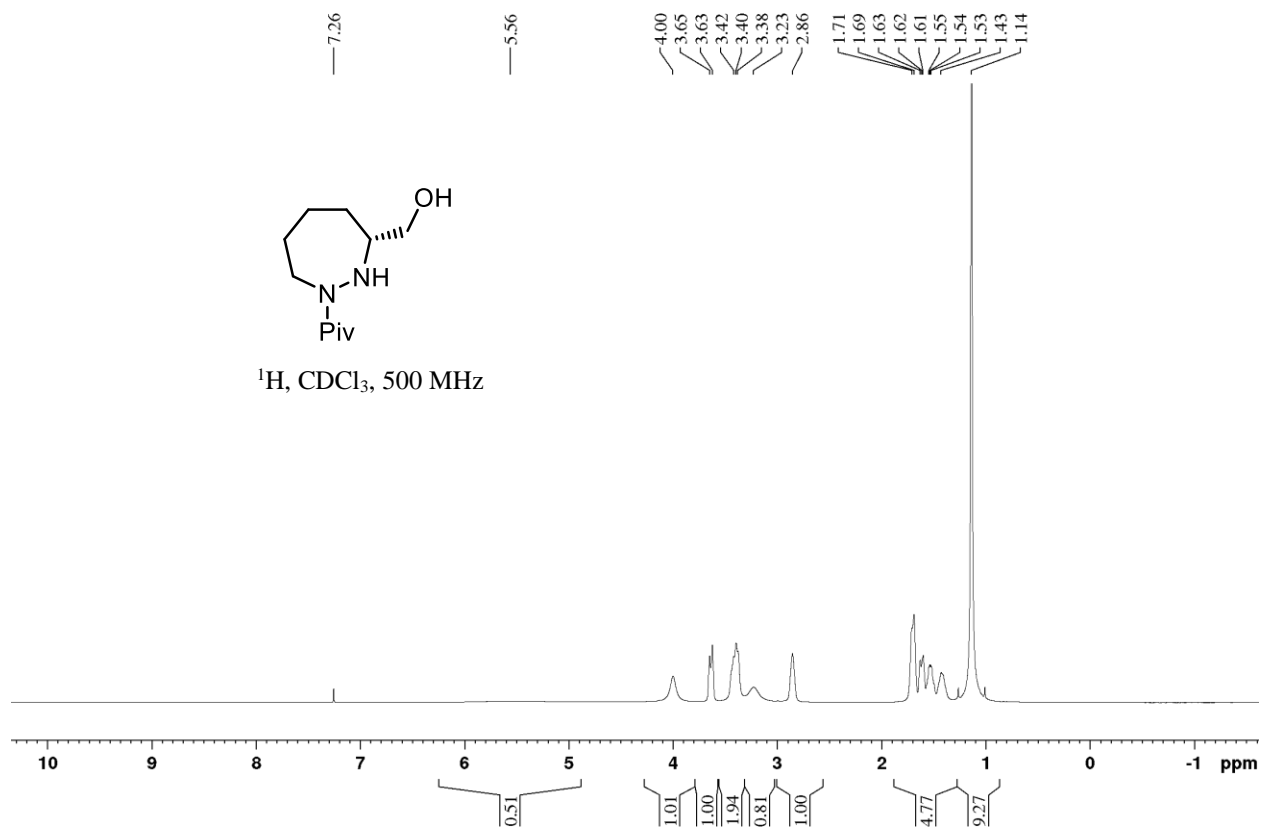


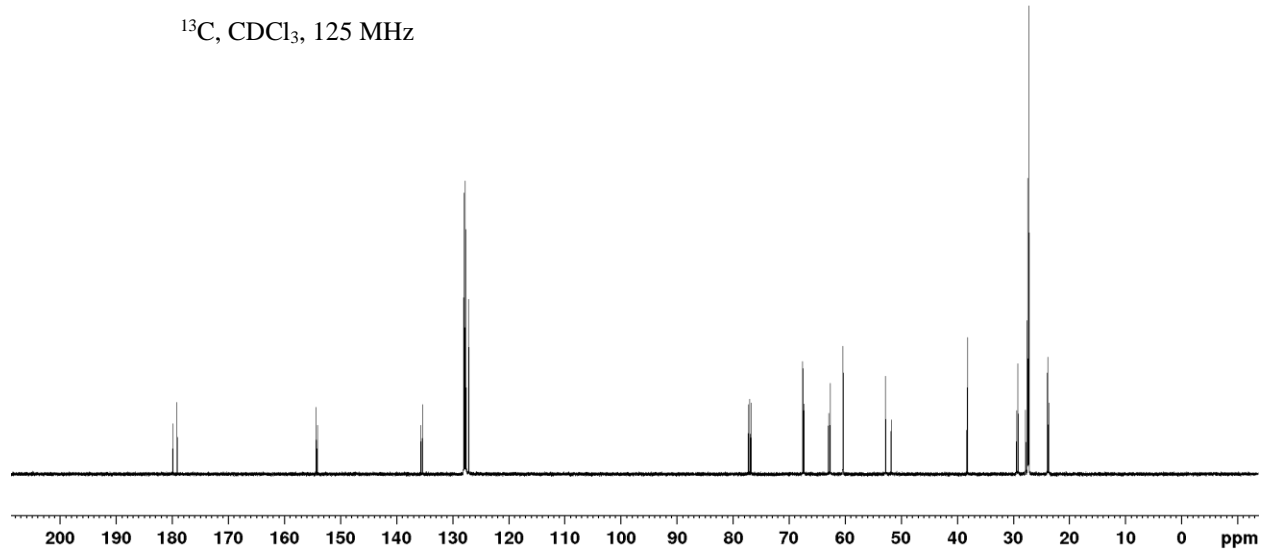
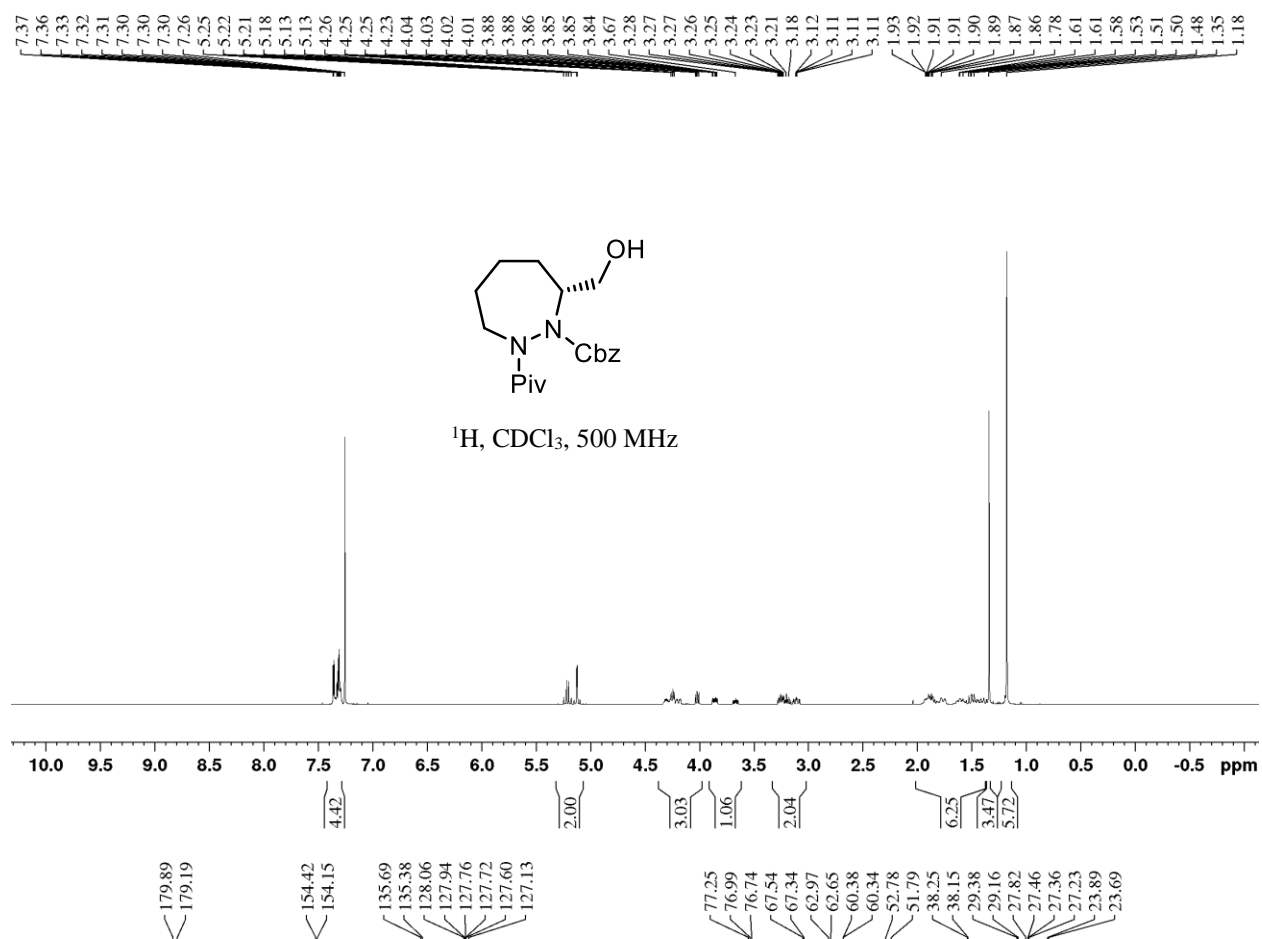


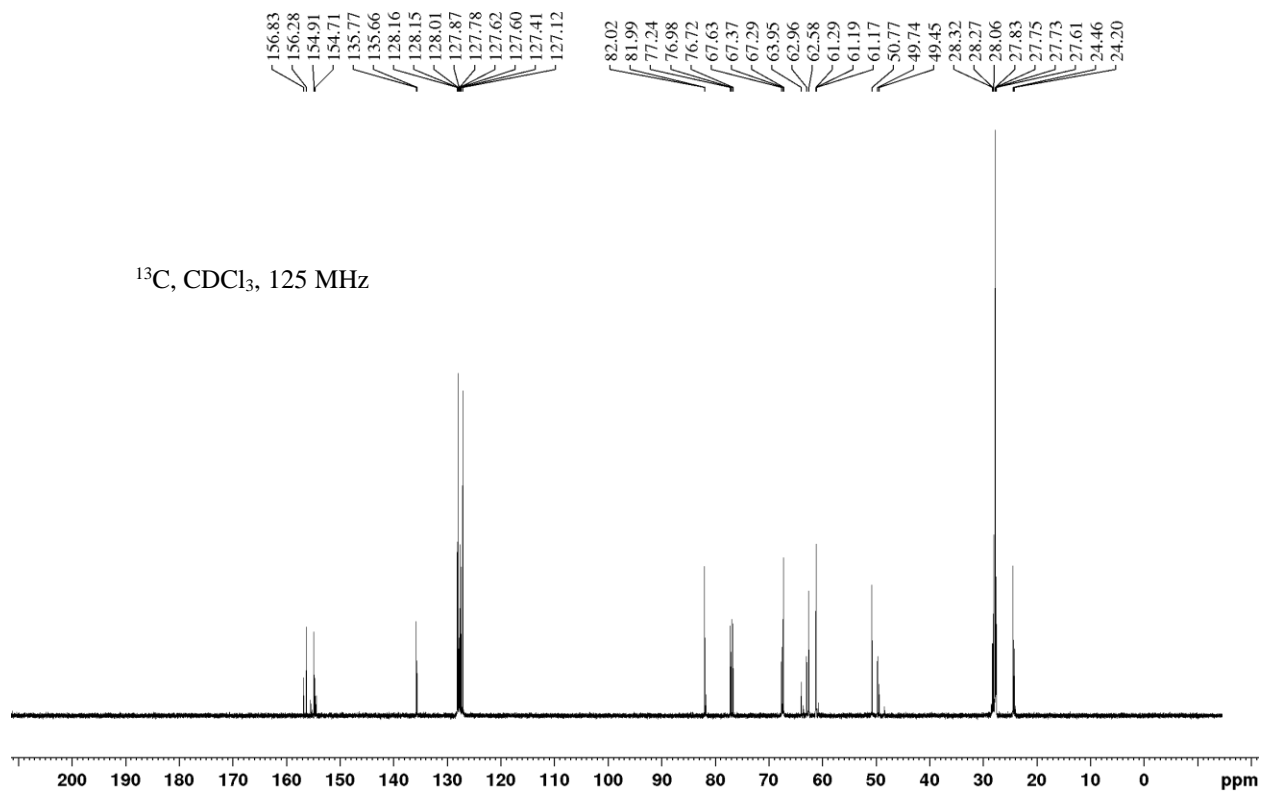
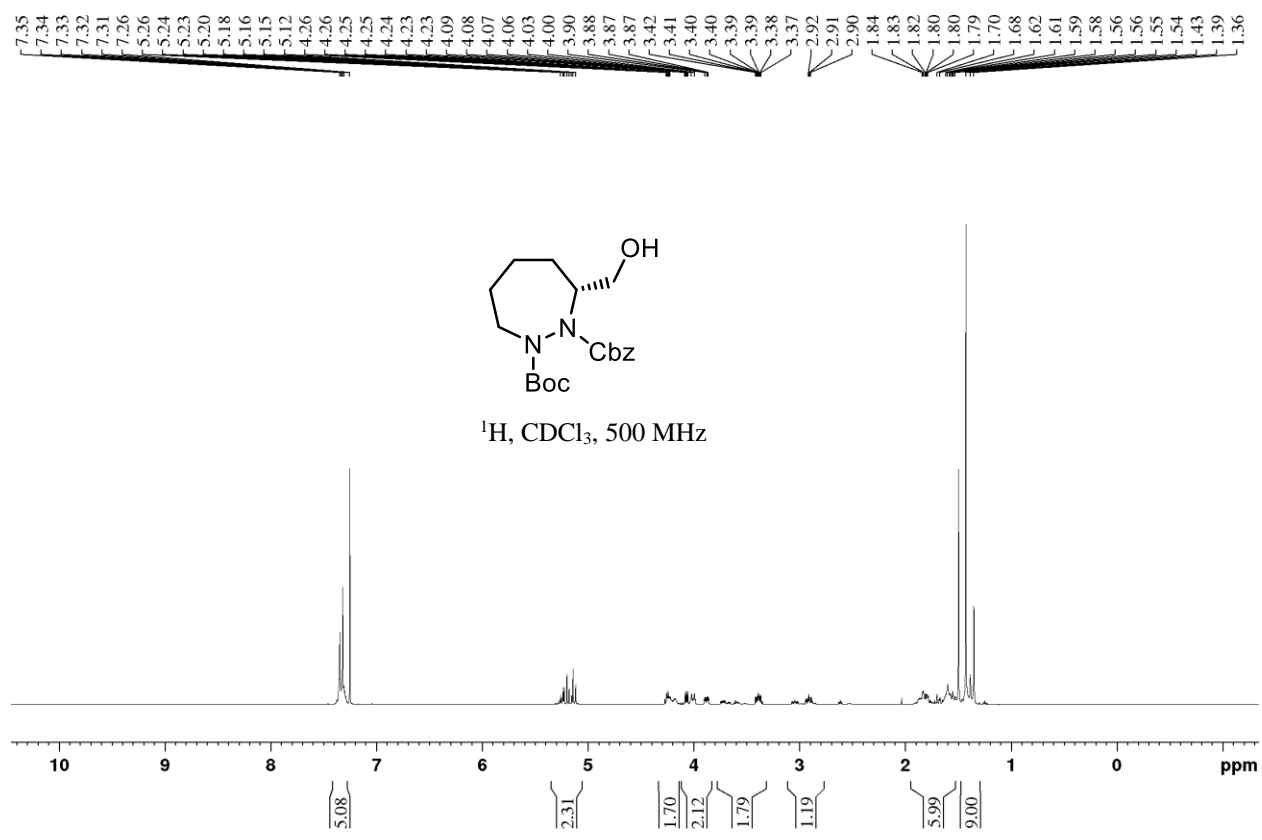


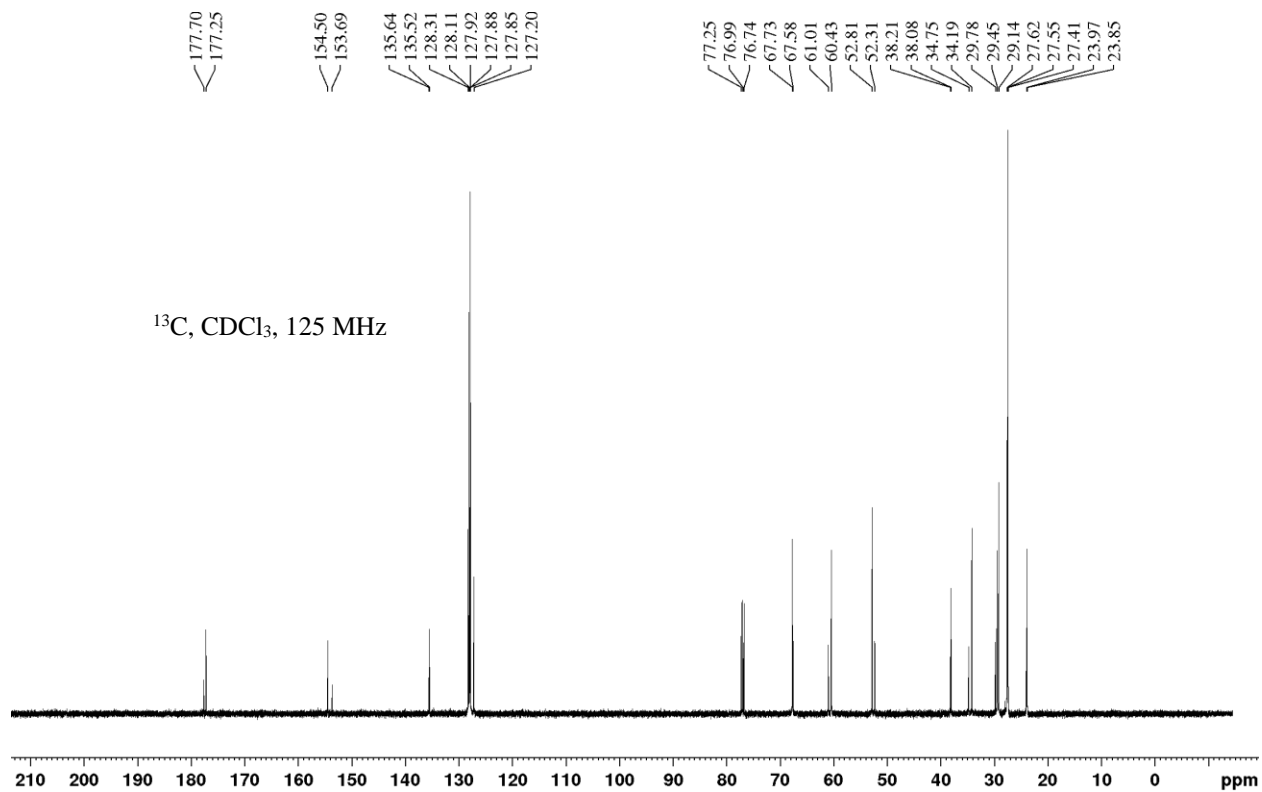
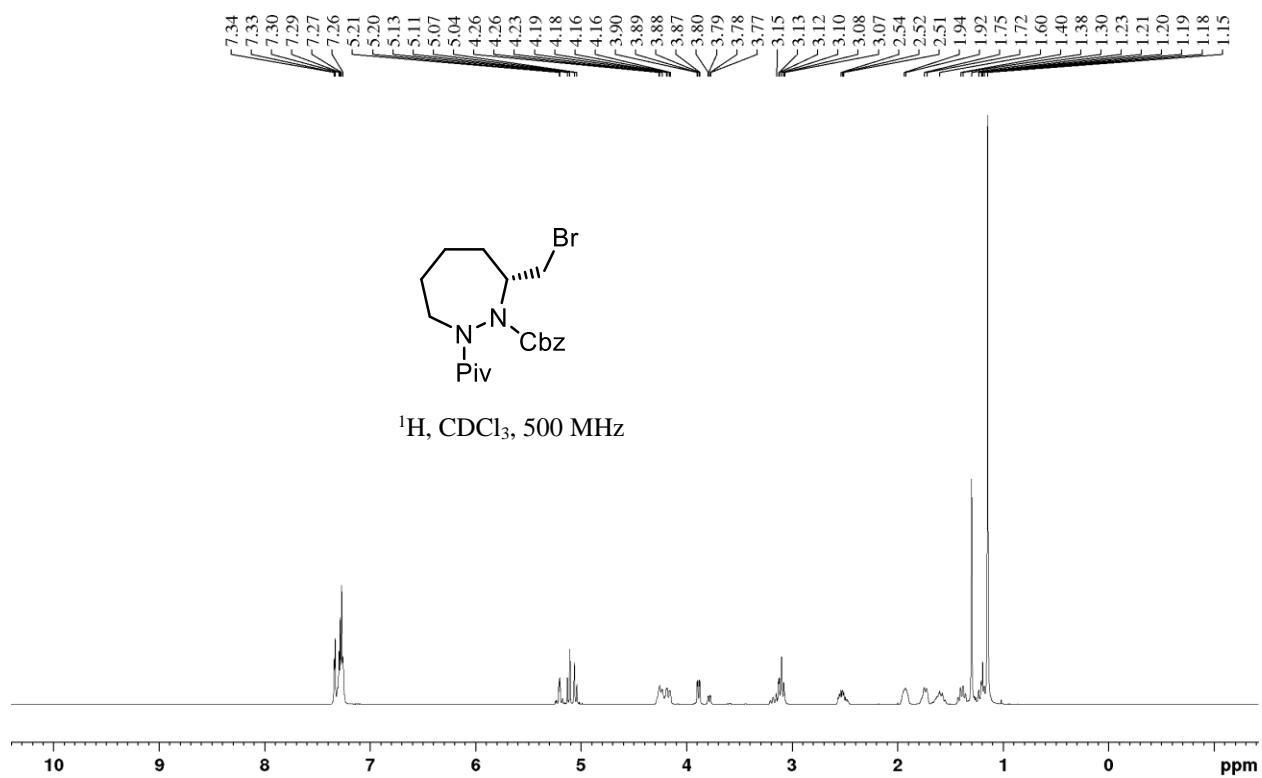


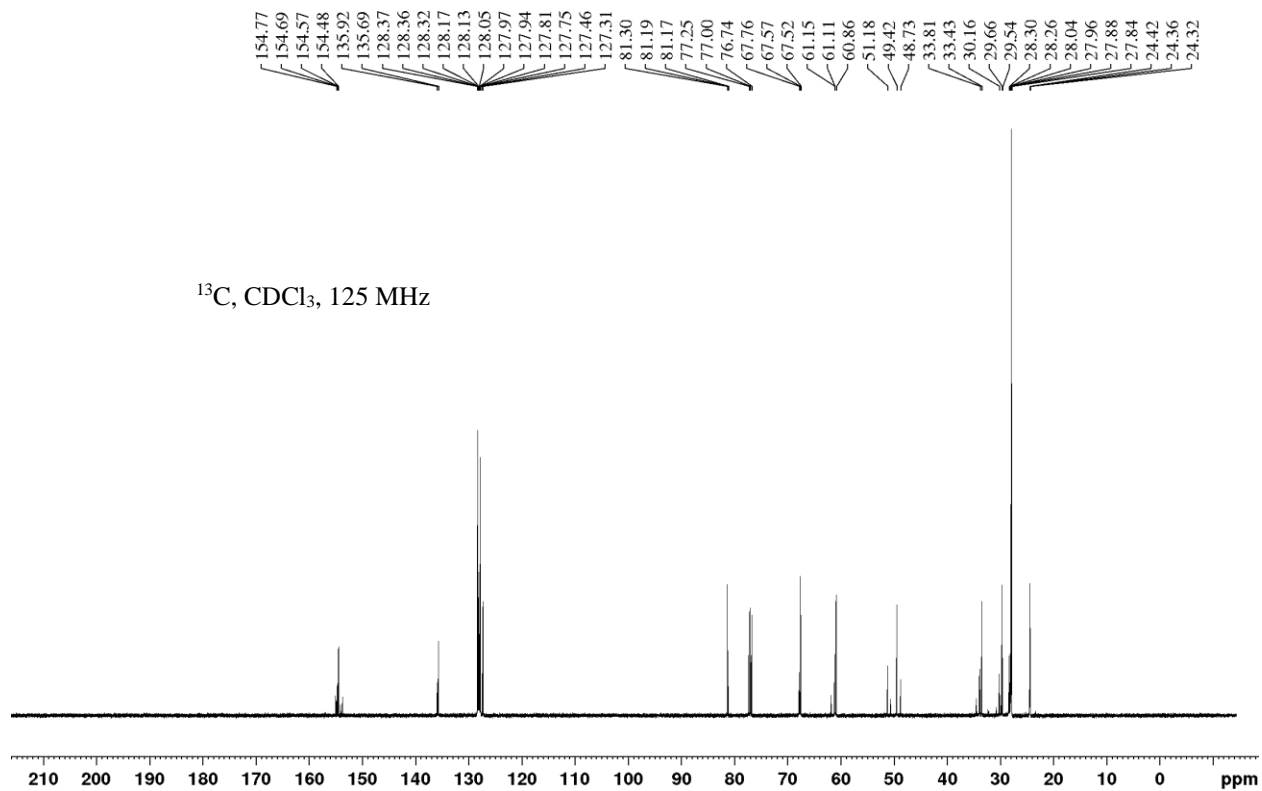
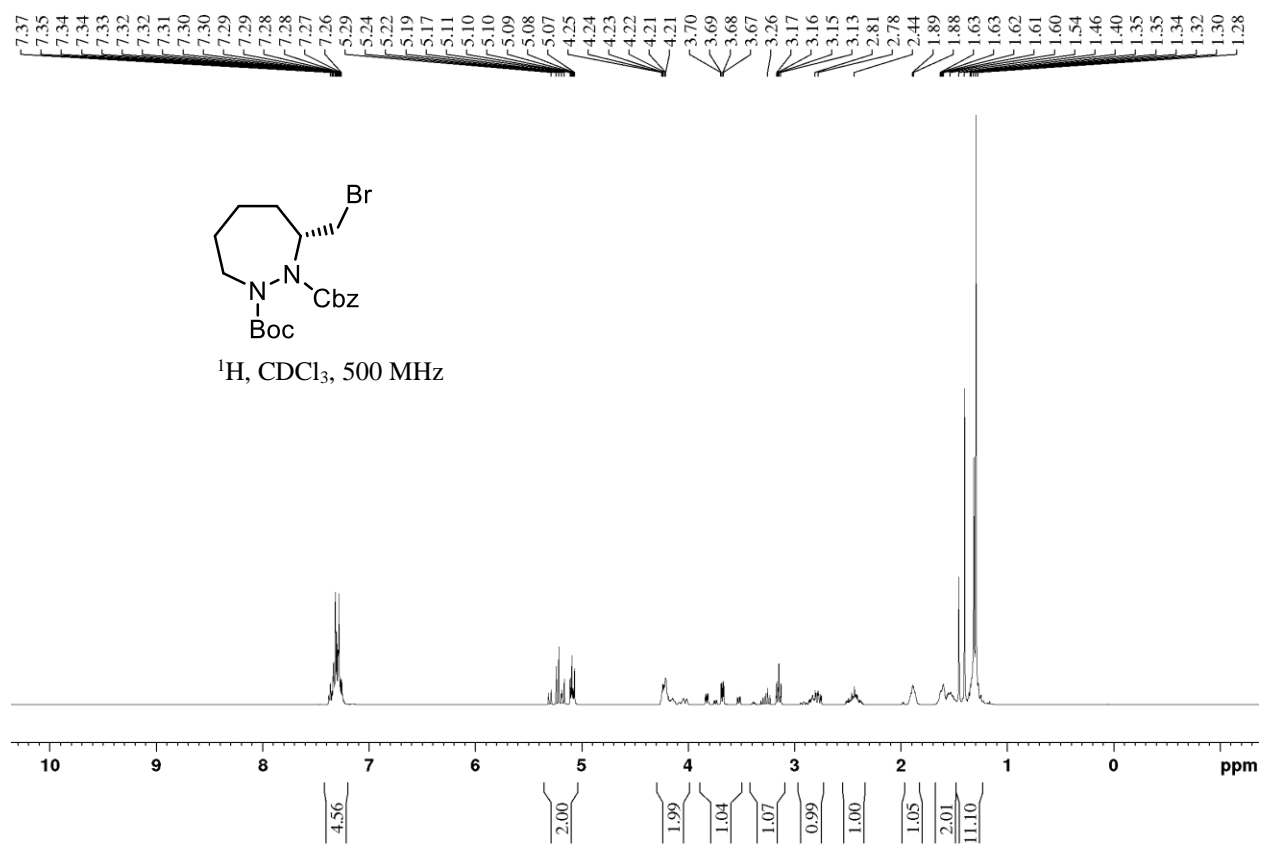


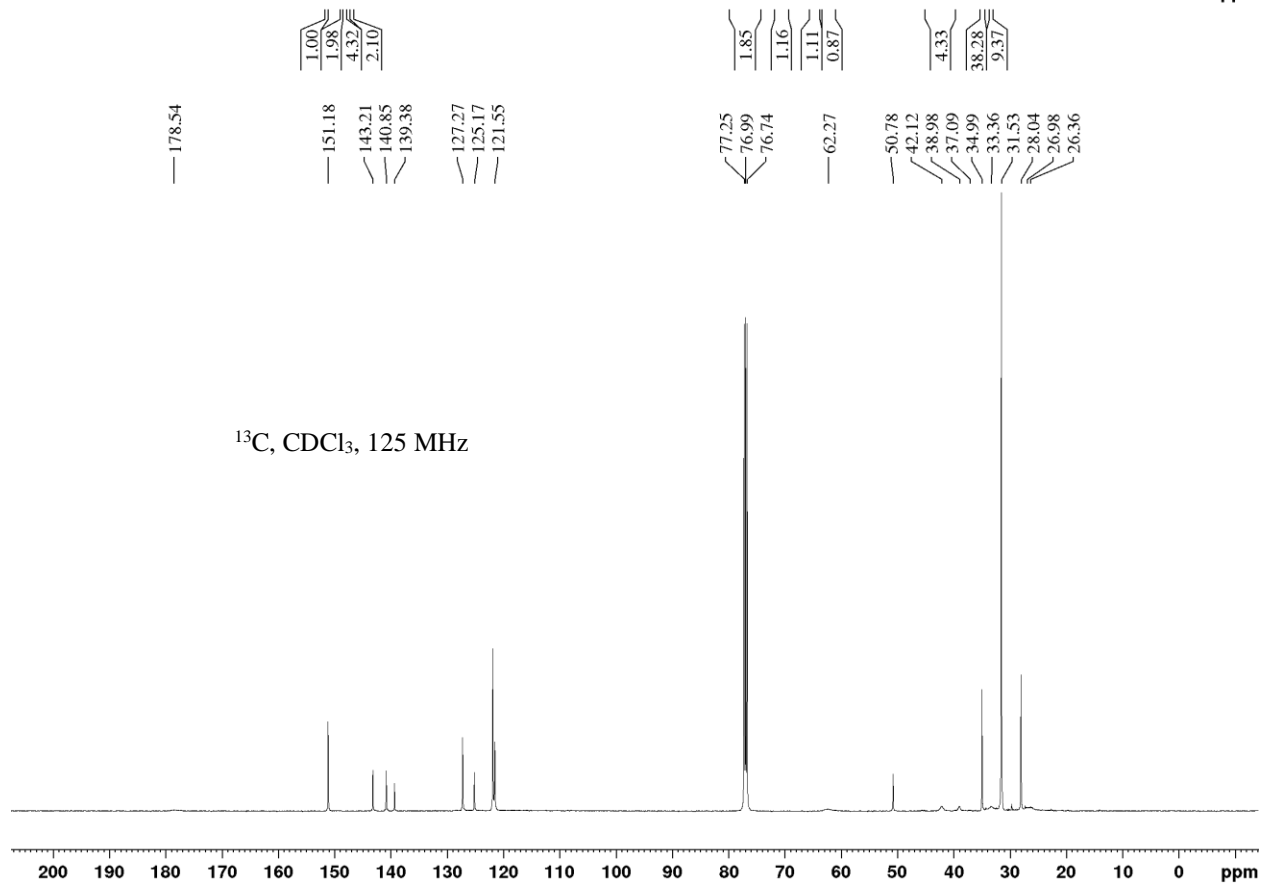
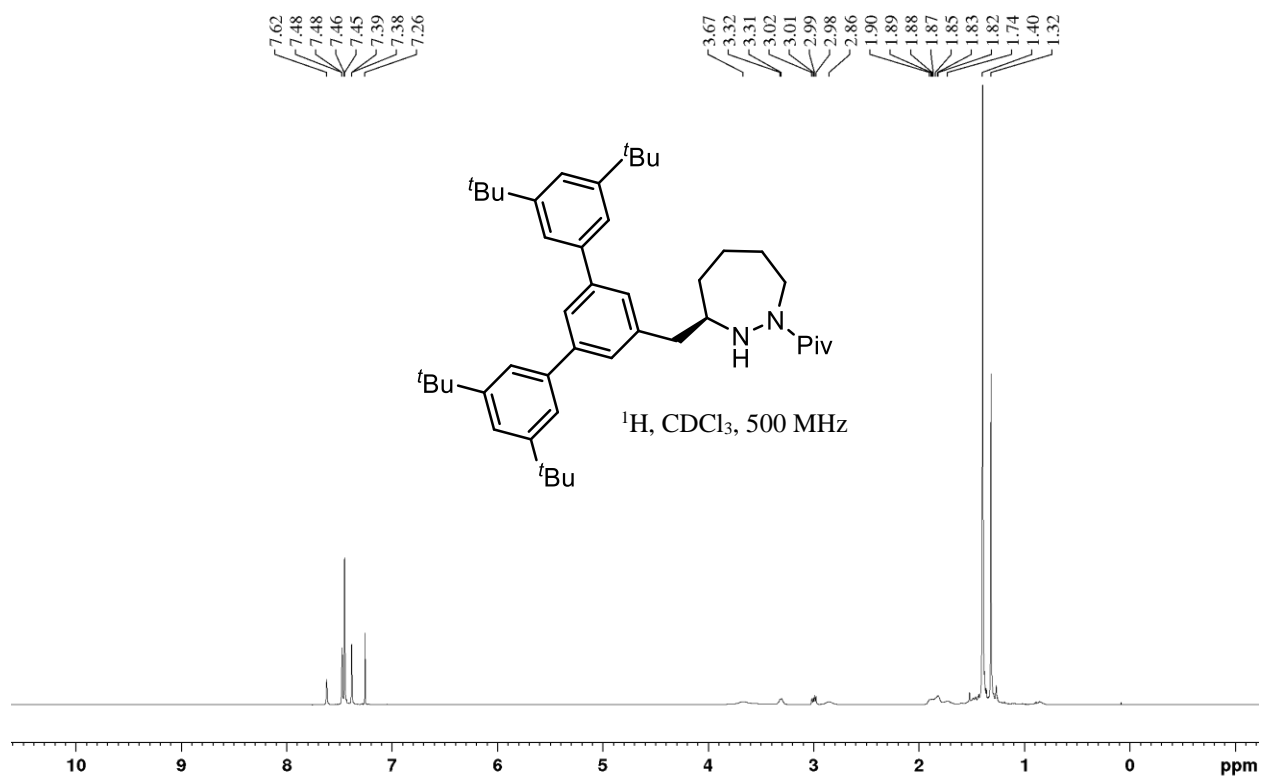


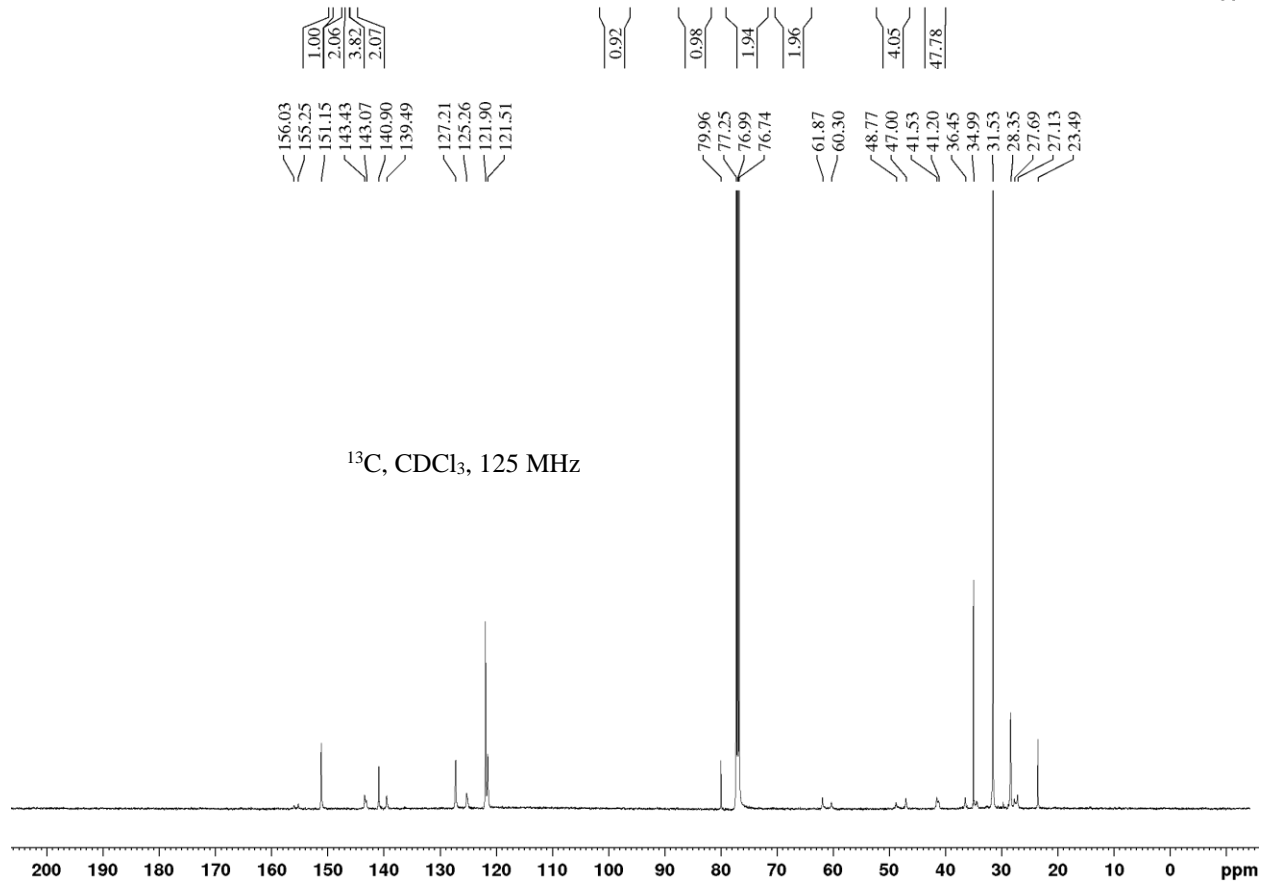
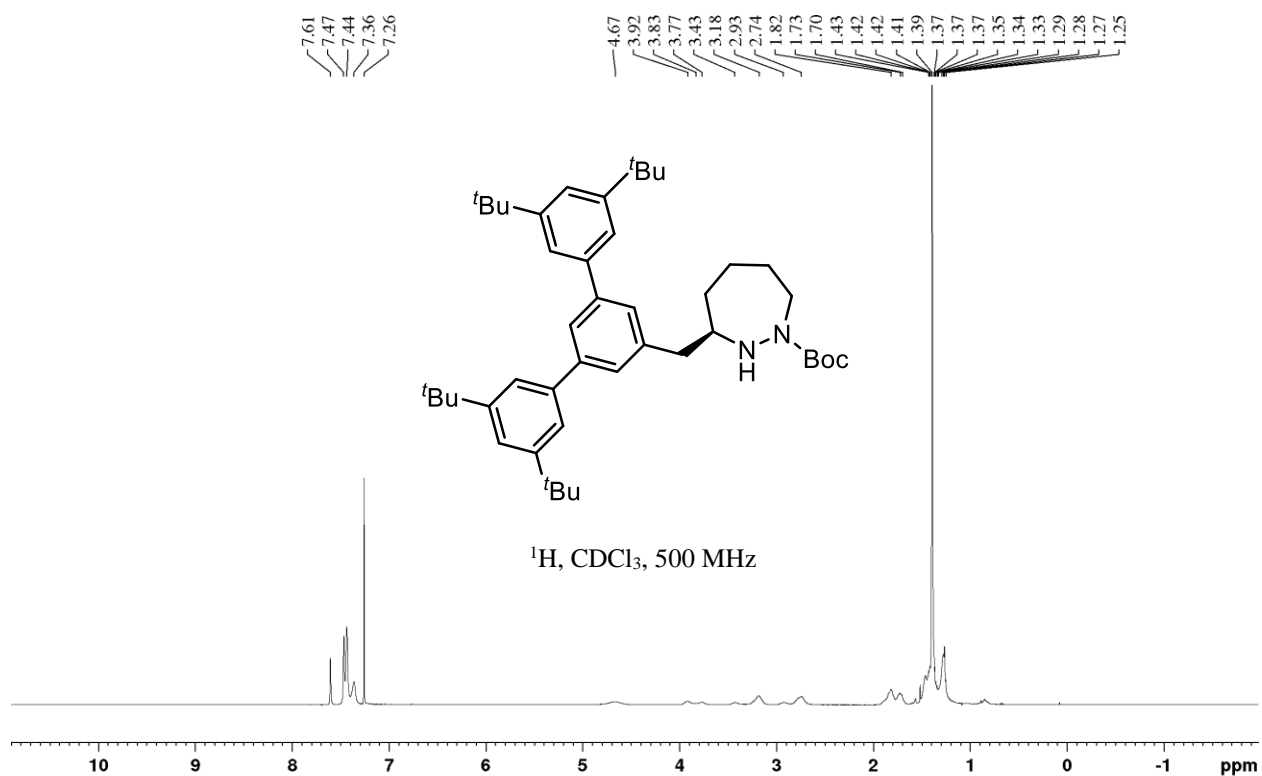


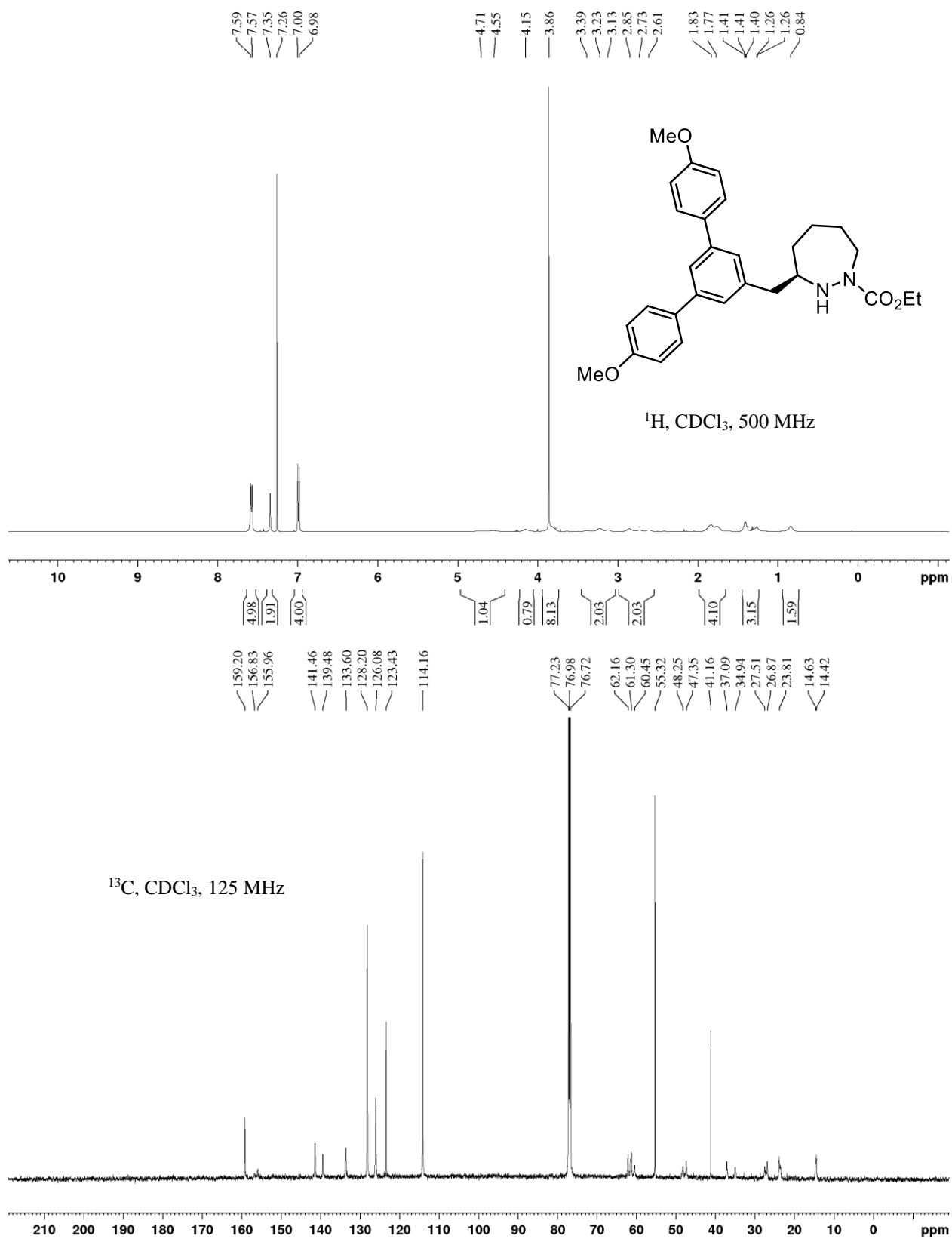


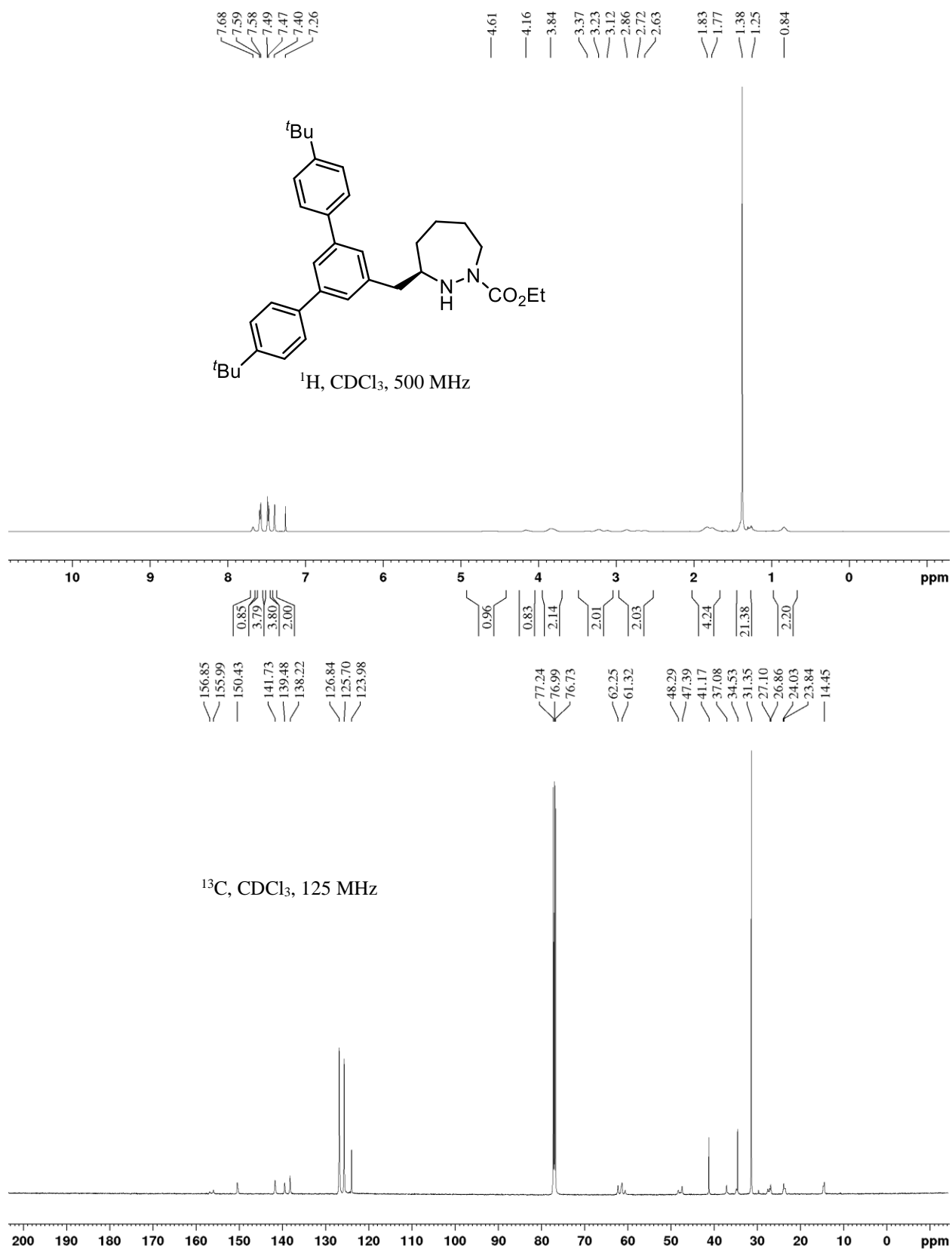


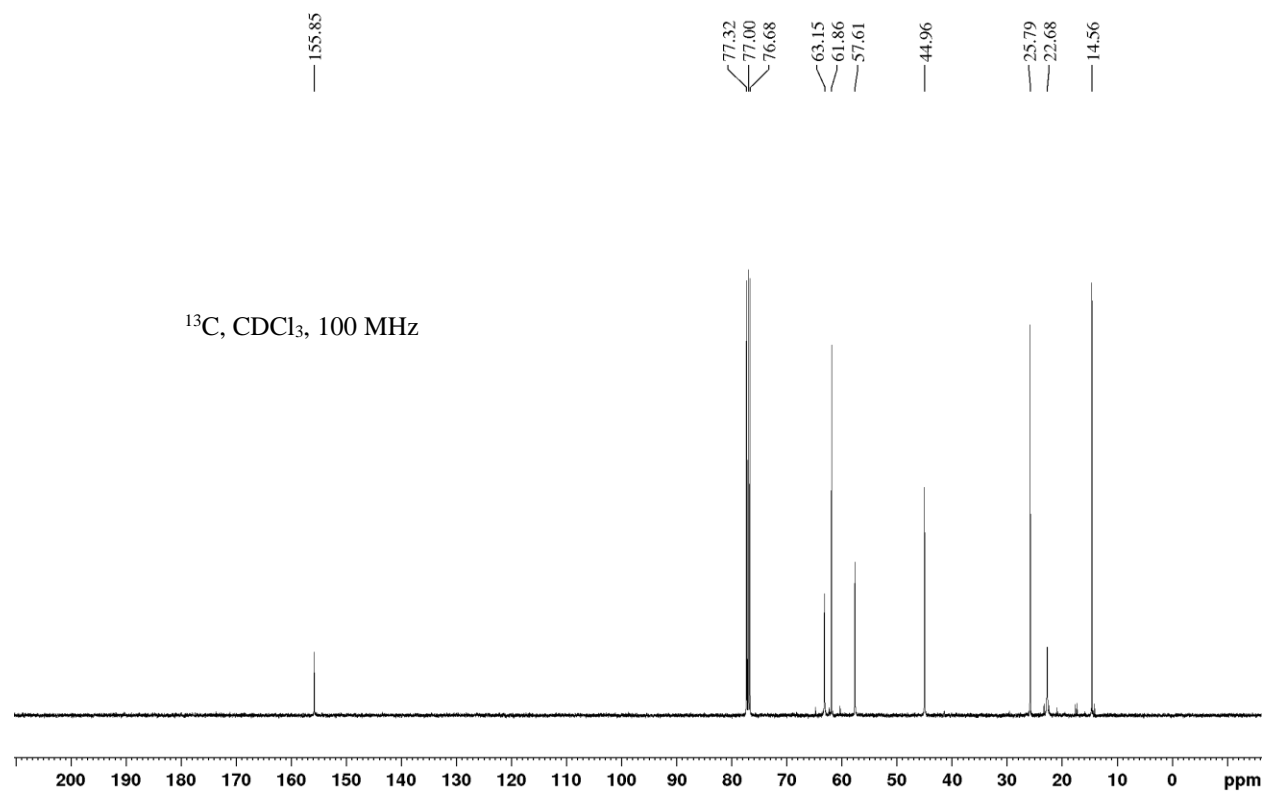
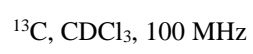
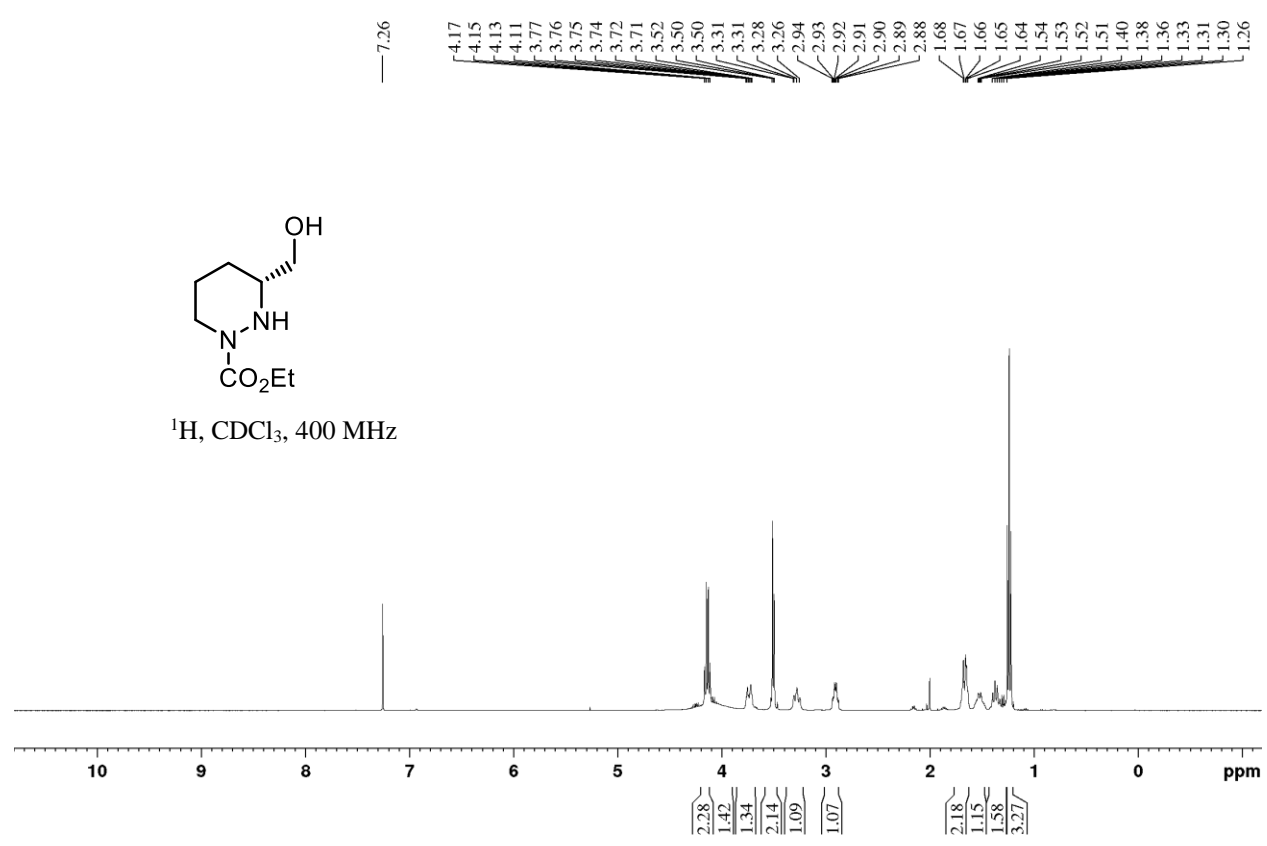
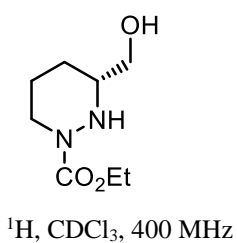


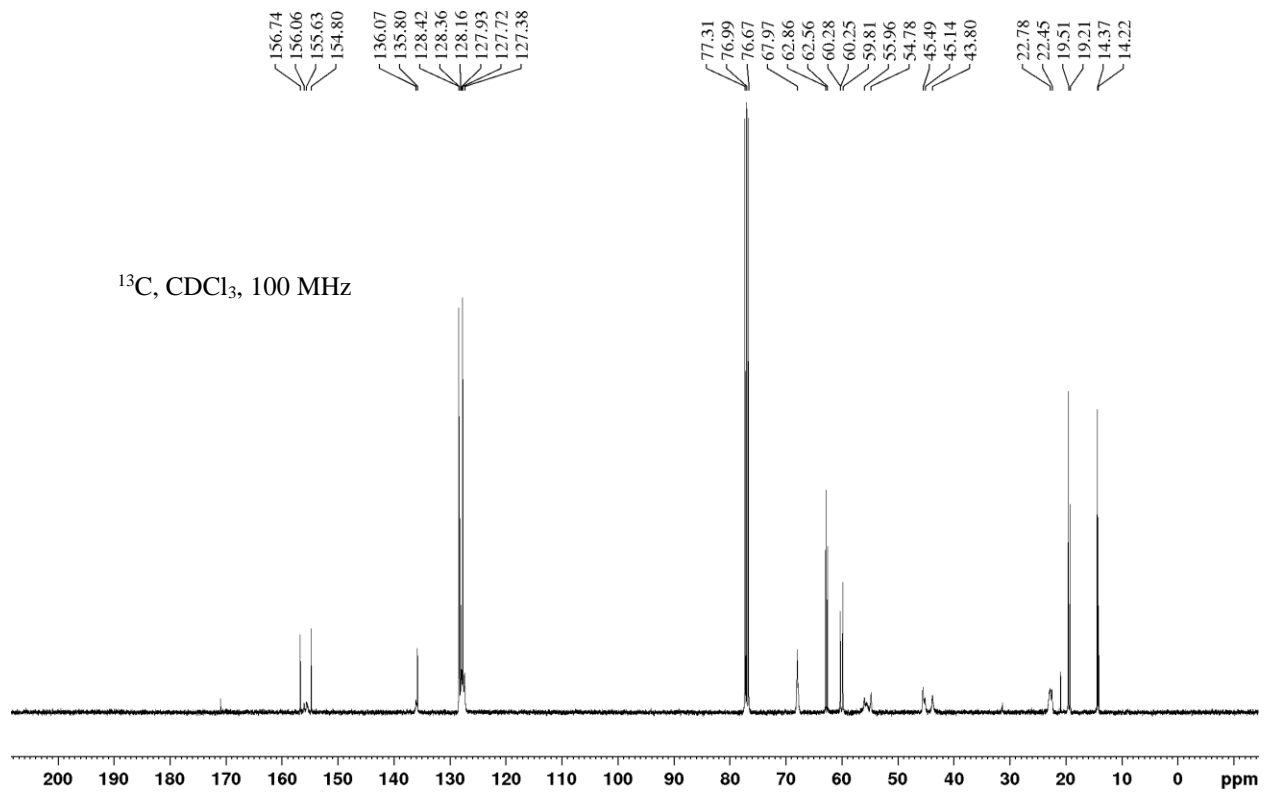
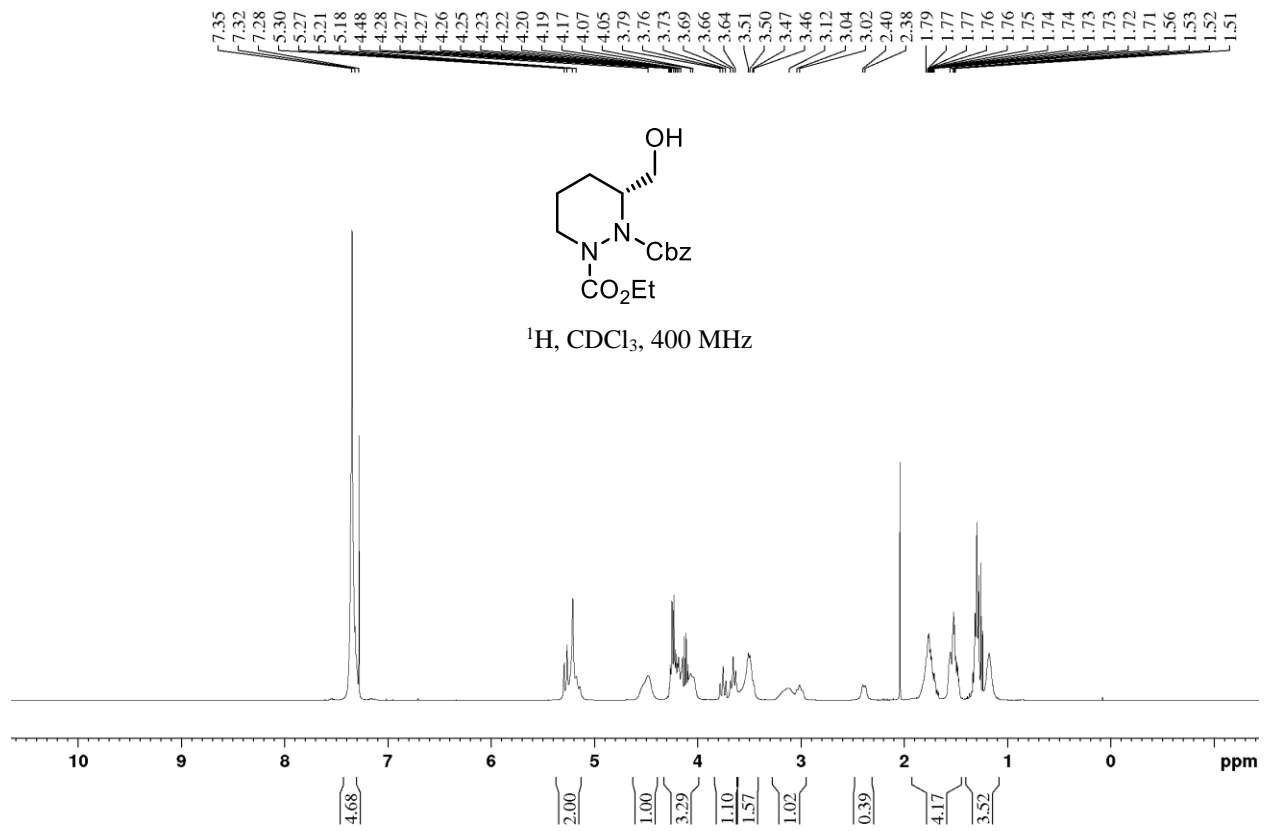


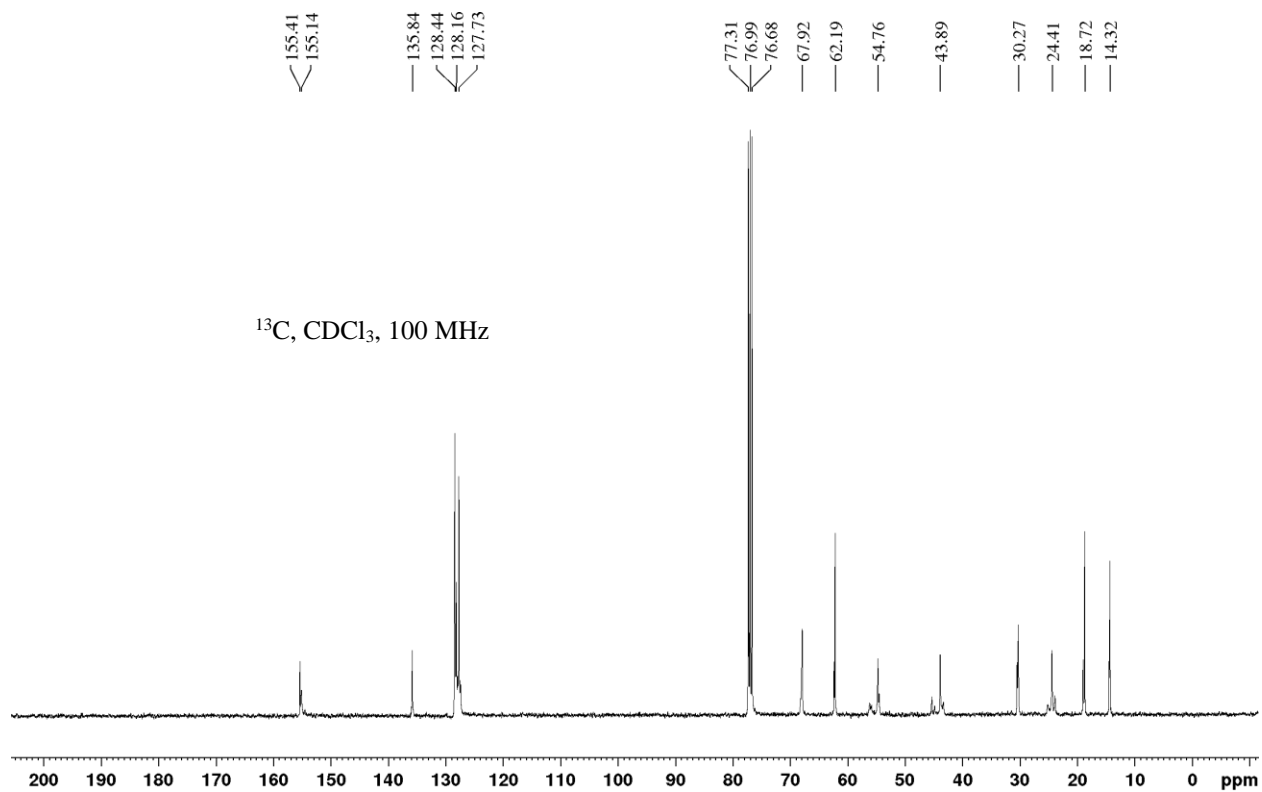
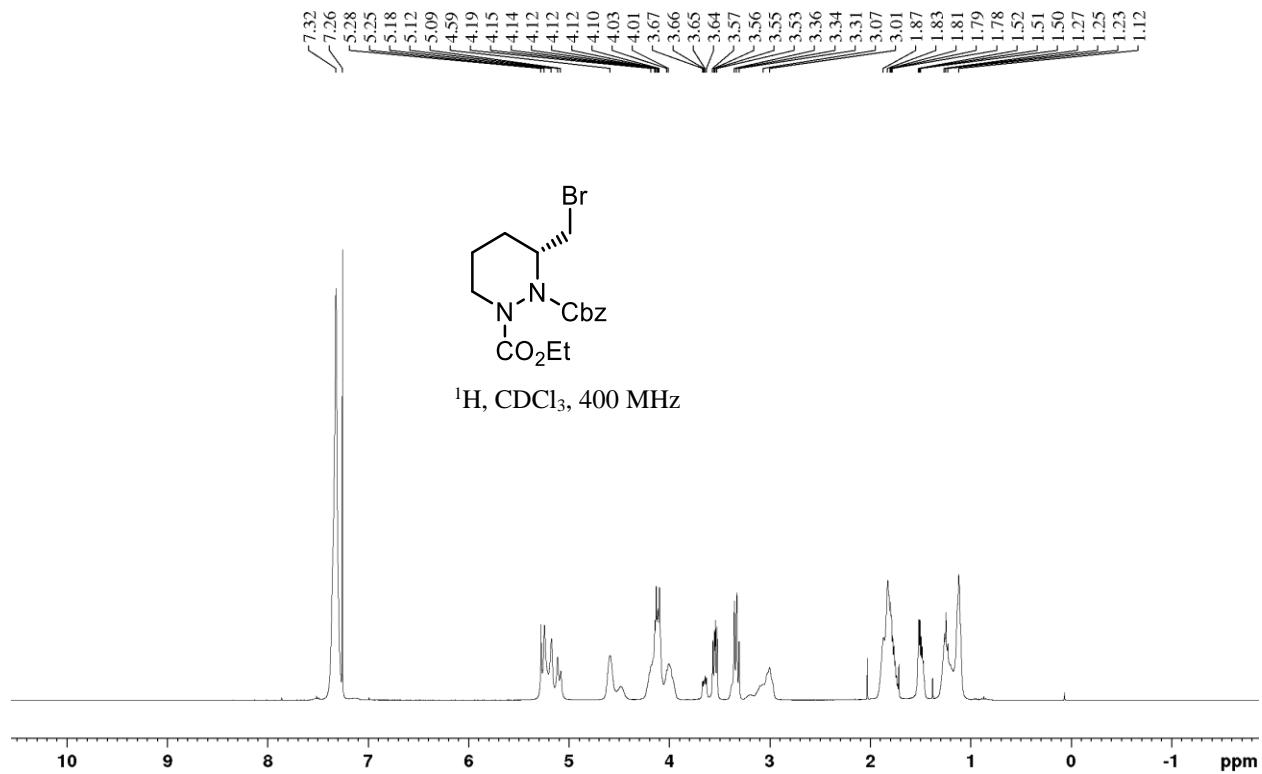


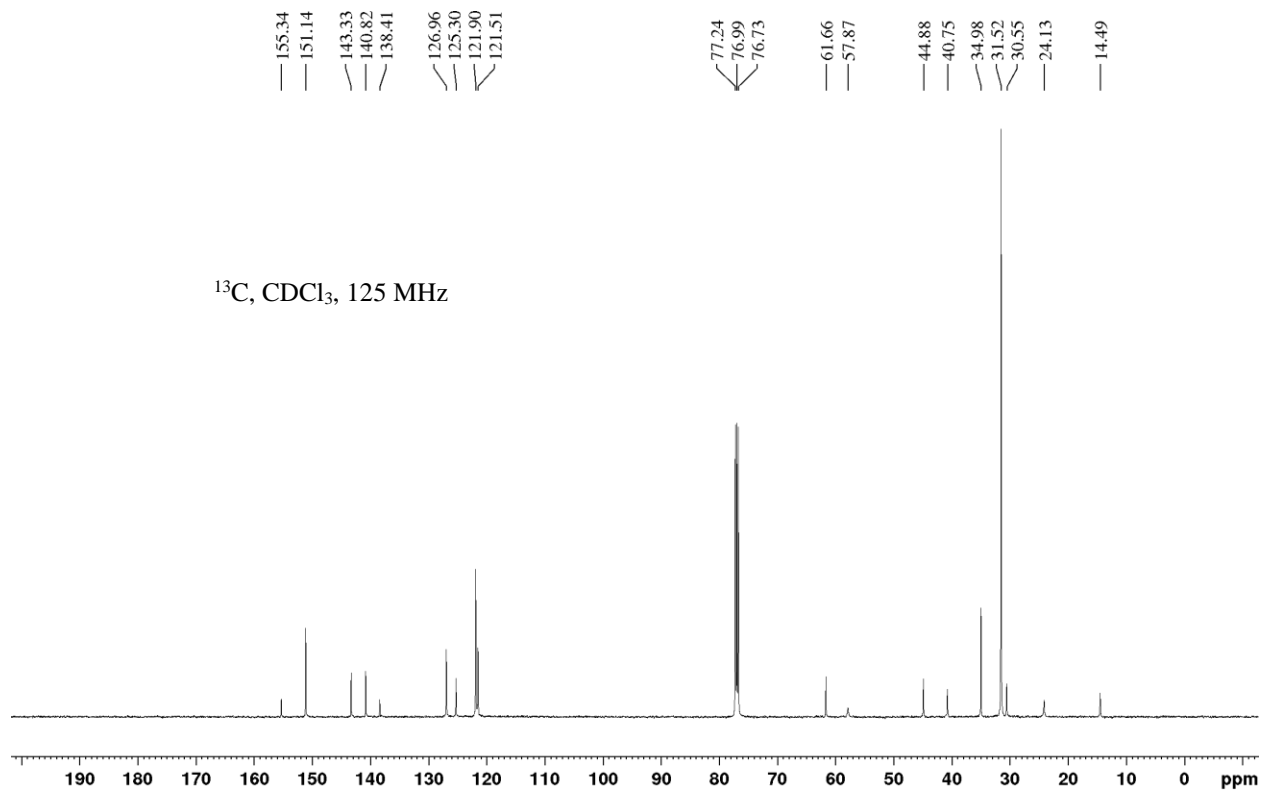
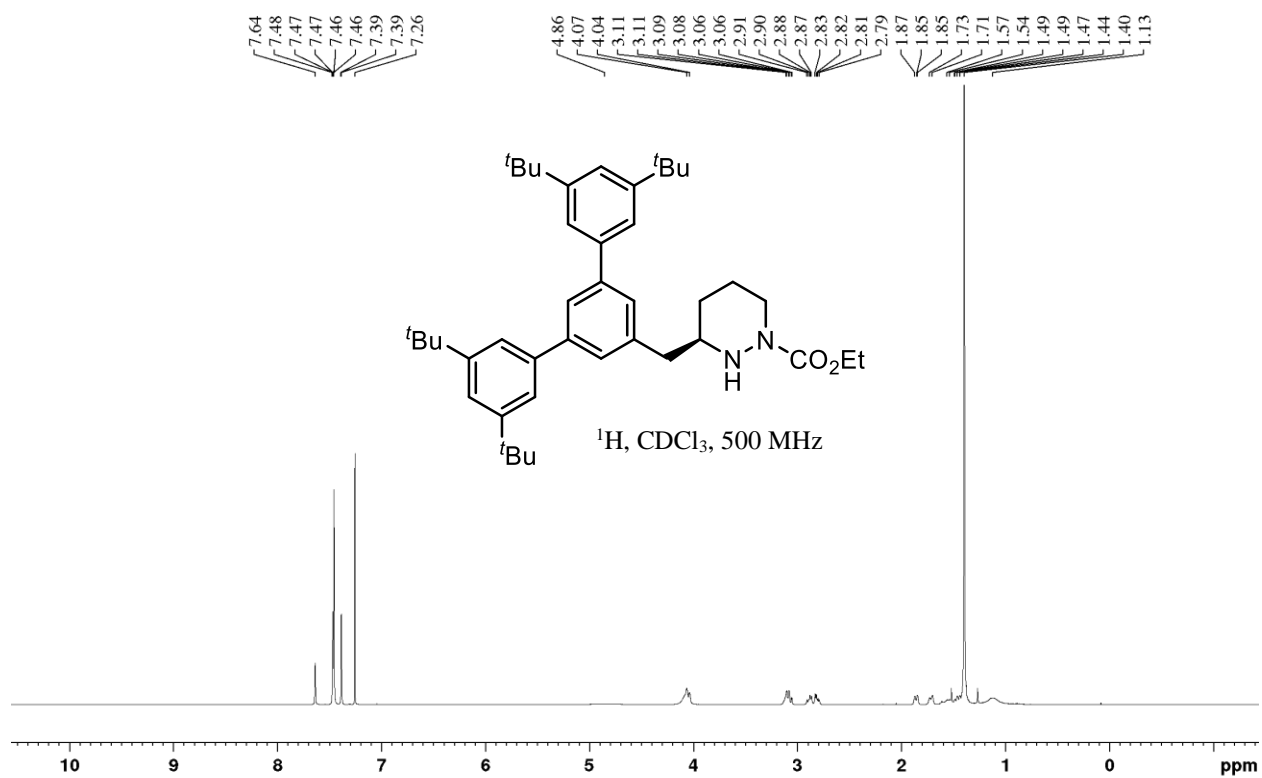


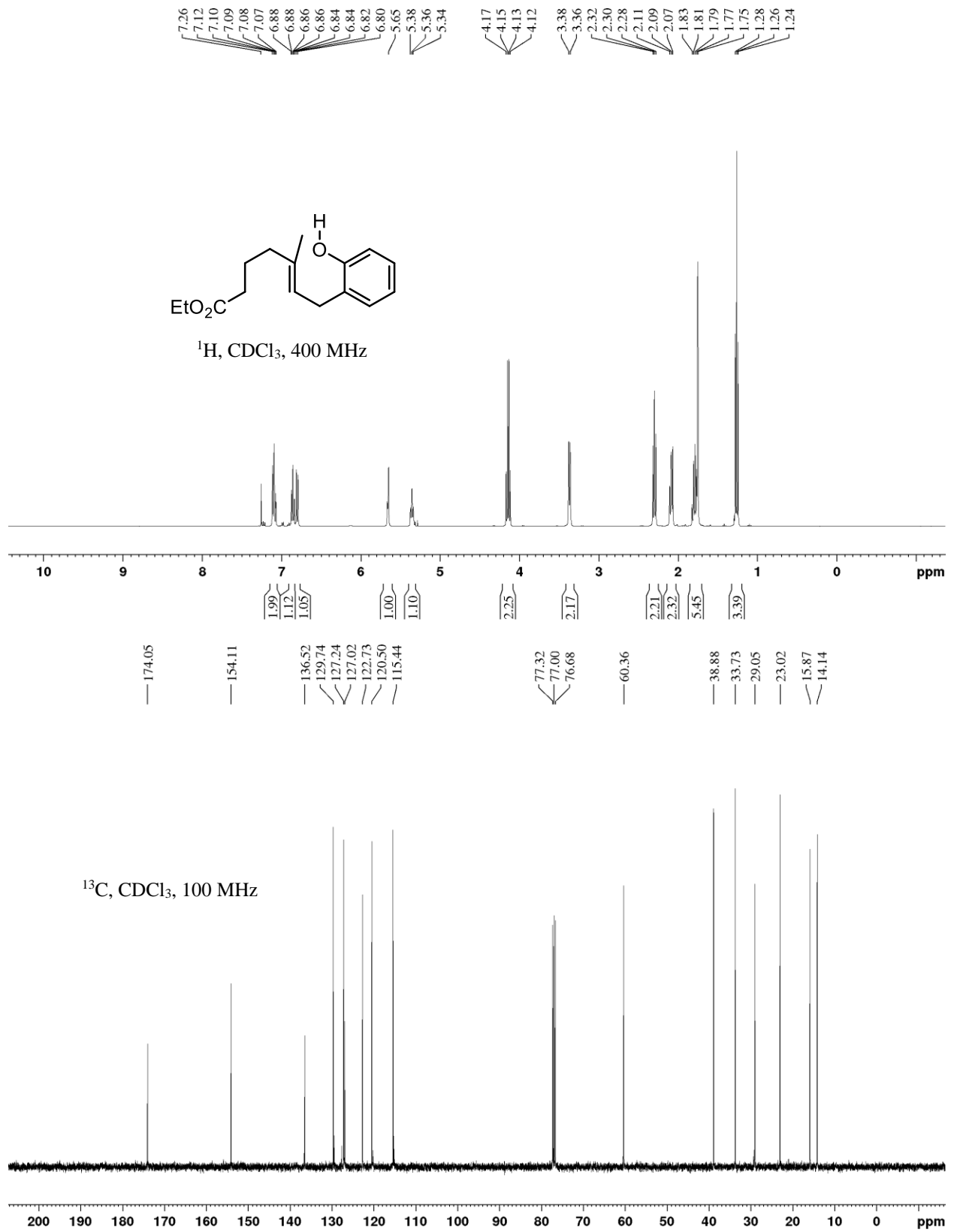


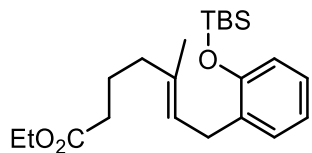
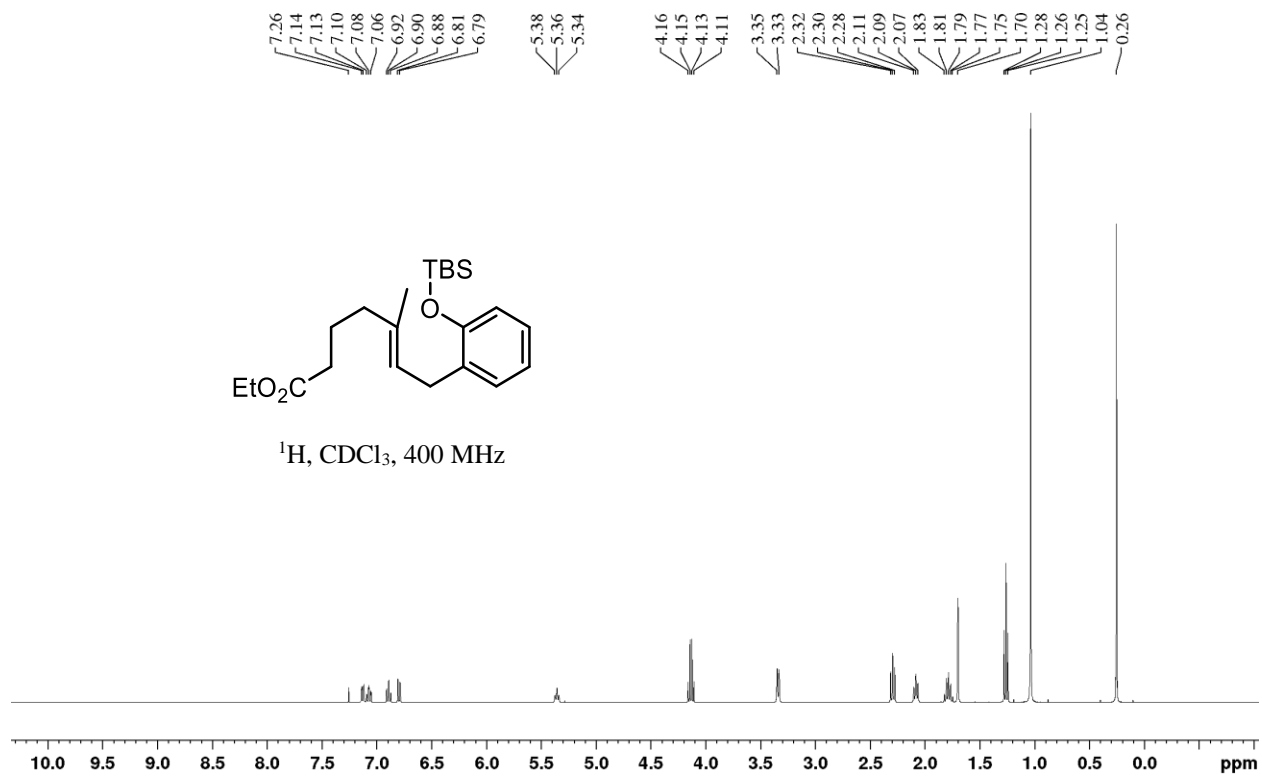




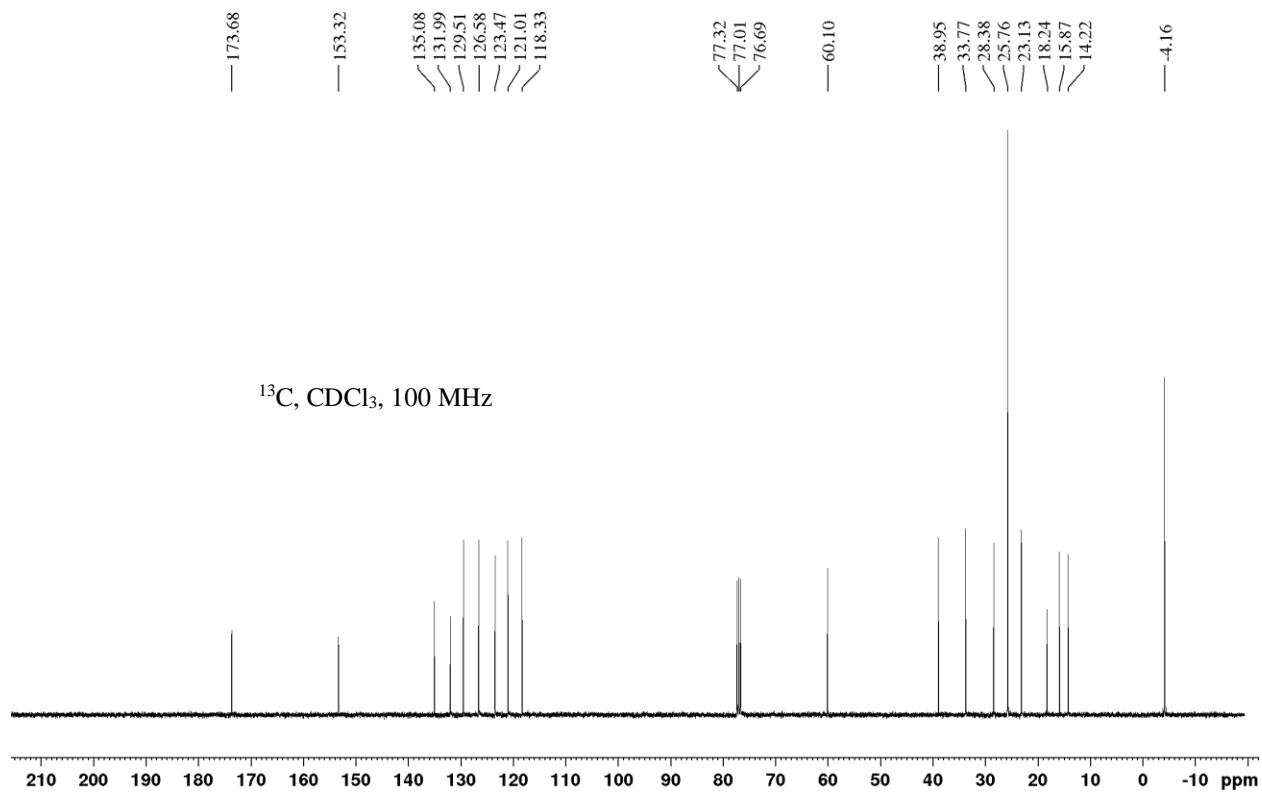


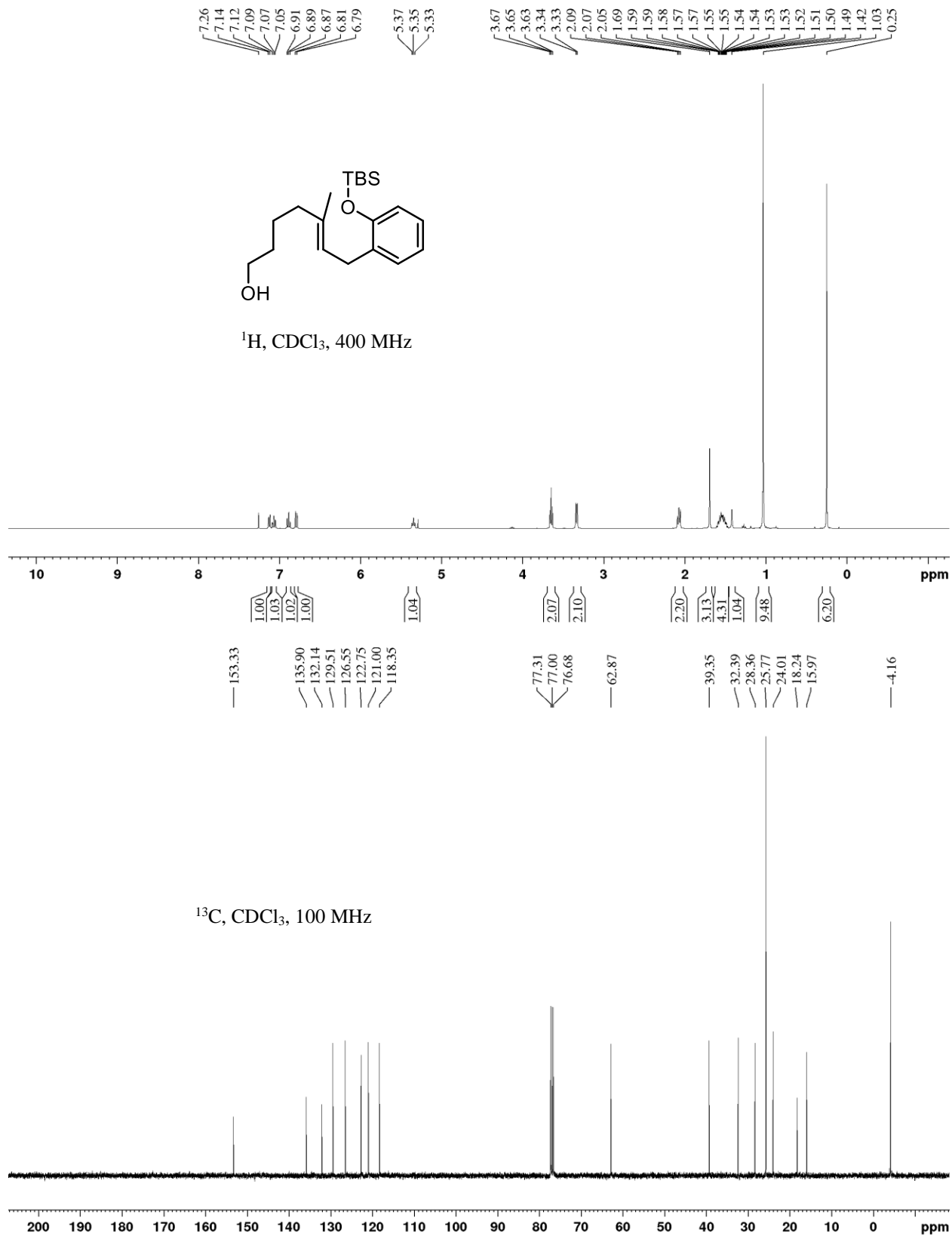


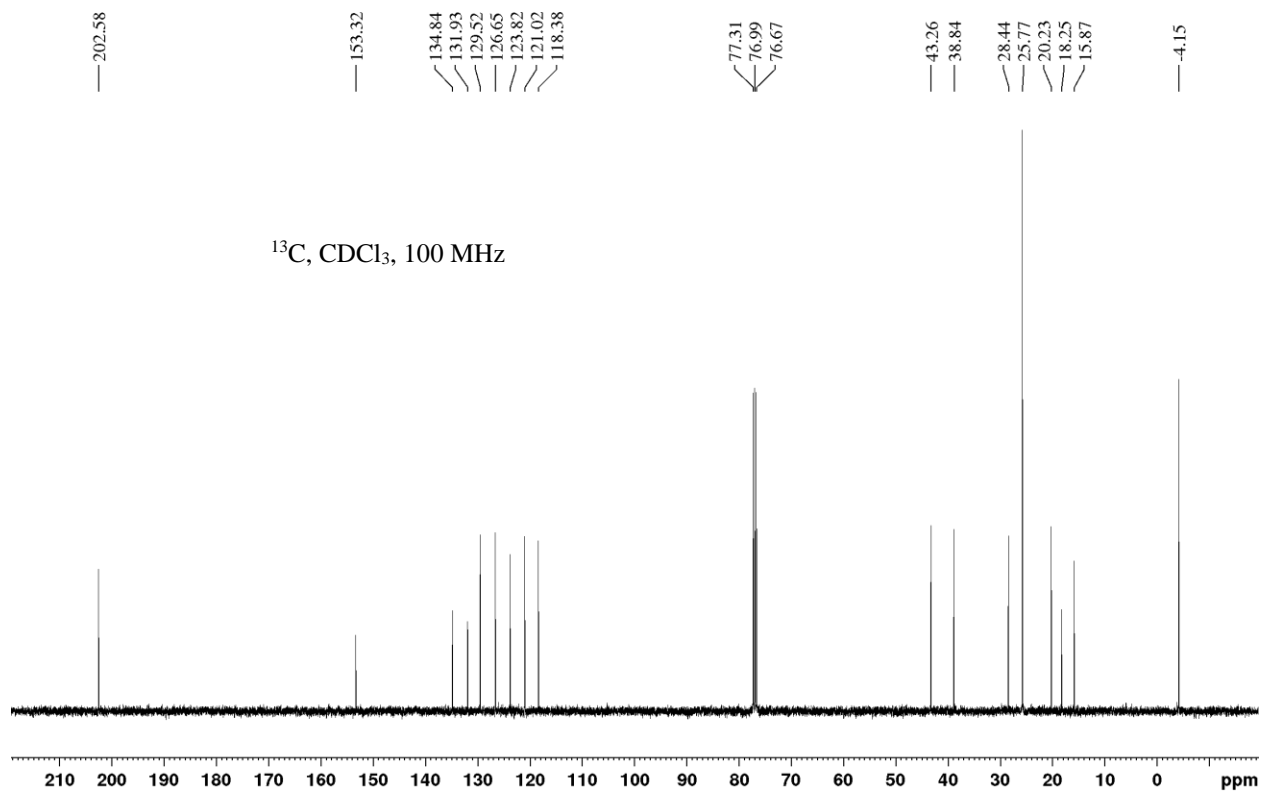
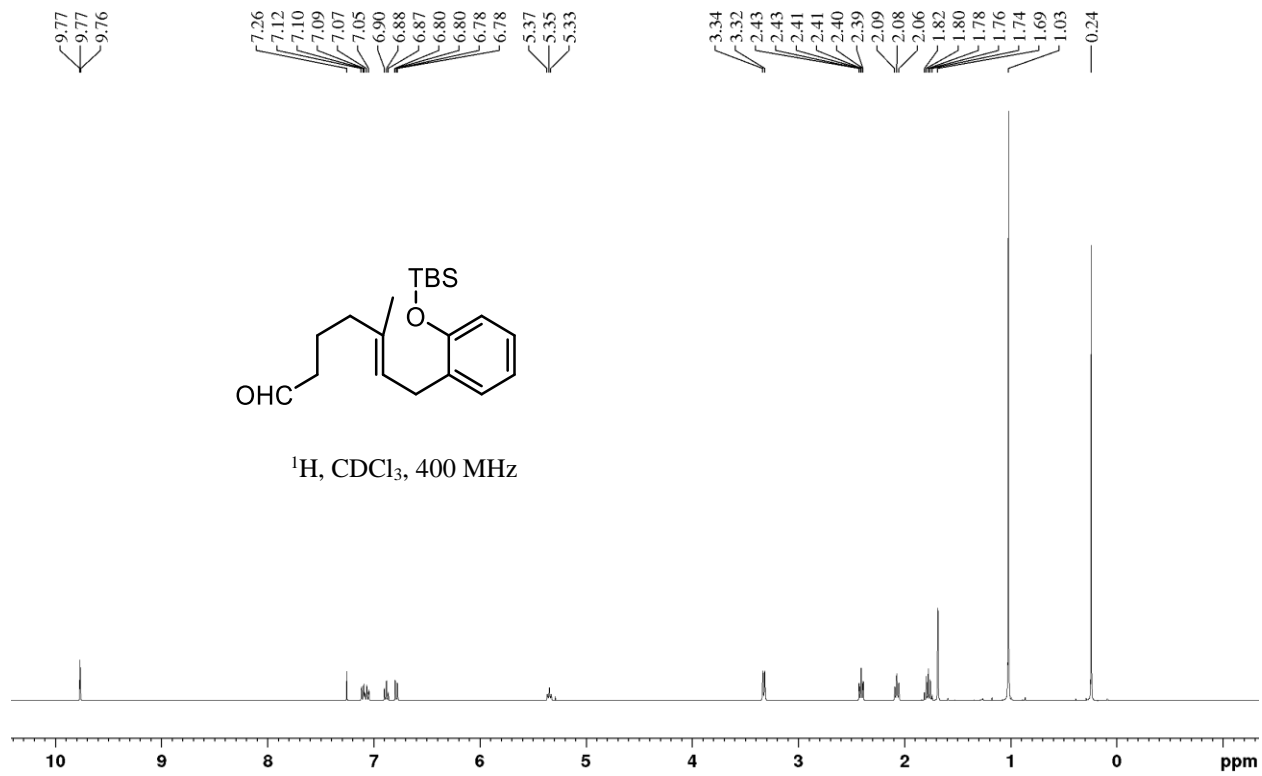


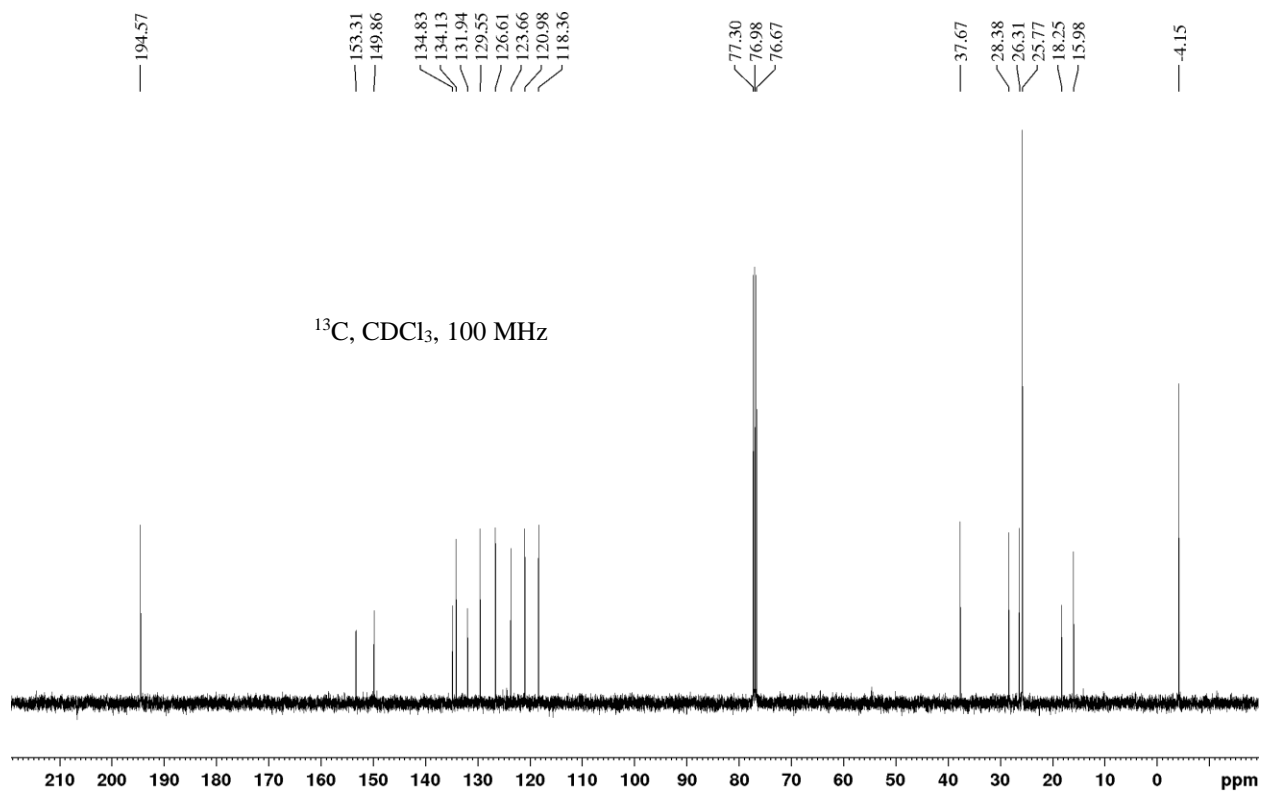
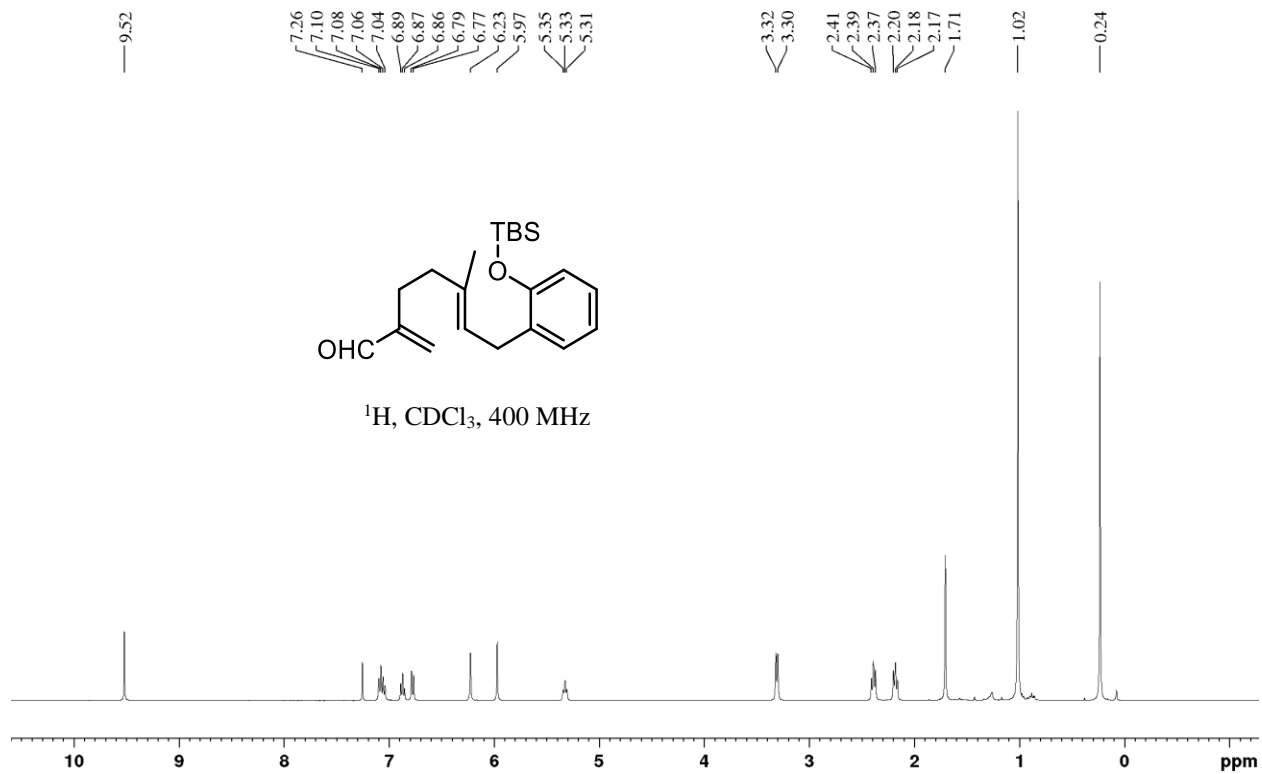


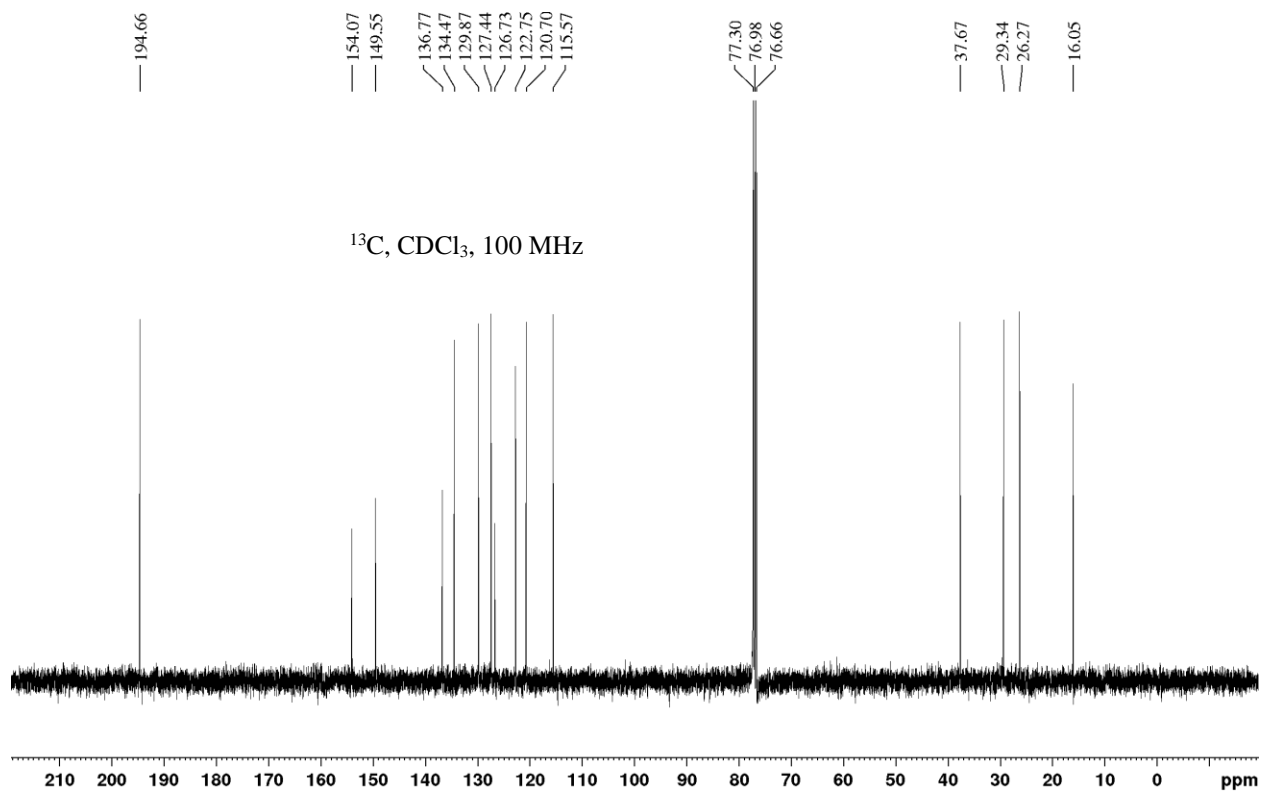
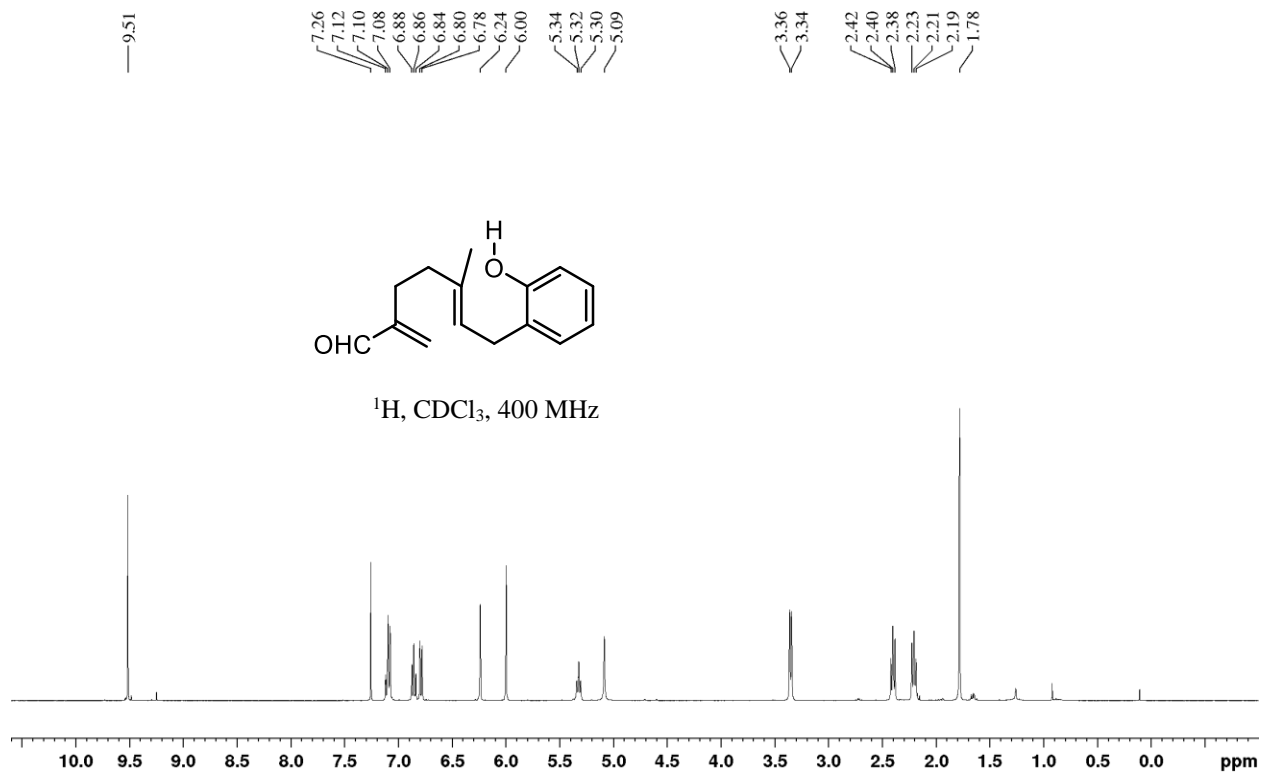
¹H, CDCl₃, 400 MHz

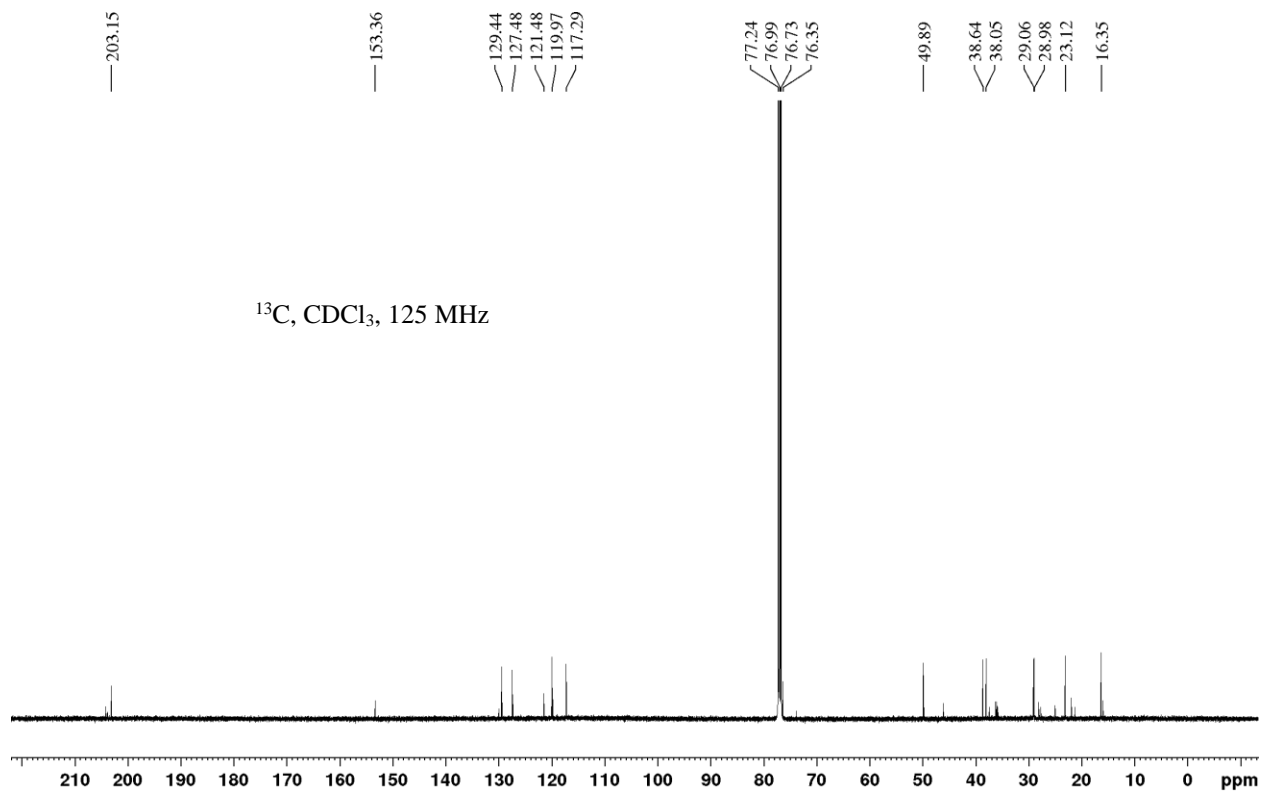
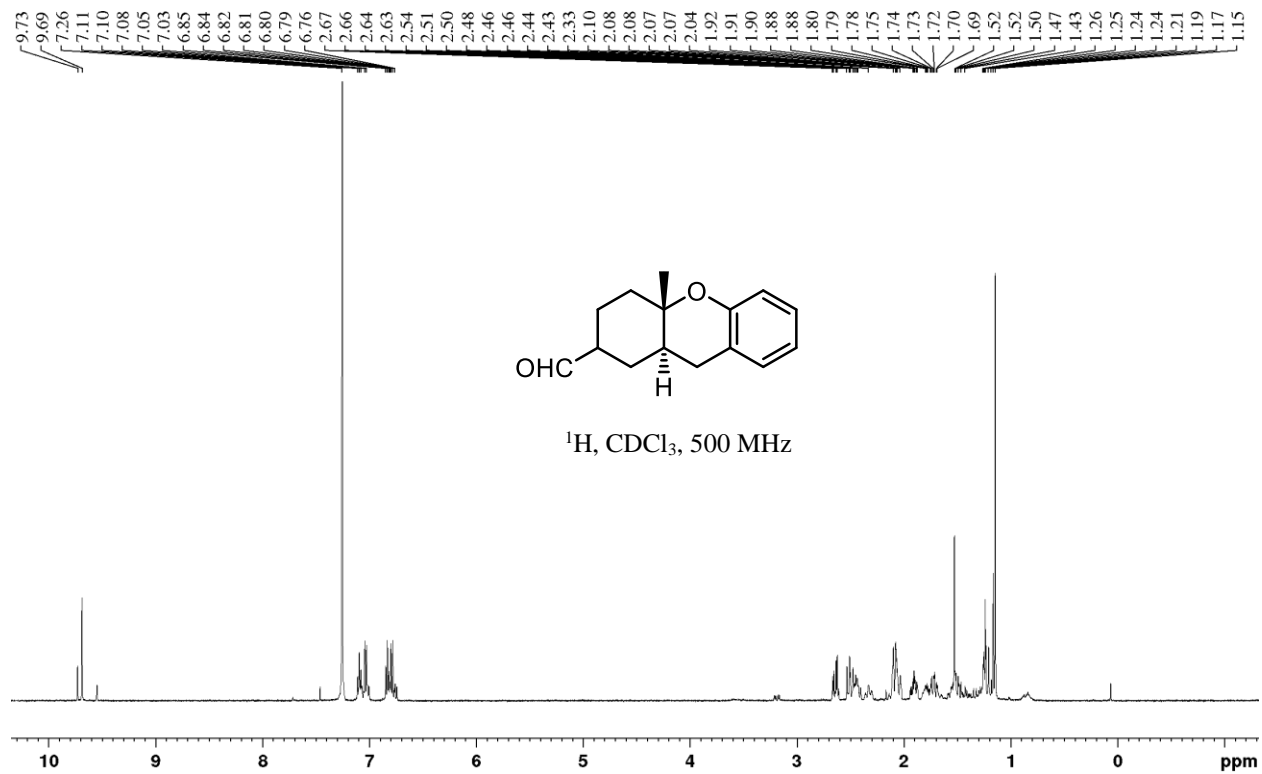


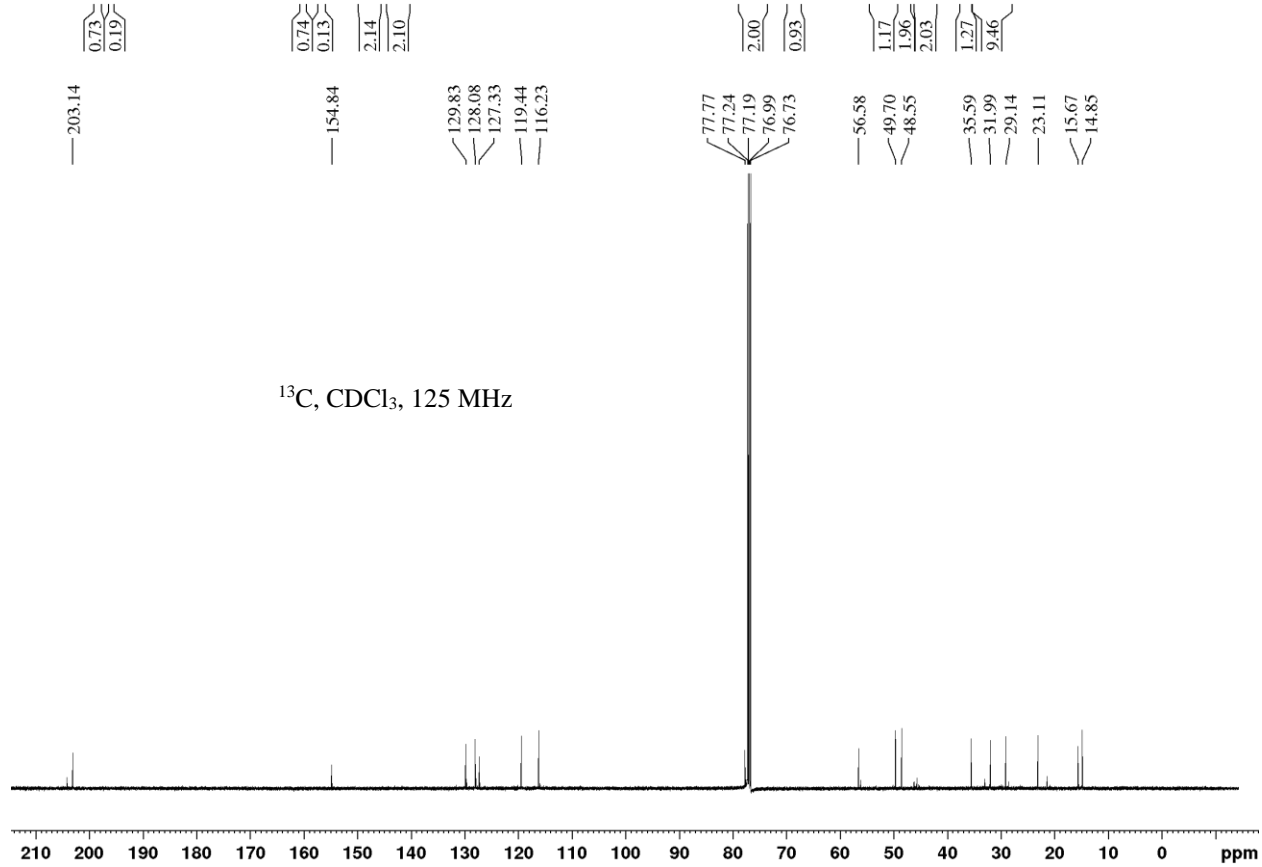
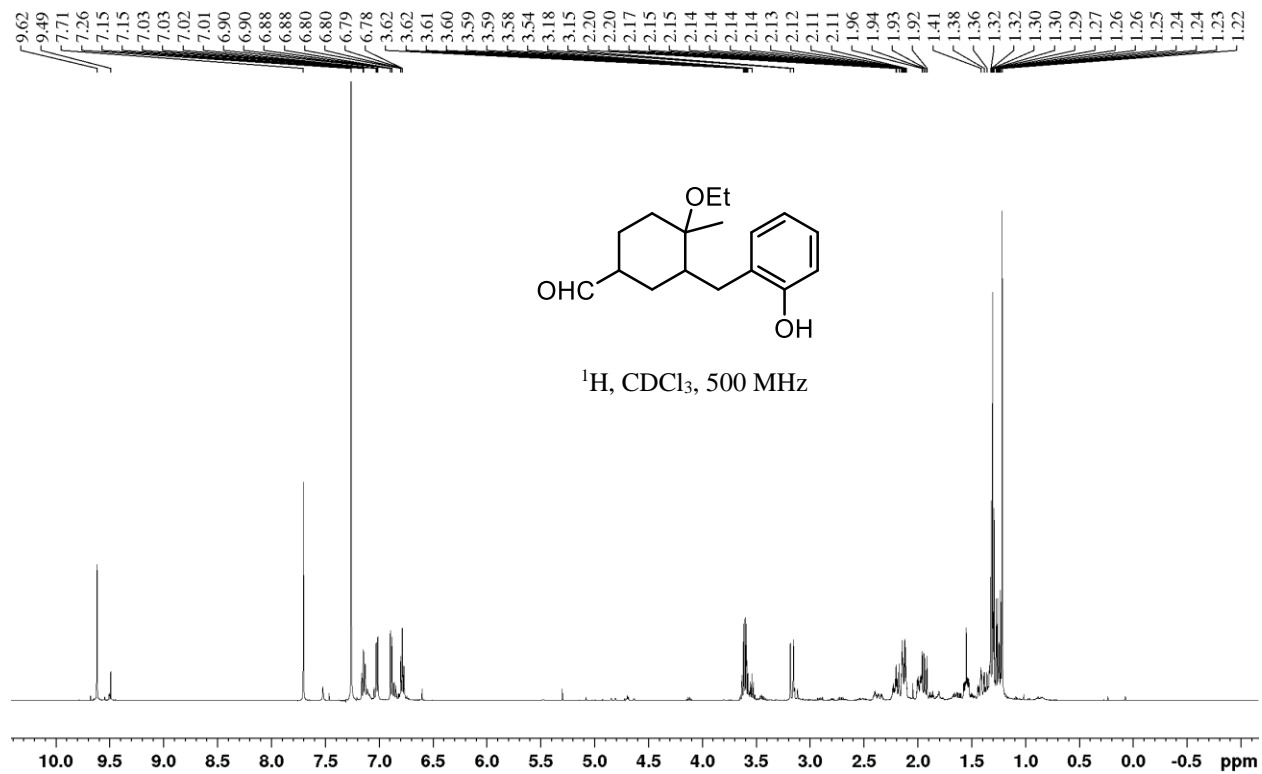


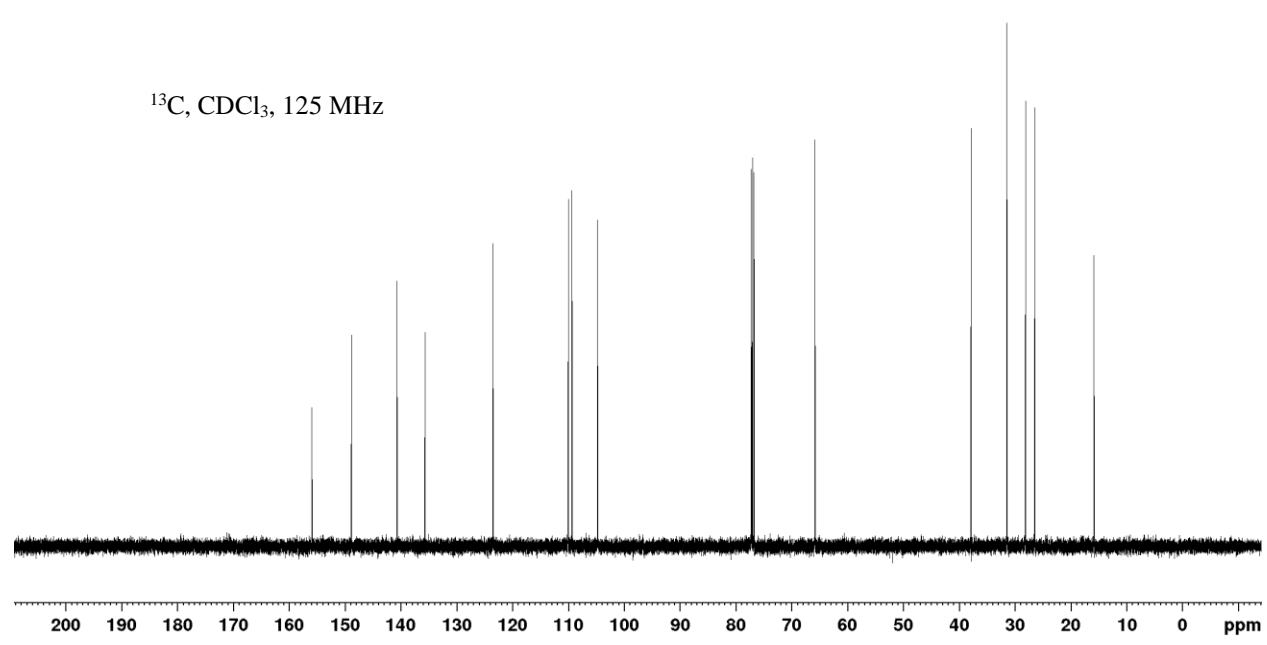
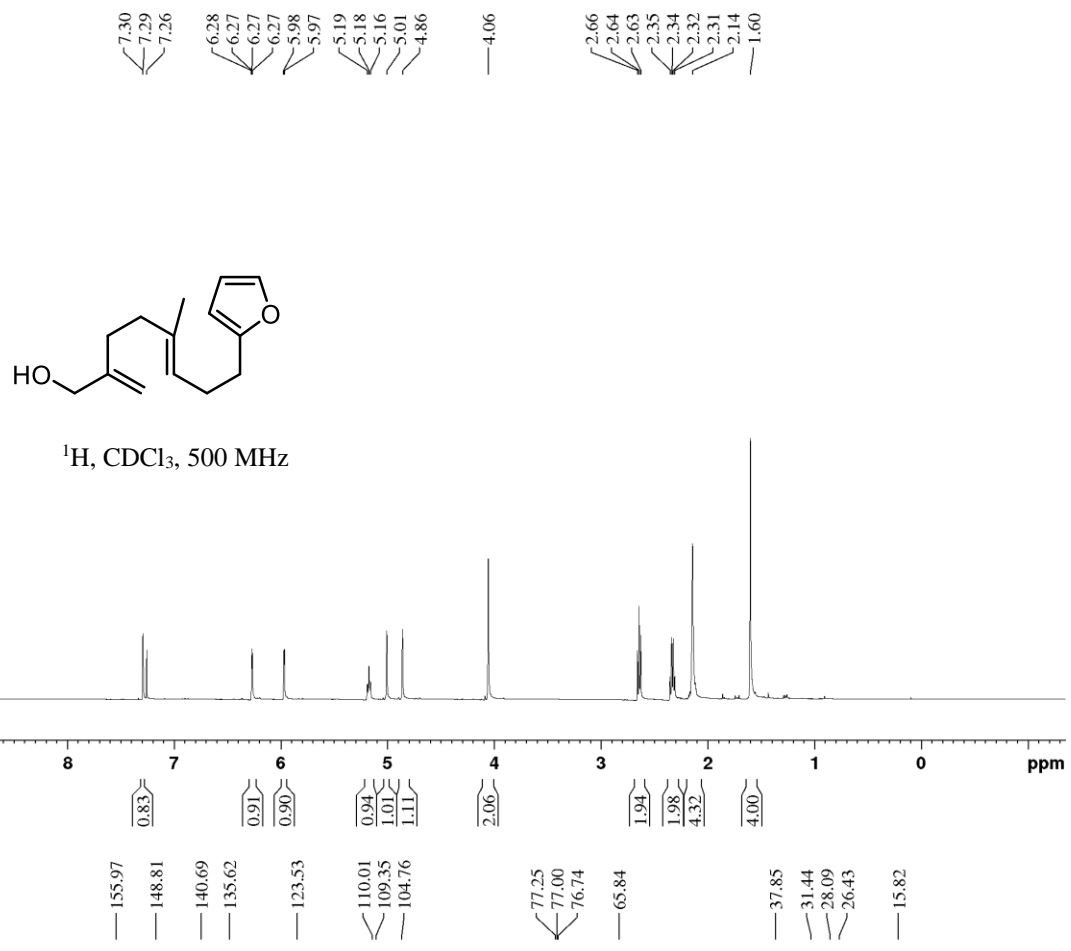


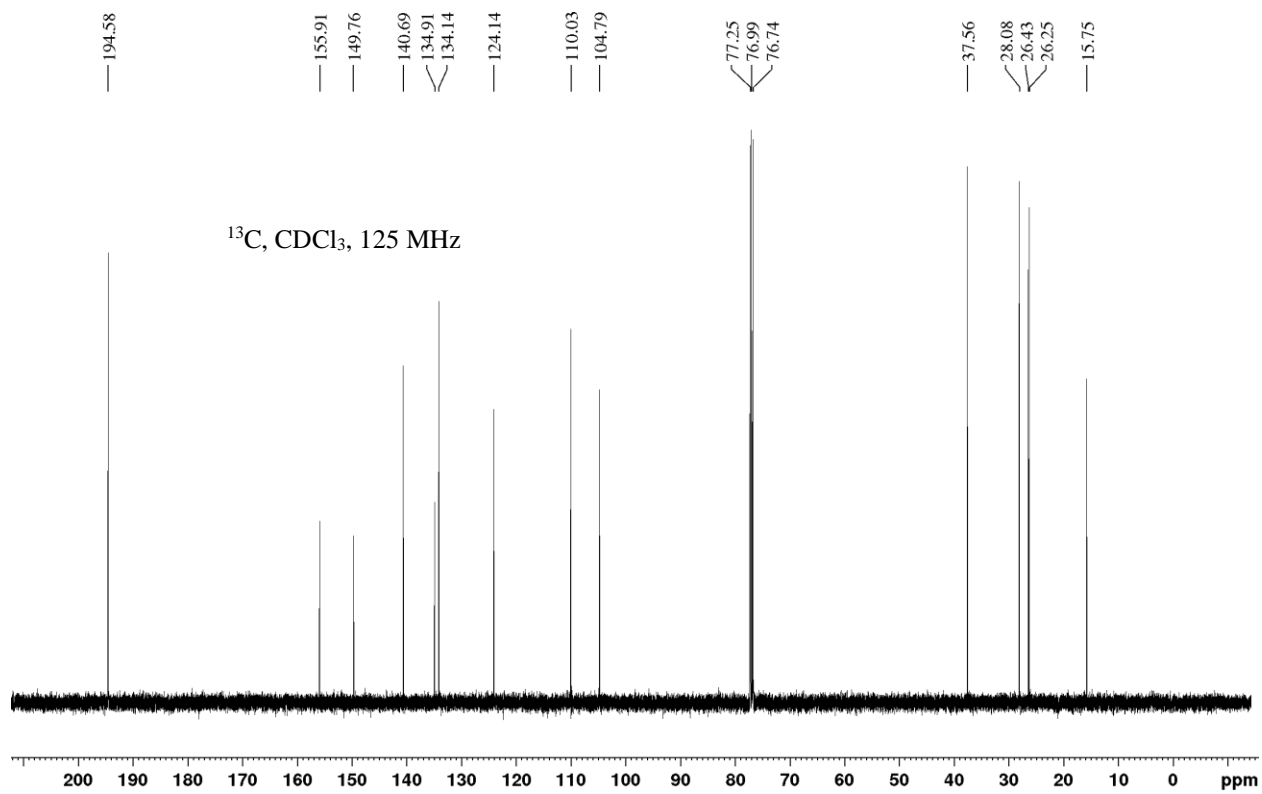
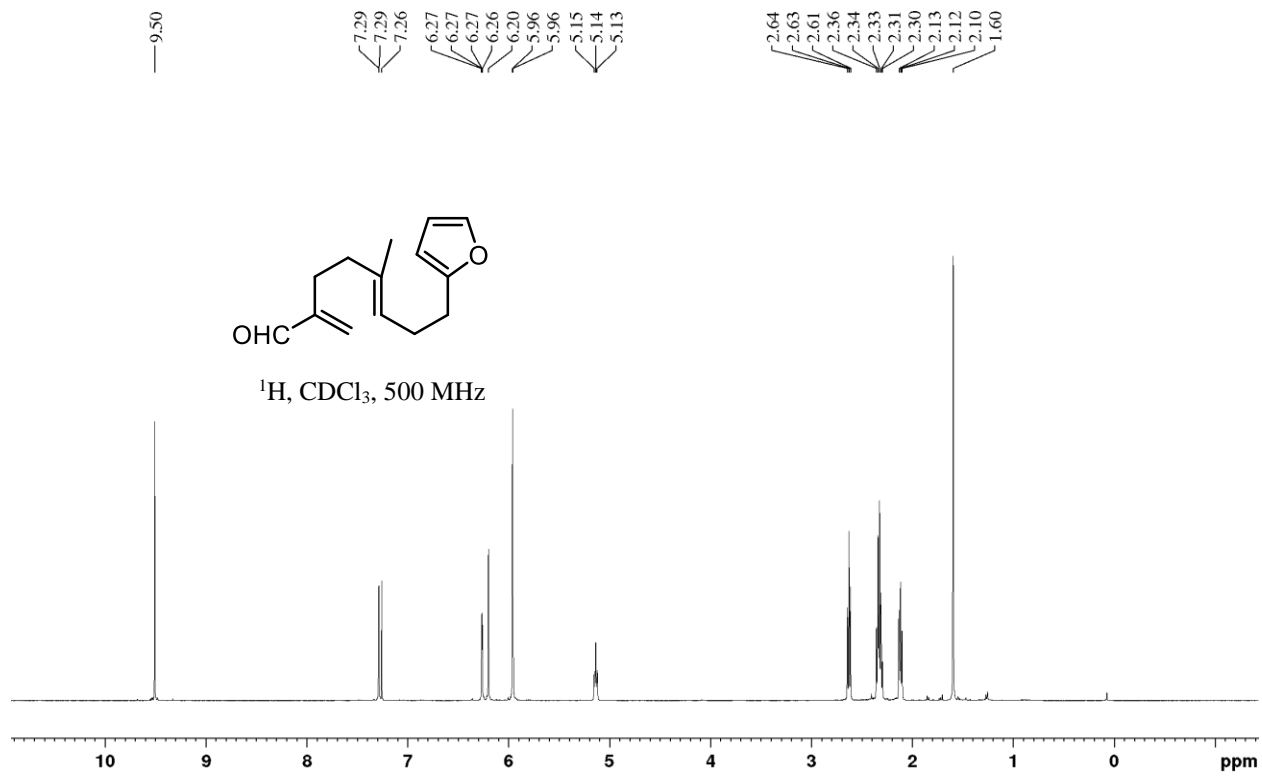


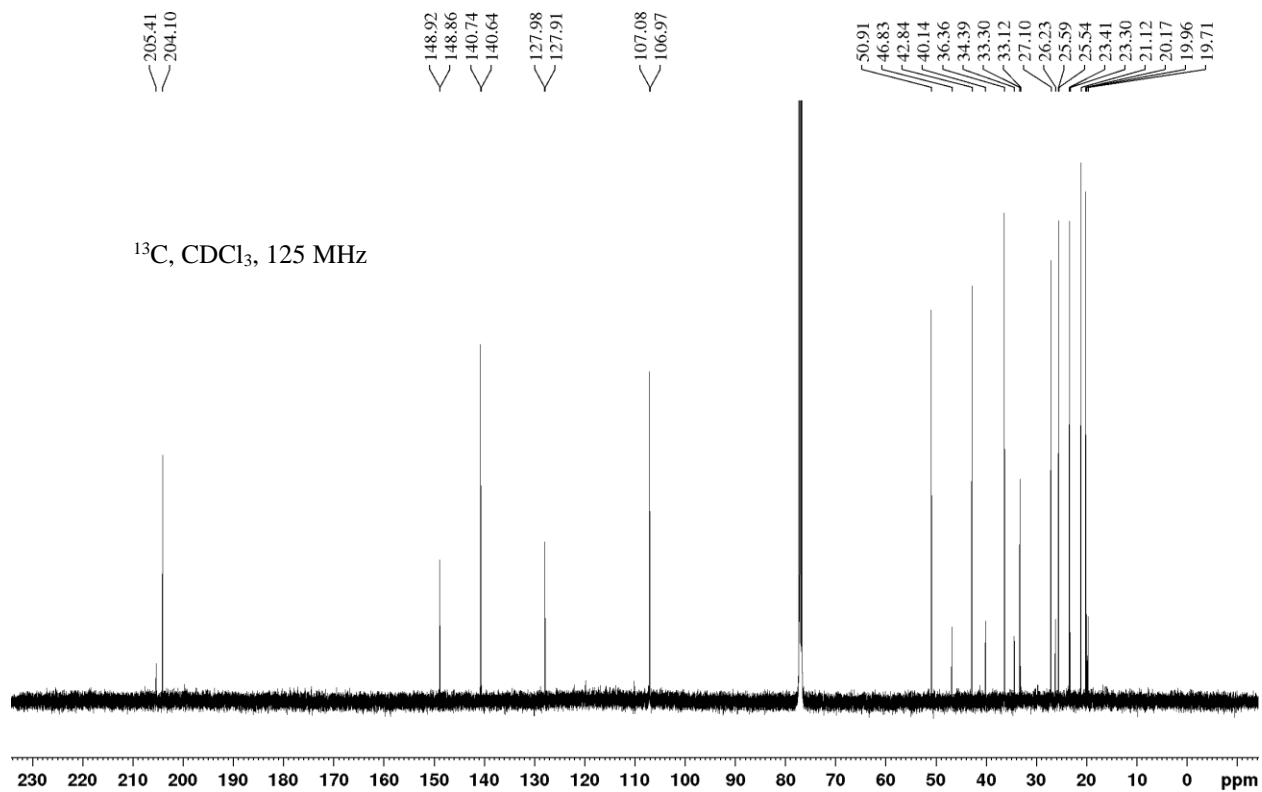
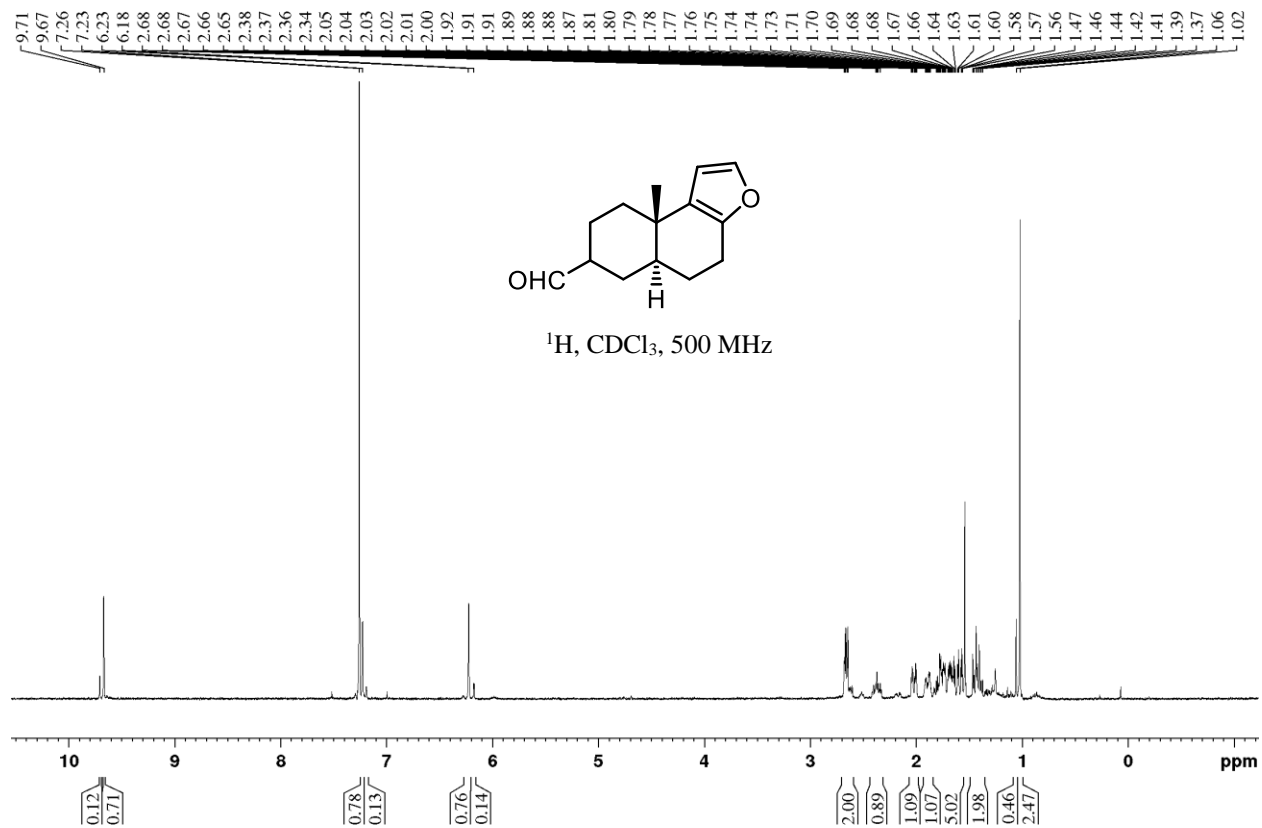












7.2. HPLC Chromatograms

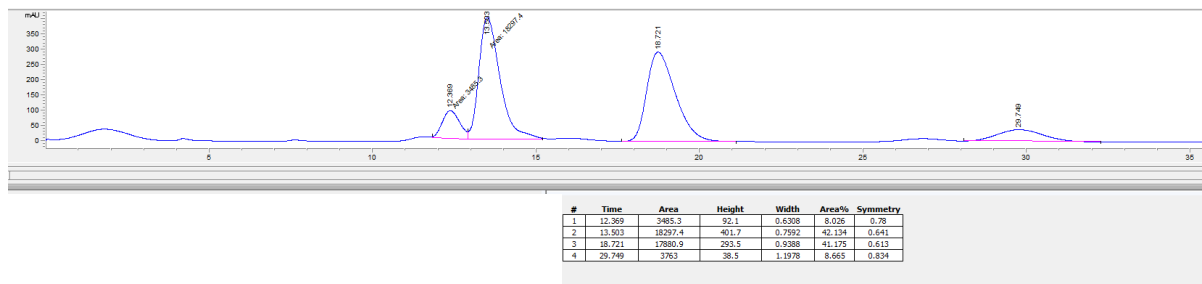
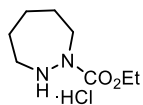
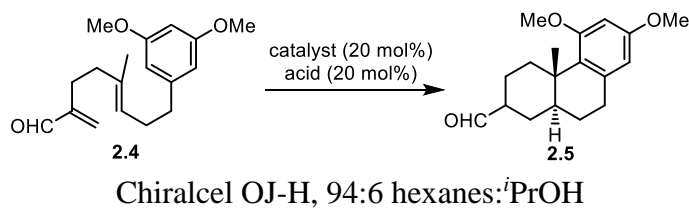
In all cases, HPLC was run on either a Daicel Chiralcel OJ-H or Chiral OD column, flow rate was 1 mL/min and UV absorbance was observed at 220 nm.

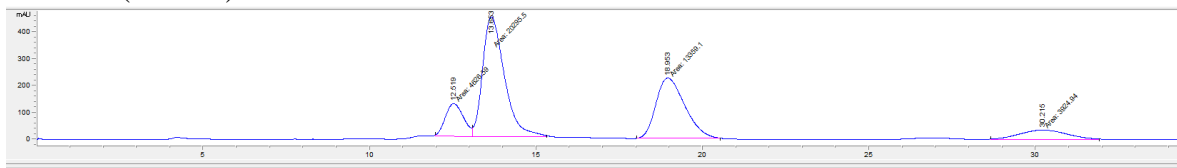
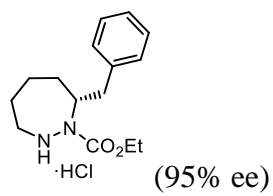
Aldehydes were derivatized to the corresponding α and β alcohols by reduction with NaBH_4 in MeOH. As the enantiomeric ratio differed between the α and β alcohols in some cases, the overall enantiomeric ratio was calculated as follows:

Enantiomeric excess = [(area of major HPLC peak of α alcohol x ^1H NMR ratio of α aldehyde) + (area of major HPLC peak of β alcohol x ^1H NMR ratio of β aldehyde) - (area of minor HPLC peak of α alcohol ^1H NMR ratio of α aldehyde) + area of minor HPLC peak of β alcohol x ^1H NMR ratio of β aldehyde)]/total peak area

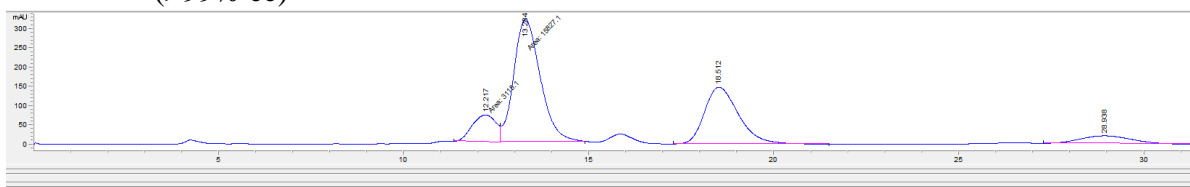
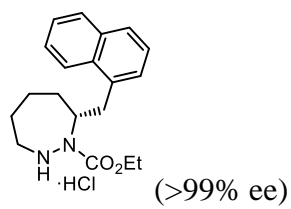
Or

Enantiomeric excess = (area of major HPLC peak of α/β alcohol - area of minor HPLC peak of α/β alcohol)/total peak area

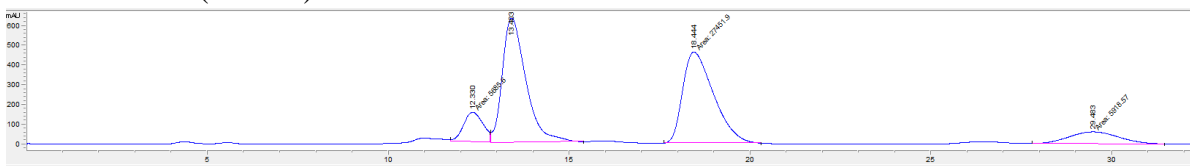
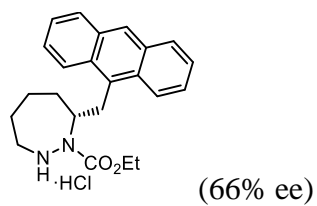




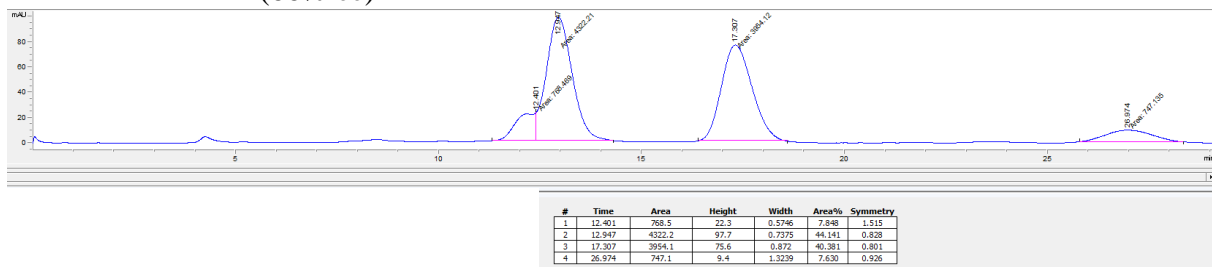
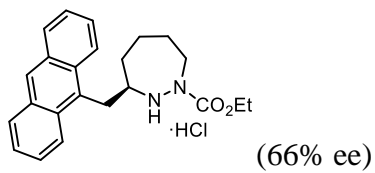
#	Time	Area	Height	Width	Area%	Symmetry
1	12.519	4026.5	121.2	0.6352	10.962	0.808
2	13.653	20295.5	446.5	0.7596	48.087	0.646
3	18.953	13359.1	223.6	0.9957	31.652	0.677
4	30.215	3924.9	37.1	1.7618	9.299	0.935



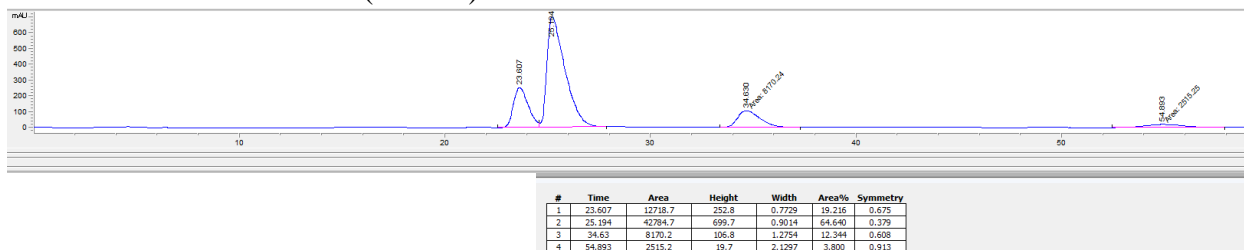
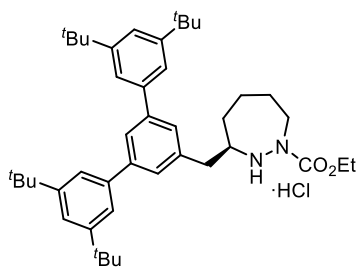
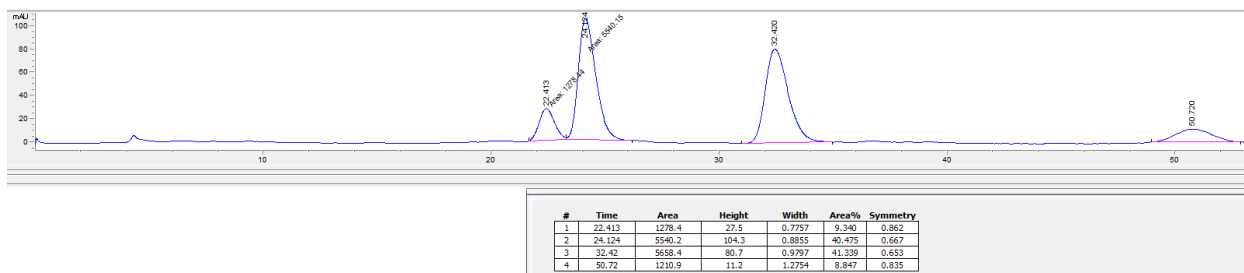
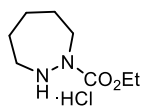
Time	Area	Height	Width	Area%	Symmetry
12.217	3115.1	69.3	0.7487	10.262	1.227
13.284	15827.1	317.6	0.8306	52.138	0.755
18.512	9444.4	147.5	0.985	31.112	0.686
28.938	1969.4	20.4	1.1345	6.488	0.893

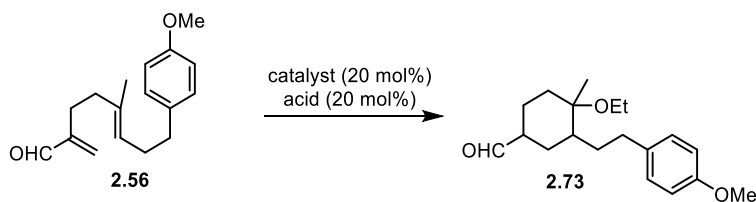
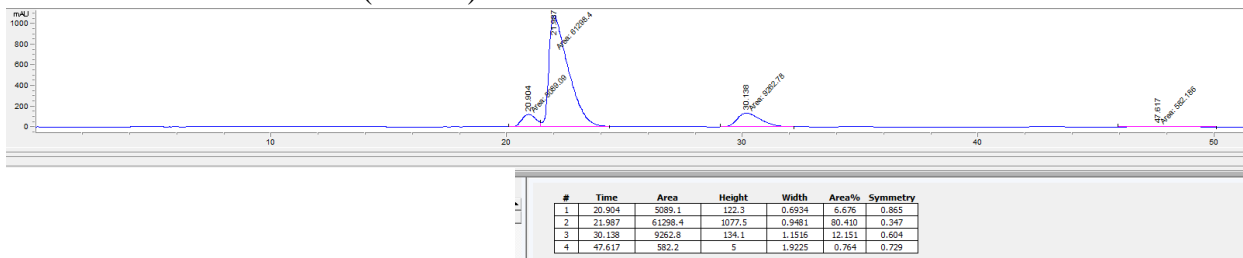
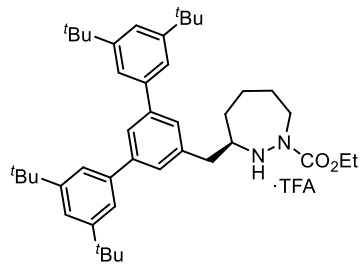


#	Time	Area	Height	Width	Area%	Symmetry
1	12.33	5685.6	150.3	0.6305	8.414	0.845
2	13.463	28517.6	630.4	0.6938	40.202	0.606
3	18.444	27451.9	462.7	0.8888	40.625	0.659
4	29.483	5918.6	60.9	1.6194	8.759	0.91

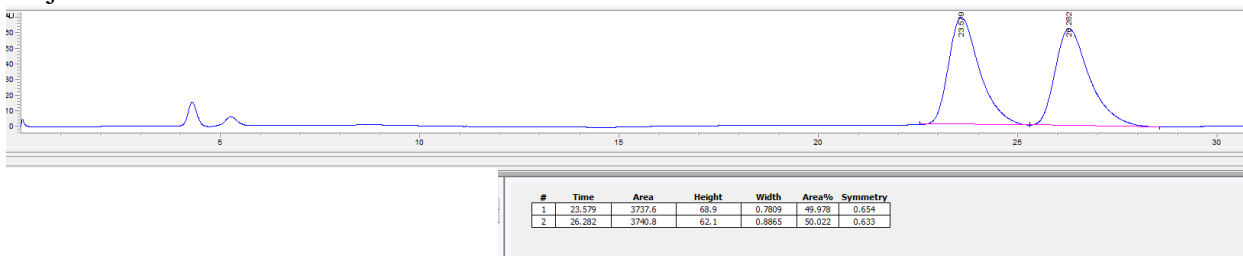
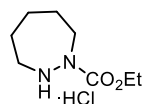


Chiralcel OJ-H, 97:3 hexanes:ⁱPrOH



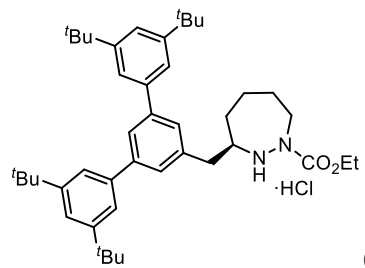


Separation of diastereomers by semi-prep HPLC, 99:1 hexanes:^tPrOH
Chiralcel OD, 98:2 hexanes:^tPrOH

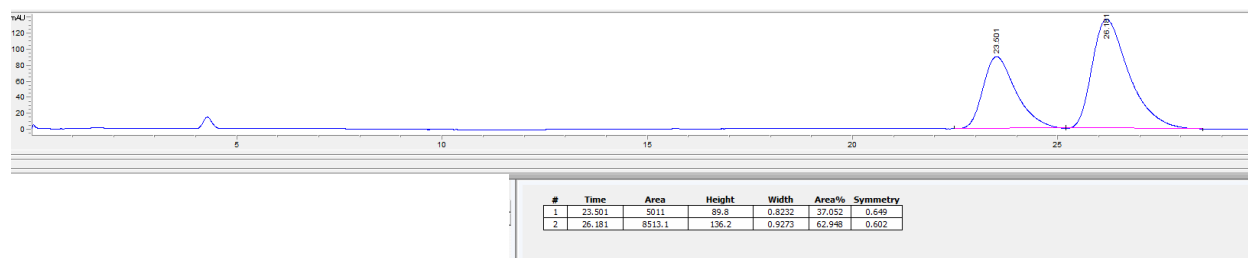


Minor diastereomer



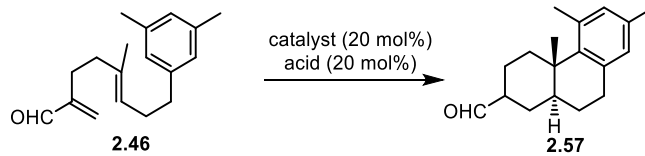


Major diastereomer

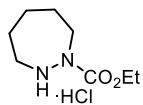


Minor diastereomer

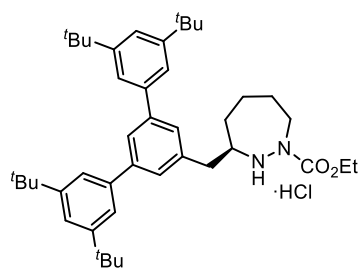
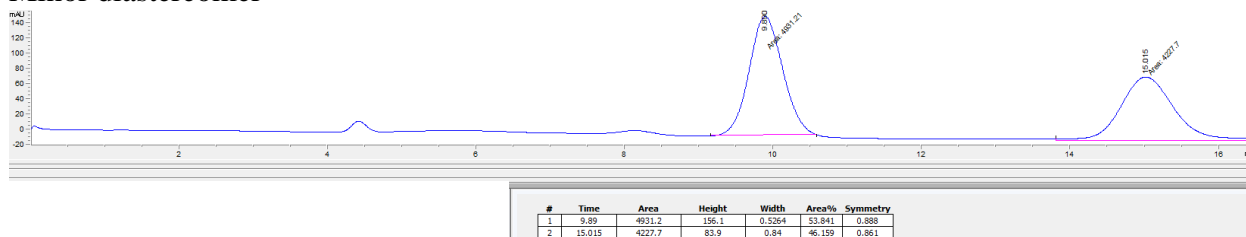




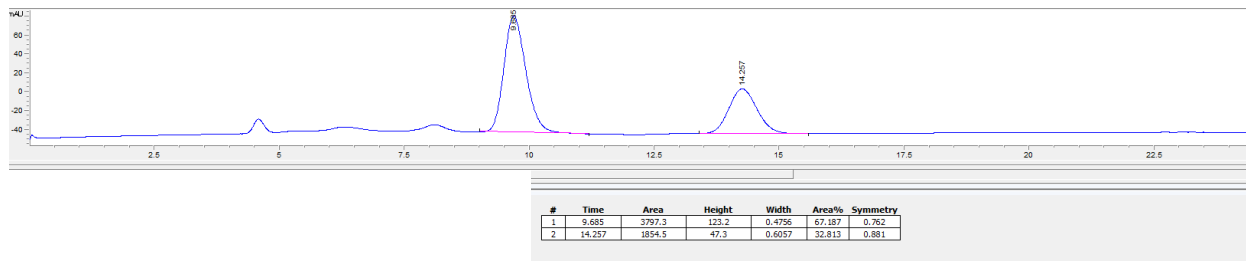
Separation of diastereomers by semi-prep HPLC, 98:2 hexanes:^tPrOH
 Chiralcel OJ-H, 97:3 hexanes:^tPrOH

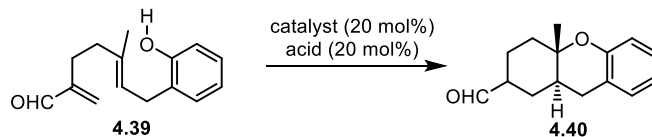


Minor diastereomer

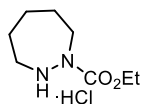


Minor diastereomer

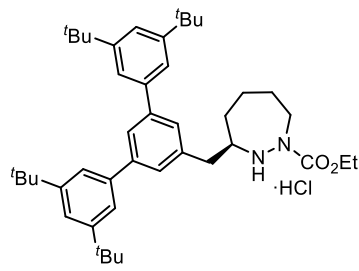
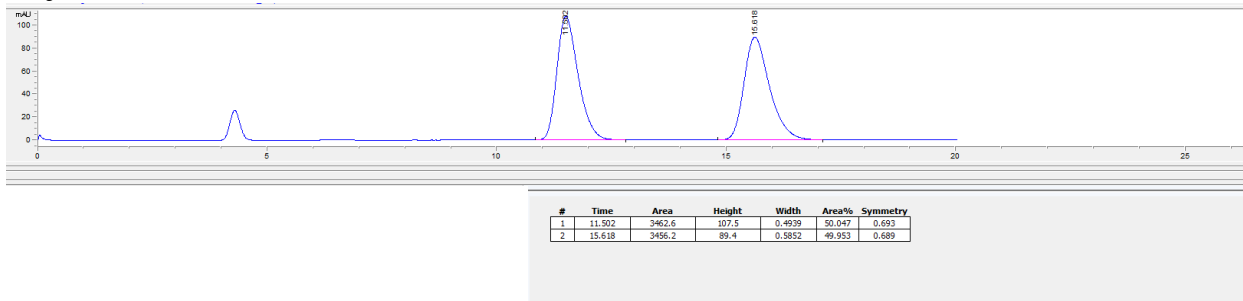




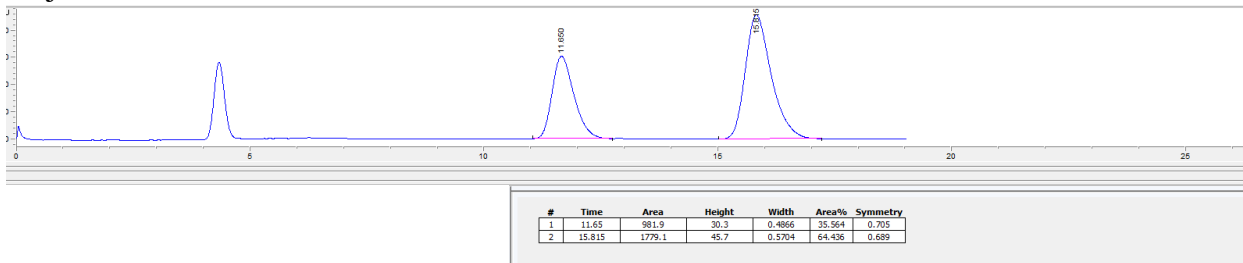
Separation of diastereomers by semi-prep HPLC, 99:1 hexanes:^tPrOH
 Chiralcel OD, 95:5 hexanes:^tPrOH

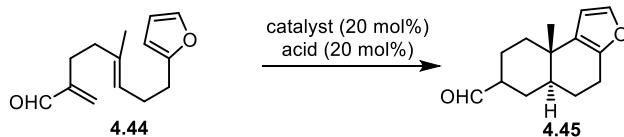


Major diastereomer

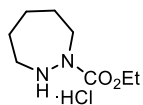


Major diastereomer

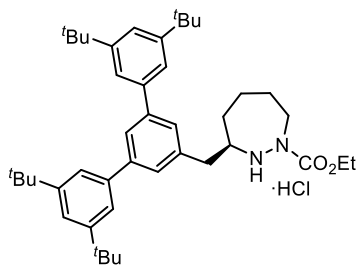
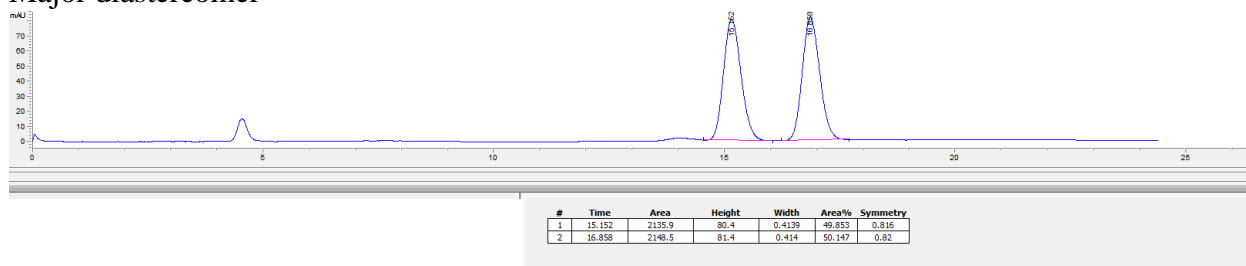




Separation of diastereomers by semi-prep HPLC, 99:1 hexanes:^tPrOH
 Chiralcel OJ-H, 97:3 hexanes:^tPrOH

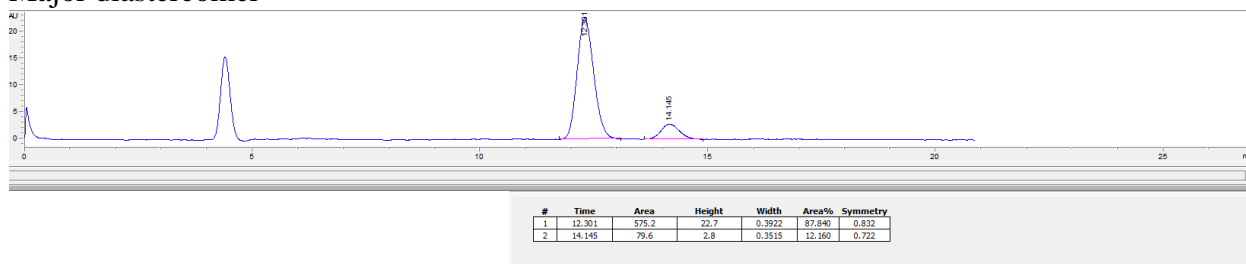


Major diastereomer

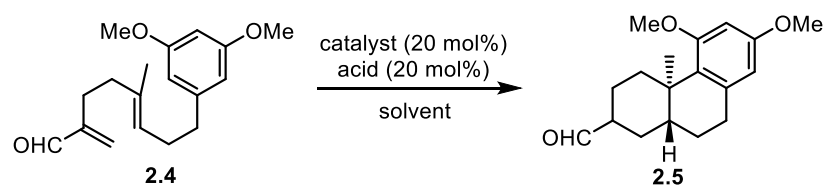


(>99% ee)

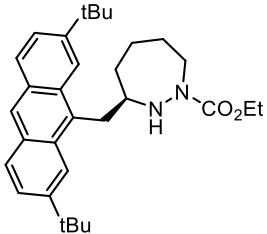
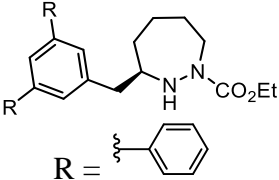
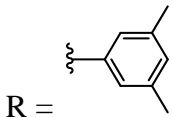
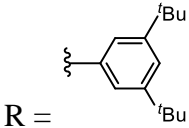
Major diastereomer

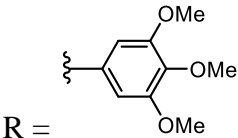
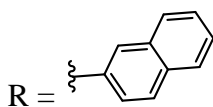
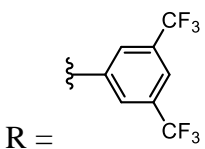
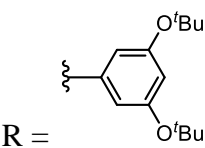
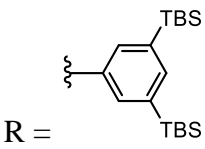
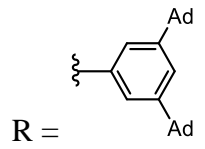
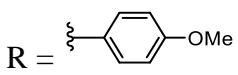


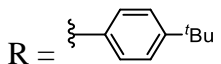
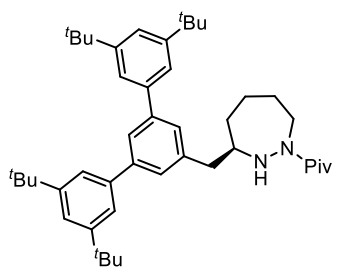
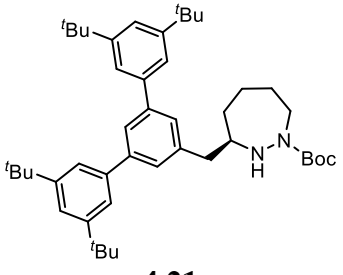
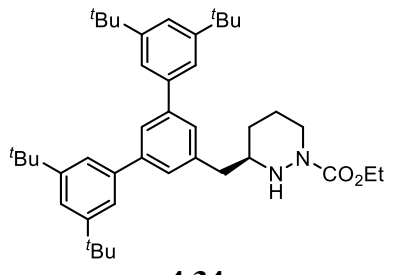
Appendix I. Table of results for the model (*E*)-polyene cyclization with chiral hydrazide catalysts



Catalyst	Solvent	Acid	Reaction Time	Yield	% ee
<p>3.17 (result from Dr. Samuel Plamondon)</p>	EtOH	HCl	48 h	36%	-51
<p>3.21 (result from Dr. Samuel Plamondon)</p>	EtOH	HCl	48 h	42%	7
<p>3.16</p>	2% HFIP/DCM	HCl	72 h	16%	19
<p>3.38</p>	2% HFIP/DCM	HCl	72 h	43%	25
<p>3.46</p>	2% HFIP/DCM	HCl	4 h	67%	2

 <p>3.47</p>	2% HFIP/DCM	HCl	1 h	66%	6
 <p>4.4</p>	2% HFIP/DCM	HCl	1 h	44%	5
	EtOH	HCl	5 days	19%	2
 <p>4.5</p>	2% HFIP/DCM	HCl	24 h	78%	2
	EtOH	HCl	24 h	32%	28
 <p>4.12</p>	EtOH	HCl	8 h	41%	53
 <p>4.13</p>	EtOH	HCl	8 h	50%	73
	10% H ₂ O/EtOH		28 h	56%	75
	MeNO ₂		5 days	63%	38
	2% HFIP/DCM		7 days	32%	29
	toluene		7 days	70%	-29
	cyclohexane		5 days	48%	-27
	EtOH	Tf ₂ NH	3h	69%	67

4.13	EtOH	TFA	6 days	48%	80
	MeOH		24h	59%	75
	ⁱ PrOH		11 days	51%	72
	^t BuOH		9 days	53%	53
 R = 4.14	EtOH	HCl	48 h	57%	56
 R = 4.15	EtOH	HCl	24 h	51%	45
 R = 4.16	EtOH	HCl	24 h	60%	15
 R = 4.17	EtOH	HCl	8 h	25%	43
 R = 4.18	EtOH	HCl	8 h	57%	66
 R = 4.19	EtOH	HCl	24 h	29%	46
 R = 4.28	EtOH	HCl	24 h	38%	56

 <p>4.29</p>	EtOH	HCl	24 h	52%	50
 <p>4.20</p>	EtOH	HCl	30 h	30%	66
 <p>4.21</p>	EtOH	HCl	6 h	62%	75
 <p>4.34</p>	EtOH	HCl	21 h	66%	0